COLLECTED REPRINTS

1985

VOLUME II
K - Z

NATIONAL MARINE FISHERIES SERVICE
SOUTHWEST FISHERIES CENTER

Library
NOAA, National Marine Fisheries Service
SWFC Honolulu Laboratory F/SWC2
2570 Dole Street
Honolulu, HI 96822-2396

LIBRARY

FEB 1, 1990

National Marine Fisheries Service
2570 Dole Street
Honolulu, Hawaii

NATIONAL MARINE FISHERIES SERVICE
SOUTHWEST FISHERIES CENTER

COLLECTED REPRINTS

1985

VOLUME II

K: 8550
Z: 8596

Library
NOAA, National Marine Fisheries Service
SWFC Honolulu Laboratory F/SWC2
2570 Dole Street
Honolulu, HI 96822-2396

SEPTEMBER 1989

The COLLECTED REPRINTS of the
Southwest Fisheries Center,
National Marine Fisheries Service,
La Jolla, California
are not copyrighted
and may be reprinted freely.

TABLE OF CONTENTS

ALVARIÑO, ANGELES.
1985. Predation in the plankton realm; mainly with reference to fish larvae. Inv. Mar. CICIMAR 2 (NGm. Esp. 1):1-122. 8501

ALVARIÑO, ANGELES.
1985. Las surgencias en la region de California-Baja California relaciones con el zooplancton y poblaciones de *Engraulis mordax* (Pisces). Inv. Mar. CICIMAR 2(1):81-102 (in Spanish). 8502

ALVARIÑO, ANGELES.
1985. Distribucion batimetrica de especies del genero *Lensia* en aguas de California y Baja California (Diphyidae, Siphonophorae, Coelenterata). Inv. Mar. CICIMAR 2(1):59-80. 8503

ANKENBRANDT, LISA.
1985. Food habits of bait-caught skipjack tuna, *Katsuwonus pelamis*, from the southwestern Atlantic Ocean. Fish. Bull., U.S. 83(3):379-393. 8504

AU, DAVID W.K. AND WAYNE L. PERRYMAN.
1985. Dolphin habitats in the eastern tropical Pacific. Fish. Bull., U.S. 83(4):623-643. 8505

BAKUN, ANDREW.
1985. Comparative studies and the recruitment problem: Searching for generalizations. Calif. Coop. Oceanic Fish. Invest. Rep. 26:30-40. 8506

BALAZS, GEORGE H.
1985. History of sea turtles at Polihua Beach on northern Lanai. 'Elepaio 46(1):1-3. 8507

BALAZS, GEORGE H.
1985. Retention of flipper tags on hatchling sea turtles. Herp. Rev. 16(2):43-45. 8508

ALAZS, GEORGE H.
1985. Sea turtles and debris: Ingestion and entanglement. Mar. Turtle Newsl. 32:8-9. 8509

ALAZS, GEORGE H.
1985. Status and ecology of marine turtles at Johnston Atoll. Atoll Res. Bull. 285, 46 p. 8510

ALAZS, GEORGE H. AND WILLIAM G. GILMARTIN.
1985. A suggested modification of tagging pliers. Mar. Turtle Newsl. 34:2-3. 8511

ARLOW, JAY.
1985. Variability, trends, and biases in reproductive rates of spotted dolphins, *Stenella attenuata*. Fish. Bull., U.S. 83(4):657-669. 8512

TABLE OF CONTENTS (CONTINUED)

BARTOO, NORMAN AND TOSHIO SHIOHAMA.
1985. A production model analysis of the North Pacific albacore population including estimates of the sensitivity of results to measurement errors in input data. Bull. Far Seas Fish. Res. Lab. 22:109-117. 8513

BENVILLE, P. E., JR., J. A. WHIPPLE, AND M. B. ELDRIDGE.
1985. Acute toxicity of seven alicyclic hexanes to striped bass, *Morone saxatilis*, and bay shrimp, *Crangon franciscorum*, in seawater. Calif. Fish Game 71(3):132-140. 8514

BERKSON, J.M. AND D.P. DeMASTER.
1985. Use of pup counts in indexing population changes in pinnipeds. Can. J. Fish. Aquat. Sci. 42(5):873-879. 8515

BERNARD, HANNAH J., JOHN B. HEDGEPETH, AND STEPHEN B. REILLY.
1985. Stomach contents of albacore, skipjack, and bonito caught off southern California during summer 1983. Calif. Coop. Oceanic Fish. Rep. 26:175-182. 8516

BOEHLERT, GEORGE W.
1985. Using objective criteria and multiple regression models for age determination in fishes. Fish. Bull., U.S. 83(2):103-117. 8517

BOEHLERT, GEORGE W. AND JOHN B. MORGAN.
1985. Turbidity enhances feeding abilities of larval Pacific herring, *Clupea harengus pallasi*. Hydrobiologia 123:161-170. 8518

BOEHLERT, GEORGE W. AND MARY M. YOKLAVICH.
1985. Larval and juvenile growth of sablefish, *Anoplopoma fimbria*, as determined from otolith increments. Fish. Bull., U.S. 83(3):475-481. 8519

BOEHLERT, GEORGE W., DENA M. GADOMSKI AND BRUCE C. MUNDY.
1985. Vertical distribution of ichthyoplankton off the Oregon coast in spring and summer months. Fish. Bull., U.S. 83(4):611-621. 8520

BRAINARD, RUSTY E. AND D. R. McLAIN.
1985. Subsurface temperature variability along the west coast of North and South America. Trop. Ocean-Atmos. Newsl., May issue:1-2. 8521

CASS, VIRGINIA L.
1985. Exploitation of California sea lions, *Zalophus californianus*, prior to 1972. Mar. Fish. Rev. 47(1):36-38. 8522

TABLE OF CONTENTS (CONTINUED)

CASTILLO, GONZALO, EDUARDO AGUILERA, GUILLERMO HERRERA, PATRICIO A. BERNAL, JOHN L. BUTLER, JAVIER CHONG, HUMBERTO GONZALEZ, CIRO OYARZUN, AND CARLOS VELOSO.

1985. Larval growth rates of the Pacific sardine *Sardinops sagax* off central Chile, determined by daily ring counts in otoliths. Biologia Pesquera 14:3-10. 8523

DeMASTER, DOUGLAS P.

1985. An analysis of a hypothetical population of walruses, pp. 77-80. *In:* F.H. Fay and G.A. Fedoseev (eds.), Soviet-American Cooperative Research on Marine Mammals, Vol. 1-Pinnipeds. NOAA Tech. Rep. NMFS-12. 8524

DeMASTER, D., D. MILLER, J.R. HENDERSON, AND J.M. COE.

1985. Conflicts between marine mammals and fisheries off the coast of California, pp. 111-118. *In:* J.R. Beddington, R.J.H. Beverton, and D.M. Lavigne (eds.), Marine Mammals and Fisheries. George Allen Univ., Boston, MA. 8525

DUFFY, JOHN M. AND HANNAH J. BERNARD.

1985. Milkfish, *Chanos chanos* (Forsskal, 1775), taken in southern California adds new family (Chanidae) to the California marine fauna. Calif. Fish Game 71(2):122-125. 8526

FIEDLER, PAUL C., GARY B. SMITH, AND R. MICHAEL LAURS.

1985. Fisheries applications of satellite data in the eastern North Pacific. Mar. Fish. Rev. 46(3):1-13. 8527

GENIN, AMATZIA AND GEORGE W. BOEHLERT.

1985. Dynamics of temperature and chlorophyll structures above a seamount: An oceanic experiment. J. Mar. Res. 43:907- 924. 8528

GERRODETTE, TIM, DANIEL GOODMAN, AND JAY BARLOW.

1985. Confidence limits for population projections when vital rates vary randomly. Fish. Bull., U.S. 83(3):207-217. 8529

GOODING, REGINALD M.

1985. Predation on released spiny lobster, *Panulirus marginatus*, during tests in the Northwestern Hawaiian Islands. Mar. Fish. Rev. 47(1):27-35. 8530

GUILLEMOT, PATRICK J., RALPH J. LARSON, AND WILLIAM H. LENARZ.

1985. Seasonal cycles of fat and gonad volume in five species of northern California rockfish (Scorpaenidae: *Sebastes*). Fish. Bull., U.S. 83(3):299-311. 8531

TABLE OF CONTENTS (CONTINUED)

HEWITT, ROGER P.
1985. A protocol for designing a sea survey for anchovy biomass assessment, pp. 51-53. *In*: R. Lasker (ed.), An egg production method for estimating spawning biomass of pelagic fish: Application to the northern anchovy, *Engraulis mordax*. NOAA Tech. Rep. NMFS-36. 8532

HEWITT, ROGER P.
1985. Comparison between egg production method and larval census method for fish biomass assessment, pp. 95-99. *In:* R. Lasker (ed.), An egg production method for estimating spawning biomass of pelagic fish: Application to the northern anchovy, *Engraulis mordax*. NOAA Tech. Rep. NMFS-36. 8533

HEWITT, ROGER P.
1985. Reaction of dolphins to a survey vessel: effects on census data. Fish. Bull., U.S. 83(2):187-193. 8534

HEWITT, ROGER P.
1985. The 1984 spawning biomass of the northern anchovy. Calif. Coop. Oceanic Fish. Invest. Rep. 26:17-25. 8535

HEWITT, ROGER P., GAIL H. THEILACKER, AND NANCY C.H. LO.
1985. Causes of mortality in young jack mackerel. Mar. Ecol. Prog. Ser. 26:1-10. 8536

HIGHTOWER, JOSEPH E. AND GARY D. GROSSMAN.
1985. Comparison of constant effort harvest policies for fish stocks with variable recruitment. Can. J. Fish. Aquat. Sci. 42(5):982-988. 8537

HOHN, ALETA A. AND P.S. HAMMOND.
1985. Early postnatal growth of the spotted dolphin, *Stenella attenuata*, in the offshore eastern tropical Pacific. Fish. Bull., U.S. 83(4):553-566. 8538

HOHN, ALETA A., SUSAN J. CHIVERS, AND JAY BARLOW.
1985. Reproductive maturity and seasonality of male spotted dolphins, *Stenella attenuata*, in the eastern tropical Pacific. Mar. Mamm. Sci. 1(4):273-293. 8539

HOLLAND, KIM, RICHARD BRILL, SCOTT FERGUSON, RANDOLPH CHANG, AND REUBEN YOST.
1985. A small vessel technique for tracking pelagic fish. Mar. Fish. Rev. 47(4):26-32. 8540

HOLLAND, KIM, RANDOLPH CHANG, AND SCOTT FERGUSON.
1985. Progress report on tuna tracking. South Pac. Comm. Fish. Newsl. 32:19-23 8541

TABLE OF CONTENTS (CONTINUED)

OLTS, DAVE.
1985. Recreational albacore, *Thunnus alalunga*, fishery by U.S. west coast commercial passenger fishing vessels. Mar. Fish. Rev. 47(3):48-53. 8542

UNTER, J. ROE.
1985. Preservation of northern anchovy in formaldehyde solution, pp. 63-64. *In:* R. Lasker (ed.), An egg production method for estimating spawning biomass of pelagic fish: Application to the northern anchovy, *Engraulis mordax*. NOAA Tech. Rep. NMFS-36. 8543

UNTER, J. ROE AND BEVERLY J. MACEWICZ.
1985. Measurement of spawning frequency in multiple spawning fishes, pp. 79-94. *In:* R. Lasker (ed.), An egg production method for estimating spawning biomass of pelagic fish: Application to the northern anchovy, *Engraulis mordax*. NOAA Tech. Rep. NMFS-36. 8544

UNTER, J. ROE AND BEVERLY J. MACEWICZ.
1985. Rates of atresia in the ovary of captive and wild northern anchovy, *Engraulis mordax*. Fish. Bull., U.S. 83(2):119-136. 8545

UNTER, JOHN AND RAGAN NICHOLL.
1985. Visual threshold for schooling in northern anchovy *Engraulis mordax*. Fish. Bull., U.S. 83(3):235-242. 8546

UNTER, J. ROE, NANCY C.H. LO, AND RODERICK J.H. LEONG.
1985. Batch fecundity in multiple spawning fishes, pp. 67-77. *In:* R. Lasker (ed.), An egg production method for estimating spawning biomass of pelagic fish: application to the northern anchovy, *Engraulis mordax*. NOAA Tech. Rep. NMFS-36. 8547

UPPERT, DANIEL D.
1985. Pacific coast groundfish management: Evolution and prospects, pp. 309-335. *In:* T. Frady (ed.), Proceedings of the Conference on Fisheries Management: Issues and Options. Univ. Alaska, Alaska Sea Grant Rep. 85-2, April 1985. 8548

UPPERT, DANIEL D., ROGER D. FIGHT, AND FRED H. EVEREST.
1985. Economic considerations, chapter 14, pp. 1-27. *In:* William Meehan (ed.), Influence of Forest and Rangeland Management on Anadromous Fish Habitat in Western North America. U.S. Dep. of Agriculture, Forest Service. Pacific Northwest Forest and Range Experiment Station, General Technical Report PNW-181, Portland, Oregon. 8549

ATO, SUSUMU AND STEPHEN C. SCHROETER.
1985. Biology of the red sea urchin, *Strongylocentrotus franciscanus*, and its fishery in California. Mar. Fish. Rev. 47(3):1-20. 8550

TABLE OF CONTENTS (CONTINUED)

KIRSCHVINK, J. L., M. M. WALKER, S-B CHANG, A. E. DIZON, AND K. A. PETERSON.
1985. Chains of single-domain magnetite particles in chinook salmon, Oncorhynchus tshawytscha. J. Comp. Physiol. A 157:375-381. 8551

LASKER, REUBEN.
1985. What limits clupeoid production? Can. J. Fish. Aquat. Sci. 42 (Suppl. l):31-38. 8552

LAURS, R.M.
1985. Application of satellite remote sensing to U.S. fisheries, pp. 755-763. *In:* Ocean Space Utilization '85. Proceedings of the International Symposium, Nihon Univ., Tokyo, Japan, June 1985. Springer-Verlag, Tokyo. 8553

LAURS, R. MICHAEL AND JOHN T. BRUCKS.
1985. Living marine resources applications, pp. 419-452. *In:* Barry Saltzman (ed.), Satellite oceanic remote sensing. Adv. Geophy. 27, Acad. Press. 8554

LAURS, R.M., R. NISHIMOTO, AND J.A. WETHERALL.
1985. Frequency of increment formation on Sagittae of North Pacific albacore *(Thunnus alalunga)*. Can. J. Fish. Aquat. Sci. 42(9): 1552-1555. 8555

LO, NANCY C.H.
1985. Egg production of the central stock of northern anchovy, *Engraulis mordax*, 1951-82. Fish. Bull., U.S. 83(2):137-150. 8556

LO, NANCY C. H.
1985. A model for temperature-dependent northern anchovy egg development and an automated procedure for the assignment of age to staged eggs, pp. 43-50. *In:* R. Lasker (ed.), An egg production method for estimating spawning biomass of pelagic fish: Application to the northern anchovy, *Engraulis mordax*. NOAA Tech. Rep. NMFS-36. 8557

MacCALL, ALEC D., RICHARD A. KLINGBEIL, AND RICHARD D. METHOT.
1985. Recent increased abundance and potential productivity of Pacific mackerel *(Scomber japonicus)*. Calif. Coop. Oceanic Fish. Invest. Rep. 26:119-129. 8558

McLAIN, DOUGLAS R., RUSSELL E. BRAINARD, AND JERROLD G. NORTON.
1985. Nomalous warm events in eastern boundary current systems. Calif. Coop. Oceanic Fish. Invest. Rep. 26:51-64. 8559

TABLE OF CONTENTS (CONTINUED)

MACKETT, DAVID J.

1985. Strategic planning for research and management of the albacore tuna fishery. Systems Res. 2(3):201-210. 8560

MOSER, H. GEOFFREY, ELAINE M. SANDKNOP, AND DAVID A. AMBROSE.

1985. Larvae and juveniles of aurora rockfish, *Sebastes aurora*, from off California and Baja California, pp. 55-64. *In:* A. W. Kendall, Jr. and J. B. Marliave (eds.), Descriptions of early life history stages of selected fishes. Third International Symposium on the Early Life History of Fishes and 8th Annual Larval Fish Conference, May 1984, University of British Columbia, Vancouver, Canada. Can. Tech. Rep. Fish. Aquat. Sci. 1359. 8561

MOSER, H. GEOFFREY AND ELBERT H. AHLSTROM.

1985. Staging anchovy eggs, pp. 37-41. *In:* R. Lasker (ed.), An egg production method for estimating spawning biomass of pelagic fish: Application to the northern anchovy, *Engraulis mordax*. NOAA Tech. Rep. NMFS-36. 8562

MOSER, MIKE, JUDY A. SAKANARI, CAROL A. REILLY, AND JEANNETTE WHIPPLE.

1985. Prevalence, intensity, longevity, and persistence of *Anisakis* sp. larvae and *Lacistorhynchus tenuis* metacestodes in San Francisco striped bass. NOAA Tech. Rep. NMFS-29, 4 8563

NJOKU, E.G., T.P. BARNETT, R.M. LAURS, AND A.C. VASTANO

1985. Advances in satellite sea surface temperature measurement and oceanographic applications. J. Geophys. Res. 90(C6):11,573-11,586. 8564

NORTON, J., D. McLAIN, R. BRAINARD, AND D. HUSBY.

1985. The 1982-83 El Niño event off Baja and Alta California and its ocean climate context, pp. 44-72. *In:* Warren S. Wooster and David L. Fluharty (eds.), El Niño north: Niño effects in the eastern subarctic Pacific Ocean. Washington Sea Grant Program, Univ. Washington, Seattle, WA 98195 USA. 8565

PARKER, KEITH.

1985. Biomass model for the egg production method, pp. 5-6. *In*: R. Lasker (ed.), An egg production method for estimating spawning biomass of pelagic fish: Application to the northern anchovy, *Engraulis mordax*. NOAA Tech. Rep. NMFS-36. 8566

PARRISH, R.H., D.L. MALLICOATE, AND K.F. MAIS.

1985. Regional variations in the growth and age composition of northern anchovy, *Engraulis mordax*. Fish. Bull., U.S. 83(4): 483-496. 8567

TABLE OF CONTENTS (CONTINUED)

PERRIN, WILLIAM F.

1985. The former dolphin fishery at St Helena. Rep. Int. Whal. Commn 35:423-428. 8568

PERRIN, WILLIAM F., MICHAEL D. SCOTT, G. JAY WALKER, AND VIRGINIA L. CASS.

1985. Review of geographical stocks of tropical dolphins (*Stenella* spp. and *Delphinus delphis)* in the eastern Pacific. NOAA Tech. Rep. NMFS-28, 28 p. 8569

PERRY, ANJANETTE, GORDON B. BAUER, AND ANDREW E. DIZON.

1985. Magnetoreception and biomineralization of magnetite in amphibians and reptiles, pp. 439-453. *In:* J. L. Kirschvink, D. S. Jones, and B. J. MacFadden (eds.), Magnetite biomineralization and magnetoreception in organisms. Plenum Press, New York, NY. 8570

PERRY, S. F., C. DAXBOECK, B. EMMETT, P. W. HOCHACHKA, AND R. W. BRILL.

1985. Effects of exhausting exercise on acid-base regulation in skipjack tuna *(Katsuwonus pelamis)* blood. Physiol. Zool. 58(4):421-429. 8571

PERRY, S. F., C. DAXBOECK, B. EMMETT, P. W. HOCHACHKA, AND R. W. BRILL.

1985. Effects of temperature change on acid-base regulation in skipjack tuna *(Katsuwonus pelamis)* blood. Comp. Biochem. Physiol. 81A(1):49-53. 8572

PICQUELLE, SUSAN.

1985. Sampling requirements for the adult fish survey, pp. 55-57. *In:* R. Lasker (ed.), An egg production method for estimating spawning biomass of pelagic fish: Application to the northern anchovy, *Engraulis mordax*. NOAA Tech. Rep. NMFS-36. 8573

PICQUELLE, SUSAN AND GARY STAUFFER.

1985. Parameter estimation for an egg production method of northern anchovy biomass assessment, pp. 7-15. *In:* R. Lasker (ed.), An egg production method for estimating spawning biomass of pelagic fish: Application to the northern anchovy, *Engraulis mordax*. NOAA Tech. Rep. NMFS-36. 8574

PITMAN, ROBERT L.

1985. The marine birds of Alijos Rocks, Mexico. Western Birds 16:81-92. 8575

PITMAN, ROBERT L. AND MICHAEL R. GRAYBILL.

1985. Horned puffin sightings in the eastern Pacific. Western Birds 16:99-102. 8576

TABLE OF CONTENTS (CONTINUED)

POLOVINA, J.
1985. Variation in catch rates and species composition in handline catches of deepwater snappers and groupers in the Mariana Archipelago. Proc. Fifth Int. Coral Reef Congress, Tahiti, 5:515-520. 8577

POLOVINA, JEFFREY J.
1985. Artificial reef technology in Japan. ONRFE Sci. Bul. 10(4):15-20. 8578

POLOVINA, JEFFREY J. AND MARK D. OW.
1985. An approach to estimating an ecosystem box model. Fish. Bull., U.S. 83(3):457-460. 8579

POLOVINA, JEFFREY J., ROBERT B. MOFFITT, STEPHEN RALSTON, PAUL M. SHIOTA, AND HAPPY A. WILLIAMS.
1985. Fisheries resource assessment of the Mariana Archipelago, 1982-85. Mar. Fish. Rev. 47(4):19-25. 8580

RALSTON, STEPHEN.
1985. A novel approach to aging tropical fish. ICLARM Newsl. 8(1):14-15. 8581

SEAGARS, DANA J. AND JOHN R. HENDERSON.
1985. Cephalopod remains from the stomach of a short-finned pilot whale collected near Santa Catalina Island, California. J. Mamm. 66(4):777-779. 8582

SCOTT, MICHAEL D., WAYNE L. PERRYMAN, AND WILLIAM G. CLARK.
1985. The use of aerial photographs for estimating school sizes of cetaceans. Inter-Am. Trop. Tuna Comm., Bull. 18(5):383-419. 8583

SHOMURA, RICHARD S.
1985. Drift bottle makes long journey. Hawaii Fishing News 10(1):12 8584

SMITH, PAUL E.
1985. A case history of an anti-El Niño to El Niño transition on plankton and nekton distribution and abundances, pp. 121-142. *In:* Warren S. Wooster and David L. Fluharty (eds.), El Niño north: Niño effects in the eastern subarctic Pacific Ocean. Washington Sea Grant Program, Univ. Washington, Seattle, WA 98195 USA. 8585

SMITH, PAUL E. AND ROGER P. HEWITT
1985. Anchovy egg dispersal and mortality as inferred from close-interval observations. Calif. Coop. Oceanic Fish. Invest. Rep. 26:97-110. 8586

TABLE OF CONTENTS (CONTINUED)

SMITH, PAUL E. AND ROGER P. HEWITT.
1985. Sea survey design and analysis for an egg production method of anchovy biomass assessment, pp. 17-26. *In:* R. Lasker (ed.), An egg production method for estimating spawning biomass of pelagic fish: Application to the northern anchovy, *Engraulis mordax*. NOAA Tech. Rep. NMFS-36. 8587

SMITH, PAUL E., WILLIAM FLERX, AND ROGER P. HEWITT.
1985. The CalCOFI vertical egg tow (CalVET) net, pp. 27-32. *In:* R. Lasker (ed.), An egg production method for estimating spawning biomass of pelagic fish: Application to the northern anchovy, *Engraulis mordax*. NOAA Tech. Rep. NMFS-36. 8588

SQUIRE, JAMES L., JR.
1985. Relationship of sea surface temperature isotherm patterns off northwestern Mexico to the catch of striped marlin, *Tetrapturus_audax*, off southern California. Mar. Fish. Rev. 47(3):43-47. 8589

STAUFFER, GARY AND SUSAN PICQUELLE.
1985. Procedures for sorting, staging, and ageing eggs, pp. 33-35. *In:* R. Lasker (ed.), An egg production method for estimating spawning biomass of pelagic fish: Application to the northern anchovy, *Engraulis mordax*. NOAA Tech. Rep. NMFS-36. 8590

SUMIDA, BARBARA Y., H. GEOFFREY MOSER, AND ELBERT H. AHLSTROM.
1985. Descriptions of larvae of California yellowtail, *Seriola lalandi*, and three other carangids from the eastern tropical Pacific: *Chloroscombrus orqueta*, *Caranx caballus*, and *Caranx sexfasciatus*. Calif. Coop. Oceanic Fish. Invest. Rep. 26:139-159. 8591

WAHLEN, BRUCE E. AND TIM D. SMITH.
1985. Observer effect on incidental dolphin mortality in the eastern tropical Pacific tuna fishery. Fish. Bull., U.S. 83(4):521-530. 8592

WALKER, MICHAEL M., JOSEPH L. KIRSCHVINK, AND ANDREW E. DIZON.
1985. Magnetoreception and biomineralization of magnetite fish, pp. 417-437. *In:* J. L. Kirschvink, D. S. Jones, and B. J. MacFadden (eds.), Magnetite biomineralization and magnetoreception in organisms. Plenum Press, New York, NY.9592 8593

WALKER, MICHAEL M., JOSEPH L. KIRSCHVINK, ANJANETTE PERRY, AND ANDREW E. DIZON.
1985. Detection, extraction, and characterization of biogenic magnetite, pp. 155-166. *In:* J. L. Kirschvink, D. S. Jones, and B. J. MacFadden (eds.), Magnetite biomineralization and magnetoreception in organisms. Plenum Press, New York, NY. 8594

TABLE OF CONTENTS (CONTINUED)

WHITTOW, G. CAUSEY AND GEORGE H. BALAZS.
1985. The thermal ecology of basking green turtles *(Chelonia mydas)*. Natl. Geographic Soc. Res. Rep. - 1977 Projects, pp. 789-796. 8595

ZUG, GEORGE R. AND GEORGE H. BALAZS.
1985. Skeletochronological age estimates for Hawaiian green turtles. Mar. Turtle Newsl. 33:9-10. 8596

The following publications are not included in the *Collected Reprints* 1985:

BALAZS, GEORGE H.
1985. Impact of ocean debris on marine turtles: Entanglement and ingestion, p. 387-429. *In:* R. S. Shomura and H. O. Yoshida (eds.), Proceedings of the Workshop on the Fate and Impact of Marine Debris, 26-29 November 1984, Honolulu, Hawaii. U.S. Dep. Commer., NOAA Tech. Memo., NOAA-TM-NMFS-SWFC-54.

GERRODETTE, TIM.
1985. Toward a population dynamics of marine debris, pp. 508-518. *In:* R. S. Shomura and H. O. Yoshida (eds.), Proceedings of the Workshop on the Fate and Impact of Marine Debris, 26-29 November 1984, Honolulu, Hawaii. U.S. Dep. Commer., NOAA Tech. Memo., NOAA-TM-NMFS-SWFC-54.

HENDERSON, JOHN R.
1985. A review of Hawaiian monk seal entanglements in marine debris, pp. 326-335. *In:* R. S. Shomura and H. O. Yoshida (eds.), Proceedings of the Workshop on the Fate and Impact of Marine Debris, 26-29 November 1984, Honolulu, Hawaii. U.S. Dep. Commer., NOAA Tech. Memo., NOAA-TM-NMFS-SWFC-54.

LASKER, REUBEN. (Editor).
1985. An egg production method for estimating spawning biomass of pelagic fish: Application to the northern anchovy, *Engraulis mordax*. NOAA Tech. Rep. NMFS-36, 99 p.

LENARZ, WILLIAM H.
1985. Theoretical first approximations of densities of discarded webbing in the eastern North Pacific Ocean and Bering Sea, pp. 213- 217. *In:* R. S. Shomura and H. O. Yoshida (eds.), Proceedings of the Workshop on the Fate and Impact of Marine Debris, 26-29 November 1984, Honolulu, Hawaii. U.S. Dep. Commer., NOAA Tech. Memo., NOAA-TM-NMFS-SWFC-54.

MORROW, ROBERT J. AND ELIZABETH. K. BUELNA.
1985. The Hawaiian monk seal and green turtle on Necker Island, 1983. U.S. Dep. Commer., NOAA Tech. Memo., NOAA-TM-NMFS-SWFC-55, 11 p.

TABLE OF CONTENTS (CONTINUED)

PARRISH, RICHARD H.
1985. Operational plan for NMFS albacore program. U.S. Dep. Commer., NOAA Tech. Memo., NOAA-TM-NMFS-SWFC-52, 31 p.

SHOMURA, RICHARD S. AND HOWARD O. YOSHIDA (EDITORS).
1985. Proceedings of the workshop on the fate and impact of marine debris, 26-29 November 1984, Honolulu, Hawaii. U.S. Dep. Commer., NOAA Tech. Memo., NOAA-TM-NMFS-SWFC-54, 580 p.

SUND, PAUL N.
1985. Albacore fishing and windspeed. U.S. Dep. Commer., NOAA Tech. Memo., NOAA-TM-NMFS-SWFC-53, 18 p.

UCHIDA, RICHARD N.
1985. The types and estimated amounts of fish net deployed in the North Pacific, pp. 37-108. *In:* R. S. Shomura and H. O. Yoshida (eds.), Proceedings of the Workshop on the Fate and Impact of Marine Debris, 27-29 November 1984, Honolulu, Hawaii. U.S. Dep. Commer., NOAA Tech. Memo., NOAA-TM-NMFS-SWFC-54.

Biology of the Red Sea Urchin, *Strongylocentrotus franciscanus*, and Its Fishery in California

SUSUMU KATO and STEPHEN C. SCHROETER

Introduction

Since Kato (1972) reported on the beginning of the sea urchin fishery in California, it has grown dramatically. The catch has exceeded 11,000 metric tons (t) in 1981 in California, and up to 500 t have been harvested in 1 year in Washington. Most of the product of the fishery, the roe (both male and female gonads), is marketed in Japan, where the sea urchins as well as the roe are called "uni."

Inevitably, development of the fishery has raised questions about the status of populations, and effects of the fishery on the urchins and environment. Because fishermen, processors, potential investors, and management officials all require information, several scientific studies were initiated by researchers in Canada and the United States to answer some of these needs. This report presents relevant information from the literature, much of which is not readily accessible to persons in the industry, as well as from our own investigations. A review of red sea urchin, *Strongylocentrotus franciscanus* (Fig. 1), biology is given to promote understanding of natural processes which can have a bearing on the commercial use of sea urchins. Descriptions of the harvesting, processing, and marketing sectors of the industry are also presented. We hope that this information will aid in maintaining a commercially viable and environmentally sound fishery for many years. We hope that this report will fill the needs of the hundreds of persons from throughout the United States as well as other countries who have requested information to help them develop fisheries for their species of sea urchins.

Description of Sea Urchins

Sea urchins belong to the phylum Echinodermata, which also includes starfish, sea cucumbers, sea lilies, and brittle stars. All sea urchins have a hard calcareous shell called a test, which is covered with a thin epithelium and is usually armed with spines. The mouth, located on the underside, consists of five calcareous plates called "Aristotle's lantern" in honor of the Greek naturalist and philosopher. The mouth leads to the digestive tract which empties through the anus located on the top of the test.

Five skeins of roe comprise the most prominent structures in the internal cavity of sea urchins. Sea urchins are

Susumu Kato is with the Tiburon Laboratory, Southwest Fisheries Center, National Marine Fisheries Service, NOAA, Tiburon, CA 94920, and Stephen C. Schroeter is with the Department of Biological Sciences, University of Southern California, University Park, CA 90089.

ABSTRACT—The California fishery for the red sea urchin, Strongylocentrotus franciscanus, *has grown steadily since its inception in 1972, and the maximum annual catch has exceeded 11,000 metric tons. Most of the product of the fishery, the roe, is exported to Japan, though a significant amount is also consumed in the United States. This paper describes aspects of red sea urchin life history, distribution, abundance, ecology, and management. A detailed description of the fishery, including harvesting, processing, shipping, and marketing methods, is also given.*

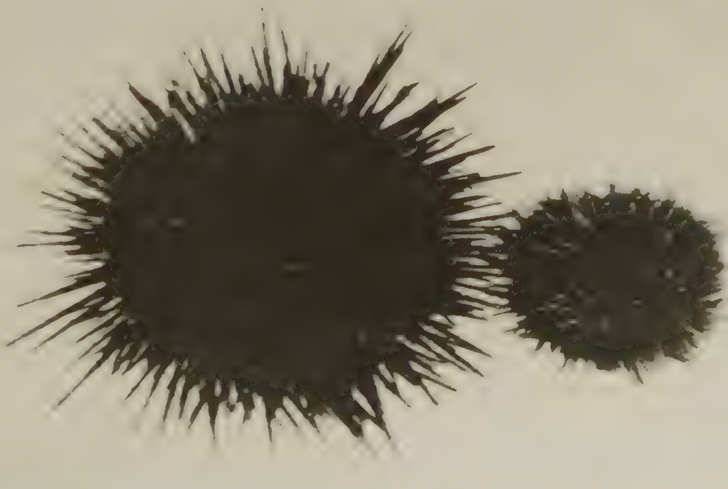

Figure 1.—The red sea urchin, *Strongylocentrotus franciscanus* (left), and the smaller purple sea urchin, *S. purpuratus*.

unisexual, being either male or female, but cases of hermaphroditism (i.e., with both male and female gonads) have been recorded in several species (Boolootian and Moore, 1956). Between the skeins of roe are gill-like structures which are part of the water vascular system, important in movement, respiration, and food gathering. The gut is dark and often filled with partially digested plant material.

Two species of sea urchins are common in shallow coastal waters off California: The red, *S. franciscanus*, and purple, *S. purpuratus*, sea urchins (Fig. 1). Several other species also occur in California, but they are either too small or too rare to be of economic significance. In fact, only the red sea urchin is presently harvested, although the purple sea urchin offers potential because of its abundance. The red sea urchin is one of the largest species of sea urchins in the world, growing to a test diameter of about 18 cm. Its test and spine color is usually dark purple. Not infrequently, however, either the test or spines—or both—are reddish or light purple. The length of the spines may be correlated with the habitat; sea urchins in deeper, calmer waters tend to have longer spines than those in shallower waters where greater abrasion of spines occurs (Silver and Brierton, 1974). The purple sea urchin, which has relatively short spines, is usually light purple or lavender.

Sea urchin roe contains an assortment of nutrients. Major components of the roe of red and purple urchins are given in Table 1. The percentages of various constituents are likely to change, depending on the nutritional and reproductive states of the urchins. Sea urchin roe also contains calcium, phosphorus, iron, Vitamins A, B_1, B_2, B_{12}, nicotinic acid, pantothenic acid, folic acid, and carotenes (Higashi et al. 1959, 1965).

Table 1.—Proximate analyses of red and purple sea urchin roe (percent of total roe weight)[1].

	Red sea urchin		Purple sea urchin	
Item	1	2	3	2
Moisture	70.0	70.8	68.6	71.8
Protein	7.7	9.6	9.5	12.3
Lipid	7.6	8.3	5.4	5.2
Ash	1.6	1.5	1.3	1.7
Glycogen	1.3		1.7	
Nonprotein nitrogen	0.1	0.5	0.1	0.5

[1] Sources: 1. Modified after Greenfield et al., 1958; 2. from Kramer and Nordin, 1979; 3. Modified after Giese et al., 1958

Since polychlorinated biphenols (PCB) and other potentially toxic hydrocarbons are of major concern to the Japanese, an analysis was undertaken to learn the extent of pollution from these noxious compounds. Red sea urchins collected at Fort Bragg, Calif., in 1973 were found to have no detectable amounts of DDT, but contained an average of 0.026 ppm (parts per million of wet weight) of DDE (range 0.006-0.050 ppm). Amounts of PCB averaged 0.04 ppm and ranged from 0.01 to 0.09 ppm[1]. Tolerance levels for PCB set by the Japanese government vary depending on the foodstuff. In flesh of coastal fishes a level of 3.0 ppm is allowed[2]. In the United States, the maximum allowable in "shellfish" is 2 ppm. Thus the California sample fell well within acceptable levels.

Distribution and Abundance

Red sea urchins are found on the west coast of North America as far south as the tip of Baja California, although their abundance declines south of lat. 27°N (Malagrino Lumare, 1972). They range northward to Sitka and Kodiak, Alaska, and along the Asiatic coast as far south as the southern tip of Hokkaido Island, Japan (McCauley and Carey, 1967). Off the California coast, dense concentrations occur patchily throughout the state. Notable exceptions are those areas off central California where sea otters, *Enhydra lutris*, a major predator of sea urchins, are abundant (McLean, 1962; E. E. Ebert, 1968; Lowry and Pearse, 1973).

Both the red sea urchin and its close relative, the purple sea urchin, usually occupy shallow waters, from the mid to low intertidal zones to depths in excess of 50 m, but red sea urchins have been found as deep as 125 m (McCauley and Carey, 1967). Individuals of both species prefer rocky substrates, particularly ledges and crevices (Schroeter, 1978), and avoid sand and mud.

Both species are often found in and around stands of the giant kelp, *Macrocystis* spp., and other brown algae. Typically, sea urchins are most abundant near the outer edges of kelp beds and less numerous inside (Pearse et al., 1970; Low, 1975; Pace, 1975; Mattison et al., 1977; Tegner and Dayton, 1981). Adult sea urchins that live within kelp beds are larger than those outside, and recent recruits (<10-20 mm) are much more abundant outside than inside the beds (Pearse et al., 1970; Bernard and Miller, 1973; Tegner and Dayton, 1981). Similar patterns have been documented for green sea urchins, *S. drobachiensis*) on the coast of Nova Scotia, Canada (Bernstein et al., 1981). Several hypotheses have been advanced to account for these patterns. Individuals within kelp beds may be larger either because they grow faster, survive longer, or both (Pearse et al., 1970). T. A. Ebert's work (1968) supports the conjecture that individuals inside are larger because they have more food. He studied intertidal populations of purple sea urchins and found that the maximum size attained by individuals in a population is influenced directly by food supply. Additional studies on red sea urchins in southern California (Pearse et al., 1970; Baker, 1973) also support this hypothesis.

The much greater abundance of very small individuals outside of kelp beds may be due to higher rates of settlement, higher survival after settlement, or both (Pearse et al., 1970; Ebert, 1983). Higher rates of settlement could result from active selection by larvae or from the passive concentration of larvae. Alternatively, larvae may be equally abundant inside and outside of beds, but may suffer higher mortality in the former habitat (Pearse et al., 1970).

Juvenile red sea urchins are frequently found under the spines of larger red urchins, and are scarce elsewhere in the same habitat (Low, 1975; Breen et al., 1976; Tegner and Dayton, 1977; Schroeter, 1978). One possible explanation for this distributional pattern is that larvae selectively settle in areas where adults are abundant, and soon find shelter under the larger sea urchins. This hypothesis was tested and rejected by Cameron and Schroeter (1980), who conducted laboratory and field larval selectivity experiments with red and purple sea urchins. They concluded that the pattern of juvenile distribution was due either to increased survival rates under adults, or to migration of young sea urchins under adults following settlement. Hinegardner (1969, 1975) and Cameron and Hinegardner (1974) found that the larvae of white sea urchins, *Lytechinus anamesus*, selectively settle and metamorphose on bacterial films. These films are ubiquitous (Sheer, 1945) and are probably abundant inside as well as outside kelp beds.

---

[1] Reuben Lasker, National Marine Fisheries Service, NOAA, La Jolla, Calif. Personal commun.

[2] Katsutoshi Miwa, Tokai Regional Fisheries Research Laboratory, Tokyo, Japan. Personal commun.

An hypothesis that higher mortality of larvae or juveniles inside versus outside kelp beds accounts for patterns of juvenile abundance remains untested; however, the higher abundance of filter-feeding organisms, known to eat sea urchin larvae, inside kelp beds suggests that predation of larvae may be significant (Pearse et al., 1970).

The importance of predation after settlement is suggested by a number of studies which have identified sea urchin predators that are abundant inside or near the edges of kelp beds. These predators include rock crabs, *Cancer* spp. (MacGinitie and MacGinitie, 1968); leather starfish, *Dermasterias imbricata* (Rosenthal and Chess, 1972); sun stars, *Pycnopodia helianthoides* (Tegner and Dayton, 1981); agile sea stars, *Astrometis sertulifera* (Leighton, 1966); bat stars, *Patiria miniata* (Schroeter et al., 1983); and spiny lobsters, *Panulirus interruptus* (Tegner and Dayton, 1981; Tegner and Levin, 1983). Among fishes, the horn shark, *Heterodontus francisci* (Limbaugh[3]) and wolf-eels, *Anarrhichthys ocellatus* (Bernstein et al., 1981), have been observed to feed on sea urchins. In southern California, however, the most significant fish predator is the California sheephead, *Semicossyphus pulcher* (Quast, 1968; Feder et al., 1974; Tegner and Dayton, 1981; Cowen, 1983).

In and near the boundaries of kelp beds, Tegner and Dayton (1977, 1981) and Tegner and Levin (1983) found bimodal size distributions which they attributed to size-specific predation by spiny lobster and California sheephead. Red sea urchins larger than 80 mm in test diameter are less vulnerable to predators because of their size; those smaller than 50 mm take shelter from predators beneath the spines of adults or in cryptic habitats. Because shelter sites are relatively scarce for urchins between 50 and 80 mm (these animals are too large to hide under larger urchins), they suffer high mortality. The mode of larger sea urchins therefore consists of those survivors which accumulate over time. The other mode is made up primarily of small sea urchins <2 years old.

Although bimodal size distribution (with only very small and large sea urchins being represented) can be explained by size-selective predation in areas where spiny lobsters and sheephead are prevalent, studies over many years by the Kelp Habitat Improvement Project[4] have shown that size distribution can vary markedly in different habitats and over time. Local populations in southern California consisted of all small or all large individuals, and any number of combinations of small, medium, and large individuals (State Water Quality Control Board, 1964; Pearse et al., 1970; Anonymous, 1977). Bernard and Miller (1973) also noted varied size distribution patterns for red sea urchins in British Columbia where major predators of small sea urchins are not so prominent. Progressions in size distribution over time in a particular habitat have been well documented by Pearse et al. (1970) and Ebert (1983) who found that food availability and rates of settlement and survival of juveniles were important in determining distribution patterns.

The rate at which existing populations are replenished and the regularity of this recruitment increase from north to south along the west coast of North America. Annual recruitment rates of red sea urchins were lower and often more variable in British Columbia, Canada (Bernard and Miller, 1973; Breen et al., 1978), than in southern California (Mitchell et al., 1969; Pearse et al., 1970; Tegner and Dayton, 1981; Ebert, 1983). The mechanisms underlying such patterns are poorly understood, but latitudinal gradients in temperature, predation, and disease, or interactions of these factors have been hypothesized (Frank, 1975; Fawcett, 1984).

Two other patterns of distribution and abundance are of interest to those engaged in the red sea urchin fishery. The first is clumping, and the second is possible competitive interactions. We've already noted that red sea urchins are often found in high abundance around the edges of kelp beds (Fig. 2). Rosenthal et al. (1974) found that even within kelp beds where adult sea urchins are comparatively rare, individuals occur in aggregations rather than being randomly or uniformly distributed. Low (1975) noted that red sea urchins in British Columbia often occurred in groups or clumps of 50 or more. Smaller groups, as well as solitary sea urchins, tended to merge with the other groups until this apparently critical number was reached. Low (1975) speculated that clumping may be a mechanism to increase the chances of fertilization, to compete with macroalgae for space, or for protection of adults as well as juveniles from predators.

Interspecific competition between abalones, *Haliotis* spp., and sea urchins is known to affect the distribution and well-being of both groups. Abalones seem to outcompete sea urchins for space (Lowry and Pearse, 1973; Shepherd, 1973), although sea urchins may be more efficient in feeding (Tegner, 1980). In southern California, both groups prefer giant kelp, *Macrocystis pyrifera*, to other seaweeds (Leighton, 1966, 1971), so competition for food is likely to occur. Selective fishing for abalones, both in Australia and, in the past, in California, may have [illegible]tributed to increases in numbers of urchins (Lowry and Pearse, 1973; Shepherd, 1973). Under present condi-

---

[3] C. Limbaugh, 1959, personal commun. cited by Leighton (1971).

[4] W. K. Keck Laboratory of Environmental Health Engineering, California Institute of Technology, Los Angeles, Calif.

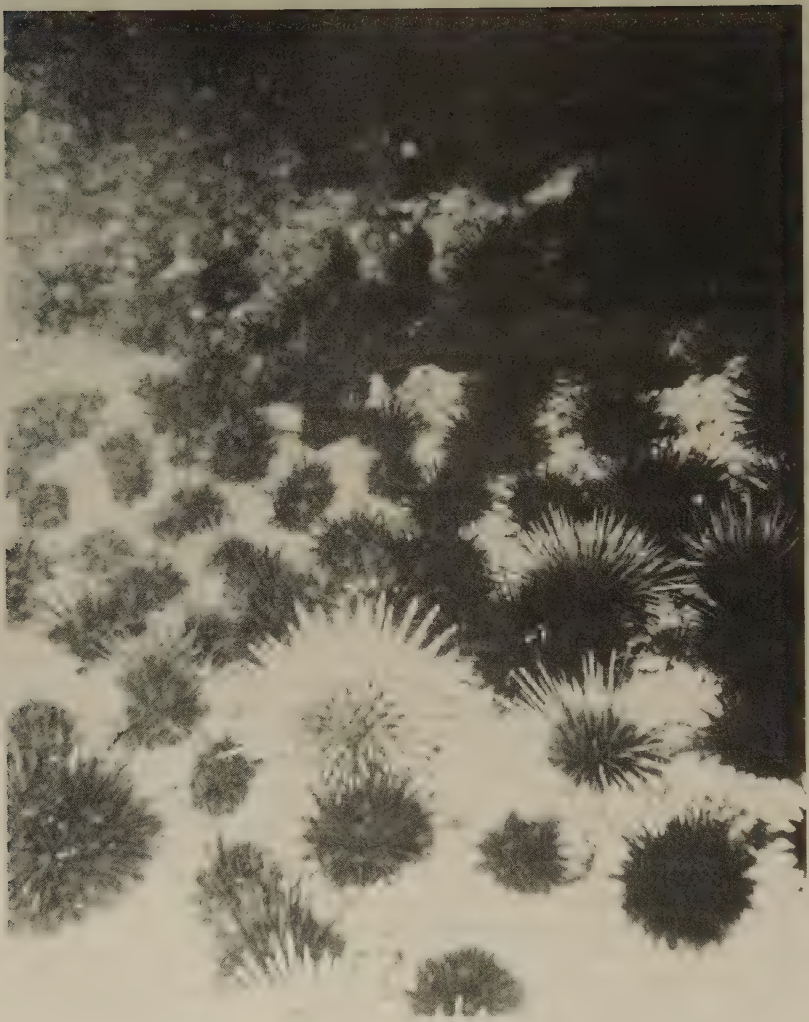

Figure 2.—A group of red sea urchins near kelp beds at Santa Cruz Island, southern California.

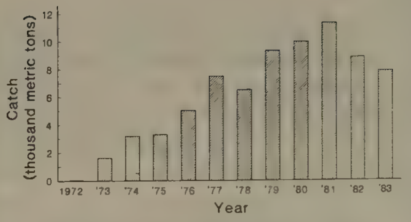

Figure 3.—Annual landings of red sea urchins in California. Source: California Department of Fish and Game.

tions in southern California, however, environmental factors, as well as fishing pressure and predation on sea urchins—rather than on abalones—may be more important than competition in determining distributional patterns and abundance of sea urchins and abalones (Tegner and Levin, 1982).

Schroeter (1978) studied red and purple sea urchins near Santa Barbara, Calif., and at nearby Santa Cruz Island, and concluded that competition for space plays an important role in determining the distribution and abundance of purple sea urchins. The distributions of the two species overlap, but purples dominate in harsh habitats (e.g., mid-intertidal and intertidal, as well as subtidal habitats exposed to waves and surge) while reds dominate in benign habitats (sheltered habitats in the low intertidal and subtidal areas). Purples are more abundant than reds in the harsher habitats because they are more tolerant of physiological stress and wave and surge action. Although purples actually prefer benign to harsh habitats, reds outcompete them there and so reduce their abundance. Because the two species compete, the selective removal of reds by the sea urchin fishery may cause an increase in the abundance of purples in the subtidal habitat. This in fact happened following small-scale experimental removals of reds in the shallow subtidal zone.

Any discussion of sea urchin distribution would be incomplete without inclusion of the effects of predation on sea urchins by sea otters, *Enhydra lutris*. Once almost extinct in California, sea otters now inhabit much of the central California coast, and it is not coincidental that sea urchins are scarce wherever sea otters are present. Sea urchins are among the most common food items of sea otters, and those sea urchins remaining in subtidal waters where otters are present are usually found deep in crevices (McLean, 1962; North, 1965; Leighton, 1966; E. E. Ebert, 1968; Lowry and Pearse, 1973).

No data are available on the abundance of red sea urchins along the California coast, but annual catch totals (Fig. 3) give some measure of harvestable populations. At first glance it would appear that the California fishery reached its harvest potential in 1981, when 11,300 t were landed. The lower catches in 1982 and 1983 may not have been directly related to abundance of sea urchins, however, and the declining catch may not signify that the maximum catch has been attained.

A major climatological event, commonly called "El Niño," occurred in 1982, affecting fisheries throughout the west coast, and indeed the whole Pacific Ocean. Unusually warm water invaded the southern California coast and weakened or killed kelp, the major food of sea urchins. Later in the year, severe storms associated with El Niño finished the job by tearing the weakened kelp from the seafloor[5]. The same storms made it impossible for divers to work in the winter and spring of 1982-83. Too, during much of 1983 the roe yield of red sea urchins was lower than normal, often to the point of making processing uneconomical[6]. The small gonads might also be linked to lower feeding activity. For red sea urchins, feeding rate is greatest at 16°C. The rate declines as the temperature increases (Leighton, 1971). During most of 1982-83 bottom temperatures were significantly above 16°C in red sea urchin habitats (Shelton et al., 1982). Several processors had to close their plants, while others continued operating at lower production levels. Thus, whether or not the southern California populations are presently being fished to their maximum potential is open to question. However, northern California fishing grounds have certainly not been worked to any extent, and expansion of the fishery is likely to occur there when conditions warrant.

Movements and Aggregating Behavior

Patterns of movement and aggregation of red sea urchins are important to fishermen and resource managers, as moving hordes of sea urchins can sometimes decimate large fields of algae (Leighton et al., 1966; Leighton, 1971; Dean et al., 1984). In many cases, however, red sea urchin populations are stationary and highly aggregated where food is abundant; they are less aggregated and move more when food is scarce (Vadas, 1968; Pace, 1975; Russo, 1979; Harrold and Reed, In press). Mattison et al. (1977) found such a pattern and documented differences in rates of movement. Movement of red sea urchins inside a kelp bed where food was abundant averaged about 7.5 cm per day. In comparison, in areas some distance from the kelp bed (15-100 m away) where food was relatively scarce, movement averaged over 50 cm per day. Experimental studies by Lees (1970) in Mission Bay in San Diego, Calif., also showed that food scarcity stimulates the movement of both red and purple sea urchins. On the other hand, Silver and Brierton (1974) found no mixing between two groups of red sea urchins which were located close together in depths of 3 and 11 m, separated by a nearly vertical rock face. The shallow group had an abundant supply of kelp, while the deeper group lived in an area with much less food and devoid of attached kelp.

Reproduction

Knowledge of sea urchin reproductive biology is valuable to those conducting the fishery; the yield of roe is greatest just before spawning when it may reach 20 percent of the total body weight. However, during the peak of reproductive activity, uptake of water by the gonads causes them to exude a great deal of gonadal material (Miller and Mann, 1973), and the roe has low marketability. Thus, the best quality roe is found just before the onset of proliferation of sex cells and before the mature gonads absorb water. After spawning, the gonads are small and the yield is too low for economic use, being 50 percent or less of the peak yield (Kramer and Nordin, 1975).

Increase in gonad size is actually related to feeding, rather than to some intrinsic reproductive cycle, and to storage of glycogen (a carbohydrate) in the gonads (Giese et al., 1958). Bernard (1977) explained the somewhat complicated processes that occur during the development of mature gametes, and concluded that food availability is the key to synchronization of the reproductive cycle in red sea urchins. The reproductive events of sea urchins follow a more or less annual cycle, but there are significant and interesting variations in the pattern.

The spawning season of red sea urchins appears to vary depending on locality and sometimes even from year to year at the same place. In various coastal localities from Papalote Bay, Mexico (near central Baja California), to Whites Point, Calif. (near Los Angeles), Pearse et al. (1970) found indications of spawning between June and November. Most of the populations showed no large increases in gonad size prior to spawning, and the gonad weight was usually less than 10 percent of the body weight. In these populations the gonads underwent a sharp decrease in weight during some time of the year, however, indicating that the populations had spawned. An exception was the population at Point Loma, in San Diego, Calif., which maintained large gonads throughout the year (March 1969-March 1970) and failed to show the marked decrease in gonad size which accompanies spawning. This population was thought to spawn throughout the year. The Point Loma population was the only one of those studied that existed in an area with abundant food.

Baker (1973) also studied red sea urchins at Point Loma in 1972-73 and found a similar lack of a well-defined period in which the decreased gonad weight indicated spawning. On the other hand, he found a lower gonad weight during summer in populations inhabiting nearby Mission Bay. Evidently the populations at the two areas were in different physiological condition; gonads of Point Loma sea urchins averaged 11.58-15.71 percent of the total weight of the sea urchin throughout the year, while those from Mission Bay sea urchins averaged 8.60-10.75 percent. Bennett and Giese (1955) found a late spring-early summer spawning season in central California; workers in Canada detected possible spawning periods from spring to fall (Bernard and Miller, 1973; Kramer and Nordin, 1975, 1979; Bernard, 1977).

A measurement commonly used to estimate a sea urchin's reproductive state on a gross (nonmicroscopic) level is the "gonad index." The index, a relative measure of gonad size, is simply the ratio (expressed as a percentage) of the gonad weight or volume to the total weight or volume of the sea urchin. An abrupt loss of gonadal bulk evidenced by a decline in the gonad index indicates that spawning has taken place.

To determine the reproductive condition of red sea urchins harvested by the

---

[5] Ron McPeak, Kelco Co., San Diego, Calif. Personal commun.

[6] Neal Matsushita, S/M Uni Co., Los Angeles, Calif. Personal commun.

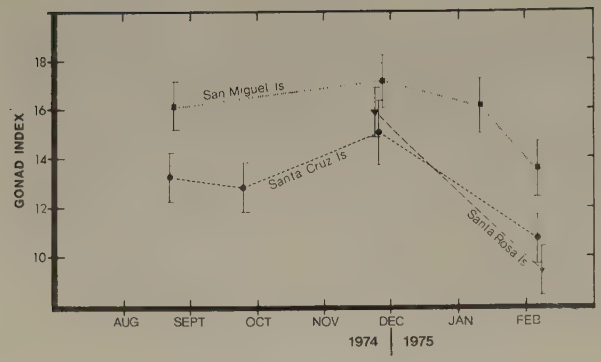

Figure 4.—Means and standard error for gonad indices of commercially caught red sea urchins (percent gonad weight of total weight of drained sea urchins).

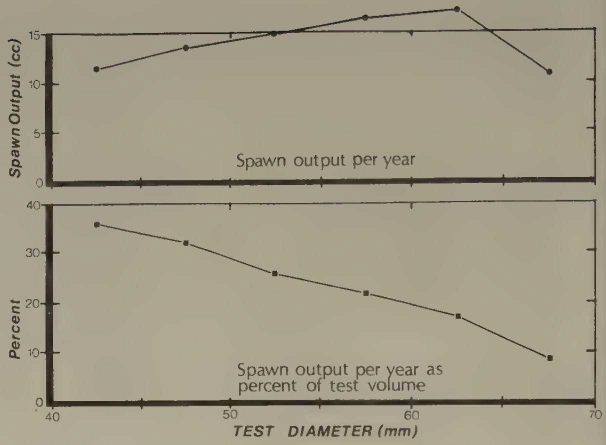

Figure 5.—Spawn output related to test diameter for the white sea urchin, *Lytechinus variegatus* (after Moore et al., 1963).

fishery, we calculated gonad indices (100 × gonad weight ÷ drained body weight) of red sea urchins harvested in 1974-75 by commercial divers from the northern Channel Islands (Santa Cruz, Santa Rosa, and San Miguel Islands). When these samples were taken, spawning was fairly synchronous among the different sites. The gonad indices were high from August to December, but they dropped from December to February (Fig. 4), thus indicating spawning during the latter period.

It should be noted that our samples were not representative of the whole population because spawned-out animals are usually not collected by divers; thus, on the whole, harvested sea urchins are likely to have a higher gonad index than the general population. Even with this bias toward higher indices, the results clearly indicate a discrete spawning period lasting at least from December through January. Red sea urchins that we sampled from commercial landings in 1976 in northern California (Fort Bragg) (unpubl. data) also indicated a winter-to-spring spawning period.

The maximum gonad size attained differs not only from locality to locality (Leighton, 1967; Pearse et al, 1970; present study, Fig. 4), but also from year to year at the same locality (Bennett and Giese, 1955). The causes of this variability have yet to be determined, but according to several sea urchin divers, differences in food supply may be most important. Divers often report that sea urchins near lush algal stands have much larger gonads than individuals located several meters away where algae are scarce or absent. Others have also noted the importance of food to the growth of gonads, which are not only reproductive organs, but also sites for food storage (Giese et al., 1958; Bernard, 1977; Dean et al., 1984).

The amount of gametes produced (usually measured by size of gonads) may not be directly correlated with size or age of the urchins. Bernard and Miller (1973) indicated that red sea urchins in British Columbia probably first spawn at age 2 at around 50 mm test diameter. We were able to induce spawning in red sea urchins as small as 40 mm at Santa Cruz Island. The production of gametes by these tiny individuals is, of course, very low.

Bernard (1977) found that the ratio of gonad weight to shell diameter increases with size, until red sea urchins attain 95 mm; the ratio then decreases slightly. Moore et al. (1963) found similar results in their study of the east coast's white sea urchin, *Lytechinus variegatus*. The total spawn output (Fig. 5, above) was greatest for large sea urchins (but not the largest size class), but smaller sea urchins were relatively more productive when spawn output was expressed as a percentage of test volume (Fig. 5, below). Thus, to assess the spawning potential of a sea urchin population, one must know the relative abundance of different sized sea urchins, as well as the amount of spawn produced by individuals in the size range.

Another reproductive process important to the sea urchin fishery is the length of time it takes for gonads to regain their bulk after spawning. Data we obtained from a commercial sea urchin processing firm in 1975-76 indicate a rather protracted recovery period lasting from spring to early summer, after the sea urchins had spawned from December through February or March. On the other hand, Bernard (1977) found that in British Columbia the gonad index of red sea urchins returned to 80 percent of maximal levels by October, only 1 month after spawning. The gonads attained their greatest size several months later in May. Kramer and Nordin (1975), however, found an intermediate interval of time between spawning and recovery in their study of British Columbia red sea urchins. The differences may be due to the amount of food available in the respective habitats.

Development and Growth

Development of red sea urchins from fertilization through various free-swimming larval stages to settling of the juvenile takes about 6-8 weeks, depending primarily on water temperature (Johnson, 1930). Depending on a host of environmental and genetic factors, young sea urchins can grow to sexual maturity between 1 and 2 years after they settle on the bottom (Bernard and Miller, 1973; Tegner[7]).

Marks on hard parts have commonly been used to study the age of animals. In sea urchins, rings similar to those found in tree trunks can be seen in the spines, and growth lines or zones also occur in the plates that make up the test. Both have been used to ascertain the age of certain species (Jensen, 1969; Pearse and Pearse, 1975). Detailed studies of the formation of growth zones in the tests of purple sea urchins have disclosed, however, that rings or zones do not necessarily correlate with seasonal phenomena, and are thus not useful for indicating age (Pearse and Pearse, 1975). Breen and Adkins (1976) reported similar negative results for red sea urchins, and our attempts using Jensen's (1969) methods failed to find reliable age indicators in the test plates.

Growth of red sea urchins, measured by increases in test diameter, has been studied in the laboratory (Leighton, 1967, 1971), in cages in the field (Swan, 1961; Schroeter, 1978), and with uncaged field populations (Baker, 1973; Bernard and Miller, 1973). The studies indicated an annual growth increment of 13-25 mm, with smaller individuals showing faster gains in test diameter, as expected. Thus, on the average, red sea urchins probably attain harvestable size (90-100 mm) in around 4-5 years.

Many factors affect growth rates of sea urchins and the maximum size attained by individuals in a local population. These include availability and nutritional value of algae, competition, temperature, and the severity of wave and surge action (Bennett and Giese, 1955; Swan, 1961; Ebert, 1967, 1968; Leighton, 1971; Baker, 1973; Schroeter, 1978).

Food and Feeding

Although red sea urchins feed on many species of algae, they clearly prefer the giant kelp, *Macrocystis* spp., when it is available (Leighton, 1966, 1971). Off the coasts of Washington and British Columbia, red sea urchins prefer the bull kelp, *Nereocystis leutkeana* (Vadas, 1968, 1977).

As one might expect, diets consisting of preferred foods result in much higher growth rates (Leighton, 1971; Vadas, 1968, 1977). A striking demonstration of this phenomenon can be found in southern California, where locally dense populations of red sea urchins eliminated all fleshy algae, forcing individuals to feed on less preferred and nutritionally inferior encrusting coralline algae (e.g., *Lithothamnion* spp. and *Bosiella* spp.). Sea urchins in such areas typically have only the rudiments of gonads and appear to be starved (State Water Quality Control Board, 1964).

Plankton, as well as organic suspensions produced by sewage outfalls, are also utilized by sea urchins. In fact, the latter source seems to have relatively high nutritional value, and may be the primary factor responsible for persistence of dense sea urchin populations even after they have overgrazed and eliminated their normal algal food source (Pearse et al., 1970). Finally, when food is scarce or absent, sea urchins can derive energy necessary for maintenance by resorbing their gonadal and gut tissues.

Feeding rates of red sea urchins are influenced by temperature. The optimum feeding temperature is about 16°C, and red sea urchins feed as long as the temperature remains between 6° and 25°C. In southern California, at depths where red sea urchins are most abundant, bottom temperatures are generally higher and nearer the 16°C optimum in winter than in the summer (Leighton, 1971).

Ecology and Management

As noted above, grazing by red sea urchins has a profound influence on the types of algae that ultimately dominate a particular habitat. This is because sea urchins prefer to eat certain species, thereby leading to the dominance of the less preferred species. In some cases, the less preferred species are poor competitors, and owe their persistence in the community to the grazing activity of sea urchins. Experimental removal of sea urchins often results in local competitive elimination of the less preferred species of algae (Vadas, 1968; Paine and Vadas, 1969; Palmisano, 1975; Pearse and Hines, 1979; Duggins, 1980).

The influence of sea urchin grazing on giant kelp in southern California has received a great deal of attention, since sea urchins have been held responsible for the widespread disappearance of this economically and environmentally valuable species (North and Pearse, 1970; Leighton, 1971; North, 1974). Researchers from the California Department of Fish and Game, Scripps Institution of Oceanography, California Institute of Technology, and Kelco[8] (a commercial kelp harvesting firm), and groups of recreational divers have worked on the restoration of kelp beds for over 20 years. Almost without exception, attempts to restore kelp forests have started with the eradication of sea urchins, and successful results of some of these efforts seem to demonstrate that sea urchin grazing is a principal reason for failure of giant kelp to become reestablished in certain habitats (North, 1974). Of course, other factors such as competing vegetation, other grazers, and adverse environmental conditions also act to hold down kelp growth (Wilson et al., 1978).

In areas where the standing crop of algae is well established, sea urchin presence is not necessarily detrimental to the plant community (Rosenthal et al., 1974), and removal of large numbers of sea urchins may not affect the algal abundance or distribution (Breen et al., 1978).

From the point of view of those favoring kelp propagation, it is clear that reduction in numbers of red sea urchins would be beneficial. Indeed it has even been suggested that sea otters be reintroduced into southern California for this purpose. It would seem, however, that the commercial fishery is a more satisfying means of controlling growth in populations of red sea urchins, which are valuable renewable natural resources. The fishery brings income to the industry as well as helping in some measure to lower our deficit in the balance of trade of seafood products. On the other hand, selective removal of red sea urchins may allow growth in the population of purple sea urchins, which can also cause overgrazing when large numbers are present. These two species overlap to a great degree (except at the shallow end of the range), and their food preferences are similar.

---

[7] Scripps Institution of Oceanography, La Jolla, Calif. Personal commun.

[8] Mention of trade name or commercial firms does not imply endorsement by the authors or by the National Marine Fisheries Service, NOAA

To maintain a long-term fishery, some management measures may need to be instituted, for it is clear from studies by Canadian researchers that recovery of exploited red sea urchin populations is a slow process (Breen et al., 1978). In the absence of regulations, divers should take it upon themselves to ensure that enough large sea urchins are left in harvest areas to support recruitment of young urchins, which need the protection afforded by the spines of larger individuals. Perhaps a maximum size limit would help in this regard.

Most persons involved in the California fishery feel that management is called for to prevent damage to sea urchin stocks. One management option favored by many divers, according to two polls, is a limit on the number of persons allowed to fish for sea urchins[9]. Some processors we interviewed also felt that economic returns should be considered in any management scheme. For example, they advocate closure of the fishery during spawning season when the roe is soft and unappealing, and until the gonads recover to near maximum bulk.

Since the precise time of spawning may vary from year to year and at different locations, however, it would be unwise to set prescribed open and closed seasons. Obviously, divers and processors have the best and earliest knowledge of these events when they occur, and it behooves them to work together to stop fishing in areas where gonad quality and quantity are low. Another period of marginal profitability is during spring and early summer when the roe yield is still rather low, as are the prices in Japan. However, market conditions do vary, and in some years it has been profitable to export roe even in summer.

Not all processors and fishermen advocate long seasonal closures of the fishery. They point to the difficulty of keeping key personnel during the off-season, or counting on their return when processing resumes, and also to the fact that some good sea urchins can be found throughout the year. Those firms that supply the domestic market especially need to operate throughout the year or chance the loss of their markets to imports.

The State of Washington has a rather simple management system, whereby the coast is divided into three zones, one of which is closed to sea urchin fishing each year to foster repopulation[10]. In Japan, seasonal, depth, and gear restrictions are all used to help ensure against overfishing, and habitat improvement programs are also employed to encourage settlement and growth of sea urchins (Mottet, 1976).

In the absence of State-mandated fishery regulations, members of the California industry might well impose self-regulatory measures to ensure the future of the fishery. The collapse of the sea urchin fishery in northwest France in the 1960's (Southward and Southward, 1975) should serve as amble reminder to all that sea urchins are susceptible to overfishing, and the authors pointed out that sea urchins are important for maintaining a balance in the ecosystem. They plead: "The lowly sea urchin is strongly in need of friends to come to its rescue."

History of the Fishery

In the 1960's, a few individuals harvested small numbers of sea urchins for home consumption and for the domestic market in California. With increasing numbers of Japanese restaurants opening in the United States to serve the growing Japanese business communities in the financial centers—New York, Chicago, Los Angeles, San Francisco—the demand for exotic (at least to conventional American tastes) fish products increased. Much of the fare served in these restaurants was traditional Japanese, including raw fish and shellfish, fish eggs (including uni, or sea urchin roe), eels, jellyfish, and the like. Since many of these were not readily available in the United States, they were imported from Japan. And, owing to the high cost of air freight, most of these items were transported by ship in the frozen state which, although unacceptable in Japan, was the only form available in the United States.

In 1968, the NMFS Southwest Fisheries Center started looking into the feasibility of developing a sea urchin fishery to supply the growing domestic markets and for export to Japan. The decision to try to initiate a fishery was prompted not only by the demand for the product, but also because sea urchins were considered pests by kelp harvesters, recreational fishermen, and the abalone industry. In fact, groups of sport divers regularly held organized "urchin kills," whereby divers armed with hammers would smash any and all sea urchins found in selected habitats. Quicklime (calcium oxide) was also used to control sea urchins in commercial kelp beds. Now, however, state regulations prohibit the use of quicklime because of strong objections by sea urchin divers and other fishermen.

Since the processing of sea urchins requires a large number of low-skilled workers, a new fishery also offered increased employment opportunities for such workers. Other advantages of a sea urchin fishery included reduction in fishing pressure on abalone, possible improvement in the habitat for abalone and other invertebrates and fishes that depend on seaweed for shelter or food, and lowered deficit in the U.S. international seafood trade.

In the early phases of development in 1972, we sent trial shipments of frozen roe to Japan, the principal market. Because the defrosted roe became soft and unappealing due to cell rupture, no interest was shown by the Japanese market for the frozen product. Since the prevail-

---

[9] David Parker, California Department of Fish and Game, Long Beach, Calif. Personal commun.

[10] Richard Burge, Washington Department of Fisheries, Shellfish Laboratory, Brinnon, Wash. Personal commun.

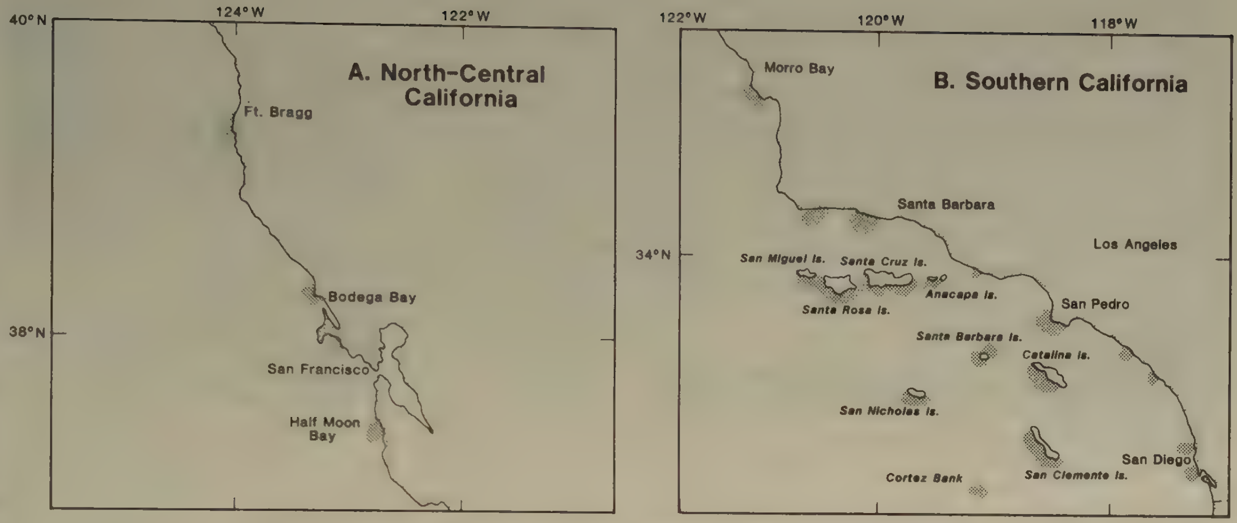

Figure 6.—Major California fishing grounds (shaded) for red sea urchins.

ing monetary climate prohibited air freight of fresh roe to Japan, we decided to concentrate on supplying the domestic market while experimenting with means of preserving the roe in better condition. First, we had to experiment with processing methods since we were unable to find descriptions in the literature. Time and motion studies and cost analyses were carried out in a pilot operation at Avila Beach, Calif., to determine if the business had potential profitability. All studies indicated good potential, especially if initial investment was low (Kato, 1972). In 1972 a trip to Japan by the senior author provided detailed information on the processing and marketing of sea urchin roe and contacts with potential buyers. This new information, and the right monetary conditions (the Japanese yen had just been raised in value relative to the dollar by 25 percent), convinced a Los Angeles processor to open the first major sea urchin processing plant in late 1972. A technician from Japan was hired by the firm to provide processing expertise in handling fresh roe, and the industry was underway.

Since its inception in 1972, the fishery has grown steadily to become one of the leading fisheries in California. Annual landings increased to 11,000 t in 1981, but declined somewhat in the next 2 years. The following sections describe the harvesting, processing, and marketing sectors of the California sea urchin fishery.

Harvesting

The bulk of the California sea urchin catch comes from the northern Channel Islands (Fig. 6) off the southern California coast. Anacapa and Santa Cruz Islands were formerly the areas of highest production, but presently San Miguel, Santa Rosa, San Nicolas, and Santa Barbara Islands produce most of the catch. Divers are forced to seek new localities as sea urchin density becomes too low for economic harvesting, or when the quality and quantity of roe fall below acceptable levels. Santa Catalina and San Clemente Islands, as well as Cortez Bank, have also provided some sea urchins, as have many localities along the mainland coast from San Diego to Fort Bragg. The relative amounts landed in various regions in California are shown in Table 2. The fishery now appears to be harvesting those sea urchins that have reached marketable size in areas previously exploited.

Table 2.—Annual California landing of sea urchin by district (percent of total landings).

Year	Eureka[1]	San Francisco	Monterey	Santa Barbara	San Pedro	San Diego
1973	<1	<1	<1	96	4	<1
1974	<1	<1	<1	97	1	1
1975	<1	<1	<1	95	3	2
1976	<1	<1	<1	94	1.3	4
1977	2	<1	<1	78	10	9
1978	<1	<1	<1	70	19	11
1979	1	<1	<1	76	18	5
1980[2]						
1981	<1	<1	<1	71	16	12
1982	<1	<1	<1	74	15	10
1983	<1	<1	<1	72	18	10

[1] Most of these landings were made at Fort Bragg and Albion

[2] Statistics for 1980 were not available

Vessels and diving gear in the sea urchin fishery are similar to those used by the abalone fishery. All harvesting is done by divers using conventional "hookah" gear, i.e., a low-pressure air compressor connected to a reservoir which feeds air through a hose to a faceplate. The compressor is usually rated at 80-125 p.s.i., and most can accomodate up to three divers. Divers wear 6-10 mm thick rubber "wet suits" or thinner "dry suits" to ward off the cold.

The most popular diving boats are

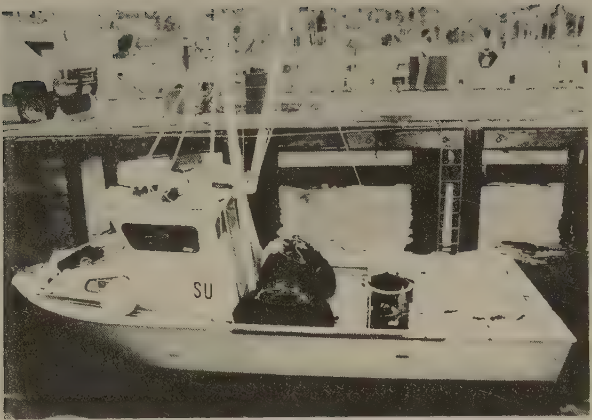

Figure 7.—A 9.1 m (30 foot) Wilson drive boat; note the two large mesh bags full of sea urchins.

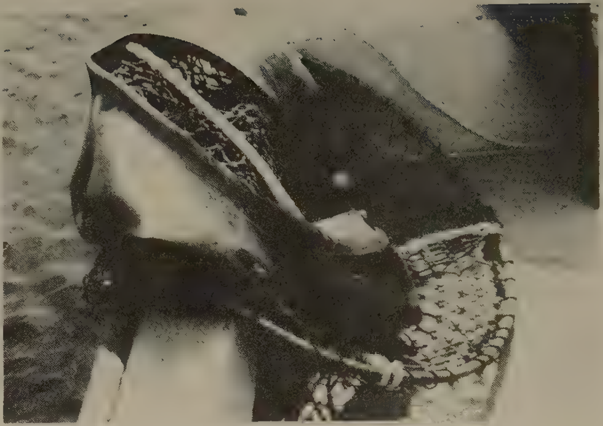

Figure 8.—Sea urchin collecting bag with rubber tube.

made by Radon and Wilson (Fig. 7). The vessels are made of fiberglass, usually around 8-9 m long, and powered with diesel engines. The carrying capacity is 1.5-3 tons. The chief criterion, besides adequate carrying capacity, appears to be speed, which is important because some of the fishing grounds are a considerable distance from port. Most sea urchin boats can cruise at 15-20 knots. In the past, vessels with large capacity, such as albacore trollers, were used as carriers for transporting sea urchins from the fishing grounds to dockside. Some divers operate by themselves, while those in larger vessels usually work in pairs or threes. All the divers on a boat may be in the water at the sime time, or one may act as a tender, loading the catch into the boat. Major home ports of the sea urchin diving boats are Santa Barbara, Oxnard, Port Hueneme, and San Pedro.

Diving operations begin with preliminary searches for concentrations of sea urchins. After finding an area with adequate numbers, the diver cracks open a few sea urchins to check the quality of roe. If satisfactory, harvesting begins. Most divers have their own methods for collecting sea urchins. One effective method is to use a short-handled rake to dislodge sea urchins and scoop them into a small collecting bag or wire cage. As this is filled, the sea urchins are transferred underwater into a larger mesh bag, about 2 m long, with a 1.4 m ring opening (Fig. 8).

After the first batch of sea urchins is transferred, air is pumped from the breathing apparatus into a rubber tube attached to the ring. This causes the ring to rise, and the bag is maintained at a convenient height, anchored by the weight of the sea urchins. As the bag is filled with more sea urchins, additional air is put into the tube to increase the height of the bag. When the collecting bag is completely filled with 50-70 kg of sea urchins, the tube is filled with enough air to float the bag to the surface. A line attached to the boat keeps the bag from drifting away[11]. This method is especially useful for single-diver operations. Boats with tenders (or diver-tenders) often store collected sea urchins in large cargo nets, which facilitates unloading (Fig. 9).

All harvesting is currently done by hand, although an airlift system was tested by one firm, with reported success. In our own experiments, we successfully pumped red sea urchins through a 25 cm hose from depths of 15 m, but we found it difficult to get enough force with an airlift system at shallower depths. Further, we found the hose too cumbersome and impractical to use in areas of dense kelp.

Because of the hard physical labor, cold water, and pressure, divers are forced to surface often to rest, and actual diving time is restricted to a few hours (usually 3-4) per day. Weather conditions and other factors further limit a diver's fishing time to around 80 days per year. Although most divers make daily fishing trips, some with large vessels make 2-day trips. On these occasions, collected sea urchins are kept in mesh bags underwater in sheltered spots until the trip home.

Divers were interviewed periodically between July 1974 and February 1975, and again in January and February 1977 to get catch data. These divers fished at the Channel Islands and at mainland sites just north of Santa Barbara. Data thus obtained revealed that catch rates did not change significantly during the two periods (Table 3). Boats with a single diver averaged around 250 kg/hour during both periods, and diving

Table 3.—Comparison of catch per day by single-diver boats during two periods.

Item	July 1974-Aug. 1975 N = 38	Jan.-Feb. 1977 N =12
Average catch per day (kg)	918	922
Average time spent underwater (hours)	3.4	3.7
Average catch per hour underwater (kg/hour)	269	249

---

[11] Jerome Betts, commercial sea urchin diver, Lompoc, Calif. Personal commun.

time averaged about 3.5 hours per day. Data from 48 deliveries made by single-diver boats (including the 38 in Table 3) and 16 deliveries by two-diver boats showed that the latter were somewhat more productive. The single-diver boats averaged 986 kg/day while the two-diver boats averaged 2,258 kg/d (or 1,129 kg/diver). In 1983 the average catch for single-diver boats was lower, probably on the order of 780-900 kg/day[11]. In some areas, such as near San Diego, the daily catch is usually even lower.

The average depth fished during 1974-75 was 8.2 m (range 4.0-15.2 m). Most divers interviewed recently reported diving a bit deeper on the average.

The number of boats engaged in the fishery varies considerably by year. During the peak year of 1981, 271 boats reported sea urchin landings. Of these, 42 boats (15 percent) landed 56 percent of the total catch, and 85 boats landed 85 percent[9].

In port the catch is weighed and loaded directly into waiting trucks which haul the sea urchins to processing plants. The unloading booms are usually equipped with scales to weigh the catch. Some divers sell their catch through a "middleman" who handles unloading and transport, as well as market orders and dispatching boats.

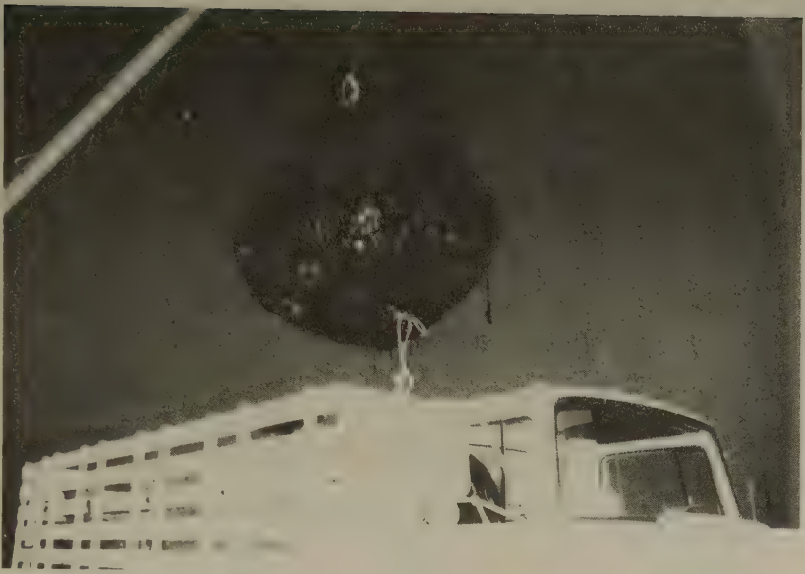

Figure 9.—Sea urchins retained in cargo nets on dive boats are easily and quickly unloaded into trucks.

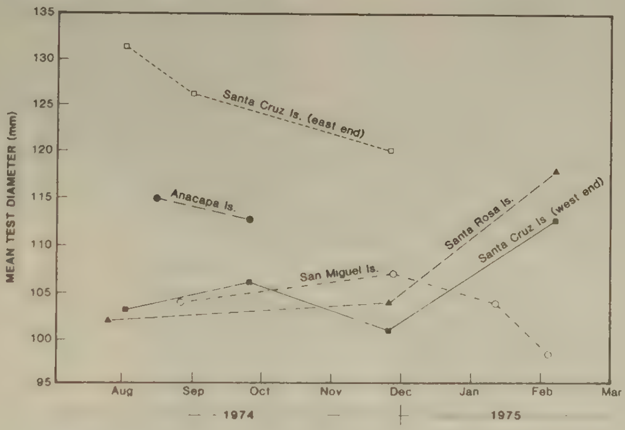

Figure 10.—Mean test diameter of red sea urchins taken by the commercial fishery at the northern Channel Islands in 1974-75.

The average size of red sea urchins changes with harvesting intensity, becoming progressively smaller with time. At times, however, the size increases (Fig. 10, Santa Rosa and Santa Cruz) rather than declining. This can probably be explained by the movement of divers into deeper waters as the number of large sea urchins decreases in shallower depths. Thus, a longer sampling period would probably have shown a second decrease in the size of the sea urchins harvested from the same area, as indicated by the San Miguel Island sea urchins (Fig. 10).

The mean test diameter of red sea urchins sampled from the commercial landings at Santa Barbara from July 1974 to February 1975 was 108 mm (95 percent measured 102-114 mm and 99 percent measured 100-116 mm). Recently, however, the average size has been considerably lower; the diameter of 27 red sea urchins measured at a processing plant in October 1983 averaged 87 mm. All processors interviewed at that time agree that the size has decreased considerably.

Those wishing to harvest sea urchins in California must obtain a commercial fishing license ($40). A revocable sea urchin fishing permit is also now required under a State law enacted in 1984. All vessels used in commercial fishing operations require a certificate of boat registration ($125). These fees are assessed each license year (1 April-31 March).

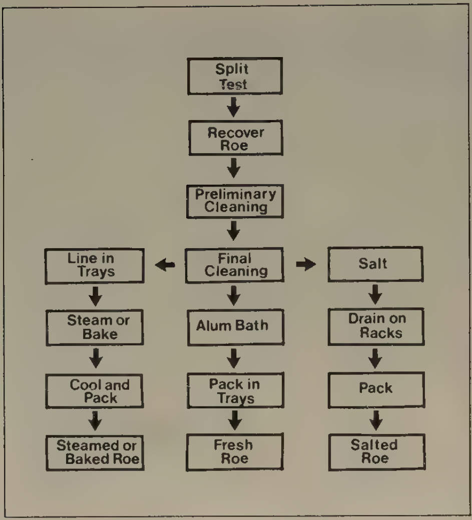

Figure 11.—Flow diagram of sea urchin processing steps. Frozen roe is treated similarly to fresh roe.

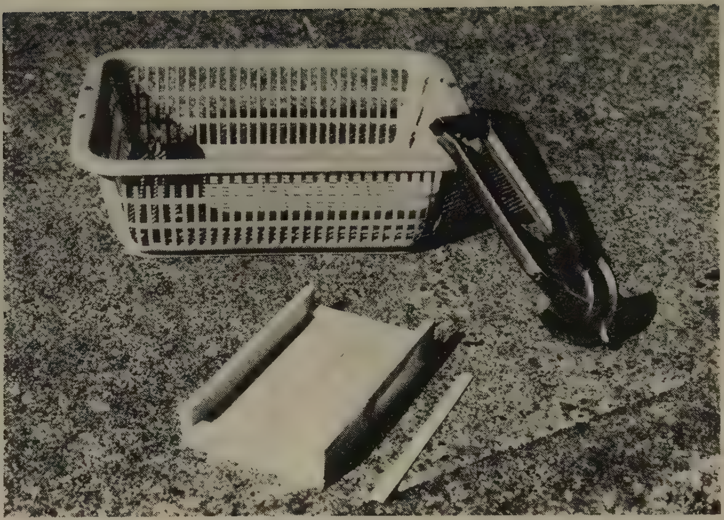

Figure 12.—Some tools of the trade: Stackable plastic strainer for cleaning roe, metal shell-cracking device, wood tray for packing roe.

Processing

Sea urchin processing has not changed appreciably since the earlier report of Kato (1972). Because the product is now primarily sold fresh rather than frozen, however, packing methods are different, and a chemical treatment is used to improve the appearance of the roe. Only a small amount of roe is salted, steamed, baked, or frozen.

Sea urchins delivered to processing plants in the evening are kept overnight. During warm weather, sea urchins must be stored in refrigerated rooms. Sea urchins kept at 2°C for 1.5 days stay alive, but the roe is noticeably softer and darker (Kramer and Nordin, 1979). Processing consists of several steps which readily lend themselves to an assembly-line operation (Fig. 11). The test is split with a cleaver or a special tool (Fig. 12). The instrument's tip is forcibly inserted into the top of the shell, which is cracked open when the handles are squeezed, forcing the flat blades outward. The roe is removed with a spoon and placed in plastic strainers, then rinsed in cold saltwater to remove viscera and extraneous matter. Final cleaning of attached membranes is done with tweezers or small forks. From this point, processing methods depend on the type of product. The Japanese name is given for each of the products described here.

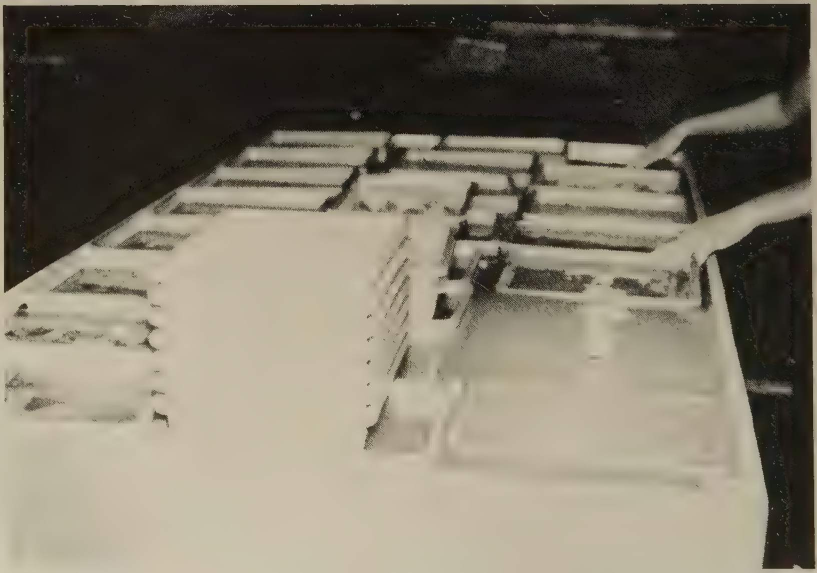

Figure 13.—Sea urchin roe becomes firm when soaked in a saltwater solution containing alum.

1) Fresh roe (uni or nama uni):

A) The roe is placed in stackable plastic strainers.

B) The strainers are placed in tanks containing a solution of anhydrous potassium alum, $KAl(SO_4)_2$, in cold

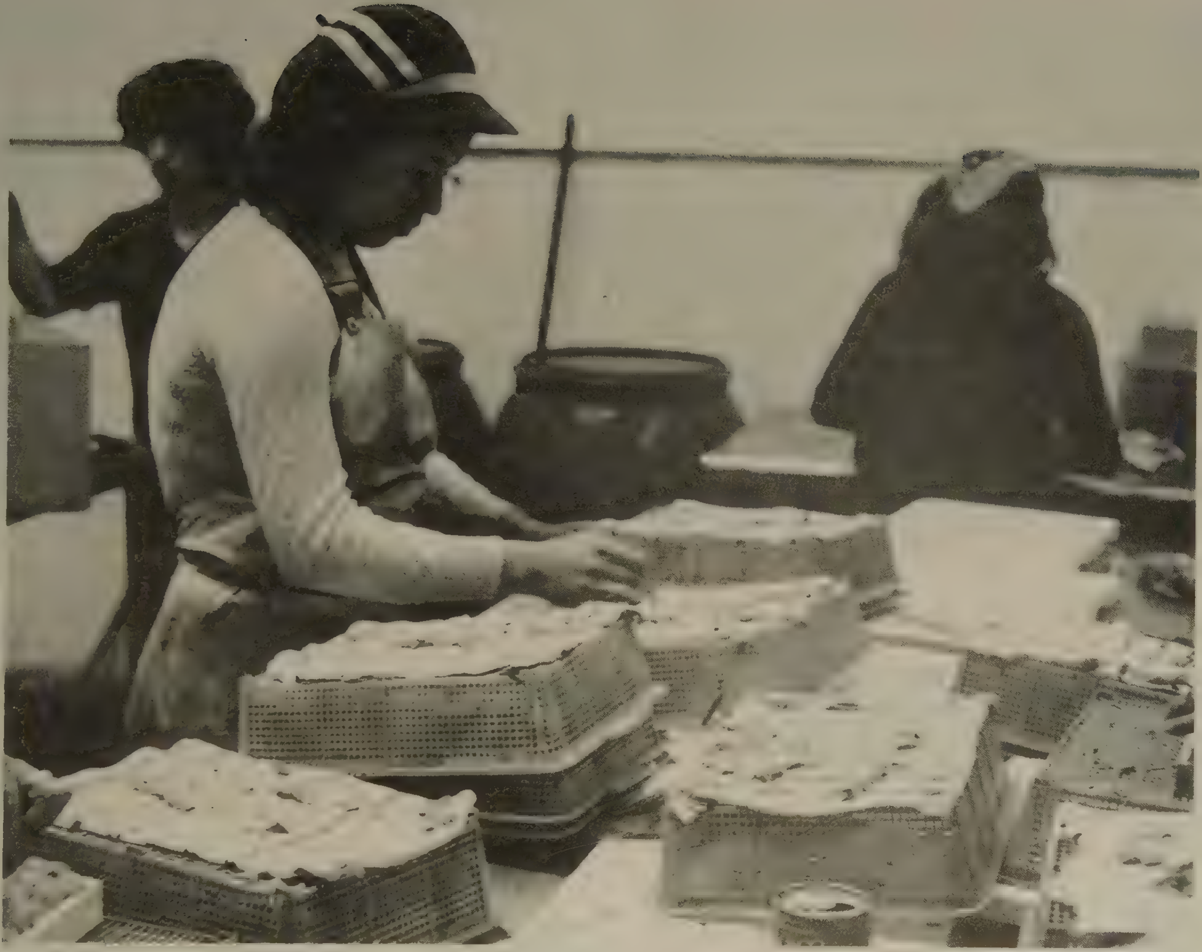

Figure 14.—Roe is drained thoroughly before packing; a layer of cloth helps absorb moisture.

saltwater until the roe becomes firm (Fig. 13). Concentrations used vary from 0.4-0.7 percent, and soak times vary from 15 minutes to 1 hour.

C) The roe is then drained (Fig. 14) and packed in small wood trays. At least 250 g, and up to 280 g, of roe are packed in a standard tray (Fig. 15). A medium-sized tray containing around 170 g is gaining in popularity, however. Occasionally, smaller trays holding 100, 50, or 30 g are also used. The standard trays measure about 9 cm × 16 cm × 1.3 cm deep (inside

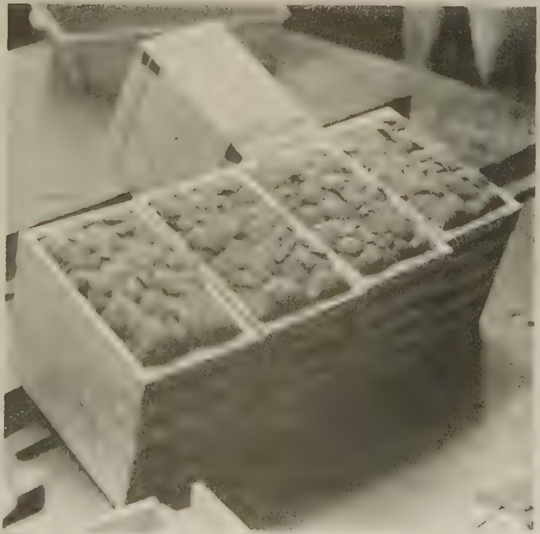

Figure 15.—Wood trays, each packed with around 250 g of red sea urchin roe.

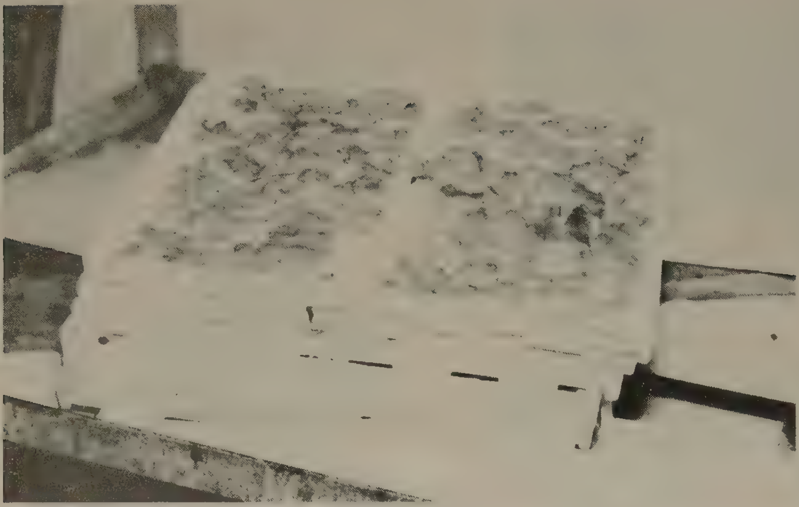

Figure 16.—Roe bulk-packed in foam trays. This roe will probably be used in salted or cooked products.

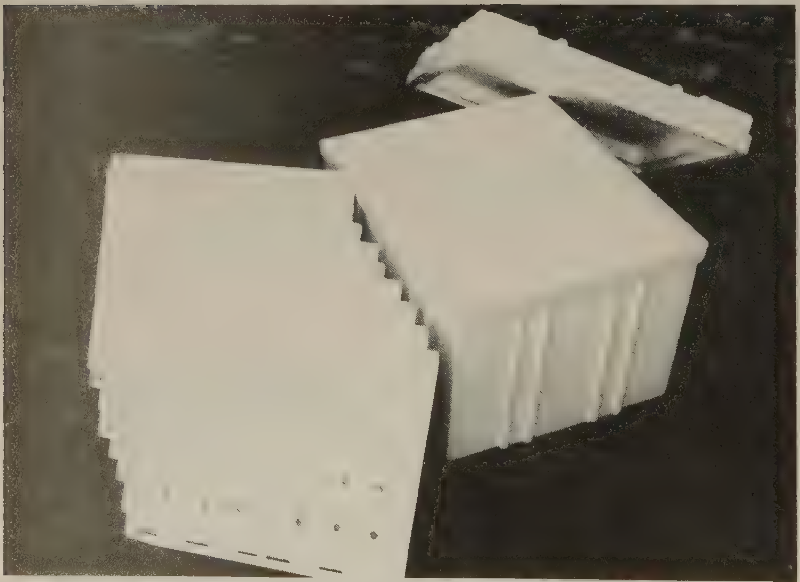

Figure 17.—Insulated master carton used to ship sea urchin roe packed in wood or foam trays. Source of cartons: Plasti Personalities, 1214 W. 252nd St., Harbor City, CA 90710.

dimensions) and cost about $0.30 each

D) Alternately, the drained roe is bulk-packed in larger perforated foam trays, 32 cm × 40 cm × 2 cm deep (Fig. 16), sometimes lined with absorbent cloth to prevent sliding and damaging of roe in transit. Only one layer of roe is packed in a tray. These trays normally hold about 1 kg of roe.

E) The wood trays are tied in bundles of 8 to 13 trays, with a wooden cover over the top. These are placed in a plastic bag and the roe is allowed to drain further in a refrigerator. It is important that the roe not be exposed to drafts while draining.

F) Just prior to shipment, the trays are placed in insulated master cartons (Fig. 17), each holding 50-54 trays. The bulk-pack foam trays are also stacked and placed in insulated master cartons with about 8-9 trays in each carton. Artificial coolant (commonly called "jelly ice") is added prior to shipment (about 1.4 kg per carton in winter and twice as much in summer).

2) Salted roe (shio uni): Methods of salting vary, depending on the requirements of buyers. Generally, the steps are as follows.

A) Layers of cheesecloth are placed on a wire rack.

B) A layer of roe is placed on the cheesecloth and covered thoroughly with salt; about 25 percent salt to weight of roe is used.

C) More layers of roe and salt are placed on the rack, sometimes with cheesecloth between layers, until the thickness reaches about 5 cm.

D) The roe is allowed to drain for several hours or overnight; about 40-50 percent of moisture is removed, and salt uptake is 10-15 percent.

E) The salted roe is packed in plastic-lined wooden kegs or plastic containers, sometimes with the addition of 10 percent by weight of ethyl alcohol (95 percent).

Recently a new type of shio uni has been produced using less salt but requiring freezing for preservation. This product apparently brings a high price if good quality roe is used[12].

3) Steamed roe (mushi uni):

A) Fresh roe is placed in wood or screen containers of various sizes.

B) The containers are stacked and

---

[12] K. Yanagita, California Uni Co., Los Angeles, Calif. Personal commun.

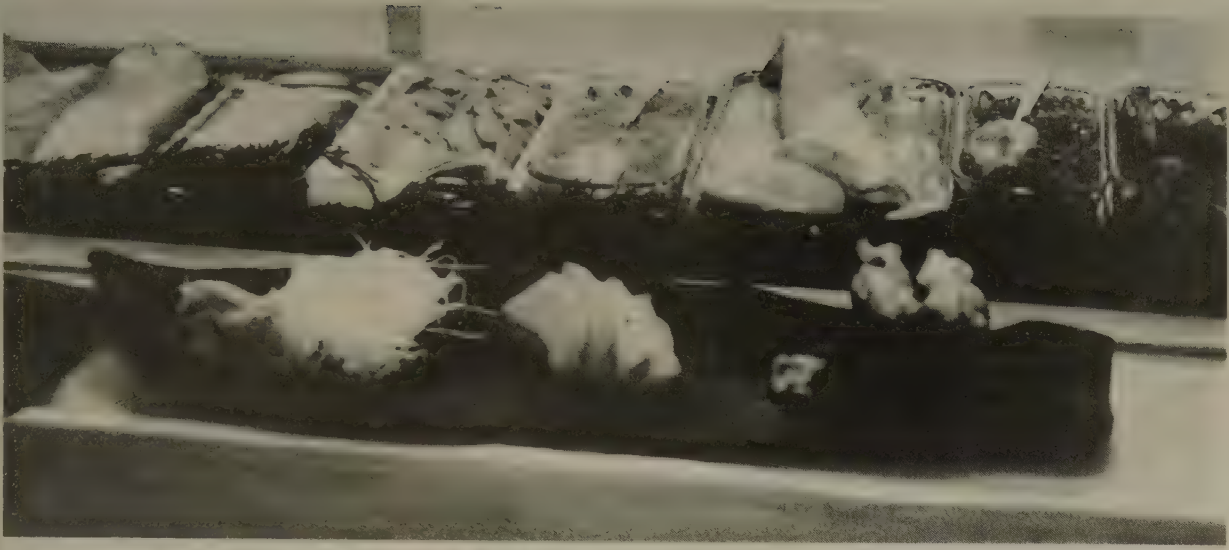

Figure 18.—Showcase in a sushi shop. A wood tray filled with red sea urchin roe is seen to the left; two pieces of "uni sushi" are on the counter on the right.

placed in a large steamer.

C) The roe is steamed for about 30 minutes; about 20-30 percent of moisture is removed during the process. Some processors steam roe under pressure, reducing cooking time to 15 minutes or less.

D) The roe is bulk-packed or packed in small wooden or plastic trays, and frozen.

4) Baked roe (yaki uni):

A) Fresh roe is placed in shallow oven-proof dishes.

B) The roe is baked in an oven at 190°C for 30 minutes. About 30-40 percent of moisture is removed in the process.

C) The cooked roe is then packed in small wooden trays (around 30 g) or in plastic imitation "scallop shells" and frozen.

5) Frozen roe (reito uni):

A) Fresh roe of good quality is packed in standard wood trays or bulk plastic trays.

B) The trays are stacked and inserted in a plastic bag, then frozen at −17°C.

C) The frozen roe, still in the plastic bag, is stored in insulated master cartons in the freezer.

This method is used when the product is to be sold later as raw-thawed sea urchin roe, and only good roe is acceptable. If the roe is destined to be salted or processed further, second-grade roe may be used, and it is often simply placed in plastic bags and frozen in bulk.

California firms have experimented with other processing methods in attempts to service specialty markets. Two such items produced were canned roe and freeze-dried roe. In addition, sea urchin roe has been used as feed for aquarium animals, particularly for sea anemones and other invertebrates.

The best quality roe is reserved for the fresh product, which brings the best prices. Secondary products are made from broken roe, or roe that is off-color, too large, or leaking fluids excessively. Salted roe is usually produced in the summer, when the price of fresh roe is low in Japan.

Because appearance is important to the Japanese, who are said to "eat with their eyes," the packing process is critical. In Japan as well as in the United States, most of the roe is bought by "sushi" shops, which are Japanese seafood restaurants specializing in fresh seafood. Customers in sushi shops usually sit at a counter in front of refrigerated showcases which contain many seafoods, mostly raw, in plain view (Fig. 18). Sea urchin roe is displayed in the same wooden trays used by the processor. To maintain good appearance, broken pieces of roe are placed on the bottom, and only whole, firm roe is placed on the top layers of wood trays. The best size is 40-50 mm, but California sea urchin roe is usually larger. Skeins of roe are separated according to their color. Very large skeins are used in other than fresh products, or broken up into smaller pieces and packed on the bottom of trays. Bright yellow roe was historically considered the highest quality in Tokyo, although consumers in different areas of Japan often prefer bright orange roe. Since the late 1970's, orange roe has equalled yellow roe in price in Tokyo.

Trays used for the Japanese market were formerly imported from Japan because only certain types of wood are ac-

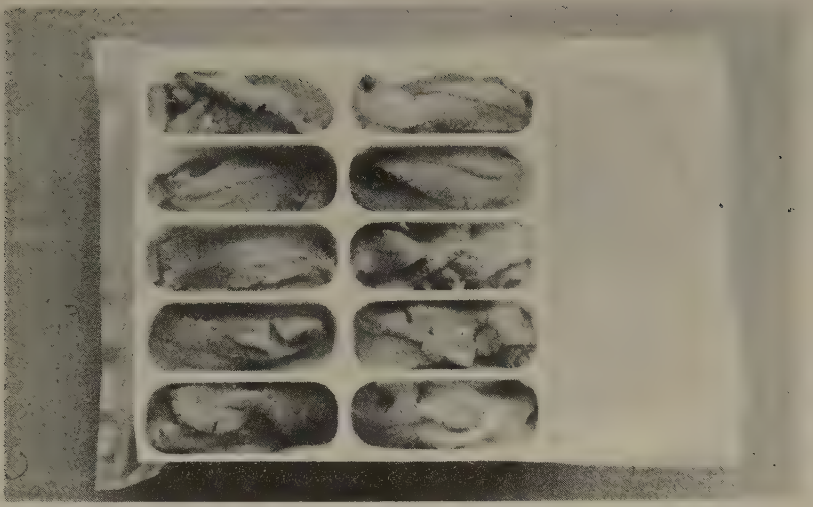

Figure 19.—Sea urchin roe packed for the domestic retail market in an "oyster tray".

ceptable, as they impart some odor or flavor to the roe. Now, however, a firm in Los Angeles manufactures nearly all wood trays used by the U.S. industry[13].

Sanitation is important because sea urchin roe, which is usually sold fresh out of the shell, can easily pick up bacterial and fungal contamination. To counteract bacteria, some processors use ultraviolet-treated water in all phases of processing, and disinfectants are used by all to maintain a sanitary environment. Good refrigeration is also critical, especially during summer.

Labor costs are rather high in an operation which calls for meticulous cleaning, sorting, and packing. Thus several processors turned to bulk-packing methods. In addition to savings in labor costs, bulk-packing also offered lower costs for trays (plastic instead of wood), as well as lower shipping costs, because the plastic trays were considerably lighter, and only a few were needed compared to wood trays. Once in Japan, the roe is repacked in the traditional wood trays and marketed through normal channels.

The proximity of the markets and the use of experienced labor ensured that the appearance of the repacked product was good. The only drawback was the extra time and cost needed to transport and repack the roe. Presently, fresh red sea urchin roe is being shipped to Japan primarily in wood trays, but some foam bulk trays are also used. The product form is largely determined by the current prices of both, and, recently, roe packed in wood trays has generally yielded higher profits.

For the domestic market, wood trays and plastic "oyster" trays (Fig. 19), which are partitioned, have 5 or 10 depressions, and hold 100 or 200 g of roe, are used for sale through retail markets. Nearly all sushi restaurants prefer the wood trays, however.

Several attempts have been made to process sea urchins aboard vessels at sea. The principal advantages are proximity to the sea urchin supply, access to clean salt water, and easy disposal of waste products. Apparently the cost of maintaining crews and workers aboard the vessels for extended periods proved uneconomical.

In the early days of the fishery, processing plants were concentrated in Santa Barbara, but by 1984 plants were located in Los Angeles (four), Long Beach (two), Ventura (one), and Oxnard (one). Several plants stopped processing recently in San Diego, Los Angeles, Oxnard, and Santa Barbara. These are likely to resume processing when conditions are favorable. Periodically, red sea urchins are harvested in northern California near Fort Bragg and trucked to central and southern California for processing.

Several attempts have been made to process sea urchins in northern California, but none has proved successful for a sustained period. The chief problem appears to be inclement weather during winter when the market is most favorable. In addition to high seas, visibility is extremely poor during and after winter storms, making diving for sea urchins rather difficult and hazardous. Nevertheless, some small-scale processing is being carried out with sea urchins from Half Moon Bay to Fort Bragg to supply local sushi shops.

Processors indicate that about 35-45 experienced workers are needed to clean and pack 10 t of whole red sea urchins in wood trays in an 8-hour work day. When larger foam trays are used, the same amount can be processed by 25 workers if the roe need not be aligned in the trays. If careful packing is required, however, only a slight savings in labor is realized.

The plants process sea urchins around 200 days annually. In a typical operation, 4 persons crack the shells open, 12 remove the roe and do preliminary cleaning, 6 do the final cleaning, and 16 pack the roe in wood trays[6]. During periods of full production, some plants have 80 persons working 10-12 hours per day.

The quantity and quality of roe contained in sea urchins is vital to processors. Quantity is by and large a seasonal phenomenon, as the amount of roe depends in part on the reproductive state of the sea urchins. However, nutritional state is important, and areas devoid of preferred algae produce sea urchins with poor yield or poor color.

We were fortunate in being allowed to examine the production log of a southern California processor, and we have constructed a graph (Fig. 20) of the yield of premium roe processed in 1975-76. The figure includes only roe packed in trays for the fresh roe market.

---

[13] The only known domestic tray maker is Matsumoto, Inc., 411 E. 5th St., Los Angeles, Calif.

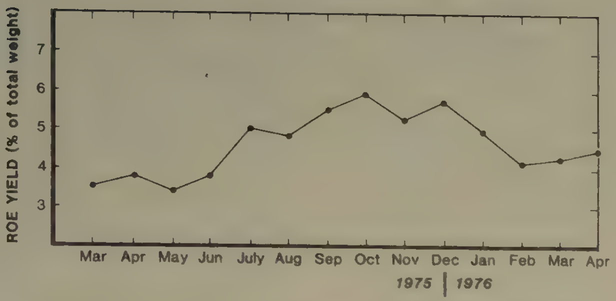

Figure 20.—Yield of sea urchin roe at a commercial processing plant. Only good quality roe sold fresh is included in the yield.

The production curve is similar to the reproductive cycle of red sea urchins (Fig. 4). The yield is lower because off-colored roe is discarded, some roe is inevitably lost during processing, and cooked and salted roe are not included in the data. Further, the gonad index given in Figure 4 is based on drained weight of sea urchins, while the production yield is based on total weight at dockside.

Roe color is exceedingly important in marketing. Clear, bright yellow or orange roe is best for the fresh market. As many as eight color grades are used by California processors, and all dark or discolored roe is discarded. For salted roe, the preferred color is orange, which is the color of high quality bottled salted roe made with Japanese sea urchins.

In the California fishery we noted that orange roe was exclusively from male red sea urchins while yellow roe was usually found in females. Bernard (1977) and Kramer and Nordin (1975) found the same relationship in red sea urchins from British Columbia, and the latter found no cyclic changes in color of the roe. Dark brown roe represents gonads degenerated because of starvation.

In addition to having good color and appearance, best quality roe is firm, small (less than 5 cm), and free of leaking fluids. Some processors feel that poor quality roe tends to occur in greater frequency in large (old) urchins, and for this reason they discourage harvest of the very large red sea urchins.

Persons in California wishing to buy and process sea urchins must obtain a wholesale fish dealers and preservers license ($65) from the Department of Fish and Game. In addition, the wholesaler is responsible for keeping records of all sea urchins purchased, and for paying a tax of $2.87/t of whole sea urchins bought.

Shipping and Marketing

Fresh roe is shipped to Japan by air freight, principally from Los Angeles International Airport. A freight forwarder consolidates products from several firms to take advantage of lower bulk-rate charges for air freight. Since carriers do not use refrigerated containers, each processor must include adequate artificial coolant in individual shipping cartons. Unit cost for air freight depends on the quantity shipped. Amounts under 100 kg are charged $5.08/kg; between 100 and 200 kg, $4.40/kg; 200-300 kg, $2.85/kg; and over 300 kg, $2.16/kg. To this are added handling charges of $17 to $45 per shipment, depending on the number of cases of roe shipped[14].

Steamed roe is often air-shipped to Japan, but it can also be frozen and sent by sea, as are all salted and frozen products. The basic shipping charge is presently $388/t. Other charges (insurance, labor, overland freight, etc.) are additional costs, as are surcharges for adjustments based on current fuel and currency rates[15].

Sea urchin roe for the domestic market is shipped in insulated cartons containing coolants similar to those used in overseas shipment. Both truck and air transport are used, depending on distance.

The short shelf life of fresh sea urchin roe makes it imperative that the product be handled expeditiously. Fresh roe is usually shipped by air freight to Japan within 30 hours after delivery of the sea urchins at dockside by divers. Shipment timing is important because all imported food undergoes agricultural inspection and customs clearance at the receiving airport in Japan. Spot checks are also made by health officials to monitor levels of bacterial contamination. It is best to ship sea urchins from Los Angeles on flights that depart around midnight, as they arrive before dawn in Tokyo after 11-12 hours. Shipments that arrive late in the day are held over for inspection the following day. Shipments are not made on Fridays, because arrival date is Sunday in Japan, or on Sundays, when most U.S. processors suspend operations.

After official clearance, the roe is held overnight in refrigerators until early the next morning when auctions are held at the Metropolitan Central Wholesale Fish Market, located in Tsukiji, Tokyo. Bulk-packed roe is trucked directly from the airport to outlying regions, particularly to Miyagi Prefecture, about 325 km from Tokyo. There the roe is repacked in standard wood trays before being marketed.

Most of the sea urchin roe produced in California is marketed fresh in Japan, but an increasing amount of fresh roe is being packed in wood trays for the growing domestic sushi trade. Small amounts packed in plastic oyster trays are also sold in U.S. retail outlets. The total amount sold in the United States is unknown, but is thought to be on the order of 30-40,000 wood trays per month, which we estimate to be about 25 percent of the average amount sent to Japan.

In Japan, fresh U.S. roe packed in wood trays is sold primarily at the Tsukiji Market through auction. The roe is sold in lots (bundles) of 11-13 trays. In other cities, sea urchin roe is sold through auction or directly to major wholesalers. Bulk-pack fresh roe, repacked in Japan in traditional wood trays, is sold in many cities through auction and direct sales. Salted, steamed, or baked roe is usually sold through brokers to manufacturers that specialize in preserved sea urchin roe products.

---

[14] Mr. Kagawa, "K" Line Air Service, Inc., Redondo Beach, Calif. Personal commun.

[15] T. Saito, Pacific Marine Products Corporation, Ventura, Calif. Personal commun.

Several American processors sell sea urchin roe to Japanese trading firms at a fixed price so they are not subjected to the vagaries of auctioning. Some processors sell their own products at auction through brokers, however. These brokers receive about 5 percent of the sales price for their services. The auctioneers, called primary wholesalers, receive 5.5 percent of the auction price for handling the product. In addition, an import customs duty of 10 percent is assessed on fresh roe, and 7 percent on salted roe. These duties are paid on the basis of the bill of sale if the roe has been sold outright. If not, a small down payment is required, and the balance of the duty is paid after the primary wholesaler reports the selling price to the customs office.

As of 1984, divers were paid about $400-500/t for red sea urchins. The prices usually correspond to the high demand in winter, low yield during spring, and low demand in summer. To encourage harvesting of good quality sea urchins, some processors offer bonuses when high roe yields are achieved.

As mentioned, the prices paid at the auctions in Japan are based on supply and demand. Of course, quality is always of primary importance, and domestic roe always brings the highest prices. As the Japanese sea urchin fishery is mainly a spring-summer fishery, prices are generally lower during those months because of high domestic production (Mottet, 1976). Around the middle of August, seasonal monsoons depress fishing effort; at the same time, several species of sea urchins start reproductive activity, and fisheries for those species are curtailed. Then imports need to be increased to fill the demand.

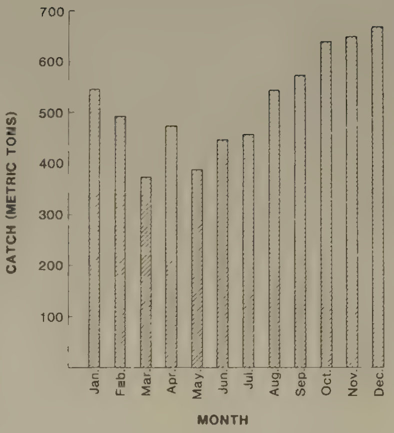

Figure 21.—Average California catch, by month, of red sea urchins, 1973-83. Source: California Department of Fish and Game.

The United States and the Republic of South Korea are presently the largest exporters of sea urchin roe to Japan. The demand and price are especially high during the holiday season near the end of the year. Thus the average catch by month in the California sea urchin fishery (Fig. 21) reflects the price structure. But the lower catches from March through July are also related to low gonad yields after the spawning season.

Processors in the United States sometimes sell their products to Japanese brokers at a flat annual price which reflects the value at both the high and low demand periods. Often by agreement the volume is kept minimal in the spring and summer to avoid big losses. However, the plants have to operate even during unprofitable periods, because of the need to keep key personnel employed.

Processors and buyers sometimes resort to freezing roe during the summer when Japanese prices are low. The frozen roe is held several months until prices are better, and though premium prices are never paid for frozen roe, the profits are a bit better than selling fresh roe in summer.

Acknowledgments

We received help from many people in preparing this report. Fishermen, processors, brokers, researchers from the California Department of Fish and Game (CDFG), Scripps Institution of Oceanography, San Diego State University, and the Washington Department of Fisheries contributed materially to the contents, and we are grateful for their time and cooperation. Useful comments were provided by David Parker (CDFG), who reviewed the manuscript and also provided much data on the harvesting section. Susan Smith (NMFS), John Dixon (University of Southern California), and F. R. Bernard (Pacific Biological Station, Nanaimo, B.C.) also critically reviewed the manuscript, improving it considerably. Sennen Salapare (NMFS) helped gather most of the statistics, and Rahel Fischer provided extensive editorial and secretarial aid. The junior author thanks Jerolyn Bleak and John Dixon for field assistance. We owe many thanks also to the Canadian scientists whose research has added substantially to little-known aspects of the biology as well as the commercial fishery for red sea urchins.

Literature Cited

Anonymous. 1977. Operations in San Diego County. *In* W. J. North (principal investigator), Kelp habitat improvement project, Annu. Rep. 1974-75, p. 15-29. Calif. Inst. Technol.

Baker, S. L. 1973. Growth of the red sea urchin, *Strongylocentrotus franciscanus* (Agassiz) in two natural habitats. M.S. thesis, Calif. State Univ., San Diego, 83 p.

Bennett, J., and A. C. Giese. 1955. The annual reproductive and nutritional cycles in two western sea urchins. Biol. Bull. (Woods Hole) 109: 226-237.

Bernard, F. R. 1977. Fishery and reproductive cycle of the red sea urchin, *Strongylocentrotus franciscanus*, in British Columbia. J. Fish. Res. Board Can. 34:604-610.

________, and D. C. Miller. 1973. Preliminary investigation on the red sea urchin resources of British Columbia (*Strongylocentrotus franciscanus*, Agassiz). Fish. Res. Board Can., Tech. Rep. 400, 37 p.

Bernstein, B. B., B. E. Williams, and K. H. Mann. 1981. The role of behavioral responses to predators in modifying urchins' (*Strongylocentrotus drobachiensis*) destructive grazing and seasonal foraging patterns. Mar. Biol. 63:37-49.

Boolootian, R. A., and A. R. Moore. 1956. Hermaphroditism in echinoids. Biol. Bull. (Woods Hole) 111:328-335.

Breen, P. A., and B. E. Adkins. 1976. Growth rings and age in the red sea urchin, *Strongylocentrotus franciscanus*. Fish. Res. Board Can., Pac. Biol. Sta., Nanaimo, B.C., Manuscr. Rep. Ser. 1413, 17 p.

________, ________, and D. C. Miller. 1978. Recovery rate in three exploited sea urchin populations from 1972 to 1977. Can. Fish. Mar. Serv. Pac. Biol. Sta., Resour. Serv. Branch, Nanaimo, B.C., Manuscr. Rep. 1446, 27 p.

________, D. C. Miller, and B. E. Adkins. 1976. An examination of harvested sea urchin populations in the Tofino area. Fish. Res. Board Can., Manuscr. Rep. Ser. 1401, 22 p.

Cameron, R. A., and R. Hinegardner. 1974. Initiation of metamorphosis in laboratory-cultured sea urchins. Biol. Bull. (Woods Hole) 146:335-342.

________, and S. C. Schroeter. 1980. Sea urchin recruitment: Effect of substrate selection on juvenile distribution. Mar. Ecol.-Prog. Ser. 2:243-247.

Cowen, R. K. 1983. The effect of sheephead (*Semicossyphus pulcher*) on red sea urchin (*Strongylocentrotus franciscanus*) populations: An experimental analysis. Oecologia (Berlin) 58:249-255.

Dean, T. A., S. C. Schroeter, and D. D. Dixon. 1984. Effects of grazing by two species of sea urchins (*Strongylocentrotus franciscanus* and *Lytechinus anamesus*) on recruitment and survival of two species of kelp (*Macrocystis pyrifera* and *Pterogophora californica*). Mar. Biol. 78:301-313.

Duggins, D. O. 1980. Kelp beds and sea otters: An experimental approach. Ecology 61(3):447-453.

Ebert, E. E. 1968. California sea otter - census and habitat survey. Underwater Nat. 5(3): 20-22.

Ebert, T. A. 1967. Negative growth and longevity in the purple sea urchin *Strongylocentrotus purpuratus* (Stimpson). Science (Wash., D.C.) 157: 557-558.

________. 1968. Growth rates of the sea urchin *Strongylocentrotus purpuratus* related to food availability and spine abrasion. Ecology 49: 1075-1091.

________. 1983. Recruitment in echinoderms. *In* M. Jangoux and J. M. Lawrence (editors), Echinoderm Studies I, p. 169-203. A. A. Balkeema, Rotterdam.

Fawcett, M. H. 1984. Local and latitudinal variation in an herbivorous marine snail. Ecology 65(4):1214-1230.

Feder, H. M., C. H. Turner, and C. Limbaugh. 1974. Observations on fishes associated with kelp beds in southern California. Calif. Dep. Fish Game, Fish Bull. 160, 144 p.

Frank, P. W. 1975. Latitudinal variation in the life history features of the black turban snail *Tegula funebralis* (Prosobranchia: Trochidae). Mar. Biol. 31:181-192.

Giese, A. C., L. Greenfield, H. Huang, A. Farmanfarmaian, R. Boolootian, and R. Lasker. 1958. Organic productivity in the reproductive cycle of the purple sea urchin. Biol. Bull. (Woods Hole) 116(1):49-58.

Greenfield, L., A. C. Giese, A. Farmanfarmaian, and R. A. Boolootian. 1958. Cyclic biochemical changes in several echinoderms. J. Exp. Zool. 139(3):507-524.

Harrold, C., and D. Reed. In press. Food availability, sea urchin grazing, and kelp forest community structure. Ecology.

Higashi, H., R. Kikuchi, and K. Tabei. 1959. Nutritive elements in salted marine appetizers. Nutrition and Foods 11(6):62-65. Tokyo. (in Jpn.)

________, T. Yamakawa, M. Yanase, T. Kinumaki, Y. Shimizu, K. Sugii, and H. Iida. 1965. Vitamins in salted sea urchin gonad. Nutrition and Foods 18(2):66-69. Tokyo. (In Jpn.)

Hinegardner, R. T. 1969. Growth and development of the laboratory cultured sea urchin. Biol. Bull. (Woods Hole) 137:465-475.

________. 1975. Morphology and genetics of sea urchin development. Am. Zool. 15:679-689.

Jensen, M. J., 1969. Age determination of echinoids. Sarsia 37:41-44.

Johnson, M. W., 1930. Notes on the larval development of *Strongylocentrotus franciscanus*. Publ. Puget Sound Biol. Sta. (Seattle) 7: 401-411.

Kato, S. 1972. Sea urchins: A new fishery develops in California. Mar. Fish. Rev. 34(9-10): 23-30.

Kramer, D. E., and D. M. A. Nordin. 1975. Physical data from a study of size, weight and gonad quality for the red sea urchin (*Strongylocentrotus franciscanus* (Agassiz)) over a one-year period. Can. Fish. Mar. Serv., Vancouver Lab., Manuscr. Rep. Ser. 1372, 91 p.

________, and ________. 1979. Studies on the handling and processing of sea urchin roe. I. Fresh product. Can. Fish. Mar. Serv., Tech. Rep. 870, Vancouver, B.C., 47 p.

Lees, D. C. 1970. The relationship between movement and available food in the sea urchins *Strongylocentrotus franciscanus* and *S. purpuratus*. M.S. thesis, Calif. State Univ., San Diego, 117 p.

Leighton, D. L. 1966. Studies of food preferences in algivorous invertebrates of southern California kelp beds. Pac. Sci. 20(1):104-113.

________. 1967. Ecological investigations of sea urchin populations along the Palos Verdes peninsula. *In* W. J. North (principal investigator), Kelp habitat improvement project, Annu. Rep. 1966-67, p. 41-54. Calif. Inst. Technol., Pasadena.

________. 1971. Grazing activities of benthic invertebrates in southern California kelp beds. *In* W. J. North (editor), The biology of giant kelp beds (*Macrocystis*) in California, p. 421-453. Beiheptezur Nova Hedwigia 32, Verlag von J. Cramer, Lehre, Ger.

________, L. G. Jones, and W. J. North. 1966. Ecological relationships between giant kelp and sea urchins in southern California. *In* E. G. Young (editor), Proc. 5th Int. Seaweed Symp., Halifax (Aug. 25-28), p. 141-153. Pergamon Press, Oxford, Engl.

Low, C. J. 1975. The effect of grouping of *Strongylocentrotus franciscanus*, the giant red sea urchin, on its population biology. Ph.D. thesis, Univ. British Columbia, Vancouver, 126 p.

Lowry, L. F., and J. S. Pearse. 1973. Abalones and sea urchins in an area inhabited by sea otters. Mar. Biol. 23(3):213-219.

McCauley, J. E., and A. G. Carey, Jr. 1967. Echinoidea of Oregon. J. Fish. Res. Board Can. 24(6):1365-1401.

MacGinitie, G. E., and N. MacGinitie. 1968. Natural history of marine animals. McGraw-Hill, New York, 473 p.

McLean, J. H. 1962. Sublittoral ecology of kelp beds of the open coast area near Carmel, California. Biol. Bull. (Woods Hole) 122:94-114.

Malagrino Lumare, G. 1972. Extraccion y preservacion de las gonadas de erizo. M.S. thesis, Universidad Autonoma de Baja California, Escuela Superior de Ciencias Marinas, Ensenada, Mexico, 79 p.

Mattison, J. E., and J. D. Trent, A. L. Shanks, T. B. Akin, and J. S. Pearse. 1977. Movement and feeding activity of red sea urchins (*Strongylocentrotus franciscanus*) adjacent to a kelp forest. Mar. Biol. 39:25-30.

Miller, R. J., and K. H. Mann. 1973. Ecological energetics of the seaweed zone in a marine bay on the Atlantic coast of Canada. III. Energy transformation by sea urchins. Mar. Biol. 18: 99-114.

Mitchell, C. T., L. G. Jones, and W. J. North. 1969. Studies on urchin larvae and recruitment of juveniles. *In* W. J. North (principal investigator), Kelp habitat improvement project, Annu. Rep. 1968-69, p. 106-115. Calif. Inst. Technol.

Moore, H. B., T. Jutare, J. C. Bauer, and J. A. Jones. 1963. The biology of *Lytechinus variegatus*. Bull. Mar. Sci. Gulf Carib. 13(1):23-53.

Mottet, M. G. 1976. The fishery biology of sea urchins in the family Strongylocentrotidae. Wash. Dep. Fish. Tech. Rep. 20, 66 p.

North, W. J. 1965. Urchin predation. *In* W. J. North (principal investigator), Kelp habitat improvement project, Annu. Rep. for 1964-65, p. 57-61. Calif. Inst. Technol.

________. 1974. A review of the studies supporting sea urchin control as a means of restoring kelp beds. *In* W. J. North (principal investigator), Kelp habitat improvement project, Annu. Rep. 1973-74, p. 95-108. Calif. Inst. Technol.

________, and J. S. Pearse. 1970. Sea urchin population explosion in southern California coastal waters. Science (Wash., D.C.) 167:209.

Pace, D. R. 1975. Environmental control of red sea urchin (*Strongylocentrotus franciscanus*) vertical distribution in Barkley Sound, British Columbia. Ph.D. thesis, Simon Fraser Univ., Burnaby, B.C., 98 p.

Paine, R. T., and R. L. Vadas. 1969. The effects of grazing by sea urchins, *Strongylocentrotus* spp., on benthic algal populations. Limnol. Oceanogr. 14(5):710-719.

Palmisano, J. F. 1975. Sea otter predation: Its role in rocky intertidal community structure at Amchitka and other Aleutian Islands. Ph.D. thesis, Univ. Wash., Seattle, 193 p.

Pearse, J. S., M. E. Clark, D. L. Leighton, C. T. Mitchell, and W. J. North. 1970. Marine waste disposal and sea urchin ecology. *In* W. J. North (principal investigator), Kelp habitat improvement project, Annu. Rep. 1969-70, p. 1-93. Calif. Inst. Technol.

________, and A. H. Hines. 1979. Expansion of a central California kelp forest following the mass mortality of sea urchins. Mar. Biol. 51: 83-91.

________, and V. B. Pearse. 1975. Growth zones in the echinoid skeleton. Am. Zool. 15:731-763.

Quast, J. C. 1968. Observations on the food of the kelp-bed fishes. Calif. Dep. Fish Game, Fish Bull. 139:109-142.

Rosenthal, R. J., and J. R. Chess. 1972. A predator-prey relationship between the leather star, *Dermasterias imbricata*, and the purple urchin, *Strongylocentrotus purpuratus*. Fish. Bull. (U.S.) 70(1):205-216.

________, W. D. Clark, and P. K. Dayton. 1974. Ecology and natural history of a stand of giant kelp, *Macrocystis pyrifera*, off Del Mar, California. Fish. Bull. (U.S.) 72(3):670-684.

Russo, A. R. 1979. Dispersion and food differences between two populations of the sea urchin *Strongylocentrotus franciscanus*. J. Biogeogr. 6:407-414.

Schroeter, S. C. 1978. Experimental studies of competition as a factor affecting the distribution and abundance of purple sea urchins, *Strongylocentrotus purpuratus* (Stimpson). Ph.D. thesis, Univ. Calif. Santa Barbara, 184 p.

________, J. D. Dixon, and J. Kastendick. 1983. Effects of the starfish, *Patiria miniata*, on the distribution of the sea urchin *Lytechinus anamesus* in a southern Californian kelp forest. Oecologia (Berlin) 56:141-147.

Sheer, B. T. 1945. The development of marine fouling communities. Biol. Bull. (Woods Hole) 89:103-121.

Shelton, D. B., P. A. Bernal, and J. A. McGowan. 1982. Large-scale interannual physical and biological interactions in the California Current. J. Mar. Res. 40:1095-1125.

Shepherd, S. A. 1973. Competition between sea urchins and abalone. Austral. Fish. 32(6):4-7.

Silver, G. R., and A. Brierton. 1974. Some indicators which suggest that vertical movement does not occur in *Strongylocentrotus franciscanus* (Agassiz). Lambda 1:15-18.

Southward, A., and E. Southward. 1975. Endangered urchins. New Sci. 10 April 1975:70-72.

State Water Quality Control Board. 1964. An investigation of the effects of discharged wastes on kelp. State Water Qual. Control Board, Sacramento, Calif., Publ. 26, 124 p.

Swan, E. F. 1961. Some observations on the growth rate of sea urchins in the genus *Strongylocentrotus*. Biol. Bull. (Woods Hole) 120: 420-427.

Tegner, M. J. 1980. Multispecies considerations of resource management in southern California kelp beds. *In* J. D. Pringle, G. J. Sharp, and J. F. Caddy (editors), Proceedings of the workshop on the relation between sea urchin grazing and commercial plant/animal harvesting. Can. Tech. Rep. Fish. Aquat. Sci. 954:125-143.

________ , and P. K. Dayton. 1977. Sea urchin recruitment patterns and implications of commercial fishing. Science (Wash., D.C.) 196: 324-326.

________ , and ________ . 1981. Population structure, recruitment and mortality of two sea urchins (*Strongylocentrotus franciscanus* and *S. purpuratus*) in a kelp forest near San Diego, California. Mar. Ecol. Progr. Ser. 5:255-268, Fed. Rep. Germany.

________ , and L. A. Levin. 1982. Do sea urchins and abalones compete in California kelp forest communities?, p. 265-271. *In* J. M. Lawrence (editor), Int. Echinoderms Conf., Tampa Bay. A. A. Balkema, Rotterdam.

________ , and ________ . 1983. Spiny lobsters and sea urchins: Analysis of a predator-prey interaction. J. Exp. Mar. Biol. Ecol. 73: 125-150.

Vadas, R. L. 1968. The ecology of *Agarum* and the kelp bed community. Ph.D. thesis, Univ. Wash., Seattle, 280 p.

________ . 1977. Preferential feeding: An optimization strategy in sea urchins. Ecol. Monogr. 47:337-371.

Wilson, K. C., P. L. Haaker, and D. A. Hanan. 1978. Kelp restoration in southern California. *In* R. Krauss (editor), The marine plant biomass of the Pacific Northwest coast, p. 183-202. Pac. Northw. Reg. Comm., Oreg. State Univ. Press.

J Comp Physiol A (1985) 157:375–381

Journal of Comparative Physiology A Sensory, Neural, and Behavioral Physiology

© Springer-Verlag 1985

Chains of single-domain magnetite particles in chinook salmon, *Oncorhynchus tshawytscha*

J.L. Kirschvink[1], M.M. Walker[2], S-B Chang[1], A.E. Dizon[3], and K.A. Peterson[1]

[1] Division of Geological and Planetary Sciences, California Institute of Technology, Pasadena, California 91125, USA
[2] Southwest Fisheries Center Honolulu Laboratory, National Marine Fisheries Service, NOAA, Box 3830,
Honolulu, Hawaii 96812, USA
[3] Southwest Fisheries Center La Jolla Laboratory, National Marine Fisheries Service, NOAA, P.O. Box 271,
La Jolla, California 92038, USA

Accepted June 3, 1985

Summary. Although the presence of magnetite in their tissues is correlated with the ability of different species to detect magnetic fields, proof that the magnetite is involved in magnetoreception has not yet been provided. Using the approach employed to localize and isolate magnetic particles in the yellowfin tuna, we found that single-domain magnetite occurs in chains of particles in tissue contained within the dermethmoid cartilage of adult chinook salmon, *Oncorhynchus tshawytscha.* The particles are present in sufficient numbers to provide the adult fish with a very sensitive magnetoreceptor system. Magnetite in the chinook can be correlated with responses to magnetic fields in a congeneric species, the sockeye salmon. Based on the presence of the chains of particles, we propose behavioral experiments that exploit the responses of sockeye salmon fry to magnetic fields to test explicit predictions of the ferromagnetic magnetoreception hypothesis.

ntroduction

Discoveries of fine-grained magnetite in the bodies of honeybees and homing pigeons (Gould et al. 978; Walcott et al. 1979) stimulated theoretical nalyses of the suitability of the particles for use n magnetoreception (e.g. Yorke 1979, 1981; Kirschvink 1979; Kirschvink and Gould 1981) and ttempts to demonstrate magnetite and magnetosensory abilities in other species. For example, recent studies found conditioned responses to magnetic field stimuli and approximately 100 million nteracting particles of pure single-domain magneite, possibly associated with nervous tissue, in tissue contained within the dermethmoid bone of the skull of the yellowfin tuna, *Thunnus albacares* (Walker 1984; Walker et al. 1984). Magnetic material, at least some of which is fine-grained magnetite, has been found in tissue from the premaxilloethmovomerine block of bones in the skull of the European eel, *Anguilla anguilla* (Hanson et al. 1984a, b), which also responds to magnetic fields (Branover et al. 1971; Tesch 1974). These results from phylogenetically distant species imply that magnetite and magnetosensory abilities are widespread among teleost fishes.

Proof that magnetite mediates magnetoreception, however, will depend on behavioral tests of predictions of the magnetite-based magnetoreception hypothesis. Such tests require identification of species that make appropriate responses to magnetic fields in experimental situations and that also possess magnetite suitable for use in magnetoreception. One possibility is juvenile sockeye salmon, *Oncorhynchus nerka*, which exhibit spontaneous directional preferences in orientation arenas that generally correspond to the axis of the nursery lake to which newly emerged fry migrate (Brannon 1972). In a series of investigations into the behavior of sockeye salmon, Quinn and his colleagues (Quinn 1980; Quinn et al. 1981; Quinn and Brannon 1982) have shown that the directional preferences in orientation arenas of lake-migrating sockeye salmon fry and smolts can be controlled by magnetic fields. Quinn et al. (1981) were able to predict from their behavioral observations that the magnetoreceptor of the salmon must be capable of operating in the dark, in the absence of water flow in both fresh and sea water, and be adaptable to geomagnetic field changes occurring over geologic time. These predictions are compatible with the hypothesis that the magnetoreceptor of the salmon is based on magnetite. Demonstration of magnetite in salmon, therefore, should open the way for adaptation of currently available procedures for behavioral tests of predictions of the ferromagnetic magnetoreception hypothesis.

Here we report that single-domain magnetite occurs in tissue from the same area of the skull of adult chinook salmon, *Oncorhynchus tshawytscha*, as it has been found in the yellowfin tuna and the European eel. We also have isolated chains of the particles from the tissue where previously we could not, although the particles had been inferred to lie in small clumps or chains from their magnetic properties (Walker et al. 1984). Sufficient numbers of the particles are present to form a very sensitive magnetoreceptor organ. We conclude by proposing behavioral tests of the magnetite-based magnetoreception hypothesis that exploit the responses of sockeye salmon fry to magnetic field polarity in the orientation arenas used by Quinn et al. (1981).

The magnetite-based magnetoreception hypothesis predicts, *inter alia*, that for magnetic particles to be used in magnetoreception they, or groups of them, must (1) be magnetized uniformly and be large enough to align with the geomagnetic field against the randomizing effects of thermal buffeting (Kirschvink 1983; Kirschvink and Walker, in press), and (2) be biochemical precipitates to provide the uniform magnetophysical properties necessary for magnetoreception. Magnetic material that could be used for detecting both magnetic field direction and intensity (see Discussion) therefore should have a high remanent magnetic moment concentrated in a small volume of sample, a consistent anatomical position, and similar bulk magnetic properties within and among species (Walker et al. 1984). Magnetic material has been located most consistently in the heads of vertebrates (Walcott et al. 1979; Mather and Baker 1981; Zoeger et al. 1981; Baker et al. 1983; Beason and Nicholls 1984; Perry et al., in press), and in the front of the skull in particular in fishes. From these results we predict that magnetite should be located in the front of the skull of the salmon.

Materials and methods

Heads from four adult, net-caught chinook salmon were dissected using glass knives and non-metallic tools in a magnetically-shielded, dust and magnetic particle-free clean laboratory at the California Institute of Technology. The techniques for conducting non-magnetic dissections and avoiding contamination of samples have been described extensively, elsewhere (Kirschvink 1983; Walker et al. in press). Tissue samples were removed from each head, washed in glass distilled water, and rapidly frozen in liquid nitrogen. Each sample was exposed to a 4 ms duration, unidirectional magnetic pulse with a peak magnetic field of 0.7 Tesla (7,000 Gauss) generated by an impulse magnetizer (Furth and Waniek 1956; Kirschvink 1983) and immediately assayed for Isothermal Remanent Magnetization (IRM, a measure of the total volume of ferromagnetic material present) in the zero field environment of a superconducting magnetometer of the type described by Goree and Fuller (1976). The procedure was repeated for each sample, after which the mass of each sample was measured to the nearest 0.1 g. Tissues sampled in all fish included muscle, eye, brain, cartilage from the skull, and fatty tissue from within the anterior portion of the skull (the dermethmoid region). Other samples not taken in all fish included the olfactory rosette, the olfactory nerve, and gills.

The background signal in the magnetometer fluctuated at or below 5 pA^2 (5×10^{-9} emu), while the empty sample holder was kept below the 50 pA^2 level by regular washing and ultrasonic cleaning. A tissue sample was judged to be magnetic when the signal from the magnetometer, the magnetometer's signal to noise ratio at the time of measurement, and the calculated intensity of magnetization (moment/volume) were high compared with those obtained from other tissues taken from the same fish. Samples that were magnetic in all fish then were subjected to progressive alternating field (Af) demagnetization and IRM acquisition experiments similar to those done to geological samples by Cisowski (1981) and to yellowfin tuna by Walker et al. (1984). In these experiments, samples were frozen to and suspended from a thin, non-magnetic cotton thread as described by Kirschvink (1983). The advantage of this technique is that the measurement sensitivity is limited only by the noise of the vertical field sensor ($\simeq 5$ pA^2) rather than the sample holder. While frozen, the samples were Af demagnetized completely by placing them in a strong, 400 Hz vertically oscillating magnetic field produced by an air core solenoid which was itself in a zero-field environment. As the alternating field decays linearly from an initial amplitude of 0.1 Tesla to zero over about 15 s, it leaves equal numbers of the still fully magnetized particles with their magnetic moments oriented in opposite directions, leaving the sample with no net magnetic moment. The frozen samples then were exposed to a series of progressively stronger magnetic impulses, and their moments remeasured after each step. After the samples reached saturation (that is, they gained no further remanence with increasing pulse strength), they were sequentially demagnetized and remeasured in a similar fashion using progressively stronger peak oscillating fields.

We extracted the magnetic material for other experiments by grinding the magnetic tissues from several fish in a glass tissue grinder, separating the released fats by dissolving them in ether, and digesting the remaining tissue in nitrocellulose (0.42 μm pore size)-filtered 5% sodium hypochlorite solution (commercial bleach). Aggregates of magnetic particles released by this procedure were treated briefly with EGTA solution (rather than with EDTA as done previously; Walker et al. 1984). After washing, centrifugation, and magnetic separation, the fine powder obtained was identified by X-ray diffraction. Particles then were dispersed magnetically in an alternating magnetic field and mounted on carbon-coated copper mesh grids for transmission electron microscope (TEM) analysis.

Results

We found inducible remanent magnetization in several of the tissue samples examined (Table 1).

Table 1. Magnetic survey of selected tissues in four chinook salmon. For each tissue type examined, the mass is reported in g, the moment in units of 10^{-12} A^2 (10^{-9} emu), the intensity in pT, and the S/N quantity gives the signal to noise ratio of the sample holder and instrument at the time of measurement. A 0.6 g sample of the olfactory rosette from fish no. 1 also had low values (moment, intensity, and S/N) of 4.0, 6.6, and 0.8 respectively

	Muscle				Eye				Brain				Dermethmoid			
	Mass (g)	Moment 10^{-12} A^2	Int. pT	S/N	Mass (g)	Moment 10^{-12} A^2	Int pT	S/N	Mass (g)	Moment 10^{-12} A^2	Int. pT	S/N	Mass (g)	Moment 10^{-12} A^2	Int. pT	S/N
Fish #1	1.3	50	3.9	0.7	9.0	163	1.8	3.3	1.4	52	3.7	1.1	0.5	895	178.0	11.9
Fish #2	1.8	140	7.8	2.8	6.3	3,300	52.4	97	1.3	51	3.9	0.8	1.0	517	51.7	14.6
Fish #3	2.1	730	34.7	40.7	6.9	270	3.9	20.9	1.9	25	1.4	2.5	0.3	320	106.7	24.8
Fish #4	2.0	140	7.0	10.9	5.0	551	11.0	42.7	1.3	776	59.7	60.2	1.2	300	25.0	10.1

Measures of magnetization were sufficiently low for most muscle and brain samples to permit the conclusion that these tissues were non-magnetic in these fish and could serve as control samples. Although the eye was sufficiently magnetic in at least two fish to invite more detailed study, two features of the data suggested it was unlikely to be the site of magnetoreception. First, the magnetic moment acquired by the eye was more variable from individual to individual than were the muscle and brain samples and, because the eye is in contact with the environment, the possibility that magnetic contaminants contributed to the moments acquired by the eyes examined can not be excluded. Second, the eye was the most massive sample measured in all fish. Eyes for three of the animals examined had intensities of magnetization, a measure of the concentration of magnetic particles in a sample, in the same range as the muscle and brain samples from the same fish. In contrast, moments acquired by the dermethmoid tissues were far less variable among fish and the intensities of magnetization were consistently higher for these samples than for muscle and brain samples from the same individuals. These results are consistent with the prediction that magnetic particles involved in magnetoreception should be concentrated in a small volume of tissue in a consistent anatomical position and led us to focus more detailed studies on the dermethmoid tissue.

Upon warming to room temperature, the dermethmoid tissues lost much of their remanent magnetization, indicating that the magnetic particles were at least partly free to rotate under the influence of thermal agitation in the low field environment of the magnetometer enclosure. When the dermethmoid tissue samples were subjected to the progressive IRM acquisition and Af demagnetization procedure described above, they acquired virtually all their remanence in fields less than 200 mTesla (mT), and lost it again in alternating fields of less than 100 mT (Fig. 1). Acquisition and loss of remanence over this range of fields is consistent with the presence in the dermethmoid tissue of large numbers of single-domain crystals of magnetite. The flattening of the IRM acquisition curve at fields above 200 mT rules out most of the common ferromagnetic contaminants such as hematite (α Fe_2O_3) or metallic iron alloys, which continue to acquire remanence in much higher fields, and also multi-domain magnetite particles, which acquire and lose remanence at much lower fields than observed here (Zoeger et al. 1981; Kirschvink 1983; Walker et al. in press).

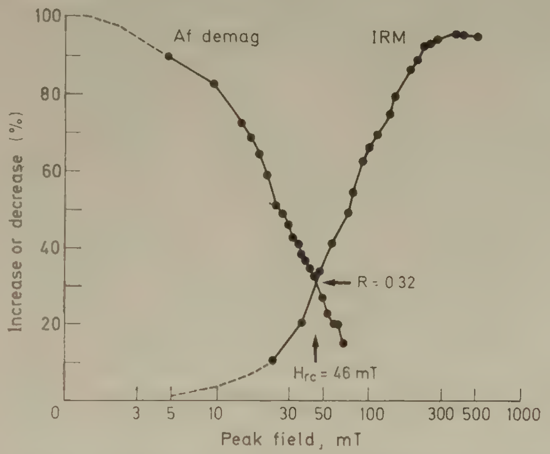

Fig. 1. Progressive acquisition and Af demagnetization of IRM for dermethmoid tissues from four chinook salmon. The intersection point of the two curves yields an estimate of the remanent coercive field (H_{rc}) of 46 mT, as well as the R value of interaction described in the text. These data are consistent with an assemblage of moderately interacting single-domain magnetite crystals

As shown by Cisowski (1981) and Walker et al. (1984) for the magnetite particles in chiton teeth and the dermethmoid tissue of the yellowfin tuna respectively, the intersection of the Af demagnetization and IRM acquisition curves falls below the 50% magnetization point. For samples with completely non-interacting single-domain particles these curves should be symmetrical about the 50% magnetization point because particle moments will be aligned or randomized equally easily by unidirectional or alternating fields of equal intensities. The interactions between the fields produced by the particles themselves increase and decrease the fields necessary to align and randomize the particle moments respectively (Dunlop and West 1969), causing the IRM acquisition and Af demagnetization curves to shift apart and their intersection to fall below the 50% magnetization point. These data therefore imply that the magnetic particles in the dermethmoid tissue of the salmon are close enough to some of their neighbors to interact with each other (e.g. within one grain diameter).

Limited constraints on the average size and shape of the particles are provided by the abscissa of the intersection point of the IRM acquisition and Af demagnetization curves. This value approximates the remanent coercive field (H_{rc}) for the particles (Cisowski 1981) and is about 46 mT for the salmon. From Fig. 2, which combines the single-domain stability field boundaries of Butler and Banerjee (1975) with the contours of equal coercivity given by McElhinny (1973), a tentative length range of 40–100 nm can be established for the particles. Depending on the distribution of particle sizes, somewhere between 1 and 100 million such crystals would be necessary to produce the magnetic remanence observed in the salmon dermethmoid tissue. These numbers compare favorably with those reported for honeybees (Gould et al. 1978), homing pigeons (Walcott et al. 1979) and yellowfin tuna (Walker et al. 1984) and, if organized into interacting groups of several particles, would be more than enough to provide the salmon with a magneto-sensory system capable of responding to both magnetic field direction and intensity (Yorke 1979, 1981; Kirschvink 1979, 1981; Kirschvink and Gould 1981).

An X-ray diffraction pattern uniquely identified magnetic particles extracted from the dermethmoid tissue as crystalline magnetite. When viewed in TEM the particles were not completely dispersed but were arranged in linear chains of particles having similar dimensions to those found in the yellowfin tuna (Fig. 3). The particles appear to be bound in some form of organic matrix, which yields an occasional electron-transparent gap between adjacent crystals. The matrix apparently prevents the particles from contacting each other as a result of magnetic attractions but preserves

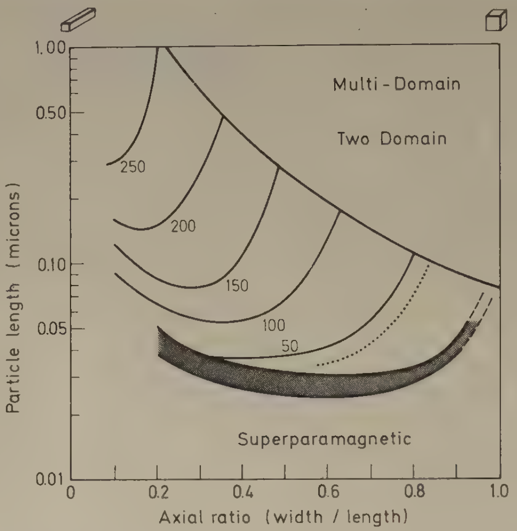

Fig. 2. Approximate contours of equal microscopic coercive force in mT (from McElhinny 1973) superimposed on the size and shape boundaries for single-domain magnetite of Butler and Banerjee (1975). Magnetite particles which spontaneously display single-domain behavior are those which have lengths and widths which plot in the central area of the diagram, between the areas labelled superparamagnetic and multi-domain. Kirschvink (1983) provides a further description of this figure. Single-domain crystals with remanent coercive fields of 46 mT, as measured here for the salmon (Fig. 1), should lie approximately in the region indicated by the dotted line. These inferred crystal sizes and shapes agree well with biogenic magnetite crystals reported from bacteria by Blakemore (1975) and Towe and Moench (1980) and from yellowfin tuna by Walker et al. (1984)

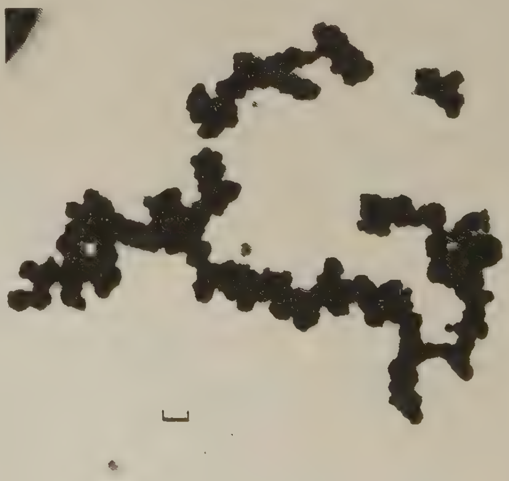

Fig. 3. Chains of magnetite particles isolated from the chinook salmon dermethmoid tissue. Scale bar 100 nm

their linear arrangement. However, folding of the chains, possibly occurring after extraction, is evident.

Discussion

The experiments reported here clearly show that adult chinook salmon possess large numbers of single-domain magnetite particles suitable for use in magnetoreception. Their narrow coercivity distribution, which indicates a restricted size range, and their presence in linear chains imply that the magnetite particles detected in the dermethmoid tissue of the salmon are produced as biochemical precipitates. As in the yellowfin tuna (Walker et al. 1984), the magnetite particles are too small to be used individually in magnetoreception as their magnetic to thermal energy ratio in the earth's magnetic field is only about 0.5. The inter-particle interaction effects detected in both the tuna and the salmon indicate that the particles are organized into arrays that could attain easily the size required for magnetoreception. Because the magnetite particles extracted from the salmon were dispersed before mounting using the same alternating magnetic field that produced isolated particles in samples taken from the yellowfin tuna, it is unlikely that the chains of particles observed in TEM in this study arose as an artifact. The hypothesis that magnetite particles in the dermethmoid tissues of the salmon and the tuna are organized in chains like those in the magnetosomes of bacteria (Balkwill et al. 1980) therefore seems reasonable. Mechanoreceptors such as hair cells could have the dimensions and sensitivity (e.g. Hudspeth 1983) to monitor the movements of the particle groups accurately.

Final demonstrations that the magnetite particles are organized as we infer can only be achieved by their identification in situ. It will be difficult to locate any such structures with normal transmission electron microscopy, however, as our magnetometry study constrains their volume fraction to be less than 5 parts per billion in the dermethmoid tissue. Each particle chain is likely to be no more than a few micrometers in length and a few hundredths of a micrometer wide. There is only a small probability of locating such a structure in a normal 0.1 micrometer thick TEM section.

It is interesting to note that many studies of other vertebrates have converged on regions of the skull close to the ethmoid bones as the likely site of a vertebrate magnetoreceptor organ (Walcott et al. 1979; Mather and Baker 1981; Zoeger et al. 1981; Baker et al. 1983; Beason and Nicholls 1984; Hanson et al. 1984a, b; Perry et al., in press). As in many of these other studies (e.g. Quinn et al. 1981; Presti and Pettigrew 1980; Baker et al. 1983), we also detected magnetic material that was not always in the same place in all individuals sampled. Some of this material, particularly that associated with tissues such as the gills and gut of the salmon, was clearly contamination that could be removed by thorough cleaning, but other magnetic samples could well have contained true biochemical precipitates. If so, the functions of these deposits remain unknown. A magnetoreceptive role seems unlikely, however, since they usually are not reproducible in all individuals (Walker et al. 1984, this study), often are detected from their natural remanent magnetization (e.g. Zoeger et al. 1981), or are magnetically unsuited to magnetoreception (Presti and Pettigrew 1980; Zoeger et al. 1981; Vilches-Troya et al. 1984).

Our results using adult chinook salmon are at variance with those of Quinn et al. (1981) who failed to find magnetic material anywhere except contaminants within the gastrointestinal tract of sockeye salmon fry. The most likely explanation for this discrepancy is that Quinn et al. (1981) carried out their studies on samples at room temperature (T.P. Quinn, personal communication). We have found in both the chinook salmon and the yellowfin tuna (Walker et al. 1984) that the dermethmoid tissue loses remanence on warming from liquid nitrogen to room temperature. Such loss of remanence is understandable based on the assumption that the magnetite particles must be at least partly free to rotate if they are to be used in magnetoreception (Yorke 1979, 1981; Kirschvink and Gould 1981). Thus magnetite suitable for use in magnetoreception can be detected consistently only by using frozen samples. The presence of IRM or natural remanent magnetization in samples at room temperature suggests the presence of magnetic material serving other functions or arising from external sources.

A second possible explanation is that magnetic material is present in salmon fry in quantities sufficient to mediate the observed responses of fry to magnetic field direction but too small to be detected by currently available superconducting magnetometers. Animals respond either to magnetic field direction (the compass response; Wiltschko 1972; Lindauer and Martin 1972; Walcott and Green 1974) or to some feature related to intensity (the inferred map response; Walcott 1980; Gould 1982). Yorke (1979) and Kirschvink and Gould (1981) found that only a few hundred single-domain crystals would be necessary to determine accurately the direction of the geomagnetic field; the small IRM produced by this number could not be detected with present superconducting magnetometers. In contrast, detection of magnetic field intensity during movements requiring the ability to determine both position and direction, as seems to occur in homing pigeons (Walcott 1980; Gould 1982), requires millions of magnetite-based magnetoreceptors. It is possible that magnetite is present in sockeye salmon fry in quantities sufficient to provide them with the ability to determine magnetic field direction but not sufficient to be detected by a superconducting magnetometer. The movements of adult salmon from the ocean to the outlet of their natal stream could require sensitivity to magnetic field intensity, and so require millions of magnetite particles. We suggest the hypothesis that magnetite is produced continuously throughout the life of the organism and so could be detected more easily in adult than in juvenile fish. A controlled magnetometric study of an ontogenetic series to distinguish among these alternative explanations of the different results for sockeye and chinook salmon is presently in progress.

Thus the presence of magnetite can be correlated with magnetic sensitivity in representatives of three orders of fishes: the European eel and yellowfin tuna, which are known to respond to magnetic fields, and a congener of a third magnetically sensitive fish, the sockeye salmon. The critical tests of the magnetite-based magnetoreception hypothesis, however, will be of behavioral constraints on magnetoreception caused by the properties of the magnetite particles themselves. The behavioral assay developed by Quinn et al. (1981) could be used to test the prediction that accuracy of compass orientation should be poor in very weak fields (<10 μT or 0.1 Gauss), should increase rapidly in fields up to earth-strength, and asymptotically in fields up to a few times earth-strength. This result holds for magnetotactic algae and bacteria (Kalmijn 1981; Lins de Barros et al. 1981) and also for honeybees (Kirschvink 1981). The response of sockeye salmon fry to magnetic field polarity also can be used in a powerful test of ferromagnetic effects on their magnetic orientation. A short magnetic impulse strong enough to reverse the moments of any magnetite particles present will cause the fry to exhibit reversed magnetic field directional preferences in orientation arenas only if the magnetite particles form the basis for their magnetoreceptor system. Thus the opportunity exists to link magnetite suitable for magnetoreception to the behavior of animals that are known to respond to magnetic fields.

Acknowledgments. This work was jointly supported by the National Marine Fisheries Service and through NSF grants PCM82-03627 and BNS83-00301. Contribution No. 3816 from the Division of Geological and Planetary Sciences, California Institute of Technology, Pasadena California 91125. We gratefully acknowledge Ron Dotson (NMFS) and Dave Ptak (Chesapeake Fish Company) for obtaining the samples.

References

Baker RR, Mather JG, Kennaugh JH (1983) Magnetic bones in human sinuses. Nature 301:78–80

Balkwill DL, Maratea D, Blakemore RP (1980) Ultrastructure of a magnetotactic spirillum. J Bacteriol 141:1399–1408

Beason RC, Nicholls JC (1984) Magnetic orientation and magnetically sensitive material in a transequatorial migratory bird. Nature 309:151–153

Brannon EL (1972) Mechanisms controlling migration of sockeye salmon fry. Int Pac Sal Fish Comm Bull 21:1–86

Branover GG, Vasil'yev AS, Gleyzer SI, Tsinober AB (1971) A study of the behavior of the eel in natural and artificial magnetic fields and an analysis of its reception mechanism. J Ichthyol 11:608–614

Butler RF, Banerjee SK (1975) Theoretical single-domain size in magnetite and titanomagnetite. J Geophys Res 80:4049–4058

Cisowski S (1981) Interacting vs non-interacting single-domain behavior in natural and synthetic samples. Phys Earth Planet Interiors 26:56–62

Dunlop DJ, West GF (1969) An experimental evaluation of single-domain theories. Rev Geophys 7:709–757

Furth HP, Waniek RW (1956) Production and use of high transient magnetic fields. Rev Sci Instr 27:195–203

Goree WS, Fuller M (1976) Magnetometers using RF-driven SQUIDS and their applications in rock magnetism and paleomagnetism. Rev Geophys Space Phys 14:591–608

Gould JL (1982) The map sense of pigeons. Nature 296:205–211

Gould JL, Kirschvink JL, Deffeyes KS (1978) Bees have magnetic remanence. Science 201:1026–1028

Hanson M, Karlsson L, Westerberg H (1984a) Magnetic material in European eel, (*Anguilla anguilla* L.). Comp Biochem Physiol 77A:221–224

Hanson M, Wirmark G, Oblad M, Strid L (1984b) Iron-rich particles in European eel (*Anguilla anguilla* L.). Comp Biochem Physiol 79A:311–316

Hudspeth AJ (1983) Mechanoelectrical transduction by hair-cells in the acousticolateralis sensory system. Annu Rev Neurosci 6:187–216

Kalmijn AJ (1981) Biophysics of geomagnetic field detection. IEEE Trans Mag 17:1113–1124

Kirschvink JL (1979) PhD Thesis. Princeton University. Xerox Univ Microfilms Internat, NY

Kirschvink JL (1981) The horizontal magnetic dance of the honeybee is compatible with a single-domain ferromagnetic magnetoreceptor. Biosystems 14:193–203

Kirschvink JL (1983) Biogenic ferrimagnetism: A new biomagnetism. In: Williamson SJ, Romani G-L, Kaufman L, Modena I (eds) Biomagnetism: An interdisciplinary approach. NATO Adv Study Inst Ser, Plenum Publ Corp, New York, pp 501–531

Kirschvink JL, Gould JL (1981) Biogenic magnetite as a basis for magnetic field detection in animals. Biosystems 13:181–201

Kirschvink JL, Walker MM (in press) Particle-size considerations for magnetite-based magnetoreceptors. In: Kirschvink

JL, Jones DS, MacFadden BJ (eds) Magnetite biomineralization and magnetoreception in living organisms: A new biomagnetism. Plenum Publ Corp, New York

Lindauer M, Martin H (1972) Magnetic effect on dancing bees. In: Galler SR. Schmidt-Koenig K, Jacobs GJ, Belleville RE (eds) Animal orientation and navigation. Nat Aeronaut Space Adminstr, Special Publ 262, Washington DC USA

Lins De Barros HGP, Esquivel DMS, Danon J, De Oliveira LPH (1981) Magnetotactic algae. Acad Brasileria Notas de Fisica CBPF-NF-48

Mather JG, Baker RR (1981) Magnetic sense of direction in woodmice for route-based navigation. Nature 291:152–155

McElhinny MW (1973) Paleomagnetism and plate tectonics. Cambridge Univ Press, London New York

Perry A, Bauer GB, Dizon AE (in press) Magnetoreception and biomineralization of magnetite in amphibians and reptiles. In: Kirschvink JL, Jones DS, MacFadden BJ (eds) Magnetite biomineralization and magnetoreception in living organisms: A new biomagnetism. Plenum Publ Corp, New York

Presti D, Pettigrew JD (1980) Ferromagnetic coupling to muscle receptors as a basis for geomagnetic field sensitivity in animals. Nature 285:99–101

Quinn TP (1980) Evidence for celestial and magnetic compass orientation in lake-migrating sockeye salmon fry. J Comp Physiol 137:243–248

Quinn TP, Brannon EL (1982) The use of celestial and magnetic cues by orienting sockeye salmon smolts. J Comp Physiol 147:547–552

Quinn TP, Merrill RT, Brannon EL (1981) Magnetic field detection in sockeye salmon. J Exp Zool 217:137–142

Towe KM, Moench TT (1981) Electron-optical characterization of bacterial magnetite. Earth Planet Sci Letters 52:213–220

Vilches-Troya J, Dunn RF, O'Leary DP (1984) Relationship of the vestibular hair cells to magnetic particles in the otolith of the guitarfish sacculus. J Comp Neurol 226:489–494

Walcott C (1980) Magnetic orientation in homing pigeons. IEEE Trans Magn 16:1008–1013

Walcott C, Green RP (1974) Orientation of homing pigeons altered by a change in the direction of an applied magnetic field. Science 184:180–182

Walcott C, Gould JL, Kirschvink JL (1979) Pigeons have magnets. Science 205:1027–1029

Walker MM (1984) Learned magnetic field discrimination in yellowfin tuna, *Thunnus albacares*. J Comp Physiol A 155:673–679

Walker MM, Kirschvink JL, Chang RS-B, Dizon AE (1984) A candidate magnetoreceptor organ in the yellowfin tuna, *Thunnus albacares*. Science 224:751–753

Walker MM, Perry A, Dizon AE, Kirschvink JL (in press) Detection, extraction, and characterization of biogenic magnetite. In: Kirschvink JL, Jones DS, MacFadden BJ (eds) Magnetite biomineralization and magnetoreception in living organisms: A new biomagnetism. Plenum Publ Corp, New York

Yorke ED (1979) A possible magnetic transducer in birds. J Theor Biol 77:101–105

Yorke ED (1981) Sensitivity of pigeons to small magnetic field variations. J Theor Biol 89:533–537

Zoeger J, Dunn J, Fuller M (1981) Magnetic material in the head of a common Pacific dolphin. Science 213:892–894

8552

What Limits Clupeoid Production?[1]

Reuben Lasker

Southwest Fisheries Center, National Marine Fisheries Service, NOAA, P.O. Box 271, La Jolla, A 92038, USA

Lasker, R. 1985. What limits clupeoid production? Can. J. Fish. Aquat. Sci. 42 (Suppl. 1): 31–38.

This review paper explores a number of hypotheses on the control of clupeoid populations. The following are discussed: the effect of fishing; egg mortality (predation); larval mortality (the critical period) with a consideration of starvation and predation and the biotic and abiotic factors that may be involved; larval transport and the oceanographic features that cause it; variable egg production; interspecific competition; and the effect of localized (e.g. storms and upwellings) and widespread (El Niño) oceanographic events. A review of the paleosedimentary record is also given showing the magnitude of natural fluctuations when no fishing occurred. Recent resurgences in clupeoid populations are reviewed and suggested causes are analyzed.

Le document aborde un certain nombre d'hypothèses concernant le contrôle des populations de clupéidés. Il y est question entre autres des conséquences de la pêche, du taux de mortalité parmi les oeufs (activité des prédateurs), de la mortalité des larves (période critique) de sous-alimentation, des prédateurs, des facteurs biotiques et abiotiques qui peuvent entrer en ligne de compte, du transport des larves et des facteurs océanographiques connexes, des variations au niveau de la production des oeufs, de la lutte entre les espèces, de même que des conséquences de certains faits océanographiques localisés (tempêtes, remontées d'eau, etc) et plus étendus (courant El Niño). L'auteur traite également des facteurs paléo-sédimentaires, illustrant l'amplitude des fluctuations normales en l'absence d'exploitation commerciale. Le document étudie enfin les réapparitions récentes de populations de clupéidés et analyse les causes qui expliqueraient pareils phénomèmes.

Received September 26, 1983
Accepted February 17, 1984
(J7537)

Reçu le 26 septembre 1983
Accepté le 17 fevrier 1984

Research devoted to the subject of recruitment mechanisms has been growing in the last few years. The fluctuations in populations of clupeoids in particular have given impetus to these investigations because of the great economic and food value of these fishes. For example, anchovy and menhaden fish meal are used as a protein source in poultry and cattle feed, and sardines, herring, anchovy, and a variety of other clupeoids are used directly for human food. In all, clupeoids make up about 30% of the 70 million metric ton (t) world fish catch alone. The importance to individual nations is exemplified by the fishery for the Peruvian anchoveta, *Engraulis ringens*, which at its height accounted for over 12 million t/yr or 15% of the world fish catch. The rise and fall of this great fishery and the economic changes that occurred in the fishmeal and soybean markets when fishmeal became scarce and a protein substitute was needed are shown in Fig. 1a. A number of other examples of the rise and fall (Murphy 1977) and sometimes rise again of specific clupeoid fisheries are available, e.g. the sardine fishery in Japan (Kondo 1980), the herring fishery in the North Sea (Hempel 1978), the Peruvian–Chilean sardine (Lasker and MacCall 1983) and anchoveta (Barber et al. 1980), and the Pacific sardine off California (Marr 1960). My paper reviews a number of hypotheses on the control of clupeoid populations.

The Paleosedimentary Record

There is little question today that there are natural fluctuations of great magnitude in fish populations which are attributable to causes other than fishing. The best evidence for naturally occurring increases and declines is from the sedimentary record of anaerobic basins. For example, Soutar and Isaacs (1969) reconstructed the population fluctuations of some of the common fishes occurring off California by identifying and counting fish scales in cores taken from anaerobic sediments of the Santa Barbara Basin. The Pacific sardine, *Sardinops sagax* (also *S. caerulea*), was greatly abundant about 1000 yr ago, much more so than in the recent history of the fishery when peak biomass was estimated to be only about 2 million t. Similarly, the northern anchovy, *Engraulis mordax*, while always abundant, also declined in biomass from 1600 yr ago to the present. Of greater interest, perhaps, is the 19th and 20th century history of anchovy and sardine fluctuations which was presented in a later paper by Soutar and Isaacs (1974). They showed that the modern decline of the Pacific sardine started about 1890, 30 yr before the inception of a fishery off the west coast of the United States. Exceptional year classes could be seen as having occurred in 1855 and 1865, yet these were not sufficient to prevent "a precipitous and natural decline" in the 1870s. In considering the paleosedimentary record, Lasker and MacCall

---

[1] This paper was presented at the International Symposium on the Biological Characteristics of Herring and Their Implication for Management, convened at Nanaimo, B.C., June 20–22, 1983, commemorating the 75th anniversary of the Pacific Biological Station.

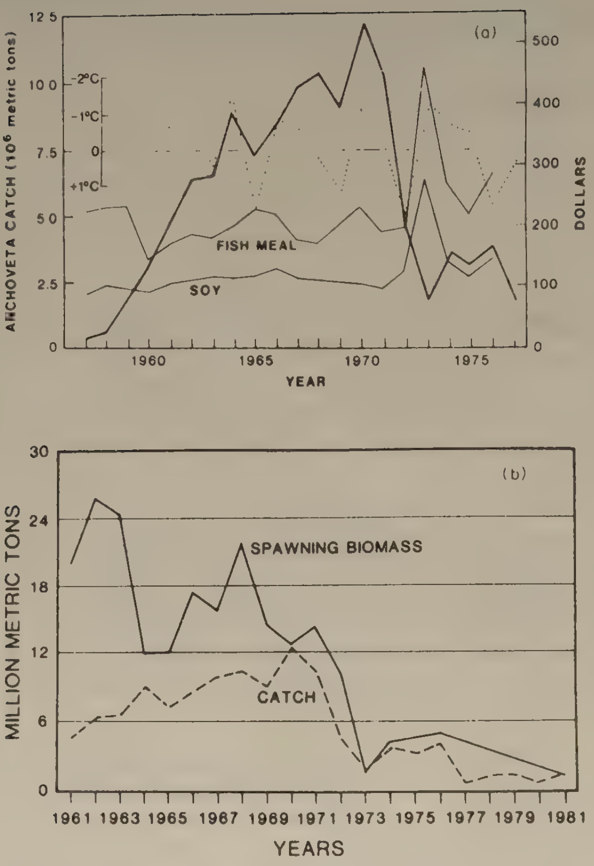

FIG. 1 (a) Peruvian anchoveta catch from 1957 to 1977. The temperature anomaly around a 19-yr mean of 23.8°C is shown with a dotted line. The El Niño of 1972 corresponds with a sharp decrease in catch. This is discussed in the text. Fish meal and soybean prices are plotted to indicate the possible effect of the diminished Peruvian anchoveta catch on the world protein market (after Barber et al. 1980). (b) Peruvian anchoveta catch from 1961 through 1981 compared with the spawning biomass (after Csirke 1980; Tsukayama 1982).

(1983) concluded that the Soutar and Isaacs (1969, 1974) data were probably too insensitive to detect below 500 000 to 1 million t sardine biomasses. The most recent (1983) biomass figures put the Pacific sardine in California waters at less than 20 000 t (Klingbeil 1983). Thus, the decline of the sardine in the 1870s and 1890s was not the same phenomenon as that which occurred off California in the 1940s. The latter was undoubtedly much more drastic and obviously had a component of heavy exploitation which appeared to force the population below its minimum spawning stock size.

Following the recent sardine population decline, there was an increase in the anchovy population off California (Huppert et al. 1980), but the anchovy was also at much higher population levels in the late 19th and early 20th centuries. In comparison, off Peru, DeVries and Pearcy (1982), using the techniques of Soutar and Isaacs, showed that the clupeoid biomass off Peru has also fluctuated greatly; the stocks of anchoveta and sardine were not as abundant in the late Pleistocene (11 000 yr ago) as they have been in recent times.

The Effect of Fishing on Clupeoid Production

For many years there have been two schools of thought on the effect of fishing on clupeoid year class survival and its ultimate effect on the fishery. In their joint paper, Clark and Marr (1955) held diametrically opposing views on the merits of density dependency versus independency, but there were a few points upon which they did agree. First, they believed that there must be some minimum spawning stock size below which year class size is a function of stock size, and second, that the magnitude of additions to a population is not determined by the number of eggs spawned but rather the degree of mortality between the time of spawning and when the juveniles or adult fish enter the fishery.

The history of clupeoid fisheries is long enough now to suggest that man has fished near the critical minimum stock size many times. A clupeoid collapse can be due to heavy fishing mortality, which reduces the mean age of the population and forces the very young fish to sustain the reproductive load of the population. If the environment intervenes in some way to cause excessive mortality of the eggs, larvae, or even small juveniles, then at the most, only two successively poor year classes with continued fishing on the adult stock will reduce the population below the critical minimum stock size. This appears to have happened to the Pacific sardine population in 1949 and 1950 (Murphy 1974) and to the Peruvian anchoveta (Fig. 1b). Thus, part of the solution to the "stock–recruitment problem" is to determine for a species the population level below which it will no longer sustain a future fishery should there be some subsequent poor year classes. More important is the need to discover what environmental conditions cause a year class to succeed or fail.

It might also be argued that there is no definable minimum stock size as judged from the observation that clupeoid recoveries are common, albeit unpredictable. An excellent example is the resurgence of the Japanese sardine, *Sardinops melanosticta*, a small, unfishable population (Kondo 1980). In 1972 this residual population gave rise to a formidable year class which has led 11 yr later, to a 3 million t fishery. This is double the tonnage taken at the previous peak of the fishery in 1936 (Fig. 2). Similar year class successes arising from small to virtually nonexistent populations occur from time to time and are not limited to clupeoids, although some other clupeoid species provide similarly spectacular examples, e.g. the Peruvian–Chilean sardine, *S. sagax*. Therefore, barring the unlikely event of the complete extinction of any clupeoid species, there may always be enough fertilized eggs produced, no matter how small the population, to produce a good year class if conditions are right. Just what the "right conditions" may have to be will be examined below.

Hjort's Hypothesis

Johann Hjort, the famous Norwegian fishery biologist, is remembered best for the idea of the "critical period," which he proposed in his 1913 review of the Norwegian herring and cod fisheries (Hjort 1913). He believed that year classes were most probably established in the early post yolk-sac stage of fish larvae when feeding was just beginning (see May 1974 for a discussion of the critical period concept). Hjort felt that spring-spawned herring larvae could not find enough food at the early post yolk-sac stage, and for the most part the larvae were

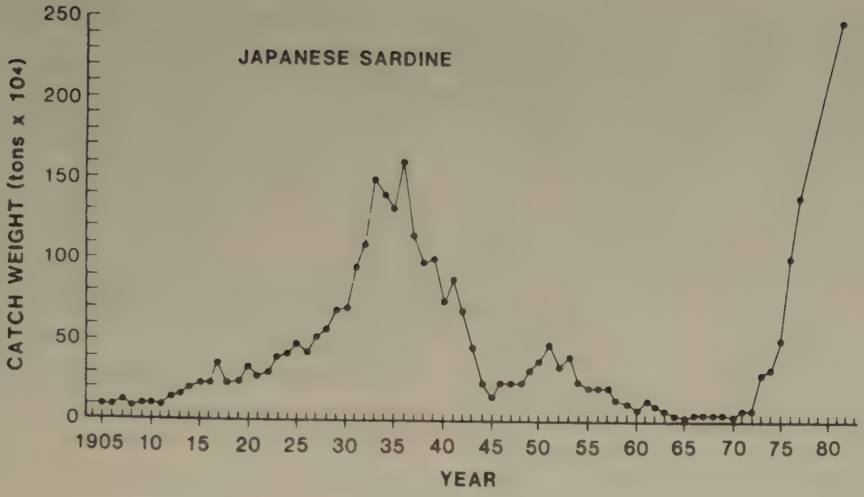

FIG. 2 Catch of the Japanese sardine *Sardinops melanosticta* (after Kondo 1980; Tanaka 1983).

doomed to starve. He reiterated this idea in a provocative paper in 1926 (Hjort 1926). In the latter the suggestion also was made that larval drift could be a mechanism for carrying eggs and larvae out of good food areas.

It has been only in the last three decades that fishery biologists have amassed enough information to begin to tell us whether Hjort was on the right track or not (see review by Blaxter and Hunter 1982). Despite the accumulation of data on the feeding behavior and physiology of the larval herring, sardine, and anchovy, the ultimate experiment, a test of the "critical period" hypothesis, is yet to be done for the herring or any clupeoid. The reason for this is clear: very large data sets on egg production, larval mortality, the larva's environment, and the resulting juvenile survivors are needed over long time periods (probably decades) to obtain the statistical reliability needed with which to test the Hjort critical period hypothesis. However, enough information has accrued in recent years to provide us with the protocol for these studies, and fishery scientists are now in the best position they have ever been to carry them out.

In recent years a number of other ideas have been published on possible year class determinants including interspecific interaction (Lasker and MacCall 1983), cannibalism (MacCall 1980), elaborations of the larval drift idea (Parrish et al. 1981; Nelson et al. 1977), variation in egg survival (Lo 1984), changes in fish fecundity (Picquelle and Hewitt 1983), and the effect of localized oceanographic events (Lasker 1975, 1978) such as stormy periods and upwellings or widespread events such as the unusual warming of the ocean (El Niño) (Valdivia 1978). Some of these depend on the concept of the critical period, i.e. starvation of first-feeding larvae, as the ultimate determinant of the year class, while others emphasize the role of larval survival in density-dependent population regulation.

Food and Feeding of the Clupeoid Larva

There are some generalizations by which the clupeoid larva can be characterized. As hatching it is weak, blind, and depends on endowed yolk to survive. There is evidence that mortality of yolk sac larvae is very great (Picquelle and Hewitt 1983), presumably from predation. At first feeding, a day or so after yolk sac absorption, the larva instinctively snaps at and tries to capture bite-size food particles. However, if it is unsuccessful it will give up trying (Blaxter and Hempel 1963), i.e. there is a "point of no return" behaviorally, and physiologically in a few days if no food (or too little food) is obtained (Blaxter and Hempel 1963; Blaxter and Ehrlich 1974; Lasker et al. 1970; O'Connell and Raymond 1970). What then must the ocean provide to insure larval survival and a good year class? Obviously, nutritious food of the right size must be present in sufficient quantity during the initial feeding of a larva. This is a necessary condition for the larva to pass its first hurdle. Subsequently, predation and transport may increase in importance, but first-feeding larvae clearly face the immediate danger of starvation.

If we accept this premise, recognizing that the quantitative and qualitative details may differ from species to species, a discussion of recent experiments is useful to see if it is possible to derive some predictive principles of recruitment from our knowledge of what a clupeoid larva needs to eat to survive.

The Stability Hypothesis

In a study of anchovy larvae off California (Lasker 1975, 1978, 1981a) I tried to apply laboratory- and field-derived information to the prediction of the relative strength of an anchovy year class. My approach was to determine the threshold number of food particles needed for successful first feeding (Lasker 1975), and then to sample the ocean to find where food concentrations were at, or higher than, the concentrations needed. Off southern California the waters along the coast were usually rich enough to feed anchovy larvae, particularly where there were strong chlorophyll maximum layers. This changed depending on oceanographic conditions, sometimes resulting in the expansion of the geographical area suitable for larval feeding, but at other times limiting successful feeding to the water immediately adjacent to the coast. Occasionally, within the anchovy's spawning season a variety of conditions prevailed such that only a portion of the season could insure a supply of food particles for first-feeding larvae to insure their survival (Lasker 1981a). In another paper (Lasker 1981b) I pointed out that a stable environment is usually needed to allow aggregations of food organisms to form and be maintained, and that it is these dense concentrations that must be exploited by anchovy larvae to survive. These investigations led me to suggest that with a knowledge of threshold numbers of food organisms needed for first feeding, and with information on what effect the environment has on preserving or destroying concentrations of food during the anchovy spawning season, the basic principles for prediction of recruitment are available and could be used to test the critical period hypothesis.

Another point of view has been expressed by Houde (1978) who observed in laboratory experiments with the subtropical bay anchovy, *Anchoa mitchilli*, that there are always survivors and some growth of individuals at extremely low food concentrations, and that food concentrations needed to produce 10% survival are generally available in the fish's normal habitat, Biscayne Bay, Florida. However, at low food concentrations larvae lost weight the first few days of feeding and most died soon after (Houde and Schekter 1981).

Recently, Methot (1983) devised an experiment to test the critical period and stability hypothesis simultaneously. He was able to determine very precisely the birthdates of juvenile anchovies by counting the number of daily rings on their otoliths (Brothers et al. 1976; Methot and Kramer 1979) and estimated seasonal changes in larval survival by comparing the monthly age composition of juveniles with earlier larval production and the changes in the physical environment encountered by the larvae. This was analyzed for the 1978 and 1979 year classes. Because the northern anchovy has a protracted spawning season (December through May), changes in the environment over the time of spawning should be reflected in the birthdates of the surviving juveniles. Methot found that survival of larvae from December 1977 to March 1978 was less than survival of larvae from April to May 1978, yet larval production was greater in the first part of the season (Fig. 3a). In 1979 this was reversed with survival coinciding with the heaviest larval production in the latter part of the season (Fig. 3b). Because of the violent storms that occurred in the winter of 1977–78, I predicted that there should be poor survival in the first half of the spawning season for that year with comparatively better survival as a reflection of calm conditions which prevailed from mid-March 1978 to the end of the spawning season in May.

The violent ocean conditions caused by the early 1978 storms kept the ocean sufficiently mixed and too dilute with respect to larval fish food organisms until March when aggregations of potential food organisms appeared (Lasker 1981b). Methot (1983) pointed out, however, that recruitment of the 1979 year class was poorer than in 1978, especially during the latter portion of the spawning season. This pattern seems better explained to him by indices of offshore transport than by indices of food availability for larvae, but the seasonal pattern of survival in 1978 could not be explained by transport. He suggested that both conditions may account for the differences found.

Mechanisms of Larval Transport

Parrish et al. (1981) investigated the reproductive strategies of the most successful fish stocks off California and how these relate to a variety of oceanographic conditions. They concluded that successful fish in the California coastal region minimize their offshore loss of reproductive products by choosing to spawn in areas and at times when upwelling and offshore transport are at a minimum. Thus, they hypothesized that deviations from "normal" transport conditions could have profound detrimental effects on a year class by carrying eggs and larvae to areas where there is not enough food to survive. A variant of this idea is the report by Shelton and Hutchings (1982) that the eggs and larvae of the South African anchovy, *Engraulis capensis*, are carried from an area of poor productivity to one of high productivity by a surface frontal jet. When transport slackens, high mortality is the rule.

One of the more interesting studies of larval transport was published by Nelson et al. (1977). They presented convincing evidence that good year classes of menhaden, *Brevoortia tyrannus*, depend on environmental conditions that favor the drift of eggs into estuaries of the east coast of the United States where the larvae presumably find good feeding conditions. They produced a multiple regression model relating recruitment to the following environmental variables: (1) Ekman transport rates from three areas where menhaden abound, (2) the minimum mean sea surface temperature at the mouth of Delaware Bay in the year class year, and (3) the sum of monthly average discharge rates from three rivers in July–September of the year preceding the year class year. These authors used a data

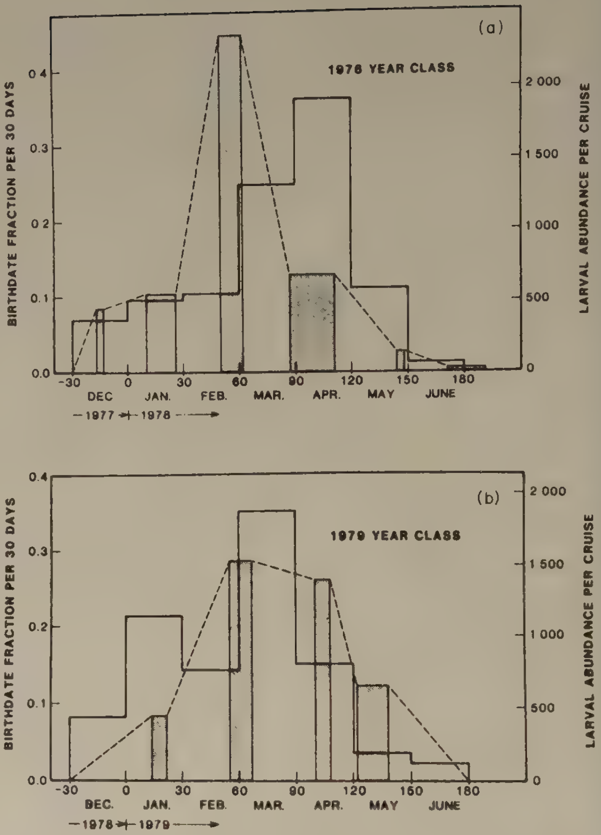

FIG. 3. Comparison of the seasonal distribution of birthdates of juvenile anchovy (open histogram) to the seasonal distribution of larval abundance (stippled bars; the width of these bars indicates individual survey duration). Note that survivorship did not coincide with major larval production in 1978 (a) but did so in 1979 (b). However, total survivorship was better in 1978 than 1979, causing a twofold greater recruitment in the earlier year relative to the latter (after Methot 1983).

set covering the years 1955–70 with remarkable correlations. However, in recent years the model has not been successful in predicting year class success (W. E. Schaaf, pers. comm.).

Another variation of the hypothesis that suggests that larval transport may regulate populations was described by Iles and Sinclair (1982). In this study they presented the interesting idea that the magnitude of herring subpopulations may depend on the size of oceanographically isolated but stable larval retention areas.

In summary, larval transport may be an effective way of sweeping relatively helpless clupeoid larvae into unfavorable areas or conversely of moving them to areas where they can find optimal survival conditions. Either way the basis for survival is the coincidence of larvae with food for them to survive, as suggested in the Hjort hypothesis of the critical period.

Predation or Starvation? Evidence from Mortality Curves

The literature on clupeoids has blossomed with information on their predators and in some cases how much is eaten. The review by Blaxter and Hunter (1982) provides an excellent summary on predation of eggs and larvae by invertebrates and fishes, including a discussion of the incidence of cannibalism. Undoubtedly, predation at all stages of the life of any planktonic organism must rank high among those factors that regulate its population size. The difficulty has been and continues to be the quantification of predation. Population dynamicists have usually resorted to indirect measures considering the fraction of mortality not accounted for by other means as being due to predation. Hunter (1982) in a recent review article concluded from a series of mortality curves obtained for the northern anchovy that the smooth monotonic exponential decrease in numbers of eggs and larvae "lays to rest the Hjort hypothesis of a high larval mortality resulting from starvation beginning at yolk absorption" at least for the Northern anchovy. His thesis is that egg and larval mortality is most probably a density-dependent result of predation, particularly if the predators are invertebrates that appear in blooms (e.g. the jellyfish *Aurelia*, Möller 1982), or due to filter-feeding fishes, as anchovy adults eating their own eggs and larvae (cannibalism, Hunter and Kimbrell 1980). However, mortality rates are too imprecise to afford us a definite conclusion on this point, and I believe it is premature to discard the "critical period" idea. The mortality curve shown in Fig. 4 is typical of those obtained for the northern anchovy. It is derived from the number of eggs and larvae obtained over a 40-d period in the midst of the anchovy spawning season and from an area over thousands of square kilometres. Corrections are made for a variety of factors, such as extrusion of a proportion of the eggs and larvae through the meshes of the plankton net used to collect them, avoidance of the collecting net as the larvae grow older, adjustment for the individual larval growth rates, and the application of two models, one age-independent instantaneous mortality rate for eggs and an age-dependent mortality rate for larvae (Lo 1984). Since the most precise mortality curves show no apparent critical period, it either does not exist as a distinct portion of the mortality curve or it is essentially not provable by current field methods. Blooms of predators, such as jellyfish in Kiel Bight (Möller 1982), should in themselves provide a break in the mortality curve that we would normally ascribe to a critical period, particularly if predators are size-selective in their feeding and the spawning season is a protracted one. However, none has been detected thus far.

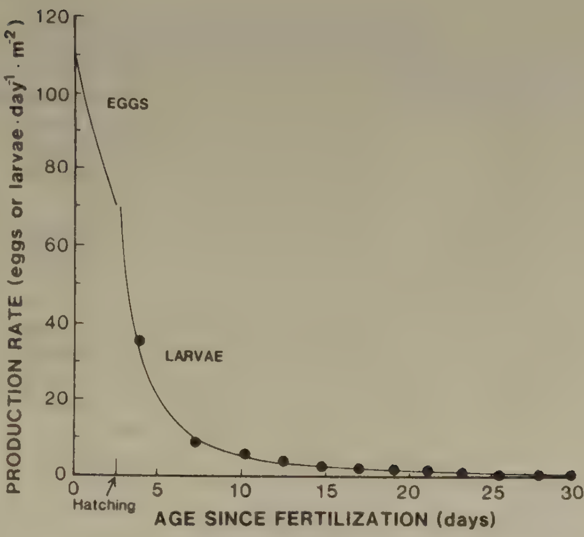

Fig. 4. Mortality curve for eggs and larvae of *Engraulis mordax*, 1983 (after Picquelle and Hewitt 1983). See text for explanation.

Oceanographic Events

It is impossible to consider the fate of pelagic fish without an examination of the effect of the environment on mortality. Parrish et al. (1983) examined a number of environmental processes in relation to anchovy and sardine reproduction in Eastern Boundary currents. They concluded that, in general, upwelling centres seem to be avoided by spawning clupeoids. Yet they also pointed out that the large Peruvian anchoveta population is an exception, since it spawns in an area of strong upwelling. However, upwelling is much stronger off Peru in the summer when spawning is weak as compared with the winter spawning season. In other words the anchoveta lives in an upwelling area known to be extremely rich in forage but minimizes the detrimental effects of upwelling, e.g. offshore transport, by choosing the least oceanographically energetic time to deposit its eggs. These authors showed that spawning tends not to occur in regions where wind conditions would cause turbulent mixing of the upper water column, and this is characteristic of the Peruvian upwelling area. The conclusion from their study is that there has been a strong natural selection acting on clupeoid populations to produce a massive number of eggs over a long spawning season during times and in latitudes where the eggs and larvae are at least risk.

Variable Egg Production and Differential Mortality

Since 1980, scientists at the Southwest Fisheries Center have been perfecting a technique for biomass assessment of the northern anchovy, the egg production method first described by Parker (1980) and now used routinely on an annual basis (Picquelle and Hewitt 1983). Table 1, derived from four years of egg and larva sampling in the California Current, encompassing the entire spawning range of the central population of the northern anchovy, shows the results of differential spawning and mortality of eggs and larvae from year to year. For example, a comparison between 1980 and 1982 shows markedly different egg production between the two years, with 1982 total egg

TABLE 1. Average daily production ($\times 10^{12}$/d) of eggs and larvae by the northern anchovy population off California during the major portion of each spawning season (1980–83) (R. Hewitt, pers. comm.).

Production	1980	1981	1982	1983
Eggs	26.34	20.96	13.51	17.25
Yolk-sac larvae	7.18	14.34	8.53	10.78
10-d-old larvae	0.74	1.59	1.04	0.69
30-d-old larvae	0.10	0.24	0.16	0.07

production being about half that of 1980. Because of very heavy egg mortality in 1980, as compared with 1982, both years had about the same daily production of hatching eggs (yolk-sac larvae). Despite the similar production of yolk-sac larvae an increased rate of larval mortality in 1980 resulted in fewer 30-d-old larvae per day than in 1982. In other words, the number of larvae remaining to metamorphose from any spawn is the result of several mortality rates, each of which may be different from year to year and all are probably the result of both biotic (predation) and abiotic (oceanographic) factors. This is dramatically illustrated in Fig. 5, which shows to what degree the average daily egg production over the entire area of northern anchovy spawning can change from year to year. Lo's (1984) analysis of 30 yr of anchovy egg production off the west coast of the United States and Mexico shows that there have been occasional bumper crops of anchovy eggs but not necessarily concomitant good year classes. For example, 1975 was an enormously successful year for egg producton (Fig. 5) and primary production (Smith and Eppley 1982), but the end result was a disastrous year class (Lasker 1981a), the worst of 16 consecutive year classes analyzed. Lasker (1981a) believes that the root cause of this poor year class could be attributed to the presence of a dominant but nutritionally poor larval food source, the dinoflagellate *Gonyaulax polyedra*, which was above the threshold-for-feeding concentrations during the first half of the spawning season, and to the untimely onset of strong upwelling thereafter, which resulted in high production of inedible diatoms.

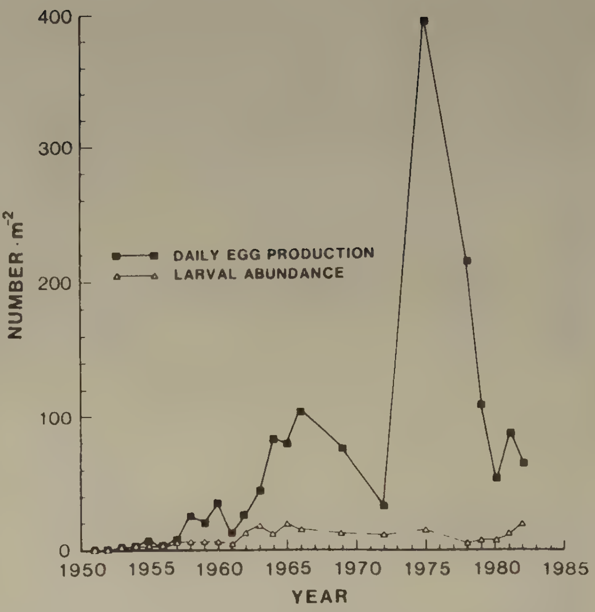

FIG. 5. Daily egg and larval production of *Engraulis mordax* in the California Current over a 30-yr period. The year 1975 was characterized by an enormous spawning but poor larval survival (after Lo 1984).

El Niño Events

The waters off Ecuador, Peru, and Chile historically have had exceptionally large clupeoid fisheries. Upwelling of nutrient-rich water has been the trophic underpinning of these fisheries by supporting an extremely rich phytoplankton fauna fed upon directly by filter-feeding anchoveta and sardines. From time to time, invasions of unusually warm nutrient-depleted water occur, an El Niño, which have, on some occasions, coincided with the collapse of the coastal clupeoid stocks off these nations (Fig. 1a). As Valdivia (1978) pointed out, there is a behavioral modification of anchovy movement and subsequent distribution during an El Niño. Off Peru, the anchoveta drastically reduced the area it occupied during the 1972 El Niño, so that in March, April, and May 1972, large concentrations of fish schooled close to the coast and became unusually available to the coastal fishery. Anomalous spawning of the anchoveta also occurred from September 1971 through May 1972, with a markedly reduced production of eggs. The combination of extremely heavy fishing, which undoubtedly pushed the anchoveta population below its minimum stock size, and the obvious failure of one or more of the following year classes caused the collapse of the fishery with its attendant disastrous economic consequences (Murphy 1974).

While there has been a gradual but persistent return of the sardine to Peruvian and Chilean waters in recent years, there have also been several El Niño events. The severe El Niño of 1983, which began in September–October 1982, was characterized by disruption of anchoveta and sardine schools. In some instances, sardines accumulated "in some small areas" according to Jordan (1983), which made it appear that sardines were abundant, but these were rapidly fished out.

Whether El Niño events affect the survival of fish eggs and larvae is currently undocumented and remains to be investigated. In California the El Niño of 1983 was manifested by a much wider distribution of spawning anchovies than occurred in previous years contrary to the contraction found in Peru. Per capita egg production seemed to be relatively unaffected in California. The amount and extent of surface warming with which the fish had to contend was much different between Peru and California, the habitat in Peru always exhibiting a greater temperature differential and more drastic effects on the behavior of the fish (Fig. 1a).

Competition

Do coexisting species of pelagic fish that inhabit thousands of square miles of ocean compete for food resources and space? This intriguing question has never been answered satisfactorily. Lasker and MacCall (1983) investigated this question indirectly by inferring the relative mean sardine and anchovy size from frequency distributions of sardine and anchovy scales found in anaerobic sediments. The average anchovy size from periods of high sardine abundance was found to be significantly smaller than in periods when sardine populations were low. The authors pointed out that this result is consistent with a competition hypothesis but that there are other possible explanations, e.g.

offshore distribution of small anchovies. An occasional response of an ecosystem when sardines are low in abundance (e.g. off California) is an increase in the population of anchovies, and alternatively, some ecosystems where anchovies are reduced (e.g. Peru–Chile), sardines have increased in number remarkably. Whether competition on a large geographic scale is the causal mechanism has yet to be decided.

Conclusion

The answer to the question, "what limits clupeoids?," seems to be "almost everything." More realistically, the question should be phrased "what limits clupeoids mostly?" Other questions follow this one: When, in the life cycle, does this occur? What are the interrelationships between limiting factors and between species? What can be learned from species life histories and fishery oceanography that will allow us to predict recruitment?

A review of the literature shows that we are on the threshold of significant investigations that may provide the answers to these questions. Studies, such as those conducted by Methot (1983), seem to be the most promising for isolating the factors affecting the recruitment of a year class. The Methot experiment allows us to look back at the environment to see which factors were present or absent when there was good or poor survival within a spawning season when a year class was produced. With a time series of such studies on the same species it seems likely that the factors that are responsible for formation of a year class can eventually be identified.

In the international sphere this approach has been suggested for IREP, the International Recruitment Program, by Working Group 67 of SCOR (Scientific Committee on Ocean Research), intending that several nations work simultaneously on the same fish species group so that data bases could be amassed and compared throughout the world. The essential data can be collected through the use of the newest technological tools available in fisheries research, which include determination of birthdates, growth rates, and ages of fish larvae and recruits using counts of daily rings of the otoliths, the egg producton method to obtain total population fecundity, sampling of the biotic environment by sophisticated nets, pumps, and high frequency sonar, and the monitoring of oceanic parameters with the variety of ocean measuring devices perfected by physical oceanographers in recent years.

References

Barber, R. T., W. W. Kirby Smith, and P. E Parsley. 1980 Wetland alteration for agriculture, p. 632–651. *In* P. E. Greeson, J. R. Clark, and J. E. Clark [ed.] Wetland functions and values. American Water Research Association, Minneapolis, MN.

Blaxter, J. H. S., and K. F. Ehrlich. 1974. Changes in behaviour during starvation of herring and plaice larvae, p. 575–588. *In* J. H. S. Blaxter [ed.] The early life history of fish. Springer Verlag, Berlin.

Blaxter, J. H. S., and G. Hempel. 1963. The influence of egg size on herring larvae (*Clupea harengus* L.). J. Cons. Cons. Int. Explor. Mer 38: 211–240

Blaxter, J. H. S., and J. R. Hunter. 1982. The biology of the clupeoid fishes. Adv. Mar. Biol. 20: 1–223.

Brothers, E. B., C. P. Mathews, and R. Lasker. 1976. Daily growth increments in otoliths from larval and adult fish. U.S. Natl Mar. Fish. Serv. Fish. Bull. 74: 1–8

Clark, F. N., and J. C. Marr. 1955. Population dynamics of the Pacific sardine, p. 11–48. Prog. Rep. Calif. Coop. Oceanic Fish. Invest., 1 July 1953 to 31 March 1955.

Csirke, J. 1980. Recruitment in the Peruvian anchovy and its dependence on the adult population. Rapp. P.-V. Reun. Cons. Int. Explor. Mer 177: 307–313.

DeVries, T. J., and W. G. Pearcy. 1982. Fish debris in sediments of the upwelling zone off central Peru: a late Quaternary record. Deep-Sea Res. 28(1A): 87–109.

Hempel, G 1978. North sea fisheries and fish stocks — A review of recent changes. Rapp P.-V. Reun. Cons. Int. Explor. Mer 173: 145–167.

Hjort, J. 1913. Fluctuations in the great fisheries of northern Europe. Rapp. P.-V. Reun. Cons. Perm. Int. Explor. Mer 19: 1–228.

1926. Fluctuations in the year classes of important food fishes. J. Cons. Cons. Int. Explor. Mer 1: 5–38.

Houde, E. D. 1978. Critical food concentrations for larvae of three species of subtropical marine fishes. Bull. Mar. Sci. 28(3): 395–411.

Houde, E. D., and R. C. Schekter. 1981. Growth rates, rations and cohort consumption of marine fish larvae in relation to prey concentratons. Rapp. P.-V. Reun. Cons. Int. Explor. Mer 178: 441–453.

Hunter, J. R. 1982. Predation and recruitment, p. 172–209. *In* Rothschild and Rooth [ed.] Fish ecology. III. A foundation for — REX. A recruitment experiment. Univ. Miami Tech. Rep. No. 82008.

Hunter, J. R., and C. A. Kimbrell. 1980. Egg cannibalism in the northern anchovy, *Engraulis mordax*. U.S. Natl. Mar. Fish. Serv. Fish. Bull. 78: 811–816.

Huppert, D. D., A. D. MacCall, G. D. Stauffer, K. R. Parker, J. A. McMillan, and H. W. Frey. 1980. California's northern anchovy fishery: biological and economic basis for fishery management. U.S. Dep Commer. NOAA Tech. Memo. NOAA-TM-NMFS-SWFC-1: 121 p. + 113 p. appendix.

Iles, T. D., and M. Sinclair. 1982. Atlantic herring: stock discreteness and abundance. Science (Wash., DC) 215: 627–633.

Jordan, R. 1983. Preliminary report of the 1982–83 Niño effects in Ecuador and Peru. Trop. Ocean–Atmos. Newslett. No. 19: 8–9

Klingbeil, R. A. 1983. Status of the spawning biomass of the Pacific sardine, 1982–83. Calif. Dep. Fish Game Mar. Resour. Admin. Rep. 83–1: 5 p.

Kondo, K. 1980. The recovery of the Japanese sardine — the biological basis of stock size fluctuations. Rapp. P.-V. Reun. Cons. Int. Explor. Mer 177: 332–345.

Lasker, R. 1975. Field criteria for survival of anchovy larvae: the relation between inshore chlorophyll maximum layers and successful first feeding U.S. Natl. Mar. Fish. Serv. Fish. Bull. 73: 453–462.

1978. The relation between oceanographic conditions and larval anchovy food in the California current: identification of factors contributing to recruitment failure. Rapp. P.-V. Reun. Cons. Int. Explor. Mer 173: 212–230.

1981a. Factors contributing to variable recruitment of the northern anchovy (*Engraulis mordax*) in the California Current: contrasting years, 1975 through 1978. Rapp. P.-V. Reun. Cons. Int. Explor. Mer 178. 375–388.

1981b. The role of a stable ocean in larval fish survival and subsequent recruitment. *In* R. Lasker [ed.] Marine fish larvae: morphology, ecology, and relation to fisheries. University of Washington Press, Seattle, WA

Lasker, R., H. M. Feder, G. H. Theilacker, and R. C. May 19 Feeding, growth and survival of *Engraulis mordax* larvae reared in the laboratory. Mar. Biol. (Berl.) 5: 345–353.

Lasker, R., and A. MacCall. 1983. New ideas on the fluctuations of clupeoid stocks off California, p. 110–120. Proc Joint Oceanogr Assembly 1982 — General Symposia, Can. Nat Comm S Comm. Ocean. Res., Ottawa, Ont.

Lo, N. C. H. 1984. Egg production of the central stock of northern anchovy Fish. Bull. (U.S.) 82. (In press)

MacCall, A. D. 1980. The consequences of cannibalism in the stock ment relationship of planktivorous pelagic fishes such as *Engrau* 201–220. *In* G. Sharp [ed.] Workshop on the effects of environmen variation on the survival of larval pelagic fishes. UNESCO. Intergove mental Oceanographic Commission. Workshop Report 28

Marr, J. C. 1960. The causes of major variations in the catch of the sardine. Proc. World Sci. Meeting Biology of Sardines an Species 3: 667–791

May, R. C. 1974 Larval mortality in marine fishes and the critica concept, p. 3–19. *In* J. H. S. Blaxter [ed.] The early life history of fis Springer-Verlag, Berlin

Methot, R. D. 1983. Seasonal variation in survival of larval *Engraul* estimated from the age distribution of juveniles. U.S. Natl Mar Fis Serv. Fish. Bull. 81

Methot, R. D., and D. Kramer. 1979. Growth of *Engraulis mordax*, larvae in the sea. U.S. Natl. Ma Bull. 77: 413–423.

Möller, H. 1982. Effect of jellyfish predation on larval herring in Kiel Bight. Int. Coun. Explor. Sea, Baltic Fish Comm. Rep. C.M. 1982/J:11: 8 p.

Murphy, G. T. [Chairman]. 1974. Report of the fourth session of the panel of experts on stock assessment on Peruvian anchoveta. Bol. Inst. Mar Peru (Callao) 2: 605–719.

Murphy, G. I. 1977. Clupeoids, p. 283–308. *In* J.A. Gulland [ed.] Fish population dynamics. John Wiley, London.

Nelson, W. R., M. C. Ingham, and W. E. Schaaf. 1977. Larval transport and year-class strength of Atlantic menhaden, *Brevoortia tyrannus*, U.S. Natl. Mar. Serv. Fish. Bull. 75: 23–41.

O'Connell, C. P., and L. R. Raymond. 1970. The effect of food density on survival and growth of early post yolk-sac larvae of the northern anchovy *Engraulis mordax* Girard in the laboratory. J. Exp. Mar. Biol. Ecol. 5: 187–197.

Parker, K. 1980. A direct method for estimating northern anchovy, *Engraulis mordax*, spawning biomass. U.S. Natl. Mar. Fish. Serv. Fish. Bull. 78: 541–544.

Parrish, R. H., A. Bakun, D. M. Husby, and C. S. Nelson. 1983. Comparative climatology of selected environmental processes in relation to eastern boundary current pelagic fish reproduction. *In* G. D. Sharp and J. Csirke [ed.] Proceedings of the expert consultation to examine changes in abundance in species composition of neritic fish resources. FAO Fish. Rep. No. 291, Vol. 3: 731–778. Rome.

Parrish, R. H., C. S. Nelson, and A. Bakun. 1981. Transport mechanisms and reproductive success of fishes in the California Current. Biol. Oceanogr. 1: 175–203.

Picquelle, S. J., and R. P. Hewitt. 1983.The northern anchovy spawning biomass for the 1982–83 California fishing season. Calif. Coop. Oceanic Fish. Invest. Rep. 24: 16–28.

Shelton, P. S., and L. Hutchings. 1982. Transport of anchovy, *Engraulis capensis* Gilchrist, eggs and early larvae by a frontal jet current. J. Cons. Cons. Int. Explor. Mer 40: 185–198.

Smith, P. E., and R. W. Eppley. 1982. Primary production and the anchovy population in the Southern California Bight. Limnol. Oceanogr. 27: 1–17.

Soutar, A., and J. D. Isaacs. 1969. History of fish populations inferred from fish scales in anaerobic sediments off California. Calif. Coop. Oceanic Fish. Invest. Rep. 13: 63–70.

1974. Abundance of pelagic fish during the 19th and 20th centuries as recorded in anaerobic sediment off the Californias. U.S. Natl. Mar. Fish. Serv. Fish. Bull. 72: 257–273.

Tanaka, S. 1983. Variation of pelagic fish stocks in waters around Japan. *In* G. D. Sharp and J. Csirke [ed.] Proceedings of the expert consultation to examine changes in abundance in species composition of neritic fish resources. FAO Fish. Rep. No. 291, Vol. 2: 17–36. Rome.

Tsukayama, I. 1982. Recursos pelagicos y sus pesquerias en Peru. Seminario Regional sobre Recursos Pelagicos y sus Pesquerias en el Pacifico Sudeste, Guayaquil, Ecuador, 25-26 Oct. 1982.

Valdivia, J. E. 1978. The anchoveta and El Niño. Rapp. P.-V. Reun. Cons. Int. Explor. Mer 173: 196–202.

8553

Application of Satellite Remote Sensing to U.S. Fisheries

R.M. Laurs

National Marine Fisheries Service, Southwest Fisheries Center, La Jolla, CA 92038, USA

ABSTRACT

Satellite oceanic remote sensing is beginning to play important roles in fishery research and fish harvesting. Spaceborne sensors are being used to make synoptic oceanic measurements for use in determining variations in ocean conditions which play key roles in causing fluctuations in stocks of fishes and in their vulnerability to harvesting.

INTRODUCTION

The use of satellite remote sensing to provide synoptic measurements of the ocean is becoming increasingly important in fisheries applications. Variations in ocean conditions play key roles in natural fluctuations of fish stocks and in their vulnerability to harvesting. Information on the changing ocean, rather than on average ocean conditions, is necessary to understand and to eventually predict the effects of the marine environment on fish populations. The evolving capabilities of satellite sensor and data-processing technology, combined with conventional data collection techniques, provide a powerful tool toward ensuring the wise-use of living marine resources.

Laurs and Brucks (1985) review fisheries applications of satellite oceanic remote sensing in the U. S. Examples of recent and potential uses of satellite imagery in U. S. fisheries in the eastern North Pacific are given in Fiedler et al. (1985). Yamanaka (1982) describes the utilization of satellite imagery in Japanese fisheries. Gower (1982) gives an overview of the different kinds of remote sensing data relevant to fisheries science and oceanography, and Montgomery (1981) discusses the utility of satellite imagery to ocean industries, including fisheries.

SATELLITE DATA USED IN FISHERIES

Satellite remote sensing applications in U. S. fisheries have concentrated on the measurements of ocean temperature and color, and computation of ocean transport based on satellite measured wind stress.

Ocean Temperature

Virtually all fisheries studies employing satellite ocean temperature measurements have utilized imagery from thermal infrared sensors. The advanced infrared sensors, notably the Advanced Very High Resolution

Radiometer (AVHRR) aboard the TIROS orbiting meteorological satellites, are characterized by high sensitivity in narrow wave lengths, fine ground resolution and an extensive data archival (Fiedler et al. 1985). These sensors yield high quality data which, except for some limitations, meet the requirements for most fishery investigations.

There have been a very limited number of attempts to apply ocean temperature measurements made from microwave instruments aboard satellites to fisheries studies. These attempts have been only marginally successful, mostly because of the large footprint of the measurements and the contamination of the data in the vicinity of land. However, an adequate evaluation of the utility of satellite microwave ocean temperature measurements in fisheries problems has yet to be conducted. Efforts to do so have been hampered because of difficulties in obtaining microwave temperature data and lack of high speed data processing capabilities to process it.

Ocean Color

The Coastal Zone Color Scanner (CZCS) on board the NIMBUS-7 satellite, launched in October 1978, is the only sensor in orbit that is specifically designed to study living marine resources (Hovis et al. 1980). The CZCS is capable of measuring very subtle variations in water color resulting primarily from variations in phytoplankton concentrations. Ocean color measurements from the CZCS are being used in fishery resource applications (a) to determine the locations of oceanic fronts, effluents, and water masses, (b) to determine circulation patterns, and (c) to make quantitative measurements of chlorophyll and sestonic concentrations.

Ocean Winds

The scatterometer (SASS) aboard the SEASAT-A satellite provided data which demonstrate the importance to fisheries of high resolution surface wind stress measurements made from space. Winds stress measurements made by satellite can be used to calculate ocean surface layer transport which controls the distribution of larval stages and the subsequent recruitment and harvests of many marine fishes and shrimps (Brucks et al. 1984). Satellite measurements of winds are also important in the detection of wind conditions that affect the safety and performance of fishing vessels at sea (Hawkins and Black 1983). While the data record of satellite measured winds is very limited due to the unfortunate, premature failure of SEASAT, extensive global coverage of oceanic surface winds will be made by satellite systems planned for launch in the late 1980's (Li et al. 1984)

USE OF SATELLITE MEASUREMENTS IN FISHERIES RESEARCH

Variations in environmental conditions affect the recruitment, distribution, abundance, and availability of fishery resources. It is not possible to measure remotely from satellites the entire spectrum of information needed to assess changes in the marine environment. However, knowledge of important oceanographic conditions and processes affecting fish populations may often be deduced using ocean measurements made by satellite e.g., distribution of surface isotherms, locations of oceanic frontal boundaries, information on currents and circulation patterns, regions of upwelling, etc.

Ocean measurements made by satellite remote sensing can be extremely useful in defining the distribution of marine fish habitats. Lasker et al.

(1981) and Fiedler (1983) have demonstrated that the northern boundary of northern anchovy spawning habitat in the Southern California Bight may be delimited using AVHRR imagery from NOAA polar orbiting satellites (Figure 1). In general, the northern extent of spawning in the Bight and the offshore extent of spawning north of Santa Catalina Island are limited by cold, upwelled waters advected south of Point Conception. The cold waters are readily evident in satellite infrared imagery of the region. The southern limit of spawning may be defined using ocean color measurements made by the CZCS aboard the NIMBUS-7 satellite showing low chlorophyll concentrations (Fiedler 1983).

The distribution and availability of albacore tuna off the west coast of the U. S. have been found to be related to oceanic fronts seen in AVHRR infrared and CZCS imagery (Laurs et al. 1984) (Figure 2). Commercially fishable aggregations of albacore are found in warm, blue oceanic waters near temperature and color fronts on the seaward edge of coastal water masses. These oceanic boundary features, which are believed to result primarily from coastal upwelling, are clearly observable in satellite imagery collected along the U. S. Pacific coast. The distribution of albacore during winter time in regions hundreds of miles off the coast has also been related to sea surface temperature fronts, believed to mark the outer boundary of the California Current, observed in AVHRR imagery (Laurs et al. 1981).

Satellite infrared measurements have also been used to trace the development and duration of the various bluefin tuna fisheries along the east coast of the U. S. (Roeffer et al. 1982). These fisheries follow the movement of seasonal warming of near-surface waters which are monitored by observing the northerly progression of the 19-20°C isotherms in satellite infrared imagery. Limited success has been achieved during winter months in relating the distribution of tuna longline fishing in the Gulf of Mexico with the position of the Loop Current deduced from temperature frontal patterns observed in Geostationary Orbiting Earth Satellite (GOES) infrared imagery (Leming, Internal Report, NMFS). In summer months after seasonal warming has occurred, it is not possible to resolve temperature frontal structure in the GOES infrared imagery of the Gulf of Mexico.

Satellite remote sensing has been an especially important tool during the recent El Niño for monitoring anomalous ocean conditions along the U. S. Pacific coast (Fiedler 1984a). The satellite imagery contains invaluable information for use in assessing the effects of the El Niño conditions on U. S. west coast fisheries. Virtually all of the fisheries were affected in varying degrees with some fisheries showing benefits from the El Niño, and others being harmed substantially. Many fish populations experienced changes in their distribution and centers of abundances. For example, there were shifts in the usual distribution of anchovy spawning which Fiedler (1984b) found could be delineated using AVHRR infrared imagery.

USE OF SATELLITE MEASUREMENTS IN FISHERIES-AID PRODUCTS FOR FISHERMEN

Several projects and programs have used or are using satellite derived ocean data in fisheries-aid products which are distributed to U. S. fishermen by a variety of mechanisms, including radio facsimile transmission, voice broadcast, U. S. mail, and telephone telecopier. A prime motivation leading to the expanded use of satellite observations in fisheries-aid products was provided by the SEASAT Commercial Demonstration Program sponsored by the National Aeronautics and Space Administration/Jet

Propulsion Laboratory. This program led to the development of an operational Satellite Data Distribution System used to distribute oceanographic products to ocean users (Montgomery 1981).

Charts showing the locations of oceanic thermal boundaries are derived from AVHRR infrared imagery from polar orbiting satellites and are provided to commercial and recreational fishermen for use in locating potentially productive fishing grounds along the Pacific coast from central Baja California to British Columbia, Canada (Breaker 1981) (Figure 3). Fishermen use these charts to save time in searching for productive fishing areas associated with oceanic frontal features (Short 1979 and Breaker 1981). High resolution infrared images from the GOES satellite and ship reports are used in the preparation of charts for waters off the Atlantic Coast, which are distributed to fishermen and other interested users (Chamberlain 1981). Of particular interest to fishermen these charts show (a) the outer limit of the shelf water mass, in which many fishery resource species reside, and (b) the numbers, sizes and persistence of warmcore Gulf Stream rings, which can markedly alter conditions on the fishing grounds. These charts have been particularly useful to lobster fishermen in reducing loss of fishing pots due to strong currents of the Gulf Stream warmcore eddies. Charts based on GOES infrared imagery are also prepared to show the path of the Loop Current in the Gulf of Mexico and are used mostly by recreational fishermen (Lowry and Leaky 1982).

Experimental ocean color boundary charts based on CZCS imagery are distributed to U. S. west coast fishermen (Montgomery 1981). These charts show four categories of ocean color---green coastal, transition green, transition blue and deep ocean blue (Figure 4). They are produced at almost weekly intervals depending on cloud conditions, and cover coastal areas up to 700,000 km^2 between Guadalupe Island and Vancouver Island. NIMBUS-7 CZCS passes along the Pacific coast are collected and processed in near-real time, and transmitted by radio facsimile the following day to fishing boats at sea. Color photographs of the satellite images are also distributed by express mail to various fishing ports and to Sea Grant marine advisors in daily contact with fishermen. The color boundary charts and photographs are used primarily by commercial albacore and salmon fishermen, and recreational fishermen in southern California.

Sea ice forecast charts derived from NIMBUS-7 Scanning Multichannel Microwave Radiometer (SMMR) and AVHRR infrared imagery are prepared for regions of Alaska and transmitted by radio facsimile to fishermen and other marine users.

References

1. Breaker, L.C.: The application of satellite remote sensing to west coast fisheries. J. Mar. Tech. Soc. 15 (1981) 32-40.

2. Brucks, J.T.; Leming, T.D.; Buokett, S.B.Jr.: A model investigation using high resolution SASS wind stress measurements to derive wind surface layer transport properties in the Gulf of Mexico. NOAA Tech. Rpt. (1984) In press.

3. Chamberlain, J.L.: Application of satellite infrared data to analysis of ocean frontal movements and water mass interactions off the northeast coast. N.W. Atlantic Fish. Organ. Doc. 8/1/123, Ser. No. 429 (1981) 15 p.

4. Fiedler, P.C.: Satellite remote sensing of the habitat of spawning anchovy in the Southern California Bight. CALCOFI Rep. 24 (1983) 202-CALCOFI Rep. 25 (1983) 53-58.

5. Fiedler, P.C.: Some effects of El Niño 1983 on the northern anchovy. CalCOFI Rep. 25 (1984a) 53-58.

6. Fiedler, P.C.: Satellite observations of El Niño along theU.S. Pacific Coast. Science 224 (1984b) 1251-1254.

7. Fiedler, P.C.; Smith, G.B.; and Laurs, R.M.: Fisheries applications of satellite data in the eastern North Pacific. Mar. Fish. Rev. 46 (1985) 1-13.

8. Gower, J.F.R.: General overview of the nature and use of satellite remote sensing data for fisheries application. NAFO Sci. Counc. Studies 4 (1982) 7-19.

9. Hawkins, J.D.; Black, P.G.: SEASAT scatterometer detection of gale force winds near tropical storms. J. Geophys. Res. 88 (1983) 1674-1682.

10. Hovis, W.A.; Clark, D.K.; Anderson, F.; Austin, R.W.; Wilson, W.H.; Baker, E.T.; Ball. D.; Gordon, H.R.; Mueller, J.L.; El-Sayed, S.Z.; Sturn, B.; Wrigley, R.C.; Yentsch, C.S.: NIMBUS-7 Coastal Zone Color Scanner: System description and initial imagery. Science 210 (1980) 60-63.

11. Lasker, R.; Pelaez, J.; Laurs, R.M.: The use of satellite infrared imagery for describing ocean processes in relation to spawning of the northern anchovy (Engraulis mordax). Remote Sensing Environ. 11 (1981) 439-453.

12. Laurs, R.M.; Brucks, J.T.: Living Marine Resource Applications. Advances in Geophysics 27 (1985) In press.

13. Laurs, R.M.; Lynn, R.J.; Nishimoto, R.; Dotson, R.: Albacore trolling and longline exploration in eastern North Pacific waters during mid-winter 1981. NOAA-TM-NMFS-SWFC 10 (1981) 40 p. plus appen. 52p.

14. Laurs, R.M.; Fiedler, P.C.; Montgomery, D.R.: Albacore tuna catch distributions relative to environmental features observed from satellites. Deep-Sea Res. 31 (1984) 1085-1099.

15. Leming. T.D.: Ocean pelagics remote sensing applications. Interim Rpt. NMFS Internal Document (1981).

16. Li, R.; Winn, C.; Long, D.; Geuy, C.: NROSS scatterometer - an instrument for global oceanic wind observations. Proc. SPIE 481 Recent Advances in Civil Space Remote Sensing (1984) 193-197.

17. Lowry, B.; Leaky, I.: Cooperation produces a flow of Gulf Stream information. Sea Grant Today 12 (1982) 3-5.

18. Montgomery, D.R.: Commercial applications of satellite oceanography. Oceanus 24 (1981) 56-65.

19. Roeffer, M.; Carl, M.; Williams, F.: Atlantic bluefin tuna-oceanography remote sensing. Proc. 32nd Annual Tuna Conf. IATTC, La Jolla, CA (1982)

20. Short, K.: How satellites can help you catch more fish and cut costs. Nat. Fisherman 60 (1979) 38-39.

21. Yamanaka, I.: Application of satellite remote sensing to fishery studies in Japan. NAFO Sci. Counc. Studies 4 (1982) 41-50.

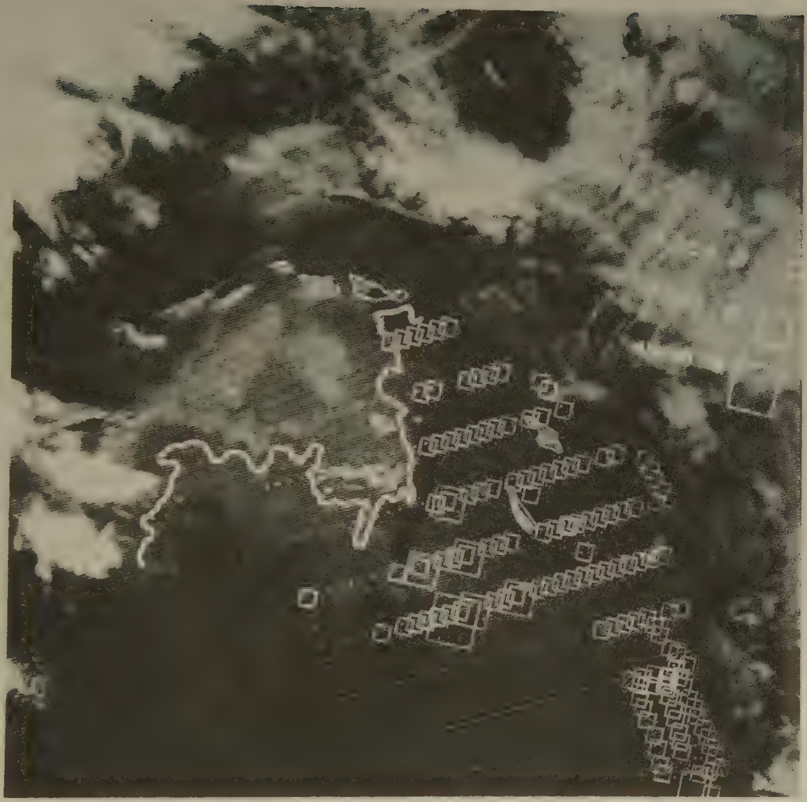

Figure 1. Distribution of anchovy eggs superimposed on the thermal image of the Southern California Bight taken 6 April, 1980. The 14°C isotherm plotted from satellite gray-scale calibration has been drawn in. Feathery white objects are clouds. Squares indicate number of anchovy eggs under one square meter of sea surface (from Lasker et al., 1981).

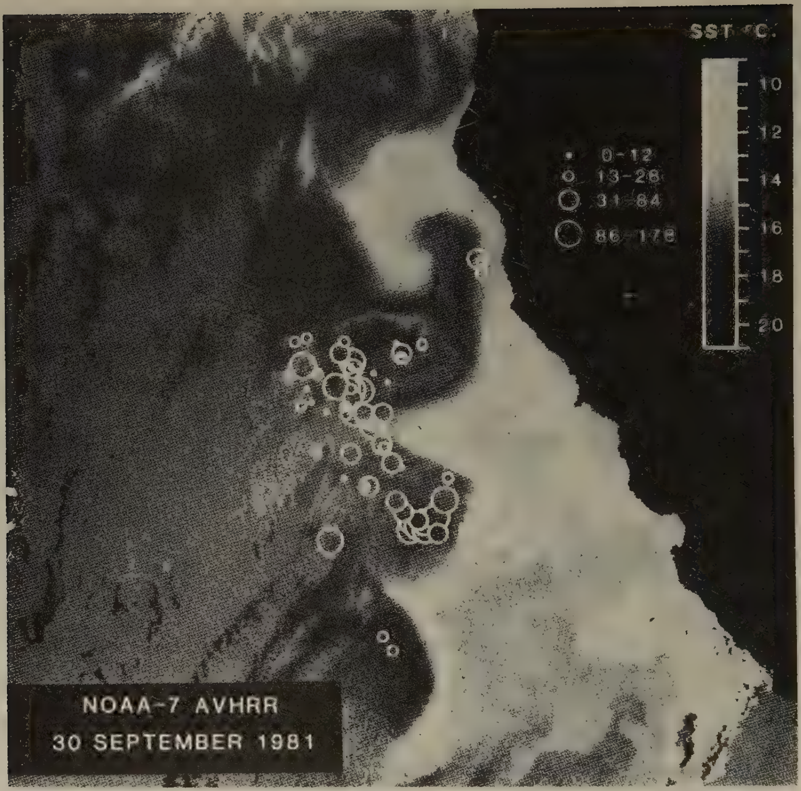
SST °C
10
12
14
16
18
20
0-12
13-28
31-84
86-178
NOAA-7 AVHRR
30 SEPTEMBER 1981

Figure 2. Central California daily albacore catches, Sept. 27-Oct. 2, 1981 and NOAA-7 AVHRR sea surface temperatures, Sept. 30, 1981 (from Laurs et al., 1984).

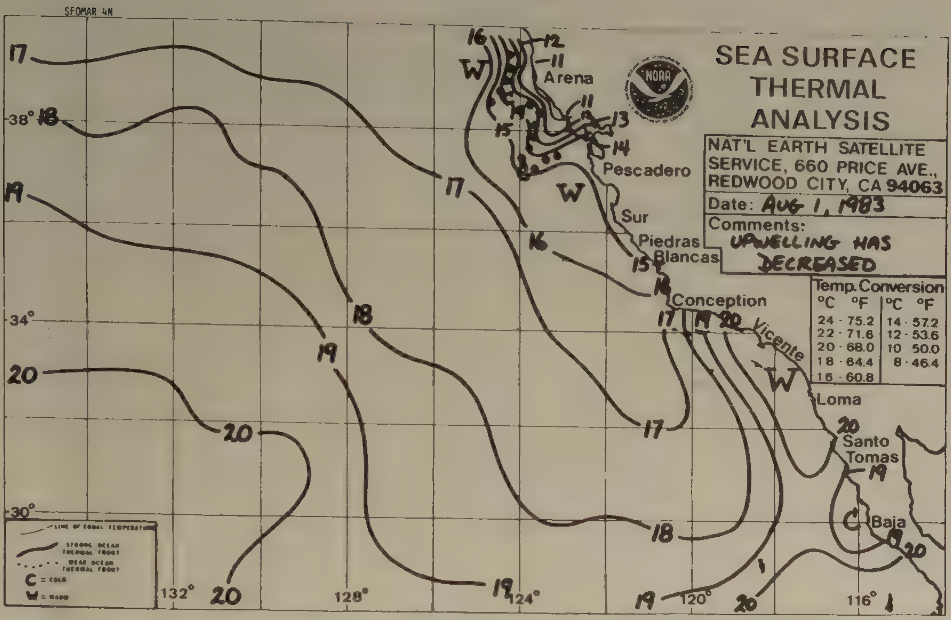
SFOMAR 4N
SEA SURFACE THERMAL ANALYSIS
NAT'L EARTH SATELLITE SERVICE, 660 PRICE AVE., REDWOOD CITY, CA 94063
Date: AUG 1, 1983
Comments: UPWELLING HAS DECREASED
Temp. Conversion
°C °F °C °F
24 - 75.2 14 - 57.2
22 - 71.6 12 - 53.6
20 - 68.0 10 50.0
18 - 64.4 8 - 46.4
16 - 60.8
Arena
Pescadero
Sur
Piedras Blancas
Conception
Vicente
Loma
Santo Tomas
Baja
38°
34°
30°
132°
128°
124°
120°
116°
17
18
19
20
16
15
14
13
12
11
W
C
LINE OF EQUAL TEMPERATURE
STRONG OCEAN THERMAL FRONT
WEAK OCEAN THERMAL FRONT
C = COLD
W = WARM

Figure 3. Sea surface temperature charts based on satellite infra-imagery and ship reports issued by U.S. National Weather Service (from Fiedler et al., 1985).

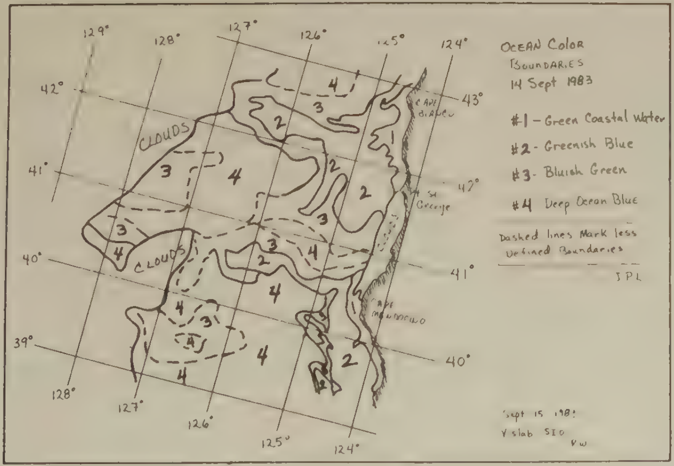
OCEAN Color
Boundaries
14 Sept 1983
#1 – Green Coastal Water
#2 - Greenish Blue
#3 - Bluish Green
#4 Deep Ocean Blue
Dashed lines Mark less Defined Boundaries
JPL
Sept 15 1983
Vislab SIO
RW
CLOUDS
CLOUDS
CAPE BLANCO
St George
CAPE MENDOCINO
129°
128°
127°
126°
125°
124°
43°
42°
41°
40°
39°
1
2
3
4

Figure 4. Ocean color boundary chart off northern California and Oregon (R. Wittenberg, Scripps Institution of Oceanography, Visibility Laboratory).

Chapter 11

LIVING MARINE RESOURCES APPLICATIONS

R. Michael Laurs
National Marine Fisheries Service
Southwest Fisheries Center
La Jolla, California

John T. Brucks
National Marine Fisheries Service
Fishery Engineering and Development Division
National Space Technology Laboratories
NSTL Station, Mississippi

1. Introduction . . . 419
2. Satellite Ocean Remote-Sensing Applications in Fisheries Research . . . 421
 2.1. Use of Satellite Infrared Thermal Data in Fisheries Research . . . 421
 2.2. Modeling Larval Transport Mechanisms Using High-Resolution SASS Wind-Stress Measurements . . . 429
 2.3. Use of Coastal Zone Color Scanner Data in Fisheries Research . . . 436
3. Utilization of Satellite Data in Fisheries-Aids Products Distribution to Fishermen . 443
 3.1. Thermal Boundary Charts . . . 443
 3.2. Sea-Ice Forecast Charts . . . 447
 3.3. NASA/JPL Satellite Data Distribution System and Fisheries Demonstration Program to U.S. West Coast Fisheries . . . 447
References . . . 450

1. Introduction

Satellite oceanic remote sensing is beginning to play an important role in fishery research and fishery management by providing synoptic oceanic measurements for use in evaluating environmental effects on the abundance and availability of fish populations. Variations in ocean conditions play key roles in natural fluctuations of fish stocks and in their vulnerability to harvesting (Hela and Laevastu, 1961, 1970). Information on the changing ocean, rather than on average ocean conditions, is necessary to understand and eventually model the effects of the ocean environment on fish stocks (Sette, 1961). This knowledge is required to provide the best possible advice in making fishery management decisions and to develop efficient harvesting strategies for fishery resources.

The use of satellite remote sensing in oceanography expanded considerably in the 1970s and satellites with dedicated oceanographic sensors were first launched in 1978. Coincident with the developments in satellite oceanography, there have been substantial increases in demand on the marine waters of the United States for activities such as fisheries development and utilization, recreation, and offshore oil exploration. With these increased activities have

ISBN 0-12-018827-9

come expanded requirements for living marine resource-management programs through legislative mandates such as the Marine Mammal Protection Act of 1972, the Fisheries Conservation and Management Act of 1976, and the Ocean Pollution Research Development and Monitoring Act of 1978. With these responsibilities, there has been an increasing need to design and initiate improved ocean-monitoring programs for resource management. The capabilities of evolving satellite remote-sensing technology, combined with conventional data collection techniques, provide a powerful tool for the efficient, cost-effective management of living marine resources.

Remote sensing is not entirely new to fishery scientists nor to fishermen harvesting living marine resources. Mariners learned long ago they could increase their perspective by elevating themselves above the water's surface. Fishermen have done this by use of crow's nests on ships, hot-air balloons, and aircraft. The sensor often used has been the naked eye, usually aided by a telescope or binoculars. Visual forms of remote sensing are common today in many fisheries, e.g., the use of helicopters operating from modern tuna purse seiners fishing on the high seas. In addition, aircraft carrying instruments for making oceanographic measurements have been used for supporting fisheries research studies (Pearcy, 1973; Thomas, 1981; and others), for locating areas favorable for fishing (Squire, 1961, 1972; and others), and for locating schools of fishes (Squire, 1982; and others).

The era of space technology brought new perspectives in remote sensing for fisheries. Man acquired the ability to view entire oceans and seas in a matter of minutes. Early satellite remote-sensing investigations for fisheries used information gathered over the ocean by systems designed for making terrestrial and meteorological observations. The objectives of these studies were to determine if certain satellite sensors could measure or identify selected oceanographic features believed to influence the distribution of fish. For example, early feasibility investigations were conducted to evaluate if fish distribution patterns may be related to temperature and color measurements made by satellites, e.g., the ERTS-1 menhaden investigation (Kemmerer *et al.*, 1974), the Skylab-3 game fish investigation (Savastano *et al.*, 1974), and the Landsat menhaden and thread herring investigation (Brucks *et al.*, 1977).

The recent development of satellite remote-sensing techniques for fisheries applications employs data from active and passive instrumentation which has been or is presently aboard a number of satellites. A wealth of satellite remote-sensing systems exists today. For the most part, however, satellite remote-sensing applications in fisheries have concentrated on the measurements of ocean temperature and color, and computation of ocean transport based on satellite-measured wind stress. Synoptic coverage of ocean temperature, color, and wind stress by no means represents the entire spectrum of environmental information necessary or required for fisheries applications.

However, knowledge of key oceanographic conditions and processes affecting the recruitment, distribution, abundance, and harvests of fishery resources may often be deduced using these data.

The purpose of this chapter is to review published living marine resource applications of ocean measurements made by Seasat and the Nimbus-7 Coastal Zone Color Scanner (CZCS). In addition, recent U.S. research involving the use of satellite infrared thermal data in fisheries is described. Satellite ocean remote-sensing applications in fisheries research is treated first and then the utilization of satellite data in fisheries-aid products that are distributed to fishermen.

2. Satellite Ocean Remote-Sensing Applications in Fisheries Research

The resolution capabilities of remote-sensing systems carried by spacecraft are not adequate for direct detection of fish schools. This has necessitated fishery scientists to examine ocean features that can be measured with spaceborne sensors and in turn can be used in fishery resource investigations. The use of satellite infrared thermal data, scatterometer wind-stress measurements, and Coastal Zone Color Scanner measurements in fisheries research investigations is yielding results which demonstrate that satellite oceanic remote sensing can be an important tool in fisheries research.

2.1. Use of Satellite Infrared Thermal Data in Fisheries Research

Satellite infrared thermal data are playing an increasingly important role in fisheries research. It is being used by U.S. fishery scientists to (1) define marine habitats of fishery resources using satellite data, which are collected contemporaneously with fishery/biological data and ground truth measurements gathered by research and fishing vessels; and (2) describe and explain variability in circulation and water mass distributions using satellite data alone or in conjunction with physical oceanographic measurements, with a view toward understanding the influence of ocean variability on fishery resources and fishing grounds.

2.1.1. Use of Satellite Infrared Imagery for Describing Ocean Processes in Relation to Spawning of the Northern Anchovy. Satellite infrared imagery was used by Lasker *et al.* (1981) for describing ocean processes in relation to spawning of the northern anchovy (*Engraulis mordax*). In this study NOAA-6 satellite thermal imagery of the Pacific Ocean adjacent to the United

States–Mexico west coast was collected on a daily basis coincident with fine-grid oceanographic ship observations. Shipboard observations included sampling of anchovy eggs, larvae, and adults as well as physical oceanographic measurements, e.g., continuous monitoring of temperature and salinity, discrete surface temperature measurements, and measurement of subsurface temperature profiles. The objectives of the investigation were to relate variations in mesoscale sea surface-temperature distributions with anchovy spawning and to identify and delineate ocean processes that might be important to the survival of fish eggs and larvae, e.g., upwelling (Lasker, 1978) and offshore transport (Parrish and MacCall, 1978).

Based on satellite imagery and confirmed by shipboard observations during the study, which was conducted during a peak period in anchovy spawning, there were distinct temperature regimes in the general geographic region where anchovy spawning normally takes place. There were (1) a cold area resulting from upwelling off Point Conception and north, (2) a large warm area which extended from Baja California into the Southern California Bight and approximately 185 km offshore, and (3) a large area of the bight with intermediate surface temperatures. The mesoscale features of surface temperature changed slowly so that for a given day the temperature distribution apparent in a satellite image did not appear to be markedly different from the preceding or following few days.

Figure 1 (from Lasker *et al.*, 1981) is an infrared thermal image which has superimposed on it the geographic distribution of anchovy egg catch. The distribution of just-spawned anchovy eggs clearly showed that nearly all spawning was confined to the Southern California Bight and to a band 40 km wide, parallel to the Baja California coast. The seaward extent of spawning in the bight was apparently abridged by the southward intrusion of recently upwelled water indicated by the 14°C isotherm. Also, anchovies were excluded from the water warmer than 17°C beyond 40 km of the Baja California coast. The satellite temperature/anchovy egg relationships were corroborated by mapping the distribution of first-day eggs on sea surface temperature observations made concurrently aboard ship.

Relatively high numbers of anchovy larvae were found in plankton hauls taken by another research vessel in the coastal area north of Point Conception in February 1980. Temperatures were very warm for this entire zone in February, with progressively warmer conditions to the south. Winds were light and from the south prior to March 11 and upwelling was minimal. Winds from the north increased on March 12 and persisted. When the area north of Point Conception, where anchovy larvae had been collected in February, was sampled in March, no larvae of any age were found. This suggested to the authors that the extensive upwelling, as indicated by wind data and observed by satellite, carried anchovy larvae out of the coastal zone

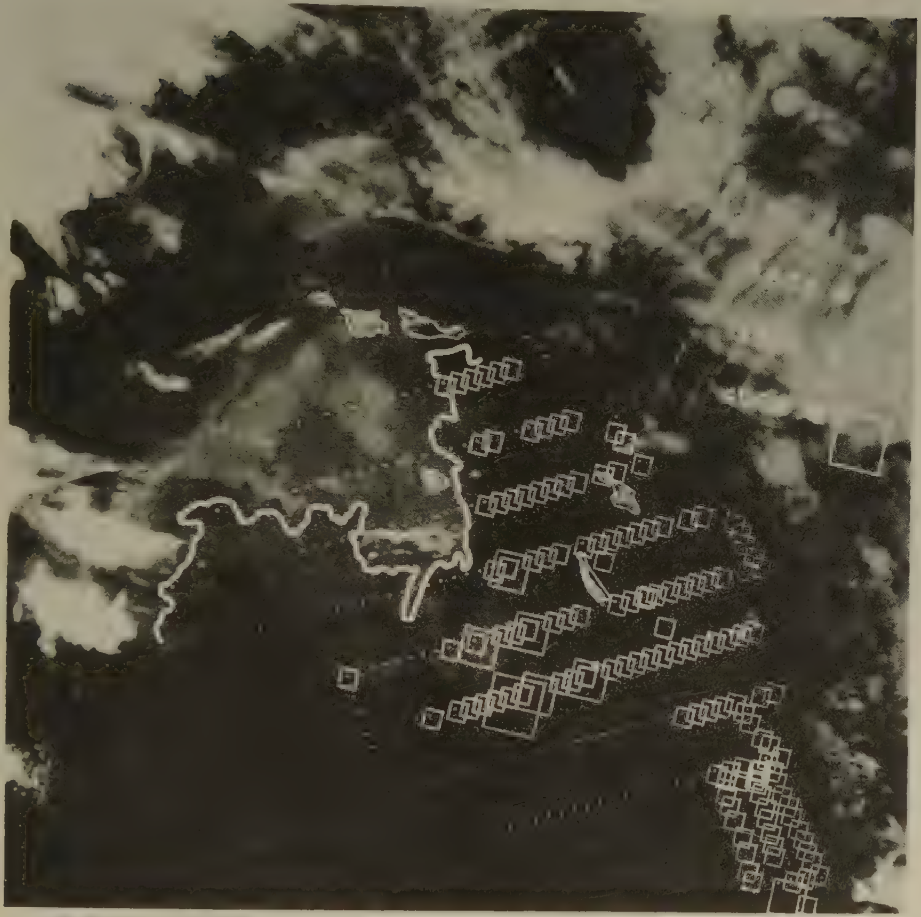

FIG. 1. Distribution of anchovy eggs superimposed on NOAA-6 infrared thermal image of the Southern California Bight. The 14°C isotherm plotted from satellite gray-scale calibration has been drawn in. Feathery objects are clouds. Square indicates number of anchovy eggs under 1 m^2 of sea surface. (From Lasker *et al.*, 1981.)

and into the California Current. At the same time adult anchovies were excluded, as was evidenced by lack of fish in trawl samples. The start of upwelling on March 14 and the progressively colder temperatures appeared to have excluded anchovies from that time on. Lasker *et al.* concluded that anchovy avoid recently upwelled water and that the areal extent of upwelled water may be mapped using infrared satellite imagery. They stated:

> Because satellites can see vast areas of the ocean day in and day out, they provide the scientist with a synoptic look at processes only seen heretofore on smaller scales and restricted to the time when a ship or ships can cover the area of interest. In this study only a

> satellite could have provided us with a synoptic picture of the large scale oceanographic events which were happening over the entire spawning area of the anchovy during the peak of the spawning season. The extensive ground truth provided by the R/V *David Starr Jordan* confirmed that the 0.5°C accuracy of the infrared radiometer aboard most of the NOAA satellites detects accurately the movement of surface layers and shows the sequential development of upwelling along the California coast over large areas of ocean [Lasker *et al.*, 1981].

Satellite remote sensing has also been utilized by Fiedler (1983) to investigate variations in spawning habitat of the northern anchovy in the Southern California Bight. He found that spawning in the northwestern region of the bight is excluded from a cold-water mass apparent in infrared satellite imagery south of Point Conception, corroborating the earlier findings of Lasker *et al.* (1981), and that spawning to the south is confined to coastal waters with moderately high phytoplankton pigment levels as measured by the CZCS. (The latter will be discussed further in Section 2.3.) Fiedler (1983) also concluded that satellite images can be used to improve the sampling efficiency of ichthyoplankton surveys. The effectiveness of using satellite infrared and CZCS imagery (see Section 2.3) to monitor shifts in anchovy spawning habitat off California associated with the 1982–1983 El Niño warm-water conditions have been demonstrated by Fiedler (1984a,b).

2.1.2. Use of Satellite Infrared Thermal Imagery in Tuna and Billfish Studies. Satellite infrared thermal imagery has proved to be a valuable tool in tuna research. This has been especially true in studies designed to investigate relationships between tuna distribution and availability and ocean temperature fronts and sea surface temperature.

2.1.2.1. North Pacific albacore tuna distribution in relation to ocean temperature fronts. Albacore tuna (*Thunnus alalunga*), which are highly mobile and widely distributed in the North Pacific, migrate seasonally into waters off the coast of North America during July through October where they support important commercial and recreational fisheries. Laurs *et al.* (1984) used Advanced Very High Resolution Radiometer (AVHRR) infrared thermal data from the NOAA-7 satellite and fishery data from logbooks kept by commercial albacore tuna fishermen to investigate relationships between albacore fishing success and oceanic temperature fronts in waters off California. Relationships to ocean-color boundaries were also examined using CZCS imagery (Section 2.3). Laurs *et al.* found that fishing effort and highest catch rates for albacore tended to be concentrated in the vicinity of temperature fronts, which are believed to result from coastal upwelling (Fig. 2). High catch rates were observed on the warm side of the temperature boundaries, usually very near the boundary but sometimes extending up to 100 km offshore from the boundary or front. Fishing activity was markedly less and catch rates were

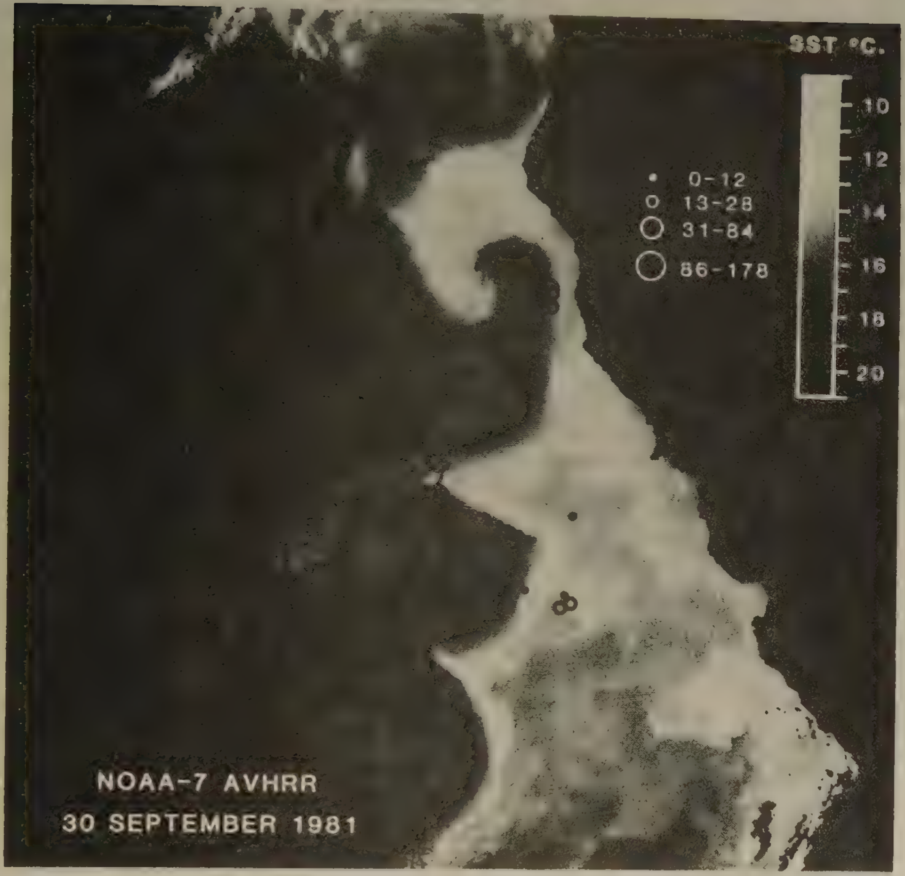

FIG. 2. Distribution of mean daily albacore tuna catches made by commercial fishing vessels superimposed on NOAA-7 AVHRR image of water off central California. Albacore catch rates are expressed as number of albacore caught per 150-line hours of fishing and are shown as varying sizes of circles. (From Laurs *et al.*, 1984.)

usually nil on the cold side of the temperature fronts (Fig. 2). While it is generally believed by fishermen and fishery scientists that tuna may aggregate in the vicinity of upwelling temperature fronts to feed (Laurs *et al.*, 1977), the use of satellite imagery is allowing fishery scientists to investigate this relationship on space and time scales hitherto not possible.

Laurs and Austin (1985) investigated the small-scale migration patterns of albacore in relation to oceanic frontal boundaries using ocean color and infrared satellite data collected contemporaneously with observations made from ships at sea. Nimbus-7 CZCS and NOAA-6 satellite AVHRR infrared data were collected in conjunction with field experiments where acoustic telemetering methods were used to track the horizontal and vertical movements of free-swimming albacore, and expendable bathythermograph (XBT) observations were made to determine subsurface ocean thermal structure. Three albacore were tracked for approximately 24 hr and one for about 15 hr. The results showed that (1) total distances tracked ranged from about 40 to 60 km, with all fish remaining in the same parcel of warm water that was separated from waters to the north, south, and inshore by about a 2°C temperature gradient as shown by infrared thermal imagery; (2) tracked fish spent most of the time in waters within and below the thermocline, and only small amounts of time in the upper mixed layer; (3) the fish exhibited marked vertical excursions in depth, with the range being larger during the day than at night; (4) the fish spent most time in waters with temperatures considerably lower than what has been generally believed to be the preferred temperature range for albacore; and (5) when changing depth, the fish, frequently within a 20-min period, passed through a vertical gradient of temperature amounting to 6–7°C or about 3+ times greater than the horizontal temperature gradient at the surface indicated by ship measurements and the infrared thermal imagery.

These findings indicate that the reasons tuna aggregate on the warm side of surface temperature fronts—an economically significant phenomenon that has been observed on scientific cruises and is well known by fishermen—may not be related to thermal–physiological mechanisms (Neill, 1976). Instead, Laurs and Austin speculate that one or more behavioral mechanisms related to feeding may be responsible. Ocean-color measurements made by the CZCS in conjunction with the tracking study and with catches made by commercial fishing vessels (Laurs *et al.*, 1984) provide data that support this hypothesis (see Section 2.3).

Laurs *et al.* (1981) report on another study involving albacore tuna which was conducted in winter several months after albacore emigrate from waters near the North American coast. In this study NOAA-6 infrared thermal imagery was used in conjunction with fish catch information and ground truth measurements made by chartered commercial albacore fishing vessels. The investigators found that a marked temperature front observed in the satellite imagery appeared to be a boundary to albacore distribution. There was up to a 20-fold decrease in catch rate on the cool side of a temperature front believed to mark the outer edge of the California Current approximately 700 miles off southern California.

2.1.2.2. Gulf of Mexico tuna longline fishery and the Loop Current. Leming (1981) evaluated the feasibility of using satellite imagery to locate the position of the Loop Current in the eastern Gulf of Mexico in an investigation of relationships between the Loop Current and tuna caught by the Japanese longline fishery. The locations of longline sets and species composition of the catches were recorded by National Marine Fisheries Service (NMFS) observers on board selected vessels of the Japanese longline fleet operating in the Gulf of Mexico. GOES-East satellite infrared images composited weekly and analyzed for major thermal boundaries by the NESS Satellite Field Service Station in Miami, Florida, were used to estimate the position of the Loop Current. An apparent strong correlation was found in early May 1978 between sets targeted on bluefin tuna and the location of surface thermal boundaries of the Loop Current (Fig. 3; Leming, 1981). However, after late May or early June, surface temperature gradients in the Gulf of Mexico were of insufficient magnitude to be detected in the GOES imagery. Curiously, during this period, all fishing for bluefin tuna ceased, and fishing was targeted for yellowfin tuna in the western Gulf of Mexico. For the most part Leming had only limited success finding a relationship between the Loop Current and tuna longline fishing in 1979.

According to Leming (1981) the thermal boundary charts he used based on GOES infrared imagery did not contain sufficient resolution in time and space for use in an analysis of catch-rate differences for major pelagic groups of fish in relation to satellite data. He concluded that to correlate catch rates with satellite data the thermal boundary analyses must be expanded to include secondary thermal gradients, ground resolution less than 8 km must be used, and composite time scales less than 1 week are necessary. The GOES provides overall the best data source, however, because the frequency of data allows compositing for cloud-cover removal, a more serious problem than spatial resolution (Maul *et al.*, 1984).

2.1.2.3. Atlantic bluefin tuna distribution in relation to seasonal ocean warming. Roffer *et al.* (1982) used satellite remote sensing in conjunction with shipboard observations and fishing logbook records in an investigation of Atlantic bluefin tuna (*Thunnus thynnus thynnus*) off the coasts of the mid-Atlantic states. Using satellite infrared imagery to follow the seasonal northerly progression of the 19–20°C surface isotherms, Roeffer *et al.* found that the development and duration of the various bluefin tuna fisheries along the East Coast follow the movement of seasonal warming of near-surface waters.

2.1.2.4. Movements of Atlantic swordfish in relation to ocean features. Carey and Robinson (1981) conducted tracking experiments of a swordfish with acoustic telemetry instruments to investigate the daily patterns in activity. Satellite infrared imagery was collected in conjunction with the tracking to study the movements of swordfish in relation to ocean features. Among the oceanic features apparent in satellite imagery were cold shelf water, warm Gulf Stream waters, and a streamer of cold shelf water pulled off by the Gulf Stream moving past Cape Hatteras. The swimming direction of

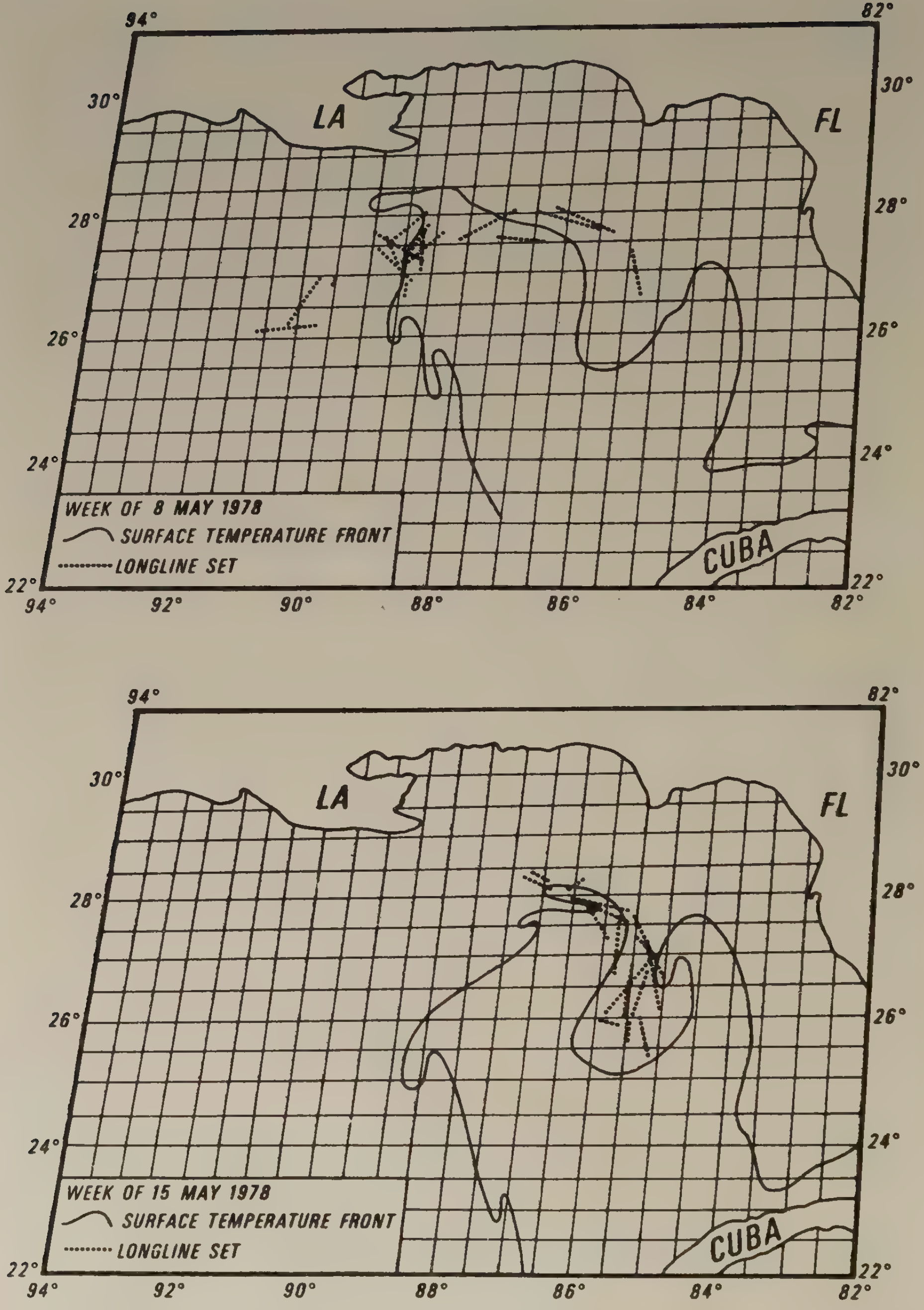
94°
82°
30°
28°
26°
24°
22°
LA
FL
CUBA
WEEK OF 8 MAY 1978
SURFACE TEMPERATURE FRONT
LONGLINE SET
94°
92°
90°
88°
86°
84°
82°
WEEK OF 15 MAY 1978
SURFACE TEMPERATURE FRONT
LONGLINE SET

FIG. 3. Distribution of longline sets relative to the May 1978 position of the Loop Current boundary in the Gulf of Mexico deduced from GOES infrared satellite imagery. (From Leming, 1981.)

the swordfish for the 3-day period it was tracked was not correlated with oceanic surface thermal boundaries obvious in the infrared image. The tracked fish was tagged on the north side of entrained cold shelf water and after tagging it swam across the cold shelf water and the Gulf Stream, and then into the Sargasso Sea.

The horizontal swimming pattern of the swordfish did not appear to be influenced by oceanic boundaries between different types of waters as has been observed in albacore tuna (Laurs and Austin, 1985). This difference in the relationships between oceanographic environmental conditions and the movements of swordfish and albacore tuna became apparent largely because satellite imagery was collected contemporaneously with the tracking experiments.

2.2. Modeling Larval Transport Mechanisms Using High-Resolution SASS Wind-Stress Measurements

Brucks *et al.* (1984) conducted a case study using Seasat-A Satellite Scatterometer (SASS) wind data to establish, quantify, and document the extent and variability of wind-induced ocean-flow indices on surface-layer transport. Knowledge of surface-layer transport processes is important in fisheries research because dispersal mechanisms control the distribution of early life stages and thereby influence the recruitment and future harvest of marine organisms with planktonic life stages. The purpose of the case study was to determine whether high-resolution SASS measurements of wind stress could improve estimates of surface layer and larval transport based on geophysical models.

The study was conducted in the Gulf of Mexico where surface layer transport plays a key role in the early survival of shrimp and menhaden. Fisheries on these species in the Gulf produce the major portions of the highest U.S. dollar and largest U.S. volume fishery. In addition, several other economically important commercial fisheries in the Gulf have planktonic life stages which are influenced by prevailing dispersal mechanisms common to all. A schematic representation of the penaeid shrimp life cycle is given in Fig. 4 showing transport of developmental stages from offshore regimes to coastal estuarine zones and the adults returning offshore to spawn.

2.2.1. Description of Model and Preparation of SASS Input Data. Brucks *et al.* (1984) developed a model to use sea surface wind stress measured by the SASS to calculate surface-layer transport. The Seasat approach developed by Brucks *et al.* compared to the standard technique for deriving surface transport is shown in Fig. 5. The Seasat approach reduces the number

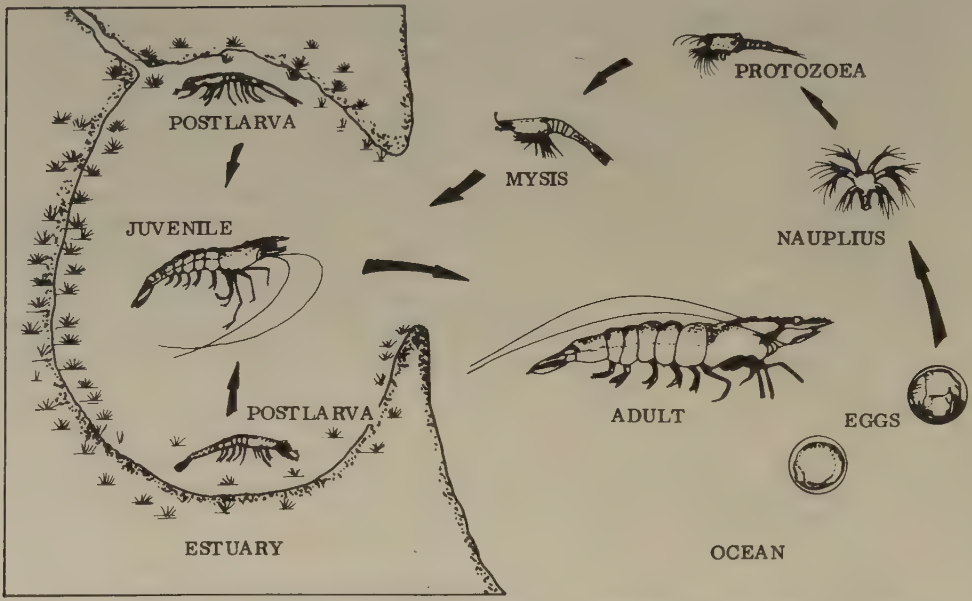

FIG. 4. Life cycle of penaeid shrimp showing transport of developmental stages from offshore to coastal estuarine zones and adults returning offshore to spawn. (From Brucks *et al.*, 1984.)

of assumptions involved in the calculation of the wind-stress vector and presumably provides more accurate estimates of surface circulation. The model is composed of offshore and coastal modules to satisfy deep and shallow water responses to meteorologic driving forces. Hydrographic boundary conditions are essentially fixed by monthly and/or seasonal averages of historical temperature and salinity data. Surface transport is thus a function of the varying wind field.

The SASS data set for input to the model of surface-layer transport was compiled by extracting scatterometer wind measurements from 70 revolutions over the Gulf of Mexico during September 1978. The spatial distribution of these 11,248 SASS measurements in the study area available for analyses is shown in Fig. 6.

The geophysical data records for scatterometer wind measurements with the direction alias removed were stratified into 26 5-day running averages grided by $\frac{1}{2}^\circ$ square. Analyses showed that sufficient coverage of the Gulf is attained within 5 days. Longer periods added to the data density, but did not improve the distribution of data.

The SASS-measured wind-stress field was used to calculate surface currents by the standard homogeneous, steady-state Ekman (1905) solution.

Model outputs consist of 5-day mean current vectors on a $\frac{1}{2} \times \frac{1}{2}^\circ$ grid. A trajectory analysis package is also available to portray current pathways of

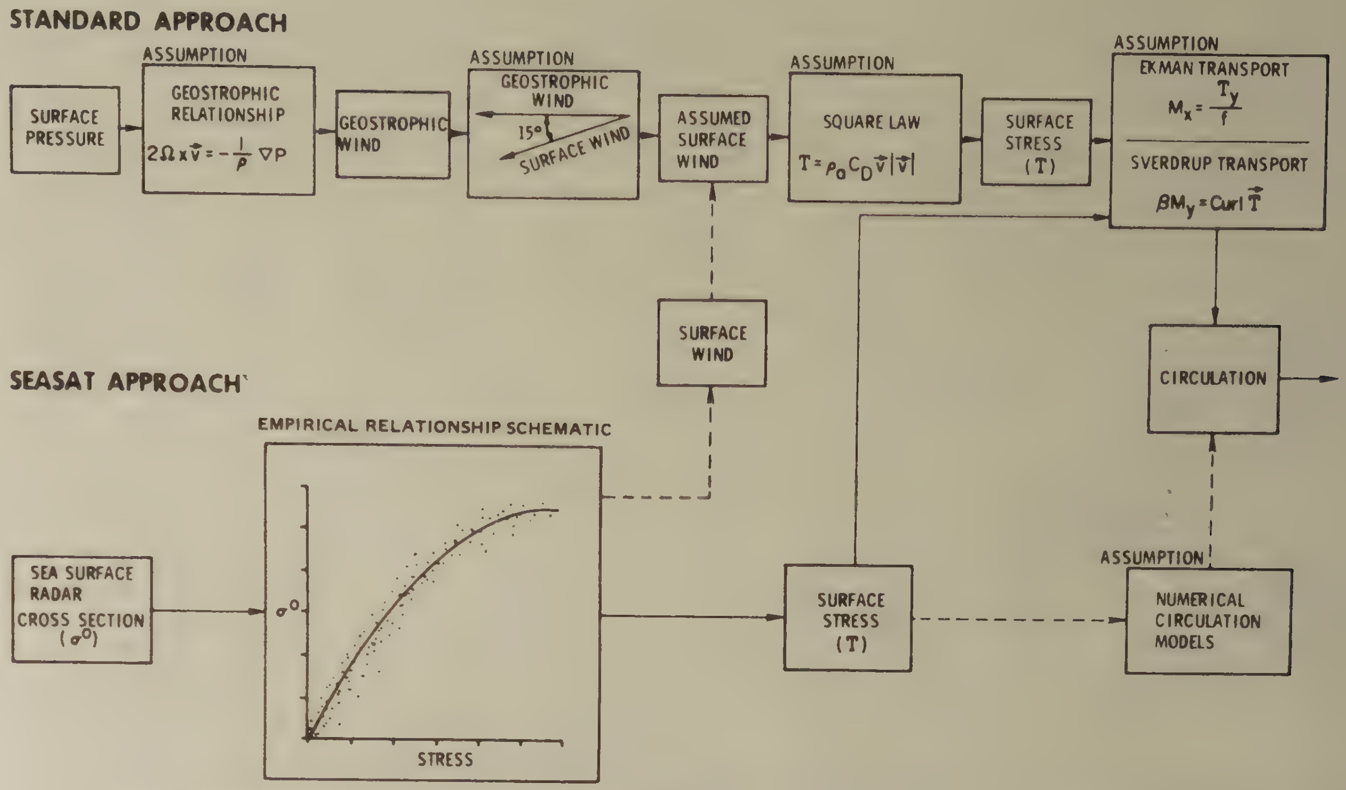
STANDARD APPROACH
SURFACE PRESSURE
ASSUMPTION
GEOSTROPHIC RELATIONSHIP
$2\Omega \times \vec{v} = -\frac{1}{\rho} \nabla P$
GEOSTROPHIC WIND
ASSUMPTION
GEOSTROPHIC WIND
15°
SURFACE WIND
ASSUMED SURFACE WIND
ASSUMPTION
SQUARE LAW
$T = \rho_a C_D \vec{v} |\vec{v}|$
SURFACE STRESS (T)
ASSUMPTION
EKMAN TRANSPORT
$M_x = \frac{T_y}{f}$
SVERDRUP TRANSPORT
$\beta M_y = \text{Curl}\, \vec{T}$
SURFACE WIND
CIRCULATION
SEASAT APPROACH
EMPIRICAL RELATIONSHIP SCHEMATIC
SEA SURFACE RADAR CROSS SECTION (σ^0)
σ^0
STRESS
SURFACE STRESS (T)
ASSUMPTION
NUMERICAL CIRCULATION MODELS

FIG. 5. Comparison of Seasat and standard technique for deriving surface-layer transport. (From Brucks *et al.*, 1984.)

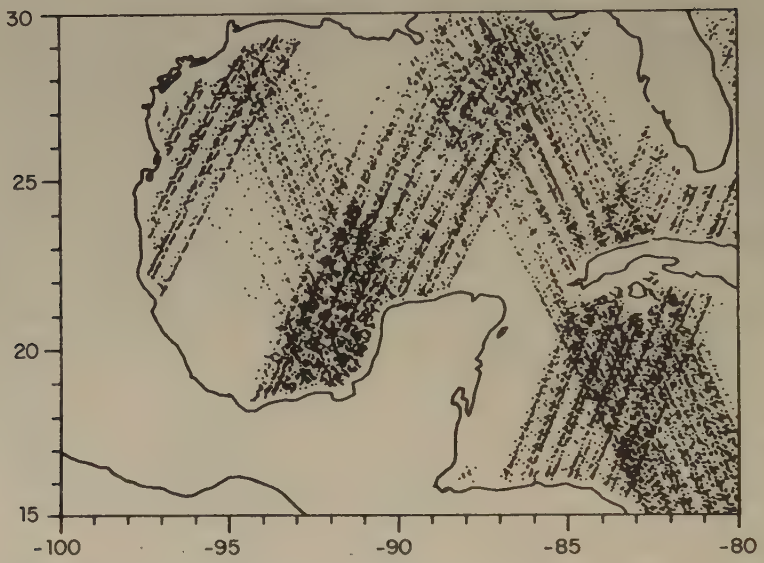

FIG. 6. Spatial distribution of 11,248 SASS measurements of the Gulf of Mexico for September 1978. (From Brucks *et al.*, 1984.)

eggs and larvae and to define impact areas. The trajectory analysis allows random selection of any number of starting points, tracking of the dispersal routes, and demonstration of the impact area of particle location between 1 and 30 days of drift. The wind-driven surface currents derived from SASS observations can be used independently for studies of wind-driven circulation or can be combined with surface flow estimates from thermohaline models to produce total current transport at the ocean surface.

Fields of vertical velocity representing upward velocity into the Ekman layer required to balance the computed Ekman divergence induced by the wind-stress curl may also be output from the model. The vertical movement of water due to wind-stress curl provides insight for the enumeration of environmental factors relevant to dispersal mechanisms for fisheries. Divergence in Ekman transport will cause upwelling of waters possibly rich in nutrients, thereby creating areas of high productivity. Conversely, convergence in the Ekman layer will produce downwelling, forming areas of accumulation of planktonic organisms. The relationship between the curl of wind stress and the vertical movement of water is important also in the delineation of spawning areas. Historically, geographic boundaries of spawning areas are identified generally by those zones high in egg and larvae concentrations and/or high in adult specimens laden with mature eggs or possessing mature, "ripe" ovaries (i.e., ready to spawn). Correlation between wind-stress curl and concentrations of planktonic eggs and larvae could assist in the definition of spawning areas. In this fashion, source ambiguities could be resolved to show that the observed concentration is due to local spawn or is due to a consequence of environmental redistribution and accumulation of distant spawn.

2.2.2. Estimates of Surface-Layer Transport and Vertical Movement of Water Using SASS Wind Data. Using SASS wind stress to calculate surface-layer transport processes showed striking spatial and temporal variability in wind-drift patterns and regions of convergence/divergence in the Gulf of Mexico. During the first half of September, surface wind drift was most pronounced in the northwestern Gulf. Initially, surface flow was oriented toward the northwest (Fig. 7a). By midmonth the wind-drift regime increased in aerial coverage and changed direction such that anticyclonic flow prevailed in the western Gulf (Fig. 7b). An obvious change occurred again in the third week as evidenced by the regional shift of predominant wind drift to the southwest quadrant of the Gulf, including the Yucatan Straits, and a change in wind-drift direction to the northwest and north (Fig. 7c). Additionally, the magnitude of the wind-driven circulation throughout the Gulf increased approximately twofold with a mean and maximum velocity of 10.50 and 45.71 $\mathrm{cm\,sec^{-1}}$, respectively. At the close of the month (Fig. 7d), the wind-driven circulation regime was sluggish. A southwest drift current, indicating a current reversal, was present in the northwest Gulf, replacing a northerly current identified previously, and an area of prominent wind-driven activity was apparent for the first time in the northeast Gulf.

Estimates of the curl of the wind stress based on the SASS measurements showed the Gulf to have a highly dynamic oceanic system of regional convergence and divergence. Using the Seasat data base the Gulf was convergent and divergent about equal amounts of time (approximately 1.5:1), with mean and maximum vertical velocities ($\mathrm{cm\,sec^{-1}}$) of 5.2×10^{-4} and 31.4×10^{-4}, respectively. Using the standard method and data base the Gulf was almost always convergent (approximately 4:1), with lower mean and maximum vertical velocities ($\mathrm{cm\,sec^{-1}}$) of 3.0×10^{-4} and 14.2×10^{-4}, respectively.

Brucks *et al.* used the SASS model derivations of wind-driven surface-layer transport processes to define potential enrichment zones of spawn material and predict the areas of coastal impact of eggs and larvae as controlled by environmental forces. Processes conducive for the offshore accumulation of planktonic organisms were found mainly in the western and eastern Gulf (Fig. 8). The western distribution was concentrated generally in the west central Gulf with projections to the south, west, and north. Distributions in

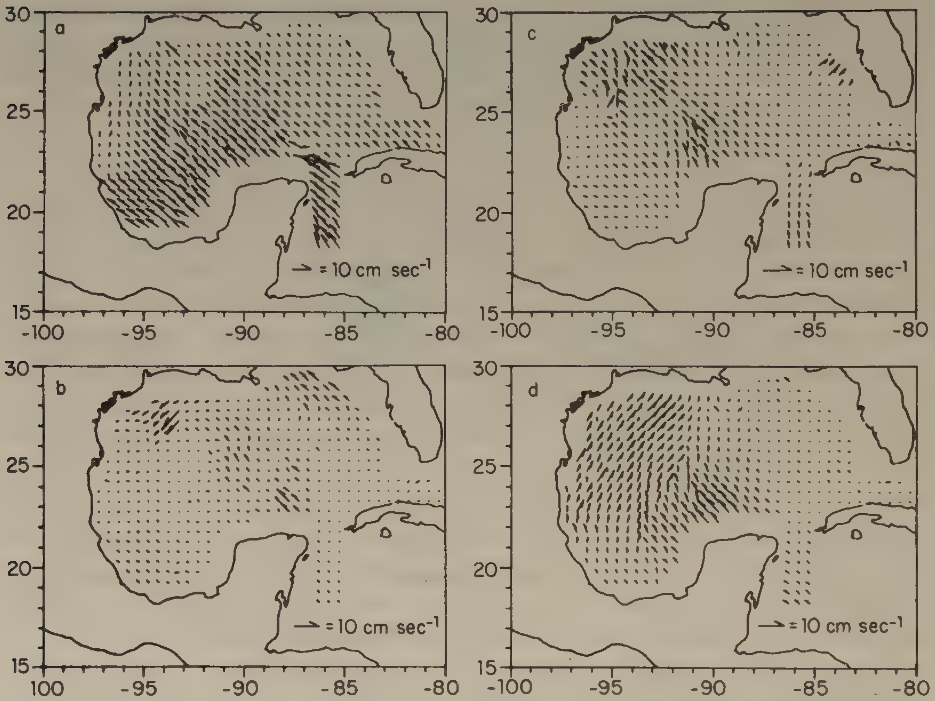

FIG. 7. Wind-driven circulation patterns show variability resulting from SASS data for four 5-day periods during September 1978. (a) Day 263 = days 261–265 (or September 20 = September 18–22); wind-stress average (dynes cm^{-2}) = mean 0.93, max 4.00; current-speed average (cm sec^{-1}) = mean 10.50, max 45.71. (b) Day 270 = days 268–272 (or September 27 = September 25–29); wind-stress average (dynes cm^{-2}) = mean 0.29, max 2.75; current-speed average (cm sec^{-1}) = mean 3.14, max 31.44. (c) Day 250 = days 248–252 (or September 7 = September 5–9); wind-stress average (dynes cm^{-2}) = mean 0.48, max 1.83; current-speed average (cm sec^{-1}) = mean 5.42, max 20.87. (d) Day 256 = days 254–258 (or September 13 = September 11–15); wind-stress average (dynes cm^{-2}) = mean 0.60, max 2.04; current-speed average (cm sec^{-1}) = mean 6.87, max 23.28. (From Brucks *et al.*, 1984.)

the east were separated although large, discrete areas prevailed in the eastern Gulf and Yucatan Straits. Coastal accumulations, summarized in Fig. 9, occurred in the northwest Gulf off Texas, Louisiana, and Mississippi; the southwest Gulf off Mexico; and in the east Gulf off Florida. Trajectories due to oceanic and wind effects shown in Fig. 8 were merged to compare final impact areas to areas of known nursery grounds (Fig. 10). It was shown that predicted impact areas were in close proximity to nursery grounds in Louisiana, Texas, and Florida.

2.2.3. Usefulness of Seasat SASS Wind-Stress Measurements in Modeling Larval Transport Mechanisms. Brucks *et. al.* concluded that Seasat afforded

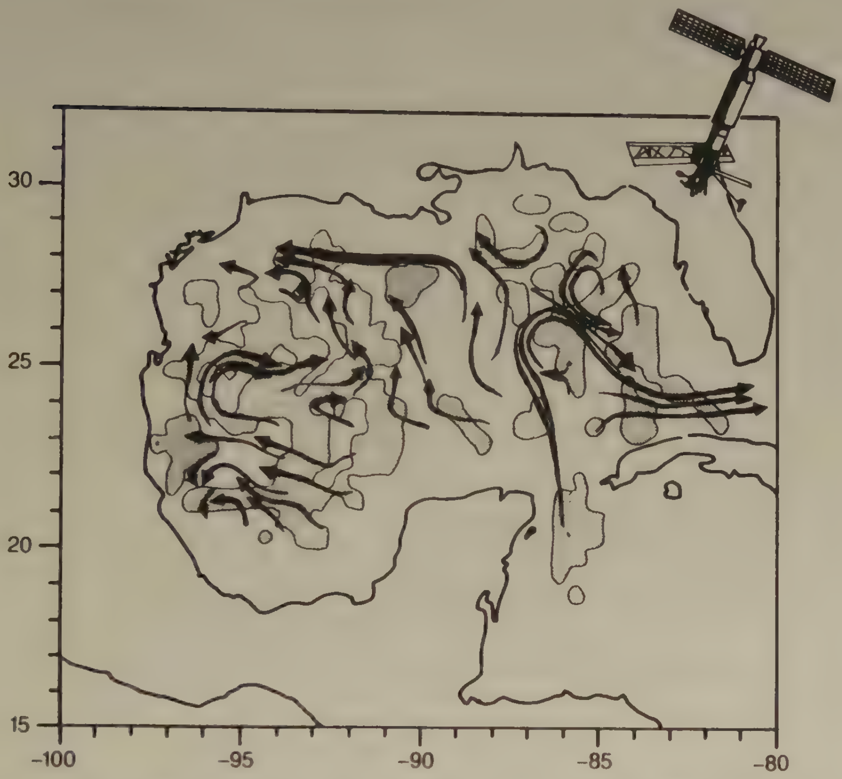

FIG. 8. High-probability area for offshore waters rich in planktonic eggs and larvae due to accumulations by wind-driven convergence of surface waters (shaded regions). Surface current trajectories are superimposed to show 30-day dispersal pathways for September 1978. (From Brucks *et al.*, 1984.)

new technology for fisheries application to monitor, model, and predict environmental pathways by which offshore spawn of estuarine-dependent shellfish and finfish find their way into coastal nursery grounds. Synoptic and repetitive direct measurements of wind stress provided enhanced capability to determine wind-driven environmental events, including a pertinent measure of inherent variability, that influence recruitment processes of marine organisms and provide a means to correlate significant interactions between subregions in the Gulf of Mexico. The effect of dispersal mechanisms is common to all major fisheries that have planktonic life stages and knowledge of transport processes can, therefore, help satisfy basic mission requirements of the NMFS for management of national fisheries and for the negotiation and establishment of international agreements concerning fisheries that span national boundaries.

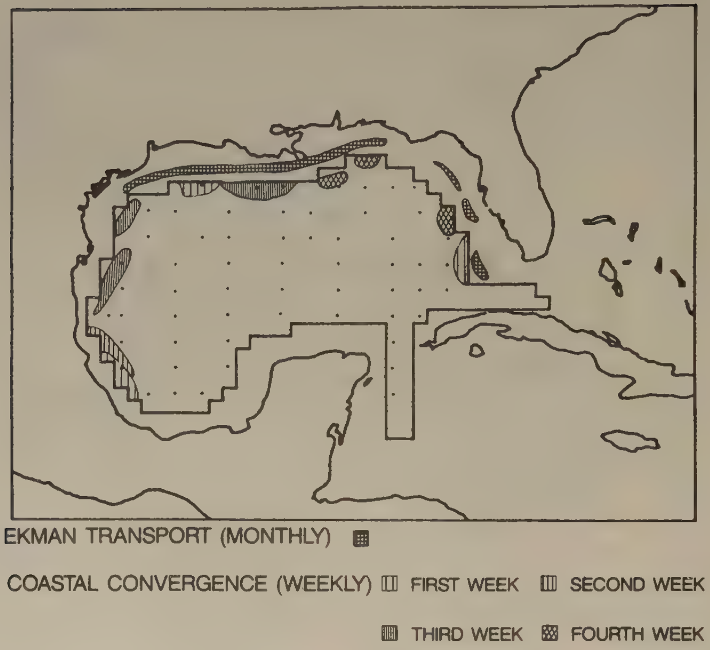
EKMAN TRANSPORT (MONTHLY) ▦
COASTAL CONVERGENCE (WEEKLY) ▥ FIRST WEEK ▥ SECOND WEEK
▥ THIRD WEEK ▩ FOURTH WEEK

FIG. 9. High-probability area for coastal waters rich in eggs and larvae for September 1978. (From Brucks *et al.*, 1984.)

2.3. Use of Coastal Zone Color Scanner Data in Fisheries Research

The concept of using ocean color for finding fishing grounds is not new. Fishermen have used variations in ocean color for centuries to locate oceanic areas believed to be favorable for catching fish. The potential value to fishermen of synoptically acquired ocean-color data from space was first demonstrated by Kemmerer *et al.* (1974). In this study ocean-color measurements from Landsat were used to predict areas of high probability of occurrence of menhaden in the Gulf of Mexico.

When the Nimbus-7 satellite with the CZCS was launched in 1978 there was increased enthusiasm and interest by fishery scientists to utilize satellite ocean-color measurements in fisheries research. Cram (1979) speculated on the use of CZCS measurements in the management of a pelagic fishery. However, applications of CZCS imagery to fisheries research has only recently been realized with the increased availability of CZCS data and improved access to hardware and software to process the color imagery.

Ocean-color measurements from the CZCS are being used in fishery resource applications for (1) the location of ocean fronts, effluents, and circulation features, (2) quantitative determinations of ocean color that are

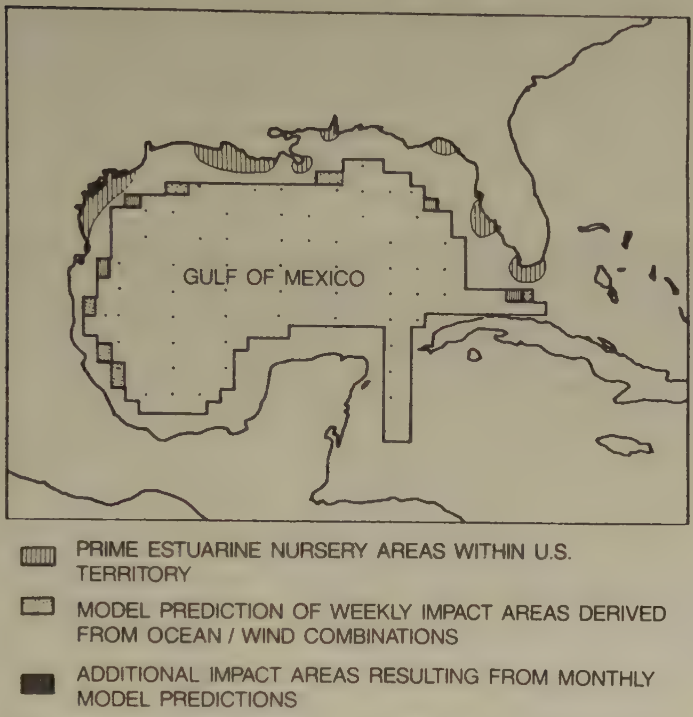
GULF OF MEXICO
PRIME ESTUARINE NURSERY AREAS WITHIN U.S. TERRITORY
MODEL PREDICTION OF WEEKLY IMPACT AREAS DERIVED FROM OCEAN / WIND COMBINATIONS
ADDITIONAL IMPACT AREAS RESULTING FROM MONTHLY MODEL PREDICTIONS

FIG. 10. Predicted coastal recruitment areas compared to known locations of estuarine nursery grounds for shrimp and fishes. (From Brucks *et al.*, 1984.)

directly related to chlorophyll and sestonic concentrations, and (3) the identification of water masses.

2.3.1. Use of CZCS Measurements in Albacore Tuna Studies. Distribution of albacore catches in relation to color boundaries. CZCS imagery and albacore tuna catch data obtained from daily logs submitted by fishermen were used by Laurs *et al.* (1984) to investigate the relationships between albacore fishing success and ocean color boundaries off the U.S. Pacific west coast. The ratios of CZCS channel 1 to channel 3 radiance [blue/green ratio or $R(13)$] were used to determine the locations of ocean color boundaries after atmospheric contamination was removed from the imagery using the algorithm of Smith and Wilson (1981). $R(13)$ was also converted to phytoplankton pigment concentration using the algorithms of Clark (1981) and Smith and Baker (1982). Normalized catch data for 5-day periods, from 2 days before to 2 days after each Nimbus-7 pass, were plotted on the CZCS images.

In nearshore waters color imagery showed a sharp color front marking the boundary between the coastal and oceanic water masses and corresponding to the temperature front visible in the AVHRR images (see Section 2.1.2). The boundary generally had a meandering north–south distribution with intrusions of oceanic water into coastal water. Chlorophyll concentrations were usually less than 0.30 mg m^{-3} offshore of the color front and were greater than 0.50 mg m^{-3} inshore of the front. Strong color fronts and chlorophyll concentrations > 1.0 mg m^{-3} were also observed in the waters nearer the coast associated with aged upwelled waters. Albacore fishing effort was distributed mostly in the oceanic waters with lesser amounts in the coastal waters. The fishing effort tended to be highest along or in the vicinity of the color boundary separating coastal and oceanic waters and in some cases up to about 100 km from the boundary in oceanic waters. Also, high fishing effort was concentrated in the fingers of oceanic water that intruded into the coastal water. Figure 11 (from Laurs *et al.*, 1984) shows a plot of albacore catch rates superimposed on a false color image of the blue/green color ratio, $R(13)$. The catch rates were highest in the bluish oceanic waters near the color boundary marking the interface between oceanic and coastal waters. The shoreward intrusions of oceanic waters had particularly large catches concentrated at the color boundary. Catch rates within the greenish coastal waters were low or nil. Satellite data and albacore fishery data were also examined from a large oceanic region centered about 500 miles off the coasts of Washington and Oregon. No temperature fronts were visible in AVHRR imagery; however, a diffuse and broken color front was apparent in the center of a CZCS image covering the region. The oceanographic boundary defined by the color front marked an area of high fishing activity and large mean catches in relatively productive water with chlorophyll concentrations of 0.30–0.40 mg m^{-3}. Sea surface temperature was observed to increase gradually from 12 to 20°C over about 8° of latitude.

The satellite images and concurrent albacore catch data examined by Laurs *et al.* (1984) clearly demonstrate that the distribution and availability of albacore are related to oceanic fronts. They also substantiate the conventional wisdom of many fishermen who use temperature and/or color "breaks" to locate potentially productive fishing areas for albacore. The results show that in nearshore regions commercially fishable aggregations of albacore are found in warm, blue oceanic waters near temperature and color fronts on the seaward edge of coastal water masses. Shoreward intrusions of oceanic water are particularly favorable sites for albacore aggregation. In offshore waters during late summer, commercial concentrations of albacore were found associated with oceanic boundaries that are marked by color

---

FIG. 11. Distribution of mean daily albacore tuna catches made by commercial fishing vessels superimposed on Nimbus-7 CZCS blue/green color ratio and phytoplankton pigment concentration in waters off central California. (From Laurs *et al.*, 1984.)

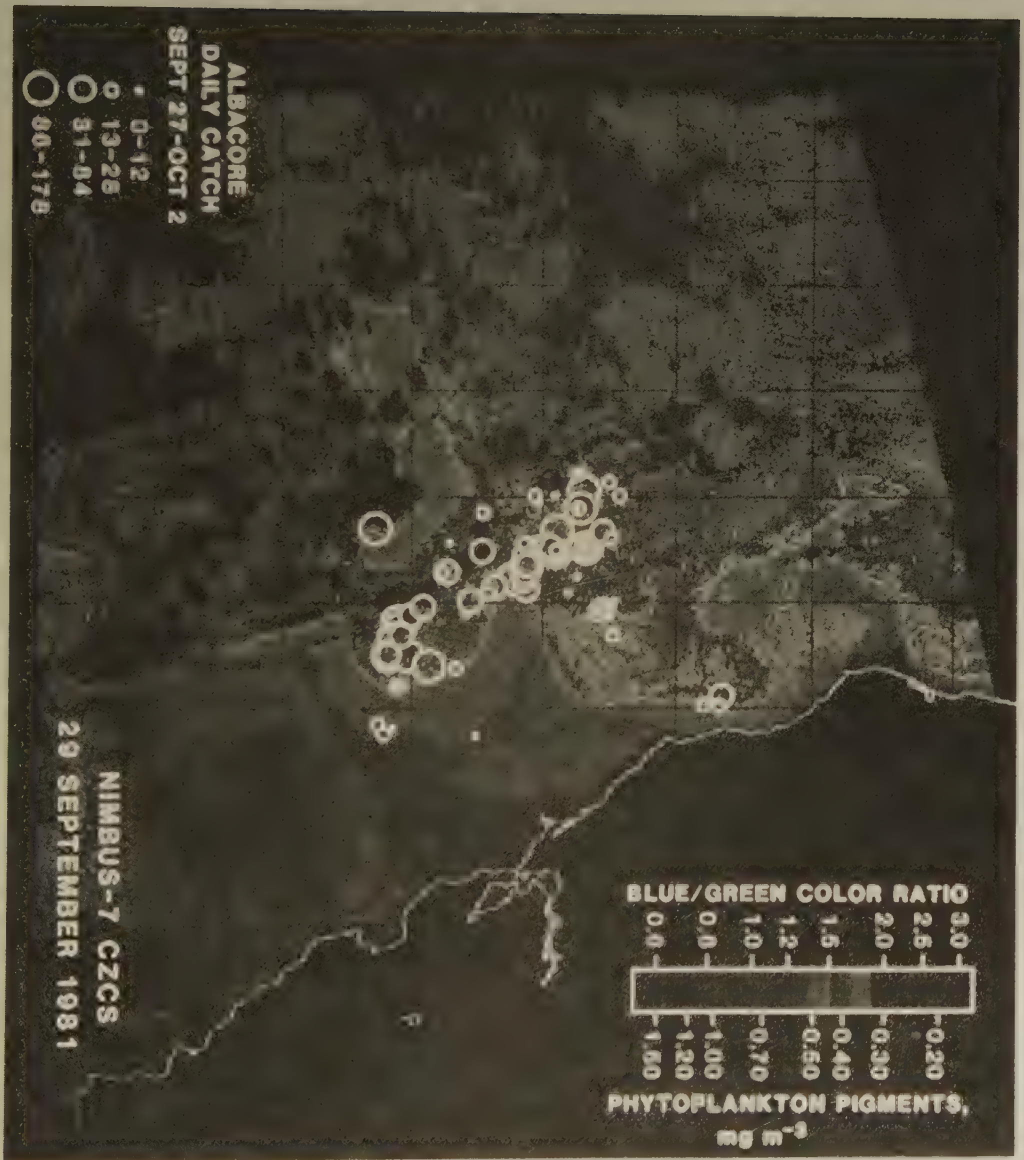
ALBACORE
DAILY CATCH
SEPT 27-OCT 2
0-12
13-25
31-84
80-178
NIMBUS-7 CZCS
29 SEPTEMBER 1981
BLUE/GREEN COLOR RATIO
0.6
0.8
1.0
1.2
1.5
2.0
2.5
3.0
1.50
1.20
1.00
0.70
0.50
0.40
0.30
0.20
PHYTOPLANKTON PIGMENTS,
mg m-3

fronts detectable from satellites but lacking sea surface temperature gradients. The availability of albacore in offshore waters appears to be higher in relatively productive waters. The temperature signature denoting the boundaries of the relatively more productive waters, if present earlier, may be lost due to seasonal warming.

It was noted earlier (Section 2.1.2.1) that Laurs and Austin (1985) speculate that behavior mechanism(s) related to feeding may be responsible for tuna aggregating on the warm side of temperature boundaries. To support this argument, the authors used CZCS measurements along with a knowledge that tuna are visual feeders. The distribution of ocean color boundaries, apparent in CZCS imagery collected concurrently with albacore acoustic tracking, showed a gradient nearly coincident with the sea surface temperature gradient patterns visible in AVHRR imagery. The diffuse attenuation coefficient (k) and chlorophyll concentration measured by the CZCS also showed a similar pattern to the gradient in sea surface temperature, with lower values in the warmer waters and higher values in the cooler waters. All tracked albacore remained in clear, warm oceanic waters and did not cross the boundaries into turbid, cool coastal waters. However, the tracked fish moved vertically through water temperatures that were 3+ times greater than the gradients in surface temperature apparent in the AVHRR imagery (Section 2.1.2.1). These results suggested to the authors that the influence of water clarity on the detection and capture of prey may play a key role in the mechanism(s) underlying the aggregation of tuna on the warm side of ocean fronts. The aggregation of commercial concentration of albacore in clear water on the oceanic side of fronts in nearshore areas found by Laurs *et al.* (1984) may reflect an inability of albacore to capture efficiently large, mobile prey in turbid coastal water and a dependence on food that has migrated or has been dispersed across the coastal–oceanic boundary. In offshore regions, the aggregation of albacore in relatively productive waters presumably occurs because relatively higher amounts of food organisms are present, yet the waters are clear enough for the albacore to detect them.

Studies have shown that both infrared and visible color data from satellites can define environmental limits on the spatial distribution of fishable aggregations of albacore and can do so more effectively than ship or aircraft data as used in the past. No other observational perspective so convincingly reveals the shapes, sizes, and continuity of mesoscale oceanic features, which are important in determining the distribution and availability of this highly migratory species.

2.3.2. Use of CZCS Imagery in a Study of Spawning of the Northern Anchovy. Fiedler (1983) extended the study of Lasker *et al.* (1981) in an investigation of the distribution of northern anchovy spawning observed on four intensive egg surveys of the Southern California Bight. AVHRR and CZCS data were used to describe mesoscale patterns of sea surface temperature and phytoplankton pigment concentration. Spawning anchovy were excluded from cold (<13.5–14°C) upwelled water to the south of Point Conception, a feature defining the northern boundary of this spawning area. This pattern was observed in February–April 1981 and February 1982, corroborating the results of Lasker *et al.* for April 1980.

Anchovy spawning to the south of San Diego in 1980–1982 was confined to a narrow band along the coast, with occasional extensions farther offshore. Sea surface temperature increased gradually offshore, sometimes exceeding 17°C, but no temperature fronts were observed in the AVHRR imagery to explain the spawning distribution. CZCS images, however, showed relatively high phytoplankton pigment concentrations in a coastal band with a sharp chlorophyll front defining the seaward extent of spawning activity (Fig. 12). In February 1982, spawning extended farther offshore in a jet of cool water with a high pigment concentration.

The spatial distribution of northern anchovy spawning can thus be defined by mesoscale patterns in satellite sea surface temperature and phytoplankton pigment images (Lasker *et al.*, 1981; Fiedler, 1983). While neither parameter alone is sufficient, both together may define the spatial distributions nearly completely. In general, the northern extent of spawning in the Southern California Bight, and the offshore extent north of Santa Catalina Island, are limited by cold, upwelled water advected south of Point Conception (Figs. 1 and 13). Spawning activity to the south is limited by low phytoplankton pigment levels in oceanic water found 20–100 km offshore, rather than by temperature (Fig. 12). However, these factors do not directly determine spawning success. Larval anchovy survival is thought to depend upon aggregations of nutritionally suitable food organisms in a stratified water column (Lasker, 1981). Satellite observations of relatively warm surface temperatures along with moderately high pigment levels may indicate a stratified water column with a mature phytoplankton community dominated by dinoflagellates. On the other hand, a well-mixed water column would be indicated by colder surface temperatures caused by upwelling or storm mixing; unsuitable food conditions would be indicated either by the low phytoplankton pigment levels of unproductive oceanic water or by very high levels associated with surface diatom blooms in recently upwelled water (Fiedler, 1983).

2.3.3. Pelagic Fishery in the Southern Benguela Current. Shannon *et al.* (1983) report on ocean-color experiments conducted off South Africa to relate satellite radiance measurements to the distribution of chlorophyll and to fish shoals. In the study, CZCS images were selected as being representative of seasons and events in the southern Benguela Current. Based on a relatively

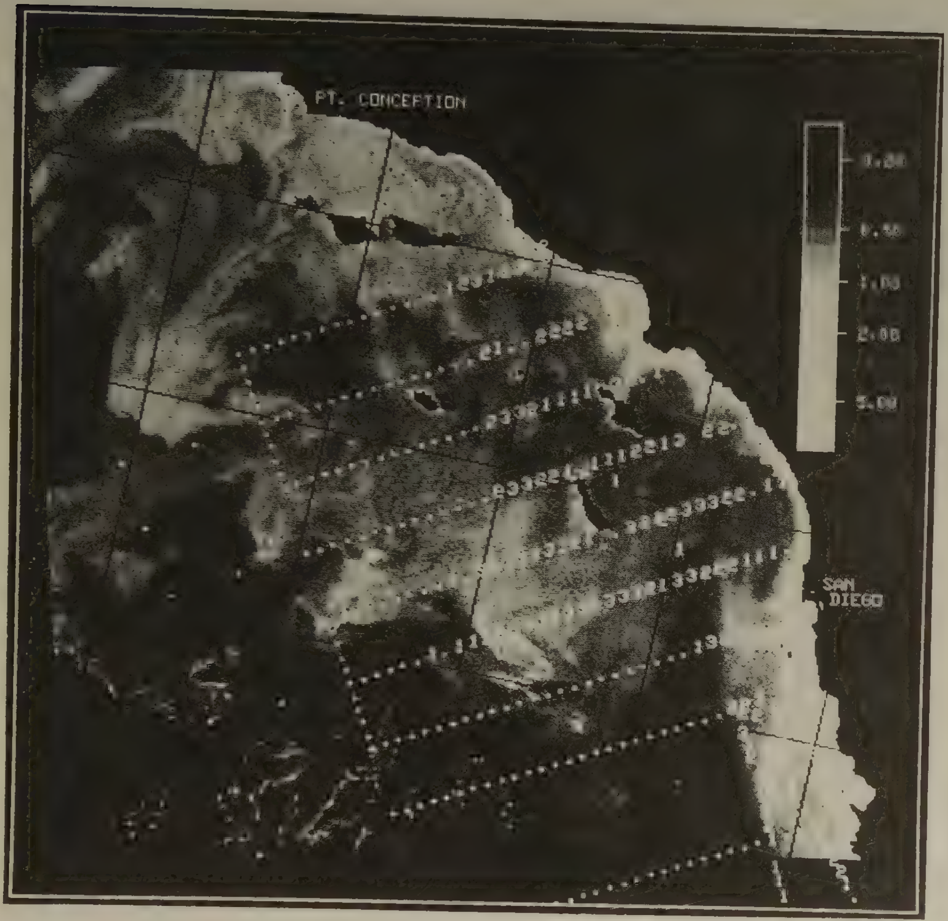

FIG. 12. Distribution of anchovy eggs superimposed on phytoplankton pigments (mg m^{-3}) from Nimbus-7 CZCS for the Southern California Bight. (From Fiedler, 1983.)

high correlation ($r = +0.89$) between near-surface chlorophyll concentrations measured aboard ship and those determined from CZCS data, the authors concluded that the satellite method could be used with confidence in the Benguela Current region to produce contoured fields of chlorophyll concentrations. The chlorophyll distribution patterns deduced from the CZCS radiances were found to be generally consistent with the known distribution and migration patterns of the main pelagic fish species off South Africa. For example, the location of a color front observed in the southern region between Cape Agulhas and Cape Point coincided approximately with the outer limit of the fish-catch locations of the five fish species that comprise the South Africa pelagic fishery.

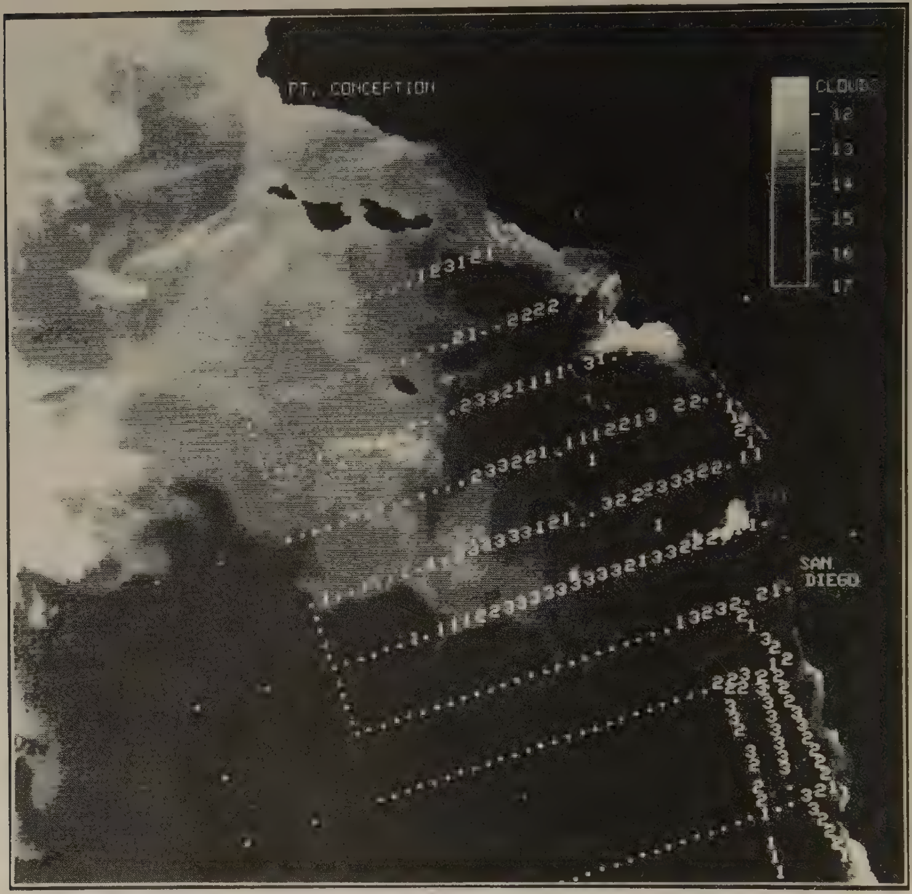

FIG. 13. Distribution of anchovy eggs superimposed on sea surface temperature from NOAA-6 AVHRR for the Southern California Bight. (From Fiedler, 1983.)

The authors caution that before definite conclusions can be drawn about the usefulness of satellite ocean-color imagery for the management of pelagic fish stocks in the southern Benguela Current, more CZCS images must be examined and additional work is needed on the feeding requirements of the different life stages of the various fish species. They do go on to state:

> Nevertheless, it does seem from the information available that the CZCS is a potentially powerful management tool. It could be used to provide an environmental index for fish availability, which in turn could be used to refine CPUE (catch-per-unit-effort) estimates or to direct fishing effort. It is also possible that chlorophyll measured by satellite could be used as a biological environmental input for fish recruitment models. Most certainly the accuracy of chlorophyll determination from satellites is adequate for it to be used in conjunction with thermal imagery and limited *in situ* monitoring to detect anomalous or episodic events [Shannon *et al.*, 1983].

3. Utilization of Satellite Data in Fisheries-Aids Products Distribution to Fishermen

Commercial fishermen have always been concerned about safety at sea and in making the best catch for the amount of time expended in search of productive fishing areas. In the last decade, commercial fishing on the high seas has become an increasingly competitive and economically risky business. To ensure a profit it has become necessary for the fishermen to utilize available technological and scientific knowledge to improve their catches. Accordingly, modern commercial fishermen require timely, reliable, and accurate meteorological and oceanographic information. Although the use of satellite imagery in the preparation of fisheries-aids products has been limited, it has the potential to contribute significantly in meeting the increased needs of fishermen for environmental information.

The first application of satellite-received data in fisheries-aids products was in a program initiated in 1971, wherein San Diego-based purse seine tuna fishermen operating in the eastern tropical Pacific were provided oceanographic and weather products prepared specifically to meet their requirements (Laurs, 1971). The tailored fisheries-aids products were transmitted via radio facsimile to cooperating fishermen on the fishing grounds who in turn radioed ashore surface weather observations and expendable bathythermograph subsurface temperature observations. In this program visual and infrared satellite images received by automatic picture transmission (APT) at the NMFS Laboratory in La Jolla, California, were analyzed in conjunction with surface observations. The APT photos were used to assist in determining the locations and movements of severe weather conditions which affected safety and/or hampered fishing operations. In addition they were used to define the location of the Intertropical Convergence Zone and regions of ocean surface temperature gradients which are important indicators in locating potential fish-productive ocean areas.

Subsequent to this endeavor, other projects and programs have used or are using satellite data in fisheries-aids products which are distributed to fishermen by a variety of mechanisms, including radio facsimile transmission, voice broadcast, U.S. mail, and telephone telecopier. Fiedler *et al.* (1984) review fisheries applications of satellite data in the eastern North Pacific.

3.1. Thermal Boundary Charts

Operational application of satellite data to commercial fishing operations began along the Pacific coast in 1975 (Breaker, 1981). Charts showing the locations of oceanic thermal boundaries are derived from satellite infrared imagery and provided to commercial and recreational fishermen for use in locating potentially productive fishing areas. Initially the charts were distributed by telephone telecopier and the U.S. mail to locations where fishermen would have the opportunity to examine them before starting a fishing trip. Radiofasimile has also been used to broadcast the charts directly to boats at sea since 1980. The thermal boundary charts are produced by the (1) NOAA Satellite Field Services Station in Redwood City, California, which produces two charts for the area between 28°N and 40°N; (2) NOAA National Ocean Services Center in Seattle, Washington, which produces a chart for the area between 40°N and 52°N; and (3) NOAA Alaska Ocean Services Unit in Anchorage, Alaska, which produces charts covering the area from 48°N to 75°N. Examples of sea surface thermal analysis charts off the Pacific west coast are found in Fig. 14.

The charts are prepared one to three times a week and are distributed primarily by USCG radiofacsimile broadcast. Fishermen use these charts to save time in searching for productive fishing areas associated with frontal features (Short, 1979; Breaker, 1981).

On the east coast, charts depicting oceanographic features and sea surface temperatures derived from satellite infrared thermal imagery and ship reports are available by mail to interested fishermen through the NMFS Atlantic Environmental Group (AEG) in Narragansett, Rhode Island (Chamberlain, 1981). These products are produced from interpretations and detailed environmental analyses done at AEG on the Oceanographic Analysis Charts which are produced routinely as a joint effort by the National Weather Service and National Environmental Satellite, Data, and Information Service (NESDIS). High-resolution infrared images from NOAA GOES satellite and ship reports are used in the preparation of the charts for waters off the Atlantic coast (see Fig. 15). Of particular interest to fishermen, these charts show (1) the offshore limit of shelf-water mass, in which most of the fishery resource species reside, and (2) the numbers, measurements, and persistence of warm-core Gulf Stream rings and the influence of these dynamic deep-ocean features on the relatively shallow waters of the fishing grounds.

NESDIS field stations in Miami, Florida, and Washington, D.C., prepare regionally oriented flow charts of the Gulf Stream from Florida to Maine three times weekly during October through May from GOES infrared images. In addition, a chart is prepared depicting the path of the Loop Current in the Gulf of Mexico from the Mississippi Delta to the east coast of Florida. The charts are distributed in cooperation with Sea Grant marine advisory serivce agents along the Atlantic coast and Gulf of Mexico by mail and telephone telecopiers and in some cases a narrative version is prepared for voice broadcast by local radio stations (Lowry and Leaky, 1982 and Flimlin, 1982). The charts have been particularly useful to lobster fishermen in reducing gear loss due to strong currents of Gulf Stream warm-core eddies, and to swordfish and recreational fishermen (Lowry and Leaky, 1982).

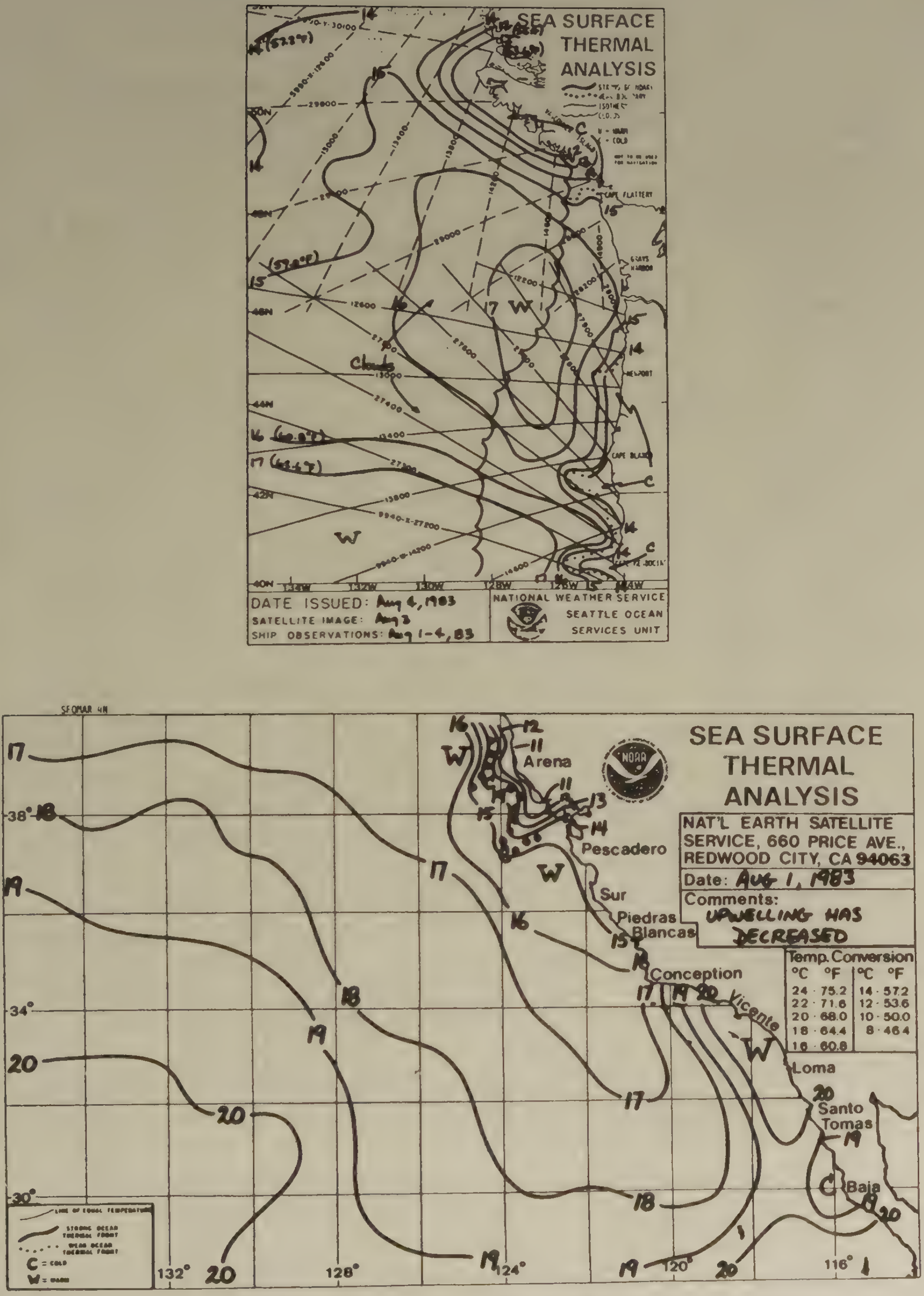
SEA SURFACE
THERMAL
ANALYSIS
ISOTHERM
CLOUDS
W = WARM
C = COLD
CAPE FLATTERY
GRAYS HARBOR
NEWPORT
CAPE BLANCO
CAPE MENDOCINO
Clouds
W
C
17 W
(57.2°F)
(57.2°F)
16 (60.8°F)
17 (62.6°F)
50N
48N
46N
44N
42N
40N
134W
132W
130W
128W
126W
124W
DATE ISSUED: Aug 4, 1983
SATELLITE IMAGE: Aug 3
SHIP OBSERVATIONS: Aug 1-4, 83
NATIONAL WEATHER SERVICE
SEATTLE OCEAN
SERVICES UNIT
SFOMAR 4N
SEA SURFACE
THERMAL
ANALYSIS
NAT'L EARTH SATELLITE
SERVICE, 660 PRICE AVE.,
REDWOOD CITY, CA 94063
Date: AUG 1, 1983
Comments:
UPWELLING HAS
DECREASED
Temp. Conversion
°C °F °C °F
24 · 75.2 14 · 57.2
22 · 71.6 12 · 53.6
20 · 68.0 10 · 50.0
18 · 64.4 8 · 46.4
16 · 60.8
Arena
Pescadero
Sur
Piedras
Blancas
Conception
Vicente
Loma
Santo
Tomas
Baja
W
W
W
C
17
18
19
20
16
15
14
13
12
11
38°
34°
30°
132°
128°
124°
120°
116°
LINE OF EQUAL TEMPERATURE
STRONG OCEAN THERMAL FRONT
WEAK OCEAN THERMAL FRONT
C = COLD
W = WARM

FIG. 14. Ocean frontal analysis charts for waters off the Pacific west coast.

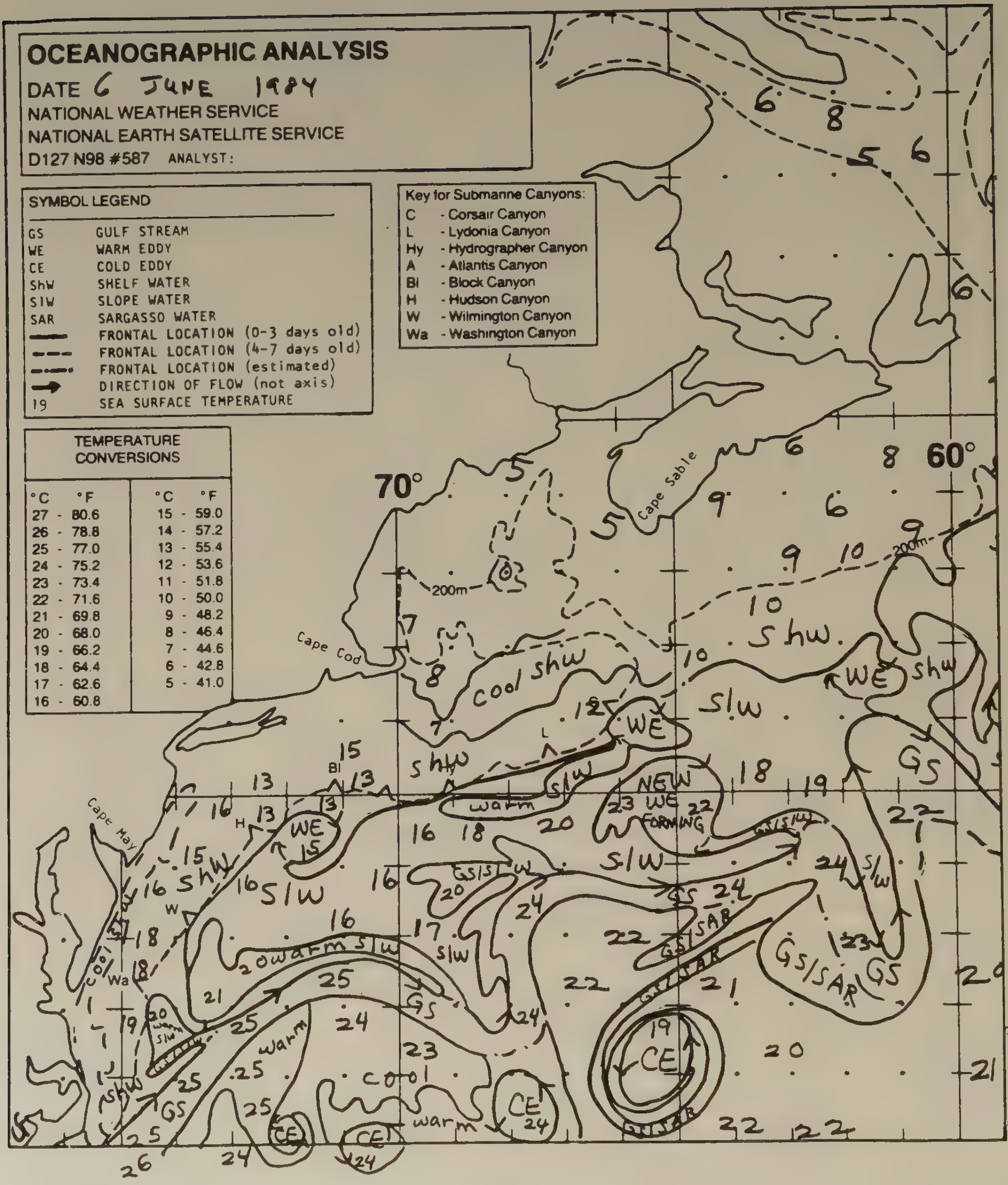
OCEANOGRAPHIC ANALYSIS
DATE 6 JUNE 1984
NATIONAL WEATHER SERVICE
NATIONAL EARTH SATELLITE SERVICE
D127 N98 #587 ANALYST:
SYMBOL LEGEND
GS GULF STREAM
WE WARM EDDY
CE COLD EDDY
ShW SHELF WATER
SlW SLOPE WATER
SAR SARGASSO WATER
FRONTAL LOCATION (0-3 days old)
FRONTAL LOCATION (4-7 days old)
FRONTAL LOCATION (estimated)
DIRECTION OF FLOW (not axis)
19 SEA SURFACE TEMPERATURE
Key for Submarine Canyons:
C - Corsair Canyon
L - Lydonia Canyon
Hy - Hydrographer Canyon
A - Atlantis Canyon
Bl - Block Canyon
H - Hudson Canyon
W - Wilmington Canyon
Wa - Washington Canyon
TEMPERATURE CONVERSIONS
°C °F
27 - 80.6
26 - 78.8
25 - 77.0
24 - 75.2
23 - 73.4
22 - 71.6
21 - 69.8
20 - 68.0
19 - 66.2
18 - 64.4
17 - 62.6
16 - 60.8
15 - 59.0
14 - 57.2
13 - 55.4
12 - 53.6
11 - 51.8
10 - 50.0
9 - 48.2
8 - 46.4
7 - 44.6
6 - 42.8
5 - 41.0
70°
60°
Cape Sable
Cape Cod
Cape May
200m
cool shw
shw
slw
WE
NEW WE FORMING
GS
GS/SAR
CE
warm
cool
20 warm slw

FIG. 15. Ocean frontal analysis chart for waters off the U.S. northeast coast.

3.2. Sea-Ice Forecast Charts

Sea-ice forecast charts derived from Nimbus-7 SMMR and polar-orbiting satellite infrared imagery are prepared by the NOAA Alaska Ocean Services Unit and transmitted by USCG radiofacsimile to fishermen and other marine users. Sea ice is an important seasonal feature in the Alaskan environment that can be monitored by satellite measurements (Weeks, 1981; McNutt, 1981). Sea ice affects commercial fishing activities by threatening vessel safety, limiting navigation and access, and damaging fishing gear. However, sometimes waters near the edge of pack ice can offer shelter or rich fishing grounds.

3.3. NASA/JPL Satellite Data Distribution System and Fisheries Demonstration Program to U.S. West Coast Fisheries

The prime motivation leading to the expanded use of satellite observations in fisheries-aids products has been provided by the Seasat Commercial Demonstration Program (SCDP) sponsored by NASA/JPL.[1] The SCDP offered a unique opportunity to evaluate the use of oceanographic satellite observations for support of commercial fisheries. The program led to the development of an operational Satellite Data Distribution System (SDDS) used to distribute oceanographic products to various components of the oceanographic user community (Montgomery, 1981). The distribution of products to fishermen included transmission of fishery advisory charts via radiofacsimile to tuna purse seiners operating in the eastern tropical Pacific, albacore tuna and salmon fishing vessels working along the Pacific west coast, and king crab vessels fishing in the Bering Sea.

The SDDS was planned and initially designed to distribute to marine users oceanographic products derived from measurements made by Seasat. When the Seasat prematurely failed, an alternative plan was devised to distribute subsets of the basic marine numerical analyses prepared at Navy Fleet Numerical Oceanographic Center (FNOC) in Monterey, California. The SDDS serves as a pilot demonstration from which general system requirements are being developed for future operational ocean-oriented satellite programs. The system also provides support for limited real-time experiments that test the utility of satellite observations in various maritime applications, including fisheries. The SDDS became operational in 1979 with products originating at FNOC. For fisheries users, the products consisted of numerically analyzed fields of winds, waves, and sea surface temperature. Although these products were operationally useful, they contained few or no satellite measurements and they were not tailored toward specific fisheries applications. Nevertheless, fishermen who utilized the products and kept evaluation logs estimated a 10–15% savings in search time as the result of using the products (Hubert, 1981).

---

[1] Capt. Paul M. Wolff (USN Retired) has played a key role in the development of operational techniques to integrate satellite observations of the ocean with conventional data to produce unique environmental charts for use by commercial fishermen.

In 1981, a plan was adopted to distribute new fisheries support products which built upon the existing SDDS system. The new products were tailored toward specific fisheries applications. They were prepared using a man/computer mix wherein additional knowledge and information, including satellite measurement, were incorporated. The program involved cooperative facilities and expertise in government, university, and commercial organizations. A schematic drawing showing the data sources and routing of the experimental fisheries-aids products, taken from Montgomery (1981), is given in Fig. 16.

Beginning in 1983, the responsibility for preparation of most of the marine advisory products was transferred to the NOAA National Ocean Service. Charts continue to be distributed to fishermen at sea by the radiofacsimile facilities shown in Fig. 15. However, except for the thermal boundary charts (Section 3.1), the products are now in a format for general use by marine users.

3.3.1. Ocean Color-Boundary Charts. Experimental ocean-color boundary charts based on Nimbus-7 CZCS imagery are distributed to U.S. West Coast fishermen under the auspices of the NASA/JPL Fisheries Demonstration Program (Montgomery, 1981). These charts (see example in Fig. 17) delineate strong gradients in the blue/green color ratio (channel 1/channel 3 radiances). They are produced at almost weekly intervals depending on cloud conditions, and cover coastal areas up to 700,000 km^2 between Guadalupe Island and Vancouver Island. Nimbus-7 CZCS passes along the Pacific coast are collected at the Scripps Institution of Oceanography (SIO) Satellite Oceanography Facility, processed in near-real time at the SIO Visibility Laboratory and transmitted by radiofacsimile the following day to fishing boats at sea from radio station WWD in La Jolla, California. Color photographs of the satellite images are also distributed by express mail to various fishing ports and to Sea Grant marine advisors in daily contact with fishermen. The color boundary charts and photographs are used primarily by commercial albacore and salmon fishermen, and recreational fishermen in southern California. Fishermen use the color boundary charts to locate color gradients or "breaks" which are important in determining potentially productive fishing areas.

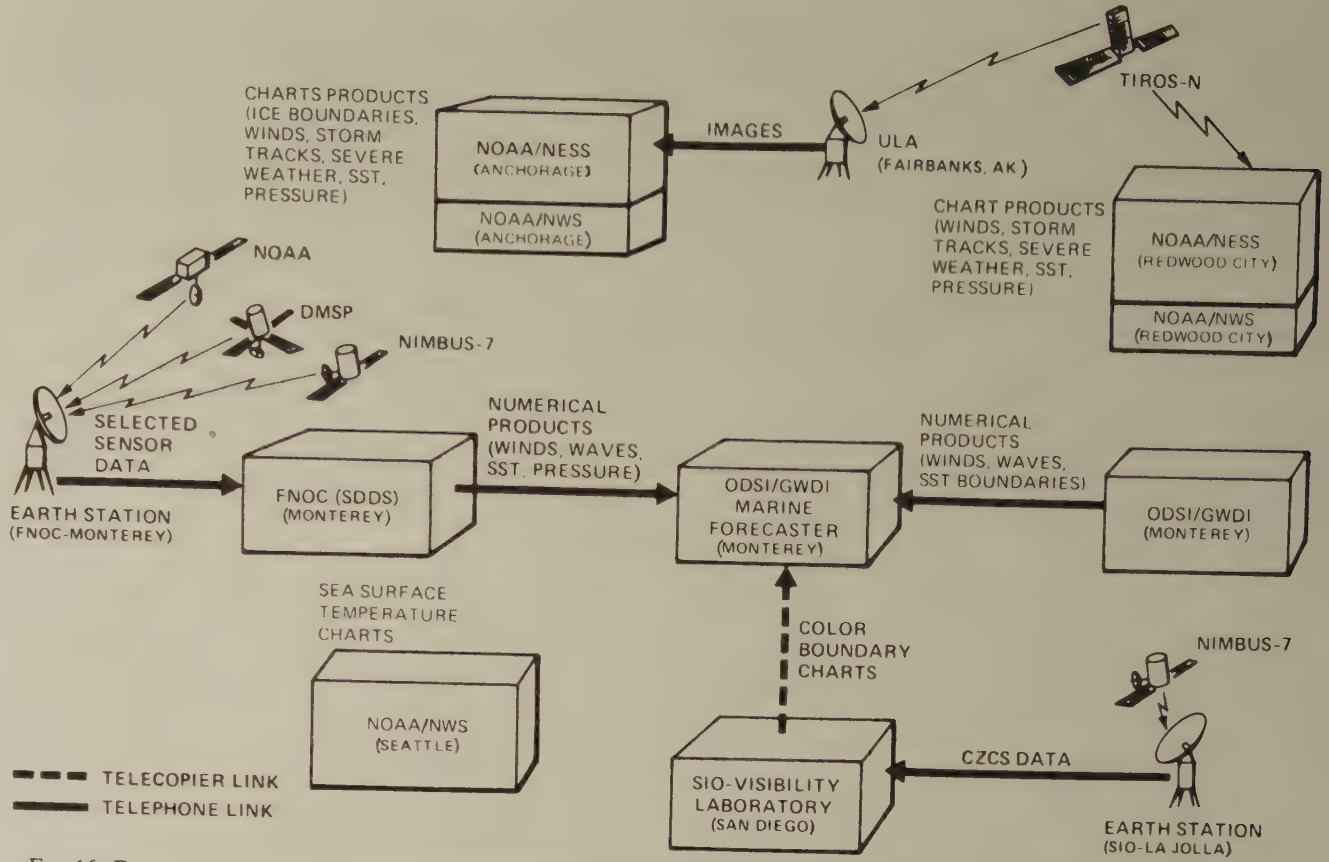
TIROS-N
CHARTS PRODUCTS (ICE BOUNDARIES, WINDS, STORM TRACKS, SEVERE WEATHER, SST, PRESSURE)
NOAA/NESS (ANCHORAGE)
NOAA/NWS (ANCHORAGE)
IMAGES
ULA (FAIRBANKS, AK)
CHART PRODUCTS (WINDS, STORM TRACKS, SEVERE WEATHER, SST, PRESSURE)
NOAA/NESS (REDWOOD CITY)
NOAA/NWS (REDWOOD CITY)
NOAA
DMSP
NIMBUS-7
SELECTED SENSOR DATA
EARTH STATION (FNOC-MONTEREY)
FNOC (SDDS) (MONTEREY)
NUMERICAL PRODUCTS (WINDS, WAVES, SST, PRESSURE)
ODSI/GWDI MARINE FORECASTER (MONTEREY)
NUMERICAL PRODUCTS (WINDS, WAVES, SST BOUNDARIES)
ODSI/GWDI (MONTEREY)
SEA SURFACE TEMPERATURE CHARTS
NOAA/NWS (SEATTLE)
COLOR BOUNDARY CHARTS
NIMBUS-7
SIO-VISIBILITY LABORATORY (SAN DIEGO)
CZCS DATA
EARTH STATION (SIO-LA JOLLA)
TELECOPIER LINK
TELEPHONE LINK

FIG. 16. Data sources and monitoring of experimental fisheries-aids products for the NASA/JPL Fisheries Demonstration Program to the U.S. West Coast fisheries. (From Montgomery, 1981.)

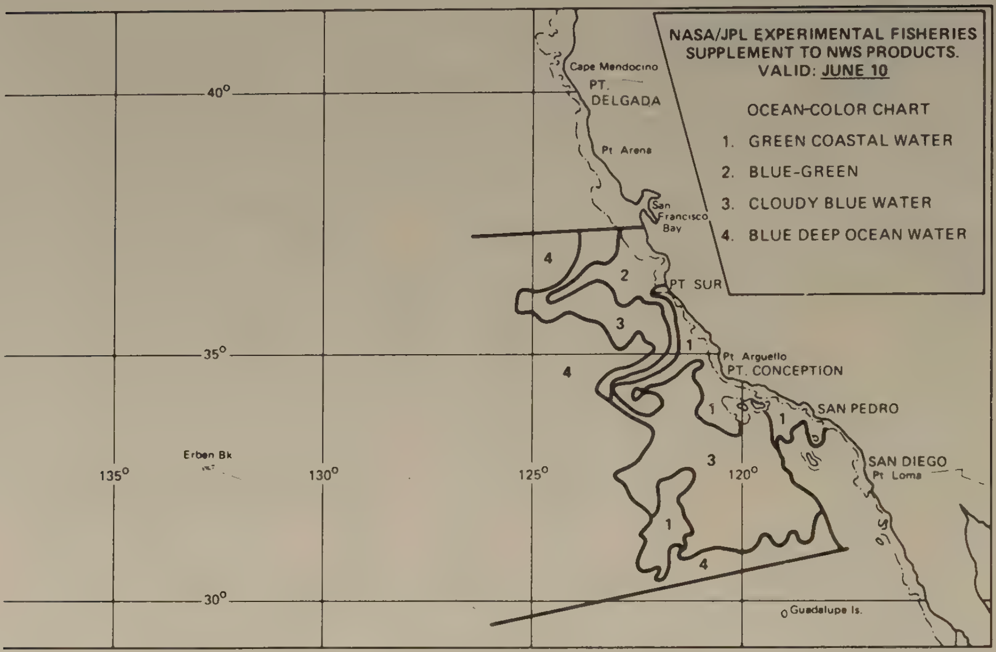
NASA/JPL EXPERIMENTAL FISHERIES
SUPPLEMENT TO NWS PRODUCTS.
VALID: JUNE 10
OCEAN-COLOR CHART
1. GREEN COASTAL WATER
2. BLUE-GREEN
3. CLOUDY BLUE WATER
4. BLUE DEEP OCEAN WATER
Cape Mendocino
PT. DELGADA
Pt Arena
San Francisco Bay
PT SUR
Pt Arguello
PT. CONCEPTION
SAN PEDRO
SAN DIEGO
Pt Loma
Guadalupe Is.
Erben Bk
40°
35°
30°
135°
130°
125°
120°
1
2
3
4

FIG. 17. Nimbus-7 CZCS-derived ocean-color chart tailored for commercial fishing applications. (From Montgomery, 1981.)

REFERENCES

Breaker, L. C. (1981). The application of satellite remote sensing to west coast fisheries. *J. Mar. Tech. Soc.* **15,** 32–40.

Brucks, J. T., Butler, J. A., Faller, K. H., Holley, H. J., Kemmerer, A. J., Leming, T. D., Savastano, K. J., and Vanselous, T. M. (1977). LANDSAT menhaden and thread herring resources investigation, final report. *NOAA, Nat. Mar. Fish. Serv., Southeast Fish. Center* Contr. No. 77-16F.

Brucks, J. T., Leming, T. D., and Burkett, S. B., Jr. (1984). A model investigation using high resolution SASS wind stress measurements to derive wind driven surface layer transport properties in the Gulf of Mexico. *NOAA Tech. Rep.* In press.

Carey, F. G., and Robinson, B. H. (1981). Daily patterns in the activities of swordfish, *Ziphias gladuis,* observed by acoustic telemetry. *Fish. Bull., U.S.* **79,** 277–292.

Chamberlain, J. L. (1981). Application of satellite infrared data to analysis of ocen frontal movements and water mass interactions off the northeast coast. *NW Atlantic Fish. Organ. NAFO Scr. Doc. 81/IX/123, Ser. No. 429.*

Clark, D. K. (1981). Phytoplankton pigment algorithms for the NIMBUS-7 CZCS. *In* "Oceanography from Space" (J. F. R. Gower, ed.), pp. 227–238. Plenum Press, New York.

Cram, D. L. (1979). A role for the NIMBUS-6 Coastal Zone Color Scanner in the management of a pelagic fishery. *Fish. Bull. S. Afr.* **11,** 1–9.

Ekman, V. W. (1905). On the Influence of the earth's rotation on ocean currents. *Ark. Mat. Astron. Fys.* 2, 1–53.

Fiedler, P. C. (1983). Satellite remote sensing of the habitat of spawning anchovy in the Southern California Bight. *CalCOFI Rep.* **24,** 202–209.

Fiedler, P. C. (1984a). Some effects of El Niño 1983 on the northern anchovy. *CalCOFI Rep.* **25,** 53–58.

Fiedler, P. C. (1984b). Satellite observations of El Niño along the U.S. Pacific coast. *Science* **224,** 1251–1254.

Fiedler, P. C., Smith, G. B., and Laurs, R. M. (1984). Fisheries applications of satellite data in the eastern North Pacific. *Mar. Fish. Rev.* **46**(3), 1–13.

Flimlin, G. (1982). A call saves time and fuel. *Sea Grant Today* **12,** 6.

Hela, L., and Laevastu, T. (1961). Fisheries hydrography. *Fish. News (London).*

Hela, L., and Laevastu, T. (1970). Fisheries oceanography. *Fish. News (London).*

Hubert, W. (1981). An evaluation of the utility of Seasat data to ocean industries. Final Report, Seasat Commercial Demonstration Program. *Jet Propulsion Laboratory Document No. 622-225.*

Kemmerer, A. J., Benigno, J. A., Reese, G. B., and Minkler, F. C. (1974). Summary of selected early results from ERTS-1 Menhadden experiment. *Fish. Bull.* **72,** 375–389.

Lasker, R. (1978). The relation between oceanographic conditions and larval anchovy food in the California Current: Identification of factors contributing to recruitment failure. *Rapp. P. v. Re'un. Cons. Int. Explor. Mer.* **173,** 212–230.

Lasker, R. (1981). Factors contributing to variable recruitment of the northern anchovy (*Engraulis mordax*) in the California Current: Contrasting years, 1975–1978. *Rapp. P. v. Re'un Cons. Int. Mer.* **179,** 375–388.

Lasker, R., Peláez, J., and Laurs, R. M. (1981). The use of satellite infrared imagery for describing ocean processes in relation to spawning of the northern anchovy (*Engraulis mordax*). *Remote Sens. Environ.* **11,** 439–453.

Laurs, R. M. (1971). Fishery-advisory information available to tropical Pacific tuna fleet via radio facsimile broadcast. *Comm. Fish. Rev.* **33,** 40–42.

Laurs, R. M., and Austin, R. (1984). Small-scale movements of albacore tuna in relation to oceanic frontal features observed in satellite. In preparation.

Laurs, R. M., Yuen, H. S. H., and Johnson, J. H. (1977). Small-scale movements of albacore, *Thunnus alalunga,* in relation to ocean features as indicated by ultrasonic tracking and oceanographic sampling. *Fish. Bull. U.S.* **73,** 347–355.

Laurs, R. M., Lynn, R. J., Nishimoto, R., and Dotson, R. (1981). Albacore trolling and longline exploration in eastern North Pacific waters during mid-winter 1981. *NOAA Tech. Memo. NMFS, NOAA-TM-NMFS-SWFC-10.*

Laurs, R. M., Fiedler, P. C., and Montgomery, D. C. (1984). Albacore tuna catch distributions relative to environmental features observed from satellite. *Deep-Sea Res.* **31**(6).

Leming, T. D. (1981). Ocean pelagics remote sensing applications. *Interim. Rep. NMFS* Intern. Document.

Lowry, B., and Leaky, T. (1982). Cooperation produces a flow of Gulf Stream information. *Sea Grant Today* **12,** 3–5.

McNutt, S. L. (1981). Remote sensing analysis of ice growth and distribution in the eastern Bering Sea. *In* "The Eastern Bering Sea Shelf: Oceanography and Resources (D. W. Hood and J. A. Calder, eds.), Vol. pp. 1, 141–165. U.S. Govt. Printing Office, Washington, D. C.

Maul, G. A., Williams, F., Roeffer, M., and Sousa, F. (1984). Remotely sensed patterns and variability of bluefin tuna catch in the Gulf of Mexico. *Oceanol. Acta* 7(4), 469–480.

Montgomery, D. R. (1981). Commercial applications of satellite oceanography. *Oceanus* **24,** 56–65.

Neill, W. H. (1976). Mechanisms of behavioral thermoregulation in fishes. Report of Workshop on the Impact of Thermal Power Plant Cooling Systems in Aquatic Environments. *Electric Power Res. Inst. Spec. Rep.* **38,** 156–169.

Parrish, R. H., and MacCall, A. D. (1978). Climatic variation and exploitation in the Pacific mackerel fishery. *Calif. Dept. Fish. Game, Fish. Bull.* **167,** 1–110.

Pearcy, W. G. (1973). Albacore oceanography off Oregon—1970. *Fish. Bull.* **71,** 489–504.

Roffer, M., Carl, M., and Williams, F. (1982). Atlantic bluefin tuna-oceanography-remote sensing. *Proc. Annu. Tuna Conf., 32nd, Inter-Am. Trop. Tuna Comm., La Jolla,* Ca.

Savastano, K. J., Pastula, E. J., Jr., Woods, E. G., and Faller, K. J. (1974). Preliminary results of fisheries investigation associated with Skylab-3. *Int. Symp. Remote Sens. Environ., 9th, Environ. Res. Inst. Mich.* (unpublished report).

Sette, O. E. (1961). Problems in fish population fluctuations. *CalCOFI Rep.* **8,** 21–24.

Shannon, L. V., Mostert, S. A., Walters, N. M., and Anderson, F. P. (1983). Chlorophyll concentrations in the southern Benguela current regions as determined by satellite (NIMBUS-7 Coastal zone colour scanner). *J. Plankton Res.* **5,** 565–583.

Short, K. (1979). How satellites can help you catch more fish and cut costs. *Natl. Fisherman* **60,** 38–39.

Smith, R. C., and Baker, K. S. (1982). Oceanic chlorophyll concentration as determined by satellite (NIMBUS-7 Coastal Zone Color Scanner). *Mar. Biol.* **66,** 269–279.

Smith, R. C., and Wilson, W. H. (1981). Ship and satellite bio-optical research in the California Bight. *In* "Oceanography from Space" (J. F. R. Gower, ed.), pp. 281–294. Plenum, New York.

Squire, J. L., Jr. (1961). Aerial fish spotting in the United States commercial fisheries. *Comm. Tech. Rev.* **23,** 1–7.

Squire, J. L., Jr. (1972). Apparent abundances of some pelagic marine fishes off the southern and central California coast as surveyed by an airborne monitoring program. *Tech. Bull. U.S.* **70,** 1005–1019.

Squire, J. L., Jr. (1982). Catch temperature for some important marine species off California: *NOAA Tech. Rep.* NMFS SSRF-759.

Thomas, J. P. (1981). Assessment of superflux relative to fisheries research and monitoring. *In* "Chesapeake Bay Plume Study" (J. W. Campbell and J. P. Thomas, eds.), *NASA Conf. Publ.* **2188,** 503–509.

Weeks, W. F. (1981). Sea ice: The potential of remote sensing. *Oceanus* **24,** 39–48.

8555

NOTES

Frequency of Increment Formation on Sagittae of North Pacific Albacore (*Thunnus alalunga*)

R. M. Laurs and R. Nishimoto

Southwest Fisheries Center La Jolla Laboratory, National Marine Fisheries Service, NOAA, La Jolla, CA 92038, USA

and J. A. Wetherall

Southwest Fisheries Center Honolulu Laboratory, National Marine Fisheries Service, NOAA, Honolulu, HI 96812, USA

Laurs, R. M., R. Nishimoto, and J. A. Wetherall. 1985. Frequency of increment formation on sagittae of North Pacific albacore (*Thunnus alalunga*). Can. J. Fish. Aquat. Sci. 42: 1552–1555.

An examination of sagittae from 116 albacore (*Thunnus alalunga*) caught in the North Pacific, injected with tetracycline, tagged, released, and subsequently recaptured in sport and commercial fisheries showed that detectable increments are formed on these otoliths at an average rate of 0.954 per day. We take this as a confirmation of daily increment formation in North Pacific albacore sagittae. The slight departure of observed mean increment counts from the expected rate of one per day may be due to an occasional interruption of otolith growth, or to a systematic bias in detecting daily increments or interpreting otolith microstructure. The estimated rate of detectable increment formation applies explicitly to albacore of fork lengths between about 50 and 100 cm. If the same rate holds for fish smaller than 50 cm, as is likely, most albacore taken in sport or commercial catches can be aged accurately by applying our methods and expanding the increment count by 5%.

Un examen des sagittae recueillies chez 116 germons (*Thunnus alalunga*) capturés dans le Pacifique nord — qui ont reçu une injection de tétracycline, puis ont été étiquetés, relâchés et recapturés au cours de pêches sportives et commerciales — a révélé que des zones de croissance discernables se forment sur ces otolithes à un taux moyen quotidien de 0,954. Les auteurs considèrent ce taux comme une confirmation de la formation d'une zone de croissance par jour dans les sagittae du germon du Pacifique nord. Le faible écart entre les dénombrements moyens observés de zones de croissance et le taux escompté, soit une zone par jour, peut être dû à un arrêt occasionnel de la croissance des otolithes ou à un biais systématique dans le dénombrement des zones de croissance quotidienne ou l'interprétation de la microstructure otolithique. Le taux estimatif de formation de zones de croissance discernables ne s'adresse qu'aux germons dont la longueur à la fourche varie d'environ 50 à 100 cm. Si le même taux s'applique, comme il est probable, aux poissons de taille inférieure à 50 cm, on pourra déterminer l'âge précis de la plupart des germons capturés par les pêcheurs sportifs et commerciaux à l'aide des méthodes présentées en ajoutant 5 % aux dénombrements des zones de croissance.

Received October 18, 1984
Accepted May 22, 1985
(J7985)

Reçu le 18 octobre 1984
Accepté le 22 mai 1985

In the decade since Pannella's pioneering studies of otolith microstructure (Pannella 1971, 1974), the validation and counting of daily growth increments on otoliths have enabled precise age determination in several species of teleosts, and more accurate modeling of life histories and the biological phenomena shaping them. In species with well-defined increments, it is now possible to study growth and other processes in considerable temporal detail. Under ideal circumstances one can estimate age-specific vital rates, and associate changes in these with coincident, small-scale perturbations of environmental factors or other influential variables. However, use of the otolith techniques must be preceded by rigorous testing of basic assumptions about increment identification and interpretation. In particular, as emphasized recently by Beamish and McFarlane (1983), the true frequency of increment formation must be established.

The otolith daily increment approach has shown particular promise for aging of tunas. Other methods based on scales, spines, or vertebrae have often produced inconclusive results (Shomura 1966). Daily formation of increments on tuna sagittae was first postulated for two tropical species, yellowfin tuna (*Thunnus albacares*) by Wild and Foreman (1980) and skipjack tuna (*Katsuwonus pelamis*) by Uchiyama and Struhsaker (1981). In experiments to estimate rates of increment deposition, Wild and Foreman confirmed the daily formation of increments in yellowfin tuna between 40 and 110 cm fork length

(FL), but rejected the hypothesis for skipjack tuna of 42–64 cm FL. Radtke (1983) demonstrated daily formation of increments on sagittae of skipjack larvae hatched and maintained for 5 d in captivity. He concluded that the first daily increment in skipjack is formed 1 d after hatching. Brothers et al. (1983) studied otolith microstructure in larvae of the Atlantic bluefin tuna (*T. thynnus*). They hypothesized that increments are deposited daily on bluefin sagittae, but were unable to pinpoint the age that the first increment appears. They found two or three diffuse increments which were presumably deposited prior to the onset of exogenous feeding, suggesting that the first increment is laid down at hatching or even earlier.

Our aim was to estimate the rate of increment deposition on sagittae of North Pacific albacore (*T. alalunga*), a temperate-water migratory tuna, with the ultimate objective of developing an accurate aging method. We based our study on a large sample of experimental fish growing in the wild over an extended period of time. These tuna may range over 40° of latitude between subtropical waters and those of the subarctic and undertake migrations as long as 6000 km in the span of a few months. In other species, similar investigations have usually been with a relatively small number of captive fish under controlled laboratory conditions (e.g. Campana and Neilson 1982; Neilson and Geen 1982; Volk et al. 1984). Only a few studies have been carried out in natural settings (e.g. the mark-and-recapture experiments by Wild and Foreman (1980) and Victor (1982)).

Experimental Methods

The increment deposition rate was estimated, in the manner of Wild and Foreman (1980), by counting increments on sagittae of albacore which had been caught at sea, injected with tetracycline, tagged, released, and later recaptured by fishermen, and then comparing the counts with the known periods of liberty.

In 1977 and 1978 albacore were caught in the eastern North Pacific, primarily by pole-and-line fishing, aboard the commercial fishing vessel *Linda*, chartered by the American Fishermen's Research Foundation.[1] Of those fish landed in good condition, 2544 were measured, injected intramuscularly with a 1.5-mL titre of 100 mg/mL oxytetracycline hydrochloride solution, tagged with a Floy[2] FT-1 "spaghetti" dart, and returned to the sea. The tetracycline, a calciphilic fluorochrome compound, was incorporated rapidly into the growing periphery of each sagitta, creating a mark on the developing otolith increment which could later be detected by its fluorescence under ultraviolet light (Milch et al. 1957; Weber and Ridgway 1962, 1967). By the end of 1982, 182 of the tagged albacore had been recaptured, and 125 returned with intact otoliths. The sagittae were dissected from these specimens, cleaned in household bleach, rinsed in distilled water, dried, and stored in darkness.

Without further preparation, the otoliths were mounted distal-side up in Plasticene, placed on a culture microslide, and viewed through a compound microscope at magnifications of 480 and 1250× under a 200-W mercury burner ultraviolet lamp. Immersion oil ($n_d 23^\circ\text{C} = 1.515$) was used to improve transparency and resolution. The excitation wavelength was restricted by BG-12, B(50-nm), and U(400-nm) filters. A 530-nm barrier filter reduced autofluorescence.

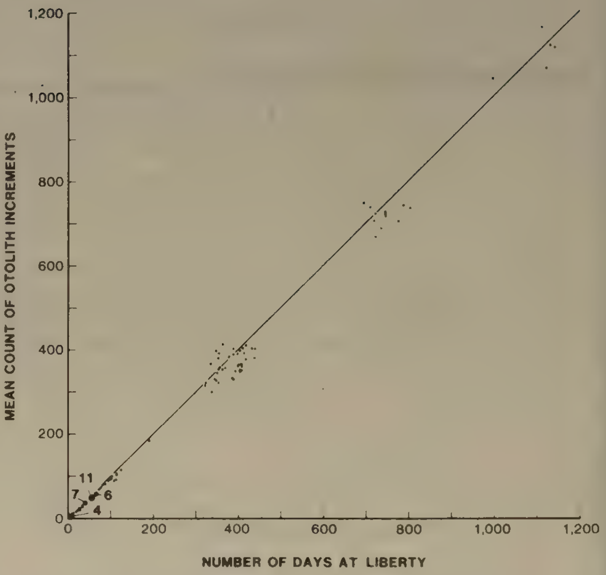

FIG. 1. Observed relationship between mean increment count on sagittae of albacore and days at liberty (points) after injection with tetracycline, and expected relationship under hypothesis of daily increment formation (line). Numerals indicate multiple observations at certain points.

Counts of increments were made by R.N. on a single otolith selected randomly from each pair of sagittae. When the selected otolith was damaged or otherwise unusable, the remaining one was read. Earlier experiments showed there was no difference between average increment counts on left and right sagittae. Increments were counted along the major axis of the post-rostrum, where definition of increments was best, from the proximal edge of the fluorescent mark to the margin of the otolith. The counting path was usually not linear. Rather, it varied with otolith topography and was selected to maximize the clarity of apparent growth structures. On thick otoliths, or on otoliths in which the growing surface had obscured (or had been obscured by) increments deposited earlier, frequent refocusing was necessary.

The fluorescing tetracycline marks were unmistakable in 116 of the 125 sagittae examined, and were nearly always confined to a single increment. Absence of a fluorescent mark could be attributed to procedural errors. In one batch of fish, the tetracycline solution used was outdated and improperly handled. In another, incorrect injection technique led to extrusion of the titre.

On sagittae from most smaller albacore or those recaptured within approximately a year of release, eight independent counts were made; otherwise four replicate counts were taken. Replicate increment counts and the exact time at liberty were known for 116 albacore. The number of days at liberty within the sample ranged from 7 to 1142. The smallest fish was 51 cm FL at release, the largest 97 cm FL at recapture.

Analysis and Discussion

Our analysis of increment counts showed that increment formation on sagittae of North Pacific albacore is almost certainly a daily event; an average of about 0.95 increments were counted for every day at liberty. The slight departure from a 1:1 relationship could be due to systematic undercounting of indistinct increments, or to periodic interruption of increment deposition.

---

[1] The American Fishermen's Research Foundation administers revenues derived from a landing assessment paid by the U.S albacore industry on U.S.-caught albacore.

[2] Reference to trade names does not imply endorsement by the National Marine Fisheries Service, NOAA.

Assuming a constant average rate of increment formation, we expected to find a linear relationship between mean increment count and days at liberty. Further, we supposed that both additive and multiplicative systematic counting errors could occur, as well as random errors proportional to the expected count. Preliminary statistical tests showed that the additive bias component was insignificant. Apparently there was no significant lag between injection and appearance of the tetracycline mark, and no other significant additive error (e.g. consistently misjudging the position of the tetracycline mark, or undercounting peripheral increments at a rate independent of the total number of increments present). An appropriate statistical model of the observed mean increment count for the ith fish was therefore established as

$$y_i = \alpha x_i\{1 + \beta + \epsilon_i\}$$

where

y_i = mean increment count
x_i = days at liberty
α = true increment deposition rate, assumed constant
β = proportional counting bias, assumed constant
ϵ_i = proportional counting error, with mean 0 and variance σ^2/m_i
m_i = number of replicate counts on the ith fish.

When constants are combined, the model reduces to a zero-intercept linear regression

$$y_i = \theta x_i + \epsilon_i'$$

where

$$\theta = \alpha(1 + \beta) \quad \text{and} \quad \epsilon_i' = \alpha x_i \epsilon_i .$$

Note that α and β are confounded; systematic undercounting will therefore introduce a negative bias into estimates of the deposition rate. The theoretical variance of the mean count is

$$V(y_i) = (\alpha x_i)^2\sigma^2/m_i ,$$

consistent with empirical estimates of $V(y_i)$ computed from the replicates. Assuming a normal distribution of the ϵ_i, we computed a maximum likelihood estimate of θ using an iteratively reweighted Gauss–Newton algorithm, minimizing

$$\sum_{i=1}^{n} w_i\{\epsilon_i'\}^2,$$

where w_i is a statistical weight proportional to $V^{-1}(y_i)$ and n is the number of fish in the sample (116).

For the entire sample the estimate of θ was $\hat{\theta} = 0.954$, with a computed standard error of $\hat{\sigma}_{\hat{\theta}} = 0.006$ (Fig. 1). The high precision in $\hat{\theta}$ reflects the low counting variability; the coefficient of variation among replicate counts was about 3%. Similar estimates of $\hat{\theta}$ were obtained when the data were partitioned by days at liberty; for albacore recaptured within 200 d of release, $\hat{\theta} = 0.941$ ($n = 51$), and for fish at large over 200 d, $\hat{\theta} = 0.969$ ($n = 55$). In each case the hypothesis that $\theta = 1$ was rejected (t-test, $P < 0.01$).

The significant departure from a 1:1 relationship could arise in at least two ways. First, increment deposition could occur with a daily rhythm, but be subject to occasional interruptions, so that the average rate of increment formation is less than 1 per day. Second, increments could be added daily, but be systematically undercounted by about 5% (i.e. assume $\beta = -0.05$). A reasonable case could be made for either undercounting or growth interruption, and indeed both factors could be involved.

We have no evidence to dismiss the possibility of systematic undercounting. However, if such a bias exists it apparently arises from difficulties in increment detection related to characteristics of the otolith or otolith preparation technique, rather than from systematic reader error. In analyses of the variation in mean increment counts recorded by different readers examining the same otoliths, between-reader differences were not significant when considered over a large number of otolith specimens. Because of the difficulties inherent in increment identification and interpretation, indistinct or atypical daily increments could have escaped detection, particularly with sagittae of the larger albacore, on which increments near the margin are usually thinner than those closer to the otolith core and detectable in whole mounts only by careful focusing. In other studies of tuna otoliths, further treatments, e.g. acid etching and acetate replication, have sometimes been applied to sagittae from larger fish in an effort to improve increment definition. However, the etching techniques carry the risk of removing increments from the otolith margin. This would have been particularly troublesome in our case, since counts were made from a mark sometimes quite near the edge.

Growth interruption might also have contributed to the slight departure of the average increment count from the expected count under the daily deposition hypothesis, but without further experiments this can only be surmised. Wild and Foreman (1980) reviewed the literature on frequency of increment formation, and noted that whereas daily formation of increments may be the rule for many species, in some fish subdaily structures are formed under certain conditions, and in some the deposition of increments is apparently interrupted due to starvation, maturation, or other factors.

The physiological basis of increment formation in sagittae is only sketchily known for a few species (Pannella 1980; Mugiya et al. 1981), and has not been studied in albacore. Experiments with a variety of species exposed to different light–dark cycles support the view that this process occurs with a daily periodicity tied to an internal clock whose pulse is entrained by diurnal cycles in various environmental factors (Taubert and Coble 1977; Tanaka et al. 1981). Some subdaily patterns of otolith growth have also been observed and irregular and periodic interruptions may occur (Pannella 1980). Studies involving diet manipulation in captive fish suggest that the regular deposition of identifiable increments may be checked by starvation, temporary chemical imbalances, or by competing nutritional or energetic needs. In some experiments, feeding schedules have been shown to affect the number of increments deposited per day (e.g. Brothers 1978; Methot and Kramer 1979; Neilson and Geen 1982). Since albacore are highly active, migratory fish (Graham and Laurs 1982), it is conceivable that in the natural environment, patchiness of food supply may produce fluctuations in growth rate, and disturb the regular deposition of increments. This view is supported by the striking patterns of variability in observed increment width, which could mirror, to some degree, changing growth conditions. In laboratory studies with other species it has been shown that food ration and prey type affect average increment width and rate of fish growth (e.g. Taubert and Coble 1977; Volk et al. 1984).

In their experiments with tagged skipjack tuna, Wild and Foreman (1980) found that otolith growth had been interrupted, to the extent that increment counts on sagittae underestimated days at large by about 25%. However, they considered it unlikely that in skipjack tuna growth retardation of such magnitude could be due to starvation, or to energy demands of migration. Instead, judging their fish to be sexually mature, they considered maturation and reproductive activity to be likely causes of the interruption in increment deposition. We found no evidence that this was so in albacore. Although all 116 fish in our analysis were considered immature (<85 cm FL) when tagged, 11 of these were presumed mature when recaptured, the largest being 97 cm FL. For these large fish the average ratio of mean increment count to days out was 0.954, identical to our estimate of θ for the whole sample.

The calibration of increment counts on sagittae of North Pacific albacore has been accomplished. Provided otolith increments accumulate at the same rate on albacore <51 cm FL as they do on larger ones, our results may be used to convert increment counts on albacore sagittae to estimates of absolute age (in days). The conversion factor, corrected for statistical bias in θ, is

$$\begin{aligned} C &= \hat{\theta}^{-1}\{1 - (\hat{\sigma}_{\hat{\theta}}/\hat{\theta})^2\} \\ &= 1.05. \end{aligned}$$

The assumption of daily increment deposition in very small fish will be difficult to test because North Pacific albacore have not been spawned in captivity and wild prejuveniles are rarely caught. However, the studies of otolith development in larvae of skipjack tuna by Radtke (1983), and in Atlantic bluefin tuna by Brothers et al. (1983), suggest it is reasonable to assume daily increment formation on albacore sagittae, at least from the time of yolk-sac absorption, i.e. within the first few days posthatching. Therefore, there is little doubt that counts of increments on sagittae of harvested albacore, adjusted upward by 5%, provide accurate estimates of absolute age.

Acknowledgments

We thank R. Dotson for conducting tagging operations, A. Wild and T. J. Foreman for advice on increment counting, A. Wild, R. D. Methot, and anonymous reviewers for helpful criticism of the manuscript, M. Yong for assistance with computing, the American Fishermen's Research Foundation for charter of the tagging vessel, and commercial and recreational fishermen for recovery and return of tagged and injected albacore.

References

BEAMISH, R. J., AND G. A. MCFARLANE. 1983. The forgotten requirements for age validation in fisheries biology. Trans. Am. Fish. Soc. 112: 735–743.

BROTHERS, E. B. 1978. Exogenous factors and the formation of daily and subdaily growth increments in fish otoliths. Am. Zool. 18(3): 631.

BROTHERS, E. B., E. D. PRINCE, AND D. W. LEE. 1983. Age and growth of young-of-the-year bluefin tuna, *Thunnus thynnus*, from otolith microstructure. U.S. Dep. Commer. NOAA Tech. Rep. NMFS 8: 49–59.

CAMPANA, S. E., AND J. D. NEILSON. 1982. Daily growth increments in otoliths of starry flounder (*Platichthys stellatus*) and the influence of some environmental variables in their production. Can. J. Fish. Aquat. Sci. 39: 1340–1347.

GRAHAM, J. B., AND R. M. LAURS. 1982. Metabolic rate of the albacore tuna *Thunnus alalunga*. Mar. Biol. (Berl.) 72: 1–6.

METHOT, R. D., JR., AND D. KRAMER. 1979. Growth of northern anchovy, *Engraulis mordax*, larvae in the sea. U.S. Natl. Mar. Fish. Serv. Fish. Bull. 77: 413–423.

MILCH, R. A., D. P. RALL, AND S. E. J. TOBIE. 1957. Bone localization of the tetracyclines. Natl. Cancer Inst. Monogr. 19: 87.

MUGIYA, Y., N. WATABE, J. YAMADA, J. M. DEAN, D. G. DUNKELBERGER, AND M. SHIMIZU. 1981. Diurnal rhythm in otolith formation in the goldfish, *Carassius auratus*. Comp. Biochem. Physiol. 68A: 659–662.

NEILSON, J. D., AND G. H. GEEN. 1982. Otoliths of chinook salmon (*Oncorhynchus tshawytscha*): daily growth increments and factors influencing their production. Can. J. Fish. Aquat. Sci. 39: 1340–1347.

PANNELLA, G. 1971. Fish otoliths: daily growth layers and periodical patterns. Science (Wash., DC) 173: 1124–1127.

1974. Otolith growth patterns: an aid in age determination in temperate and tropical fishes, p. 28–39. *In* T. B. Bagenal [ed.] Proceedings of an International Symposium on the Ageing of fish. Unwin Brothers, Surrey, England.

1980. Growth patterns in fish sagittae, p. 519–560. *In* D. C. Rhoads and R. A. Lutz [ed.] Skeletal growth of aquatic organisms. Plenum Press, New York, NY.

RADTKE, R. L., 1983. Otolith formation and increment deposition in laboratory-reared skipjack tuna, *Euthynnus pelamis*, larvae. U.S. Dep. Commer. NOAA Tech. Rep. NMFS 8: 99–103.

SHOMURA, R. S. 1966. Age and growth studies of four species of tunas in the Pacific Ocean, p. 203–219. *In* T. A. Manar [ed.] Proceedings of Governor's Conference on Central Pacific Fishery Resources, State of Hawaii.

TANAKA, K., Y. MUGIYA, AND J. YAMADA. 1981. Effects of photoperiod and feeding on daily growth patterns in otoliths of juvenile *Tilapia nilotia*. U.S. Natl. Mar. Fish. Serv. Fish. Bull. 79: 459–466.

TAUBERT, B. D., AND D. W. COBLE. 1977. Daily rings in otoliths of three species of *Lepomis* and *Tilapia mossambica*. J. Fish. Res. Board Can. 34: 332–340.

UCHIYAMA, J. H., AND P. STRUHSAKER. 1981. Age and growth of skipjack tuna, *Katsuwonus pelamis*, and yellowfin tuna, *Thunnus albacares*, as indicated by daily growth increments of sagittae. U.S. Natl. Mar. Fish. Serv. Fish. Bull. 79: 151–162.

VICTOR, B. C. 1982. Daily otolith increments and recruitment in two coral-reef wrasses, *Thalassoma bifasciatum* and *Halichoeres bivittatus*. Mar. Biol. (Berl.) 71: 203–208.

VOLK, E. C., R. C. WISSMAR, C. A. SIMENSTAD, AND D. M. EGGARS. 1984. Relationship between otolith microstructure and the growth of juvenile chum salmon (*Oncorhynchus keta*) under different prey rations. Can. J. Fish. Aquat. Sci. 41: 126–133.

WEBER, D. D., AND G. J. RIDGWAY. 1962. The deposition of tetracycline drugs in bones and scales of fish and its possible use for marking. Prog. Fish-Cult. 24: 150–155.

1967. Marking Pacific salmon with tetracycline antibiotics. J. Fish. Res. Board Can. 24: 849–865.

WILD, A., AND T. J. FOREMAN: 1980. The relationship between otolith increments and time for yellowfin and skipjack tuna marked with tetracycline. [In Engl. and Span.] Inter-Am. Trop. Tuna Comm. Bull. 17: 509–560.

8556

EGG PRODUCTION OF THE CENTRAL STOCK OF NORTHERN ANCHOVY, *ENGRAULIS MORDAX*, 1951-82

NANCY C. H. LO[1]

ABSTRACT

A model was developed for estimating daily production of eggs of northern anchovy from counts of the total numbers of eggs and size-frequency distribution of larvae. Estimates of egg production using this model were compared with three estimates based on the mortality rates of staged (aged) eggs. The model was used to calculate daily egg production of anchovy for a 24-year time series (1951-82) (data were collected each year from 1951 to 1966 and 1979 to present and every 3 years from 1966 to 1979). Comparisons of this index of stock abundance with ones based on the standing stock of larvae indicate that the present model is a better index of spawning biomass. It was found from the 1979-81 data that the eggs and larvae (<20 days) have different forms of instantaneous mortality rate (IMR): The larval IMR was age dependent, i.e., $z(t) = \beta/t$ for $t_c < t$ whereas the egg IMR was constant $z(t) = \alpha$ for $t < t_c$ where t_c is incubation time or yolk-sac absorption. Based upon this model, the daily egg production, and egg-larval mortality rates for larvae <20 days (<8 mm preserved length), were estimated for 1951-82 from data collected with 1 m ring nets and bongo nets. Egg production varies with stock size proportionally if the reproduction effort remains constant. The egg production is a better index of stock size than the larval abundance because the latter is subject to the inherent egg and larval mortality in addition to reproductive output.

Ichthyoplankton data have been used extensively for estimating biomass (or spawning biomass) of marine fish stocks (Murphy 1966; Ahlstrom 1968; Smith 1972). One of the tacit assumptions underlying most of the methods used for estimating biomass from ichthyoplankton data is that egg or larval mortality is constant among years. In recent years, however, it has become increasingly evident that egg and larval mortality is quite variable among years and among life stages (Ahlstrom 1954; Marr 1956; Colton 1959; Burd and Parnell 1972; Cushing 1973; Fager 1973; Harding and Talbot 1973). As a result, biomass indices based on standing stock of eggs or larvae are subject to a considerable bias if the interannual variability in mortality is not taken into account. In order to eliminate the bias, attempts were made to estimate the spawning biomass by using the egg production and reproduction parameters (Saville 1964; Beverton and Holt 1965; Ciechomski and Capezzani 1973). The basic model is

$$P_0 = B_a R(E/W) \qquad (1)$$

where P_0 = egg production at age zero,
B_a = spawning biomass,
R = proportion of spawning biomass being female,
E = average batch fecundity,
W = average mature female weight.

Equation (1) is adequate for species that spawn only once during a season. But for the multiple spawners, like northern anchovy, *Engraulis mordax*, one needs to include another adult parameter, the proportion of mature spawning female (F), in the equation (Parker 1980). Moreover, Parker chose to use egg production per day, as this could be easily estimated from a single cruise. Thus, the egg production model (EPM) for northern anchovy (or any multiple spawning stock) becomes

$$P_0 = B_a R \cdot F(E/W). \qquad (2)$$

Staged eggs are used to estimate the daily egg production (number of eggs per day) of the population (P_0) while adult fish are sampled to estimate the number of eggs produced per fish weight (E/W), sex ratio (R), and proportion of mature spawning female (F). This method is, without doubt, the best of all ichthyoplankton biomass estimation techniques. It is, however, a data rich method requiring both ichthyoplankton and adult sampling plus staging of eggs and various laboratory measurements which may not be available. In this report, I present an alternative method for

---

[1] Southwest Fisheries Center La Jolla Laboratory, National Marine Fisheries Service, NOAA, P.O. Box 271, La Jolla, CA 92038.

Manuscript accepted April 1984.
FISHERY BULLETIN: VOL. 83, NO. 2, 1985.

estimating biomass using conventional ichthyoplankton data rather than the extensive sets of specialized information required by the EPM method. This alternative method provides estimates of the daily egg production (P_0) and is referred to as the historical egg production (HEP) to distinguish it from the current EPM. This model for HEP requires only the standing stock of unstaged eggs, and the numbers of larvae in various length classes subsequently transformed into age classes using Gompertz growth curve (Zweifel and Hunter[2]; Methot and Hewitt[3]; Lo 1983). Daily egg production varies proportionally with the stock size if the reproduction effort of the population remains constant. The production of eggs by a stock is certainly a better index of stock size than the standing stock of larvae (Smith 1972) because both egg and larval mortality rates are considered in the former case.

In addition to development of the model, I provide a time series of northern anchovy HEP for 1951-82. This historical record of daily egg production rather than the EPM (Equation (2)) was used to estimate anchovy biomass for these past years because data were not available for all the female reproductive parameters until 1980 and none of the eggs have been staged. It would be unpractical and take years to do all the staging of eggs that would be required for all the years. The HEP is an unbiased index for the spawning biomass (B_a) of the anchovy population for those years if the annual reproductive output per fish weight has remained constant. I do not have sufficient data to validate the assumption of constant reproductive output although 1981-82 data do indicate so.

ASSEMBLY AND BIAS CORRECTION OF EGG AND LARVAL DATA

The northern anchovy spawning area lies off central and southern California and Baja California. The sampling area was divided into 23 regions covering 17.556×10^{11} m^2 (Fig. 1). The central anchovy stock is enclosed by eight regions (4, 5, 7, 8, 9, 11, 13, and 14) with a total of 5.703×10^{11} m^2 (Duke 1976[4]; Huppert et al. 1980). Because the peak spawning season of northern anchovy was usually February-April, daily egg production for the central stock northern anchovy was computed from egg and larval data (CalCOFI[5]) collected in January-April within these eight regions. The CalCOFI survey was conducted each year until 1966 after which the survey was conducted every 3 yr. Owing to various improvements in the design of the plankton nets over the past 20 yr (Smith and Richardson 1977; Stauffer and Picquelle 1980[6]), different calibration factors were necessary to standardize the catch of eggs and larvae taken in different nets: A 1 m ring net with 0.55 mm silk mesh was used until 1969 when it was replaced by a 1 m ring net with 0.505 mm nylon mesh; this net was used until 1978 when it was replaced by the bongo net of 0.505 mm nylon mesh. Beginning in 1979, a vertical tow of the 0.333 mm mesh, 25.23 cm diameter CalVET net (CalCOFI vertical egg net) (Hewitt 1983) was used along with the 0.505 mm mesh bongo net to collect egg and larval samples in order to estimate the northern anchovy spawning biomass using the egg production method (EPM) (Parker 1980). In addition to the bias in catch caused by the different mesh sizes, biases also existed due to avoidance of the net, water volume filtered through the net (measured by water flowmeter readings), growth rate of larvae, temperature dependent incubation time (in days), and proportion of larvae from each plankton sample sorted (Zweifel and Smith 1981; Lo 1983). All data (counts of eggs and larvae) were adjusted for the above biases, when it was appropriate, following the procedures outlined by Zweifel and Smith (1981).

Egg Data

The counts of unstaged eggs from each tow were adjusted to a standardized volume of water filtered per unit depth (0.05 m^3/1 m depth = 0.05 m^2 sea surface area = area sampled by the CalVET net). The adjusted egg counts per 0.05 m^2 sea surface area were then stratified by CalCOFI regions. A weighted mean egg count per 0.05 m^2 was computed as

---

[2] Zweifel, J. R., and J. R. Hunter. Unpubl. manuscr. Temperature specific equations for growth and development of anchovy, *Engraulis mordax*, during embryonic and larval stages.

[3] Methot, R. D., and R. P. Hewitt. 1980. A generalized growth curve for young anchovy larvae; derivation and tabular example. Natl. Mar. Fish. Serv., Southwest Fish. Cent. Admin. Rep. LJ-80-17, 8 p.

[4] Duke, S. 1976. CalCOFI station and region specifications. Natl. Mar. Fish. Serv., Southwest Fish. Cent. Admin. Rep. LJ-76-3, 37 p.

[5] CalCOFI. California Cooperative Ocean Fisheries Investigation, a program sponsored by the State of California. The cooperating agencies in the program are California Department of Fish and Game, National Marine Fisheries Service, and Scripps Institution of Oceanography, University of California.

[6] Stauffer, G. D., and S. J. Picquelle. 1980. Estimates of the 1980 spawning biomass of central subpopulation of northern anchovy. Natl. Mar. Fish. Serv., Southwest Fish. Cent. Admin. Rep. LJ-80-09.

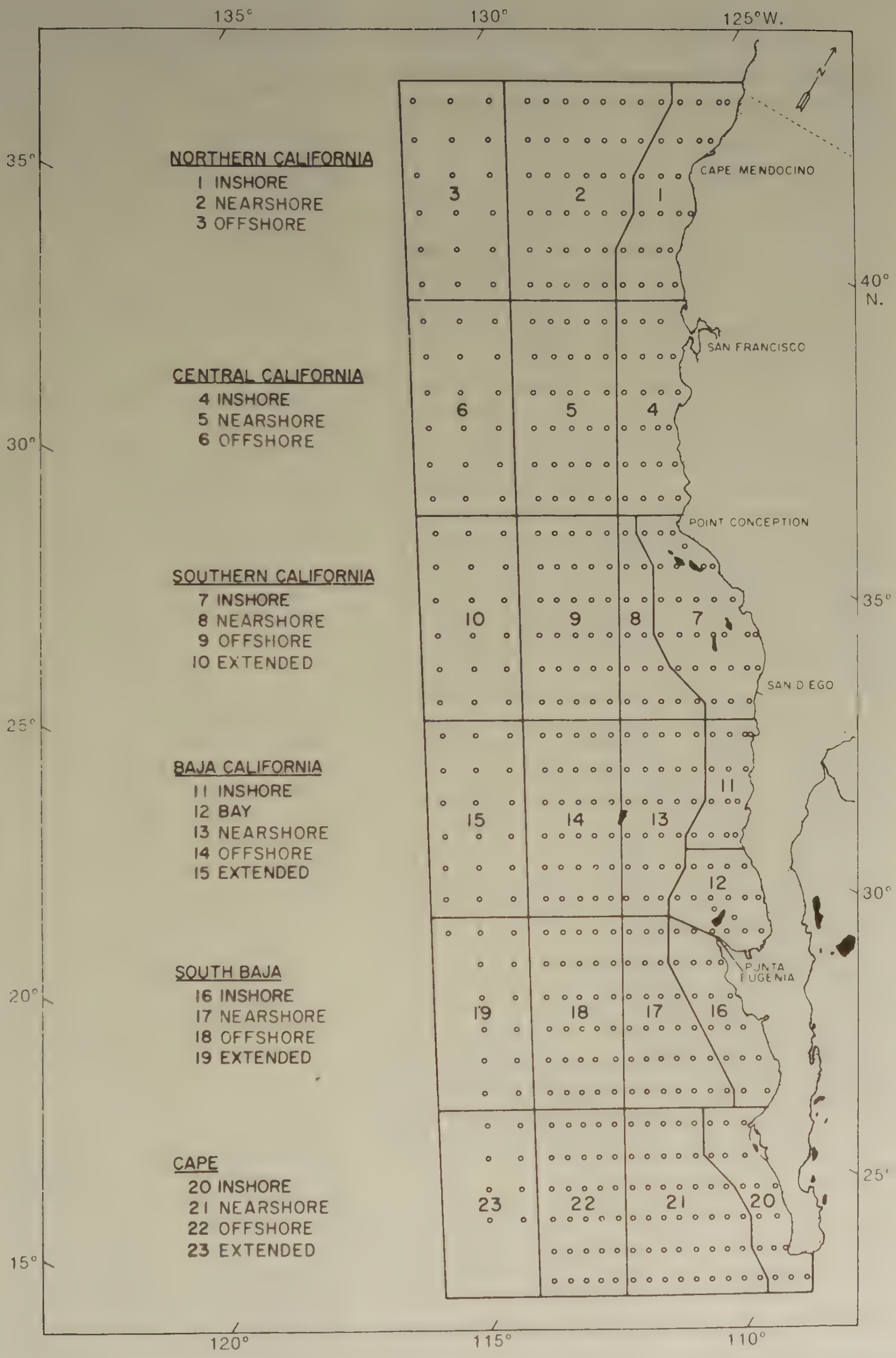
135°
130°
125°W.
35°
30°
25°
20°
15°
40° N.
35°
30°
25°
120°
115°
110°
N
NORTHERN CALIFORNIA
1 INSHORE
2 NEARSHORE
3 OFFSHORE
CENTRAL CALIFORNIA
4 INSHORE
5 NEARSHORE
6 OFFSHORE
SOUTHERN CALIFORNIA
7 INSHORE
8 NEARSHORE
9 OFFSHORE
10 EXTENDED
BAJA CALIFORNIA
11 INSHORE
12 BAY
13 NEARSHORE
14 OFFSHORE
15 EXTENDED
SOUTH BAJA
16 INSHORE
17 NEARSHORE
18 OFFSHORE
19 EXTENDED
CAPE
20 INSHORE
21 NEARSHORE
22 OFFSHORE
23 EXTENDED
CAPE MENDOCINO
SAN FRANCISCO
POINT CONCEPTION
SAN DIEGO
PUNTA EUGENIA
1
2
3
4
5
6
7
8
9
10
11
12
13
14
15
16
17
18
19
20
21
22
23

FIGURE 1.—Sampling area for estimating northern anchovy spawning biomass with CalCOFI sampling stations denoted by the open circles, and CalCOFI regions denoted by numbers (from Duke text footnote 4).

$$\bar{x}_w = \sum_i \bar{x}_i W_i, \quad \sum_i W_i = 1$$

where $\bar{x}_i$ is the adjusted mean egg count for region i and W_i is the relative area weight for region i.

Region	$nmi^2 \times 10^{-3}$	$m^2 \times 10^{-10}$	W_i
4	18	6.105	0.107
5	29	9.878	0.174
7	20	6.896	0.119
8	12	4.116	0.072
9	29	9.878	0.174
11	9	3.171	0.0538
13	21	7.122	0.126
14	29	9.866	0.174
Total	167	[1]57.031	1.00

[1] Sum is not equal to the total due to rounding error.

Zero catch was assumed for regions where no samples were taken because historical records show those regions usually had low densities of eggs and larvae. The weighted $\bar{x}_w$'s were also corrected for extrusion through the mesh by multiplying the catch by the ratio of the catch in a 0.150 mm CalVET net to the catch in the net used in a particular survey (r): $r = 3.6$ for 0.55 mm mesh silk 1 m ring net (1951-68), $r = 3.04$ for 0.505 mm mesh Nitex[7] 1 m ring net (1969-76), $r = 12.76$ for 0.505 mm mesh Nitex bongo net (1978-present) (Lo 1983). The 0.505 mm mesh bongo net seems to catch 4 times that of a 1 m ring net. The reason is unknown. (A field experiment was conducted in April 1983 to reestimate the extrusion rate of anchovy eggs from 0.505 mm mesh bongo net. The data have not been analyzed at the time of writing. Although the egg samples from bongo nets were used to compute the HEP, the bongo net is primarily used for catching anchovy larvae, whereas the CalVET net is the egg sampler. The discrepancy between bongo and 1 m ring net is not of major concern for the current anchovy biomass estimation.) The standing stock of eggs per 0.05 m² is then

$$m_{t_I} = \bar{x}_w \cdot r$$

and

$$\mathrm{var}(m_{t_I}) = \mathrm{var}(\bar{x}_w) r^2 + \bar{x}_w^2 \,\mathrm{var}(r)$$

where m_t is the standing stock of eggs (and larvae) up to age t days from fertilization. Here t_I is the duration of incubation.

The size of standing stock of eggs depends on not only egg production rate and mortality rate but also the duration of incubation (or the incubation time), which is a function of sea temperature. The average temperature for all positive egg tows (tows which contain one or more anchovy eggs) over January-April in each year was used to estimate incubation time (t_I) using the equation (Lo 1983)

$$t_I = (18.73\, e^{-0.125\, \mathrm{temp}})$$

where t_I = incubation time in days,
temp = temperature in degrees centigrade.

Both the standing stock of eggs (m_{t_I}) and the incubation time (t_I) are essential in computing the time series of daily egg production. The temperature in January-April ranges from 11° to 19°C. The long-term average temperature from January to April is 14.25°C, thus the average incubation time is 3.15 d.

Larval Data

The anchovy larvae from all years were measured to the nearest 0.5 mm preserved length. For the purpose of estimating mortality rate, larval data were grouped into 2.5 mm, ranging 2-3.0 mm; 3.75 mm, 3.5-4.0 mm; 4.75 mm, 4.5-5.0 mm; ... for larvae < 30 mm. Each preserved length was first converted to a live standard length using a shrinkage formula based on the tow duration (Theilacker 1980), and then converted to age (t days) using a two-cycle Gompertz growth curve. The first cycle is from hatching to yolk-sac absorption, a temperature-dependent growth curve, and the second cycle is from yolk-sac absorption to 22 mm larvae, a food-dependent growth curve (Zweifel and Hunter footnote 2; Methot and Hewitt footnote 3; Lo 1983). Larval abundance by length (age) group was estimated using a negative binomial weighted model (Bissell 1972; Zweifel and Smith 1981) which incorporates the "effective sampler size" (relative sampler bias). All larval abundance data were adjusted to conform to the following standard conditions: no extrusion, no day-night difference in avoidance, and a constant water volume filtered per unit depth. These data were converted to daily production (P_t) by dividing the total number of larvae in each length group by the duration (the number of days larvae remain within each length group). It was necessary to compute a weighted mean of larval production ($_wP_t$) because the number of net tows was not proportional to the area size: The daily larval production (P_{t_j}, t_j) was estimated first for each of the three subareas (j = 1: inshore = regions 7 and 11; j = 2: nearshore = regions 4, 8, and 13; and j = 3: offshore = regions 5, 9, and 14) (Fig. 1). The data set ($_wP_t, t$) was used for final fitting of the mortality curve where $_wP_t = \sum_{j=1}^{3} P_{t_j} u_j$, and u_j = 0.17, 0.31, and 0.52 for j = 1, 2, and 3, the relative area sizes. The unweighted average age $\bar{t}$ over three areas was used because little variation exists among t_j's (Fig. 2).

---

[7] Reference to trade names does not imply endorsement by the National Marine Fisheries Service, NOAA.

DAILY LARVAL PRODUCTION PER 0.05 m^2 ($_wP_t$) AT AGE t, 1979

PRESERVED SIZE (mm)	LIVE SIZE (mm)	(t) AVE AGE (day)	($_wP_t$) DAILY LARVAL PROD /0.05 m^2
2.50	3.26	4.91	0.518
3.75	4.57	8.60	0.121
4.75	5.69	11.58	0.0838
5.75	6.27	14.15	0.0665
6.75	7.63	16.41	0.0481
7.75	8.87	18.62	0.036

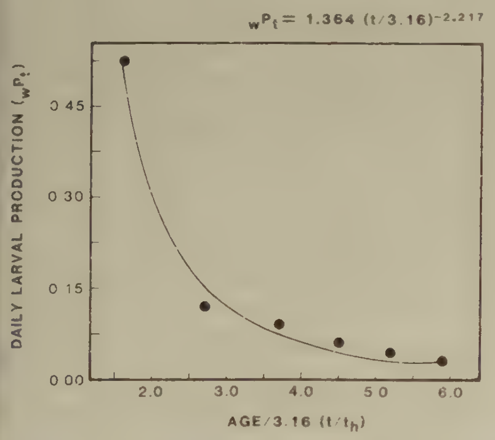

FIGURE 2.—Weighted daily larval production ($_wP_t$) and age in days (t) of northern anchovy and the fitted larval mortality curve based upon Equation (8B) for larvae < 20 d old, 1979.

MODEL

If a cohort of eggs (larvae) is followed and N_t s defined as the number of eggs (larvae) at age days), then the ratio N_t/N_0 measures the survival probability at age t: $S(t; z(t)) = P(T > t; z(t))$. The sample ratio n_t/n_0 estimates he survival probability $S(t)$ where $z(t)$, the instantaneous mortality rate (IMR), is defined as $\lim_{\Delta t \to 0} \frac{P(t < T < t + \Delta t \mid T > t)}{\Delta t}$. If the sample data n_t, t) are taken from a single cohort and the form of $S(t)$ is known, both N_0 and $z(t)$ can be estimated through $n_t = n_0\ S((t); z(t))$. Assuming that the standing stock of eggs and larvae represents a single cohort (with stable age distribution) as it ages, then (N_t, t) can be estimated from the number of eggs and larvae in various stages (lengths) which are later converted to age in the sample. Hewitt (1982) conducted a simulation study to check for possible bias in larval mortality rate caused by seasonal changes in the intensity of spawning of northern anchovy which violates the assumption of a stable age distribution. He found that mortality was overestimated in the beginning (January-February) of a season when spawning was increasing and underestimated at the end (May-July) when spawning was decreasing. When the larval numbers were accumulated over the entire season, these two biases tended to cancel out. Therefore, the stable age distribution is a reasonable assumption if the egg and larval sample covers the entire season. To compute larval mortality for each year, I chose larval data from January to April to be consistent with the current sampling scheme. According to Hewitt's study, the larval mortality may be overestimated. However, because only young larvae (<8 mm preserved length) were considered in the model, the upward bias is slight. The number of eggs and larvae at various stages or length classes (n_{t_i}), as mentioned in a previous section, was further adjusted for the duration in days that eggs (larvae) remained in a particular stage or length class (d_i), i.e., $P_{t_i} = n_{t_i}/d_i$. The quantity P_{t_i} is egg (larval) production per day per unit area (e.g., 0.05 m^2) at age t_i, the average age of eggs (larvae) in the ith stage (length) class (Farris 1960; Saville 1964; Harding and Talbot 1973; Ciechomski and Capezzani 1973). (In later sections, the subscript i is dropped, thus (P_t, t) is used in place of (P_{t_i}, t_i).)

The model is based on the form of the mortality curves of northern anchovy eggs and those for anchovy larvae, the form of the curve for eggs and larvae being distinctly different. The daily egg and larval production P_t is modeled by three survivorship functions S_1, S_2, and S_3:

$$P_t = P_0 S(t) = \begin{cases} P_0\, S_1(t; z_1(t)) & t \le t_c \quad \text{(3A)} \\ P_{t_c}\, S_2(t; z_2(t) \mid T > t_c) & t_c < t < 20\,\text{d} \quad \text{(3B)} \\ P_{t_k}\, S_3(t; z_3(t) \mid T > t_k) & t_k < t \quad \text{(3C)} \end{cases}$$

with the IMR

$$z(t) = \begin{cases} z_1(t) & t \leq t_c \\ z_2(t) & t_c < t < 20\ \mathrm{d} \\ z_3(t) & t_k < t \end{cases}$$

where $S_2(t; z(t) \mid T > t_c) = P(T > t; z(t) \mid T > t_c)$,
t_c is the age when the form of IMR changes,
t_k is max t_i for $t_i < 20$ d where t_i is the average age for the ith length class.

The quality of larval data for larvae older than 20 d is questionable because older larvae avoid the net (Hewitt 1982). The forms of $z_3(t)$ and $S_3(t)$ for $t > 20$ d are unknown at the present time. Therefore, only the mortality of eggs and larvae < 20 d old was assessed.

The IMR, $z(t)$, relates to the survivorship function $S(t)$, by definition, in the form of

$$\begin{aligned} S(t) &= e^{-\int_0^t z(u)du} \\ &= \begin{cases} e^{-\int_0^t z_1(u)du} = S_1(t) & t \leqslant t_c \\ e^{-\int_0^t z(u)du} = e^{-\int_0^{t_c} z_1(u)du - \int_{t_c}^{t} z_2(u)du} & t_c < t < 20 \\ \phantom{e^{-\int_0^t z(u)du}} = S_1(t_c)\, S_2(t \mid T > t_c) & \\ \phantom{e^{-\int_0^t z(u)du}} = S_2(t). & \end{cases} \end{aligned} \tag{4}$$

The critical age t_c was defined as the age before which $z(t) = z_1(t)$, after which $z(t) = z_2(t)$. P_t and t from larval data were used to estimate both P_{t_c} and $z_2(t)$ through Equation (3B) after $S(t)$ is specified. Both larval production (P_{t_c}) and the standing stocks of eggs and larvae up to age t_c (m_{t_c}) were then used to estimate P_0 and $z_1(t)$ through Equation (3A) as below:

$$m_{t_c} = \int_0^{t_c} P_t\, dt = \int_0^{t_c} P_0\, S_1(t; z_1(t))\, dt \tag{5A}$$

and

$$P_{t_c} = P_0\, S_1(t_c; z_1(t)). \tag{5B}$$

Now I have two Equations (5A) and (5B) to be solved simultaneously for the unknowns P_0 and the parameters in $z_1(t)$. An iterative procedure was used to obtain estimates of P_0 and $z_1(t)$. Clearly, the selection of the function forms of $z_1(t)$ and $z_2(t)$ are important in obtaining accurate estimates of P_0 and P_{t_c}.

Anchovy Mortality Curves and Estimation of Egg Production

Daily egg and larval production per 0.05 m^2 and their ages (P_t, t) were estimated for 1979-81 to model the mortality curves $P_0\, S_1(t)$ and $P_{t_c}\, S_2(t \mid T > t_c)$ (Equation (3)). The egg data were collected in vertical net tows from 70 m with the

TABLE 1.—Daily egg and larval production per 0.05 m^2 (P_t) at various ages in days (t) sampled from CalVET and bongo tows, and the estimates of five parameters: egg production at age zero ($\hat{P}_0$), egg mortality ($\hat{\alpha}$), larval mortality coefficient ($\hat{\beta}$), larval production at hatching ($\hat{P}_I$) and incubation time in days (t_I) in CalCOFI regions 4, 7, 8, and 11, January-April 1979-81.

	1979[1]		Live standard length (mm)	1980		1981		Live standard length (mm)[2]	
	t	P_t		t	P_t	t	P_t		
Eggs	0.4167	10.79		0.4167	9.34	0.4167	5.64		CalVET net
	0.9167	4.36		0.9167	9.22	0.9167	7.66		
	1.4167	4.91		1.4167	6.34	1.4167	4.87		
	1.9167	4.58		1.9167	4.71	1.9167	6.05		
	2.4167	6.87		2.4167	5.14	2.4167	4.84		
	2.9167	3.63							
Larvae	3.73	2.64	3.03	2.94	2.26	3.14	3.23	3.03	
				4.08	2.39	4.35	2.99	3.59	
				5.91	0.99	6.25	2.10	4.13	
				7.69	0.86	8.08	1.84	4.66	
	4.72	1.96	3.26	3.05	2.35	3.10	5.29	2.97	Bongo net
	8.32	0.48	4.17	5.65	1.04	5.86	1.96	4.00	
	11.49	0.35	5.69	8.90	0.49	9.22	1.10	5.13	
	13.90	0.25	6.77	11.47	0.39	11.79	0.72	6.23	
	16.24	0.19	7.83	13.83	0.26	14.01	0.54	7.30	
	18.31	0.13	8.87	15.91	0.21	16.01	0.53	8.35	
				17.99	0.15	18.22	0.41	9.38	
$\hat{P}_c$		9.76	[3](2.82)	11.46	(1.27)	6.73	(1.32)		
$\hat{\alpha}$		0.33	(0.28)	0.38	(0.09)	0.11	(0.13)		
$\hat{\beta}$		1.83	(0.14)	1.24	(0.17)	1.19	(0.17)		
$\hat{P}_I$		3.59	(0.18)	2.51	(0.19)	4.81	(0.42)		
t_I		3.21		2.96		2.85			

[1] Not weighted by area size.
[2] For both 1980 and 1981 larval data.
[3] Asymptotic standard error in parentheses.

CalVET net, and the larval data were collected with both bongo oblique tows and the CalVET nets. The egg and larval catches by age group were standardized, that is, corrected for possible biases caused by extrusion through the mesh, day-night difference in avoiding the net, variation in the amount of water filtered, and the variation of larval growth rates which is both temperature and food dependent (Methot 1981; Lo 1983). The standardized daily egg and larval production estimates per 0.05 m^2 sea surface area in CalCOFI regions 4, 7, 8, and 11 for January-April 1979-81 are given (Table 1, Fig. 3).

The IMR for the egg stage was believed to be constant, $z_1(t) = \alpha$, (Stauffer and Picquelle footnote 6), whereas the IMR for larval stage was found to be age dependent $z_2(t) = \beta/t$ (a Pareto hazard function, Johnson and Kotz 1970). I first calculated sample IMR $z(t_i) = (P_{t_{i-1}} - P_{t_i})/(t_i - t_{i-1})/P_{t_i}$ which is an approximation of $dS(t)/dt/S(t)$ at various t for $0 < t < 20$ d using 1980 standardized egg and larval data listed in Table 1. The 1980 egg and larval production and age data were further combined so that $z(t) > 0$ for all t. The relationship between $z(t)$ and t determined the function form of $z(t)$ (Table 2). The $z(t)$'s were

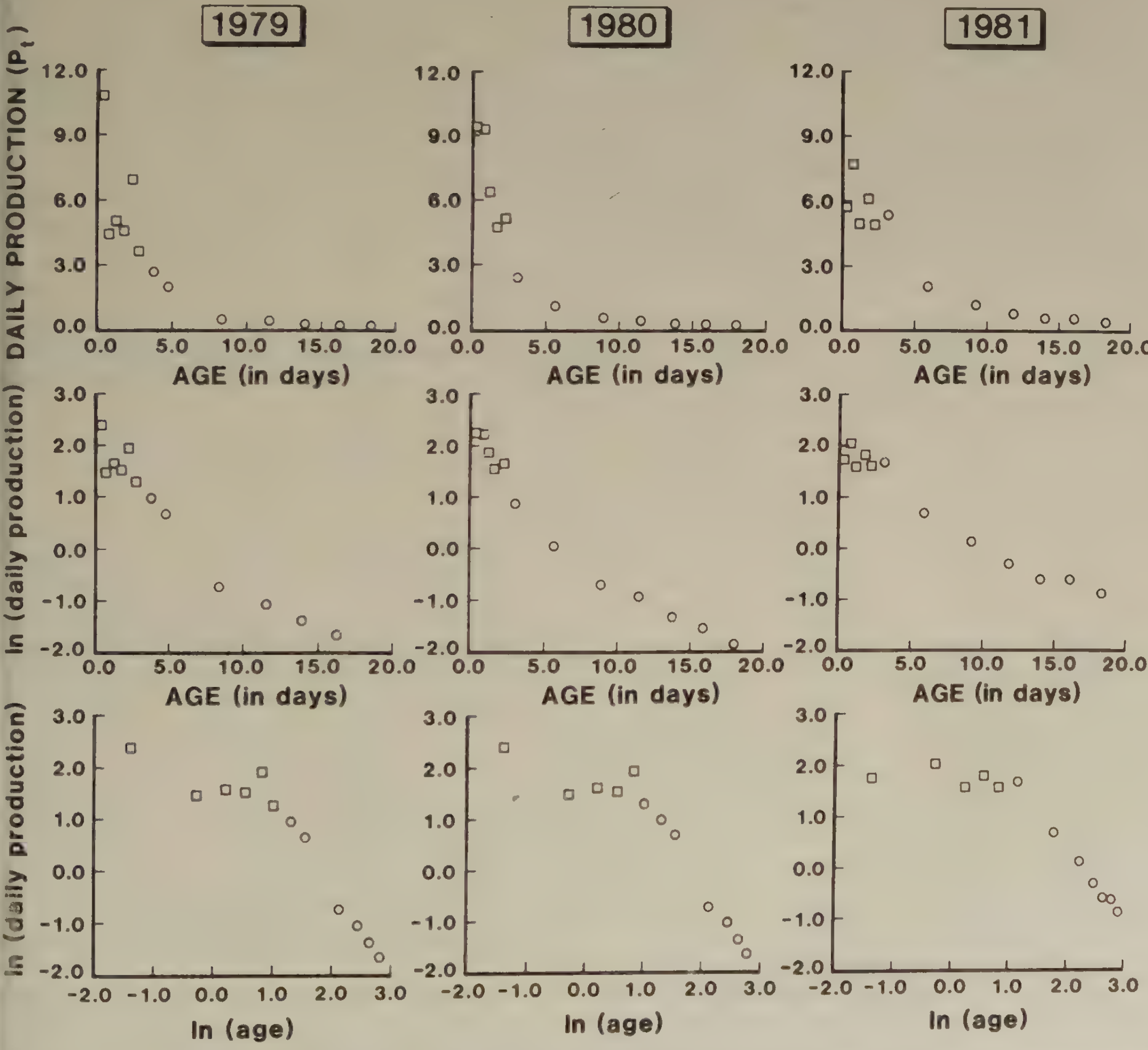

FIGURE 3.—Daily egg and larval production of northern anchovy per 0.05 m^2 (P_t) by age in days (t) and their log transformations ($\ln(P_t)$), 1979-81. A linear relationship between $\ln(P_t)$ and t indicates a constant instantaneous mortality rate (IMR) and a curvilinear relationship between $\ln(P_t)$ and t indicates an age dependent IMR. Squares are egg data and open circles are larval data.

TABLE 2.—The instantaneous mortality rates of anchovy eggs and larvae <20 days ($z(t_i)$) by age in days ($\bar{t}_i$) computed from the daily egg and larval production estimates (P_{t_i}) and age (t_i), 1980. $z(t) = 0.0060 + 1.63/t$ is the function fitted to the data in the last two columns for $t > 4.5$ d.

i	t_i (d)	Daily egg and larval production P_{t_i}	$P_{t_{i-1}} - P_{t_i}$	$t_i - t_{i-1}$	$\bar{t}_i = (t_i + t_{i-1})/2$	$z(t_i)$[1]
1	0.67	9.28				
2	1.67	5.53	3.75	1.00	1.17	0.40
3	2.60	3.70	1.83	0.93	2.14	0.36
4	3.57	2.37	1.33	0.97	3.09	0.37
5	5.65	1.04	2.28	2.08	4.61	0.46
6	5.91	0.99	0.05	0.26	5.78	0.18
7	7.69	0.86	0.13	1.78	6.80	0.07
8	8.90	0.49	0.37	1.21	8.30	0.36
9	11.47	0.39	0.10	2.57	10.19	0.08
10	13.83	0.26	0.13	2.36	12.65	0.14
11	15.91	0.21	0.05	2.08	14.87	0.09
12	17.99	0.15	0.06	2.08	16.95	0.14

[1] $z(t_i) = (P_{t_{i-1}} - P_{t_i})/(t_i - t_{i-1})/P_{t_i}$.

quite constant for egg and larvae <4.5 d old and decreased thereafter. For t values >4.5 d, the function $z(t) = a + b/t$ fit the data best. Based upon the function relationship $z(t) = b/t$ (the intercept a is not distinguishable from zero and thus was dropped), I have the IMR $z(t)$:

$$z(t) = \begin{cases} \alpha & t \leq t_c \\ \beta/t & t_c < t < 20. \end{cases} \tag{6}$$

Applying Equation (6) to Equation (4) leads to

$$S(t) = \begin{cases} S_1(t) = e^{-\alpha t} & t \leq t_c \\ S_2(t) = e^{-\alpha t_c}\left(\dfrac{t}{t_c}\right)^{-\beta} & t_c < t < 20. \end{cases} \tag{7}$$

Combining Equations (3) and (7) one has

$$P_t = \begin{cases} P_0\, e^{-\alpha t} & t \leq t_c \\ P_0\, e^{-\alpha t_c}\left(\dfrac{t}{t_c}\right)^{-\beta} & t_c < t < 20 \end{cases} \tag{8A}$$

$$= P_{t_c}\left(\frac{t}{t_c}\right)^{-\beta}. \tag{8B}$$

To validate both Equations (8A) and (8B), logarithms of P_t and t were plotted: $\ln(P_t)$ against t should be a straight line for $t \leq t_c$ (Equation (8A)) and $\ln(P_t)$ against $\ln(t)$ should be a straight line for $t_c < t < 20$ (Equation (8B)) (Fig. 3). This was true for egg and larval production from 1979 to 1981. The determination of t_c, the age at which IMR changes, was subjective. Two values of t_c were used: One was the time of hatching or the duration of incubation (t_I) which is temperature dependent and the other was the average age of yolk-sac larvae (embryonic period) $t_c = t_{ys} : t_{2.5\,\text{mm}}$ = age at preserved length 2.5 mm (about 5 d old). When t_c was considered equivalent to the incubation time ($t_c = t_I$), the egg stages were considered as one group with constant IMR; and when t_c was equivalent to average age of the yolk-sac larvae ($t_c = t_{ys}$), egg stages and yolk-sac length class(es) were considered as one group with constant IMR. In either case, P_{t_c} was estimated from the fitted curve

$$P_t = P_{t_I}\left(\frac{t}{t_I}\right)^{-\beta}, \text{i.e., } \hat{P}_{t_c} = \hat{P}_{t_I}\left(\frac{t_c}{t_I}\right)^{-\hat{\beta}}.$$

Substitution of Equation (7) in Equation (5) gives

$$m_{t_c} = \begin{cases} \displaystyle\int_0^{t_c} P_0\, e^{-\alpha t}\, dt = P_0(1 - e^{-\alpha t_c})/\alpha & \alpha > 0 \\ t_c \cdot P_0 & \alpha = 0 \end{cases} \tag{9A}$$

$$P_{t_c} = P_0\, e^{-\alpha t_c} \tag{9B}$$

where m_{t_c} is the standing stock of eggs and larvae up to age t_c. Equation (9A) divided by Equation (9B) results in

$$q = \begin{cases} m_{t_c}/P_{t_c} = (e^{\alpha t_c} - 1)/\alpha = \mathrm{h}(\alpha) & \alpha > 0 \\ t_c & \alpha = 0 \end{cases} \tag{10}$$

where $t_c = t_I$ or t_{ys} and q is the ratio of standing stock of eggs and larvae up to age t_c to the larval production P_{t_c}. The estimated IMR, $\hat{\alpha}$, was obtained by an iterative procedure using Equation (10). The estimated egg production obtained by rearranging the terms in Equation (9B):

$$\hat{P}_0 = \hat{P}_{t_c} \cdot e^{\hat{\alpha} t_c}.$$

The approximate variance of $\hat{\alpha}$ and $\hat{\beta}$ were computed in the appendix.

TIME SERIES ESTIMATES OF HISTORICAL EGG PRODUCTION (HEP)

The HEP per 0.05 m^2 (P_0) and the egg IMR (α) for the central stock of northern anchovy in the first 4 mo of the year, 1951-82, were estimated based upon Equations (9B) and (10). For years after 1978, catch data were available for CalVET and bongo nets, but I chose to use samples from bongo nets because only bongo or similar nets (1 m ring nets) were used for sampling eggs and larvae prior to 1978.

Two series of HEP estimates were constructed. Series 1 assumed a constant IMR for the egg stage with $t_c = t_I$, whereas series 2 with $t_c = t_{ys}$ assumed a constant IMR throughout the embryonic period (Table 3). Both P_{t_I} and $P_{t_{ys}}$, the daily larval production at hatching and yolk-sac stage, were obtained from the fitted line of Equation (8B) with $t_c = t_I$.

Under series 1, nearly half of the egg IMR ($\hat{\alpha}$) were negative (11 out of 24 yr). This was because the egg IMR depended on the value of q through Equation (10) where $q = m_{t_I}/P_{t_I}$. However, judging from Equation (10), $q = t_I$ for $\alpha = 0$. Therefore for those years where $q < t_I$, egg IMR would be less than 0. The small q's could result from the underestimated m_{t_I} or overestimated P_{t_I} or both. The poor results of IMR ($\hat{\alpha}$) were likely due to the underestimation of m_{t_I}. As a result, the standing stock of eggs and that of yolk-sac larvae were combined into one group in series 2, to eliminate the negative IMR's.

TABLE 3.—Two time series of estimated historical egg production ($\hat{P}_0$), and egg mortality ($\hat{\alpha}$), larval mortality coefficient ($\hat{\beta}$), mean egg abundance (m_{t_I}), mean egg and yolk-sac larval abundance ($m_{t_{ys}}$), January-April, and mean larval abundance (L_a) per 0.05 m², 1951-82 with standard error in parentheses.

	[1]Series 1		[1]Series 2					
Year	Daily egg production $\hat{P}_0$	Egg mortality $\hat{\alpha}$	Daily egg production $\hat{P}_0$	Egg mortality $\hat{\alpha}$	Larval mortality coeff. $\hat{\beta}$	Mean egg abundance m_{t_I}	Mean yolk-sac larval abundance $m_{t_{ys}}$	Mean larval abundance[2] L_a
1951	0.006 (0.024)	0.03 (1.34)	0.012 (0.116)	0.23 (2.18)	0.85 (0.15)	0.02 (0.03)	0.03 (0.03)	0.04
1952	0.002 (0.003)	−0.57 (0.35)	0.017 (0.107)	0.09 (1.27)	0.88 (0.20)	0.02 —	0.07 (0.01)	0.04
1953	0.026 (0.019)	−0.08 (0.20)	0.066 (0.180)	0.19 (0.54)	0.95 (0.10)	0.11 (0.03)	0.21 (0.03)	0.011
1954	0.031 (0.026)	−0.48 (0.26)	0.168 (0.188)	0.12 (0.24)	1.16 (0.07)	0.24 (0.08)	0.61 (0.08)	0.17
1955	0.026 (0.028)	−0.77 (0.32)	0.316 (0.393)	0.07 (0.26)	1.01 (0.17)	0.39 (0.12)	1.27 (0.14)	0.19
1956	0.122 (0.114)	0.33 (0.26)	0.146 (0.647)	0.33 (0.88)	0.88 (0.24)	0.25 (0.12)	0.36 (0.12)	0.11
1957	0.148 (0.040)	−0.12 (0.31)	0.364 (0.423)	0.20 (0.25)	0.94 (0.10)	0.54 (0.23)	1.09 (0.24)	0.26
1958	0.966 (0.481)	0.40 (0.18)	1.274 (1.182)	0.43 (0.23)	0.88 (0.08)	1.61 (0.45)	2.44 (0.93)	0.33
1959	0.444 (0.267)	−0.11 (0.21)	0.992 (0.822)	0.23 (0.20)	1.18 (0.16)	1.47 (0.36)	2.68 (0.38)	0.34
1960	0.678 (0.535)	−0.18 (0.26)	1.765 (0.774)	0.24 (0.10)	1.80 (0.06)	2.78 (0.99)	4.85 (0.99)	0.34
1961	0.446 (0.669)	0.25 (0.43)	0.653 (0.635)	0.29 (0.22)	1.55 (0.16)	0.94 (0.28)	1.59 (0.28)	0.26
1962	0.443 (0.297)	−0.18 (0.18)	1.314 (1.171)	0.19 (0.18)	1.08 (0.23)	2.09 (0.50)	4.15 (0.58)	0.67
1963	1.404 (0.690)	0.16 (0.15)	2.275 (0.991)	0.28 (0.09)	0.81 (0.04)	3.57 (0.93)	5.92 (0.93)	0.95
1964	3.681 (1.956)	0.43 (0.15)	4.147 (2.681)	0.42 (0.13)	1.44 (0.21)	6.39 (1.80)	8.55 (1.81)	0.65
1965	0.778 (0.559)	−0.45 (0.21)	4.019 (1.176)	0.19 (0.06)	2.42 (0.12)	6.48 (1.75)	12.78 (1.75)	1.04
1966	3.540 (1.660)	0.26 (0.14)	5.256 (1.799)	0.42 (0.07)	1.84 (0.04)	7.82 (2.11)	10.61 (2.11)	0.80
1969	0.876 (0.557)	−0.42 (0.19)	3.821 (1.062)	0.19 (0.06)	2.15 (0.08)	6.16 (1.53)	12.14 (1.53)	0.67
1972	0.639 (0.356)	−0.09 (0.16)	1.657 (0.804)	0.25 (0.11)	1.73 (0.11)	2.56 (0.66)	4.52 (0.67)	0.62
1975	15.320 (11.608)	0.36 (0.22)	19.691 (10.364)	0.44 (0.11)	1.88 (0.20)	30.06 (4.40)	39.14 (14.41)	0.81
1978	10.524 (4.566)	0.64 (0.15)	10.738 (4.484)	0.59 (0.10)	1.66 (0.10)	13.58 (3.67)	16.60 (3.67)	0.29
1979	4.258 (2.215)	0.36 (0.16)	5.426 (2.616)	0.48 (0.10)	2.22 (0.15)	8.06 (2.39)	10.05 (2.39)	0.39
1980	2.338 (1.427)	0.37 (0.22)	2.671 (1.260)	0.36 (0.08)	1.22 (0.03)	4.12 (1.46)	6.48 (1.46)	0.40
1981	3.95 (2.658)	0.36 (0.24)	4.376 (2.084)	0.38 (0.08)	1.53 (0.03)	6.88 (2.70)	10.29 (2.70)	0.63
1982	1.941 (1.230)	0.15 (0.20)	3.294 (1.367)	0.36 (0.09)	1.81 (0.04)	4.93 (1.70)	7.33 (1.70)	0.46

[1] Series 1 and 2 are two methods used for estimating daily egg production (P_0). Series 1 assumed a constant IMR for egg stage whereas series 2 assumed a constant IMR for egg through yolk-sac larval stage.

[2] Computed from annual larval abundance for the central subpopulation (Table 2, Stauffer and Charter 1982).

Under series 2, P_0 and α were estimated based upon $q = m_{t_{ys}}/P_{t_{ys}}$ (Equations (9B) and (10)), with $t_c = t_{ys}$. The average age of yolk-sac larvae ($t_{ys} = t_{2.5\ \mathrm{mm}}$) was 4.7 d. All q's were greater than t_{ys}, thus $\hat{\alpha}$'s were all positive.

The HEP (P_0) for both series have the same trend: a gradual increase from the early 1950's to middle 1960's, thereafter fluctuating until 1975 when it reached the peak value at 15.32/day per 0.05 m^2 (series 1) or 19.69/day per 0.05 m^2 (series 2). From 1978, HEP decreased to the present level of 1.94/day per 0.05 m^2 (series 1) and 3.29/day per 0.05 m^2 (series 2) (Table 3, Fig. 4). The approximate standard error of the estimated HEP (P_0) and egg mortality ($\hat{\alpha}$) is large for the early years and small for the recent years, possibly because of the poor quality of early egg data, or an insufficiency of the delta method to estimate the variance.

For the purpose of verification, HEP (P_0) from the two series based upon the egg-larval mortality model and the egg production at age 0 estimated from the current EPM (Stauffer and Picquelle footnote 6) were compared for 1980-82 where adequate egg and larval samples were available (Table 4). The P_0's from the two series of HEP and the current EPM were not significantly different, nor were the egg mortality rates. However, the point estimates of P_0's from the current EPM were lower than those estimated from the two series. The reason for the lower values is unknown at the moment. This could be due to random fluctuation of the statistics. The current EPM estimates of P_0 were much more precise than those derived from the historical egg-larval mortality model, whereas the precision of egg mortality rate from both methods was similar.

TABLE 4.—Daily egg production per 0.05 m^2 ($\hat{P}_0$), egg instantaneous mortality ($\hat{\alpha}$), egg abundance (m_{t_I}) of northern anchovy, and number of tows (n) in CalCOFI regions 4, 5, 7, 8, 9, 11, 13, and 14, January-April 1980-82.

	1980		1981		1982	
	$\hat{P}_0$ (SE)	$\hat{\alpha}$ (SE)	$\hat{P}_0$ (SE)	$\hat{\alpha}$ (SE)	$\hat{P}_0$ (SE)	$\hat{\alpha}$ (SE)
Historical egg production						
Series 1	2.33 (1.46)	0.37 (0.21)	3.95 (2.70)	0.36 (0.24)	1.94 (1.70)	0.15 (0.20)
Series 2	2.67 (1.46)	0.36 (0.08)	4.37 (2.70)	0.38 (0.08)	3.29 (1.70)	0.36 (0.09)
Current egg production method[1]	2.29 (0.51)	0.45 (0.11)	1.82 (0.31)	0.14 (0.08)	1.18 (0.32)	0.15 (0.104)

	1980		1981		1982	
Egg abundance per 0.05 m^2 (m_{t_I})	n	m_{t_I} (SE)	n	m_{t_I} (SE)	n	m_{t_I} (SE)
CalVET (0.333 mm)[2]	961	3.20 (0.52)	1,134	4.72 (0.72)	992	3.48 (0.62)
Bongo (0.505 mm)	97	4.12 (1.46)	403	6.88 (2.70)	113	4.93 (1.70)

[1] Picquelle, see text footnote 8.
[2] Mesh size.

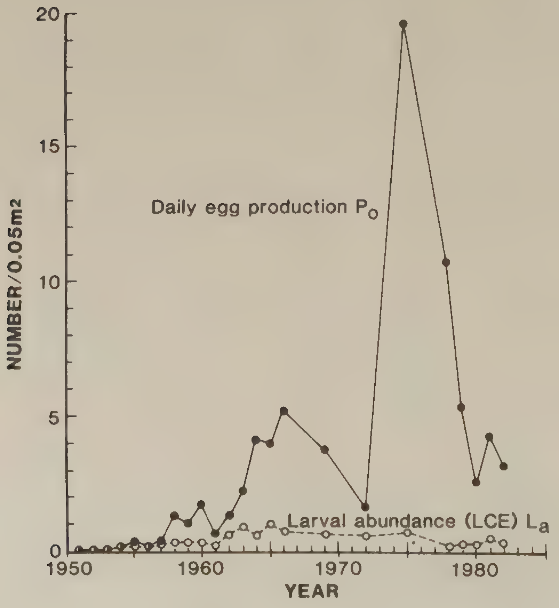

FIGURE 4.—Estimates of historical egg production of the central stock of northern anchovy using the series 2 method (P_0) and the larval abundance (L_a) of the larval census estimates, 1951-82.

As to the estimates from the two series of HEP, the point estimates of P_0 from series 2 were always higher than those estimated from series 1. Recall that the assumption of series 2 was that the egg through yolk-sac larval stage suffers a constant mortality rate. However, if in fact the yolk-sac larvae suffer a higher mortality rate than eggs, the mortality rate of eggs and larvae when combined (series 2) would overestimate egg mortality as well as egg production (P_0) (Equation (9B)).

DISCUSSION

Historical production (P_0) and egg IMR (α) of the central stock of northern anchovy for the first 4 mo of the year from 1951 to 1982 were estimated based upon the information of total number of eggs and yolk-sac larvae per 0.05 m^2 and the egg-larval mortality model. Two series of P_0 and α were produced. Series 1 assumed a constant IMR for only the egg stage whereas series 2 assumed a constant IMR for the entire embryonic period. Both series of P_0 showed the same trend (Table 3, Fig. 4) with a peak in 1975. The high daily egg production estimate (P_0) in 1975 was caused by the high standing stock of eggs ($m_{t_I} = 30.06/0.05$ m^3 per m depth) which was more than 10 times that of other years, and the high egg IMR ($\hat{\alpha} = 0.36$) (Table 3). The high daily egg production in 1975 reflects either a high fecundity (high spawning frequency) or a high spawning biomass or some combination of these effects. The present level of egg production is the same as that in the middle 1960's. Both egg IMR ($\hat{\alpha}$) and larval IMR coefficient $\hat{\beta}$, $z(t) = \beta/t$, vary from year to year (Fig. 5).

In addition to providing a 24-yr time series of HEP for the northern anchovy, two important conclusions can be drawn from this analysis:

1. The form of IMR of eggs (and yolk-sac larvae) is different from that of older larvae (6-20 d).
2. Egg production is a better index of stock abundance than is the standing stock of larvae.

Little doubt exists that mortality rates change sometime between the hatching of the eggs and the onset of feeding. Analysis of the daily egg and larval production by age for 1979-81 (Fig. 3) suggested a constant IMR for eggs (or eggs and yolk-sac larvae) and an age-dependent IMR of Pareto form for older larvae ($z(t) = \beta/t$ for $t_c < t < 20$ d) (Table 2). The age t_c in Equation (3) could be considered to mark the end of the critical period after which mortality decreases (Ahlstrom 1954; Marr 1956; Farris 1960; Saville 1964). Series 1 assumed t_c = incubation time and series 2 assumed t_c = average age of yolk-sac larvae. From the existing data, I could not ascertain which assumption was the more likely, but it was evident that larvae at hatching or near first-feeding (yolk absorption) suffer higher mortality than do older larvae.

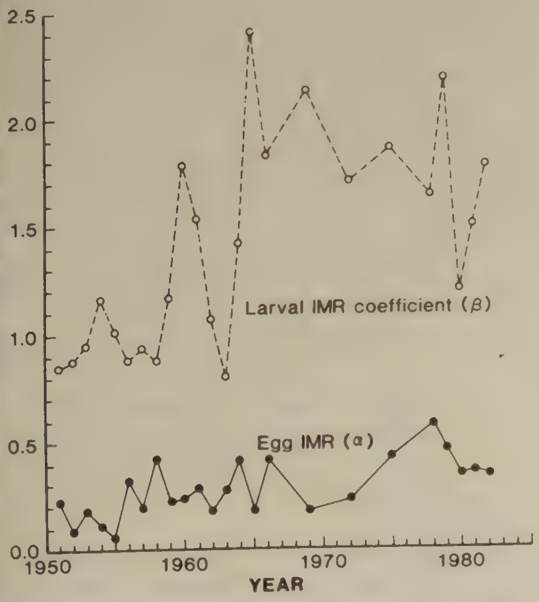

FIGURE 5.—Estimated egg instantaneous mortality rate (IMR) ($\hat{\alpha}$) from series 2 method of estimating egg production and the larval mortality coefficient ($\hat{\beta}$) of the central stock of northern anchovy, 1951-82.

The HEP (P_0) is certainly preferable to larval standing stock (larval census estimate = LCE) for use as an index of spawning biomass. Egg production is related to the spawning biomass through Equation (2), i.e., $P_0 = B_a \cdot C$, where the proportionality C is the reproductive output ($R \cdot F \cdot E/W$). If the reproductive output remains constant between years, as shown by 1980-82 anchovy data (Picquelle[8]), the HEP will be an unbiased index of the spawning biomass. The LEC assumes $B_a = K \cdot L_a$ where L_a is the larval abundance and K is a constant proportionality (Smith 1972; Stauffer and Charter 1982) (Table 3, Fig. 4). Thus to provide an unbiased index of biomass, the method requires that not only the reproductive output be constant from year to year but also the egg and larval mortality must remain constant as well. Using Equation (8), the larval abundance (age <30 d old) can be written as

$$\begin{aligned} L_a &= \int_{t_I}^{30} P_t \, dt \\ &= \int_{t_I}^{30} P_0 \, S(t; z(t)) \, dt \\ &= B_a \left(\frac{R \cdot F \cdot E}{W}\right) g(\alpha, \beta, t_I) \end{aligned}$$

$$\text{where } g(\alpha, \beta, t_I) = \begin{cases} e^{-\alpha t_I} \dfrac{t_I}{\beta - 1}\left[1 - \left(\dfrac{30}{t_I}\right)^{-(\beta-1)}\right] & \text{for } \beta \neq 1 \\ e^{-\alpha t_I} (\ln 30 - \ln t_I) & \beta = 1 \end{cases}$$

α is the egg IMR and β is the larval mortality coefficient.

The larval abundance (L_a) is proportional to the spawning biomass (B_a) with constant proportionality only if the reproductive output

---

[8] S. J. Picquelle, Statistician, Northwest and Alaska Fisheries Center, National Marine Fisheries Service, NOAA, 2725 Montlake Boulevard E, Seattle, WA 98112, pers. commun. July 1983.

$(R \cdot F \cdot E/W)$ and the egg and larval mortality rates through the function $g\ (\alpha, \beta, t_I)$ remain constant from year to year. It is clear that from 1951 to 1982 time series (Table 3) that the assumption of constant egg and larval mortality has not been met by the central California anchovy population. The HEP requires constant reproductive output. The validity of this assumption can only be tested with future data.

In addition to the ichthyoplankton data, several other indices of anchovy biomass exist: acoustic trawl surveys conducted by California Department of Fish and Game, aerial survey records from aircraft associated with the fishery, catch-effort analysis (CPUE), and cohort analysis from the catch of the United States and Mexican fishery. In a recent management plan, all of these indices except cohort analysis have been calculated and compared with the time series of egg production presented in this paper (MacCall et al.[9]). The estimates of egg production covaried with these other indices from year to year and appeared to be the most consistent index of spawning biomass among these indices (Table 5).

Selection of the appropriate method for estimating biomass depends upon the data availability and knowledge of the growth of eggs and larvae. If nothing is known of the age of eggs and larvae and no information exists on reproductive parameters, the LCE is the only method available although subject to major biases. If egg and larval age data exist but no data on reproductive parameters are available, then the HEP is the preferable method. The EPM is the best method; it requires not only knowledge of egg mortality but accurate estimates of adult reproductive parameters as well. In many time series, both growth and abundance of eggs and larvae are available but reproductive parameters are not. In these cases, the HEP is probably the most accurate means of creating a historic time series of biomass.

TABLE 5.—Correlations among various indices of anchovy spawning biomass. Upper value is correlation coefficient, lower value is number of observations. (Reproduced from table 4.3-2 of MacCall et al. (text footnote 9).)

Historical egg production					
0.458 (23)	Larval census				
0.807 (8)	0.708 (7)	Acoustic survey			
0.818 (9)	0.327 (9)	0.659 (9)	Aerial index		
0.791 (4)	0.004 (4)	0.512 (10)	0.379 (9)	Spring CPUE	
0.395 (4)	0.865 (4)	0.290 (10)	0.655 (10)	0.256 (9)	Fall CPUE

Spawning biomass index	Consistency[1]	Rank
Historical egg production	0.654	1
Larval census	0.480	5
Acoustic survey	0.606	2
Aerial index	0.583	3
Spring CPUE	0.388	6
Fall CPUE	0.517	4

[1] Consistency is average of correlation coefficients.

ACKNOWLEDGMENTS

I thank John Hunter, Roger Hewitt, Paul Smith, Rick Methot, Alec MacCall, Jay Barlow, National Marine Fisheries Service; David Farris, San Diego State University; Grace Yang, University of Maryland; two referees for reviewing the manuscript and making valuable suggestions. I also thank Barry Finzel, Cynthia Meyer, Carol Miller, and Richard Charter for compiling historical egg and larval data files, and Mary DeWitt and Debra Brown for typing the manuscript.

LITERATURE CITED

AHLSTROM, E. H.
1954. Distribution and abundance of egg and larval populations of the Pacific sardine. U.S. Fish Wildl. Serv., Fish. Bull. 56:83-140.
1968. An evaluation of the fishery resources available to California fishermen. *In* D. Gilbert (editor), The future of the fishing industry of the United States. Univ. Wash. Publ. Fish. New Ser. 4:65-80.
BEVERTON, R. J. H., AND S. J. HOLT.
1965. On the dynamics of exploited fish populations. Fish. Invest. Minist. Agric. Fish. Food (G.B.) Ser. II, 19: 1-533.
BISSEL, A. F.
1972. A negative binomial model with varying element sizes. Biometrika 59:435-441.
BURD, A. C., AND W. G. PARNELL.
1972. The relationship between larval abundance and stock in the North Sea herring. Rapp. P.-v. Réun. Cons. Perm. int. Explor. Mer 164:30-36.
CIECHOMSKI, J. D. DE, AND D. A. CAPEZZANI.
1973. Studies on the evaluation of the spawning stocks of the Argentinean anchovy, *Engraulis anchoita*, on the basis of egg surveys. Rapp. P.-v. Réun. Cons. Perm. int. Explor. Mer 164:293-301.
COLTON, J. B.
1959. A field observation of mortality of marine fish larvae due to warming. Limnol. Oceanogr. 4:219-222.
CUSHING, D. H.
1973. Dependence of recruitment on parent stock. J. Fish. Res. Board Can. 30:1965-1976.
FAGER, E. W.
1973. Estimation of mortality coefficients from field sam-

---

[9] MacCall, A. D., R. D. Methot, D. D. Huppert, H. W. Frey, and O. Mathisen. 1983. Northern anchovy second draft revised fishery management plan incorporating DEIS/RIR. Pac. Fish. Manage. Counc.

ples of zooplankton. Limnol. Oceanogr. 18:297-301.

FARRIS, D. A.
1960. The effect of three different types of growth curves on estimates of larval fish survival. J. Cons. Perm. Int. Explor. Mer 25:294-306.

HARDING, D., AND J. W. TALBOT.
1973. Recent studies on the eggs and larvae of the plaice (*Pleuronectes Platressa* L.) in the southern Bight. Rapp. P.-v. Réun. Cons. Perm. int. Explor. Mer 164:261-269.

HEWITT, R. P.
1982. Spatial pattern and survival of anchovy larvae: implications of adult reproductive strategy. Ph.D. Thesis, Univ. California, San Diego, 187 p.
1983. Roll, heave and vertical ichthyoplankton tows. Ocean Sci. Eng. 8(1):41-51.

HUPPERT, D. D., A. D. MACCALL, G. D. STAUFFER, K. R. PARKER, J. A. MCMILLAN, AND H. W. FREY.
1980. California's northern anchovy fishery: Biological and economic basis for fishery management. U.S. Dep. Commer., NOAA Tech. Memo., SWFC-TM-NMFS-1, 234 p.

JOHNSON, N. L., AND S. KOTZ.
1970. Distributions in statistics: continuous univariate distributions. Houghton Mifflin Co., Boston, 300 p.

LO, N. C. H.
1983. Re-examination of three parameters associated with anchovy egg and larval abundance: Temperature dependent of incubation time, yolk-sac growth rate and egg larva retention in mesh nets. U.S. Dep. Commer., NOAA Tech. Memo., SWFC-TM-NMFS-31, 32 p.

MARR, J. C.
1956. The critical period in the early life history of marine fish. J. Cons. Perm. Int. Explor. Mer 21:160-170.

METHOT, R. D.
1981. Growth rates and age distributions of larval and juvenile northern anchovy, *Engraulis mordax*, with inferences on larval survival. Ph.D. Thesis, Univ. California, San Diego, 203 p.

MURPHY, G. I.
1966. Population biology of the Pacific sardine (*Sardinops caerulea*). Proc. Calif. Acad. Sci., Ser. 4(34):1-84.

PARKER, K.
1980. A direct method for estimating northern anchovy, *Engraulis mordax*, spawning biomass. Fish. Bull., U.S. 78:541-544.

SAVILLE, A.
1964. Estimation of the abundance of a fish stock from egg and larval surveys. Rapp. P.-v. Réun. Cons. Perm. int. Explor. Mer 155:164-170.

SEBER, G. A. F.
1973. The estimation of animal abundance and related parameters. Hafner Press, N.Y., 506 p.

SMITH, P. E.
1972. The increase in spawning biomass of northern anchovy, *Engraulis mordax*. Fish. Bull., U.S. 70:849-874.

SMITH, P. E., AND S. L. RICHARDSON.
1977. Standard techniques for pelagic fish egg and larva surveys. FAO Fish. Tech. Pap. 174, FIR/T175, 100 p.

STAUFFER, G. D., AND R. L. CHARTER.
1982. The northern anchovy spawning biomass for the 1981-82 California fishing season. CalCOFI Rep. 23: 15-19.

THEILACKER, G. H.
1980. Changes in body measurements of larval northern anchovy, *Engraulis mordax*, and other fishes due to handling and preservation. Fish. Bull., U.S. 78:685-692.

ZWEIFEL, J. R., AND P. E. SMITH.
1981. Estimates of abundance and mortality of larval anchovies (1951-75): application of a new method. Rapp. P.-v. Réun. Cons. Perm. int. Explor. Mer 178:248-259.

APPENDIX

The approximate variances of $\hat{\alpha}$ and $\hat{P}_0$ were derived from the delta method (Seber 1973):

$$\operatorname{var}[f(x_1,\ldots,x_I)] \doteq \sum_{i=1}^{I}\left[\frac{\partial}{\partial x_i} f(x_1,\ldots,x_I)\right]^2 \operatorname{var}(x_i) + 2\sum_{i<j} \frac{\partial}{\partial x_i} f(x_1,\ldots,x_I)\,\frac{\partial}{\partial x_j} f(x_1,\ldots,x_I)\operatorname{cov}(x_i,x_j)\Bigg|_{\hat{E}x_i,\, i=1,\ldots,I}$$

var $(\hat{\alpha})$ was computed based upon Equation (10), i.e.,

$$\operatorname{var}(q) \doteq \left(\frac{\partial h(\alpha)}{\partial \alpha}\right)^2 \operatorname{var}(\hat{\alpha}).$$

Thus $\mathrm{var}(\hat{\alpha}) \doteq \mathrm{var}(q) \cdot \left(\frac{\partial h(\alpha)}{\partial \alpha}\right)^{-2}$

$$\doteq \mathrm{var}(\hat{m}_{t_c}/\hat{P}_{t_c}) \left(\frac{\partial h(\alpha)}{\partial \alpha}\right)^{-2}$$

$$= \frac{\mathrm{var}(\hat{m}_{t_c}) + q^2\,\mathrm{var}(\hat{P}_{t_c}) - 2\,q\,\mathrm{cov}(\hat{m}_{t_c}, \hat{P}_{t_c})}{\hat{P}_{t_c}{}^2} \cdot \left[\hat{\alpha}^4 / \left\{ e^{\hat{\alpha} t_c}(\hat{\alpha} t_c - 1) + 1 \right\}^2\right]$$

where cov (m_{t_c}, P_{t_c}) was estimated from the 1951-82 time series. Var (P_0) was computed based upon Equation (9B)

$$\hat{P}_0 = \hat{P}_{t_c} e^{\hat{\alpha} t_c}$$

$$\mathrm{var}(\hat{P}_0) \doteq \left\{\frac{\partial P_0}{\partial \alpha}\right\}^2 \mathrm{var}(\hat{\alpha}) + \left\{\frac{\partial P_0}{\partial P_{t_c}}\right\}^2 \mathrm{var}(\hat{P}_{t_c}) + 2\left(\frac{\partial P_0}{\partial \alpha}\right)\left(\frac{\partial P_0}{\partial P_{t_c}}\right) \mathrm{cov}(\hat{P}_{t_c}, \hat{\alpha}) \Big|_{\hat{\alpha},\, \hat{P}_{t_c}}$$

$$= e^{2\hat{\alpha} t_c}\left[t_c{}^2\, \hat{P}_{t_c}{}^2\, \mathrm{var}(\hat{\alpha}) + \mathrm{var}(\hat{P}_{t_c}) + 2\hat{P}_{t_c} \cdot t_c \cdot \mathrm{cov}(\hat{P}_{t_c}, \hat{\alpha})\right]$$

where cov $(\hat{P}_{t_c}, \hat{\alpha})$ was estimated from the 1951-82 time series.

8557

A Model for Temperature-Dependent Northern Anchovy Egg Development and an Automated Procedure for the Assignment of Age to Staged Eggs

NANCY C. H. LO
Southwest Fisheries Center,
National Marine Fisheries Service, NOAA,
P.O. Box 271, La Jolla, CA 92038

ABSTRACT

A functional relationship between age and developmental stage of northern anchovy, *Engraulis mordax*, eggs for various temperatures was determined based upon data collected in two laboratory experiments. The age of an egg was found to be a mixed exponential and power function of temperature and stage. An automated procedure was also developed using a reference table to assign age to staged eggs for any given time of tow and sea temperature ranging from 10° to 22°C. A comparison between the manual system and the automated procedure was made based on 1980-83 data, and the difference was found to be minimal.

INTRODUCTION

In the first section of this paper, I discuss the modelling of temperature-dependent anchovy egg development based on data from two laboratory experiments conducted at the Southwest Fisheries Center (SWFC). This temperature-dependent egg development curve is used to assign ages to the field-collected eggs after they are staged according to their anatomical development. In the second section, I discuss an automated procedure for accomplishing the assignment of ages.

TEMPERATURE AND DEVELOPMENT

Both laboratory and field-collected anchovy egg data indicate that the developmental rate of eggs is temperature-dependent. The higher the temperature, the shorter the time required to reach a given stage. The relationship between the age of eggs and temperature for a given stage has been studied in the past (Zweifel and Lasker 1976; Zweifel pers. comm.[1]) and a Gompertz growth curve fitted to the laboratory egg development data of both anchovy and sardine.

To improve our knowledge of the relationship between temperature and development of anchovy eggs and yolksac larvae, in 1981 a laboratory experiment was conducted at three temperatures (13.5°, 15.0°, and 16.5°C) using eggs from a captive brood stock (Lo 1983). These egg data were used along with those collected at temperatures ranging from 13.8° to 20.8°C for stages III, VI, VIII, IX, and XI in an earlier experiment to develop a revised model for expressing the development of anchovy eggs at a given temperature (Table 1). Stages are described by Moser and Ahlstrom (1985), and procedures for sorting and staging eggs by Stauffer and Picquelle (1985).

Table 1.—Average age (in hours.minutes) of northern anchovy eggs for each of 10 developmental stages (Stage I not observed) at various temperatures (°C) from laboratory experiments conducted at the SWFC.

	Temperature (°C)								
	(Lo 1983)			Zweifel and Lasker (1976)					
Stage	13.9	15.2	16.2	13.8	15.2	16.6	18.0	19.4	20.8
II	6.82	6.42	6.40						
III	16.36	13.55	13.14	20	15	10	9	8	6
IV	24.91	21.12	20.18						
V	35.88	30.7	25.56						
VI	44.63	39.24	33.20	42	35	26	24	21	9
VII	49.64	47.13	38.56						
VIII	52.5	52.07	43.64						
IX	61.1	56.28	50.48	58	50	39	35	33	28
X	66.09	62.63	54.78						
XI	69.79	65.65	56.10	78	65	55	44	39	35

MODEL DEVELOPMENT AND RESULTS

To choose an appropriate model for the relationship between age and temperature for a particular stage, I examined the age-temperature relationship empirically for stages III, VI, VIII, IX, and XI, because data on these stages were available for a wide temperature range (data for stages VIII and IX were combined to increase the sample size).

---

[1] J. R. Zweifel, Southeast Fisheries Center, National Marine Fisheries Service, NOAA, 75 Virginia Beach Drive, Miami, FL 33149, pers. commun. July 1983.

In: R. Lasker (editor), An Egg Production Method for Estimating Spawning Biomass of Pelagic Fish: Application to the Northern Anchovy, *Engraulis mordax*. NOAA Tech. Rep. NMFS 36. U.S. Dep. Commer., Wash., D.C., 99 p.

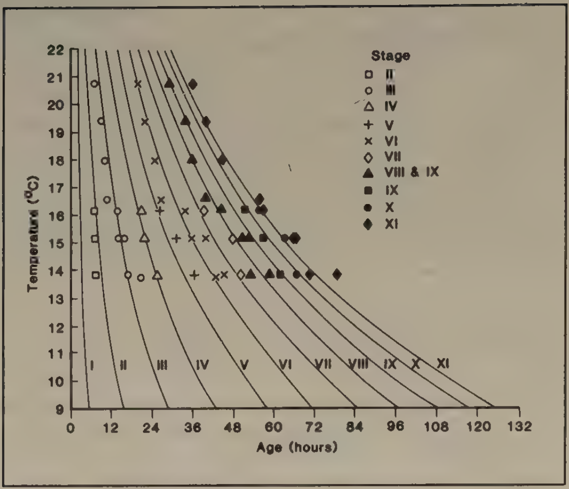

Figure 1.—Observed (denoted by various symbols) and predicted ages (smooth lines) of time to the *i*th stage as a function of temperature (°C) based on egg development data collected from two laboratory experiments conducted at SWFC. The predicted values are computed from Equation (4).

For all four stages, the exponential function fitted the data well, i.e.,

$$y_{i,t} = a_i e^{b_i t} \qquad (1)$$

where $y_{i,t}$ is the average age of the *i*th-stage anchovy eggs at temperature t°C. The coefficients $(a_i b_i)$ are for the *i*th stage only. The initial fitting of the model was accomplished by linear regression of the natural logarithm of the ages on the temperatures ($\ln y_{i,t} = \ln a_i + b_i t$). The coefficient of determination (R^2) ranges from 0.82 to 0.98:

Stage	$\ln a_i$	b_i	R^2
III	5.02	−0.155	0.95
VI	5.50	−0.126	0.82
VIII, IX	5.54	−0.107	0.95
XI	5.88	−0.113	0.98

Next, the development data were examined for a given temperature where ages were available for most of the stages. In this analysis, only the latest laboratory data were included because the other data set had only four or five egg stages. The temperatures used were 13.9°, 15.2°, and 16.2°C (mean temperature experienced by all egg stages). For each of the three temperatures, the development curves were more complicated than time-to-stage curves described above. A simple exponential function was not sufficient. Instead, the function was a combination of an exponential and a power function:

$$y_{i,t} = a_t\, e^{b_t i}\, (i)^{c_t} \qquad (2)$$

All the coefficients are temperature specific; a_t, b_t, and c_t are for temperature t°C. Linear regressions of the natural logarithms of average age on stage ($\ln y_{i,t} = \ln a_t + b_t \cdot i + c_t \ln(i)$) show an excellent fit with R^2 ranging from 0.96 to 0.99 for each of the three temperatures:

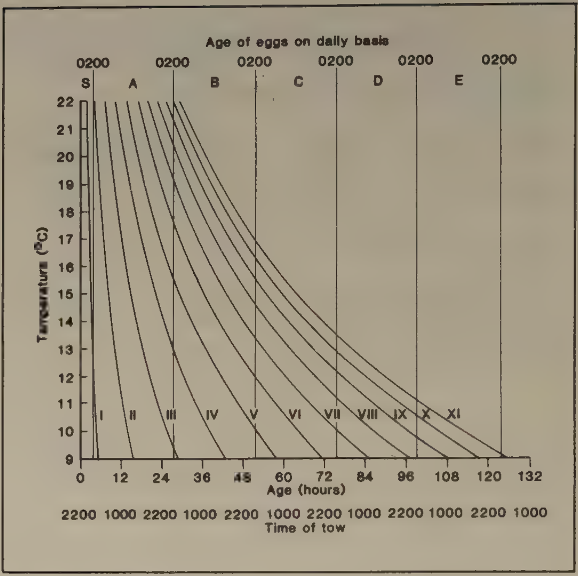

Figure 2.—Function relationship of average age of eggs for the *i*th stage based upon time of tow and sea surface temperature (°C).

Temperature (°C)	$\ln a_t$	b_t	c_t	R^2
13.9	0.717	−0.206	2.4	0.96
13.5	0.731	−0.153	2.13	0.96
16.2	0.793	−0.206	1.94	0.99

In order to include all the existing data on anchovy egg development in a single model, Equations (1) and (2) were combined into one equation:

$$y_{i,t} = a\, e^{(bt+ci)}\, i^{d} \qquad (3)$$

where the coefficients a, b,c, and d were common for all stages and all temperatures. Equation (3) was then fitted to all temperature-specific egg development data (Table 1). The resulting model is:

$$y_{i,t} = 16.07\, e^{-(0.1145t+0.0098i)}\, i^{1.74}. \qquad (4)$$

The observed and predicted ages of anchovy eggs were plotted in Figure 1.

For each of the 11 stages, the average age of anchovy eggs can be estimated from Equation (4) for a given temperature. A family of 11 temperature-age curves was used as the key to determine the ages of anchovy eggs collected in the field in conjunction with the time of tow and sea surface temperature, assuming 1800-0200 was the spawning time with 2200 as the peak (Fig. 2).

To use Figure 2 to assign age to anchovy eggs after they are staged, the following is done. First, time zero was assumed to be 2200, the midpoint of the daily spawning period. All the eggs observed between 1800 and 0200 were classified as newly spawned eggs (S). Eggs that fall in the consecutive 24-h intervals from 0200 to 0200 are classified as day 0, day 1, day 2, and day 3 eggs (or A-day, B-day, C-day, D-day eggs), depending on the time of tow and the sea surface temperature. For example, the eggs collected from a tow taken at 1800 h at 16°C should have the age assignment as below (theoretically no stage II should be observed):

Stage	I	II	III	IV	V	VI	VII	VIII	IX	X	XI
Age	S	—	A	A	A	B	B	B	B	B	B,C

The above assignment of ages to staged eggs is on a daily basis. With the information of time of tow, the age of eggs can be expressed in hours, e.g., A-day eggs are 20 h old (20 h from 2200) and B-day eggs are 44 h old in this example.

AN AUTOMATED PROCEDURE

The automated procedure for assigning an age to a staged anchovy egg is a FORTRAN computer program (STAGEAGE) coded for VAX[2] computer. It takes input data of staged eggs along with sea temperature and time of tow and assigns ages to eggs according to a reference table (see Table 3). This reference table contains the estimated ages of eggs for each of the 11 egg stages (see Moser and Ahlstrom 1985) at temperatures ranging from 10° to 22°C for any time throughout a day. In the following paragraphs, I describe the construction of the reference table.

The estimated ages ($y_{i,t,k}$) in the reference table are the average ages ($y_{i,t}$) computed from Equation (4) adjusted for the time of tow (k) assuming that the peak spawning time is 2200. If the eggs are observed before their expected time, an age younger than $y_{i,t}$ will be assigned. Otherwise, an older age will be assigned. The basic formula of determining the age of eggs ($y_{i,t,k}$) is

$$y_{i,t,k} = y_{i,t} + k - \hat{T} \tag{5}$$

where $y_{i,t}$ is from Equation (4), k is time of tow, and $\hat{T}$ is the expected time of observing stage i eggs. $\hat{T}$ is obtained from the peak spawning time (st) (=2200 for northern anchovy) and average age ($y_{i,t}$):

$$\hat{T} = \text{remainder of } (y_{i,t} + st)/24.$$

The basic formula is used for samples taken between $\hat{T}$-G and $\hat{T}$+G h. The quantity G is chosen to be 2× the standard deviation of ages within stage (sd). If $y_{i,t,k}<2\times sd$, G is set to be equal to $y_{i,t,k}$, or

$$G = \begin{cases} 2\times sd & \text{if } y_{i,t,k}>2\times sd \\ y_{i,t,k} & \text{otherwise.} \end{cases}$$

The average standard deviation over three temperatures (13.9°, 15.2°, 16.2°C) is between 2 and 5 h.

Stage	I	II	III	IV	V	VI	VII	VIII	IX	X	XI
sd (h)	—	2	4	4	4	4	3	3	5	3	3

The average age ($y_{i,t}$) and the expected time of tow ($\hat{T}$) for each stage and temperature combination are given in Table 2. The assignment of ages of eggs as a function of the time of tow (k) and sea surface temperature (t) is computed as below:

$$y_{i,t,k} = \begin{cases} y_{i,t}-G & \text{if } k<\hat{T}-G \\ y_{i,t}+k-\hat{T} & \hat{T}-G<k<\hat{T}+G \\ y_{i,t}+G & \hat{T}+G<k. \end{cases} \tag{7}$$

Notice Equation (7) is a modified version of Equation (5).

Table 2.—Average age and expected time of tow for each combination of stages (i) and temperatures (t) ranging from 10° to 22°C.

Temp. (°C)	Stage I	II	III	IV	V	VI	VII	VIII	IX	X	XI
					Average ($y_{i,t}$) (in hours.minutes)						
10	4.23	13.16	24.21	36.25	48.40	60.36	71.51	82.11	91.27	99.36	106.36
11	3.54	11.50	21.43	32.28	43.24	54.03	64.05	73.17	81.34	88.50	95.04
12	3.29	10.33	19.22	28.57	38.43	48.12	57.09	65.22	72.44	79.13	84.47
13	3.06	9.24	17.16	25.50	34.31	42.59	50.58	58.17	64.52	70.39	75.36
14	2.46	8.23	15.24	23.02	30.47	38.20	45.27	51.59	57.51	63.00	67.26
15	2.28	7.29	13.44	20.32	27.27	34.11	40.32	46.22	51.36	56.11	60.08
16	2.12	6.40	12.15	18.19	24.29	30.29	36.09	41.21	46.01	50.07	53.38
17	1.58	5.57	10.55	16.20	21.50	27.11	32.14	36.52	41.02	44.41	47.49
18	1.45	5.18	9.44	14.34	19.28	24.15	28.45	32.53	36.36	39.51	42.39
19	1.34	4.44	8.41	13.00	17.22	21.38	25.38	29.19	32.38	35.32	38.02
20	1.24	4.13	7.45	11.35	15.29	19.17	22.52	26.09	29.06	31.42	33.55
21	1.15	3.46	6.55	10.20	13.49	17.12	20.23	23.19	25.57	28.16	30.15
22	1.06	3.21	6.10	9.13	12.19	15.20	18.11	20.48	23.09	25.13	26.59
					Expected time of tow ($\hat{T}$) (in hours.minutes)						
10	2.23	11.16	22.21	10.25	22.40	10.36	21.51	8.11	17.27	1.36	8.36
11	1.54	9.50	19.43	6.28	17.24	4.03	14.05	23.17	7.34	14.50	21.04
12	1.29	8.33	17.22	2.57	12.43	22.12	7.09	15.22	22.44	5.13	10.47
13	1.06	7.24	15.16	23.50	8.31	16.59	0.58	8.17	14.52	20.39	1.36
14	0.46	6.23	13.24	21.02	4.47	12.20	19.27	1.59	7.51	13.00	17.26
15	0.28	5.29	11.44	18.32	1.27	8.11	14.32	20.22	1.36	6.11	10.08
16	0.12	4.40	10.15	16.19	22.29	4.29	10.09	15.21	20.01	0.07	3.38
17	23.58	3.57	8.55	14.20	19.50	1.11	6.14	10.52	15.02	18.41	21.49
18	23.45	3.18	7.44	12.34	17.28	22.15	2.45	6.53	10.36	13.51	16.39
19	23.34	2.44	6.41	11.00	15.22	19.38	23.38	3.19	6.38	9.32	12.02
20	23.24	2.13	5.45	9.35	13.29	17.17	20.52	0.09	3.06	5.42	7.55
21	23.15	1.46	4.55	8.20	11.49	15.12	18.23	21.19	23.57	2.16	4.15
22	23.06	1.21	4.10	7.13	10.19	13.20	16.11	18.48	21.09	23.13	0.59

---

[2] VAX is a trademark of Digital Equipment Corporation.

Thus, the age for eggs of stage *i* observed at temperature *t* is always within $y_{i,t} \pm G$ (i.e., between two standard deviations of age within a stage). Equation (7) eliminates the possibility of assigning either too young or too old an age to eggs that were sampled at the time which is more than *G* hours before or after the expected time of tow. Occasionally, the eggs are taken 12 h away from the expected time of spawning. These eggs can be either the youngest or the oldest eggs for that stage. In this case, the maximum and minimum ages are then randomly assigned to those eggs because there is no way of distinguishing eggs between the young and old ages within stage.

The reference table for stage IV anchovy eggs is given (Table 3). In the table, the first column is the time of tow (01-24 h). The rows corresponding to 25 h are the maximum ages used for random selection of ages for eggs observed at 12 h away from the expected time. Row 1 contains temperatures ranging from 10° to 22°C. Each entry from row 2 and on is the estimated age for a combination of time of tow and sea temperature. For a given temperature, and time of tow, ages are assigned to each stage according to the reference table. The reference table for all stages is included in FORTRAN program STAGEAGE (Hewitt et al. 1984).

Use of Computer Program STAGEAGE

Input Data File—The input data file of eggs should include tow identification (ID) information, e.g., cruise number, location (line and station for CalCOFI survey), stratum, weighting factor (Hewitt et al. 1984), tow number, tow time, sea surface temperature, number of eggs for each stage, and total number of eggs. Variables in tow ID and total eggs are useful for data checking. The other variables are essential for estimating the ages of eggs (Table 4).

Output Data Files—Several output data files are available from STAGEAGE. STAGEAGE can be used not only to assign ages to staged eggs, but also to stratify the survey area into regions as desired. Regions are defined as area between line numbers. The user can choose output data file(s) and the number of regions in the execution instructions (see next section). The major output data file names in logic unit numbers are FOR026.DAT, FOR029.DAT, FOR036.DAT, FOR037.DAT, FOR038.DAT (Tables 5a-e).

Table 3.—Partial listing of the reference table. Estimated age (in hours.minutes) for stage IV for each combination of time of tow (1-24 h) and temperature (10°-22°C). Asterisks (*) indicate the estimated age corresponding to expected time of tow ($\hat{T}$) (see Tables 2a, b). Row 25 is for random assignment of ages for eggs observed at 12 h before or after expected time of tow.

Time of tow (k)	Temperature (°C)												
	10	11	12	13	14	15	16	17	18	19	20	21	22
1	28. 25	27. 28	27. 57	27. 50	27 02	27. 32	26 19	24. 20	6. 34	4. 60	3 35	3. 20	3. 13
2	28 25	28 28	28 57*	28 50	28. 02	28. 32	26. 19	8 20	6. 34	4. 60	4 35	4. 20	4. 13
3	29. 25	29. 28	29 57	29. 50	29. 02	28. 32	26. 19	8 20	6. 34	5. 60	5. 35	5. 20	5. 13
4	30 25	30. 28	30 57	30. 50	30. 02	28. 32	10. 19	8 20	6. 34	6. 60	6 35	6. 20	6. 13
5	31. 25	31. 28	31. 57	31 50	31 02	28. 32	10 19	8. 20	7. 34	7. 60	7. 35	7. 20	7. 13
6	32. 25	32. 28*	32. 57	32. 50	31. 02	12. 32	10. 19	8. 20	8 34	8. 60	8 35	8. 20	8. 13
7	33 25	33. 28	33 57	33 50	31 02	12 32	10. 19	9. 20	9. 34	9. 60	9 35	9. 20	9 13*
8	34 25	34 28	34 57	33 50	31 02	12 32	10. 19	10 20	10. 34	10. 60	10 35	10 20*	10. 13
9	33 25	35 28	35 57	33. 50	15 02	12. 32	11. 19	11. 20	11 34	11. 60	11. 35*	11 20	11 13
10	36. 25*	36. 28	36. 57	33 50	15. 02	12. 32	12. 19	12 20	12. 34	12. 60*	12 35	12. 20	12. 13
11	37. 25	37. 28	36 57	17. 50	15 02	13 32	13. 19	13. 20	13. 34	13 60	13. 35	13. 20	13 13
12	38. 25	38. 28	36. 57	17. 50	15. 02	14. 32	14. 19	14. 20	14. 34*	14. 60	14. 35	14. 20	14 13
13	39. 25	39. 28	36. 57	17. 50	15. 02	15. 32	15. 19	15. 20	15. 34	15. 60	15 35	15. 20	15. 13
14	40. 25	40. 28	20. 57	17. 50	16. 02	16. 32	16. 19	16. 20*	16. 34	16. 60	16 35	16. 20	16. 13
15	41. 25	40. 28	20. 57	17. 50	17. 02	17. 32	17. 19	17. 20	17. 34	17. 60	17. 35	17. 20	17. 13
16	42 25	40. 28	20. 57	18 50	18 02	18. 32	18. 19*	18. 20	18. 34	18 60	18. 35	18 20	17. 13
17	43 25	40. 28	20. 57	19. 50	19. 02	19. 32	19. 19	19. 20	19. 34	19. 60	19 35	18 20	17 13
18	44. 25	24. 28	20. 57	20. 50	20 02	20 32*	20. 19	20. 20	20. 34	20. 60	19 35	18 20	17. 13
19	44. 25	24. 28	21. 57	21. 50	21 02	21. 32	21. 19	21. 20	21. 34	20 60	19. 35	18. 20	1. 13
20	44. 25	24. 28	22. 57	22. 50	22. 02	22. 32	22. 19	22. 20	22. 34	20. 60	19. 35	2. 20	1. 13
21	44 25	24. 28	23 57	23. 50	23 02*	23 32	23. 19	23. 20	22. 34	20. 60	3. 35	2. 20	1. 13
22	28. 25	24. 28	24. 57	24. 50	24 02	24 32	24. 19	24. 20	22. 34	4. 60	3 35	2. 20	1. 13
23	28 25	25. 28	25 57	25 50*	25 02	25. 32	25. 19	24. 20	22. 34	4. 60	3. 35	2 20	1 13
24	28 25	26 28	26. 57	26 50	26 02	26 32	26. 19	24. 20	6 34	4. 60	3 35	2. 20	2 13
25	44. 25	40. 28	36. 57	33. 50	31. 02	28. 32	26. 19	24. 20	22. 34	20. 60	19 35	18. 20	17 13

FOR026.DAT contains tow ID, region, tow time, temperature, and number of eggs and age grouped by 24-h increments: 0-3, 4-27, 28-51, 52-75, and 76-99 as S, A, B, C, and D-day categories for each tow. The program assigns number 0 to an age if it is impossible to observe eggs that belong to such a day category for a given time of tow. For example, S-day eggs are never observed at 1200 (Table 5a).

FOR029.DAT contains the same data as FOR026.DAT except the age is not included and this file was formatted for the CalCOFI data base for the SWFC (Table 5b).

FOR036.DAT contains tow ID, region, tow time, temperature, and number of eggs and age for each stage by tow (Table 5c).

FOR037.DAT contains records in which at least one stage was observed outside the normal range of expected time, i.e., $\hat{T} \pm G$. This file is useful for double-checking the accuracy of data on eggs observed at unusual times (Table 5d).

FOR038.DAT contains tow ID and two variables: number of eggs and age for A, B, and C-day eggs. The day categories with age >2.5 d are excluded. Therefore, the total number of records is <3 × the number of tows. This file can be used directly for regression estimates of egg production and egg mortality rates (Table 5e).

Execution Instructions—The program may be executed interactively or as a batch job. An example of a set of commands for VAX is given below with input data file FILENAME:

```
$ASSIGN FILENAME FOR025
$RUN STAGEAGE
(...enter 1 for each of the output files needed:FOR026,028,029,
036,037, and 038. Enter 2, otherwise.)
1 2 1 2 1 1
(enter number of regions)
3
(enter max (CalCOFI) line number for each region, separated by
space.)
826 950 1500
```

This set of commands takes FILENAME as the input file and asks for output files FOR026, 029, 037, and 038. Commands in parentheses are prompted by the machine. Other lines are inputs by the user. The input and output data files for 1983 anchovy eggs are listed in Tables 4 and 5 for illustration.

Table 4.—Partial listing of input data file for 1983 northern anchovy eggs (N8302.DAT) for the computer program STAGEAGE. (Cruise no. is 8302; 8 was deleted from printout.)

Cruise no.	Tow no.	CalCOFI line	CalCOFI stn.	Stratum	Weighting factor	Date	Tow time (h)	Temp. (°C x 10)	Egg stages I	II	III	IV	V	VI	VII	VIII	IX	X	XI	Disintegrated eggs	Total no eggs/tow
302	1	733	500	0	1. 000	830205	408	150	0	0	0	0	0	0	0	0	0	0	0	0	0
302	2	733	510	0	1. 000	830205	545	149	0	0	0	0	0	0	0	0	0	0	0	0	0
302	3	733	520	0	1. 000	830205	631	149	0	0	0	0	0	0	0	0	0	0	0	0	0
302	4	733	530	0	1. 000	830205	837	148	0	0	0	0	0	0	0	0	0	0	0	0	0
302	5	733	540	0	1. 000	830205	1028	146	0	0	0	0	0	0	0	0	0	0	0	0	0
302	6	733	550	1	1. 000	830205	1113	148	0	0	0	0	0	0	0	0	0	1	0	0	1
302	7	733	560	0	1. 000	830205	1159	148	0	0	0	0	0	0	0	0	0	0	0	0	0
302	8	733	570	0	1. 000	830205	1245	150	0	0	0	0	0	0	0	0	0	0	0	0	0
302	9	733	580	0	1. 000	830205	1328	148	0	0	0	0	0	0	0	0	0	0	0	0	0
302	10	733	590	0	1. 000	830205	1416	147	0	0	0	0	0	0	0	0	0	0	0	0	0
302	11	733	600	0	1. 000	830205	1633	147	0	0	0	0	0	0	0	0	0	0	0	0	0
302	12	741	600	0	1. 000	830205	1831	146	0	0	0	0	0	0	0	0	0	0	0	0	0
302	13	741	590	0	1. 000	830205	2035	147	0	0	0	0	0	0	0	0	0	0	0	0	0
302	14	741	580	0	1. 000	830205	2109	147	0	0	0	0	0	0	0	0	0	0	0	0	0
302	15	741	570	0	1. 000	830205	2144	147	0	0	0	0	0	0	0	0	0	0	0	0	0
302	16	741	560	0	1. 000	830205	2231	147	0	0	0	0	0	0	0	0	0	0	0	0	0
302	17	741	550	1	1. 000	830205	2328	146	0	0	0	0	1	0	0	0	0	0	0	0	1
302	18	741	540	1	1. 000	830206	20	146	0	0	0	0	0	0	0	1	0	0	0	0	1
302	19	741	530	1	1. 000	830206	113	146	0	0	0	0	0	0	0	3	0	0	0	0	3
302	20	741	520	0	1. 000	830206	151	148	0	0	0	0	0	0	0	0	0	0	0	0	0
302	21	741	510	0	1. 000	830206	228	149	0	0	0	0	0	0	0	0	0	0	0	0	0
302	22	741	500	0	1. 000	830206	312	149	0	0	0	0	0	0	0	0	0	0	0	0	0
302	23	741	492	0	1. 000	830206	417	148	0	0	0	0	0	0	0	0	0	0	0	0	0
302	24	750	485	1	1. 000	830206	619	146	0	0	0	0	0	0	0	0	0	0	0	0	0
302	26	750	500	1	1. 000	830206	1539	151	0	0	0	0	0	0	0	0	0	2	0	0	2
302	27	750	510	1	1. 000	830206	1717	151	0	0	0	0	0	0	0	0	0	0	0	0	0
302	29	750	520	1	1. 000	830206	2232	151	0	0	0	0	0	0	0	0	0	0	0	0	0
302	30	750	530	1	1. 000	830206	2311	148	0	0	0	0	0	0	0	0	0	0	0	0	0
302	31	750	540	1	1. 000	830207	8	143	0	0	0	0	0	0	0	0	2	0	0	1	3
302	32	750	550	1	1. 000	830207	49	143	0	0	0	0	0	0	0	0	0	2	0	0	2
302	33	750	560	1	1. 000	830207	147	144	0	0	0	0	0	0	0	0	0	2	0	0	2
302	34	750	570	1	1. 000	830207	231	145	0	0	0	0	0	0	0	0	0	1	0	0	1
302	35	750	580	0	1. 000	830207	309	144	0	0	0	0	0	0	0	0	0	0	0	0	0
302	36	750	590	0	1. 000	830207	350	146	0	0	0	0	0	0	0	0	0	0	0	0	0
302	37	750	600	0	1. 000	830207	441	146	0	0	0	0	0	0	0	0	0	0	0	0	0
302	38	758	600	1	1. 000	830207	616	146	0	0	0	0	0	0	0	2	0	0	0	0	2
302	39	758	590	1	1. 000	830207	720	146	0	0	0	0	0	0	0	2	0	0	0	0	2
302	40	758	580	1	1. 000	830207	807	146	0	0	0	0	0	0	0	0	2	0	0	0	2
302	41	758	570	1	1. 000	830207	852	144	0	0	0	0	0	0	0	0	0	0	0	0	0

Table 5a.—Partial listing of output data file (FORO26.DAT) for 1983: Number of northern anchovy eggs and estimated ages (in hours) grouped by S(0-3 h), A(4-27 h), B(28-51), C(52-75 h), D(76-99 h). Disintegrated eggs are obtained by subtraction. E-day eggs (100-123 h) are not observed for northern anchovy and thus are not included in the output. (Cruise no. is 8302.)

Cruise no.	Tow no.	CalCOFI line	CalCOFI stn.	Stratum	Weighting factor	Date	Region	Tow time (h)	Temp. (°C)	No. eggs and ages (h)/day catagories										Total
										S		A		B		C		D		
										N	h	N	h	N	h	N	h	N	h	
302	17	741	550	1	1. 000	830205	1	23 28	14	0.	1.	1.	25.	0.	48.	0.	71.	0.	0.	1.
302	18	741	540	1	1. 000	830206	1	24 20	14	0.	2.	0.	20.	1.	50.	0.	71.	0.	0.	1.
302	19	741	530	1	1. 000	830206	1	1 13	14	0.	3.	0.	20.	3	51.	0.	65.	0.	0.	3.
302	24	750	485	1	1. 000	830206	1	6 19	14	0.	0.	0.	7.	0.	37.	0.	53.	0.	0.	0.
302	26	750	500	1	1. 000	830206	1	15 39	15	0.	0.	0.	16.	0.	41.	2	62.	0.	0.	2.
302	27	750	510	1	1. 000	830206	1	17 17	15	0.	2.	0.	19.	0.	43.	0	64.	0.	0.	0.
302	29	750	520	1	1. 000	830206	1	22 32	15	0.	2	0.	24.	0.	48	0.	66.	0.	0.	0.
302	30	750	530	1	1. 000	830206	1	23 11	14	0.	1.	0.	19.	0.	48.	0.	71.	0.	0.	0.
302	31	750	540	1	1. 000	830207	1	24 8	14	0.	2.	0.	20.	2.	50.	0	71.	0.	0.	3.
302	32	750	550	1	1. 000	830207	1	24 49	14	0.	2.	0.	20.	0.	49.	2.	69.	0.	0.	2.
302	33	750	560	1	1. 000	830207	1	1 47	14	0.	3.	0	20	0.	46.	2	57.	0.	0.	2.
302	34	750	570	1	1. 000	830207	1	2 31	14	0.	0	0.	5.	0.	34.	1.	57.	0.	0.	1.
302	38	758	600	1	1. 000	830207	1	6 16	14	0.	0.	0.	7.	0.	37	2	56.	0.	0.	2
302	39	758	590	1	1. 000	830207	1	7 20	14	0.	0.	0.	7.	0	34.	2	57.	0.	0.	2.
302	40	758	580	1	1. 000	830207	1	8 7	14	0.	0.	0	8.	0	35.	2.	58.	0.	0.	2.
302	41	758	570	1	1. 000	830207	1	8 52	14	0.	0.	0.	8.	0.	35.	0.	59.	0.	0.	0.
302	42	758	560	1	1. 000	830207	1	9 34	14	0.	0.	0.	10.	0.	36.	0.	59.	0.	0.	0.
302	43	758	550	1	1. 000	830207	1	10 39	14	0.	0.	0.	11.	0.	37	2.	60.	0.	0.	2
302	44	758	540	1	1. 000	830207	1	11 22	14	0.	0.	0.	11.	0	38	2.	61.	0.	0.	2.
302	45	758	530	1	1. 000	830207	1	12 0	15	0.	0.	0	13.	1	38.	1.	62.	0.	0.	2
302	46	758	520	1	1. 000	830207	1	12 35	15	0.	0.	0.	13	0.	38	3	61.	0.	0.	3
302	47	758	510	1	1. 000	830207	1	13 16	15	0.	0	0.	15.	0.	40.	0	63	0.	0.	0
302	49	758	495	1	1. 000	830207	1	14 30	15	0.	0.	0.	16.	0.	40.	0.	63.	0.	0.	0.
302	50	767	480	1	1. 000	830207	1	17 9	15	0	0.	0.	17.	0.	43.	0.	64.	0.	0.	0
302	51	767	490	1	1. 000	830207	1	18 28	15	0.	2.	0	20.	1.	44.	0.	64.	0.	0.	1.
302	52	767	500	1	1. 000	830207	1	20 46	15	0.	2.	0.	23.	0.	47.	0.	66.	0.	0.	0
302	53	767	510	1	1. 000	830207	1	22 25	15	0.	2.	3	24.	1.	48.	0.	66.	0.	0.	4.
302	54	767	520	1	1. 000	830208	1	24 43	15	0.	3	0	21.	0.	49.	0.	54.	0.	0.	0.
302	55	767	530	1	1. 000	830208	1	1 31	15	0	3.	0	22.	0	50.	0.	54.	0.	0.	0.
302	56	767	540	1	1. 000	830208	1	2 17	15	0.	0	0.	4.	1.	28.	0.	53.	0.	0.	1.
302	57	767	550	1	1. 000	830208	1	3 6	15	0.	0.	1.	5.	1.	29.	0.	53.	0.	0.	2.
302	58	767	560	1	1. 000	830208	1	5 28	15	0.	0.	0.	6.	1.	31.	0.	54.	0.	0.	1.
302	59	767	570	1	1. 000	830208	1	6 22	14	0.	0.	0.	7.	1.	32.	0.	58	0.	0.	1.
302	64	775	590	1	1. 000	830208	1	14 14	14	0.	0.	0	15.	1.	38.	0.	64.	0.	0.	1.
302	65	775	580	1	1. 000	830208	1	14 53	14	0.	0.	0.	15.	0.	41.	0.	64.	0.	0.	0.
302	66	775	570	1	1. 000	830208	1	15 29	15	0.	0.	0	16.	0.	41	1.	62.	0.	0.	1.
302	67	775	560	1	1. 000	830208	1	16 15	15	0.	0.	0.	17.	1.	42.	1	66.	0.	0.	2
302	68	775	550	1	1. 000	830208	1	17 3	14	0.	0.	0	18.	0.	44.	0.	67.	0.	0.	0.

Table 5b.—Partial listing of output data file (FORO29.DAT). Number of northern anchovy eggs grouped by S(0-3 h), A(4-27 h), B(28-51 h), C(52-75 h), D(76-99 h), and E(100-123 h).

Cruise no.	Tow no.	CalCOFI line	CalCOFI stn.	Stratum	Weighting factor	Date	Tow time (h)	Temp. (°C x 10)	No. eggs/ day categories						Disintegrated eggs	Total no. eggs in tow
									S	A	B	C	D	E		
8302	19	741	530	1	1. 00	830206	113	146	0	0	3	0	0	0	0	3
8302	24	750	485	1	1. 00	830206	619	146	0	0	0	0	0	0	0	0
8302	26	750	500	1	1. 00	830206	1539	151	0	0	0	2	0	0	0	2
8302	27	750	510	1	1. 00	830206	1717	151	0	0	0	0	0	0	0	0
8302	29	750	520	1	1. 00	830206	2232	151	0	0	0	0	0	0	0	0
8302	30	750	530	1	1. 00	830206	2311	148	0	0	0	0	0	0	0	0
8302	31	750	540	1	1. 00	830207	24 8	143	0	0	2	0	0	0	1	3
8302	32	750	550	1	1. 00	830207	2449	143	0	0	0	2	0	0	0	2
8302	33	750	560	1	1. 00	830207	147	144	0	0	0	2	0	0	0	2
8302	34	750	570	1	1. 00	830207	231	145	0	0	0	1	0	0	0	1
8302	38	758	600	1	1. 00	830207	616	146	0	0	0	2	0	0	0	2
8302	39	758	590	1	1. 00	830207	720	146	0	0	0	2	0	0	0	2
8302	40	758	580	1	1. 00	830207	8 7	146	0	0	0	2	0	0	0	2
8302	41	758	570	1	1. 00	830207	852	144	0	0	0	0	0	0	0	0
8302	42	758	560	1	1. 00	830207	934	144	0	0	0	0	0	0	0	0
8302	43	758	550	1	1. 00	830207	1039	149	0	0	0	2	0	0	0	2
8302	44	758	540	1	1. 00	830207	1122	149	0	0	0	2	0	0	0	2
8302	45	758	530	1	1. 00	830207	12 0	151	0	0	1	1	0	0	0	2
8302	46	758	520	1	1. 00	830207	1235	151	0	0	0	3	0	0	0	3
8302	47	758	510	1	1. 00	830207	1316	153	0	0	0	0	0	0	0	0
8302	49	758	495	1	1. 00	830207	1430	150	0	0	0	0	0	0	0	0
8302	50	767	480	1	1. 00	830207	17 9	150	0	0	0	0	0	0	0	0
8302	51	767	490	1	1. 00	830207	1828	151	0	0	1	0	0	0	0	1
8302	52	767	500	1	1. 00	830207	2046	152	0	0	0	0	0	0	0	0
8302	53	767	510	1	1. 00	830207	2225	151	0	3	1	0	0	0	0	4
8302	54	767	520	1	1. 00	830208	2443	152	0	0	0	0	0	0	0	0
8302	55	767	530	1	1. 00	830208	131	152	0	0	0	0	0	0	0	0
8302	56	767	540	1	1. 00	830208	217	151	0	0	1	0	0	0	0	1
8302	57	767	550	1	1. 00	830208	3 6	151	0	1	1	0	0	0	0	2
8302	58	767	560	1	1. 00	830208	528	151	0	0	1	0	0	0	0	1
8302	59	767	570	1	1. 00	830208	622	143	0	0	1	0	0	0	0	1
8302	64	775	590	1	1. 00	830208	1414	145	0	0	1	0	0	0	0	1
8302	65	775	580	1	1. 00	830208	1453	145	0	0	0	0	0	0	0	0
8302	66	775	570	1	1. 00	830208	1529	153	0	0	0	1	0	0	0	1
8302	67	775	560	1	1. 00	830208	1615	151	0	0	1	1	0	0	0	2
8302	68	775	550	1	1. 00	830208	17 3	148	0	0	0	0	0	0	0	0
8302	69	775	540	1	1. 00	830208	1824	148	0	0	0	0	0	0	0	0
8302	70	775	530	1	1. 00	830208	2044	152	0	0	1	0	0	0	0	1
8302	71	775	520	1	1. 00	830208	2121	152	0	0	0	0	0	0	0	0
8302	72	775	510	1	1. 00	830208	2315	152	0	0	0	0	0	0	0	0
8302	73	775	500	1	1. 00	830209	2410	151	0	2	2	0	0	0	0	4
8302	74	775	495	1	1. 00	830209	150	149	0	7	1	0	0	0	0	8
8302	75	783	510	1	1. 00	830209	314	151	0	0	1	0	0	0	0	1

Table 5c.—Partial listing of output data file (FORO36.DAT). Number of northern anchovy eggs and estimated ages (in hours) are grouped by developmental stages I-XI. (Cruise no. is 8302.)

Cruise no.	Tow no.	CalCOFI line	CalCOFI stn.	Stratum	Weighting factor	Date	Region	Tow time (h)	Temp. (°C)	No. eggs and ages (h)/egg stages																					
										I		II		III		IV		V		VI		VII		VIII		IX		X		XI	
302	19	741	530	1	1. 000	830206	1	113	14	0.	3.	0	4	0	23.	0	27.	0.	27	0	30	0	51	3	51	0	51	0	57.	0.	73.
302	24	750	485	1	1 000	830206	1	619	14	0	4	0	8	0	8	0	31.	0	32	0	32	0	51	0	56	0	56	0	57	0.	61
302	26	750	500	1	1 000	830206	1	1539	15	0	0	0	11	0	17	0.	17.	0	19	0	41	0	41	0	41	0	41	2	62	0	65
302	27	750	510	1	1 000	830206	1	1717	15	0	0	0	3	0	19	0	19.	0	19	0	42	0	43	0	43	0	43	0	62	0	66
302	29	750	520	1	1. 000	830206	1	2232	15	0	0	0	3	0	21	0	24	0	24.	0	26.	0	46	0	48.	0	48	0	50	0.	66.
302	30	750	530	1	1 000	830206	1	2311	14	0	1	0	4	0	23	0	25.	0	25	0	46	0	49	0	49	0	49	0	69	0	73
302	31	750	540	1	1 000	830207	1	24 8	14	0	2	0	4	0	23	0	26.	0	26	0.	46	0	50	0	50	2	50	0	69	0.	73
302	32	750	550	1	1 000	830207	1	2449	14	0	2	0	4	0	23	0	26.	0	26	0	46	0	50	0	50	0	50	2	69	0.	73
302	33	750	560	1	1 000	830207	1	147	14	0	3	0	4	0	23	0	27.	0	27	0.	30	0	51	0	51	0.	51	2	57	0	73
302	34	750	570	1	1 000	830207	1	231	14	0	4	0	4	0	7	0	28.	0	28	0	30	0	51	0	52	0	52	1	57	0	73
302	38	758	600	1	1 000	830207	1	616	14	0	4	0	8	0	8	0	31	0	32	0	32	0	51	2	56	0	56	0	57	0	61
302	39	758	590	1	1 000	830207	1	720	14	0	4	0	9	0	9	0	31.	0	33	0	33	0	39	2	57	0	57	0	57	0	61
302	40	758	580	1	1 000	830207	1	8 7	14	0	4	0	10	0	10	0	31.	0	34	0	34	0	39	0	57	2	58	0	58	0.	61
302	41	758	570	1	1 000	830207	1	852	14	0	4	0	10	0	10	0	31.	0	34	0	34	0	39	0	57	0	58	0	58	0.	61
302	42	758	560	1	1 000	830207	1	934	14	0	4	0	11	0	11	0	15.	0	35	0	35	0	39	0	57	0	59	0	59	0	61
302	43	758	550	1	1 000	830207	1	1039	14	0	4	0	12	0	12	0	15	0	36	0	36	0	39	0	57	2	60	0	60	0	61
302	44	758	540	1	1 000	830207	1	1122	14	0	4	0	12	0	13	0	15	0	37	0	37	0	39	0	57	2	61	0	61	0.	61.
302	45	758	530	1	1 000	830207	1	12 0	15	0	0	0	11	0	14	0	14.	0	35	1	38	0	38	0	40	0	61	1	62	0	62
302	46	758	520	1	1 000	830207	1	1235	15	0	0	0	11	0	14	0	14.	0	35	0	38	0	38	0	40	2	61	1	62	0	62.
302	47	758	510	1	1 000	830207	1	1316	15	0	0	0	11	0	15	0	15	0	19	0	39	0	39	0	40	0	41	0	62	0	63
302	49	758	495	1	1 000	830207	1	1430	15	0	0	0	11	0	16	0	16	0.	19	0	40	0	40.	0	40	0	41	0	62	0	64
302	50	767	480	1	1 000	830207	1	17 9	15	0	0	0	11	0	19	0	19.	0	19	0	42	0	43	0	43	0	43	0	62	0.	66
302	51	767	490	1	1 000	830207	1	1828	15	0	0	0	3	0	20	0	20	0	20	0	42	1	44	0	44	0	44	0	62	0.	66
302	52	767	500	1	1 000	830207	1	2046	15	0	0	0	3	0	21	0	22	0	22	0	26	0	46	0	46	0	46	0	50	0	66
302	53	767	510	1	1 000	830207	1	2225	15	0	0	0	3	0	21	3	24	0	24.	0	26	0	46	1	48	0	48	0	50	0	66
302	54	767	520	1	1 000	830208	1	2443	15	0	2	0	3	0	5	0	26	0	26	0	26	0	46	0	50	0	50	0	50	0	54
302	55	767	530	1	1 000	830208	1	131	15	0	3	0	3	0	5	0	27	0	27	0	27	0	46	0	51	0	51	0	51	0	54
302	56	767	540	1	1 000	830208	1	217	15	0	4	0	4	0	5	0	28	1	28	0	28	0	34	0	52	0	52	0	52	0	54
302	57	767	550	1	1 000	830208	1	3 6	15	0	4	1	5	0	5	0	28	1	29	0	29	0	34	0	52	0	53	0	53	0	54
302	58	767	560	1	1 000	830208	1	528	15	0	4	0	7	0	7	0	28	1	31	0	31	0	34	0	52	0	55	0	55	0	55
302	59	767	570	1	1 000	830208	1	622	14	0	4	0	8	0	8	0	31	1	32	0	32	0	51	0	56	0	56	0	57	0.	61
302	64	775	590	1	1 000	830208	1	1414	14	0	0	0	12	0	16	0	16	1	38	0	40	0	40	0	45	0	64	0	64	0.	64
302	65	775	580	1	1 000	830208	1	1453	14	0	0	0	12	0	16	0	16	0	38	0	40	0	40	0	45	0	64	0	64	0	64
302	66	775	570	1	1 000	830208	1	1529	15	0	0	0	11	0	17	0	17	0	19	0	41	0	41	0	41	0	41	1	62	0	65
302	67	775	560	1	1 000	830208	1	1615	15	0	0	0	11	0	18	0	18	0	19	0	42	1	42	0	42	0	42	0	62	1	66
302	68	775	550	1	1 000	830208	1	17 3	14	0	0	0	12	0	19	0	19	0	22	0	43	0	43	0	45	0	67	0	67	0	67
302	69	775	540	1	1 000	830208	1	1824	14	0	0	0	12	0	20	0.	20	0	22	0	44	0	44	0	45	0	67	0	68	0	68
302	70	775	530	1	1 000	830208	1	2044	15	0	0	0	3	0	21	0	22	0	22	0	42	0	46	1	46	0	46	0	50	0	66
302	71	775	520	1	1 000	830208	1	2121	15	0	0	0	3	0	21	0	23	0	23	0	26	0	46	0	47	0	47	0	50	0.	66
302	72	775	510	1	1 000	830208	1	2315	15	0	1	0	3	0	21	0	25	0	25	0	26	0	46	0	49	0	49	0	50	0	54
302	73	775	500	1	1 000	830209	1	2410	15	0	2	0	3	0	5	2	26	0	26	0	26	0	46	0	50	2	50	0	50	0	54
302	74	775	495	1	1 000	830209	1	150	14	0	3	2	4	0	23	0	27	5	27	0	30	0	51	0	51	1	51	0	57	0	73
302	75	7[illegible]3	510	1	1 000	830209	1	314	15	0	4	0	5	0	5	0	28	0	29	0	29	1	34	0	52	0	53	0	53	0	54

Table 5d.—Partial listing of the output data file (FORO37.DAT): estimated age (h) and number of northern anchovy eggs for those egg stages observed within or beyond the normal ranges of expected tow time ($\hat{T}$±G, see text). (Cruise no. is 8302.)

Cruise no.	Tow no.	CalCOFI line	CalCOFI stn.	Stratum	Weighting factor	Date	Region	Tow time (h)	Temp. (°C)	Est. age (h)	Lower limit of age	Upper limit of age	Egg stage	No. of eggs	Expected tow time (h)
302	26	750	500	1	1. 000	830206	1	15 39	15	62	50	62	10	2.	6.
302	32	750	550	1	1. 000	830207	1	24 49	14	69	57	69	10	2.	13.
302	33	750	560	1	1. 000	830207	1	1 47	14	57	57	69	10	2.	13.
302	34	750	570	1	1. 000	830207	1	2 31	14	57	57	69	10	1.	13.
302	39	758	590	1	1. 000	830207	1	7 20	14	57	45	57	8	2.	2.
302	45	758	530	1	1. 000	830207	1	12 0	15	62	50	62	10	1.	6.
302	46	758	520	1	1. 000	830207	1	12 35	15	61	41	61	9	2	1.
302	46	758	520	1	1. 000	830207	1	12 35	15	62	50	62	10	1.	6.
302	64	775	590	1	1. 000	830208	1	14 14	14	38	22	38	5	1.	4.
302	66	775	570	1	1 000	830208	1	15 29	15	62	50	62	10	1.	6.
302	67	775	560	1	1. 000	830208	1	16 15	15	66	54	66	11	1.	10.
302	74	775	495	1	1. 000	830209	1	1 50	14	4	4	12	2	2.	6.
302	75	783	510	1	1. 000	830209	1	3 14	15	34	34	46	7	1.	14.
302	76	783	520	1	1 000	830209	1	4 5	15	34	34	46	7	1.	14.
302	86	791	590	1	1. 000	830209	1	12 43	15	62	50	62	10	2.	6.
302	92	791	530	1	1. 000	830209	1	16 45	15	42	26	42	6	3.	8.
302	92	791	530	1	1. 000	830209	1	16 45	15	62	50	62	10	3.	6.
302	98	800	540	1	1. 000	830210	1	4 12	15	4	0	4	1	3.	24.
302	98	800	540	1	1. 000	830210	1	4 12	15	52	40	52	8	2.	20.
302	100	800	560	1	1. 000	830210	1	9 0	15	11	3	11	2	3.	5.
302	100	800	560	1	1. 000	830210	1	9 0	15	35	19	35	5	2.	1
302	102	800	580	1	1. 000	830210	1	11 30	15	11	3	11	2	1.	5.
302	108	808	570	1	1. 000	830210	1	19 53	15	66	54	66	11	1.	10.
302	133	817	580	1	1. 000	830214	1	2 33	15	4	0	4	1	10.	24.
302	133	817	580	1	1. 000	830214	1	2 33	15	28	12	28	4	3.	18.
302	133	817	580	1	1. 000	830214	1	2 33	15	34	34	46	7	1.	14.
302	133	817	580	1	1. 000	830214	1	2 33	15	52	40	52	8	1.	20.
302	134	817	590	1	1. 000	830214	1	3 10	15	4	0	4	1	2.	24.
302	139	825	570	1	1. 000	830214	1	7 20	15	4	0	4	1	1.	24.
302	146	825	490	1	1. 000	830214	1	12 32	15	61	41	[illegible]1	9	1	1.
302	155	833	406	1	1 000	830214	2	19 36	15	0	0	4	1	10.	24.
302	155	833	406	1	1. 000	830214	2	19 36	15	3	3	11	2	4.	5.
302	165	841	450	1	1. 000	830215	2	9 20	16	10	2	10	2	11.	4.
302	165	841	450	1	1 000	830215	2	9 20	16	56	44	56	10	5.	[illegible]4.
302	165	841	450	1	1. 000	830215	2	9 20	16	59	47	59	11	3.	3.
302	166	841	440	1	1 000	830215	2	10 5	16	59	47	59	11	3.	3.
302	172	850	410	1	1. 000	830215	2	16 0	16	42	30	42	7	2.	10.
302	173	850	420	1	1 000	830215	2	16 35	16	42	30	42	7	4.	10.
302	178	850	470	1	1. 000	830215	2	20 54	15	0	0	4	1	1.	24.
302	178	850	470	1	1. 000	830215	2	20 54	15	3	3	11	2	1.	5.
302	178	850	470	1	1. 000	830215	2	20 54	15	66	54	66	11	2.	10.
302	179	850	480	1	1. 000	830215	2	22 20	15	0	0	4	1	2.	24.

Table 5e.—Partial listing of data file (FORO38.DAT): Number of eggs and age (in days) excluding eggs >2.5 d old. (Cruise no. is 8302.)

Cruise no.	Tow no.	CalCOFI line	CalCOFI stn.	Date	Number of eggs	Age (in days)
302	6	0733	0550	830205	0.0000	0.4583
302	6	0733	0550	830205	0.0000	1.5694
302	6	0733	0550	830205	1.0000	2.5417
302	17	0741	0550	830205	1.0000	1.0417
302	17	0741	0550	830205	0.0000	2.0104
302	17	0741	0550	830205	0.0000	2.9583
302	18	0741	0540	830206	0.0000	0.8229
302	18	0741	0540	830206	1.0000	2.0833
302	18	0741	0540	830206	0.0000	2.9583
302	19	0741	0530	830206	0.0000	0.8438
302	19	0741	0530	830206	3.0000	2.1250
302	19	0741	0530	830206	0.0000	2.7083
302	24	0750	0485	830206	0.0000	0.2778
302	24	0750	0435	830206	0.0000	1.5208
302	24	0750	0485	830206	0.0000	2.3958
302	26	0750	0500	830206	0.0000	0.6667
302	26	0750	0500	830206	0.0000	1.7083
302	26	0750	0500	830206	2.0000	2.5833
302	27	0750	0510	830206	0.0000	0.7917
302	27	0750	0510	830206	0.0000	1.7813
302	27	0750	0510	830206	0.0000	2.6667
302	29	0750	0520	830206	0.0000	0.9896
302	29	0750	0520	830206	0.0000	2.0000
302	29	0750	0520	830206	0.0000	2.7500
302	30	0750	0530	830206	0.0000	0.8021
302	30	0750	0530	830206	0.0000	2.0104
302	30	0750	0530	830206	0.0000	2.9583
302	31	0750	0540	830207	0.0000	0.8229
302	31	0750	0540	830207	2.0000	2.0833
302	31	0750	0540	830207	0.0000	2.9583
302	32	0750	0550	830207	0.0000	0.8229
302	32	0750	0550	830207	0.0000	2.0417
302	32	0750	0550	830207	2.0000	2.8750
302	33	0750	0560	830207	0.0000	0.8438
302	33	0750	0560	830207	0.0000	1.9063
302	33	0750	0560	830207	2.0000	2.3750
302	34	0750	0570	830207	0.0000	0.2083
302	34	0750	0570	830207	0.0000	1.4271
302	34	0750	0570	830207	1.0000	2.3750
302	38	0758	0600	830207	0.0000	0.2778
302	38	0758	0600	830207	0.0000	1.5208
302	38	0758	0600	830207	2.0000	2.3333
302	39	0758	0590	830207	0.0000	0.3056
302	39	0758	0590	830207	0.0000	1.4167
302	39	0758	0590	830207	2.0000	2.3750
302	40	0758	0580	830207	0.0000	0.3333
302	40	0758	0580	830207	0.0000	1.4375

Table 6.—Number of northern anchovy eggs per tow grouped by days S(0-3 h), A (4-27 h), B (28-51 h), C (52-75 h), and D (76-99 h) from the manual system (m) and the proposed automated system (a) for each year in 1980-83.

		No. eggs/day categories					Disintegrated		No.
		S[1]	A	B	C	D	eggs	Total[2]	tows[3]
1980	m	2.72	13.65	8.86	4.91	0.16	0.82	31.14	312
	a	2.61	13.74	9.78	4.08	0.03		30.24	
1981	m	2.76	12.32	10.33	6.91	0.47	0.85	33.72	564
	a	1.81	13.86	12.00	4.98	0.13		32.78	
1982	m	2.49	9.00	7.00	4.44	0.31	0.89	24.23	308
	a	1.13	10.50	7.77	3.78	0.16		23.34	
1983	m	1.95	9.16	8.42	2.88	0.002	0.67	23.07	482
	a	2.01	9.31	8.51	2.61			22.44	

[1] S eggs from manual system (m) include some disintegrated eggs.

[2] Difference between "m" and "a" is the disintegrated eggs which were included in "m," but not in "a."

[3] Positive tows only.

DISCUSSION

The automated procedure should be fully tested before being implemented. For the anchovy egg data, 1980-83 data of aged eggs from both manual and automated procedures were compared based upon positive tows (tows with at least one egg sampled) (Table 6). Although there were some differences between the results of these two procedures, the results from the automated procedure are encouraging. The differences are due to different methods of age assignment and to subjective elements in the manual age assignment method. In the manual system, day category (S, A, B, C, D, and E) was first assigned to eggs (Stauffer and Picquelle 1985). An actual age was then computed based upon the time of tow (*k*) and day category:

$$\text{age} = k+2+24\times f \qquad (8)$$

where $f = 0,1,2,\ldots$ for A,B,C,. . .-day eggs. In the automated system, the age was assigned according to Equation (7) before the day category was assigned. Equation (8) yields a range of ages larger than that from Equation (7) and thus gives larger values for maximum ages. This difference affects the ages of older eggs, particularly in the case where eggs older than 2.5 d are excluded in computation of egg mortality. For example, at temperature 15°C, the maximum age for stage XI is 66 h using Equation (7), and the maximum age is 72 h using Equation (8) for eggs that were sampled at 0100. Thus, more eggs would be assigned to older age groups when Equation (8) was used rather than Equation (7). The subjectivities of human judgment or human errors of the manual system are evident in several steps in the manual methods. These include 1) misassignment of age from the key structure due to inexperience or the fatigue of the worker; 2) determination of age for eggs which were observed at a time significantly different from the expected time (Table 2); and 3) assignment of age to eggs observed around 0200 which is the break point of A, B, C, D, and E-day categories (Fig. 2).

To adopt the program for other species would require 1) a model for the temperature-dependent egg development, e.g., Equation (4); 2) the distribution of age within each egg stage to obtain G in Equation (6); and 3) the peak spawning time (*st*) for Equation (5), so that a reference table can be constructed which is the base of the automated procedure.

LITERATURE CITED

HEWITT, R., A. BINDMAN, and N. LO.
1984. Procedures for calculating the egg production estimate of spawning biomass. Natl. Mar. Fish. Serv., NOAA, Southw. Fish. Cent., La Jolla, CA, Admin. Rep. LJ-84-19, 46 p.

LO, N. C. H.
1983. Re-examination of three parameters associated with anchovy egg and larval abundance: Temperature dependent incubation time, yolk-sac growth rate and egg and larval retention in mesh nets. Natl. Mar. Fish. Serv., NOAA, Southw. Fish. Cent., La Jolla, CA, NOAA-TM-NMFS-SWFC-31, 33 p.

MOSER, H. G., and E. H. AHLSTROM.
1985. Staging anchovy eggs. *In* R. Lasker (editor), An egg production method for estimating spawning biomass of pelagic fish: Application to the northern anchovy, *Engraulis mordax*, p. 37-41. U.S. Dep. Commer., NOAA Tech. Rep. NMFS 36.

STAUFFER, G., and S. PICQUELLE.
1985. Procedures for sorting, staging, and ageing eggs. *In* R. Lasker (editor), An egg production method for estimating spawning biomass of pelagic fish: Application to the northern anchovy, *Engraulis mordax*, p. 33-35. U.S. Dep. Commer., NOAA Tech. Rep. NMFS 36.

ZWEIFEL, J. R., and R. LASKER.
1976. Prehatch and posthatch growth of fishes—A general model. Fish. Bull., U.S. 74:609-621.

8558

RECENT INCREASED ABUNDANCE AND POTENTIAL PRODUCTIVITY OF PACIFIC MACKEREL (*SCOMBER JAPONICUS*)

ALEC D. MACCALL
National Marine Fisheries Service
Southwest Fisheries Center
P.O. Box 271
La Jolla, California 92038

RICHARD A. KLINGBEIL
California Department of Fish and Game
245 W. Broadway
Long Beach, California 90802

RICHARD D. METHOT
National Marine Fisheries Service
Southwest Fisheries Center
P.O. Box 271
La Jolla, California 92038

ABSTRACT

Cohort analysis (VPA) of recent Pacific mackerel catches off southern California and northern Baja California shows that total biomass (age 1+) increased sharply beginning in 1977. The increase followed a period of extreme depletion, and continued for several years, reaching a peak of 300,000 to 500,000 MT in 1982. Abundance decreased substantially in 1983 and 1984 because of very weak recruitment. The 1978 year class was considerably stronger than the previous largest year class. The recent pattern of reproductive success has been more variable than was seen historically, although the underlying cycle seems to continue.

We investigate potential productivity of the Pacific mackerel resource by simulating the fishery from 1929 o 1968. The model assumes a Ricker stock-ecruitment relationship, and retains the historical pat-ern in anomalies in reproductive successes, logarithm f recruits per spawner. We examine sensitivity of the mulation results to several alternative models of ock-recruitment compensation; the results are most obust to these assumptions if exploitation rates annual catch divided by total biomass) are near 0.2. yield isopleth diagram summarizes average annual elds for linear harvest formulas of the type: harvest quals a *fraction* of the total biomass in excess of a *utoff* level. The present California Pacific mackerel shery regulations (*fraction* = 0.2, *cutoff* = 18,144 T total biomass) should produce an average yield of 7,000 MT/yr with an annual standard deviation of bout 15,000 MT. Average yield could be increased to bout 29,000 MT/yr if the *fraction* is increased to 28, but the annual standard deviation would increase about 19,000 MT, and the average total biomass ould decrease by about 25 percent. Because present lifornia fishery regulations do not include all catch- of Pacific mackerel in the harvest formula, the esent effective value of the *fraction* exceeds its minal value of 0.2.

RESUMEN

Análisis de las cohortes en capturas recientes de la caballa del Pacífico a la altura del sur de California y norte de Baja California indican que la biomasa total (edad 1+) aumentó abruptamente desde 1977. El incremento sucedió a un período de gran pauperización y continuó durante varios años, alcanzando, en 1982, un máximo de 300,000 a 500,000 toneladas métricas (TM). En 1983 y 1984 la abundancia disminuyó considerablemente debido al escaso reclutamiento. La clase anual de 1978 fué considerablemente más robusta que la clase anual anterior de mayor magnitud. El reciente patrón de éxito reproductivo fué más variable de lo registrado históricamente, pero el ciclo subyacente parece continuar. Investigamos el potencial reproductivo del recurso de la caballa del Pacífico mediante la simulación de la pesquería desde 1929 hasta 1968. El modelo presupone una relación Ricker de stock-reclutamiento, y conserva el patrón histórico de anomalías en el éxito reproductivo, i.e., logaritmo de reclutas por desovante. Examinamos la sensibilidad de los resultados de la simulación con respecto a varios modelos alternativos de compensación stock-reclutamiento; los resultados mas coherentes frente a estos supuestos se obtienen si los ritmos de explotación (captura anual sobre biomasa total) se mantienen en alrededor de 0.2. Un diagrama de isolíneas de rendimiento resume los rendimientos anuales medios para fórmulas de cosechas lineales del siguiente tipo: la cosecha es igual a una fracción de la biomasa total la cual excede un valor límite dado. Las reglamentaciones californianas actuales sobre la pesca de la caballa del Pacífico (fracción = 0.2, valor límite = 18,144 TM de biomasa total) deberían producir un rendimiento promedio de 27,000 TM por año, con una desviación estándar anual de aproximadamente 15,000 TM. La captura promedio podría ser aumentada a alrededor de 29,000 TM por año si la fracción fuera incrementada a 0.28, pero esto llevaría a un aumento de la desviación estándar anual a unas 19,000 TM, y la biomasa media total disminuiría en un aproximadamente 25%. Dado que las actuales reglamenta-

---

nuscript received February 15, 1985.]

ciones pesqueras de California no incluyen todas las capturas de caballa del Pacífico en la fórmula del rendimiento, el valor actual efectivo de la fracción excede su valor nominal de 0.2.

INTRODUCTION

The Pacific mackerel (*Scomber japonicus*) resource off California is one of the most thoroughly studied in world fisheries. Its population dynamics, nonetheless, remain enigmatic in many respects. Fishery data have allowed cohort analyses to extend from the beginning of the fishery in 1929 to its collapse in the late 1960s, a period of about 40 years (Parrish and MacCall 1978). The California fishery was closed by legislation in 1970 and reopened in 1977, when abundance increased (Klingbeil 1983). Lack of fishery data during this closed period prevents detailed analysis of the collapsed population. However, the relatively large fishery since 1977 once again has supplied data sufficient for population estimates, the results of which are reported here.

In 1972 the California legislature enacted an innovative management law that established Pacific mackerel catch quotas according to a formula based on estimated resource abundance. The formula was changed in 1978 to its present wording, whereby seasonal harvest is to be no more than 20 percent of the excess over 20,000 short tons (18,144 MT). Klingbeil (1983) gives a detailed history of the fishery's management, including provisions for incidental catch allowances and size limits. Recent biological and economic conditions have caused both the southern and central California purse seine fleets to increase reliance on Pacific mackerel. The result has been that during recent seasons (1983-84 and 1984-85), quotas have been met much earlier than they otherwise would have been. Fishermen were then faced with several months of interseason restrictions on the catch of Pacific mackerel with virtually no alternative species available for redirected effort. Fishery managers have been faced with imposing short-term economic hardships on fishermen or else increasing quotas above the quantity dictated by the harvest formula and current abundance estimate.

Accordingly, some parts of industry and management have expressed interest in either modifying the harvest formula or replacing it with other management measures (e.g., constant quotas) in order to allow higher catch rates and/or lessen the need for in-season quota adjustments. Because the formula adopted in 1978 was not based on extensive fishery analysis, we have undertaken an evaluation of that formula in comparison with a range of alternative management measures. This analysis provides a guide for revising the management regime as well as an assessment of reasonable expectations for future catch levels and patterns.

ABUNDANCE ESTIMATES

Method

Because many segments of the Pacific mackerel fishery are highly seasonal, we have compiled catches on a quarterly basis beginning with the fourth quarter of 1976, when incidental catches rose to a level allowing monitoring (Table 1). Accuracy of abundance estimates by cohort analysis requires that all catches be accounted for, so we have included estimates of the northern Baja California commercial catch (provided by Biol. Walterio Garcia, Instituto Nacional de Pesca, Ensenada, B.C.N., Mexico), and the recreational catch on the Pacific coast of the United States. Some of these source data were aggregated by year, and others are not yet available; reasonable assumptions (documented in Table 1) were employed where necessary to complete the catch information base. Errors in cohort analysis that arise from converting annual

TABLE 1
Season (July-June) Catches (MT) for Commercial and Recreational Segments of the Pacific Mackerel Fishery

	California		Mexico [a]		Fraction sampled (California
Season	Comm.	Recr.[b]	Comm.	Total	comm./total)
1976-77	2603	190	1271	4064	0.64
1977-78	7787	872	5168	13827	0.56
1978-79	18249	1678	7376	27303	0.67
1979-80	27753	1648	5153	34554	0.80
1980-81	27910	1910	3368	33179	0.84
1981-82	37950	(1366)[c]	3045	42361	0.90
1982-83	30045	(1412)	(4518)	35975	0.84
1983-84	35908	(1412)	(4518)	41838	0.86

All fish for which ages were determined were sampled from the California commercial landings.

[a] Annual Mexican commercial catches and estimates of recent catches were supplied by Walterio Garcia (personal communication, Instituto Nacional de Pesca, Ensenada, Mexico). We calculated seasonal values by assuming 40% of the annual catch is taken in January-June.

[b] California partyboat catch is converted to total recreational catch based on the Marine Recreational Surveys of 1979 and 1980 (Holliday et al. 1984).

[c] Monthly partyboat catches are known through August 1981. Annual catch is known for 1981 and 1982. Annual catches for 1983 and 1984 are assumed to be the same as in 1982.

catches to nominal seasonal catches are not likely to be large (Sims 1982). Because age composition estimates are lacking for the Mexican and recreational fishery segments, their age compositions were assumed to be the same as that of the commercial fishery monitored at San Pedro, California. Although there are errors associated with these assumptions, much larger errors would necessarily result from omitting catch estimates for these incompletely reported segments.

The cohort analyses were conducted similarly to earlier estimates, except that the solution uses an accounting season beginning July 1 rather than May 1, as was used by Parrish and MacCall (1978). As before, fish 4 years old or older (age 4+) are assumed to be fully and equally available to the fishery; fishing mortality rates of age 4+ and age 5+ fish are equated in each season in order to "link" the solutions for adjacent cohorts. The instantaneous natural mortality rate (*M*) was assumed to be 0.5/yr (Parrish and MacCall 1978).

Current values of fishing mortality rates (*F*) need to be assumed in order to obtain *F* estimates for earlier time periods. The current values are imprecise, not being based on direct evidence; fortunately, estimates of fishing mortality rates for earlier periods become less arbitrary because of converging properties of cohort analysis (Parrish and MacCall 1978, 38-39). Lacking independent indices of mackerel abundance, we must base the estimate of current *F* (and hence the current biomass) on internal consistency and experience with fishery analysis; it would be misrepresentation to claim this to be more than an elaborate educated guess.

TABLE 2
Fishing Mortality Rate Estimates for Age 4+ Fish, for Various Initial Assumed Values

Season	Annual *F* estimate for age 4+		
1978-79	0.264	0.279	0.289
1979-80	0.417	0.450	0.473
1980-81	0.295	0.330	0.355
1981-82	0.292	0.341	0.378
1982-83	0.282	0.348	0.403
1983-84 (assumed)	0.3	0.4	0.5

Our rationale for postulating initial values of *F* is as follows:

Fully available ages (4+). Trial solutions using a variety of current (1983-84 season) *F* estimates (Table 2) showed that a value of 0.3/yr produced consistently similar values for the preceding three seasons, and would correspond to roughly constant fishing mortality rates generated by the fishery. However, since mid-1983 jack mackerel (*Trachurus symmetricus*, the main alternative species in the fishery) have been much less available than usual, suggesting that fishing has been directed more specifically toward Pacific mackerel than in previous periods. Also, the abundance of Pacific mackerel has declined in the 1982-83 and 1983-84 seasons for all trial solutions (Figure 1),

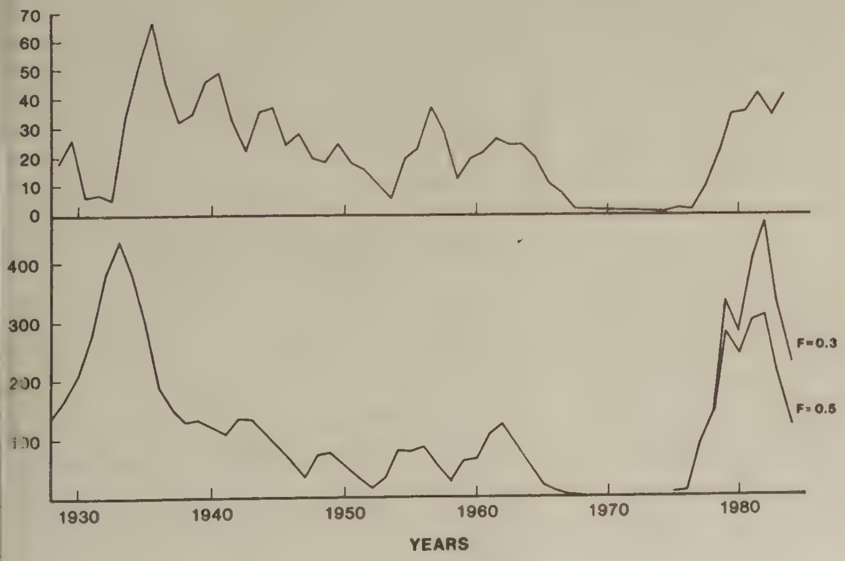

Figure 1. History of total harvest and total abundance (age 1+) of Pacific mackerel. Recent abundances reflect the range of assumed current fishing mortality rates (*F*) used in the analysis.

and *F* may have increased because of an abundance-dependent increase in the catchability coefficient, as is typical for coastal pelagic fisheries (cf MacCall 1976). Associated with this decline is a much older age composition, which in itself should result in higher average availability and consequently higher fishing mortality rates given similar levels of nominal fishing effort. Moreover, total catches during 1984 reached nearly 41,000 MT, one of the highest levels since the recovery began (Figure 1). On the other hand, the Pacific mackerel population extended northward much farther than normal in 1983 and 1984, probably in association with warm oceanic conditions. This would have reduced the available fraction of the stock, and would have reduced *F* accordingly. An *F* approaching 0.5/yr was generated on fully available fish in the 1979-80 season (Table 2), indicating that a value this high is clearly possible. We concluded that a range of current *F* from 0.3/yr to 0.5/yr is roughly consistent with these observations. These values provide nominal upper and lower abundance estimates, respectively (Figure 1). We feel that true abundance probably lies somewhere between these levels, but only future catch patterns can confirm these estimates.

Partially available ages (0,1,2,3). We obtained estimates of historical abundance of the 1980 and earlier year classes by assuming values of current *F* for fully available fish. We then evaluated availability of younger ages relative to age 4+ for the 1979-80 through 1982-83 seasons. Mean availabilities differed very little for the three solutions, and were 0.026, 0.153, 0.380, and 0.717 for ages 0 through 3 in the current $F = 0.4$/yr solution. Current *F* values for the partially available ages were obtained by multiplying estimated *F* for fully available ages by mean availability at age. These estimates become very imprecise for the younger age groups, but the effect on the 1984 abundance estimate is relatively small because the contribution from the 1982 and 1983 year classes is unusually small. Nominal estimates for age 0 fish are inaccurate because the fish appear in the catch only toward the end of the season.

Annual biomasses are calculated for July 1 of each year, using estimated abundances (Table 3) and observed mean weights at age for the third quarter of that year. We calculated spawning biomasses according to the spawning fractions at age given by Parrish and MacCall (1978, 26-27). Where comparisons with the historical fishery were desired, we projected numerical abundances back to May 1 by multiplying by EXP $[(F+M)/6]$, and calculated biomasses based on mean weights at age from the second quarter of the year.

Results

Pacific mackerel abundance from 1977 to 1984 was of a magnitude that has not been experienced for nearly 50 years in California (Figure 1). The high biomasses estimated by Parrish and MacCall for the 1930s were based on length-composition information that they considered unreliable. Thus the reality of those extremely high abundance estimates seemed questionable. However, the similar abundances estimated for the recent period confirm that the resource can attain such high levels. The contrast between recent abundances and those of the previous decade (1967-76) is even more remarkable. In view of this apparently unusual behavior of the resource, it is reasonable to inquire whether the recent patterns of Pacific mackerel population dynamics are similar to, or different from those of the preceding period.

The historical relationship between recruitment and spawning biomass has been nebulous, even when viewed on a log-log scale (Figure 2). Yet the recent estimates are variable even by historical standards: many of the new observations fall on the periphery or outside the "cloud" of points established during the previous 40 years of fishery analysis. The 1976 year class that initiated the fishery recovery was moderately strong, but was produced by a spawning biomass much smaller than any parental abundance previously

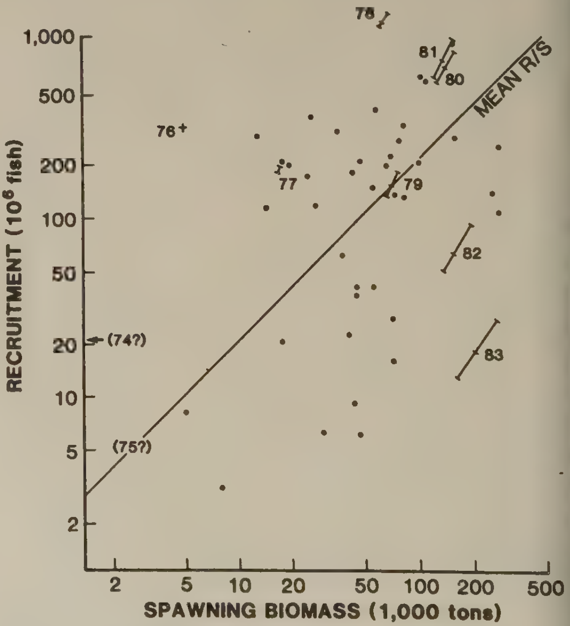

Figure 2. Relationship between Pacific mackerel recruitment and spawning biomass (log-log scale). Ranges of recent estimates reflect the range of assumed current fishing mortality rates (*F*) used in the analysis. Historical values (dots) are included for comparison.

TABLE 3
Annual Catches at Age (*C*, 10^6 Fish), Estimated Fishing Mortality Rates (*F*, $Year^{-1}$), and Initial Abundances at Age (*N*, 10^6 Fish on July 1) for the Current *F* = 0.4/yr Solution

	Age						
Season	0	1	2	3	4	4+	5+
1976-77							
C	15.5	0.05	1.3				
F	0.041	0.015	0.156				
N	—	5.0	11.7				
1977-78							
C	7.9	38.3	0.08	0.21			
F	0.034	0.172	0.036	0.045			
N	—	304.8	3.0	6.1			
1978-79							
C	64.2	20.9	30.8	0.85	0.68	0.68	
F	0.041	0.165	0.286	0.894	0.279	0.279	
N	—	173.7	155.6	1.8	3.5	3.5	
1979-80							
C	0.1	105.3	14.2	13.5	0.13	0.60	0.47
F	0.001	0.120	0.224	0.273	0.451	0.451	0.451
N	—	1181.8	89.4	70.9	0.4	2.1	1.6
980-81							
C	16.2	1.4	77.7	7.6	7.3	7.5	0.18
F	0.019	0.012	0.167	0.249	0.330	0.330	0.330
N	—	141.6	636.1	43.3	32.7	33.5	0.8
981-82							
C	6.1	33.8	5.8	66.6	4.7	8.1	3.4
F	0.007	0.069	0.090	0.296	0.341	0.341	0.341
N	—	641.7	84.8	326.3	20.5	35.1	14.6
982-83							
C	0.6	19.9	23.7	7.4	34.5	38.1	3.6
F	0.008	0.037	0.086	0.221	0.348	0.348	0.348
N	—	693.9	363.2	47.0	147.2	162.4	15.2
983-84							
C	0.2	2.8	45.3	40.2	6.0	—	18.4
F	0.010	0.061	0.152	0.287	0.400	—	0.400
N	—	59.9	405.6	202.1	22.9	—	69.6
uly 1, 1984							
N	—	16.5	34.2	211.3	92.0	—	37.6

he 1974 year class (upper right diagonal) includes all older ages.

een to have produced such a level of recruitment. The ecruitment strength of the 1978 year class (1.21 to 44 billion fish on May 1) was 27% to 52% larger an the previous record 1932 year class (0.95 billion sh). Indeed, three of the four largest year classes on cord (1978, 1980, and 1981) may have occurred nce the recovery. In contrast, the 1982 and 1983 year asses appear to be unusually weak with respect to the rge spawning biomasses that produced them. This lies the previous impression (Parrish and MacCall 1978, 42) that recruitment strength is much less variable when spawning biomass exceeds 100,000 MT, and that this abundance provides insurance against recruitment failure.

The temporal pattern of reproductive success, measured as the logarithm of recruits per spawning biomass, historically followed a roughly cyclic pattern (Figure 3). As expected from Figure 2, the amplitude of recent fluctuations is larger than was seen in the historical pattern. The decline in reproductive success

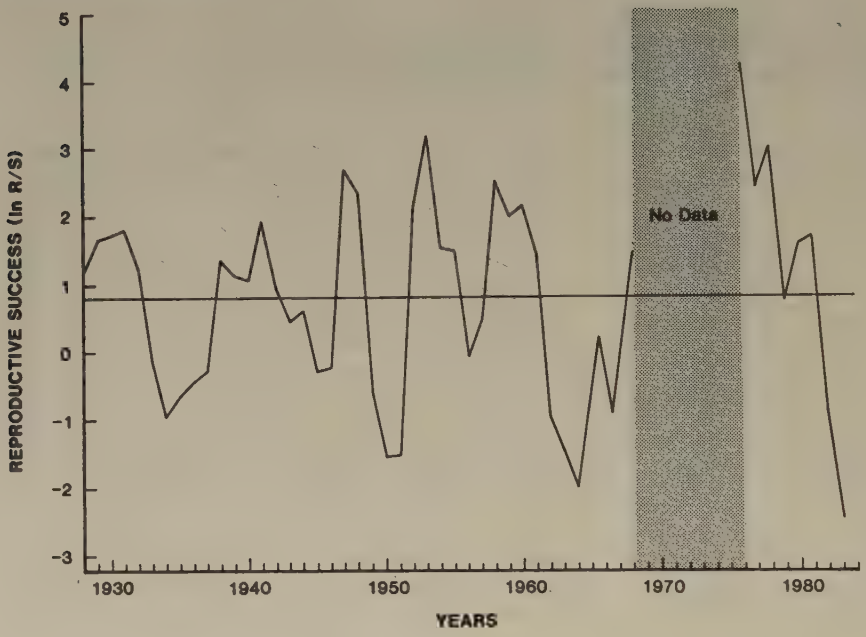

Figure 3. Time series of Pacific mackerel reproductive successes, based on an assumed current F of 0.4/yr. R is recruitment in numbers of fish; S is spawning biomass in kg.

from 1976 to 1983 shows a multiyear decline similar to previous declines, but with short-term reversals that have not been common previously. The presumptive cycle is not yet complete; early catches of the 1984 year class indicate that it is stronger than the two preceding year classes. Of course, a prolonged series of poor reproductive success is possible, especially in view of the historical pattern of poor recruitments from 1933 to 1938, immediately following the very high abundances of the early 1930s. The recent decline from the top (1976) to the bottom (1983?) of the present cycle in reproductive success has taken at least eight years, which is one year longer than the previous longest decline (from 1957 to 1964). The reproductive success at the top of the recent cycle was approximately 750 times that at the presumptive bottom of the cycle, making Pacific mackerel off California one of the more variable cases known to fishery science. The temporal pattern of reproductive success since the recovery is roughly congruent with the previous historical pattern, but the scale appears to be different. The unreliability of the values estimated by Parrish and MacCall for the 1930s limits our ability to draw definitive comparisons.

POTENTIAL PRODUCTIVITY

Method

The Pacific mackerel resource is by nature highly variable. Standard fishery models, most of which are based on equilibrium assumptions, are inappropriate for addressing this variability and its consequences. Here we assess potential productivity by means of computer simulations. We re-create the fishery from 1929 to 1968 under various harvesting policies, basing the simulated resource response on the observed history of reproductive successes, and thus preserving the important temporal pattern of the fluctuations (cf Figure 3). The calculations use Pope's (1972) approximation to the catch equation, whereby annual catches are removed from the simulated stock instantaneously at midseason. Weights at age are taken from Parrish and MacCall (1978, Table 7), and availabilities at age are based on the average F relative to that of age 4+ for the 1945-46 to 1964-65 seasons, during which period the resource was fully exploited. The natural mortality rate (M) was assumed to be 0.5, and ages 4 and older are combined into a single age group. Table 4 gives age-specific parameter values used in the simulations.

Treatment of the stock-recruitment relationship (SRR) has a strong influence on estimates of productivity, and deserves extensive discussion. Because the simulated spawning biomass is usually different from the historical spawning biomass for a particular year, the simulated recruitment should be correspondingly different from the historical recruitment. The nature and extent of that difference is given by the SRR. Unfortunately, the historical reproductive successes do not show a clear functional SRR (Figures 2,4).

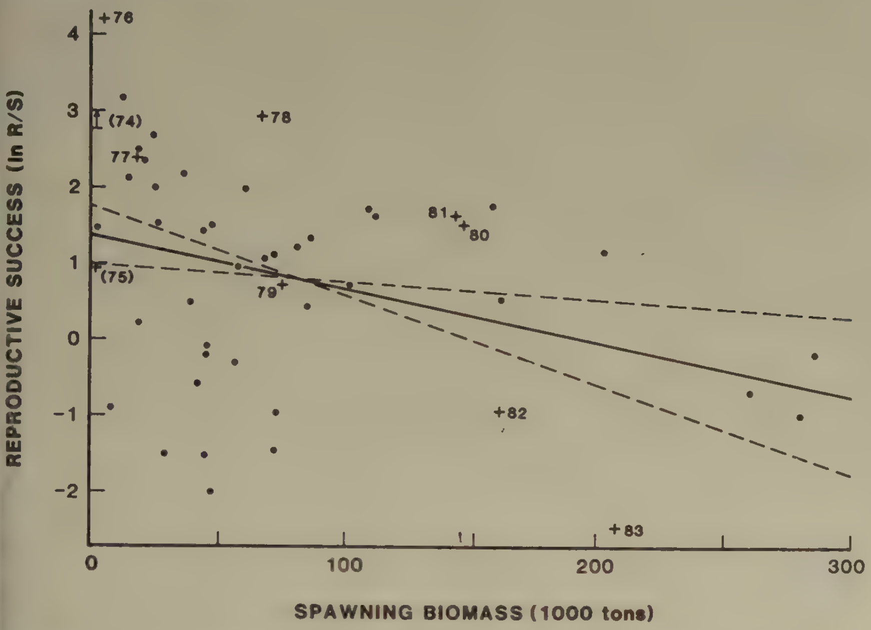

Figure 4. Relationship between Pacific mackerel reproductive success and spawning biomass, showing the linear regression estimates. Dashed lines show a nominal 90 percent confidence interval for the slope, *b*.

Therefore we consider two null models: first, that of "constant reproductive success" (CR/S), where historical reproductive successes are used without compensatory modification, and at the other extreme, "constant recruitment" (CR), where the historical recruitments themselves are used without modification, i.e., complete compensation. The true response must lie between the two extremes given by these null models, so they provide reasonable bounds on the estimated productivity of the resource. An intermediate level of compensation is represented by the Ricker SRR, which can be defined by a linear regression of ln(*R*/*S*) on spawning biomass (*S*). Some degree of compensation seems necessary because the abundance trajectory of the 40-year simulation reaches unreasonably high levels in the absence of harvest, whereas use of the Ricker SRR produces an abundance trajectory with upper bounds similar to the abundance levels observed in the 1930s and 1980s (Figure 5). It is important that we have no objective evidence that a Ricker SRR is appropriate. However, the model agrees with the trend in the data (Figure 4), and is mathematically convenient.

TABLE 4
Age-Specific Parameters Used in the Pacific Mackerel Fishery Simulations

	Age 1	 2	 3	 4	 5+
Availability	0.366	0.494	0.711	1.000	1.000
Weight (kg)	0.192	0.317	0.448	0.574	0.725
Fraction spawning	*	0.77	0.88	1.00	1.00
Initial abundance (10^6 fish)	229.6	207.0	33.2	24.4	0.0

*Fraction age 1 is 0.54/EXP(15.8*B*), where *B* is total biomass age 1+) in 10^6MT (Parrish and MacCall 1978).

The Ricker SRR used in the simulations retains the observed time series of anomalies in historical reproductive success,

$$\ln(R/S)_i = a - bS_i + e_i$$

where R_i is recruitment (in numbers) from the spawning in year i,
S_i is spawning biomass (kg),
a and b are parameters estimated from the historical data from 1929 to 1983,
and e_i is the anomaly in year i.

Although this regression estimate of parameters may be assumed to provide the best estimates of resource productivity from the simulations, the extreme variability of reproductive success (Figure 4) makes sensitivity analysis appropriate. In addition to the best-fitting Ricker SRR ($a = 1.352$, $b = 6.788/10^6$MT, $SE_b = 2.818/10^6$MT, $46df$), we examined cases corresponding to the upper and lower 90% con-

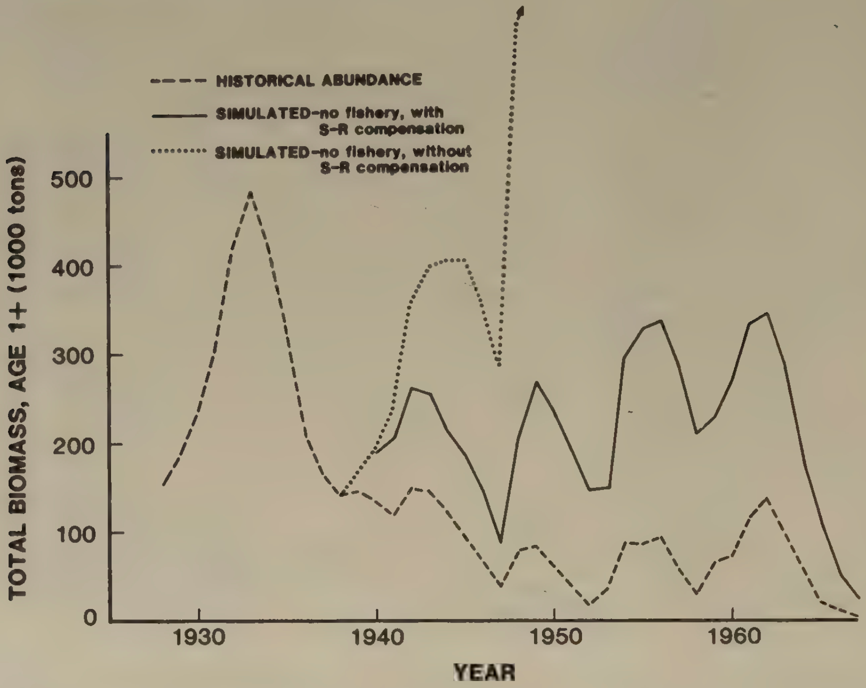

Figure 5. Time trajectories of simulated total biomass of Pacific mackerel. Solid line is based on the best-fitting Ricker SRR; dashed line is based on the CR/S model.

fidence limits of the slope parameter from the regression ($b_{\text{upper}} = 11.521/10^6\text{MT}$, $b_{\text{lower}} = 2.055/10^6\text{MT}$). Besides imprecision arising from natural variability, estimates of b are also influenced by systematic biases resulting from violations of simplifying assumptions. For example, Ludwig and Walters (1981) showed that random error in measurement of spawner abundance (S_i) tends to produce underestimates of b. In contrast, Walters (1985) showed that the time-series dynamics of propagation of environmental perturbations (e_i) tend to lead to overestimation of b. The extent of, and interaction among, these systematic biases is unknown.

Results

Although a wide variety of management policies could be evaluated by our simulation procedure, we present results for only one type of policy—that corresponding to the linear harvest formula of the present California management law. This type of policy can be written as

$$H = p(B\text{-}B_{\min}) \qquad \text{if } B > B_{\min}$$
$$H = O \text{ otherwise.}$$

Thus, the harvest (H) is specified by two parameters, and is given by the fraction (p, the *fraction*) of the excess of the total biomass (B) over a minimum total biomass ($B_{\min}$, the *cutoff*). Note that if the formula implies a negative harvest, no harvest is allowed. A *cutoff* of zero abundance is analogous to a constant effort policy. *Cutoff* values greater than zero approach a constant escapement policy, whereas *cutoff* values less than zero approach a constant harvest policy.

For the purpose of sensitivity analysis, we compare yields averaged over the 40-year simulation, given the five different stock-recruitment compensation models discussed above (Figure 6). This comparison examines the set of harvest formulas consisting of various *fractions*, given a *cutoff* of 18,144 MT (20,000 short tons) total biomass. The average annual yields are very consistent for *fractions* from 0.2 to 0.25; simulated spawning biomasses are most near their historical values (average is 80,573 MT); spawning successes are most near their historical values; and the influence of different assumed models of compensation is minimal. Accordingly, we should be able to place our greatest confidence in this region of the yield curves. Unlike the other models, the CR model produces an asymptotic yield curve because the model lacks feedback of harvests on subsequent recruitments. The CR/S model behaves badly at low fishing intensities, because it allows the simulated abundance to become unreasonably large, as was mentioned previously. As might be expected, the yield curve corre-

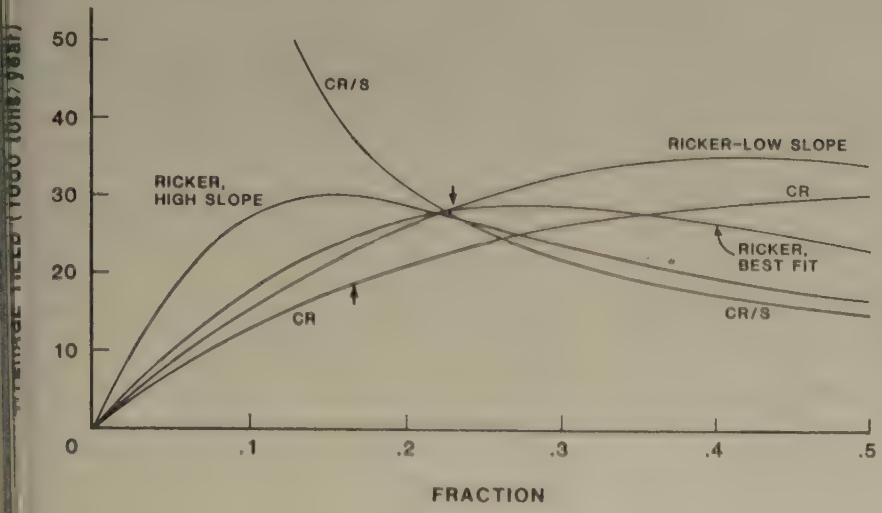

Figure 6. Comparison of average Pacific mackerel yields from linear harvest policies with a *cutoff* of 18,414 MT (20,000 short tons), and five assumed models of stock-recruitment compensation. The arrow denotes the simulations with greatest robustness, where simulated average spawning biomass is equal to the historical average.

onding to the upper confidence limit for parameter (i.e., the most compensation) tends to resemble the R yield curve, and the lower confidence limit (i.e., ast compensation) produces a yield curve closely sembling the CR/S curve at higher fishing intensies. Although the fishing intensity needed to produce e maximum average yield is sensitive to the assumed mpensation model, the maximum average yield itlf is much less sensitive, ranging from 29,000 to ,000 MT (within the 90% confidence limits of the cker SRR).

Our simulation results are summarized by a yield opleth diagram showing the average yields for vars combinations of the *cutoff* and *fraction* parameters the linear harvest formula (Figure 7). The region of eatest confidence in the simulation results, where erage simulated spawning biomass is equal to the storical average, extends across the center of the agram, rising slightly toward the right. Maximum erage yield for a given *cutoff* appears as a ridge also ing toward the right. Maximum average yield for a ro-*cutoff* (constant effort) policy is 28,500 MT/year, ereas it exceeds 30,000 MT/year at large *cutoff* lues.

In general, the standard deviation of annual harvest reases with larger *fractions*, but is nearly indepent of *cutoffs* in the range of values examined here. e standard deviation of annual harvest rises in prortion to the *fraction* to about 15,000 MT at a *fracn* of 0.2, and then becomes roughly asymptotic at out 20,000 MT for *fractions* above 0.3. Because her *cutoffs* require higher fractions to maximize ld, variability also increases with maximum avere yield.

Formulas with negative *cutoffs* do not curtail harvest at low abundances, and therefore run a high risk of depleting the resource. The region of Figure 7 marked "collapse" shows those parameter values that result in total loss of the resource within the 40-year period of the simulation; the actual region of potential collapse extends to much lower *fractions*, but does not extend to positive values of *cutoff*, which serve to protect against total loss of the resource. Also, the isopleths of average yield for negative *cutoffs* do not recognize the long period of no yield following a collapse, so actual isopleths must bend downward much more sharply than is shown by the upper left section of Figure 7.

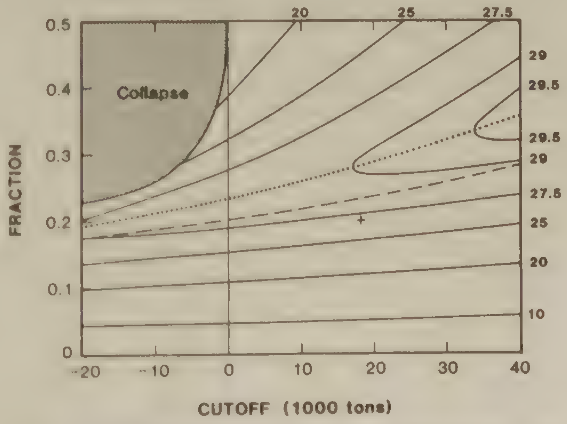

Figure 7. Average yield isopleths for linear harvest policies and the best-fitting Ricker SRR. Dotted line is maximum average yield, given the *cutoff*. Dashed line is the locus of greatest robustness, where simulated average spawning biomass is equal to the historical average. The cross denotes present management policy.

DISCUSSION

The high abundances of the 1930s and 1980s are remarkable events in the history of the fishery (Figure 1). We are now able to attempt to estimate how often these events occur. The paleosedimentary record of Pacific mackerel scales in the Santa Barbara Basin (Soutar and Isaacs 1974) shows two peak periods of deposition since 1800. One is in 1925-35, corresponding to the known abundance peak at that time. The other event occurred about 1830. Albeit imprecise, the simulated trajectory of Pacific mackerel abundances in the absence of a fishery (Figure 5) suggests that none of the post-1930 peaks would have been as large. Thus we can tentatively identify three major eruptions of the resource in the last 185 years, and conclude that the recent level of abundance is a rare event.

The ecological effects of increased Pacific mackerel abundance are confounded with other recent changes in the environment and fisheries. Mackerel extended their range far to the north during the 1980s, but the migratory effects of population pressure are difficult to separate from the influence of the strong 1982-84 oceanic warming. During 1983 and 1984 Pacific mackerel schools were reported in Puget Sound and Queen Charlotte Sound (Canada), and frequently were caught off Oregon in ''blind'' purse seine sets sampling nekton (W. Pearcy, Oregon State Univ., pers. comm.). Mackerel were abundant in Monterey Bay and the Gulf of the Farallons, off San Francisco. James Messersmith (CDF&G, Sacramento, California, pers. comm.) identified a very small juvenile Pacific makerel caught in 1984 in Humboldt Bay, near Eureka. This is clear evidence for at least marginally successful spawning over 400 nmi north of Point Conception, the usual northern boundary of spawning (Kramer and Smith 1970).

Mais (1981) reported a sudden change toward a much younger age composition of northern anchovies (*Engraulis mordax*) in southern California beginning about 1977. He suspected increased predation by Pacific mackerel and increased fishing pressure from the expanding Mexican anchovy fishery to be the major causes of this shift. Also, anchovy abundance has declined severely from the levels of the mid-1970s (ca. 2 million MT spawning biomass) to 1984 (ca. 0.3 million MT). In view of the Pacific mackerel abundances estimated in this paper, which are much larger than the previous estimates available to Mais, an increased mortality rate of anchovies due to mackerel predation is a very likely cause of these changes in the anchovy stock. Anchovy age composition analysis by Methot (1983) indicated large changes in the natural mortality rate of anchovies, but a conclusive statistical demonstration of this phenomenon is difficult.

The northerly extension of Pacific mackerel has been popular with commercial fishermen at Monterey, where landings have reached record levels. On the other hand, recreational fishermen seeking salmon in the Gulf of the Farallons have complained about interference and gear losses caused by mackerel. Salmon biologists in Canada have been concerned about potential increased predation on salmon smolts in Queen Charlotte Sound. To the south, recreational fishermen often spurn Pacific mackerel in the pursuit of more esteemed sportfish. Indeed, some recreational fishermen blame increased abundance of Pacific mackerel for the increased harassment of recreational fishermen by California sea lions (*Zalophus californianus*). The importance of Pacific mackerel as forage aside, these perceptions combine with the harvesting desires of southern and central California commercial fishermen to form an unusually unified public opinion that allowable catches should be increased. This opinion is strengthened by the prevailing industry opinion—confirmed by the estimates in this paper—that Pacific mackerel abundance, and hence allowable harvest, have been underestimated for several years.

Evaluation of the present management policy requires consideration of both interacting components of this policy: the harvest formula, and the abundance estimates used to implement it. Within the framework of the present linear harvest formula there is little reason to change the present *cutoff* level of 18,144 MT (20,000 short tons). This level provides sufficient protection from severe depletion while allowing a fishery in nearly all years. The latter consideration is additionally important because the present method of estimating abundance depends entirely on fishery information.

The present *fraction* of 0.2 is more amenable to change. The simulations, which assume all catches are accounted for in the harvest formula, indicate that a higher *fraction* is likely to increase average yield up to a maximum of about 29,000 MT/yr at a *fraction* of 0.28 (Figure 7). The sensitivity analysis showed that the optimal *fraction* is strongly influenced by the assumed model of compensation. However, for simplicity the following discussion will consider only the results of the best-fitting Ricker SRR, the case that best corresponds to available information.

Strict maximization of yield is often undesirable because the last increments in yield are achieved at the cost of relatively large decreases in abundance and correspondingly large increases in fishing effort. Of course, if Pacific mackerel are perceived as pests, this reduction in abundance may be desirable in its own right. Assuming we wish to conserve the resource, a popular rule of thumb is the ''$F_{0.1}$'' policy suggested

TABLE 5
Yield and Biomass Statistics for Various *Fractions*, Given a *Cutoff* of 18,144 MT (20,000 Short Tons), Based on Simulations Using the Best-Fitting Ricker Stock-Recruitment Model

	Yield		Biomass	
Fraction	Average	Standard deviation	Average total	Average spawning
0.00	0.0	0.0	236	160
0.01	2.14	1.02	232	157
0.20	27.1	15.4	153	90
0.24	28.6	17.3	137	78
0.28	29.0	18.7	122	67
0.30	29.0	19.2	115	63
0.40	26.7	20.4	85	44

(Values in 1000 MT).

by Gulland and Boerema (1973), whereby fishing effort should not be greater than the intensity at which the marginal yield from an additional unit of effort is ten percent of the marginal yield at very low levels of fishing. For the present case of Pacific mackerel, *fraction* may be substituted for "effort", giving a *fraction*$_{0.1}$ of 0.24. Table 5 gives some values of *fraction* together with comparative statistics from the simulation results. It is important that these yield estimates assume that all catches are accounted for by the harvest formula, whereas present management policy gnores recreational catches, incidental catches during he closed commercial season, and foreign fishery catches—all of which add up to many thousand tons. Thus the effective *fraction* must be considered to be somewhat larger than the nominal *fraction* in the wording of the official management policy. Finally, he 40,000 MT harvests that have been taken from 1979 to 1984 must not be expected to continue for long under the present, or any, management policy.

ACKNOWLEDGMENTS

We wish to thank Walterio Garcia and the Instituto Nacional de Pesca for supplying catch data for the Ensenada fishery. Also, we thank Gordon Broadhead for valuable ideas, which we have used in estimating Pacific mackerel abundances.

LITERATURE CITED

Gulland, J.A., and L.K. Boerema. 1973. Scientific advice on catch levels. Fish. Bull., U.S. 71:325-335.

Holliday, M.C., D.G. Deuel, and W.M. Scogin. 1984. Marine recreational fishery statistics survey, Pacific coast, 1979-1980. U.S. Dept. Commerce, Current Fishery Statistics (8321), 224 p.

Klingbeil, R.A. 1983. Pacific mackerel: A resurgent resource and fishery of the California Current. CalCOFI Rep. 24:35-45.

Kramer, D., and P.E. Smith. 1970. Seasonal and geographic characteristics of fishery resources. California Current region—I. Jack mackerel. Commer. Fish. Rev. 32(5):27-31.

Ludwig, D., and C.J. Walters. 1981. Measurement errors and uncertainty in parameter estimates for stock and recruitment. Can. J. Fish. Aquat. Sci. 38:711-720.

MacCall, A.D. 1976. Density dependence of catchability coefficient in the California Pacific sardine, *Sardinops sagax caerulea*, purse seine fishery. CalCOFI Rep. 18:136-148.

Mais, K.F. 1981. Age-composition changes in the anchovy, *Engraulis mordax*, central population. CalCOFI Rep. 22:82-87.

Methot, R. 1983. Age-specific abundance and mortality of northern anchovy. *In* A.D. MacCall and R. Methot, The historical spawning biomass estimates and population model in the 1983 anchovy fishery management plan. SWFC Admin. Rept. LJ-83-17. Southwest Fisheries Center, P.O. Box 271, La Jolla, CA 92038, p. 14-40.

Parrish, R.H., and A.D. MacCall. 1978. Climatic variation and exploitation in the Pacific mackerel fishery. Calif. Dept. Fish Game Fish Bull. 167, 110 p.

Pope, J.G. 1972. An investigation of the accuracy of virtual population analysis using cohort analysis. Res. Bull., Int. Comm. No. Atlantic Fish. 9:65-74.

Sims, S.E. 1982. The effect of unevenly distributed catches on stock-size estimates using virtual population analysis (cohort analysis). J. Cons. Int. Explor. Mer 40:47-52.

Soutar, A., and J.D. Isaacs. 1974. Abundance of pelagic fish during the 19th and 20th centuries as recorded in anaerobic sediment off the Californias. Fish. Bull. U.S. 72:257-273.

Walters, C.J. 1985. Bias in the estimation of functional relationships from time series data. Can J. Fish. Aquat. Sci. 42:147-149.

8559

McLAIN ET AL.: ANOMALOUS WARM EVENTS IN EASTERN BOUNDARY CURRENT SYSTEMS
CalCOFI Rep., Vol. XXVI, 1985

ANOMALOUS WARM EVENTS IN EASTERN BOUNDARY CURRENT SYSTEMS

DOUGLAS R. McLAIN, RUSSELL E. BRAINARD, AND JERROLD G. NORTON
Pacific Fisheries Environmental Group
Southwest Fisheries Center
National Marine Fisheries Service
P.O. Box 831
Monterey, California 93942

ABSTRACT

Monthly means of sea-surface temperature are computed for 3° blocks of latitude and longitude along the eastern coasts of the Pacific and Atlantic oceans from March 1971 to June 1984. Long-term mean, between-year standard deviation, and monthly anomaly values are computed and used to describe major anomalous warm events in the California, Peru, Canary, and Benguela eastern boundary current systems. Possible causes of warm events include anomalous local onshore transport, propagation of coastally trapped waves, and anomalous solar radiation.

RESUMEN

Se computan las medias mensuales de temperatura superficial del agua para sectores de 3° de latitud y longitud a lo largo de las costas orientales de los oceanos Pacífico y Atlántico desde marzo de 1971 hasta junio de 1984. Los cálculos de la media de este período, la desviación estándar interanual y las anomalías mensuales se utilizan para describir los principales eventos anómalos de calentamiento en los sistemas de corrientes de margen oriental de California, Perú, Canarias, y Benguela. Las causas posibles de los fenómenos de calentamiento incluyen transporte local anómalo hacia la costa, propagación de ondas retenidas por las costas, y anomalías en la radiación solar.

INTRODUCTION

The four major eastern boundary current systems—California, Peru, Canary, and Benguela—are characterized by equatorward surface flow; persistent coastal upwelling of cold, nutrient-rich waters; high biological productivity; and similar marine populations (Parrish et al. 1983). In certain years, anomalous warming events occur to disrupt the normal upwelling of nutrients and to reduce the surface water's productivity. Severe impacts on local fish populations may occur. In the California Current, warm events have occurred many times in the past, but major recent events have been in 1931-32, 1940-41, 1957-58, 1972-73 1976-77, and 1982-83. Warm events have been studied intensely in the California Current (e.g., Sette and Isaacs 1960). This paper will describe anomalous events in the California Current and extend the analysis to the other eastern boundary current systems.

During warm events in the California Current, the surface layer warms and deepens and may remain warmer and deeper than normal for a year or more (Table 1). The greatest interannual variability of oceanic conditions off California occurs in winter. Thus, to compare conditions in different years, we computed winter quarterly means (December to February) using the years 1971 to 1984 as a normal. We chose these years because later we will present sea-surface temperature (SST) data for these years. During the winters of 1957-58 and 1982-83, the SST at Scripps Pier was 1.2° to 1.7°C above normal, and positive anomalies persisted into the following winter. Deepening of the surface layer can be represented by the depth of the 14°C isotherm, which is near the top of the thermocline off San Diego (Barilotti et al. 1984). During winter 1957-58, the 14°C isotherm was about 20 m deeper than normal off San Diego, and positive depth anomalies persisted into the following winter. During the 1982-83 winter, the 14°C isotherm was over 40 m deeper than normal and remained deeper than normal the following winter. Deepening of the thermal structure also causes sea level, as

TABLE 1
Winter Quarterly Mean Ocean Conditions During Warm Winters and Comparison with 1971-84

	December-February Quarterly Means				
	Mean winter 1971-84	1957-58	1958-59	1982-83	1983-84
SST at Scripps Pier (°C)	14.5	16.2 (1.7)	15.9 (1.4)	15.7 (1.2)	15.3 (0.8)
Depth of 14°C isotherm off San Diego (m)	48	69 (21)	65 (17)	91 (43)	58 (10)
Sea level at San Diego (cm)	201	204 (3)	203 (2)	215 (14)	202 (1)

Quarterly means were computed as means of monthly mean values for the months December to February. Quarterly anomalies from the mean winter 1971-84 are shown in parentheses. SST data from Scripps Pier, Scripps Institution of Oceanography, La Jolla, California. Depth of 14°C isotherm off San Diego computed from data of Fleet Numerical Oceanography Center (Barilotti et al. 1984). Sea-level data from National Ocean Service, NOAA, Rockville, Maryland.

observed at tide gages, to stand higher. Monthly mean sea level at San Diego was about 6 cm higher than normal in 1957-58 and up to 16 cm higher than normal in 1982-83.

Two biologically significant processes occur during warm events (McLain and Thomas 1983). One is an intensification of the normal seasonal poleward flow of undercurrents over and along the edge of the continental shelf. Current-meter observations in five winters off the central Oregon coast (Table 2) suggest that during winter 1982-83, the speed of poleward flow over the continental shelf (13.0 cm/sec) was almost twice the mean speed observed in the other four winters (7.5 cm/sec). This increased poleward flow advected warm southern water poleward, further increasing coastal temperatures. The strong poleward flows and warm coastal waters allowed warm-water fish species to extend their ranges poleward along the coast or inshore from warmer waters offshore. Occurrences of warm-water species in the California Current during warm years have been described by many authors (e.g., Radovich 1961). Bonito, barracuda, white sea bass, and others have been caught far north of their normal ranges during warm years. Whereas the larger animals may swim northward in the warm waters, many warm-water planktonic organisms also have been observed far north of their normal ranges, suggesting that poleward transport is a contributing factor in range extension.

A second major effect observed during warm events has been decreased biological productivity of the surface waters. The thickened and warmed surface layer reduces the ability of upwelling-favorable winds to cause upwelling of nutrients into lighted surface waters. Chelton et al. (1982) showed that zooplankton volumes observed on CalCOFI surveys during 1957-59 were much lower than on later surveys during the 1960s and 1970s. Although fewer observations of this type have been made in recent years, available data do suggest similar low zooplankton volumes and decreased productivity in the California Current in 1983 (McGowan 1984). Biological observations of poor reproduction of many species of fish and sea birds (Ainley 1983) and the extremely low harvest of kelp off southern California (Barilotti et al. 1984), for example, all suggest a sharp drop in biological productivity following the winter of 1982-83.

TABLE 2
Mean Poleward Speed of California Undercurrent Observed with Current Meters at Midshelf off Central Oregon

Winter	Poleward speed (cm/sec)
1973-74	7.5
1977-78	10.2
1981-82	5.8
1982-83	13.0
1983-84	7.0
Mean of four winters 1973-74, 1977-78, 1981-82, and 1983-84	7.5

Mean speeds are for the 93-day period October 30 to January 30. Current meters were about 25 m off the bottom in water depths of 90 to 120 m. Data from Dr. Robert Smith, Oregon State University, Corvallis, Oregon.

CAUSES OF ANOMALOUS WARM EVENTS

Two major hypotheses have been suggested to explain anomalous warm events in the California Current system: (1) propagating coastal waves in the ocean, and (2) atmospheric circulation changes. The ocean hypothesis suggests that during periods of strong trade winds over the tropical Pacific, warm surface water piles up in the western tropical Pacific, causing a rise in sea level there (Wyrtki 1975). When the trade winds relax or reverse, sea level falls and a pulse of warm surface water flows eastward toward South America, propagating as an equatorially trapped Kelvin wave. El Niño occurs as the warm water intrudes against the South American coast, causing a rise in sea level, and depressing the thermocline along the coast. The depression of the thermocline may be as large as 150 m (at 0°N, 85°W in October 1982, Toole 1984).

Wave theory (Gill 1982) suggests that the depression can propagate in two ways: (1) westward along the equator as equatorially trapped Rossby waves, and (2) poleward along the coast as both coastally trapped waves and coastal Kelvin waves. Since the trapping distance of coastal Kelvin waves is limited to the Rossby radius of deformation, they narrow as they proceed poleward and eventually become coastally trapped waves. Therefore, we will refer to the two types of poleward-propagating waves as coastally trapped waves. As they propagate poleward the coastally trapped waves lose energy by numerous processes, including generation of very slow, westward-propagating planetary Rossby waves. As the depression of the thermocline propagates poleward along the coast, it geostrophically forces an intensification of normal poleward coastal countercurrents. After the depression passes a point on the coast, the countercurrent may reverse to equatorward. The poleward flows commonly occur in winter, and the reversals, called spring transitions, are most intense following warm winters (Breaker 1983).

One shortcoming with the ocean hypothesis is that it does not explain the very wide expanse of anomalousy warm water observed off the West Coast in early 1983 and the simultaneous formation of a pool of colder than normal water in the central North Pacific. Published SST anomaly charts for winter 1982-83 U.S. Dept. Commer. 1983) show that SSTs were above normal for over 800 km seaward of the California coast. A coastally trapped wave would be restricted to within about 50 km of the coast and thus could cause positive anomalies only near the coast, leaving he offshore cold pool unexplained. Simpson[1] suggests hat the westward-propagating Rossby waves generted by the poleward-propagating coastally trapped waves cannot explain the offshore cold anomalies observed in winter 1982-83.

Coastally trapped waves of higher than annual freuency are generated by tropical storms and have been observed off Central America in hourly sea level records (Christensen et al. 1983). As these waves propagate poleward, they become trapped in the Gulf of California and do not propagate poleward past the tip of Baja California. Evidently, coastally trapped waves must be of very large spatial scale and of several months' or longer duration to propagate past the Gulf of California.

Subsurface temperature data provide empirical evidence for the existence of poleward-propagating hermal depressions. Brainard and McLain (in press) computed anomalies of temperature at 100 m for areas long the west coast of North and South America. They analyzed over 115,000 temperature profiles from he files of Fleet Numerical Oceanography Center for series of 3° blocks of latitude along the coast from 0°S to 50°N from 1951 to 1984. Anomalies of month mean temperature at 100 m computed from these rofiles show that regions of anomalously warm water 100 m occurred along the coast during 1957-58, 1972-73, 1976-77, and 1982-83. The regions appeared expand poleward from near the equator, with their eading edges occurring progressively later in time with distance away from the equator. Although this ould be evidence of a poleward-propagating coastally apped wave, the leading edges of the anomalies aveled at speeds of 6 to 44 km/day, much less than he theoretical speeds of coastally trapped waves. ikewise, other authors (e.g., Enfield and Allen 1980; helton and Davis 1982) have found relatively low peeds of coastally propagating disturbances. The low opagation speed of the anomalies suggests that hanges in advection may also occur (Chavez et al. 1984). Brainard and McLain (in press) also showed a general warming trend along the whole coast at 100 m beginning in 1976 and culminating in the extremely strong warm event in 1982-83. This warming trend was described by McLain (1983) and is similar to that described by Huang (1972) for the years 1958-69 relative to the years 1948-57.

Sea-surface temperature observations are more abundant than subsurface profiles and show the same general pattern of anomalies. Figure 1 shows the locations of 39 3° blocks of latitude and longitude in the Pacific, and 37 3° blocks in the Atlantic where monthly mean SST was computed. The SST reports used were received in real time by Fleet Numerical Oceanography Center from March 1971 to June 1984. The monthly means of SST were made for the 3° blocks by first averaging the reports by 1° blocks each month and then making 3° means of the 1° submeans. The number of observations in each 1° block varied widely from 0 to over 50 reports per month. Thus, making the 3° means from the 1° submeans reduced the spatial bias of sampling. A 3° mean was made if there was at least one 1° submean available. Because of the inhomogeneous distribution of the reports, this may have caused spurious 3° means in areas of sparse data. The number of reports used in each 3° block (shown in Table 3) varies from over 40,000 in the California and Canary currents to fewer than 100 in the Peru Current. Anomalies of SST were computed relative to the long-term mean for the period March 1971 to June 1984.

The long-term mean annual cycle of SST in the California Current region (Figure 2, left) is dominated by seasonal migration of a region of closely packed SST isotherms along the coast of Mexico between 18° to 28°N (Blocks 27 to 31 in Figure 1). This region represents a frontal zone between the colder water to the north (where the seasonal cycle of heating and cooling is strong) and the warmer water to the south (where seasonal fluctuations are small). A similar frontal region migrates seasonally in the Peru Current region from 0° to 10°S off Ecuador. The two frontal regions lie at the equatorward end of the California and Peru eastern boundary currents where the currents leave the coast and turn to the west.

Interannual variability of SST is described by between-year standard deviations of the individual monthly mean SST values (Figure 2, right). The greatest interannual variability of SST along the coast is in the Southern Hemisphere, with between-year standard deviations of over 1.0°C from the equator to at least 40°S. Peak variability (over 2.0°C standard deviation) occurs in a region from 15°S to 25°S from November to February, representing El Niño fluctuation. This

---

mpson, J.J. MS. The Aleutian Low teleconnection between equatorial and midude "El Niño-type" events. Submitted to J. Geophys. Res.

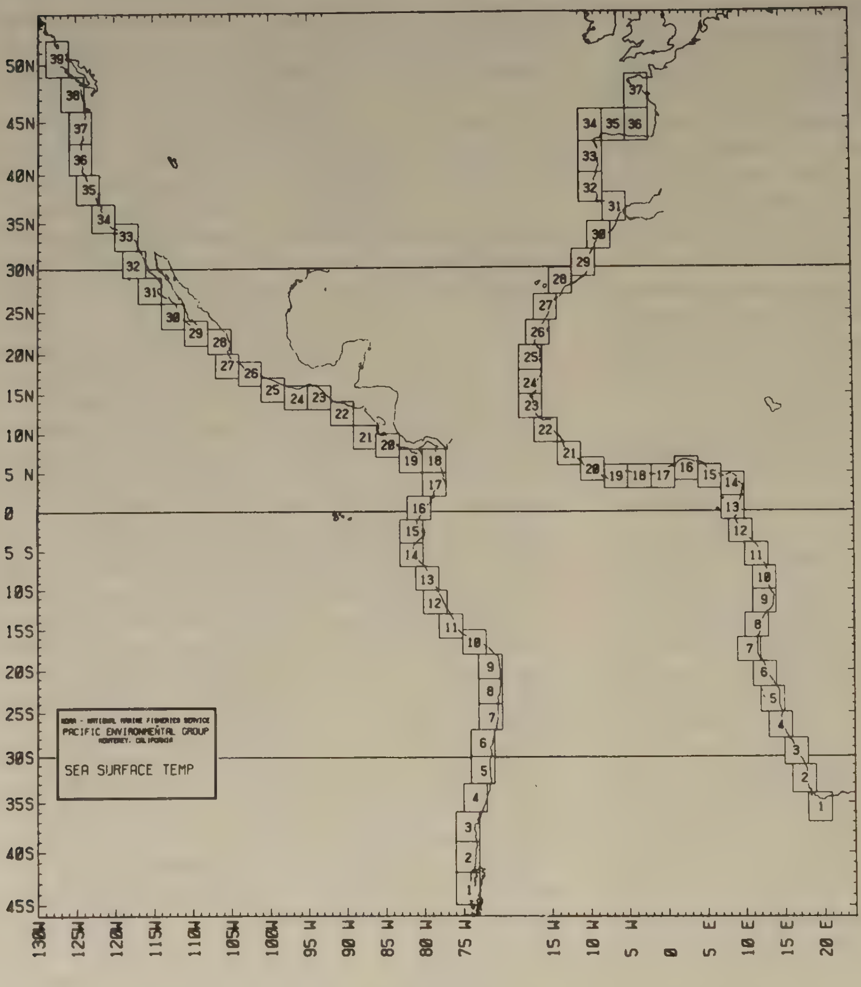

Figure 1. Locations of 3° blocks of longitude and latitude along eastern boundaries of Pacific and Atlantic oceans where monthly mean sea-surface temperature was computed for the period March 1971 to June 1984.

region is somewhat south of the region off Ecuador and Peru where El Niño is normally thought to be strongest. Perhaps the extreme scarcity of reports off Peru and Chile caused the apparent center of greatest interannual variability to be shifted southwards. Interannual variability in the California Current is lower than in the Peru Current and has between-year standard deviations of 0.5° to 0.8°C. The standard deviation is locally highest near the frontal zone off Mexico, representing interannual changes in the seasonal migration of the zone.

The computed anomalies of SST along the eastern Pacific were very noisy, with many small regions of positive and negative anomaly. Anomalies in the Peru Current were particularly noisy, perhaps because of the extreme scarcity of reports there. To smooth the array of SST anomalies, we applied two filters to the array in succession. First, we eliminated spikes with a 3 × 3 nonlinear or median filter in which the central value of each 3 × 3 subarray was replaced by the median of the 9 values in the subarray. Second we passed a 3 × 3 linear smoother with an arbitrarily chosen smoothing factor of 0.5 over the array. After this filtering, only the major anomalies remain.

Regions of positive anomaly of great coastwise extent occurred in the eastern Pacific in 1972-73 and 1982-83 (Figure 3), with peak values of about +4.0°C in December 1982 and January 1983 off Ecuador and Peru, and smoothed values of greater than +2.5°C. A positive coastwise anomaly of lesser magnitude and extent occurred in 1976-77. Because these coastwise anomalies are contemporaneous with major tropical El Niño events, they are probably of tropical origin. Negative coastwise anomalies occurred from 1973 to

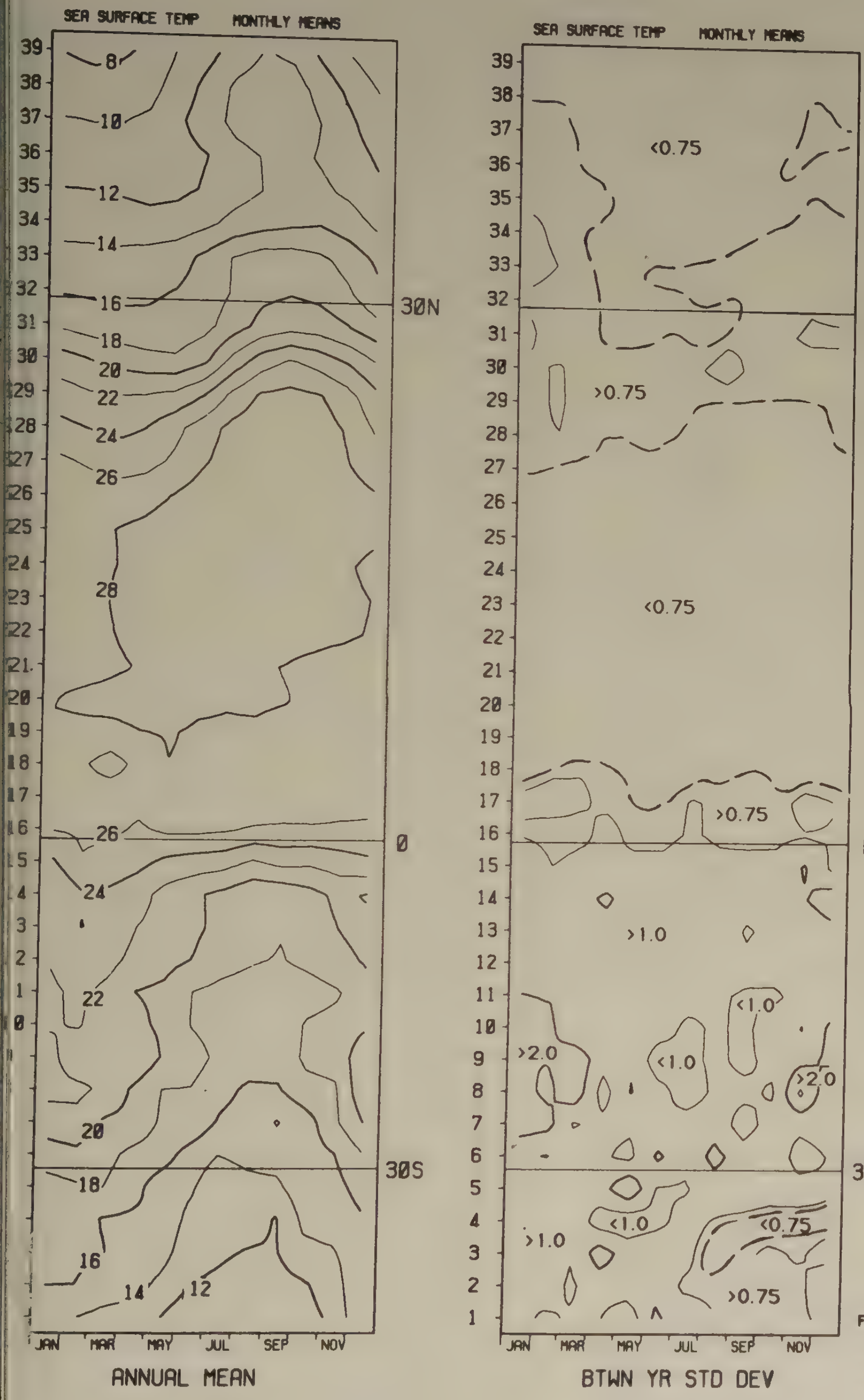

Figure 2. Annual cycle of long-term monthly mean SST (*left*) and between-year standard deviation (*right*) along eastern boundary of Pacific Ocean. Contour intervals are 2°C for the annual means and 1°C for the standard deviations (dashed line is 0.75°C).

TABLE 3
Total Number of SST Observations in 3° Blocks in the Eastern Atlantic and Pacific Oceans from March 1971 to June 1984

Block number	Pacific	Atlantic
39	5,710	—
38	47,092	—
37	20,581	15,980
36	30,149	5,415
35	82,056	14,797
34	42,885	46,279
33	35,568	46,759
32	8,107	30,665
31	8,956	21,035
30	10,559	10,817
29	10,020	6,510
28	5,427	11,503
27	8,886	19,488
26	9,763	59,190
25	9,103	32,198
24	8,600	24,063
23	5,592	22,255
22	7,126	9,426
21	8,016	15,075
20	8,067	5,466
19	7,122	5,030
18	1,475	3,825
17	332	2,201
16	985	1,121
15	673	930
14	879	553
13	636	456
12	477	452
11	305	1,453
10	120	5,946
9	62	4,659
8	70	1,661
7	73	12,238
6	150	15,424
5	115	6,113
4	81	3,269
3	115	7,258
2	110	10,693
1	198	8,440
Total	386,243	488,643

1975. Because of the large coastwise extent of these anomalies, the California and Peru current systems may have had similar anomalies simultaneously.

Large positive anomalies occur in regions such as off Baja and Alta California, where SST normally decreases rapidly with distance poleward along the coast. Stronger than normal poleward coastal flow during anomalous warm events would tend to cause positive SST anomalies in these regions. In contrast, off Central America, reduced positive or even negative SST anomalies occur as gaps in the coastwise positive anomalies. Negative SST anomalies also appear in maps of SST anomaly off Central America during February 1983 (U.S. Dept. Commer. 1983). A possible explanation for negative SST anomalies off Central America at a time when one might expect positive anomalies is that the mean coastwise SST gradient is small or negative in this region. A stronger than normal poleward flow along this coast would have little tendency to cause positive SST anomalies. Other possible reasons for gaps in positive coastwise SST anomaly might be: (1) wind mixing by Tehuantepec and Papagallo winds, which occur in this region and cause local cooling, and (2) upwelling of cold waters off Costa Rica. Douglas and Englehart (1983) found that cold anomalies off Mexico and Central America were correlated with alterations in the paths of tropical hurricanes.

In contrast to the coastwise warm events of 1972-73, 1976-77, and 1982-83 and the cold events of 1973-75, other anomalous periods occurred locally in the California Current and were not associated with tropical warm events. These included positive anomalies in the winters 1977-78, 1979-80, and 1980-81, and the negative anomalies in the winters of 1970-71, 1971-72, and 1978-79. Near-zero anomalies occurred in winter 1981-82. Similarly, many local SST anomalies occurred in the Peru Current that were not related to the major El Niño tropical warm events.

The second major ocean warm-event hypothesis—atmospheric circulation changes—suggests that the local anomalies in the California Current are caused by variations in wind-induced, onshore transport in midlatitudes. Recent work of Simpson (1983, 1984a, 1984b) and others emphasizes the importance of onshore transport of warm surface waters during local warming events. Horel and Wallace (1981) showed that a particular pattern of midlatitude upper atmospheric circulation, the "Pacific/North America" pattern, is associated with, or "teleconnected" to El Niño warming events in the Pacific. When there is anomalous warming in the tropical Pacific, there often is an associated shift in the upper atmospheric circulation, which causes a trough over the central North Pacific, a ridge over western Canada, and a trough over the eastern United States. This pattern of upper-atmospheric circulation is associated on the surface with an intensification of the Aleutian Low. Emery and Hamilton (in press) present maps of the winter mean surface atmospheric pressure over the North Pacific and show that years with a strengthened Aleutian Low are often associated with anomalous warmings in the tropics. During winter 1982-83, the Aleutian Low was several standard deviations deeper than normal and was shifted 10° to 20° of longitude east of its normal position over the central Aleutians, causing

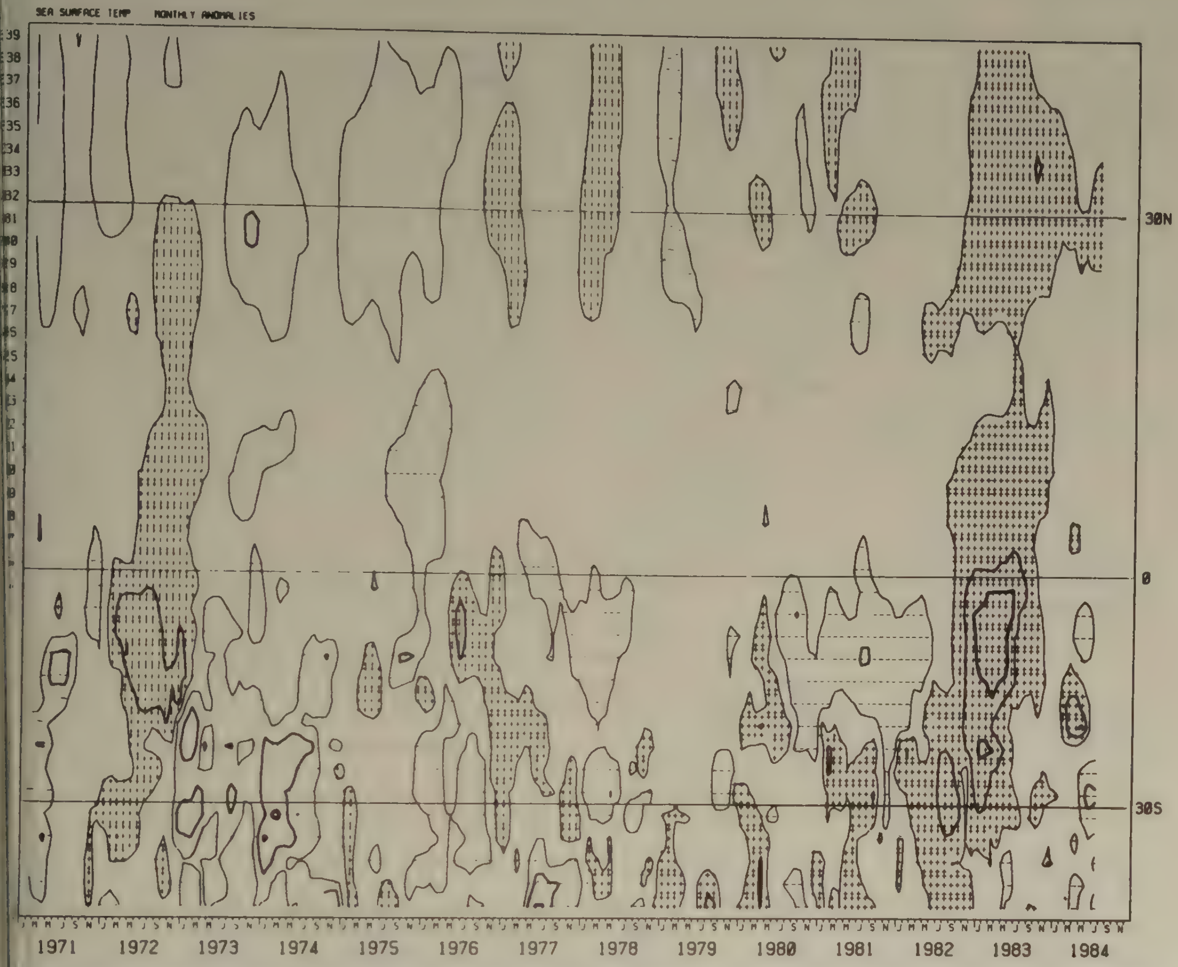

gure 3. Anomaly of monthly mean SST along eastern boundary of Pacific Ocean. Small plus and minus signs represent anomalies before smoothing of greater than +0.5°C and less than −0.5°C, respectively. Contouring was performed after median and linear filtering. Light contour lines represent +0.5° and −0.5°C; dark contour lines represent −2.5°, −1.5°, +1.5°, and +2.5°C.

very strong negative pressure anomaly over the Gulf Alaska. The strong Aleutian Low combined with a eakened North Pacific High to cause a change in rface winds that resulted in very strong onshore nsport of surface waters against the California ast.

Evidence of the importance of onshore transport in using anomalous warm events off California can be n in indices of upwelling intensity computed for 15 ns along the west coast of North America (Figure using methods of Bakun (1973). The strong upwell- off central California in summer has peak upwell- index values of greater than +200 m^3/sec/100 m stline (Figure 5). During winter, tongues of negative upwelling index, representing onshore transport or downwelling, intrude southward along the coast from the Gulf of Alaska, where onshore transport occurs during much of the year. The tongues of onshore transport did not generally extend south of about 36°N in the early 1970s except in winter 1972-73. From 1976 to 1980, however, onshore transport extended south to about 33°N each winter. Increased frequency of onshore transport of warm surface water off central California in winter may thus have been a cause of the general warming along the coast during 1976-80.

During winter 1982-83, there was an extremely strong pulse of onshore transport with upwelling index

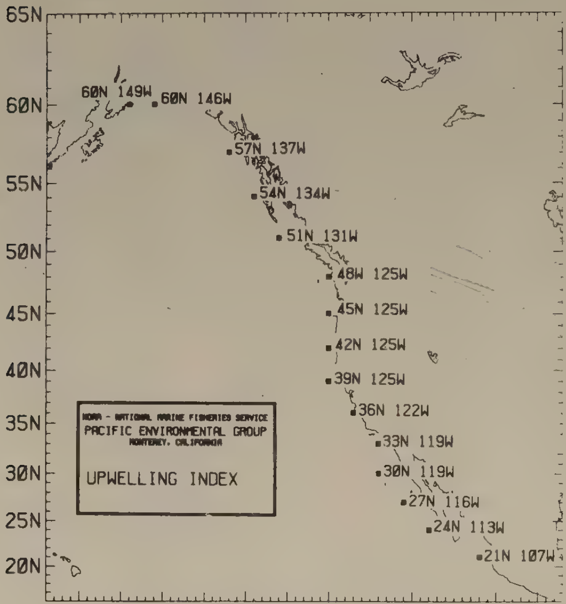
65N
60N
55N
50N
45N
40N
35N
30N
25N
20N
60N 149W
60N 146W
57N 137W
54N 134W
51N 131W
48W 125W
45N 125W
42N 125W
39N 125W
36N 122W
33N 119W
30N 119W
27N 116W
24N 113W
21N 107W
NOAA - NATIONAL MARINE FISHERIES SERVICE
PACIFIC ENVIRONMENTAL GROUP
MONTEREY, CALIFORNIA
UPWELLING INDEX
155W
150W
145W
140W
135W
130W
125W
120W
115W
110W
105W
100W

Figure 4. Locations of 15 points along west coast of North America where upwelling indices were computed by methods of Bakun (1973).

values of less than −200 units for two consecutive months. Onshore transport in the California Current region is not normally less than −150 index units in any one month. The largest total onshore transport (sums of negative index values at 42°N) of any winter in the period of record, 1946-84, occurred in 1982-83 (Norton et al. in press). There were −765 total units of negative upwelling index that winter, three times the normal of −251 index units. During the warm winter of 1957-58, there was also strong onshore transport, with a total of −544 index units. During the warm winter of 1972-73, however, strong onshore transport did not occur (−219 index units), suggesting that warming in 1972-73 was primarily a tropically related phenomenon. Lack of local reinforcement of the tropical warming in 1972-73 prevented positive SST anomalies from extending as far north as in 1982-83 and from persisting as long. During the more normal winter of 1981-82, the total onshore transport was −215 index units, and SST anomalies were near zero. Only very weak onshore transport occurred off California in winter 1978-79 (−99 index units), and negative anomalies (Figure 3) resulted.

The mechanism of onshore transport can explain a number of other features of anomalous coastal events. For example, it can explain the large offshore extent of the warm water along the coast in 1982-83 and the

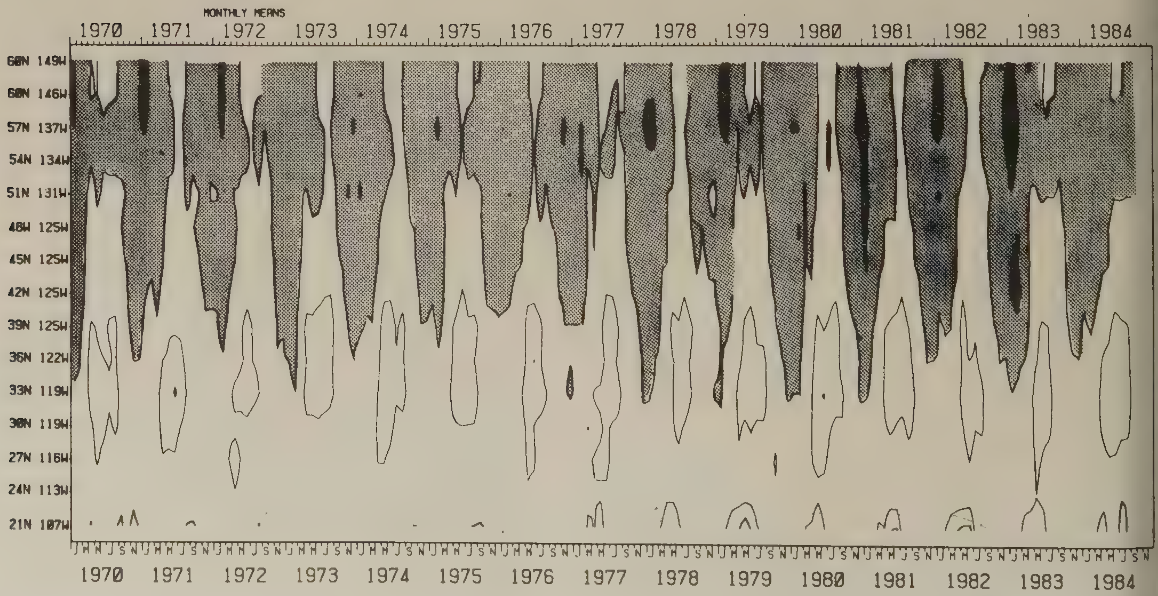

Figure 5. Monthly mean indices of upwelling intensity computed for 15 points along the west coast of North America. Units are m³/sec/100 m of coastline. Heavy contour lines are zero index and enclose tongues of onshore transport or negative upwelling index. Black areas are less than −200 index units. Fine contour lines are +200 index units and enclose areas of strong upwelling off central California in summer.

simultaneous formation of a pool of anomalously cold water in the central North Pacific. The onshore transport mechanism can also explain the low-salinity, high-dissolved-oxygen water observed in early 1983 on CalCOFI line 90 off San Diego (Simpson 1984a). Low-salinity waters have also been observed at frequently occupied coastal monitoring stations after periods of onshore transport (McLain and Thomas 1983).

In some years, local heating may contribute to anomalous warming events. In 1976-77, a blocking high-pressure system persisted over much of the western United States, causing record drought. The many warm, calm days associated with this high-pressure system probably caused increased solar radiation and warming of the surface waters. Solar heating cannot, however, explain the 1982-83 subsurface temperature anomalies, which were larger than those at the surface.

Thus it appears that anomalous warming events in Pacific eastern boundary current systems may be either—or both—tropical or locally forced events. El Niño events in the tropics can cause poleward-propagating coastally trapped waves, but because they narrow and lose energy, these waves do not seem to explain the large coastwise SST anomalies. Both processes may occur in the same year, and when they occur together, local onshore transport can reinforce the effects of coastally trapped waves to create the observed large anomalies in midlatitudes. Interannual variations in local onshore transport can cause local warm and cold events in the California Current. Onshore transport itself could generate coastally trapped waves, which would propagate the effects of the onshore transport poleward. To an observer at a point along the coast, both tropical and local processes could cause apparent depression of the thermal structure and intensified poleward coastal currents. When local reinforcement occurs, these effects may be additive. During 1982-83, for example, both processes were unusually intense, and combined to cause an extremely strong warm event in the California Current: warming in the tropics was the greatest in many decades, and local onshore transport was the strongest of any winter during the period of record 1946-83 (Norton et al. in press). The resulting depression of the thermal structure and poleward currents along the coast were very large (Tables 1 and 2). In contrast, during the tropical warm event of 1972-73, when local reinforcement was not strong, SST anomalies in the California Current were of short duration and did not extend far up the coast. Local reinforcement by onshore transport in the Peru Current has not been demonstrated (Fonseca 1984).

SST FLUCTUATIONS IN THE EASTERN ATLANTIC

The long-term mean annual cycle of SST fluctuations in the eastern Atlantic (Figure 6, left) is dominated by seasonal migration of frontal zones between 10°N and 20°N between Cape Vert and Cape Blanc in the Canary Current (Wooster et al. 1976) and between 10°S and 20°S near Cape Fria in the Benguela Current (Wooster, in Picaut 1983). As in the Pacific, the frontal zones represent regions where the eastern boundary current turns offshore. Seasonal heating and cooling is strong poleward of the frontal zones, and seasonal variations are weak equatorward of the zones.

Interannual variability of SST in the eastern Atlantic (Figure 6, right) is similar to that of the Pacific, with low values of between-year standard deviation in the Northern Hemisphere and large values in the Southern Hemisphere. Local, weak maxima of variability occur in the Canary Current near the frontal zone. Interannual variability in the Benguela Current is high, and between-year standard deviations range up to 2.2°C near 10°S, reflecting large interannual variations in the front. A band of high interannual variability occurs from 25° to 30°S as a result of multiyear anomalous periods.

The anomalies of SST in the eastern Atlantic (Figure 7) appear somewhat similar to those of the Pacific, except that no large coastwise anomalies occur. Anomalies in the Canary Current are weak and of local nature. There was a general warming trend evident during 1971-84 in the Canary Current; it was cool in 1972 and 1974 and then warming in 1976 and remaining generally warm thereafter, with positive anomalies occurring in 1978, 1979-80, 1981-82, and 1983-84.

SST values in the Benguela Current were above normal from 1971 to early 1979 and below normal from 1979 to 1983. Greatest negative anomalies (less than −1.0°C) occurred off Namibia from November 1981 to May 1982, in rough agreement with the cold period observed there during February to September 1982 by Boyd and Agenbag (1984). The persistence of these anomalous periods is unusual. Whereas in the other eastern boundary current systems, SST anomalies are more coherent with distance along the coast than in time (causing the generally vertical features in Figures 3 and 7), in the Benguela Current, anomalies were very persistent in time (causing the more horizontal features at the bottom of Figure 7). This suggests that the upwelling-related winds over the Benguela Current must be very persistent, but Picaut (1983) mentions that south of about 20°S in the Benguela Current the correlation between winds and SST anomalies is low. Perhaps the large persistence of the

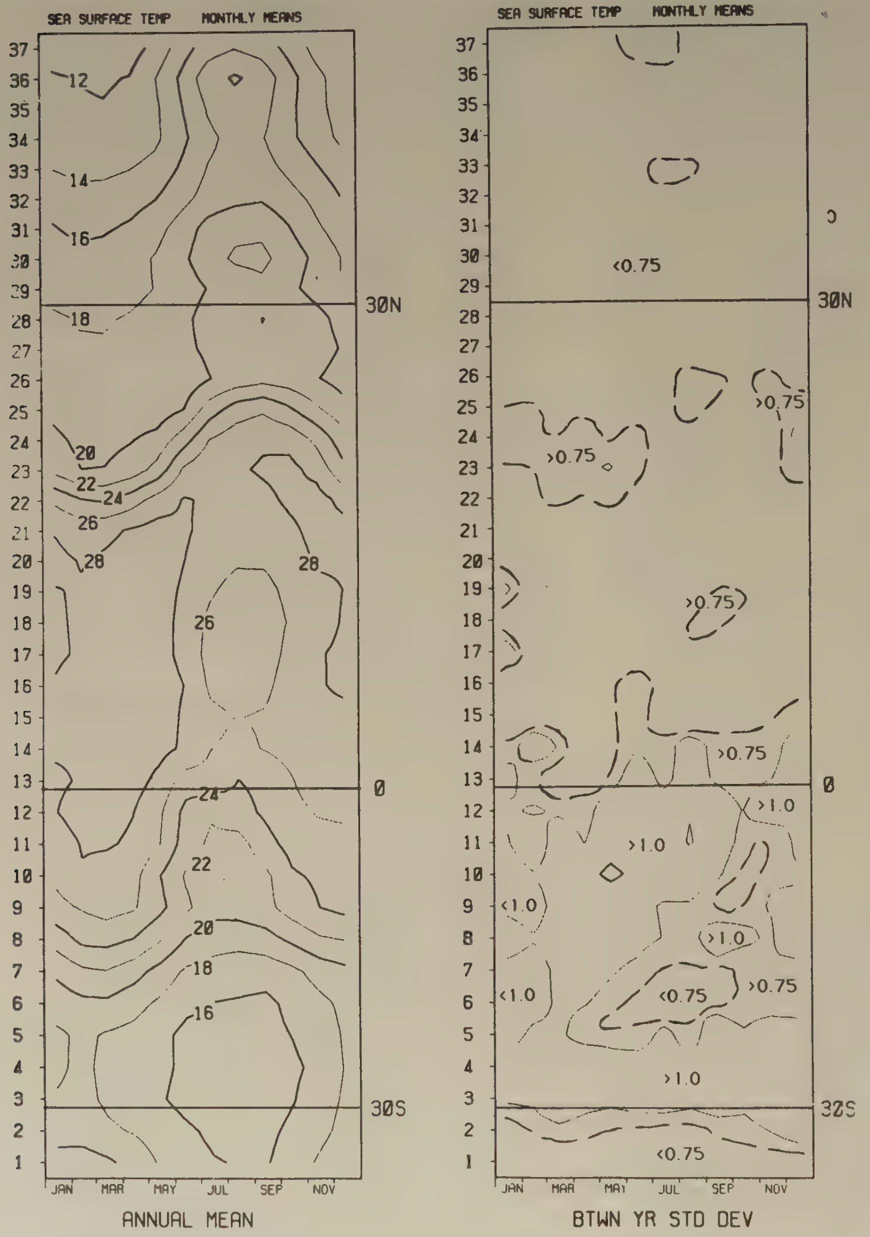

Figure 6. Annual cycle of long-term monthly mean SST (*left*) and between-year standard deviation (*right*) along eastern boundary of Atlantic Ocean. Contour intervals are 2°C for the annual means and 1°C for the standard deviations (dashed line is 0.75°C).

anomalies in this region is related to very slow changes in advection in the South Atlantic gyre.

An intense local warming occurred in the Benguela Current from March to at least May 1984. SSTs greater than 29°C intruded as far south as latitude 15°S. The warm event started along the coast near Cape Fria (12° to 19°S) and expanded equatorward, becoming most intense near Point Noire, Congo (5° to 10°S), in June 1984, with anomalies of up to 3.5°C. In contrast, Boyd and Thomas (1984) examined hydrographic data taken within 1° of the coast from 18° to 26°S and found water up to 6°C warmer than normal, particular-

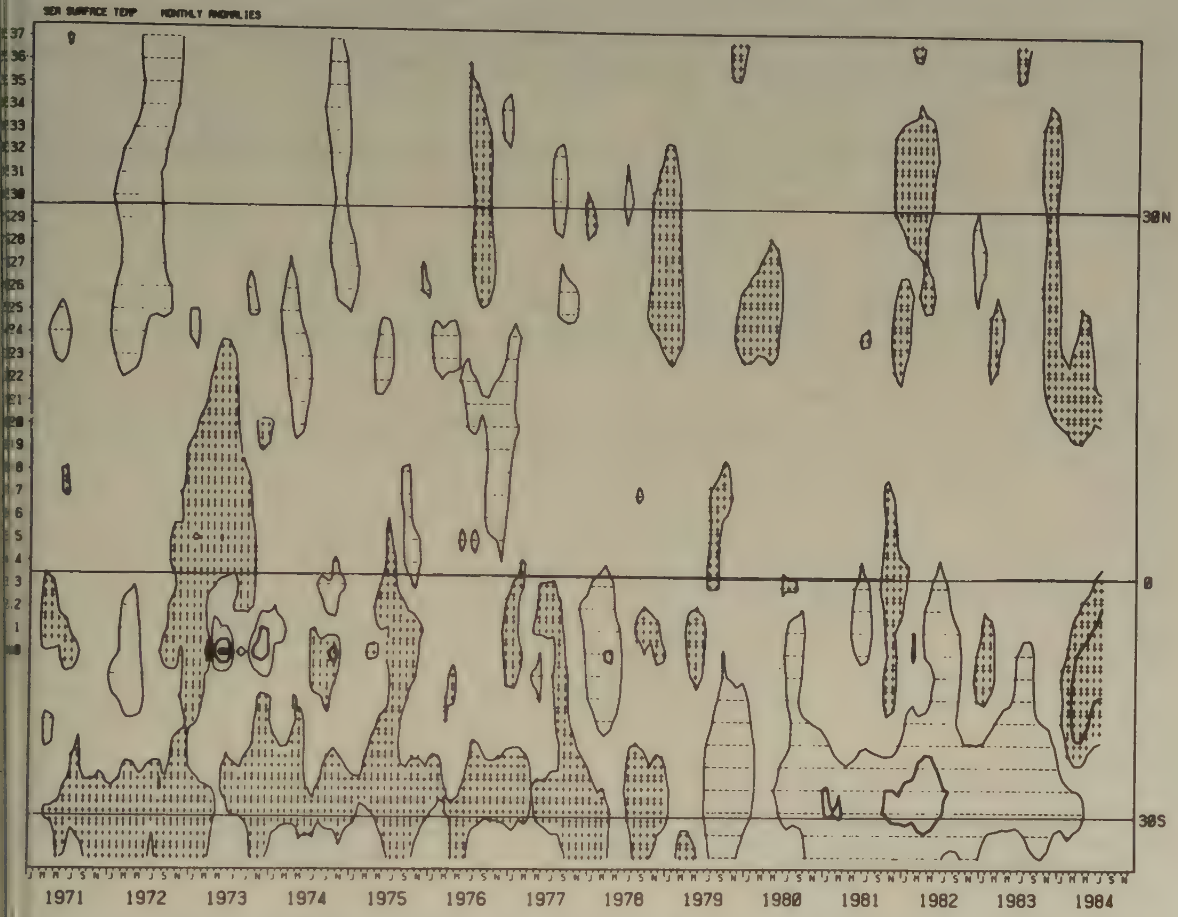

igure 7. Anomaly of monthly mean SST along eastern boundary of Atlantic Ocean during the period March 1971 to June 1984. Small plus and minus signs represent anomalies before smoothing of greater than +0.5°C and less than −0.5°C, respectively. Contouring was performed after median and linear filtering. Light contour lines represent +0.5° and −0.5°C; dark contour lines represent −2.5°, −1.5°, +1.5°, and +2.5°C.

v near the coast. They suggest that the warm event vas caused by a southward intrusion of equatorial vater. If so, the intrusion may have come from ffshore, reaching the coast near Cape Fria, and then xpanding generally northward, as seen in the 3°-lock SST data. It may also have expanded southward nd been seen in the hydrographic data, very close to e coast.

In contrast to the large coastwise extent of SST nomalies in the Pacific, anomalies in the eastern tlantic are more local and do not have the large astwise extent. The Atlantic anomalies generally ere restricted to one of the three regions: Benguela urrent, Gulf of Guinea, and Canary Current. Only e warm events in 1972-73 and mid-1981 in the Benela and Gulf of Guinea regions spanned more than one region. This suggests that different oceanic or atmospheric processes affect the three regions. Also, SST anomalies in the Pacific tended to occur in northern winters, but Atlantic anomalies occurred throughout the year.

RELATION OF TROPICAL ATLANTIC AND PACIFIC ANOMALIES

Because there was an anomalous warm event in the tropical Atlantic in early 1984, one year after the major warm event in the Pacific in 1982-83, it was thought that similar Atlantic warm events might have occurred following earlier Pacific warm events. To examine this question, we made time series of monthly mean SST for the years 1946 to 1979 by 5° blocks for the eastern tropical Pacific and Atlantic from the

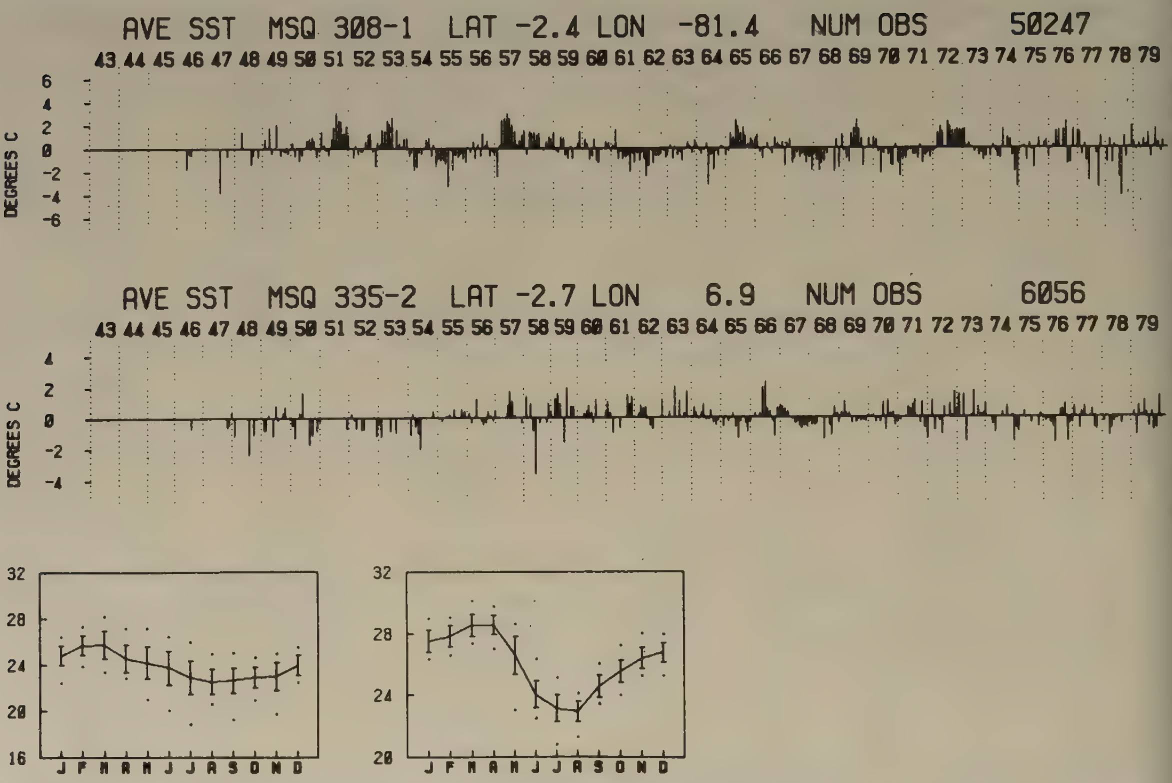

Figure 8. Time series of anomaly of SST in 5° blocks in eastern tropical Pacific (*upper*) and Atlantic (*lower*) oceans for the years 1943 to 1979. Mean annual cycle of SST and range and standard deviation of interyear variability are shown in small boxes (Pacific, *left*, Atlantic, *right*). Areas are Marsden 5° blocks 308-1 off Ecuador in the eastern tropical Pacific (0° to 5°S, 80° to 85°S) and 335-2 off Gabon in the eastern tropical Atlantic (0° to 5°S, 5° to 10°E).

Consolidated Data Set of Fleet Numerical Oceanography Center (FNOC). This data set comprises marine weather reports from two sources: (1) historical logbook reports in the TDF-11 data file from the National Climatic Data Center for the years 1946 to about 1976, and (2) the reports received in real time by FNOC for 1971 to 1979. Time series of SST anomalies (Figure 8) were made for an area off Ecuador (Marsden 5° block 308-1) and an area off Gabon in the tropical Atlantic (5° block 335-2). Although the Atlantic data are very sparse, there is no obvious lag relationship between the two series.

The most obvious difference between the Atlantic and Pacific SST time series is the generally greater persistence of anomalies in the tropical Pacific relative to the tropical Atlantic. We examined this in greater detail by computing autocorrelation functions for the two series (Figure 9). The autocorrelation function of the Atlantic series drops to less than 0.1 in 3 months, whereas it takes 8 months in the Pacific. The slower response time in the Pacific reflects the larger size of the Pacific and the greater energy required to displace the thermocline vertically.

CONCLUSIONS

Although sampling density was extremely nonhomogeneous, we computed monthly mean SSTs and anomalies from the long-term mean for series of 3° blocks along the coast in the eastern boundary current systems of the Pacific and Atlantic oceans. From these data, anomalous warm and cold events can be seen in all four major eastern boundary current systems. In the Pacific, coherent anomalies can extend over great stretches of coast from Chile to British Columbia, causing the California and Peru current systems to have similar SST anomalies simultaneously. Other local anomalies can occur in the California and Peru currents as well. There was less coastwise coherence of SST anomalies in the Atlantic than the Pacific, and thus the Canary and Benguela current systems do not generally have similar SST anomalies simultaneously.

Two major hypotheses for formation of anomalous

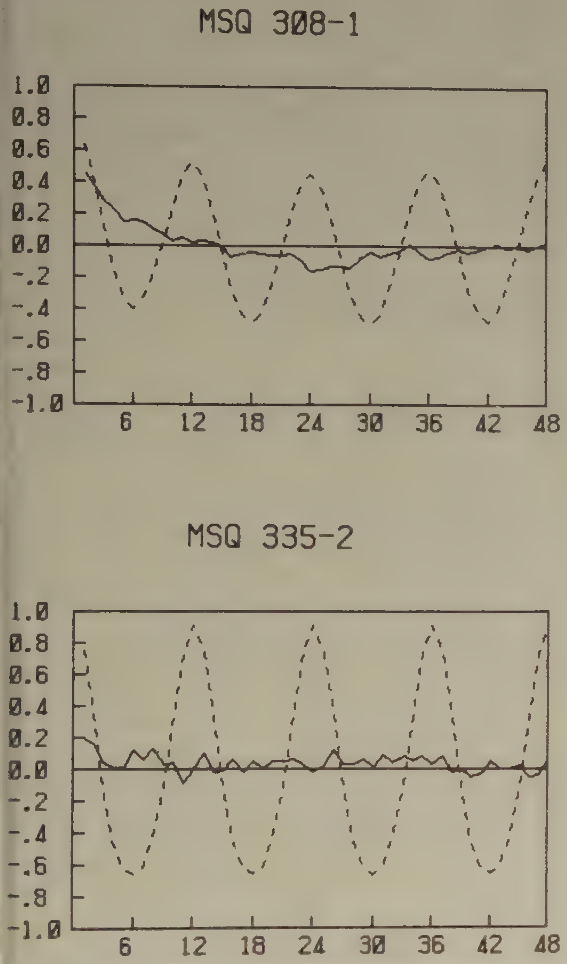

Figure 9. Autocorrelation function of monthly mean SST anomaly series for lags up to 48 months in 5° blocks in the eastern tropical Pacific (*upper*) and the eastern tropical Atlantic (*lower*). The dashed curves are the autocorrelation functions of the original SST time series, and the solid lines are the autocorrelation functions of the time series of SST anomalies.

warm events in the California Current have been suggested: (1) onshore transport of warm surface waters by strong southwesterly winds warms the surface water and depresses the thermal structure; (2) poleward-propagating coastally trapped waves from tropical El Niño events cause depressions of the thermocline to propagate poleward. Propagating coastally trapped waves narrow and lose energy with distance poleward from the tropics and do not explain the observed large coastwise anomalies. Onshore transport may occur in the same year as tropical warming events and cause local reinforcement of the effects of propagating coastally trapped waves in midlatitudes. Local heating by solar radiation is a third possible hypothesis for formation of anomalous warm events.

Two important effects of the anomalous warming events have biological significance: (1) geostrophic adjustments to the deepened thermal structure cause an intensification of normal seasonal poleward flow over the continental shelf. This intensification causes increased advection of warm water poleward and allows warm-water organisms to extend their ranges poleward. (2) A thickened surface layer reduces the ability of upwelling-favorable winds to upwell nutrients into the lighted surface waters, lowering the biological productivity.

An extremely anomalous warming event occurred in the California and Peru current systems during 1982-83. Off California exceptionally strong onshore transport of warm waters from offshore reinforced propagating coastally trapped waves from an exceptionally strong tropical El Niño. Anomalies were as large as +4°C at the surface and as large as +5° to +6°C at 100 m (Brainard and McLain in press), reflecting a deepening of the thermocline along the coast by 50 to 100 m. Off California the biological productivity of the surface waters was greatly reduced, and strong poleward flows advected many warm-water species northward.

SST anomalies in the Canary Current during 1971-84 have been relatively small but showed a general warming trend similar to that observed in the Pacific. Anomalies in the Benguela Current were extremely persistent and were positive during the years 1971-78 and cool during 1979-83. Anomalies then became strongly positive in early 1984, possibly because of an intrusion of equatorial water. There was no obvious lag relationship of SST anomalies in the Atlantic following similar warm events in the Pacific. SST anomalies are generally more persistent in the tropical Pacific than in the tropical Atlantic, but anomalous conditions in the Benguela Current can persist for five or more years.

The interannual variability of SST fluctuations in eastern boundary current systems is high near the frontal regions where the eastern boundary currents leave the coast. SST gradients are strong in these regions, and interannual variability of SST is locally high because of interannual variations in the seasonal migration of the fronts. Interannual variability of SST is higher in the Southern Hemisphere than in the Northern Hemisphere, but the anomalies in the Southern Hemisphere tend to be more persistent. Thus SSTs in the Northern Hemisphere tend to vary about a mean state, whereas Southern Hemisphere anomalies tend to switch between different regimes, lasting for a year or longer.

LITERATURE CITED

Ainley, D. 1983. El Niño in California? Point Reyes Bird Observatory, Stinson Beach, Calif., Newsletter 62.

Bakun, A. 1973. Coastal upwelling indices, west coast of North America, 1946-71. NOAA Tech. Rept. NMFS SSRF 671, 103 p.

Barilotti, D.C., D.R. McLain, and R.A. Bauer. 1984. Forecasting standing crops of *Macrocystis pyrifera* from the depth of the 14°C isotherm. (Abstract L 032A-06) EOS-Trans. Amer. Geophys. Union 65(45):909.

Boyd, A.J., and J.J. Agenbag. 1984. Seasonal temperature and salinity trends off central Namibia between 1978 and 1983 with particular reference to the cool winter of 1982. South African J. Sci. 80(2):77-79.

Boyd, A.J., and R.M. Thomas. 1984. A southward intrusion of equatorial water off northern and central Namibia in March 1984. Tropical Ocean-Atmosphere Newsletter 27:16-17.

Brainard, R., and D.R. McLain. In press. Subsurface temperature variability along the west coast of North and South America. Tropical Ocean-Atmosphere Newsletter.

Breaker, L. 1983. The space-time scales of variability in oceanic thermal structure off the central California coast. Ph.D. dissertation, Naval Postgraduate School, Monterey, Calif., 483 p.

Chavez, F.P., R.T. Barber, and H.S. Soldi. 1984. Propagated temperature changes during onset and recovery of the 1982-83 El Niño. Nature 309(5963):47-49.

Chelton, D., and R. Davis. 1982. Monthly mean sea-level variability along the west coast of North America. J. Phys. Oceanog. 12:757-784.

Chelton, D., P. Bernal, and J.A. McGowan. 1982. Large scale interannual physical and biological interactions in the California Current. J. Mar. Res. 40(4):1095-1125.

Christensen, N., Jr., R. de La Paz, and G. Gutierrez. 1983. A study of sub-inertial waves off the west coast of Mexico. Deep Sea Res. 30(8A):835-850.

Douglas, A., and P. Englehart. 1983. Factors leading to the heavy precipitation of 1982-83 in the United States. Proceedings of the Eighth Climate Diagnostics Workshop, NOAA Dept. of Commerce, Wash., D.C. p. 42-54.

Emery, W.J., and K. Hamilton. In press. Atmospheric forcing of interannual variability in the northeast Pacific Ocean, connections with El Niño. J. Geophys. Res.

Enfield, D., and J. Allen. 1980. On the structure and dynamics of monthly mean sea level anomalies along the Pacific coast of North and South America. J. Phys. Oceanog. 10(4):557-578.

Fonseca, T. 1984. On the origin of anomalies in the Humboldt Current during the 1982-83 El Niño. Tropical Ocean-Atmosphere Newsletter 28:12-13.

Gill, A.E. 1982. Atmosphere-ocean dynamics. Academic Press, New York, 662 p.

Horel, J.D., and J.M. Wallace. 1981. Planetary-scale atmospheric phenomena associated with the Southern Oscillation. Mon. Wea. Rev. 109:813-829.

Huang, J.C.K. 1972. Recent decadal variation in the California Current system. J. Phys. Oceanog. 2:382-390.

McGowan, J. 1984. The California El Niño, 1983. Oceanus 27(2):48-51.

McLain, D.R., 1983. Coastal ocean warming in the northeast Pacific, 1976-83. *In* W. G. Pearcy (ed.) The influence of ocean conditions on the production of salmonids in the North Pacific, a workshop. Sea Grant College Program. Rep. ORESU-W-83-001. Oregon State Univ. Newport, p. 61-86.

McLain, D.R., and D.H. Thomas. 1983. Year-to-year fluctuations of the California Countercurrent and effects on marine organisms. CalCOFI Rep. 23:165-181.

Norton, J., D.R. McLain, R. Brainard, and D. Husby. In press. The 1982-83 El Niño event off Baja and Alta California and its ocean climate context. *In* W. Wooster and D. Fluharty (eds.), Proceedings of workshop on El Niño effects in the Eastern Subarctic Pacific. Univ. Wash., Seattle.

Parrish, R.H., A. Bakun, D.M. Husby, and C.S. Nelson. 1983. Comparative climatology of selected environmental processes in relation to eastern boundary current pelagic fish reproduction. *In* G.D. Sharp and J. Csirke (eds.), Proceedings of the expert consultation to examine changes in abundance and species composition of neritic fish resources. San José, Costa Rica, April 1983. FAO Fish. Rep. 291(3):731-777.

Picaut, J. 1983. Propagation of the seasonal upwelling in the eastern equatorial Atlantic. J. Phys. Oceanog. 13(1):18-37.

Radovich, J. 1961. Relationships of some marine organisms of the northeast Pacific to water temperatures, particularly during 1957 through 1959. Calif. Dept. Fish Game, Fish Bull. 112:1-62.

Sette, O.E., and J. Isaacs, eds. 1960. Symposium on the changing Pacific Ocean in 1957 and 1958. CalCOFI Rep. 7:14-217.

Simpson, J.J. 1983. Large-scale thermal anomalies in the California Current during the 1982-83 El Niño. Geophys. Res. Lett. 10(10):937-940.

———. 1984a. El Niño-induced onshore transport in the California Current during 1982-83. Geophys. Res. Lett. 11(3):241-242.

———. 1984b. A simple model of the 1982-83 Californian "El Niño." Geophys. Res. Lett. 11(3):243-246.

Toole, J.M. 1984. Near equatorial CTD observations at 85°W in October 1982. (Abstract 4713 Circulation). EOS-Trans. Amer. Geophys. Union 65(49):1208.

U.S. Dept. Commer. 1983. Oceanographic monthly summary. February 1983. NOAA National Weather Serv., Wash., D.C. 20233, 24 p.

Wooster, W.S., A. Bakun, and D.R. McLain. 1976. The seasonal upwelling cycle along the eastern boundary of the North Atlantic. J. Mar. Res. 34(2):131-141.

Wyrtki, K. 1975. El Niño—the dynamic response of the equatorial Pacific Ocean to atmospheric forcing. J. Phys. Oceanog. 5:572-584.

8560

Systems Research Vol. 2, No. 3, pp. 201–210, 1985.
Printed in Great Britain.

0731-7239/85 $3.00 + 0.00
Pergamon Press Ltd.

Strategic Planning for Research and Management of the Albacore Tuna Fishery

DAVID J. MACKETT

National Oceanic and Atmospheric Administration, National Marine Fisheries Service,
Southwest Fisheries Center, P.O. Box 271, La Jolla, CA 92038, U.S.A.

(*Received* 26 *July* 1984; *revised* 25 *January* 1985)

Key Words—Management; organizations; consensus; fisheries; planning; forecasting.

Abstract—The National Marine Fisheries Service (NMFS) employed the principles of interactive management, supported by consensus building techniques for facilitating meetings, to produce a strategic plan for research on and management of an important fishery. A technically oriented task force aided by a planner was assigned the task of facilitating the production of the plan; an important first step was the production of a probable future scenario of the fishery. Interested citizens, informed by the scenario, were invited to state their goals for the fishery and to list what they considered desirable future trends and events. An options field for the research and management strategy consisting of 17 design categories was produced by the task force and knowledgeable members of NMFS management. The pros and cons for including each option in the NMFS strategy were discussed in a meeting of NMFS Headquarters, Regional and Laboratory management. A set of options was chosen by consensus to represent the NMFS strategic plan for its research and management of the north Pacific albacore fishery.

INTRODUCTION

THIS PAPER presents a description of the process employed by the National Marine Fisheries Service (NMFS) to develop a strategic plan for its program of research and management for the U.S. north Pacific albacore fishery.

The National Marine Fisheries Service, an agency of the U.S. Department of Commerce's National Oceanic and Atmospheric Administration (NOAA), is responsible for conducting research and management programs for the nation's fisheries resources. Its mission includes ensuring the long-range viability of populations of marine fish to help sustain American fishermen's catches and consumer supplies at reasonable levels and prices.

An important U.S. fishery of concern to the NMFS is the north Pacific albacore tuna fishery. The north Pacific albacore is harvested primarily by the Japanese and American fishing fleets but Taiwanese and Canadians also participate in the fishery. The fish are caught as they migrate throughout the temperate north Pacific Ocean from the coast of Japan to the coast of North America.

Total catches of all countries have averaged 93,000 metric tons annually for the 10-year period 1971–1980. During the same period the U.S. portion of the annual catch has averaged 18,300 metric tons caught by approx. 900 small boats that fish along the U.S. west coast from Mexico to Washington state and as far west as Hawaii and Midway Island. At current ex-vessel prices ($1300/ton), the average annual U.S. catch was worth $23.8 million. Although there is a growing fresh fish market, presently, nearly all of the albacore that is caught is canned and sold as white meat tuna.

In addition to the domestic catch large quantities of foreign caught albacore are imported for canning; for example, during 1983 nearly 23,000 mt of north Pacific albacore were imported and canned by U.S. owned companies. The international north Pacific fishery currently yields about 42% of the U.S. canned supply of white meat tuna or nearly 10% of the entire supply of U.S. canned tuna. The north Pacific albacore fishery currently contributes over 100 million cans of tuna to the U.S. consumer annually [2].

NMFS faces several management and research problems concerning the albacore resource and fishery. First, the life history of the albacore is complex; for example, the species migrates in complicated patterns throughout the north Pacific. Second, the dynamics and interactions of the multinational tuna fisheries and the ebb and flow of world-wide economics can affect the intensity of U.S. fishing and thereby the levels of the resource. Superimposed on the already complex problem is the lack of adequate understanding of the effects of environmental elements.

Perhaps most importantly, recent analyses show that the average annual American catch has dropped to about 9000 mt—a situation that warrants increased attention and closer monitoring of the albacore fishery situation by NMFS.

With this background information in mind, the NMFS's Southwest Regional Office (SWR) and Southwest Fisheries Center (SWFC)—the NMFS offices responsible for fisheries management and research in the Southwestern Region of the U.S. respectively—decided in 1980 to increase their monitoring of and research on the albacore fishery. As a result of the need for increased monitoring and the growing complexity of the situation, it became clear that a comprehensive long-range plan for research and management of the albacore would be of benefit to both NMFS and its constituents.

Simultaneously, the SWFC was investigating better ways and means to evaluate, plan, and carry out its research programs. The SWFC installed an interactive planning and management system which integrated the results of normative, strategic and operational planning and put an emphasis on long-run efficiency through consensus building [4]. The key elements of the SWFC's interactive management approach are broad participation by constituents and staff in the planning and management of the Center's research objectives and programs and the formulation of ideals (normative planning) as a starting point for developing strategic and operational plans. Another important feature of the SWFC's system is the training and development of staff members as meeting facilitators skilled in the application of several interactive, consensus-building processes for conducting meetings.

The interactive management system was installed to help the Center approach important management and planning problems, especially those involving inter-disciplinary complexities of biology, economics, oceanography, sociology, domestic politics and international affairs. Subsequently, the SWR and SWFC began the planning for the albacore program based on this interactive planning and management process as it is described in this paper. The formation of the planning organization, the planning and meeting processes that were followed and examples of the intermediate and final results of the strategic planning are described.

THE BASES FOR EMPLOYING THE INTERACTIVE MANAGEMENT APPROACH

The interactive management approach used to develop the albacore strategic plan was applied to help NMFS solve an apparent planning and management dilemma. The dilemma arises when, on the one hand, management tries to overcome the well-known failure of homogeneous groups to solve problems adequately and, on the other hand, in trying to avoid groupthink, is faced with the problem of establishing heterogeneous and therefore potentially more effective groups and getting them to work cooperatively and efficiently in solving problems and developing plans [6]. The trade-off is between quickly determined but deficient decisions and more deliberate but better decisions.

It is important to the long-range viability of an organization to solve this dilemma. A homogeneous group formed to study a problem and offer solutions deceptively appears efficient, because it predictably reaches decisions quickly, never mind if the decision or solution is based on a limited number of possibilities, ignores risks and drawbacks, avoids evaluation of minority opinions, neglects cost–benefit information, and selectively perceives outside criticism. These deficiencies of groupthink can lead to long-run inefficiencies or even disastrous results for the organization [6].

The interactive approach tries to avoid these problems by employing a group whose members collectively possess all the disciplines and points of view needed for better decisions and solutions. However, the operation of such a heterogeneous group presents another set of problems for management. The heterogeneous group's work may at first appear to be inefficient because more time is required for overcoming the shortcomings mentioned previously: more ideas are entertained, risks and drawbacks are discussed, minority opinions are evaluated, cost–benefit information is integrated and outside values and opinions are taken seriously. In addition, members may need time to learn each other's technical language and jargon. However, all of these actions contribute to increasing the probability of finding better solutions to complex problems and to making good decisions. One of the challenges to management then, is to find a means of making the work of heterogeneous groups efficient as well as effective. The SWFC and SWR attempted to do just that in undertaking the strategic planning program described in the following sections.

THE FORMATIVE STAGES

After the independent decisions to increase research activities related to the albacore fishery and to install an interactive planning and management system at the SWFC, the SWFC and SWR directors agreed that a comprehensive planning operation should be undertaken for the albacore program. Although other planning needs were also apparent, especially for the Pacific coast groundfish fishery, lack of experience in the new system and the relatively small number of trained facilitators on hand, made it prudent to undertake only one major planning activity at this stage, and the albacore fishery problem was chosen. It was further agreed that the Center's interactive management system would serve as a model for the planning and that the joint planning endeavor would offer an opportunity to evaluate the effectiveness and efficiency of the interactive management system for planning involving a number of different people, responsibilities, disciplines and points-of-view.

The Directors of the SWFC and the SWR initiated the albacore strategic planning process by appointing a task force whose duty was first to facilitate the strategic planning and then to carry out operational planning and program execution. The task force was made up of scientists and technically oriented individuals all of whom were working on various aspects of albacore fishery research or management; the planning officer for the SWFC was assigned to assist the task force. The task force members were responsible for the content and technical aspects of the work while the planning officer was responsible for establishing and facilitating the planning processes employed by the task force.

The original task force was made up of three biologists, an oceanographer and a fishery management specialist. However, it was apparent after the first meeting that fishery economics and systems analysis expertise were also needed for proper planning, and individuals with these disciplines were added to the task force. The task force members were of very high caliber, nearly all with a Ph.D. degree and each one with several years of experience in his field. The task force members, besides representing a variety of disciplines, also represented five different organizational elements each of which was responsible for an aspect of current albacore research or management. Thus four SWFC Laboratories or Divisions and the SWR office were represented. The individuals on the task force had no previous experience working as a team although from time to time two or more had collaborated on short-term research projects or in writing a scientific paper. Concurrently, with the strategic planning project, most of the SWFC task force members were also assigned to a technical committee which began to work towards its objective of building a computer-oriented model of the dynamics of the north Pacific albacore fishery.

THE PLANNING PROCESS

There were seven major steps in the development of the National Marine Fisheries Service's (NMFS) strategic plan for research and management of the north Pacific albacore fishery (Fig. 1):

1. An analysis of the current situation and the definition of issues that needed to be addressed.
2. The definition of probable trends and events in the fishery and its related entities.
3. The writing of a probable scenario incorporating the issues and projections of the current trends into the future.
4. The definition and structure of the constituents' desirable objectives for the fishery.
5. The definition of trends and events that would obtain if the desirable objectives were being achieved.
6. Development of an Options Field, i.e. the specification of the viable options that could be made a part of NMFS's strategy for meeting the objectives and a classification of the options into similar groups called design categories.
7. Selection of the best option(s) within each design category.

The features of each of these steps along with a description of the process used to accomplish them are provided in the following sections.

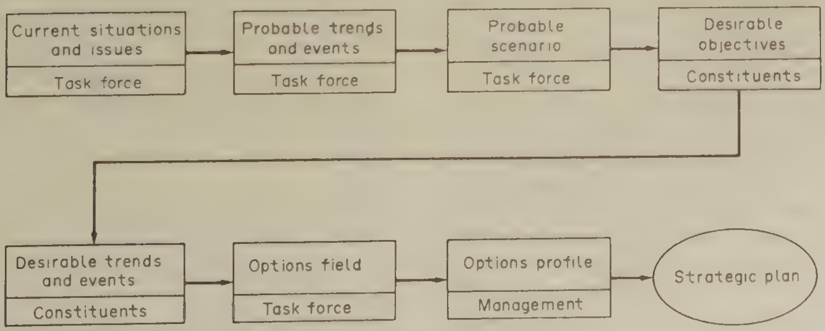

Fig. 1. The seven major steps in the development of the National Marine Fisheries Service's (NMFS) strategic plan for research and management of the north Pacific albacore fishery. The responsibility for the completion of the steps shifted among the task force, constituents and NMFS management.

ANALYSIS OF CURRENT SITUATION AND ISSUES

One of the first activities of the joint SWFC/SWR Task Force for Albacore Program Planning was to explore the issues involved with improving the situation in the north Pacific albacore fishery and to document the existing situation of the fishery and its related entities. At its first meeting the task force discussed the purpose and nature of its assignment and the overall status of the fishery. The group was engaged in a Nominal Group Technique (NGT) process to elicit the issues that the group felt needed to be addressed. The NGT process is a group decision-making process led by a meeting facilitator who usually does not have a personal stake in the outcome of the meeting. The NGT process [1] consists of the following four major steps:

1. Silent generation of ideas in writing in response to a pertinent question about the problem at hand.
2. Round-robin feedback from group members and recording of each idea.
3. Discussion and clarification of each idea.
4. Individual voting on priority ideas with the group decision derived through rank-ordering or rating.

The NGT question which the task force addressed was: 'What issues (concerns) do you think will need to be addressed in planning and carrying out a program for research and management of albacore?'

In response to this trigger question, the group generated 58 issues which were classified into seven categories. Learning and team-building began very early in the discussion period of this first NGT process. As examples, it was agreed to standardize a number of technical terms and, as the issues were discussed, agreements and disagreements were voiced which allowed members to judge the extent to which colleagues understood or appreciated their particular insights or points of view. The generation, discussion, clarification and classification of these issues occupied the first day of the two-and-a-half day meeting.

Probable trends and events

After the issues were set forth and classified, the task force identified the current and probable trends in the fishery. A facilitated brain-storming session was employed to identify important trends in the fishery that would help to characterize the present and probable future situation in the fishery. Systematic discussions of each trend resulted in (1) consensus on the current and future direction and magnitude of the trend, based on the facts on hand, (2) an agreement that sufficient data were available to quantify the trend through subsequent analysis, or (3) that pure speculation was required. The facilitator kept the group's discussion notes and graphs on a flip-chart. The group's work on trends took a full day.

Development of a probable scenario

After these discussions, task force members were assigned, on the basis of expertise and interest, the job of further analyzing some of the trends, making judgements about their future projections, and describing the trends and their probable effects in more detail. This work, which was actually the beginning of the development of the probable scenario, presented difficulties for some task force members. It is hard to identify exact causes, but the difficulties seemed to have stemmed from:

1. an uneasiness on behalf of some scientists in going outside of the scientific method and beyond the range of the data to speculate on the trends;
2. the lack of a clear precedent or model for the probable scenario; and
3. an insufficient initial explanation by the planning officer of how the scenario was to be used, accompanied by a possible fear that mere projections of trends for the probable scenario would somehow make their way into the scientific peer-review process and be misjudged as an individual's scientifically based forecast of what actually will happen.

When these difficulties were settled (through the provision of example scenarios from other planning problems and further explanations by the planning officer, coupled with strong support from upper management) the members did write a probable scenario of the future of the north Pacific albacore fishery to 1993 based on the projection of current trends. The scenario was divided into five interrelated sectors of the fishery and a chapter describing each sector was written. Albacore resources, international and domestic harvesting, domestic processing and consumption, research on the resource and fishery, and national policies and management comprised the five sectors.

A sub-committee of the task force reviewed the draft to assure that the probable scenario was internally consistent from chapter to chapter. The scenario revealed the possible problems and opportunities that the fishery might encounter in the future if current trends were allowed to continue uninterrupted. Thus it represented a picture of the status quo projected to the future.

The scenario was presented to constituents as part of the background information to prepare them for the long-range planning workshop. It helped focus the workshop participants' attention on the future of the fishery and helped them develop their ideas about a desirable or ideal future.

CONSTITUENTS' WORKSHOP ON LONG-RANGE PLANNING

A Workshop on Long-range Planning for the north Pacific albacore fishery was convened at the SWFC during June 1983. It was attended by a number of invited citizens who represented a cross-section of points of view or interests in the albacore fishery; commercial and recreational fishermen, canners, boat owners, industry spokesmen and a State legislator were represented at the meeting. All the participants were individuals outside of the Federal government. As a result of the workshop, NMFS hoped to gain valuable information about what interested citizens would like to see happen in the north Pacific albacore fishery over the next decade; this information would help NMFS plan its programs. At the same time, it was hoped that the workshop participants would feel that they had contributed in a useful way toward improving their government and in helping to create the future they desired for a valuable fishery [3].

The constituents' long-range planning workshop was arranged by the task force and conducted by a facilitator contracted by the SWFC and SWR. One of the most important steps in arranging the workshop was deciding who was to be invited as a participant. The task force began to solve this problem in its first meeting by brainstorming to develop a list of attributes and specialized knowledge required to be represented at the meeting for the constituents' group to achieve a comprehensive overview of the fishery's problems and possible solutions. Thus, about 20 categories of specialized knowledge or experience were listed, e.g. long-range fishermen, boat owners, recreational fishermen, food processors, canners, economic expertise, consumer requirements, financing, population dynamics, etc.

With the categories specified, a matrix was formed by listing names of individuals or organizations and checking-off the attributes possessed by the person or a representative from an organization. In some cases the people that were identified could represent two or more attributes.

The task force worked for approx. half a day to complete the list of categories and to identify the individuals. Afterwards, however, considerable time and effort was spent on logistics by support staff to invite the participants and make the other arrangements for the workshop. A group of 11 citizens representing all the required attributes was invited to attend the workshop on a volunteer basis; 10 actually attended. Travel expenses but no honoraria or fees were paid.

The two-and-a-half day workshop began with an overview of the probable scenario and a discussion of the problems in the fishery. An NGT session produced a list and discussion of the constituents' desirable objectives for the albacore fishery. The NGT trigger question to elicit these objectives was: what are desirable goals and objectives for the future of the north Pacific albacore fishery? Following the NGT session the objectives were structured into a support relationship using Interpretive Structural Modeling (ISM) (Fig. 2).

ISM is a computer-assisted group learning process that culminates in the development of a structure displaying the relationships among the elements of an issue, problem, plan or project. The structure is developed in a meeting assisted by a skilled facilitator. The ISM methodology allows the structuring of a large set of elements, often involving a very large number of possible combinations and permutations, while the group considers at any one time only the relationship between two elements [7, 8]. Inferential logic is applied in the ISM computer program to reduce considerably the number of queries that need to be addressed.

As in the NGT process, a 'trigger' question is used in the ISM process to focus the discussion and to establish the relationship between pairs of elements. The question used in this case was: 'In the context of a desirable future for the north Pacific albacore fishery, will the achievement of objective X significantly support objective Y?'

When the objective statements are substituted for X and Y the question can only be answered with a yes or no. However, a great deal of discussion may ensue before the group can answer the question. The pairs of objectives that were considered were selected by the ISM computer program with the text of the objectives displayed on a large television screen. A typical question from this ISM session would be as follows: 'In the context of a desirable future for the north Pacific albacore fishery, will the achievement of the objective *improve forecasting of annual and geographic fluctuations in the fish stock* significantly support the objective *conduct research to improve efficiency of fishing methods of domestic fishermen*?'

With the support relationship among the objectives identified and displayed, the participants were then asked to describe what desirable trends and events one would experience in the future if indeed the objectives were being pursued. To accomplish this, the objectives were grouped into four major categories. Two categories were assigned to each of two sub-groups of workshop participants. Each sub-group was then engaged in an NGT and an idea writing session to produce a list of desirable trends and events for each category.

The workshop resulted in two major sets of information that formed the basis for further planning: (1) a set of desirable goals and objectives for the future of the albacore fishery from the

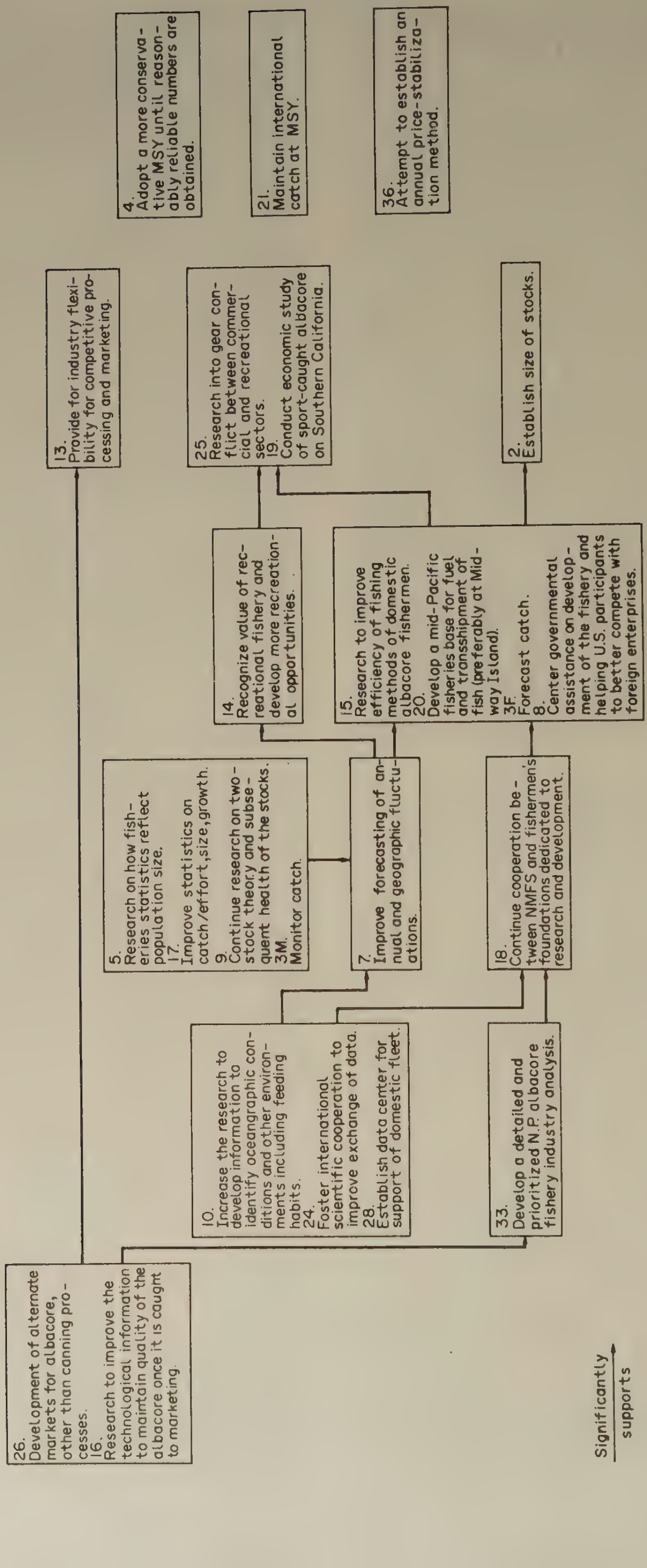
4. Adopt a more conservative MSY until reasonably reliable numbers are obtained.
21. Maintain international catch at MSY.
36. Attempt to establish an annual price-stabilization method.
13. Provide for industry flexibility for competitive processing and marketing.
25. Research into gear conflict between commercial and recreational sectors.
19. Conduct economic study of sport-caught albacore on Southern California.
2. Establish size of stocks.
14. Recognize value of recreational fishery and develop more recreational opportunities.
15. Research to improve efficiency of fishing methods of domestic albacore fishermen.
20. Develop a mid-Pacific fisheries base for fuel and transshipment of fish (preferably at Midway Island).
3F. Forecast catch.
8. Center governmental assistance on development of the fishery and helping U.S. participants to better compete with foreign enterprises.
5. Research on how fisheries statistics reflect population size.
17. Improve statistics on catch/effort, size, growth.
9. Continue research on two-stock theory and subsequent health of the stocks.
3M. Monitor catch.
7. Improve forecasting of annual and geographic fluctuations.
18. Continue cooperation between NMFS and fishermen's foundations dedicated to research and development.
10. Increase the research to develop information to identify oceangraphic conditions and other environments including feeding habits.
24. Foster international scientific cooperation to improve exchange of data.
28. Establish data center for support of domestic fleet.
33. Develop a detailed and prioritized N.P. albacore fishery industry analysis.
26. Development of alternate markets for albacore, other than canning processes.
16. Research to improve the technological information to maintain quality of the albacore once it is caught to marketing.
Significantly supports

Fig. 2. Desirable goals and objectives for the future of the north Pacific albacore fishery.

constituents' point of view, and (2) a set of desirable trends and events that, if realized over the next 10 years, would indicate to the workshop participants that the desirable goals and objectives were actually being pursued and realized.

These sets of information, together with the information from the probable scenario and an examination of the issues, formed the basis for the options that were later developed for the design of the strategic plan for the NMFS albacore program. The participants in the workshop also completed an evaluation of the workshop itself. Their remarks made it clear that a large majority of the participants regarded the workshop as an efficient one and as being beneficial to both NMFS and themselves.

PREPARATION OF INFORMATION AND THE OPTIONS FIELD

Following the constituents' workshop, the task force combined the desirable trends and events developed by the constituents with the probable trends and events developed earlier by the task force. These trend statements, numbering about 130, were then grouped into 17 categories on the basis of similarities; duplicates were eliminated. The meaning and implications of the various trends were discussed during this process which was carried out in a facilitated ISM session. In this way, the task force members were able to learn a great deal about the citizens' requirements and desires and the interrelationships among the trends and issues.

With the detailed trends and events classified, the SWFC senior staff was able to develop a set of options for the NMFS strategy. Option statements were formulated by consolidating individual detailed statements of desirable trends and events within each category. Table 1 shows a portion of this original set of options arrayed by category into what is called an Options Field. In this case, the options in each category are annotated by the original statements of desirable trends and events obtained from the constituents or from the probable scenario. This preliminary options field for guiding the design of the NMFS program for albacore research and management was used as a background document for the Directors' meeting on strategic planning for the NMFS Program for North Pacific Albacore Research and Management.

The NMFS Directors' meeting

A meeting attended by NMFS Directors was held for the purpose of establishing program objectives and selecting the options to form the NMFS strategic plan for albacore research and management. The objectives and strategy were to be established in light of the constituents' desirable goals and objectives, and in support of these objectives to the extent that the NMFS mission and capabilities could accommodate them. The NMFS managers at the meeting were asked to:

—consider the issues and opportunities involved with the north Pacific albacore resources and fisheries;

—discuss the pros and cons of the possible and feasible options for resolving the issues or taking advantage of the opportunities;

—reach a consensus on the preferred options to be included in the long-range NMFS program for albacore research and management; and

—determine the roles and responsibilities of the various NMFS offices for carrying out the NMFS albacore program.

The participants were provided with background materials before the meeting, including reports on the fishery, a draft of the options field and the report of the constituents' workshop.

The meeting was facilitated by a professional, non-government facilitator, the same person who conducted the constituents' workshop. All of the options were displayed on a magnetic board visible at all times to the participants (Fig. 3). The participants first discussed the meaning of each of the options within each of the design categories, one at a time. SWFC and SWR technical staff from the albacore planning task force were available to answer questions and to explain the significance of options, issues or opportunities based on material from the constituents' workshop or based on known facts. After NMFS Directors were satisfied that the meanings of the options were understood, they reorganized the options field slightly by combining the four research categories into a single category and by adding a few additional options.

When the final options field was established, the group discussed the pros and cons of including each option in the NMFS strategy and selected those to be included in the NMFS albacore program. A combination of facilitated discussion and voting was used to arrive at a consensus for selecting or rejecting individual options for the strategy.

Because there were logical relationships among some of the options or categories, it was possible that selections of certain options in one category could eliminate choices in the remaining categories. Therefore, during the meeting, logically inconsistent options in the remaining categories were removed from consideration after the selections were made for a category. Only a few options were thus affected. From the Directors' point of view, the final choices in each of the design categories constituted the best alternative design of the NMFS albacore strategy (Fig. 4).

Table 1. The Options Field for three of the 17 original design categories. The options were developed by SWFC Management from the individual statements of desirable trends and events from the constituents (asterisked items) and some of the probable trends and events from the probable scenario (non-asterisked items)

4. FISHERY DEVELOPMENT

—Investigate potential for increasing: total catch, U.S. share of total catch, efficiency (lower costs)
—Conduct gear research and development program
—Conduct research program on fishing strategies
—Continue cooperation with S-K projects

1. Number of Japanese pole-and-line vessels declines. (PH)
2. Decrease in U.S. pole-and-line vessels. (PH)
3. U.S. vessels move farther west. (PH)
4. U.S. longline fleet increases. (PH)
5. Increase in gillnet vessels. (PH)
6. Increase in larger combination vessels. (PH)
7. Indirect constraints on albacore fishery determined. (I)
8. Fishing efficiency increases. (PH)
9. Determine if albacore fishery can be used to absorb fishing effort diverted from other U.S. fisheries. (I)
10*. Assistance for development of U.S. high seas longline and gillnet fleets through the use of S-K, AFRF, or other funds for charter vessels. (1DD) (2DD) (3DD) (6DD)
11*. Continue close communication and cooperation between government and industry for fishery development. (1DP)
12*. Establish SWFC and Navy assistance to obtain oceanographic and fishery data in support of longline and gillnet development. (1DD–6DD)
13*. R & D for domestic high-seas gillnet albacore fishery. (3DD)
14*. R & D for domestic high-seas longline fishery. (3DD)
15*. Continue R & D on new types of fishing gear. (14DR)
16*. Improve vessel and machinery designs. (19DD)
17*. Develop new materials for vessels and gear. (4DD)
18*. Develop an effective longer-lasting fish aggregation buoy (FAB). (37DD)
19*. Test fish aggregation devices with fishermen/government participation. (4DP) (5DP)
20*. Place aggregating devices in oceanic and mid-Pacific waters. (11DP)
21*. R & D on new methods for fishing albacore at depth. (12DD)
22*. Expand aquaculture research to assist commercial fisheries, e.g. baitfish culture in sea-holding pens.
23*. Engineer a breakthrough in rearing mullet for use as a baitfish. (10DD–40DD)
24*. Increase congressional support for fishery development. (29DD)

5. CENTRAL PACIFIC FISHERY BASE

—Promote development of Fishery Base
—Monitor the State/industry efforts
—Oppose development of base at Midway

1. Infrastructure is required to develop a U.S. fishery in more distant fishing grounds. (I)
2*. Develop statistical data to show benefits of Midway base development. (11DD)
3*. Develop a plan for the necessary infrastructure in Hawaii to support the Midway Island fishing port. (20DD)
4*. Feasibility study to determine various economic development plans to use Midway Island as a fishing port. (15DD)
5*. Develop a Midway fishing base to increase fleet efficiency. (27DD)
6*. Assess level of proper government participation in developing Midway base. (28DD)
7*. Provide NMFS assistance for establishing Midway base. (11DD)
8*. State of Hawaii assistance for establishing Midway base. (11DD)
9*. U.S. Navy assistance for establishing Midway base. (11DD)
10*. Establish a fuel and transshipment base at Midway Island. (17DD)
11*. Establish a cooperative or association, to manage the Midway facility. (25DD)
12*. Develop a mothership operation at Midway if feasible. (29DD)
13*. Use of U.S. Navy mothballed fleet (refrigeration and cargo) for development of U.S. fishery. (30DD)

6. NEW PRODUCTS

—Actively develop new albacore seafood products (utilization labs)
—Assist industry through grants (e.g. S-K)

1. Canned tuna consumption at 93,000 tons by 1988; 104,000 tons by 1993. (PP)
2. Existing processing plants produce domestic demand through 1993. (PP)
3. Domestic retail demand for albacore in all product forms approaches 119,000 tons annually by 1993. (PP)
4. Increased industry R & D funds devoted to fresh-frozen and 'over the counter' items. (PP)
5*. Develop alternative albacore products. (11DA)
6*. Analysis of all possible ways of using albacore for the market. (11DA)
7*. Develop albacore sandwich spread. Develop sliced albacore (bologna-like). (14DA)
8*. Establish a fishery product development and utilization laboratory in Hawaii. (36DD)
9*. Establish a utilization lab outside of Hawaii. (12DA)

CONCLUDING REMARKS

The NMFS strategic plan developed for the north Pacific albacore fishery research and management—or more specifically the collective experience of the planning process—is already guiding the programming, budgeting and operations within NMFS. For example, the Southwest Fisheries Center and Southwest Regional Office are reviewing their albacore fishery-related operations, making better operational plans (some involving fishermen) and making program decisions based on the planning experience.

The strategic planning process also lead to a great deal of learning by all of the people involved. The task force members learned many technical facts and scientific approaches from each other; they learned to trust each other more, and to work together more as a team. The task force also learned the explicit desires of the constituents and NMFS management. Thus the people who shared a common planning experience gained a common understanding of the albacore fishery situation and of NMFS goals and strategy for the fishery.

The citizens who were invited to participate in the long-range planning workshop also learned, as did a number of other constituents who later became informed about the results of the planning. Recreational and commercial interests learned that they shared some explicit common goals and desires for the fishery and that they both could and should provide their thoughts to the NMFS planning process. NMFS management learned explicitly what the stakeholders desired for their fishery and, as importantly, what common desires were shared by the various components of the fishery—commercial and recreational alike. Everyone, including NMFS management, learned that it is always difficult to make judgments about the directions one should take to ensure a desirable future result, but that a systematic, open consensus-building approach, involving those who will be affected by the decisions is a worthwhile approach which minimizes confusion and improves the probability of making better decisions.

This approach used to develop the strategic plan has, in the author's opinion, helped overcome the apparent planning and management dilemma mentioned previously, i.e. the problems concerning the differences in results and operations between homogeneous and heterogeneous groups.

The approach taken here attempted to establish a heterogeneous group not only for the task force but also by the involvement of constituents, management and staff in the overall solution to the problem.

Fig. 3. National Marine Fisheries Service's top management met to select the options that were to be included in the Services Strategic Plan for the north Pacific albacore fishery.

The approach also employed ways and means of running meetings efficiently, consistent with dealing with the complexity and importance of the problem and the number and difficulty of the disciplines required to solve the problem. Unfortunately, it is difficult to judge, in any particular instance, how much better or worse an interactively derived decision might be, compared to a hurried decision made in some other mode of operation. What we do know is that over the long run, if the interactive approach is pursued, better decisions should result. Thus in the case of the strategic plan for the albacore fishery we have no absolute way of knowing how much better the result would be than if the decision were derived in the traditional manner. However, we believe that we have increased the probability that the solution is a good one.

Evidence for this assertion lies in the fact that the task force members, who are, at this stage, responsible for carrying out major portions of the plan, state that they share a common understanding of objectives and the overall program which they did not have before. This improved understanding coupled with a better appreciation of their co-workers' contributions allows them to coordinate their work much better. Inter-personal relationships among the task force members have improved also. NMFS management, though still having concerns about the future of the fishery and the resource, has a more relaxed and more confident attitude about the Service's ability to meet the research and management challenges that are before it. Overall, the SWFC and SWR staffs and management are pleased with the planning result. However, the overall implementation of the plan may have been improved if the NMFS Directors' meeting in addition to the assignment of responsibilities also included the development of a managerial monitoring and reporting system for better coordinating the albacore program among the Regional Offices, Research Centers and NMFS Headquarters.

Since the albacore program planning experience the SWFC especially has been inclined to employ the principles of interactive management in many other situations. Several more staff members have been trained in the principles of interactive management and the art of facilitation. The author is confident that as more experience with the methodology is gained and more successes are realized both the frequency of the application of interactive management techniques and the quality of the results will increase. A reinforcement to the commitment comes from the many favorable comments that are received about how the Center conducts its planning meetings from people outside the SWFC who have attended planning sessions organized by the Center. It is expected that this trend will continue.

Because a lot of time and energy are needed to design and install an interactive approach the traditional approach to solving problems seems at the present time to be on the path of least resistance for many managers and many organizations. Thus it seems likely that only the problems amenable to traditional or prescriptive solutions are adequately tackled and that important complex problems are either ignored or fitted with weak solutions in a great many instances. However, it is to be hoped that good experiences with the interactive management approach such as the one described here, will be of value to other managers and organizations and be an encouragement to them to apply it for solving those important and complex problems that seem to defy satisfactory solution through traditional approaches.

Acknowledgements—Dr. Izadore Barrett, Director of the Southwest Fisheries Center, created and maintained the environment which permitted the ideas and concepts of interactive planning and management to flourish and be successful. This kind, honest, capable man has dedicated his career to excellence in government and fishery science. Every day by deed and attitude he steers a steady course towards these goals; he is an example for us all.

Richard Parrish, Chairman; Norman Bartoo, Samuel Herrick, Pierre Kleiber, R. Michael Laurs, Rodney McInnis and Jerry Wetherall comprised that task force that did most of the work, while carrying out their usual tasks as well.

Dr. Alexander Christakis, Center for Interactive Management, George Mason University, very ably taught and guided us and facilitated many of the meetings in his own inimitable style. Susan Iacometti and Christina Show, Southwest Fisheries Center, provided perfect computer assistance.

REFERENCES

1. Andre L. Delbecq, Andrew H. Van de Ven and David H. Gustafson, *Group Techniques for Program Planning—A Guide to Nominal Group and Delphi Processes*. Scott, Foresman (1975).
2. Samuel F. Herrick, Jr. and Steven Koplin, U.S. tuna trade summary, 1983. *Mar. Fish. Rev.* **46** (1984), 65–72.
3. David J. Mackett, Report of the workshop on long-range planning for the north Pacific albacore fishery. National Oceanic and Atmospheric Administration Technical Memorandum: NOAA-TM-NMFS-SWFC-37 (1983).
4. David J. Mackett and Alexander N. Christakis, Designing and installing an interactive management system for the Southwest Fisheries Center. *Proc. Third Symp. Coastal and Ocean Management*, ASCE/San Diego, CA (1983), pp. 518–537.
5. NOAA, Status report on world tuna and billfish stocks. National Oceanic and Atmospheric Administration Technical Memorandum: NOAA-TM-NMFS-SWFC-15 (1981).
6. Benjamin Schneider, An interactionist perspective on organizational effectiveness. In Kim S. Cameron and David A. Whetten (eds), *Organizational Effectiveness, A Comparison of Multiple Models*, pp. 27–54. Academic Press, New York (1983).
7. Robert J. Waller, An application of interpretive structural modeling to priority-setting in urban systems management. In M. Bladwin Maynard (ed.), *Portraits of Complexity, Applications of Systems Methodologies to Societal Problems*. Battelle Monograph No. 9 (1975), pp. 104–108. Battelle Memorial Institute, Columbus, OH.
8. John N. Warfield, Organizations and systems learning, general systems. Presidential address. *Yearbook of the Society for General Systems Research*, Vol. XXVII (1983).

FINAL OPTIONS FIELD/OPTIONS PROFILE FOR GUIDING THE DESIGN OF THE NMFS PROGRAM FOR ALBACORE RESEARCH & MANAGEMENT

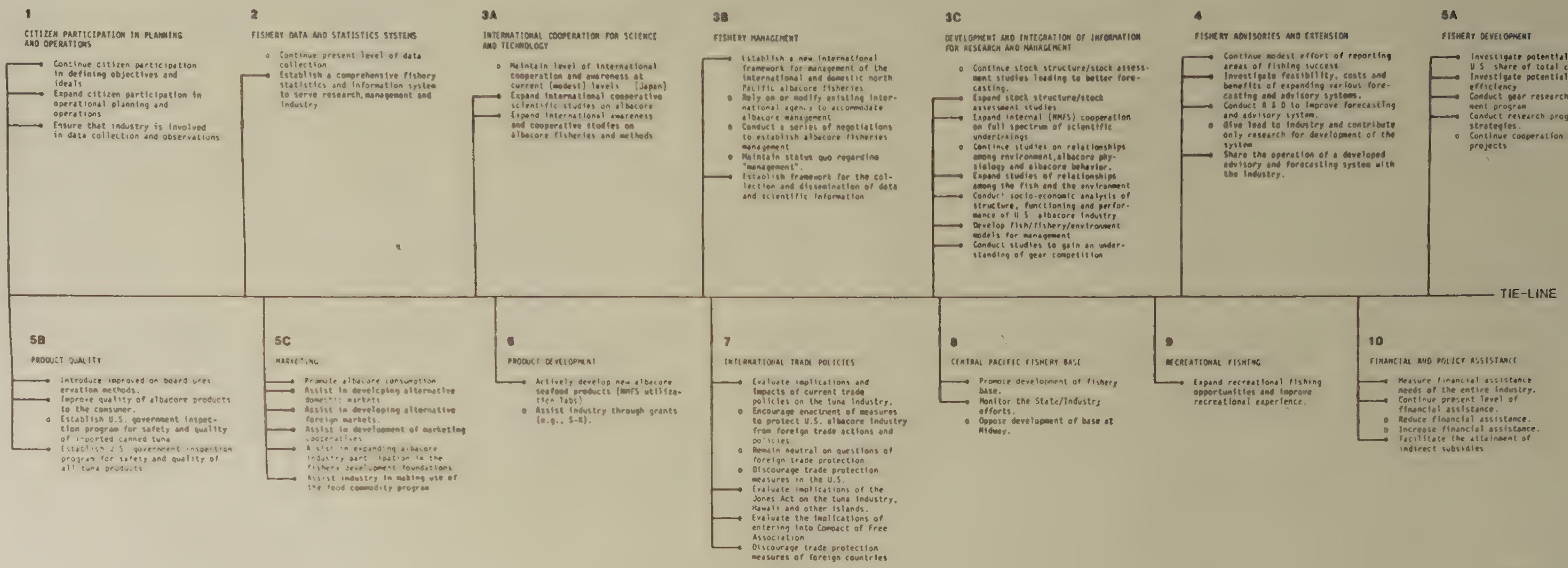

1

CITIZEN PARTICIPATION IN PLANNING AND OPERATIONS

- ● Continue citizen participation in defining objectives and ideals
- ● Expand citizen participation in operational planning and operations
- ● Ensure that industry is involved in data collection and observations

2

FISHERY DATA AND STATISTICS SYSTEMS

- ○ Continue present level of data collection
- ● Establish a comprehensive fishery statistics and information system to serve research, management and industry

3A

INTERNATIONAL COOPERATION FOR SCIENCE AND TECHNOLOGY

- ○ Maintain level of international cooperation and awareness at current (modest) levels (Japan)
- ● Expand international cooperative scientific studies on albacore
- ● Expand international awareness and cooperative studies on albacore fisheries and methods

3B

FISHERY MANAGEMENT

- ● Establish a new international framework for management of the international and domestic north Pacific albacore fisheries
- ○ Rely on or modify existing international agency to accommodate albacore management
- ○ Conduct a series of negotiations to establish albacore fisheries management
- ○ Maintain status quo regarding "management".
- ● Establish framework for the collection and dissemination of data and scientific information

3C

DEVELOPMENT AND INTEGRATION OF INFORMATION FOR RESEARCH AND MANAGEMENT

- ○ Continue stock structure/stock assessment studies leading to better forecasting.
- ● Expand stock structure/stock assessment studies
- ● Expand internal (NMFS) cooperation on full spectrum of scientific undertakings
- ○ Continue studies on relationships among environment, albacore physiology and albacore behavior.
- ● Expand studies of relationships among the fish and the environment
- ● Conduct socio-economic analysis of structure, functioning and performance of U S albacore industry
- ● Develop fish/fishery/environment models for management
- ● Conduct studies to gain an understanding of gear competition

4

FISHERY ADVISORIES AND EXTENSION

- ● Continue modest effort of reporting areas of fishing success
- ● Investigate feasibility, costs and benefits of expanding various forecasting and advisory systems.
- ● Conduct R & D to improve forecasting and advisory system.
- ○ Give lead to industry and contribute only research for development of the system
- ● Share the operation of a developed advisory and forecasting system with the industry.

5A

FISHERY DEVELOPMENT

- ● Investigate potential for increasing U S share of total catch
- ● Investigate potential for increasing efficiency
- ● Conduct gear research and development program
- ● Conduct research program on fishing strategies.
- ○ Continue cooperation with S K projects

5B

PRODUCT QUALITY

- ● Introduce improved on board preservation methods.
- ● Improve quality of albacore products to the consumer.
- ○ Establish U.S. government inspection program for safety and quality of imported canned tuna
- ● Establish U S government inspection program for safety and quality of all tuna products

5C

MARKETING

- ● Promote albacore consumption
- ● Assist in developing alternative domestic markets
- ● Assist in developing alternative foreign markets.
- ● Assist in development of marketing cooperatives
- ● Assist in expanding albacore industry participation in the fishery development foundations
- ● Assist industry in making use of the food commodity program

6

PRODUCT DEVELOPMENT

- ● Actively develop new albacore seafood products (NMFS utilization labs)
- ○ Assist industry through grants (e.g., S-K).

7

INTERNATIONAL TRADE POLICIES

- ● Evaluate implications and impacts of current trade policies on the tuna industry.
- ○ Encourage enactment of measures to protect U.S. albacore industry from foreign trade actions and policies
- ○ Remain neutral on questions of foreign trade protection
- ○ Discourage trade protection measures in the U.S.
- ● Evaluate implications of the Jones Act on the tuna industry, Hawaii and other islands.
- ● Evaluate the implications of entering into Compact of Free Association
- ● Discourage trade protection measures of foreign countries

8

CENTRAL PACIFIC FISHERY BASE

- ● Promote development of fishery base.
- ● Monitor the State/Industry efforts.
- ○ Oppose development of base at Midway.

9

RECREATIONAL FISHING

- ● Expand recreational fishing opportunities and improve recreational experience.

10

FINANCIAL AND POLICY ASSISTANCE

- ● Measure financial assistance needs of the entire industry.
- ● Continue present level of financial assistance.
- ○ Reduce financial assistance.
- ○ Increase financial assistance.
- ● Facilitate the attainment of indirect subsidies

January 1984

FIGURE 4

8561

LARVAE AND JUVENILES OF AURORA ROCKFISH, *Sebastes aurora,* FROM OFF CALIFORNIA AND BAJA CALIFORNIA

H. GEOFFREY MOSER, ELAINE M. SANDKNOP AND DAVID A. AMBROSE

National Oceanic and Atmospheric Administration
National Marine Fisheries Service
Southwest Fisheries Center
P.O. Box 271
La Jolla, California 92038

r. and J.B. Marliave (editors). 1985. Descriptions of early life history
elected fishes: from the 3rd International Symposium on the Early Life
Fishes and 8th Annual Larval Fish Conference, May 1984, University of
mbia, Vancouver, Canada. Can. Tech. Rep. Fish. Aquat. Sci. 1359: 82 p.

INTRODUCTION

Adults of Sebastes aurora are uniformly pink-red in coloration, moderate in size (up to 40 cm) and have been reported from Amphridite Pt., Vancouver Island, to San Diego, California, in depths of 180-768 m (Miller and Lea 1972; Eschmeyer et al. 1983). They are a minor component of trawl catches from deep soft-bottom habitats (W.H. Lenarz, NMFS, Tiburon Lab., pers. comm.). Published fishery and life history information of this species is lacking.

Sebastes aurora is the eighth eastern Pacific Sebastes species for which complete life history stages are known. Others are S. cortezi, S. dallii, S. jordani, S. levis, S. macdonaldi, S. melanostomus and S. paucispinis (Moser et al. 1977; Moser and Ahlstrom 1978; Moser and Butler 1981). Five other species have been reared to the stage of notochord flexion--S. rufus and S. constellatus (Moser and Butler, In press); S. caurinus and S. auriculatus (Stahl-Johnson, this volume); S. melanops (G.W. Boehlert, NMFS, Honolulu Lab., pers. comm.). Postflexion stages have been described for seven species--S. crameri, S. helvomaculatus and S. pinniger (Richardson and Laroche 1979); S. flavidus and S. melanops (Laroche and Richardson 1980); S. entomelas and S. zacentrus (Laroche and Richardson 1981). Information on pre-extrusion, newborn or first-feeding larvae is available for 28 other species (Moser et al. 1977; Kendall 1982; Washington et al. 1984), leaving 22 eastern North Pacific species for which life history stages have not been described. The use of ichthyoplankton surveys in estimating spawning biomass and recruitment of Sebastes species is impaired by the large species complement and the inadequate knowledge of their early life histories. This paper employs specimens from ichthyoplankton and trawl collections and the technique of tracing larval series backward from identifiable juveniles. The companion paper (Stahl-Johnson, this volume) describes larval stages of two nearshore species reared from larvae extruded from identified females. Extensive use of these techniques is necessary to fill in the gaps in our knowledge of Sebastes life histories.

MATERIALS AND METHODS

Material for early life history description was based on the 415 larvae and early pelagic juvenile specimens (3.0-21.5 mm in length) collected on California Cooperative Oceanic Fisheries Investigations (CalCOFI) plankton surveys from 1949 to 1981. Eleven pelagic juveniles (14.4-34.4 mm SL) were obtained from midwater trawl collections of the Natural History Museum of Los Angeles County (LACM Cat. Nos. 9369-17, 9674-16, 9677-11, 9943-17, 30202-7, 30203-3, 30270-9, 30526-13, 36303-1, and 36313-1). Two benthic juveniles (38.3 and 38.9 mm SL) were obtained from bottom trawl samples of Scripps Institution of Oceanography (SIO Cat. Nos. 70-350 and 84-47). Descriptive methods and terminology follow Moser et al. (1977) and Moser and Ahlstrom (1978).

Fresh specimens for aging were obtained from the stomach contents of albacore (Thunnus alalunga) taken in August 1977 about 129 km south-southwest of San Diego, California. The otoliths were prepared and analyzed according to the methods of Brothers et al. (1976).

DESCRIPTION OF DEVELOPMENT

GENERAL DEVELOPMENT

Larvae of S. aurora are released principally during the winter and spring and are about 4.0 mm long at birth (Fig. 1). Notochord flexion occurs in a size interval of about 6.5-8.6 mm and transformation to the pelagic juvenile stage occurs at about 13 mm SL (Table 1). Our largest pelagic juvenile was 34.4 mm SL; the smallest benthic juvenile was 38.3 mm SL (Fig. 2).

MORPHOLOGY

Larvae have a distinctive shape; the head and mouth are large and the produced snout has a concave dorsal profile. The snout-anus distance is relatively greater than in other species studied (Table 2). Pelagic juveniles have a relatively large head and mouth; however, the dorsal snout profile is slightly convex.

Sebastes aurora develops a nearly complete complement of head spines; the sequence of their appearance is listed in Table 3. The parietal spines are relatively small, weakly serrated and lie flat against the head. The 2nd and 3rd anterior preopercular spines, and the 1st and 4th upper infraorbitals are lost during the pelagic juvenile stage; the pterotic, lower posttemporal and cleithral spines are lost in the benthic juvenile stage.

FIN DEVELOPMENT/MERISTICS

The principal caudal fin rays are the first rays to begin ossification, at about 5.3 mm. The full complement of 8 + 7 rays is present at 8.0 mm at which size the procurrent caudal rays begin ossifying (Table 4). Ossification of the pectoral fin rays begins at about 5.6 mm and the full complement is ossifying at about 8.3 mm. The pectoral fin attains a moderate size compared with that in other Sebastes species (Table 2). Ossifying dorsal and anal fin rays are present during notochord flexion and the full complements are present in early postflexion larvae. The gill rakers on the lower limb of each arch appear at about 5.6 mm and the full complement on both limbs (24-28) is ossifying at the end of the larval period. Only one other species of eastern Pacific Sebastes, S. rastrelliger, has a lower count. The

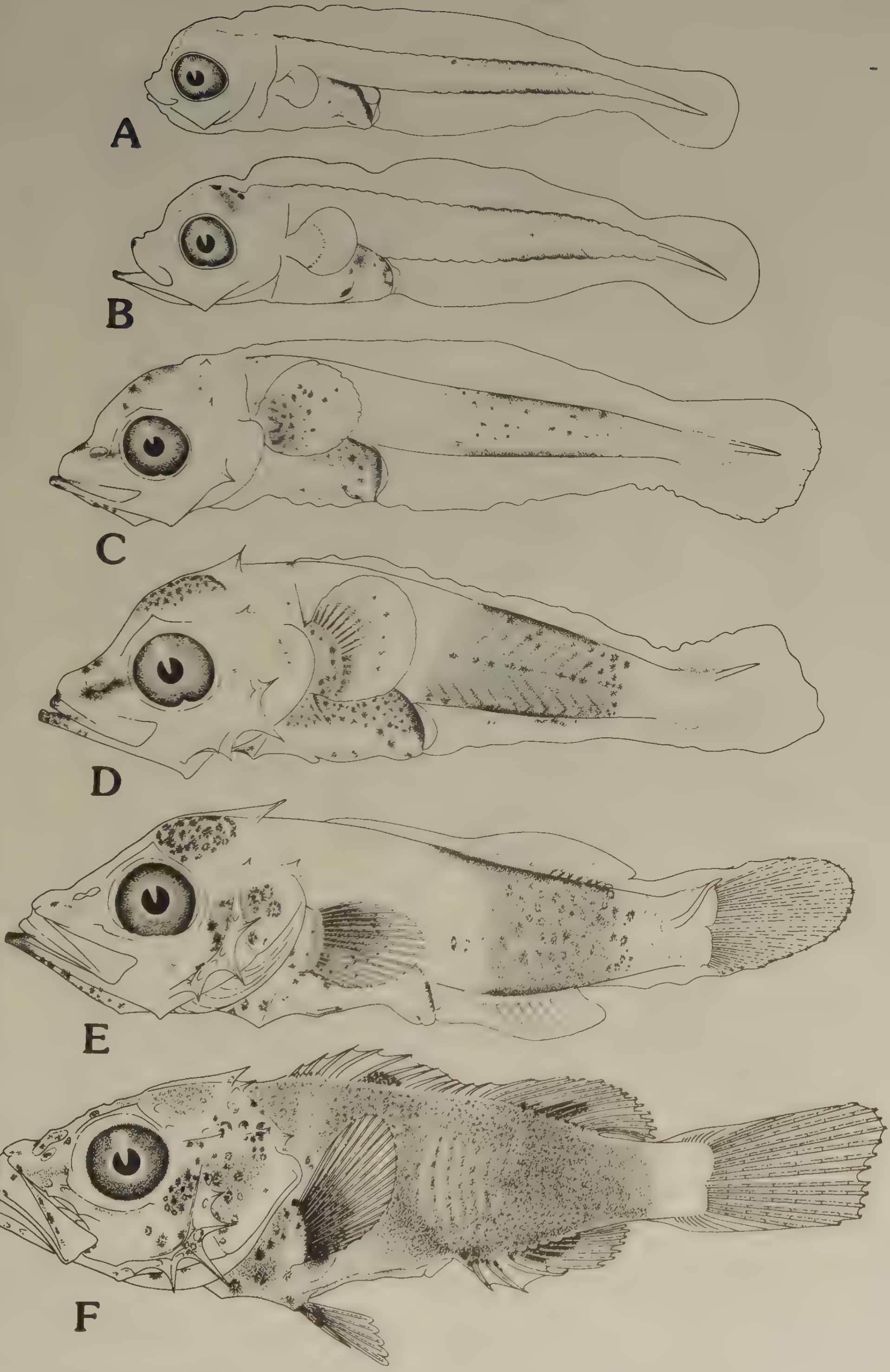

gure 1. Developmental series of *S. aurora*. (A) 4.4 mm larva, Scripps 2-6-B, Sta. 3-1-A; (B) 4.8 mm larva, CalCOFI 4908 (H6) 802; (C) 6.5 mm larva, Scripps 2-6-B, Sta. 3-1-A; (D) 6.7 mm larva, CalCOFI 5005 Sta. 130.40; (E) 8.3 mm larva, CalCOFI 7507 Sta. 90.70; (F) 13.5 mm pelagic juvenile, LACM 30270-9.

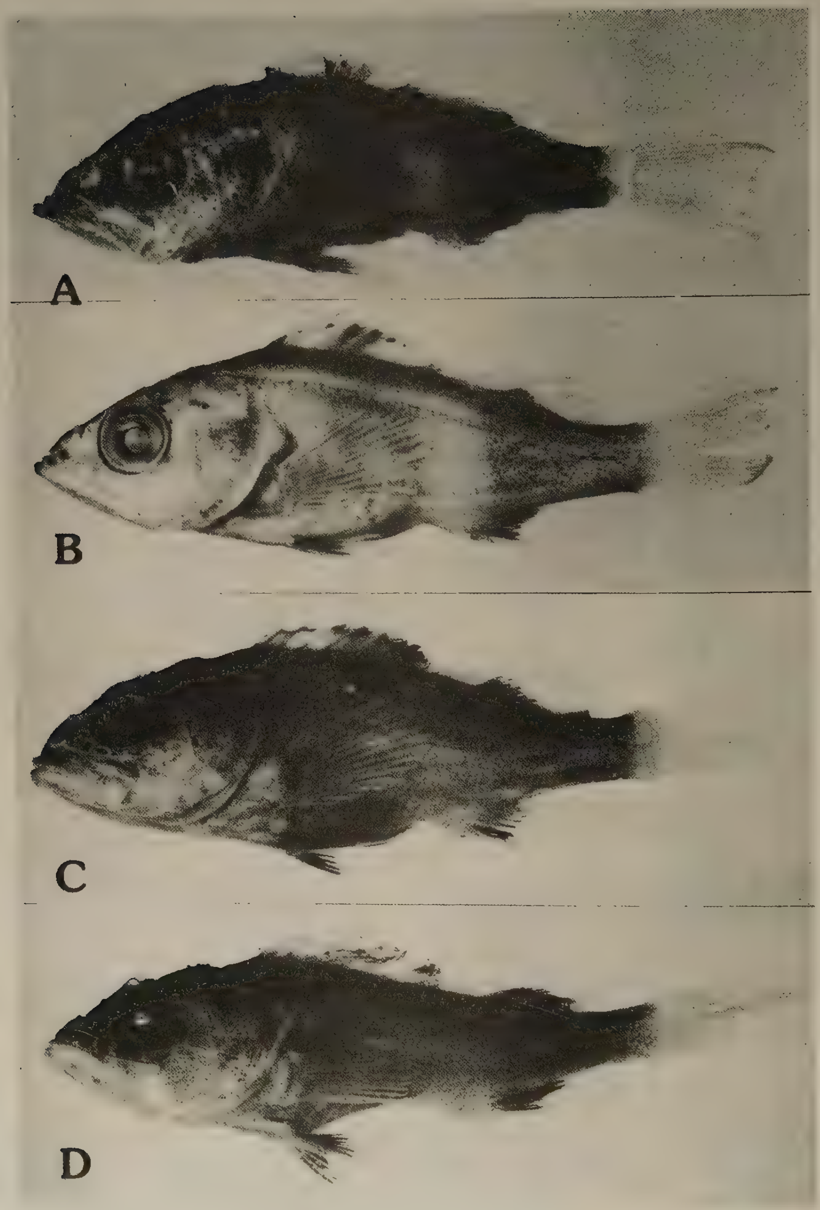

Figure 2. Developmental series of *S. aurora*. (A) 18.6 mm pelagic juvenile, LACM 30202-7; (B) 28.3 mm pelagic juvenile, LACM 36313-1; (C) 34.4 mm pelagic juvenile, LACM 36303-1; (D) 38.9 mm benthic juvenile, SIO 70-350.

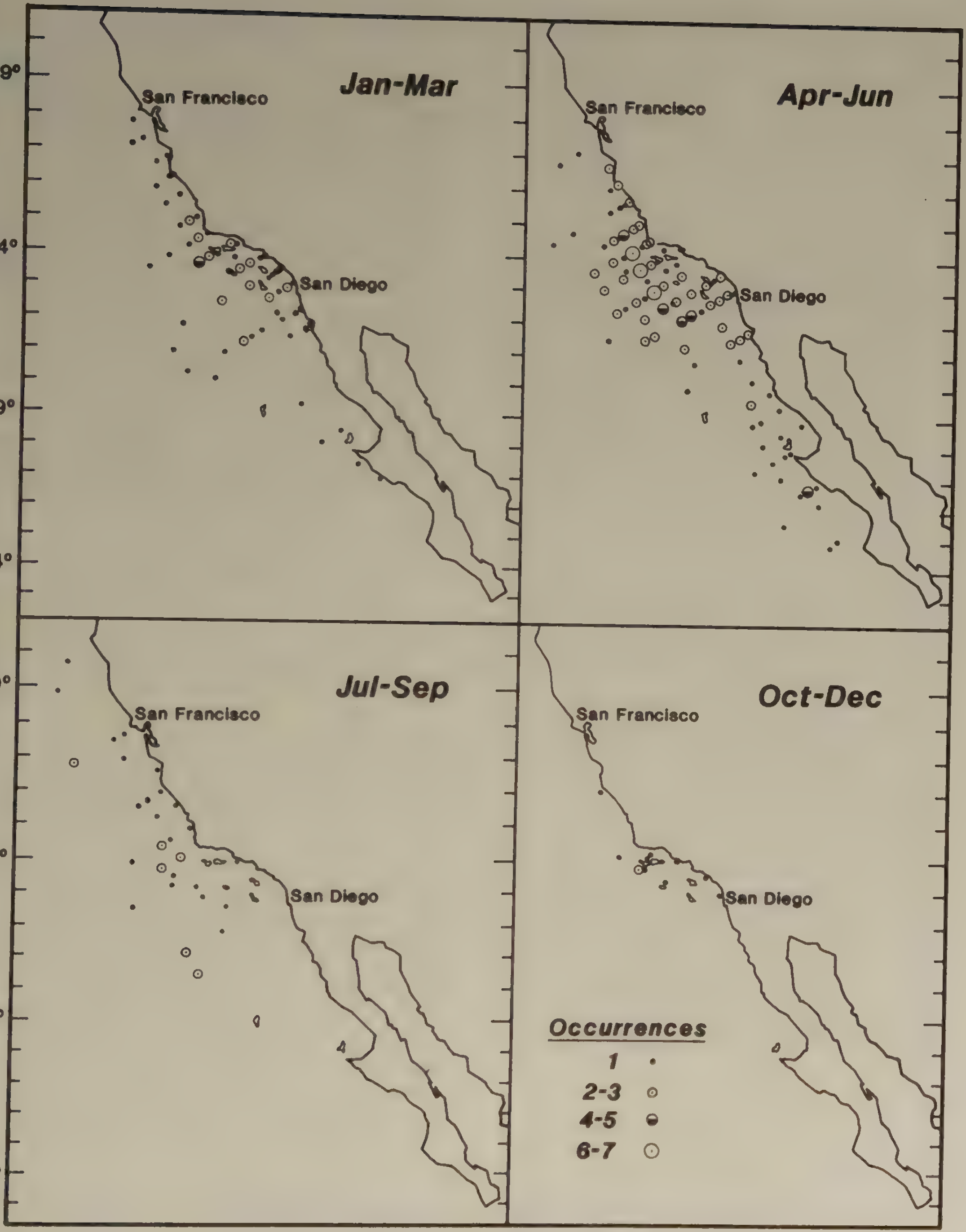
39°
34°
29°
24°
Jan-Mar
Apr-Jun
Jul-Sep
Oct-Dec
San Francisco
San Diego
Occurrences
1
2-3
4-5
6-7

Figure 3. Numbers of occurrences of larvae of S. aurora in standard CalCOFI tows taken during 1959-1981 and pooled by season.

full complement of 27-30 lateral line scales, the lowest count among eastern Pacific Sebastes, is present about mid-way through the pelagic juvenile stage. The combination of these two counts is diagnostic for the species.

PIGMENTATION

Larvae of S. aurora have an unusual pigment pattern. Newborn larvae have a melanistic sheath above the gut and a distinctive band extending from the 4th or 5th postanal myomere to the 14th or 15th. Most of the melanophores are concentrated near the dorsal and ventral midlines but some occur laterally and many are deeply embedded in the myomeres (Fig. 1). Melanophores can be counted in only a few specimens in which the pigment cells are contracted. A 3.8 mm larva had about 45 melanophores above the horizontal septum and 35 below. In four specimens between 4.5 mm and 6.1 mm the counts range from about 63-100 above the septum and 44-73 below. The band enlarges and becomes more prominent in later larval stages and appears as a dusky bar in pelagic and benthic juveniles (Fig. 2). The head becomes heavily pigmented in preflexion larvae as pigment develops above the brain, on the nape, upper jaw, lower jaw, gular region, isthmus, otic region, cleithral region and snout. The deeply embedded pigment in the snout is a diagnostic feature. During the preflexion stage, groups of melanophores appear posterior to the eye on the preopercle and opercle. The pectoral fin becomes heavily pigmented during the preflexion period; the fin base develops solid pigmentation on both medial and lateral surfaces and the blade is pigmented except in the distal region. During notochord flexion pigment begins to develop on the proximal regions of the pelvic fins and the anal fin. Transition to the pelagic juvenile stage involves an expansion of the tail bar posteriorly and anteriorly and the appearance of pigment over the entire head and body. A second dusky bar appears at midbody below the 5th-11th spinous dorsal rays and a small pigment saddle forms below the 1st-3rd spinous rays. Three blotches form on the membrane of the spinous dorsal at rays 1-3, 5-7, and 9-11. A large blotch develops on the proximal region of the soft dorsal. In large pelagic juveniles the distal margin of the spinous dorsal fin develops a series of black markings.

DISTRIBUTION AND GROWTH

Adults of S. aurora have been reported from central Baja California to southern British Columbia. Distribution of the larvae collected on CalCOFI surveys indicates that the southern limits of the distribution are south of Punta Eugenia, Baja California (Fig. 3). Larvae of S. aurora occurred in 292 of 14,124 CalCOFI samples taken at 136 stations from 1949 to 1981 in a region extending from Cape Mendocino, California, to off Thetis Bank, Baja California. Seasonal fluctuations in abundance were evident with occurrences most numerous in April-June (166 occurrences in 4762 tows, 3.5%) followed by January-March (79 occurrences in 4083 tows, 1.9%), July-September (36 occurrences in 2928 tows, 1.2%), and October-December (11 occurrences in 2351 tows, 0.5%). Individuals ranged in size from 2.8-21.5 mm; 92% were 8.5 mm or less. Larval size was independent of season and distance offshore.

Examination of the otoliths of specimens taken from albacore stomachs showed an estimated age of 68 days for a 17.6 mm SL pelagic juvenile, 76 days for one 25.3 mm SL and 80 days for one 26.8 mm SL (Fig. 4). This is similar to age estimations for pelagic juveniles of S. melanostomus, a species with a similar early life history (Moser and Ahlstrom 1978). Adults of both species occupy deep slope habitats and have distinctively banded pelagic juveniles which attain a length of 35-40 mm SL and an age of 3-4 months before settling. The pigment pattern of strong dark bands alternating with almost transparent body regions is also found in pelagic juveniles of the subgenus Sebastomus and the genus Sebastolobus and may function to conceal the juveniles during their extended midwater life (Moser and Ahlstrom 1978).

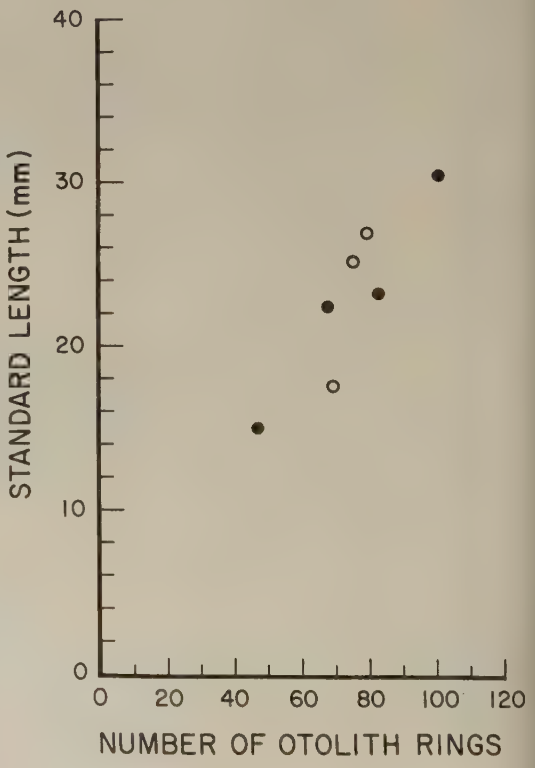

Figure 4. Estimated ages of pelagic juveniles of S. aurora and S. melanostomus based on counts of daily growth rings of sagittae.

ACKNOWLEDGMENTS

Barbara Sumida MacCall, Elizabeth Stevens and Morgan Busby helped identify and measure larvae of S. aurora from the CalCOFI collections. Henry Orr illustrated the larvae. Typing services were provided by Mary DeWitt. Pelagic juveniles were obtained from trawl samples provided by Dr. R. J. Lavenberg (Natural History Museum of Los Angeles County); Dr. R. H. Rosenblatt and W. Wakefield (Scripps Institution of Oceanography) loaned demersal juveniles. Susan Longinotti prepared and aged the otoliths. Rich Charter and Larry Zins helped with the CalCOFI data base.

REFERENCES

Brothers, E.B., C.P. Mathews, and R. Lasker. 1976. Daily growth increments in otoliths from larval and adult fishes. U.S. Fish. Wildl. Serv., Fish. Bull. 29:1-8.

Eschmeyer, W.N., E. Herald and H. Hammann. 1983. A field guide to Pacific Coast fishes of North America. Peterson Field Guide Series 28. Houghton Mifflin Co., Boston.

Kendall, A.W., Jr. 1982. A catalog of information, primarily illustrative, on larval development of Sebastes. NOAA NMFS Northwest and Alaska Fisheries Center Processed Rep. 82-01.

Laroche, W.A. and S.L. Richardson. 1980. Development and occurrence of larvae and juveniles of the rockfishes Sebastes flavidus and Sebastes melanops (Scorpaenidae) off Oregon. Fish. Bull., U.S. 77: 901-924.

__________. 1981. Development of larvae and juveniles of the rockfishes Sebastes entomelas and S. zacentrus (Family Scorpaenidae) and occurrence off Oregon, with notes on head spines of S. mystinus, S. flavidus and S. melanops. Fish. Bull., U.S. 79: 231-257.

Miller, D.J. and R.N. Lea. 1972. Guide to the coastal marine fishes of California. Calif. Dep. Fish Game Bull. 157.

Moser, H.G., E.H. Ahlstrom, and E.M. Sandknop. 1977. Guide to the identification of scorpionfish larvae in the eastern Pacific with comparative notes on species of Sebastes and Helicolenus from other oceans. NOAA Tech. Rep. NMFS Circ. 402.

Moser, H.G., and E.H. Ahlstrom. 1978. Larvae and pelagic juveniles of blackgill rockfish, Sebastes melanostomus, taken in midwater trawls off southern California. J. Fish. Res. Board Can. 35: 981-996.

Moser, H.G., and J.L. Butler. 1981. Description of reared larvae and early juveniles of the calico rockfish, Sebastes dallii. Calif. Coop. Oceanic. Fish. Invest. Rep. 22:88-95.

__________. In Press. Description of reared larvae of six species of Sebastes (S. constellatus, S. entomelas, S. ovalis, S. rubrivinctus, S. rufus, S. serranoides).

Richardson, S.L. and W.L. Laroche. 1979. Development and occurrence of larvae and juveniles of rockfishes, Sebastes crameri, Sebastes pinniger and Sebastes helvomaculatus (Family Scorpaenidae) off Oregon and Washington. Fish. Bull., U.S. 77:1-41.

Washington, B.B., H.G. Moser, W.A. Laroche, and W.J. Richards. 1984. Scorpaeniformes: Development, p. 405-428. In: Ontogeny and systematics of fishes. H.G. Moser, W.J. Richards, D.M. Cohen, M.P. Fahay, A.W. Kendall, Jr., and S.L. Richardson (eds.). Spec. Publ. No. 1. Amer. Soc. Ichthyol. Herpetol.

Table 1. Measurements (mm) of larvae and juveniles of Sebastes aurora. Specimens between dashed lines are in the notochord flexion stage and specimens between solid lines are pelagic juveniles.

Station	Body length	Snout-anus length	Head length	Snout length	Eye diameter	Body depth	Pectoral fin length	Pectoral fin base depth	Pelvic fin length	Snout-anal fin distance
5404 117.37.5	3.8	1.5	0.80	0.22	0.31	0.64	0.25	0.22		
5206 90.33	4.0	1.5	0.84	0.22	0.30	0.60	0.21	0.24		
5305 77.60	4.2	1.7	0.94	0.22	0.32	0.73	0.24	0.26		
Scripps 36B-31A	4.4	1.8	1.0	0.24	0.38	0.76	0.28	0.27		
7805 87.60	4.6	2.0	1.2	0.34	0.43	0.88	0.34	0.34		
4908 802	4.8	2.1	1.2	0.40	0.41	0.94	0.38	0.34		
6504 83.51Reg	5.0	2.1	1.2	0.34	0.40	0.90	0.35	0.32		
5104 130.3 .34	5.2	2.2	1.4	0.44	0.49	1.2	0.43	0.36		
7203 100.80	5.5	2.4	1.6	0.45	0.49	1.1	0.46	0.40		
8104 83.3 .42	5.7	2.7	1.5	0.45	0.46	1.1	0.47	0.40		
7807 77.60	5.9	2.8	1.8	0.58	0.58	1.3	0.58	0.56		
5404 127.37	6.1	2.9	1.8	0.66	0.53	1.4	0.54	0.50	0.02	3.3
5305 113.45	6.3	3.1	1.8	0.61	0.60	1.7	0.59	0.52	0.03	3.6
Scripps 36B-21A	6.5	3.0	1.9	0.59	0.59	1.4	0.54	0.53	0.03	3.6
5005-130.40	6.7	3.5	2.2	0.80	0.71	1.8	0.72	0.53	0.07	3.8
5206 80.60	6.9	3.3	2.2	0.78	0.62	1.7	0.60	0.60	0.06	4.1
5604 83.70	7.0	3.6	2.3	0.81	0.76	1.8	0.70	0.66	0.08	4.2
5206 93.50	7.4	4.0	2.5	0.89	0.75	1.8	0.80	0.75	0.12	4.5
5306 85.60	7.6	4.2	2.5	0.91	0.79	2.1	0.84	0.84	0.13	4.5
5704 100.60	7.7	4.6	3.1	1.1	0.80	2.2	1.0	0.80	0.18	5.0
5303 80.60	7.9	4.7	2.8	1.1	0.86	2.2	0.91	0.86	0.18	5.0
5605 93.70	8.0	4.7	3.0	1.1	0.85	2.2	1.0	0.83	0.24	5.0
7507 90.70	8.3	5.0	3.1	1.1	1.0	2.4	1.0	0.95	0.18	5.3
5706 73.90	8.6	5.0	3.2	1.2	0.90	2.2	1.0	0.86	0.30	5.4
7712 90.26	8.8	4.9	2.9	1.0	0.95	2.3	1.0	0.91	0.22	5.4
5304 127.40	9.4	5.3	3.2	1.2	0.92	2.7	1.1	1.0	0.34	5.6
7807 63.60	9.8	6.1	3.8	1.4	1.1	2.9	1.3	1.1	0.50	6.1
8107 70.90	10.3	6.5	4.1	1.4	1.2	3.2	1.4	1.1	0.68	6.5
LACM 9674-16	10.5	6.9	4.2	1.5	1.2	3.4	1.8	1.0	0.90	6.9
8107 76.7.70	11.3	6.9	4.3	1.6	1.3	3.8	1.8	1.2	1.0	6.9
7808 93.60	11.9	7.7	4.7	1.6	1.3	3.6	2.1	1.2	1.0	7.7
H49 123.50	12.4	7.9	4.8	1.7	1.4	4.0	1.9	1.2	1.4	7.9
LACM 302-70-9	13.5	8.8	5.5	2.0	1.4	4.3	2.6	1.2	1.5	8.8
8101 76.7.50	13.7	8.3	5.4	1.9	1.6	4.3	2.4	1.2	1.7	8.3
LACM 30202-7	14.2	8.8	5.4	1.8	1.6	4.6	2.9	1.3	1.6	8.8
7510 83.60	14.7	9.5	5.8	1.8	1.8	4.6	3.1	1.5	2.1	9.5
LACM 9677-11	15.7	9.8	6.2	2.2	1.8	4.8	3.2	1.3	2.2	9.8
LACM 9497-11	17.9	11.3	6.8	2.2	1.8	5.2	4.1	1.7	2.7	11.3
LACM 30202-7	18.6	11.3	7.1	2.5	2.0	5.6	4.1	1.6	2.9	11.5
5103 93.40	21.5	14.4	7.8	2.5	2.2	7.0	4.8	1.9	3.4	14.4
LACM 30203-3	23.1	15.2	9.6	---	2.5	6.8	5.5	1.8	4.0	15.9
LACM 9943-17	27.3	16.9	10.0	2.8	2.9	9.2	6.7	2.5	4.8	17.7
LACM 36313-1	28.3	17.9	10.0	3.2	2.8	9.2	6.9	2.5	4.6	18.6
LACM 36303-1	34.4	22.0	12.8	4.2	3.3	11.2	8.6	2.9	5.9	23.3
SIO 84-47*	38.3	23.7	13.2	3.4	4.1	11.3	10.1	3.2	6.9	25.5
SIO 70-350*	38.9	23.0	13.8	3.2	4.2	11.8	8.6	3.2	6.2	25.5

*Benthic juvenile.

Table 2. Comparative morphometry of six species of Sebastes. Data from Moser et al. 1977, Moser and Butler 1981, and this study.

Species		Snout to anus distance / Body length	Head length / Body length	Snout length / Head length	Eye diameter / Head length	Body depth / Body length	Pectoral fin length / Body length	Pectoral fin base depth / Body length	Pelvic fin length / Body length
S. aurora	A	43.6 ± 3.46(38-49)	25.9 ± 3.38(21-30)	29.5 ± 3.86(23-37)	33.7 ± 2.87(29-39)	19.9 ± 3.20(15-27)	7.6 ± 1.34(5-10)	7.0 ± 0.96(6- 9)	<1
	B	56.3 4.69(48-62)	35.2 2.66(32-40)	36.2 1.40(35-39)	30.0 2.36(26-33)	27.0 1.70(25-29)	11.4 1.26(9-13)	9.9 0.99(8-11)	1.9 ± 0.74(1- 3)
	C	61.6 3.81(56-66)	37.8 2.71(33-40)	35.6 1.60(34-38)	29.5 1.51(28-33)	30.5 2.39(26-34)	14.5 2.45(11-18)	10.5 0.53(10-11)	7.0 2.78(3-11)
	D	63.4 1.98(61-67)	38.2 1.96(35-41)	32.9 2.30(28-36)	28.0 1.91(25-31)	31.2 1.60(29-34)	21.9 2.35(18-25)	8.8 0.58(8-10)	14.8 2.38(11-18)
S. dallii	A	42.4±0.52(42-43)	22.6±1.06(21-24)	25.6±3.02(19-29)	38.0±1.85(35-41)	17.6±1.85(15-20)	5.6±0.52(5- 6)	5.9±1.36(3- 7)	—
	B	45.7 2.07(43-48)	26.5 1.38(25-29)	28.7 1.86(27-32)	37.8 1.33(36-40)	20.7 2.07(18-23)	8.0 0.63(7- 9)	8.3 0.82(7- 9)	1.26±0.73(0.3-2)
	C	50.8 3.27(48-56)	30.6 1.95(28-33)	30.4 0.89(29-31)	36.8 1.92(34-39)	23.8 2.68(22-28)	11.0 2.45(9-14)	10.2 0.84(9-11)	4.0 2.83(2- 9)
	D	57.0 1.41(56-58)	29.5 0.71(29-30)	33.0 0.00(33)	33.5 0.71(33-34)	25.0 0.00(25)	23.5 0.71(23-24)	8.0 0.00(8)	15.5 0.71(15-16)
S. jordani	A	36.5 0.84(36-38)	22.3 1.51(21-25)	26.8 3.43(23-31)	37.7 0.82(36-38)	17.0 1.26(16-19)	6.7 0.52(6- 7)	6.5 0.55(6- 7)	—
	B	42.4 1.67(41-45)	28.4 2.19(26-30)	35.5 1.29(34-37)	32.2 2.50(29-35)	21.0 1.00(20-22)	8.4 1.14(7-10)	7.8 0.45(7- 8)	1.4 0.55(1- 2)
	C	51.0 2.86(46-54)	32.3 1.44(31-36)	34.4 1.98(31-39)	29.3 2.10(27-34)	23.8 1.19(22-26)	16.8 3.25(11-20)	7.9 1.00(7-10)	9.0 3.62(3-13)
	D	53.3 1.03(52-55)	31.2 1.94(28-33)	34.0 2.83(30-38)	26.5 1.52(24-28)	22.2 0.84(21-23)	20.5 1.05(19-22)	7.0 0.00(7)	13.5 1.22(12-15)
S. levis	A	39.6 2.30(37-44)	24.7 1.60(23-28)	30.7 2.63(27-35)	33.1 2.67(29-36)	21.7 1.11(20-23)	17.4 5.29(11-24)	10.9 1.57(8-13)	—
	B	48.9 3.44(45-56)	30.5 1.85(28-33)	34.8 0.87(34-36)	32.5 1.77(30-35)	28.5 3.51(24-35)	34.9 6.96(24-46)	12.9 0.64(12-14)	6.1 3.27(2-12)
	C	59.2 2.87(57-63)	35.0 2.00(34-38)	30.2 2.22(28-33)	30.5 1.73(28-32)	34.0 1.41(33-36)	45.0 3.74(41-50)	11.2 0.96(10-12)	21.0 4.76(16-26)
	D	63.0 0.82(62-64)	33.8 0.96(33-35)	30.5 2.38(28-33)	27.0 3.37(25-32)	35.0 1.41(34-37)	40.8 7.09(32-47)	10.2 0.96(9-11)	24.2 2.87(22-28)
S. macdonaldi	A	42.4 3.53(36-47)	27.6 2.25(24-31)	30.6 4.16(25-36)	34.6 2.34(31-37)	23.1 3.99(13-27)	8.4 1.21(6-10)	—	1.8 0.84(1- 3)
	B	51.8 3.56(48-56)	35.6 1.52(34-38)	34.0 4.00(30-38)	32.0 1.41(31-34)	31.6 2.07(30-35)	13.0 1.22(12-15)	—	5.8 2.39(3- 9)
	C	60.3 3.06(55-64)	37.5 1.84(34-41)	32.9 3.00(29-37)	33.0 1.33(31-35)	34.4 1.17(33-36)	19.3 3.65(15-26)	—	14.3 3.77(10-21)
	D	64.2 2.44(61-68)	35.1 2.37(32-38)	27.9 2.09(25-32)	30.7 2.74(26-34)	31.4 1.59(30-34)	30.4 1.74(28-34)	—	21.9 1.36(21-25)
S. paucispinis	A	41.0 2.74(37-44)	26.8 2.28(24-29)	27.4 3.21(24-32)	32.8 3.77(29-37)	19.6 1.67(17-21)	16.4 4.56(11-21)	9.0 0.71(8-10)	5.3 4.93(2-11)
	B	44.8 3.70(40-49)	29.6 1.95(27-32)	30.6 1.82(29-33)	30.2 1.64(29-33)	23.0 1.41(21-24)	27.2 2.49(25-31)	9.0 0.71(8-10)	13.6 9.28(9-26)
	C	57.3 3.82(51-61)	37.1 1.07(36-39)	32.2 0.98(31-33)	31.3 1.70(28-33)	29.6 0.98(28-31)	35.7 1.25(34-37)	7.6 0.53(7- 8)	35.1 2.79(31-39)
	D	62.3 2.73(60-66)	36.2 1.72(33-38)	30.5 2.95(26-33)	27.8 1.72(26-30)	27.3 0.52(27-28)	28.2 3.40(25-34)	6.0 0.89(5- 7)	25.2 2.71(22-30)

A = preflexion larvae; B = larvae undergoing notochord flexion; C = postflexion larvae; D = pelagic juveniles

Table 3. Sequence of Development of Head Spines of Sebastes aurora.

Spine	Order of appearance	Size (mm) (body length) at appearance	Size (mm) (body length) when lost
pterotic	1	5.0	---
2nd anterior preopercular	2	5.3	18.6
3rd posterior preopercular	2	5.3	---
4th anterior preopercular	3	5.6	18.6
2nd posterior preopercular	3	5.6	---
parietal	3	5.6	---
postocular	3	5.6	---
4th posterior preopercular	4	6.1	---
5th posterior preopercular	5	8.0	---
lower posttemporal	5	8.0	---
1st upper infraorbital	5	8.0	27.3
1st lower infraorbital	5	8.0	---
upper opercular	5	8.0	---
nuchal	6	8.9	---
1st posterior preopercular	7	10.5	---
2nd lower infraorbital	7	10.5	---
supracleithrum	7	10.5	---
preocular	7	10.5	---
4th upper infraorbital	8	12.7	27.3
nasal	8	12.7	---
upper posttemporal	9	15.2	---
interopercular	9	15.2	---
lower opercular	10	18.6	---
supraocular	10	18.6	---
tympanic	10	18.6	---
coronal	10	18.6	---
cleithral	11	34.4	---

Table 4. Meristics of Cleared and Stained Specimens of Sebastes aurora.

Length (mm)	Principal caudal fin rays		Procurrent caudal fin rays		Branchiostegal rays		Pectoral fin rays		Gill rakers (right arch)		Anal fin rays	Dorsal fin rays	Pelvic fin rays		Vertebrae
	superior	inferior	superior	inferior	left	right	left	right	upper limb	lower limb			left	right	
5.3	1	1	--	--	1	1	--	--	--	--	--	--	--	--	1
5.6	3	3	--	--	4	4	2	2	--	5	--	--	--	--	2
6.1	4	4	--	--	4	4	5	5	--	5	--	--	--	--	4
6.2	5	5	--	--	5	4	6	6	--	6	--	--	--	--	7
6.6	6	6	--	--	6	6	7	7	--	7	--	--	--	--	14
7.2	7	7	--	--	7	7	12	12	--	7	--	--	--	--	22
7.5	7	7	--	--	6	6	9	9	--	7	--	--	--	--	21
8.0	8	7	1	2	7	7	14	14	2	12	I,4	I, 9	I,2	I,2	24
8.3	"	"	4	4	"	"	16	17	3	14	III,5	XII,12	I,4	I,4	26
8.9	"	"	3	3	"	"	16	16	3	12	III,5	XII,13	I,4	I,4	25
9.4	"	"	4	4	"	"	17	17	3	12	III,6	XIII,13	I,4	I,4	26
10.5	"	"	7	7	"	"	17	17	5	15	III,6	XIII,13	I,5	I,5	"
11.3	"	"	7	7	"	"	18	18	4	14	III,7	XIII,13	"	"	"
12.7	"	"	8	8	"	"	18	18	5	14	III,6	XIII,13	"	"	"
13.7	"	"	9	9	"	"	17	18	7	17	"	XIII,12	"	"	"
14.2*	"	"	10	10	"	"	17	17	7	17	"	XIII,13	"	"	"
15.2*	"	"	10	10	"	"	17	17	6	16	"	XIII,13	"	"	"
18.6*	"	"	10	11	"	"	17	17	8	18	"	XIII,13	"	"	"
21.5*	"	"	10	10	"	"	18	18	8	18	"	XIII,13	"	"	"
27.3*	"	"	10	10	"	"	18	18	7	17	"	XIII,13	"	"	"
28.3*	"	"	10	10	"	"	17	17	8	17	"	XIII,13	"	"	"
34.4*	"	"	10	10	"	"	18	18	9	18	"	XIII,12	"	"	"
38.9**	"	"	10	9	"	"	18	18	7	18	"	XIII,13	"	"	"

*Pelagic juvenile.
**Demersal juvenile.

8562

Staging Anchovy Eggs

I. GEOFFREY MOSER and ELBERT H. AHLSTROM
outhwest Fisheries Center,
ational Marine Fisheries Service, NOAA,
O. Box 271, La Jolla, CA 92038

BSTRACT

e developmental period of northern anchovy eggs is divided into eleven stages. ese stages are defined by structural criteria chosen from the sequence of mor- ological changes which occur during embryogenesis. Samples of eggs, preserved 3% formaldehyde solution, are examined under a dissecting microscope using t transmitted light. In Stage I eggs, cell division has not yet begun and the oplasm appears as a cap at one pole of the elliptical yolk mass. Cell division urs during Stage II to produce a blastodisc. At Stage III the size of the in- idual blastomeres is greatly reduced and the blastodisc has the appearance of ue. Stages IV, V, and VI are defined by the fraction of the yolk mass covered the blastoderm. The proportion of tail length to head length defines Stages and VIII, and the proportion of tail length to yolk mass length defines Stages X, and XI. The procedure for staging eggs with disintegrated embryos is cribed.

INTRODUCTION

The eleven egg stages used since 1980 in egg production biomass estimates are modified from stages established by Ahlstrom (1943) for the Pacific sardine, *Sardinops sagax*. Northern anchovy eggs differ markedly from those of the Pacific sardine in size, shape, and in the absence of an oil globule. The strongly elliptical eggs of *Engraulis mordax* measure 1.23-1.55 mm at the major axis and 0.65-0.82 mm at the minor axis (Bolin 1936), whereas developing sardine eggs range from 1.35 to 2.05 mm with a mean of 1.70 mm (Ahlstrom 1943). The sardine embryo, however, is only slightly larger than the embryo of the anchovy since the wide perivitelline space of the sardine accounts for almost half the total egg diameter. Also, the rates of development of major embryonic features and organ systems are comparable in the two species.

METHODS

Eggs are sorted from the plankton samples as described by Stauffer and Picquelle (1985) and preserved in 3% buffered Formalin in 2-dr vials. For staging, each sample is placed in a watch glass with water and examined under a dissecting microscope, using the microscope mirror to produce a soft transmitted light. A direct light source does not allow one to distinguish fine structures of the embryos.

Most samples contain several groups of eggs representing widely separated stages from several days' spawnings. An initial cursory examination allows one to sort most of the eggs into these several subgroups, which can then be assigned to stages. The stages are based on structural criteria chosen from the sequence of morphological changes which occur during embryogenesis. These are described below and illustrated in Figures 1 and 2.

EGG STAGES

Stage I

Cell division has not yet begun. In intact eggs the cytoplasm of the single cell appears as a clear hemisphere at one pole, easily differentiated from the yolk mass which is divided into granules. The cytoplasm may be displaced to other locations around the periphery of the yolk mass, but there is usually some accumulation at one pole, which allows the stage to be identified.

Stage II

This begins with the division of the single cell into two cells or blastomeres. The division is first noticeable when a furrow develops in the middle of the cytoplasmic cap. Small bubble-like structures (probably artifacts) are often visible along the furrow and help identify it. The next cleavage plane is at right angles to the first, and subsequent synchronous divisions in both meridional and latitudinal planes produce a hemispherical mound of cells, termed the blastodisc. After the 5th or 6th division, the blastodisc has a berry-like appearance, the so-called "mulberry stage," and with subsequent divisions the blastomeres become increasingly smaller and more difficult to distinguish individually. During a certain phase of the early divisions the blastomeres are about the same size as the yolk granules. If the blastodisc and yolk mass become disrupted during collection or preservation, the blastomeres may become distributed among the yolk granules. They may be distinguished from one another since they have different refractive indices and the blastomeres appear darker when viewed with transmitted light.

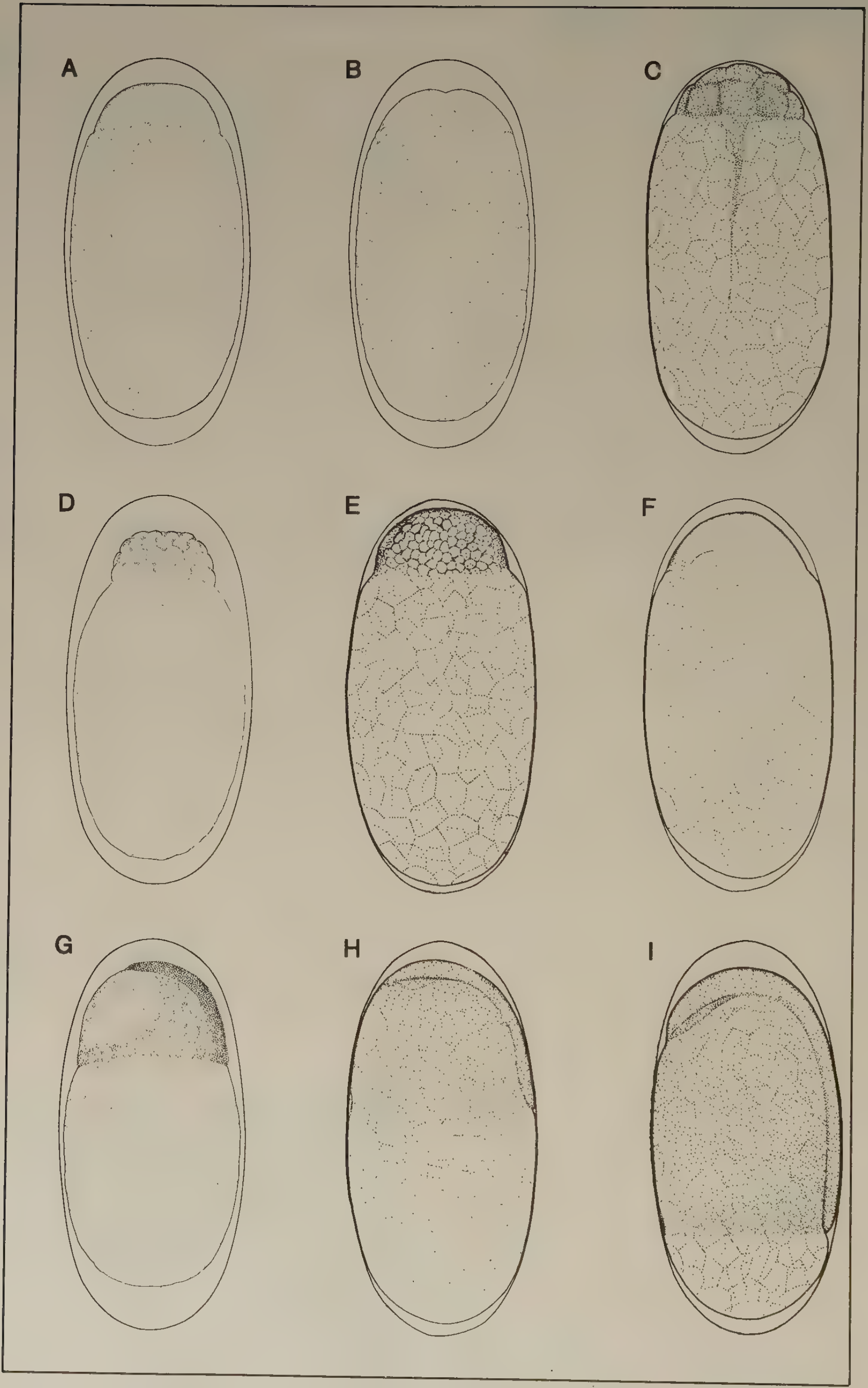

Figure 1.—Stages of northern anchovy eggs. A. Stage I; B. Stage II (2 cells); C. Stage II (16 cells); D. Stage II ("Mulberry"); E. Stage II (late); F. Stage III (mid); G. Stage III (late); H. Stage IV (mid); I. Stage V (mid). Original illustrations of A, B, D, G, by G. Mattson; C, E, F, H, I from Bolin (1936).

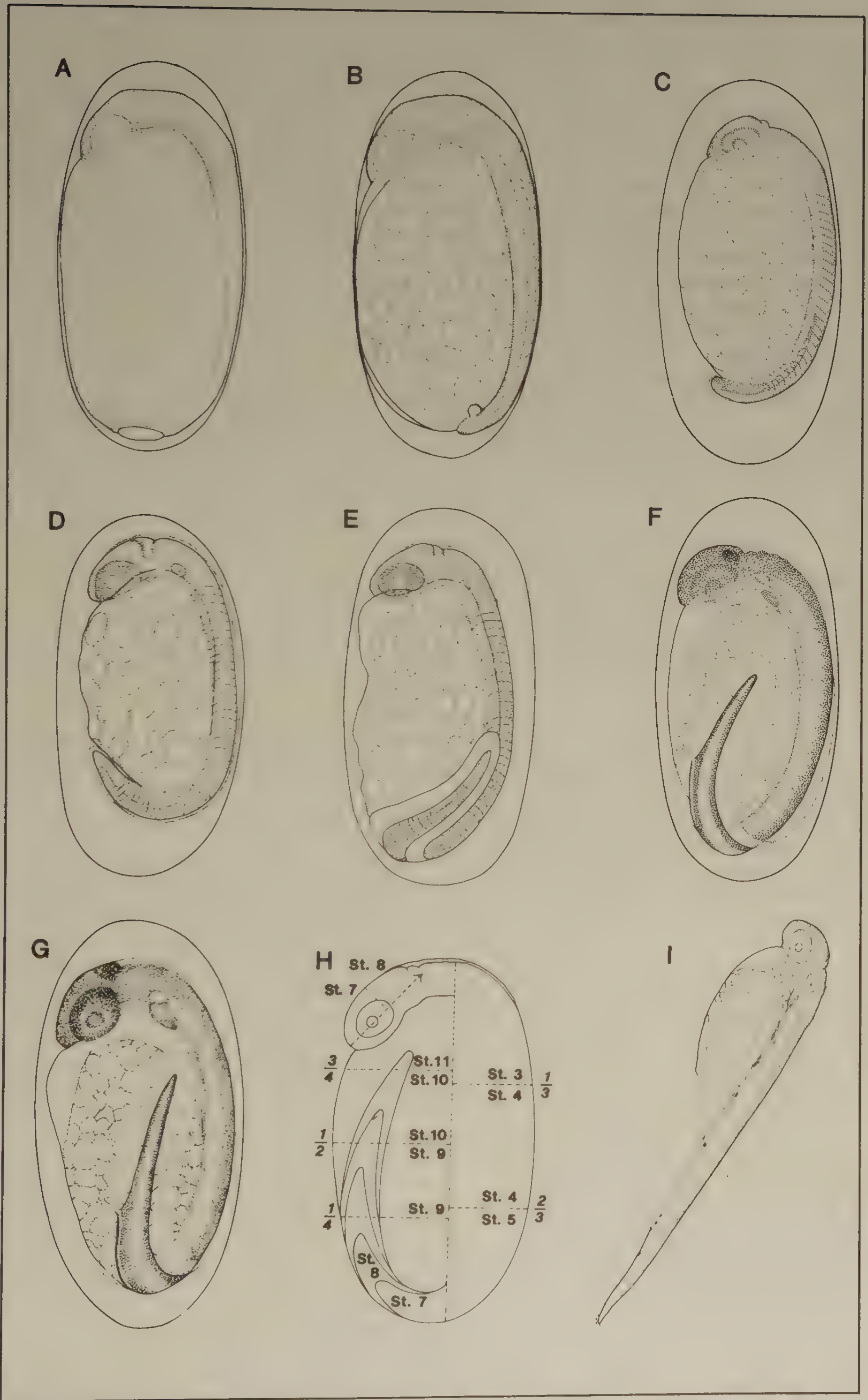

Figure 2.—Stages of northern anchovy eggs. A. Stage V (late); B. Stage VI; C. Stage VII; D. Stage VIII; E. Stage IX; F. Stage X; G. Stage XI; H. Diagrammatic egg showing relationship of epiboly and tail length to stage; right side indicates fraction of the yolk mass covered by the blastoderm in Stages III, IV, and V; left side shows tail length/head length proportions which define Stages VII and VIII and tail length/yolk mass length proportions which define Stages IX, X, and XI; I. Newly hatched anchovy. Original illustrations of A, C, and F by G. Mattson; B from Bolin (1936); original illustrations of D and E by H. Orr; original illustration of G by G. Moser; H prepared by B. Sumida; I from Kramer and Ahlstrom (1968).

Stage III

Ahlstrom (1943) defined this stage in sardine eggs as beginning with the appearance of the segmentation cavity. The segmentation cavity of teleost eggs is the space formed between the blastodisc and the yolk mass during late cleavage. In most anchovy eggs in our collections the blastodisc is shrunken and somewhat cup-shaped and consequently the segmentation cavity, which is a delicate structure, is obliterated. We have found it preferable to define the beginning of Stage III on the basis of the appearance of the blastoderm, i.e., when it has the appearance of tissue rather than of a collection of individual cells. This stage marks the beginning of gastrulation. The margin of the blastodisc becomes slightly thickened and is termed the germ ring. At one region of the germ ring the thickening extends inward to form the embryonic shield, which defines the future axis of the embryo. Gastrulation proceeds by further proliferation and downward movement of cells in the region of the germ ring by a process known as epiboly. Simultaneously, proliferation and inward migration (emboly) of cells from the margin of the embryonic shield produce the organ-forming cell layers of the primordial embryo. At the end of Stage III the germ ring is one-third down the yolk mass and the bilateral nature of the primordial embryo is apparent.

Stage IV

At the beginning of this stage the germ ring has enclosed one-third of the yolk mass and the embryo is beginning to form along the median region of the embryonic shield. At the end of this stage, defined by the germ ring enveloping two-thirds of the yolk, the head region of the embryo is becoming apparent.

Stage V

This stage begins with the germ ring two-thirds down the yolk and ends with the closure of the blastopore and the complete enclosure of the yolk by the cellular sheath of the embryo. The stage is characterized by rapid differentiation resulting in the formation of several somites in the midregion of the embryonic axis, development of the notochord which can be seen from a dorsal viewpoint, and differentiation of the optic vesicles from the brain.

Stage VI

This stage begins with the closure of the blastopore and ends when the tail starts to separate from the yolk mass. The embryonic sheath of cells is extremely thin and, in some samples, it may be difficult to determine the point of blastopore closure. In these cases the event can be estimated from the position of the caudal terminus of the embryonic axis, since it grows toward the pole with the edge of the cellular sheath. Initially the caudal region lies flat against the polar region of the yolk, then gradually thickens and becomes more rounded at the tip until it is clearly separate from the yolk. During this stage the somites are apparent along the entire body axis (except at the caudal portion), the lens primordium appears in the eye, and the regions of the brain begin to differentiate.

Stage VII

At the beginning of this stage the tip of the tail free from the yolk is broadly rounded, then begins to narrow as it elongates. The notochord extends almost to the tip and the finfold is just becoming visible. At the end of this stage the length of the free tail is one-half the length of the head. For this purpose, head length is considered the distance from the tip of the snout to the back of the cerebellum (see Fig. 2H). Relative tail length is the criterion for each remaining stage.

Stage VIII

This stage begins when the free tail length is greater than one-half the head length and ends when tail length equals head length. The tail becomes pointed during this stage and begins to bend away from the axis of the body, to the right or left side. The curvature of the tail generally increases with development, but is subject to individual variability (Fig. 2). Judgement is required in compensating for curvature in estimating relative tail length; however, accuracy and precision increase rapidly with practice.

Stage IX

This stage begins with the tail extending one-quarter the length of the yolk sac and ends when it reaches one-half the yolk sac length. The gut is now apparent along the ventral surface of the tail, and its terminal section passes through the finfold which is now considerably wider than in the previous stage. The pectoral fin buds appear as lateral thickenings as do the otic vesicles.

Stage X

This stage starts when the tail is one-half the length of the yolk sac and ends when it reaches three-quarters of the yolk sac length.

Stage XI

This is the final stage before hatching and is defined by a tail length greater than three-quarters of the length of the yolk sac.

Disintegrated (Dis) Eggs

Eggs with embryos in various states of disintegration are found in many samples, and some samples contain a large proportion of disintegrated eggs. Despite some preliminary field and laboratory experiments, we are not able to determine whether disintegration is caused by net damage, fixation, mortality prior to capture, or some combination of these. The sampling design requires that all eggs be assigned a stage regardless of condition. Empty egg shells and eggs which have no identifiable morphological features are assigned the "Dis" (disintegrated) category. These are later assigned a stage, by pro rating, during the aging procedure (see Lo 1985). With detailed examination, eggs containing damaged or shrunken embryos can be staged. Usually they are part of a mode which is present in the sample and thus can be staged by comparison with the groups of intact eggs. In the early-stage disintegrated eggs, the blastomeres and yolk granules are intermingled but can be distinguished since the former appear darker in transmitted light. In eggs beyond Stage III, the embryos are rarely disassociated but may be distorted or shrunken and oriented abnormally because of the disintegration of the yolk mass. Despite their condition, these embryos have the morphological features described for intact embryos and can be staged, although this requires more attention to morphological details; particularly useful are careful observations on the degree of differentiation of myomores, median finfold, and head structures such as eyes, brain lobes, and otic vesicles.

LITERATURE CITED

AHLSTROM, E. H.

1943. Studies on the Pacific pilchard or sardine (*Sardinops caerulea*). 4. Influence of temperature on the rate of development of pilchard eggs in nature. U.S. Fish. Wildl. Serv., Spec. Sci. Rep. 23, 26 p.

BOLIN, R. L.

1936. Embryonic and early larval stages of the California anchovy *Engraulis mordax* Girard. Calif. Fish Game 22(4):314-321.

KRAMER, D., and E. H. AHLSTROM.

1968. Distributional atlas of fish larvae in the California Current region: Northern Anchovy, *Engraulis mordax* Girard, 1951 through 1965. Calif. Coop. Oceanic Fish. Invest. Atlas 9, 269 p.

LO, N C. H.

1985. A model for temperature-dependent northern anchovy egg development and an automated procedure for the assignment of age to staged eggs. *In* R. Lasker (editor), An egg production method for estimating spawning biomass of pelagic fish: Application to the northern anchovy, *Engraulis mordax*, p. 43-50. U.S. Dep. Commer., NOAA Tech. Rep. NMFS 36.

STAUFFER, G., and S. PICQUELLE.

1985. Procedures for sorting, staging, and ageing eggs. *In* R. Lasker (editor), An egg production method for estimating spawning biomass of pelagic fish: Application to the northern anchovy, *Engraulis mordax*, p. 33-35. U.S. Dep. Commer., NOAA Tech. Rep. NMFS 36.

8563

Prevalence, Intensity, Longevity, and Persistence of *Anisakis* sp. Larvae and *Lacistorhynchus tenuis* Metacestodes in San Francisco Striped Bass

MIKE MOSER, JUDY A. SAKANARI, CAROL A. REILLY,[1] and
JEANNETTE WHIPPLE[2]

ABSTRACT

Thirteen hundred and seventy-three striped bass, *Morone saxatilis*, were collected from the San Francisco Bay-Delta area to correlate host diet with parasitic infections and to determine the prevalence, intensity, longevity, and persistence of larval *Anisakis* sp. nematodes and the metacestode *Lacistorhynchus tenuis*. There is an increase in the prevalence and intensity of *Anisakis* sp. and in the intensity of *L. tenuis* with increase of age of the host. These increases are probably related to the diet and the persistence of the parasites. The infections of both species are overdispersed. San Francisco Bay striped bass are an incompatible host for both species of parasites. Degenerated *Anisakis* sp. will remain in the host for at least 8 months and *L. tenuis* metacestodes for 22 months. The occurrence of several other species of parasites and a tumor are also reported.

INTRODUCTION

Striped bass, *Morone saxatilis*, is a popular sportfish in the San Francisco Bay, CA, area. Anglers have often reported the presence of parasites in the mesenteries and muscle of striped bass and questioned the public health aspects of the parasitic infections. The purpose of this study was to determine the prevalence (no. hosts infected/no. hosts examined), intensity (total no. parasites/no. infected hosts), longevity (time parasites remain alive), and persistence (time degenerated parasites are detectable) of the two most commonly seen parasites: the metacestode *Lacistorhynchus tenuis* (Cestoda) and the larval nematode *Anisakis* sp. (probably *A. simplex*).

MATERIALS AND METHODS

Collection

Thirteen hundred and seventy-three striped bass were collected from the San Francisco Bay-Delta area between June 1979 and December 1983 by hook and line, gill net, and otter trawl. Fish were frozen or Formalin-fixed and autopsied for parasites and stomach content analyses at Long Marine Laboratory, University of California, Santa Cruz.

Aging

The age of the fish was determined by scale ring counts by the California Department of Fish and Game and the use of growth curves.

Diet Analysis

The stomach contents of the fish were analyzed to determine possible correlations between diet and parasite infections. Stomach contents of 831 striped bass collected between January and September 1981 from San Pablo Bay and Suisun Slough were examined for possible intermediate hosts. The Index of Relative Importance (IRI) of food items was determined by methods suggested by Cailliet (1976). The young-of-the-year (YOY) and most of the 1-yr-olds had similar diets, hence were combined for analysis. The age groups for diet analysis were: YOY and 1-yr-old (10 to 230 mm SL); subadult females and adult males (2 to 3 yr); and adults (4+ yr).

Statistical Analysis

The coefficient of dispersion (overdispersed distribution) was determined to indicate possible clumping in parasite distributions, hence the possible need for nonparametric analysis (Sokal and Rohlf 1969). Within each age class seasonality did not significantly change the prevalance or intensity of the parasitic infections. Therefore, all seasons were combined within each age class (ANOVA, regression analysis).

Serial Infections

Serial infections were performed to determine whether nematode larvae can be transferred from fish to fish. The striped bass used in both infection experiments were YOY hatchery fish provided by the California Department of Fish and Game, Elk Grove, CA. The third stage larval *Anisakis* sp. used were from bocaccio, *Sebastes paucispinis*. The fish were force-fed (Wootten and Smith 1975) with washed larvae (Tanaka and Torisu 1978). Fifty larvae were fed to each of six striped bass. As a control, four YOY yellowtail rockfish, *Sebastes flavidus*, were infected in a similar manner.

---

[1] Coastal Marine Studies, University of California, Santa Cruz, Santa Cruz, CA 5064.

[2] Physiological Ecology Investigations, Southwest Fisheries Center Tiburon Laboratory, National Marine Fisheries Service, NOAA, Tiburon, CA 94920.

Longevity and Persistence

Striped bass collected from the field were observed to have degenerated larval nematodes in their mesenteries and tissues. The purposes of this experiment were to determine how long the larval *Anisakis* sp. remain alive in striped bass, therefore potentially harmful to humans, and to determine the persistence of dead larvae in the mesenteries and muscle. The third stage *Anisakis* sp. larvae used were prepared as above but were from sablefish, *Anoplopoma fimbria*. To insure that all fish were infected with equal numbers of larvae, 25 larvae were inserted into the coelomic cavity through a small cut on the sides of 178 striped bass. This wound was sealed with a nontoxic biological glue, Histoacryl (Tri-Hawk, Los Angeles, CA). Previous tests showed that striped bass reacted similarly to larvae infected by this technique, to those force-fed, and to those seen in field fish. The hosts were periodically autopsied during a 33-wk period.

RESULTS

Diet Analysis

The fullness of the stomachs and the percent IRI for the dominant food item or items are given for each age class. No stomachs contained larvae or metacestodes (Fig. 1).

Anisakis sp.

Host reaction.—The larval *Anisakis* from field fish were found on the mesenteries and internal organs. Rarely were they found in the muscle tissue. Most larvae were dead or degenerating with dark brown cuticles. The larvae were often seen as solid, round masses of fibrous tissue. When several larvae were in close proximity in the mesenteries, they were often encapsulated to form a fibrous "raft." In field fish with high intensity infections, numerous degenerated larvae were found embedded in the posterior end of the stomach (Fig. 2).

Prevalance and intensity.—The prevalence and intensity of larval nematode infections in striped bass begin to increase at 4 yr and continue to increase throughout the life of the host. The mean to variance ratios (year classes 3 to 8+ are: 1.3, 14.2, 58.8, 33.7, 49.9, 39.5, respectively) show the infections to be increasingly overdispersed with time (Fig. 3).

Serial infection.—Autopsies showed that after 5 wk, two of six striped bass were infected by one and four larvae, respectively.

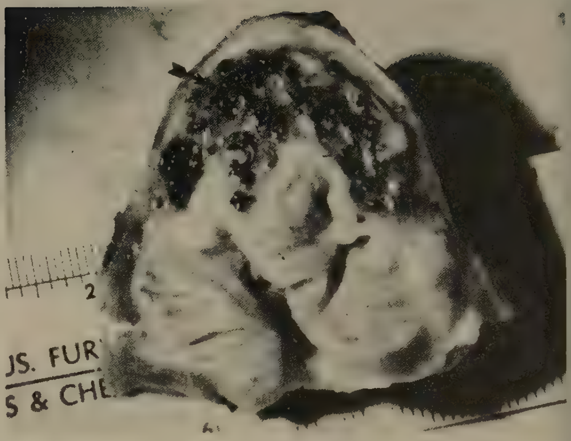

Figure 2.—Cross section of posterior end of stomach with embedded larval nematodes.

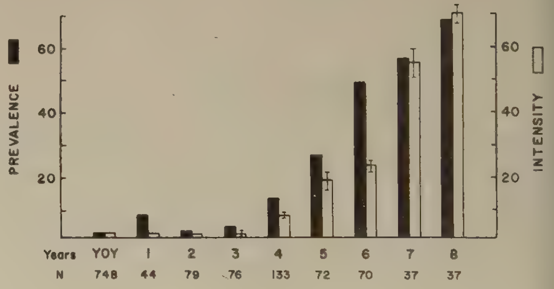

Figure 3.—Prevalence and intensity of larval nematodes compared with age of host. Bar = standard error.

Although the larvae from the striped bass responded weakly to tactile stimuli, the cuticle had darkened, resembling the dead larvae recovered from field-captured striped bass. In contrast, three of the four rockfish were infected with an average of four larvae. The larvae from the rockfish were more active, and the cuticle was flesh colored, similar to larvae from field-collected *Sebastes paucispinis* and other fish hosts.

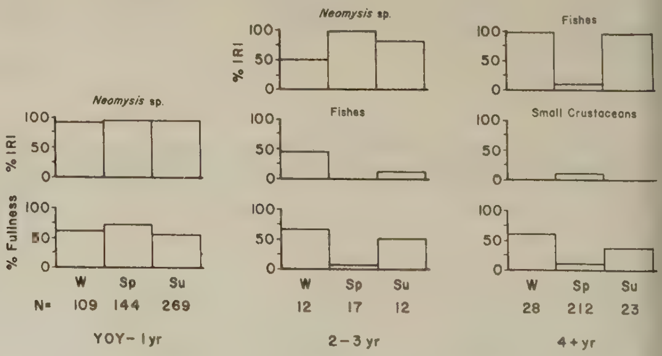

Figure 1.—Stomach content analysis of striped bass in the three major age groups in winter (W), spring (Sp), and summer (Su).

Longevity and persistence.—At the end of 2 wk most larvae had been encapsulated into a fibrous "raft." In the following 31 wk, in addition to the "raft," one to five larvae were recovered in the coelom or attached to the mesenteries. These larvae usually responded weakly to tactile stimuli, but became progressively darker and weaker with time (Fig. 4).

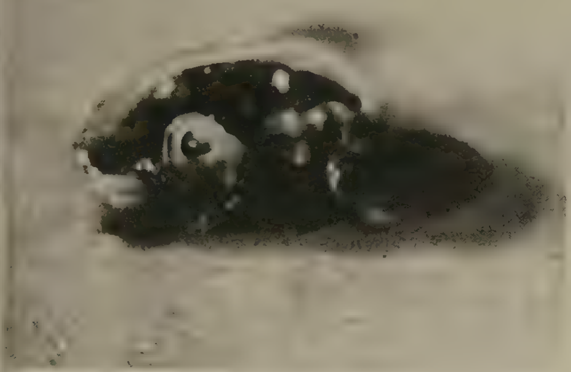

Figure 4.—*Anisakis* sp. larvae encapsulated in fibrous "raft."

Lacistorhynchus tenuis

Host reaction.—Moser, Sakanari, Wellings, and Lindstrom (1984) described the inflammatory response of the striped bass to these "rafts." The metacestodes from field fish appeared degenerated. The outer surface of the blastocyst was brown and the metacestode was a hardened mass. Often, the metacestodes, similar to the nematode larvae, were encapsulated into fibrous "rafts."

Prevalance and intensity.—During the first year the prevalence of larval cestode infections reached 81.6% and remained approximately at this level throughout the year. However, the mean intensity of infection slowly increases with the age of the host. The mean to variance ratios (age classes YOY to 8+ are: 14.4, 23.2, 38.9, 9.2, 48.6, 36.7, 59.3, 51.2, 73.0, respectively) indicate the infections were increasingly overdispersed with time (Fig. 5).

Persistence.—Four field fish kept in the laboratory for 22 mo still retained their dead metacestodes and "rafts."

Other Parasites and a Tumor

Occasionally other helminth parasites were encountered during autopsies. However, because of the overall goal of this study and the method of preservation of field fish, no attempt was made to quantify these helminths. Parasites reported from the San Francisco Bay-Delta include: Acanthocephala—*Southwellina* (D. Woodbury[3]); Cestoda—Tetraphyllidae larvae, in mesenteries, (this study); Digenea—*Stephanostomum tenue* (D. Woodbury footnote 3), *Lepocreadium californianum* (Edwards and Nahhas 1968); Monogenea—*Cleidodiscus pricei* (Hensley and Nahhas 1975); Nematoda—*Thynnascaris brachyurum* (as *Contracaecum b.*, Hensley and Nahhas 1975), *Spiroxys* sp. larva (Hensley and Nahhas 1975), and *Phocanema* sp. larvae, in mesenteries, (this study); a tumor, in coelom, (this study, Fig. 6, National Museum of Natural History-Registry of Tumors in Lower Animals (NMNH-RTLA) #3173).

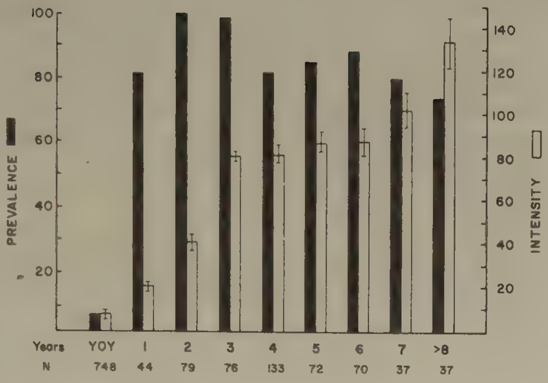

Figure 5.—Prevalence and intensity of metacestodes compared with age of host. Bar = standard error.

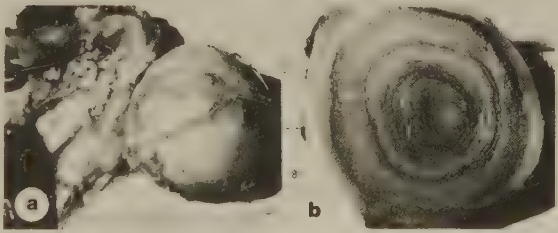

Figure 6.—Tumor a) attached to mesenteries, b) cross section.

DISCUSSION

The food habits of San Francisco Bay-Delta striped bass have been reported by Turner and Kelley (1966), Thomas (1967), Orsi (1971), Moriguchi (1973), Moyle (1976), and Orsi and Knutson (1979). The present study and the above reports show that YOY consume primarily shrimp (*Neomysis* sp. and *Crangon* sp.), amphipods (*Corophium* sp.), and copepods. By the end of the first year the fish begin to switch from feeding on invertebrates to eating fish (striped bass, shad, salmon, flatfish, herring, perch, bait). This trend continues in the subadults. Although adults are primarily piscivorous, striped bass continue to eat some invertebrates, such as crabs. The adults, and perhaps the subadults, reduce their feeding in the spring and early summer during the spawning season.

The life cycle of *Anisakis* sp. usually includes a marine crustacean as the first intermediate host, a fish or squid as the second host, and a marine mammal as the definitive host. The larva of *Anisakis* sp. is well known as a potential hazard to human health if consumed in raw or improperly prepared seafood (Moser, Love, and Sakanari 1984). San Francisco Bay striped bass infected with larval *Anisakis* do not appear to be a major health hazard. Rarely were these larvae found in the muscle tissue. In addition, most of the larvae degenerate in the body cavity after a few weeks. The results of this study suggest that some degenerating larvae and the fibrous "rafts" can persist in striped bass for at least 33 wk. This slow turnover rate of larvae probably contributes to the increase in intensity of infection with time.

---

[3] D. Woodbury, Seasonal Aide, California Department of Fish and Game, 203 Tall Trees Drive, Vallejo, CA 94589, pers. commun. March 1983.

Wootten and Smith (1975) showed that trout can be serially infected with *Anisakis* sp. larvae from herring. Many of the fish consumed by striped bass are infected by *Anisakis* sp. larvae (Love and Moser 1983). The serial infection experiments with *Anisakis* sp. larvae may explain the increase in prevalence and intensity as striped bass become more piscivorous at 4 yr. Although numerous fibrous "rafts" were found in the mesenteries and next to the peritoneum of field fish, they did not form open lesions as described for the metacestodes of *L. tenuis* in San Francisco Bay striped bass (Moser, Sakanari, Wellings, and Lindstrom 1984).

The life cycle of *Lacistorhynchus tenuis*, although not completely described, most probably includes the adult in an elasmobranch, such as the leopard shark, *Triakis semifasciata*, common to San Francisco Bay, the procercoid in a crustacean, and the metacestode in fish. *Lacistorhynchus tenuis* metacestodes have been reported worldwide from more than 60 species of hosts (Moser 1983), including striped bass from the east coast and other San Francisco Bay fish, with no apparent harm to the host. However, Moser, Sakanari, Wellings, and Lindstrom (1984) have shown that these metacestodes are pathological to striped bass found in the San Francisco Bay-Delta area.

The sharp rise in prevalence of *L. tenuis* metacestodes in the 1-yr-olds may be related to the movement of this age class from the Delta area into San Francisco Bay where they are more likely to encounter the infected intermediate hosts. The continued increase in the intensity of metacestodes through time may reflect both the acquisition of new metacestodes and their persistence in the host. Preliminary studies (Sakanari, Moser) suggest that metacestodes of *L. tenuis* can be transfered serially from white croaker, *Genyonemus lineatus*, to striped bass. These studies suggest that the prevalence of metacestodes from the YOY to the 1 yr class may also be related to increased piscivory. The increased clumped distribution of parasites with the age of the host may indicate striped bass vary in their susceptibility to these parasites. Some hosts may eliminate the parasites before they can become embedded in the mesentaries or muscle tissue. Striped bass were introduced into San Francisco Bay from the east coast approximately 100 yr ago. The type of incompatibility shown here has not been described between east coast striped bass and their helminth parasites. Current studies are investigating the possibility that the west coast striped bass are immunologically incompatible with the indigenous strain of parasite.

ACKNOWLEDGMENTS

We thank the staffs at Marine Studies, University of California, Santa Cruz, and the National Marine Fisheries Service, Tiburon, CA; Marvin Jung, State Water Resources Control Board; Frank Fisher and the California Department of Fish and Game, Kinnetics Laboratory; Elmer Noble, University of California, Santa Barbara; James Berry, Scripps Institute of Oceanography, La Jolla, CA; Donald Gruber, Pinole, CA; Thomas Tucker, Steinhart Aquarium, California Academy of Sciences.

LITERATURE CITED

CAILLIET, G. M.
1976. Several approaches to the feeding ecology of fishes. First Pac. N.W. Tech. Workshop. Sess. 1. Workshop Proc., Astoria, Oreg., October 13-15, 1976.

EDWARDS, S. R., and F. M. NAHHAS.
1968. Some endoparasites of fishes from the Sacramento-San Joaquin Delta, California. Calif. Fish Game 54:247-256.

HENSLEY, G. H., and F. M. NAHHAS.
1975. Parasites of fishes from the Sacramento-San Joaquin Delta, California. Calif. Fish Game 61:201-208.

LOVE, M. S., and M. MOSER.
1983. A checklist of parasites of California, Oregon, and Washington marine and estuarine fishes. U.S. Dep. Commer., NOAA Tech. Rep. NMFS SSRF-777, 576 p.

MORIGUCHI, M. N.
1973. Food habits of the striped bass, *Roccus saxatilis*, (Walbaum) in San Francisco Bay with notes on the major areas of the fishery. M.A. Thesis, San Francisco State Univ., San Francisco, CA, 61 p.

MOSER, M.
1983. Parasites of San Francisco Bay-Delta area stripped bass (*Morone saxatilis*) and other San Francisco Bay fishes. Final Rep., Calif. State Water Res. Control Board, Sacramento, CA, 114 p.

MOSER, M., M. LOVE, and J. SAKANARI.
1984. Common parasites of California fishes. Calif. Dep. Fish Game, 20 p.

MOSER, M., J. SAKANARI, S. WELLINGS, and K. LINDSTROM.
1984. Incompatibility between San Francisco striped bass, *Morone saxatilis* (Walbaum), and the metacestode, *Lacistorhynchus tenuis* (Beneden 1858). J. Fish Dis. 7:397-400.

MOYLE, P. B.
1976. Inland fishes of California. Univ. Calif. Press, Berkeley, 405 p.

ORSI, J. J.
1971. The 1965-1967 migrations of the Sacramento-San Joaquin Estuary striped bass population. Calif. Fish Game 57:257-267.

ORSI, J. J., and A. C. KNUTSON.
1979. The role of mysid shrimp in the Sacramento-San Joaquin estuary and factors affecting their abundance and distribution. *In* T. J. Conomos (editor), San Francisco Bay: The urbanized estuary, p. 401-408. Pac. Div./A.A.A.S., San Francisco State Univ., CA, June 12-16, 1977.

SOKAL, R. R., and F. J. ROHLF.
1969. Biometry. The principles and practice of statistics in biological research. W. H. Freeman and Co., San Francisco, CA, 776 p.

TANAKA, J., and M. TORISU.
1978. *Anisakis* and eosinophil. I. Detection of a soluble factor selectively chemotactic for eosinophils in the extract from *Anisakis* larvae. J. Immunol. 120:745-749.

THOMAS, J. L.
1967. The diet of juvenile and adult striped bass, *Roccus saxatilis*, in the Sacramento-San Joaquin River system. Calif. Fish Game 53:49-62.

TURNER, J. L., and D. W. KELLEY.
1966. Ecological studies of the Sacramento-Joaquin Delta. Calif. Dep. Fish Game, Fish Bull. 136, Part II, Fishes of the Delta, 168 p.

WOOTTEN, R., and J. W. SMITH.
1975. Observational and experimental studies on the acquisition of *Anisakis* sp. larvae (Nematoda: Ascaridida) by trout in fresh water. Int. J. Parasitol. 5:373-378.

8564

JOURNAL OF GEOPHYSICAL RESEARCH, VOL. 90, NO. C6, PAGESS 11,573–11,586, NOVEMBER 20, 1985

Advances in Satellite Sea Surface Temperature Measurement and Oceanographic Applications

E. G. Njoku,[1] T. P. Barnett,[2] R. M. Laurs,[3] and A. C. Vastano[4]

Satellite techniques for measurement of sea surface temperature (SST) are reviewed briefly, and a discussion of satellite SST applications and recent research in oceanography is provided. These applications include the areas of climate, mesoscale oceanography, and fisheries. Examples given focus mainly on the Pacific and California Current regions. Satellite SST data are currently used operationally for fisheries applications and, in conjunction with in situ data, are providing new insights into mesoscale oceanographic phenomena. Requirements for sensor precision and calibration accuracy are more stringent in air-sea interaction studies and climate research, thus satellite data have gained only qualified acceptance for these applications. Improvements in future satellite instruments, more comprehensive in situ sensor deployments, and better data management procedures should eventually satisfy most oceanography and climate SST requirements.

1. Introduction

From the early days of satellite environmental remote sensing, efforts have been made to measure sea surface temperature (SST) from space with scientifically useful accuracy. The synoptic view from space allows SST to be mapped globally in regions where ships and in situ measuring devices are sparse or nonexistent. Furthermore, the coverage can be complete and frequent, enabling the motion of current eddies and meanders to be studied in detail. Nevertheless, it had to be demonstrated that the measurement accuracies and spatial and temporal resolutions available from satellites were adequate for the specific applications in which the data were to be used. Some generations of instruments later, the process of evaluating the scientific usefulness of satellite-derived SST's is still in progress. However, the satellite instruments and algorithms are now considerably improved, the scientific applications and requirements are much better understood, and the potential benefits of satellite observations have been widely recognized.

In this paper we present some of the major applications and requirements for satellite SST data, discuss how the satellite instruments have evolved to meet these requirements, and outline where improvements to SST data processing and assimilation procedures are needed. For convenience the applications have been separated into the broad areas of climate, mesoscale oceanography, and fisheries. Put together, these cover the full range of temporal and spatial resolutions for which satellite data are required and illustrate the accuracies needed for research and operational purposes. A more general review of applications of satellites to oceanography has been provided by *Brown and Cheney* [1983].

2. Satellite Instruments

Early environmental satellites of the 1960's carried infrared radiometers primarily for mapping nighttime cloud cover and estimating cloud heights. In the absence of clouds the infrared measurements provided useful estimates of the earth's surface temperature [*Rao et al.*, 1972]. With present-day infrared radiometers, highly accurate (~0.5 K) measurements of SST are possible if the atmosphere is clear, but the opacity of clouds is still a major obstacle to obtaining accurate SST measurements in overcast conditions. On the other hand, microwave measurements have been shown to be less affected by clouds, but they have other problems in accounting for variable ocean emissivity and obtaining a precise instrument calibration [*Njoku*, 1985]. For both types of sensor, satellite orbit configurations and instrument scanning geometries must be optimized to achieve the desired temporal and spatial resolution and coverage. Retrieval methods used to derive SST's from the measured radiances must be robust and flexible enough to account for environmental factors without being so complex as to render them useless for operational purposes. None of the satellite techniques currently used for measuring SST are entirely satisfactory on the above counts. However, some are particularly suited for specific applications, and there is promise that various combinations of satellite and in situ techniques may eventually satisfy all applications for which SST data are required.

The variety of satellite techniques presently available for SST measurement is illustrated by the four sensors primarily discussed in this issue. The advanced very high resolution radiometer (AVHRR) is a descendant of the early imaging visible and infrared sensors on polar-orbiting satellites that provides high spatial resolution and measures radiation in two visible and two or three infrared spectral bands [*McClain et al.*, this issue]. The high-resolution infrared sounder/microwave sounding unit (HIRS/MSU) is a polar-orbiting, sounding instrument that measures radiation at several infrared and microwave wavelengths, allowing better correction for atmospheric effects but with poorer spatial resolution [*Susskind and Reuter*, this issue]. The scanning multichannel microwave radiometer (SMMR) is a polar-orbiting, low-spatial-resolution sensor that is comparatively insensitive to clouds and other atmospheric effects [*Milman and Wilheit*, this issue]. The visible-infrared spin-scan radiometer atmospheric sounder (VAS) is a combination imaging/sounding instrument placed in geostationary orbit and has medium spatial resolution and a fixed-earth-disk field of view, but it can make measurements with high temporal frequency (~every 30 min) [*Bates and Smith*, this issue]. The characteristics of these instruments are summarized in Table 1. Instruments with capabilities similar to or approaching the above are also planned for satellites of

---

[1] Jet Propulsion Laboratory, California Institute of Technology, Pasadena, and Department of Engineering, Harvey Mudd College, Claremont, California.

[2] Climate Research Group, Scripps Institution of Oceanography, La Jolla, California.

[3] Southwest Fisheries Center, National Oceanic and Atmospheric Administration, La Jolla, California.

[4] Department of Oceanography, Texas A & M University, College Station.

Copyright 1985 by the American Geophysical Union.

Paper number 5C0634.
0148-0227/85/005C-0634$05.00

TABLE 1. Characteristics of Satellite Sensors Used in Measurement of SST

Spacecraft	Orbit Type	Sensor	Spectral Channels‖	Sensor Spatial Resolution, km	Spatial Resolution of Global SST Product,§ km	Swath Width	Research/ Operational Status of SST Product
NOAA 6–9	Polar, 98.8° inclination, 850-km altitude	AVHRR	Visible plus 3.7, 11, 12* μm (infrared)	1	50–250	2500 km†	operational (several products)
NOAA 6–9	Polar, 98.8° inclination, 850-km altitude	HIRS/MSU	2.7–15 μm (20 channels, infrared), 50.3–58.0 GHz (four channels, microwave)	20	60–250	2200 km	research
Nimbus 7	Polar, 99.3° inclination, 955-km altitude	SMMR‡	6.6, 10.7, 18, 21, 37 GHz (microwave)	150	150	800 km	research
GOES 4–6	Geosynchronous 0°N, 75°W latitude (GOES-East) 0°N, 135°W latitude (GOES-West)¶	VAS	Visible, plus 3.9, 11, 12.6 μm (infrared)**	14	50–75	Earth disk†	research

*This channel not included on NOAA 6 and 8.
†Useful area reduced by viewing angle constraints.
‡SMMR was also carried on the Seasat satellite.
¶Nominal positions (spacecraft failure may necessitate repositioning of remaining active satellite).
§Depending on method used to generate product.
‖Not all channels used in SST determination.
**Additional infrared channels available in dwell-sounding scan mode.

other countries, including those of the Soviet Union, Europe, Japan, and India.

2.1. *Infrared Techniques*

For a cloud-free atmosphere, infrared radiation emitted from the ocean surface can propagate relatively unattenuated through the atmosphere at wavelengths for which gaseous absorption is small. The variability in attenuation at a given wavelength is primarily due to water vapor. At these "window" frequencies (~3.5–4 μm and 10–12 μm), atmospheric transmission can range from ~90% for a dry atmosphere (~1 cm precipitable H_2O) to only 30% for a humid atmosphere (~5.5 cm precipitable H_2O). The transmittance depends on the vertical distribution of water vapor as well as the total water vapor amount. The total infrared radiance $I(\lambda, \theta)$ measured by the sensor at wavelength λ and viewing angle θ is the sum of components from the ocean surface, from the atmosphere itself, and from background solar radiation reflected at the ocean surface. This can be expressed by the equation

$$I(\lambda, \theta) = \varepsilon(\lambda, \theta)B(\lambda, T_s)\tau_0(\lambda, \theta) + I_a(\lambda, \theta) + \tau_0(\lambda, \theta) \iint_{2\pi} \gamma(\lambda, \theta; \theta') \cdot [I_d(\lambda, \theta') + \tau_0(\lambda, \theta') I_s(\lambda, \theta')]\, d\Omega' \qquad (1)$$

where ε is surface emissivity, B is the Planck blackbody emission function, T_s is the ocean surface temperature, τ_0 is atmospheric transmittance, γ is the surface scattering coefficient, I_a is the upward component of atmospheric emission at the satellite, I_d is the downward component of atmospheric emission at the surface, and I_s is the extraterrestrial radiation (including solar radiation). Expressions for the dependence of τ_0, I_a, and I_d on atmospheric temperature, absorption, and scattering are provided in the literature [e.g., *Chahine et al.*, 1983].

In practice, to obtain the radiation component emitted by the surface—$\varepsilon(\lambda, \theta)B(\lambda, T_s)$—corrections must be made to the measured radiance for the atmospheric and reflected solar contributions. Once the surface radiation is known, the surface temperature can be determined from knowledge of the surface emissivity and the form of the Planck function (as weighted by the spectral filter response of the receiver).

The simplest approach for atmospheric correction is to measure radiation from a given field of view at two or more window frequencies having different atmospheric absorptions. The SST can then be estimated as a linear combination of measured brightness temperatures at these frequencies:

$$\mathrm{SST} = a_0 + \sum_{i=1}^{N} a_i T_i \qquad (2)$$

where T_i is the brightness temperature at the ith frequency or channel, and N is the number of channels (usually two or three). The coefficients a_0 and a_i are determined by regression, either theoretically, by using the model of (1), or empirically, by using satellite and in situ data. This type of algorithm has the advantage of simplicity and under ideal conditions performs surprisingly well. It forms the basis of the MCSST (multichannel sea surface temperature) approach used operationally by NOAA [*Strong and McClain*, 1984]. Its possible disadvantage is that two or three channels combined linearly may not be sufficient to account adequately for all the independent environmental variables, and the sources of errors observed when using the algorithm in a practical situation are difficult to determine. Small errors might be expected, for example, from any or all of the following: nonlinearity of the dependence of τ_0 on total water vapor content and on the vertical distribution of water vapor; dependence of surface emissivity on wavelength, angle, and roughness; residual cloud or aerosol absorption and scattering; reflected solar radiation; uncertainties in molecular absorption coefficients; and regression errors caused by theoretical model inaccuracies, in situ data errors, or incomplete statistical representation of the operating environment. Some of these errors may be negligible, some can be rendered negligible by appropriate viewing or operating configurations, and others are very difficult to model physically in any case. Nevertheless, under the small but significant percentage of conditions when erroneous results are produced, it is not easy to determine why algorithm errors have occurred or how to remedy the situation.

An alternative approach to regression is to use an iterative method [e.g., *Susskind et al.*, 1984] in which initial estimates of ocean and atmosphere parameters are used to compute radiances at the instrument operating wavelengths according to (1). These initial parameters are then modified iteratively according to a chosen relaxation scheme until the computed radiances match the observed radiances to within a given tolerance. The attractiveness of this scheme is that the physics contained in (1) is maintained for each retrieval, since a separate iteration is carried out at each retrieval point rather than using a general set of prederived coefficients, as with the regression approach. This method, however, can be computationally more demanding, and there may be subtle reasons for nonconvergence, such as model errors or channel calibration biases. In principle it is easier to simulate the causes of errors produced by such physically based algorithms and hence more fully understand their operation. In practice, ad-hoc "tuning" of the procedures is often necessary to achieve adequate performance, in the process of which the user may lose some of the advantages of this method.

Variations of the above retrieval methods are used for most satellite infrared SST retrievals. Other differences between retrieval schemes lie in the methods used to account for clouds. These are basically cloud avoidance schemes, in which radiance measurements containing cloud emission are detected and rejected, or cloud correction schemes in which a correction is attempted for effects of clouds up to some upper threshold of cloudiness. Whatever the case, some clouds always remain undetected or imperfectly corrected, and SST accuracies degrade accordingly in persistently cloudy regions of the oceans. For examples of other development and applications of infrared SST algorithms, see *Bernstein* [1982], *Barton* [1983], and *Brown and Cheney* [1983].

2.2. *Microwave Techniques*

The emission of microwave radiation by the ocean and atmosphere can also be represented by (1). Atmospheric transmission in the microwave frequency range suitable for SST measurements (~5–10 GHz) is generally greater than ~98% and, even in the presence of heavy clouds, does not fall below ~95%. However, the microwave surface emissivity varies considerably as a function of wind speed on account of the generation of waves and foam (in contrast to infrared surface emissivity, which remains essentially constant ≃1). Thus additional channels must be introduced into a retrieval algorithm such as (2) in order to provide a correction for wind speed [*Wilheit and Chang*, 1980].

Similar comments apply to microwave retrievals as were discussed above for infrared methods; these comments concern the merits of regression and iterative retrieval algorithms. The major sources of error are different for microwave methods, however. Variability of surface roughness rather than atmospheric water vapor and aerosols is the principal uncertainty factor in determining SST, although clouds can cause erroneous retrievals also if they contain precipitation. For examples of other development and applications of microwave SST algorithms, see *Hofer and Njoku* [1981], *Wilheit et al.* [1984], and *Wentz* [1983].

2.3. *Sensors and Systems*

As shown in Table 1, satellite instruments currently exist that individually, or in combination, satisfy a variety of oceanographic requirements in terms of spatial resolution, temporal resolution, and global or regional coverage. What is required is a reliable mechanism for transforming or combining the satellite data into useful SST products and verifying the accuracy of these products. In most cases the accuracies need to be improved. As will be discussed in other papers in this issue, presently achievable SST accuracies are estimated to be in the range of 0.5°–1.5°C, depending on the prevailing atmospheric and surface conditions, the amount of temporal and spatial averaging involved, and the method used for evaluation (which may involve sampling errors and in situ measurement errors).

The contributing error sources arise mainly from uncertainties in the physical radiation models and imperfections in the retrieval procedures. However, in some cases, instrument noise and calibration drifts may dominate the error budget and must be carefully monitored. In situations where high-resolution satellite imagery is required for detection of localized SST gradients, absolute calibration can be less important than ensuring that instrument rms noise is small in comparison to the desired signal. In other situations, such as for climate studies, absolute calibration accuracy is essential in order to observe small SST changes over long time periods and large spatial scales. Noise and calibration problems vary in severity with specific sensors. Thus, for example, excessive noise in the AVHRR 3.7-μm channels has consistently occurred, and calibration drifts associated with instrument thermal cycles and component degradation have been observed in the SMMR channels. It is often difficult, if not impossible, for a user to get adequate information on how satellite instruments have been calibrated, usually resulting in a need for some kind of "end-calibration," i.e., adjustment of bias drifts in measured SST by periodic comparisons with XBT's, buoys, or other sensors of supposedly stable accuracy. This provides motivation for blended products in which data from two or more sensors are combined to produce an optimum SST field. The algorithms for performing such blending, and the sense in which the resultant fields are optimum, are areas of current research.

In the following sections the uses of satellite-derived SST's will be discussed for applications in mesoscale oceanography, fisheries, and climate. The requirement for high spatial resolution in determining temperature fronts for fisheries applications has dictated the use of primarily high-resolution (~1 km) AVHRR data to provide images of SST in coastal regions. Also for reasons of spatial resolution, mesoscale oceanography applications have used predominantly high-resolution AVHRR data for studying eddies and currents. Geostationary satellite data from infrared radiometers on the GOES and Meteosat satellites have also been used for this purpose. For climate applications, low-resolution sensors are useful, since these can be composited into well-calibrated weekly or monthly global fields of SST on appropriate grid scales, e.g., 2°–5° latitude and longitude. Thus the SMMR and HIRS/MSU, in addition to the AVHRR, are potentially well suited for this purpose.

3. Mesoscale Oceanography Applications

3.1. *Introduction*

The role of satellite sensors in mesoscale oceanographic studies can be examined on the basis of two questions: Does this method of observing the ocean disclose new phenomena and processes, and do these observations contribute new ways of understanding mesoscale phenomena? In the case of sensors detecting SST, research during the past decade has answered the first question affirmatively. Qualitative descriptions using satellite images have altered mesoscale concepts and modified experimental approaches. The second question concerns the extraction of quantitative information and its effect on the representation of dynamics and processes. The answer here, though not as definite, is positive and reflects the present stage in which the development of methods and verification of measurements are taking place.

A general mesoscale characteristic length given by the Rossby radius of deformation is 100 km, and the associated wave period is approximately 60 days. Features on these scales include fronts and eddies that are the first-order expressions of oceanic turbulence. Investigations of mesoscale oceanographic phenomena in the last two decades have produced regional surveys as well as studies of specific features and processes. Satellite and surface observations have revealed a pervasive mesoscale presence as well as dynamic and structural elements of these features. Continued progress requires multiple-platform sampling schemes with increased spatial and temporal resolution and coverage. The simultaneous attainment of these requirements is difficult to achieve using surface platforms alone. The polar-orbiting and geostationary satellites listed in Table 1 that employ infrared sensors are particularly suited to this objective and can contribute quantitative as well as qualitative data pertaining to surface expressions and their evolutions. Infrared sensors are emphasized in this discussion, since microwave sensors for SST have not yet attained the necessary spatial resolution.

3.2. *Mesoscale Studies*

Satellite infrared imagery can provide information on distributions, relationships, structure, dynamics, and thermodynamics of the surface layer. As with all instruments and their observations, unique advantages and inherent limitations exist. The seasonal development of an isothermal surface layer tends to obliterate detectable temperature patterns in mid-latitudes. Depending on the strengths of initial temperature perturbations, this factor can inhibit use of AVHRR images during summer months. Obscuring clouds associated with storm systems tend to be seasonal also and can interrupt observations for periods of time that are critical in some mesoscale studies. However, the resolution and coverage of the AVHRR and VAS instrument systems aboard the recent NOAA satellites are examples of the significant capabilities now afforded researchers. Mesoscale analyses using satellite infrared imagery often require independent bulk temperature measurements, since infrared radiometers measure the temperature of the upper millimeter of the ocean surface only. Dynamic interpretations of satellite SST pattern evolution tend to focus on surface shear [*Mueller and LaViolette*, 1980] or baroclinic instabilities [*Bernstein et al.*, 1977]. Analyses often require subsurface data to define vertical continuity and depth of the surface layer in order to estimate advective heat exchange [*Brown et al.*, 1983]. While historical data can be used for this purpose, most studies of specific mesoscale features and processes depend on surface platforms for information coincident with the satellite observations. *Vastano and Bernstein* [1984*a*] have shown that combinations of satellite and XBT observations can yield synoptic understanding of front and eddy evolution in the Tohoku area of the northwest Pacific between the Kuroshio and Oyashio fronts.

Infrared SST data gathered over the world oceans by satellites have shown a variety of mesoscale features in regions near strong current systems and within adjacent gyres. Major surveys of such mesoscale SST features [e.g., *Legeckis*, 1978] illustrate that qualitative studies can confirm circulation features, provide initial detection, and support new hypotheses on the role of dynamic and thermodynamic balances. The seaward deflection of the Gulf Stream by topography off Charleston, South Carolina [*Vukovitch and Crissman*, 1980], upwelling along the northwest coast of Africa, and eddy production at the juncture of the Brazil and Falkland currents are examples.

Studies with infrared images have derived quantitative estimates that pertain to specific events. Information has been extracted about size, shape, translation, generation, and surface temperatures of mesoscale features. *Brown et al.* [1983] employed a sequence of 42 images in a study of a ring (81-D) in the Mid-Atlantic Bight. The translation of this ring and variations in its shape were correlated with Gulf Stream interactions. A time series of near-shore meanders and eddies off Vancouver Island contributed to the verification of a quasi-geostrophic numerical model [*Ikeda et al.*, 1984]. In this case the AVHRR imagery provided evidence for the selection of model dynamic mechanisms and confirmed the production of predicted eddy features. *Maul et al.* [1978] studied time series of Gulf Stream positions observed with GOES infrared imagery. Observations over a 9-month interval were used to determine the spatial and temporal variability of meanders from the Yucatan Straits to Grand Banks.

Considerable effort has been made to develop algorithms that compute SST corrected for atmospheric water vapor and free of cloud contamination [e.g., *McClain*, 1981; *Maul*, 1981; *Bernstein*, 1982]. The production of synoptic, mesoscale-resolving SST maps is now possible with accuracies of less than 1°C. *Vastano and Bernstein* [1984*b*] presented a case study that compared satellite and XBT SST values for a complex mesoscale field in the Tohoku area. An rms scatter of 0.8°C was found about a mean bias of 0.6°C, with the satellite estimates warmer. SST maps of this nature can contribute to studies of mesoscale features as well as ocean environmental reports.

Progress has been made on the extraction of mesoscale flow maps and related information from infrared imaging. *Vukovitch* [1985] has obtained surface geostrophic flow vectors by starting with atmospherically corrected, cloud-free satellite SST values and associating salinity values from statistical temperature-salinity relations. Surface density distributions are calculated from an equation of state, and flow components on a uniform grid are derived from an integrated form of the thermal wind equation. Comparisons of satellite results with geostrophic currents derived from coincident hydrographic transects in the Gulf of Mexico show an average correlation coefficient for surface current magnitudes of 0.82. This utilization of temperatures from infrared observations is an extension of the standard Eulerian oceanographic procedure. Other methods are under study that utilize corrected as well as uncorrected image patterns and include a Lagrangian procedure for sea surface features that is related to cloud tracking developed by meteorologists. Submesoscale feature displacements in sequential satellite SST patterns can be interpreted in terms of advection by the general mesoscale motion. *La Violette* [1984] has estimated motion around the Alboran Sea gyre in this manner. *Kelly* [1983] has developed a procedure based on an analytical model that includes the thermal wind relation and conservation of temperature. The computations provide a

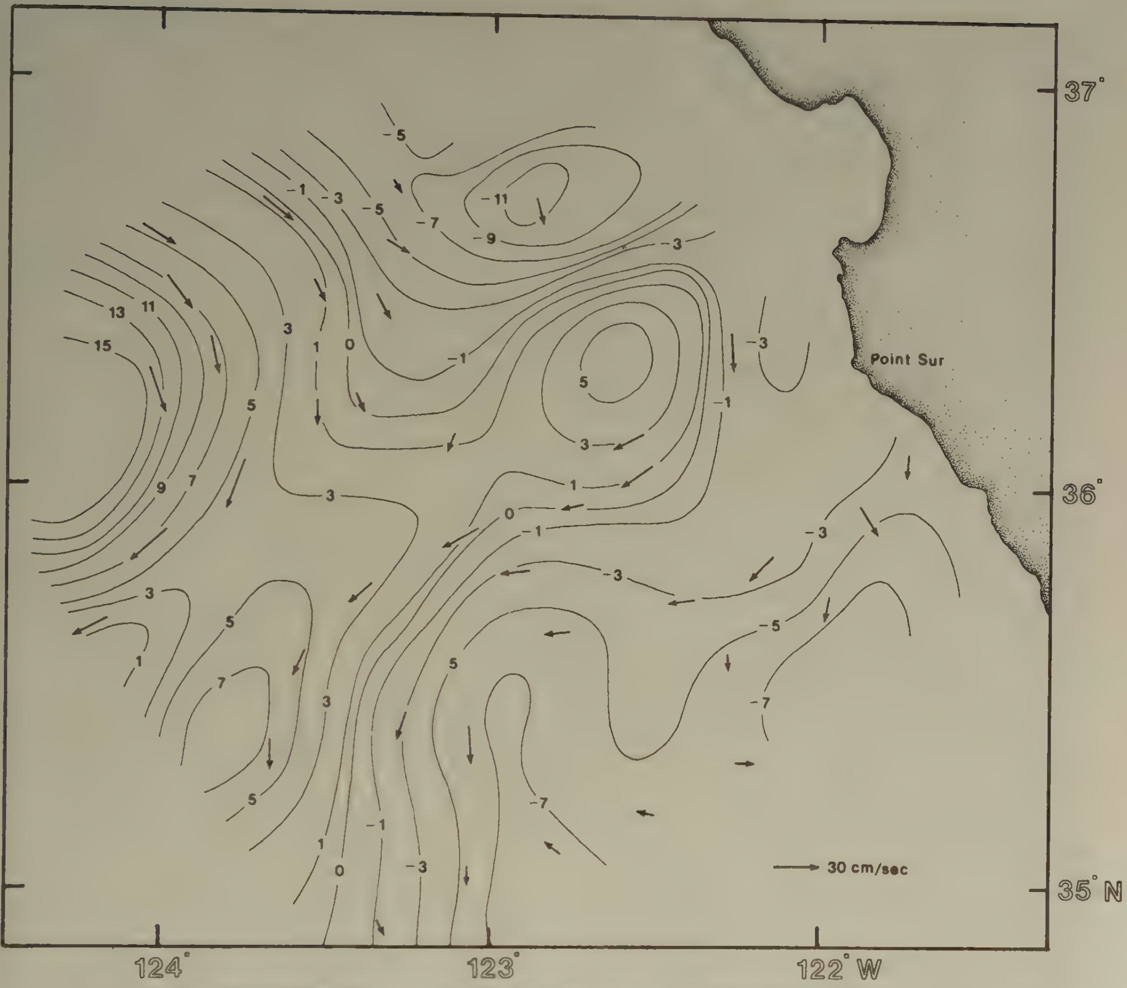

Fig. 1. Surface flow (cm/s) and topography (cm) derived from sequential AVHRR images for March 31 to April 1, 1982.

uniform distribution of along-isotherm and cross-isotherm flow components for an infrared image. Application to the California Current region showed good qualitative agreement with velocities obtained from coincident shipborne Doppler acoustic log velocities and surface drifter tracks. *Vastano and Borders* [1984] have used an interactive algorithm for flow that computes a nonuniform distribution of vectors by tracking submesoscale feature displacements in sequential imagery. This method can accommodate image patterns formed by discrete scalar values from infrared or visible observations and identifies small feature displacements in the direction of a scalar gradient. The flow vectors in Figure 1 were obtained with the interactive method from two sequential NOAA 7 infrared (channel 4, 11 μm) images of a California Current region taken during March 31 to April 1, 1984. The flow estimates are for portions of a warm core eddy (36°N, 124°W) and a cold water plume (35°30′N, 123°20′W) extending offshore from Point Sur.

Flow vector estimates obtained from infrared images can be used to find stream function representations for the flow fields. As an example, *Vastano and Reid* [1985] use a nonuniform distribution of vectors to derive coefficients of a two-dimensional stream function expansion. By invoking a geostrophic approximation, the sea surface topography in Figure 1 was computed from the stream function. Although coincident hydrography or surface flow observations are not available, these satellite estimates of topography and the associated topographic gradients are in close agreement with similar estimates taken from historical CalCOFI (California Cooperative Oceanic Fisheries Investigation) dynamic topography maps given by *Hickey* [1979].

3.3. *Discussion*

The computation of dynamic and thermodynamic fields from infrared imagery is a major step in mesoscale studies. Research is required to improve their accuracy and range of applicability. A more thorough investigation of alternative SST techniques and accuracies has developed in comparison with the relatively new flow studies. The latter are currently derived with restrictive assumptions regarding the absence of external forcing and lateral flow. In the future these fields will form intermediate results in surface layer studies. For example, their analysis with XBT observations can be applied to research on surface layer heat content (Q), the material or sub-

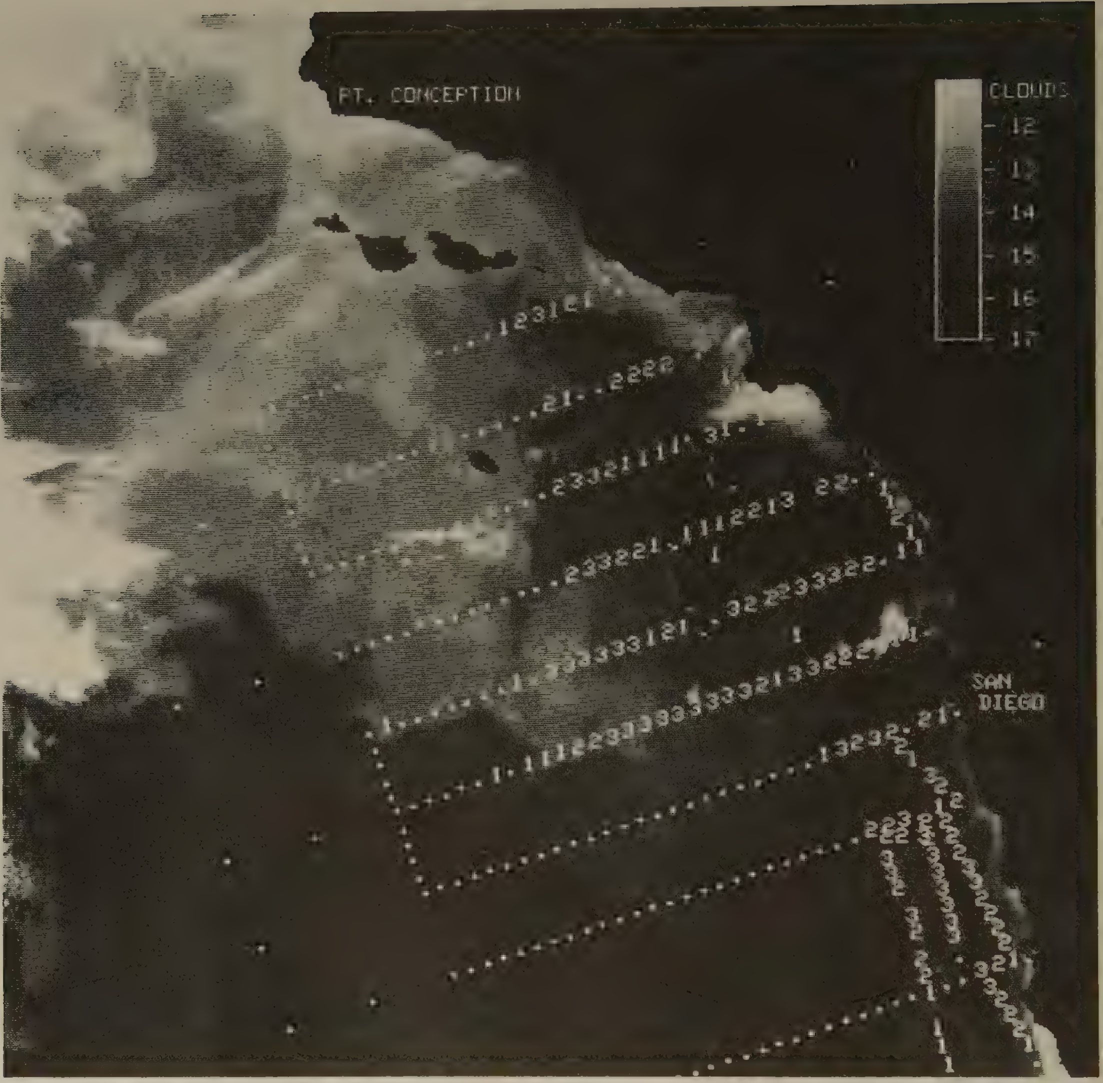

Fig. 2. Northern anchovy egg distribution based on plankton net hauls made during March 20 to April 10, 1980, and sea surface temperature from NOAA 6 AVHRR, channel 4, April 7, 1980. The number of eggs per 0.05 m^2 are given, where · = 0, 1 = 1–4, 2 = 5–17, and 3 = 18–245 eggs per 0.05 m^2 [from *Fiedler*, 1983].

stantial derivative (dQ/dT), and the local and advective components of dQ/dT at mesoscale resolution and coverage. Results from such studies will be pertinent to climatic research concerned with spatial and temporal variability of air/sea interactions.

4. FISHERIES APPLICATIONS

4.1. *Introduction*

The use of satellite remote sensing to provide synoptic measurements of the ocean is becoming increasingly important in fisheries research and fishing operations. Variations in ocean conditions play key roles in natural fluctuations of fish stocks and in their vulnerability to harvesting. Information on the changing ocean, rather than on average ocean conditions, is necessary to understand and to eventually predict the effects of the ocean environment on fish populations. The evolving capabilities of satellite sensors and data-processing technology, combined with conventional data collection techniques, provide a powerful tool toward ensuring the wise use of living marine resources.

Satellite remote sensing applications in fisheries have concentrated on the measurement of ocean temperature and color and computation of ocean transport based on satellite-measured wind stress. *Laurs and Brucks* [1985] review fisheries applications of satellite oceanic remote sensing in the U.S. Examples of recent and potential uses of satellite imagery in eastern North Pacific fisheries are given in *Fiedler et al.* [1985]. *Yamanaka* [1982] describes the utilization of satellite imagery in Japanese fisheries. *Gower* [1982] gives an overview of the different kinds of remote sensing data relevant to fisheries science and oceanography, and *Montgomery* [1981] dis-

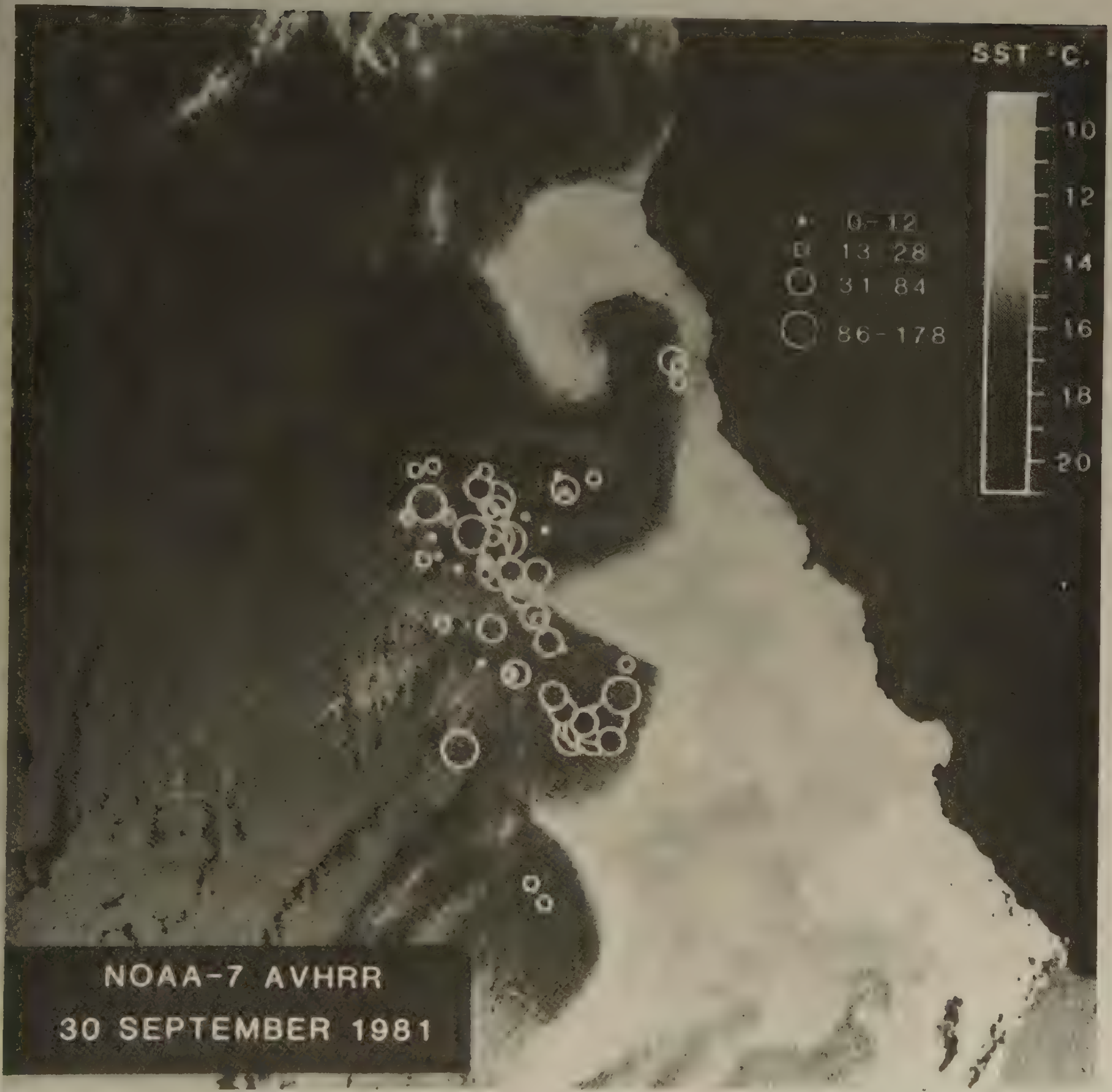

Fig. 3. Central California daily albacore tuna catches, September 27 to October 2, 1981, and sea surface temperature from NOAA 7 AVHRR, channels 4 and 5, September 30, 1981 [from *Laurs et al.*, 1984].

usses the utility of satellite imagery to ocean industries, including fisheries. This section will concentrate on fisheries applications of satellite sea surface temperature measurements.

2 *Measurement of Environmental Conditions Affecting ishery Resources*

Variations in environmental conditions affect the reruitment, distribution, abundance, and availability of fishery esources. It is not possible to measure remotely from satellites he entire spectrum of information needed to assess changes in he marine environment. However, information about importnt oceanographic conditions and processes affecting fish opulations, such as surface temperature isotherms, oceanic ontal boundaries, current and circulation patterns, and astal upwelling, may often be deduced by using ocean surce temperature measurements made by satellite.

Ocean temperature measurements made by satellite remote sensing can be extremely useful in defining the distribution of marine fish habitat conditions. *Lasker et al.* [1981] and *Fiedler* [1983] have demonstrated that the northern boundary of northern anchovy spawning habitat in the Southern California Bight may be delimited by using AVHRR imagery from NOAA polar-orbiting satellites (Figure 2). In general the northern extent of spawning in the bight and the offshore extent of spawning north of Santa Catalina Island are limited by cold, upwelled waters advected south of Point Conception. The cold waters are readily evident in satellite infrared imagery of the region. The southern limit of the anchovy spawning corresponds to low chlorophyll concentrations apparent in ocean color imagery from the coastal zone color scanner (CZCS) aboard Nimbus 7 [*Fiedler*, 1983].

The distribution and availability of albacore tuna off the

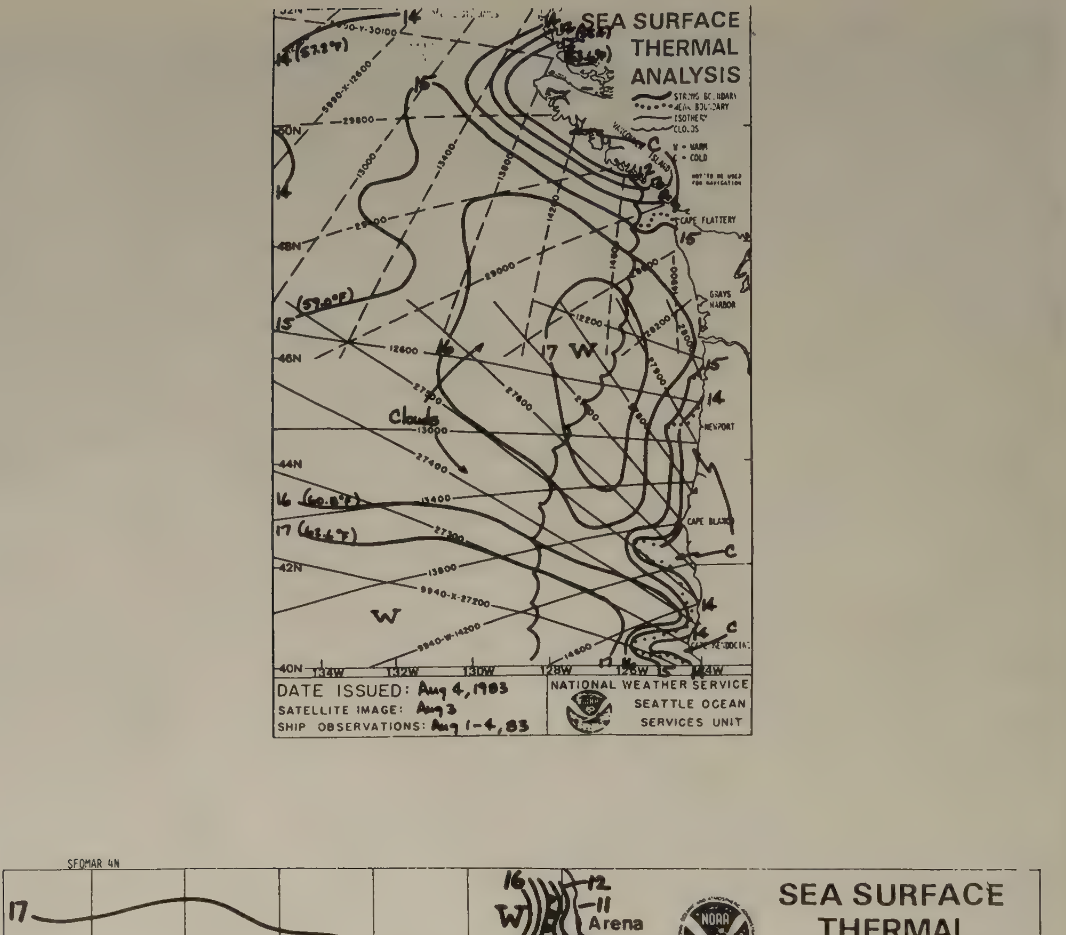
SEA SURFACE THERMAL ANALYSIS
STRONG BOUNDARY
WEAK BOUNDARY
ISOTHERM
CLOUDS
W = WARM
C = COLD
NOT TO BE USED FOR NAVIGATION
CAPE FLATTERY
GRAYS HARBOR
NEWPORT
CAPE BLANCO
CAPE MENDOCINO
VANCOUVER ISLAND
Clouds
(57.0°F)
16 (60.8°F)
17 (62.6°F)
50N
48N
46N
44N
42N
40N
134W
132W
130W
128W
126W
124W
DATE ISSUED: Aug 4, 1983
SATELLITE IMAGE: Aug 3
SHIP OBSERVATIONS: Aug 1-4, 83
NATIONAL WEATHER SERVICE
SEATTLE OCEAN SERVICES UNIT
SFOMAR 4N
SEA SURFACE THERMAL ANALYSIS
NAT'L EARTH SATELLITE SERVICE, 660 PRICE AVE., REDWOOD CITY, CA 94063
Date: AUG 1, 1983
Comments: UPWELLING HAS DECREASED
Temp. Conversion
°C °F
24 - 75.2
22 - 71.6
20 - 68.0
18 - 64.4
16 - 60.8
14 - 57.2
12 - 53.6
10 - 50.0
8 - 46.4
Arena
Pescadero
Sur
Piedras Blancas
Conception
Vicente
Loma
Santo Tomas
Baja
38°
34°
30°
132°
128°
124°
120°
116°
LINE OF EQUAL TEMPERATURE
STRONG OCEAN THERMAL FRONT
WEAK OCEAN THERMAL FRONT
C = COLD
W = WARM

Fig. 4. Examples of fishery advisory charts showing sea surface thermal analysis for waters off the West Coast. Upwelling during this period was nonexistent along the Washington coast and strong along the central and southern Oregon coast.

TABLE 2. Data Requirements for Satellite Sea Surface Temperature Measurements for Fisheries Applications [adapted from *Sherman*, 1980]

	Accuracy, °C	Precision, °C	Spatial Resolution, km	Temporal Resolution, days	Acceptable Time Delay, days	Areal Coverage
Research	0.5	0.15	2–10	0.1–1	0.5–5	selected coastal and mid-ocean
Fishing operations	0.5	0.15	2–10	1	0.5	selected coastal and mid-ocean

west coast of the United States have been related to oceanic fronts seen in AVHRR infrared and color imagery [*Laurs et al.*, 1984] (Figure 3). Infrared thermal and visible color data from satellites can define environmental limits on the spatial distribution of fishable aggregations of albacore and can do so more effectively than ship or aircraft data used in the past. Commercially fishable aggregations of albacore are found in warm, blue oceanic waters near temperature and color fronts on the seaward edge of coastal water masses. These oceanic boundary features, which are believed to result primarily from coastal upwelling, are clearly observable in satellite imagery collected along the U.S. Pacific coast. The distribution of albacore during winter in regions hundreds of miles off the coast has also been related to sea surface temperature fronts observed in AVHRR imagery from the NOAA 7 polar-orbiting satellite [*Laurs et al.* 1981]. These fronts are believed to mark the outer boundary of the California Current.

Satellite infrared measurements have also been used to trace the development and duration of the various bluefin tuna fisheries along the east coast of the United States [*Roffer et al.*, 1982]. These fisheries follow the movement of seasonal warming of near-surface waters; this movement is monitored by observing the northerly progression of the 19°–20°C isotherms n satellite infrared imagery. Limited success has been achieved in relating the winter distribution of tuna longline ishing in the Gulf of Mexico with the position of the Loop Current deduced from temperature frontal patterns observed n GOES infrared imagery [*Maul et al.*, 1984]. In summer months, after seasonal warming, it is not possible to resolve emperature frontal structure in the GOES infrared imagery om the Gulf of Mexico.

Satellite remote sensing played an especially important role uring the recent El Nino for monitoring anomalous ocean emperatures along the U.S. Pacific coast [*Fiedler*, 1984*a*]. The satellite imagery contains invaluable information for use assessing the effects of the El Nino conditions on West oast fisheries. Virtually all of the fisheries were affected in arying degrees: some fisheries benefited from the El Nino, nd others were harmed substantially. Many fish populations perienced changes in their latitudinal and onshore-offshore stribution. For example, shifts in the distribution of anchovy pawning could be delineated by using NOAA 7 AVHRR frared satellite imagery [*Fiedler*, 1984*b*].

3. *Use of Satellites in Collection and terpretation of Ship Data*

Satellite ocean temperature data can save time and money the planning and the execution of fishery research field udies involving vessel operations. This important application satellite remote sensing usually requires direct reception d processing of satellite data in real time. The cost savings n be significant, since a single satellite image from data received and processed in a matter of a few hours can save days of expensive ship time by locating significant environmental features and permitting optimum allocation of sampling effort [*Fiedler et al.* 1985]. In addition, satellite data collected concurrently with field studies at sea can be especially valuable. It can be used to validate the interpolation and extrapolation of shipboard measurements and as a basis for interpretation of mesoscale patterns and possible mechanisms responsible for spatial and temporal variability observed in shipboard observations [*Lasker et al.*, 1981].

4.4. *Fisheries-Aid Products for Fishermen*

Several projects and programs have used or are using satellite-derived ocean temperature data in fisheries-aid products distributed to fishermen by radio facsimile transmission, voice broadcast, U.S. mail, and telephone telecopier. The first utilization of satellite data in fisheries-aid products was in the early 1970's when visual and infrared imagery received by automatic picture transmission (APT) were employed in the preparation of advisory charts transmitted to tuna purse seine fishermen operating in the eastern tropical Pacific [*Laurs*, 1971]. A prime motivation leading to the expanded use of satellite observations in fisheries-aid products was provided by the Seasat Commercial Demonstration Program sponsored by NASA/JPL. This program led to the development of an operational satellite data distribution system to distribute oceanographic products to users [*Montgomery*, 1981].

Charts showing the locations of oceanic thermal boundaries are derived from AVHRR infrared imagery and are provided to commercial and recreational fishermen for use in locating potentially productive fishing grounds along the Pacific coast from central Baja California to British Columbia and Canada [*Breaker*, 1981]. Fishermen use these charts (example shown in Figure 4) to save time in searching for productive fishing areas associated with oceanic frontal features [*Short*, 1979; *Breaker*, 1981]. Lower-resolution infrared images from the GOES satellites and ship reports are used to prepare charts for waters off the Atlantic coast that are distributed to fishermen and other interested users [*Chamberlain*, 1981]. Of particular interest to fishermen, these charts show (1) the outer limit of the shelf water mass in which many fishery resource species are concentrated, and (2) the numbers, sizes, and persistence of warm-core Gulf Stream rings, which can markedly alter conditions on the fishing grounds. These charts have been particularly useful to lobster fishermen in reducing loss of fishing pots caused by strong currents of the Gulf Stream warm-core eddies. Charts based on GOES infrared imagery are also prepared to show the path of the Loop Current in the Gulf of Mexico and are used notably by recreational fishermen [*Lowry and Leaky*, 1982]. The multichannel sea surface temperature (MCSST) charts [*Strong and McClain*, 1984], improved versions of the former global operational sea surface temperature computation (GOSSTCOMP) charts, are also used by fishermen in locations around the world where both historically and operationally there is little information on the distribution of sea surface temperature because of low ship traffic.

Finally, sea ice forecast charts derived from Nimbus 7 scanning multichannel microwave radiometer (SMMR) and AVHRR imagery are prepared for regions off Alaska and are transmitted by radio facsimile to fishermen and other marine users.

4.5. *Data Requirements, Sources, and Limitations*

Data requirements. The data requirements for satellite sea surface temperature measurements for fisheries applications have been specified in several satellite program documents [e.g., *Sherman*, 1980] and are summarized in Table 2.

While the requirements of satellite sensor measurements for fisheries applications have been treated extensively, specification of requirements for ground processing and data delivery systems have been neglected and require further development. There are pressing needs to increase the availability of ocean temperature measurements made by satellite for use in fisheries applications. In some cases, direct reception and processing of the satellite data are required. In others the routine distribution of earth-located and geographically rectified charts of level 3 data will suffice.

Data sources. Virtually all fisheries studies employing satellite ocean temperature measurements have utilized data from thermal infrared sensors. The advanced infrared sensors, notably the advanced very high resolution radiometer (AVHRR) aboard the NOAA polar-orbiting meteorological satellites, are characterized by high sensitivity in narrow frequency bands, fine ground resolution, and extensive data archiving [*Fiedler et al.*, 1985]. These sensors yield high-quality data but do have some limitations.

There have been a very few attempts to apply ocean temperature measurements made from microwave instruments aboard satellites to fisheries studies. These attempts have been only marginally successful, mostly because of the large footprint of the measurements and the contamination of the data in the vicinity of land. However, the utility of satellite microwave ocean temperature measurements in fisheries problems has yet to be adequately evaluated. Efforts to do so have been severely hampered by difficulties in obtaining high-quality microwave temperature data and lack of high-speed data-processing capabilities.

Data limitations. The major inadequacy of satellite infrared technology is that it can measure sea surface temperature only through a cloud-free atmosphere. This has hampered its utilization and acceptance for fisheries research and fish-harvesting applications because many important fisheries are in areas that have dense cloud cover much of the time. *Fiedler et al.* [1985] examined the seasonal and areal distribution of cloud conditions over the eastern North Pacific and discussed the probabilities of conditions suitable for satellite coverage. They found that (1) south of latitude 27°N, mean cloud cover is consistently less than 50%; (2) from latitude 30°N to 38°N the most favorable conditions for remote sensing are between October through April, whereas a dense layer of low stratus clouds covers the coastal waters during the summer upwelling season; (3) from latitude 40°N to 50°N the best conditions for remote sensing occur from August to October; and (4) north of latitude 50°N, mean cloud cover increases and is consistently 70% or greater in the Gulf of Alaska, although March and April may be relatively clear.

Another drawback to satellite ocean temperature measurements is their restriction to the uppermost skin of the ocean surface. Although AVHRR measurements in some situations can be representative of general temperature conditions in the upper mixed layer [*Bernstein et al.*, 1977; *Maul et al.*, 1984], many important species live below the thermocline or on the bottom, where temperature patterns are not necessarily apparent at the surface. Another shortcoming of infrared imagery is that its use to detect fronts in open ocean areas may be limited to periods prior to the onset of seasonal warming. The use of ocean color imagery from the coastal zone color scanner (CZCS) on the Nimbus 7 satellite can help circumvent this problem [*Laurs et al.*, 1984].

In spite of the limitations noted, data from advanced infrared sensors on satellites meet the general needs for many fisheries applications. However, the development of reliable microwave radiometers that can measure sea surface temperature with high resolution through clouds is required in addition to infrared to make full utilization in fisheries of ocean temperatures measured from space.

5. CLIMATOLOGICAL USES OF SATELLITE SST DATA

This section broadly outlines ways in which satellite-derived SST products can be used to study both regional and global-scale climate phenomena. A brief summary is then given of some of the instrumental problems that appear serious for climatic studies.

5.1. *Regional Climate Studies*

Contrary to popular belief, many climate studies deal with areas a few thousand kilometers in dimension, not the entire global domain. An example of how satellite SST fields can assist in this type of study occurs off the coast of western South America. It is here that the largest El Nino signals are observed, exhibiting SST anomalies of order 6°C. How these anomalies first appear and evolve is a problem that appears soluble only by incorporation of remote sensing data. Ships and drifting buoys have provided the limited knowledge that we now have regarding evolution of the SST anomalies off South America, but most would agree this description is far from adequate. Without an adequate description it is difficult to test the various theories that now exist for SST variability in this oceanographically complicated area.

By contrast there are some areas where the satellite products may not be adequate in their current state for the study of regional climate variations. Good examples of such areas are the North Atlantic Ocean and western equatorial Pacific, where the rms variability away from the boundaries is only of order 0.3°C. Without some type of calibration to an in situ data field it is unlikely that current satellite products will be capable of achieving this accuracy on a consistent basis.

5.2. *Global Studies*

Satellites offer perhaps the only hope of obtaining a truly global view of changes in the sea surface temperature field. This is because ships do not adequately sample all of the world's oceans. However the combination of ship and satellite data together offers exciting possibilities. For instance, *Weare* [1982] has used the existing data base to study what appears to be the propagation of sea surface temperature anomalies from the region of Australia to the coast of western South America across the entire south Pacific Ocean. He suggests that the ability to track these anomalies may allow the possibility of long lead-time forecasts for El Nino events. Weare also notes that the data available to support his studies were meager at best. A good coherent set of satellite SST fields would permit further analyses to be performed in a more complete manner.

Monitoring changes in global SST will become particularly important in the future as the research community searches for an expected CO_2-induced increase in the planet's atmosphere and, presumably, ocean temperature. It is clear that the only hope of obtaining such a globally averaged number lies in the application of satellite technology. Here again, the instrumental problems noted below can be critical and may lead to misguided conclusions, unless they are adequately addressed.

5.3. *Modeling Studies*

Meteorologists interested in constructing numerical models for climate studies often state that the information needed about the oceans is the sea surface temperature. This information is used to initialize the models for subsequent prognostic runs. Inserting observed or simulated SST patterns as initial conditions in general circulation models (GCM's) has led to a number of interesting results. Examples of this type of research are simulations of the effects of El Nino on the general circulation of the atmosphere [e.g., *Blackmon et al.*, 1983; *Lau*, 1985]. For such initializations, temperature anomalies are not the critical item. The quantity required is the absolute temperature of the ocean. Given the strong relation between surface temperature and atmospheric water vapor content, this specification of temperature becomes critical in the tropical regions, particularly the western equatorial Pacific and eastern Indian oceans. Indeed, errors as small as 0.5°C could lead to rather large differences in model responses to initial SST fields. Ironically, it is in these regions of the oceans that ome satellite SST sensors are most prone to error because of high water content of the atmosphere and the resulting large, uncertain numerical corrections to estimated SST's. It is these ocean areas that seem to be of fundamental importance in determining changes in global climate. Thus attempts to achieve the highest accuracy and reliability of SST products, using remotely sensed data, should be focused on this part of he world, as appears to be demanded by the physics of the limate system.

4. *Data Problems*

There are at least three classes of instrumentation problems hat must be addressed if one is to use satellite-derived SST's o study climatic problems. The first has to do with biases ntroduced into the satellite-estimated SST's. Such biases ake if difficult to mate the satellite-derived SST products ith the much longer historical data set derived from ship eather observations [e.g., *Barnett et al.*, 1979]. Fortunately, e bias problem seems to be partially resolved by the newer atellite sensors and algorithms.

A problem comparable to the bias can be introduced if the ns variability seen by the satellite sensor is substantially dif-rent from that associated with the historical SST fields. Any tempts to standardize the data or otherwise normalize it will gain lead to a discontinuity in the historical record that ould have misleading consequences.

Another type of instrumentation problem that has not been equately addressed has to do with the problem of sensor ift. A satellite sensor may gradually degrade in orbit while ithfully returning numbers to interested scientists on earth. ithout an external calibration, scientists could be led to the nclusion of a long-term trend in SST. If, for example, this as an increasing trend, it might be inferred that the first sign of a CO_2 warming had been detected. It seems that the only reliable way to avoid the instrument drift problem is to continually check the satellite SST products against in situ standards.

A final class of problem has to do with changes in the sensors and algorithms. If one wishes to study the behavior of SST over, say, 20 years, with satellite-borne devices, then it is fair to expect that improvements will be made in both the sensors and the algorithms over that period of time. Without care, however, each improvement could result in a "jump" in the SST time history associated with each satellite launch. Clearly, this problem can be overcome by allowing the sensor deployments to overlap. Alternatively, tying the satellite product to a consistent in situ data set also would avoid the problem.

5.5. *Recommendations*

The preceding text seems to justify one recomendation above most others. This has to do with finding methods to optimally blend satellite and in situ information into an estimate of a global SST field. Use of the ship and buoy data in such a product will alleviate the instrument problems alluded to earlier as well as allow a blend between the improved, mixed product and the historical SST fields that are currently available from ships alone. The satellite data will, of course, provide the data coverage and homogeneity of observing technique that the ship observations cannot provide.

The best methods for use in developing an optimal blend of satellite and in situ data are not known. However, recent work on this problem has produced promising results [*Reynolds and Gemmill*, 1984]. Still it appears that less resources are available to solve this problem than are required. A program needs to be established to optimally blend various types of satellite and in situ information into an SST product that will benefit a wide range of the scientific community as well as be a practical input to numerical weather and climate forecasts.

6. Discussion

The preceding discussions have shown that satellite-derived SST measurements are being increasingly utilized for a variety of oceanographic applications. In some cases, however, particularly for climate research, satellite data will not be widely accepted unless data availability, precision, and calibration accuracy can be maintained continuously for several years, even decades. Thus one must look to the future to plan specific sensors and data-processing capabilities required to provide the desired SST products.

Table 3 shows satellite sensors planned for launch during the next decade that will be useful for SST measurements. The NOAA satellite series G through J provides a continuation of the present operational capabilities with the AVHRR and HIRS/MSU sensors essentially unchanged from their present configurations. Starting from the early 1990's, the next satellites in the NOAA series, designated K through M, will carry a modified AVHRR with the addition of a 1.6-μm channel and will replace the MSU with a new instrument, the advanced microwave sounding unit (AMSU). The 1.6-μm AVHRR channel may improve the capability of the AVHRR to correct for aerosol contamination in the SST retrievals. The AMSU will have 20 microwave channels in the range 23–183 GHz and is primarily intended for atmospheric sounding. However, it should enhance the capabilities of the HIRS/(A)MSU combination for SST measurement.

Three more satellites in the present GOES series are planned, with no changes to the VAS instruments on board.

TABLE 3. Future Satellite Sensors for SST Measurement

Spacecraft	Time Frame	Sensors	Sensor Characteristics or Modifications	Projected Improvements Over Present SST Capability
NOAA G–J (U.S.)	1985–1990	AVHRR HIRS/ MSU	Same instruments as present (NOAA G is last four-channel AVHRR) (HIRS on NOAA H–J will have two modified channels)	
GOES 7–9 (U.S.)	1985–1991	VAS	Same instrument as present	
MOS-1 (Japan)	1987	VTIR	Infrared (6.3, 11, 12 μm) plus visible; polar-orbiting, 1-km resolution, 500-km swath, limited on-board recording	
ERS-1 (Europe)	1989	ATSR*	Infrared (3.7, 11, 12 μm), microwave (24, 36 GHz); polar-orbiting, dual-look, 1-km resolution, 500-km swath	improved water vapor and aerosol corrections
N-ROSS (U.S. Navy)	1989	LFMR/ SSMI	Microwave (5.2, 10.4 GHz)/(19.3, 22.2, 37, 85 GHz); polar-orbiting, 25-km resolution, 1400-km swath	ability to derive SST in cloud-covered areas
NOAA "Next" (K–M) (U.S.)	1990	AVHRR HIRS/ AMSU	AVHRR: additional 1.6-μm channel, switchable with 3.7 μm, AMSU: 20 microwave channels (23–183 GHz), 50-km resolution	AVHRR: better correction for aerosols; HIRS/AMSU: better humidity and cloud correction, operational product (?)
GOES "Next" (U.S.)	1991	VAS	Added 3.7-μm channel, modified 11- and 12.6-μm channels; sounder independent of imager	correction for reflected solar radiation, improved split-window retrieval rms; increased data availability, operational product (?)
Radarsat (Canada)	1991	AVHRR†	Same instrument as on NOAA K–M, polar-orbiting	
MOS-2 (Japan)	1992	OCTS†	3.7, 11, 12 μm plus five other visible/infrared channels.	
ERS-2 (Europe)	1992/3	TBD‡	TBD	
EOS/Polar Platform† (U.S.)	1993(?)	MODIS	Several visible and narrow-band infrared channels (3–5 μm, 8–14 μm), 1-km resolution;	improved spatial resolution, cloud filtering, and atmospheric corrections
		HMMR	several microwave channels (1.4–183 GHz), three subsystems	
Meteosat "Next" (Europe)	1994	VAS type† IR imager† MW sounder†	Geostationary Instruments in conceptual stage	improved SST from geostationary orbit, global coverage (with GOES and GMS).
GMS "Next" (Japan)	199?	VAS type†	Geostationary	see Meteosat

*Possibly also a 1.6 μm channel switchable with the 3.7 μm as in the AVHRR (NOAA K-M).
†Proposed.
‡To be determined.

The GOES "Next" satellites will carry a modified VAS, with an additional 3.7-μm channel and slightly shifted 11- and 12.6-μm channels. These changes should improve the SST measurement capability. There is a possibility that NOAA may produce an operational geostationary SST product when this new VAS instrument becomes available.

Two new instruments will also become available in the 1990's. The European satellite ERS-1 will carry an along-track scanning radiometer (ATSR), which will have infrared channels similar to the AVHRR but with two viewing angles: one at nadir and one at a forward incidence angle of 55°. This will provide an additional capability for correcting path attenuation through the atmosphere in deriving SST. The U.S. Navy Research Oceanographic Satellite System (NROSS) will carry a low frequency microwave radiometer (LFMR) as well as a special sensor microwave imager (SSMI) of a type scheduled for prior launch on an Air Force satellite (DMSP) in 1985. These two instruments, in conjunction, should provide an improvement over the SST-sensing capabilities of the SMMR.

In addition to the above, several other sensors that may be useful for SST measurement are planned for the 1990–1995 time frame. Most of these are presently in the proposal stage.

The increased data volume provided by these sensors will require superior capabilities for archiving, retrieval, and validation to those that are currently available to most researchers. Various scientific committees are now addressing these issues as part of the larger problem of satellite data management. Clearly, much work lies ahead in coordinating satellite SST data sets for specific research and operational programs and in determining optimum methods for producing validated SST products.

Acknowledgments. The research described in this paper was carried out, in part, by the Jet Propulsion Laboratory, California Institute of Technology, under contract with the National Aeronautics and Space Administration. Andrew Vastano was supported by grant OCE 80-26037 of the National Science Foundation and the Office of Naval Research under contract N00014-75-0537.

REFERENCES

Barnett, T. P., W. C. Patzert, S. C. Webb, and B. R. Bean, Climatological usefulness of satellite-determined sea surface temperatures in the tropical Pacific, *Bull. Am. Meteorol. Soc.*, *60*(3), 197–205, 1979.

Barton, I. J., Dual channel satellite measurements of sea surface temperature, *Q. J. R. Meteorol. Soc.*, *109*, 365–378, 1983.

Bates, J. J., and W. L. Smith, Sea surface temperature observations from geostationary satellites, *J. Geophys. Res.*, this issue.

Bernstein, R. L., Sea surface temperature estimation using the NOAA 6 satellite advanced very high resolution radiometer, *J. Geophys. Res.*, *87*(C12), 9455–9465, 1982.

Bernstein, R. L., L. Breaker, and R. H. Whritner, California Current eddy formation: Ship, air, and satellite results, *Science*, *195*, 353–359, 1977.

Blackmon, M. L., J. Geisler, and E. Pitcher, A general circulation model study of January climate anomaly patterns associated with interannual variation of equatorial Pacific sea surface temperature, *J. Atmos. Sci.*, *40*, 1410–1425, 1983.

Breaker, L. C., The application of satellite remote sensing to West Coast fisheries, *J. Mar. Tech. Soc.*, *15*, 32–40, 1981.

Brown, O. B., and R. E. Cheney, Advances in satellite oceanography, *Rev. Geophys.*, *21*(5), 1216–1230, 1983.

Brown, O. B., D. B. Olson, J. W. Brown, and R. H. Evans, Satellite infrared observation of the kinematics of a warm core ring, *Aust. J. Freshwater Res.*, 535–545, 1983.

Chahine, M. T., D. J. McCleese, P. W. Rosenkranz, and D. H. Staelin, Interaction mechanisms within the atmosphere, in *Manual of Remote Sensing*, vol. 1, edited by D. S. Simonett and F. T. Ulaby, chap. 5, American Society of Photogrammetry, Falls Church, Va., 1983.

Chamberlain, J. L., Application of satellite infrared data to analysis of ocean frontal movements and water mass interactions off the northeast coast, *Doc. 8/1/123*, *Ser. 429*, 15 pp., N.W. Atl. Fish. Org., Dartmouth, N. S., Canada, 1981.

Fiedler, P. C., Satellite remote sensing of the habitat of spawning anchovy in the Southern California Bight, *CalCOFI Rep. 24*, pp. 202–209, Calif. Coop. Fish. Invest., La Jolla, Calif., 1983.

Fiedler, P. C., Some effects of El Nino 1983 on the northern anchovy, *CalCOFI Rep. 25*, pp. 53–38, Calif. Coop. Fish. Invest., La Jolla, Calif., 1984*a*.

Fiedler, P. C., Satellite observations of El Nino along the U.S. Pacific Coast, *Science*, 224, 1251–1254, 1984*b*.

Fiedler, P. C., G. B. Smith, and R. M. Laurs, Fisheries applications of satellite data in the eastern north Pacific, *Mar. Fish. Rev.*, *46*, 1–13, 1985.

Gower, J. F. R., General overview of the nature and use of satellite remote sensing data for fisheries application, *Sci. Counc. Stud. 4*, pp. 7–19, N.W. Atl. Fish. Org., Dartmouth, N. S., Canada, 1982.

Hickey, B. M., The California Current System—Hypotheses and facts, *Progr. Oceanogr.*, *8*(4), 191–279, 1979.

Hofer, R., and E. G. Njoku, Regression techniques for oceanographic parameter retrieval using space-borne microwave radiometry, *IEEE Trans. Geosci. Remote Sensing*, *GE-19*, 178–189, 1981.

Ikeda, M., L. A. Mysak, and W. J. Emery, Observation and modeling of satellite-sensed meanders and eddies off Vancouver Island, *J. Phys. Oceanogr.*, *14*(1), 3–21, 1984.

Kelly, K. A., Swirls and plumes or application of statistical methods to satellite-derived sea surface temperatures, *CODE Tech. Rep. 18*, 209 pp., Coastal Ocean Dyn. Exp., Scripps Inst. of Oceanogr., La Jolla, Calif., 1983.

La Violette, P. E., The advection of submesoscale thermal features in the Alboran Sea Gyre, *J. Phys. Oceanogr.*, *14*, 550–565, 1984.

Lasker, R., J. Peláez, and R. M. Laurs, The use of satellite infrared imagery for describing ocean processes in relation to spawning of the northern anchovy (*Engraulis mordax*), *Remote Sensing Environ.*, *11*, 439–453, 1981.

Lau, N-C, Modeling the seasonal dependence of the atmospheric response to observed El Ninos in 1962–1976, *J. Atmos. Sci.*, in press, 1985.

Laurs, R. M., Fishery-advisory information available to tropical Pacific tuna fleet via radio facsimile broadcast, *Commer. Fish. Rev.*, *33*(4), 40–42, 1971.

Laurs, R. M., and J. T. Brucks, Living marine resource applications, *Adv. Geophys.*, *27*, 419–452, 1985.

Laurs, R. M., R. J. Lynn, R. Nishimoto, and R. Dotson, Albacore trolling and longline exploration in eastern North Pacific waters during midwinter, *NOAA-TM NMFS-SWFC 10*, 52 pp., 1981.

Laurs, R. M., P. C. Fiedler, and D. R. Montgomery, Albacore tuna catch distributions relative to environmental features observed from satellites, *Deep Sea Res.*, *31*, 1085–1099, 1984.

Legeckis, R., A survey of worldwide sea surface temperature fronts detected by environmental satellites, *J. Geophys. Res.*, *83*(C9), 4501–4522, 1978.

Lowry, B., and I. Leaky, Cooperation produces a flow of Gulf Stream information, *Sea Grant Today*, *12*, 3–5, 1982.

Maul, G. A., Application of GOES visible-infrared data to quantify mesoscale ocean surface temperatures, *J. Geophys. Res.*, *86*(C9), 8007–8021, 1981.

Maul, G. A., M. Roffer, and F. M. Sousa, Remotely sensed oceanographic patterns and variability of bluefin tuna catch in the Gulf of Mexico, *Oceanol. Acta.*, *7*, 469–479, 1984.

Maul, G. A., P. W. de Witt, A. Yanaway, and S. R. Baig, Geostationary satellite observations of Gulf Stream meanders: Infrared measurements and time series analysis, *J. Geophys. Res.*, *83*, 6123–6135, 1978.

McClain, E. P., Multiple atmospheric window techniques for satellite sea surface temperatures, in *Oceanography from Space*, edited by J. F. R. Gower, Plenum, New York, 1981.

McClain, E. P., W. G. Pichel, and C. Walton, Comparative performance of AVHRR-based multichannel sea surface temperatures, *J. Geophys. Res.*, this issue.

Mueller, J. L., and P. E. La Violette, Color and temperature signatures of ocean fronts observed with the Nimbus-7 CZCS, in *Oceanography from Space*, edited by J. F. R. Gower, Plenum, New York, 1981.

Milman, A. S., and T. T. Wilheit, Sea surface temperature from the scanning multichannel microwave radiometer on Nimbus 7, *J. Geophys. Res.*, this issue.

Montgomery, D. R., Commercial applications of satellite oceanography, *Oceanus*, *24*, 56–65, 1981.

Njoku, E. G., Satellite-derived sea surface temperature: Workshop comparisons, *Bull. Am. Meteorol. Soc.*, *66*(3), 274–281, 1985.

Rao, P. K., W. L. Smith, and R. Koffler, Global sea-surface temperature distribution determined from an environmental satellite, *Mon. Weather Rev.*, *100*, 10–14, 1972.

Reynolds, R. W., and W. H. Gemmill, A sea surface temperature analysis based on in-situ and satellite data, in *Proceedings of the 9th Climate Diagnostics Workshop*, pp. 408–416, National Oceanic and Atmospheric Administration, Washington, D.C., 1984.

Roffer, M., M. Carl, and F. Williams, Atlantic bluefin tuna-oceanography remote sensing, in *Proceedings of the 32nd Annual Tuna Conference*, edited by Alec Wild, Inter-Am. Trop. Tuna Comm., La Jolla, California, 1982.

Sherman, J. W., III (Ed.), *NOAA Workshop on Oceanic Remote Sensing*, vol. 2, *Workshop Support Documentation*, National Oceanic and Atmospheric Administration, Washington, D.C., 1980.

Short, K., How satellites can help you catch more fish and cut costs, *Nat. Fish.*, *60*(4), 38–39, 1979.

Strong, A. E., and E. P. McClain, Improved ocean surface temperature from space—Comparisons with drifting buoys, *Bull. Am. Meteorol. Soc.*, *65*(2), 138–142, 1984.

Susskind, J., and D. Reuter, Retrieval of sea surface temperatures from HIRS2/MSU, *J. Geophys. Res.*, this issue.

Susskind, J., J. Rosenfield, D. Reuter, and M. T. Chahine, Remote sensing of weather and climate parameters from HIRS2/MSU on TIROS-N, *J. Geophys. Res.*, *89*, 4677–4697, 1984.

Vastano, A. C., and R. L. Bernstein, Mesoscale features along the First Oyashio Intrusion, *J. Geophys. Res.*, *89*(C1), 587–596, 1984*a*.

Vastano, A. C., and R. L. Bernstein, Comparison of ship and satellite SST in the Kuroshio-Oyashio region, Satellite-Derived Sea Surface Temperature Workshop 2, *JPL Publ. 84-5*, 150 pp., Jet Propul. Lab., Pasadena, Calif., 1984*b*.

Vastano, A. C., and S. E. Borders, Sea surface motion over an anticyclonic eddy on the Oyashio Front, *Remote Sensing Environ.*, *16*(1), 87–90, 1984.

Vastano, A. C., and R. O. Reid, Sea surface topography estimation with infrared satellite imagery, *J. Atmos. Oceanic Technol.*, in press, 1985.

Vukovitch, F. M., and R. W. Crissman, Some aspects of Gulf Stream western boundary eddies from satellite and situ data, *J. Phys. Oceanogr.*, *10*(11), 1792–1813, 1980.

Vukovitch, F. M., Comparison of surface geostrophic currents calculated using satellite data and hydrographic data, final report, *Contr. N402730*, Fla. Inst. Oceanogr., Miami, Fla., 1985.

Weare, B. C., El Nino and tropical Pacific ocean surface temperature, *J. Phys. Oceanogr.*, *12*, 17–27, 1982.

Wentz, F. J., A model function for ocean microwave brightness temperatures, *J. Geophys. Res.*, *88*, 1892–1908, 1983.

Wilheit, T. T., and A. T. C. Chang, An algorithm for retrieval of ocean surface and atmospheric parameters from the observations of the scanning multichannel microwave radiometer, *Radio Sci.*, *15*, 525–544, 1980.

Wilheit, T. T., J. Greaves, J. Gatlin, D. Han, B. M. Krupp, A. S. Milman, and E. S. Chang, Retrieval of ocean surface parameters from the scanning multichannel microwave radiometer (SMMR) on the Nimbus-7 satellite, *IEEE Trans. Geosci. Remote Sensing, GE-22*, 133–143, 1984.

Yamanaka, I., Application of satellite remote sensing to fishery studies in Japan, *Sci. Counc. Stud. 4*, pp. 41–50, N.W. Atl. Fish. Org., Dartmouth, N. S., Canada, 1982.

T. P. Barnett, Climate Research Group, Scripps Institution of Oceanography, La Jolla, CA 92093.

R. M. Laurs, Southwest Fisheries Center, National Oceanic and Atmospheric Administration, La Jolla, Ca 92038.

E. G. Njoku, Jet Propulsion Laboratory, California Institute of Technology, Pasadena, CA 91109, and Department of Engineering, Harvey Mudd College, Claremont, CA 91711.

A. C. Vastano, Department of Oceanography, Texas A&M University, College Station, TX 77843.

(Received January 31, 1985;
accepted June, 13, 1985.)

8565

The 1982–83 El Niño Event off Baja and Alta California And Its Ocean Climate Context

J. Norton, D. McLain, R. Brainard, and D. Husby
National Marine Fisheries Service

Introduction

The 1982-83 El Nino brought extremely warm water to the coast of Alta and Baja California as part of one of the most intense ocean-atmosphere events of the century. This report describes this event in terms of surface and subsurface temperature, sea level, and large scale atmospheric pressure changes. The 1982-83 event is examined as part of the continuum of events occurring over the past 13 years (1971-83), a period containing two other tropical El Ninos (1972-73, 1976-78) and two California warming events seemingly unrelated to tropical warmings (1979-80, 1980-81). The 1976-77, 1977-78, 1979-80, 1980-81, and 1982-83 winters have been warmer than normal. Consequently, the period before 1976 was anomalously cool compared to the 13 year mean. These interannual variations are discussed in terms of physical characteristics of the California Current System and associated coastal upwelling, which are the predominant ocean features within 1000 km of the coast. The extreme nature of the 1982-83 event is examined by comparison with other winters of the series. Time-distance contour plots are used to graphically interpret interannual variations over the 13 year period and over the 2123 km distance from the southern tip of Baja California to the Alta California northern border.

The oceanographic term "El Nino", historically, has been applied to ocean surface warming events in the equatorial Pacific off the coasts of Peru and Ecuador. These events generally begin during the Christmas season. Hence, the Spanish words El Nino refer to the Christ Child. Since El Nino lasts through the northern winter, common terminology refers to two or more calendar years. More recently, El Nino became a generic term describing anomalous warm events in eastern boundary current regions of the world's ocean (Wooster 1960). Current understanding is that El Nino is part of a global ocean-atmosphere perturbation called "El Nino-Southern Oscillation" (ENSO) (Quinn 1974, Rasmusson and Wallace 1983). The Southern Oscillation is a quasi-periodic cycle (2-10 years) observed in the atmospheric pressure differences between Pacific and Indian Oceans and the Tahiti minus Darwin, Australia sea level pressure difference is a commonly used Southern Oscillation Index (SOI). Bjerknes (1969) found that El Nino events occur as the trade winds relax and the SOI drops sharply.

ENSO may include the tropical El Nino (TEN) and a California El Nino (CEN). Like the TEN, the CEN is characterized by warming in the coastal ocean's surface layers and both warm events may be synchronous. Other oceanic warming events also occur along the greater California coast (see below). These are mid-latitude warm (MLW) events. CEN events occur in concert with the TEN events: MLW events do not.

Major Geographic and Oceanic Features

The coast of Baja and Alta California extends 19.1 degrees of latitude from Cabo San Lucas at 22.9^{0}N, to the northern California border at 42^{0}N. East to west, the distance from Cabo San Lucas at 109.9^{0}W to Cape Mendocino at 124.4^{0}W is 14.5^{0} (1363 km). In the following "California" refers to Alta California (USA).

The California Current transports cool, low salinity subarctic water southward along the greater California coast (Sverdrup, et al. 1942, Reid et al. 1958). Warmer, more saline, eastern North Pacific Central Water lies west of the California Current creating a positive temperature gradient from east to west as well as north to south. Consequently, warming along the coast can result from local heating and/or increased transport from the south and/or west.

Off central, southern and Baja California, a countercurrent flows northward inshore of the southward flowing California Current where it frequently becomes the dominant nearshore circulation feature (Wooster and Jones 1970, Wickham 1975). North of Pt. Conception, the surface countercurrent is generally most intense in late fall and winter (34.3^{0}N). However, recent studies by Wickham and Tucker show countercurrent activity throughout the year during the warm 1978-80 period (Bird et al. 1984). South of Point Conception, the countercurrent is an important nearshore feature throughout the year, but it is not necessarily continuous with the surface Counter Current to the north (Reid 1960). The California Current System is characterized at depth by a weak poleward countercurrent having maximum speed and persistence over the continental slope. The California Current thickens seaward of 200 km resulting in a deeper countercurrent (Reid 1965, Hickey 1979).

The California Current System's western edge is a broad complex transition zone joining the subarctic transition on the north to the subtropical transition on the south as shown in Figure 1 (Saur 1980, Bernal and McGowan 1981).

Upwelling, caused by northerly winds and resulting offshore Ekman transport is a dominant oceanographic process in spring and summer along the entire California and Baja California coast (Sverdrup et al. 1942). Cooler, higher salinity subsurface waters are brought to the surface in a relatively narrow coastal band and then mixed and carried offshore by other advective processes (Smith 1968, Hickey 1979). The resulting density distribution enhances southward California Current flow. Upwelling occurs year-round off Baja California under the influence of the North Pacific High pressure system. Off central and northern California, however, the atmospheric high weakens and moves south in the winter as the Aleutian Low pressure system intensifies. The winds off central and northern California reverse as these pressure systems change. Downwelling occurs in winter under southerly winds asso-

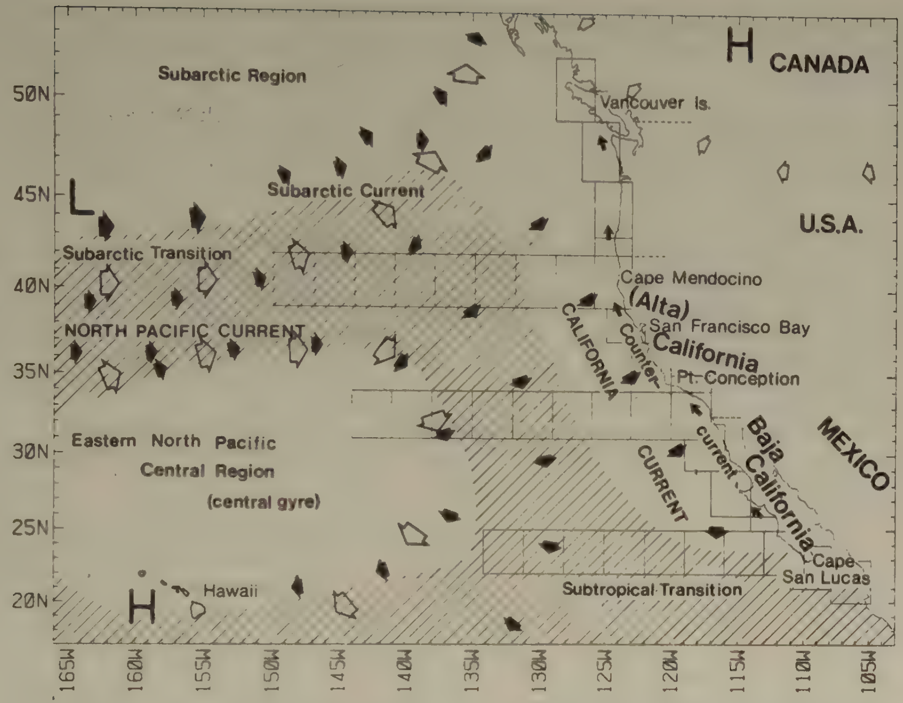
Subarctic Region
H
CANADA
Vancouver Is.
50N
45N
L
Subarctic Current
U.S.A.
Subarctic Transition
40N
Cape Mendocino
(Alta)
San Francisco Bay
California
NORTH PACIFIC CURRENT
CALIFORNIA
Counter
35N
Pt. Conception
30N
Eastern North Pacific
Central Region
(central gyre)
current
CURRENT
Baja
California
MEXICO
25N
Cape
San Lucas
Subtropical Transition
20N
H
Hawaii
165W
160W
155W
150W
145W
140W
135W
130W
125W
120W
115W
110W
105W

Figure 1. Schematic representation of northeastern Pacific Ocean climatology showing surface winds (open arrows), surface currents (solid arrows), and dominant atmospheric pressure systems: Aleutian Low, North Pacific High, and North American High. Letters "H" and "L" are near centers of action defined by Wallace and Gutzler (1981). Subarctic, California Current and Subtropical transition zones are indicated by hatching. Also shown are locations of $3^{o}x3^{o}$ areas where surface and subsurface temperature are summarized.

ciated with intensified Aleutian Low, deepening the mixed layer and facilitating poleward flow along the coast.

Connections Between Tropical and California El Niños

El Nino years on the California coast coincide with El Nino years along the South American coast because of energy transfer from the tropics to mid-latitudes by both oceanic and atmospheric processes. Each process has received considerable attention in the literature (McCreary 1976, Picaut 1984, Rasmusson and Wallace 1983, Wallace and Gutzler 1981).

Tropical El Nino's are associated with slackening of trade winds blowing from east to west over the tropical Pacific. As the trade winds relax, the Southern Oscillation Index (SOI) falls, and even reverses, resulting in a downwelling disturbance which propagates eastward toward South America with characteristics of an equatorially trapped Kelvin wave (Halpern et al. 1983, Cane 1983). The energy transfer that occurs along the equator is the result of the radiation of many Kelvin waves that superimpose to form a beam of energy that propagates eastward and downward (Picaut 1984). When the eastern boundary is reached, poleward and downward-propagating, coastal Kelvin waves are formed. These Kelvin wave packets bring downwelling perturbations to the California coast. This wave energy with subsequent advective adjustment can produce a remotely forced CEN event. This is consistent with subsurface temperature observations from the California coast shown below.

The atmospheric connection to mid-latitudes involves a mechanism originally postulated over fifty years ago by Walker (Rasmusson and Wallace 1983). As the Kelvin wave propagates eastward along the equator, it is accompanied by anomalously high sea surface temperature (SST). Through evaporation and condensation processes, the warm water transfers increased energy to the atmosphere. This energy appears to set up a quasi-stationary tropospheric wave pattern as it propagates northward in great circle arcs (Wallace and Gutzler 1981, Horel and Wallace 1981). In this way, extensive tropical SST anomalies can be teleconnected to mid-latitudes through the atmosphere, altering wind forcing on the eastern subtropical Pacific, thousands of miles to the north (Bjerknes 1969, Quiroz 1983, Pan and Oort 1983). These teleconnections appear most significant in winter and their impact at mid-latitude depends upon ongoing subtropical processes (Wallace and Gutzler 1981, Rasmusson and Wallace 1983, Haney 1984).

The Pacific/North American (PNA) Index was developed to measure tropical to mid-latitude teleconnection (Wallace and Gutzler 1981). This index is derived from a linear combination of 500 millibar atmospheric height anomalies at "centers of action" along the great circle standing wave pattern from the tropics through the North-Pacific High, Aleutian Low, North American Continental High and Florida Low pressure systems. Each is intensified by the standing wave, so that higher highs and deeper lows will contribute positively to the index value. Three of these pressure systems are indicated schematically in Figure 1.

Horel and Wallace (1981) have presented important correlations between the PNA pattern and TEN activity. However, Douglas et al. (1982) point out that PNA type circulation can occur without TEN as it did in the winters of 1958-59, 1960-61, 1962-63, 1967-68, 1979-80 and 1980-81. Conversely, the intense TEN of 1972-73 occurred without a fully distinctive PNA pattern. It is probable that tropical forcing through the PNA pattern has maximum effect when in phase with pressure patterns brought about by complementary subtropical processes (Rasmusson and Wallace 1983). There also seems to be a time lag in the atmosphere's response to equatorial SST forcing (Pan and Oort 1983). The 1982-83 ENSO brought extreme El Nino conditions to the eastern tropical Pacific and the characteristic PNA pattern was formed over the North Pacific (Rasmusson and Wallace 1983, Halpern et al. 1983, Toole 1984).

Data Sources and Methods

El Nino is of large space and time scale and thus we based our analyses on historical data files of weather observations and ocean temperature profiles. The data were averaged by month for 3^{0} longitude-latitude areas.

Surface and subsurface temperature and atmospheric pressure data were obtained from the archives of the U.S. Navy Fleet Numerical Oceanography Center in Monterey, California (FNOC). Sea surface temperatures (SST) were obtained from the file of surface marine weather observations received in real-time at FNOC. The wind speed and upwelling index data were derived from the 6-hourly northern hemisphere pressure analyses (Bakun 1973, 1975).

The SST data were averaged by month in 1° latitude-longitude areas and then further aggregated to provide means for the 3° latitude-longitude areas in transects along the coast and westward from the coast (Figure 1). The total number of observations in the study area for the 1971-83 period exceeded 300,000. Over half of the observations were taken within 100km of the coast. Monthly means for SST may represent several thousand values depending on location.

Subsurface temperature profiles were taken from the FNOC Master Oceanographic Observations Data Set, which is an archive of bottle casts, mechanical and expendable bathythermographs, and CTD casts. Although the number of subsurface observations is an order of magnitude less than that of surface observations, the improved accuracy of the individual observations yields a more accurate data set.

Sea level data for tide stations along the west coast of the United States were obtained from Mr. Ray Smith of the National Ocean Survey, Rockville, Maryland. Sea level data for two Canadian stations were obtained from Dr. S. Tabata, Institute of Ocean Science, Sidney, British Columbia and data from Baja California were obtained from Ing. Francisco Grivel Pina, Instituto de Geofisica, Mexico, D.F. Monthly means of sea level were computed from daily values.

Time-distance plots of the variables under study were produced to display large-scale fluctuations in time and space (e.g., Figure 2a). In each plot, time is on the horizontal axis with years and months indicated. The vertical axis is distance, either along the coast (as in Figure 2a) or offshore (as in Figure 4a). The monthly mean values are contoured allowing objective assessment of major patterns. Each contour line is interpreted as the excursion of an isopleth through time and space. Areas north of California and south of Baja California are often included in alongshore plots to allow greater spatial continuity of features. Anomalies of variables from the long-term mean were computed and plotted in time-distance form (as in Figure 2b) to show interannual changes.

Sea Surface Temperature

Figure 2a is a time-distance plot of sea surface temperature along the coast from south of the tip of Baja California to Vancouver Island. A pronounced annual cycle is shown by the large excursions of each contour line (isotherm). Farthest northward isotherm extension or maximum SST occurs in summer and fall. Minimum SSTs, as shown by farthest southward isotherm excursions, occur in winter or spring. Isotherms at higher latitude have larger annual excursions, eg. the 12°C isotherm crosses 12-18 degrees of latitude while the 20°C isotherm has about half this latitudinal excursion. The subtropical transition zone off southern Baja California is shown by the denser packing of isotherms south of 29°N. Interannual spatial variation in SST is weak south of 23°N.

The extreme nature of the 1982-83 CEN is reflected in the 16°C isotherm which extended as far north as San Francisco (37.8°N) in October 1983. This extension was unprecedented in the previous 11 years and represents an anomaly of 1.2-2.0°C or 2 to 2.2 times the between-year standard deviation (sdu) for that month and latitude. The minimum SST

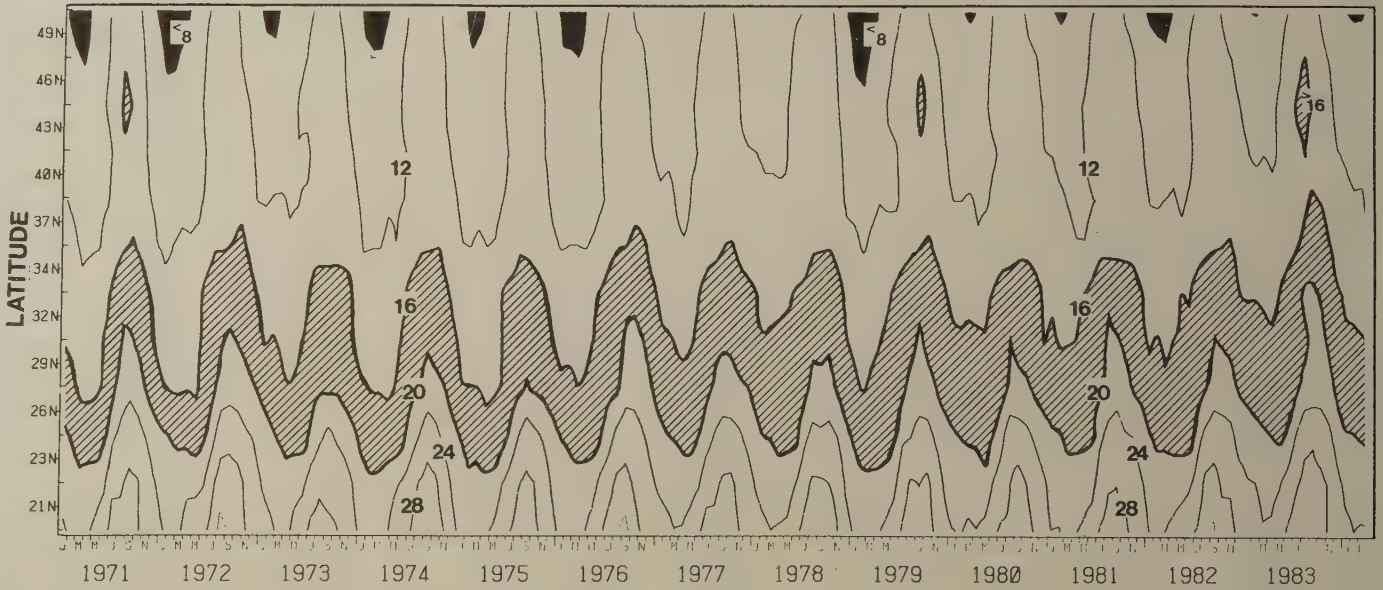

Figure 2a. Time-distance contour plot of monthly mean sea surface temperature (^{o}C) at 12 $3^{o}x3^{o}$ blocks of latitude and longitude on the alongshore transect from Baja California to Vancouver Island. Values are mean SST for $3^{o}x3^{o}$ blocks of sub-means for 1^{o} blocks. Contour interval is 4^{o}C.

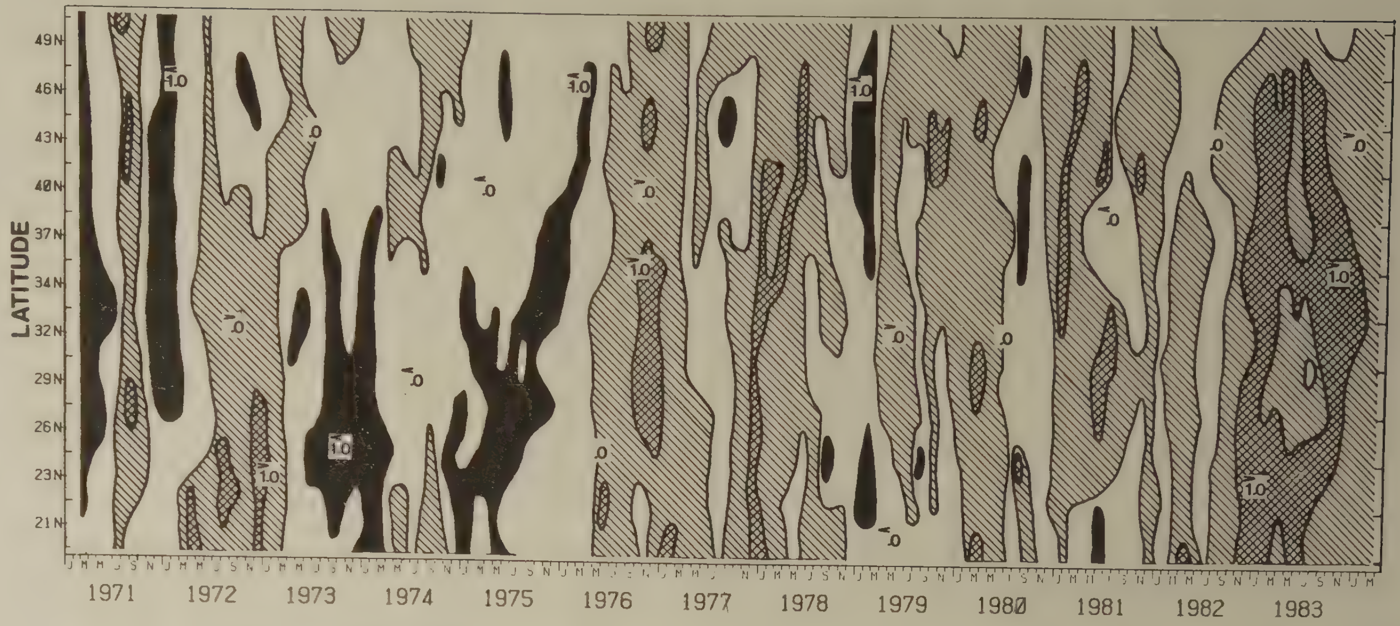

Figure 2b. Anomaly of monthly mean sea surface temperature on alongshore transect from Baja California to Vancouver Island. Hatched areas indicate anomaly between 0 and +1^{0}C and cross-hatched areas greater than +1^{0}C. Unshaded areas indicate anomaly between 0 and -1^{0}C and areas shaded black anomaly less than -1^{0}C. Block locations are the same as in Figure 2a.

during the previous spring was much warmer than usual. The maximum SST during fall 1982 was unusually high, equalled only by the fall seasons of 1979, 1976 and 1972, a MLW and two CEN years, respectively. Water of greater than 16°C was also present in an unusually large closed cell near 43°N. Warmer winters since 1976 are indicated by the reduction in areas less than 8°C near 49°N and by the greater distance between the 16°C and 20°C isotherms off Baja and southern California (23° -34°N). The maxima of the 20°C isotherm tend to follow those of the 16°C isotherm, but the 20°C minima are much more stable, causing the 16°-20°C band to widen in winter (Figure 2a).

The extreme nature of the 1982-83 event becomes more evident when the annual cycle is removed by taking anomalies from monthly mean values (Figure 2b). Areas representing anomaly greater than 1°C have wider meridional distribution and persist longer during the 1982-83 event than in any of the other warm events during 1971-83. The CEN winter of 1976-77 shows a comparable pattern. Figure 2b shows that during 1982-83, anomaly exceeding 1°C appears as two vertical bands connected at 24°N and 36°N by persistent periods lasting from November 1982 through November 1983. These vertical bands represent almost simultaneous occurrence of the anomaly over the range from 29°N to 49°N. Anomalies greater than 1°C occur first in the subtropical transition. The extreme anomaly (2.0°C or 2.0 sdu) south of 29°N represents a northward shift of the 20°C isotherm due to decreased or displaced input of cooler California Current water. Because of the steep SST gradient in the subtropical transition, a small geographical change in isotherm position will create relatively large anomalies. The area of anomaly persistence near 36°N on the central California coast probably reflects a relatively large decrease in seasonal upwelling and climatological tendency toward negative wind stress curl at these latitudes (Nelson 1977). Increased input of offshore water into the coastal region north of 46°N may have been responsible for persistence of the anomaly greater than 1°C in these areas.

CEN warming effects were partially negated in spring and summer 1983 by spring upwelling when anomalies remained positive but less than 1°C. Maximum SSTs normally occur in the inshore California Current System in the fall when both the California Current and the countercurrent are near minimum intensity and insolation has had maximum effect (Sverdrup et. al. 1942, Reid et al. 1958). The second period of extreme anomaly corresponds to this period of maximum seasonal SST. The tropical El Nino of this period also had two maxima in temperature (Smith 1984).

Generally warmer SSTs since mid-1976 are indicated by Figure 2b. Much of the period after 1976 had positive SST anomaly and much of the period before 1976 had negative SST anomaly. Extensive periods with positive anomaly during the 1979-80 and 1980-81 winters indicate MLW events, since there was no corresponding TEN activity.

The SST anomalies were summed for the entire coast for each 6 month period during 1971-84 to show large-scale features of the alongshore anomalies. Scaled values are plotted in Figure 3. A succession of warm events after the first half of 1976 produced a positive shift in SST involving the entire California Current System's inshore component. In the winter of 1976-77, there was a California El Nino accompanied by a tropical El Nino. In 1977-78, CEN and ENSO conditions reoccurred. Winter and spring of 1978-79

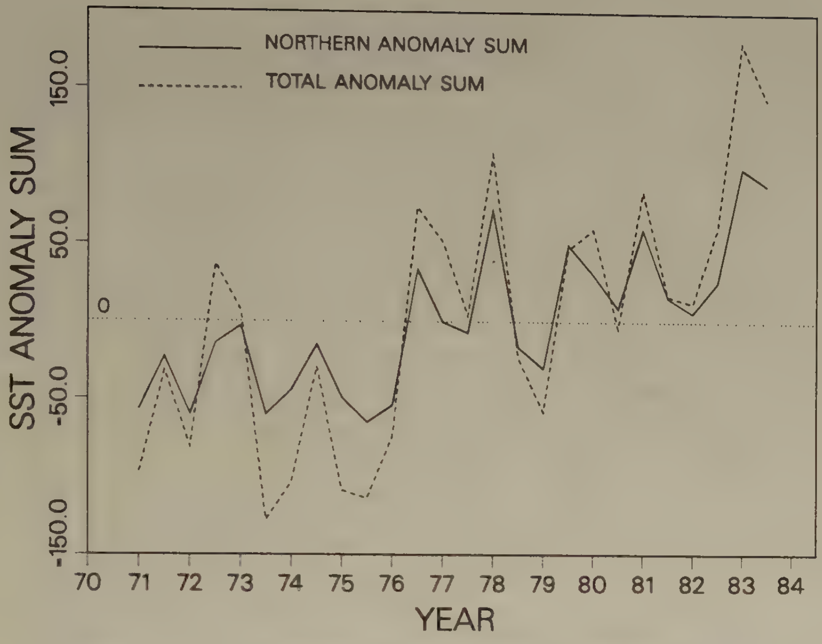

Figure 3. Six-month sums of SST anomaly on alongshore transect from Baja California to Vancouver Island. Abstract of data presented in Figure 2b. Northern Anomaly Sum is for northernmost 7 blocks of transect and Total Anomaly Sum is for all 12 blocks of transect.

were relatively cool, but temperatures remained above pre-1976 levels. In 1979-80, a MLW event occurred off California and Baja California. Similar though less extreme atmospheric and oceanic conditions occurred in 1980-81. The 1981-82 winter temperatures were near normal for the 13 year period. More recently, the extreme CEN and TEN 1982-83 season elevated coastal temperature to a 13 year high. In 1983-84 SSTs remained above normal through fall 1984. Note that during CEN years, the northern and southern portions of the transect both contribute to the total but during MLW years, the northern portion is dominant.

To examine the offshore extent of SST fluctuations, the data were abstracted to form three transects of nine 3^{0} blocks extending from the coast 3000 km westward (Figure 1). A time-distance plot for the transect off Southern California (Figure 4a) shows warm fingers reaching in from offshore during summer and fall and cold fingers of California Current water extending offshore to near 126^{0}W during the winter months.

Regions of cool water (less than 14^{0}C) are prominent features from February through May in 1971, '72, '74, '75, '76, but appear in only one year after 1976 and this occurrence in 1979 is minor compared to the previous years. Cool water is brought into the coastal area from the north by the California Current. Upwelling is less important at the one month-3^{0} scales. Lack of water less than 14^{0}C since 1976 suggests a diminished California Current since 1976. During the third quarter of 1972, '76, '78, '79, '82 and '83 SSTs of greater than 18^{0}C occurred over the entire zonal range (Figure 4a). In general these events precede MLW and CEN winters, and probably represent early surface countercurrent influence. Normally the areas within the 16°C isotherm are broken into inshore and offshore regions by the cool California Current maximum which occurs 200 - 400 km offshore. The absence of persistently strong California Current flow since 1976 has allowed the area greater than 16°C to become zonally continuous in summer and fall during five of the last eight years.

In 1980 and 1983 offshore water was cooler than in other years; SSTs greater than 22°C were absent at the western end of the Southern California transect (Figure 4a). Negative SST anomalies were widespread offshore in fall (Figure 4b). Both events followed winters of intense PNA-type atmospheric circulation. In both preceding winters, a deep Aleutian Low created high winds of long fetch blowing eastward across the Pacific. These intense and persistent winds may have redistributed the warm surface water of the central gyre and transition zone, decreasing horizontal density gradients in the upper layers and thereby decreasing the baroclinicity of the California Current Region. The warm water displaced onshore by southwesterly winds near the coast would tend to increase poleward countercurrent activity which would in turn bring more warm water into the coastal zone from the south. Comparison of Figures 4a and 4b shows that the absence of 22°C water offshore in 1980 and 1983 represents extreme negative anomaly (to -1.8°C, sdu to 2.4). Nearshore, positive SST anomaly is associated with each event. During 1983, the shoreward extension of the 20°C isotherm was the most extreme of the series, as shown by anomalies to 1.2°C (sdu to 2.5) in fall 1983 (Figure 4b).

The SST anomalies along the offshore transect tend to be of opposite sign in nearshore and offshore areas (Figure 4b). Note similarities among 1971, 1973, 1974 and 1975, which were cool years. Negative anomaly occurred in nearshore areas from 1971 through 1976, accompanied by positive anomaly offshore; producing horizontal density structure conducive to an enhanced California Current. In 1976 and the years following, negative anomaly commonly occurred offshore, accompanied by positive anomaly nearshore; opposing California Current baroclinicity.

Warm winters since 1971 were compared by summarizing the three offshore transects (Table 1). Offshore areas were divided into three 1000 km zones, with the nearshore zone containing most of the California Current System and the middle zone in the transition region (Figure 1). The outer zone of the northern transect extends into and sometimes through the northerly meander in the North Pacific and Subarctic Currents (Kirwan et al. 1978) where temperatures are more characteristic of the Subarctic Region. The transect off southern California reaches into the central gyre and the offshore zone of the Baja California transect remains in the subtropical transition.

In Table 1, the 1982-83 winter is shown to have the warmest SSTs of the series inshore and the coolest offshore. If the full length of each transect is considered, the 1982-83 CEN must be considered a cool SST event. In the inshore zone, the 1976-77 and 1983-84 winters were as warm as in 1982-83. Winter 1983-84 probably represents residual warming of the 1982-83 CEN. Note, the inshore zone remained warm in 1983-84, but offshore the cool anomaly of the previous year was lost in the southern and Baja California transects.

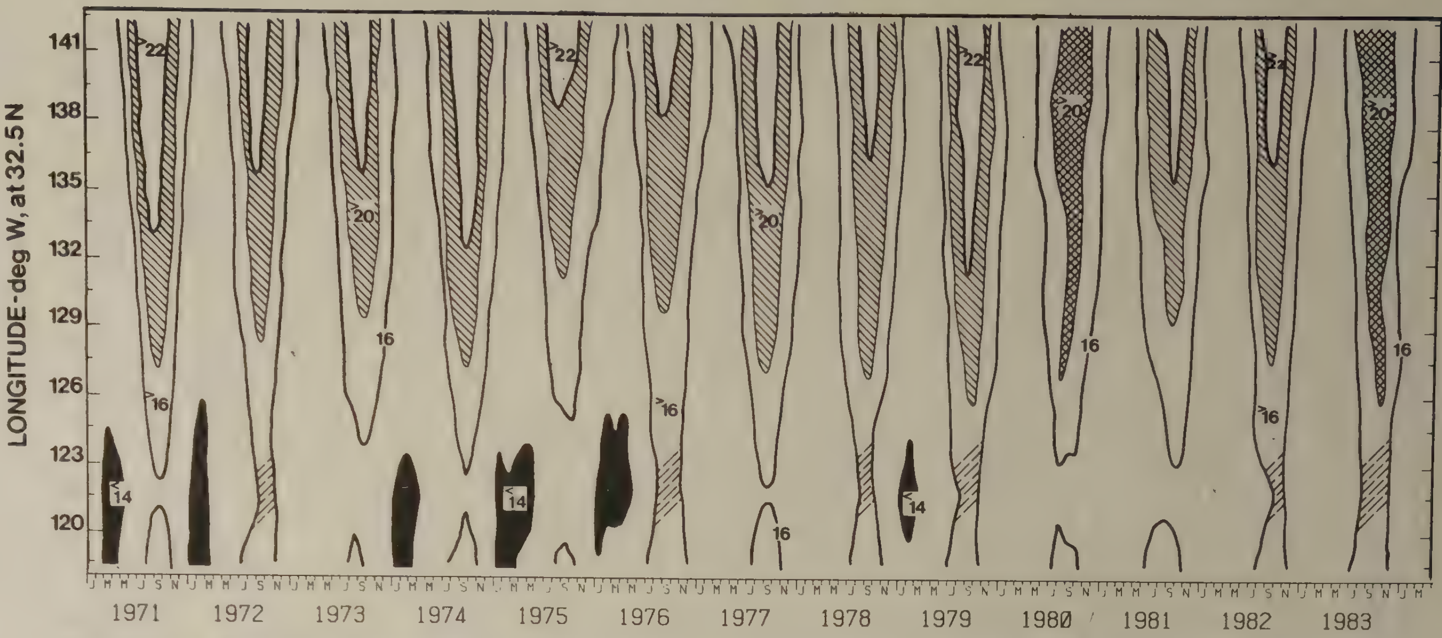

Figure 4a. Sea surface temperature of offshore transect west from southern California. The coast is at the bottom of the figure and the top of the figure is a point 2900 km offshore. The contour interval is 2°C except that the 18°C line is omitted. SSTs between 20°C and 22°C are hatched except for the two years 1980 and 1983 when SST greater than 22°C was not present offshore and the area greater than 20°C cross-hatched for emphasis (see text). Diagonal dashes near 122°W indicate years when SSTs greater than 16°C occurred continuously along the entire transect.

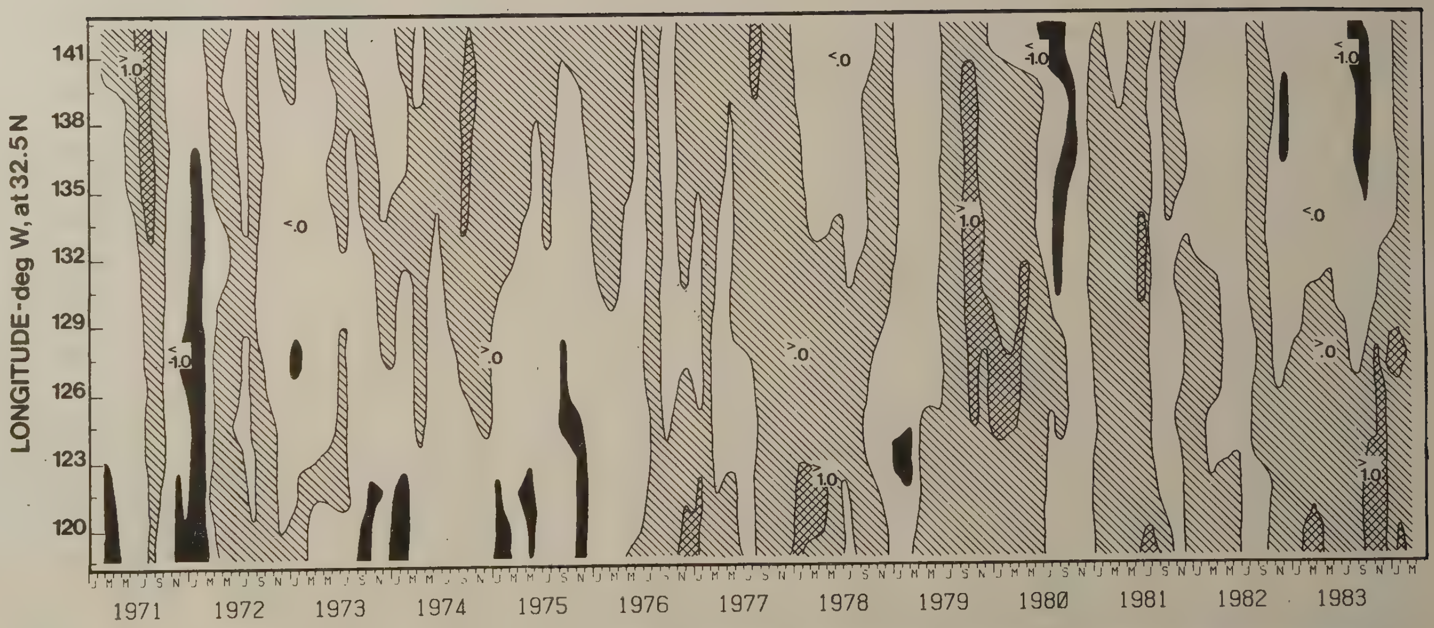

Figure 4b. Anomaly of sea surface temperature of offshore transect from southern California. Hatched areas indicate anomaly 0 to +1°C and cross-hatched areas anomaly greater than +1°C. Unshaded areas indicate anomaly between 0 and -1°C, and areas shaded black anomaly less than -1°C. Block locations are the same as Figure 4a.

Table 1. Summary table of SST anomaly during warm event winters (Nov.-Feb.) since 1971 along the three offshore transects; Northern California, Southern California, and Baja California. SST anomalies are summarized for 1000 km zones along each transect. The symbols represent SST anomaly in each zone along a transect; "W" represents areas having more than 50% positive SST anomaly and "C" represents areas having more than 50% negative anomaly. The numbers under each column are weighted average SST anomaly indices in each zone for each of the three transects; positive numbers representing positive anomalies and negative numbers representing negative anomalies. The anomaly indices are summed by winter in the sixth column and compared to event type (see text).

Winter (Nov-Mar)	Transect	Offshore 2000-3000	Zone Middle 1000-2000	Inshore 0-1000 km	Event Type (Warm Index Total)
1972-73	North	W	W	C	CEN
	South	C (10)	C (-15)	W (-4)	(-9)
	Baja	W	C	W	
1976-77	North	W	W	W	CEN
	South	W (12)	C (15)	W (25)	(53)
	Baja	W	W	W	
1977-78	North	C	C	W	CEN
	South	W (1)	W (15)	W (19)	(35)
	Baja	W	W	W	
1979-80	North	C	W	W	MLW
	South	W (10)	W (20)	W (10)	(40)
	Baja	W	W	C	
1980-81	North	C	W	W	MLW
	South	W (-4)	W (19)	W (12)	(27)
	Baja	W	W	W	
1982-83	North	C	C	W	CEN
	South	C (-9)	C (-19)	W (27)	(-1)
	Baja	W	C	W	
1983-84	North	C	C	W	CEN
	South	W (2)	W (10)	W (26)	(38)
	Baja	W	W	W	

The 1976-77 CEN occurred at the end of a cool onshore - warm offshore period (McLain 1983). It appears that in this winter the central gyre remained warm from the previous period and that the inshore zone warmed under CEN influence. Overall, the SSTs of the 1976-77 CEN were the warmest of the series.

Since 1976-77, each warm winter has shown a tendency to negative SST anomaly offshore in the northern transect (Table 1). This could be the result of increased mixing by high winds in this area and/or a southward shift of the subarctic transition under the influence of basin-wide forcing due to persistent PNA circulation.

During the 1979-80 and 1980-81 MLW winters, warming occurred in the middle zone of all three offshore transects. Since this also occurred under

PNA pattern influence, the suggestion is that surface water is being transported from west to east under the influence of the intensified Aleutian Low. In the case of the MLW winters, warm surface water is moved from offshore into the middle zone. The Aleutian Low was even stronger in winter 1982-83 (Quiroz 1983). More water moved to the south and east in the offshore and middle zones bringing cooler water to the surface in the middle zone and extreme Ekman convergence at the coast. This is indicated by the 1982-83 pattern shown in Table 1. When extreme wind forcing relaxed in 1983-84, a more stable pattern returned offshore even though the inshore zone remained warm.

Subsurface Temperature

Mean monthly temperature time-distance plots at 100 and 200m depths for the same alongshore transect used for SST are shown in Figure 5. The seasonal cycle at 100m is influenced by vertical motion of the thermocline, especially off northern California where turbulent mixing causes mixed layer depths greater than 80m in winter (Husby and Nelson 1982). As with SST, subsurface isotherms make greater latitudinal excursion in the north (see Figure 2a). Isotherms are also more closely packed in the south, but the temperature gradient of the subtropical transition is not as large at 100m as it is at the surface.

In 1982-83, two northward excursions of the 10°C isotherm mark anomalous warming at 100m associated with the 1982-83 CEN (Figure 5). The first warming occurred in winter 1982-83 and after cooling in spring and summer, the second major warming occurred in late summer, fall and winter 1983. Resulting positive anomalies of up to 1.5°C (3.1 sdu) occurred between 46°N and 49°N in the first warming episode. The extreme excursions of the 10°C isotherm off central California in 1982-83 caused anomalies to 1.5°C (3.0 sdu) and 1.4°C (2.8 sdu) for the 1982-83 winter and 1983 fall respectively. Farther south between 29°N and 34°N, anomalies were 2.3 to 3.0°C (2.8 to 3.0 sdu) in winter 1983 and to 1.8°C (3.6 sdu) the following fall. These were the most extreme positive anomalies encountered in the study. The 8°C isotherm was depressed below the 100m level for the entire 1982-83 event (Figure 5). Relative extent of the two northward isotherm excursions varies with latitude and depth. The TEN associated first peak is more persistent with depth and distance south. This persistence is clearly suggestive of oceanic connection between tropical El Nino and California El Nino.

Extreme excursions of the 10°C isotherm at 100m are also seen during the 1972-73 CEN and the 1979-80 MLW winters. If northward excursion of this isotherm is considered alone, the 1979-80 winter is the most extreme, producing an anomaly of 1.6°C (2.7 sdu) at 43°N. The extremity of this winter was also evident at the surface (Figures 2a,b and 4a,b). These two events represent extremes of quite different forcing processes. The 1972-73 CEN was unaccompanied by a fully developed PNA pattern and the 1979-80 MLW event was unaccompanied by anomalous equatorial Kelvin wave activity (Douglas et al. 1982, Cane 1983).

The excursions of the 8°C isotherm during the 1972-73 CEN were as large at 200m as they were at 100m in the 10°C isotherm (Figure 5). The 1972-73 signal was also strong to the south in the subtropical transition, where

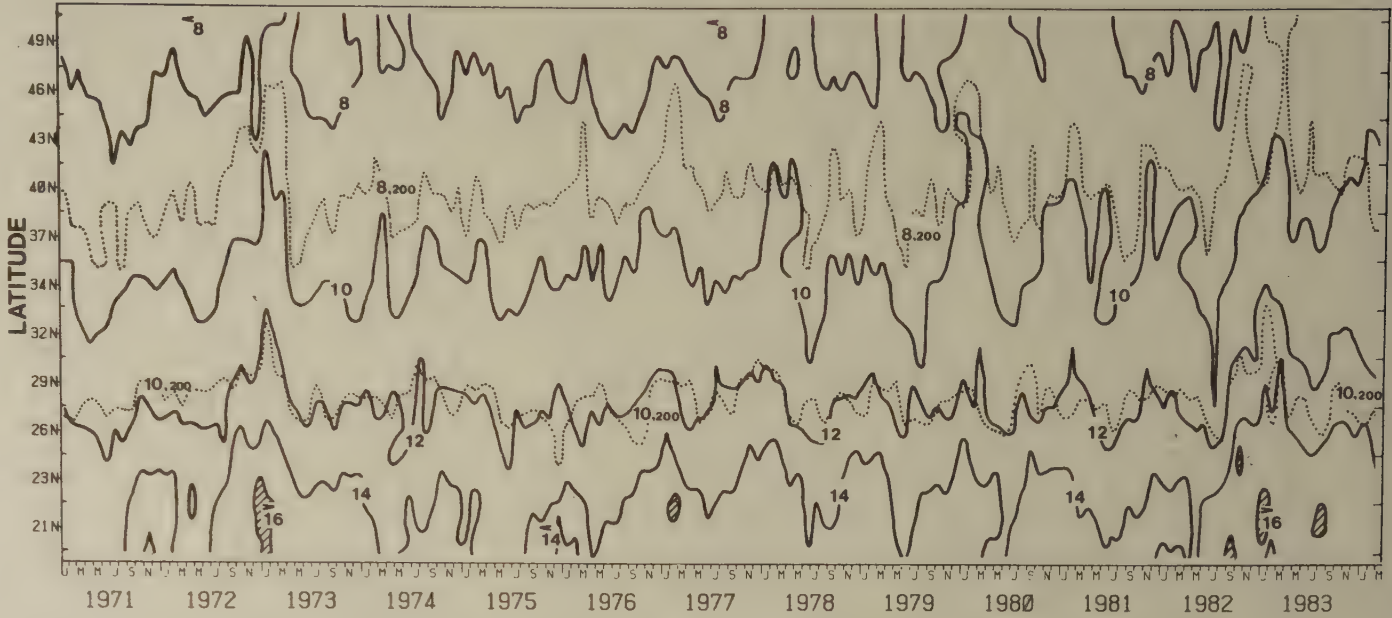

Figure 5. Monthly mean temperature at 100 m depth (solid lines) of alongshore transect from Baja California to Vancouver Island. Contour interval is 2°C. The 8° and 10°C isotherms at 200m (dotted lines) are also shown for comparison.

Table 2. Summary table of temperature at 100 m during warm event winters since 1971 along the three offshore transect. Symbols and numbers are the same as in Table 1.

Winter (Nov-Mar)	Transect		Zone		Event Type (Warm Index)
		Offshore	Middle	Inshore	
1972-73	North	W	W	W	CEN
	South	W (8)	C (0)	W (19)	(27)
	Baja	C	-	W	
1976-77	North	W	C	C	CEN
	South	W (16)	C (-16)	C (-7)	(-7)
	Baja	-	-	C	
1977-78	North	W	C	C	CEN
	South	C (-6)	C (-4)	C (-12)	(-22)
	Baja	-	-	C	
1979-80	North	W	W	W	MLW
	South	C (1)	C (2)	C (-14)	(-11)
	Baja	W	W	C	
1980-81	North	C	W	W	MLW
	South	C (-3)	W (17)	C (-9)	(5)
	Baja	W	-	C	
1982-83	North	C	C	W	CEN
	South	C (-2)	C (-4)	W (20)	(14)
	Baja	W	-	W	
1983-84	North	C	C	W	CEN
	South	C (-1)	W (-5)	W (16)	(10)
	Baja	W	-	-	

the extent of 16°C water at 100m was as great in this period as at any other time in the series.

In contrast to the 1972-73 CEN, the 1979-80 MLW event's signal was halved at 200m and it appears not to have had pronounced influence in the south. This mid-latitude warming event is an example of locally forced coastal warming. Its signal is attenuated with depth and distance from areas of direct energy transfer.

The 100m and 200m alongshore temperature data for the 1972-73 CEN clearly suggest remote forcing from the south. The persistence of signal with depth without apparent attenuation indicates poleward and downward propagating coastal Kelvin waves (McCreary 1976). Although strong MLW events affect temperature at 200m, attenuation occurs with depth. Anomaly computations show the signal for the 1972-73, 1976-77 and 1982-83 CEN events to be stronger in terms of sdu below the thermocline than above. This trend is also shown in Figure 5 where the 1976-77 CEN appears stronger at 200m in the 8°C isotherm than at 100m in the 10°C isotherm. These are the years when a strong Kelvin wave signal would be expected (Cane 1983, Picaut 1984).

Table 2 summarizes the offshore 100m temperature anomaly in the same form as Table 1. The 1982-83 event produced a temperature anomaly pattern at 100m similar to that observed at the surface. The patterns at the surface and 100m were also similar during the following warm winter, 1983-84.

In contrast to the 1982-83 CEN, the inshore zone was cool at 100m during the 1976-77, 1977-78, 1979-80 and 1980-81 warming events. This may represent a large scale density adjustment with depth. Presumably similar adjustment occurred below 100m during the 1982-84 period.

Figure 5 shows conspicuous coastal warming at 100m during the 1976-77, 1977-78, 1979-80 and 1980-81 winters in the alongshore 3° blocks. However, the 3° latitude by 9° longitude areas summarized in Table 2 show that these winters have predominantly negative anomaly at 100m. Quite possibly, this points to the distinction between the coastal countercurrent, which appears instrumental in increased coastal warming in warm winters, and the diffuse offshore countercurrent or undercurrent. Kelvin wave influence would be expected to occur first in the region of the countercurrent. Offshore, it appears that the undercurrent becomes weaker as the California Current weakens (Table 1, Figure 4a) during warm events, leading to cool anomalies at depth in the inshore zone (Table 2).

The persistence of negative winter SST anomaly offshore on the northern transect as shown in Table 1 may represent a southward shift of the subarctic transition. It appears that a similar shift occurs in the 100m index four years later in winter 1980-81 and persists through winter 1983-84. This is shown by negative anomaly index in the offshore zones of the two northern transects. Examination of more detailed data shows that the cooling in this region began in 1977. This trend to cooler water in the offshore zone may represent a time-dependent deepening of the mean oceanic circulation brought by increased frequency of the PNA atmospheric pattern over the north Pacific. This climatic shift, which apparently favors warmer coastal water, undoubtedly contributed to the extremity and persistence of the 1982-83 CEN.

Sea Level

To examine the effects of the 1982-83 California El Nino on sea level, 6-month sums of sea level anomaly for Neah Bay, Washington and for Crescent City, San Francisco, Monterey, Los Angeles and San Diego, California were added together to give a value for the entire west coast of the United States. These scaled values are plotted with the corresponding scaled SST anomaly sum in Figure 6. The extremely high sea level anomaly values that occurred during the 1982-83 CEN event suggest an anomalously warm water column as the result of atmospheric and oceanic forcing of convergent ocean currents along the greater California coast.

The 1982-83 CEN resulted in the most extreme sea level anomaly in the 1971-83 record. If cool negative anomaly events are excluded, the 1972-73 CEN was next in extremity followed by the 1976-77 (CEN), 1977-78 (CEN) and 1979-80 (MLW) events. Greatest anomalies were in winter 1982-83 when anomalies greater than 20 cm occurred from San Francisco north to Sitka, Alaska. Anomalies of this magnitude and duration are unique in the National Ocean Survey's records for the west coast of the USA. A 90 year daily sea-level height maximum for San Francisco occurred on January 27, 1983. The 26 cm monthly anomalies for February and March 1983 at San Francisco were

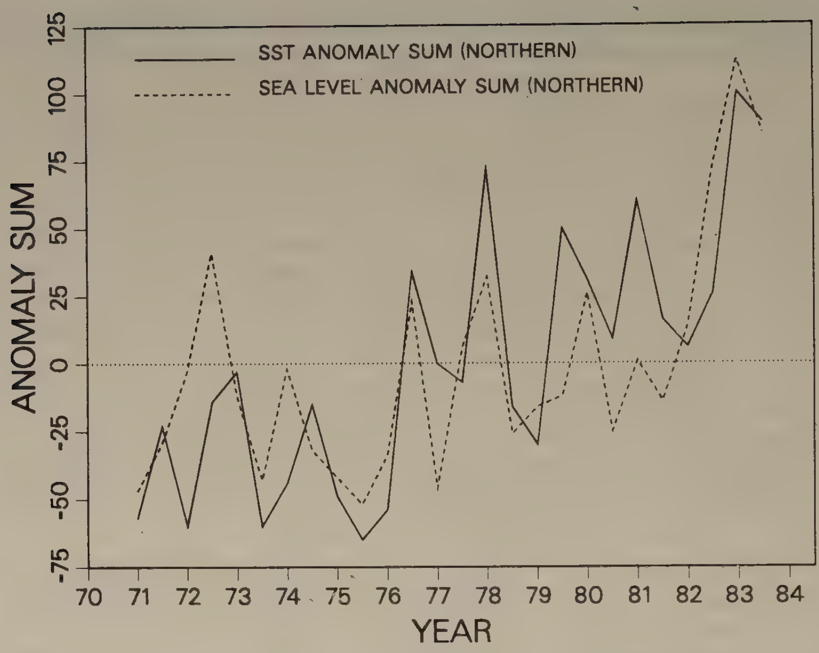

Figure 6. Six-month sums of anomaly of sea level at 6 tide stations along the northern portion of coast from San Diego, CA. to Neah Bay, WA. Six-month SST anomaly for the northern portion of coast are also included from Figure 1 for comparison.

without precedent in the 90 year record. High positive anomalies also made the 1983 yearly mean unique in the 90 year series. In southern California anomalies were less extreme with the largest monthly anomalies ranging from 10 to 15 cm.

Chelton and Davis (1982) related the first empirical orthogonal function of monthly sea level anomaly along the coast of North America to bifurcation of the North Pacific Current as it approaches the eastern boundary under the influence of basin-wide atmospheric forcing. When bifurcation favors northerly flow, there is sea level rise along the coast of Alta and Baja California. This represents the warm oceanic event response characterized by the years since 1976 (Figure 6). In the opposite extreme, the cool subarctic water flows south in an anomalously cool California Current and there are lower sea level heights.

This analysis agrees well with the implications of the above temperature data. Northerly winds in the western Pacific basin bring more cool subarctic water into the North Pacific Current allowing the subarctic transition to move south. This brings cool water to the offshore end of the northern transect (Tables 1, 2). The PNA-associated intensified Aleutian Low favors an increased northward flow of subarctic water. Consequently, the California Current System receives less cool water.

Wind Mixing and Upwelling Index

Wind stress on the sea surface mechanically mixes the ocean's surface layers and induces surface currents. The mixing effect of the wind is directionally independent and the rate at which turbulent kinetic energy becomes available to mix the upper ocean is proportional to the third power of the wind speed (Niiler and Kraus 1977).

An index of the turbulent wind events along the California coast was calculated from the 6-hourly northern hemisphere pressure/wind analyses of the Fleet Numerical Oceanography Center at six coastal locations from 24° to 39°N for the period 1974-84. The daily mean wind speed cubed was calculated from the mean of the four 6-hourly wind speed cubed values. To investigate the interannual variability in the atmospheric forcing, these daily time series of wind speed cubed were examined in terms of the number of daily means greater than a threshold value of 400 m^3/s^3 and the persistence of events above the threshold. It is emphasized that these wind speed values are representative of the large-scale wind forcing, characteristic of the approximate 3°x3° grid spacing of the northern hemisphere analysis.

Wind events for the central California coast (36°N) during the winter quarter (Dec. - Feb.) from 1974-75 to 1983-84 are described by the product of the number of daily means greater than the 400 m^3/s^3 threshold times the mean value of the wind speed cubed for these days (Table 3). This product is a relative index of the turbulent energy added to the water column during the various winters. The greatest turbulent mixing appears to have occurred in the CEN winters of 1977-78 and 1982-83. The third most turbulent winter was the mid-latitude warming event winter of 1979-80. These three winters occurred in winters when the PNA-type atmospheric circulation was strong (Wallace and Gutzler 1981, Quiroz 1983). This pattern was also observed at the other coastal locations, but with smaller magnitudes in the extreme events.

Equatorward winds blowing parallel to the California coast cause surface water to be moved offshore and subsurface water to rise in the upwelling process. Conversely, poleward winds cause surface water to be pushed toward shore, causing downwelling and northward flow. The upwelling index (Bakun 1973, 1975) provides a large-scale estimate of the onshore/offshore Ekman transport based on FNOC pressure/wind fields.

A time-distance plot of monthly mean upwelling index (Figure 7) shows that in the area south of 33°N, winds favoring coastal upwelling occur throughout most of the year. North of 33°N, winter winds favor onshore transport and resulting downwelling. These areas are seen in Figure 7 as cusps that extend southward to latitudes from 33° to 39°N. The hatched areas within the negative regions represent extreme downwelling of less than -200 cubic meters per second per 100m of coastline (m^3/s/100m). At 42°N the upwelling index exceeded this negative value for only two months in the entire 13 year record. These occurred during the anomalously warm 1982-83 winter. The shaded cells centered near 33°N represent periods of strong upwelling in spring and summer when the monthly values are greater than +200 (m^3/s/100m). Note the increase in upwelling at 21°N which occur in the spring and summer after 1976. These may be the result of a southward shift and/or intensification of the North Pacific High pressure center.

To examine the interannual variability in the upwelling index the consecutive positive values of the index greater than +200 at 33°N were summed for summer seasons during the 1951-84 period. The negative

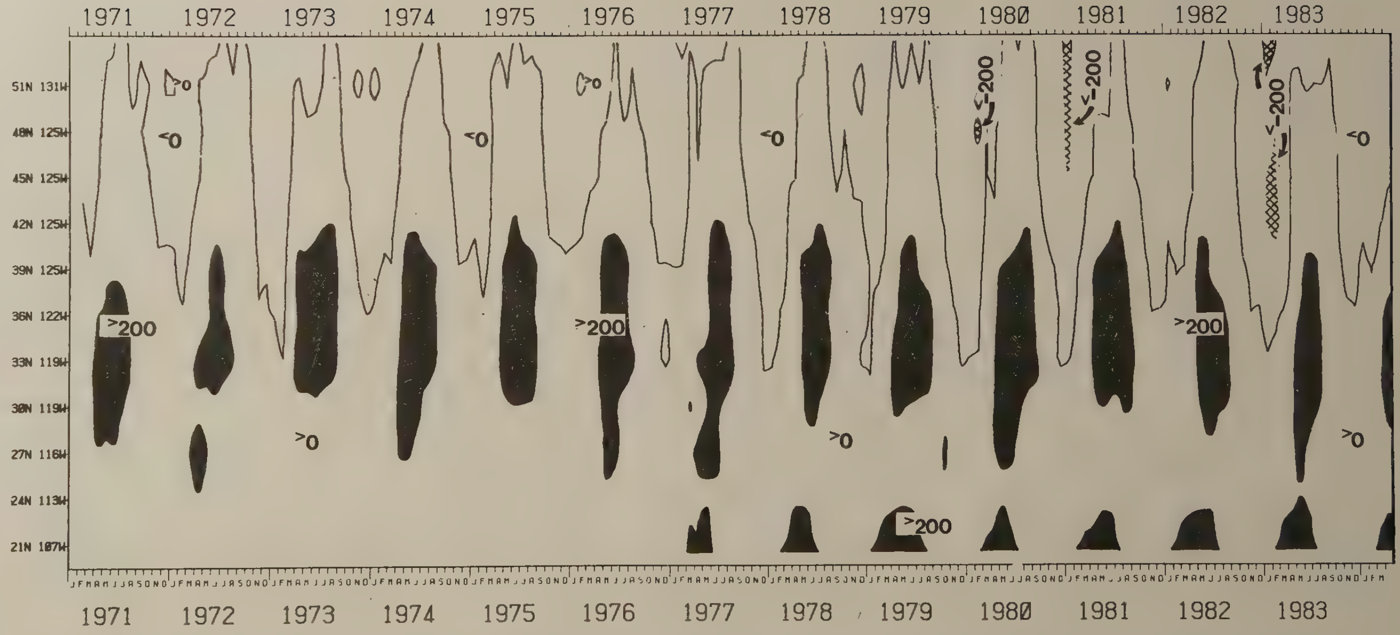

Figure 7. Upwelling Index computed by methods of Bakun (1973) for 12 locations along west coast from Baja California to Vancouver Island. Units are m^3/s/100 m of coastline. Solid lines represent zero upwelling index and enclose regions of negative upwelling or downwelling. Cross-hatched areas represent downwelling stronger than -200 upwelling index units. Areas shaded black represent cells of strong upwelling (greater than +200 units) along central and Baja California in spring and summer.

Table 3. Summary of severe winter (Dec.-Feb.) turbulent wind events off central California (36°N) during winters from 1974-75 to 1983-84. Computed from 6-hourly pressure fields from Fleet Numerical Oceanography Center. The first column gives the number of days when the daily mean wind speed cubed was greater than 400 m^3/s^3 and the second column gives the mean wind speed cubed value for those days. The third column gives the product of number of days times the mean wind speed cubed and indicates the amount of turbulent energy added to the water column. The last three columns summarize the turbulent energy transfer as events by giving the number of events of wind speed greater than 400 m^3/s^3, the mean duration of the events, and the standard deviation of the duration of the mean.

	WIND SPEED CUBED > $400m^3/s^3$					
SEASON	(1) NO. OF DAYS	(2) MEAN FOR DAYS>400	(3) (1)x(2)	(4) NO. OF EVENTS	(5) DURATION MEAN	(6) OF EVENT S.D.
1974-75	26	1096	28496	9	2.8	0.7
1975-76	9	760	6840	3	2.3	0.3
1976-77	4	516	2064	2	2.0	0.0
1977-78	27	1462	39474	5	4.6	8.8
1978-79	19	836	15884	6	2.2	0.2
1979-80	24	1388	33312	6	3.3	3.9
1980-81	11	1548	17028	4	2.3	0.3
1981-82	16	854	13664	5	2.4	0.8
1982-83	31	1261	39091	8	3.3	0.8
1983-84	12	1610	19320	3	2.3	0.3

upwelling index values at 42°N were also summed for each winter downwelling season (Table 4). The most extreme downwelling of the last 33 years occurred during the 1957-58 and 1982-83 fall and winter seasons which were two and three times the mean, respectively. During the winters of 1979-80 and 1980-81, the PNA-type circulation occurred over the North Pacific. They also had higher than average downwelling values at 42°N. The 1979-80 and 1980-81 winters were probably important in maintaining the anomalously warm SST regime since 1976.

Large negative values of the downwelling at 42°N are associated with the occurrence of PNA atmospheric circulation. Upwelling in the following spring and summer appear decoupled from winter downwelling. However, upwelling can also influence the overall impact of warm anomalies. Note that in the 1982-83 two seasonal influences related to upwelling lead to high California coastal SSTs. First, there appears to have been unprecedented downwelling which promoted northward coastal flow and warming during winter 1982-83. This was followed by indication of below average upwelling during the following spring and summer. This, in turn, was followed by the highest SSTs and highest SST anomalies (in sdu.) during fall 1983 (see Figures 2a,b).

Table 4. Summary of monthly upwelling index for winter and summer seasons from 1951-52 to 1983-84. The second column is the sum of negative monthly mean upwelling index values at 42°N during the winter downwelling season. Seasons with downwelling sums more negative than -300 units at 42°N are marked with double minus (--). The third column is a similar sum of positive upwelling index values during the following spring and summer at 33°N. These are the sum of consecutive monthly mean values greater than +200 units . Upwelling seasons with sums greater than +1500 units are marked with double plus (++). The fourth column indicates the occurrence of tropical El Nino (TEN) and Pacific/North American circulation (PNA).

MONTHLY MEAN UPWELLING INDEX ABSTRACT
1951-1984

SEASON	42N NEG.	33N POS.	EVENT
51-52	(194)	448	
52-53	(413)--	814	TEN
53-54	(215)	491	
54-55	(246)	1813++	
55-56	(230)	1656++	
56-57	(60)	1439	
57-58	(544)--	1535++	TEN, PNA
58-59	(139)	1955++	PNA
59-60	(101)	349	
60-61	(409)--	809	PNA
61-62	(64)	792	
62-63	(204)	1053	PNA
63-64	(168)	2261++	
64-65	(210)	1161	
65-66	(197)	1211	TEN
66-67	(165)	1319	
67-68	(189)	1511++	PNA
68-69	(269)	1584++	
69-70	(353)--	1404	TEN, PNA
70-71	(131)	1354	
71-72	(92)	1209	
72-73	(219)	1310	TEN
73-74	(198)	1383	
74-75	(121)	1217	
75-76	(54)	1055	
76-77	(128)	1266	TEN, PNA
77-78	(366)--	798	TEN, PNA
78-79	(99)	1446	
79-80	(369)--	1629++	PNA
80-81	(383)--	1546++	PNA
81-82	(215)	1157	
82-83	(765)--	984	TEN, PNA
83-84	(278)	1191	

DOWN 42:	MIN.	(60)
	MEAN	(251)
	MAX.	(765)
	--LT.	(300)
UP 33:	MIN.	349
	MEAN	1224
	MAX	2261
	++ MT	1500

Discussion and Conclusions

Our analyses suggest that the severity of the 1982-83 CEN was the result of several warming factors. Remote forcing occurred both through the atmosphere and through the ocean to cause warming in the California Current System which had already been warmed by remotely forced and local events of lesser, but similar nature.

Two maxima characterized 1982-83 warming that occurred within 300km of shore (Figures 2a,2b,4a,4b). The first maxima occurred nearly in phase with the tropical El Nino at all depth levels studied. At the surface the second peak which occurred in late summer and early fall 1983 was the most extreme. At the 100 and 200m depths, the first peak, which was most likely associated with coastal Kelvin wave activity, was the most extreme. The second maxima at 100m was reduced in expression south of 32°N and with depth (Figure 5).

Maximum temperature anomalies of 2°C, 3°C and 1.2°C occurred at the surface, 100m and 200m respectively. In terms of sdu, the highest value was 3.6 off Baja California with values to 3.0 throughout the alongshore transect at 100m. Anomalies with sdu values ranging to 2.0 and 2.5 at the surface and 200m, respectively, indicate a relatively unattenuated signal below the thermocline consistent with coastal Kelvin wave theory.

Comparison of the 1982-83 CEN with other warm events of the series has allowed considerable insight into the causes of its severity and persistence. The 1972-73 CEN occurred without the PNA atmospheric adjustment which occurred in 1976-77, 1977-78 and 1982-83. The 1972-73 CEN, which has a number of similarities to the 1982-83 event (Figure 5) provided an example of the oceanic tropical to mid-latitude connection. In contrast, the 1979-80 MLW event was accompanied by the distinctive PNA atmospheric pattern in a period without tropical El Nino activity. This coastal warming event also had several points of similarity to the 1982-83 CEN (Figures 4a,b). Overall, the 1977-78 CEN is similar to the 1982-83 event, though less extreme (Figure 4b, Table 3).

The 1982-83 event brought anomalous cooling in an area reaching from 1000-3000 km offshore. If the 3000 km area adjacent to the coast is considered, the 1982-83 CEN was a cool event rather than a warm one (Figure 4b, Table 1). This was the result of unprecedented development of the Aleutian low that occurred in winter 1982-83. As noted above, this low was probably the result of extra-tropical forces acting in concert with the tropical atmospheric connection. Cooling in the area 2000-3000 km offshore at 40.5N appears characteristic of years when anomalously warm water occurs at the coast (Tables 1, 2). However, no other offshore cooling event of the 13 year series was as extensive as the one that occurred during the 1982-83 CEN (Figure 4b, Table 1).

Coastal subsurface temperature patterns at 100m and 200m during the 1976-77, 1977-78 and 1982-83 CENs suggest downward and poleward propagating coastal Kelvin wave influences, since the signal at 200m appears stronger, in terms of sdu, than at the surface (Figure 5). The warming signal decreased with depth for the 1979-80 warm event, which appeared unrelated to tropical warming.

Coastal winds during 1982-83 winter were extreme (Figure 7, Tables 3,4). In terms of negative upwelling index, indicating a general tendency to Ekman convergence at the coast, the 1982-83 CEN winter was the most extreme of the 33 year series (Table 4). The 1957-58 CEN winter which also occurred with PNA atmospheric adjustment was second. Although the 1957-58 event is considered extreme, the accumulated seasonal downwelling index at 42°N was only 70% of that obtained for the 1982-83 winter. Extreme downwelling index or negative upwelling index is associated with the PNA atmospheric pattern, though not absolutely (Table 4).

Atmospheric and oceanic remote forcing appear to produce California El Ninos by enhancing normal processes that lead to warming, according to the following scenario. Coastal Kelvin wave activity depresses the thermocline along the coast. This in turn facilitates northward coastal countercurrent flow, which will bring anomalously warm water into the coastal zone, as indicated by Figures 2a, 2b, 3, 4a and 4b. Basin-wide forcing deflects subarctic water north away from the California Current. Consequently, more warm water reaches the California coast (Figure 6). Atmospheric patterns associated with mid-latitude adjustment to tropical influences may also cause local downwelling winds (Table 4) causing Ekman convergence at the coast, thereby inducing northward surface currents (Figure 6). These three warming processes contribute to positive temperature anomalies occurring at the coast during CEN years.

The data presented suggest that a climatic change occurred after the winter of 1976-77. The period before 1976 was characterized by positive SST anomaly offshore (Figure 4b), negative anomaly in the California Current System (Figure 3, 4a, b), negative sea level anomaly (Figure 6) and coastal winds favoring upwelling (Table 4). Four of the six winters since 1976 are classified as anomalously warm on the coast. These were accompanied by positive sea level anomaly and downwelling winds. The 1982-83 CEN occurred in an already warm period. This also contributed to its severity.

The 1972-73 CEN appears equal in positive anomaly to the 1982-83 CEN in subsurface temperature (Figure 5) and sea level (Figure 6). However, its expression, particularly at the surface (Figure 2b), was attenuated in the California Current System because it was opposed by locally forced processes rather than augmented by them.

Summary

1. Coastal ocean warming associated with the 1982-83 California El Nino was the most extreme of 1971-83 period. This warming appears to have been the result of at least two remote connections to the tropical El Nino, one through the ocean and the other through the atmosphere. Two major peaks of anomalous subsurface warming occurred. The earlier peak may primarily reflect oceanic propagation while the latter peak seems to be the result of the atmospheric tropical to mid-latitude connection.

2. Atmospheric patterns associated with the 1982-83 event brought extreme cooling in an area reaching from 1000 to 3000 km offshore. The 1982-83 period was a cool rather than a warm year if the entire 3000 km offshore area is considered. Offshore cooling is characteristic of

other coastal warming events (eg. 1979-80 and 1980-81) that can occur without tropical El Nino activity.

3. Persistence of warm anomaly below 100m during the 1982-83 event suggests the presence of oceanic propagation from the tropics consistent with coastal Kelvin wave activity. Similar strong persistence at depth occurred during the 1972-73 California El Nino, which was unaccompanied by atmospheric patterns associated with 1976-77, 1977-78 and 1982-83 California El Ninos. In contrast, the strong surface warming which occurred during 1979-80 unaccompanied by tropical El Nino activity, attenuated rapidly with depth.

4. In winter 1982-83 monthly anomalies based on 3^0 latitude-longitude areas exceeded 2.5^0C at 100m with lesser magnitudes at surface and 200m.

5. Maximum alongshore SST warming occurred in fall 1983. During winter 1982-83 accumulated downwelling index at 42^0N was three times the average value indicating a tendency to extreme Ekman convergence. This is the largest accumulated downwelling index recorded (33 year series). Non-directional wind mixing parameter for winter 1977-78 was as great as for 1982-83, but the downwelling index value was only half that recorded for 1982-83. The extreme accumulated downwelling value for 1982-83 represents local expression of the PNA pattern circulation.

6. Indirect evidence points to weakening of the cool California Current, onshore transport of offshore water, increased downwelling and counter current intensification as primary local mechanisms through which the oceanic and atmospheric remote forcing bring warming to the California coast. Atmospheric and oceanic forcing of warming processes occurred together during the 1982-83 California El Nino.

7. The second half of the 1971-83 study period is warm relative to the first half. The change occurred rather abruptly in winter 1976. Since five of the next seven winters were characterized by warm coastal waters and characteristic atmospheric circulation, residual warm effects have accumulated so that the 1982-83 California El Nino occurred in an already warm period with an atmospheric circulation already favorable to coastal warming. This warm setting also contributed to the extreme nature of the 1982-83 event.

References

ARKIN, P.A.
1984. Tropical circulation anomalies associated with the 1982-83 ENSO Event. Proceedings of the Eighth Annual Climate Diagnostics Workshop, U.S. Dep. Commer., NOAA, pp. 111-121.

BAKUN, A.
1973. Coastal upwelling indices, west coast of North America, 1946-71. U.S. Dep. Commer., NOAA Tech. Rep., NMFS SSRF-671, 103 p.

1975. Daily and weekly upwelling indices, west coast of North America, 1967-73. U.S. Dep. Commer., NOAA Tech. Rep., NMFS SSRF-693, 114 p.

BERNAL, P.A. and J.A. McGOWAN
1981. Advection and upwelling in the California Current. In Coastal Upwelling, F. A. Richards, (Ed.), Coastal and Estuarine Science 1, Amer. Geophys. Union, Washington, D.C., pp. 381-399.

BIRD, A.A., R.J. KOOB, J.B. WICKHAM and C.N.K. MOOERS
1984. Hydrographic data from the slope waters off central California. 26 November 1978 - 26 June 1980., Dep. of Oceanography, Tech. Rep. NPS 68-84-010, Naval Postgraduate School, Monterey, CA.

BJERKNES, J.
1969. Atmospheric teleconnections from the equatorial Pacific. Mon. Wea. Rev., 97:163-172.

CANE, M.A.
1983. Oceanographic events during El Nino. Science, 222: 1189-1194.

CHELTON, D.B.
1981. Interannual variability of the California Current-physical factors. Cal. Coop. Ocean. Fish. Inv. Rep. 22: 34-47.

CHELTON, D.B. and R.E. DAVIS
1982. Monthly mean sea-level variability along the west coast of North America. J. Phys. Oceanog., 12: 757-784.

DOUGLAS, A.V., D.R. CAYAN and J. NAMIAS
1982. Large-scale changes in North Pacific and North American weather patterns in recent decades. Mon. Wea. Rev., 110: 1851-1862.

EMERY, W.J. and K. HAMILTON
1984. Atmospheric forcing of interannual variability in the Northeast Pacific Ocean, connections with El Nino. J. Geophys. Res. (In press) (see also this volume).

HALPERN, D., P. HAYES, A. LEETMAA, D.V. HANSEN and S.G.H. PHILANDER
1983. Oceanographic observations of the 1982 warming of the tropical eastern North Pacific. Science, 221: 1173-1175.

HANEY, R.L.
1984. Comment on "Seasonality in the associations between surface temperatures over the United States and the North Pacific Ocean". Mon. Wea. Rev., 112: 868-869.

HICKEY, B.M.
1979. The California Current System-hypotheses and facts. Prog. Oceanog., 8: 191-279.

HOREL, J.D. and J.M. WALLACE
1981. Planetary atmospheric phenomena associated with the Southern Oscillation. Mon. Wea. Rev., 109: 813-829.

KIRWAN, JR.,A.D., G.J. McNALLY, E. REYNA and M.J. MERRELL, JR.
1978. The near-surface circulation of the eastern North Pacific. J. Phys. Oceanog. 8: 937-945.

McCREARY, J.
1976. Eastern tropical ocean response to changing wind systems: with application to El Nino. J. Phys. Oceanog., 6: 632-645.

McLAIN, D.R. and D.H. THOMAS
1983. Year-to-year fluctuations of the California Countercurrent and effects on marine organisms. Cal. Coop. Ocean. Fish. Inv. Rep., 24: 165-181.

McLAIN, D.R.
1983. Coastal ocean warming in the northeast Pacific, 1976-83. In The Influence of Ocean Conditions on the Production of Salmonids in the North Pacific, A Workshop. W.G. Pearcy, (Ed.), Oregon State University, Sea Grant Program. Newport, OR. ORESU-W-001. November 8-10, 1983. 61-86.

McLAIN, D.R., R.E. BRAINARD, and J. NORTON
1984. Anomalous warm years in eastern boundary current systems. Cal. Coop. Ocean. Fish. Inv. Rep., (In press)

MOREANO, H.R.
1984. The weakening of the 1982-83 El Nino in Ecuadoran waters. Tropical Ocean-Atmosphere Newsletter, 28: 13-14.

NELSON, C.S.
1977. Wind stress and wind stress curl over the California Current. U.S. Dep. Commer., NOAA Tech. Rep. NMFS SSRF-714, 87 p.

NIILER, P.P. and E.B. KRAUS
1977. One dimensional models of the upper ocean. In E.B. Kraus (Ed.), Modelling and Prediction of the Upper Layers of the Ocean. Pergamon Press, New York, pp. 143-172.

NORTON, J. and D.R. McLAIN
1984. Monitoring the California Current from daily sea surface temperature and salinity at shore stations. (Abstract) EOS Trans. Amer. Geophys. Union, 65(45): 970.

PAN, Y.H. and A.H. OORT
1983. Global climate variations connected with sea surface temperature anomalies in the eastern equatorial Pacific Ocean for the 1958-73 period. Mon. Wea. Rev., 111: 1244-1258.

PICAUT, J.
1984. Major dynamics affecting the eastern tropical Atlantic and Pacific Oceans. Cal. Coop. Ocean. Fish. Inv. Rep. (in press).

QUINN, W.H. and V.T. NEAL
1984. Recent climatic change and the 1982-83 El Nino. Proceedings of the Eighth Annual Climate Diagnostic Workshop, U.S. Dep. Commer., NOAA, pp. 148-154.

QUIROZ, R.S.
1983. The climate of the "El Nino" winter of 1982-83 - A season of extraordinary climatic anomalies. Mon. Wea. Rev., 111: 1685-1706.

RASMUSSON, E.M. and J.M. WALLACE.
1983. Meterological aspects of the El Nino/Southern Oscillation. Science, 122: 1195-1202. (see also this vol.)

REID, J.L., G.I. RODEN, and J.G. WYLLIE
1958. Studies of the California Current System. Cal. Coop. Ocean Fish. Inv. Progress Rep. 7-1-56 to 1-1-58, Marine Res. Comm., Cal. Dep. Fish and Game, Sacramento, Ca., p. 27-56.

REID, J.L.
1960. Oceanography of the Northeastern Pacific Ocean during the last ten years. Cal. Coop. Ocean. Fish. Inv. Rep., 7: 77-90.

1965. Intermediate waters of the Pacific Ocean. Johns Hopkins Oceanog. Stud., Number 2, Johns Hopkins Press, Baltimore, MD, 85 p.

SAUR, J.F.T.
1980. Surface salinity and temperature on the San Francisco-Honolulu route, June 1966-December 1970 and January 1972-December 1975. J. Phys. Oceanogr., 10: 1669-1680.

SIMPSON, J.J.
1984. El Nino-induced onshore transport in the California Current during 1982-83. Geophys. Res. Let., 11: 241-242.

SKOGSBERG, T.
1936. Hydrography of Monterey Bay, California, thermal conditions, 1929-1933. Amer. Phil. Soc., Trans., M.S., 29, 152 p.

SMITH, R.L.
1968. Upwelling. Oceanog. Mar. Biol. Ann. Rev., 6: 11-46.

1983. Peru coastal currents during El Nino: 1976 and 1982. Science, 221: 1397-1398.

1984. Coastal Currents off Peru during El Nino of 1982-83: Prenatal to Senescent Conditions. Tropical Ocean-Atmosphere Newsletter, 28: 7-8.

SVERDRUP, H.U., M.W. JOHNSON and R.H. FLEMING
1942. The oceans, their physics, chemistry and general biology. Prentice-Hall, Inc., Englewood Cliffs, N.J., 1087 p.

TABATA, S.
1984. Oceanographic conditions off the Pacific coast of Canada during the 1982-83 El Nino. Proceedings of the Eighth Annual Climate Diagnostics Workshop, U.S. Dep. Commer., NOAA pp. 92-99. (see also this vol.)

TOOLE, J.M.
1984. Near equatorial CTD observations at 85°W in October 1982. (Abstract) EOS. Trans. Amer. Geophys., 65(49): 1208.

WALLACE, J.M. and D.S. GUTZLER
1981. Teleconnections in the geopotential height field during the northern hemisphere winter. Mon. Wea. Rev., 109: 784-812.

WICKHAM, J.B.
1975. Observations of the California Counter Current. J. Mar. Res., 33: 325-340.

WOOSTER, W.S.
1960. El Nino. Cal. Coop. Ocean. Fish. Inv. Rep., 7: 43-45

WOOSTER, W.S. and J.L. REID
1963. Eastern Boundary Currents. In The Sea, 2, M.N. Hill, (Ed.), pp. 253-276., John Wiley and Sons, New York.

WOOSTER, W.S. and J.H. JONES
1970. California undercurrent off northern baja California. J. Mar. Res., 28: 235-250.

8566

Biomass Model for the Egg Production Method

EITH PARKER[1]
uthwest Fisheries Center,
utional Marine Fisheries Service, NOAA,
) Box 271,
Jolla, CA 92038

BSTRACT

e spawning fraction of multiple spawners is estimable when females exhibit mor-
ological characteristics which indicate when spawning will take (or has taken)
ce. The length of time in which characteristics remain detectable must in itself
estimable and constant over the field sampling interval. Spawning biomass is
n estimated as a function of the estimated spawning frequency and other
rameters: egg production, batch fecundity, sex ratio, and average weight of
ture females. Based on the delta method, approximate variance estimates for
wning biomass are derived and given.

The relationship between the spawning biomass of a fish stock and its production of eggs is easily derived. Simply stated, the production of eggs (P) must be equal to the female biomass that produced those eggs multiplied by the female batch fecundity:

$$P = (B \cdot R') \cdot F'. \qquad (1)$$

The female biomass is represented as the product of the total biomass of the entire stock B, both males and females, and R', the portion of the entire stock that is egg-producing females. The batch fecundity F' is the number of eggs spawned per batch per unit weight of female.

Note that R' is not the biomass of females divided by the biomass of males plus females, a simple sex ratio in terms of biomass. Rather R' is the total biomass of females that has produced eggs in a specified period of time divided by the biomass of males and females together. If females spawn more than once during the period of time in which production is measured, R' may be greater than the simple sex ratio in terms of biomass. The converse would be true if, on the average, females spawn less than once.

It is this fundamental definition of R' that allows Equation (1) to be easily derived. However, in its present form, Equation (1) is of practical value only when each mature female spawns once during the time interval over which production is measured, in which case R' becomes the simple sex ratio estimated from biomass, say R.

In its present form, Equation (1) is not useful for multiple spawners, when population spawning appears to be continuous over the period of time over which production is measured. There is no way to relate production of eggs, P, to female biomass that produced those eggs without making an adjustment for spawning frequency.

R', the proportion of female-producing biomass, is composed of two parts: R, the simple biomass-based sex ratio (the biomass of females to that of males plus females) and f, the fraction of females spawning during the time interval,

$$R' = R \cdot f. \qquad (2)$$

Parker (1980) documented the above relationship and demonstrated that spawning frequency (f) can be estimated if three conditions are met: 1) Females can be examined for a characteristic which indicates when spawning will or has taken place, 2) the length of time such a characteristic remains detectable is estimable, and 3) the spawning rate (or frequency) remains constant over the sampling interval in which f is estimated.

Under these conditions the spawning fraction (f) is the fraction of females displaying characteristic 1 above, divided by the length of time the characteristic remains detectable. For example, if from a sample of 10 females, 2 display a characteristic which lasts for 1 d and which indicates that spawning will take place in approximately 3 d, then the spawning rate can be expected to be 1/5 in 3 d. Spawning frequency so estimated is additive. For instance, a daily rate can be summed over any length of time, week, year, etc. However, if multiple spawnings occur in the time period, parameter f can exceed unity and is no longer properly a "fraction."

Having developed a condition under which the spawning frequency can be estimated, Parker (1980) rewrote Equation (1) in terms of the simple biomass sex ratio (R) and the spawning frequency (f),

$$P = B \cdot R \cdot f \cdot F'. \qquad (3)$$

---

resent address: 8263 Vista Drive, La Mesa, CA 92041.

Spawning biomass can be estimated directly,

$$B = P/(R \cdot f \cdot F'). \tag{4}$$

Equation (4) is a conventional equation relating spawning biomass to egg production. The estimate of production (P) can be for any time interval, as long as the fraction of females spawning (f) is computed for the same interval. For a species that spawns but once over the time interval in which production is measured, say a year, Equation (4) is still valid, but now greatly simplified since $f = 1$.

Stauffer and Picquelle (1980) modified Equation (4) for the northern anchovy, *Engraulis mordax*, and based the biomass equation on a daily estimate of production and fraction spawning,

$$B = P \cdot A(k \cdot W)/(R \cdot F \cdot S) \tag{5}$$

where B = spawning biomass in metric tons,
P = daily egg production, numbers of eggs produced per 0.05 m^2 per day,
W = average weight of mature females (g),
R = sex ratio, fraction of population that are mature females, by weight (g), as before,
F = batch fecundity, number of eggs spawned per mature females per batch,
S = the fraction of mature females spawning per day,
A = the total survey area (in 0.05 m^2),
k = conversion factor of grams to metric tons.

Stauffer and Picquelle (1980) found that more stable estimates of spawning biomass are achieved if Parker's batch fecundity estimate by weight is replaced by F, eggs per female per batch, and W, the average weight of mature females. Stauffer and Picquelle (1980) demonstrated estimation with an example. A detailed example is given in Picquelle and Stauffer (1985).

Based on the delta method (Seber 1973), Stauffer and Picquelle (1980) show the approximate bias and variance of the biomass estimator to be a function of sample variances and covariances. Bias (b) is given by

$$E[B] = \hat{B} + b \tag{6}$$

where $E[B]$ is the expected value of the biomass and $\hat{B}$ is the estimate from Equation (5). The bias is approximately

$$b \cong \hat{B}(CV(R)^2 + CV(F)^2 + CV(S)^2 + COVS) \tag{7}$$

where CV denotes coefficient of variation, and $COVS$ is the sum of terms involving covariances:

$$\begin{aligned} COVS = {} & COV(PW)/PW - COV(PR)/PR - COV(PF)/PF \\ & - COV(PS)/PS - COV(WR)/WR - COV(WF)/WF \\ & - COV(WS)/WS + COV(RF)/RF + COV(RS)/RS \\ & + COV(SF)/SF. \end{aligned} \tag{8}$$

Ignoring the bias, approximate variance of the estimate is given by

$$Var\ B \cong \hat{B}^2(CV(P)^2 + CV(W)^2 + CV(F)^2 + CV(S)^2 + 2\ COVS) \tag{9}$$

LITERATURE CITED

PARKER, K.
1980. A direct method for estimating northern anchovy, *Engraulis mordax*, spawning biomass. Fish. Bull., U.S. 78:541-544.

PICQUELLE, S., and G. STAUFFER.
1985. Parameter estimation for an egg production method of northern anchovy biomass assessment. *In* R. Lasker (editor), An egg production method for estimating spawning biomass of pelagic fish: Application to the northern anchovy, *Engraulis mordax*, p. 7-15. U.S. Dep. Commer., NOAA Tech. Rep. NMFS 36.

SEBER, G. A. F.
1973. The estimation of animal abundance and related parameters. Hafner Press, N.Y., 506 p.

STAUFFER, G. D., and S. J. PICQUELLE.
1980. Estimates of the 1980 spawning biomass of the subpopulation of northern anchovy. Natl. Mar. Fish. Serv., Southwest Fish. Cent., La Jolla, CA, Admin. Rep. LJ-80-09, 41 p.

8567

REGIONAL VARIATIONS IN THE GROWTH AND AGE COMPOSITION OF NORTHERN ANCHOVY, *ENGRAULIS MORDAX*

R. H. PARRISH,[1] D. L. MALLICOATE,[1] AND K. F. MAIS[2]

ABSTRACT

Data from the Sea Survey Program conducted by the California Department of Fish and Game were analyzed to describe regional variations in growth and age composition of northern anchovy, *Engraulis mordax*. Juvenile growth appeared to be greater at higher latitudes and in the offshore portion of the Southern California Bight. Adult growth was less variable; however, there were statistically significant differences between regions. In addition, the growth rate for the southern stock was markedly lower than that of the central stock. This difference in growth rates was used to characterize the area of overlap between the two stocks. Age composition varied with depth of water and geographical location within the Southern California Bight and with latitude. Young-of-the-year and yearling fish were found in larger proportions in shallow water and in the southern and inshore areas of the Southern California Bight. Age compositions of northern anchovies sampled in the California and Mexican purse seine fisheries were compared with those of the Sea Survey Program. This comparison suggests that the present California area restrictions, which exclude the fishery from the nearshore area, greatly reduces the number of young fish in the catch.

The purpose of this study is to describe regional variations in growth and age composition of the northern anchovy, *Engraulis mordax*. Data for the study were taken by the Sea Survey Program of the California Department of Fish and Game. Mais (1974) described this program and analyzed the data for the most common species taken in the survey. This report is an extension of Mais' work and focuses on geographical variations in age composition and growth rates and on depth variations in age composition.

Meristic and morphometric (McHugh 1951) and electrophoretic (Vrooman et al. 1981) studies on the stock structure of the northern anchovy suggest that there are three stocks (northern, central, and southern) and that the boundaries between the stocks occur in central California and central Baja California. There is also recent evidence (Parrish[3]) of a fourth stock which spawns in the fall in central California and in the northern and offshore areas of the Southern California Bight.

Mais (1974) showed that the southern stock of northern anchovies was smaller at age than the central stock. In addition, northern anchovies are known to be larger off central California than off southern California (Collins 1969; Mais 1974; Mallicoate and Parrish 1981), and they are larger in the offshore areas of the Southern California Bight than in the inshore areas (Mais 1974). These differences could be due to varying growth rates between regions, varying seasonality of spawning, varying age compositions, size-specific migration, or a combination of these factors.

Tagging experiments have shown that northern anchovies move from southern California to central California, from central California to southern California, and from southern California to Ensenada, Mexico; there is a northerly movement in summer and a southerly movement in winter (Haugen et al. 1969). Mais (1974) found northern anchovies to be distributed more offshore in some years and more inshore in other years, and he found them concentrated closer to shore and in the northern part of the Southern California Bight during the fall months. Mais (1974) suggested that northern anchovies begin an offshore and southeastward movement in late winter, which coincides with the onset of major spawning activity. These movements of anchovy may affect the measurement of growth rates and age compositions within the different regions.

METHODS

The data used in the study were taken from north-

---

[1] Southwest Fisheries Center Pacific Fisheries Environmental roup, National Marine Fisheries Service, NOAA, P.O. Box 831, onterey, CA 93942.

[2] California Department of Fish and Game, 1301 West 12th Street, ong Beach, CA 90813.

[3] Parrish, R. H. 1983 Evidence for a fall spawning anchovy ock. Paper presented at 1983 CalCOFI Conference.

---

anuscript accepted January 1985.

ern anchovies caught by midwater trawl. The gear and sampling procedures are described by Mais (1974). The data set covers the period 1966-1983 and consists of 101 cruises. Twenty-three cruises extended north of Point Conception, 77 cruises occurred in southern California and northern Baja California, and 8 cruises extended into southern Baja California. Several cruises extended into more than one region. There were a total of 4,166 trawl hauls, of which 3,017 contained anchovies. Standard lengths were normally taken from about 25 anchovies in each trawl haul in which they occurred; otoliths, for aging, were usually taken from a subsample of up to 10 fish. A total of 60,082 northern anchovies were measured, of which 20,772 were aged by California Department of Fish and Game personnel with methods developed by Collins and Spratt (1969).

For purposes of determining age composition and growth rates of northern anchovies, it was assumed that February was the birth month of all fish sampled. Anchovies off California and Baja California have a peak in spawning in February-March; however, some spawning does occur all year (Ahlstrom 1966). The age determinations used in this report are, of course, not accurate to the month. They are based on the number of annuli, the seasonality of annuli formation, an assumed February birth month, and the month the fish were caught. Annuli formation occurs in May in California (Collins and Spratt 1969). A 1-yr-old anchovy would therefore be an anchovy caught in February with no annuli on its otoliths. A 1½-yr-old anchovy would be a fish with one annuli which was caught in August. An anchovy born in February would be 15 mo old when its first annuli was formed. An anchovy spawned in September would be 8 mo old if it formed its first annuli in its first May and 20 mo old if it formed its first annuli in its second May.

Differences in growth between geographical regions were compared by linear regression analyses which included anchovies of 1½ yr of age and older. Evaluation of the relationship between age composition and water depth in the area of capture was made by grouping the samples into depth strata. The strata were established partially on the number of observations.

To determine growth rates, the data were processed with a computer program (Mallicoate and Parrish 1981) which calculates and plots the mean length, standard deviation of length, and length range by age and month. The program also tabulated the number of observations by age and month; these data were used for determining age composition.

Our preliminary analysis of the sea survey data showed an alongshore cline in the mean length of northern anchovies (Fig. 1). It also revealed a bias in the selection of fish to be aged. Aged fish were generally larger at all latitudes than were the unaged fish. This bias is apparently due to a consistent tendency for samplers to pick larger anchovies for the subsample which was aged. Anchovies < 100 mm SL were particularly susceptible to not being selected for aging (Table 1). On checking with the field biologists who took the data, we found a second source of bias which occurred only in trawl hauls of exclusively small fish. When trawl hauls were considered by the sampler to be "obviously" all young-of-the-year fish, there was a tendency not to take otoliths for age determination. These sampling biases affect the analyses of age composition presented in this report but do not affect the growth analyses.

TABLE 1.—Two types of length bias in sampling northern anchovies in the Sea Survey Program.

Standard length (mm)	No. fish measured	No. fish measured in hauls sampled for otoliths	No. otolith samples	[1]Bias 1	[2]Bias 2
<70	2,174	1,275	460	0.59	0.36
70-80	2,366	1,939	684	0.82	0.35
80-90	4,667	4,241	1,667	0.91	0.39
90-100	7,077	6,367	2,498	0.90	0.39
100-110	8,988	7,875	2,997	0.88	0.38
110-120	12,058	10,834	4,164	0.90	0.38
120-130	11,744	10,462	4,215	0.89	0.40
130-140	7,390	6,456	2,748	0.87	0.43
140+	3,619	3,036	1,339	0.84	0.44
Total	60,082	52,484	20,772		

[1] Bias 1 is the decision to sample for otoliths (i.e., the proportion of fish in trawl hauls which were sampled for otoliths).

[2] Bias 2 is the selection of larger fish by the sampler (i.e., the proportion of fish in trawl hauls, which were sampled for otoliths, for which otolith samples were taken).

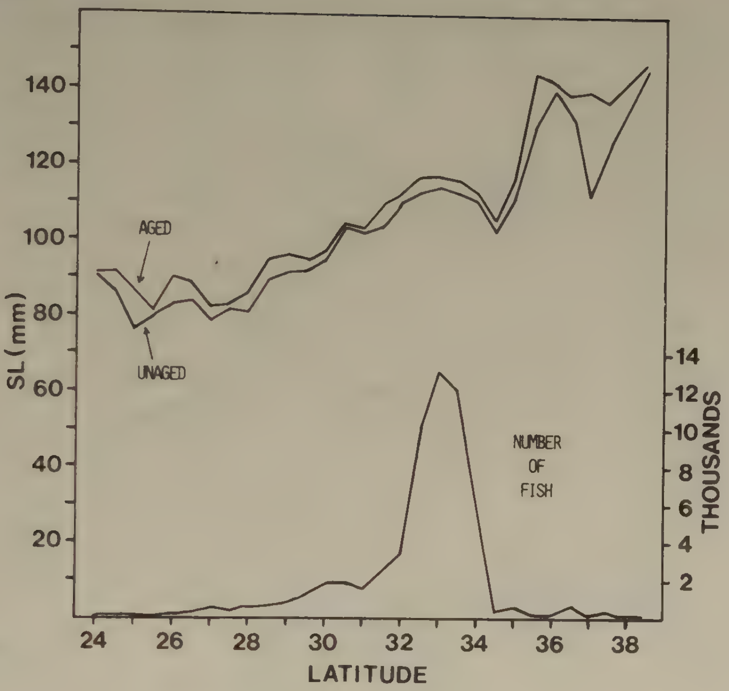

FIGURE 1.—Mean length of aged and unaged northern anchovies and the number of anchovies by half degree of latitude.

The data were inadequate to calculate growth curves or age composition on the one-half degree of latitude interval used in Figure 1; therefore, geographical regions were selected based partially on the number of observations. For example, the southern and central Baja California and central California areas, which had fewer samples, were more widely spaced than the southern California and northern Baja California areas. Nearly all of the anchovy samples taken south of lat. 32°N or north of lat. 34°N were taken within one-half degree of the coast. The lat. 32°-34°N area included a large amount of samples taken further than one-half degree from the coast. This area, the Southern California Bight, contains numerous islands and basins; we, therefore, divided it into regions which approximate the natural basins described in Emery (1954) (Fig. 2).

RESULTS

Growth

Earlier studies on northern anchovies from British Columbia (Pike 1951), northern California (Waldvogel 1977), central California (Clark and Phillips 1952), and southern California (Spratt 1975) showed considerable variation in their growth (Fig. 3A). Anchovies in British Columbia, lat. 49°N, and northern California, lat. 41°N, are of the northern stock (Vrooman et al. 1981) and have a summer spawning season. Anchovies in southern California, lat. 33°N, are of the central stock, whereas those in central California, lat. 36°N, are considered to be a mixture of northern and central stocks (Vrooman et al. 1981); anchovies in both southern and central California have a late winter (February-April) spawning season (Parrish footnote 3). Anchovies in British Columbia were the fastest growing of all the four areas in their first year of life, whereas anchovies in northern California were the slowest. Anchovies in central and southern California showed similar growth rates after their first year of life; however, the growth rate of anchovies in central California was greater than the growth rate of those in southern California in their first year.

Our study shows that the growth of anchovies has a distinct geographical pattern. Anchovies sampled in the Central California region (CC) and the offshore area of the Southern California Bight [i.e., San Nicolas (SN) and Tanner and Cortez Banks (TCB) regions] have the fastest juvenile growth (Fig. 3). Anchovies in these areas attain an average length of 120 mm before they are 1½ yr old. In the inshore areas of the Southern California Bight and in Baja California there is a continuous decline in the growth rate associated with decreasing latitude (Figs. 3, 4). Anchovies reach a mean length of 120 mm at about age 2 in the Santa Barbara Channel region (SBC)

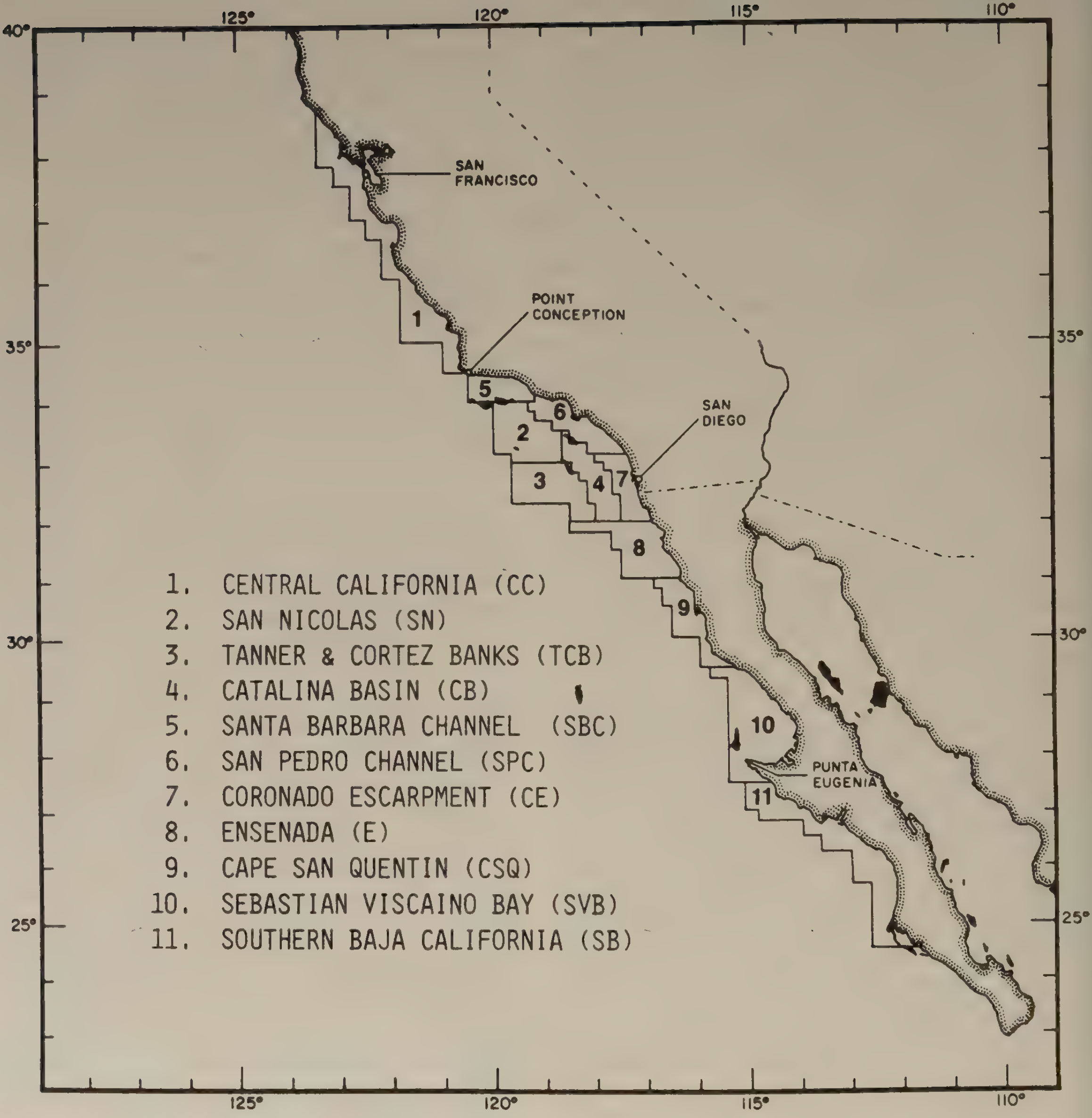
125°
120°
115°
110°
40°
35°
30°
25°
SAN FRANCISCO
POINT CONCEPTION
SAN DIEGO
PUNTA EUGENIA
1
2
3
4
5
6
7
8
9
10
11
1. CENTRAL CALIFORNIA (CC)
2. SAN NICOLAS (SN)
3. TANNER & CORTEZ BANKS (TCB)
4. CATALINA BASIN (CB)
5. SANTA BARBARA CHANNEL (SBC)
6. SAN PEDRO CHANNEL (SPC)
7. CORONADO ESCARPMENT (CE)
8. ENSENADA (E)
9. CAPE SAN QUENTIN (CSQ)
10. SEBASTIAN VISCAINO BAY (SVB)
11. SOUTHERN BAJA CALIFORNIA (SB)

FIGURE 2.—Geographical regions for which the growth and age composition of northern anchovies were determined.

and in the remaining offshore region, Catalina Basin (CB). In the San Pedro Channel (SPC), Coronado Escarpment (CE), and Ensenada (E) regions anchovies reach 120 mm at about age 3. In the Cape San Quentin (CSQ) and Sebastian Viscaino Bay (SVB) regions anchovies reach 120 mm at about age 4 or later.

The Cape San Quentin (CSQ), Sebastian Viscaino Bay (SVB), and Southern Baja California (SB) regions include anchovies from both the central and southern stocks, and there are marked differences in their growth (Fig. 4). Anchovies from the southern stock appear to reach an asymptotic mean size of about 92 mm, whereas those from the central stock continue to grow throughout their lives. Note the occurrences of 2- to 4-yr-old fish with monthly mean lengths of about 92 mm (Fig. 4 CSQ, SVB, SB). Assuming that stocks can be identified by size at age, the Cape San Quentin region appears to be dominated by the central stock; however, the

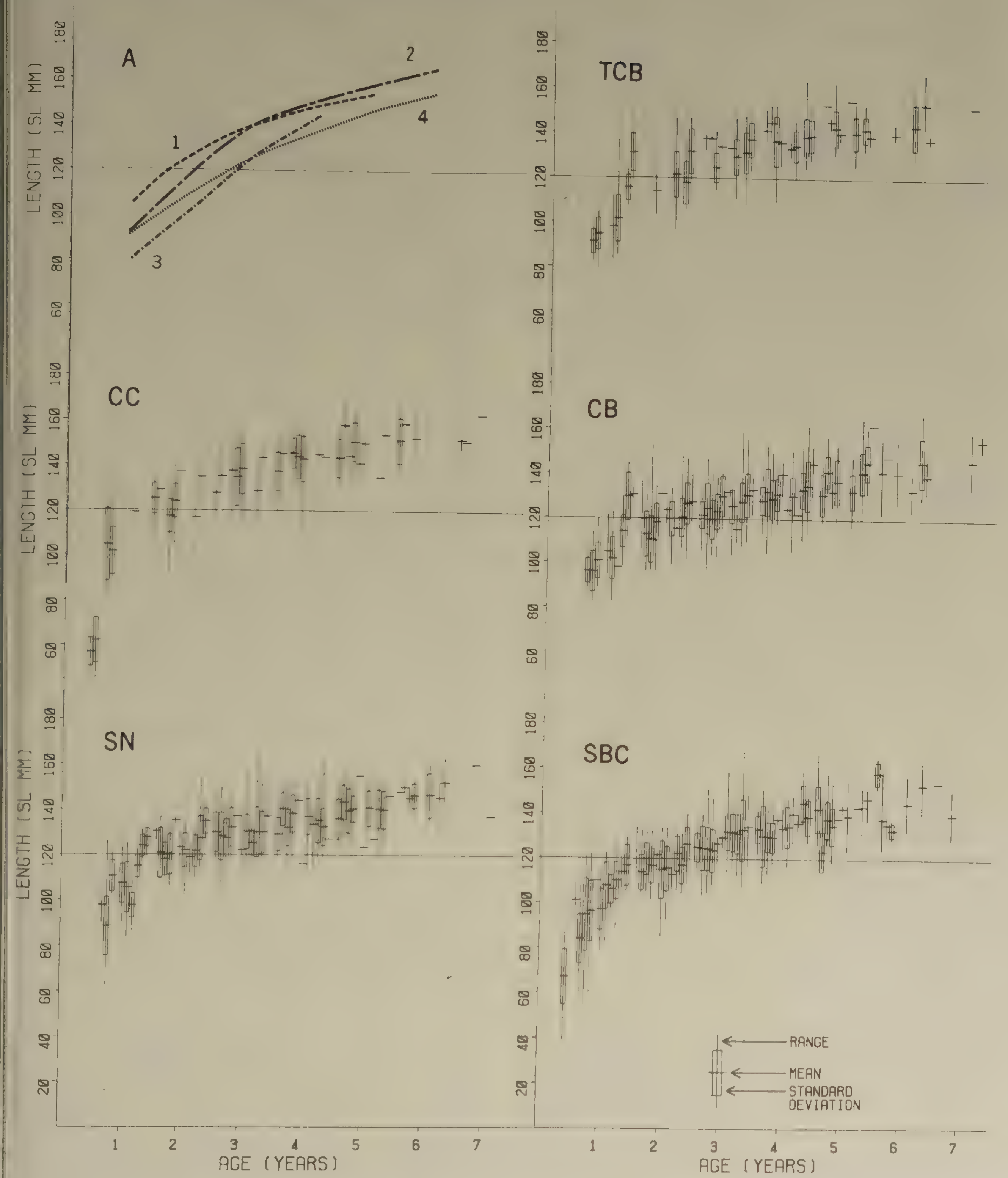

FIGURE 3.—Age-length relationships of northern anchovies taken in A. Earlier studies 1) British Columbia (Pike 1951), 2) Central California (Clark and Phillips 1952), 3) Northern California (Waldvogel 1977), and 4) Southern California (Spratt 1975), CC, Central California; SN, San Nicolas; TCB, Tanner and Cortez Banks; CB, Catalina Basin; SBC, Santa Barbara Channel.

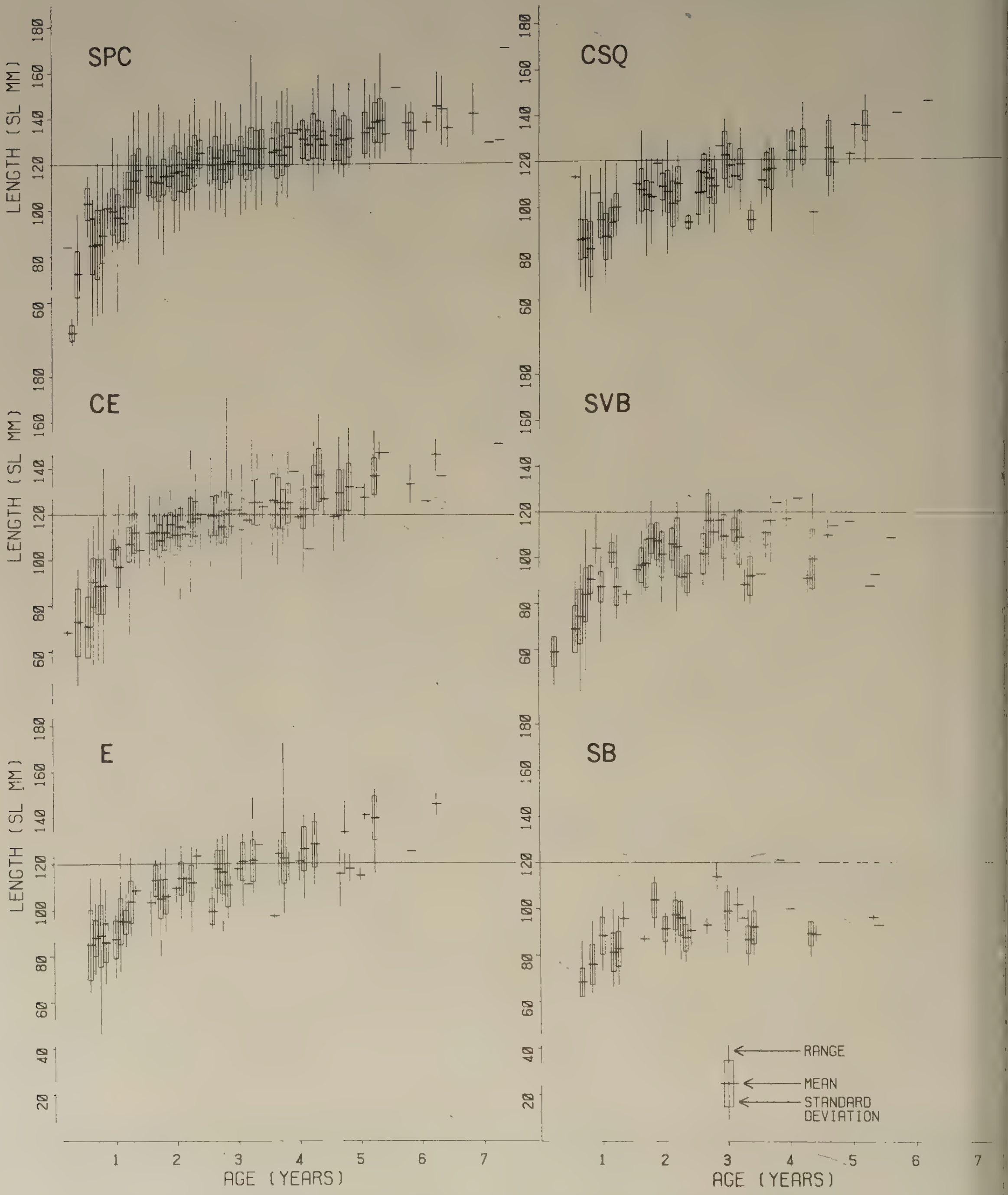

FIGURE 4.—Age-length relationships of northern anchovies taken in SPC, San Pedro Channel; CE, Coronado Escarpment; E, Ensenada; CSQ, Cape San Quentin; SVB, Sebastian Viscaino Bay; and SB, Southern Baja California.

southern stock does extend into this region. The most northerly trawl sample which could be identified, by size at age, as southern stock was a June 1971 sample taken at lat. 30.3°N. Southern and central stock anchovies broadly overlap in the Sebastian Viscaino Bay region; however, the region is occupied principally by the southern stock in the summer and by the central stock in the fall and winter. The Southern Baja California region is dominated by the southern stock; however, central stock anchovies, as identified by size at age, were taken as far south as lat. 26.5°N in November 1967. The fact that the central stock is the farthest south in winter and the southern stock the farthest north in summer suggests that the separation of the stocks is aided by different environmental preferences, possibly temperature.

The Central California region is an area of overlap between the northern and central anchovy stocks. In addition, as previously mentioned (Parrish footnote 3), a fall spawning stock may occur in central California and the offshore areas of the Southern California Bight. Vrooman et al. (1981) did not have any samples south of Monterey in central California or from the offshore and northern areas of the Southern California Bight. Samples from these areas may consist of a mixture of different stocks with different spawning seasons. Our assumption of a February birth month in these areas must therefore be evaluated.

Regression Analysis

Growth in length of anchovies in the size range sampled by the Sea Survey Program (i.e., 40-180 mm SL) can be divided into two phases. The early, juvenile phase extends until the fish are about 1 yr old. Methot (1981) found that in the Southern California Bight juvenile growth averages about 9 mm/mo, and it is at a maximum when the fish are between 40 and 50 mm SL. The second, adult phase extends from a little over 1 yr old until death. Growth during this phase is more than an order of magnitude less than the early phase (i.e., 0.48-0.69 mm/mo). Examination of the age-length relationships (Figs. 3, 4) in the central stock shows that growth in the adult phase is essentially linear. Therefore, we used linear regressions to compare growth of anchovies from different regions. These analyses included only fish of 1½ yr of age and older. This model has several advantages for comparing the growth during the two phases described above. By limiting the model to the linear segment of the age-length relationships, the slopes of the regressions can be used to compare the regional variations in growth rate during the adult phase. Another advantage is that the expected length at 1½ yr of age can be used to compare regional variation in growth during the juvenile phase.

Juvenile Growth

In the area occupied by the central stock, growth during the juvenile phase shows considerable variation among regions. There were significant differences in growth to age 1½. Fastest growth occurred in the north, and the slowest was in the south (Table 2, Fig. 5). Mean standard length at 1½ yr of age was 123.6 mm in the Central California region, 113.4 mm in the San Pedro Channel region, and 103.6 mm in the Cape San Quentin region. The three southernmost Baja California regions contain mixtures of the central and southern stocks; therefore, data from these regions were divided into central and southern stock sets, based on length and month, for the analyses. In contrast to those of the central stock, anchovies of the southern stock attain only 91.8 mm by age 1½. Within the Southern California Bight there is also an inshore-offshore gradient, with faster juvenile growth in the offshore regions and slower growth in the inshore regions (i.e., lengths at age 1½ in the Coronado Escarpment, Catalina Basin, and Tanner and Cortez Banks regions were 110.5, 116.4, and 119.2 mm respectively).

An analysis of covariance showed that the differences in size at age 1½ are not significantly different (α = 0.01) in two pairs of regions. The San Nicolas region (120.4 mm at age 1½) and the Tanner and Cortez Banks region (119.2 mm) are the first pair, and the Catalina Basin region (116.4 mm) and the Santa Barbara Channel region (116.2 mm) are the second pair. In all other pairs of regions, size at age 1½ is significantly different at the α = 0.0001 level.

Adult Growth

The regressions demonstrate that growth during the adult phase is relatively constant between the different regions occupied by the central stock, with slopes varying from a low of about 6 mm/yr to a high of about 8 mm/yr (Table 2). In contrast, anchovies of the southern stock have essentially no adult growth after age 1½ (i.e., slope = 0.07 mm/yr).

Although the differences in adult growth between regions is not large, there are statistically significant differences (Table 3). The San Nicolas region and the Tanner and Cortez Banks region have adult growth

TABLE 2.—Regression parameters and statistics for the relationship between age and length of northern anchovies older than 1½ yr: Central California (CC), San Nicolas (SN), Tanner-Cortez Banks (TCB), San Nicolas combined with Tanner-Cortez Banks (SN+TCB), Catalina Basin (CB), Santa Barbara Channel (SBC), Catalina Basin combined with Santa Barbara Channel (CB+SBC), San Pedro Channel (SPC), Coronado Escarpment (CE), Ensenada (E), Cape San Quentin (CSQ), Sebastian Viscaino Bay and Southern Baja California, central stock only (SVB+SB), and Southern Baja California, southern stock only (S).

Area	Mean age (Yr)	Mean length (SL mm)	Length at age 1½ (SL mm)	Adult growth (mm/yr)	*r*	SD of length at age 1½	SD of adult growth	*N*
				Central Stock				
CC	3.4	138.4	123.6	7.75	0.702	1.563	0.431	335
SN	3.3	131.1	120.4	5.97	0.613	0.713	0.205	1,410
TCB	3.2	130.8	119.2	6.69	0.623	0.975	0.286	860
SN+TCB	3.3	131.0	120.0	6.23	0.616	0.577	0.167	2,270
CB	3.1	126.7	116.4	6.29	0.582	0.633	0.192	2,092
SBC	2.9	125.6	116.2	6.83	0.636	0.689	0.224	1,374
CB+SBC	3.0	126.3	116.4	6.50	0.606	0.465	0.145	3,466
SPC	2.8	121.3	113.4	6.07	0.575	0.435	0.146	3,497
CE	2.7	118.7	110.5	6.89	0.569	0.666	0.235	1,798
E	2.8	116.5	106.2	8.08	0.636	0.944	0.321	934
CSQ	2.5	111.1	103.6	7.54	0.649	0.776	0.291	923
SVB+SB	2.4	106.4	101.1	5.76	0.443	1.571	0.618	358
				Southern Stock				
S[1]	2.9	91.9	91.8	0.07	0.009	1.274	0.421	335

[1] Combined from three areas: CSQ, SVB, and SB.

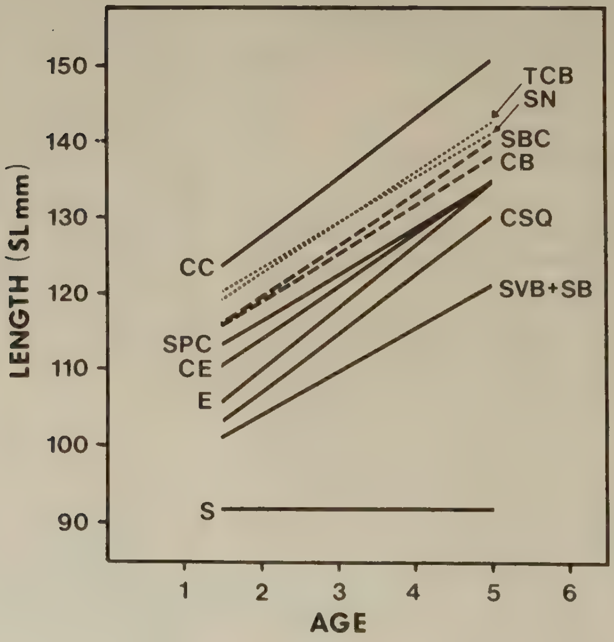

FIGURE 5.—Linear regressions showing the expected length at age (Table 1) of northern anchovies taken in CC, Central California; SN, San Nicolas; TCB, Tanner and Cortez Banks; CB, Catalina Basin; SBC, Santa Barbara Channel; SPC, San Pedro Channel; CE, Coronado Escarpment; E, Ensenada; CSQ, Cape San Quentin; SVB+SB, Sebastian Viscaino Bay and Southern Baja California, central stock only; and S, Southern Baja California, southern stock only.

patterns which are not statistically different (α = 0.01), and since the two regions are adjacent we have considered them together. Also there is no significant difference (α = 0.01) in adult growth in the Catalina Basin and the Santa Barbara Channel regions, but since these regions are geographically separated we have retained them as separate regions. The relatively large standard deviations of the regression slopes (Table 2) for fish from the Central California and the Sebastian Viscaino Bay and the Southern Baja California regions may indicate that these regions are the most likely to have mixtures of more than one stock.

There was no significant difference (α = 0.01) between growth of adults in the best growth regions (Ensenada, Cape San Quentin, and Central California). The difference between the Coronado Escarpment and the Santa Barbara Channel regions is not significant at the α = 0.1 level nor are the differences between the Catalina Basin, combined San Nicolas-Tanner and Cortez Banks, San Pedro Channel, and combined Sebastian Viscaino Bay and Southern Baja California regions.

TABLE 3.—Significance levels for differences in growth of adult northern anchovies from different geographical regions: Ensenada (E), Central California (CC), Cape San Quentin (CSQ), Coronado Escarpment (CE), Santa Barbara Channel (SBC), Tanner and Cortez Banks (TCB), Catalina Basin (CB), San Nicolas combined with Tanner and Cortez Banks (SN+TCB), San Pedro Channel (SPC), San Nicolas (SN), Sebastian Viscaino Bay and Southern Baja California, central stock only (SVB+SB), and Southern Baja California, southern stock only (S). Geographic areas are arranged in order from largest to smallest slopes.

Area	E	CC	CSQ	CE	SBC	TCB	CB	SN+TCB	SPC	SN	SVB+SB	S
E	—											
CC	0.5573	—										
CSQ	0.2217	0.6517	—									
CE	0.0019	0.0514	0.0754	—								
SBC	0.0015	0.0477	0.0629	0.9422	—							
TCB	0.0013	0.0331	0.0384	0.6516	0.6951	—						
CB	0.0000	0.0000	0.0000	0.0605	0.0628	0.2400	—					
SN + TCB	0.0000	0.0003	0.0002	0.0283	0.0280	0.0000	0.8141	—				
SPC	0.0000	0.0000	0.0000	0.0015	0.0033	0.0465	0.3560	0.4659	—			
SN	0.0000	0.0000	0.0000	0.0042	0.0042	0.0367	0.2547	0.3234	0.6902	—		
SBV + SB	0.0000	0.0085	0.0051	0.0826	0.0952	0.1616	0.3943	0.4372	0.6048	0.7379	—	
S	0.0000	0.0000	0.0000	0.0000	0.0000	0.0000	0.0000	0.0000	0.0000	0.0000	0.0000	—

Age Composition by Area

Geographical variation in age composition is one factor which could influence the observed variation in mean size of anchovies in the various regions; therefore, age composition was calculated for each of the regions used earlier (Fig. 2). Few anchovies < 60 mm SL occur in the data, and it appears that young-of-the-year fish are apparently not susceptible to capture by the midwater trawl gear used in the sea survey until they are about 6 mo old.

Central California and the three offshore regions within the Southern California Bight (San Nicolas, Tanner and Cortez Banks, and Catalina Basin) differ from the other regions in that they are dominated by fish 3 yr and older (Fig. 6A, Table 4). Central California and Tanner and Cortez Banks also have substantial percentages of young-of-the-year fish, whereas the other two regions do not.

Anchovies in the three inshore regions of the Southern California Bight (Santa Barbara Channel, San Pedro Channel, and the Coronado Escarpment) have very similar age compositions (Fig. 6B, Table 4). One- and two-yr-old fish are the most numerous in these three regions. Young-of-the-year and 3 yr-olds are slightly less abundant than 1- and 2-yr-olds, and there are fewer older fish in the samples.

Baja California is characterized by a dominance of young fish (Fig. 6C, Table 4). The age compositions in the Ensenada, Cape San Quentin, and Sebastian Viscaino Bay regions are very similar; young-of-the-year and 1-yr-old fish are the most abundant, and there is rapid decrease in the abundance of fish with increasing age. Anchovies in southern Baja California are principally from the southern stock. The age composition in this region shows a preponderance of 1-yr-olds, and like the other Baja California regions there are few fish of age 4 or older.

Age Composition by Depth Strata

Anchovies primarily live within the upper mixed layer; they occur in the surface layer over the continental shelf and over deepwater regions. Mais (1974) showed that the average size of anchovies sampled in offshore areas was greater than that of anchovies sampled near the coast. The percentage of trawl hauls containing anchovies was quite constant in areas with different water depths, varying

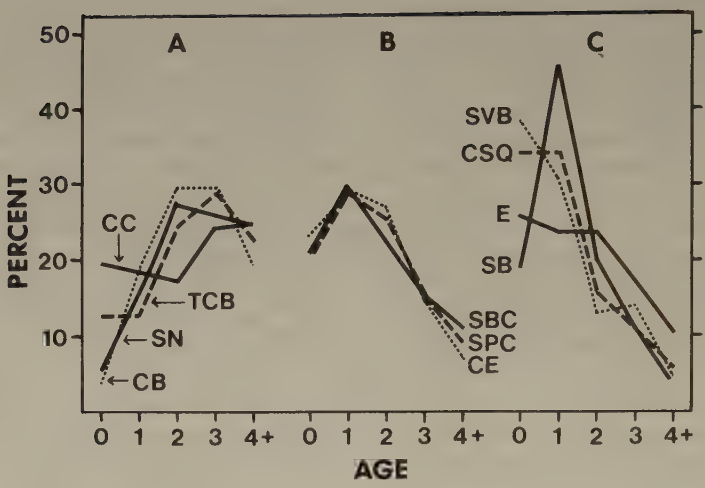

FIGURE 6.—Age composition of northern anchovies taken in the following geographical regions: A. Central California and offshore areas of the Southern California Bight; Central California (CC), San Nicolas (SN), Tanner and Cortez Banks (TCB), and Catalina Basin (CB); B. Inshore areas of the Southern California Bight; Santa Barbara Channel (SBC), San Pedro Channel (SPC), and Coronado Escarpment (CE); C. Baja California; Ensenada (E), Cape San Quentin (CSQ), Sebastian Viscaino Bay (SVB), and Southern Baja California (SB).

TABLE 4.—Percentage age composition of northern anchovies by geographical region: Central California (CC), San Nicolas (SN), Tanner-Cortez Banks (TCB), Catalina Basin (CB), Santa Barbara Channel (SBC), San Pedro Channel (SPC), Coronado Escarpment (CE), Ensenada (E), Cape San Quentin (CSQ) Sebastian Viscaino Bay (SVB), Southern Baja California (SB).

	Age							
Area	0	I	II	III	IV	V	VI+	No. fish
CC	19.3	17.2	14.7	23.9	17.7	5.7	1.6	436
SN	5.6	15.5	27.7	26.0	15.9	7.4	2.0	1,721
TCB	12.6	12.6	24.3	28.3	13.6	6.5	2.1	1,136
CB	3.7	18.7	29.2	29.2	12.8	5.2	1.1	2,538
SBC	21.8	29.6	22.2	15.2	8.2	2.4	0.6	1,989
SPC	21.6	28.6	25.4	15.6	6.3	1.9	0.5	5,439
CE	23.5	28.1	26.9	14.6	5.4	1.3	0.2	2,965
E	25.8	23.6	23.4	17.1	7.6	2.3	0.2	1,464
CSQ	33.8	33.7	15.5	11.2	4.4	1.2	0.1	1,779
SVB	38.1	30.8	12.8	13.5	4.5	0.3	—	896
SB	18.8	45.7	19.6	11.5	3.7	0.7	—	409

between 64 and 77% (Table 5). This is probably influenced by the fact that trawling (in the upper 30 m) was carried out normally in areas where fish schools had already been detected by depth recorder or sonar.

In southern California (lat. 32°-34°N) young-of-the-year anchovies comprise more than one-half of the anchovies sampled in the 5-25 fathom-depth stratum (Table 6A). One- and two-yr-olds comprise more than one-half of the anchovies in the 26-50, 51-150, 151-300, and 301-500 fathom strata. The most abundant age group in the 26-50 stratum is age 1; there are essentially equal numbers of age 1 and age 2 anchovies in the 51-150 and 151-300 strata; 2-yr-olds are the most abundant age group in the 301-500 stratum; and 3-yr-olds are the most abundant age group in the 701+ stratum. Age groups 3-6+ each show an increasing percentage with increasing depth. Collectively they comprise about 11% of the 5-25 stratum, 31% of the 51-150 stratum, and 51% of the 701+ stratum. The same general pattern occurs in northern Baja California (lat. 29.5°-32°N); however, the percentage of young fish declines more

TABLE 5.—Percentage of midwater trawl hauls taking northern anchovies by depth strata. Trawl hauls were normally within 30 meters of the surface.

Depth (fm)	Total sets	% sets with anchovies
5-25	704	75
26-50	828	69
51-150	554	69
151-300	546	76
301-500	752	77
501-700	437	73
701 +	345	64
Total	4,166	72

TABLE 6.—Age composition (%) of northern anchovies taken in shallow and deep-water areas (depth in fathoms).

A

	Lat. 32°-34°N						
Age Depth:	5-25	26-50	51-150	151-300	301-500	501-700	701 +
0	56.5	26.3	16.9	7.8	5.5	3.0	6.5
I	20.6	29.5	26.5	27.4	25.8	17.9	15.5
II	12.5	24.1	26.0	27.9	30.6	32.0	26.8
III	7.0	12.3	20.1	22.8	22.7	28.2	27.1
IV	2.5	5.8	6.8	9.1	10.5	13.3	15.3
V	0.8	1.5	3.2	3.6	3.8	4.9	7.2
VI +	0.2	0.5	0.6	1.4	1.1	0.6	1.7
n	1,579	1,492	1,102	2,199	3,704	2,091	1,086

B

	Lat. 29.5°-32°N			
Age Depth:	5-25	26-50	51-150	151 +
0	56.1	36.8	21.0	8.9
I	23.1	40.4	28.5	28.8
II	12.3	10.8	24.2	26.9
III	6.2	7.8	14.2	23.3
IV	1.9	3.6	9.4	8.7
V	0.3	0.6	2.5	3.0
VI +	—	—	0.2	0.3
n	935	619	480	1,189

C Aug.-Dec.

	Lat. 29.5°-32°N				Lat. 32°-34°N			
Age Depth:	5-25	26-50	51-150	151 +	5-25	26-50	51-150	151-300
0	62.8	52.6	38.7	24.9	66.2	37.8	26.4	16.0
I	18.2	32.3	29.2	43.0	15.6	29.0	24.7	21.0
II	11.7	10.6	19.9	24.4	12.1	22.5	25.8	32.4
III	5.7	4.0	8.2	6.4	5.0	8.6	16.1	21.2
IV	1.6	0.5	4.1	1.2	0.9	2.0	5.1	8.3
V	—	—	0.7	—	0.2	0.1	1.8	0.9
VI +	—	—	—	—	—	—	—	0.2
n	806	378	267	405	1,286	1,013	546	990

slowly with increasing depth there than in southern California (Table 6B). In both southern California and northern Baja California, there is a direct relationship between average age and depth of water in which fish were caught. In the period August-December when smaller (< 60 mm) anchovies can be caught by midwater trawls, there is a greater dominance of young-of-the-year fish in the shallower water (Table 6C). In the northern Baja California area, 63% of the 5-25 stratum and 53% of the 25-50 stratum were young-of-the-year fish. In southern California the corresponding percentages were 66 and 38.

Sea Survey - Fishery Comparisons

The purse seine fleets which harvest anchovies operate primarily out of San Pedro, California, and Ensenada, Mexico. The age composition of anchovies in the San Pedro fishery (Mallicoate and Parrish 1981) contains a smaller proportion of age 0 and age 1 fish than does the sea survey data for the San Pedro Channel region. We only had 2 years of age composition data for the Ensenada fishery available to us (Sunada and Silva 1980), but this limited information shows the same dominance of younger anchovies as in the sea survey data for this region. The San Pedro fishery had several regulations which reduced the numbers of young fish in the catch. These included a 5-in minimum size limit and a series of area closures which prevent the fleet from fishing in nearshore areas. The Ensenada fishery did not have regulations which influenced the age composition of the catch.

To evaluate the effects of the area closures and size limit on the San Pedro fishery, we broke the sea survey data into depth classifications, < 50 fathoms and > 50 fathoms. The > 50 fathom classification was intended to approximate the area of the fishery (i.e., the coastal strip is excluded). In this area the age composition of anchovies taken by the Sea Survey Program is very close to that taken by the fishery; conversely, the age composition of the fishery is unlike that taken in areas < 50 fathoms (Fig. 7). The California fishery no longer has a 5-in size limit; however, the closure of the nearshore area appears to be the dominant factor in reducing the catch of young anchovies.

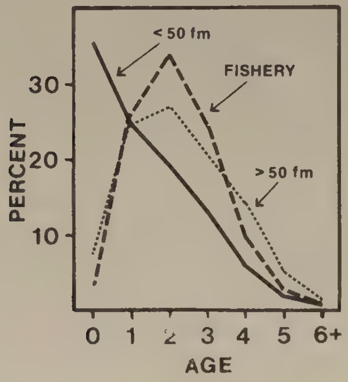

FIGURE 7.—Comparison of the age composition of northern anchovies taken in the San Pedro purse seine fishery with those taken in areas with <50 fathoms and >50 fathoms of water in the midwater trawl Sea Survey Program.

DISCUSSION

Our data show that the growth rate and the age composition of northern anchovies vary geographically. The greatest differences in growth appear to occur during the juvenile stage; growth in adults shows much less regional variation. Juvenile growth is greatest in central California and in the offshore areas of the Southern California Bight. In the inshore regions there is a trend toward reduced juvenile growth from central California to southern Baja California. Average size at age 1½ falls from 123.6 mm to 91.8 mm over this area. Growth in adult anchovies appears to be the greatest in northern California, and it is also relatively high in British Columbia (Pike 1951), central California, and northern Baja California. Adult growth appears to be relatively low in the Southern California Bight; this, however, may be an artifact as this area probably includes resident fish plus slower growing fish which have moved into this region from the south. Age composition showed a large variation among regions, and the pattern of this variation appears to be closely related to the gyral circulation within the Southern California Bight. There is also a strong relationship in age composition to the depth of water at trawl sites. Adult anchovies dominated the catches in the offshore, deepwater regions of the Southern California Bight and in central California. Age also had a strong latitudinal gradient with adult fish dominating in the north and young-of-the-year and yearling fish dominating in the shallow water areas off central and northern Baja California. Adult anchovies appear to be concentrated in areas of the Bight where prevailing currents will result in southerly and inshore larval transport (Parrish et al. 1981). At recruitment, anchovies appear to be heavily concentrated in shallow water, and young fish appear to be concentrated in the nearshore area where they will tend to be advected northward by the southern California gyre.

As will be discussed later, the interpretation of the regional differences in juvenile growth is dependent upon the stock structure in the various regions. Earlier studies (McHugh 1951; Vrooman et al. 1981) showed that the boundary between the southern and central stocks was in the northern Sebastian Viscaino Bay area. This is supported by the present study, and, as previously mentioned, the boundary is further north in the summer and fall and further south in winter and spring. We feel that there is ample evidence that the southern stock had the smallest juvenile growth rate and that growth during the adult phase is minor. Vrooman et al. (1981) suggested that the boundary between the northern and central stocks occurs in the central California area; both northern and central stocks occurred in samples taken at San Francisco (lat. 37°50′N) and Monterey (lat. 36°50′N). Their data might be interpreted to suggest that a fourth stock occurred in the San Francisco and Monterey samples, and in addition it has been suggested (Parrish footnote 3) that this fourth stock spawns during the fall in central California and the offshore areas of the Southern California Bight. Unfortunately the Vrooman et al. (1981) study did not have any samples from the region between Monterey (lat. 36°50′N) and Newport (lat. 33°30′N), nor were there any samples from the offshore areas of the Southern California Bight. It is therefore not presently possible to determine the amount of stock mixture over much of the accepted range of the central stock.

Variation in juvenile growth of northern anchovies in the different regions may be due to genetic factors, differences in the seasonality of spawning, or environmental factors. The northern stock has a relatively short spawning season with a strong peak in July (Richardson 1980). The central stock has a more extended spawning season with a broad peak from February to April, and there is some spawning all year in the central stock region. It is not yet known if the anchovies that spawn in central and southern California during the summer and fall are from the central stock, northern stock, or a possible fall spawning stock. If the anchovies in this region are predominatly from the central stock, the relatively high juvenile growth in central California and the offshore portion of the Bight might be due to a favorable feeding environment. Offshore portions of the Southern California Bight have been shown to have considerably more plankton and nutrients than the inshore portions (Reid et al. 1958; Owen 1980). If the anchovies in the area occupied by the central stock have a large component that are not central stock, the increased juvenile growth could be due to the genetic differences, due to environmental differences, or caused by the assumption of a February birth month. At our "assumed" age of 1½ yr, an anchovy spawned in the fall would be about 6 mo older than the "normal" central stock anchovy. If the growth that occurred during these additional 5 mo was at the normal adult rate (i.e., 0.48-0.69 mm/mo), there would be only a 2-4 mm difference in the size of the two fish. However, the difference in mean length between 1½-yr-old anchovies in the central California and Cape San Quentin regions is 20 mm. If, however, growth during the 5 mo is even one-half of the average juvenile rate (i.e., 9 mm/mo) the difference in size at "1½" yr could be achieved.

CONCLUSION

The interpretation of regional variations in the growth and age composition of northern anchovies in the area between central California and central Baja California and the implications of this study for fisheries management are dependent upon the stock structure of the anchovies in the area.

If a significant proportion of these fish are not from the central stock, this study suggests the following:

1. The observed regional variation in age composition may be the result of mixtures of stocks with different mortality rates.
2. The juvenile growth rate of anchovies in the central stock is lower than that of anchovies from the northern stock(s). The reason for this lower growth rate could be either genetic, environmental, or dependent upon the seasonality of spawning.
3. The southern California and Mexican fisheries are based on different stock mixtures, and thus the interactions between these fisheries would not be as great as they would be if both were based entirely on the same stock.

If essentially all of these anchovies are from the central stock, this study suggests the following:

1. The offshore regions of the Southern California Bight contain a disproportionate share of the adult anchovies; however, recruitment does not occur here to any significant extent.
2. Recruitment occurs largely in shallow water along the coast, and the northern Baja California region has the largest percentage share of young-of-the-year anchovies.
3. Larvae and juveniles recruited from the offshore regions of the Southern California Bight tend to move or be advected south and inshore.
4. The relatively high juvenile growth rates in central California and the offshore regions of the Southern California Bight are due to favorable environmental conditions.
5. As they grow older anchovies tend to move, or be advected, north and offshore.
6. Mixing of adults is not complete; otherwise length at age and age composition would be the same everywhere.
7. Due to the inferred tendency for recruitment to occur in the south, an extensive fishery on the central stock would reduce the proportion of older anchovies and result in fewer older anchovies in the northern and offshore areas.
8. The combination of the large Mexican fishery, which has been associated with a reduction in the proportion of older anchovies (Mais 1982), and the continued closure of the nearshore areas where younger fish are concentrated will severely impact the California fishery.

ACKNOWLEDGMENTS

We are grateful to Roy Mendelssohn, Alec MacCall, Janet Mason, and Rick Methot for their comments and editorial assistance. In addition we wish to thank Susie Myers for her help in completing the manuscript.

LITERATURE CITED

AHLSTROM, E. H.
1966. Distribution and abundance of sardine and anchovy larvae in the California Current Region off California and Baja California, 1951-64: A summary. U.S. Fish Wildl. Serv., Spec. Sci. Rep.—Fish. 534, 71 p.

CLARK, F. N., AND J. B. PHILLIPS.
1952. The northern anchovy (*Engraulis mordax*) in the California fishery. Calif. Fish Game 38:189-207.

COLLINS, R. A.
1969. Size and age composition of northern anchovies (*Engraulis mordax*) in the California anchovy reduction fishery for the 1965-66, 1966-67, and 1967-68 seasons. Calif. Dep. Fish Game Fish Bull. 147:56-74.

COLLINS, R. A., AND J. D. SPRATT.
1969. Age determination of northern anchovies, *Engraulis mordax*, from otoliths. Calif. Dep. Fish Game Fish Bull. 147:39-55.

EMERY, K. O.
1954. Source of water in basins off southern California. J. Mar. Res. 13:1-21.

HAUGEN, C. W., J. D. MESSERSMITH, AND R. H. WICKWIRE.
1969. Progress report on anchovy tagging off California and Baja California, March 1966 through May 1969. Calif. Dep. Fish Game Fish Bull. 147:75-89.

MAIS, K. F.
1974. Pelagic fish surveys in the California Current. Calif. Dep. Fish Game Fish Bull. 162:1-79.
1981. Age-composition changes in the anchovy, *Engraulis mordax*, central population. Calif. Coop. Oceanic Fish. Invest. Rep. 22:82-87.

MALLICOATE, D. L., AND R. H. PARRISH.
1981. Seasonal growth patterns of California stocks of northern anchovy, *Engraulis mordax*, Pacific mackerel, *Scomber japonicus*, and jack mackerel, *Trachurus symmetricus*. Calif. Coop. Oceanic Fish. Invest. Rep. 22:69-81.

McHUGH, J. L.
1951. Meristic variations and populations of northern anchovy (*Engraulis mordax mordax*). Bull. Scripps Inst. Oceanogr. 6:123-160.

METHOT, R., JR.
1981. Growth rates and age distributions of larval and juvenile northern anchovy, *Engraulis mordax*, with inferences on larval survival. Ph.D. Thesis, Univ. California, San Diego, 388 p.

OWEN, R. W.
1980. Eddies of the California Current System: physical and ecological characteristics. *In* D. M. Power (editor), The California Islands: Proceedings of a multidisciplinary symposium, p. 237-263. Santa Barbara Mus. Nat. Hist. (Calif.).

PARRISH, R. H., C. S. NELSON, AND A. BAKUN.
1981. Transport mechanisms and reproductive success of fishes in the California Current. Biol. Oceanogr. 1:175-203.

PIKE, G. C.
1951. Age, growth and maturity studies on the Pacific anchovy (*Engraulis mordax*) from the coast of British Columbia. M.A. Thesis, Univ. British Columbia, Vancouver, 44 p.

REID, J. L., G. I. RODEN, AND J. G. WYLLIE.
1958. Studies of the California Current System. Calif. Coop. Oceanic Fish. Invest. Rep., 1 July 1956 to 1 January 1958, p. 28-56.

RICHARDSON, S. L.
1980. Spawning biomass and early life of northern anchovy, *Engraulis mordax*, in the northern subpopulation off Oregon and Washington. Fish. Bull., U.S. 78:855-876.

SPRATT, J. D.
1975. Growth rate of the northern anchovy, *Engraulis mordax*, in southern California waters, calculated from otoliths. Calif. Fish Game 61:116-125.

SUNADA, J. S., AND S. SILVA.
1980. The fishery for northern anchovy, *Engraulis mordax*, off California and Baja California in 1976 and 1977. Calif. Coop. Oceanic Fish. Invest. Rep. 21:132-138.

VROOMAN, A. M., P. A. PALOMA, AND J. R. ZWEIFEL.
1981. Electrophoretic, morphometric, and meristic studies of subpopulations of northern anchovy, *Engraulis mordax*. Calif. Fish Game 67:39-51.

WALDVOGEL, J. B.
1977. Age, maturity and distribution of northern anchovy *Engraulis mordax* in Humboldt Bay, California. M.S. Thesis, Humboldt State Univ., Arcata, CA, 36 p.

8568

SC/36/SM2

The Former Dolphin Fishery at St Helena

William F. Perrin

Southwest Fisheries Center, National Marine Fisheries Service, NOAA, P.O. Box 271, La Jolla, California

ABSTRACT

The spotted dolphin exploited at St Helena is of the same species as that exploited in the eastern tropical Pacific and referred to *Stenella attenuata*. Take is now illegal, but former catches were about 50–300 annually. A few bottlenose dolphins, *Tursiops truncatus*, were also taken. Impacts on the population are uncertain, because of poor documentation of catches and lack of good estimates of current population sizes. The fishery apparently originated in 'porpoise' harpooning by 19th-century whalers. The population of spotted dolphins is apparently isolated and offers a good opportunity for observation of what happens in a dolphin population when exploitation is halted.

INTRODUCTION

The existence of a dolphin fishery at the Island of St Helena (a Crown Colony of the UK) has been known for some time (Melliss, 1875; Fraser, 1966; Taylor, 1969; Finneran, 1979), but there has been very little information available on the identity of the animals taken or on the methods and scale of the fishery (Anon., 1980; 1981). The information reported here was gathered during a visit to St Helena during April–June 1983. The primary purpose of the visit was to determine the identity of spotted dolphins (*Stenella* sp.) reported from the island by Fraser (1966), as part of a taxonomic study of spotted dolphins of the Atlantic (Perrin and Perrin, in press). A secondary goal was to document the methods, catches, history, economic aspects and present status of the dolphin fishery.

METHODS

I observed and photographed dolphins on the lee side of the island from a chartered 28 ft (8.6 m) open fishing boat on 5, 11, 16, 26 May and 2 June.

The usual observation strategy was to make multiple passes through the moving school, photographing on the down-swell legs. On 5 and 26 May, I observed and photographed the animals underwater. On the latter underwater session the fishermen chummed with live bait (small mackerel), which held the dolphins within underwater viewing range for several minutes.

On 25 May, a 35 ft (10.8 m) sailboat was chartered to circle the island to observe cetaceans on the windward side, but the weather was rough and no cetaceans were seen.

To collect information on the dolphin fishery, which was officially halted in 1979 (Anon., 1981), interviews were tape-recorded with ten fishermen and one boat owner (Table 1) concerning its history, methods, catches and economics. Informal discussions were held with an additional 35–40 individuals, including government officials and employees of the St Helena Fisheries Corporation. I was interviewed by the island radio station and a notice was inserted in the island newspaper asking for information on the dolphin fishery.

Several days were spent examining books, official records and 19th-century newspaper files maintained in the island library and the Archives, but lack of time meant that I was able to examine only a fraction of the available material.

Table 1

Recorded interviews

	Occupation	Age	Started fishing	Status
1 *	Fisherman	75	1918–19	Retired
2	Fisherman	82	1914	Retired
3	Fisherman	>70	Before 1930	Retired
4 *	Fisherman	>70	1958–60	Retired
5 *	Fisherman	>70	Before 1930	Retired
6	Fisherman	>70	1920	Retired
7	Fisherman	68	-1925	Retired
8	Fisherman	62	–	Retired
9	Boat owner	>70	Before 1950	Active
10	Fisherman	43	1954	Active
11	Fisherman	>60	Before 1940	Inactive

* Sold dolphin heads to the British Museum.

THE DOLPHINS

Pantropical spotted dolphin, *Stenella* sp.

The taxonomy of the spotted dolphins is unsettled. It is likely that two species inhabit the Atlantic, an endemic species that has been referred in recent years to *S. plagiodon* and *S. frontalis* and a pantropical species that has been referred to *S. attenuata* and *S. frontalis*. While the species-level nomenclature has not yet been resolved (Perrin and Perrin, in press), the spotted dolphins at St Helena are of the pantropical type. I clearly observed the color-pattern characteristics that are diagnostic of the pantropical species (Perrin, 1975): white-tipped beak, cape well defined and passing high over the eye and with greatest depth at level of dorsal fin, narrow light band subsidiary to the cape, flipper stripe to gape and dorso-ventral division of the peduncle into upper dark and lower light areas. Calves are unspotted, and juveniles have pronounced dark spots below. Dorsal spotting in adults is so poorly developed as to appear absent when the animals are seen at a distance of only a few meters. In this they resemble the spotted dolphins that occur in Hawaiian waters (referred to *S. attenuata*—Perrin, 1975).

This was the dolphin most commonly harpooned in the fishery. The island fishermen call it 'bottlenose porpoise' or simply 'porpoise'. Skulls that were sold to the British Museum in the 1950s and 1960s (Fraser, 1966) came from the school of this species that frequents the northern side of the island.

The school that I observed consisted of several hundred dolphins. On each of the five days that I worked with it, it came into shallow water within 0.5 km of shore along the southern half of the northern, lee side of the island (Egg Island to Lemon Valley, Fig. 1) in the early morning and moved slowly north past Jamestown and went back offshore at the northern edge of the lee of the Island, off Sugar Loaf Point, before noon. During this slow passage, the school appeared to be loosely organized and dispersed over a distance of about 0.5 km in subgroups of about 5–10 animals. Groups of animals milled and made short forays offshore. There was a great deal of aerial activity, including high leaps (mostly by juveniles), forward flips, pitch-poling and tail lobbing. I observed occasional intense flurries of surface activity involving two or more animals and evidenced by violent, confused splashing.

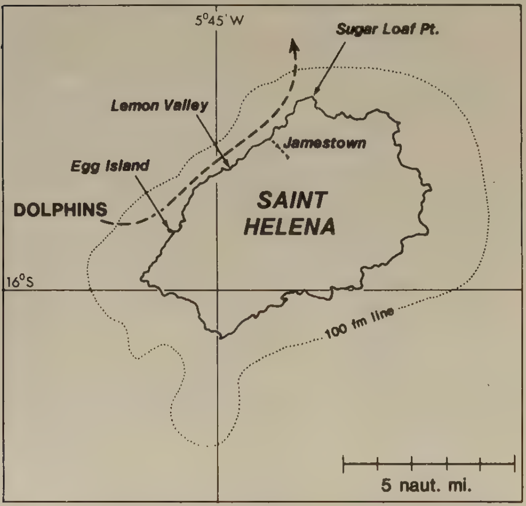

Fig. 1. Typical morning movement of the spotted dolphin school at St Helena in April–May, 1983.

Each time the school was approached, individual dolphins came to meet the boat and briefly rode the bow. They did not surface at the bow to breathe, but moved a few meters away from the boat, blew, and returned to the bow underwater. This differs from the typical bowriding behavior that I have seen in this species in other areas (e.g., Hawaii), in which the animals surface to breathe at the bow, and may be related to the fishermen's practice of harpooning dolphins from the bow.

On 11 May, I followed the dolphins to the edge of the Island's lee, off Sugar Loaf Point. Here part of the school spent several minutes 'surfing' in short steep swells coming from the northeast. It appeared that some of the dolphins made several passes in the waves, doubling back after traveling 100 m or so.

Several fishermen told me that once the school has gone offshore and out of the lee of the Island, it breaks up into several smaller schools that can be encountered up to several kilometers offshore in the afternoon. They are also occasionally seen on the windward side of the Island. Concerning seasonal variation in the daily pattern of movement of the school(s), they said that the dolphins are 'easiest to find' in April–May (the fishermen frequent the area year-round).

Bottlenose dolphin, *Tursiops truncatus*
This dolphin is called 'cowfish' or 'cow porpoise' but may be called 'angerine' by some fishermen (discussed below). It was taken in lesser numbers than the spotted dolphin. The collection at the British Museum (Natural History) contains 10 skulls from St Helena (Pilleri and Gihr, 1972).

I observed the bottlenose dolphin two (or possibly three) times. On 5 May, I saw several large dark dolphins with high falcate dorsal fins together with the school of spotted dolphins, off Lemon Valley. The fishermen said these were 'cowfish', but I did not get a good look at them. On 2 June, I photographed a small school (10–15) of bottlenose dolphins just inside Sugar Loaf Point at 0830 hours. Each time the dolphins were approached, they evaded the boat by diving for several minutes and coming up about 200 m away. On 5 June at 1420 hours, as I left the island aboard the R.M.S. *Centaur,* several bottlenose dolphins joined the ship about 5–7 km offshore, NE of the island, and rode the bow and the stern wake for about 10 minutes.

The fishermen told us that 'cowfish' sometimes frequent James Bay at night, feeding on flying fish that are attracted to lights on the waterfront.

Tursiops truncatus also occurs at Ascension Island, about 700 nmi northwest of St Helena. An officer on the R.M.S. *Centaur* (S. Bhatia) showed us a video-tape of several bottlenose dolphins riding the bow of the ship just off Ascension Island on 12 March, 1983.

Other Species
The only other species of small cetacean that can be said with certitude to occur (or have occurred) at or near St Helena is the spinner dolphin, *Stenella longirostris,* based on a skull in the Cleveland Museum of Natural History (No. 2413) labeled as collected at St Helena by the Blossom South Atlantic Expedition on 10 October, 1926. I showed photographs of spinner dolphins to several fishermen, but they did not recognize it, nor did they remember having seen its distinctive spinning behavior.

The fishermen reported occasional or seasonal occurrence of 'whale killers' (possibly killer whales, *Orcinus orca*); 'blackfish' (possibly short-finned pilot whales, *Globicephala macrorhynchus* and/or false killer whales, *Pseudorca crassidens*); 'whitebelly porpoise' (possibly common dolphins, *Delphinus delphis,* striped dolphins, *Stenella coeruleoalba,* or Fraser's dolphins, *Lagenodelphis hosei*); and 'black porpose' with blunt heads (possibly pygmy killer whales, *Feresa attenuata,* or melon-headed whales, *Peponocephala electra*).

While some fishermen may use 'angerine' (or 'angeline') when referring to the bottlenose dolphin, most use this name to refer to a quite different animal. The retired fisherman who I considered to be my most reliable and conservative informant described the 'angerine' as a little larger than a 'cow porpoise' (which he has measured as up to 2.5 m long), dark above and cream-colored below, with 4–5 white spots on each side and a short beak. He said that it occurs in groups of a dozen or so, never in the company of other dolphins. Others described the 'angerine' as larger than the 'cowfish' and with a few spots (pink or white and about an inch in diameter) and a white or pinkish belly. Murphy (1947) reported that the Yankee whalemen used the term 'algerine' (possibly derived from 'Algerian') for small beaked whales of the genus *Mesoplodon,* but the above description makes it very unlikely that this is also the usage at St Helena. The descriptions are most consistent

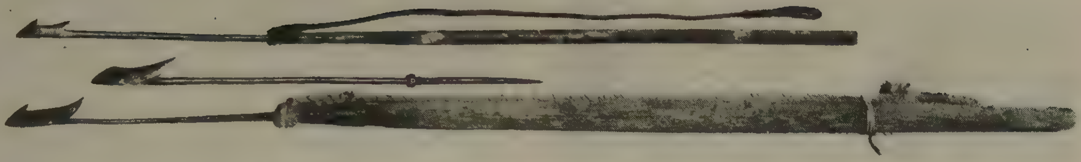

Fig. 2. Toggle-iron harpoons used for catching dolphins at St Helena into the 1960s. The top iron may have come from a Yankee sperm-whaling vessel; the bottom two were forged in Jamestown, St Helena.

with characteristics of the rough-toothed dolphin, *Steno bredanensis*; this, however, is a tentative conclusion. The 'angerine' was only rarely harpooned by the Islanders and is said to 'fight' harder than other 'porpoise'.

The inclusion by Melliss (1875) of the right whale dolphin (*Lissodelphis peronii*) in the fauna of St Helena seems questionable, as it is a cool-temperate species (Brownell, 1974) and the waters around St Helena are tropical, albeit seasonally verging on warm-temperate. It is possible that he included it on the basis of accounts by seagoers who saw the dolphins not near St Helena but while *en route* to or from the island.

METHODS AND EQUIPMENT OF THE FISHERY

In the memory of the fishermen, which extends in some cases back to shortly after the turn of the century, dolphins have been harpooned from small open fishing boats (6–12 m) that were operated out of Jamestown primarily to take tuna and other large pelagic fish. The number of these small boats has fluctuated between about 10 to about 20, with some engaged in fishing only part-time. In very recent years, island fishery operations have been upgraded (Harvey, 1980), with adoption of centralized marketing, addition of a cold-storage plant, and acquisition of two high-seas fishing vessels. Whereas formerly all fish caught were consumed locally, St Helena now exports fish (frozen and dried). The larger vessels, however, have not been significantly involved in the dolphin fishery.

Until after World War II, the fishing boats were all powered by sail. Light gasoline-powered outboard engines were tried in the late 1940s, but by the late 1960s most of the boats were equipped with small diesel engines, mounted amidships.

Most of the dolphin take was of animals harpooned at the bow while the boat was underway (called 'ironing'). Although this became easier when the boats converted from sail to engine, because the dolphins were more apt to ride the bow-waves of the faster-moving boats, it was always difficult, with fishermen sometimes hunting all day but missing on every throw.

Until the 1960s, the toggle-iron harpoon used was similar to that used for sperm whales in the 19th century (Fig. 2). Some whaling irons in use actually came from Yankee whalers, the last of which ceased whaling in the early 1920s. Others were forged on the island but patterned after sperm-whaling irons. The St Helena harpoon differed from the 19th century whaling harpoon only in having a shorter pole (about 1–1.2 m long). The locally-made irons differed chiefly in having a tang rather than a socket. Some fishermen recognized that the sperm-whaling iron was unnecessarily large for use on dolphins and commissioned scaled-down versions. Some of these were mounted on lengths of galvanized pipe rather than wooden poles. In the 1960s, visiting yachtsmen introduced a different type of harpoon, of the sort used widely for swordfish and other large fish. The line is fastened to a detachable head that separates from the rest of the harpoon when the quarry is struck (Fig. 3). The rod that carries the head is mounted on a 3 m bamboo pole. This harpoon is called by the fishermen a 'spear', as opposed to the older 'iron'. While taking of dolphins is now prohibited, the boats still carry harpoons, because they are also used for wahoo and yellowtail (*Seriola*).

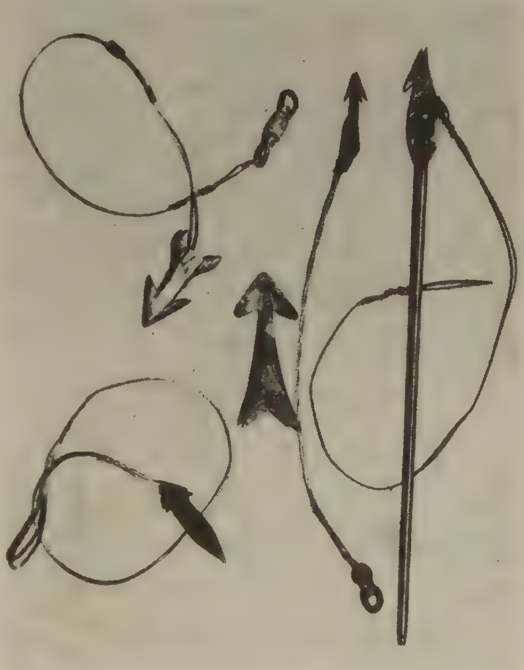

Fig. 3. Detachable harpoon heads used for dolphins, wahoo and yellowtail at St Helena since the 1960s. All were handmade.

The islanders also caught spotted dolphins while fishing for mackerel with monofilament handlines. When a dolphin seized a hooked mackerel, it was carefully eased ('dredged' in island terminology) close to the boat and then gaffed or harpooned. At times, several dolphins were taken in this manner by a single boat in one day. In some years the mackerel season has lasted several weeks or months, and in other years the mackerel have not appeared around the island at all. A few spotted dolphins were also taken in this manner on tuna handlines with live bait.

Although a few bottlenose dolphins were taken from boats, most were harpooned in the harbor at night during seasonal appearance of flying fish (Exocoetidae). A flying fish was attached to a short line on a long bamboo pole and used as a lure to attract the dolphins close to the quay (usually at 'The Steps') or a moored boat, so that they could be harpooned. Usually not more than one per night was captured with this technique.

Some of the fishermen experimented with the use of firearms (in one case a large-bore shotgun loaded with birdshot) but found that a large proportion of the dolphins shot sank before they could be retrieved.

A very few dolphins are taken accidentally when they become entangled in mooring lines in Jamestown Bay.

CATCHES

The only previously published estimate of dolphin catches is 'some 20 . . . annually' (Anon., 1981). Records of dolphins sold to the St Helena Fisheries Corporation were only kept for 1978 (T. Richards, pers. comm.) when 37 dolphins were logged (some landed dolphins were not sold to the Corporation and therefore not logged).

The pursuit of dolphins has always been an adjunct to other fishing activities. Typically, a dolphin or two was caught on the way home from the tuna grounds after a day of low catch, although on occasion as many as 12 are reported to have been caught by one boat in a day (during the 'day-mackerel' season).

Table 2

Estimates of dolphin catches at St Helena, obtained in interviews with fishermen

Parameter	Estimates
Usual catch/boat/day	1, 1, 1–2, 2, 2, 2–3
Maximum catch/boat/day	3, 3, 3–4, 4, 5–6, 6, 6, 8–9, 9–10, 12
Usual catch/boat/year	14–15, 20, 20
Usual total catch/year	-50, 50–100, <100, -100–200, ~150, ~200, >200, 200–300
Usual total catch at steps/year (*T. truncatus*)	"a few", 7–8, 15
Probable present catches/year	"a few", 5–10, ~6, 10
Number of boats in fleet	5–6, 7, 8, 8–10, -14 *, 12–15 *

* Includes part-time boats.

The casual estimates of catch levels obtained by us from the fishermen in interviews were highly variable (Table 2), as were estimates of the number of boats fishing for dolphins (5–6 to 12–15). Some of the variation can be ascribed to the fact that several of the retired fishermen interviewed had fished for dolphins at various times over the last 20–60 years. As casual and variable as the estimates are, however, there is some internal consistency. The estimate of catch per boat per year (no. 3 in Table 2) was relatively stable, and when this (~15–20) is multiplied by the approximate size of the full-time fleet (no. 7, ~5–10 boats), a very rough catch estimate of 75–200 dolphins/yr is obtained, which is consistent with the range of estimates of total annual catch (~50 to 200–300). These were mostly spotted dolphins; the catch of bottlenose dolphins would appear to have been on the order of 5–15 per year.

Some of my sources stressed the seasonal and year-to-year variability of fishing success in the waters around St Helena. The seasonal nature of the mackerel fishery is discussed above. The availability of tuna is also highly variable, and when tuna catches were low, more time was spent pursuing dolphins. These factors account for the inconsistency of the estimates of daily catch rates (no. 1 in Table 2) with the estimates of annual catches; dolphins were sought only on some days, in some seasons, and more in some years than in others.

None of the informants thought that there had been a long-term trend in dolphin catches or availability. However, several noted that harpooning dolphins became easier when diesel engines were added to the boats in the 1950s and 1960s. They believed that there had perhaps been a peak in dolphin catches at about that time.

The dolphin fishery was officially terminated in 1979. A condition of the required fishing license issued by the Fisheries Corporation is that 'no porpoise . . . be taken'; violation carries a fine of up to £1000. A very few dolphins are still taken illegally, however (Table 2), for consumption by boat crews or for family use. No dolphin meat now appears in the market.

IMPACT OF THE FISHERY

Very little information is available on the sizes of the populations of dolphins around St Helena. The school of spotted dolphins that I saw, which I was told is the 'Island school', contained several hundred animals. The size of this school was estimated by five of my informants to be >1000, 1000 or more, 1000s, 100s and 500–1000. One said that he had once seen a school offshore (~2.5 mi) that contained 'many 1000s' of animals. Assuming that the population is isolated, to support a sustained annual take of 75–200 it would have to contain about 1,250–5,000 dolphins, and perhaps more (based on a maximum sustainable yield of 0–6%—see Smith, 1983). While more information on present population size and past removals is needed before an assessment of population status or fishery impact can be made, the present very low levels of take are unlikely to affect the population adversely.

We know even less about the population of bottlenose dolphins around St Helena. The school that I saw contained no more than a few 10s of animals, but there may be more schools around the island.

UTILISATION

Dolphin meat is well liked by the islanders; there would be a ready market for it if the taking of dolphins were not illegal. In the 1950s and 1960s, the retail price was 6d per 'piece' which varied in weight between about 1 and 2 lbs depending on demand. In more recent years, up to 1979, the price was 20–30p per piece, about the same as the price for tuna and higher than that for mackerel.

Nearly the entire animal was utilised. The head and intestines were discarded at sea or given away; everything else was sold, including lungs, kidneys, stomach, liver, gonads and other organs. The favored cuts came from the ribs and the neck. The meat was often cooked with the skin and blubber attached, usually in curries. Oil extracted from the head was used for oiling tools, fishing equipment, etc.; oil extracted from the lower jaw was used for oiling watches and other fine mechanisms.

ORIGINS OF THE FISHERY

Several lines of evidence point to the 19th-century Yankee sperm whale fishery as the origin of the St Helena dolphin fishery. As noted by Mellis (1875), Mitchell (1975) and many others, the sperm whalers took 'porpoise' (dolphins) for two reasons: to provide practice for the harpooners and to obtain fresh meat for the crew.

As early as 1805, St Helena was a major way station for Yankee whalers fishing the Indian and Pacific oceans (Brooke, 1808). In 1855, for example, at least 43 whalers, mostly US-registered, called at St Helena; at least 6 called twice (St Helena newspaper files). St Helenians served as crewmen on some of these whalers. At least three times between 1830 and 1875 (and once in this century—Lea, 1929) St Helena attempted to develop its own local industry to take the seasonally occurring humpback whales; all of these ventures came to naught (Taylor, 1969; Gosse, 1938). In any case, there was extensive exposure of St Helenian seagoing men to the Yankee practice of harpooning dolphins.

There were at least three sources of sperm-whaling gear for dolphins at St Helena: 1) St Helenians who had returned after shipping on whalers may have brought harpoons or the technology to make them, 2) auctions of the equipment of the failed St Helenian whaling operations, e.g. in 1856 (*St Helena Herald* of 16 October), and 3) sales of equipment of the many whaling vessels condemned at St Helena, e.g. in 1856 a list of items to be auctioned from the condemned barque *George* (Newport, Rhode Island) included 'masts, spars, sails, stanching and running rigging; also the whale boats, and all other whaling gear, viz-trypots, casks and shooks, hooping &c., harpoons, lances, whale lines, and various other articles' (*St Helena Herald* of 1 January, 1857).

Another piece of evidence pointing to a whaling origin of the dolphin fishery is the islanders' use of Yankee whaling terms such as 'bottlenose porpoise' (applied to small dolphins), 'blackfish', 'cowfish', 'angerine' and 'iron' (used both as a noun and a verb).

There is some evidence to suggest that a dolphin fishery did not exist at St Helena before the mid-19th century. I searched an early-19th-century military midden (at Rupert's Bay) extensively for animal remains and found abundant evidence of reliance on the sea for food: in addition to remains of domestic animals and fowl, the site contains large numbers of limpet shells (*Patella*), shells of other gastropods and bones of fish, including large tunas, but no cetacean remains.

The St Helena dolphin fishery, then, probably arose as an outgrowth of Yankee whaling sometime in the latter two-thirds of the last century.

RECOMMENDATIONS FOR FURTHER RESEARCH

The dolphins at St Helena offer a very good opportunity for studying the population dynamics of dolphins. Management of dolphin populations has been based on a theorized 'surplus' or net production under exploitation, caused by increased reproductive rates and/or decreased natural mortality rates (Smith, 1983). There is as yet no empirical evidence that such net production occurs in an exploited dolphin population. The spotted dolphins at St Helena were exploited for at least 65 years and probably longer. They are of the same species as tens of thousands of dolphin taken annually in the eastern tropical Pacific (IWC, 1983).

The present size and composition of the population could be estimated using several techniques; these include additional survey and observation effort from small boats, survey from the mast of a larger vessel, aerial photography from a tethered balloon or remote-controlled drone, survey and monitoring from a cliff-top station (sea cliffs at the portion of the coast line where the dolphins come close inshore are several hundred feet high) such as has been done in studying spinner dolphins (*Stenella longirostris*) in Hawaii (Norris and Dohl, 1980) and dusky dolphins (*Lagenorhynchus obscurus*) in Argentina (Würsig and Würsig, 1980), and underwater observation and photography to determine size, structure and dynamics of subgroups and to follow naturally-marked individuals through time.

Vessel-based survey effort is needed to determine the offshore extent of the range of the resident spotted-dolphin school and to investigate the possibility that there are dolphins offshore (within, say 30 km) that do not regularly come close to shore. Survey of the windward side of the island is also needed (during the rare calm weather there).

Excavation of the many 19th and 20th century middens on the island could yield information on the beginnings, geographical distribution (e.g., in the interior vs in Jamestown) and scale of consumption of dolphins. This, coupled with the results of further interviews and archival research (to determine, for example, the number of boats operating in different periods) may make possible estimation of removals over time, a necessary task if the present status of the population is to be assessed.

Should the above studies reveal that the fishery had a significant effect on the population, this would be an excellent opportunity to see what happens when exploitation of a dolphin population stops. Will it grow? Will production of calves decline? This opportunity for a case study of an isolated and accessible population with a long history of exploitation is unique and valuable.

NON-CONSUMPTIVE UTILISATION

The spotted dolphins at St Helena also have potential as a tourist attraction. They can be found nearly every day in the same place, very near Jamestown Harbor and in quiet clear water. Despite having been pursued in the past, they are approachable and could be expected to become quite tame under conditions of sustained benign interactions with humans. They could be observed below the surface by snorkeling or with a glass-bottomed boat. Marketing research would be needed to determine the practicability of such an operation.

ACKNOWLEDGEMENTS

The research was supported by the National Geographic Society (Grant 2543-82). I was assisted by my wife, Marilyn J. Perrin. The following (in roughly the order that we met them) gave abundant help, encouragement and hospitality in St Helena: Brian and Katherine Sellwood, Basil George, Patrick Joshua, Laurie and Joan Baker, David Harrison, Joan Buckley, John and Silvia Clifford, Miriam Henry, Phillip Dale, Graham Sim, William Lawrence, Maxwell Joshua, Arthur and Molly Mawson, Donald and Joyce Thorpe, David and Sara Young, Terrence and Julia Green, Michael and Fabienne Holland, Terence Richards, Charles Wade, Fred Thomas, Humphrey and Violet Benjamin, Fred Ward, Charles Francis, John Hopkins, Charles George, John Musk, Barry Dillon, Hopewell Joshua, Nicolas and Gail Thorpe, Douglas Hudson, Trevor Benjamin, George Stevens, John Crowie, Charles Henry, Joan Scipio, Dot Leo, Brian Thomas, Mervyn Crowie, Hugh and Joyce Gibbs, Leonard Peters, Fred Young, George Benjamin and Kenneth Maggot. Governor John Massingham was off the Island while we were there but offered help and encouragement in the planning stages of the undertaking. Michael D. Scott (IATTC, Southwest Fisheries Center) and Drs J. Barlow, A. Dizon, I. Barrett and G. T. Sakagawa (SWFC) critically reviewed the manuscript and offered suggestions for its improvement.

REFERENCES

Anonymous. 1980. United Kingdom progress report on cetacean research June 1978 to May 1979. *Rep. int. Whal. Commn* 30: 173–4.

Anonymous. 1981. United Kingdom progress report on cetacean research June 1979–May 1980. *Rep. int. Whal. Commn* 31: 219–20.

Brooke, T. H. 1808. *A History of the Island of St Helena, from its Discovery by the Portugese to the Year 1806; to which is Added an Appendix*. Black, Parry and Kingsbury, London, 409 pp.

Brownell, R. L., Jr. 1974. Small odontocetes of the Antarctic. pp. 13–19 & pl. 8, 9 & 11. *In*: S. G. Brown, R. L. Brownell, Jr., A. W. Erickson, R. J. Hofman, G. A. Llano, and N. A. Mackintosh, *Antarctic Mammals*, Folio 18, American Geographical Society, New York.

Finneran, H. 1979. St Helena the unspoiled game fishing isle of the Atlantic. *South African Boating*, Mar–Apr 1979: 30–2.

Fraser, F. C. 1966. Comments on the Delphinoidea. pp. 7–31. *In*: K. S. Norris (ed.), *Whales, Dolphins and Porpoises*. Univ. California Press, Berkeley and Los Angeles, 789 pp.

Gosse, P. 1938. *St Helena 1502–1938*. Cassel & Co., London, Toronto, Melbourne and Sydney, 447 pp.

Harvey, M. 1980. Success at St Helena. *Fishing News International*, June 1980: 47–9.

International Whaling Commission. 1983. Report of the sub-committee on small cetaceans (Annex H). *Rep. int. Whal. Commn* 33: 152–70.

Lea, L. 1929. Whale fisheries. pp. 224–227. *In: A Revised Edition of the Ordinances of the Colony of Saint Helena.*

Melliss, J. C. 1875. *St Helena: a Physical, Historical, and Topographical Description of the Island, Including its Geology, Fauna, Flora, and Meteorology*. L. Reeve & Co., Ashford, Kent, 426 pp.

Mitchell, E. D. (ed.). 1975. Review of biology and fisheries for smaller cetaceans. *J. Fish. Res. Bd Can.* 32: 875–1242.

Murphy, R. C. 1947. *Logbook for Grace*. MacMillan, New York, 290 pp.

Norris, K. S. and Dohl, T. P. 1980. Behavior of the Hawaiian spinner dolphin, *Stenella longirostris, Fish. Bull.*, US 77: 821–49.

Perrin, W. F. 1975. Variation of spotted and spinner porpoise (genus *Stenella*) in the eastern tropical Pacific and Hawaii. *Bull. Scripps Inst. Oceanogr.*, 21: 1–206.

Perrin, W. F. and Perrin, M. J. In press. Investigation of the cetacean fauna and former dolphin fishery of St Helena. *Nat. Geogr. Res. Reps.*

Pilleri, G. and Gihr, M. 1972. Record and taxonomy of *Tursiops gephyreus* Lahille, 1908 from Playa Coronilla, Uruguay. *Invest. in Cetacea* 4: 173–81.

Smith, T. D. 1983. Changes in size of three dolphin populations (*Stenella* spp.) in the eastern tropical Pacific. *Fish. Bull.*, US 81: 1–14.

Taylor, M. S. 1969. *St Helena, Ocean Roadhouse*. Robert Hale, London, 192 pp.

Würsig, B. and Würsig, M. 1980. Behavior and ecology of the dusky dolphin, *Lagenorhynchus obscurus*, in the South Atlantic. *Fish. Bull.*, US, 77: 871–90.

8569

Review of Geographical Stocks of Tropical Dolphins (*Stenella* spp. and *Delphinus delphis*) in the Eastern Pacific

WILLIAM F. PERRIN,[1] MICHAEL D. SCOTT,[2] G. JAY WALKER,[1]
and VIRGINIA L. CASS[1]

ABSTRACT

Information on geographical variation is reviewed for *Stenella attenuata*, *S. longirostris*, *S. coeruleoalba*, and *Delphinus delphis* in the eastern tropical Pacific, and boundaries for potential management units are proposed. National Marine Fisheries Service and Inter-American Tropical Tuna Commission sighting records made from 1979 to 1983 which were outside boundaries used in a 1979 assessment were examined for validity. Tagging returns and morphological data were also analyzed. Several stock ranges are expanded or combined. Three management units are proposed for *S. attenuata*: the coastal, northern offshore, and southern offshore spotted dolphins. Four management units are proposed for *S. longirostris*: the Costa Rican, eastern, northern whitebelly, and southern whitebelly spinner dolphins. Two provisional management units are proposed for *S. coeruleoalba*: the northern and southern striped dolphins. Five management units (two of which are provisional) are proposed for *D. delphis*: the Baja neritic, northern, central, southern, and Guerrero common dolphins. Division into management units was based on morphological stock differences and distributional breaks.

INTRODUCTION

Tuna fishermen make use of four species of dolphins in the international purse-seine fishery for yellowfin tuna in the eastern tropical Pacific in finding and capturing the tuna (Smith 1983). These are (in order of importance to the fishery): the spotted dolphin, *Stenella attenuata*; the spinner dolphin, *S. longirostris*; the common dolphin, *Delphinus delphis*, and the striped dolphin, *S. coeruleoalba*. Perrin et al. (1983) delineated the known ranges of the species in the eastern Pacific in a recent review. The purpose of this paper is to review available information on geographical variation of the four species in the eastern Pacific and to propose boundaries for potential management units.

Geographical variation in *S. attenuata* and *S. longirostris* was first described by Perrin (1972a, b, 1975a). He placed the nominal endemic *S. graffmani* (Lönnberg 1934) (described from Acapulco, Mexico) in the synonymy of *S. attenuata* (Gray 1846) and described three subspecies from the eastern and Central Pacific: 1) the coastal spotted dolphin, *S. a. graffmani* (formerly *S. graffmani*), a relatively large and heavily spotted form thought to occur within about 20-25 km of the shore and in gulfs and embayments from southern Mexico to Colombia; 2) the offshore spotted dolphin, *S. a.* subsp. "A" (unnamed), a smaller and more lightly spotted pelagic form thought to occur from about 25 km offshore from Cabo San Lucas, Mexico, to Colombia and west to at least long. 145°W in tropical water; and 3) the Hawaiian spotted dolphin *S. a.* subsp. "B" (unnamed) from Hawaiian waters, similar to the offshore form but less spotted and with a larger skull. In the case of the spinner dolphins, specimens from the eastern tropical Pacific had been referred (by Hester et al. 1963) to *S. microps* (Gray 1846; described from an unknown locality) and animals from Hawaii referred (by Morris and Mowbray 1966) to *S. roseiventris* (Wagner 1846; described from the western Pacific). Perrin (1975a) considered the spinner dolphins to belong to a single species, *S. longirostris* (Gray 1848) (described from an unknown locality) and described four subspecies. The Costa Rican spinner dolphin, *S. l.* subsp. "A" (unnamed), is a relatively long and slender form of overall gray color and with a very long rostrum, from nearshore waters of Costa Rica and El Salvador. The eastern spinner dolphin, *S. l.* subsp. "B" (unnamed; formerly identified as *S. microps*), is a smaller but similarly colored form with a small skull and (in many adult males) with the dorsal fin canted forward almost so as to appear reversed and occurs westward from the coast of Mexico out to about 800 km. The whitebelly spinner dolphin (so called by tuna fishermen), *S. l.* subsp. "C" (unnamed), is similar to the eastern spinner dolphin in size and skull but has a ventrolateral white area extending from the flipper to the genital region and a less triangular dorsal fin; it ranges from about 800 km offshore to long. 140°W. The Hawaiian spinner dolphin, *S. l.* subsp. "D" (unnamed; formerly identified as *S. roseiventris*), is a relatively large form with large skull, sharply defined three-part color pattern and slightly falcate dorsal fin and occurs in Hawaiian waters. The first and last of these forms ("A" and "D") were at that time each known from only a few specimens, as were the coastal and Hawaiian forms of the spotted dolphin.

Perrin (1972a) described geographical variation in the color pattern of *S. longirostris* in detail and proposed a generalized model for variation in this and other delphinids. Under this scheme, the variation in the spinner dolphin is seen as variation in extent and density of a color-pattern component called the "dorsal overlay," with the overlay being modally darkest and most extensive in the Costa Rican and eastern forms and lightest and least extensive in the Hawaiian form. The color patterns of the various forms are thus perceived as variations on a theme rather than as discretely different patterns.

As more distributional data have accumulated, the known ranges of the several forms of *S. attenuata* and *S. longirostris* have expanded (Perrin 1975b; Perrin et al. 1982). Studies of material from below the Equator led to division of the offshore spotted dolphin and the whitebelly spinner dolphin each into northern and southern stocks by Perrin, Sloan, and Henderson (1979). They found the southern offshore spotted dolphin to be slightly smaller than the northern animal, with a larger skull and more distinct color pattern. The southern whitebelly spinner dolphin they found to be larger than the northern form, with coloration more resembling that of the Hawaiian form. These findings and additional distribution records were taken into account in the most recent delineation of the ranges, which was used in an exercise referred to below as "SOPS 1979" (for Status of Porpoise Stocks [Workshop], 1979) in 1979 (Smith 1983) (Figs. 1, 2). Scott (1981) and Alverson (1981) reviewed the ranges, the former incorporating data through 1980.

---

[1] Southwest Fisheries Center La Jolla Laboratory, National Marine Fisheries Service, NOAA, P.O. Box 271, La Jolla, CA 92038.

[2] Inter-American Tropical Tuna Commission, La Jolla, CA 92038.

The range of *S. coeruleoalba* in the eastern Pacific has been divided into management units based solely on apparent latitudinal gaps in distribution (Smith 1983), yielding five units: "northern temperate," "northern tropical," "central tropical," "southern tropical" and "southern temperate" (Fig. 3). To date, geographical variation in this species in the eastern Pacific has not been studied.

Delphinus delphis varies morphologically a great deal in the eastern Pacific. Banks and Brownell (1969) referred a short-beaked offshore form and a long-beaked neritic form occurring off southern California and Baja California to *D. delphis* L. and *D. bairdii* Dall 1873, respectively. Van Bree and Purves (1972) reported material that showed intergradation in skull morphology between the two forms and concluded that they belong to the single species *D. delphis*. Evans (1975, 1982) described five forms in the eastern Pacific: 1) a relatively large form inhabiting waters inside the 100-fathom curve off southern California and Baja California, with a very long rostrum and a muted color pattern (later called the "Baja neritic" form); 2) and 3) small, short-beaked northern temperate and northern tropical forms; and 4) and 5) large short-beaked central and southern tropical forms delineated by apparent latitudinal gaps in distribution. He also suggested the possible existence of an "equatorial-oceanic" population inhabiting waters west of long. 95°W. On the basis of additional distribution data, Au et al.[3] modified the boundaries of the stocks and added a "southern temperate" stock (Fig. 4). They included all animals between lat. 3° and 15°N in the "central tropical" stock, not recognizing Evans' tentative "equatorial-oceanic" stock. In the 1979 stock assessment (Smith 1983), the Baja neritic and northern temperate stocks were combined into a single management unit. The stock structure of *D. delphis* was most recently reviewed by Scott (1981).

In this paper we review developments and data collected for the four species since the 1979 stock assessment.

MATERIALS AND METHODS

Morphological Analyses

The samples and methods used in analyses of variation in skull and body length in *S. attenuata* and *S. longirostris* are described in Schnell et al.[4] and Douglas et al. (1984). In addition to considera-

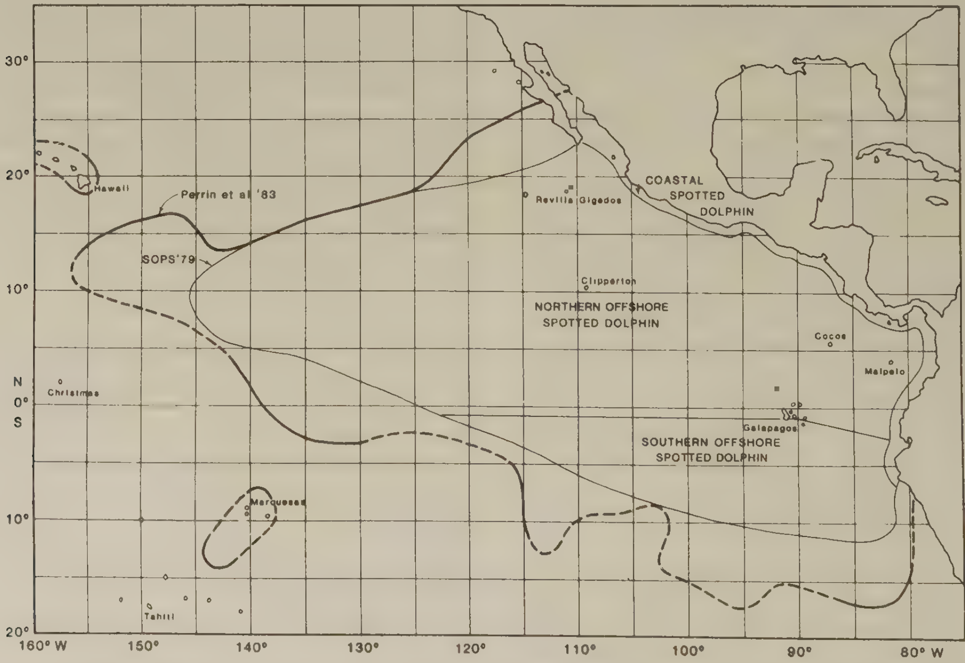

Figure 1.—Known distribution of *Stenella attenuata* in the eastern Pacific, showing SOPS '79 species range and stock boundaries, and new species range (from Perrin et al. 1983).

---

[3] Au, D. K. W., W. L. Perryman, and W. F. Perrin. 1979. Dolphin distribution and the relationship to environmental features in the eastern tropical Pacific. Southwest Fisheries Center Admin. Rep. LJ-79-43, 59 p.

[4] Schnell, G. D., M. E. Douglas, and J. D. Hough. 1982. Geographic variation in morphology of spotted and spinner dolphins (*Stenella attenuata* and *S. longirostris*) from the eastern tropical Pacific. Southwest Fisheries Center Admin. Rep. LJ-82-15C, 213 p.

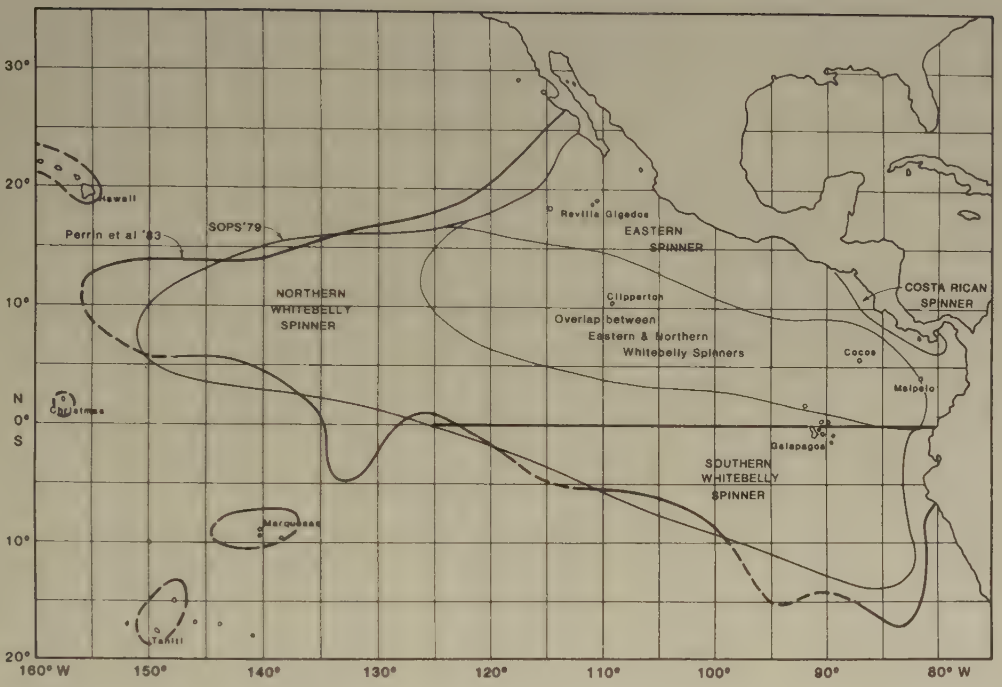
30°
20°
10°
N
0°
S
10°
20°
160° W
150°
140°
130°
120°
110°
100°
90°
80° W
Hawaii
Perrin et al '83
SOPS'79
Revilla Gigedos
EASTERN SPINNER
NORTHERN WHITEBELLY SPINNER
Clipperton
Overlap between Eastern & Northern Whitebelly Spinners
COSTA RICAN SPINNER
Cocos
Malpelo
Christmas
Galapagos
SOUTHERN WHITEBELLY SPINNER
Marquesas
Tahiti

Figure 2.—Known distribution of *Stenella longirostris* in the eastern Pacific, showing SOPS '79 species range and stock boundaries, and new species range (from Perrin et al. 1983).

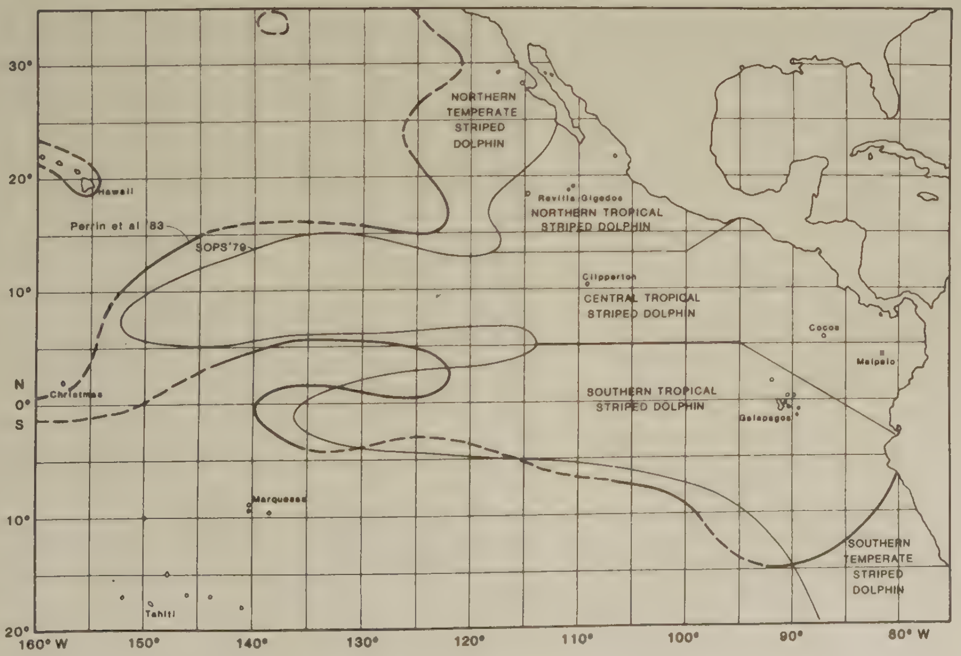
30°
20°
10°
N
0°
S
10°
20°
160° W
150°
140°
130°
120°
110°
100°
90°
80° W
NORTHERN TEMPERATE STRIPED DOLPHIN
Hawaii
Revilla Gigedos
NORTHERN TROPICAL STRIPED DOLPHIN
Perrin et al '83
SOPS'79
Clipperton
CENTRAL TROPICAL STRIPED DOLPHIN
Cocos
Malpelo
Christmas
SOUTHERN TROPICAL STRIPED DOLPHIN
Galapagos
Marquesas
SOUTHERN TEMPERATE STRIPED DOLPHIN
Tahiti

Figure 3.—Known distribution of *Stenella coeruleoalba* in the eastern Pacific, showing SOPS '79 boundaries and new species range (from Perrin et al. 1983).

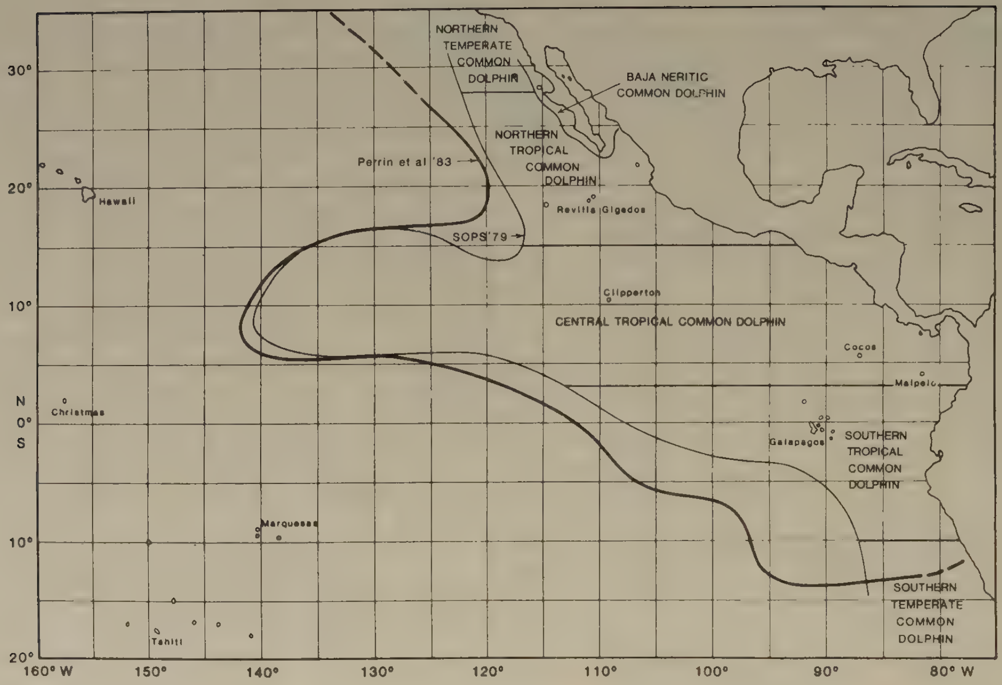
30°
20°
10°
N
0°
S
10°
20°
160° W
150°
140°
130°
120°
110°
100°
90°
80° W
NORTHERN TEMPERATE COMMON DOLPHIN
BAJA NERITIC COMMON DOLPHIN
NORTHERN TROPICAL COMMON DOLPHIN
Perrin et al '83
SOPS '79
Hawaii
Revilla Gigedos
Clipperton
CENTRAL TROPICAL COMMON DOLPHIN
Cocos
Malpelo
Christmas
Galapagos
SOUTHERN TROPICAL COMMON DOLPHIN
Marquesas
SOUTHERN TEMPERATE COMMON DOLPHIN
Tahiti

Figure 4.—Known distribution of *Delphinus delphis* in the eastern tropical Pacific, showing SOPS '79 species range and stock boundaries, and new species range (from Perrin et al. 1983).

tion of the results obtained by those authors, we reviewed all body-length data collected through 1981 (Figs. 5-8), including some data for the inshore forms of *S. attenuata* and *S. longirostris* not included in the contracted analyses, and data for *S. coeruleoalba* and *D. delphis*. We also examined data on frequencies of ovarian corpora for *S. attenuata* and *S. longirostris*. Sources of the data are described in Perrin and Oliver (1982); statistical reporting areas are defined in Appendix 1.

Distribution Data

The sources and nature of the distribution data are described in Perrin et al. (1983). Data were included for all NMFS and IATTC (Inter-American Tropical Tuna Commission) tuna/dolphin observer cruises from 1979 through most of 1983.

***Stenella attenuata*.**—We reviewed all records of spotted dolphins from within 100 nmi of the coast (or a coastal island) that were identified to stock ("coastal" or "offshore"). These comprised 1,650 sightings and collection records. Of 502 "coastal" records, we concurred with the identifications for 218; 67 were changed to "offshore," and 217 were downgraded to unidentified spotted dolphin. Of 1,147 "offshore" records, we accepted 456, changed 44 to "coastal," 640 to unidentified spotted dolphin, and 7 to unidentified dolphin. The large number of changes to unidentified spotted dolphin was occasioned by the fact that in recent years NMFS observers aboard commercial purse seiners have largely identified spotted dolphins to stock based only on locality without regard to morphological information, all those within 50 nmi of the coast being designated as "coastal" and all those outside 50 nmi as "offshore." In point of fact, the coastal form was described on the basis of skull characters, body size, and coloration (Perrin 1975a).

In reviewing a sighting, we considered the morphological observations recorded by the observer and any photographs, body-length data, life history data, and osteological specimens collected in association with the sighting. If the observer noted that the animals seemed larger and/or more heavily spotted than those seen far offshore, or, better, if the photos, length data, or specimens indicated this (based on the published information for the two forms), we considered the record to be a confirmed record of the coastal form. Because the question is one of modal differences between forms within a species, the identification was judgmental in many cases, especially if only a few animals were measured or if the observer's recorded comments were sketchy or ambiguous and voucher data and specimens were absent. We tried to err on the side of conservatism, relegating the more weakly supported sightings to the unidentified category, but undoubtedly we classified some sightings of the coastal form as "offshore" and vice versa.

In evaluating the observer's recorded information, we also considered such factors as sighting distance and conditions, experience of the observer, and quality of documentation and identifications for other sightings made by the same observer. In

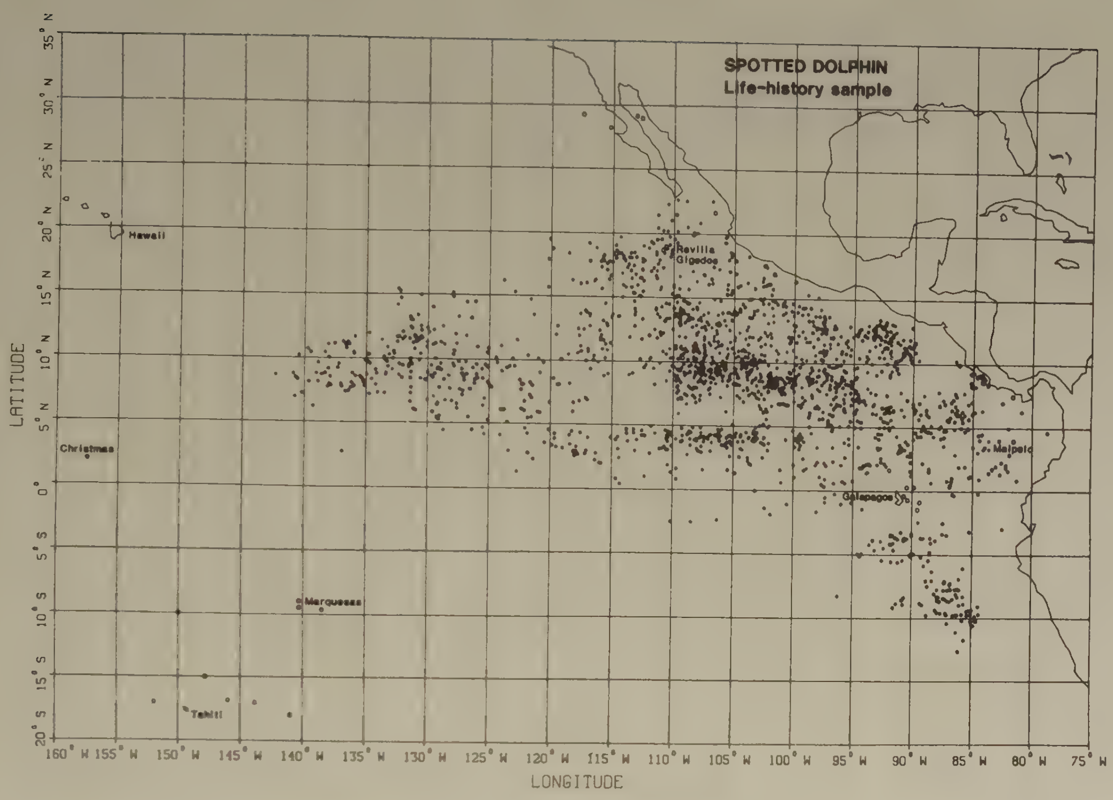

Figure 5.—Collection localities for adult specimens of *Stenella attenuata* included in body-length analyses. Adults defined as males with testis-epididymis weight of 100 g or more and females with at least one ovarian corpus. Open dots are small islands.

addition, we considered the context of the sighting record. If, for example, one net set (a sighting record) was made on the same school or near the same time and in the same area as a previous set assignable to stock based on recorded observations or specimens, we considered the second record to be of the same form.

Stenella longirostris.—To examine the distribution of the Costa Rican spinner, we reviewed all records of *S. longirostris* within 50 nmi of the coast. The number of confirmable records was small, mainly because the Costa Rican form differs externally from the eastern form only in total body length and relative length of the rostrum and apparently not in coloration. Also, the Costa Rican spinner dolphin is only very rarely captured by tuna fishermen (Perrin 1975b). Of 42 "Costa Rican" records, we confirmed 33, assigning the rest to unidentified spinner. Of these confirmed records, 24 were based on aerial photographs taken during a photogrammetric experiment by the IATTC in 1980. One of 196 "eastern" records was judged to be "Costa Rican"; 28 were confirmed as "eastern," 157 changed to unidentified spinner, and 10 were accepted. One of 118 unidentified records was changed to "eastern."

We also reviewed all records of eastern spinner dolphins and whitebelly spinner dolphins outside the respective SOPS '79 boundaries (see Fig. 2). We again adopted a conservative stance because of the necessarily judgemental nature of the identifications in many cases. Of 198 "eastern" records, we confirmed 115 (8 supported by specimen data), assigned 40 to "whitebelly," 41 to unidentified spinner, and 2 to *S. attenuata*. Of 280 outlying "whitebelly" records, 184 were confirmed (1 with specimen data), 35 assigned to "eastern," 49 to unidentified spinner, 1 to *S. attenuata*, 1 to *Delphinus delphis*, and 10 to unidentified dolphin.

In addition to considering the sighting factors discussed above, we found it necessary to "second-guess" the observer's understanding of the modal nature of the differences between the two forms, as a large number of sightings of "mixed" schools of eastern and whitebelly spinner dolphins were reported. In some cases, this designation was likely valid, because the observer noted separate groups of the two forms in the net. In other cases we assigned the "mixed" sighting to one or the other of the two forms because only a very few individuals of the "other" type were seen, as would be expected in the case of subspecific-level modal difference. There were a large number of "mixed" sightings, however, where it was unclear from the information recorded if the record should be assigned to both forms. In some cases, color-pattern "intergrades" were reported, again something to be expected in the case of subspecific variation but difficult to evaluate when

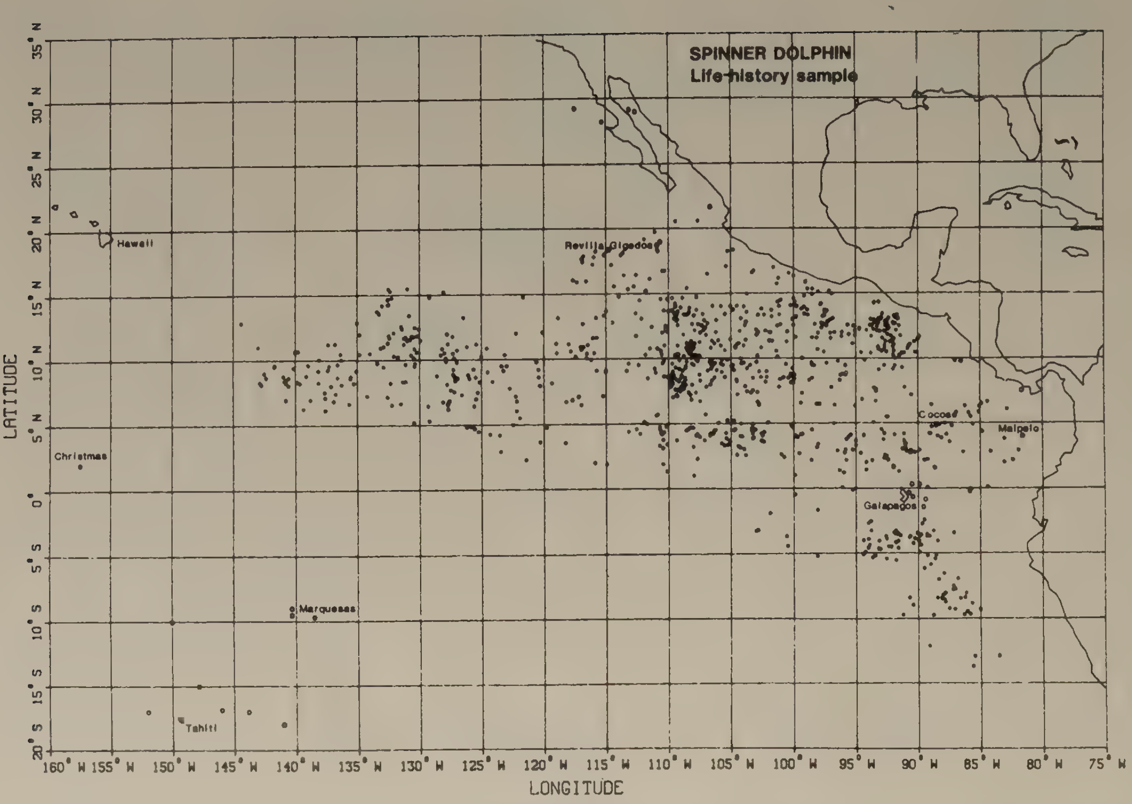

Figure 6.—Collection localities for adult specimens of *Stenella longirostris* included in body-length analyses. Adults defined as for *S. attenuata*. Specimens not identified to stock are not included.

assigning a school to one mode or the other or both. In these situations, we made judgmental decisions based on other aspects of the sightings, giving heavy weight to the experience and apparent knowledgability of the observer.

We noted three additional problems primarily encountered in sightings made by inexperienced observers, usually during the first few days of a first cruise:

1) Juvenile eastern spinner dolphins appear whitebelly-like in having a light ventrum (Perrin 1972a), and some were clearly misidentified in the sighting records. Where specimens were collected, we were able to detect the error; other instances probably remain in the whitebelly spinner dolphin records that we accepted.

2) Adult eastern spinner dolphins when seen at a distance, especially when spinning, appear slightly lighter ventrally then dorsally. In some cases it was clear that the observer had not yet seen whitebelly spinners and was mistaking this muted countershading for the sharply demarcated dark-gray and white pattern of the whitebelly form. Again, some instances of this have probably gone undetected in our review.

3) New observers in some cases clearly confused the similar fishermen's terms "whitebelly" (*Delphinus delphis*, *S. coeruleoalba* or *Lagenodelphis hosei*) and "whitebelly spinner" (*S. longirostris*). In an earlier review of species ranges (Perrin et al. 1983), we found that this had led to obviously spurious records of *S. longirostris* far north of the tropical habitat. Again, in the present review we found sightings (made at a distance) which members of the crew identified as "whitebellies" but the inexperienced observer identified as "whitebelly spinners," most likely misunderstanding the crewman's identification.

In view of these difficulties, and because of the rather unusual broad overlap of the ranges of geographical forms (which usually, by definition, are allopatric but may not be in these highly mobile and socially complex cetaceans), we consider the allocation of outlying sightings to whitebelly and eastern spinners on balance to be less reliable than the allocations for the other stocks and species reviewed in this study.

Tagging.—The tagging methods and operations (except for the tag releases listed in Table 1) have been described previously

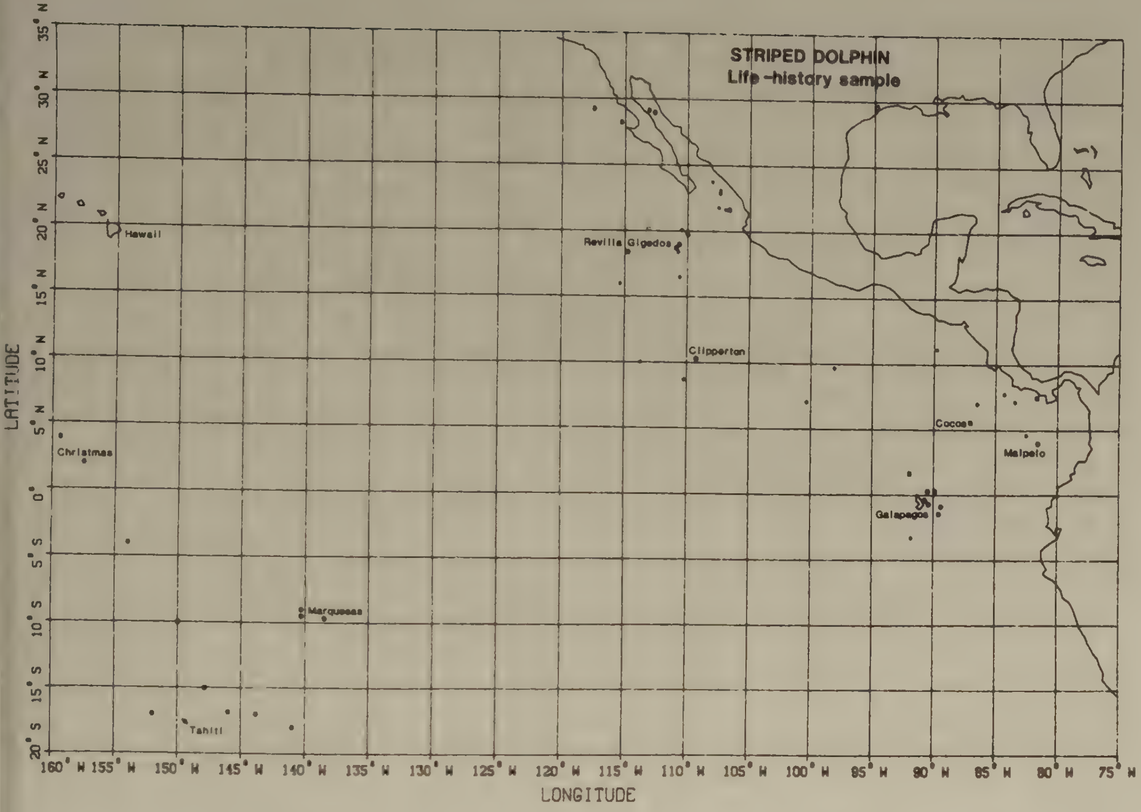
STRIPED DOLPHIN
Life-history sample
Hawaii
Revilla Gigedos
Clipperton
Cocos
Malpelo
Galapagos
Christmas
Marquesas
Tahiti
LATITUDE
35° N
30° N
25° N
20° N
15° N
10° N
5° N
0°
5° S
10° S
15° S
20° S
LONGITUDE
160° W
155° W
150° W
145° W
140° W
135° W
130° W
125° W
120° W
115° W
110° W
105° W
100° W
95° W
90° W
85° W
80° W
75° W

Figure 7.—Collection localities for adult specimens of *Stenella coeruleoalba* included in body-length analyses. Adults defined as for *S. attenuata*.

Table 1.—Releases of spaghetti tags (metal dart, type d—Perrin, Evans, and Holts 1979) by Martini and Nilson aboard the private vessel *Serenity* in 1975 and 1976. The species identifications are tentative.

Species	Tag no.	Date	Position (lat., long.)	Species	Tag no.	Date	Position (lat., long.)
S. attenuata	05002	27DEC75	8°20′N, 78°45′W	*Tursiops truncatus*[1]	05009	3JAN76	0°42′S, 89°30′W
	05004	27DEC75	8°13′N, 78°47′W		05010	3JAN76	0°42′S, 89°30′W
	05006	27DEC75	8°08′N, 78°50′W		05011	3JAN76	0°46′S, 89°30′W
	05007	27DEC75	8°07′N, 78°50′W		05012	3JAN76	0°46′S, 89°30′W
	05008	27DEC75	8°06′N, 78°50′W		05013	3JAN76	0°46′S, 89°30′W
	05017	27DEC75	8°07′N, 78°50′W		05015	3JAN76	0°46′S, 89°30′W
S. longirostris	05034	11MAR76	8°23′S, 137°36′W		05019	3JAN76	0°46′S, 89°30′W
	05036	12MAR76	8°42′S, 139°20′W		05021	3JAN76	0°46′S, 89°30′W
	05038	12MAR76	8°42′S, 139°40′W		05025	22JAN76	1°16′S, 90°22′W
	05040	20MAR76	8°58′S, 140°09′W		05028	24JAN76	0°50′S, 89°41′W
	05041	21MAR76	8°57′S, 140°03′W		05030	5FEB76	0°06′S, 90°52′W
	05043	21MAR76	8°56′S, 140°01′W		05033	16FEB76	0°38′S, 91°33′W
	05044	21MAR76	8°56′S, 140°01′W	Unidentified dolphin (*T. truncatus* or *Delphinus delphis*)	05022	7JAN76	0°48′S, 90°11′W
	05046	22MAR76	8°55′S, 140°01′W		05029	24JAN76	0°50′S, 89°41′W
	05047	23MAR76	8°57′S, 140°06′W		05031	16FEB76	0°38′S, 91°32′W

[1] Included here for completeness; these tagging data have not been published elsewhere.

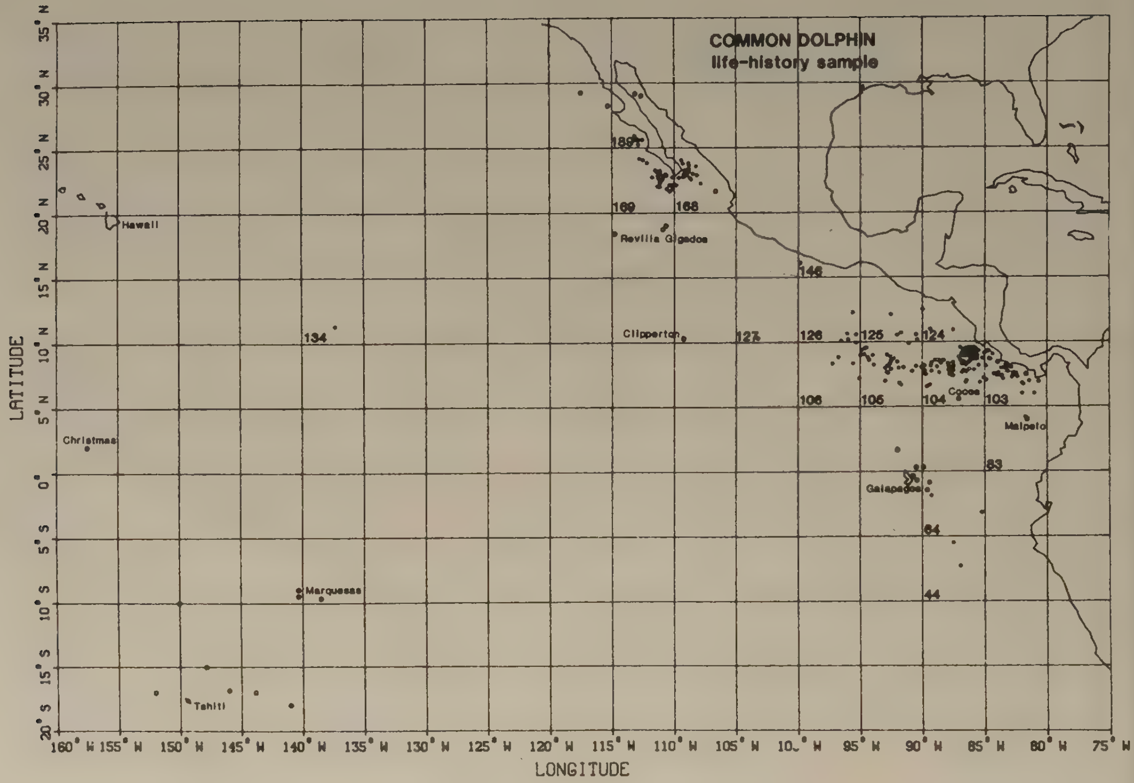
COMMON DOLPHIN
life-history sample
Hawaii
Christmas
Marquesas
Tahiti
134
189
169
168
Revilla Gigedos
146
Clipperton
127
126
125
124
106
105
104
Cocos
103
Malpelo
83
Galapagos
64
44
LATITUDE
35° N
30° N
25° N
20° N
15° N
10° N
5° N
0°
5° S
10° S
15° S
20° S
LONGITUDE
160° W
155° W
150° W
145° W
140° W
135° W
130° W
125° W
120° W
115° W
110° W
105° W
100° W
95° W
90° W
85° W
80° W
75° W

Figure 8.—Collection localities for adult specimens of *Delphinus delphis* included in body-length analyses. Adults defined as for *Stenella attenuata*. See Appendix 2 for square-numbering guide.

(Perrin, Evans, and Holts 1979; White et al. 1981; Jennings and Stives[5], Powers et al.[6]). Part of the results (tag recapture and resights) were presented and analyzed in Perrin, Evans, and Holts (1979) and Jennings and Stives (footnote 5).

SPECIES ACCOUNTS

Stenella attenuata

Our results for this species agree with those of similar earlier studies (Perrin 1975a, b; Perrin, Sloan, and Henderson 1979) and the results of the multivariate analyses by Schnell et al. (footnote 4). Our review of records within 100 nmi of the coast confirmed the existence of a relatively large-bodied, heavily spotted form living near the coast from northern Mexico to Ecuador (Fig. 9). The nearshore zone is not inhabited exclusively by the coastal form, however. There are well-supported records of the smaller, less-spotted offshore form within 20 nmi of the coast, in close proximity to well-supported records of the coastal form (Fig. 10A, B, C). Conversely, there are some well-supported records of the coastal form fairly well offshore, surrounded by records of the offshore form. The greatest distance from shore for a "coastal" record supported by body-length data was 70 nmi (off central Mexico), and the supported offshore record closest to the coast was at 16 nmi (also off central Mexico) (Figs. 10, 11). The transition from "coastal" to "offshore" is relatively regular out to about 60 nmi, with a continuing low frequency of sightings of the coastal form out to 90 nmi (Fig. 11). The distance at which the number of included records east of the line which are "offshore" is equal to the number of "coastal" records excluded (offshore of the line) is about 35 nmi. This, of course, is based on the distance-from-shore frequency distribution in the sample considered here. Within 50 nmi, the boundary used in the past in stock assessment and management, the composition (based on the stratification in Figure 11) was 52.7% "coastal" and 47.3% "offshore." A line drawn at 100 nmi from shore could safely be said to encompass all of the coastal range.

The coastal form may also occur around some of the oceanic islands in the eastern Pacific (Revilla Gigedos, Clipperton Island,

---

[5] Jennings, J. G., and R. K. Stives. 1979. Summary of preliminary results of a dolphin tagging feasibility study. Unpublished meeting document 79/32, Status of Porpoise Stocks Workshop, August 29-31, 1979, La Jolla, California, 22 p.

[6] Powers, J. E., R. W. Butler, J. G. Jennings, R. McLain, C. B. Peters, and J. DeBeer. 1979. Summary of research results from the fourth cruise of the Dedicated Vessel, September 12 to October 31st, 1978. Southwest Fisheries Center Admin. Rep LJ-79-14, 46 p.

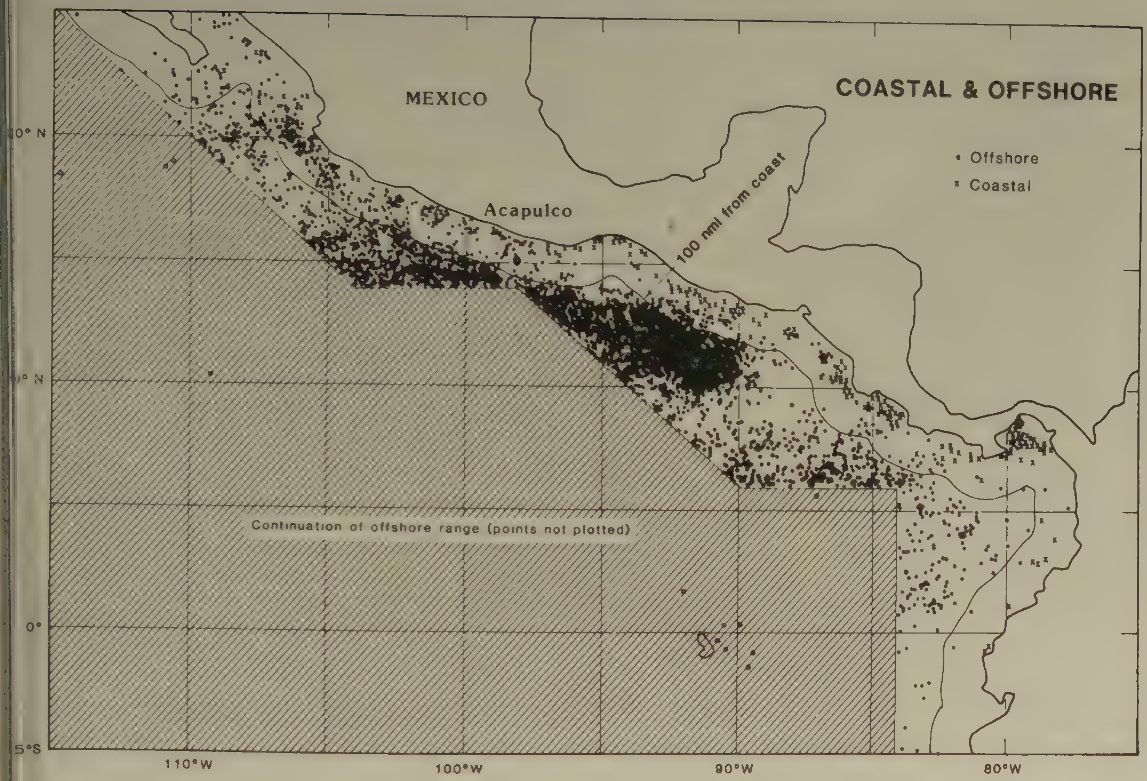

Figure 9.—Records of offshore (dots) and coastal (x's) spotted dolphins in the far-eastern Pacific.

os Island, and Malpelo Island), but there is only one sighting
rd indicating this. An IATTC technician aboard a commercial
er approximately 60 nmi off Malpelo Island in 1983 observed
hool of 15-30 robust and heavily spotted dolphins that "look-
ike coastals." The distance from the mainland was approx-
ely 240 nmi. Without more records, it is difficult to say
her the observer just happened to see a few heavily spotted
ore animals (which would be expected under the racial
digm, given enough observation effort) or the animals around
sland are similar to those close to the mainland. We assume
ormer, pending availability of more information.

lult male coastal spotted dolphins average about 23 cm longer
offshore males (those north of SOPS '79 north/south boun-
—Fig. 1—and east of long. 120°W) and coastal females
t 19 cm longer than offshore females (Fig. 12), although there
oad overlap in length. The standard deviations for the coastal
les are appreciably larger than those for the offshore samples
= 5.07 and 3.91, respectively). This and the right-skew in the
al female distribution may mean that some animals classified
coastal" should have been identified as "offshore," or that
rades are more common in "coastal" schools than in "off-
" schools, i.e., that the coastal form is more variable, perhaps
ting proportionately greater introgression of offshore genes
he coastal population than the reverse. Another possible
nation is that coastal females continue to grow longer after
ment of sexual maturity than do offshore females.

The coastal form has been characterized as occurring in relatively ". . . small groups or schools or (sic) fewer than 100 individuals" (Perrin 1975a:127). In our review of sighting records, we found that while most records were of small groups of animals, there were also several records of very large schools of the coastal form (Table 2). Estimated school sizes ranged to 20,000 animals. Most of the very large schools were seen off Costa Rica, south of Puntarenas (lat. 8°-10°N and long. 83°-85°W), while some were seen off central Mexico (lat. 15°N).

Schnell et al. (footnote 4) concluded that the results of their multivariate analyses of skull data "fully warrant(s) the recognition of the southern *S. attenuata* as a distinct stock." They found the skulls of spotted dolphins from south of the Equator to be, on the average, larger and to have a smaller temporal fossa than those of animals from north of the Equator. They reached the same conclusion from analysis of body-length data; they found the southern animals to be, on the average, shorter than the northern animals. The results of our review of body-length data are the same (Fig. 12). Males from the eastern portion of the SOPS '79 "northern offshore" range were modally about 3.5 cm longer than those from the "southern offshore" range (this difference and others between the offshore samples are statistically significant at $P < 0.001$); the difference for females is 2.5 cm. When the southern sample is compared with the portion of the northern sample from west of long. 120°W, the difference is smaller, 2.0 cm for males and 1.3 cm for females, a result consistent with the finding by

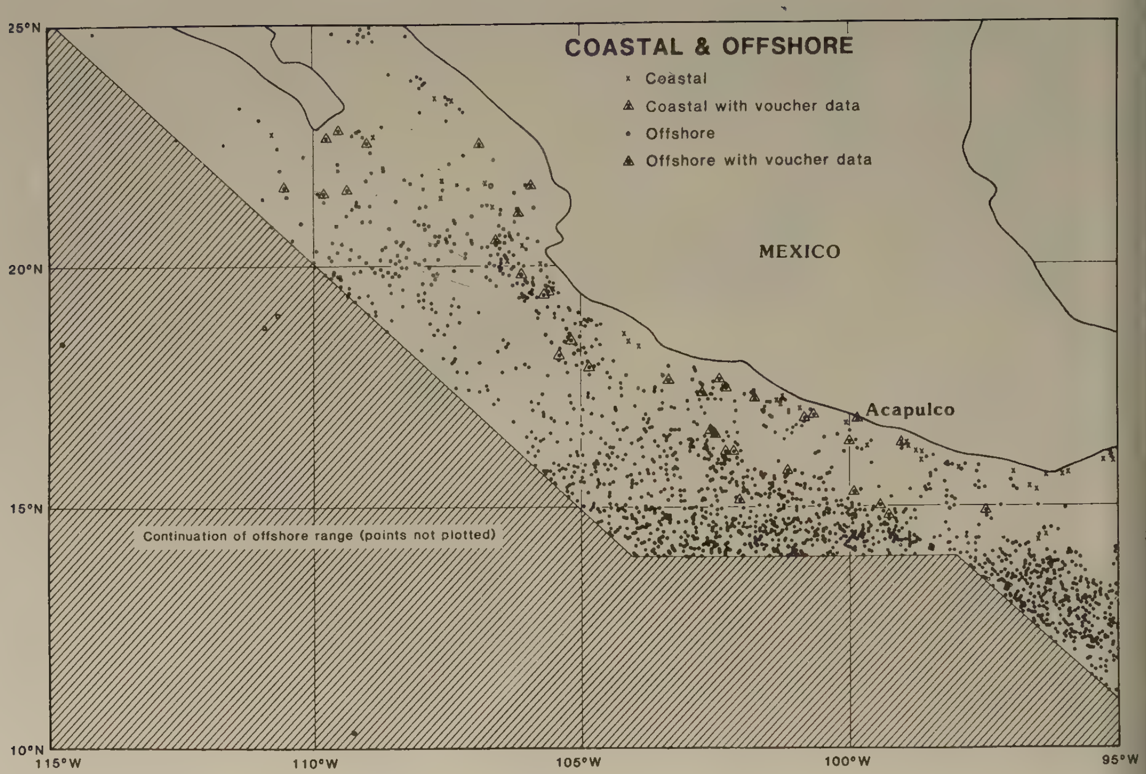
25°N
20°N
15°N
10°N
115°W
110°W
105°W
100°W
95°W
COASTAL & OFFSHORE
× Coastal
▲ Coastal with voucher data
• Offshore
▲ Offshore with voucher data
MEXICO
Acapulco
Continuation of offshore range (points not plotted)

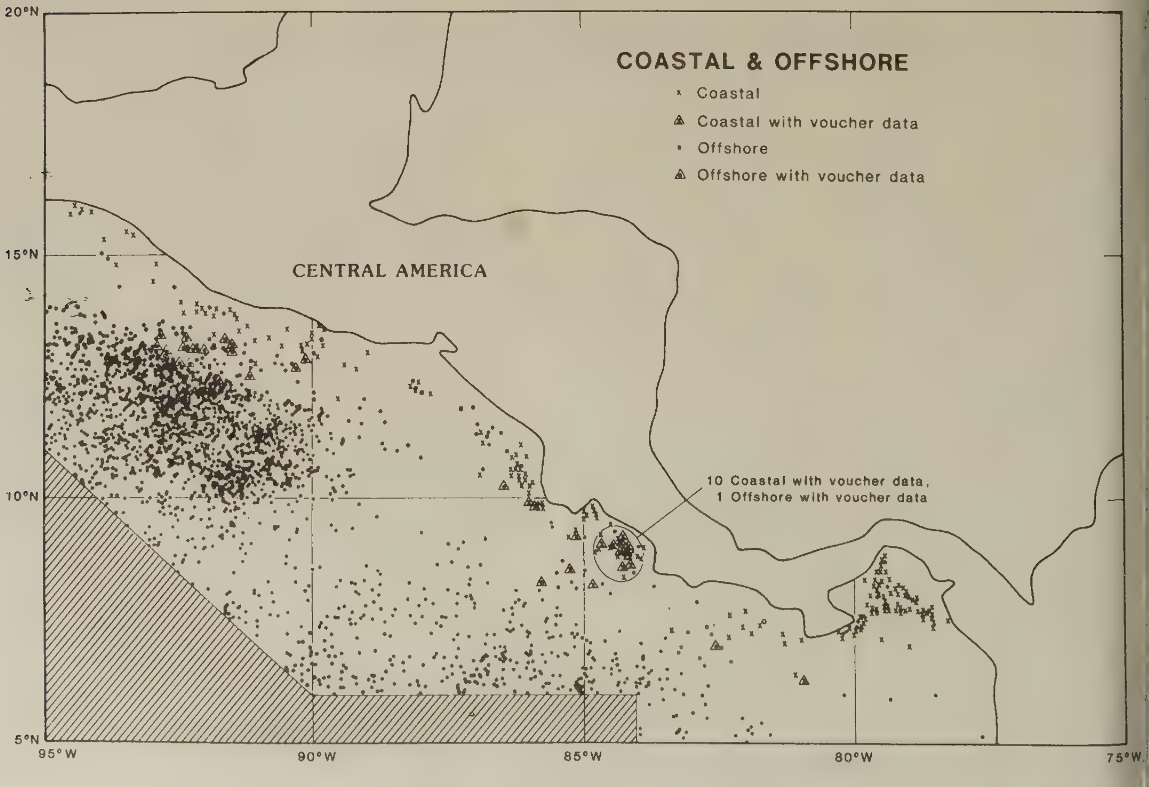
20°N
15°N
10°N
5°N
95°W
90°W
85°W
80°W
75°W
COASTAL & OFFSHORE
× Coastal
▲ Coastal with voucher data
• Offshore
▲ Offshore with voucher data
CENTRAL AMERICA
10 Coastal with voucher data, 1 Offshore with voucher data

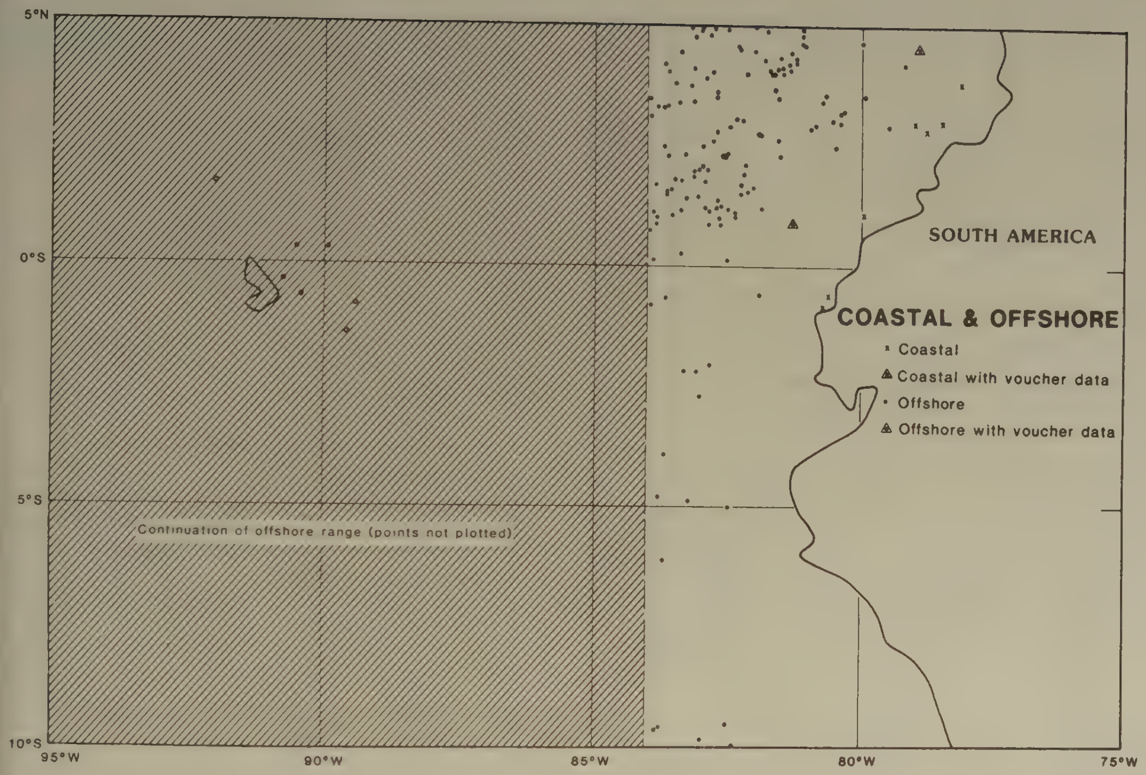
5°N
0°S
5°S
10°S
95°W
90°W
85°W
80°W
75°W
SOUTH AMERICA
COASTAL & OFFSHORE
x Coastal
▲ Coastal with voucher data
• Offshore
▲ Offshore with voucher data
Continuation of offshore range (points not plotted)

Figure 10.—Records of offshore (small dots) and coastal (x's) spotted dolphins off A) North America (upper left), B) Central America (lower left), and C) South America (above), with records that are supported by photos, measurements, or osteological specimens indicated (triangles).

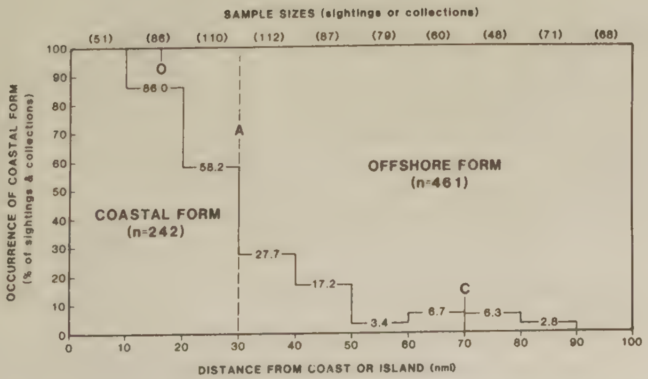

Figure 11.—Relative abundance of records of offshore and coastal spotted dolphins by distance from coast. "C" is most offshore "coastal" record supported by photos, measurements, or osteological specimens; "O" is most inshore "offshore" record with such support. "A" is distance from coast at which the proportion of included records that are offshore equals the proportion of coastal records that are excluded.

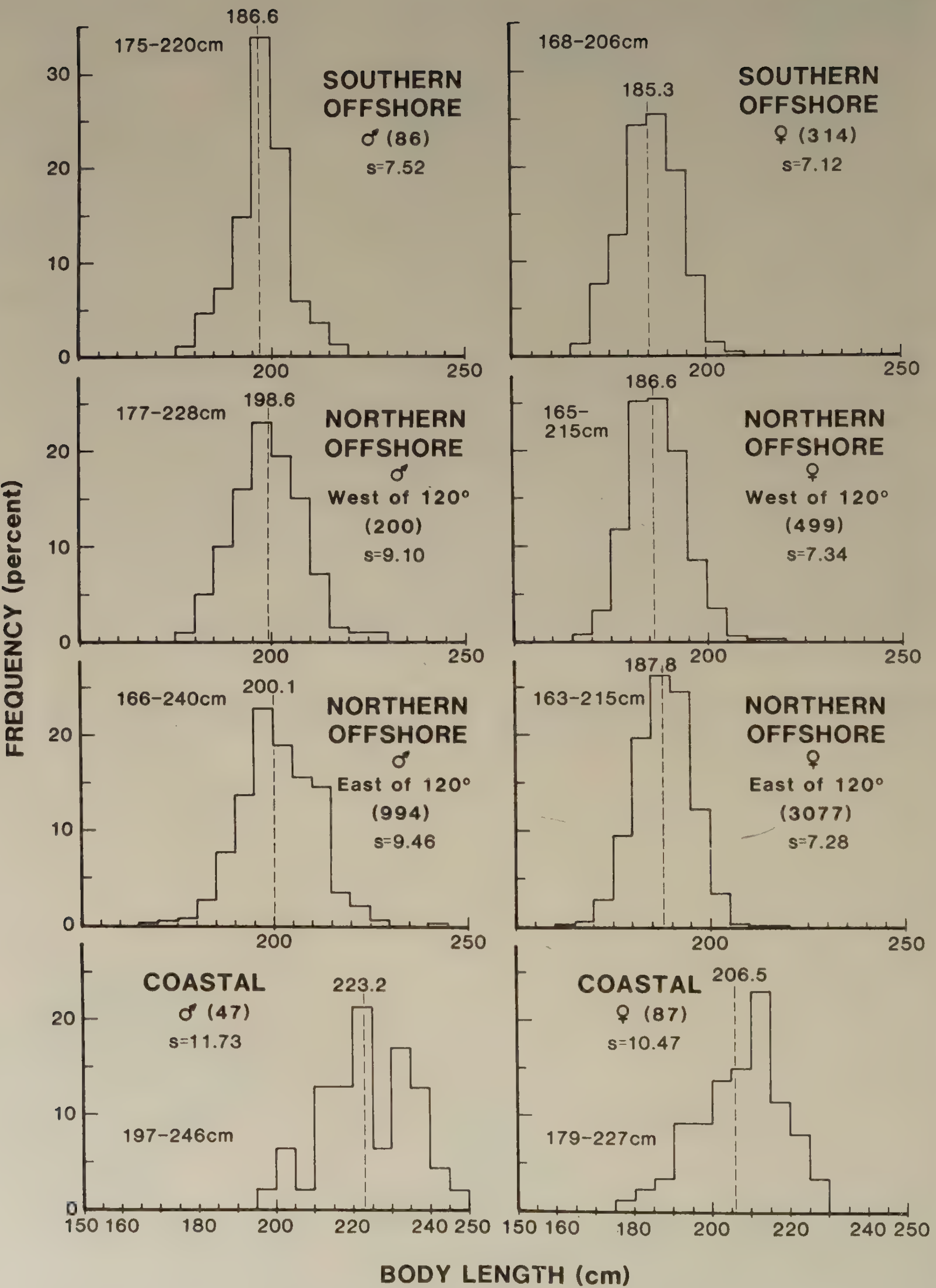

Figure 12.—Frequency distributions, ranges, means, and standard deviations of body length for male and female spotted dolphins, *Stenella attenuata*, from four geographical areas. Sample sizes in parentheses.

ble 2.—Estimated school sizes for sightings of coastal and offshore spotted olphins within 100 nmi of the coast. Ranges of school sizes in parentheses.

School size › of dolphins)	Coastal form		Offshore form	
	n	%	n	%
<100	144	63.2	59	13.2
	(min. <10)		(min. <10)	
100-1,000	64	28.1	270	60.3
>1,000	20	8.8	119	26.6
	(max. >20,000)		(max. >20,000)	
Total	228		448	

hnell et al. (footnote 4) of affinities between southern skulls and very small sample of skulls from the far-western part of the rthern range. The samples used in our body-length comparison vered the geographic range of the species more completely than d the samples of skulls available to Schnell et al. (Fig. 5).

Two additional lines of evidence suggest that the southern imals are smaller than the northern animals: 1) Hohn and Hamond[7] estimated length at birth from northern offshore samples at .4 cm. Their estimate from southern offshore samples was 83.2 . Their conclusion that the southern form is about 2 cm shorter n the northern form at birth is tentative because of the rather all sample size for the southern form. 2) Average length at ainment of sexual maturity was estimated at 177-180 cm 74-82) and 175 cm (1973-82) for northern and southern nples, respectively (Barlow in press).

Because both females and males can continue to grow after aining sexual maturity (Perrin et al. 1976), we considered the sibility that the differences between the northern and southern nples in average lengths of adults reflect not inherent racial difence in size but difference in age structure in the two regions. nples from the southern region have not been aged, so direct nparison of age structures was not possible. We were able, wever, to compare the frequency distributions of ovarianous count for the two samples (Fig. 13). If ovulation rates are umed to be similar in the two regions, it is clear that the age ctures for adult females are not radically different. In any case, difference is in a direction opposite that which would be exted were the adult southern animals smaller because of being, he average, younger.

he results of tagging studies (Perrin, Evans, and Holts 1979; nings and Stives footnote 5, and unpublished data—J.G. Jens[8]) indicate considerable east-west movement within the hern offshore range. Of 206 tag recoveries or resights of tags in notches, 9 indicated movement from east to west of the h meridian; three involved movement of at least 1,300 nmi, a period of 9-10 mo. While this inference of long east-west ement must remain provisional (none of the 3 cases involved actual recovery of a tag), when it is considered in the context possible east-west cline in morphology (body-length, colora- and skull measurements), it suggests that such morphological rentiation is maintained despite at least temporary long-range ements of individuals and perhaps schools. One tag released n of lat. 10°N was resighted by a tuna-seiner crewman (but not recovered) at lat. 10°37′S, some 4-5 mo later. This result, if confirmed, would suggest that the apparent north-south morphological differences may actually reflect a clinal situation similar to that (east-west) which may exist in the northern offshore portion of the range, rather than a substantial separation of populations north and south of the Equator.

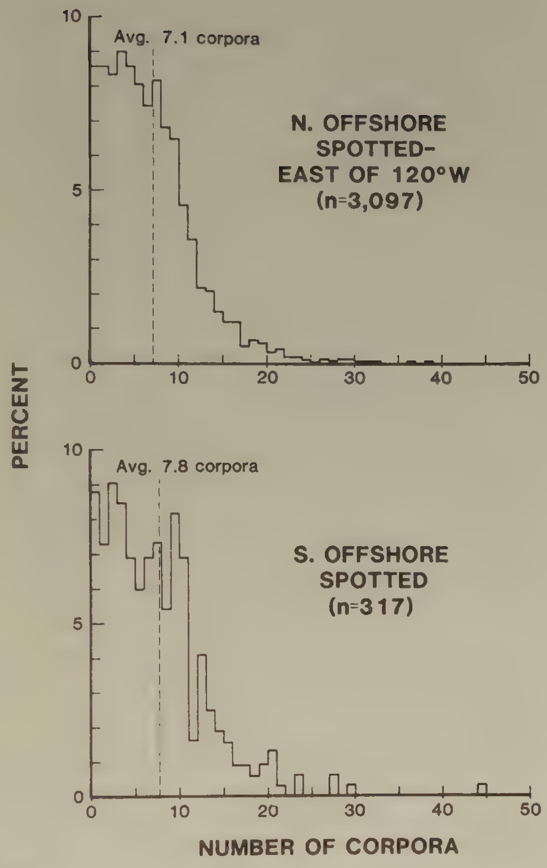

Figure 13.—Frequency distributions of ovarian-corpus count for northern and southern offshore samples of adult female spotted dolphins.

The results of a study of breeding seasonality (Barlow 1984) show very different distributions of birth dates in southern and northern offshore spotted dolphins (SOPS '79 boundaries). In the south the single calving season is quite short, March to May, whereas in the north there are two diffuse breeding peaks, in the spring and in the autumn. Barlow stratified the northern sample into two subsamples, from lat. 0°-5°N and from north of lat. 5°N, and found an intermediate pattern in the equatorial stratum of a single but diffuse calving peak from March to June, statistically different from the patterns both to the south and the north. He concluded that these results support the view of a separate population south of the Equator but that the transition from a diffuse bimodal breeding pattern in the north to a single sharp peak in the south may not be abrupt. He offered two possible explanations for the apparent patterns: 1) if seasonality in reproduction is determined by the timing of oceanographic or trophic factors, the dif-

---

hn, A. A., and P. S. Hammond 1983. Growth in the first year of the offspotted dolphin, *Stenella attenuata*, in the eastern tropical Pacific. Southwest ies Center Admin. Rep. LJ-83-08, 33 p.

Jennings, Fishery Biologist, Southwest Fisheries Center La Jolla Laboratory, al Marine Fisheries Service, NOAA, P.O. Box 271, La Jolla, CA 92038, pers. un. January 1983.

ference could reflect geographical change in the timing of the environmental determinants, or 2) the area between lat. 0° and 5°N could represent an area where two populations can occur, with the apparent distribution of birthdates actually being a composite of two different distributions. He noted that if a previously noted relative hiatus in sightings in the vicinity of the Equator (Perrin, Sloan, and Henderson 1979) is real, the latter explanation would be the least likely. The band of low density of sightings for 2°-3° south of the Equator is still present (Perrin et al. 1983) but not as well defined as previously.

Hohn and Hammond (footnote 7) have confirmed Barlow's results with modal-progression analysis of monthly distributions of length (after adjusting for use of different growth curves in the two studies), finding birth of two annual seasonal cohorts in the north but only one in the south. They also found a pattern of variation within the northern range; data from the far west and from along the Equator do not fit well with the pattern in data from the more easterly and northerly major part of the range. They concluded that while spotted dolphins may have different calving seasons depending on area of capture, this seasonality is probably "not actually a function of area but of schools or groups of schools which tend to inhabit different areas with different environmental conditions."

Resolution of the nature of the east-west and north-south variation must await study of more material from west of long. 120°W and from near the Equator (see also the discussion below on origins of the geographical forms).

Stenella longirostris

In our review of records within 50 nmi of the coast, we found only 33 convincing "Costa Rican" records, all south of the Gulf of Tehuantepec (Fig. 14) and north of the Bay of Panama. Of these, 16 were supported by photos or measurements of specimens (Fig. 15, Table 3). We found no coastal records of eastern spinner dolphins with such support below the Gulf of Tehuantepec and only six unsupported records there. It appears that the eastern spinner dolphin is largely, or possibly totally, replaced on the coast below about lat. 15°N by the larger, longer beaked Costa Rican form. We ascribe the relatively small number of convincing records of either form to the difficulty of estimating size of animals at sea; the two forms are not known to differ in coloration. The sample of body lengths for the Costa Rican form taken directly from specimens is very small (Fig. 16), but it is probable that modal adult length differs from that of the eastern form by about 30-40 cm in both sexes. A very large sample of photogrammetric lengths for both forms supports this conclusion (unpubl. data, M. D. Scott).

We found several well-supported records of the eastern form outside the SOPS '79 boundary (Fig. 14); the range of this form

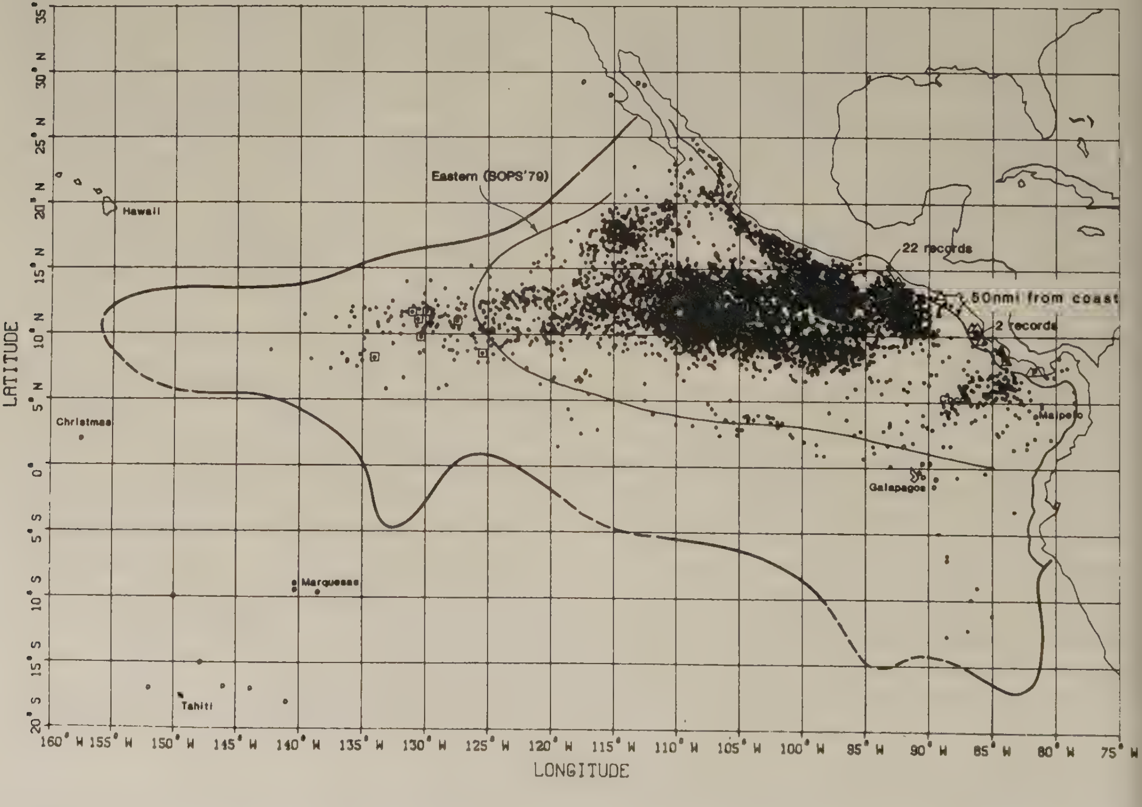

Figure 14.—Distribution of eastern and Costa Rican spinner dolphins in the eastern tropical Pacific, showing records outlying the SOPS '79 boundary for the eastern form. Outlying records enclosed in squares are supported by specimen data.

Table 3.—Records of Costa Rican and eastern forms of *Stenella longirostris* within 50 nmi of the coast (or a coastal island), north and south of Gulf of Tehuantepec (~ lat. 15°N). Number of records supported by photos, body-length data, or skull specimens in parentheses.

Gulf of Tehuantepec	Distance from coast (nmi)	Costa Rican form (records)	Eastern form (records)	Total
North of Gulf	0- 9	0	0	0
	10-19	0	8(1)	8(1)
	20-29	0	13(2)	13(2)
	30-39	0	7(0)	7(0)
	40-49	0	11(4)	11(4)
	Subtotal	0	39(7)	39(7)
South of Gulf	0- 9	3(2)	0	3(2)
	10-19	1(1)	1(0)	2(1)
	20-29	7(3)	5(0)	12(3)
	30-39	[1]19(9)	0	[1]19(9)
	40-49	3(1)	1(0)	4(1)
	Subtotal	33(16)	7(0)	40(16)
	Total	33(16)	46(7)	79(23)

[1] Includes 17 sightings made in a small area off southern Mexico during an aerial hotogrammetric experiment by the Inter-American Tropical Tuna Commission in 980 (see Fig. 15). Other intervals contain records from this source as follows 20-29 mi, 6; 40-49 nmi, 1 (all Costa Rican).

extends farther to the west than previously documented, to at least long. 134°W, albeit in apparent very low density relative to that of the whitebelly form (Fig. 17). We found only one well-supported record of the whitebelly form to the east of the SOPS '79 boundary (Fig. 17). We attribute the large number of unsupported whitebelly sightings to the identification difficulties discussed in the Materials and Methods section and believe that many of them probably represent sightings of misidentified eastern spinners. In any case, the inshore density of whitebelly spinner sightings is very low relative to that of the eastern form (Fig. 14).

Rather than draw boundaries around what are believed to be the major ranges of the two forms, as has been done in the past, we instead present a summary of relative frequency of records by 5° square (Fig. 18; values in Appendix 2). The sample sizes on the fringe of the continous range of the species in the eastern tropical Pacific are small, but those in the major zone of overlap are very large, and the proportions likely reflect the true relative abundances of schools of the two forms. As discussed above, the real levels of whitebelly-spinner-dolphin records in the northeastern reaches of the eastern range are likely lower than indicated, e.g., we believe that the anomalously high proportion in the square at

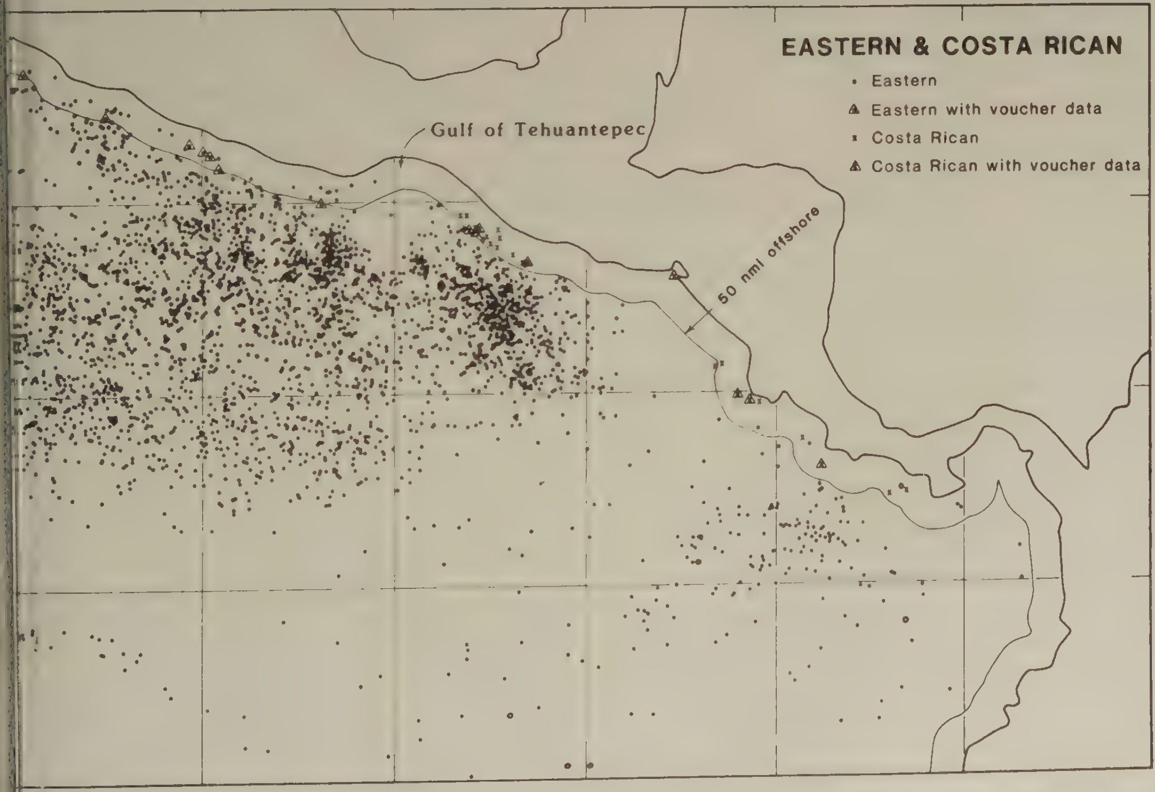

gure 15.—Distribution of eastern (dots) and Costa Rican (x's) spinner dolphins off Central America, with records inside 50 nmi supported by photos, measurements, or osteological specimens indicated (triangles).

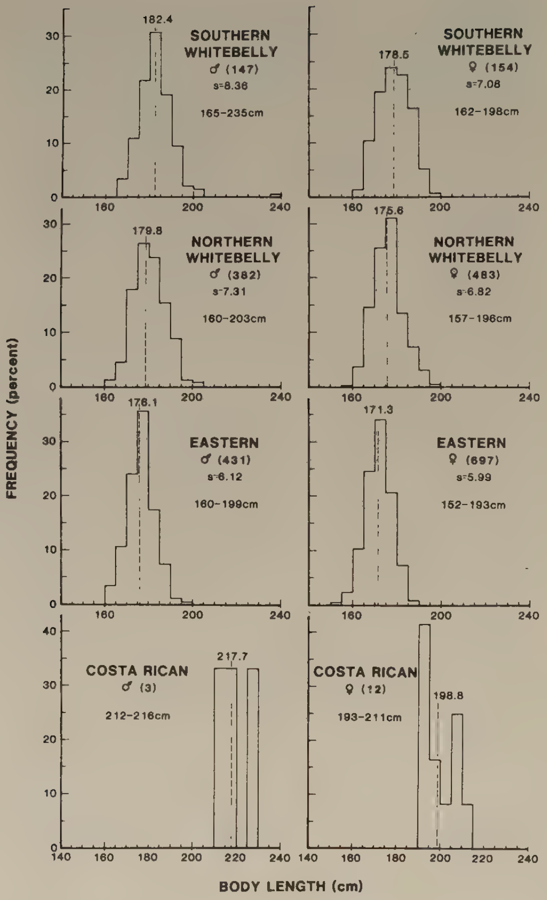

Figure 16.—Frequency distributions, ranges, means, and standard deviations of body length in samples of adult specimens of *Stenella longirostris* of four stocks. Sample sizes in parentheses.

the tip of Baja California may be the result of unfamiliarity with the two kinds of spinner dolphins by south-bound first-time observers.

Eastern spinner dolphins are, on the average, about 3-4 cm smaller (significant at $P < 0.001$) than (northern) whitebelly spinner dolphins (Fig. 16). The length-frequency distributions for the two forms are very similar in shape, and the variances are small compared with those for other samples examined here, suggesting that the two populations are well delineated and accurately represented by the samples.

Schnell et al. (footnote 4) found "marked differentiation of a southern form from populations to the north" based on multivariate analysis of skull measurements. They found skulls from the south to be larger, with a proportionately larger temporal fossa, than skulls from the north, a situation exactly the opposite of that found in *S. attenuata* (smaller skulls, with larger fossa, in the south). As was the case of *S. attenuata*, they noted morphological affinities, in some of the analyses, between southern specimens and those from west of long. 120°W. They also found southern spinners to be longer than northern specimens. However, they did not distinguish between the eastern and whitebelly color forms. Our comparison of body length for northern and southern whitebelly spinner dolphins using the SOPS '79 ranges showed a difference of about 2-3 cm (significant at $P < 0.01$) in males and females (Fig. 15). No new information is available on color pattern of the southern spinner dolphins beyond that given in Perrin, Sloan, and Henderson (1979).

Because of the possibility that the difference in average body length could be caused by a difference in age structure (i.e., relatively more younger and smaller adult females in the northern region), we examined the frequency distributions of ovarian-corpus count for the two samples (Fig. 19), again assuming similar ovulation rates. The distributions do indeed differ, with a higher proportion having fewer than three corpora in the northern sample than in the southern sample. This may reflect differing age structures or differing ovulation rates; resolution of the question will require comparison of aged samples (not yet available for the southern form).

Tag returns for *S. longirostris* from the eastern tropical Pacific have been few and suggest less extensive movement than do those for *S. attenuata* (Perrin, Evans, and Holts 1979). There has been one sighting (by a yachtsman) of a tagged animal in the Marquesas (a spaghetti tag of unspecified type; J. G. Jennings footnote 8), where nine spinner dolphins were tagged in 1976 (Table 1). There have been no tag returns indicating movement across the Equator or between the far-eastern and far-western parts of the eastern tropical Pacific above the Equator.

Barlow (in press a) found a single sharp seasonal breeding peak in the eastern spinner dolphin and at least two modes in the northern whitebelly spinner dolphin. He also found a regional difference in timing of the peak in the eastern spinner dolphin, with offshore animals calving earlier in the year than inshore animals. He noted that distributional studies indicated that there are inshore and offshore population centers for eastern spinner dolphins with a decreased density of sightings in between (Fig. 14 and Au et al. footnote 3) and suggested that a further subdivision of the eastern spinner into two populations/stocks would be meaningful. He did not examine seasonality in spinner dolphins south of the Equator.

Stenella coeruleoalba

Very little new information is available for this species. Delineation of the three tropical stocks was based on apparent latitudinal gaps in distribution, pending availability of adequate series of morphometric data (Smith 1983; Au et al. footnote 3). The band of relatively low density of sightings between lat. 10° and 15°N is apparent in the data (Fig. 20), but the distribution now appears relatively continuous south of lat. 15°N and east of about long. 115°W, with a region of lower apparent density around the Galapagos Islands (which may only reflect the lesser sighting effort there—Perrin et al. 1983, Fig. 1). It would seem that there is now little or no justification for dividing the animals in this area (south of lat. 15°N and east of long. 115°W) into two stocks based on distribution data alone. The same applies to the eastern and western concentrations within the "central tropical" range; sighting effort has been relatively lower in the region between them. Only the low-density band between lat. 10° and 15°N at this point can be said with some confidence to be real. There is a 200-300 nmi wide swath extending northeastward from long. 105°W where no striped dolphins have been sighted despite extremely high levels of sighting effort. We conclude that direct interchange between the population centers to the north and south probably occurs so seldom as to be negligible. In the region im-

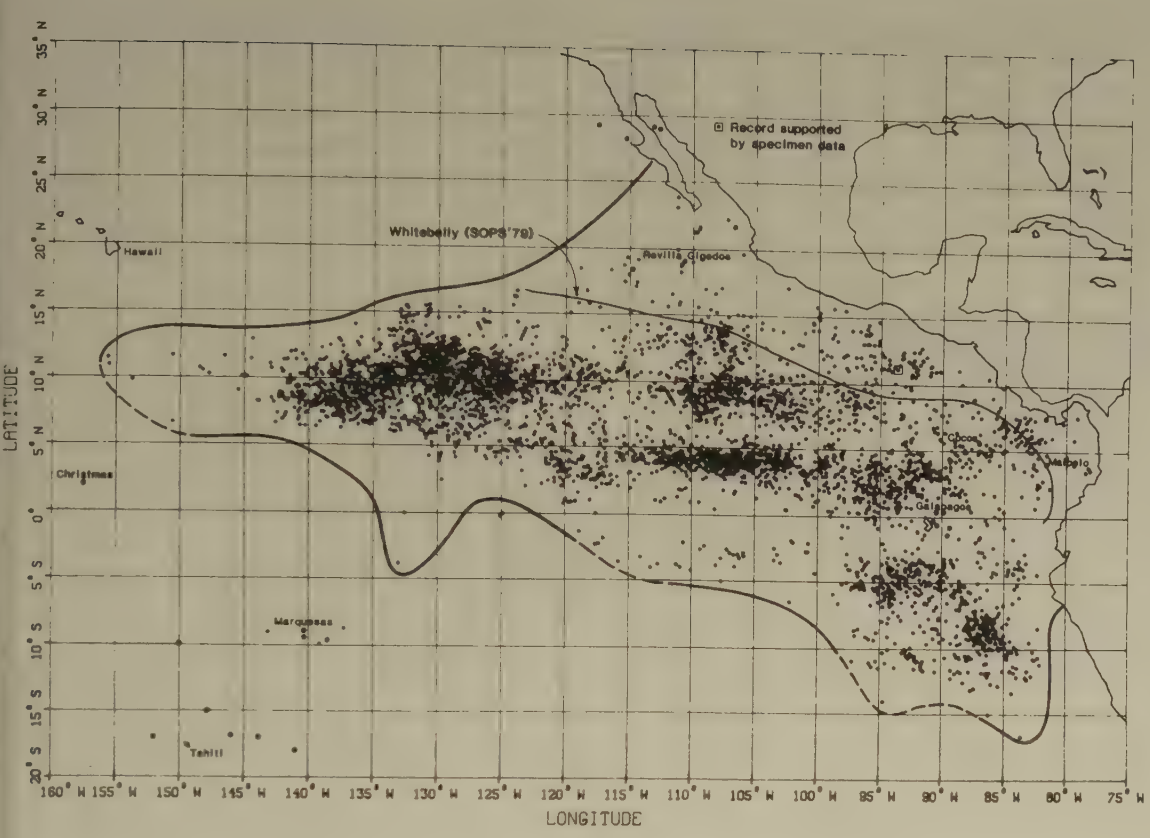

gure 17.—Distribution of whitebelly spinner dolphins (northern and southern) in the eastern Pacific, showing records east of the SOPS '79 boundary. Record enclosed in square is supported by specimen data.

ediately to the west (between about lat. 10° and 15°N and long. 5° to 120°W), where sighting effort has also been extremely avy, there are only a few records of the species; the density here apparently also very low.

In the area north of lat. 25°N, where sighting effort has been tremely heavy to at least lat. 31°N, scattered sightings of striped lphins have continued to accumulate (Perrin et al. 1983), but it uld appear that the animal occurs rarely in this warm-temper- part of its range in the eastern Pacific. It seems to us unlikely t this represents a separate population center. Similarly, the duction of the existence of a "southern temperate" stock south lat. 10°S is probably also not justified.

The very limited adult body-length data (most of the animals led have been juveniles) do not suggest a modal difference in gth between animals from the northern and central tropical ges (Fig. 21). Only one adult (a 204 cm female) from the thern tropical range has been measured.

lphinus delphis

Although "Baja neritic" and "northern tropical" stocks were ined by Evans (1975, 1982) based on morphology and color terns (Fig. 4), these have been pooled in assessment and nagement (Holt and Powers 1982; Smith 1983). Common dolphins sampled in the fishery and tropical sightings have been identified only as "*Delphinus delphis*" and allocated by position to the "northern tropical" (3°N-10°S) latitudinal management units. This pooling is evident in the "northern tropical" (between lat. 15° and 28°N), "central tropical" (lat. 3°-15°N), or "southern tropical" body-length data (Fig. 22); the Baja neritic form is about 30 cm longer than the northern tropical form (Evans 1982). The animals included in the "northern tropical" sample came from two areas: Baja California (Squares 168, 169, and 189 in Figure 8), and off southern Mexico (Square 146). Those from north of Magdalena Bay (Square 189) appear from their lengths (shaded portions of histograms in Figure 20) to have been of the Baja neritic form, whereas those from south of Magdalena Bay and around Cabo San Lucas into the Gulf of California (Squares 168 and 169 in Figure 8) appear to have been of the short-beaked northern tropical form. Evans (1982) showed the range of the Baja neritic form as including the Gulf of California. Some of the Baja neritic common dolphins on the outer coast were taken more than 50 nmi offshore, and some of the short-beaked "offshore" animals were captured within 10 nmi of the coast (Table 4). When this is considered in the context of the pooled distribution data (Fig. 23), it is clear that common dolphins off Baja California cannot be identified to stock on the basis of an inshore-offshore criterion alone. The two forms are, however, fairly easily identi-

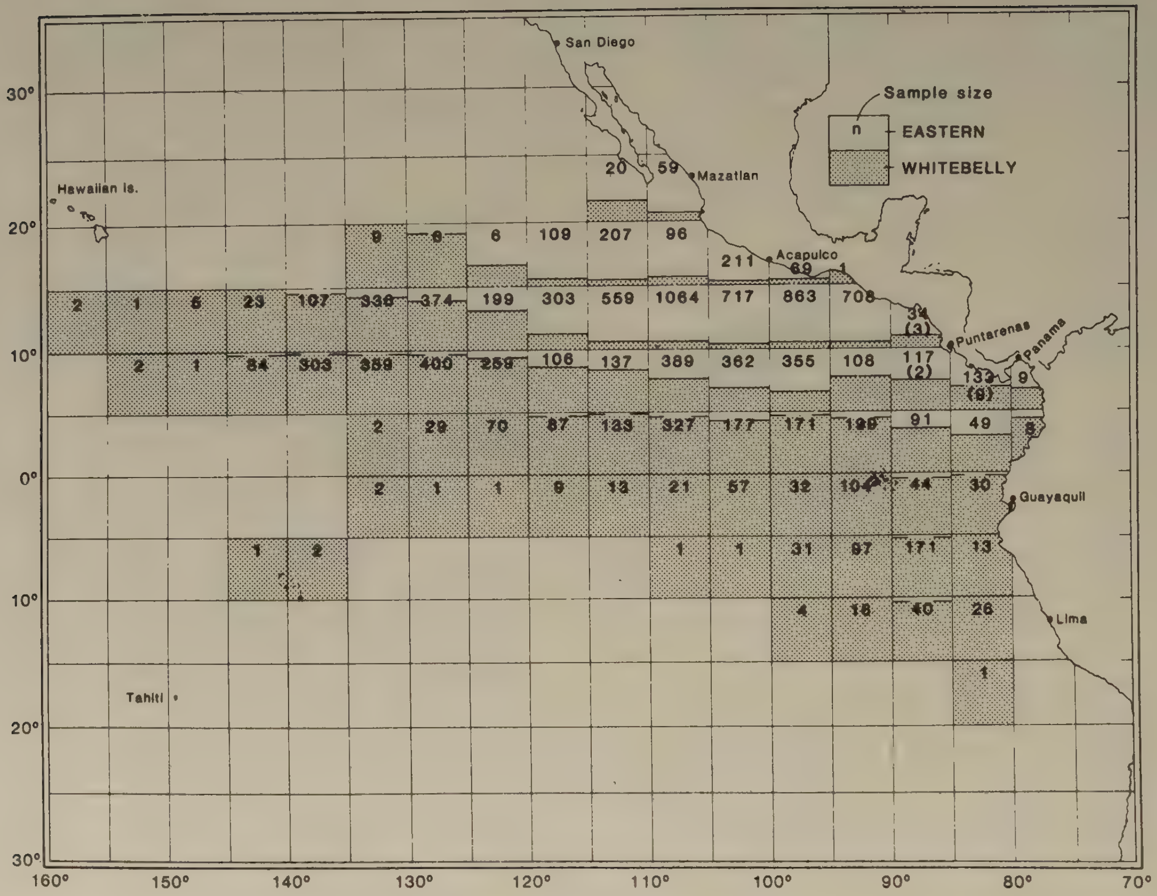
San Diego
Mazatlan
Acapulco
Puntarenas
Panama
Guayaquil
Lima
Hawaiian Is.
Tahiti
Sample size
n
EASTERN
WHITEBELLY
30°
20°
10°
0°
10°
20°
30°
160°
150°
140°
130°
120°
110°
100°
90°
80°
70°

Figure 18.—Racial composition by 5° square of sightings of *Stenella longirostris* identified to geographical race. Open areas of squares represent eastern form (and, for four squares, Costa Rican); shaded areas represent whitebelly form (northern and southern). Sample size given for each square. Number of Costa Rican records in parentheses.

Figure 19.—Frequency distributions of ovarian-corpus counts in northern and southern samples of adult female spotted dolphins.

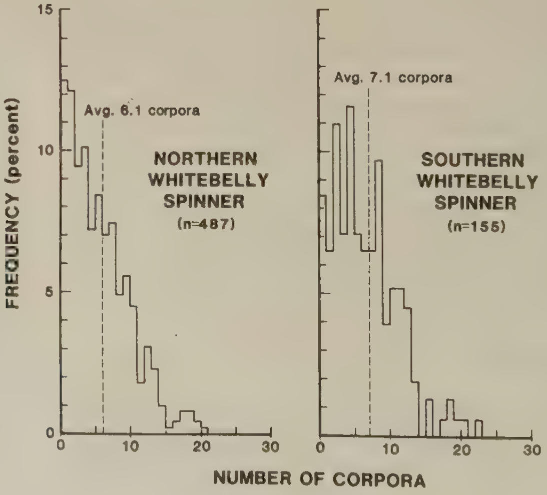

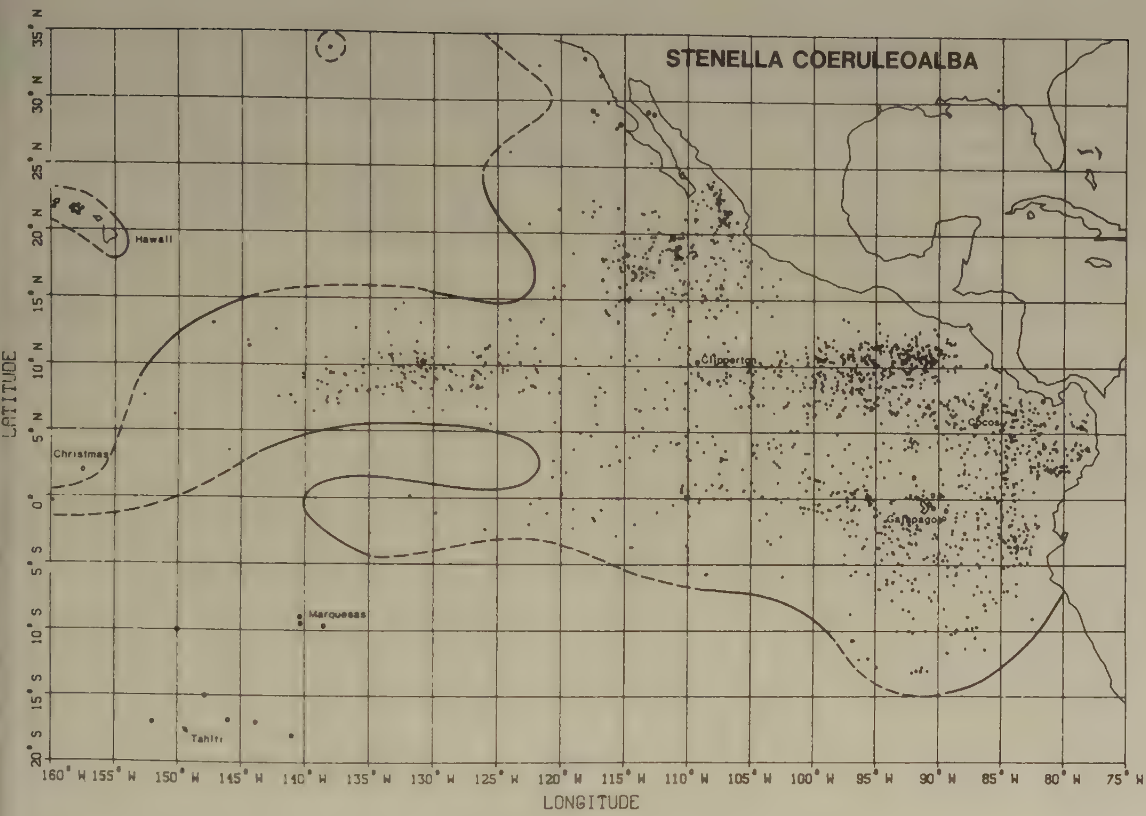
STENELLA COERULEOALBA
Hawaii
Christmas
Clipperton
Cocos
Galapagos
Marquesas
Tahiti
35° N
30° N
25° N
20° N
15° N
10° N
5° N
0°
5° S
10° S
15° S
20° S
LATITUDE
160° W
155° W
150° W
145° W
140° W
135° W
130° W
125° W
120° W
115° W
110° W
105° W
100° W
95° W
90° W
85° W
80° W
75° W
LONGITUDE

Figure 20.—Records of *Stenella coeruleoalba* in the eastern Pacific. Boundary from Perrin et al. (1983).

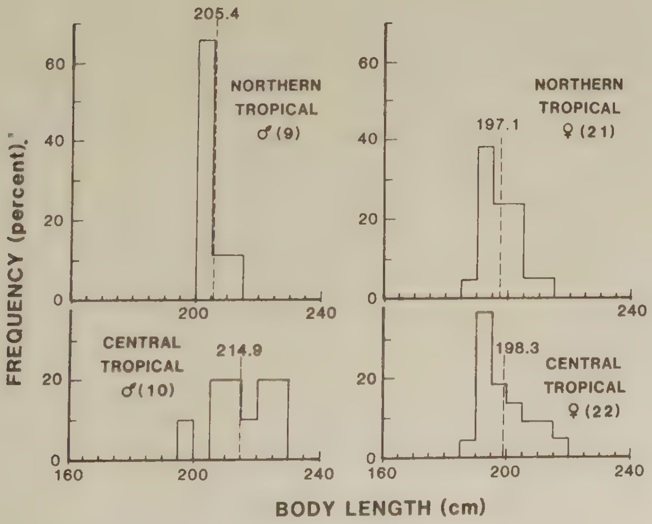

igure 21.—Length-frequency distribution and means of body ength for nothern tropical and central tropical adult males and emales of *Stenella coeruleoalba*. Sample sizes in parentheses.

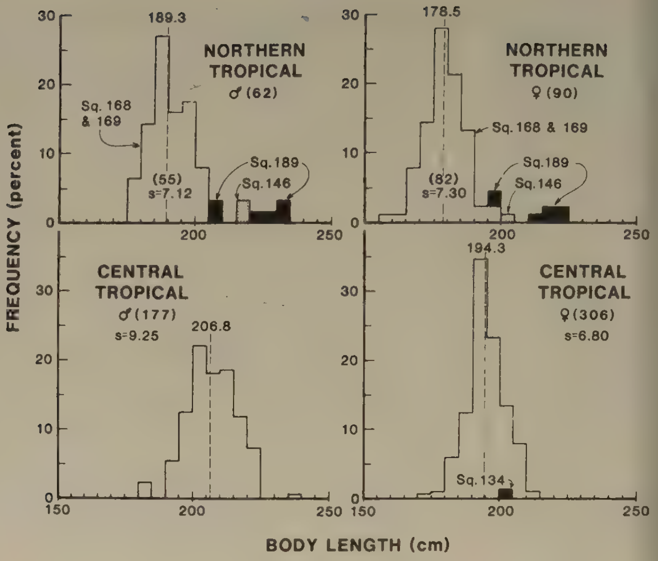

Figure 22.—Frequency distributions, ranges, means and standard deviations of length in two stocks of *Delphinus delphis*. Sample sizes in parentheses.

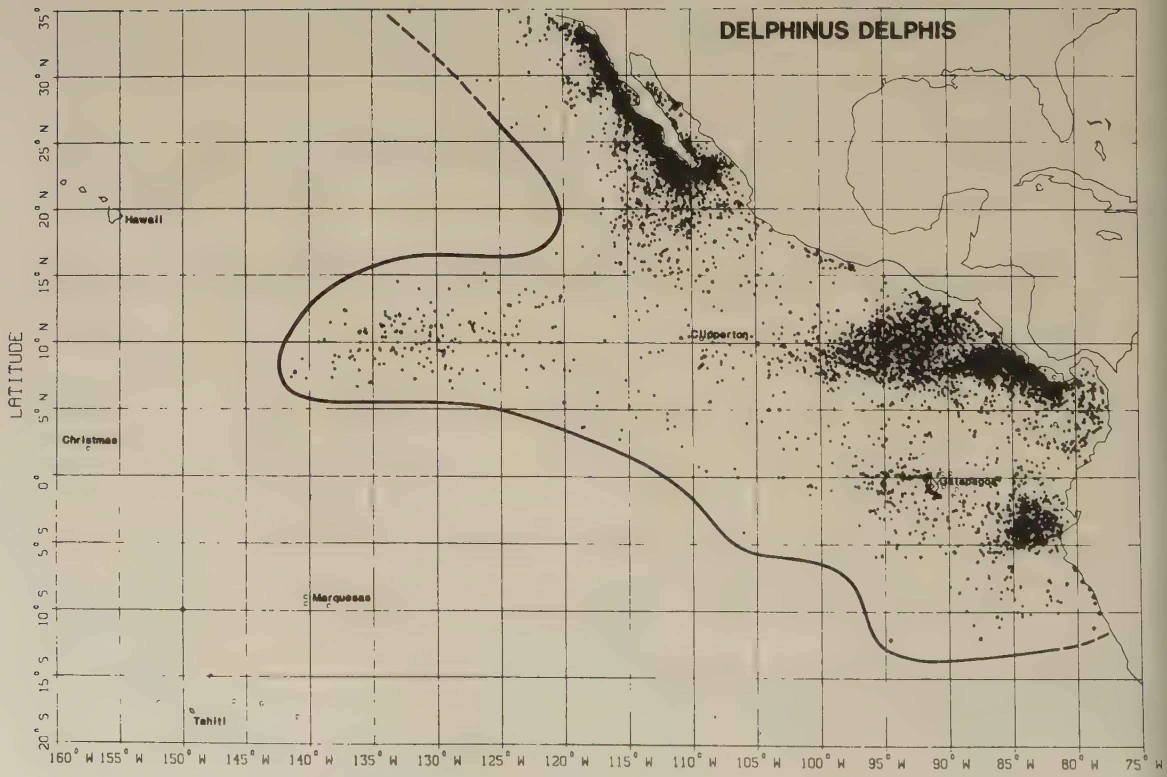

DELPHINUS DELPHIS
LATITUDE
35° N
30° N
25° N
20° N
15° N
10° N
5° N
0°
5° S
10° S
15° S
20° S
Hawaii
Christmas
Marquesas
Tahiti
Clipperton
Galapagos
160° W
155° W
150° W
145° W
140° W
135° W
130° W
125° W
120° W
115° W
110° W
105° W
100° W
95° W
90° W
85° W
80° W
75° W

Figure 23.—Records of *Delphinus delphis* in the eastern tropical Pacific. Boundary from Perrin et al. (1983).

Table 4.—Distances from coast of specimen records of *Delphinus delphis* in Square 189 (Baja neritic form; north of lat. 25°N) and Squares 168-169 (northern tropical form; south of lat. 25°N). Most offshore record of Baja neritic at 51 nmi; most inshore northern tropical at 51 nmi. See Figure 8 for locations of squares and Figure 22 for specimen data.

Distance from coast (nmi)	Records: Baja neritic in Square 189 (no.)	Records: Northern tropical in Squares 168 & 169 (no.)
0- 9		1
10-19	1	7
20-29	2	7
30-39	2	10
40-49	4	12
50-59	1	12
60-69		8
70-79		9
80-89		4
90-99		6
Total	10	76

fied at sea by size, shape, and coloration (Leatherwood et al. 1982).

In addition to the specimens indicated in Figures 8 and 2, there were 21 animals measured from Square 189 for which gonadal material was not collected that would allow them to be classified as adult or immature. The lengths of 11 males were 153, 164, 195, 208, 218, 225(2), 227, 228, 230, and 236 cm. The lengths of 10 females were 181, 197(2), 199, 205, 206(2), 209, 213, and 215 cm. These lengths more likely belong to the same frequency distributions as the adult animals from Square 189 than to those of the animals from Squares 168 and 169 just to the south. Therefore, maximum length of the Baja neritic form can be assumed to be at least 236 cm.

The sample from off the state of Guerrero in southern Mexico (Square 146) is too small (2 males and 3 females, cross-hatched in Figure 22) to allow a firm conclusion to be made, but it apparently does not belong to the same distribution as the animals from Squares 168 and 169.

Evans initially (1975) did not subdivide the short-beaked "temperate-subtropical" animals north of lat. 20°N into temperate and tropical stocks. He later (1982) defined a "northern" stock in the eastern tropical Pacific extending from about lat. 6°-18°N to just below Cedros island (about lat. 28°N) but did not delineate a "temperate" stock to the north. The 1979 assessment used "northern temperate" and "northern tropical" management units divided at lat. 28°N. The very extensive distribution data do not now suggest a gap or transition of any sort down the entire length of Baja California, and the "northern tropical" body-length data (Fig. 22) accord precisely with Evans' (1975) pooled sample of all short-beaked "temperate-subtropical" animals from north of lat. 20°N. Thus no evidence exists to support dividing the short-beaked common dolphins at lat. 28°N.

Evans (1975) found short-beaked common dolphins from south of lat. 15°N ("central tropical") to be modally longer than those from north of lat. 20°N as well as differing from them in skull features and possibly in color pattern. The present larger sample of central-tropical length data (177 males and 306 females, vs. 40 males and 48 females in Evans (1975)) confirms this; the difference is approximately 18 cm in males and 16 cm in females. With the exception of the local concentration of records off southern Mexico between about long. 97° and 103°W (Fig. 23), the central-tropical concentration (centered around lat. 8°-10°N) is separated from the northern-tropical concentration by an 800 nmi wide zone in which sighting effort has been heavy and sightings of common dolphins rare (only a dozen or so, compared with several thousand sightings of other species). This separation and the morphological differences speak strongly for treating the two populations as separate stocks. The coastal animals from between long. 97° and 103°W are problematical; their lengths do not accord well with the distributions for either the "northern tropical" or the "central tropical" samples, although they fit best with the latter. Determination of their affinities with any confidence must await study of osteological material and accumulation of more length data. Provisionally, they could be included in the central-tropical unit. They may prove to comprise a separate population, however, and it would be equally reasonable to treat them separately at this time.

Length was available for only one (female) common dolphin from the far-western portion of the central-tropical range (Square 134 in Figure 8); it is within the central-tropical range of length (shaded in Figure 22). The number of records of the species from west of long. 120°W is small (Fig. 23), despite heavy sighting effort (Perrin et al. 1983), and the distances separating the area from the denser population centers to the east are large. Determination of affinities must await more information.

Evans (1975, 1982) did not examine material from south of lat. 3°N, the "southern tropical" range. Length data are available for only 6 adults (females: 180, 182, 188, 189, 194, and 198 cm). These accord about equally well with the length distributions for the central tropical and the northern tropical samples (Fig. 22). Since the distribution of the common dolphin in this area exhibits a largely reciprocal relationship with that of the spotted and spinner dolphins, being abundant in regions likely to have lower sea-surface temperatures (near the Galapagos Islands and near the coast of Peru at lat. 0°-5°S) than do the areas where those species are abundant (Perrin et al. 1983), it is possible that the concentration near and below the Equator represents a temperate-tropical stock analogous to the short-beaked northern temperate-tropical stock. There is fairly good separation from the central-tropical center by a band of heavy sighting effort and few sightings between lat. 0° and 5°N.

ORIGINS OF THE GEOGRAPHICAL FORMS

The results for *Stenella* spp. suggest that a concept of radially patterned geographical variation in the eastern tropical Pacific may be more appropriate than the primarily latitudinal approach that has held sway to date. The radial pattern also meshes better with our developing understanding of the ecology of pelagic dolphins in the eastern tropical Pacific. Perrin (in press) has suggested that the variation between central Pacific and eastern Pacific races of *Stenella attenuata* and *S. longirostris* may actually constitute ecological character displacement between the two species in the eastern tropical Pacific, where they school and feed together. (They school and feed separately elsewhere.) Under this hypothesis, the animals forage together because of mutual advantage gained in finding prey or in avoiding predators[9] in the special conditions of the oceanographically anomalous eastern tropical Pacific,[10] and their divergence in coloration, tooth size, jaw muscles, etc. reflects divergent specializations in feeding (species, size, and depth of prey) that minimize direct competition between the components of the multispecies "school" (which also often includes yellowfin tuna). The two species (and the tuna) do indeed have different feeding habits in the eastern tropical Pacific, even in the same "school" (Perrin et al. 1973). In addition, Schnell et al. (footnote 4) found that expression of characters of the skull in *S. attenuata* that are associated with feeding is correlated with environmental parameters over long distances in the eastern tropical Pacific. For example, a correlation exists between size of the temporal fossa (through which the main jaw-closing muscle passes) and sea-surface temperature, solar insulation, and thickness of the oxygen-minimum layer. *Stenella longirostris* varies in a similar way. Schnell et al. concluded that "the rather marked morphological covariation between *S. attenuata* and *S. longirostris* involving a number of characters could reflect common causes associated with environmental spatial variation."

---

[9] Norris and Dohl (1980) have suggested that Eastern Tropical Pacific spinner dolphins may use the shelter of spotted dolphin schools as a surrogate for the shallow bays in which they spend their daytime resting hours in the central Pacific.

[10] The eastern Pacific is peculiar in having a relatively thin, warm mixed layer (50 m thick) above a stable steep thermocline and a thick oxygen minimum layer. This establishes an effective shallow habitat much like the nearshore habitat in other tropical waters (see Perrin et al. 1976 and Au et al. footnote 3).

A conceptual model of the radial nature of the pattern of variation can be based on what we now know in a general way (Fig. 24). In this view, the animals in the far eastern Pacific (the eastern or Costa Rican spinner dolphins and, for the sake of argument, the offshore spotted dolphins north of the Equator and east of long. 120°W), and the dolphins in the central Pacific (Polynesia and points west) comprise the purest populations of the ecologically differentiated forms. Those in between (whitebelly spinner and offshore spotted dolphins south of the Equator and west of long.

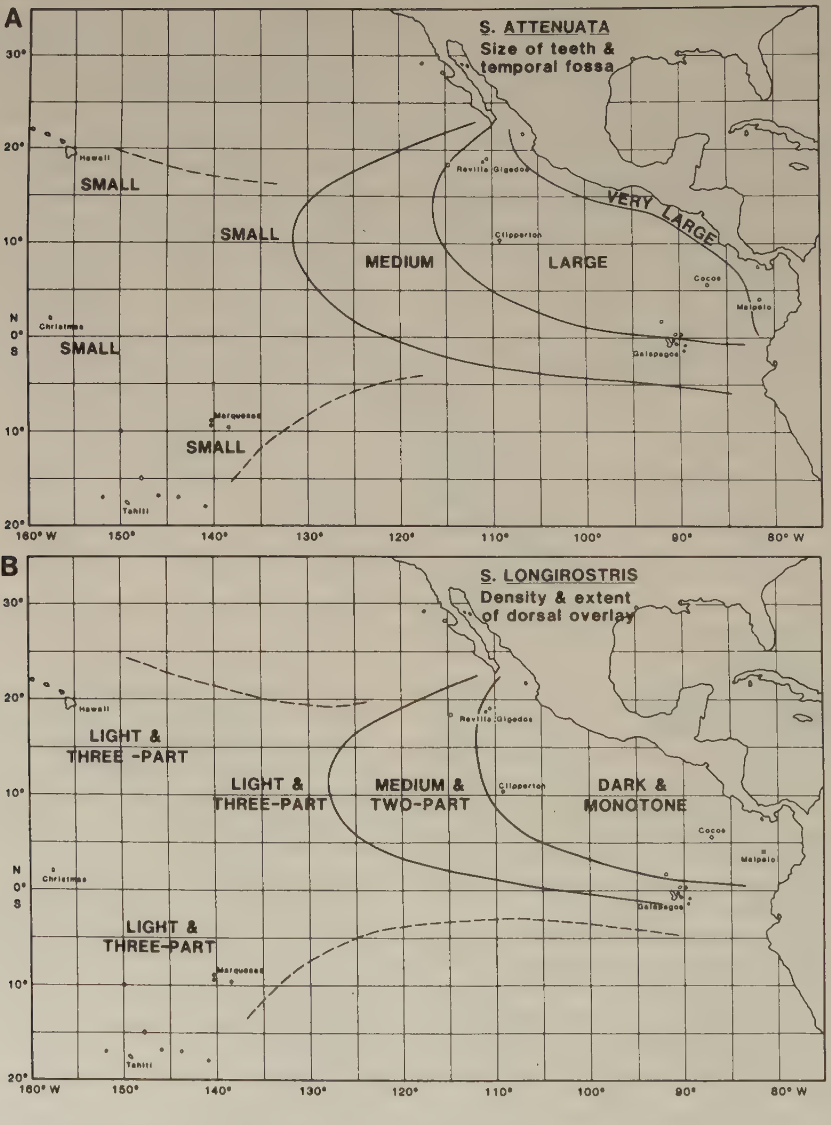
A
S. ATTENUATA
Size of teeth & temporal fossa
SMALL
SMALL
MEDIUM
LARGE
VERY LARGE
SMALL
SMALL
Hawaii
Revilla Gigedos
Clipperton
Cocos
Malpelo
Galapagos
Christmas
Marquesas
Tahiti
B
S. LONGIROSTRIS
Density & extent of dorsal overlay
LIGHT & THREE-PART
LIGHT & THREE-PART
MEDIUM & TWO-PART
DARK & MONOTONE
LIGHT & THREE-PART
Hawaii
Revilla Gigedos
Clipperton
Cocos
Malpelo
Galapagos
Christmas
Marquesas
Tahiti
30°
20°
10°
N
0°
S
10°
20°
160° W
150°
140°
130°
120°
110°
100°
90°
80° W

Figure 24.—Conceptual model of radial pattern of geographical variation in pelagic populations of *Stenella* A) *S. attenuata* and B) *S. longirostris* in the eastern tropical Pacific. Color pattern information from Perrin (1972a) and Perrin, Sloan, and Henderson (1979).

20°W) would thus comprise "hybrid" swarms. At least two storical scenarios can be suggested: differentiation during isolaon of populations in the far-eastern Pacific by cool-water comunication between the hemispheres during the glacial epoch (as s been suggested for the tropical Atlantic—Perrin et al. 1978), existence, now or in the past, of selection pressures in the far-stern Pacific sufficiently strong to give rise to differentiation thout isolation by a physical barrier. In either case, the present uation of pronounced polymorphism could be stable or could be namic, e.g., introgression of central Pacific genes from the west uld be neutralized by continuing strong selection pressures in e ecologically different eastern-Pacific, or the Indo-Pacific pool uld be in the process of swamping out the eastern-Pacific differtiation. Lacking historical data, this of course is only speculaon. Analysis of more osteological material from Polynesia may ed some light in relationships between animals there and those the outer reaches of the eastern tropical Pacific.

RECOMMENDATIONS

enella attenuata

1) Schools should not be identified as "coastal" or "offshore" the basis of position alone, because the ranges of the two forms erlap. Any school within 100 nmi of the coast for which size d degree of spotting of the animals is not determined should be egated to unidentified status. If a management boundary is set side 100 nmi to balance errors of identification based exclusive-on position, it should take into account relative school sizes for e two forms as well as relative abundance of schools, in order to ow what proportion of the population would be protected at rious distances from the coast.

2) The northern and southern samples are clearly morphologilly distinct. Although the spotted dolphins west of long. 120°W ow affinities with those south of the Equator, and though the st-west and north-south variation may be broadly rather than arply clinal, the present division of offshore populations into rthern and southern units should be retained pending study of aterial from west of long. 120°W, from the equatorial region, d from Hawaii. Consideration should also be given to seasonal d year-to-year variation in oceanographic regimes north and uth of the Equator and in the area between the two apparent nters of distribution.

enella longirostris

1) South of lat. 16°N, north of lat. 7°N, and within 50 nmi of coast, schools of spinner dolphins should be assigned to "Costa can" or "eastern" based on modal body length and relative beak gth. If this is not possible, they should be called unidentified nner.

2) Identification of spinner schools as "eastern" (or "Costa can") or (northern or southern) "whitebelly" should be based modal adult color pattern and modal dorsal-fin shape in adult les. Assessment and management of the two forms in the overping portions of their range should be an area-by-area basis ., 5° squares, as in Figure 18).

3) As in the case of the spotted dolphin, the division of whitely spinners into northern and southern management units uld be retained pending study of material from areas poorly resented in previous studies (near the Equator and in the far-stern area) and comparison of the age structures of the northern and southern samples. Osteological material from Hawaii should be analyzed to determine relationships with animals in the eastern tropical Pacific. Seasonal and year-to-year oceanographic variation should also be considered in future definition of units.

Stenella coeruleoalba

A single provisional division into northern and southern stocks is recommended (Fig. 25). This is based solely on a hiatus in distribution, and existing osteological material should be analyzed.

Delphinus delphis

1) Within 100 nmi of the Pacific coast of Baja California and in the Gulf of California, schools of common dolphins should be identified as "Baja neritic" or "northern" (temperate/tropical) based on modal length, coloration, and relative beak length. If these features are not observable, the school should be classified as unidentified common dolphin.

2) Division into northern, central, and southern units is recommended (in addition to the Baja neritic stock, which is contained within the northern range) (Fig. 26). As the central-southern division is based on distribution alone, material from the southern area should be collected and compared with existing material from the central area.

3) Delineation of a "Guerrero" unit of common dolphins off southern Mexico is marginally justified pending study of material from the area.

ACKNOWLEDGMENTS

Nearly all of the data and specimens analyzed here were collected by government-employed biologists and technicians aboard commercial tuna seiners. Individual cruises lasted as long as 5 mo, and there have been more than 800 cruises. The labors and dedication of these people and the cooperation and assistance by the owners, operators, and crews of the tuna boats made this study possible.

We thank the following for critical review of the manuscript and the useful suggestions for its improvement: J. G. Mead, K. S. Norris, F. G. Alverson, G. D. Schnell, D. W. K. Au, A. E. Dizon, G. T. Sakagawa, and I. Barrett.

LITERATURE CITED

ALVERSON, F. G

1981. Comments on the distribution of spotted, spinner, common and striped dolphin in the tropical Pacific Ocean. *In* P. S. Hammond (editor), Report on the Workshop on Tuna-Dolphin Interactions, Managua, Nicaragua, April 6-10, 1981. Inter-American Tropical Tuna Commission, La Jolla, CA, 259 p.

BANKS, R. C., and R. L. BROWNELL

1969. Taxonomy of the common dolphins of the eastern Pacific Ocean. J. Mammal. 50.262-271

BARLOW, J

1984. Reproductive seasonality in pelagic dolphins (*Stenella* spp.): implications in measuring rates. *In* W. F. Perrin, R. L. Brownell, Jr., and D. P. DeMaster (editors), Reproduction in whales, dolphins and porpoises. Rep. Int. Whaling Comm. (Spec. Issue 6), p. 191-198.

In press. Variability, trends and biases in reproductive rates of spotted dolphins (*Stenella attenuata*). Fish. Bull., U.S.

DOUGLAS, M. E., G. D. SCHNELL, and D. J. HOUGH.

1984. Differentiation between inshore and offshore spotted dolphins in the eastern tropical Pacific Ocean. J. Mammal. 65:375-387.

EVANS, W. E

1975. Distribution, differentiation of populations, and other aspects of the

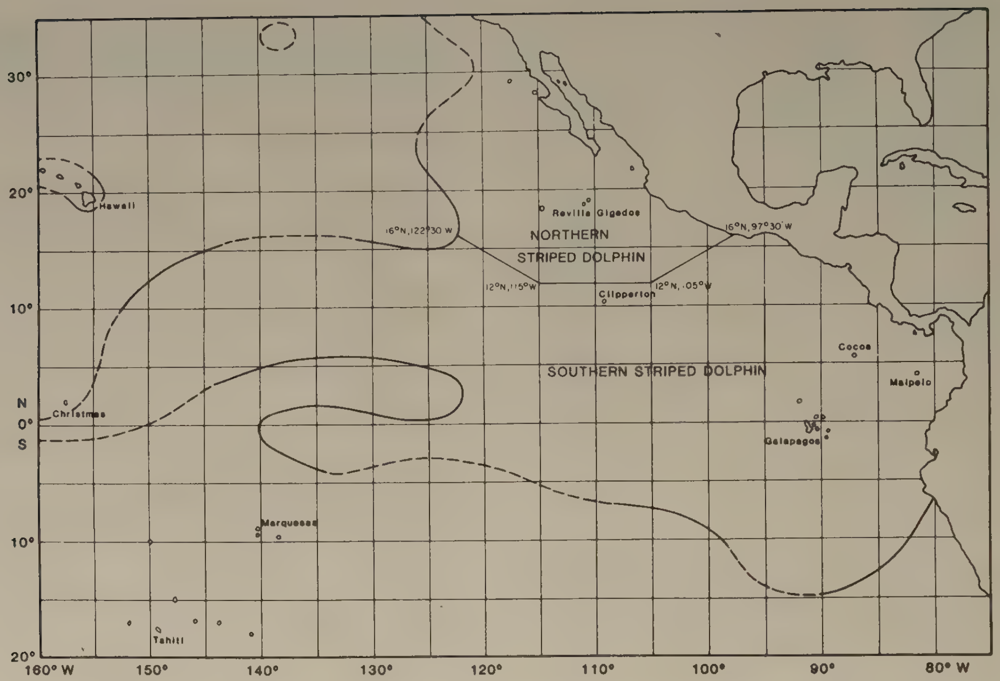
30°
20°
10°
N
0°
S
10°
20°
160° W
150°
140°
130°
120°
110°
100°
90°
80° W
Hawaii
Christmas
Marquesas
Tahiti
Revilla Gigedos
16°N,122°30 W
16°N,97°30'W
NORTHERN STRIPED DOLPHIN
12°N,115°W
12°N,105°W
Clipperton
SOUTHERN STRIPED DOLPHIN
Cocos
Malpelo
Galapagos

Figure 25.—Recommended management units for *Stenella coeruleoalba*.

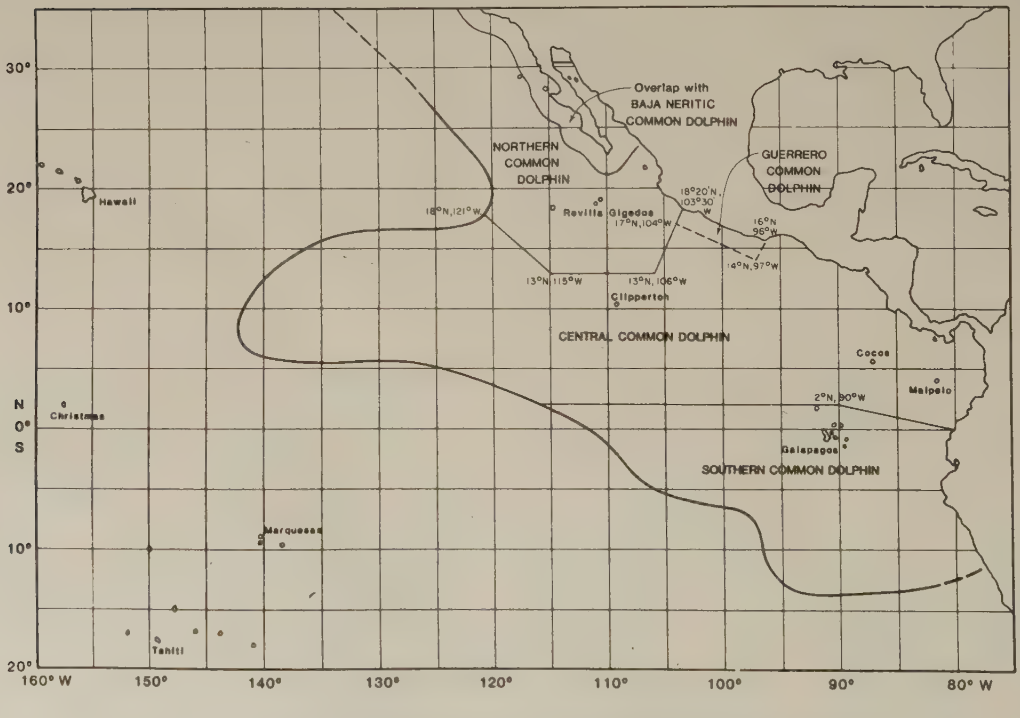
30°
20°
10°
N
0°
S
10°
20°
160° W
150°
140°
130°
120°
110°
100°
90°
80° W
Hawaii
Christmas
Marquesas
Tahiti
Overlap with BAJA NERITIC COMMON DOLPHIN
NORTHERN COMMON DOLPHIN
GUERRERO COMMON DOLPHIN
18°N,121°W
Revilla Gigedos
18°20'N, 103°30' W
17°N,104°W
16°N 96°W
14°N,97°W
13°N,115°W
13°N,106°W
Clipperton
CENTRAL COMMON DOLPHIN
Cocos
Malpelo
2°N,90°W
Galapagos
SOUTHERN COMMON DOLPHIN

Figure 26.—Recommended management units for *Delphinus delphis* in the eastern tropical Pacific.

natural history of *Delphinus delphis* Linnaeus in the northeastern Pacific. Ph.D. Thesis, Univ. California, Los Angeles, 145 p.

1982. Distribution and differentiation of stock of *Delphinus delphis* Linnaeus in the northeastern Pacific. *In* Mammals in the seas, Vol. IV, p. 45-66. FAO, Rome.

HESTER, F. J., J. R. HUNTER, and R. R. WHITNEY.

1963. Jumping and spinning behavior in the spinner porpoise. J. Mammal. 44:586-588.

HOLT, R. S., and J. E. POWERS.

1982. Abundance estimation of dolphin stocks involved in the eastern tropical Pacific yellowfin tuna fishery determined from aerial and ship surveys to 1979. NOAA Tech. Memo. NMFS-SWFC-23, 95 p.

LEATHERWOOD, S., R. R. REEVES, W. F. PERRIN, and W. E. EVANS.

1982. Whales, dolphins, and porpoises of the eastern North Pacific and adjacent Arctic waters. U.S. Dep. Commer., NOAA Tech. Rep. NMFS Circ. 444, 245 p.

MORRIS, R. A., and L. S. MOWBRAY.

1966. An unusual barnacle attachment on the teeth of the Hawaiian spinner dolphin. Norsk Hvalfangst-tidende 55:15-16.

NORRIS, K. S., and T. P. DOHL.

1980. Behavior of the Hawaiian spinner dolphin, *Stenella longisrostris*. Fish. Bull., U.S. 77:821-849.

PERRIN, W. F.

1972a. Color patterns of spinner porpoises (*Stenella* cf. *S. longirostris*) of the eastern Pacific and Hawaii, with comments on delphinid pigmentation. Fish. Bull., U.S. 70:983-1003.

1972b. Variation and taxonomy of spotted and spinner porpoises (genus *Stenella*) of the eastern tropical Pacific and Hawaii. Ph.D. Thesis, Univ. California, Los Angeles, 490 p.

1975a. Variation of spotted and spinner porpoise (genus *Stenella*) in the eastern Pacific and Hawaii. Bull. Scripps Inst. Oceanogr. 21, 206 p.

1975b. Distribution and differentiation of populations of dolphins of the genus *Stenella* in the eastern tropical Pacific. J. Fish. Res. Board Can. 32:1059-1067.

In press. Patterns of variation in small cetaceans. Acta Zool. Fennica.

ERRIN, W. F., J. M. COE, and J. R. ZWEIFEL.

1976. Growth and reproduction of the spotted porpoise, *Stenella attenuata*, in the offshore eastern tropical Pacific. Fish. Bull., U.S. 74:229-269.

ERRIN, W. F., W. E. EVANS, and D. B. HOLTS.

1979. Movements of pelagic dolphins (*Stenella* spp.) in the eastern tropical Pacific as indicated by results of tagging, with summary of tagging operations, 1969-76. U.S. Dep. Commer., NOAA Tech. Rep. NMFS SSRF-737, 14 p.

PERRIN, W. F., E. D. MITCHELL, and P. J. H. van BREE.

1978. Historical zoogeography of tropical pelagic dolphins. [Abstr.] II. Congr. Theriol. Int., Brno, Czechoslovakia, June 20-27, 1978, p. 73.

PERRIN W. F., and C. W. OLIVER.

1982. Time/area distribution and composition of the incidental kill of dolphins and small whales in the U.S. purse-seine fishery for tuna in the eastern tropical Pacific, 1979-80. Rep. Int. Whaling Comm. 32:429-444.

PERRIN, W. F., M. D. SCOTT, G. J. WALKER, F. M. RALSTON, and D. W. K. AU.

1983. Distribution of four dolphins (*Stenella* spp. and *Delphinus delphis*) in the eastern tropical Pacific, with an annotated catalog of data sources. NOAA Tech. Memo. NMFS-SWFC-38, 65 p.

PERRIN, W. F., P. A. SLOAN, and J. R. HENDERSON.

1979. Taxonomic status of the 'south-western stocks of spinner dolphin *Stenella longirostris* and spotted dolphin *S. attenuata*.' Rep. Int. Whaling Comm. 29:175-184.

PERRIN, W. F., T. D. SMITH, and G. T. SAKAGAWA.

1982. Status of populations of spotted dolphin, *Stenella attenuata*, and spinner dolphin, *S. longirostris*, in the eastern tropical Pacific. *In* Mammals in the seas. Vol. IV, p. 67-83. FAO, Rome.

PERRIN, W. F., R. R. WARNER, C. H. FISCUS, and D. B. HOLTS.

1973. Stomach contents of porpoise, *Stenella* spp., and yellowfin tuna, *Thunnus albacares*, in mixed-species aggregations. Fish. Bull., U.S. 71: 1077-1092.

SCOTT, M. D.

1981. Dolphin stocks in the eastern tropical Pacific. *In* P.S. Hammond (editor), Report on the Workshop on Tuna-Dolphin Interactions, Managua, Nicaragua, April 6-10, 1981. Inter-American Tropical Tuna Commission, La Jolla, CA, 259 p.

SMITH, T. D.

1983. Changes in size of three dolphin (*Stenella* spp.) populations in the eastern tropical Pacific. Fish. Bull., U.S. 81:1-13.

van BREE, P. J. H., and P. E. PURVES.

1972. Remarks on the validity of *Delphinus bairdii* (Cetacea, Delphinidae). J. Mammal. 53:372-374.

WHITE, M. J., Jr., J. G. JENNINGS, W. F. GANDY, and L. H. CORNELL.

1981. An evolution of tagging, marking, and tattooing techniques for small delphinids. NOAA Tech. Memo. NMFS-SWFC-16, 142 p.

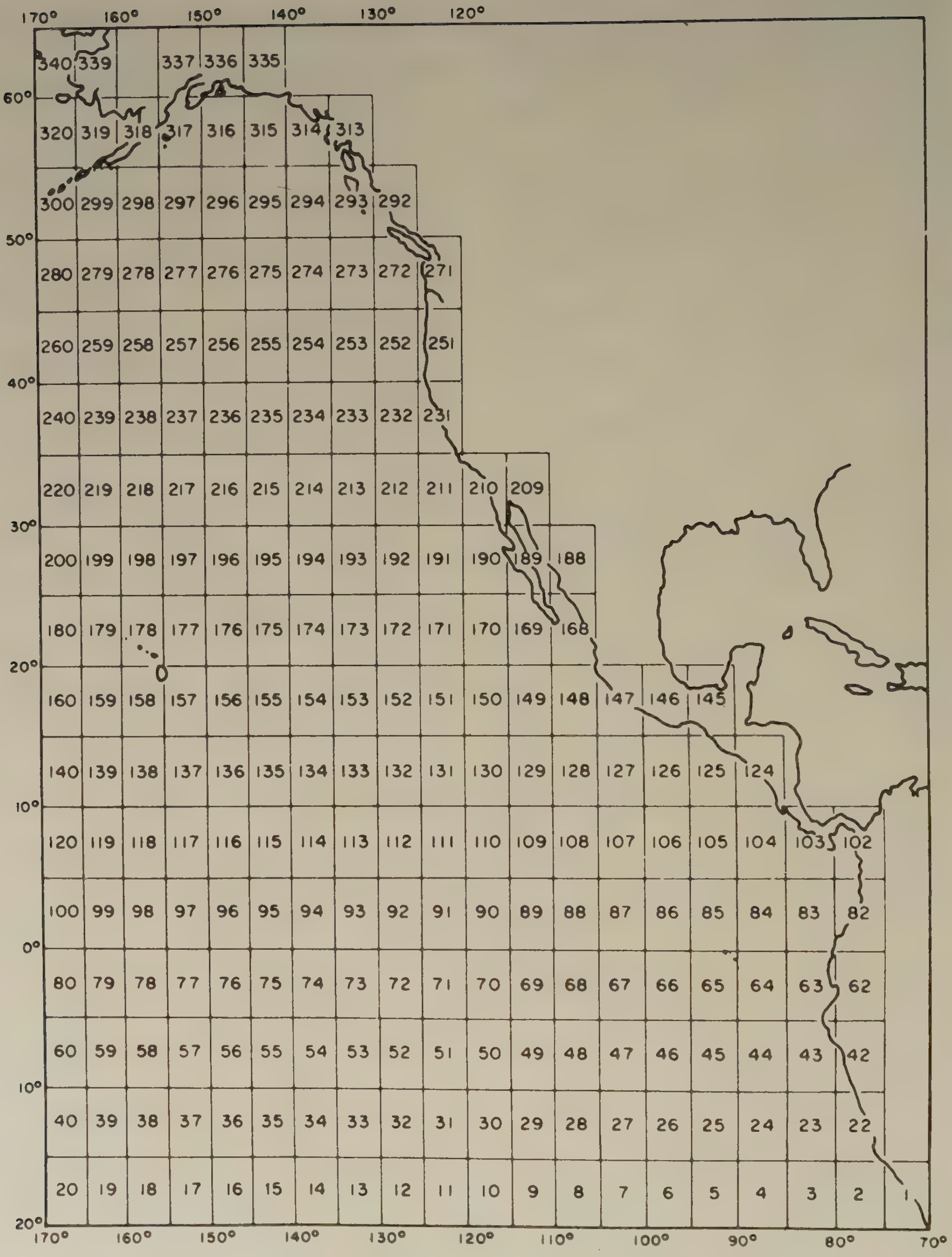

170°
160°
150°
140°
130°
120°
60°
50°
40°
30°
20°
10°
0°
10°
20°
170°
160°
150°
140°
130°
120°
110°
100°
90°
80°
70°
340 339 337 336 335
320 319 318 317 316 315 314 313
300 299 298 297 296 295 294 293 292
280 279 278 277 276 275 274 273 272 271
260 259 258 257 256 255 254 253 252 251
240 239 238 237 236 235 234 233 232 231
220 219 218 217 216 215 214 213 212 211 210 209
200 199 198 197 196 195 194 193 192 191 190 189 188
180 179 178 177 176 175 174 173 172 171 170 169 168
160 159 158 157 156 155 154 153 152 151 150 149 148 147 146 145
140 139 138 137 136 135 134 133 132 131 130 129 128 127 126 125 124
120 119 118 117 116 115 114 113 112 111 110 109 108 107 106 105 104 103 102
100 99 98 97 96 95 94 93 92 91 90 89 88 87 86 85 84 83 82
80 79 78 77 76 75 74 73 72 71 70 69 68 67 66 65 64 63 62
60 59 58 57 56 55 54 53 52 51 50 49 48 47 46 45 44 43 42
40 39 38 37 36 35 34 33 32 31 30 29 28 27 26 25 24 23 22
20 19 18 17 16 15 14 13 12 11 10 9 8 7 6 5 4 3 2 1

Appendix 1.—Statistical reporting blocks (5°) for eastern tropical Pacific.

Appendix 2.—Stock composition of records of *Stenella longirostris* by 5° block (see Appendix 1 for locations).

Block no.	Costa Rican		Eastern		Whitebelly		Total identified	Unidentified		Total
	No.	% of ID'ed	No.	% of ID'ed	No.	% of ID'ed		No.	% of total	
3	0	—	0	—	1	100	1	0	—	1
23	0	—	0	—	26	100	26	1	4	27
24	0	—	3	7	37	92	40	2	5	42
25	0	—	0	—	16	100	16	0	—	16
26	0	—	0	—	4	100	4	0	—	4
43	0	—	0	—	13	100	13	5	28	18
44	0	—	4	2	167	98	171	16	9	187
45	0	—	0	—	97	100	97	5	5	102
46	0	—	0	—	31	100	31	1	3	32
47	0	—	0	—	1	100	1	0	—	1
48	0	—	0	—	1	100	1	0	—	1
54	0	—	0	—	2	100	2	1	33	3
55	0	—	0	—	1	100	1	10	90	11
63	0	—	1	3	29	98	30	29	49	59
64	0	—	3	7	41	93	44	13	23	57
65	0	—	0	—	102	100	102	22	18	124
66	0	—	0	—	32	100	32	6	16	38
67	0	—	0	—	57	100	57	6	10	63
68	0	—	0	—	21	100	21	1	5	22
69	0	—	0	—	13	100	13	0	—	13
70	0	—	0	—	9	100	9	0	—	9
71	0	—	0	—	1	100	1	0	—	1
72	0	—	0	—	1	100	1	0	—	1
73	0	—	0	—	2	100	2	0	—	2
82	0	—	1	13	7	87	8	2	20	10
83	0	—	18	37	31	63	49	37	43	86
84	0	—	24	26	67	74	91	49	35	140
85	0	—	15	8	183	92	198	55	22	253
86	0	—	9	5	162	95	171	31	15	202
87	0	—	22	12	155	88	177	24	12	201
88	0	—	17	5	310	95	327	23	7	350
89	0	—	2	2	131	98	133	13	9	146
90	0	—	4	5	82	95	86	17	17	103
91	0	—	0	—	70	100	70	4	5	74
92	0	—	0	—	29	100	29	2	6	31
93	0	—	0	—	2	100	2	2	50	4
102	0	—	6	67	3	33	9	14	61	23
103	9	6	75	56	49	37	133	82	38	215
104	2	2	60	51	55	47	117	80	41	197
105	0	—	51	47	57	53	108	70	39	178
106	0	—	236	70	99	30	335	164	33	499
107	0	—	220	61	142	39	362	167	32	529
108	0	—	169	43	220	57	389	172	31	561
109	0	—	42	31	95	69	137	46	25	183
110	0	—	25	24	81	76	106	34	24	140
111	0	—	26	10	233	90	259	62	19	321
112	0	—	21	5	378	95	399	57	13	456
113	0	—	12	3	345	97	357	57	14	414
114	0	—	8	3	294	97	302	28	9	330
115	0	—	1	1	81	99	82	7	8	89
116	0	—	0	—	1	100	1	0	—	1
117	0	—	0	—	2	100	2	0	—	2
124	3	9	25	74	6	17	34	36	51	70
125	0	—	653	92	54	7	707	494	41	1,201
126	0	—	789	91	74	9	863	294	25	1,157
127	0	—	664	93	53	7	717	190	21	907
128	0	—	932	88	132	12	1,064	297	22	1,361
129	0	—	481	86	78	14	559	132	19	691
130	0	—	229	76	74	24	303	88	23	391
131	0	—	70	35	129	65	199	58	23	257
132	0	—	60	16	312	84	372	73	16	445
133	0	—	27	8	306	92	333	55	14	388
134	0	—	6	6	101	94	107	6	6	113

Appendix 2.— *Continued.*

	Costa Rican		Eastern		Whitebelly		Total	Unidentified		
Block no.	No.	% of ID'ed	No.	% of ID'ed	No.	% of ID'ed	identified	No.	% of total	Total
135	0	—	0	—	23	100	23	4	15	27
136	0	—	0	—	5	100	5	1	17	6
137	0	—	0	—	1	100	1	0	—	1
138	0	—	0	—	2	100	2	0	—	2
145	0	—	0	—	1	100	1	3	75	4
146	0	—	65	94	4	6	69	44	39	113
147	0	—	203	96	8	4	211	132	38	343
148	0	—	86	90	10	10	96	45	32	141
149	0	—	192	93	15	7	207	104	33	311
150	0	—	97	89	12	11	109	46	30	155
151	0	—	4	67	2	33	6	2	45	8
152	0	—	1	17	5	83	6	3	33	9
153	0	—	0	—	9	100	9	0	—	9
168	0	—	0	—	5	8	5	46	44	51
169	0	—	0	—	6	30	6	9	31	15
Total	14	0.1	5,659	50.7	5,496	49.3	11,169	3,579	24.1	14,748

8570

Chapter 21

Magnetoreception and Biomineralization of Magnetite in Amphibians and Reptiles

ANJANETTE PERRY, GORDON B. BAUER,
and ANDREW E. DIZON

1. Introduction . . . 439
2. Amphibians . . . 440
3. Reptiles . . . 443
   3.1. Magnetoreception in Sea Turtles . . . 443
   3.2. Isolation and Identification of Magnetite in Sea Turtles . . . 447
4. Conclusion . . . 452
   References . . . 452

1. Introduction

Many amphibians and reptiles are seasonally migratory, traveling to and from suitable breeding, feeding, or hibernation grounds. These creatures also carry out small-scale directed movements in local areas. As juveniles, they must locate appropriate areas for growth and maturation, often in environments vastly different from those into which they hatched. Thus, soon after hatching, sea turtles scrabble up through the sand and find their way down the beach to the ocean, while tadpoles, after spending several weeks in an aquatic environment, metamorphose into frogs and climb out of their ponds onto dry land. As adults, the amphibians and reptiles slither, stalk, or swim about in search of food and shelter and to escape predators.

The distances covered by amphibians and reptiles in all of these movements are, with notable exceptions, not of great extent, and in most cases the use of sight, smell, hearing, and touch are probably sufficient for direction finding. In order to orient in familiar areas while engaged in foraging, escaping from predators, or other routine movements, these animals probably depend upon reference to learned landmarks, routes, and features of topography (Ferguson, 1971). The occasional longer foray into unfamiliar territory, unusual weather or other adverse environmental conditions, and ontogenetic and seasonal migrations may, on the other hand, require the use of a host of sensory capabilities. Studies have shown that amphibians and reptiles can call on multiple sensory bases for direction

---

ANJANETTE PERRY • Department of Oceanography, University of Hawaii, Honolulu, Hawaii 96822. GORDON B. BAUER • Department of Psychology, University of Hawaii, Honolulu, Hawaii 96822. ANDREW E. DIZON • Southwest Fisheries Center La Jolla Laboratory, National Marine Fisheries Service, National Oceanic and Atmospheric Administration, California 92038.

finding (reviewed in Adler, 1982), and are capable of employing alternative cues and sensory mechanisms when circumstances dictate or when denied use of a normally functional sense.

The use of magnetic information for orientation has been demonstrated in other vertebrates, including homing pigeons (Keeton, 1971), salmon (Quinn, 1980), elasmobranchs (Kalmijn, 1978), eels (Tesch, 1974), and woodmice (Mather and Baker, 1981). Only preliminary studies, however, have looked specifically at magnetic sensitivity as a component of amphibian and reptile orientation. Magnetic cues could be of particular importance to amphibians and reptiles in environments where visual cues are limited, as is the case for two of the animals discussed below, the cave-dwelling salamander and the marine turtle.

2. Amphibians

Amphibian movements are generally restricted to distances less than a few kilometers. Within their limited range, seasonal migrations and movements around local areas are well oriented (Schmidt-Koenig, 1975), and, in displacement studies, amphibians have exhibited remarkable homing abilities. In one of many such experiments designed to examine amphibian orientation, Twitty *et al.* (1967) displaced red-bellied newts up to 8 km away from their native stream segment, either to other segments of the same stream or across a ridge to some foreign stream. Over 60% of the displaced newts were able to find their way back to their home stream segment, usually in the next breeding season. To account for such homing accuracy among amphibians, researchers have investigated the use of olfaction, vision, extraoptic receptors, and sun and celestial compasses, but have rarely questioned whether magnetoreception may also be involved.

Phillips (1977) provided evidence for a learned directional response to earth-strength magnetic fields in the cave salamander, *Eurycea lucifuga*. His objective was to determine if animals trained to move through passageways under specific magnetic field conditions would, when tested, use the learned magnetic information as an orientation cue. For training, he confined two groups of 15 salamanders each in two separate training corridors. Each corridor consisted of two compartments filled with pieces of limestone, connected by a darkened central passageway. Moisture was supplied alternately to one of the two end compartments, forcing the animals to move at intervals from one compartment to the other through the passageway. The two corridors were aligned along the same topographical axis, parallel to the earth's N–S magnetic field, with one, the "a" corridor, enclosed in a coil which rotated the magnetic field 90° clockwise, and the other, the "b" corridor, in the normal field. Movement of the A group was therefore perpendicular to the magnetic N–S axis, while that of the B group was parallel to the earth's field. For testing, the two groups were released simultaneously into the center of a cross-shaped assembly made up of the two training corridors connected perpendicularly to one another. Animals were released into the center of the testing assembly, and after 40 min the location of each salamander was recorded. Animals were tested in both the natural and the altered magnetic field, and with the cross assembly positioned with either the "a" or the "b" corridor parallel to the topographical axis along which both were aligned in training.

In 6 of 16 tests there was a significant difference between the groups in their choice of corridors, with the difference resulting from the groups moving in the direction predicted from training, that is, perpendicular to the N–S magnetic axis for the A group and parallel to the N–S magnetic axis for the B group (Fig. 1). In these cases the animals' distribution shifted in the manner predicted by the orientation of the magnetic field only. Although a directional response to magnetic fields was clear in these six tests, in the majority of tests the distribution of the two groups was not significantly different. Phillips believes this

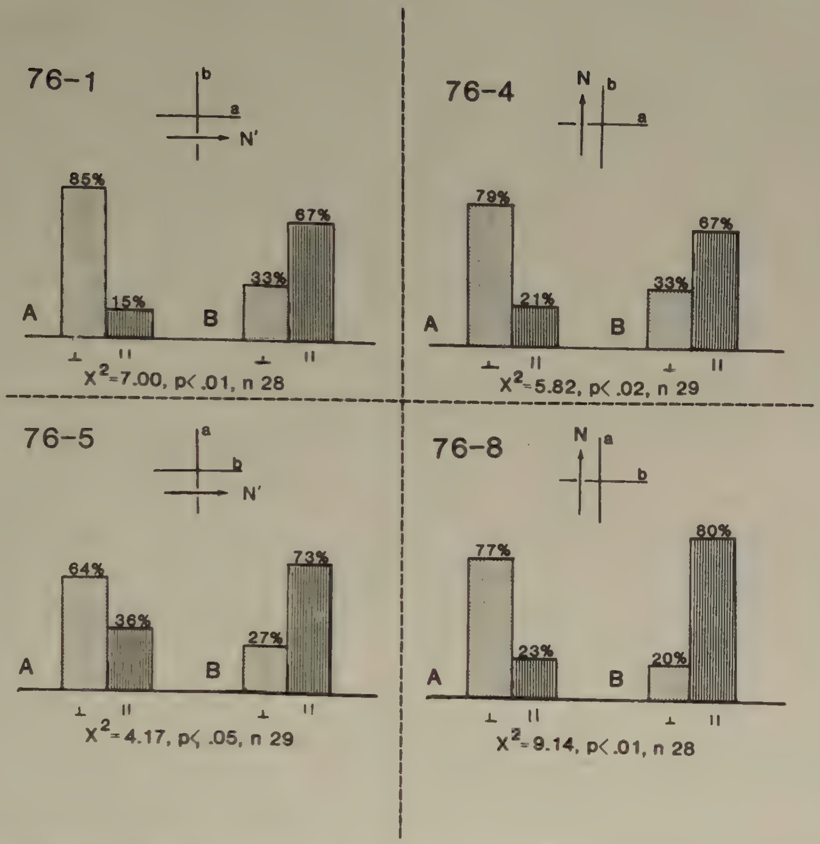

Figure 1. Results of tests with salamander groups A and B, previously trained in corridors a and b, respectively. These tests represent the four possible combinations (insets) of the expected magnetic directions relative to the home corridors and the topographical axis. The histograms show the percentage of each group of animals which moved perpendicular and parallel to the natural or altered field. For example, in test 76-1, animals in group A, which were originally trained to move perpendicularly to the magnetic field, do so preferentially (85%) even though the corridor perpendicular to the magnetic axis (b) is not their home corridor; this preferred movement also coincides with the topographical axis (represented by the vertical axis in each inset). For statistical purposes, the combined number of A- and B-group animals which moved along the expected axis is tested (chi-square, one-tailed, one degree of freedom) against the null hypothesis of a 50:50 distribution of both groups along the two perpendicular axes. From Phillips (1977).

discrepancy may have been due to different factors for each group. The A group may have been influenced by familiar vibrations, as the tests were carried out in the location where this group had been trained. Natural disturbance in the earth's magnetic field appeared to affect the B group's performance, with increased deterioration in performance correlated with the magnitude of disturbance.

Related experiments were carried out by Phillips and Adler (1978) with eastern red-spotted newts (*Notophthalmus viridescens*), to determine if newts exhibit a locomotor or positional response when placed in a magnetic gradient. Newts were individually tested by placing them in aquaria oriented along the earth's N–S magnetic axis. As in Phillips's

Table I. Mean Positions of Newts under Three Magnetic Conditions[a]

Test sequence	Date	A	B	C	D	E	F	Test mean
Mag-0 tests								
1	July 14	N 18.47	N 22.07	*N 22.10*	N 12.12	N 15.85	N 0.84	N 15.21
4	July 18	N 9.02	S 4.75	*N 1.17*	*N 18.87*	S 2.54	1.27	N 3.43
7	July 21	N 10.43	N 18.77	*excluded*	*excluded*	N 9.22	*excluded*	N 12.78
10	July 27	N 23.06	*S 24.40*	*N 13.46*	S 22.23	*S 20.19*	N 1.35	S 4.83
Mag-N tests								
2	July 15	S 0.43	N 8.46	*N 17.04*	N 9.07	N 0.97	N 5.08	N 6.68
5	July 19	N 1.45	N 15.75	S 13.72	*S 2.06*	*S 13.54*	N 1.14	S 4.45
8	July 22	N 6.02	S 11.18	N 0.18	S 13.64	*N 13.49*	*N 5.97*	N 0.15
11	July 29	N 2.79	*S 22.10*	*S 6.02*	S 23.70	S 3.18	N 17.70	S 5.74
Mag-S tests								
3	July 16	N 23.55	N 4.75	*excluded*	N 16.08	N 11.35	N 15.06	N 14.15
6	July 20	N 6.81	N 18.47	S 3.56	S 9.96	N 16.69	*N 5.46*	N 5.66
9	July 25	N 15.32	S 18.47	*excluded*	S 12.19	*N 23.29*	S 0.28	N 1.52
12	August 1	X	X	N 13.84	*excluded*	*excluded*	S 8.89	N 2.49

[a] Six newts (animals A–F) were tested in the sequence noted, with the bar magnet absent (Mag-0) or present at the north (Mag-N) or south (Mag-S) end of the tank corridor. Individual means are corrected to exclude positions when newts climbed on the tank wall and the mean is excluded altogether if the number of data points is less than 10. Climbing animals, i.e., those climbing on the tank walls 10 or more times during a given test, are indicated by italics. Mean values are given in centimeters, north (N) or south (S) of the center of the tank where each animal was released. Animals A and B died of unknown causes on August 1. From Phillips and Adler (1978).

salamander experiments, light was kept dim and diffuse to avoid influencing the response. Newts were exposed to three magnetic conditions: (1) the natural magnetic field, (2) magnetic north tests (Mag-N) in which a bar magnet was placed horizontally 5 cm beyond the north end of the tank, and (3) magnetic south tests (Mag-S) in which the magnet was placed an equal distance from the tank's south end. Newts were observed for a 90-min period under each condition, and their position, as well as whether they were on the floor or climbing the walls, was noted. From comparison of the mean floor positions of six animals (Table I), and of the positions on the wall of climbing animals relative to the placements of the bar magnet, the authors concluded that newts are capable of perceiving magnetic cues and prefer positions where the field strength and inclination approximate ambient values.

The apparent existence of magnetic sensitivity in newts and cave salamanders suggests that the capability may be present in salamanders generally (Phillips and Adler, 1978). The two salamanders studied belong to markedly different habitats, thus their magnetic sensitivity probably did not evolve simply in response to specific environmental constraints, such as cave dwelling. While the terrestrial cave salamanders probably perceive the magnetic field directly, the newts, like other aquatic vertebrates, could indirectly perceive the field through electric induction. The two species studied thus far, however, are phylogenetically related rather closely, and it is likely that they share a common type of magnetoreceptor, possibly involving magnetite.

At this time, the two papers discussed above comprise the published research on magnetic sensitivity in amphibians. Many questions still remain to be answered. Are other amphibians sensitive to magnetic fields? How is such sensitivity used in orientation? Is magnetic perception in amphibians magnetite-mediated, or is some other sensory mechanism responsible? Studies under the direction of Dr. J. B. Phillips and Dr. K. Adler are currently in progress to examine magnetoreception in amphibians in greater detail.

3. Reptiles

Most reptile movements are confined within small-scale natural boundaries, such as the shores of a pond for aquatic turtles, or to a few kilometers of desert or forest terrain for the terrestrial snakes, lizards, and turtles. Only the sea snakes, the saltwater crocodile, and the marine turtles travel across long distances.

Little is known about the migratory patterns and mechanisms of the sea snakes (Dunson, 1975) or the crocodile (Minton and Minton, 1973). Sea snakes are without well-defined musculature, and are not capable of vigorous or prolonged swimming. It appears that these snakes are almost planktonic and drift passively with the currents, sometimes over hundreds or thousands of kilometers when they are caught up in the major ocean gyres. The crocodiles may be more adept at charting a course than the snakes, but their movements are almost wholly unresearched. Of course, long-distance migration is not a prerequisite for magnetic sensitivity in reptiles. Nonmigratory snakes, alligators, crocodiles, lizards, and turtles may use a magnetic sense for short-range orientation, but studies have not yet been conducted to test this hypothesis.

Among the reptiles, the best-researched long-distance migrant is the green turtle, *Chelonia mydas*. Green turtles can accurately navigate in open ocean waters over distances up to a few thousands of kilometers. Tagged individuals from populations throughout the world have been shown to migrate from coastal feeding pastures to far-removed breeding and nesting grounds on remote island beaches, returning to the same nesting sites repeatedly (Carr and Carr, 1970; Pritchard, 1973; Balazs, 1976). Hirth (1971) has suggested that green turtles employ a multiplicity of cues and several senses, possibly including magnetoreception, for navigation. Magnetic cues available to the turtles include the geomagnetic field's intensity, polarity, and inclination. Sea turtles could also use magnetic anomalies such as the striped pattern on the ocean bottom that is a result of continuous seafloor spreading during epochs of normal and reversed magnetic field direction, and volcanic islands and seamounts that are sites of magnetic anomaly due to the high iron content of the basaltic lavas that formed them.

A small amount of pilot work with green turtles and another of the migratory sea turtles, the loggerhead *Caretta caretta*, has produced some results which could be supportive of a magnetic sensitivity in these species.

3.1. Magnetoreception in Sea Turtles

Baldwin (1972) compared the headings in the wild of four radio-equipped green turtles that had magnets attached to their plastrons with their headings when equipped with nonmagnetic brass bars. On clear days or in shallow water, no differences in headings before and after magnet placement were apparent. However, the heading of one turtle tested in deep water under overcast conditions suggested that where the bottom is not visible, sensing of the magnetic field could be important in turtle orientation. Further experiments with the remaining turtles were hampered by difficulties with weather and with the radio-tracking equipment, and to our knowledge these experiments have not been repeated.

We have conducted preliminary learning experiments to test for magnetoreception in sea turtles. All our experiments were carried out at the National Marine Fisheries Service Laboratory in Honolulu, Hawaii. We first tested the ability of two 1-year-old green turtles to discriminate between normal and altered magnetic field conditions (Pèrry, 1982). The turtles were tested for magnetic sensitivity using a discrete-trials/fixed-interval conditioning technique (Woodward and Bitterman, 1974). Experiments were conducted in a 6-m-diameter, circular, nonmagnetic pool that was wrapped with a Helmholtz coil constructed of 100 turns of magnet wire. A 1-A dc current through the coil added a vertical field of from 0.30 G at tank center to 0.50 G along the periphery to the Hawaiian magnetic field of about 0.35 G. The turtles were trained to repeatedly press a paddle presented at tank edge. At the end of 30-sec trial periods, they were rewarded with a small piece of fish. The paddle was manually lowered into the tank at the beginning of each trial by the experimenter, who was stationed behind a screen. A bar attached perpendicularly to the paddle handle enabled the experimenter to lower the paddle while remaining out of the turtle's view. A microswitch attached to the back of the paddle and connected to an automatic counter recorded the number of presses per trial.

For discrimination testing, the turtles were rewarded for pressing the paddle only during stimulus-present (S^+) trials. One turtle (turtle A) was rewarded for paddle presses in the altered magnetic field, the other (turtle B) for presses in the normal field. Each trial began after a random interval of 20–60 sec with simultaneous presentation of the paddle and the altered or normal magnetic field. For S^+ trials, the first paddle press after 30 sec had elapsed resulted in reward presentation and paddle removal. During stimulus-absent (S^-) trials, presses during the 30-sec period earned nothing and, as punishment, the paddle was not removed for another 20 sec, thus delaying the start of a new trial. Paddle presses during this punishment period resulted in subsequent 20-sec delays in paddle removal, up to 60 sec total. S^+ and S^- trials were presented in quasi-random order, with no more than three trials of one type in a row. Each day's session consisted of 20 S^+ and 20 S^- trials.

After the first 3 days of discrimination testing, turtle A's response rate during the S^+ condition was significantly greater than during S^- trials for 5 days (200 trials), using a *t*-test for paired comparisons ($t_4 = 6.4$, $p < 0.01$). In later trials, however, correct responding by turtle A did not exceed 50%, and the experiment was halted (Fig. 2a). Although there were no changes in the experimental setup for trials with turtle B, except to reverse the rewarded and unrewarded conditions, turtle B never showed the ability to discriminate between the two field conditions (Fig. 2b).

We also conducted learning experiments with an adult male loggerhead turtle of approximately 20–25 years of age. The experiments were conducted in one arm of a U-shaped concrete tank. A free operant conditioning format was used in which the subject was reinforced for pressing a paddle in the presence of a magnetic stimulus and was not reinforced for pressing in the absence of the stimulus. A buzzer (secondary reinforcer) followed by a fish (primary reinforcer) was delivered after every correct paddle press, i.e., a continuous reinforcement (CRF) schedule was employed. Presentation of magnetic stimuli and recording of data were fully automated; food was delivered by an experimenter blind to the stimulus condition. There were no adversive experimental contingencies for incorrect responding. S^+ and S^- trials were counterbalanced over groups of 30 trials for experiment I and of 12 trials for experiment II. It should be noted that the S^- condition was not equivalent to the normal Hawaiian magnetic intensity of about 0.35 G. Steel reinforcing bars in the walls of the tank distorted the inclination and reduced the intensity to 0.27 G at the experimental paddle.

In experiment I a small Helmholtz coil was placed perpendicularly to the N–S axis of the experimental tank. This generated a graded field which amplified the horizontal component of the ambient field and produced an overall intensity of 0.77 G at the point of response, the paddle. Dc current was used to reduce acoustic artifacts, as ac generates a 60-cycle hum.

As in the green turtle trials, the results from this experiment were somewhat ambiguous. Approximately 540, 30-sec trials were run over 6 days before performance stabilized at 50% correct response. Over the following 4 days of trials (90 trials a day), performance exceeded 50% on 3 of 4 days (range 48–54%). There was some indication of a deterioration in performance at the end of each session, perhaps due to reduced motivation. If the last

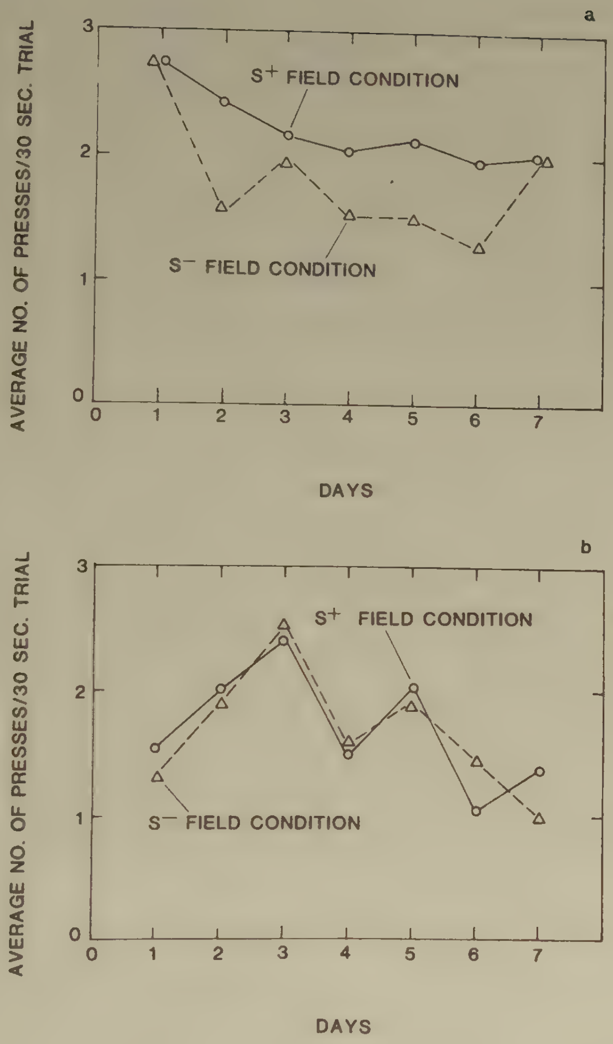

Figure 2. Daily averaged rate of paddle presses by turtle A (a) and turtle B (b) after the first 3 days of discrimination testing.

30 trials for each session are dropped from consideration, the subject exceeded 50% on all 4 days (range 51–60%). Data considered over counterbalanced groups of 30 trials (15 S^+ and 15 S^- trials) indicated a significant difference using a t-test for paired comparisons ($t_7 = 2.67$, $p < 0.05$).

In experiment II the same free operant procedure was used, but the coil was suspended horizontally above the subject. A field was generated which added to the vertical component of the ambient field and produced an intensity of 0.58 G at the point of response. Because of the turtle's relative stability in the horizontal plane, we felt that a vertical field alteration would present the subject with a more stable stimulus as it moved within the experimental area. Performance over 266 discrimination trials, however, remained at approximately 50%. In other words, the turtle was responding equally in S^+ and S^- conditions, i.e., at chance levels.

Although there were differences in inclination and intensity between the two loggerhead experiments, and between the loggerhead and green turtle experiments, methodological deficiencies preclude any intelligent discussion of differences in our results based on these factors. The results of the experiments were equivocal from several standpoints:

1. The slow consummatory response of the loggerhead deprived it of response time during the S^+ period, possibly artificially depressing discriminative performance.
2. A free operant procedure, especially using a CRF, allows the subject to track reinforcement, i.e., the act of rewarding a response increases the probability of another response no matter what the state of the discrimination stimulus. In other words, a better than 50% performance might be attained solely by using reinforcement cues rather than magnetic cues.
3. The effect, when present at all, was small.

Due to differences in experimental design, items (1) and (2) were not problems in the green turtle study, but the effect was also small (54–58% correct response) during trials with turtle A, and was absent in turtle B's experiment. Under such circumstances, one has to be concerned with subtle alternative cues or chance effects.

If one keeps the results of these discrimination experiments in perspective, they can be considered promising pilot work. There are various procedural changes that can be employed in future experiments which will reduce the ambiguity of results.

1. There are a number of learning formats which can reduce or eliminate reinforcement cues. These include lean partial reinforcement schedules, testing on extinction trials, and the discrete-trials/fixed-interval method reported by Woodward and Bitterman (1974) and used in the green turtle experiments (see also Walker *et al.*, Chapter 20, this volume).

2. Punishment, e.g., time-out, or delays before the beginning of another trial, has been shown to be effective in reducing incorrect responses in discriminatory learning by green turtles (Manton *et al.*, 1972) and in discriminatory learning of magnetic cues by tuna (M. Walker, personal communication). Mild punishment procedures (delay of paddle removal) were used in the green turtle experiment, and might prove effective in training loggerheads and other turtles in magnetic discrimination formats.

3. The use of only one or two subjects and a single two-choice format leaves open to question the influence of nonexperimental cues, i.e., discriminative cues other than the magnetic field which may bias responding. Using single subject designs, the influence of alternative cues can be lessened by reversals of reinforcement contingencies. For example, initially reward responses during the presence of a magnetic field but not in its absence. After a criterion percentage correct is attained, reverse the contingencies, reward only responses in the absence of the magnetic field, but not in its presence. In this manner, cues that might accompany one magnetic condition but not the other are equated over the experiment. Another alternative is to increase the sample size and make reward contingencies differ for different groups, i.e., one group is only rewarded in the presence of a magnetic stimulus, the other is rewarded only in the absence of the magnetic stimulus.

4. Fixing the presentation of food at a given site and fully automating the feeding procedure can reduce potential experimenter cues as well as encourage a more time efficient consummatory response by the subject.

5. The use of more magnetically clean procedures can enhance the likelihood of a subject detecting a stimulus as well as giving the experimenter a clearer picture of exactly what stimulus characteristics are salient. For example, in the loggerhead experiments the steel reinforcing bars in the tank walls created a disorderly ambient field and distorted the gradient of the experimental field.

Additional issues in discrimination learning experiments using magnetic stimuli are discussed in Ossenkopp and Barbeito (1978) and in the chapter on cetaceans (Bauer *et al.*) in this volume.

We are presently conducting a study on the resting orientation of green turtles in response to altered magnetic field conditions. In these experiments, individual turtles are placed in a small, indoor tank that is enclosed in black plastic to eliminate light and visual distractions. Helmholtz coils outside the tank are supplied with power to alter the normal magnetic field. Turtles are kept in the tank overnight in complete darkness, except for a brief flash every 20 min to provide light for an overhead camera that records their positions. The turtles are being tested for orientation responses to shifts in both the horizontal and the vertical components of the magnetic field. Similar experiments conducted with eels (Tesch, 1974) demonstrated a clear orientation shift with changes in the horizontal field components. We hope that the results from these tests will be less ambiguous than those obtained in our learning experiments, and that they will aid us in designing future experiments to determine what aspects of the field might be relevant to migrational navigation in the sea turtles.

3.2. Isolation and Identification of Magnetite in Sea Turtles

During the course of our operant conditioning experiments, we conducted magnetometry studies to look for magnetic material in *Chelonia mydas*. Specimens of hatchling, juvenile, and adult green turtles were examined for magnetic remanence using SQUID magnetometers. To reduce the risk of contamination, the magnetometer enclosure was thoroughly cleaned, and only nonmagnetic glass and wood instruments were used in all handling and dissection. Whole hatchlings and samples of tissue from all age classes were rinsed with glass-distilled water, frozen in liquid nitrogen, and saturated with a 3000-G cobalt/samarium magnet. Saturation isothermal remanent magnetization (sIRM) was then measured in the SQUID. Background signal measurements were taken periodically for comparison with tissue signals, and to ensure that the magnetometer enclosure remained magnetically clean.

Magnetic remanence was found in the head region of all turtles examined (four hatchlings, three juveniles, and two adults; Table II). The greatest concentration of magnetic material occurred in the anterior portion of the dura mater, although it was also present diffusely throughout the facial muscle. sIRM in the adult turtle duras was 9×10^{-6} emu, about 50 times greater than background. Because of this high remanence, dura tissue was the primary material examined in further tests.

Remanence was also found in whole hatchlings. When these were further dissected, the highest readings were obtained from the stomach; they probably came from magnetic particles present in sand and dirt ingested by the turtles. Remanence associated with surface tissues, such as carapace scutes, could be the result of external contamination and was therefore not measured separately or examined in subsequent tests.

The sIRM measured in the turtle is within the range of that found in other vertebrate species (see Bauer *et al.*; Presti; Walker *et al.*, Chapter 20, this volume). Adult turtles contain more magnetic material than juveniles, a phenomenon also observed in yellowfin tuna (Walker *et al.*, Chapter 20, this volume), honeybees (Gould *et al.*, 1978), and woodmice (J. Mather, personal communication).

Remanence in the dura was found from alternating-field demagnetization to be magnetically hard. The median unblocking field for net magnetic alignment in the dura was approximately 225 G, which indicates that single-domain magnetite crystals are present in the dura samples (Kirschvink and Lowenstam, 1979).

Table II. sIRM in Three Age Classes of Green Turtles

Sample	emu
Whole hatchlings	3.8×10^{-6}
	8.7×10^{-6}
	1.3×10^{-5}
	2.3×10^{-5}
Hatchling heads	1.4×10^{-6}
	1.6×10^{-6}
Hatchling necks	7.0×10^{-8}
	8.3×10^{-8}
Juvenile heads	1.1×10^{-6}
	3.0×10^{-6}
	9.5×10^{-6}
Juvenile flippers	
Front left	3.7×10^{-7}
Front right	2.8×10^{-7}
Rear left	9.7×10^{-7}
Rear right	6.3×10^{-7}
Adult brain	3.2×10^{-7}
	6.0×10^{-7}
Adult eyeball	6.3×10^{-7}
Adult facial muscle blocks	
1 × 1 × 1 cm	4.4×10^{-7}
1 × 1 × 2 cm	5.5×10^{-7}
1 × 2 × 3 cm	4.4×10^{-6}
1 × 3 × 3 cm	6.1×10^{-6}
Adult dura mater	
Posterior	1.0×10^{-6}
Posterior	1.5×10^{-6}
Anterior	9.0×10^{-6}
Anterior	9.2×10^{-6}
Empty sample holder	4.2×10^{-8}–2.3×10^{-7}

In order to identify the source of magnetic remanence in turtle tissue, we extracted and analyzed magnetic particles from adults and juveniles (for methods used see Walker *et al.*, Chapter 5, this volume). Particle samples were examined via X-ray diffraction, electron microprobe analysis, EDAX line spectra analysis, and scanning electron microscopy.

The X-ray diffraction pattern produced by aggregated particles from turtle duras is that expected for magnetite (Fig. 3). The lattice spacing parameter estimate calculated from this pattern was 0.8375 ± 0.004 nm, which compares well to the reference parameter for magnetite of 0.8396 nm, indicating that we had extracted a very pure magnetite sample from the turtles. The number and relative intensities of rings in the pattern, specific for each crystal type, also closely match the reference values (Joint Committee on Powder Diffraction Studies, 1974).

Electron microprobe analysis revealed that the extracted particles were very rich in iron and contained no measurable titanium or chromium, as would be expected for magnetite isolated from rock. Unlike geologic magnetite, small amounts of manganese and calcium oxides were persistently associated with the crystals (Table III). Tissue residue often found associated with the magnetite particles after extraction (see Walker *et al.*, Chapter 5, this volume) may account for the presence of these oxides. Analysis by EDAX probe corroborated the microprobe data, exhibiting strong peaks only for iron, and showing

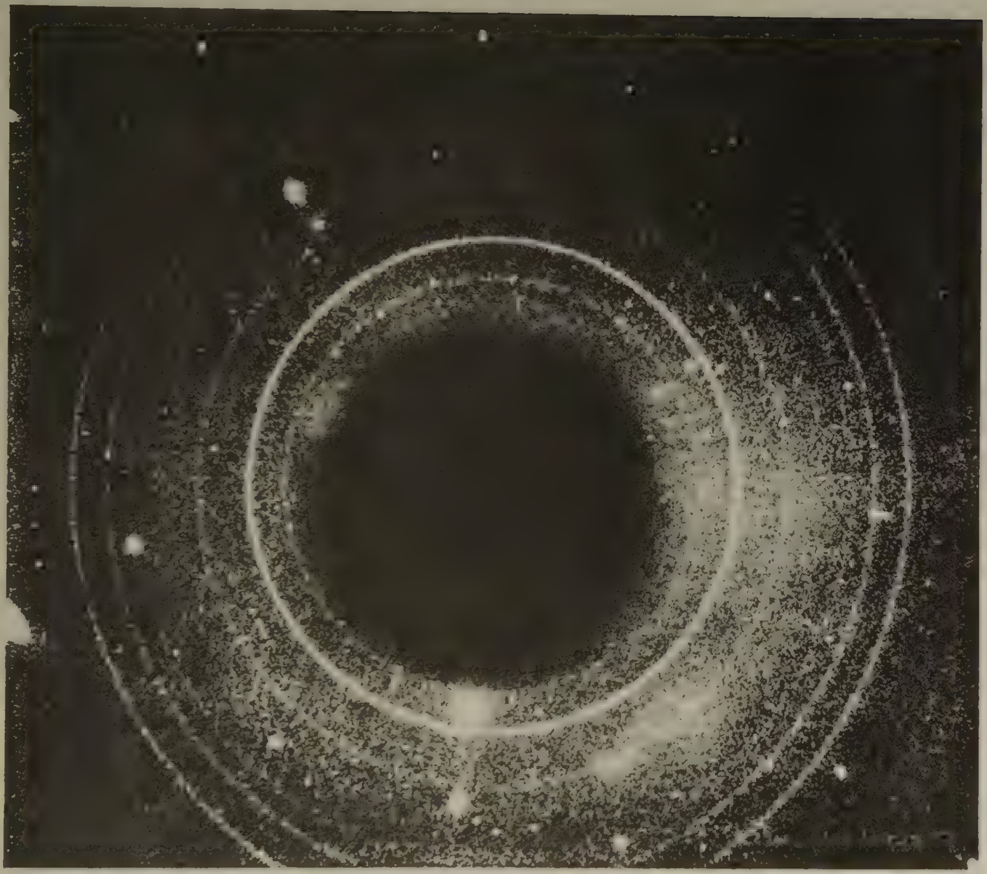

Figure 3. X-ray diffraction pattern of magnetite extracted from green turtle dura maters.

Table III. Electron Microprobe Analysis of Magnetite Particles Isolated from Green Turtles

Oxide	Weight % of sample Magnetite standard (NMNH 11487)	 Turtle
FeO	90.9	85.5 ± 1.7
TiO_2	0.2	0.0 ± 0.0
Cr_2O_3	0.2	0.0 ± 0.0
MnO	0.0	0.3 ± 0.0
CaO	—	0.3 ± 0.1
Total	91.3	86.1

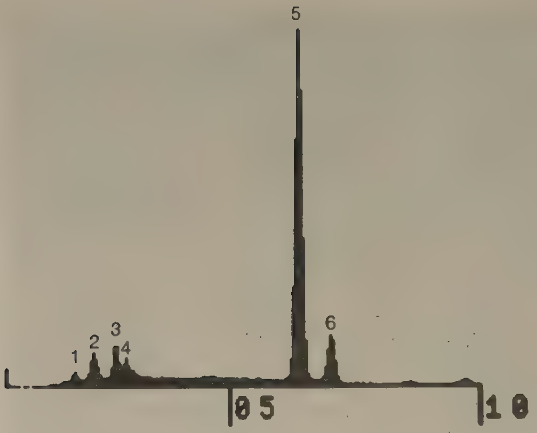

Figure 4. EDAX spectrum for magnetite sample from green turtle dura maters. Numbered peaks correspond to the following elements: 1, silica (from glass coverslip sample was placed on); 2, gold (from gold/paladium coating sprayed on sample to increase conductivity for scanning electron microscopy); 3, chlorine (from bleach used to digest dura membrane tissue); 4, paladium (from gold/paladium coating); 5 and 6, iron.

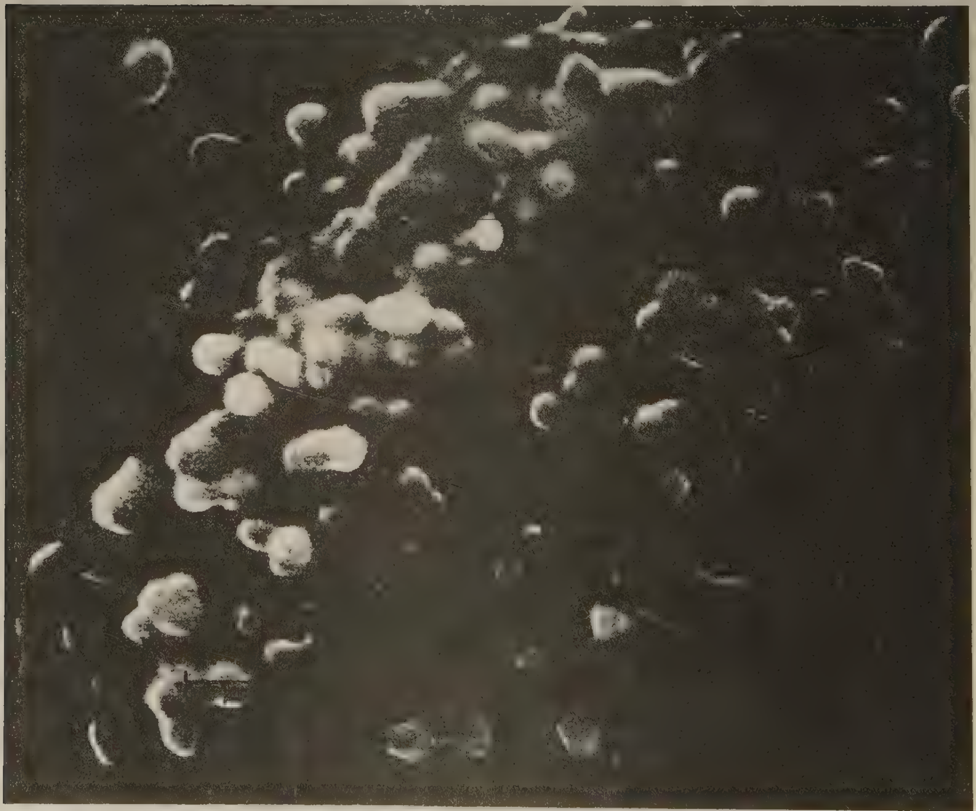

Figure 5. Scanning electron micrograph of colloidal crystal structure from green turtle dura mater sample.

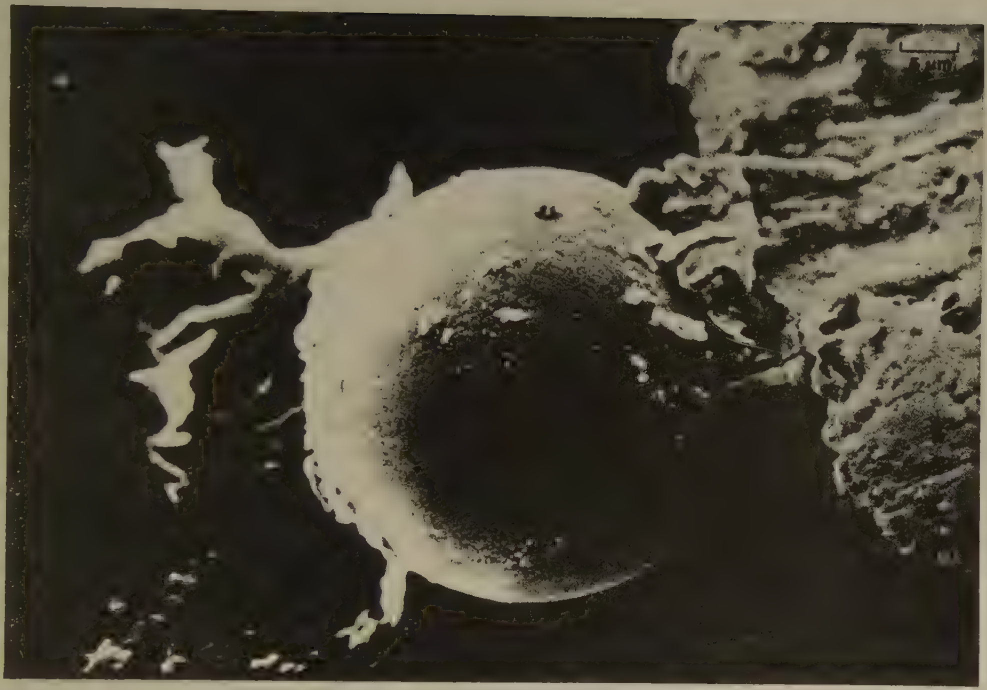

Figure 6. Scanning electron micrograph of sphere from green turtle dura mater sample.

no presence of other metals that would be expected as geologic contaminants, including nickel (Fig. 4).

Scanning electron microscopy revealed two types of crystal structure in dura samples: colloids (Fig. 5), and spheres (Fig. 6). The colloidal structures may comprise clusters of single-domain magnetite crystals. Although the apparent size of each nodule in the cluster is larger than that which would produce single-domain behavior in magnetite, each crystal may be surrounded by an organic coat. The spheres of magnetite, such as the one depicted in Fig. 6, have not previously been observed in organisms, although magnetite-containing cosmic spherules are common (Parkin *et al.*, 1977). It is possible that the turtle dura spheres are not of biological origin, but are contaminating cosmic spherules. We believe, however, that the spheres we observed are the result of biologic precipitation rather than cosmic contamination for several reasons. Our sample preparations were carried out in two different laboratories at different times, and as cosmic spherules are not a common laboratory contaminant it seems unlikely that they would appear in both sample sets. Cosmic spherules usually contain high proportions of magnesium and nickel, neither of which were present in our samples. Our strongest evidence for *in situ* information was that the spheres were not seen in control samples or in tissues other than dura. At this time the function of the large (10–50 μm) spheres is unknown. Dr. J. L. Kirschvink speculates that they may be involved in a system that detects geoelectric fields (Cromie, 1982).

The green turtle is a threatened species, and we therefore use only specimens that have died from natural causes in our magnetometry studies. As specimens become available, we hope to isolate more spheres from the duras and to study their properties in greater detail. We can then attempt to elucidate the role the spheres play, if any, in turtle magnetoreception.

4. Conclusion

The amphibians and reptiles form an evolutionary link between higher and lower vertebrates. Because of this phylogenetic position, the examination of magnetic perception and the sensory apparatus responsible for such perception is of particular interest in these classes. Evidence is accumulating for magnetoreception and magnetite biomineralization among fish, mammals, and birds. Preliminary work on magnetic susceptibility in salamanders and turtles, and the discovery of magnetite in turtles, is an important step toward understanding the evolutionary processes involved in magnetic sensitivity in all vertebrates. As demonstrated by this chapter, research on magnetoreception in the amphibians and reptiles has just begun. Additional studies are needed if the role of magnetite and magnetic sensitivity in vertebrates as a group is to be clearly understood.

ACKNOWLEDGMENTS. We wish to thank William G. Gilmartin and the National Marine Fisheries Service for providing turtles, equipment, and research facilities. John McIntosh, Kathleen Sobon, and Catherine Uyehara gave freely of their time to help in carrying out the behavioral experiments. Personnel of the Hawaii Institute of Geophysics, University of Hawaii, provided paleomagnetic laboratory facilities and assistance with electron microscopy and diffraction analyses. Joseph L. Kirschvink introduced us to the use of paleomagnetic techniques to look for magnetite in organisms, and gave us much-needed advice and instruction. Research funds were generously provided by the Southwest Fisheries Center Honolulu Laboratory, National Marine Fisheries Service. The loggerhead studies were supported in part by Sea Grant Project NA79AA-D-00085.

References

Adler, K., 1982, Sensory aspects of amphibian orientation and navigation, *Vertebr. Hung.* **21**:7–18.

Balazs, G. H., 1976, Green turtle migrations in the Hawaiian archipelago, *Biol. Conserv.* **9**:125–140.

Baldwin, H. R., 1972, Long-range radio tracking of sea turtles and polar bear: Instrumentation and preliminary results, in: *Animal Orientation and Navigation* (S. R. Galler, K. Schmidt-Koenig, G. J. Jacobs, and R. E. Belleville, eds.), NASA SP-262, U.S. Government Printing Office, Washington, D.C., pp. 19–37.

Carr, A., and Carr, M. H., 1970, Modulated reproductive periodicity in *Chelonia*, *Ecology* **5**:335–337.

Cromie, W. J., 1982, Born to navigate, *Mosaic* July/August:17–23.

Dunson, W. A. (ed.), 1975, *The Biology of Sea Snakes*, University Park Press, Baltimore.

Ferguson, D. E., 1971, The sensory basis of orientation in amphibians, *Ann. N.Y. Acad. Sci.* **188**:30–36.

Gould, J. L., Kirschvink, J. L., and Deffeyes, K. S., 1978, Bees have magnetic remanence, Science **201**:1026–1028.

Hirth, H. F., 1971, Synopsis of Biological Data on the Green Sea Turtle (*Chelonia mydas* Linnaeus 1758), FAO Fish. Syn. No. 85.

Joint Committee on Powder Diffraction Studies, 1974, *Selected Powder Diffraction Data for Minerals*, Swathmore, Pa.

Kalmijn, A. J., 1978, Experimental evidence of geomagnetic orientation in elasmobranch fishes, in: *Animal Migration, Navigation, and Homing* (K. Schmidt-Koenig and W. T. Keeton, eds.), Springer-Verlag, Berlin, pp. 347–353.

Keeton, W. T., 1971, Magnets interfere with pigeon homing, *Proc. Natl. Acad. Sci. USA* **68**:102–106.

Kirschvink, J. L., and Lowenstam, H. A., 1979, Mineralization and magnetization of chiton teeth: Paleomagnetic, sedimentologic, and biologic implications of organic magnetite, *Earth Planet. Sci. Lett.* **44**:193–204.

Manton, M., Karr, A., and Ehrenfeld, D. W., 1972, An operant method for the study of chemoreception in the green turtle, *Chelonia mydas*, *Brain Behav. Evol.* **5**:188–201.

Mather, J. G., and Baker, R. R., 1981, Magnetic sense of direction in woodmice for route-based navigation, *Nature* **291**:152–155.

Minton, S. A., Jr., and Minton, M. R., 1973, *Giant Reptiles*, Scribner's, New York.

Ossenkopp, K.-P., and Barbeito, R., 1978, Bird orientation and the geomagnetic field: A review, *Neurosci. Biobehav. Rev.* **2**:255–270.

Parkin, D. W., Sullivan, R. A. L., and Andrews, J. N., 1977, Cosmic spherules as rounded bodies in space, *Nature* **266**:515–517.

Perry, A., 1982, Magnetite and magnetic sensitivity in the green turtle, *Chelonia mydas*, Master's thesis, Department of Oceanography, University of Hawaii, Honolulu.

Phillips, J. B., 1977, Use of the earth's magnetic field by orienting cave salamanders (*Eurycea lucifuga*), *J. Comp. Physisol. A* **121**:273–288.

Phillips, J. B., and Adler, K., 1978, Directional and discriminatory responses of salamanders to weak magnetic fields, in: *Animal Migration, Navigation, and Homing* (K. Schmidt-Koenig and W. T. Keeton, eds.), Springer-Verlag, Berlin, pp. 325–333.

Pritchard, P. C. H. 1973, International migrations of South American sea turtles (Cheloniid and Dermochelidid), *Anim. Behav.* **21**:18–27.

Quinn, T. P., 1980, Evidence for celestial and magnetic compass orientation in lake migrating sockeye salmon fry, *J. Comp. Physiol. A* **137**:243–248.

Schmidt-Koenig, K., 1975, *Migration and Homing in Animals*, Springer-Verlag, Berlin.

Tesch, F. W., 1974, Influence of geomagnetism and salinity on the directional choice of eels, *Helgol. Wiss. Meeresunters.* **26**:382–395.

Twitty, V. C., Grant, D., and Anderson, O., 1967, Initial homeward orientation after long-distance displacements in the newt *Taricha rivularis*, *Proc. Natl. Acad. Sci. USA* **57**:342–348.

Woodward, W. T., and Bitterman, M. E., 1974, A discrete-trials/fixed-interval method of discrimination training, *Behav. Res. Methods Instrum.* **6**:389–392.

8571

EFFECTS OF EXHAUSTING EXERCISE ON ACID-BASE REGULATION IN SKIPJACK TUNA (KATSUWONUS PELAMIS) BLOOD[1]

S. F. PERRY,[2] C. DAXBOECK,[3] B. EMMETT,[4] P. W. HOCHACHKA,[4] AND R. W. BRILL

Southwest Fisheries Center, National Marine Fisheries Service, National Oceanic
and Atmospheric Administration, Honolulu, Hawaii 96812

(Accepted 1/2/85)

The effects of exhausting exercise on acid-base balance of skipjack tuna blood were investigated. Following exercise, tuna displayed a mixed respiratory/metabolic acidosis with blood pH being reduced by ~0.4 units. The respiratory component (51% of the initial acidosis) was compensated following 20 min of recovery, while the blood metabolic acid load (H^+m; ~8 mM) was cleared after only 50 min. At that time, there was a great discrepancy between blood lactate load and H^+m load because blood lactate levels were still increasing. The significance of these results is discussed with reference to the tuna's habitat, behavior, and physiology.

INTRODUCTION

Skipjack tuna (*Katsuwonus pelamis*) have a remarkable capacity to maintain high cruising speeds for long periods of time. The estimated maximum sustainable speed for this species is 6–10 body lengths/s (Yuen 1970; Dizon, Brill, and Yuen 1978). While the sustainable velocities greatly exceed those of most other fish examined, the maximum swimming speeds attainable by skipjack tuna (15–20 body lengths/s; Brill and Dizon [1979]) do not differ greatly from those of other active teleosts (e.g., *Salmo gairdneri*, 15 body lengths/s [Webb 1971; Mosse 1979; Johnston 1982]). Similarly, the amount of time it takes to reach exhaustion during burst activity also does not differ greatly from those of other active fish. However, there are reasons to believe that tuna may be better adapted for recovery from burst-swimming activity than are other teleosts: tuna exhibit relatively rapid lactate clearance (1–2 h; [Barrett and Connor 1964]) compared to the 8–12 h or even longer period seen in other teleosts (e.g., 24 h for flounder [Wood, McMahon, and McDonald 1977] and >12 h for rainbow trout [Turner, Wood, and Clark 1983*a*]). Rapid acid-base recovery following burst swimming clearly would be advantageous to skipjack tuna, considering that they inhabit the open ocean (an environment that provides little shelter) and that high swimming speeds are a skipjack tuna's most potent defense against predators.

In the present study we have investigated blood acid-base changes in skipjack tuna blood following exhausting exercise. In these experiments we were interested in determining the respiratory and metabolic components of the acid-base disturbance following burst swimming and the method and time course of recovery. Particularly, our interest was in determining if protons and lactate formed in equimolar amounts by muscular anaerobic metabolism (Hochachka and Mommsen 1983) are cleared at the same rate or whether a discrepancy in proton/lactate loads develops, as has been observed in other fish species (Piiper et al. 1972; Turner et al. 1983*a;* Turner, Wood, and Hobe 1983*b*).

---

[1] This study was funded by National Marine Fisheries Service, Pacific Gamefish Foundation, and an NSERC operating grant to P.W.H. The authors would like to thank Dr. C. M. Wood and Dr. D. J. Randall for providing some necessary equipment. As visitors to the Kewalo Research Facility, S.F.P., C.D., B.E., and P.W.H. wish to express thanks to the entire staff for their hospitality and support during this study. We are grateful to Dr. C. M. Wood, Dr. R. B. Boutilier, and Dr. P. J. Walsh for critically reading the manuscript. S.F.P. was supported by an E. B. Eastburn Postdoctoral Fellowship.

[2] Present address: Department of Biology, University of Ottawa, 30 Somerset E., Ottawa, Ontario, Canada K1N 6N5.

[3] Present address: Pacific Gamefish Foundation, P.O. Box 3189, Kailua-Kona, Hawaii 96740.

[4] Present address: Department of Zoology, University of British Columbia, 6270 University Blvd., Vancouver, British Columbia, Canada V6T 2A9.

Physiol. Zool. 58(4):421–429. 1985.
© 1985 by The University of Chicago. All rights reserved. 0031-935X/85/5804-8486$02.00

MATERIAL AND METHODS

Skipjack tuna (*Katsuwonus pelamis*) were captured on hook and line by local fishermen and transported to Kewalo Research Facility (National Marine Fisheries Service, Southwest Fisheries Centre, Honolulu Laboratory), where all subsequent experiments were performed. Fish of either sex, weighing 1.2–2.3 kg (mean ± SE weight = 1.7 kg ± 0.2; $n = 10$) were maintained outdoors in large circular holding tanks and supplied with rapidly flowing seawater (temperature = 25 C). Animals were used within the first 3 days of capture and were not fed while in captivity.

EXPERIMENTAL PROTOCOL

Blood buffering capacity.—In order to sample blood, a fish was netted and quickly injected intramuscularly with 2.4–4.8 mg/kg body weight of the neuromuscular blocking agent gallamine triethiodide (Flaxedil; 20 mg/ml). On cessation of swimming, the fish was transferred to an operating table and submerged in water, and a tube that allowed continuous irrigation of the gills with aerated seawater (10–12 liters/min) was inserted into the mouth. The fish was surrounded by a tent of opaque plastic to eliminate visual disturbances. One milliliter of sodium heparin (10,000 U.S.P. units) was injected into the ventral aorta, and, following a 5-min mixing period, as much blood as possible (usually 30–50 ml) was withdrawn via "blind" ventral aortic or cardiac puncture.

To determine nonbicarbonate blood buffering value (β) and to construct CO_2 combining curves at various hematocrit (HCT) levels, blood from four fish was centrifuged and plasma removed. Erythrocytes were resuspended in plasma to give a range of HCTs of 0%–60%. Blood samples were placed into 50-ml tonometer shaker flasks (5 ml/flask) that were suspended in a constant-temperature (25 C) bath. Blood was equilibrated with humidified gas mixtures of CO_2 diluted with air (using flowmeters) to produce a range of P_{CO_2} ~0 to ~15 torr. Following a 45-min equilibration, 1-ml samples of blood or plasma were analyzed for pH, total CO_2 content (C_{CO_2}), and HCT. The pH measurements were made with a Radiometer PHM-71 digital acid-base analyzer and associated "micro" pH electrode at 25 C. C_{CO_2} was determined according to the method of Cameron (1971). P_{CO_2} and bicarbonate concentration $[HCO_3^-]$ were calculated using a reorganization of the Henderson-Hasselbalch equation. The pK′ values of carbonic acid were obtained from Severinghaus, Stupfel, and Bradley (1956), and the solubility coefficients of CO_2 (αCO_2) were obtained from Albers (1970). Separate buffer curves for each HCT ($n = 18$) were plotted and β values ($dHCO_3^-/dpH$) determined. Finally, a curve relating buffering capacity to HCT was constructed using linear regression.

Effects of exhausting exercise.—Individual fish were exercised to exhaustion by chasing them around their holding tank, usually for periods of 5–10 min. Earlier studies (Hochachka, Hulbert, and Guppy 1978) have established that under such conditions skipjack tuna reach burst-swimming speeds of 20 body lengths/s and that white-muscle lactate concentration, $[La^-]$, rises to extremely high levels. Following this exercise period, the fish was injected with Flaxedil (2.4–4.8 mg/kg body weight), transferred to an operating table, and maintained as described above. As quickly as possible (usually within 1 min of placement of the fish on the operating table) a 1-ml blood sample was taken from the ventral aorta and analyzed for pH, C_{CO_2}, $[La^-]$, and HCT. The ventral aorta then was cannulated using an indwelling catheter, a procedure that took ~20 min. Additional blood samples were drawn immediately following cannulation and then at 10-min intervals for a further 30 min, at which time experiments were terminated and the fish sacrificed. Once again, blood was analyzed for pH, C_{CO_2}, $[La^-]$, and HCT. Lactate levels were determined enzymatically according to the method of Hochachka et al. (1978). The concentration of metabolic H^+ ions added to the blood over any time period, $[\Delta H_m^+]$, was calculated according to the following equation (McDonald, Boutilier, and Toews 1980):

$$[\Delta H_m^+] = [HCO_3^-]_1 - [HCO_3^-]_2 - \beta(pH_1 - pH_2), \tag{1}$$

where β equals the nonbicarbonate buffering capacity of whole blood as determined in vitro. Blood metabolic H^+ load (H_m^+) was determined at any given time by summing the [ΔH_m^+]'s, signs considered, from the preexercise sample onward. Blood lactate load was determined in a similar fashion.

Blood acid-base values for nonexercised (control) fish were obtained in a similar manner as were those for exercised fish, but care was taken to avoid stressing the animal prior to Flaxedil injection.

In the figures, variability of the data is indicated by ±1 SE. Sample means have been statistically analyzed using Student's *t*-test, and 5% was taken as the fiducial limit of significance.

RESULTS

CO_2 combining curves for separated plasma and whole blood at various HCTs are shown in figure 1A. The upward displacement of the curves with decreasing HCT indicates that the major fraction of total CO_2 in skipjack blood is carried in the plasma and not in erythrocytes. Similarly, the positive relationship between HCT and slope of the CO_2 combining curves reflects the greater buffering capacity as hemoglobin levels increase. Figure 1B illustrates the relationship between HCT

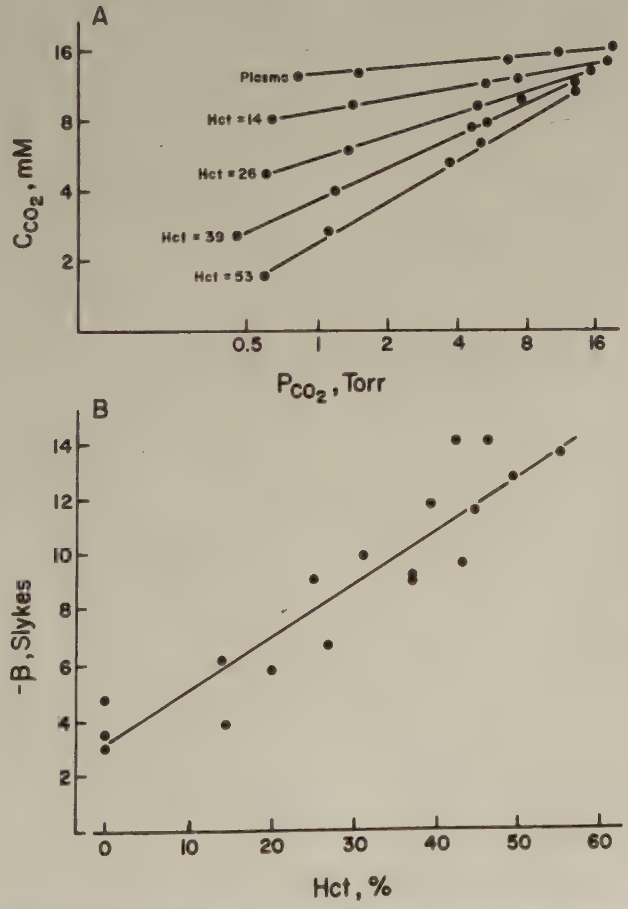

FIG. 1.—(*A*) CO_2 combining curves (log P_{CO_2} vs. log C_{CO_2}) for skipjack tuna blood of various hematocrit (HCT) values ($n = 4$, same fish for each curve) and (*B*) the relationship between nonbicarbonate buffering value (β) and HCT (18 determinations from blood of four fish). The regression equation is $-\beta = 0.196$ HCT $+ 3.11$, $r = 0.93$.

TABLE 1

NONBICARBONATE BUFFERING CAPACITY (β) OF SKIPJACK TUNA BLOOD COMPARED WITH THAT OF VARIOUS OTHER FISH SPECIES

Species	$-\beta$ (slyke)	HCT (%)	Source
Katsuwonus pelamis	11.2	41	This study
Salmo gairdneri	10.3	26	Wood and Jackson (1980)
S. gairdneri	9.7	25	Wood, McDonald, and McMahon (1982)
S. gairdneri	8.5	. . .	Eddy (1976)
Salvelinus fontinalis	7.5	35	Packer and Sunkin (1979)
Catostomus commersoni	8.5	28	Wilkes et al. (1981)
Ictalurus punctatus	14.3	25	Cameron and Kormanik (1982)
Platichthys stellatus	5.2	16	Wood et al. (1977)
Hippoglossoides elassodon	6.7	14	Turner et al. (1983*b*)
Parophrys vetulus	6.1	25	McDonald et al. (1982)
Protopterus aethiopicus (water-breathing)	12.6	. . .	DeLaney et al. (1977)

and β and is given by the regression equation $-\beta = 0.196\,(\mathrm{HCT}) + 3.11$. From in vivo determinations, HCT was 41% ± 2.2% ($n = 7$), giving a mean β of -11.2 slykes ($dHCO_3^-/dpH$; table 1). Plasma β is equal to the y-intercept of the regression line and is -3.11 slykes.

The effects of exhausting exercise on the acid-base status of tuna blood are shown in figure 2. After ~5 to ~10 min of forced burst-swimming activity, blood pH was greatly depressed from a preexercise value of 7.97 to a postexercise value of 7.54 (fig. 2A). The pH recovery following exercise was extremely rapid, taking only 30 min. When experiments were terminated, after 50 min of recovery, blood pH appeared to be greater than the preexercise value. This may indicate a slight acidosis in nonexercised (control) fish, probably owing to the stress of netting and Flaxedil injection. Alternatively, the higher pH following recovery from exercise may have been a result of overcompensation.

P_{CO_2} was greatly elevated following exercise (fig. 2D), but after 20 min of recovery P_{CO_2} had returned to the preexercise level. P_{CO_2} remained constant for the next 30 min, although at a lower level than the preexercise value, possibly indicating a condition of mild respiratory acidosis in nonexercised animals.

The changes in C_{CO_2} after exercise are shown in figure 2B. C_{CO_2} was lowered immediately postexercise and continued to decline for the initial 20 min of recovery. C_{CO_2} then increased during the next 30 min and was still rising on termination of the experiment.

Blood lactate concentration was significantly elevated following burst swimming and remained elevated throughout the postexercise period (fig. 2C). The preexercise blood [La$^-$] is seemingly high (9.2 mM ± 2.4) when compared with blood [La$^-$] of free-swimming skipjack tuna (4.7 mM; Hochachka et al. [1978]).

A pH-[HCO_3^-] diagram displaying the temporal changes in blood acid-base status following exhausting exercise in skipjack tuna is illustrated in figure 3. The dashed line, AB_1, represents the in vitro buffer line (slope = -11.2 slykes). It is clear that the postexercise acidosis is both respiratory and metabolic in origin. Using an approach outlined in detail by Wood et al. (1977), we evaluated the relative contributions of alterations of P_{CO_2} and lactic acid to the total pH change observed. Immediately postexercise (fig. 3, point *B*) the metabolic component of the acidosis equaled 49% and the respiratory component of the total acidosis equaled 51%. After 20 min the respiratory acidosis was completely compensated, whereas blood H_m^+ load (see eq. [1]) remained elevated until 50 min postexercise, at which time there was a slight base excess (fig. 3). The changes in blood [H_m^+] and [La$^-$] during recovery from exercise are shown in figure 4. By definition, $\Delta[H_m^+]$ and $\Delta[La^-]$ in fish at rest were equal to 0. Immediately postexercise, La^- load was significantly greater than H_m^+ load. La^- load continued to increase throughout the recovery period, while H_m^+ load declined gradually and was actually below the preexercise value at 50 min postexercise. The discrepancy between $\Delta[La^-]$ and $\Delta[H_m^+]$ could be caused by preferential removal of protons from the blood space and/or by a slower release of H^+ ions (with respect to La^-) from white muscle.

DISCUSSION

In the present study, a somewhat unorthodox method for blood sampling was employed. Clearly, this procedure did not allow us to measure true resting blood acid-base values or enable an analysis of blood acid-base changes in freely swimming animals following the forced exercise. Unfortunately, because of the fragile nature of skipjack tuna, all our attempts to anesthetize, catheterize, and recover tuna resulted in failure. Until very recently such a procedure was considered impossible by most tuna researchers. However, since completion of this study, successful recoveries of skipjack tuna from dorsal aortic catheterization have been reported (D. R. Jones, personal communication); however, 12 h was the longest that any fish survived following surgery and generally fish began to deteriorate after 3–4 h (D. R. Jones, personal communication), so it is also unlikely that true resting acid-base values can be obtained in this manner. Thus, it is apparent that until new surgical proce-

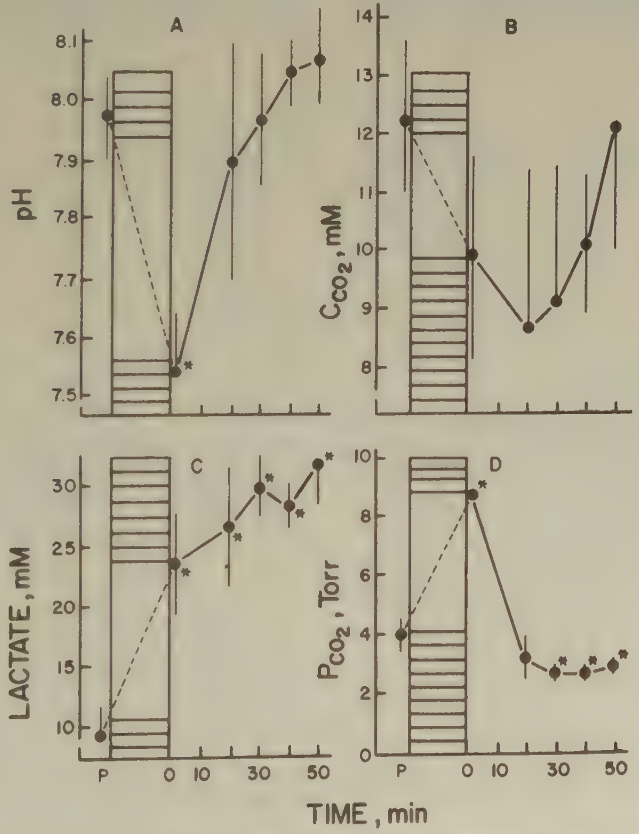

FIG. 2.—In vivo blood acid-base status of skipjack tuna at 25 C before and following exhausting exercise (burst swimming). Two separate groups of fish were used to determine preexercise (*P*) and postexercise values (*n* = 3 in both cases). Exercise period is represented by the striped bar; an asterisk indicates a significant difference from preexercise value.

dures are developed it will not be possible to use routine methodology to study blood acid-base status of tuna before and following exercise. It should be pointed out, however, that the methodology employed in the present study allowed arterial oxygen tension to be maintained at 70–80 torr, which is similar to values reported for freely swimming tuna (D. R. Jones, personal communication). Therefore, it would appear that forced ventilation does not limit gill O_2 transfer. Moreover, nonexercised tuna did not exhibit a marked blood acidosis (pH = 7.97), a condition normally associated with stressed fish.

The β of skipjack tuna blood (−11.2 slykes) is among the highest of all fish species examined (table 1). That the β is not greater is surprising, considering the high HCT (~40%) and hemoglobin concentration (14–20 g/100 ml; Klawe, Barrett, and Klawe [1963]) in this species. It is apparent, however, that hemoglobin is the major blood buffer (fig. 1). It also is clear from the negative relationship between CO_2 combining capacity and HCT in vitro that the major fraction of total CO_2 in the blood resides in the plasma, not in the erythrocytes. Similar results have been reported for trout (Eddy 1974) and flounder (Wood et al. 1977).

The changes in blood acid-base status immediately following strenuous exercise in skipjack tuna were similar to those reported for other active fish (e.g., *Scyliorhinus stellaris* [Piiper, Meyer, and Drees 1972]; *Salmo gairdneri* [Turner et al. 1983*a;* Wood, Turner, and Graham 1983]). The large initial decrease in pH (~0.4 units) was a result of equal respiratory and

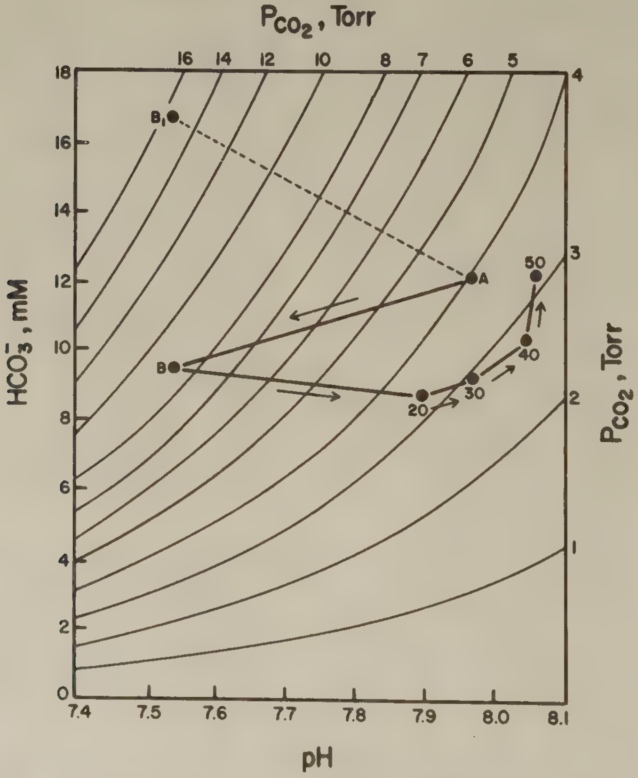

FIG. 3.—pH-[HCO_3^-] diagram showing temporal changes in blood acid-base status following exhausting exercise in skipjack tuna at 25 C (n = 3). A = the preexercise value from a separate group of fish (n = 3). B = the value immediately following exercise (usually within 1 min). Times (in min) of later blood samples are indicated at each successive data point. The dashed line AB_1 represents the in vitro buffer curve. See text for further details.

metabolic contributions. The respiratory component of the acidosis was compensated quickly, and following 20 min of recovery only the metabolic component remained. The increase in P_{CO_2} of venous blood during exercise probably is caused by greater aerobic metabolism as well as buffering of metabolic protons by HCO_3^-.

The ability of paralyzed skipjack tuna to recover from exhausting exercise is remarkable; after only 30 min blood pH was restored to preexercise levels, while H_m^+ load was cleared after only 50 min. Clearly, this is the most rapid metabolic acid clearance following burst-swimming activity ever reported for a fish. Normally, metabolic acid clearance in freely swimming fish requires ≥8 h (see review by Jones and Randall [1978]). The metabolic acid load immediately postexercise (~8 mM) was similar to values reported for rainbow trout (Turner et al. 1983*a;* Wood et al. 1983). The relatively low metabolic acid load is surprising considering that the tuna white-muscle contribution to burst swimming is supported almost entirely by the most intense glycolysis thus far known in nature (Hochachka et al. 1978). Typical values for white muscle [La⁻] following burst swimming are ~100 µmol/g in skipjack tuna (Hochachka et al. 1978) versus ~40 µmol/g in rainbow trout (Turner et al. 1983*a*). The difference in white-muscle lactate levels between tuna and trout probably accounts for the much higher blood lactate concentration in skipjack tuna following exercise. As has been shown for dogfish and rainbow trout (Piiper et al. 1972; Turner et al. 1983*a*), blood lactate levels in skipjack tuna exceed blood metabolic acid levels during the recovery phase, which is exactly opposite to the situation observed in sluggish species (e.g., starry flounder [Wood et al. 1977]; flathead sole [Turner et al. 1983*b*]). However, the magnitude of the discrepancy between

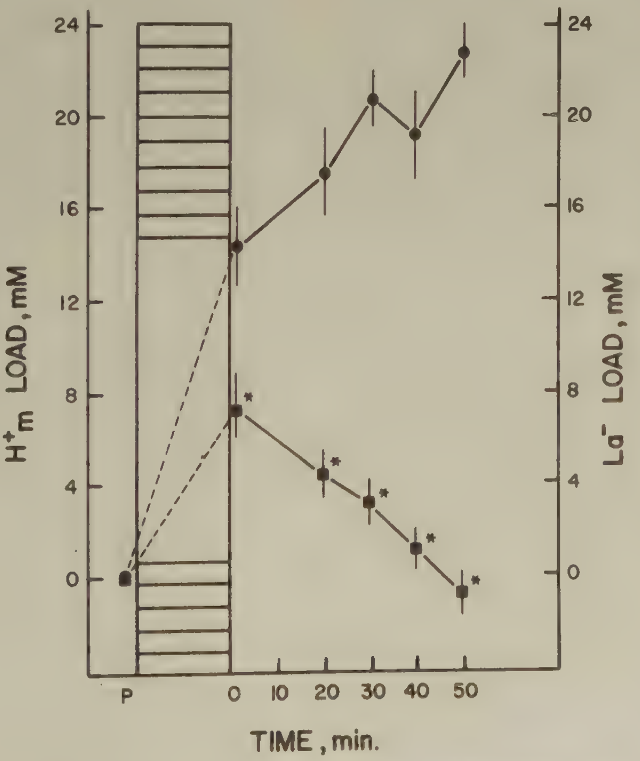

FIG. 4.—Changes in blood metabolic acid load (H_m^+ load; ■——■) and lactate load (La⁻ load; ●——●) following exhausting exercise in skipjack tuna (*n* = 3). *P* = preexercise; an asterisk indicates a significant difference between H_m^+ load and La⁻ load at the same sample time.

$[La^-]$ and $[H^+_m]$ in skipjack tuna is far greater than other studies have shown (Piiper et al. 1972; Turner et al. 1983*a;* Wood et al. 1983). Since lactate ions and H^+ ions are produced in stoichiometrically equal amounts (Hochachka and Mommsen 1983), this discrepancy must be due to differential release of La^- and H^+ ions from white muscle and/or their differential removal from blood. Although it is difficult to differentiate between these two possibilities, our results do indicate that skipjack tuna are able to remove H^+ ions from the blood at a much faster rate than are other fish (50 min for tuna compared to 8–12 h for rainbow trout [Turner et al. 1983*a*]). Whether the metabolic acid is being excreted across the gills into the water (see Heisler 1980) or being translocated to another tissue (e.g., red muscle) is unclear. However, the large blood volume, cardiac output, and gill surface area in skipjack tuna (Muir 1969; Laars, Ulevitch, and Morrison 1978) are all factors that could enhance acid excretion. Nevertheless, we cannot ignore the possibility that the rapid acid-base regulation following exercise was in some way due to muscle paralysis, although we consider this unlikely. Indeed, muscular movements are thought to enhance local blood flow (Randall and Daxboeck 1982) and therefore would, if anything, probably enhance acid clearance. Hochachka et al. (personal communication) have proposed that the major site of lactate oxidation is red muscle. Thus, movement of H^+ ions from white muscle to red muscle could be important for the ultimate remetabolism of lactate. In trout, the discrepancy between $[La^-]$ and $[H^+_m]$ is believed to be due to differential release from white muscle (Turner et al. 1983*a;* Turner and Wood 1983). Studies using a perfused trunk preparation (Turner and Wood 1983) have shown that H^+ ions are retained in white muscle as a result of a continuing blood acidosis that inhibits proton efflux; under resting conditions, La^- and H^+ ions are released at similar rates. This would suggest that in skipjack tuna metabolic acid is not retained in white muscle, since blood pH is restored to resting levels in 30 min. It seems more likely that H^+ ions formed during anaerobic metabolism are eliminated rapidly from white muscle and removed from the blood by excretion and/or translocation. The fact that skipjack white muscle is well vascularized compared to that of other teleosts (Hulbert et al. 1979) supports this theory. A slower release of lactate ions from white muscle and/or their slower removal from the blood would explain the discrepancy between blood levels of these two ions following exercise. Clearly, measurements of acid excretion as well as intracellular pH of white and red muscle following burst activity and lactic acid infusion would help clarify this problem.

LITERATURE CITED

Albers, C. 1970. Acid-base balance. Pages 173–208 *in* W. S. Hoar and D. J. Randall, eds. Fish physiology. Vol. **4.** Academic Press, New York.

Barrett, I., and A. R. Connor. 1964. Muscle glycogen and blood lactate in yellowfin tuna, *Thunnus albacares,* and skipjack tuna, *Katsuwonus pelamis,* following capture and tagging. Inter-Am. Trop. Tuna Comm. Bull. **9:**219–268.

Brill, R. W., and A. E. Dizon. 1979. Effect of temperature on isotonic twitch of isolated muscle and predicted maximum speeds of skipjack tuna. Environ. Biol. Fishes **4:**199–205.

Cameron, J. N. 1971. Rapid method for determination of total carbon dioxide in small blood samples. J. Appl. Physiol. **31:**532–534.

Cameron, J. N., and G. A. Kormanik. 1982. The acid-base responses of gills and kidneys to infused acid and base loads in the channel catfish, *Ictalurus punctatus.* J. Exp. Biol. **99:**143–160.

DeLaney, R. G., G. Lahiri, R. Hamilton, and A. P. Fishman. 1977. Acid-base balance and plasma composition in the aestivating lungfish (*Protopterus*). Am. J. Physiol. **232:**10–17.

Dizon, A. E., R. W. Brill, and H. S. H. Yuen. 1978. Correlations between environment, physiology and activity and its effects on thermoregulation in skipjack tuna, *Katsuwonus pelamis.* Pages 233–259 *in* G. D. Sharp and A. E. Dizon, eds. The physiological ecology of tunas. Academic Press, New York.

Eddy, F. B. 1974. *In vitro* blood carbon dioxide of the rainbow trout, *Salmo gairdneri.* Comp. Biochem. Physiol. **47A:**129–140.

———. 1976. Acid-base balance in rainbow trout (*Salmo gairdneri*) subjected to acid stresses. J. Exp. Biol. **64:**159–171.

Heisler, N. 1980. Regulation of the acid-base status in fishes. Pages 123–162 *in* M. A. Ali, ed. Environmental physiology of fishes. Ser. A, vol. **35.** Nato Advanced Study Institute Series. Plenum, New York.

Hochachka, P. W., W. C. Hulbert, and M. Guppy.

1978. The tuna power plant and furnace. Pages 153–174 *in* G. D. SHARP and A. E. DIZON, eds. The physiological ecology of tunas. Academic Press, New York.

HOCHACHKA, P. W., and T. P. MOMMSEN. 1983. Protons and anaerobiosis. Science **219**:1391–1397.

HULBERT, W. C., M. GUPPY, B. MURPHY, and P. W. HOCHACHKA. 1979. Metabolic sources of heat and power in tuna muscles. I. Muscle fine structure. J. Exp. Biol. **82**:289–301.

JOHNSTON, I. A. 1982. Physiology of muscle in hatchery raised fish. Comp. Biochem. Physiol. **13B**:105–124.

JONES, D. R., and D. J. RANDALL. 1978. The respiratory and circulatory systems during exercise. Pages 425–501 *in* W. S. HOAR and D. J. RANDALL, eds. Fish physiology. Vol. 7. Academic Press, New York.

KLAWE, W. L., I. BARRETT, and B. M. H. KLAWE. 1963. Haemoglobin content of the blood of six species of scombroid fishes. Nature **198**:96.

LAARS, R. M., R. J. ULEVITCH, and D. C. MORRISON. 1978. Estimates of blood volume in the albacore tuna. Pages 135–139 *in* G. D. SHARP and A. E. DIZON, eds. The physiological ecology of tunas. Academic Press, New York.

MCDONALD, D. G., R. G. BOUTILIER, and D. P. TOEWS. 1980. The effects of enforced activity on ventilation, circulation and blood acid-base balance in the semi-terrestrial anuran, *Bufo marinus*. J. Exp. Biol. **84**:273–287.

MCDONALD, D. G., R. L. WALKER, P. R. H. WILKES, and C. M. WOOD. 1982. H^+ excretion in the marine teleost, *Parophrys vetulus*. J. Exp. Biol. **98**:403–414.

MOSSE, P. R. L. 1979. Capillary distribution and metabolic histochemistry of the lateral propulsive musculature of pelagic teleost fish. Cell Tissue Res. **203**:141–160.

MUIR, B. S. 1969. Gill dimensions as a function of fish size. J. Fisheries Res. Board Can. **26**(1):165–170.

PACKER, R. K., and A. L. SUNKIN. 1979. Blood acid-base balance in brook trout (*Salvelinus fontinalis*). J. Exp. Biol. **79**:115–126.

PIIPER, J., M. MEYER, and F. DREES. 1972. Hydrogen ion balance in the elasmobranch, *Scyliorhinus stellaris*, following exhausting activity. Respir. Physiol. **16**:290–303.

RANDALL, D. J., and C. DAXBOECK. 1982. Cardiovascular changes in the rainbow trout (*Salmo gairdneri*) during exercise. Can. J. Zool. **69**:1135–1142.

SEVERINGHAUS, J. W., M. STUPFEL, and A. F. BRADLEY. 1956. Variations of serum carbonic acid pK′ with pH and temperature. J. Appl. Physiol. **9**: 197–200.

TURNER, J. D., and C. M. WOOD. 1983. Factors affecting lactate and proton efflux from pre-exercised, isolated, perfused rainbow trout trunks. J. Exp. Biol. **105**:395–401.

TURNER, J. D., C. M. WOOD, and D. CLARK. 1983*a*. Lactate and proton dynamics in the rainbow trout (*Salmo gairdneri*). J. Exp. Biol. **104**:247–268.

TURNER, J. D., C. M. WOOD, and H. HOBE. 1983*b*. Physiological consequences of severe exercise in the inactive benthic flathead sole (*Hippoglossoides elassodon*): a comparison with the active pelagic rainbow trout (*Salmo gairdneri*). J. Exp. Biol. **104**:269–288.

WEBB, P. W. 1971. The swimming energetics of trout. I. Thrust and power output at cruising speeds. J. Exp. Biol. **55**:489–520.

WILKES, P. R. H., R. L. WALKER, D. G. MCDONALD, and C. M. WOOD. 1981. Respiratory, ventilatory, acid-base and ionoregulatory physiology of the white sucker, *Catostomus commersoni:* the influence of hyperoxia. J. Exp. Biol. **91**:239–254.

WOOD, C. M., and E. B. JACKSON. 1980. Blood acid-base regulation during environmental hyperoxia in the rainbow trout. Respir. Physiol. **42**:351–372.

WOOD, C. M., D. G. MCDONALD, and B. R. MCMAHON. 1982. The influence of experimental anaemia on blood acid-base regulation in vivo and in vitro in the starry flounder (*Platichthys stellatus*) and the rainbow trout (*Salmo gairdneri*). J. Exp. Biol. **96**:221–237.

WOOD, C. M., B. R. MCMAHON, and D. G. MCDONALD. 1977. An analysis of changes in blood pH following exhausting activity in the starry flounder, *Platichthys stellatus*. J. Exp. Biol. **69**:173–185.

WOOD, C. M., J. D. TURNER, and M. S. GRAHAM. 1983. Why do fish die after severe exercise? J. Fish Biol. **22**:189–201.

YUEN, H. S. H. 1970. Behavior of skipjack tuna, *Katsuwonus pelamis*, as determined by tracking with ultrasonic devices. J. Fisheries Res. Board Can. **27**:2071–2079.

8572

Comp. Biochem. Physiol. Vol. 81A, No. 1, pp. 49–53, 1985
Printed in Great Britain

0300–9629/85 $3.00 + 0.00
© 1985 Pergamon Press Ltd

EFFECTS OF TEMPERATURE CHANGE ON ACID–BASE REGULATION IN SKIPJACK TUNA (*KATSUWONUS PELAMIS*) BLOOD

S. F. Perry,* C. Daxboeck,† B. Emmett,‡ P. W. Hochachka‡ and R. W. Brill

Southwest Fisheries Center, National Marine Fisheries Service, National Oceanic and Atmospheric Administration, Honolulu, Hawaii 96812. USA

(*Received* 24 *July* 1984)

Abstract—1. The effects of temperature change (*in vitro*) on acid–base balance of skipjack tuna blood were investigated.

2. By examining the relationship between blood pH and temperature (*in vitro*) under conditions of constant CO_2 tension (open system), it was observed that dpH/dT = −0.0131 U/°C.

3. This value falls well within the range of *in vivo* values reported for other ectothermic vertebrates, and is only slightly different than results obtained *in vitro* under conditions of constant CO_2 content (closed system; dpH/dT = −0.0165 U/°C).

4. It is concluded that changes in pH following temperature changes can be accounted for solely by the passive, *in vitro* behaviour of the chemical buffer system found in the blood, so that active regulatory mechanisms of pH adjustment need not be postulated for skipjack tuna.

INTRODUCTION

Tuna are extraordinary teleosts with respect to their ability to maintain muscle temperature above ambient temperature (1–11°C higher). The mechanism by which tuna conserve heat is by retention of metabolic heat through vascular counter-current heat exchangers or retia (see Carey *et al.*, 1971). Very steep thermal gradients develop within the body musculature and thus blood temperature varies during circulation through the systemic vasculature. Behaviour patterns of tuna also may lead to rapid temperature changes of the blood. Indeed, Dizon *et al.* (1978) have shown that extensive vertical migrations (surface to 273 m) are continuous features of the daylight activity pattern of skipjack tuna in areas where water temperature ranged from 25°C at the surface to less than 12°C at 270 m depth. These temperature changes also would appear to place extraordinary demands on acid-base regulatory systems.

In air-breathing ectotherms blood pH changes with a temperature slope of approx. −0.016 to −0.018 U/°C by ventilatory adjustments of P_{CO2} (see review by Reeves, 1977). Generally, air-breathing ectotherms behave as constant CO_2 content (C_{CO2}) systems or closed systems, *in vitro* and dpH/dT parallels the neutral pH of water (dpN/dT = −0.016U/°C, range 20–37°C; *Handbook of Chemistry and Physics*, 56th edn). Such pH changes allow maintenance of constant relative alkalinity (Rahn, 1967) or constant fractional dissociation of alpha imidazole groups on protein histidine residues (Reeves, 1977). Similar changes in pH with temperature have been observed in water-breathers (*Salmo gairdneri*, −0.017; Randall and Cameron, 1973; *Cancer magister*, −0.018; McMahon *et al.*, 1978; *Carcinus maenas*, −0.019; Howell *et al.*, 1973; −0.0162; Truchot, 1973; *Callinectes sapidus*, −0.015; Wood and Cameron, 1984). However, a significant number of aquatic species (primarily fish) display dpH/dT of blood slightly lower than dpN/dT such that constant relative alkalinity is not maintained (e.g. *Scyliorhinus stellaris*, Heisler, *et al.*, 1976; Heisler, *et al.*, 1980; *Ictalurus punctatus*, Cameron and Kormanik, 1982; *Cynoscion arenarius*, Cameron, 1978; *Anguilla rostrata*, Walsh and Moon, 1982). Also, the situation in water-breathers is complicated further because, depending on the species, they may behave as constant CO_2 tension (P_{CO2}) systems (e.g. *Salmo gairdneri*, Randall and Cameron, 1973) or as a combination of the two types (i.e. changes in both P_{CO2} and C_{CO2}; see Heisler, 1980) following temperature changes. While acid–base adjustments following temperature changes take place rapidly in air-breathers (< 2 hr), they take as long as 24 hr in water-breathers. Such prolonged adjustments would seem ill-suited to the active life-style of the tuna which imposes the simultaneous acid–base challenges of temperature fluctuations and exercise. In the present study we have investigated blood acid–base changes in skipjack tuna blood during temperature changes. These experiments were designed to determine whether skipjack blood, *in vitro*, obeys the rule of constant relative alkalinity (i.e. dpH/dT = −0.016 U/°C such that the ratio of OH^-/H^+ remains constant, Rahn, 1967) under conditions of constant CO_2 content (closed system) as one would predict (Rosenthal, 1948; Reeves, 1972, 1976a, b), as well as to determine blood pH temperature dependence under conditions of constant CO_2 tension (open system) which may more closely resemble the situation in fish. In particular, the experiments test the possibility that acid–base adjustments following temperature changes occur passively.

---

*Department of Biology, University of Ottawa, 30 Somerset E., Ottawa, Ontario, Canada K1N 6N5.

†Pacific Gamefish Foundation, PO Box 3189, Kailua-Kona, Hawaii 96740, USA.

‡Department of Zoology, University of British Columbia, 6270 University Blvd., Vancouver, British Columbia, Canada V6T 2A9.

MATERIALS AND METHODS

Skipjack tuna (*Katsuwonus pelamis*) were captured on hook and line by local fishermen and transported to Kewalo Research Facility (National Marine Fisheries Service, Southwest Fisheries Centre, Honolulu Laboratory) where all subsequent experiments were performed. Fish of either sex, weighing between 1.2 and 2.3 kg (mean wt = 1.7 kg ± 0.2 SE, $N = 10$) were maintained outdoors in large circular holding tanks and supplied with rapidly flowing seawater (temperature = 25°C). Animals were used within the first three days of capture and were not fed while in captivity.

Experimental protocol

In order to sample blood, a fish was netted and quickly injected intramuscularly with 0.2–0.4 ml of the neuromuscular blocking agent, gallamine triethiodide (Flaxedil). Upon cessation of swimming, the fish was transferred to an operating table, submerged in water and a tube was inserted into the mouth which allowed continuous irrigation of the gills with aerated seawater (10–12 l/min). One ml of sodium heparin (10,000 U.S.P. units) was injected into the ventral aorta and, following a five min mixing period, as much blood as possible (usually 30–50 ml) was withdrawn via "blind" ventral aortic or cardiac puncture. Blood was centrifuged in order to obtain plasma and to prepare blood of approximately 40% haematocrit (hct). Blood or plasma then was transferred to tonometer flasks (50 ml) and equilibrated with humidified mixtures of CO_2 in air (using flowmeters) in a temperature controlled water bath. Three different experiments were performed. In the first, the blood or plasma was warmed from 15° to 30°C in 5-degree increments every 60 min under conditions of constant P_{CO_2} (approximately 1% CO_2 in air). pH and total CO_2 content (C_{CO_2}) were determined at each temperature and from these values, P_{CO_2} and the molar concentration of CO_2 (S_{CO_2}; $\alpha CO_2 \times P_{CO_2}$) were calculated. pH measurements were made with a Radiometer PHM-71 digital acid–base analyser and associated micro pH electrode at 25°C. C_{CO_2} was determined according to the method of Cameron (1971). P_{CO_2} and bicarbonate concentration (HCO_3^-) were calculated using a reorganization of the Henderson–Hasselbalch equation. pK′ values of carbonic acid were obtained from Severinghaus *et al.* (1956) and the solubility coefficients of CO_2 (α_{CO_2}) were obtained from Albers (1970). In the second series of experiments, blood again was warmed in 5-degree increments, but under conditions of constant C_{CO_2}, in sealed syringes. Temperature equilibration was slow in these experiments and 60 min was required to reach stable water and blood temperatures. pH and C_{CO_2} were measured as described previously. Because of the long time blood remained sealed in syringes, it was possible that red blood cell (rbc) metabolism alone, might cause changes in pH and P_{CO_2}. To test for the effect of rbc metabolism, blood was sealed in syringes for identical time periods as before, but at constant temperature (25°C). The results of these control experiments made it possible to correct the results obtained during the temperature change experiments for the effects of rbc metabolism. In the final series of experiments, blood was equilibrated first with 1% CO_2 (in air) at 15°C and pH and C_{CO_2} were determined. After making these measurements, samples of blood were quickly warmed to 30°C (20 min) in sealed syringes and pH and C_{CO_2} measured again. Open and closed system experiments were performed on blood obtained from different sets of animals ($N = 3$ in each case).

In the figures, variability of the data is indicated by ± 1 SE. Sample means have been statistically analysed using Student *t*-test and 5% was taken as the fiducial limit of significance.

RESULTS

The results of changing temperature under conditions of constant P_{CO_2} (open system) in blood (hct ≃ 40%) and plasma are illustrated in Fig. 1. The effects of temperature change on pH and C_{CO_2} for plasma and whole blood are strikingly different. In blood, pH fell as temperature increased with a slope of -0.0131 U/°C. In contrast, plasma pH increased with increasing temperature ($dpH/dT = +0.004$ U/°C). This increase in pH was a result of the ratio $[HCO_3^-]/S_{CO_2}$ increasing from 26.7 at 15°C to 37.1 at 30°C and the change in pK′ being so small that the overall effect was an increase in pH. Similarly, blood C_{CO_2} decreased greatly with increasing temperature ($dC_{CO_2}/dT = -0.339$ mM/°C) whereas plasma C_{CO_2} was affected only slightly ($dC_{CO_2}/dT = -0.100$ mM/°C). The minor changes of P_{CO_2} in both blood and plasma during conditions of supposed constant P_{CO_2} were probably due to small variations in air or CO_2 flow which were undetectable using flowmeters as monitoring devices. In both cases, S_{CO_2} decreased with increasing temperature and simply reflects the inverse relationship between αCO_2 and temperature.

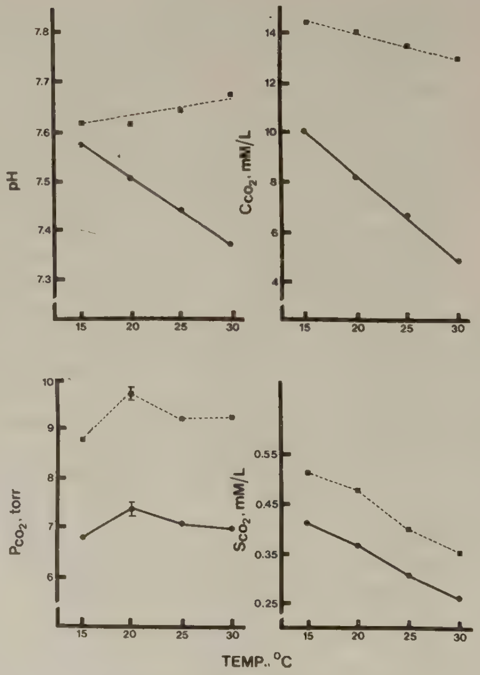

Fig. 1. The effect of temperature change on *in vitro* blood (hct ≃ 40) (● — ●; $n = 3$) and plasma (■ -- ■; $n = 2$) acid–base status under conditions of constant P_{CO_2} (open system). S_{CO_2} = the molar concentration of CO_2 ($\alpha_{CO_2} \times P_{CO_2}$). Where not shown, standard error bars lie within the data points. See text for further details.

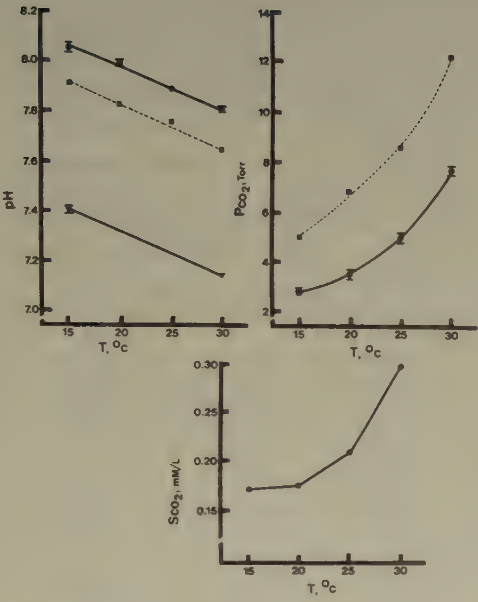

Fig. 2. The effect of temperature change on *in vitro* blood (●—●; $n=3$) and plasma (■—■; $n=2$) acid–base status under conditions of constant CO$_2$ content (closed system). S_{CO_2} = the molar concentration of CO$_2$ ($\alpha_{CO_2} \times P_{CO_2}$). All values have been corrected for the effects of metabolism with time (see text) except for blood subjected to rapid temperature change (▼—▼; $n=3$). Where not shown, standard error bars lie within the data points. Curves of P_{CO_2} vs T were fitted by eye.

Figure 2 summarises the effects of temperature change under conditions of constant C_{CO_2} (closed system). Unlike the open system experiments, blood (hct ≃ 40%) and plasma were affected in a similar fashion; for plasma dpH/dT was −0.0162 U/°C and for whole blood dpH/dT was −0.0165 U/°C. This value for whole blood was obtained by correcting for the effects of metabolism, as described earlier. The effect of metabolism alone, caused pH to change with a slope of −0.0355 U/hr. Since temperature was changed every hour, the measured pH values were corrected by subtracting 0.0355 × *t* (hr). To check the validity of this correction, samples of blood were warmed from 15 to 30°C as quickly as possible (20 min). In this instance pH changed with a temperature slope of −0.0174 U/°C, a value very similar to our corrected value of −0.0165 U/°C (Fig. 3). The slight difference between the temperature slopes was probably due to a small effect of metabolism during the 20 min it took to warm the blood 15°C. Indeed, if we correct the slope of the rapid temperature change as before, the resultant slope (−0.0168 U/°C) is almost identical to that obtained (−0.0165 U/°C) using the longer equilibration technique. In the constant content system, P_{CO_2} increased for both blood and plasma in a similar manner (blood; $dP_{CO_2}/dT = 0.32$ Torr/°C; plasma; $dP_{CO_2}/dT = 0.48$ Torr/°C). Correction of blood P_{CO_2} for the effect of metabolism was made using a correction factor of 1.0 Torr/hr. As expected, S_{CO_2} increased with temperature as a result of a large increase in P_{CO_2} compared to only a small decrease in α_{CO_2}.

DISCUSSION

Since the observations of Rahn (1967), a great body of evidence has been accumulated showing that blood pH in fish varies inversely with temperature with a slope ranging between −0.012 and −0.017 U/°C (see review by Reeves, 1977; Heisler, 1980). A notable exception is the blood of the American eel (*Anguilla rostrata*), which changes with a temperature slope of only −0.0076 U/°C (Walsh and Moon, 1982).

Alpha-imidazole is the most concentrated blood buffer and its dissociation constant is affected by temperature (dpK/dT ≃ −0.017 U/°C) in a similar manner as the blood of a great variety of ectothermic vertebrates (Reeves, 1977), although to a greater extent in fish (Heisler, 1980). It is clear, however, that regulation of the CO$_2$/HCO$_3^-$ buffer system represents the principal physiological control of blood acid–base status. Since the pK′ of carbonic acid is only slightly affected by temperature (dpK′/dT ≃ −0.005), it is apparent when viewing the Henderson-Hasselbalch equation,

$$\mathrm{pH} = \mathrm{pK}' + \log \frac{(\mathrm{HCO_3}^-)}{\alpha_{CO_2} \times P_{CO_2}},$$

that either the demoninator ($\alpha_{CO_2} \times P_{CO_2}$) or the numerator (HCO$_3^-$) must be adjusted following a temperature alteration in order to explain the observed changes in blood pH. Air-breathing ectotherms behave as constant CO$_2$ content systems and adjust P_{CO_2} by ventilatory changes (Reeves, 1977). In water-breathers, the high ventilation–perfusion ratio required for adequate oxygen uptake precludes ventilation as a means of regulating P_{CO_2}. Alternatively, water-breathers primarily manipulate bicarbonate levels to achieve the final adjustment of blood pH. Strictly speaking, water-breathers do not behave as constant CO$_2$ content systems or constant P_{CO_2} systems but as a combination of the two types, depending on the species in question (Cameron and Kormanik, 1982). What is clear however, is that generally, adjustment of (HCO$_3^-$) is the method by which fish manipulate blood pH following temperature changes. The adjustment of blood HCO$_3^-$ levels is a slow process that likely involves manipulations of active ion-exchange mechanisms (see review of Heisler, 1980).

The results of the present study demonstrate, that in skipjack tuna, there is no need for gradual active regulation of blood bicarbonate levels following temperature changes. The blood pH change observed *in vitro*, under conditions of constant P_{CO_2} (dpH/dT = −0.0131 U/°C, Fig. 1) falls well within the range of values noted for other ectothermic vertebrates (Reeves, 1977) and is only slightly different than the pH change observed under conditions of constant C_{CO_2} (dpH/dT = −0.0165 U/°C, Fig. 2). The large decrease in pH with increasing temperature in the open system is a result of a pronounced reduction in blood C_{CO_2} (and hence HCO$_3^-$) compared to only a small decrease in S_{CO_2} (Fig. 1). That dpH/dT in the open system was not closer to the closed system value may have been due to the fact that blood was equilibrated with 1% CO_2 (7.5 Torr). Clearly, similar changes in HCO_3^- concentration at physiological P_{CO2} (2–3 Torr) would cause greater changes in pH.

Our results differ from a similar *in vitro* experiment performed on sand-trout (*Cynoscion arenarius*) blood (Cameron, 1978). In that study a temperature slope of only -0.0048 U/°C was observed, which is the value one would predict based solely on the effect of temperature on pK′, as discussed previously. Similarly, C_{CO2} decreased only slightly as a result of the change in αP_{CO2} ($dC_{CO2}/dT = -0.05$ mM/°C) compared to $dC_{CO2}/dT = -0.34$ mM/°C in the present study. Why does tuna blood act so differently than sand-trout blood? More specifically, why does bicarbonate decrease so greatly in tuna blood and only slightly in sand-trout blood? It is highly unlikely that the dissimilarities are related to differences in α_{CO2} or pK′. We believe that the large reduction in C_{CO2} as temperature increases, under conditions of constant P_{CO2}, is caused by dissociation of haemoglobin (presumably histidine residues) which allows H^+ ions to combine with HCO_3^- and thereby removing HCO_3^- from the system as gaseous CO_2. This idea is supported by the fact that in plasma, under identical conditions, pH actually increased with increasing temperature. That this process does not occur in *Cynoscion* and presumably other fishes may be a reflection of the greater amount of haemoglobin present in tuna blood which would allow more protons to be released. Haemoglobin levels as high as 14–20 g/100 ml have been measured in skipjack blood (Klawe *et al.*, 1963; Perry and Daxboeck, unpublished observations) whereas most fish have haemoglobin levels in the area of 4–6 g/100 ml. Alternate possibilities are that tuna haemoglobin contains more histidine residues than in haemoglobins of other fish or that the temperature sensitivity of imidazole dissociation is somehow greater in tuna haemoglobin.

Given the results of the present study on skipjack tuna, it is not necessary to postulate extrinsic mechanisms that can add or subtract base to or from the system in response to temperature change, unlike the situation in other fish. Instead, the changes in pH and C_{CO2} can be accounted for solely by the passive, *in vitro* behaviour of the chemical buffer system found in the blood. A similar passive mechanism has recently been identified by Wood and Cameron (1984) in blue crab haemolymph. The rapid nature of such a passive system clearly is advantageous to skipjack tuna considering they make frequent vertical migrations through waters of greatly varying temperature. Rapid pH changes would not be possible if active adjustment of blood bicarbonate levels was responsible for blood pH regulation.

Acknowledgements—This study was funded by National Marine Fisheries Service, Pacific Gamefish Foundation and an NSERC operating grant to P.W.H. The authors would like to thank Dr. C. M. Wood and Dr. D. J. Randall for providing some necessary equipment. As visitors to the Kewalo Research Facility, S.F.P., C.D., B.E. and P.W.H. wish to express our thanks to the entire staff for their hospitality and support during this study. We are grateful to Dr. C. M. Wood, Dr. R. B. Boutilier and Dr. P. J. Walsh for critically reading the manuscript. S.F.P. was supported by an E.B. Eastburn Postdoctoral Fellowship.

REFERENCES

Albers C. (1970) Acid–base balance. In *Fish Physiology*, (Edited by Hoar W. S. and Randall D. J.), Vol. IV, pp. 173–208, Academic Press, New York.

Cameron J. N. (1971) Rapid method for determination of total carbon dioxide in small blood samples. *J. appl. Physiol.* **31**, 532–534.

Cameron J. N. (1978) Regulation of blood pH in teleost fish. *Respir. Physiol.* **33**, 129–144.

Cameron J. N. and Kormanik G. A. (1982) The acid–base responses of gills and kidneys to infused acid and base loads in the channel catfish, *Ictalurus punctatus*. *J. exp. Biol.* **99**, 143–160.

Carey F. G., Teal J. M., Kanwisher J. W., Lawson K. D. and Becket J. S. (1971) Warm-bodied fish. *Am. Zool.* **11**, 135–143.

Dizon A. E., Brill R. W. and Yuen H. S. H. (1978) Correlations between environment, physiology and activity and its effects on thermoregulation in skipjack tuna, *Katsuwonus pelamis*. In *The Physiological Ecology of Tunas* (Edited by Sharp G. D. and Dizon A. E.), pp. 233–259. Academic Press, New York.

Heisler N. (1980) Regulation of the acid–base status in fishes. In *Environmental Physiology of Fishes*, (Edited by Ali M. A.), Series A, Vol. 35. Nato Advanced Study Institute Series. Plenum Press, New York.

Heisler N., Weitz H. and Weitz A. M. (1976) Extracellular and intracellular pH with temperature in the dogfish, *Scyliorhinus stellaris*. *Respir. Phyisol.* **26**, 249–263.

Heisler N., Neumann P. and Holeton G. F. (1980) Mechanisms of acid–base adjustment in dogfish (*Scyliorhinus stellaris*) subjected to long-term temperature acclimation. *J. exp. Biol.* **85**, 89–98.

Howell B. J., Rahn H., Goodfellow D. and Herreid C. (1973) Acid–base regulation and temperature in selected invertebrates as a function of temperature. *Am. Zool.* **13**, 557–563.

Klawe W. L., Barrett, I. and Klawe B. M. H. (1963) Haemoglobin content of the blood of six species of scombroid fishes. *Nature, Lond.* **198**, 96.

McMahon B. R., Sinclair F., Hassall C. D., deFur P. L. and Wilkes P. R. H. (1978) Ventilation and control of acid –base status during temperature acclimation in the crab, *Cancer magister*. *J. comp. Physiol.* **128**, 109–116.

Rahn H. (1967) Gas transport from the external environment to the cell. In *Development of the Lung* (Edited by de Reuck A. V. S. and Porter R.), CIBA Foundation Symposium, pp. 3–23. Churchill, London.

Randall D. J. and Cameron J. N. (1973) Respiratory control of arterial pH as temperature changes in rainbow trout, *Salmo gairdneri*. *Am. J. Physiol.* **225**, 997–1002.

Reeves R. B. (1972) An imidazole alphastat hypothesis for vertebrate acid–base regulation: tissue carbon dioxide content and body temperature in bullfrogs. *Respir. Physiol.* **14**, 219–236.

Reeves R. B. (1976a) Temperature induced changes in blood acid–base status: pH and P_{CO2} in a binary buffer. *J. appl. Physiol.* **40**, 752–761.

Reeves R. B. (1976b) Temperature induced changes in blood acid–base status: Donnan r_{Cl} and red cell volume. *J. appl. Physiol.* **40**, 762–767.

Reeves R. B. (1977) The interaction of body temperature and acid–base balance in ectothermic vertebrates. *Ann. Rev. Physiol.* **39**, 559–586.

Rosenthal T. B. (1948) The effect of temperature on the pH of blood and plasma *in vitro*. *J. biol. Chem.* **173**, 25–30.

Severinghaus J. W., Stupfel M. and Bradley A. F. (1956) Variations of serum carbonic acid pK′ with pH and temperature. *J. appl. Physiol.* **9**, 197–200.

Truchot J. P. (1973) Temperature and acid–base regulation in the shore crab *Carcinus maenas*. *Respir. Physiol.* **17**, 11–20.

Walsh P. J. and Moon T. W. (1982) The influence of temperature on extracellular and intracellular pH in the American eel (*Anguilla rostrata*). *Respir. Physiol.* **50,** 129–140.

Wood C. M. and Jackson E. B. (1980) Blood acid–base regulation during environmental hyperoxia in the rainbow trout, *Salmo gairdneri*. *Respir. Physiol.* **42,** 351–372.

Wood C. M. and Cameron J. N. (1984) Temperature and the physiology of intracellular and extracellular acid–base regulation in the blue crab *Callinectes sapidus*. *J. exp. Biol.*, in press.

8573

Sampling Requirements for the Adult Fish Survey

SUSAN PICQUELLE[1]
Southwest Fisheries Center,
National Marine Fisheries Service, NOAA,
P.O. Box 271, La Jolla, CA 92038

ABSTRACT

The question of how many fish should be collected to estimate population fecundity parameters is addressed. The goal is to determine the optimal combination of the number of stations to occupy (*n*) and the number of fish to subsample per station (*m*) that will provide the minimum variance of parameter estimates. The collection of mature fish for this purpose is considered to be a two-stage sample design in which the total number of fish processed is equal to *n* times *m*. In most cases, the subsample of fish taken from a trawl station can be treated as a cluster sample, and a simple relationship between variance of the parameters and the sample sizes, *n* and *m*, may be established. Spawning fraction, the parameter with the largest relative variance, is chosen to evaluate alternative combinations of *n* and *m*. In terms of the total number of fish processed, it is generally more efficient in a statistical sense to occupy more trawl stations and to subsample fewer fish per station than vice-a-versa. If the major cost of collecting data is associated with ship operations, then it is cheaper to occupy fewer trawl stations and subsample more fish per station. The equations and Figure 1, based on northern anchovy data from California, provide criteria for determining the combination of *n* and *m* which achieves desired levels of variance.

INTRODUCTION

The number of independent observations directly impacts the estimated variance of a parameter; the higher the number of observations, the smaller the variance. A trawl survey is usually a two-stage sample design; hence the number of observations is determined by the number of trawls taken (n) and the number of fish subsampled from each trawl (m). However, for a fixed total sample size (nm), varying combinations of n and m will produce varying values of the estimated variance because the fish within a trawl are typically more similar than fish between trawls, that is, fish within trawls are positively correlated and hence are not independent observations. For example, the intratrawl correlation coefficient for female weight data collected during the 1980 survey was 0.60. Thus it is advantageous to find the optimal combination of n and m that will produce the minimum variance.

SAMPLE SIZE RELATIONSHIPS

In two-stage sampling, the estimates of the population mean and variance are (Cochran 1963),

$$\bar{\bar{x}} = \sum_{i=1}^{n} \frac{\bar{x}_i}{n} \quad \text{where } \bar{x}_i = \sum_{j=1}^{m} \frac{x_{ij}}{m} \tag{1}$$

$$\text{and} \quad \hat{var}(\bar{\bar{x}}) = (1-f_1)\frac{s_1^2}{n} + f_1(1-f_2)\frac{s_2^2}{nm} \tag{2}$$

$$\text{where} \quad s_1^2 = \frac{\sum_{i=1}^{n} (\bar{x}_i - \bar{\bar{x}})^2}{n-1} = \text{intertrawl component of variance,}$$

$$s_2^2 = \frac{\sum_{i=1}^{n}\sum_{j=1}^{m} (x_{ij} - \bar{x}_i)^2}{n\,(m-1)} = \text{intratrawl component of variance,}$$

$f_1 = n/N$, where N is the total number of stations, and
$f_2 = m/M$, where M is the total number of elements at each station.

(Note: for simplicity's sake, two-stage sampling with stations of equal size is used here for illustration purposes.) Equation (2) relates variance to the values of n and m, and this equation can be used to find the optimal values of n and m which will produce the minimum variance.

But first, some simplifications can be made. In the majority of fisheries surveys, the sampling fraction f_1 is negligibly small so that the value $f_1 = 0$ may be substituted into equation (2). This reduces to

$$\hat{var}(\bar{\bar{x}}) = \frac{s_1^2}{n} \tag{3}$$

and the intratrawl component of variance disappears. Because of this simplification, the trawl sample may be treated like a cluster sample. In cluster sampling, the trawl average, $\bar{x}_1$, is measured without error, i.e., every fish is measured. In two-stage sampling, the trawl average is estimated with error, but in this case that error is negligible and does not impact the total variance estimate.

By considering the subsample of fish taken from a trawl as a cluster sample, a simpler relationship between variance and values of n and m may be established. The intracluster correlation (ρ) may be expressed as a function of the ratio of the cluster-sample variance to the random-sample variance:

---

[1] Present address: Northwest and Alaska Fisheries Center, National Marine Fisheries Service, NOAA, 7600 Sand Point Way NE, Seattle, WA 98115.

$$\frac{\sigma^2_{\bar{\bar{x}}_{cluster}}}{\sigma^2_{\bar{\bar{x}}_{random}}} = 1 + \rho\,(m-1) \qquad (4)$$

where
$$\sigma^2_{\bar{\bar{x}}_{cluster}} = \frac{\sum_{i=1}^{n} (\bar{x}_i - \bar{\bar{x}})^2}{n\,(n-1)} \qquad (5)$$

and
$$\sigma^2_{\bar{\bar{x}}_{random}} = \frac{\sum_{i=1}^{n}\sum_{j=1}^{m} (x_{ij} - \bar{\bar{x}})^2}{nm\,(nm-1)}\,. \qquad (6)$$

The fish sampled during the trawl survey are used to estimate several parameters, i.e., sex ratio, spawning fraction, fecundity, and female weight. The optimal combination of m and n will not be the same for all parameters. Hence, the parameter with the largest relative variance is chosen to pick the values of m and n. This parameter is spawning fraction for the northern anchovy example.

Spawning fraction is distributed approximately as a binomial distribution. We can simplify equation (4) by substituting the variance of a binomial distribution for the random-sample variance

$$\sigma^2_{\bar{\bar{x}}_{random}} = \sigma^2_{\bar{\bar{x}}_{binomial}} = \frac{\bar{\bar{x}}\,(1-\bar{\bar{x}})}{nm}\,. \qquad (7)$$

Solving equation (4) for m after substituting equation (7) for $\sigma^2_{\bar{\bar{x}}\ random}$ gives

$$m = \frac{\bar{\bar{x}}\,(1-\bar{\bar{x}})(1-\rho)}{n\sigma^2_{\bar{\bar{x}}_{cluster}} - \bar{\bar{x}}\,(1-\bar{\bar{x}})\rho}\,. \qquad (8)$$

Values for $\bar{\bar{x}}$, ρ and $\sigma^2_{\bar{\bar{x}}\ cluster}$ are needed to specify the relationship between m and n. It is more convenient to work with the coefficient of variation (cv) rather than variance directly because one can then specify the desired precision in terms of percent of the parameter rather than in absolute terms. This changes equation (8) to

$$m = \frac{(1-\bar{\bar{x}})(1-\rho)}{n\bar{\bar{x}}\,cv^2 - (1-\bar{\bar{x}})\rho} \qquad (9)$$

where
$$cv = \frac{\sigma_{\bar{\bar{x}}_{cluster}}}{\bar{\bar{x}}}\,.$$

Considering a range of values for the coefficient of variation is useful to see how n and m change as the precision of the estimate of $\bar{\bar{x}}$ changes. It is also worthwhile to consider a range of values for $\bar{\bar{x}}$, because estimates of this are not available until after the survey, but it is possible to specify a range of values within which $\bar{\bar{x}}$ is likely to fall. A value for ρ may be selected using an estimate from previous surveys.

NUMERICAL EXAMPLE

As an example, the attached series of graphs (Fig. 1) was constructed using the estimate of ρ calculated from the 1982 survey data using Equation (4) ($\rho = 0.0448$). Values of $\bar{\bar{x}}$ range from 0.06 to 0.12 in increments of 0.02, with one graph corresponding to each value of $\bar{\bar{x}}$. On each graph are five lines corresponding to five values of the desired coefficient of variation (0.100 to 0.200). The vertical axis is m, the subsample size; and the horizontal axis is n, the number of trawls.

These graphs do not serve to pinpoint the precise combination of m and n that is optimal. Instead, they illustrate how n and m together determine the precision of the estimate, given the value of the estimate. They suggest general sampling strategies rather than specific criteria.

It is generally more efficient (in terms of number of fish processed) to take more trawls and fewer fish per trawl than vice-a-versa. For example, consider a spawning fraction of 0.10 and a desired coefficient of variation of 0.125. If 80 trawls are taken, then 10 fish should be subsampled, for a total of 800 fish. On the contrary, if only 50 trawls are taken, then 26 fish need to be subsampled, for a total of 1,250 fish. This is true because the fish within each trawl tend to be positively correlated and hence are not independent observations, while the fish between trawls are uncorrelated, thus contributing more information per fish.

COST CONSIDERATIONS

The major cost of data collection is associated with ship operations, not with processing the fish in the laboratory. For a fixed number of fish sampled, it is much cheaper to take fewer trawls and larger subsamples, although this reduces the precision of the estimates. Thus, what is more efficient statistically (many trawls and small subsamples) is the exact opposite of what is more efficient financially (few trawls and large subsamples). If the costs of taking a trawl (C_1) and of processing a fish (C_2) are known, these costs may be incorporated in the relationship between n and m and a new function may be derived which minimizes total cost (C),

$$C = nC_1 + nmC_2\,. \qquad (10)$$

We wish to minimize C under the constraint of Equation (9).

$$C = nC_1 + nC_2\left[\frac{(1-\bar{\bar{x}})(1-\rho)}{n\bar{\bar{x}}\,cv^2 - (1-\bar{\bar{x}})\rho}\right]. \qquad (11)$$

C is minimized by setting $\frac{\partial C}{\partial n} = 0.$

This results in the following values for n and m:

$$n = \frac{C_1(1-\bar{\bar{x}})\rho + (1-\bar{\bar{x}})\sqrt{C_1C_2\rho(1-\rho)}}{C_1\bar{\bar{x}}\,cv^2} \qquad (12)$$

$$m = \left(\frac{(1-\rho)C_1}{\rho C_2}\right)^{1/2}. \qquad (13)$$

Consider the example presented earlier where $\bar{\bar{x}} = 0.10$ and the desired coefficient of variation is 0.125 (again using $\rho = 0.0448$ from the 1982 survey data). Suppose the cost of taking one trawl (C_1) is \$1,000 and the cost of processing one fish (C_2) is \$25. These conditions result in the values minimizing cost of $n = 45$ and $m = 29$.

Frequently the number of trawls taken is determined by factors not related to desired precision and not directly controllable, such as the number of days at sea, weather condition, and the success rate of catching the target species. Before a survey begins, only the number of days at sea is known; however, predictions about the other two factors mentioned are available, so that an approximate number of trawls can be deduced. Then the graphs may be used to find the necessary value of m to attain the desired coefficient of variation.

Another consideration of selecting n and m is the expected number of spawning females subsampled in a trawl. If the spawning fraction is 0.10, and only 10 females are subsampled from each trawl, then the expected number of spawning females sampled from each trawl is only 1, based on a binomial distribution where $n = 10$ and $p = 0.10$. This will lead to a high proportion (35% on average) of trawl subsamples with no spawning females, thus inflating the variance. By raising m to 15 females, the average percent of trawl subsamples with no spawning females drops to 21%; for 20 females the percent is 12%.

LITERATURE CITED

COCHRAN, W. G.
1963. Sampling techniques. John Wiley and Sons, N.Y., 413 p.

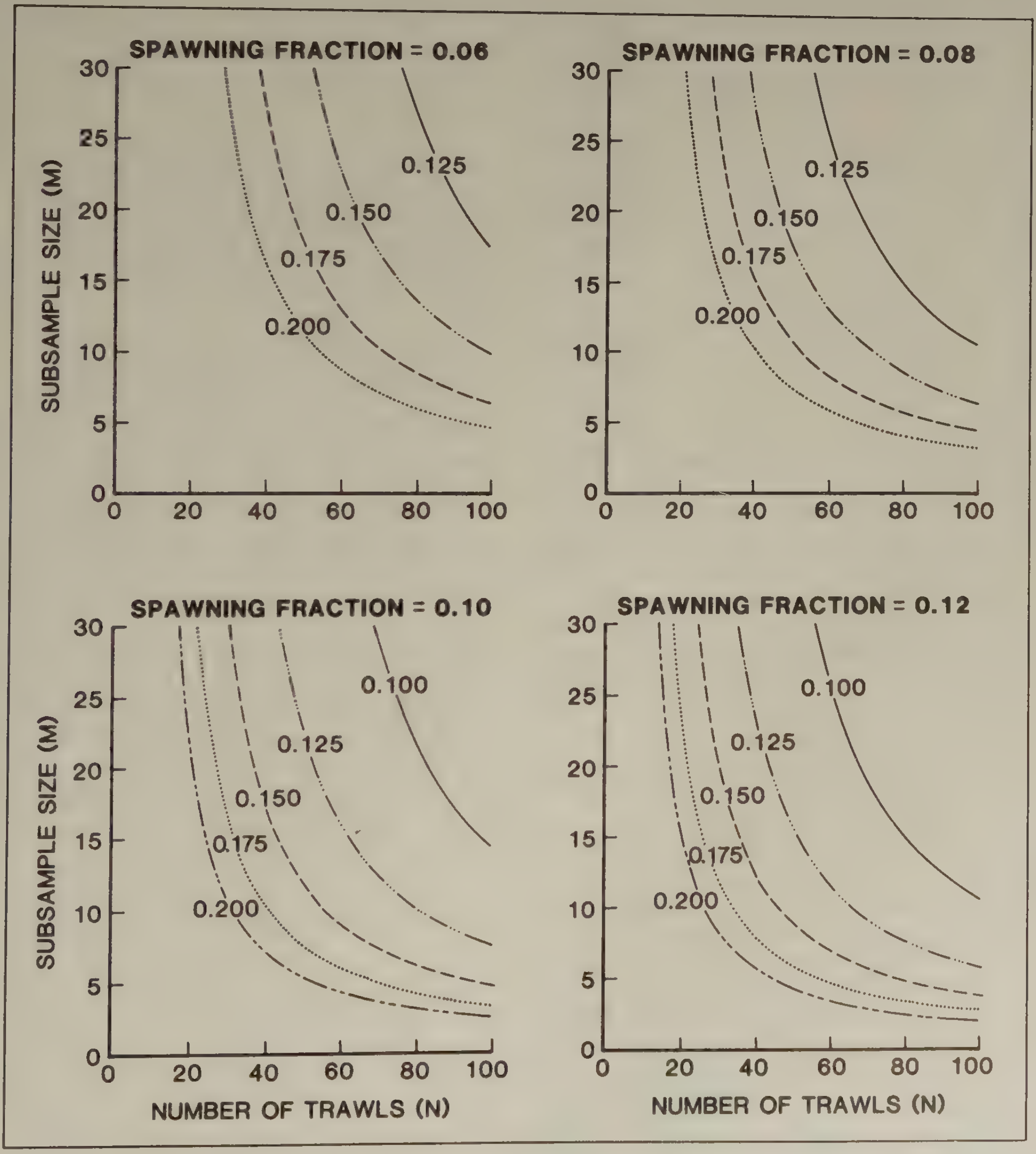

Figure 1.—Relationship between subsample size and number of trawls for a range of values for spawning fraction and coefficient of variation.

8574

Parameter Estimation for an Egg Production Method of Northern Anchovy Biomass Assessment

SUSAN PICQUELLE and GARY STAUFFER[1]
Southwest Fisheries Center,
National Marine Fisheries Service, NOAA,
P.O. Box 271,
La Jolla, CA 92038

ABSTRACT

The estimate of daily egg production is derived from the exponential mortality model fit to the egg density data generated by the plankton survey. The specific formulation of the model used in any particular application depends on the availability of computer programs to run the regression analysis. The model also provides an estimate of egg mortality. Stratification and station weighting schemes depend on survey station pattern. Poststratification of plankton stations is recommended for eliminating those plankton stations occupied that lie beyond the spawning area.

The adult spawning parameters for the northern anchovy example are estimated from trawl survey data using the equations for the sample mean and variance from cluster sampling theory. The choice of the most appropriate estimate in any particular application depends on the sample design. The need for stratifying the survey depends on whether the daily population fecundity parameters change in a consistent fashion over the range and duration of the survey.

The estimation of average weight is straightforward except that the weight of females with hydrated ovaries must be adjusted downward to correct for the temporary weight gain from the increased fluid in the ovaries. Since batch fecundity cannot be measured for each female fish, it is estimated for each individual from a regression model of batch fecundity and ovary-free body weight derived from a sample of female fish with hydrated ovaries. The station value for batch fecundity is estimated as the sample mean of the estimated fecundities. The variance of the mean fecundity, however, is adjusted to include the additional variance resulting from the regression estimation.

For the northern anchovy trawl survey, spawning fraction is the proportion of the mature females which have day-1 postovulatory follicles. Evidence from these trawl surveys indicate female fish classed as day-0 spawners are oversampled. The number of mature females per station is adjusted to compensate for this bias. The sex ratio parameter is the fraction of the mature population that is female, based on weight rather than numbers. Sex ratio data are best generated from a second subsample. For these trawl surveys, the sampling bias of day-0 spawning females occurs during the peak hours of the evening spawning period and impacts the estimates of spawning fraction and sex ratio.

INTRODUCTION

The development of equations for estimating egg production parameters is based on statistical procedures that are applicable to survey and sampling designs and that give valid estimates of the parameters and their variances. The purpose of this paper is to present the statistical equations for estimating daily egg production and daily specific[2] fecundity parameters and the associated variance estimates that have been used for the northern anchovy. For convenience, a summary of the parameter values estimated for the northern anchovy from 1980 to 1984 is included in Table 1.

Table 1.—Time series of egg production parameters (1980-84).

Parameters		1980	1981	1982	1983	1984
Daily egg production (10^{12} eggs/d)	*PA*	26.34	20.96	13.51	17.25	12.98
Average female weight (g)	*W*	17.44	13.37	18.83	11.20	12.02
Batch fecundity (no. eggs/batch per mature female)	*F*	7,751	8,329	10,845	5,297	5,485
Spawning fraction (no. spawning females per mature female)	*S*	0.142	0.106	0.120	0.094	0.160
Sex ratio (no. females/total)	*R*	0.478	0.501	0.472	0.549	0.582
Daily specific fecundity (no. eggs/g biomass per d)		30.28	33.03	32.53	24.35	42.43
Spawning biomass (10^3 t)	*B*	870	635	415	652	309

DAILY EGG PRODUCTION

The estimate of daily production of eggs released into the sea, P, by spawning adult fish is derived by regressing the counts of eggs on their age using the exponential mortality model. This model assumes a constant mortality rate.

$$P_{ijk} = P_i e^{(-Zt_{ijk})} + \epsilon_{ijk} \qquad (1)$$

where P_{ijk} = the number of eggs in day k age category from station j in stratum i,
t_{ijk} = the age in days measured as the elapsed time from the specified spawning time, t_0, to the time of sampling of station j in stratum i,
P_i = the daily egg production per unit area in stratum i,
Z = the daily rate of instantaneous egg mortality, and
ϵ_{ijk} = the additive error term.

A number of regression procedures can be used to estimate P and Z from the observations of P_{ijk} and t_{ijk} depending on the design of the survey and the availability of statistical computer programs.

First, the need to stratify the plankton survey should be evaluated. Stratification is usually undertaken to reduce the variance of parameter estimates. If more than one major spawning area exists, or if the survey is conducted over a relatively long period such that spawning rates differ among areas or over time, stratification of the data after the survey would be appropriate. This occurred in the anchovy spawning survey conducted in 1983 (Picquelle and Hewitt 1984).

---

[1] Present addresses: Northwest and Alaska Fisheries Center, National Marine Fisheries Service, NOAA, 7600 Sand Point Way NE, Seattle, WA 98115.

[2] Daily specific fecundity = number of eggs produced/gram of biomass per day.

In addition, the total survey area may be considerably larger than the spawning range. This has been the case for the anchovy resource off the California coast. The anchovy surveys are intentionally designed to sample the full range of anchovy spawning, knowing that in any one year the spawning will occur over a much smaller area within the range. As a result, many stations are beyond the spawning area of anchovies and contribute a large number of stations with zero egg counts, thus inflating the variance of the egg count data set. To reduce the impact of these zero-count stations, the total survey area is poststratified into two strata depending on the presence or absence of eggs in the sample. Stratum 0 contains the stations beyond the geographic area of spawning so that P is zero for stratum 0. The geographic area containing all the anchovy eggs and the few embedded stations with zero egg counts make up stratum 1. In this latter case, the size of the geographic area of stratum 1, A_1, and the number of occupied stations, n_1, become random variables with variances and expected values. The magnitude of this added variance is negligible if n_1 is larger than 100 (Jessen 1978). Poststratification of the stations to eliminate those stations beyond the spawning area is a recommended procedure for estimating egg production.

In addition to stratification, it is desirable to increase the density of plankton stations within the geographic area where adult spawning is expected. Increased sample size in this area will reduce the variance of P for the positive stratum. To correct for differences in station density, the egg count observations by station need to be weighted by a factor proportional to their representative area such that the sum of the station weights in the positive stratum, $i=1$, equals n_1, the total number of stations in this stratum, i.e.,

$$\sum_{j=1}^{n_1} w_{1j} = n_1 .$$

Since the egg counts in the zero stratum are zero, weighting in that stratum is unnecessary. The preferred statistical technique for estimating parameters P and Z from Equation (1) is weighted nonlinear least squares regression fit to individual egg counts and ages from stations within the positive stratum. The computer program used for the northern anchovy case was BMDPAR (Dixon and Brown 1981).

The stratified estimate of P can be calculated as the weighted average of P_0 and P_1, where P_0 is zero by definition and P_1 is estimated by regression analysis, and the weights are the relative areas of the two stratum, i.e.,

$$P = \frac{A_1}{A} P_1 + \frac{A_0}{A} P_0$$

and the variance, adjusted for postsurvey stratification (Jessen 1978) is

$$Var(P) = (1 + \frac{1}{n})(\frac{A_1}{A} Var(P_1) + \frac{A_0}{A} Var(P_0))$$

where A_i = the area of stratum i for each region,
A = $A_1 + A_0$,
n = the total number of observations for the survey,
$Var(P_1)$ = estimated for stratum 1 from the regression analysis, and
$Var(P_0)$ = 0 by definition.

In the event that a computer program for nonlinear regression is not available, the egg mortality model must be linearized so that P and Z can be estimated by linear regression methods. The linear version of the model is

$$\ln(P_{1jk}) = \ln P_1 - Zt_{1jk} + \epsilon_{ijk} .$$

This linear model gives the error structure of ε as additive in the transformed expression. This implies a multiplicative error structure in the nonlinear model. The form of the error in either case should be studied by examining the variability about P_{1jk} versus age. This can best be accomplished by examining the residuals between the observed P_{1jk} and those predicted by the model. The antilog estimate of P will be biased. An unbiased estimate can be approximated by

$$P = e^{(\ln P + s^2/2)}$$

where s^2 is the estimated residual variance from the regression analysis, usually denoted by $s_{y \cdot x}{}^2$.

If computer facilities are not readily available, the estimation of P and Z can be further simplified. This simplification involves averaging the egg counts P_{1jk} over time intervals of equal length. A minimum of three time intervals is necessary to estimate the two parameters P and Z. For the anchovy example, five intervals of 12 h were tried. The modified mortality model in this case is[3]

$$\bar{P}_{1k} = P_1 e^{-Zt'_k} (1 - e^{-Z\Delta t}) / Z\Delta t$$

where $\bar{P}_{1k}$ = the average number of eggs of age t_k sampled during the time interval (t_k, t_{k+1}),
$t'_k = t_k - t_0$ = the time elapsed (or age) between spawning and the beginning of the time interval, k,
t_0 = the midpoint of the daily spawning period, and
Δt = the length of the time interval ($t_{k+1} - t_k$) over which P_{1jk} are averaged.

The linear form of this model is

$$\ln(P_{1k}) = \ln(P_1(1 - e^{-Z\Delta t}) / Z\Delta t) - Zt'_k$$

where the regression coefficients $b_0 = \ln(P_1(1 - e^{-Z\Delta t})/Z\Delta t)$, and $b_1 = -Z$. Substituting the value of Z from b_1 into b_0 will provide an estimate of P_1. These estimates of P and Z should be useable in most cases, but their associated variance estimates will not be realistic.

DAILY SPECIFIC FECUNDITY

Station Weighting Alternatives

In sampling theory, several estimates of the population mean are described; the choice of the most appropriate estimate depends on the sample design. Trawl surveys typically consist of a three-stage sampling design: 1) the selection of the trawl stations, 2) the catch of fish at the station, and 3) the selection of the subsample of fish from the catch. The sample design, and hence the estimate, is determined by how each of the stages is executed.

There are two common methods for selecting station locations: random sampling and judgment sampling. Under the random sampling regime, the trawl stations are distributed randomly over the survey area. The exact locations of the stations are determined principally by the requirements of convenient and efficient use of ship time, and by the desire to have stations distributed evenly over the survey area. This strategy will produce station locations independent of local fish population densities.

---

[3] McCaughran, C. A., Intl. Pacific Halibut Comm., Seattle, WA., pers. commun. May 1981.

Judgment sampling uses information independent of the trawl samples to place stations where fish abundances are high. This information may consist of a historical account of the distribution of fish based on current sea temperature and salinity data, results from a recent survey, the use of sonar to detect fish schools, or observable evidence of local fish concentrations, such as their spawning products in plankton samples. The resulting distribution of stations will be patchy, with the high densities of stations coinciding with high densities of fish. This strategy approximates the sampling technique of probability proportional to a measure of size.

The second stage of sampling, the catch of fish, is ideally a random sample of fish residing at the station. However, some bias may occur due to net design, the execution of the trawl, fish behavior, and other variables. In addition to striving for a random sample, it is also advantageous if the catch size is proportional to the number of fish at the station. This is valuable information which may be incorporated into the estimate, but this situation holds only for certain species and sampling methods.

Fish are subsequently sampled randomly from the catch. The subsample size is usually constant, but may vary with the catch size to produce a self-weighting estimate for some of the estimates presented below.

Based on this sampling structure, many specific sample designs and corresponding estimates of the population mean may be considered. The following estimates all assume that the total population size is very large and the finite population correction is approximately 1. Under these conditions, the within-subsample contribution to variance disappears because this quantity is multiplied by 1/*Nn* which is approximately 0.

If stations are selected randomly, and catch size is unrelated to fish abundance, then each station should receive equal weight and equal subsample sizes should be attempted. In this case the appropriate estimate is (Cochran 1977)

$$\bar{\bar{y}} = \frac{\sum_{i=1}^{n} \bar{y}_i}{n} \quad \text{and} \quad \hat{Var}(\bar{\bar{y}}) = \sum_{i=1}^{n} \frac{(\bar{y}_i - \bar{\bar{y}})^2}{n\,(n-1)} \tag{2}$$

where $\bar{\bar{y}}$ = the estimate of the population mean,

n = the number of stations,

$\bar{y}_i = \sum_{j=1}^{m_i} \frac{y_{ij}}{m_i}$ = the mean of the *i*th station, and

m_i = the number of fish subsampled from the *i*th catch.

This estimate is a biased estimate of the true population mean and this bias does not necessarily get small as *n* gets large. The estimate is self-weighting if m_i is constant.

A better estimate exists for the case of random station selection f the catch size is proportional to the abundance of fish at the station. This is the ratio-to-size estimate:

$$\bar{\bar{y}} = \frac{\sum_{i=1}^{n} M_i \bar{y}_i}{\sum_{i=1}^{n} M_i} \quad \text{and} \quad \hat{Var}(\bar{\bar{y}}) = \frac{\sum_{i=1}^{n} M_i^2 (\bar{y}_i - \bar{\bar{y}})^2}{\left(\sum_{i=1}^{n} \frac{M_i}{n}\right)^2 n\,(n-1)} \tag{3}$$

where M_i is the total number of the target fish species caught in the *i*th trawl. This estimate is biased because it is a ratio of two random variables, but the bias is small and gets smaller as *n* gets larger. This estimate is self-weighting when the subsampling fraction m_i/M_i is constant.

Under judgment sampling, the attempt is made to sample with probability proportional to size. If this can be accomplished, or if confidence is high that this situation is closely approximated, then the unbiased estimates of the population mean and the variance are the same as Equation (2). This estimate is self-weighting when m_i is constant.

If, instead, the stations are selected with probability proportional to u_i, a measure of size, and the catch size is proportional to the population size at the station, then the appropriate estimate is

$$\bar{\bar{y}} = \frac{1}{M_0 n} \sum_{i=1}^{n} \frac{M_i \bar{y}_i}{u_i} \quad \text{and} \quad \hat{Var}(\bar{\bar{y}}) = \frac{\sum_{i=1}^{n} \left(\frac{M_i \bar{y}_i}{u_i M_0} - \bar{\bar{y}} \right)^2}{n\,(n-1)} \tag{4}$$

where M_0 is the total population size. This estimate is self-weighting if $n u_i m_i / M_i$ is constant. However, this estimate is not very useful because M_0, the total population size, is rarely known, and the estimates of station sizes, u_i, can rarely be enumerated.

A modification of Equation (2) is used for the trawl survey for the northern anchovy. As mentioned earlier, this estimate is unbiased if sampling with probability proportional to size. The information used to detect high concentrations of anchovies is the occurrence of anchovy spawning products in the plankton samples taken concurrently, and the presence of apparent schools on the sonar. Both of these factors are good indicators of local concentrations of anchovies, and the resulting sample design is assumed to be a good approximation of sampling with probability proportional to size, justifying the use of Equation (2).

Equal subsample sizes are attempted, but occasionally a station will produce a very small catch or a catch with very few mature females (mostly males or mostly immature fish). Both situations will result in a small subsample, as most of the parameters to be estimated are for mature females. This occurrence is interpreted as meaning that an error in judgment sampling has been made. The actual size of the station, based on mature females, is much smaller than was estimated at the time the trawl station was selected. Hence, the probability of selecting that station should be adjusted *a posteriori* to reflect the actual size of the station. This is accomplished by giving these stations less weight in the estimate; each station is weighted by its subsample size, m_i. Thus, Equation (2) is modified to produce the following estimate:

$$\bar{\bar{y}} = \frac{\sum_{i=1}^{n} m_i \bar{y}_i}{\sum_{i=1}^{n} m_i} \quad \text{and} \quad \hat{Var}(\bar{\bar{y}}) = \frac{\sum_{i=1}^{n} m_i^2 (\bar{y}_i - \bar{\bar{y}})^2}{\left(\sum_{i=1}^{n} \frac{m_i}{n}\right)^2 n\,(n-1)} \tag{5}$$

If m_i is constant, this estimate simplifies to Equation (2). This estimate is biased because it is the ratio of two random variables, $m_i \bar{y}_i$ and m_i. However, the bias is of the order 1/*n*, so that the bias gets smaller as *n* gets larger.

Trawl Survey Stratification

The egg production model assumes that the parameters in the model are constant over the range and duration of the survey. If this assumption is violated, the survey should be divided into regions or time spans within which the parameters are constant. The biomass is then estimated separately for each section of the survey and then summed to produce the total biomass estimate.

An example of this situation is the Spring 1983 anchovy spawning biomass survey. Two parameters of the daily specific fecundity varied significantly with geographic regions, female weight decreased from north to south, and spawning fraction increased from north to south.

The survey area was divided into three regions: north, bight, and south (Figs. 1, 2). Figure 3 illustrates the frequency distribution for female weight by region; the average female weight for the southern region was significantly smaller than the average weights for both the bight and north regions. The pattern for spawning fraction was the opposite (Fig. 4) with the estimate for the north region being significantly smaller than the estimates for the bight and south regions.

Table 2 presents the parameter estimates and biomass estimates for each region. Each of the population fecundity estimates, *W*, *S*, *F*, and *R*, was estimated separately for each region. It was impossible to estimate P_0, egg production, independently for each region because of the small sample sizes per region. Instead, the slope of the mortality curve, *Z*, was assumed to be constant for the entire survey and hence was estimated using all the data. The intercept of the mortality curve, P_0, was allowed to vary between regions and was estimated by fitting a separate but parallel mortality curve to each region while holding the mortality estimate, *Z*, fixed at the value previously estimated.

The total biomass estimate is simply the sum of the regional biomass estimates, and the total variance estimate is also just the sum of the regional variances. This variance estimate ignores any covariance terms between regions, which is probably trivially small because all parameters were estimated using separate and independent data for each region, except for the mortality, *Z*, whose contribution to covariance is probably slight.

Table 2.—Estimates of egg production parameters and spawning biomass by region for 1983. Coefficient of variation indicated by parentheses.

Parameters		North	Bight	South	Total
Daily egg production (no. eggs/0.05 m^2 per d)	*P*	1.62 (0.671)	7.28 (0.0751)	5.06 (0.332)	
Area of region (10^{12} 0.05 m^2)	*A*	0.420	1.33	1.36	
Average female weight (g)	*W*	12.9 (0.121)	11.2 (0.0705)	9.63 (0.0385)	
Batch fecundity (no. eggs/batch per mature female)	*F*	6,285 (0.140)	5,295 (0.0882)	4,423 (0.0570)	
Spawning fraction (no. spawning females per mature female)	*S*	0.0346 (0.563)	0.103 (0.174)	0.126 (0.237)	
Sex ratio (no. females/total)	*R*	0.523 (0.0949)	0.559 (0.0736)	0.549 (0.128)	
Spawning biomass (10^3 t)	*B*	77.5 (0.897)	358 (0.214)	216 (0.419)	652 (0.211)

Parameter Estimation

The parameters of the daily population fecundity are all estimated from samples of anchovies collected on a midwater trawl survey. These parameters, female weight (*W*), batch fecundity (*F*), spawning fraction (*S*), and sex ratio (*R*), and their variances, are estimated using Equation (5) developed previously:

$$\bar{\bar{y}} = \frac{\sum_{i=1}^{n} m_i \bar{y}_i}{\sum_{i=1}^{n} m_i} \quad \text{and} \quad \hat{Var}(\bar{\bar{y}}) = \frac{\sum_{i=1}^{n} m_i^2 (\bar{y}_i - \bar{\bar{y}})^2}{\left(\sum_{i=1}^{n} \frac{m_i}{n} \right)^2 n\,(n-1)}$$

where n = the number of trawls,

m_i = the number of fish subsampled from each trawl,

$\bar{y}_i = \sum_{j=1}^{m_i} y_{ij}/m_i$ = the average value for the *i*th trawl, and

y_{ij} = the observed value for the *j*th fish sampled from the *i*th trawl.

Female weight is estimated from a fixed subsample size of mature females. The subsample size has ranged from 15 to 25 mature females for the surveys taken from 1980 through 1983; however, the targeted subsample size is not always realized, due to very small catches, a high proportion of immature fish, or a high proportion of males. The y_{ij} in Equation (5) is the whole body weight of the *j*th mature females sampled from the *i*th trawl (W_{ij}). This observed weight is adjusted downward for those females whose ovaries contain hydrated eggs because their body weight is temporarily inflated due to water retention. This adjusted weight ($\hat{W}_{ij}$) is estimated from a linear regression of whole body weight regressed on ovary-free weight (W_{ij}*) which is fit only to those females that do not have hydrated eggs.

$$\hat{W}_{ij} = \hat{\alpha} + \hat{\beta}\, W_{ij}^{*} \tag{6}$$

The observed frequency distribution of the average female weight per trawl is usually symmetrical although there may occur a hint of bimodality if there is a large 1-yr-old year class. The weights within each trawl tend to be homogeneous, suggesting that the anchovy schools are homogeneous with regard to weight.

Batch fecundity can be observed only for those females whose ovaries contain hydrated eggs. There is a high correlation between the number of eggs per batch and the ovary-free body weight. This relationship is used to estimate batch fecundity for the same mature females used to estimate female weight.

The sample of hydrated females is collected throughout the trawl survey and the number of eggs per batch (F_{ij}) and ovary-free weight (W_{ij}*) are recorded for each of these females. This data are used to fit a model regressing batch fecundity on ovary-free weight

$$F_{ij} = \alpha + \beta\, W_{ij}^{*} + \epsilon_{ij}\,. \tag{7}$$

A linear regression has explained the data satisfactorily in previous surveys, although a curvilinear model should be considered depending on the shape of the data.

Using this regression, batch fecundity is estimated for each mature female subsampled. The accuracy of the estimated batch fecundity will be improved if the distribution of weights for the sample of hydrated females used to fit the regression is similar to the distribution of weights for the total sample of females.

Equation (5) is used to estimate average batch fecundity where the y_{ij} are in this case the estimates $\hat{F}_{ij}$. However, there is an added source of variance that should be included because the $\hat{F}_{ij}$ are not observed directly but are estimates with their own associated variance. Thus, the estimate of variance is adjusted to include this additional variance (Draper and Smith 1966):

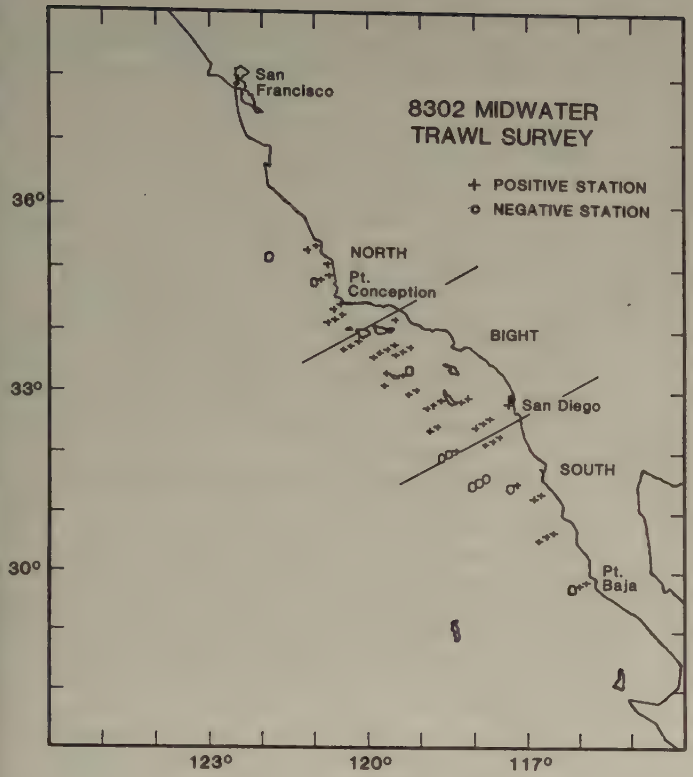
San Francisco
8302 MIDWATER TRAWL SURVEY
+ POSITIVE STATION
o NEGATIVE STATION
36°
NORTH
Pt. Conception
BIGHT
33°
San Diego
SOUTH
30°
Pt. Baja
123°
120°
117°

Figure 1.—Geographic distribution of trawl stations and positive trawls within each region.

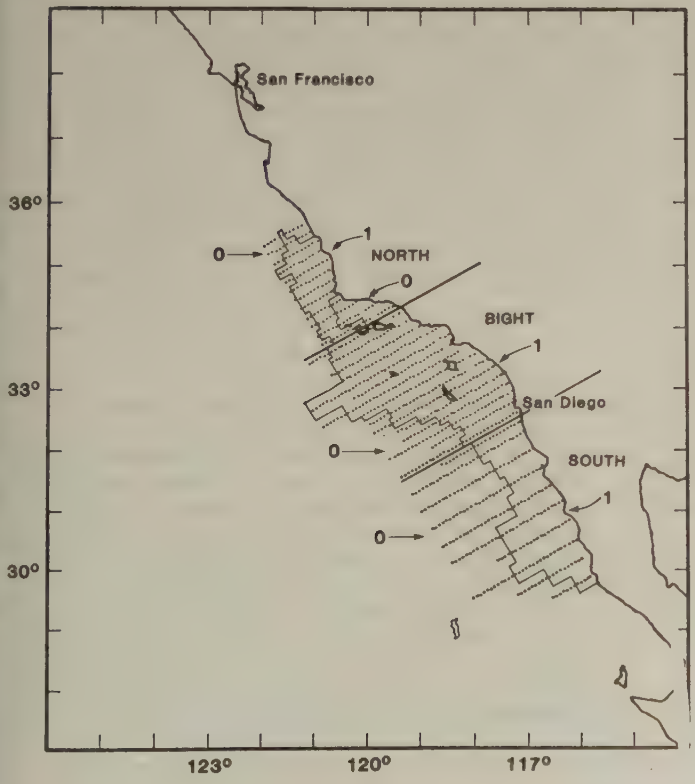
San Francisco
36°
0
1
NORTH
0
BIGHT
1
33°
San Diego
0
SOUTH
1
0
30°
123°
120°
117°

Figure 2.—Subdivision of CalVET survey into strata (0 = beyond the range of anchovy spawning; 1 = within the range of anchovy spawning) and regions (North, Bight, and South).

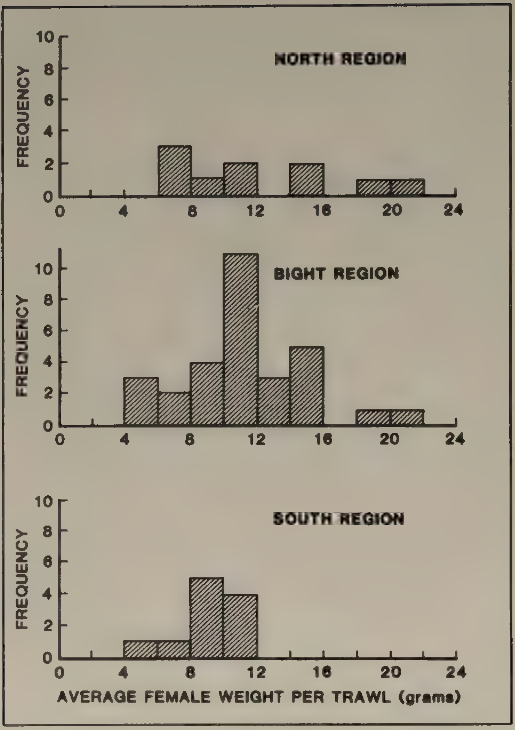

Figure 3.—Frequency distribution for average whole-body weight of mature females in grams for each region.

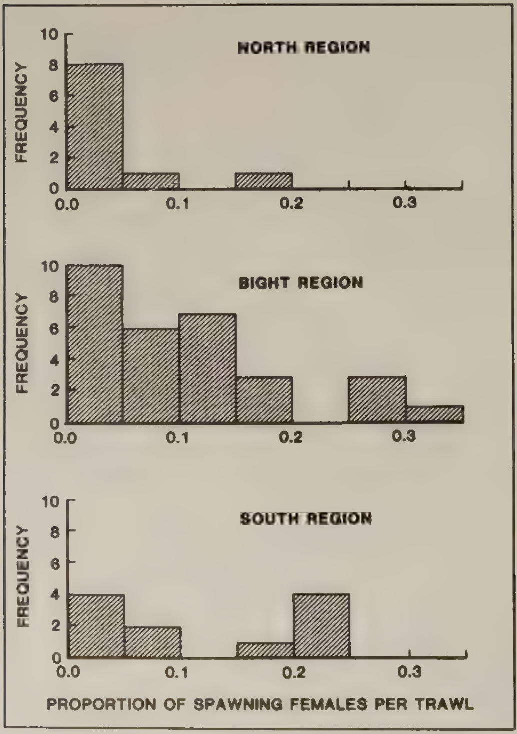

Figure 4.—Frequency distributions of spawning fractions for each region.

$$\hat{Var}(\bar{\bar{F}}) = \frac{\sum_{i=1}^{n} m_i^2 \left[\frac{(\bar{F}_i - \bar{\bar{F}})^2}{n-1} + \frac{s_h^2}{n_h} + (\bar{W}_i^* - \bar{W}_h^*)\, \hat{Var}(\hat{\beta}) \right]}{\left[\sum_{i=1}^{n} \frac{m_i}{n} \right]^2 n} \tag{8}$$

where $\bar{\bar{F}}$ = the estimate of batch fecundity for the whole population of mature females,

$\bar{F}_i$ = the average batch fecundity for the ith trawl,

$\bar{F}_i = \sum_{j=1}^{m_i} \hat{F}_{ij}/m_i$ where $\hat{F}_{ij}$ is the estimated batch fecundity for the jth female in the ith subsample,

s_h^2 = the variance about the regression (Equation (7)),

n_h = the number of hydrated females used to fit the regression (Equation (7)),

$\bar{W}_i^*$ = the average ovary-free weight for the ith trawl,

$\bar{W}_h^*$ = the average ovary-free weight for the n_h hydrated females, and

$\hat{Var}(\hat{\beta})$ = the variance of the slope of the regression (Equation (7)).

Spawning fraction is estimated using Equation (5) by setting $\bar{y}_i$ equal to the proportion of mature females in the ith trawl which have been classified as having day-1 postovulatory follicles (day-1 spawners). Thus, $\bar{\bar{y}}$ estimates the fraction of mature females in the population that are day-1 spawners, which is a measure of the fraction of mature females which are spawning on any given day.

Spawning fraction can also be estimated by the fraction of females classified as day-0 spawners. However, this fraction has been consistently higher than the fraction of day-1 spawners. Past experience has shown that using day-0 spawners may produce a biased estimate, at least for northern anchovy sampled by a trawl survey. Evidence of this conclusion will be presented in a later section.

If day-0 spawners are indeed oversampled, then day-1 spawners are undersampled. The sample of mature females from each catch may be grouped into three categories: Day-0 spawners (m_i^0); day-1 spawners (m_i^1); and day 2+ spawners (m_i^2). For a fixed subsample size, if one group is over-represented then the other two groups are under-represented. This is corrected by adjusting m_i to reflect what subsample size would have included the observed number of day-1 spawners if day-0 had not been oversampled. The number of day-0 spawners included in m_i is replaced by the observed number of day-1 spawners, since day-0 and day-1 spawners should be equal, on average, because they both measure the number of females spawning during a 24-h period. Thus, the m_i in Equation (5) is replaced by

$$m_i^* = 2m_i^1 + m_i^2 \, . \tag{9}$$

The average value of m_i^* will be smaller than the average m_i, and the resulting estimate of spawning fraction based on day-1 spawners will be larger to compensate for the bias in sampling day-0 spawners.

The parameter sex ratio is the fraction of the mature population that is female, based on weight rather than numbers. Equation (5) is again used, where m_i is the weight of the subsample rather than number, and $\bar{y}_i$ is the fraction of the subsample weight that is attributable to female fish. Both mature and immature fish are included in the estimate because it is impossible to distinguish between mature and immature males. It is assumed that sex ratio by weight is the same for both mature and immature fish.

To save effort in preserving and weighing individual fish, $\bar{y}_i$ and m_i are estimated rather than measured directly. A fixed number of fish are subsampled from each trawl and the numbers of females and males are recorded. The average weight for each sex is estimated for each trawl from a smaller fixed subsample of each sex. The total weight of each sex in the subsample is estimated by multiplying the observed number of fish of that sex by its average weight.

$$\hat{W}_i^F = m_i^F \cdot \overline{W}_i^F$$
$$\hat{W}_i^M = m_i^M \cdot \overline{W}_i^M \qquad (10)$$

where $\hat{W}_i^k$ = the total estimated weight of the kth sex in the ith subsample,
m_i^k = the number of fish of the kth sex in the ith subsample, and
$\overline{W}_i^k$ = the average weight of the kth sex in the ith subsample.

Then m_i is estimated by the sum of the estimated total weight of males plus the estimated total weight of females,

$$\hat{m}_i = \hat{W}_i^F + \hat{W}_i^M \qquad (11)$$

and $\bar{y}_i$ is the estimated total weight of females divided by m_i

$$\bar{y}_i = \hat{W}_i^F / \hat{m}_i \,. \qquad (12)$$

The parameters W_i^F and W_i^M are estimated with little error because the weights of fish within a trawl catch are quite homogeneous. Thus the added variance in estimating sex ratio, due to the fact that $\bar{y}_i$ and m_i are estimated rather than observed, is assumed to be trivial.

Sampling Bias

Spawning fraction may be estimated by either the number of day-0 spawners or the number of day-1 spawners, as each is an estimate of the number of females spawning on any given day. However, as mentioned earlier, the proportion of day-0 spawners is consistently larger than the proportion of day-1 spawners. A hypothesis on the mechanism causing this result is that females who are actively spawning are more vulnerable to capture by a midwater trawl. This hypothesis is supported by the observation that the catch of spawning females (day-0) increases significantly during the hours of the evening when spawning takes place.

This phenomenon is illustrated by Figure 5. This bar chart was calculated using data from the trawl surveys conducted from 1978 to 1980. Day-0 spawners are composed of three types of females: Females whose ovaries contain hydrated eggs which will be spawned later that evening (represented by an open bar); females whose ovaries contain postovulatory follicles indicating they have spawned earlier that evening (represented by the bar area with horizontal lines); and females whose ovaries contain both hydrated eggs and postovulatory follicles indicating they were caught during spawning (represented by vertical lines in the bars). The predominant hours of spawning are 2100-2359, when the highest number of females are caught with both hydrated eggs and postovulatory follicles in their ovaries. This is also the time period when the proportion of day-0 spawners in the catch is highest.

It should also be noted that the proportion of day-0 spawners decreases after 0300. This can be more easily seen in Figure 6, which shows the proportion of day-0 spawners by hour for each year, and all years combined. Figure 7 shows that the proportion of day-1 spawners also drops off after 0300. This is explained by an increased error rate in classifying ovaries as to the date of spawning (day-0, day-1, or later), and in subsequent years trawl catches were not made after 0300 to avoid this problem.

If one ignores the points corresponding to 0300 and later, then

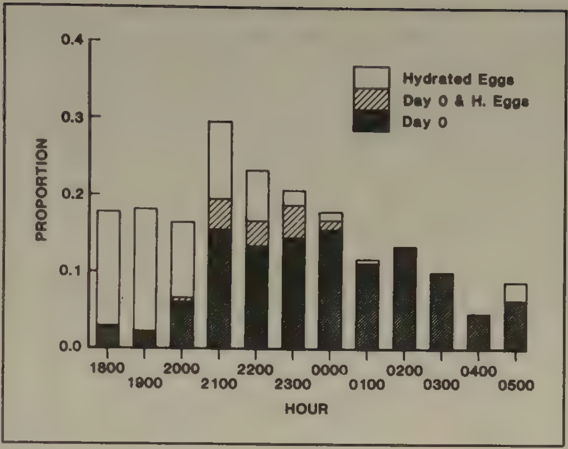

Figure 5.—Breakdown of day-0 females into ovarian categories by time of sampling.

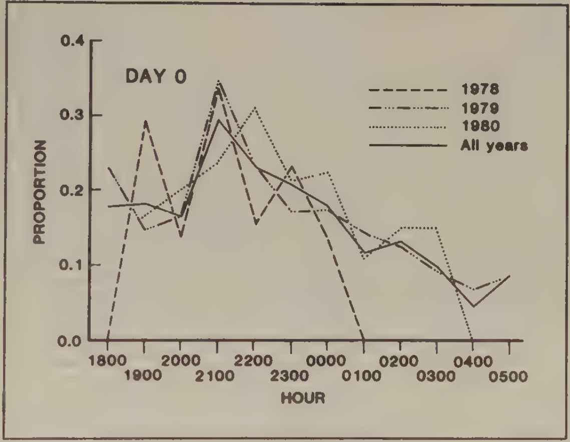

Figure 6.—Proportion of day-0 spawning females by hour for trawl surveys conducted from 1978 to 1980.

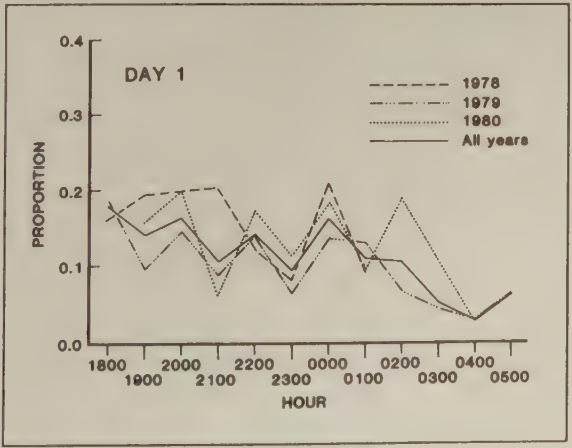

Figure 7.—Proportion of day-1 spawning females by hour for trawl surveys conducted from 1978 to 1980.

a comparison of Figures 6 and 7 shows that the plot of day-1 spawners is quite flat over time, while day-0 spawners exhibit a definite peak at 2100-2359. The comparison is highlighted in Figure 8. The proportion of day-0 females is plotted against the proportion of day-1 females for each hour, and 1-standard-error bars are drawn for day-1 proportions. The diagonal line shows the values for which the proportions of day-0 and day-1 spawners are equal. The obvious outlier points (i.e., those points furthest from the day 0=day 1 line) correspond to the time 2100-2359.

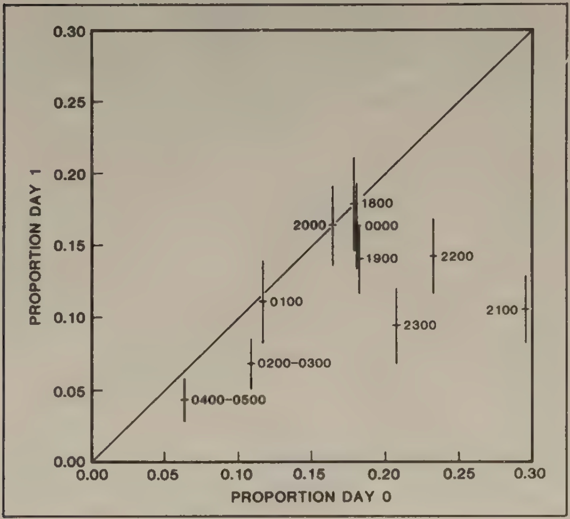

Figure 8.—Day-1 vs. day-0 females for each hook with standard error bars for day-1 females.

The effect of time on the proportion of day-0 and day-1 females in the catch can be quantified using contingency table analysis. Table 3 shows the number of females from the 1978-80 trawl survey samples, by spawning condition and time of their capture. Parentheses contain the expected number of females under the hypothesis that there is no interaction between time and spawning condition. The contribution to the χ^2 statistic by the cell is in brackets. The resulting χ^2 statistic ($\chi^2 = 38.85$, df = 16) is highly significant ($P = 0.05$), thus rejecting the hypothesis of no interaction between time and spawning condition. Examination of the individual cell's contribution to the test statistic shows that the largest deviations are due to the hour 2100-2159. Omitting this hour from the analysis produces Table 4 and a nonsignificant ($P = 0.05$) test statistic ($\chi^2 = 20.51$, df = 14). Therefore, if the hour 2100-2159 is omitted, there is no significant relationship between time and spawning condition. Based on this analysis, the conclusion is made that day-0 spawners are sampled with bias during the peak hours of spawning.

A similar scenario has been discovered for sex ratio and time. The proportion of females declines radically during the time period 2300-2359. A contingency table analysis (Table 5) shows that there is a significant interaction between time and sex ratio ($\chi^2 = 126.44$, df = 8); an examination of the individual cells shows a large deviation during time 2300-2359. When this time period is removed (Table 6), there is no significant interaction ($\chi^2 = 10.63$, df = 7). Apparently, there is a sample bias also occurring for sex ratio during the hours when spawning activity is greatest.

LITERATURE CITED

COCHRAN, W. G.
1977. Sampling techniques, 3rd ed. John Wiley and Sons, N.Y., 428 p.
DIXON, W. J., and M. B. BROWN.
1981. BMDP statistical software. Univ. Calif. Press, Berkeley, CA., 735 p.
DRAPER, N. R., and H. SMITH.
1966. Applied regression analysis. John Wiley & Sons, N.Y., 407 p.
JESSEN, R. J.
1978. Statistical survey techniques. John Wiley & Sons, N.Y., 520 p.
PICQUELLE, S. J., and R. P. HEWITT.
1984. Estimates of the spawning biomass of the northern anchovy for the 1983-84 California fishing season. Calif. Coop. Oceanic Fish. Invest. Rep. 25:16-27.

Table 3.—Contingency table analysis of spawning condition by time. Each cell contains the observed count, the expected count in parentheses, and the contribution to the χ^2 statistic in brackets.

	Time (h)									
Spawning condition	1800-1859	1900-1959	2000-2059	2100-2159	2200-2259	2300-2359	0000-0059	0100-0159	0200-0259	Total
Day-0	25 (27.5) [0.22]	42 (45.3) [0.24]	30 (35.9) [0.96]	67 (44.5) [11.36]	49 (41.4) [1.41]	30 (28.4) [0.09]	29 (31.8) [0.24]	19 (32.0) [5.26]	9 (13.3) [1.41]	300
Day-1	25 (17.8) [2.87]	31 (29.4) [0.08]	30 (23.3) [1.91]	19 (28.9) [3.41]	27 (26.9) [0.00]	12 (18.5) [2.27]	26 (20.6) [1.39]	18 (20.8) [0.37]	7 (8.7) [0.32]	195
Day-2+	90 (94.7) [0.23]	158 (156.3) [0.02]	.23 (123.8) [0.01]	141 (153.6) [1.03]	135 (142.7) [0.42]	103 (98.1) [0.25]	107 (109.6) [0.06]	126 (110.3) [2.25]	52 (46.0) [0.78]	1,035
Total	140	231	183	227	211	145	162	163	68	1,530

$\chi^2 = 38.85$, df = 16
$\chi^2_{16}(0.95) = 26.3$

Table 4.—Contingency table analysis of spawning condition by time, in which the hour 2100-2159 has been omitted. Each cell contains the observed count, the expected count in parentheses, and the contribution to the χ^2 statistic in brackets.

	Time (h)								
Spawning condition	1800-1859	1900-1959	2000-2059	2200-2259	2300-2359	0000-0059	0100-0159	0200-0259	Total
Day-0	25	42	30	49	30	29	19	9	233
	(25.0)	(41.3)	(32.7)	(37.7)	(25.9)	(29.0)	(29.1)	(12.2)	
	[0.00]	[0.01]	[0.23]	[3.37]	[0.64]	[0.00]	[3.53]	[0.82]	
Day-1	25	31	30	27	12	26	18	7	176
	(18.9)	(31.2)	(24.7)	(28.5)	(19.6)	(21.9)	(22.0)	(9.2)	
	[1.96]	[0.00]	[1.13]	[0.08]	[2.94]	[0.78]	[0.73]	[0.52]	
Day-2+	90	158	123	135	103	107	126	52	894
	(96.1)	(158.5)	(125.6)	(144.8)	(99.5)	(111.1)	(111.8)	(46.7)	
	[0.38]	[0.00]	[0.05]	[0.66]	[0.12]	[0.15]	[1.79]	[0.61]	
Total	140	231	183	211	145	162	163	68	1,303

$\chi^2 = 20.51$, df $= 14$

$\chi^2_{14}(0.95) = 23.7$

Table 5.—Contingency table analysis of sex ratio by time. Each cell contains the observed count, the expected count in parentheses, and the contribution to the χ^2 statistic in brackets.

	Time (h)									
Sex	1800-1859	1900-1959	2000-2059	2100-2159	2200-2259	2300-2359	0000-0059	0100-0159	0200-0259	Total
Female	153	349	189	271	227	189	163	187	71	1,799
	(131.2)	(331.2)	(160.3)	(268.3)	(198.7)	(321.9)	(154.4)	(175.5)	(57.4)	
	[3.62]	[0.96]	[5.13]	[0.03]	[4.03]	[54.88]	[0.48]	[0.75]	[3.23]	
Male	158	436	191	365	244	574	203	229	65	2,465
	(179.8)	(453.8)	(219.7)	(367.7)	(272.3)	(441.1)	(211.6)	(240.5)	(78.6)	
	[2.64]	[0.70]	[3.74]	[0.02]	[2.94]	[40.05]	[0.35]	[0.55]	[2.36]	
Total	311	785	380	636	471	763	366	416	136	4,264

$\chi^2 = 126.44$, df $= 8$

$\chi^2_8(0.95) = 15.5$

Table 6.—Contingency table analysis of sex ratio by time, in which the hour 2300-2359 has been omitted. Each cell contains the observed count, the expected count in parentheses, and the contribution to the χ^2 statistic in brackets.

	Time (h)								
Sex	1800-1859	1900-1959	2000-2059	2100-2159	2200-2259	0000-0059	0100-0159	0200-0259	Total
Female	153	349	189	271	227	163	187	71	1,610
	(143.0)	(361.0)	(174.8)	(292.5)	(216.6)	(168.3)	(191.3)	(62.5)	
	[0.70]	[0.40]	[1.16]	[1.58]	[0.50]	[0.17]	[0.10]	[1.14]	
Male	158	436	191	365	244	203	229	65	1,891
	(168.0)	(424.0)	(205.2)	(343.5)	(254.4)	(197.7)	(224.7)	(73.5)	
	[0.59]	[0.34]	[0.99]	[1.34]	[0.43]	[0.14]	[0.08]	[0.97]	
Total	311	785	380	636	471	366	416	136	3,501

$\chi^2 = 10.63$, df $= 7$

$\chi^2_7(0.95) = 14.1$

8575

THE MARINE BIRDS OF ALIJOS ROCKS, MEXICO

ROBERT L. PITMAN, National Marine Fisheries Service, Southwest Fisheries Center,
P.O. Box 271, La Jolla, California 92038

Alijos Rocks (24°57'N, 115°45'W) lie 185 nautical miles almost due west of Cabo San Lazaro, off southwestern Baja California, Mexico (Figures 1-5). Their jagged, volcanic spires consist of three main stacks and numerous smaller rocks. South Rock, the largest of the group, rises 34 m above the sea; North Rock is 22 m high and Middle Rock, the smallest, is approximately 18 m high. The total top surface area of the three main pinnacles is under ¼ acre (0.1 hectare).

The only published accounts of biological surveys of Alijos Rocks come from Hanna (1926) and McLellan (1926), who spent 3 hours rowing among the rocks on 24 April 1925, and Murphy (1958) who visited the area on 9 November 1956. Since 1974 I have passed by these pinnacles five times recording bird and mammal observations while aboard research vessels. A list of survey dates and pertinent comments is given in Table 1. In addition, Bayard Brattstrom visited Alijos Rocks on 10 May and 15 November 1953, and David Au surveyed them on 7 December 1976 by helicopter from a passing research vessel.

Although Alijos Rocks maintain only small populations, the composition of the avifauna, with mixed zoogeographic affinities, is unique. It therefore seems worthwhile to update the current status of marine birds that occur there.

SPECIES ACCOUNTS

EARED GREBE (*Podiceps nigricollis*). A pair was swimming close to the rocks on 14 January 1983.

LAYSAN ALBATROSS (*Diomedea immutabilis*). There are no historical accounts of any albatrosses from Alijos Rocks. I first saw Laysan Albatrosses there on 29 February 1976, when 10 were present around the rocks, including 6 on the water between two of the larger stacks. Later that year D. Au (pers. comm.) reported one in the area on 7 December. On 15 May 1982, four were present, and when I passed near the area again on 14 January 1983 approximately 15 were soaring in the updrafts of the pinnacles or swimming on the water. Up to 12 were sitting on the water next to the ship as we drifted around the rocks on 10 April 1983, and 4, probably different birds, followed the ship several miles north of Alijos Rocks.

During the January 1983 visit to Alijos Rocks small groups of 4 to 6 albatrosses were sitting on the water facing each other, clapping their bills, and bobbing their heads up and down rapidly. They were also bowing forward, turning their wings up, and dipping their bills into the water off to the side; they appeared to lock beaks occasionally. In April 1983 bill-clapping was still common and I regularly heard a whistling whinny as the birds sat on the water near the vessel. No head-bobbing was noted at that time but some head and face allo-preening was observed. These behaviors are important components of the breeding displays of the Laysan Albatross (Rice and Kenyon 1962b). In January 1983, one (or more?) albatross flew over South Rock several times and dropped its feet as it stalled less than 0.5 m over the surface of the stack in an apparent attempt to land. Each time it averted at the last moment and was never actually seen to alight.

Western Birds 16:81-92, 1985

Table 1. Surveys of Alijos Rocks, Mexico, by the author.

Date	Sea Temperature (°C)	Comments
16 Nov. 1974	21.1	Passed 1.5 nautical miles off east side of the rocks stopping <10 min.
29 Feb. 1976	18.7	Spent 5 hrs. in the morning drifting and fishing 0.5 nautical miles off rocks.
15 May 1982	18.5	Cruised along west side of rocks 0.5 nautical miles offshore without stopping; surveyed site with 25x, 150 mm mounted spotting binoculars.
14 Jan. 1983	20.4	Spent 50 min. circling the rocks at a distance of 0.5 nautical miles surveying with mounted spotting binoculars.
10 Apr. 1983	19.1	Drifted for 3.5 hrs. within 500 m of the rocks surveying with mounted spotting binoculars.

This species now occurs annually at Alijos Rocks for at least the duration of the breeding season (November-August in the Hawaiian Islands; Rice and Kenyon 1962b). None of the earlier expeditions to Alijos reported any species of albatross there and Sanger (1974) indicated that Laysans in the eastern Pacific range south only to about 28°N (northern Baja). Friedmann et al. (1950) reported they were "formerly fairly common" off central Baja but did not elaborate. Other records, however, show that Laysan Albatross does occur off southern Baja California, and occasionally further south, with some regularity. Perhaps this occurrence is recent.

Table 2 lists additional sightings of Laysan Albatrosses from Baja California and elsewhere in the southeast portion of its range. Dunn and Unitt (1977) reported an inland sighting north of Salton Sea, California, on 5 May 1976, and surmised that the bird had become "trapped" in the Gulf of California and continued overland in its northward migration. A Laysan found in Yuma, Arizona, on 14 May 1981, one found dead near Blaire Valley, California, on 28 May 1982, and one present at Salton Sea, California, on 21 May 1984 all probably suffered the same fate (McCaskie 1984). While these records may only reflect an increase in observer coverage, they and other data suggest that the Laysan Albatross may be expanding its range.

Historically all of the North Pacific albatrosses (including Black-footed Albatross, *D. nigripes*, and Short-tailed Albatross, *D. albatrus*) were considerably more numerous and widespread than they are now. Japanese feather hunters at the turn of the century, and then World War II military operations, depleted albatross populations and even eliminated some colonies (Rice and Kenyon 1962a). Although no albatross has been known to breed in the eastern North Pacific in recent times, albatross colonies in the central and western North Pacific were more widely distributed prior to human interference (Rice and Kenyon 1962a).

At present almost all Laysan Albatrosses breed in the Leeward Hawaiian Islands, but very small numbers have also nested in the main Hawaiian Islands including Moku Manu off Oahu and on Niihoa (Richardson 1957), and more recently on Kilauea Point, Kauai (see Pyle 1983). Hasegawa (1978) recently reported nesting on Bonin Island, Japan, which is the only modern record away from the Hawaiian chain.

The Laysan is now by far the most abundant albatross in the North Pacific, and some of the large protected colonies in the Leeward Hawaiian chain are likely at preexploitation levels and still growing (Rice and Kenyon 1962a, M. Naughton pers. comm.). If so, surplus birds may be available for colonization elsewhere in the North Pacific. This species typically nests on sandy atolls, but a few birds have bred on the tiny rocky stacks of Gardner Pinnacles in the Leeward Hawaiian Islands (Rice and Kenyon 1962a). Though there were no signs of actual nesting or even of adults roosting at Alijos Rocks in 1983, a breeding population may be established there in the near future.

BLACK-FOOTED ALBATROSS (*D. nigripes*). One, 20 nautical miles north of Alijos on 29 February 1976.

NORTHERN FULMAR (*Fulmarus glacialis*). Four all-dark fulmars scavenged around the boat as we fished just off the rocks in February 1976. In 1976 a huge influx of fulmars and Black-legged Kittiwakes occurred off the western United States, with large die-offs occurring at least as far south as southern California in February and March (Ainley 1976, Pitman pers. obs.). Fulmars normally venture as far south as Alijos only during "flight years."

Murphy (1958) collected a dark-phase fulmar on 12 December 1956 at 23°31'N, 111°22'W, which he felt was probably the southernmost record for a Northern Fulmar in any ocean. On 28 February 1976 I found a dead white-phase fulmar at 22°38'N, 115°15'W [San Diego Natural History Museum (SDNHM) 39789]. It was fairly fresh but may have drifted a considerable distance after dying. On 29 November 1983 I saw a dark-phase fulmar at 22°03'N, 114°55'W, and saw several others farther north.

Table 2. Laysan Albatross sightings off Baja California, Mexico.

Date	Position	Number	Observer
11 Apr. 1975	16°10'N 105°01'W	1	G. Friedrichsen
26 Feb. 1976	18°59'N 127°10'W	1	J. Dunn & P. Unitt (1977)
29 Feb. 1976	24°57'N 115°45'W (Alijos Rocks)	10	R. Pitman
7 Dec. 1976	24°57'N 115°45'W (Alijos Rocks)	1	D. Au
5 Jan. 1977	30°49'N 118°24'W	1	R. Pitman
4 Mar. 1979	19°00'N 111°00'W	2	D. Au
10 Mar. 1979	30°53'N 116°41'W	1	R. Pitman
4 Jan. 1980	29°53'N 118°03'W*	2	R. Pitman
18 Feb. 1980	10°33'N 113°40'W	1	G. Anderson
1 Mar. 1980	21°08'N 126°32'W	1	R. Pitman
3 Mar. 1980	26°50'N 121°54'W*	2	R. Pitman
4 Mar. 1980	30°25'N 120°13'W*	3	R. Pitman
22 Mar. 1980	28°11'N 115°59'W	1	R. Pitman
23 Mar. 1980	23°32'N 114°27'W	1	R. Pitman
2 Apr. 1981	20°28'N 110°35'W	1	J.R. Jehl, Jr.
21 Feb. 1982	24°49'N 113°12'W	1	R. Pitman
15 May 1982	24°57'N 115°45'W (Alijos Rocks)	4	R. Pitman
14 Jan. 1983	24°57'N 115°45'W (Alijos Rocks)	15	R. Pitman
7 Mar. 1983	29°39'N 117°20'W	1	G. Friedrichsen
25 Mar. 1983	16°32'N 105°43'W	1	G. Friedrichsen
29 Mar. 1983	11°22'N 109°25'W	1	J. Cotton
10 Apr. 1983	24°57'N 115°45'W (Alijos Rocks)	16	R. Pitman

*noon ship position

COOK'S PETREL (*Pterodroma cookii*). These petrels were abundant in the vicinity on 15 May 1982. An estimated 75 were foraging in association with a school of Common Dolphins (*Delphinus* sp.) ½ nautical mile north of the rocks. This species was noted during every survey and is a common resident off Baja during the boreal summer (Pitman unpubl. data).

SOOTY SHEARWATER (*Puffinus griseus*). One bird, 5 nautical miles north, and two others, ½ nautical mile north of the rocks, on 15 May 1982.

TOWNSEND'S SHEARWATER (*P. auricularis*). Identification of this shearwater is based on a sharply demarcated black and white color pattern, conspicuous white rump patches and fluttering flight. I saw one 5 nautical miles north of the rocks on 15 May 1982, which is as far north as this species has been known to range (Jehl 1982). Seven more were seen within 20 nautical miles south of Alijos Rocks on the same date. These birds were presumably part of a northward, post-breeding dispersal from nesting colonies on the Revillagigedo Islands.

BLACK-VENTED SHEARWATER (*P. opisthomelas*). A brownish "Manx-type" shearwater seen 46 nautical miles southeast of Alijos Rocks on 8 March 1979 was probably this species; two positively identified birds were circling in the immediate area of the rocks on 10 April 1983. Identifying characters included rapid wingbeat, brown upperparts and white below with a smudgy brown chest. This species typically requires soil for excavating nest burrows (Palmer 1962), but also nests in rock crevices (Jehl pers. obs.). Conceivably a few pair may breed on the soilless rocks of Alijos.

GALAPAGOS STORM-PETREL (*Oceanodroma tethys*). Murphy (1958) collected two of these petrels on 10 November 1956 at 22°57'N, 113°34'W, "a few miles N of the isolated Alijos Rocks" (actually 175 nautical miles southeast of Alijos). In November 1974 I saw two individuals 20 nautical miles north of the rocks and four others closer in.

LEACH'S STORM-PETREL (*O. leucorhoa*). This species has been common in the area during every visit. Murphy (1958) also found them common in the vicinity in November 1956.

On 15 May 1982, I observed at least three dark-rumped, medium-sized storm-petrels fluttering about South Rock in broad daylight (about 1400). They hovered within 10-15 cm of the cliff face at a height of up to 23 m above the sea surface and were apparently investigating nest sites. I presumed they were all Leach's Storm-Petrels. On 10 April 1983 I saw an all-dark Leach's Storm-Petrel fluttering about South Rock at 0800 while another flew from the rock out to sea.

If this species does nest here, it would be the southernmost location in the North Atlantic or the Pacific, although Imber and Lovegrove (1982) have reported a case of potential breeding off New Zealand. It also appears that the normally nocturnal Leach's Storm-Petrel has taken to visiting nest sites by day at Alijos Rocks, possibly owing to a lack of avian predators. Harris (1969) found a similar situation for Galapagos Storm-Petrels breeding in the Galapagos Islands.

BLACK STORM-PETREL (*O. melania*). Eight individuals were within 40 nautical miles of the rocks in November 1974.

RED-BILLED TROPICBIRD (*Phaethon aethereus*). Apparently this species is a year-round resident; I saw it on every trip to Alijos Rocks. Hanna (1926) saw tropicbirds in April 1925 on North Rock and presumed they were breeding. Brattstrom (pers. comm.) saw three in November 1953, and Murphy (1958) found them "in abundance" and courting in November 1956, when he collected a breeding male. I have observed roosting and nesting only on South Rock and suspect it may be the only rock where they are now breeding. The current population is about seven pairs. This is the northernmost colony for this species in the eastern Pacific, outside the Gulf of California.

MASKED BOOBY (*Sula dactylatra*). Boobies are year-round residents. They were present on North and South rocks and were presumed breeding when Hanna (1926, McLellan 1926) and company collected an immature bird in April 1925. Brattstrom (pers. comm.) estimated 25 in May 1953 and Murphy (1958) found an unspecified number of young and adults associated with the colony in November 1956.

I estimated 30 of these boobies in February 1976 and Au (pers. comm.) reported "no more than 30" in December of that year. I estimated 30 again in May 1982 and 35 in January 1983. My largest count, however, was in April 1983, when 65 (including two large downy young) were present on North Rock and 15 (including one chick) were on South Rock. The majority of the booby activity is currently centered on North Rock, where most of the roosting and nesting take place. This rock is presumably the "easternmost of the three stacks" to which Murphy (1958) refers.

The Alijos Rocks breeding population is the northernmost in the eastern Pacific and consists of approximately 50 pairs.

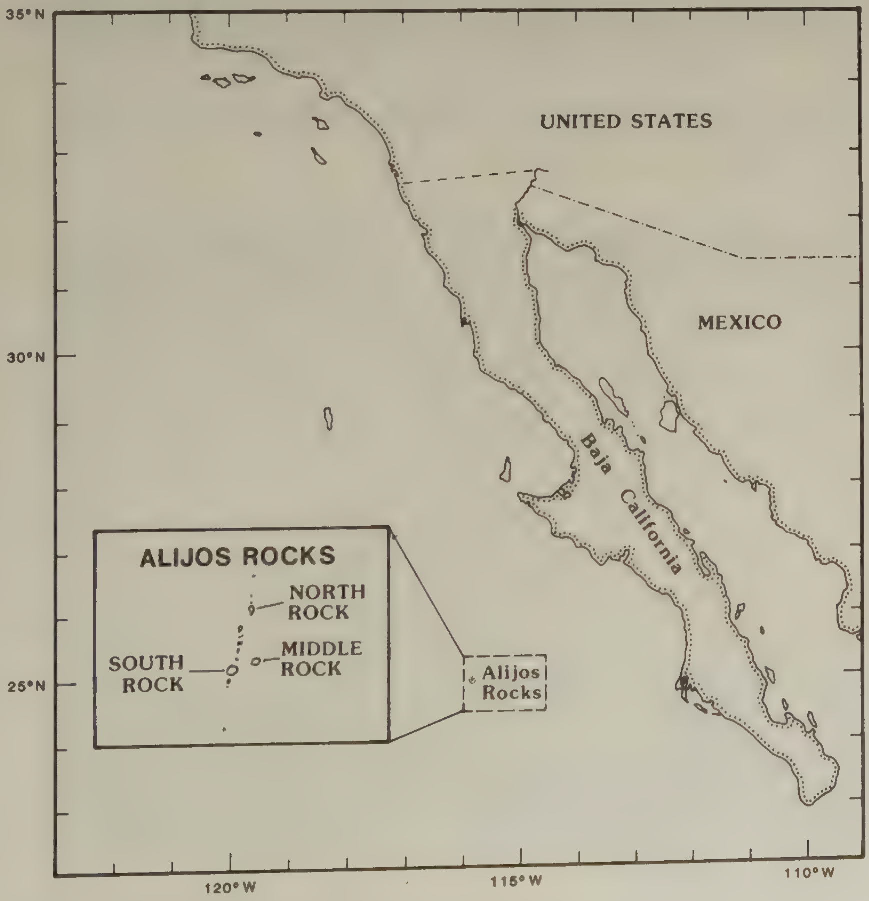

Figure 1. Alijos Rocks, Mexico, with inset showing individual rocks.

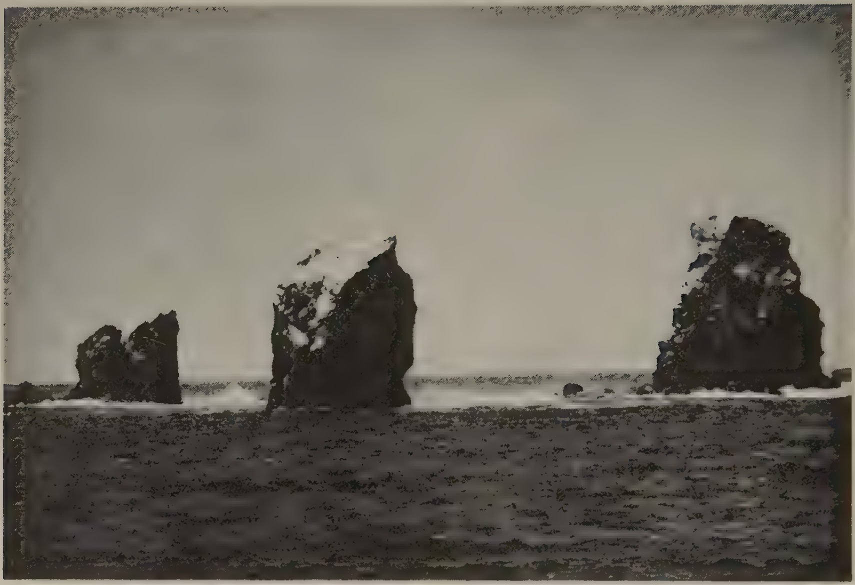

Figure 2. A relatively calm day at Alijos Rocks showing from left to right: Middle Rock, North Rock and South Rock (April 1983).

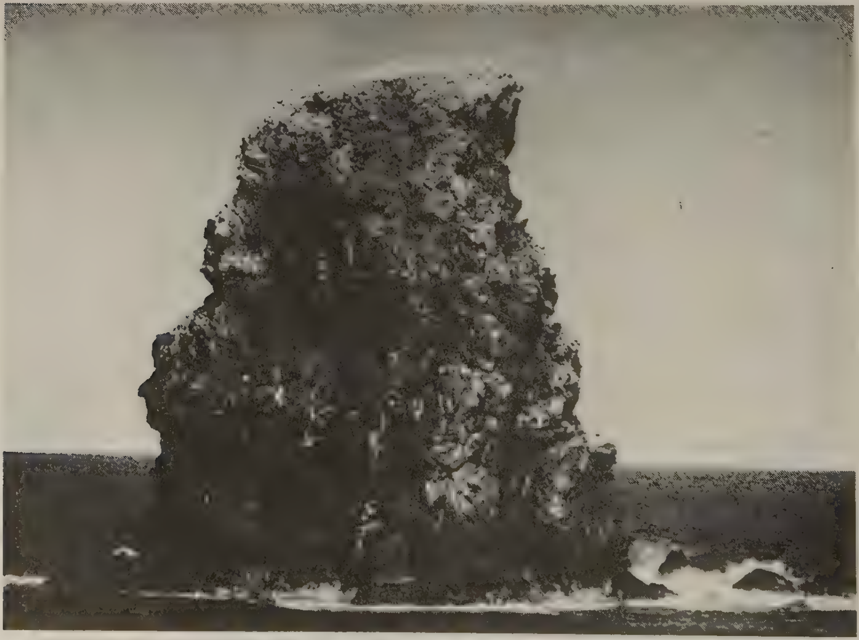

Figure 3. South Rock stands up on five legs and has daylight visible from almost any angle. Laysan Albatross can be seen flying to the right of the rock (April 1983).

CORMORANT (*Phalacrocorax* sp.). A single, large cormorant was roosting on the cliff faces in February 1976 and again in May 1982. Brandt's Cormorant (*P. penicilatus*) seems likely.

MAGNIFICENT FRIGATEBIRD (*Fregata magnificens*). Seven Magnificent Frigatebirds were present on 14 January 1983, five females and one juvenile being identified. I saw several roosting on Middle Rock, but none elsewhere. A single adult female was soaring above the rocks on 10 April 1983, but I saw no signs of nesting.

Away from the immediate area of Alijos Rocks, I saw an adult female *magnificens* and an unidentified frigatebird 80 nautical miles to the southeast in March 1979; later I observed six individual unidentified frigatebirds (probably *magnificens*) within 75 nautical miles of the area in January 1981.

It is not clear whether frigatebirds nest at Alijos Rocks. Hanna (1926, McLellan 1926) saw none in April 1925. Brattstrom (pers. comm.) reported 12 at the rocks in November 1953 though he apparently saw none in May 1953. Murphy (1958) collected two adult males in November 1956 and identified Alijos Rocks as the northernmost breeding colony for *magnificens* along the Pacific coast, but provided no evidence for breeding. My records suggest that Magnificent Frigatebirds are regular visitors to Alijos Rocks during the non-breeding season (winter) but probably do not breed there.

CATTLE EGRET (*Bubulcus ibis*). A flock of five joined the ship for a few minutes, 10 nautical miles east of the rocks on 16 November 1974.

RED PHALAROPE (*Phalaropus fulicarius*). An estimated 20 were close to the rocks and feeding in February 1976; small numbers were in the vicinity and moving north in April 1983.

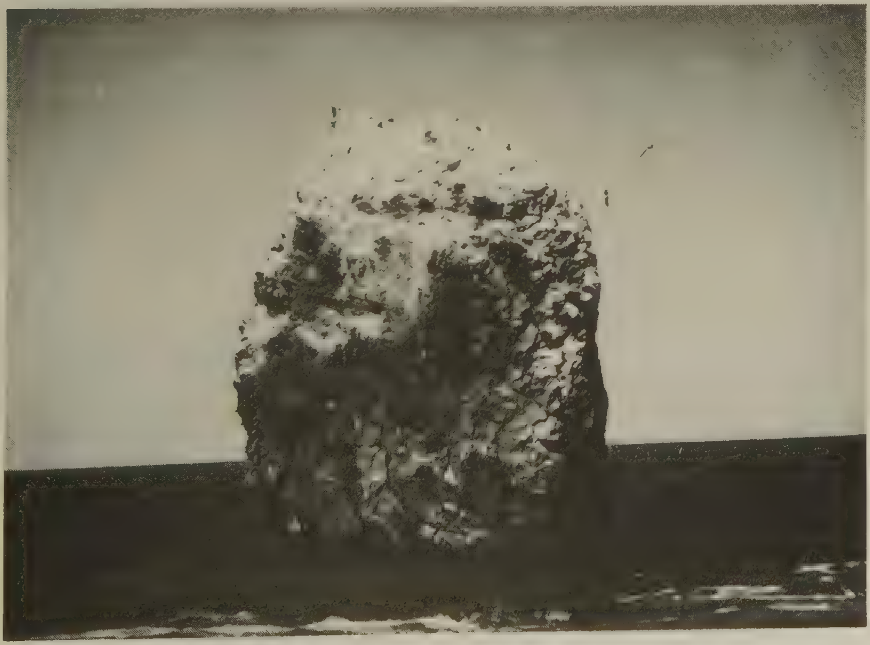

Figure 4. Masked Boobies roosting on top of North Rock and Laysan Albatross circling in the background (April 1983).

POMARINE JAEGER (*Stercorarius pomarinus*). One was 15 nautical miles south of the rocks on 15 May 1982.

PARASITIC JAEGER (*S. parasiticus*). One was 3 nautical miles north on 14 January 1983.

HERRING GULL (*Larus argentatus*). Five (2 adults, 3 subadults) were among the gulls that stayed around the ship as we fished near the rocks in February 1976.

WESTERN GULL (*L. occidentalis*). Probably a regular visitor. One subadult was among the gulls present in February 1976; a third year bird was 20 nautical miles south of the rocks on 15 May 1982, and two adults joined the ship 35 nautical miles to the northeast on 10 April 1983.

CALIFORNIA GULL (*L. californicus*). One was with the other gulls present in February 1976.

LAUGHING GULL (*L. atricilla*). One juvenile, collected 16 November 1974, was 1.5 nautical miles from the rocks (SDNHM 39578).

BLACK-LEGGED KITTIWAKE (*Rissa tridactyla*). A minimum of 10 adults and juveniles hovered around the ship in February 1976. This is the only record for Alijos Rocks and is probably as far south as this species has been known to occur in the eastern Pacific. The winter of 1975-76 was a significant "flight year" for kittiwakes in the eastern Pacific (see also Northern Fulmar).

SOOTY TERN (*Sterna fuscata*). A summer breeder, probably absent at other seasons. I saw none on trips in November, January or February, nor did Brattstrom (pers. comm.) in November 1953 or Murphy (1958) in November 1956. McLellan (1926) and Hanna (1926) reported them on both South and East rocks in late February 1925 and collected nine. Brattstrom (pers. comm.) estimated 100 "roosting, apparently nesting" in May 1953.

On 15 May 1982 I estimated a minimum of 200 terns on top of South Rock; they were evenly spaced and probably nesting. Also, I saw four more foraging ½ nautical mile to the north. On 10 April 1983 approximately 10 were flying around the rocks but none was on shore. There are very few nesting colonies of Sooty Terns in the eastern Pacific, and the Alijos Rocks colony is the northernmost, with a population of about 250 individuals.

ZOOGEOGRAPHY

As is evident from some of the comments in the species accounts, Alijos Rocks is situated at the border of two very distinct oceanographic areas. Cool, southward flowing waters of the California Current meet warm tropical waters of southern Baja California at about 25°N and then veer to the southwest to form the southeast corner of the North Pacific Gyre (Wyrtki 1966).

South-central Baja is therefore an important boundary zone for tropical and cooler water species of marine birds, mammals and fishes (Hubbs 1960), as well as euphausiids (Brinton 1962) and other epipelagic organisms (McGowan 1968). Dawson (1960) sampled marine algae at Alijos Rocks and found southern records for three northern types along with "a high proportion of tropical species."

Currently four species of marine birds nest at Alijos Rocks. Leach's Storm-Petrel (a presumed breeder) nests in more temperate waters around the North Pacific basin and has its southernmost breeding station at Alijos. The

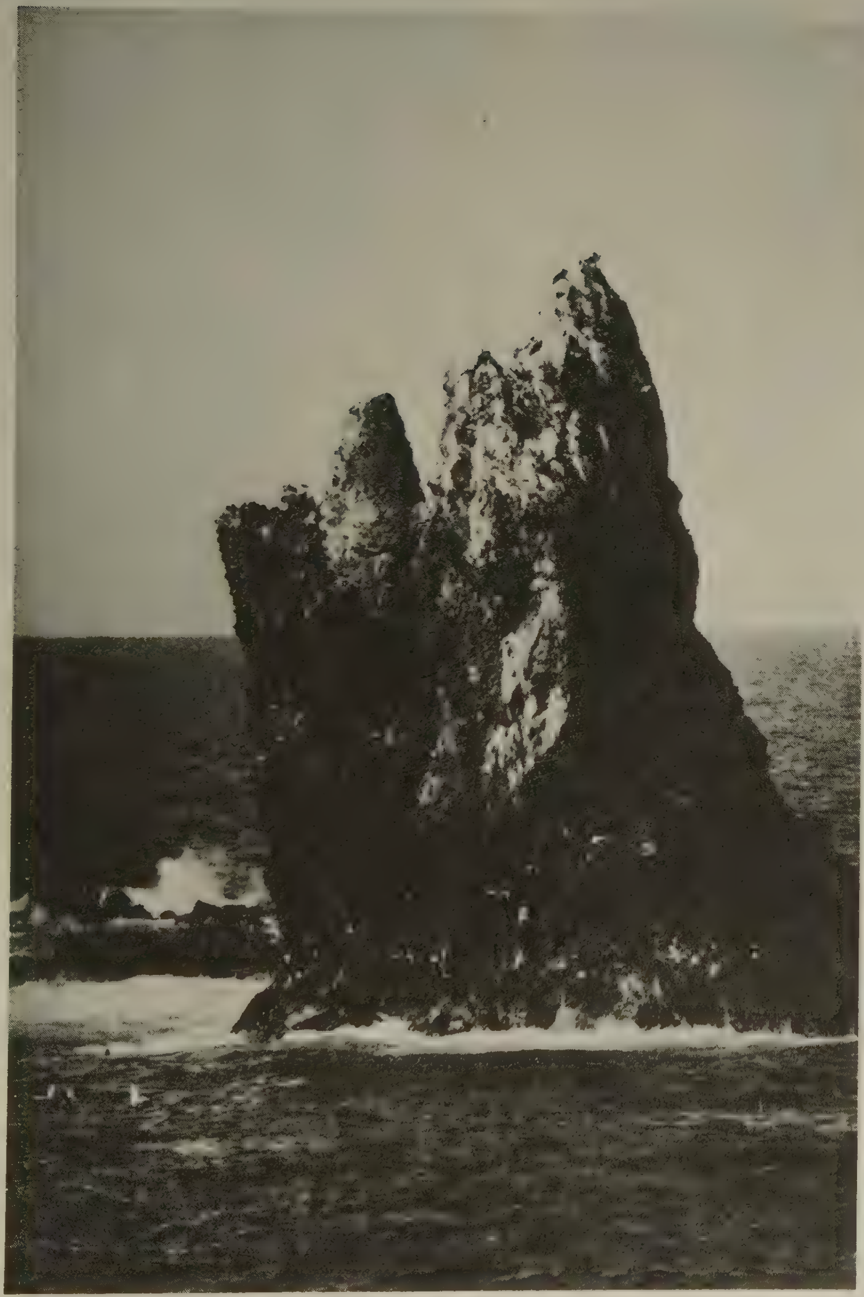

Figure 5. Middle Rock with roosting frigatebirds; California Sea Lions (*Zalophus californianus*) are hauled out in the foreground. A group of four albatrosses is on the water at the lower left (January 1983).

Photos by the author

remaining species (Masked Booby, Red-billed Tropicbird and Sooty Tern) all inhabit tropical or subtropical waters and have their northernmost breeding colony in the eastern Pacific at Alijos. The bird fauna of Alijos Rocks, then, also reflects the transitional nature of the local ocean environment.

On most of my visits to Alijos Rocks the thunderous splashes produced by swells slamming into the vertical pinnacles have been visible from many miles (see also Hanna 1926:28). Despite this relentless onslaught the three main spires appear to have remained largely unchanged since they were first illustrated nearly 150 years ago (Figure 6), or photographed almost 60 years ago (Hanna 1926). South Rock, severely undermined through wave action, is still precariously perched on five legs as it was in 1925 when Hanna (1926) described it. A recent fourth pinnacle, however, has not survived. Rudkin's (1956:100) reproduction of a drawing made on a French survey in 1837 (Figure 6) shows a fourth rock (second from right; also mentioned in his text, p. 94-95) that is about half the size of Middle Rock. This site no longer exists. The remaining stacks at Alijos Rocks will probably topple in time and several species of marine birds will forfeit a toehold at the edge of their ranges in the eastern Pacific.

SUMMARY

The breeding marine avifauna of Alijos Rocks, Mexico (24°57'N, 115°45'W), currently consists of Leach's Storm-Petrel (a presumed breeder; probably a few pairs), Red-billed Tropicbird (14 birds), Masked Booby (100), and Sooty Tern (250). Magnificent Frigatebird is a regular winter visitor but probably does not breed. Laysan Albatross is currently an annual visitor to Alijos Rocks during its winter breeding season, and may start to nest there in the near future.

ACKNOWLEDGMENTS

A number of people have been very helpful in conducting these surveys and I would particularly like to thank Jim Cotton and Gary Friedrichsen, as well as the indulgent ship captains and chief scientists who made this report possible. Dave Au and Bayard Brattstrom kindly made their unpublished field notes available to me, and Glen Dawson, Los Angeles, granted me permission to reproduce Figure 6. I am especially indebted to Joseph R. Jehl, Jr., for first taking me to Alijos Rocks, then for commenting on an earlier version of this paper.

LITERATURE CITED

Ainley, D.G. 1976. Seabirds. A spectacular seabird die-off in 1976: a beach survey report. Pt. Reyes Bird Obs. Newsletter 39:4-5.

Brinton, E. 1962. The distribution of Pacific euphausiids. Bull. Scripps Instit. Oceanogr. 8:51-270.

Dawson, E.Y. 1960. A review of the ecology, distribution and affinities of the benthic flora. Pp. 93-100 *in* Symposium on the biogeography of Baja California and adjacent seas. Part II. Marine Biotas. Syst. Zool. 9.

Dunn, J. & P. Unitt. 1977. A Laysan Albatross in interior southern California. West. Birds 8:27-28.

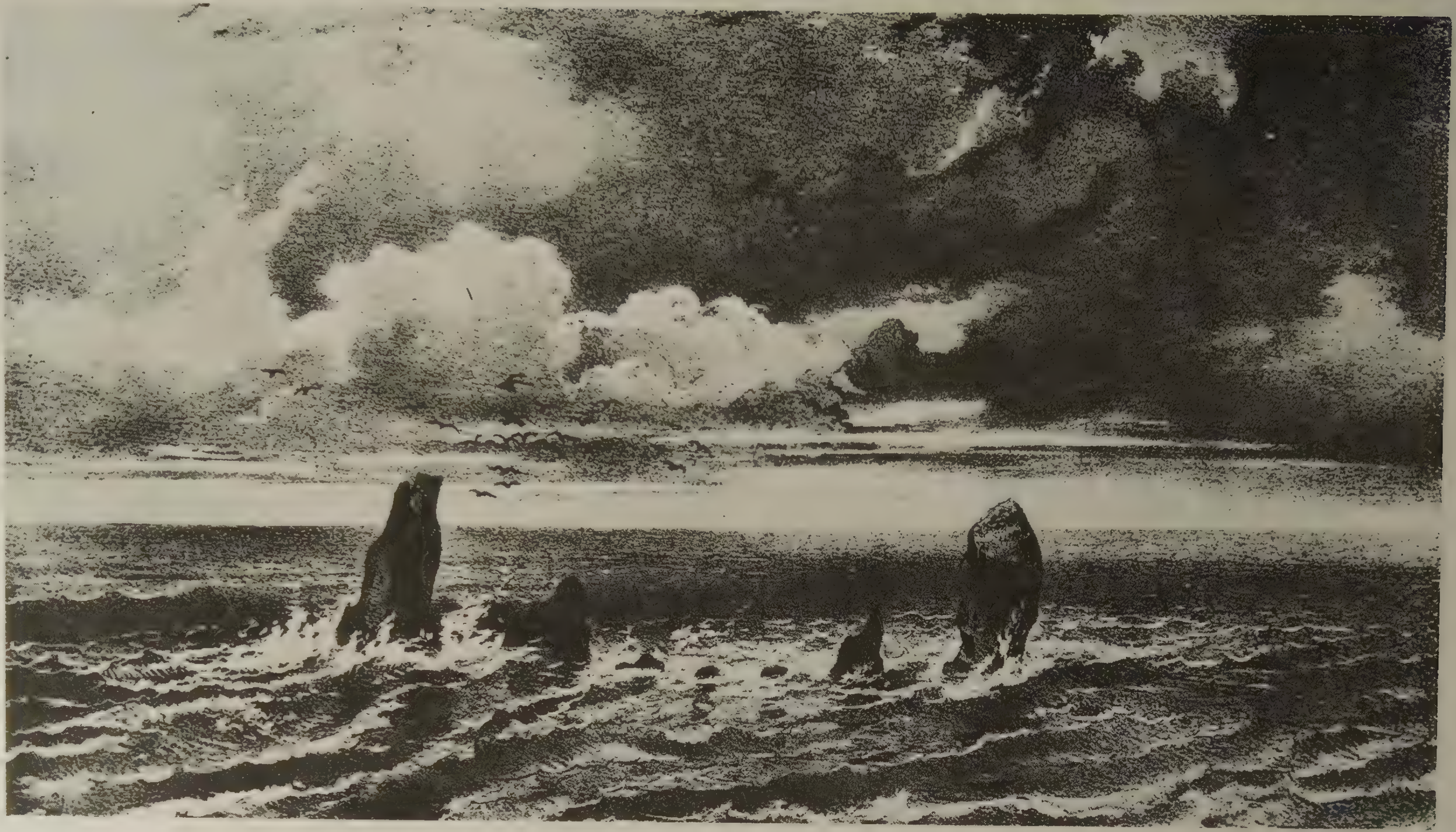

Figure 6. Alijos Rocks from an 1837 engraving; notice the birds hovering above the pinnacles (from Abel Du Petit-Thouars' *Voyage of the Venus*, courtesy Glen Dawson).

Friedmann, H., L. Griscom & R.T. Moore. 1950. Distributional checklist of the birds of Mexico, Part I. Pac. Coast Avif. 29.

Hanna, G.D. 1926. Expedition to the Revillagigedo Islands, Mexico, in 1925. I. General Report. Proc. California Acad. Sci., 4th Ser., 15:1-113.

Harris, M.P. 1969. The biology of storm-petrels in the Galapagos Islands. Proc. California Acad. Sci., 4th Ser., 37:95-166.

Hasegawa, H. 1978. The Laysan Albatross breeding in the Ogasawara Islands. Pac. Seabird Group Bull. 5:16-17.

Hubbs, C.L. 1960. The marine vertebrates of the outer coast. Pp. 134-147 *in* Symposium on the biogeography of Baja California and adjacent seas. Part II. Marine Biotas. Syst. Zool. 9.

Imber, M.J. & T.G. Lovegrove. 1982. Leach's Storm-Petrel (*Oceanodroma leucorhoa*) prospecting for nest sites on the Chatham Islands. Notornis 29:101-108.

Jehl, J.R., Jr. 1982. The biology and taxonomy of Townsend's Shearwater. Le Gerfaut 72:121-135.

McCaskie, G. 1984. Southern Pacific coast region. Am. Birds 38:957-958.

McGowan, J.A. 1968. The thecostomata and gymnostomata of California. The Veliger. Supplement to 3:103.

McLellan, M.E. 1926. Expedition to the Revillagigedo Islands, Mexico, in 1925. VI. The birds and mammals. Proc. California Acad. Sci., 4th Ser., 15:279-322.

Murphy, R.C. 1958. The vertebrates of SCOPE, November 7-December 16, 1956. USDI Fish & Wildl. Serv., Spec. Sci. Rep., Fish. No. 279.

Palmer, R.S., ed. 1962. Handbook of North American birds, Vol. I. Yale Univ. Press, New Haven, CT.

Pyle, R.L. 1983. Hawaiian Islands region. Am. Birds 37:1028-1029.

Rice, D.W. & K.W. Kenyon. 1962a. Breeding distribution, history and populations of North Pacific albatrosses. Auk 79:365-386.

Rice, D.W. & K.W. Kenyon. 1962b. Breeding cycles and behavior of Laysan and Black-footed albatrosses. Auk 79:517-567.

Richardson, F. 1957. The breeding cycles of Hawaiian sea birds. Bernice P. Bishop Mus. Bull. 218:1-41.

Rudkin, C.N. (Transl.). 1956. Voyage of the Venus: sojourn in California. G. Dawson, Los Angeles.

Sanger, G.A. 1974. Laysan Albatross (*Diomedea immutabilis*). *In* Pelagic studies of seabirds in the central and eastern Pacific Ocean. Contrib. Zool. No. 158:129-153.

Wyrtki, K. 1966. Oceanography of the eastern equatorial Pacific Ocean. Oceanogr. Mar. Biol. Ann. Rev. 4:33-68.

Accepted 14 March 1985

8576

HORNED PUFFIN SIGHTINGS IN THE EASTERN PACIFIC

ROBERT L. PITMAN, National Marine Fisheries Service, Southwest Fisheries Center, P.O. Box 271, La Jolla, California 92038

MICHAEL R. GRAYBILL, Oregon Institute of Marine Biology, Charleston, Oregon 97420

On 3 July 1979, while conducting a survey of marine bird colonies of coastal Oregon for the U.S. Fish and Wildlife Service, we saw a single Horned Puffin (*Fratercula corniculata*) roosting on Island Rock, approximately 8 km south of Port Orford, Oregon. The bird (Figure 1) was an adult in summer plumage. It roosted on a rocky outcropping 40 m above the sea surface on the east side of the island, near the south end. During the next 2 hours, while we censused nesting birds on the island from a boat, it disappeared into a crevice for up to 30 minutes at a time. Twice while we watched, it flew from its roost and circled widely around the colony several times before returning to its original site. We climbed up and inspected the crevice but were unable to determine if it was being used for nesting. As Campbell et al. (1979) pointed out, the behaviors we observed are also the activities of scouting pre-breeders and we have not inferred that this was an actual breeding attempt. At the time of our sighting, Island Rock had a population of approximately 350 Tufted Puffins (*F. cirrhata*).

On 4 August 1984, while conducting research on Hunters Island, Oregon, Graybill observed a single Horned Puffin in summer plumage circling above the island with 13 Tufted Puffins. Presumably it had been flushed from the island with the other puffins when Graybill went ashore. During the next 20 minutes it made repeated passes at the island at an altitude of less than 3 m but was never seen to land. Hunters Island is approximately 20 km south of Gold Beach, Oregon; an estimated 10 pairs of Tufted Puffins were nesting on the island at the time of the sighting.

Campbell et al. (1979) recently found Horned Puffins breeding in southern British Columbia. Their report was the first record of nesting for this species south of Alaska. Though they found only a few pairs, making it possible that the puffins were only overlooked in the past, Campbell et al. (loc. cit.) cautiously implied that some real range expansion may have been taking place. Thoresen (1981) reported a single Horned Puffin with a group of Tufted Puffins near a potential nesting colony in Rosario Strait, Washington, in July 1977, but the bird was never actually seen to land on the colony.

Since around 1970, Horned Puffins have been regularly seen off Oregon in small numbers during the summer months (e.g. Crowell and Nehls 1970, 1975, 1977; Hunn and Mattocks 1977). The only previous record of Horned Puffin roosting at a potential nesting site in the western United States outside of Alaska was from Yaquina Head, Oregon, 260 km north of Island Rock, where a single individual was seen on two consecutive days in June 1973 (Hoffman et al. 1975). Ramsey (1975), noting the change in the number and seasonal occurrence of Horned Puffins in Oregon, asked "Could it be that this species actually nests on the Oregon coast?"

Hoffman et al. (1975) reviewed the status of Horned Puffin in the eastern Pacific following 1973, when an inordinate number were recorded off the western United States. They reported that around the mid-1950s this species changed from a predominately wintering bird to a spring and early summer visitor. They suggested that possibly a long term change in the oceanic environment was causing a shift in seasonal occurrence as well as an increase in abundance of Horned Puffins in the eastern Pacific.

This suggestion of a change in seasonality and increased occurrence was given some support by the extensive seabird surveys conducted off California by the Univer-

Western Birds 16:99-102. 1985

sity of California for the Bureau of Land Management and Minerals Management Service. During regular, year-round ship and aerial surveys from 1975 to 1977, Briggs et al. (1978) recorded 108 Horned Puffins off southern California, all in the months of April, May and June. Hoffman et al. (1975) found records of only five Horned Puffins from southern California prior to 1974.

During 1980-83, Briggs et al. (1983) conducted regular aerial surveys of marine birds off northern California (Point Conception to the California/Oregon border). They found low numbers of Horned Puffins (up to seven in February 1980) from February through May; most of these were "well offshore." Single birds were sighted over the continental slope in August 1980 and November 1982, but none were seen during other months. Briggs et al. (loc. cit.) identified only 24 Horned Puffins during the northern California study but alcids are difficult to distinguish from the air. Also, their aerial surveys normally ranged only out to 200 km from shore during most of the study (and occasionally out to 350-400 km during 1982); this distance may not have been far enough offshore to sample this species adequately (see below).

On 17 February 1984, Pitman was surveying seabirds en route from San Francisco, California, to Honolulu, Hawaii, aboard the NOAA ship Discoverer using 25 power mounted spotting binoculars. During 6.5 hours of observation in Beaufort 4 sea conditions he saw 54 Horned Puffins. These birds were observed only during the last 3.5 hours of survey as the ship traveled from 185 to 260 km (100-140 nm) due W of San Francisco. Puffins became increasingly common until dusk when the survey was terminated, with 20 seen during the last half hour. During the last 2 hours of that survey, Horned Puffin was the second most abundant species, out-numbered only by Red Phalarope (*Phalaropus fulicarius*). At that time puffins were mostly seen either sitting on the water or flying away from the ship. None were seen the next morning when the ship was 726 km (392 nautical miles) from San Francisco, nor were any seen the rest of the way to Hawaii.

On the return trip from Hawaii to Seattle, Washington, in May 1984, Horned Puffins were once again abundant in the offshore zone. On 7 May during 7 hours of observation in Beaufort 5 sea conditions, Pitman counted 165 puffins. It was the most abundant species present as the ship traveled NE from 815 to 630 km (440-340 nm) off Cape Blanco, Oregon. Almost every bird seen was flying WNW, apparently heading to breeding grounds farther north.

On the following day, 8 May, the ship continued NE, traveling from 315 to 31 km (170-17 nm) off Cape Flattery, Washington. During 8 hours of observation only four puffins were seen though sighting conditions were improved (Beaufort 3-4). None of these puffins were within 185 km (100 nm) of the coast. Interestingly, no Horned Puffin records were included in the regional reports of *American Birds* from the western United States for the winter, spring or summer of 1984 (G. McCaskie and R. LeValley pers. comm.), though puffins were apparently abundant offshore.

Table 1. Records of Horned Puffins (*Fratercula corniculata*) off the western United States, south of Canada, from the regional reports of *American Birds*, 1974-1984 (n = 369; not included below are 5 puffins from months other than those listed and 3 described as long dead).

	summer: May-Aug.	winter: Dec.-Mar.
alive	324	6
dead	4	27

Since 1974, when Hoffmann et al. (1975) last summarized available records, 369 Horned Puffins have been reported off the western United States, south of Canada, in the regional reports of *American Birds* (Table 1). Winter records are sparce and usually involve dead birds on the beach. Three of the six live winter birds were 130-140 km off the coast of Washington. In contrast, summer records were almost all of live, healthy birds, often near islands or inshore areas, and usually seen during the months of May or June.

From the evidence above we suspect that Horned Puffin may be a regular and, at least sometimes, abundant visitor to the offshore waters of western North America, ranging as far south as central or southern California during the winter (see also Ainley 1976, McCaskie 1976). In May and June 1975, when an unprecedented number of Horned Puffins were reported off California, they were found as far south as northern Baja California (Punta Banda), Mexico (McCaskie 1975).

Under normal conditions, Horned Puffins probably only rarely stray onto the waters of the continental shelf during winter. In late spring/early summer, with the onset of northwesterly winds, upwelled, nutrient-rich water causes an annual peak in plankton production in the California Current (Bolin and Abbott 1963). This period of increased productivity coincides with a peak in observations of Horned Puffins off the west coast. During normal years, most wintering puffins presumably depart offshore waters and head north to summering grounds without being noticed. In other years, however, some Horned Puffins appear to move in closer to the coast just prior to their northward migration, accounting for the preponderance of May/June records.

There appears to be an increased occurrence of Horned Puffins remaining behind to spend the summer and occasionally visit roosting sites in the southern extent of their eastern range. Whether this is indicative of annual oceanographic anomolies, a longer

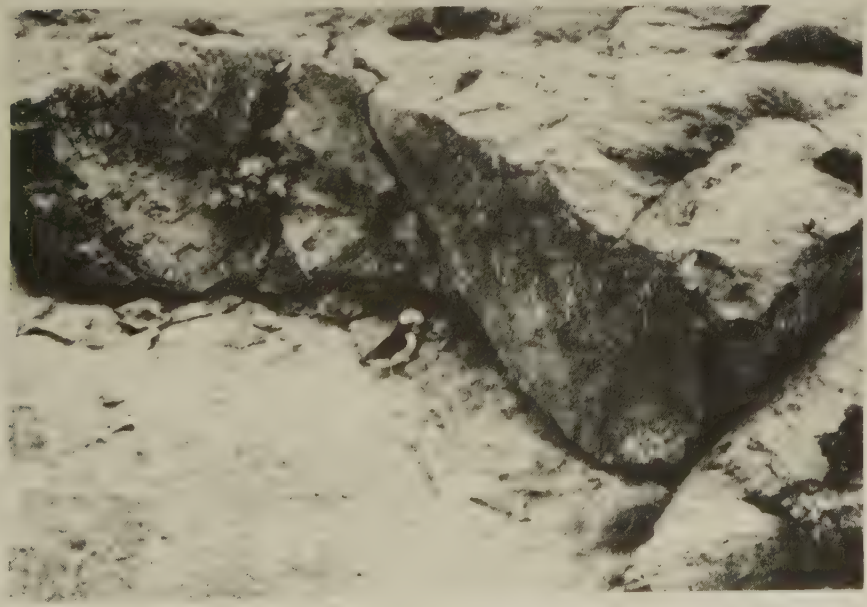

Figure 1. Horned Puffin roosting at a crevice entrance on Island Rock, Oregon, 3 July 1979.

Photo by Michael R. Graybill

term cycle that may ultimately affect their breeding range, or some other factors (e.g. a burgeoning population), is unknown. What is known is that the apparent change in status for this species closely parallels the development of increased public interest in recreational seabird watching and the advent of detailed seabird resource assessments (e.g. at-sea surveys, colony inventories, beached-bird salvaging programs). So it may also be that most of the records discussed above, including our own, are only the result of closer scrutiny by field investigators.

We would like to thank Ken Briggs and Harry Nehls for comments on an earlier draft of this paper.

LITERATURE CITED

Ainley, D.G. 1976. The occurrence of seabirds in the coastal region of California. West. Birds 7:33-68.

Bolen, R.L. & D.P. Abbott. 1963. Studies on the marine climate and phytoplankton of the central coastal area of California, 1954-1960. Calif. Coop. Ocean. Fish. Invest. Rep. 9:23-45.

Briggs, K.T., E.W. Chu, D.B. Lewis, W.B. Tyler, R.L. Pitman & G.L. Hunt, Jr. 1981. Distribution, numbers and seasonal status of seabirds of the Southern California Bight. Pages 1-212 *in* Summary report, 1975-1978: marine mammal and seabird surveys of the Southern California Bight area. Natl. Tech. Info. Service Rep. PB-81-248-197.

Briggs, K.T., W.B. Tyler, D.B. Lewis & K.F. Dettman. 1983. Seabirds of central and northern California, 1980-1983: Status, abundance, and distribution. Report prepared for Pacific OCS Region, Minerals Management Service, U.S. Dep. Int., Contract No. AA551-CT9-33.

Campbell, R.W., H.R. Carter & S.G. Sealy. 1979. Nesting of Horned Puffins in British Columbia. Can. Field-Nat. 93:84-86.

Crowell, J.B. & H.B. Nehls. 1970. North Pacific coast region. Aud. Field Notes 24:82-88.

Crowell, J.B. & H.B. Nehls. 1975. North Pacific coast region. Am. Birds 29:1020-1025.

Crowell, J.B. & H.B. Nehls. 1977. North Pacific coast region. Am. Birds 31:212-216.

Hoffman, W., W.P. Elliot & J.M. Scott. 1975. The occurrence and status of the Horned Puffin in the western United States. West. Birds 6:87-94.

Hunn, E. & P. Mattocks, Jr. 1977. North Pacific coast region. Am. Birds 31:1178-1183.

McCaskie, G. 1975. Southwest Pacific coast region. Am. Birds 29:907-912.

McCaskie, G. 1976. Southwest Pacific coast region. Am. Birds 30:886-894.

Ramsey, F. 1975. Field notes. Chat (newsletter Audubon Soc. Corvallis, Oregon) 5:7-8.

Thoresen, A.C. 1981. Mid-summer occurrence of the Horned Puffin in Rosario Strait, Washington. West. Birds 12:56.

Accepted 2 April 1985

8577

VARIATION IN CATCH RATES AND SPECIES COMPOSITION IN HANDLINE CATCHES OF DEEPWATER SNAPPERS AND GROUPERS IN THE MARIANA ARCHIPELAGO

VARIATIONS DU TAUX DE CAPTURE ET DE LA COMPOSITION SPECIFIQUE DES PRISES PAR LIGNES A MAIN DE VIVANEAUX ET MEROUS DANS L'ARCHIPEL DES MARIANNES

J. POLOVINA
Southwest Fisheries Center, Honolulu Laboratory, P.O. Box 3830,
Honolulu, HAWAII 96812, U.S.A.

ABSTRACT

A total of 7621 deepwater snappers and groupers were caught with handline gear in a systematic survey of 22 banks in the Mariana Archipelago with six cruises spanning mid-1982 through mid-1984. Variations in the catch-per-unit effort (CPUE) and catch composition at banks due to geographic and temporal factors is examined.

Both bank type and latitude explain variation in CPUE. Seamounts have higher CPUE values than the high islands at the same latitude while within bank types, CPUE increases with increasing latitude. For both bank CPUE and bank catch composition, variation between banks within a cruise period is substantially greater than variation between banks over the 2-year survey period. A relationship between the index of the diversity of the bank catch composition and an index of the area of bottom fish habitat at the bank is established. Cluster analysis applied to the bank catch composition indicates that all the banks can be grouped into one of three catch profiles which are relatively invariant over the survey period. Bank size appears to explain the catch composition and bank grouping for at least two of the three clusters.

RESUME

Un nombre total de 7621 vivaneaux et mérous des eaux profondes ont été capturés par pêche avec des lignes à main au cours d'une exploration systématique de 22 bancs dans l'archipel des Mariannes (6 croisières de mi-1982 à mi-1984). Les variations du taux de capture par unité d'effort (CPUE) et de la composition spécifique des bancs en fonction des facteurs géographiques et temporels sont examinées.

La variation de CPUE s'explique par le type de banc et aussi par la latitude. Les bancs profonds et isolés, présentent des valeurs de CPUE plus élevées que ceux situés au voisinage des îles émergeantes sous les mêmes latitudes, tandis que, dans un type de banc donné, le CPUE augmente selon la latitude. Pour le CPUE, ainsi que pour la composition spécifique d'un banc, les variations entre bancs pendant la période d'une sortie sont plus importantes que celles observées entre bancs pendant la période de 2 années d'exploration.. Une relation entre l'indice de la diversité de la composition des captures sur un banc et l'indice de l'aire de l'habitat des poissons démersaux est établi. Un groupement hiérachique de la composition des captures sur chaque banc indique que tous les bancs peuvent être groupés dans un des trois profils de capture, qui sont relativement invariables durant la période d'exploration. L'étendue d'un banc semble expliquer la composition des captures et le groupement, au moins pour deux des trois groupes.

INTRODUCTION

Variation in density and community composition of fishes associated with coral reefs has received considerable attention from ecologists (Ehrlich 1975; Goldman and Talbot 1976; Helfman 1978; Sale 1980). Studies have documented a wide variation in density of reef fish populations on nearby patch reefs but little has been learned regarding the factors which are responsible for this variation (Sale 1980). There is some dispute on the subject of stability of coral reef communities. Some researchers find evidence that fish communities associated with coral reef systems are stable over time (Molles 1978; Smith 1978; but others argue that reef fish assemblages are predominantly nonequilibrium and unstable (Talbot et al. 1978; Sale 1980).

While the shallow water reef fishes have been extensively studied, the distribution and stability of species composition due to temporal and geographic factors of deepwater bottom fishes in tropical waters has received little attention. This paper will examine variation in relative abundance and species composition for deepwater bottom fishes found in depths of 125 to 275 m caught with deep-sea handline gear in a fishing survey of 22 islands and banks in the Mariana Archipelago.

Six resource assessment cruises of 40 days each were conducted in the Mariana Archipelago during the period between May 1982 through June 1984. In the subsequent analysis, cruises will be grouped into two cruise periods--one cruise period including the three 1982 cruises, and the other cruise period including the three cruises from the latter part of 1983 and early and mid-1984. During these cruises, the deepwater snapper and grouper community was sampled at the 22 islands and banks shown in Fig. 1. Thirteen of these 22 sites were sampled at least once in each cruise period. Two sites, Pagan Island and Esmeralda Bank, were sampled on each of the six cruises.

The Mariana Archipelago consists of a chain of islands and banks on a north-south axis beginning with Galvez Banks and Santa Rosa Reef at the southernmost end and extending northward to Farallon de Pajaros (30 nmi north of Maug Island), and a chain of seamounts also on a north-south axis about 120 nmi west of the high island chain (Fig. 1). From a geological perspective, there are three distinct types of formations within the Mariana Archipelago. One is the high island chain which is composed of two subgroups. The southern islands in this chain which consist of the formations Santa Rosa Reef, Galvez Banks, Guam, Rota, Aguijan, Tinian, Saipan, and Farallon de Medinilla, are 30 to 40 million years old and represent the oldest formations in the archipelago (Scott et al. 1980). The second is the northern islands in this chain which include Esmeralda Bank and 38-Fathom Bank (lat. 15°18.5'N, long. 145°26'E) and all the islands from Anatahan north to Farallon de Pajaros. They are the youngest in the chain, about 1 million years old, and several are still active volcanoes (Scott et al. 1980). The western seamount chain is the third geological type and is approximately 10 million years old (Scott et al. 1980). The seamounts sampled in the western chain were Bank A (lat. 14°12'N, long. 142°50'E), Arakane Reef, Pathfinder Reef, Bank D (lat. 17°07'N, long. 143°20'E), and Bank C (lat. 18°06'N, long. 143°10'E).

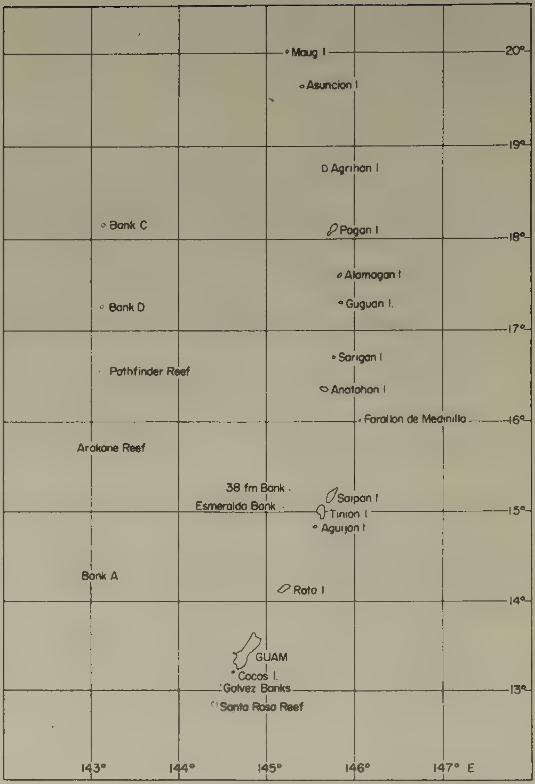

Figure 1. Hawaiian Archipelago showing the 22 islands and banks sampled.

The National Oceanic and Atmospheric Administration (NOAA) ship *Townsend Cromwell* was used as the fishing vessel for all the cruises. For sampling bottom fish, four hydraulic gurdies were used each with 365 m of braided 90 kg Dacron[1] line. The terminal rig consisted of four hooks spaced approximately 1 m apart and a 2 kg weight. Two of the rigs used No. 20 Tonkichi hooks and two rigs used No. 28 Tonkichi hooks.

At each island and bank, an attempt was made to conduct a systematic fishing survey of the bottom fish community along the 200-m contour. Fishing was conducted while the vessel drifted and targeted the 125 to 275 m depth range. Fishing effort is measured in line-hours and is defined as the product of the number of lines fishing, and the length of time in hours that they are fishing. The basic sampling unit is the fishing drift which is the fishing that occurs during an uninterrupted drift by the vessel while it is fishing in the 125 to 275 m depth range. A fishing station is the sampling unit which corresponds to a specific geographic site around an island or bank. A station may consist of only one drift or may contain multiple drifts which repeatedly fish the specific site. Numerous fishing stations are used in a systematic survey of each island and bank.

---

[1] Reference to trade names does not imply endorsement by the National Marine Fisheries Service, NOAA.

Relative Abundance

A total of 7,621 bottom fishes of over 30 species were caught with handline gear during the six cruises. *Pristipomoides zonatus* accounted for 51.2% of the catch and three species, *P. zonatus*, *P. auricilla*, and *Etelis carbunculus* accounted for 79.1% of the total catch.

Catch per unit effort (CPUE) is measured in number of fish per line-hour. For each bank, bank CPUE is computed as the mean of all the drift CPUE values where a drift CPUE is the number of fish caught during an uninterrupted drift divided by the drift line-hours. Mean drift CPUE is used as a measure of bank CPUE because to a large extent the drifts within a bank appear to represent replicates from the total bank population and as such allow for the estimation of within bank variation in CPUE. The mean drift CPUE is presented for all 22 banks and islands in Table 1.

There was considerable variation in mean drift CPUE between banks. A nested analysis of variance shows that when the variation in drift CPUE within banks is taken into account, the differences in mean drift CPUE between the two cruise periods is not significant ($P>0.10$), whereas the differences in mean drift CPUE among banks and bank types both pooled over cruise period are significant ($P<0.025$). Taken by bank type, the seamounts (Table 1) have the greatest mean drift CPUE (4.68 fish per line-hour) followed by the northern islands (3.19 fish per line-hour) and then the southern islands (2.46 fish per line-hour). The inhabited islands of the Marianas are Guam, Saipan, Rota, and Tinian--all in the southern group. Fishermen at these islands exploit the local stocks of bottom fishes which most likely accounts for the relatively low CPUE values for the populated islands. The mean of the bank CPUE for the uninhabited islands and banks in the southern group is 3.36 fish per line-hour which suggests that when islands with heavy fishing mortality are excluded, there is no difference in bottom fish standing stock between the northern and unfished southern islands. The seamounts, however, appear to support a higher standing stock than the unfished (northern and southern) islands and banks. There also appears to be a trend of increasing drift CPUE with latitude within the northern and seamount groups (Table 1). An analysis of covariance using just the drift CPUE from the seamounts and northern islands, where fishing mortality is not a factor, shows that latitude and bank type explain a statistically significant portion of variation in drift CPUE ($P = 0.0001$ for both variables). Thus, at the same latitude, the seamounts have a higher relative abundance than the high northern islands and for both types of formations, the relative abundance increases with increasing latitude.

Table 1. Bank, mean drift, catch per unit effort (CPUE), standard error (SE), and latitude over the survey period.

Bank	No. of drifts	Mean drift CPUE (numbers)	Mean drift SE	Latitude N
Northern Islands				
Maug	7	5.03	1.02	20°02'
Asuncion	17	2.16	0.49	19°40'
Agrihan	45	4.20	0.31	18°46'
Pagan	100	4.57	0.40	18°06'
Alamagan	118	2.37	0.19	17°36'
Guguan	32	3.01	0.30	17°19'
Sarigan	28	2.82	0.37	16°43'
Anatahan	38	2.31	0.23	16°21'
38-Fathom	61	3.12	0.26	16°20'
Esmeralda	114	2.29	0.15	14°58'
Average drift CPUE		3.19		
Southern Islands				
Farallon de Medinilla	32	3.29	0.65	16°01'
Saipan	17	1.72	0.34	15°10'
Tinian	20	1.96	0.29	15°00'
Aguijan	13	3.84	0.98	14°52'
Rota	19	1.91	0.40	14°10'
Guam	20	1.53	0.35	13°25'
Galvez and Santa Rosa	41	2.95	0.31	13°00'
Average drift CPUE		2.46		
Seamounts				
Bank C	8	5.91	1.57	18°08'
Bank D	20	5.85	0.51	17°09'
Pathfinder	136	4.58	0.23	16°30'
Arakane	84	3.36	0.24	15°38'
Bank A	24	3.71	0.57	14°12'
Average drift CPUE		4.68		

CATCH COMPOSITION

To facilitate analysis of the catch composition among banks and cruise sets, the catch is partitioned into seven species categories. Due to their large contribution to the overall catches, *P. zonatus*, *P. aurcilla*, and *P. flavipinnis* each represent single species categories. Other species categories are the groupers which consist of all the Serranidae, and the jacks which are composed of all the Carangidae. *Etelis carbunculus* and *E. coruscans* are combined into an *Etelis* group, and all the other snappers, *Aprion virescens*, *P. sieboldii*, *P. amoenus*, *P. filamentosus*, are combined to form the other snapper group.

The percentage of the catch in the seven species groups at each bank pooled over all cruises is given in Table 2. While most of the seven species groups are represented at all of the islands and banks there do appear to be differences in the diversity of the catch compositions between islands and banks. For example, at the seamounts three species accounted for about 90% of the catch while at many other islands and banks at least five species must be combined to account for 90% of the catch composition (Table 2).

Table 2. Bank catch composition pooled over all cruises.

Bank	*Etelis*	*Pristipomoides zonatus*	Groupers	Jacks	*P. auricilla*	Other snappers	*P. flavipinnis*
Maug	10.6	43.9	4.1	3.3	35.8	0.8	1.6
Asuncion	5.4	58.9	17.9	3.6	8.9	5.4	0
Agrihan	12.6	60.2	3.9	2.1	10.3	4.6	6.4
Pagan	14.8	70.0	2.6	1.1	8.9	1.3	1.3
Alamagan	20.2	49.6	2.9	1.4	23.3	1.4	1.1
Guguan	13.1	61.5	3.6	2.8	18.3	0.4	0.4
Sarigan	9.9	64.6	7.3	2.1	14.1	1.0	1.0
Anatahan	8.4	54.0	2.5	2.0	11.9	6.4	14.9
Farallon de Medinilla	11.5	47.9	3.7	6.3	9.4	4.7	16.7
Saipan	7.6	22.8	1.3	1.3	8.9	24.1	34.2
38-Fathom	6.4	43.4	4.5	6.6	22.8	11.7	4.7
Tinian	19.4	0	0	0	8.3	2.8	69.4
Aguijan	0	27.1	0	2.1	6.3	22.9	41.7
Esmeralda	5.4	39.7	3.0	2.0	4.0	9.3	36.6
Rota	9.5	36.2	1.9	2.9	16.2	21.9	11.4
Guam	12.9	16.1	0	6.5	25.8	25.8	12.9
Galvez and Santa Rosa	6.8	32.2	1.7	9.3	36.4	8.5	5.1
Bank C	22.9	35.6	0.9	0	39.0	1.7	0
Bank D	39.4	48.0	0	1.5	9.1	1.5	0.5
Pathfinder	21.5	50.6	0.4	8.2	17.3	1.6	0.4
Arakane	16.9	41.2	0.7	12.8	18.8	9.3	0.3
Bank A	15.9	60.7	0.4	2.5	18.4	1.3	0.8
Total	15.2	51.4	2.3	4.5	15.4	4.7	6.6

A measure of the species diversity of the catch at a bank can be computed from the Shannon-Weaver measure of the diversity (H) of the catch composition given by the equation:

$$H = -\sum_{i=1}^{7} p(i)\ln(p(i))$$

where p(i) is the proportion of the catch at a bank which belongs to the ith species category (i = 1, ..., 7 in our application) (Shannon and Weaver 1963).

A regression of H against the natural log of the length of the 200-m isobath, which is an index of the area of bottom fish habitat, indicates that there is a positive linear relationship between H and ln (length of 200-m isobath) (Table 3). The regression has a slope of 0.19 and an R^2 of 0.28 ($P = 0.013$). Thus the larger the bank the greater the diversity of the catch.

To assemble banks into groups of similar catch composition and to determine if these groups are invariant over time, a multivariate procedure known as cluster analysis was applied to form clusters of banks with similar catch composition within each of the two cruise periods. The catch composition for each bank is simply the number of fish caught in the seven species groups described earlier. The cluster analysis groups banks together based on the chi-squared distance between their catch composition.

Table 3. The Shannon-Weaver measure of diversity (H) and length of the 200-m contour for each bank.

Bank	H	Length of 200-m contour (nmi)	$\log_e$ (length of 200-m contour (nmi))
Northern Islands			
Maug	1.31	10	2.30
Asuncion	1.27	11	2.40
Agrihan	1.32	18	2.89
Pagan[1]	1.29	30	3.40
Alamagan	1.29	11	2.40
Guguan	1.14	9	2.20
Sarigan	1.15	9	2.20
Anatahan	1.42	17	2.83
Southern Islands			
Farallon de Medinilla	1.56	77	4.34
Saipan	1.57	53	3.97
38-Fathom	1.59	3	1.10
Tinian	0.89	29	3.37
Aguijan	1.31	16	2.77
Esmeralda[1]	1.42	12	2.48
Rota	1.64	32	3.47
Guam	1.70	79	4.37
Galvez and Santa Rosa	1.57	53	3.97
Western Seamounts			
Bank C	1.18	3	1.10
Bank D	1.09	3	1.10
Pathfinder	1.16	3	1.10
Arakane	1.20	3	1.10
Bank A	1.11	4	1.39

[1] For Pagan and Esmeralda most of the fishing was restricted to a 10 nmi length of 200-m contour for purpose of replicated sampling, thus H may not reflect species diversity of the entire bank.

Although selecting the number of clusters which is appropriate for a data set can be subjective, the decision rule used here is to determine the number of clusters as the minimum number of clusters which achieve the greatest relative decrease in the maximum within cluster distance. In both the 1982 and the 1983-84 cruise periods, three clusters provide the greatest relative reduction in intracluster distance. The three clusters are similar for both cruise periods in their bank composition and catch composition (Tables 4, 5, and 6). Although the clusters do not entirely segregate along the three geological bank types, there is considerable similarity. As a naming convention, it is descriptive to refer to the three clusters as northern, seamount, and southern clusters for both cruise periods, but it should be kept in mind that the clusters and the island types of the same name do not contain exactly the same set of banks. In both cruises, the southern cluster was characterized by its high proportion of *P. flavipinnis* 30% in one period and 16% in the other period,

Table 4. Banks in the three clusters from the 1982 cruise period.

Northern cluster	Seamount cluster	Southern cluster
Galvez and Santa Rosa	Pagan[1]	Esmeralda[1]
38-Fathom	Bank A[1]	Anatahan[1]
Agrihan[1]	Pathfinder[1]	Farallon de Medinilla[1]
Guguan[1]	Arakane[1]	Tinian
Maug		Aguijan
Alamagan[1]		Saipan
Asuncion		Rota[1]
Sarigan[1]		Guam[1]

[1] Banks sampled in both cruise periods.

Table 5. Banks in the three clusters from the 1983-84 cruise period.

Northern cluster	Seamount cluster	Southern cluster
Guguan[1]	Pathfinder[1]	Guam[1]
Pagan[1]	Bank D	Rota[1]
Sarigan[1]	Bank C	Arakane[1]
	Bank A[1]	Agrihan[1]
	Alamagan[1]	Anatahan[1]
		Farallon de Medinilla[1]
		Esmeralda[1]

[1] Banks sampled in both cruise periods.

Table 6. Cluster catch composition by cruise periods.

		Species catch composition in percent						
Cluster	Number of fish	*Etelis*	*Pristipomoides zonatus*	Groupers	Jacks	*P. auricilla*	Other snappers	*P. flavipinnis*
1982 Cruise Period								
Northern	1,328	6.5	48.6	5.7	4.2	24.6	6.8	3.5
Seamount	936	18.4	56.2	2.0	7.8	9.8	4.4	1.4
Southern	812	8.3	37.1	3.2	3.8	7.5	9.7	30.4
1983-84 Cruise Period								
Northern	977	13.1	71.6	2.9	1.4	9.6	0.7	0.7
Seamount	2,455	23.1	50.1	0.8	5.3	18.9	1.3	0.5
Southern	1,108	12.1	45.0	1.8	3.3	11.9	10.1	15.8

while the other clusters contained less than 4%. The seamount cluster was characterized in both cruise periods by its higher proportion of *Etelis* species, just about twice the amount in the other clusters within each cruise period. For banks in the seamount cluster essentially three species accounted for the entire catch.

Of the 13 banks sampled on both cruise periods, 9 were in the same cluster in both periods and 4 changed clusters. Under the hypothesis that banks are randomly assigned to clusters, the probability that nine or more do not change clusters between the two periods is less than 0.01.

The similarity in the catch composition and bank composition of corresponding clusters between cruise periods suggests that variation in the species composition of the archipelago over the 2-year period between cruises was less than the variation in species composition within the archipelago. When the catch composition for each cruise period was combined and cluster analysis performed on the combined data again, three clusters were selected based on their relative reduction in the maximum intracluster distance. Again, these three clusters will also be called northern, seamount, and southern (Tables 7 and 8).

Table 7. Banks grouped by three clusters when both cruise periods are combined.

Northern cluster	Seamount cluster	Southern cluster
Asuncion	Maug	Esmeralda
Agrihan	Alamagan	Tinian
Anatahan	Pagan	Saipan
Farallon de Medinilla	Guguan	Aguijan
38-Fathom	Sarigan	Rota
Galvez and Santa Rosa	Bank C	Guam
Arakane	Bank D	
	Pathfinder	
	Bank A	

The species composition of the three clusters is very similar to the composition of the clusters from each cruise period. The southern cluster is characterized by a high proportion of *P. flavipinnis*, and the seamount cluster differs from the others in its higher proportion of *Etelis* species and lower diversity. In general there is an increase in diversity measured by the Shannon-Weaver Index (H) and a corresponding increase in the index of habitat area going from the seamount to northern to southern clusters (Table 8). The fishing mortality for *P. zonatus* based on pooled length-frequency data is estimated for each cluster and used as an index of fishing pressure (Wetherall et. al. 1985). The islands and banks of the northern and seamount clusters are unfished while those of the southern cluster are fished (Table 8). The most noticeable feature of the catch composition of the southern cluster is the high proportion of *P. flavipinnis* relative to the other clusters and it is hypothesized that this is due to fishing pressure present at the southern cluster and absent from the other two clusters. Even within the southern cluster the three islands and banks, which after Tinian where no *P. zonatus* was caught, have the highest proportion of *P. flavipinnis* also have an estimate of fishing mortality for *P. zonatus* of 0.26/year which is slightly more than twice the value of

Table 8. Cluster catch compositions based on three clusters and data pooled over both cruise periods together with the Shannon-Weaver index of diversity for the cluster catch composition (H), the mean of the $\log_e$ (length of 200-m contour) (L), and the fishing mortality (F) on *Pristipomoides zonatus*.

	Percentage of catch									
Cluster	*Etelis*	*Pristipomoides zonatus*	Groupers	Jacks	*P. auricilla*	Other snappers	*P. flavipinnis*	H	L	F
Southern	9	24	1	3	11	18	34	1.62	3.32	[1]0.12
Northern	10	48	5	7	16	7	7	1.57	2.58	0.0
Seamount	19	53	3	3	20	1	1	1.25	1.16	0.0

[1] Three banks, Saipan, Esmeralda, and Aguijan, each of which have over 34% of the catch composed of *P. flavipinnus*, have a combined estimate of F of 0.26.

fishing mortality based on length-frequency data from all the islands and banks of the southern cluster pooled, further supporting the hypothesis of a relationship between fishing pressure and relative abundance of *P. flavipinnis*.

DISCUSSION

For CPUE and catch composition there was substantial variation among banks within the archipelago, and this pattern of variation was relatively invariant over the 2-year survey period.

The higher bank CPUE at the western seamounts relative to the unfished northern and southern islands and banks is intriguing. Unfortunately we can only speculate at the factors which might be responsible for the difference. One hypothesis is that the difference is due to the Taylor column effect. A model of a small pinnacle exposed to current flow indicates that a deep eddy can form above and around the pinnacle (Uda and Ishino 1958). It has been speculated that this eddy, termed a Taylor column, can entrain larvae, create an upwelling and serve to increase primary and secondary production (Shomura and Barkley 1979; Owens and Hogg 1980).

The results of cluster analysis indicate that banks can be grouped into one of three catch profiles which are relatively invariant over time. It appears that both bank size which determines the bottom fish habitat, and fishing pressure explain variation in the diversity of the catch composition. The *Etelis* group, *P. zonatus*, and *P. auricilla* are the dominant species when habitat is relatively small. As the amount of habitat increases other species increase their relative abundance. In the absence of fishing mortality, it is hypothesized, *P. flavipinnis* is not able to establish a significant population, and it is only in the presence of fishing pressure, perhaps because stocks of competing species are reduced, that *P. flavipinnis* can become established.

ACKNOWLEDGMENT

This paper is the result of the Resource Assessment Investigation of the Mariana Archipelago at the Southwest Fisheries Center Honolulu Laboratory, National Marine Fisheries Service, NOAA.

REFERENCES

Ehrlich, P.R. 1975. The population biology of coral reef fishes. Annu. Rev. Ecol. Syst. 2:211-247.

Goldman B. and F.H. Talbot. 1976. Aspects of the ecology of coral reef fishes. *In* O.A. Jones and R. Endean (eds.). Biology and geology of coral reefs: Vol. IV, Biol. 2. Pp. 125-154. New York: Academic Press.

Helfman, G.S. 1978. Patterns of community structure in fishes: Summary and overview. Environ. Biol. Fish. 3(1):129-148.

Molles, M.C., Jr. 1978. Fish species diversity on model and natural reef patches: Experimental insular biogeography. Ecol. Monogr. 48:289-305.

Owens, W.B. and N.G. Hogg, 1980. Oceanic observations of stratified Taylor columns near a bump. Deep-Sea Res. 27:1029-1045.

Sale, P.F. 1980. The ecology of fishes on coral reefs. *In* H. Barnes and M. Barnes (eds.). Oceanography and Marine Biology: Vol. 18. Pp. 367-421. Abderdeen Univ. Press.

Scott, R.B., L. Kroenke, G. Zakariadze, and A. Sharaskin. 1980. Evolution of the South Philippine Sea: Deep sea drilling project Leg 59 results. *In* L. Kroenke, R. Scott, et al. Initial reports of the deep sea drilling project. Vol. 59. Pp. 803-815. Washington: U.S. Govt. Print. Off.

Shannon, C.E. and W. Weaver. 1963. The mathematical theory of communication. 177 pp. Urbana: Univ. Illinois Press.

Shomura, R.S. and R.A. Barkley. 1979. Ecosystem dynamics of seamounts--a working hypothesis. [Abstract.] *In* Kuroshiio IV. Proceedings of the Fourth Symposium for the Cooperative Study of the Kuroshio and adjacent regions. The Japan Academy, Tokyo, Japan, 14-17 February 1979. Pp. 789-790. Compiled by the Editorial Committee for the Proceedings of the Fourth CSK Symposium. Saikon Publ. Co., Tokyo.

Smith, C.L. 1978. Coral reef communities: A compromise view. Environ. Biol. Fish. 3(1): 129-148.

Talbot, F.H., B.C. Russell, and G.R.V. Anderson. 1978. Coral reef fish communities: Unstable, high-diversity systems? Ecol. Monogr. Pp. 425-440.

Uda, M. and M. Ishino. 1958. Enrichment pattern resulting from eddy systems in relation to fishing grounds. J. Tokyo Univ. Fish. 44(1-2):105-129.

Wetherall, J.A., J.J. Polovina, and S. Ralston 1985. Estimating growth and mortality in steady state fish stocks from length-freguency data. Proceedings of the ICLARM/KISR Conference on the Theory and Application of Length-Based Methods for Stock Assessment, held at the Instituto di Technologia della della Pesca e del Pescato, Mazara del Vallo, Sicily, Italy, 11-16 February 1985.

8578

ARTIFICIAL REEF TECHNOLOGY IN JAPAN

Jeffrey J. Polovina

INTRODUCTION

This report highlights artificial reef technology in Japan emphasizing ideas which were expressed in meetings with about a dozen artificial reef researchers and obtained from a number of reports and publications which were acquired during the author's ten-day visit to Japan in August 1985.

Japan has a long history of developing fishing reefs. Historically, piles of rocks were placed in shallow waters to create fish habitat. In 1952, the government began a subsidy program to support the construction of artificial reefs. In 1976, concerned over the declaration of the 200-mile exclusive economic zones by a number of countries of the world which threatened to reduce the fish catches of Japan's far seas fleet, the government made a major commitment to increase fish production in her coastal waters. The government saw artificial reefs as one way to increase fish catches in their local waters and in 1976 initiated the a six-year program with about $40 million a year to be spent on construction and deployment of artificial reefs. In 1982, a second six-year program continued the first six-year program with annual funding for artificial reef construction and deployment at about $50 million.

Much of this funding in recent years has been directed toward large-scale artificial reef projects, those which have an enclosed volume of more than 50,000 m^3 and which are installed in areas where there is no existing fishery with the objective of creating new fishing grounds. The national government funds about 50% of the costs of the smaller projects, those which are used to enhance existing fishing grounds, and about 70% of the costs of the larger projects. The remainder of the funding comes from prefectural governments with a small contribution from fishing villages and cooperatives.

CURRENT STATUS

While the design of an artificial reef is still largely an empirical art, the Japanese feel strongly that the construction of an artificial reef at a specific site must take into account oceanographic and bottom conditions and the biological requirements of the target species. Dr. Yoshinori Ogawa of the Nansei Regional Fisheries Research Laboratory indicated that the behavior around artificial reefs of about 150 marine species has been examined and five patterns of reef usage have been identified. There are those species such as lobsters and moray eels which prefer strong physical contact with the reef structure. Then there are those species such as the rockfish which prefer close contact with a fin or belly to the reef. The third type of behavior is found with many reef fish such as the red snapper which is close proximity to the reef without actually touching it. The fourth pattern of behavior is exhibited by fishes such as mackerel and yellowtail which do not necessarily require a hard structure but use it for orientation when one is found. Finally, there are those fishes which appear to use the internal wave generated by the current over the reef structure; these fishes tend to be more pelagic in nature such as the tunas and swordfish. Artificial reefs can be used in a number of ways by fishes. Larval fishes may settle out on the reef and use it for shelter. Some fishes will use the reef for habitat and actually reside in the artificial reef while others will stay some distance from the reef and just use it for orientation. For some fishes the reef will be a foraging site while for others it will be used as a spawning site.

Prior to the construction of a large-scale artificial reef, oceanographic and fishing surveys are conducted to evaluate a potential site. Typically the artificial reef should be separated from an existing natural reef to avoid competiton for the same fish stocks. In Japan it is recommended that artificial reefs be separated by at least 1 km from natural reefs. The artificial reef should be sited on a hard bottom where subsidence will be minimal and in an area which is flat or gently sloping where the bottom contours are parallel to each other. In this type of monotonous environment, the reef will be conspicuous to fish looking for food, shelter, or a feature to provide orientation.

The artificial reef is composed of a number of modules. These modules are most frequently constructed with concrete, steel, or fiberglass. Their designs range from simple open cubes to large and intricate steel or fiberglass structures (Figure 1). The type of reef module used and the depth at which it is placed must be tailored to the behavior of the target species. For example, species such as lobsters and abalone require reefs with small intricate spaces and a rough surface while adult sea bream use reefs with large openings and vertical height.

Typically the size of an artificial reef is measured as the volume it encloses since the volume appears to be the single most important factor in influencing the abundance of fish found at the reef. Thus, a reef composed of 1000 concrete cubes 1 m on a side would have a volume of 1000 m^3. In the Japanese artificial reef design there are four levels of construction. The reef unit or module is the individual block. The size of the individual module can range from 1 m^3 to several hundred m^3. The reef set is composed of a number of reef units. It is recommended that the reef units be piled together to form a reef set to increase the spatial complexity and the vertical relief, and that the total size of the reef set be at least 1000 m^3. A reef group consists of 10 to 20 reef groups with a separation of about 400 m between each reef set in the group. The size of the reef group should be at least 50,000 m^3. In some instances, for a particularly large-scale artificial reef a number of reef, groups will be used to form a reef complex.

EFFECTIVENESS OF ARTIFICIAL REEFS

I was particularly interested in learning what the Japanese have discovered concerning the effect that artificial reefs have on the marine ecosystem and the role they play in their coastal fishery. Two of Japan's foremost experts on artificial reefs, Dr. Yoshinori Ogawa of the Nansei Regional Fisheries Research Laboratory and Dr. Hiroshi Kakimoto of the Niigata Prefectural Fisheries Laboratory, both indicated that artificial reefs in Japan generally impinge in a number of ways. They aggregate fish and thus increase the catchability of fishing vessels. This role is particularly useful for the more migratory demersal and pelagic fishes, and artificial reefs are frequently sited in migration paths where they interrupt the migration for a period of time which allows fishermen time to fish the stocks. A time series of acoustic surveys conducted along the coast of Niigata Prefecture covering both an area with and without and artificial reef indicated that usually the greatest concentrations of both demersal and pelagic fishes were found at or near the artificial reef rather than over the open bottom with similar oceanographic conditions but without an artificial reef. However, large concentrations of fishes were not always at the artificial reef site and at times the acoustic survey did not detect any fish at the artificial reef site.

A second function of the artificial reef in Japan, in areas where there are conflicts between large trawlers and small vessels which use hook and line and trammel net gear, is to use the artificial reefs which would damage a trawl net to close an area to trawling and create a fishing ground for the small vessels with more traditional gear.

A number of studies in Japan indicate that a different composition of species are caught at artificial reefs than on nearby open bottoms with the same oceanographic conditions. Thus, artificial reefs appear to produce a change in the species composition from flat bottom associated fishes to reef associated fishes and this change in species composition in many cases is beneficial because the fishes which are found associated with artificial reefs such as rockfish and red snappers often command a higher market price than the fishes caught on the flat bottoms.

One question which has yet to be resolved is the extent that artificial reefs actually increase production rather than simply aggregate fishes. Surprisingly the Japanese, even with their large expenditures on the construction of artificial reefs, have not rigorously addressed this question. In general, there were no baseline studies of catch rates in areas which received artificial reefs prior to the placement of these reefs to compare with the catch rates after the creation of the artificial reef. Even this data would not adequately address the question unless data were available on catch rates along the coast on both sides of the artificial reef to determine the extent that the artificial reef drew fishes from the adjacent areas rather than actually increased production.

The work that has been done to evaluate the extent that artificial reefs increase production has not been conclusive. Frequently a value of the increase in annual production of about 5 kg of fish biomass per cubic meter of artificial reef volume is cited, particularly in feasibility studies but this value has not been rigorously documented. Other studies such as one conducted in Makimura, Hokkaido, which compared the value of fish catches in a area prior to the placement of an artificial reef with the value of the catches after an artificial reef, found that there was no significant economic benefit from the reef.

However, relative to the other functions the artificial reef plays such as aggregating, and excluding trawlers, the increased production offered by the reef may in many cases be secondary. For example, in the Niigata area about 350,000 m^3 of artificial reefs have been installed since 1955 along about 250 km of coastline. The average annual fish landings from that area is about 100,000 metric tons. Even if the artificial reef increases production by 5 kg per cubic meter of reef volume, the increase in production from the artificial reefs will only be 1750 metric tons or less than 2% of the total annual landings from the area and not even enough to be measurable relative to the annual variation in total landings. However, the benefits from effectively aggregating migratory fishes to vessels can increase their catches and reduce their travel time and benefits to maintaining employment in coastal fisheries by providing fishing grounds for smaller vessels with more traditional gear which cannot compete with larger trawlers can make artificial reefs an effective management tool. They are popular politically because they benefit the numerous fishing villages and cooperatives which have political influence. Further, the government subsidies directly benefit large concrete, steel, and fiberglass companies which produce the reef modules as well as other industries involved in the deployment of the modules.

ACKNOWLEDGMENTS

The author met with the following individuals associated with fishery enhancement work and wishes to acknowledge their assistance and hospitality.

Asahi Chemical Industry, Osaka

Mr. S. Akasaka, manager, Artificial Reef Program

Asahi Chemical International, Tokyo

Mr. N. Chibazakura, director

Japan Sea Regional Fisheries Research Laboratory, Niigata

Dr. A. Shirota, chief of Coastal Fisheries Development Division
Mr. K. Nashida and Mr. Y. Kitano, biologists

Nansei Regional Fisheries Research Laboratory

Dr. Y. Ogawa, head, Aquaculture Division
Dr. K. Ishioka, biologist

Niigata Prefectural Fisheries Laboratory

Dr. H. Kakimoto, artificial reef biologist

Oceanautes Inc., Tokyo

Mr. S. Kobori, director, and
Mr. M. Igarashi, manager, Engineering Department

Tohoku University, Sendai

Dr. T. Kawasaki

Tokyo University of Fisheries

Dr. S. Watanabe

University of Tokyo, Ocean Research Institute

Dr. S. Tanaka

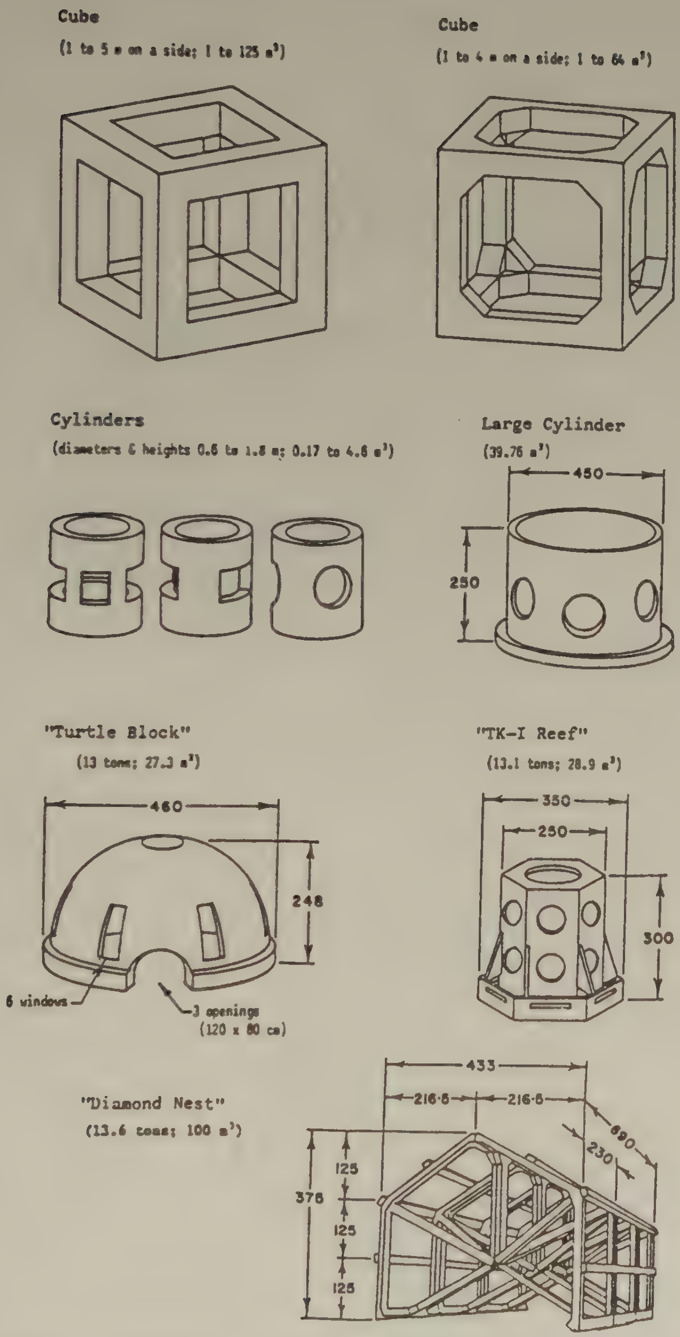
Cube
(1 to 5 m on a side; 1 to 125 m^3)
Cube
(1 to 4 m on a side; 1 to 64 m^3)
Cylinders
(diameters & heights 0.6 to 1.8 m; 0.17 to 4.6 m^3)
Large Cylinder
(39.76 m^3)
450
250
"Turtle Block"
(13 tons; 27.3 m^3)
460
248
6 windows
3 openings
(120 x 80 cm)
"TK-I Reef"
(13.1 tons; 28.9 m^3)
350
250
300
"Diamond Nest"
(13.6 tons; 100 m^3)
433
216·5
216·5
690
230
376
125
125
125

Figure 1. Selected artificial reef modules (sizes in cm)

Note: These figures are from "Enhancement of the Marine Environment for Fisheries and Aquaculture in Japan," Mottet, M. G. State of Washington, Department of Fisheries, TR No. 69 (1981).

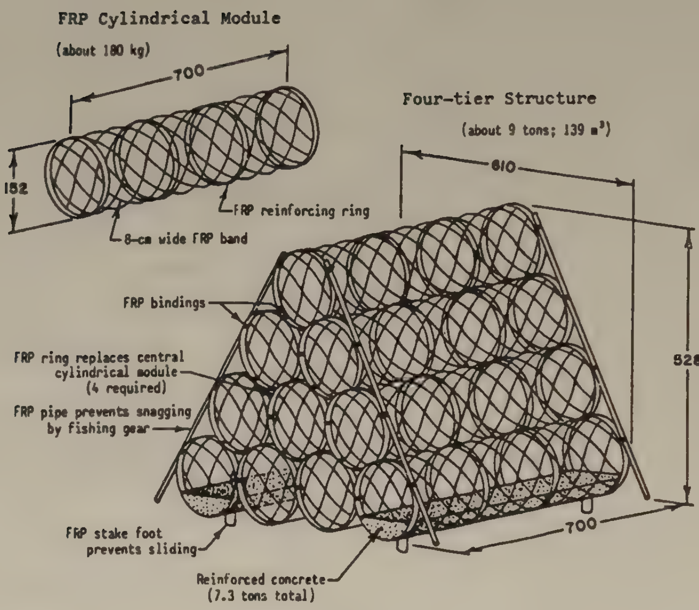
FRP Cylindrical Module
(about 180 kg)
700
152
FRP reinforcing ring
8-cm wide FRP band
Four-tier Structure
(about 9 tons; 139 m³)
610
528
700
FRP bindings
FRP ring replaces central cylindrical module (4 required)
FRP pipe prevents snagging by fishing gear
FRP stake foot prevents sliding
Reinforced concrete (7.3 tons total)

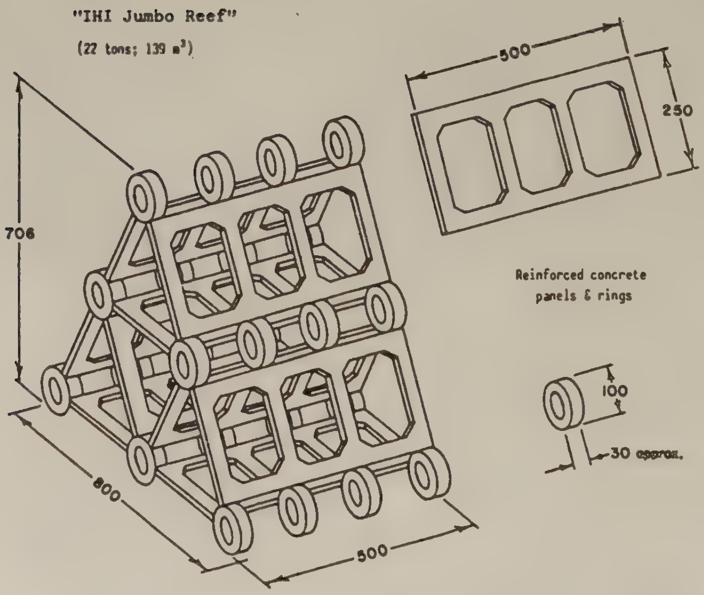
"IHI Jumbo Reef"
(22 tons; 139 m³)
706
800
500
500
250
Reinforced concrete panels & rings
100
30 approx.

Figure 1 continued.

8579

AN APPROACH TO ESTIMATING AN ECOSYSTEM BOX MODEL

Recent trends in ecosystem modeling have produced complex simulation models which are very data intensive (Andersen and Ursin 1977; Laevastu and Larkins 1981). However, in many situations the construction of a biomass budget for a box model of an ecosystem is relatively simple and can provide important information about the ecosystem standing stock and energy flow (Walsh 1981; Pauly 1982; Polovina 1984).

The ECOPATH model is an analytical procedure to estimate a biomass budget for a box model of an ecosystem given inputs which specify the components of the ecosystem, together with their mortality, diet, and energetics value. A computer program for ECOPATH has been written in BASIC-80, version 5.21, by Microsoft[1] (CP/M version). A listing of the ECOPATH computer program and a user's manual are available from the author.

The ECOPATH model produces estimates of mean annual biomass, annual biomass production, and annual biomass consumption for each of the user specified species-groups. The species-groups represent aggregations of species with similar diet and life history characteristics and which have a common physical habitat. The ECOPATH model is not a simulation model with a time component as are some more complex ecosystem models. It estimates a biomass budget for the marine ecosystem in a static situation under the assumption that the ecosystem is at equilibrium conditions.

Equilibrium conditions are defined to exist when the mean annual biomass for each species-group does not change from year to year. This condition results in a system of biomass budget equations which, for species-group i, can be expressed as

Production of biomass for species i − all predation on species i − nonpredatory biomass mortality for species i − fishery catch for species $i = 0$ for all i. (1)

The ECOPATH model expresses each term in the budget equation as a linear function of the unknown mean annual biomasses (B_i's) so the resulting biomass budget equations become a system of simultaneous equations linear in the B_i's. The mean annual biomass estimates are obtained by solving the system of simultaneous linear equations.

---

[1] Reference to trade names does not imply endorsement by the National Marine Fisheries Service, NOAA.

FISHERY BULLETIN: VOL. 83, NO. 3, 1985.

The formulation of each term of the biomass budget equation will now be presented in detail.

The Model

Biomass Production

Production (P) for a cohort of animals over 1 yr is defined as

$$P = \int_0^1 N_t \frac{d}{dt} (w_t)\, dt$$

and mean annual biomass (B) for the cohort is defined as

$$B = \int_0^1 N_t\, w_t\, dt$$

where N_t is the number of animals and w_t the mean individual weight at time t.

Allen (1971) investigated the production to biomass (P/B) ratio for a cohort over a range of mortality and growth functions. For a number of growth and mortality functions, including negative exponential mortality and von Bertalanffy growth, the ratio of annual production to mean biomass for a cohort is the annual instantaneous total mortality (Z_i). For a species-group which consists of n cohorts or species, with instantaneous annual total mortality (Z_i) for cohort or species i, where mortality is determined by a negative exponential function and growth by a von Bertalanffy growth function, the total species-group production (P) is the sum of the cohort production (P_i) and can be expresed as

$$P = \sum_{i=1}^{n} P_i = \sum_{i=1}^{n} Z_i B_i. \tag{2}$$

Under the assumption that the Z_i's are all equal to say Z, then total species-group production can be expressed as

$$P = Z \cdot B$$

where B is the mean annual species-group biomass.

Allen (1971) has also shown that when growth in weight is linear, the P/B ratio is equal to the reciprocal of the mean age for a range of mortality functions. For a number of other growth and mortality functions the ratio of cohort P/B can be the reciprocal of the mean lifespan. Thus, for a range of growth and mortality functions, total species-group production can be expressed as

$$P = C \cdot B$$

where B is the mean annual species-group biomass, and C is a parameter.

In an application of ECOPATH to an ecosystem of French Frigate Shoals where there was very little fishing mortality, the P/B ratio for fishes and crustaceans was taken as the annual instantaneous natural mortality (M); whereas, for primary and secondary producers whose growth is more likely to be linear than the von Bertalanffy, the P/B ratio was estimated as the reciprocal of the mean age (Polovina 1984).

Predation Mortality

The predation mortality is the fraction of the biomass of a species-group which is consumed by all predators excluding fishing mortality. Two types of information are needed. First the food web or predator-prey relationships must be defined. A diet composition matrix DC_{ij} must be specified where an entry DC_{ij} from this matrix refers to the proportion (by weight) of prey j in the diet of predator i. The primary source of this information is the analysis of stomach contents data. At least in one study it has been shown that there is a high correlation between diet indices based on weight, volume, and percentage of occurrence for stomach content data, and thus either index may be used to generate the DC matrix (Macdonald and Green 1983). The second type of information needed to ascertain predation mortality is the food requirements of the predator. The ECOPATH model requires the user to specify FR_i, the ratio of annual consumption to mean annual biomass. The annual food required by the predator is the product of FR_i and B_i.

Some values of daily food required as a fraction of body weight range from 0.005 to 0.02 (Laevastu and Larkins 1981). Based on these daily estimates a range of annual food required as a fraction of mean biomass (FR_i) is 1.8 to 7.3.

Nonpredation Mortality

All mortality attributable to causes other than predation and fishing is termed nonpredatory mortality. The ECOPATH model defines ecotrophic efficiency e_i as the fraction of total production which is removed by fishing and predation mortality. This was 0.95 in the French Frigate Shoals model. The nonpredator mortality rate is $(1 - e_i) \cdot Z_i$, and the amount of production which goes to nonpredation mortality is

$$(1 - e_i)\,P_i = (1 - e_i)\,C_i\,B_i.$$

For n species-groups the biomass budget Equation (1) becomes a system of n simultaneous equations as follows:

$$\begin{array}{llll}
C_1 B_1 - \sum\limits_{k=1}^{n} (FR_k) B_k DC_{k1} & - (1 - e_1) C_1 B_1 & = & \text{catch}_1, \\
\cdot \quad\quad \cdot & \cdot & & \cdot \\
\cdot \quad\quad \cdot & \cdot & & \cdot \\
\cdot \quad\quad \cdot & \cdot & & \cdot \\
C_i B_i - \sum\limits_{k=1} (\mathrm{FR}_k) B_k DC_{ki} & - (1 - e_i) C_i B_i & = & \text{catch}_i, \\
\cdot \quad\quad \cdot & \cdot & & \cdot \\
\cdot \quad\quad \cdot & \cdot & & \cdot \\
\cdot \quad\quad \cdot & \cdot & & \cdot \\
C_n B_n - \sum\limits_{k=1}^{n} (FR_k) B_k DC_{kn} & - (1 - e_n) C_n B_n & = & \text{catch}_n.
\end{array}$$

With input estimates for parameters C_i, FR_i, DC_{ij}, and e_i for all i and j, and catches (catch_i) if there is fishing, this system of equations is a system of n simultaneous equations linear in the unknown B_i's. This system of equations can be expressed in matrix form as $AB = C$, where A is an $n \times n$ matrix of coefficients, B is an n-dimensional vector of mean annual species group biomass, and C is the vector of fishery catch where the ith element is the total catch of the ith species-group.

If the matrix A is of full rank and if there are some fishery catches for some species so the vector C is not null, then there typically exists a unique nontrivial solution vector of biomass B. If there are no fishery catches then it is necessary to provide an estimate of at least one of the mean species group biomass B_i before there exists a unique nontrivial biomass vector B which solves the budget equation. In the application of ECOPATH to an ecosystem at French Frigate Schoals where there was no fishing mortality, the biomasses of three apex predators were estimated from field censuses and treated as known inputs. In this application the ith element of C vector was the annual predation by the three apex predators on the ith species-group.

Five years of field work targeting most of the components of the marine ecosystem at French Frigate Schoals in the Northwestern Hawaiian Islands provided the estimates for many of the input parameters required by the ECOPATH model as well as some estimates of biomass and production to serve to evaluate the estimates produced by the model. The estimates of biomass and production generated by the application of ECOPATH to French Frigate Shoals are given in Figure 1. In general the model's estimates of biomass and production are in good agreement with the available field data (Polovina 1984). In the application of the French Frigate Shoals, the biomasses of the top level carnivores are treated as fixed inputs thus a particularly appropriate validation of the model is the comparison of the estimate of net benthic primary production with an independent estimate from field data. The model estimated net benthic primary production, adjusted to the total 1,200 km^2 habitat of French Frigate Shoals, at 2.3×10^6 kg · km^{-2} · yr^{-1} while the estimate based on field data was 2.5×10^6 kg · km^{-2} · yr^{-1} (Grigg et al. 1984).

The Computer Program

The ECOPATH model has been implemented via two BASIC language programs. The "dialect" of the language used is BASIC-80, version 5.21, by Microsoft (CP/M version). These programs are designed to be used interactively on a terminal or a hard-copy printer. The first program is the input parameter program which accepts the input parameters and formats them into a BASIC sequential file. The second program is the ECOPATH model itself.

Literature Cited

ALLEN, K. R.
1971. Relation between production and biomass. J. Fish. Res. Board Can. 28:1573-1581.

ANDERSEN, K. P., AND E. URSIN.
1977. A multispecies extension to the Beverton and Holt theory of fishing, with accounts of phosphorus circulation and primary production. Medd. Dan. Fisk. Havunders., New Ser., 7:319-435.

GRIGG, R. W., J. J. POLOVINA, AND M. J. ATKINSON.
1984. Model of a coral reef ecosystem: Part III Resource Limitation, Community Regulation, Fishery Yield, and Resource Management. Coral Reefs 3:23-27.

LAEVASTU T., AND H. A. LARKINS.
1981. Marine fisheries ecosystem: its quantitative evaluation and management. Fishing News Books, Farnham, Surrey, Engl., 162 p.

MACDONALD, J. S., AND R. H. GREEN.
1983. Redundancy of variables used to describe importance of prey species in fish diets. Can. J. Fish. Aquat. Sci. 40:635-637.

PAULY, D.
1982. Notes on tropical multispecies fisheries, with a short

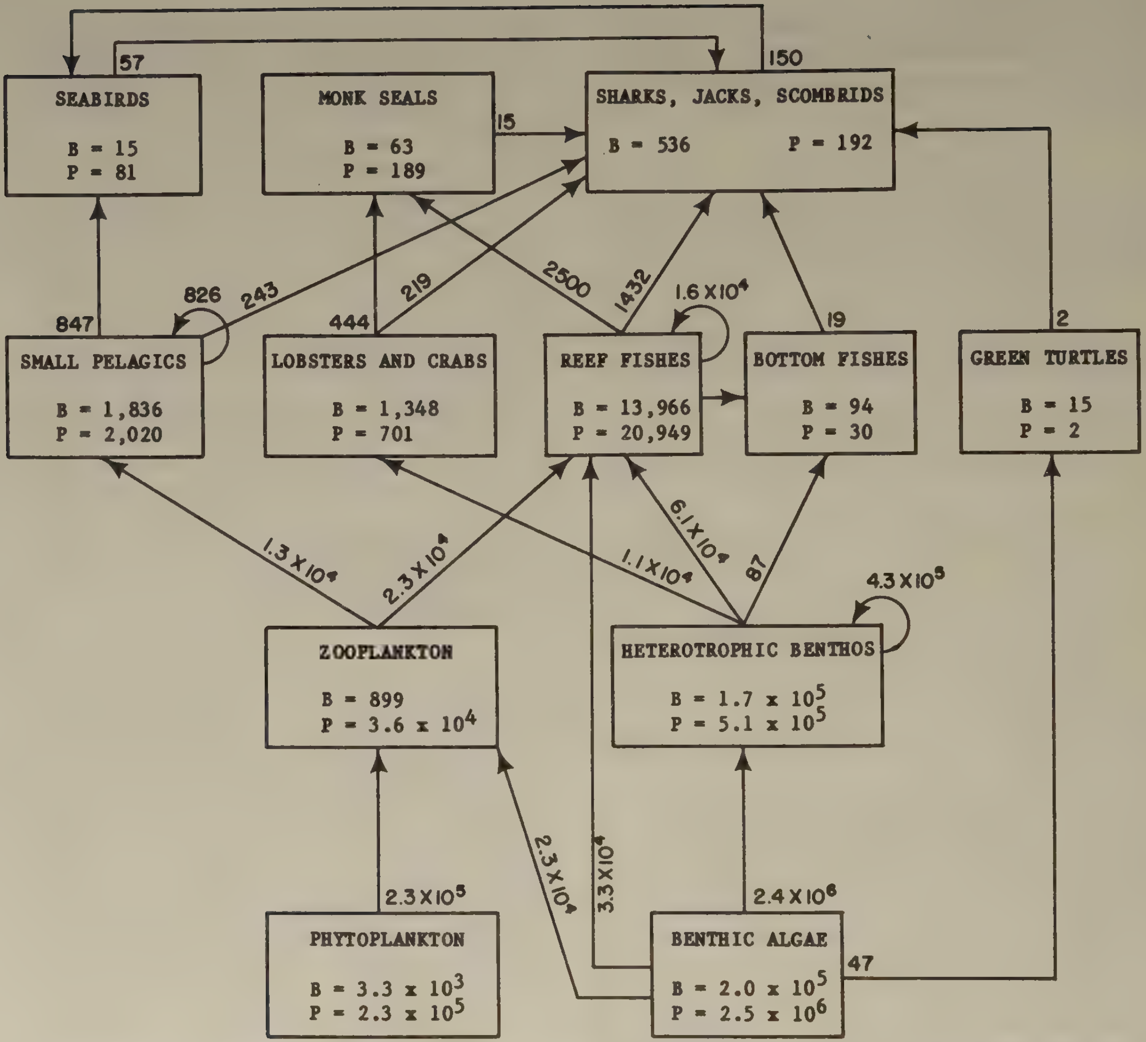
SEABIRDS
B = 15
P = 81
MONK SEALS
B = 63
P = 189
SHARKS, JACKS, SCOMBRIDS
B = 536
P = 192
57
150
15
SMALL PELAGICS
B = 1,836
P = 2,020
LOBSTERS AND CRABS
B = 1,348
P = 701
REEF FISHES
B = 13,966
P = 20,949
BOTTOM FISHES
B = 94
P = 30
GREEN TURTLES
B = 15
P = 2
847
826
243
444
219
2500
1432
1.6×10^4
19
2
1.3×10^4
2.3×10^4
1.1×10^4
6.1×10^4
87
4.3×10^5
ZOOPLANKTON
B = 899
$P = 3.6 \times 10^4$
HETEROTROPHIC BENTHOS
$B = 1.7 \times 10^5$
$P = 5.1 \times 10^5$
2.3×10^5
2.3×10^4
3.3×10^4
2.4×10^6
47
PHYTOPLANKTON
$B = 3.3 \times 10^3$
$P = 2.3 \times 10^5$
BENTHIC ALGAE
$B = 2.0 \times 10^5$
$P = 2.5 \times 10^6$

FIGURE 1.–Biomass budget schematic for major prey-predator pathways. Annual production denoted as P and mean annual biomass as B with values in units of $(kg/km)^2$ based on a habitat area of 1,200 km^2. The values associated with the arrows represent the production from the lower trophic level consumed by the higher trophic level (Polovina in press).

bibliography of the food and feeding habits of tropical fish. *In* Report on the regional training course on fishery stock assessment, 1 September-9 October 1981, Samutprakarn, Thailand, p. 30-35 and 92-98. Tech. Rep. 1, Part II, SCS/GEN/82/41, Manila.

POLOVINA, J. J.
1984. Model of a coral reef ecosystem, Part I: ECOPATH and its application to French Frigate Shoals. Coral Reefs 3:1-11.

WALSH, J. J.
1981. A carbon budget for overfishing off Peru. Nature 290: 300-304.

JEFFREY J. POLOVINA
MARK D. OW

Southwest Fisheries Center Honolulu Laboratory
National Marine Fisheries Service, NOAA
P.O. Box 3830
Honolulu, HI 96812

8580

Fisheries Resource Assessment of the Mariana Archipelago, 1982-85

JEFFREY J. POLOVINA, ROBERT B. MOFFITT,
STEPHEN RALSTON, PAUL M. SHIOTA, and HAPPY A. WILLIAMS

Introduction

The Resource Assessment Investigation of the Mariana Archipelago (RAIOMA) was a 5-year program initiated by the Honolulu Laboratory of the National Marine Fisheries Service's Southwest Fisheries Center in 1980 to quantify the distribution and sustainable yield of insular fishery resources with commercial potential in the Mariana Archipelago (Fig. 1).

To identify fishery resources with commercial value or potential, data from the commercial landings collected by the Governments of Guam and the Commonwealth of the Northern Marianas together with data from earlier research cruises were used to rank species of fish by their economic potential and importance to the subsistence fishery. Four species groups were thus identified as important fishery resources in the Marianas: 1) Tunas, 2) deepwater snappers and groupers, 3) deepwater shrimp *Heterocarpus* spp., and 4) akule or bigeye scad, *Selar crumenophthalmus* (Polovina[1]).

The tuna resource has the greatest economic potential, but an assessment of the tunas in the Marianas would require an assessment of the tuna stocks in the western Pacific which was beyond the scope of the program. Thus, information on the tuna resource in the Marianas was obtained from historical catch and effort statistics provided by Japanese longliners and baitboats operating in

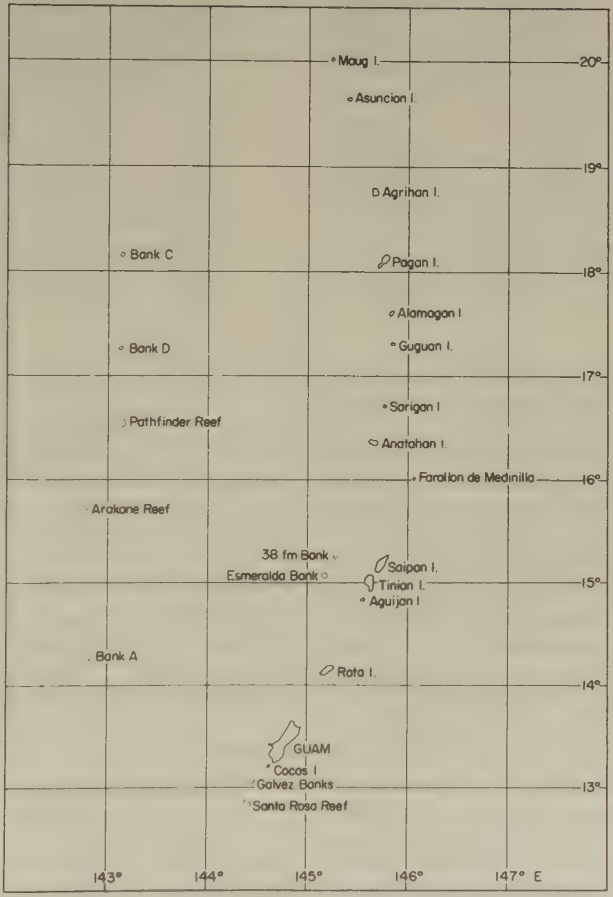
Maug I.
Asuncion I.
Agrihan I.
Bank C
Pagan I.
Alamagan I
Bank D
Guguan I.
Sarigan I
Pathfinder Reef
Anatahan I.
Farallon de Medinilla
Arakane Reef
38 fm Bank
Saipan I.
Esmeralda Bank
Tinian I.
Aguijan I
Bank A
Rota I.
GUAM
Cocos I
Galvez Banks
Santa Rosa Reef
20°
19°
18°
17°
16°
15°
14°
13°
143°
144°
145°
146°
147° E

Figure 1.—The Mariana Archipelago with the 22 islands and banks sampled during the RAIOMA Program.

---

[1] Polovina, J. J. 1981. Planning document for the assessment of marine resources around Guam and the Commonwealth of the Northern Mariana Islands. Honolulu Lab., Southwest Fish. Cent., Natl. Mar. Fish. Serv., NOAA, Honolulu, HI 96812. Admin. Rep. H-81-10, 13 p.

The authors are with the Honolulu Laboratory, Southwest Fisheries Center, National Marine Fisheries Service, NOAA, 2570 Dole Street, Honolulu, HI 96822-2396.

Table 1.—Bottom fish catch per unit effort (CPUE) and standard error (SE), by island and bank for the six cruises.

Area	No. of drifts	Mean drift CPUE (numbers)	SE	Latitude N
Northern Islands and Banks				
Maug	7	5.03	1.02	20°02′
Asuncion	17	2.16	0.49	19°40′
Agrihan	45	4.20	0.31	18°46′
Pagan	100	4.57	0.40	18°06′
Alamagan	118	2.37	0.19	17°36′
Guguan	32	3.01	0.30	17°19′
Sarigan	28	2.82	0.37	16°43′
Anatahan	38	2.31	0.23	16°21′
38-Fathom	61	3.12	0.26	16°20′
Esmeralda	114	2.29	0.15	14°58′
Average drift CPUE		3.19		
Southern Islands and Banks				
Farallon de Medinilla	32	3.29	0.65	16°01′
Saipan	17	1.72	0.34	15°10′
Tinian	20	1.96	0.29	15°00′
Aguijan	13	3.84	0.98	14°52′
Rota	19	1.91	0.40	14°10′
Guam	20	1.53	0.35	13°25′
Galvez and Santa Rosa	41	2.95	0.31	13°00′
Average drift CPUE		2.46		
Seamounts				
Bank C	8	5.91	1.57	18°08′
Bank D	20	5.85	0.51	17°09′
Pathfinder	136	4.58	0.23	16°30′
Arakane	84	3.36	0.24	15°38′
Bank A	24	3.71	0.57	14°12′
Average drift CPUE		4.68		

the fishery conservation zone (FCZ) around the Marianas (Polovina and Shippen[2]).

The insular resources were assessed by a field program which consisted of six cruises, each of 40 days, using the NOAA ship *Townsend Cromwell*, from May 1982 through June 1984. On these cruises a systematic survey was conducted to measure geographic and seasonal variation of deepwater bottom fishes and shrimps at 22 islands and banks (Fig. 1). Also, intensive fishing experiments were conducted to estimate catchability of the bottom fishes and shrimps. A collection of all specimens which appeared to represent new records was developed. Two aerial surveys were made in an attempt to estimate the abundance of akule in the Marianas. Finally bathymetric surveys were conducted and chartlets produced for 11 islands and banks where existing bathymetric data were insufficient for fishing and fishery assessment work (Polovina and Roush[3]). This report summarizes the main findings of the RAIOMA Program.

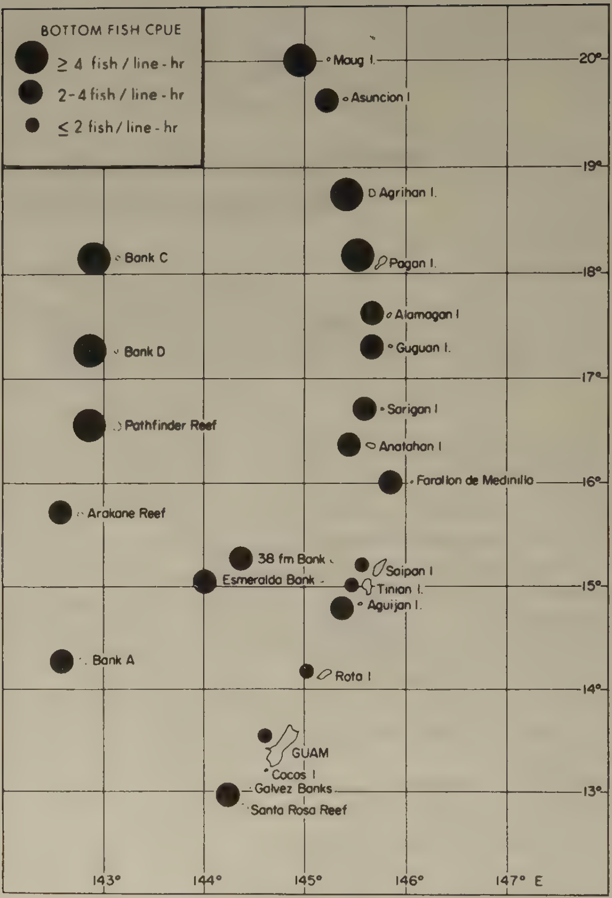

Figure 2.—The bottom fish CPUE grouped into three catch levels.

Deepwater Snappers and Groupers

At each island and bank, an attempt was made to conduct a systematic fishing survey of the bottom fish community in the 125-275 m depth range. A total of 7,621 bottom fishes of over 30 species were caught with handline gear during the six cruises. Gindai, *Pristipomoides zonatus*, accounted for 51.2 percent of the catch, and three species (gindai, yellowtail kalekale, *P. auricilla*; and ehu, *Etelis carbunculus*) accounted for 79.1 percent of the total catch (Polovina, In press).

Catch per unit effort (CPUE) was measured by the number of fish caught per line-hour. For each bank, bank CPUE was computed as the mean of all the drift CPUE values, where a drift CPUE is the number of fish caught during an uninterrupted drift of the vessel while it is fishing in the 125-275 m depth range divided by the drift line-hours. The mean drift CPUE is presented for all 22 banks and islands in Table 1 and Figure 2.

---

[2] Polovina, J. J., and N. T. Shippen. 1983. Estimates of the catch and effort by Japanese longliners and baitboats in the fishery conservation zone around the Mariana Archipelago. Honolulu Lab., Southwest Fish. Cent., Natl. Mar. Fish. Serv., NOAA, Honolulu, HI 96812. Admin. Rep. H-83-1, 42 p.

[3] Polovina, J. J., and R. C. Roush. 1982. Chartlets of selected fishing banks and pinnacles in the Mariana Archipelago. Honolulu Lab., Southwest Fish. Cent., Natl. Mar. Fish. Serv., NOAA, Honolulu, HI 96812. Admin. Rep. H-82-19, 15 p.

Taken by bank type, the seamounts have the greatest mean drift CPUE (4.68 fish/line-hour), followed by the northern islands (3.19 fish/line-hour), and then the southern islands (2.46 fish/line-hour). The main inhabited islands of the Marianas are Guam, Saipan, Rota, and Tinian—all in the southern group. Fishermen at these islands exploit the local stocks of bottom fishes which most likely account for the relatively low CPUE values for the islands. The mean of the bank CPUE for the uninhabited islands and banks in the southern group is 3.36 fish/line-hour which suggests that when islands with heavy fishing mortality are excluded, there is no difference in bottom fish standing stock between the northern and unfished southern islands. The seamounts, however, appear to support a higher standing stock than the northern or southern islands and banks.

Bottom fish species were stratified by depth. The results, summarized in Table 2, show that the centers of distribution for black ulua or black jack, *Caranx lugubris*; lehi, *Apharens rutilans*; and the yelloweye opakapaka, *P. flavipinnis*; and pink opakapaka, *P. filamentosus*, were between 164 and 183 m (90 and 100 fathoms). Similarly, yellowtail kalekale, kahala or greater amberjack, *Seriola dumerili*; and gindai were most abundant between 183 and 201 m (100 and 110 fathoms). Species with deeper depth distributions, i.e., mean depth of capture >201 m (110 fathoms), were the pink kalekale, *P. sieboldii*; black grouper, *Epinephelus* sp.; ehu, and onaga, *Etelis coruscans*. Studying each fishing bank individually showed that, overall, depth distributions were similar over the archipelago.

The approach to yield estimation for the deepwater bottom fishes is described in detail by Polovina and Ralston (In press). Using an estimate of catchability obtained from an intensive fishing experiment and a measure of bottom fish habitat together with the estimated relative abundance from the systematic survey, the total bottom fish biomass which can be exploited with handline gear was computed. The Beverton and Holt (1956) yield equation, together with estimates of growth and mortality parameters obtained from otolith and size-frequency data, was used to first determine the age of entry for each of the major species which will maximize the yield per recruit. Then with the estimate of unexploited biomass the equilibrium yield was estimated as a function of fishing mortality. Also the change in the spawning stock biomass relative to its level in the absence of exploitation can be computed with the Beverton and Holt yield equation as a function of fishing mortality.

Table 2.—Mean depth of capture for the principal bottomfish species captured during the RAIOMA cruises (N = sample size).

Scientific name	Mean depth		
	Meters	Fathoms	N
Caranx lugubris	166	91	270
Pristipomoides flavipinnis	170	93	499
P. filamentosus	170	93	191
Aphareus rutilans	174	95	81
P. auricilla	188	102	1,166
Seriola dumerili	196	107	47
P. zonatus	199	109	3,890
Epinephelus sp.	214	117	38
P. sieboldii	214	117	57
Etelis coruscans	218	119	200
E. carbunculus	225	123	950

Table 3.—Annual equilibrium bottom fish yield in metric tons (t) for the age at entry which maximizes the yield per recruit for each species.

Fishing mortality (F)	Total yield (t)
0.1	35
0.5	91
[1]1.0	109
1.5	114
2.0	116
2.5	116

[1] $F_{0.1}$ and $Y_{0.1}$ as defined by Gulland (1983).

Table 4.—Annual equilibrium bottom fish yield and yield per nautical mile of 200 m contour for the age at entry which maximizes the yield per recruit at a level of fishing mortality of $F = 1.0$.

Area	Total yield (t/year)	Yield[1]/n.mi. of 200 m contour
Northern Islands and Banks		
Maug	2.7	262.2
Asuncion	2.1	188.4
Agrihan	5.6	303.6
Pagan	7.7	255.1
Alamagan	2.0	177.6
Guguan	1.7	179.0
Sarigan	1.6	193.8
Anatahan	2.5	144.2
38-Fathom	0.5	187.3
Esmeralda	2.9	237.4
Subtotal	29.3	Mean 212.9
Southern Islands and Banks		
Farallon de Medinilla	16.7	216.6
Saipan	13.4	254.1
Tinian	8.8	303.9
Aguijan	4.2	266.7
Rota	6.1	192.2
Guam	17.2	201.6
Galvez and Santa Rosa	8.6	164.2
Subtotal	76.0	Mean 228.5
Seamounts		
Bank C	0.9	288.2
Bank D	1.1	351.2
Pathfinder	0.9	303.5
Arakane	0.6	199.6
Bank A	0.6	179.7
Subtotal	4.1	Mean 264.4

Total yield from all banks = 109 t per year.

[1] Yield in kg/year.

The equilibrium yield for the multispecies bottom fish complex fished with handline gear in the 125-275 m depth range for the 22 islands and banks of the Mariana Archipelago increases rapidly as a function of fishing mortality to a level of about 100 metric tons (t) and beyond that exhibits a gradual increase with increasing fishing mortality (Table 3). In view of the flat-topped, yield curve which assumes constant recruitment and does not incorporate any economic considerations, an approach to determining the optimum equilibrium yield has been suggested (and adopted for several North Atlantic fisheries) as the yield corresponding to that level of effort where an increase of one unit of effort will increase the catch by 0.1 of the amount caught by the very first unit of effort (Gulland, 1983; 1984).

The value of $F_{0.1}$ for the bottom fish resource in the Marianas is estimated to be $F = 1.0$, and the corresponding annual equilibrium yield is 109 t (Table 3). An approximate 95 percent confidence interval (CI) for this yield is 81-137 t (Polovina and Ralston, In press). About 70 percent of this yield would come from the southern islands and banks, 27 percent would come from the northern chain, and only 3 percent from the seamounts (Table 4; Fig. 3). At a fishing mortality of 1.0, the spawning stock biomasses for the seven major species are reduced 20-42 percent of their unexploited levels. Although the spawner recruit curve for these species is unknown, as a generic lower bound, the spawning stock biomass should not be

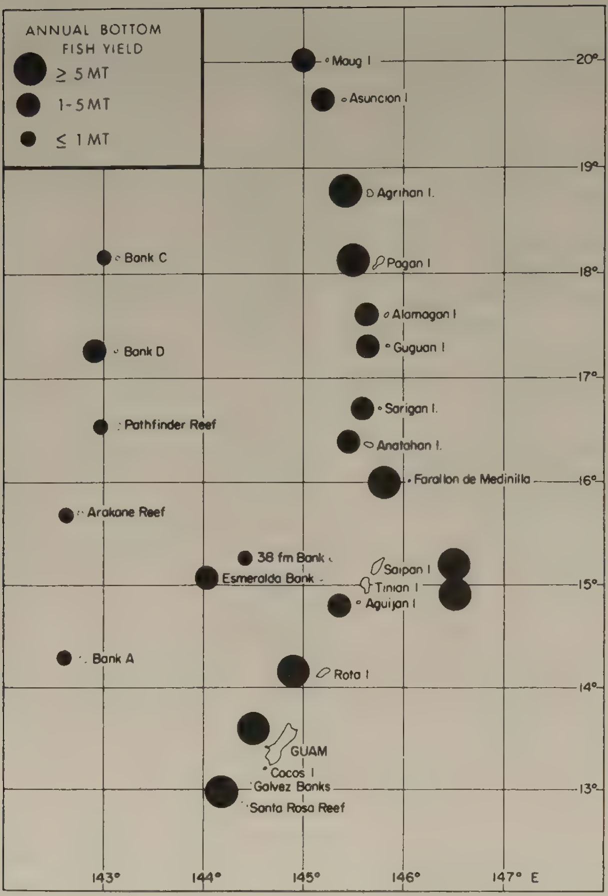

Figure 3.—Annual bottom fish yield grouped into three yield levels.

Table 5.—The percentage of annual sustainable yield by species group for fishing mortality of 1.0/year at age of entry which maximizes yield per recruit.

Species	Annual sustainable yield (percent)
Caranx lugubris	8.3
Pristipomoides filamentosus	8.2
P. auricilla	7.3
P. flavipinnis	28.7
P. zonatus	23.1
Etelis coruscans	5.0
E. carbunculus	5.9
Others	13.5

Table 6.—Estimates of Guam fish landings, 1980-84[1].

	Landings (t)	
Year	Pelagic species	Deep bottom fish
1980	198	6
1981	223	12
1982	240	9
1983	189	11
1984[2]	265	20

[1] Based on data from the Honolulu Laboratory's Western Pacific Fishery Information Network file on the Guam Division of Aquatic and Wildlife Resources offshore creel survey. Confidence interval ± 30 percent of catch for pelagics and ± 50 percent of catch for bottom fish.

[2] Estimate expanded from data from period June-September 1984.

reduced below 20 percent of its unexploited level if a serious reduction of recruitment is to be avoided (Beddington and Cooke, 1983).

The means of the annual equilibrium yield per nautical mile of 200 m contour for the northern banks, southern banks, and western seamounts are 212.9, 228.5, and 264.4 kg/n.mi., respectively. The ratio of total yield for the archipelago to the total length of the 200 m contour is 222.4 kg/n.mi. (95 percent CI of 165.3-279.6 kg/n.mi.) (Table 4). These values suggest that the stocks in the Marianas are slightly less productive than those in Hawaii where a lower-bound estimate of maximum sustainable yield of 272 kg/n.mi. of 200-m contour was obtained from a stock production model applied to commercial catch and effort data (not including the recreational fishing component) of snappers and groupers from Penguin Bank (Ralston and Polovina, 1982).

If the entire archipelago is fished, *P. flavipinnis* and *P. zonatus* together will comprise about 50 percent of the catch (Table 5).

Over the period 1980-84 it is estimated that annual bottom fish landings have increased from 6 t in 1980 to 20 t in 1984 (Table 6). Although the location data were not always obtained for these data, it appears that 65-95 percent of this catch comes from around Guam and the remainder comes from Galvez Banks and Santa Rosa Reef south of Guam or areas in the Commonwealth of the Northern Marianas. Given the estimated equilibrium yield of 17.2 t for Guam and that the CPUE around Guam is about half of the archipelago average, it appears that Guam is already fished at its maximum sustainable yield and most probably overfished on the leeward coast. There may be an opportunity to increase the yield with more fishing effort directed toward Galvez Banks and Santa Rosa Reef, but most of the additional yield potential lies in the islands and banks to the north of Guam (Table 4).

The commercial landings at Saipan have ranged from 4 to 10 t, compared with the estimate of equilibrium yield of 29 t from Saipan, Tinian, Aguijan, and Esmeralda Bank (Tables 4 and 7). These sites are all within 30 miles of Saipan suggesting that there is an opportunity to increase bottom fish landings from Saipan, Tinian, Aguijan, and Esmeralda Bank with a bottom fishing fleet operating out of Saipan and Tinian.

Based on the catchability estimated from the intensive fishing experiment,

Table 7.—Estimates of the Commonwealth of the Northern Mariana Islands commercial landings, 1981-83[1].

	Landings (t)	
Year	Pelagic species	Deep bottom fishes
1981	40.8	5.3
1982	47.2	3.7
1983	89.2	6.4
1984	123.8	9.9

[1]Data from the Honolulu Laboratory's Western Pacific Fishery Information Network.

Table 8.—Depth stratification for *Heterocarpus* spp.

Depth			Depth		
Meters	Fathoms	CPUE[1]	Meters	Fathoms	CPUE[1]
Heterocarpus ensifer			*H. laevigatus* (continued)		
320	175	0			
366	200	0.18	686	375	1.93
412	225	0.15	732	400	1.64
458	250	0.10	778	425	2.33
503	275	0.09	824	450	1.10
549	300	0.02	869	475	0.87
595	325	0.02	915	500	0.36
640	350	0.03	961	525	0.05
686	375	0	1,006	550	0.02
732	400	0	1,052	575	0.02
H. laevigatus			*H. longirostris*		
366	200	0	824	450	0
412	225	0.08	869	475	0.11
458	250	0.01	915	500	0.29
503	275	0.62	961	525	0.38
548	300	2.10	1,006	550	0.46
595	325	1.95	1,052	575	0.75
640	350	1.75	1,098	600	0.63

[1]CPUE in kg/trap.

the fishing mortality of 1.0 per year is equivalent to an annual fishing effort of 74,153 line-hours. Thus, for example, 15 small vessels each with two electric or hydraulic gurdies which fish 12 hours a day for 200 days a year can achieve this level of fishing effort and would have a fleet catch rate of 1.5 kg/line-hour with an annual average catch of 7.3 t per vessel.

Deepwater Shrimp

Deepwater shrimp, *Heterocarpus* spp., was sampled at depths from 360 to 900 m (about 200-500 fathoms). The sampling gear consisted of Quonset[4] shaped traps about 90 by 66 cm at the base and a height of 46 cm. The frame is made of rebar and is covered with a wire mesh which is then covered on the top and two sides with a canvas cover. The entrances to the trap are two cones on opposite sides of the trap. Five traps were used on a string with a separation of about 40 m between traps. The traps were baited with mackerel.

The shrimp catches were primarily *H. ensifer*, *H. laevigatus*, and *H. longirostrus* which are stratified by depth (Table 8). The catch rates of *H. laevigatus* were the highest of the three species and were greatest in the depth range 500-825 m.

The systematic survey of the relative abundance of *Heterocarpus* spp. in the 500-825 m depth range found little seasonal variation but considerable variation in CPUE between banks. As with the bottom fishes, the seamounts had the highest catch rates (2.37 kg/trap-night), followed by the northern islands and banks (2.01 kg/trap-night), and then the southern islands and banks (1.39 kg/trap-night) (Table 9; Fig. 4).

Table 9.—Catch rates and habitat for *Heterocarpus* spp. in the 500-825 m depth range.

Area	CPUE (kg/trap)	Area (n.mi.^{2}) (500-825 m)
Northern Islands and Banks		
Maug	1.88	3.83
Asuncion	2.11	5.93
Aguijan	1.96	12.39
Pagan	2.17	16.19
Alamagan	2.18	11.43
Guguan	2.52	5.60
Sarigan	1.45	4.55
Anatahan	2.36	10.89
38-Fathom	2.12	6.37
Esmeralda	1.35	2.03
Mean = 2.01		
Southern Islands and Banks		
Farallon de Medinilla	0.97	88.55
Saipan	2.06	213.99
Tinian	1.81	73.80
Aguijan	1.61	39.36
Rota	1.02	197.31
Guam	0.72	44.24
Galvez and Santa Rosa	1.78	50.77
Mean = 1.39		
Seamounts		
Bank C	2.07	2.71
Bank D	2.72	2.71
Pathfinder	2.79	2.71
Arakane	1.91	2.10
Bank A	1.43	3.33
Mean = 2.37		

Table 10.—Equilibrium yield (t) for *Heterocarpus laevigatus* in the 500-825 m depth range and relative spawning stock biomass as a function of fishing mortality (*F*).

F	Total yield (t) in 500-825 m depth	Spawning stock biomass under *F*/unexploited spawning biomass
0.1	56.3	0.70
0.2	95.6	0.51
0.3	124.2	0.37
0.4	145.1	0.27
0.5	161.5	0.20
0.6	174.1	0.15
0.7	181.1	0.11

A growth equation for *H. laevigatus* was estimated from a time-series of length-frequency data and estimates that the shrimp become susceptible to trap fishing at age 2 and that the females become sexually mature at age 4.5 (Moffitt and Polovina[5]). Yield-per-recruit analysis indicates that an age-of entry of 2 maximizes the yield per recruit. The Beverton and Holt yield equation estimates equilibrium yield as a function of fishing mortality and the ratio of spawning stock biomass under exploitation to the unexploited spawning stock biomass (Table 10). At a fishing mortality of $F = 0.5$, the spawning stock is reduced to 20 percent of its original level in the absence of exploitation which has been suggested as a generic lower bound before a substantial decrease in recruitment may occur (Beddington and Cooke, 1983). At $F = 0.5$ the equilibrium yield from the entire archipelago in the 500-825 m depth range is estimated at 162 t, with a 95 percent CI of 102-218 t, which would almost exclusively consist of *H. laevigatus*. About 85 percent of this yield would come from the southern islands and banks, 13 percent from the northern islands and banks, and about 2 percent from the seamounts (Table 11; Fig. 5).

Although there have been several short-lived attempts to harvest deepwater shrimp around Guam, there is currently no shrimp fishing around Guam or anywhere else in the Marianas. Given that the catch rates around Guam are <50 percent of the catch rates at most other banks, any shrimp fishing should target areas other than Guam. In the southern islands the best shrimp fishing areas are Saipan, Tinian, and Aguijan (Table 9). Although Galvez Banks and Santa Rosa Reef south of

---

Reference to trade names or commercial firms does not imply endorsement by the National Marine Fisheries Service, NOAA.

[5]Moffitt, R. B., and J. J. Polovina. The distribution and yield assessment of the deepwater shrimp resource in the Marianas. Manuscr. in prep.

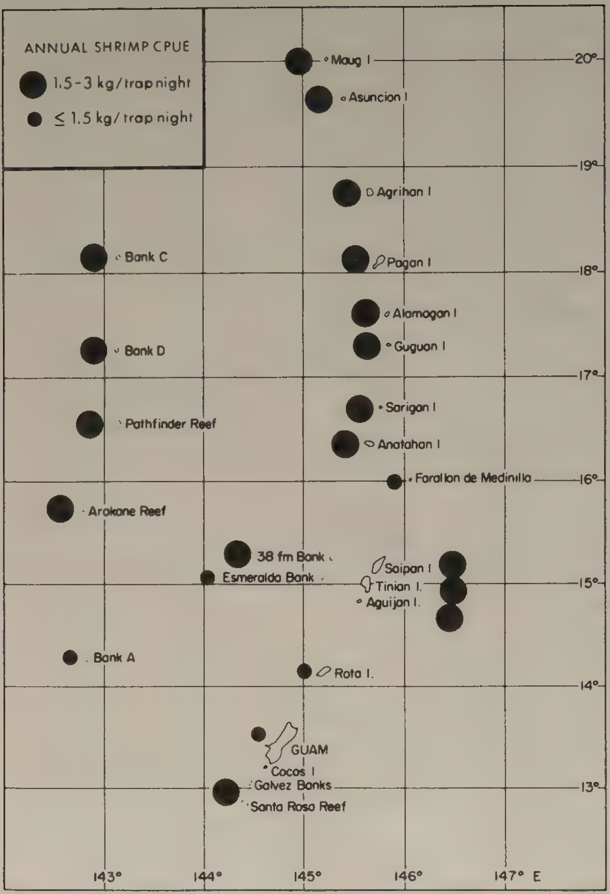
ANNUAL SHRIMP CPUE
● 1.5-3 kg/trap night
● ≤ 1.5 kg/trap night
Maug I
Asuncion I
Agrihan I
Bank C
Pagan I
Alamagan I
Bank D
Guguan I
Pathfinder Reef
Sarigan I
Anatahan I
Farallon de Medinilla
Arakane Reef
38 fm Bank
Esmeralda Bank
Saipan I
Tinian I.
Aguijon I.
Bank A
Rota I.
GUAM
Cocos I
Galvez Banks
Santa Rosa Reef
20°
19°
18°
17°
16°
15°
14°
13°
143°
144°
145°
146°
147° E

Figure 4.—Deepwater shrimp CPUE grouped into two catch levels.

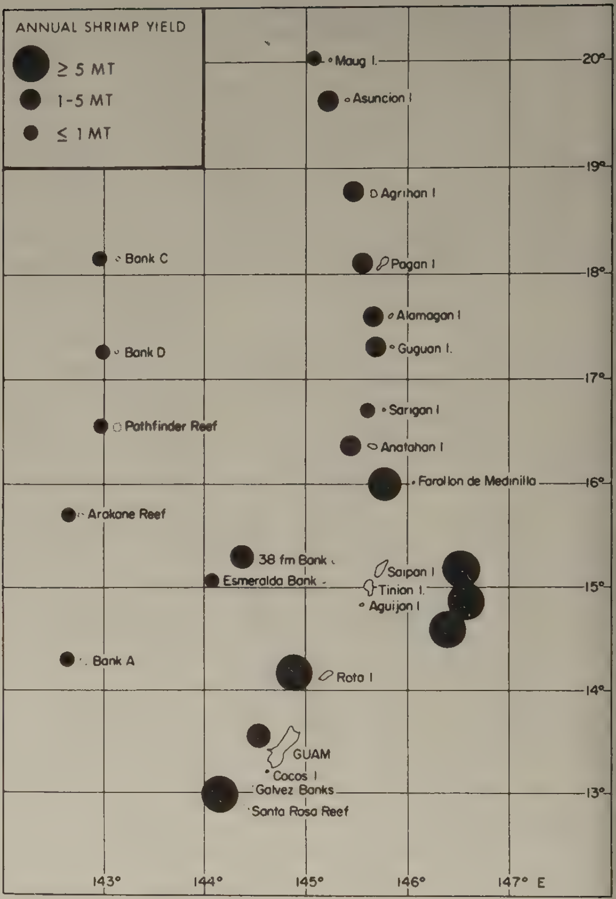
ANNUAL SHRIMP YIELD
● ≥ 5 MT
● 1-5 MT
● ≤ 1 MT
Maug I.
Asuncion I
Agrihan I
Bank C
Pagan I
Alamagan I
Bank D
Guguan I.
Pathfinder Reef
Sarigan I
Anatahan I
Farallon de Medinilla
Arakane Reef
38 fm Bank
Esmeralda Bank
Saipan I
Tinian I.
Aguijon I
Bank A
Rota I
GUAM
Cocos I
Galvez Banks
Santa Rosa Reef
20°
19°
18°
17°
16°
15°
14°
13°
143°
144°
145°
146°
147° E

Figure 5.—Annual deepwater shrimp yield grouped into three yield levels.

Guam have good catch rates, the strong currents encountered there during the assessment work resulted in considerable trap loss.

The estimated catchability from the intensive trapping and the *F* of 0.5 correspond to an effort of 280 trap-nights/n.mi.^{2}. Given a total habitat of 800 n.mi.^{2} from 500 to 825 m, an annual effort of 224,000 trap-nights would produce the fishing mortality of 0.5 for the entire archipelago. Thus, for example, 28 small vessels which each set 40 traps/night for 200 nights/year would produce this effort and have an average fleet catch rate of 0.7 kg/trap-night and an average annual landing of 5.8 t/vessel.

Other Resources

There is a substantial resource of tunas and other pelagic species around the Marianas. The Japanese longline catch and effort data for the period 1965-79 and Japanese baitboat data for the period 1970-79 within 50 n.mi. and within the FCZ around Guam and the Commonwealth of the Northern Marianas have been analyzed by Polovina and Shippen[2]. The total annual tuna catches from Japanese longliners within the FCZ around Guam ranged from 9

Table 11.—Equilibrium yield for *Heterocarpus* spp. in the 500-825 m depth range.

Area	Yield[1]	Area	Yield[1]
Northern Islands		Saipan	54.1
and Banks		Tinian	16.3
Maug	0.9	Aguijan	7.8
Asuncion	1.5	Rota	24.7
Aguijan	3.0	Guam	3.9
Pagan	4.3	Galvez and	
Alamagan	3.0	Santa Rosa	20.2
Guguan	1.7	Subtotal	137.6
Sarigan	0.8		
Anatahan	3.1	Seamounts	
38-Fathom	1.7	Bank C	0.7
Esmeralda	0.3	Bank D	0.9
Subtotal	20.3	Pathfinder	0.9
		Arakane	0.5
Southern Islands		Bank A	0.6
and Banks		Subtotal	3.6
Farallon de			
Medinilla	10.6	Archipelago total =	161.5

[1] Metric tons/year based on a fishery mortality of 0.50.

to 1,334 t, and the annual catches within the FCZ around the Commonwealth of the Northern Mariana Islands ranged from 71 to 576 t. Billfish catches typically were about 10-30 percent of the total tuna catch. The total annual tuna catches from Japanese baitboats within the FCZ around Guam ranged from 83 to 2,059 t, and the catches within the FCZ around the Commonwealth of the Mariana Islands ranged from 2,554 to 12,564 t.

Annual catches of pelagic species typically from nearshore trolling, which include tunas, mahimahi, wahoo, and billfishes, are estimated at about 200 t for Guam and varied from 40 to 124 t for Saipan (Tables 6 and 7).

Although the Japanese catches indicate that the magnitude of the pelagic resource is large it is also widely dispersed. Fish aggregating devices are widely used throughout the Pacific and appear to be useful as a means of aggregating pelagic species and hence increasing catches, but the frequency of typhoons in the Marianas is an impediment to their application. The expansion of the charter fishing industry may have potential as a means of further exploiting the tuna and billfish resources, given the strong tourist industry in both Guam and Saipan.

Akule, often called atulai or bigeye scad, is a popular resource which is usually netted or hooked in nearshore areas. Reported annual landings in Guam and the Commonwealth of the Mariana Islands are only about 5 and 1 t, respectively, but much of the resource does not go through the usual market channels and is not reported. The RAIOMA Program found akule present at most of the islands and banks but, given the seasonal nature of the resource and effect of moon phase on the catch rates, a systematic survey was not possible. Two aerial surveys were not effective in estimating the nearshore akule biomass. The estimated catch rate of akule in the Hawaiian Islands from 1948 to 1982 varies from 0.4 to 0.9 t/n.mi. of 200 m contour. If it is assumed that abundance of akule in the Marianas is equivalent to that in Hawaii, then the Marianas, where the length of the 200 m contour is 490 n.mi., would offer a range of harvest from 200 to 440 t per year. However, most of the catches in Hawaii are by small purse seiners using aerial spotters, and these catches extrapolated to the Marianas may represent upper bounds for the more traditional gear.

Literature Cited

Beddington, J. R., and J. G. Cooke. 1983. The potential yield of fish stocks. FAO Fish. Tech. Pap. 242, 47 p.

Beverton, R. J., and S. J. Holt. 1956. A review of methods for estimating mortality rates in fish populations, with special reference to sources or bias in catch sampling. Rapp. P.-v. Reun. Cons. Int. Explor. Mer 140:67-83.

Gulland, J. A. 1983. Fish stock assessment. A manual of basic methods. John Wiley & Sons, N.Y., 223 p.

________ . 1984. Advice on target fishery rates. ICLARM Fishbyte 2(1):8-11.

Polovina, J. J. In press. Variation of catch rates and species composition in handling catches of deepwater snappers and groupers in the Mariana Archipelago. Submitted to Proceedings of the 5th International Coral Reef Congress, Tahiti, 1985, Vol. 1.

________ , and S. Ralston. In press. An approach to yield assessment for unexploited resources with application to snappers and groupers in the Marianas. Fish. Bull. (U.S.).

Ralston, S., and J. J. Polovina. 1982. A multispecies analysis of the commercial deep-sea handline fishery in Hawaii. Fish. Bull., U.S. 80:435-448.

858

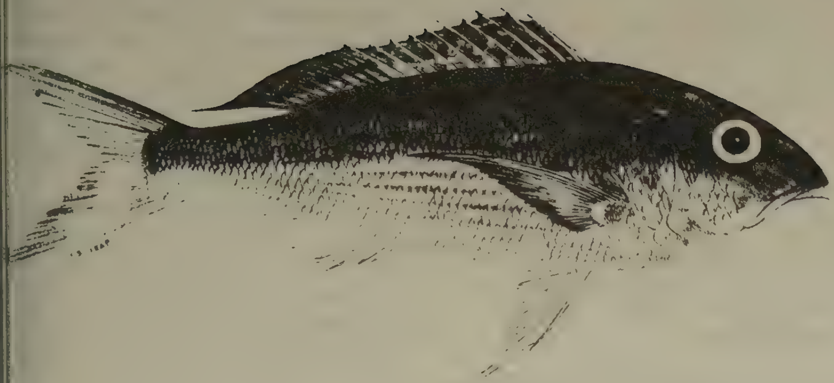

Pristipomoides typus, one of the deepwater snappers from Hawaii and Southeast Asia. Painting by Yeap Tho Seng.

A Novel Approach to Aging Tropical Fish

STEPHEN RALSTON
Research Fishery Biologist
Southwest Fisheries Center
Honolulu Laboratory
National Marine Fisheries Service, NOAA
P.O. Box 3830
Honolulu, Hawaii 96812, U.S.A.

Research has been underway for several years at the Southwest Fisheries Center Honolulu Laboratory of the National Marine Fisheries Service (NMFS) to improve upon existing methods of aging tropical fishes. Most people familiar with the subject are now aware that the otoliths of virtually all the fishes that have been studied to date grow by means of a daily episodic accretion of calcium carbonate. The episodic nature of the growth process leaves microscopic daily check marks which are commonly called "daily increments." The existence of daily increments in the otoliths of a wide variety of marine and freshwater fishes has now been shown in temperate and tropical environments.

The occurrence of daily increments in the otoliths of tropical fishes affords the opportunity of developing novel approaches to aging. Perhaps the simplest method used so far is to count all the increments present in an otolith, and to use the number obtained as an estimate of the age, in days, of the sample specimen. Although simple on theoretical grounds, there are a number of reasons why this particular approach is not always the most effective. First, for slow growing species characterized by long life spans, this method may entail counts to several thousands of increments. Work of this type is tedious, exhausting, and time-consuming. Second, it is very difficult to obtain preparations of otoliths which show the complete development of increments extending all the way from the otolith focus to the outer margin. Usually there are areas in which increment microstructure becomes unclear. Obscure areas such as these not uncommonly account for half of the visual field in a preparation. Because otoliths without a fully visible complement of increments are useless for this type of approach, undue time is spent working on sample preparations, i.e., in trying to develop perfect specimens.

Faced with these realities, I have devised a simple method which can overcome some of the difficulties which arise with daily increments. The method takes advantage of the fact that it is possible to measure the growth rate of the otolith by studying daily increments. A wide space between adjacent increments is interpreted to mean that the otolith grew rapidly in the intervening time interval. Conversely, a narrow space between adjacent increments indicates slow growth. The basic approach is to estimate the average width of daily increments at various points in the otolith. If the otolith were to grow at a constant rate, independent of the size of the otolith, then increment widths would be uniform at all points in the otolith from focus to margin. If one could estimate this rate and the total length of the otolith, then the age of the specimen could simply be estimated by dividing the otolith length by its rate of growth.

Of course, otoliths do not grow at a constant rate and neither do whole fish. Nevertheless, this same process works well if one takes into account otolith and fish size. According to the von Bertalanffy growth model, fish growth slows with age and approaches zero at an asymptotic size with increasing time. The same is true of the otolith. It is well known that the size of a fish is well correlated to the size of its otoliths. The relationship is often nonlinear but it is nonetheless relatively easy to obtain and describe statistically.

In my method, the otolith is subdivided into regions which are small enough so that the growth of the otolith can be considered constant within a subregion. I have found that within regions of about 500 microns the growth rate of the otolith is essentially uniform. The time it takes to grow through each one of these subregions is calculated exactly as outlined above. The average widths of daily increments within subregions (e.g., 0-500 microns, 500-1,000 microns, 1,000-1,500 microns, etc.) are determined by examining a number of preparations. Average increment width is then equated directly to the average growth rate of the otolith, measured in units of microns per day.

Typically, areas in which up to 25-30 increments are plainly visible are analyzed in detail. The total length of a short

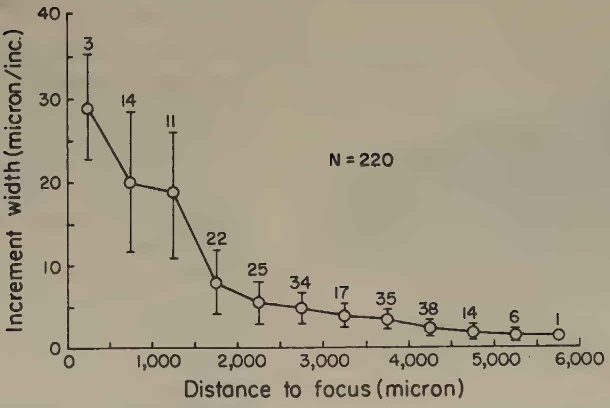

The relationship between increment width (otolith growth rate) and otolith size for *Pristipomoides auricilla*. The circles are mean values which are bracketed by standard deviations. Individual subregion sample sizes are presented above each mean.

segment containing the increments is measured with an ocular micrometer and the total number of increments within the short segment is counted. The ratio of segment length to included increments provides an estimate of the average width of increments within the short segment. If one computes a number of such ratios, categorized by subregion, their mean values will provide an estimate of the average growth rate of the otolith in the subregion of interest. Of course, a large number of points is desirable for statistical reasons, although data collected from different specimens can be pooled to reveal the species-specific pattern. Once the relationship between otolith growth rate and otolith length has been determined, one calculates the length of time it takes to grow through each subregion by simple division. Next, the time intervals necessary for growth through each of the subregions are added together sequentially to estimate the total amount of time necessary for the otolith to reach a given size. It is then possible to convert otolith lengths to fish lengths with a regression equation of these variables. Ultimately one is left with a series of age at length determinations which can be fitted to any growth model desired. The whole process outlined above is essentially a form of numerical integration of otolith growth rate data.

The accompanying figure shows a plot of increment width against distance to the otolith focus for one of the many deepwater snappers, *Pristipomoides auricilla,* we have been examining at the Honolulu Laboratory. Note that, like the whole fish, the growth rate of the otolith declines as the size of the otolith increases. One can consider increment width (microns/increment) equal to otolith growth rate (microns/day) because there is a one-to-one correspondence between days and increments, at least as long as increments are deposited daily. This is an important assumption, however, which should always be validated if possible.

The data presented in the figure were gathered after examining 220 short segments in 51 separate *P. auricilla* otolith preparations. These 220 segments contained an average of 14.25 daily increments each (s.d. = 5.6) so that a total of 3,135 increments were counted and measured in all. Furthermore, the average length of each short segment was 67.4 microns (s.d. = 43.8).

Summary of increment width and otolith growth rate analysis for *Pristipomoides auricilla.* Dat are taken from the accompanying figure.

Otolith length interval (micron)	Mean otolith growth rate (micron/day)	Time for interval growth (day)	Cumulative age through interval (day)	Length of fish-fork (cm)
0-500	29.04	17.22	17.22	3.4
500-1,000	20.05	24.94	42.16	6.4
1,000-1,500	18.88	26.48	68.64	9.3
1,500-2,000	7.99	62.56	131.20	12.1
2,000-2,500	5.55	90.04	221.24	14.9
2,500-3,000	4.92	101.57	322.81	17.6
3,000-3,500	3.92	127.42	450.23	20.3
3,500-4,000	3.41	146.74	596.97	23.0
4,000-4,500	2.28	219.35	816.32	25.6
5,000-5,500	1.64	303.95	1,401.88	30.9
5,500-6,000	1.53	326.53	1,728.41	33.4

The results in the accompanying tabl summarize the method as applied to th data presented in the figure. The amoun of time necessary to grow through length interval is simply the interva length divided by the average growth rat during the interval. Fish lengths wer estimated from an independently derive regression on otolith length.

It is apparent from the data that *auricilla* is relatively fast growing fc members of this genus, reaching 50 of its maximum size of 42 cm in roughl 1.3 years. This fast growth is not surprisin in light of its small adult size. *Pristip moides filamentosus,* one of sever larger species also under study, is know to exceed 80 cm, but does not reac 50% of its maximum size until we after three years of growth.

This simple method of aging tropic fish by estimating the widths of dai otolith increments is currently bei evaluated at the Honolulu Laborator Results to date are certainly encouragi One of the problems with using da increments to age fishes, as some p lished studies show, is that increme deposition can break down from daily periodicity, and there are lon intervals of arrested accretion in lar (older) fish. This particular probl hinders any method using daily inc ments for aging purposes. Neverthele a head start has been made towa developing a reliable and economi technique for studying the grow dynamics of a wide variety of tropi species.

8582

J. Mamm., 66(4):777–779, 1985

CEPHALOPOD REMAINS FROM THE STOMACH OF A SHORT-FINNED PILOT WHALE COLLECTED NEAR SANTA CATALINA ISLAND, CALIFORNIA

DANA J. SEAGARS AND JOHN R. HENDERSON

National Marine Fisheries Service, Southwest Region, 300 South Ferry Street,
Terminal Island, CA 90731 (DJS)
National Marine Fisheries Service, Southwest Fisheries Center, P.O. Box 271,
La Jolla, CA 92038 (JRH)
Present address of JRH: N.M.F.S., Southwest Fisheries Center, Honolulu Laboratory,
P.O. Box 3830, Honolulu, HI 96812

Considerable evidence suggests that long-finned pilot whales (*Globicephala melaena*) feed predominately on cephalopods in the Atlantic Ocean (Mercer, 1975; Norman and Fraser, 1937; Sergeant, 1962; Sergeant and Fisher, 1957). It is generally presumed that the short-finned pilot whale (*G. macrorhynchus*) of the Pacific preferentially consumes squid (Brown, 1960, 1962; Caldwell et al., 1971; Fiscus, 1982; Kritzler, 1949; Leatherwood et al., 1982; Reilly, 1977, 1978). However, squid beaks in the stomach of this delphinid have been reported only twice (Kritzler, 1952; Hall et al., 1971) and neither account identified the species of squid. Norris and Prescott (1961) described group behavior in "feeding schools" of short-finned pilot whales among schools of squid but did not identify the species. Our note provides the first identification of squid beaks from the stomach of a short-finned pilot whale collected dead from the Pacific Ocean.

Six floating dead pilot whales were observed from the air near Santa Catalina Island (ca. 35 km SSW Los Angeles, CA) on 16 and 17 December 1980. They were scattered along a 20 km area from the shoreline to 5 km off the southwestern end of the island. On 18 December we traveled by boat to this vicinity and located and examined three dead *G. macrorhynchus* and two California sea lions (*Zalophus californianus*). Two of the whales had numerous post-mortem abdominal and caudal bites, which we observed being made by feeding blue sharks (*Prionace glauca*). We collected one sea lion (JRH 091) and towed one pilot whale (JRH 089) 35 km to the Catalina Marine Science Center, Big Fisherman Cove, Santa Catalina Island, for examination.

The standard length (snout tip to fluke notch) of the pilot whale was 463.0 cm; this value could be exaggerated from its length in life because we towed the carcass by the flukes. Other external measurements were made and are on file at the Southwest Fisheries Center, La Jolla, CA. Even though the whale was in an initial stage of decomposition, we looked for gross signs of trauma or pathology. We found none, either because of the decomposition or more likely because of the absence of such. The internal parasite load was very light: only a few (<15) cestode cysts (*Monorygma* sp.) and flukes (*Nasitrema* sp.) were found and collected during a gross examination of all muscle and organ systems. The stomach and its contents, reproductive tract, complete skeleton, and parasites were collected and deposited in the collections of the Southwest Fisheries Center.

The stomach contained about 20 l of a moderately digested (or decomposed) slurry of the "market" squid, *Loligo opalescens*. We decanted (and subsequently inadvertently discarded) about 18 l of the slurry and collected and froze the stomach with the remaining, heavier contents (2,580 ml) for later analysis. The stomach and its contents were defrosted in the laboratory. The stomach was everted and contents rinsed into dishes for examination. Whole and large pieces of squid were removed by hand. All other contents were washed through 5.0 mm and 1.0 mm screens. Beaks were picked from the screens after each washing. Remaining organic material was air dried and examined for teleost otoliths. The beaks were stored in 70% ethanol for subsequent identification.

The examined contents were composed almost entirely of whole or moderately digested remains of *L. opalescens*, represented by 15 intact individuals (dorsal mantle length $\bar{X} = 128$ mm, range 112–142 mm, $n = 11$) and an additional 188 beaks (99 lowers, 89 uppers). About one-half of these beaks were picked in pairs from partially digested buccal tissue. Additionally, one upper beak of the north Pacific giant squid, *Moroteuthis robusta*, and one lower beak from *Histioteuthis dofleini* were present. No fish otoliths or bones were found.

Several lines of circumstantial evidence lead us to believe that the pilot whale we examined had been a healthy individual that had accidentally suffocated in a net while feeding on squid. 1) Our necropsy results were typical for drowned cetaceans; within the limits imposed by decomposition we did not find injuries or pathological conditions suggestive of the cause of death (the lungs of drowned cetaceans do not fill with water). At necropsy the stomach was packed with whole or only moderately digested squid, indicating very recent feeding. It is our experience that the stomachs of diseased or moribund cetaceans are generally empty, whereas stomachs of cetaceans which die accidently in fishing nets are more likely to contain prey items. 2) Reports from island residents and observations made during our aerial surveys indicated that numerous dip-net and purse-seine vessels had been fishing for spawning *L. opalescens* in this area throughout the month prior to our collection. Three of the six dead whales observed from the air and two of three observed floating at sea were without flukes and terminal vertebrae. The entangled flukes of dead whales typically are severed to facilitate removal from squid purse-seines (California Department of Fish and Game, pers. comm.). 3) The blue sharks observed feeding on the whales were utilizing them as carrion; blue sharks feed predominantly on small schooling fish such as the northern anchovy (*Engraulis mordax*), on cephalopods including *L. opalescens* and two histioteuthids (Tricas, 1979), but not on live large cetaceans.

The presence of *L. opalescens* in the stomach of our specimen confirms the presumption of others that *G. macrorhynchus* feeds predominantly on this species of squid in waters offshore southern California. *Loligo opalescens* is seasonally epipelagic, inhabiting open coastal waters most of the year and moves into nearshore waters adjacent to submarine canyons, escarpments, or islands to mate and spawn (Recksiek and Frey, 1978). Large mating and spawning schools of market squid aggregate in the upper 20 m of water during winter nights near Santa Catalina Island (Fields, 1965), thus becoming more accessible to predators such as marine mammals. The market squid found in the stomach of our specimen probably were spawning adult individuals, based on a comparison of our mantle length measurements and beak sizes with the findings of others (Hochberg and Fields, 1980; Wolff, 1982).

The cephalopods *H. dofleini* and *M. robusta* have been found previously in the stomachs of marine mammals: the northern fur seal, *Callorhinus ursinus* (Fiscus, 1982), and the sperm whale, *Physeter catodon* (Clarke and MacLeod, 1980; Rice, 1963). *Histioteuthis dofleini* also has been reported from the stomachs of one California sea lion (Antonelis and Fiscus, 1980), one spotted dolphin, *Stenella attenuata* (Perrin et al., 1973), and two beaked whales, *Mesoplodon carlhubbsi* (Mead et al., 1982). We estimate that our specimen of *H. dofleini* would have weighed about 110 g, based on a regression of lower beak rostral length (L.R.L. = 0.55 cm; Clarke, 1962). Based on the relative size (similar to *L. opalescens*), abundance, and distribution of *H. dofleini* (Voss, 1969; Young, 1972), Hochberg (pers. comm.) suspects that a reexamination of squid beaks collected from marine mammal stomachs of the eastern North Pacific, which remain unassigned or have been identified only to the familial level, will result in their identification as *H. dofleini*.

Moroteuthis robusta is a deep water inhabitant (100–500 m) considered abundant along the North Pacific rim from Japan to southern California (Clarke, 1966; Roper and Young, 1975). Fiscus (1984) and Rice (1963) identified *M. robusta* as the species of squid found most frequently in the stomachs of sperm whales off central California. There are only nine published records of *M. robusta* south of Point Conception, California (Hochberg, 1974); our beak is the only record from a marine mammal stomach for the southernmost portion of this species' range.

We thank Dr. F. G. Hochberg, Santa Barbara Museum of Natural History, for identifying the beaks and reviewing an early draft of the manuscript. Dr. R. Given provided access to the University of Southern California, Catalina Marine Science Center for our necropsy. The U.S. Coast Guard, Captain of the Port, San Pedro, provided transportation to the collection site. Drs. D. P. DeMaster, W. F. Perrin, and S. B. Reilly, Southwest Fisheries Center, and Dr. C. A. Hui, Naval Oceans Systems Center, provided comments on a draft of the manuscript.

Literature Cited

Antonelis, G. A., and C. H. Fiscus. 1980. The pinnipeds of the California current. California Coop. Oceanog. Fish. Invest. Repts., 21:68–78.

Brown, D. H. 1960. Behavior of a captive Pacific pilot whale. J. Mamm., 41:342–349.

———. 1962. Further observations on the pilot whale in captivity. Zoologica, 47:59–64.

Caldwell, D. K., M. C. Caldwell, W. F. Rathjen, and J. R. Sullivan. 1971. Cetaceans from the Lesser Antillean island of St. Vincent. Fish. Bull., 69:303–312.

Clarke, M. R. 1962. The identification of cephalopod "beaks" and the relationship between beak size and total body size. Bull. British Mus. Nat. Hist. Zool., 8:419–480.

———. 1966. A review of the systematics and ecology of oceanic squids. Adv. Mar. Biol., 4:91–300.

Clarke, M. R., and N. MacLeod. 1980. Cephalopod remains from sperm whales caught off western Canada. Mar. Biol., 59:241–246.

Fields, W. G. 1965. The structure, development, food relations, reproduction, and life history of the squid *Loligo opalescens* Berry. Calif. Dept. Fish and Game, Fish. Bull., 131:1–108.

Fiscus, C. H. 1982. Predation by marine mammals on squids of the eastern North Pacific Ocean and the Bering Sea. Mar. Fish. Rev., 44:1–10.

———. 1984. Catalogue of cephalopods at the National Marine Mammal Laboratory. NOAA Tech. Mem. NMFS, F/NWC-65, 120 pp.

Hall, J. D., W. G. Gilmartin, and J. L. Mattson. 1971. Investigation of a Pacific pilot whale stranding on San Clemente Island. J. Wildl. Dis., 7:324–327.

Hochberg, F. G. 1974. Southern California records of the giant squid, *Moroteuthis robusta*. Tabulata, 7:83–85.

Hochberg, F. G., and W. G. Fields. 1980. Cephalopoda: the squids and octopuses. Pp. 429–444, *in* Intertidal invertebrates of California (R. H. Morris et al., eds.). Stanford Univ. Press, Stanford, California, 904 pp.

Kritzler, H. 1949. The pilot whale at Marineland. Natural Hist., 58:302–308, 331–332.

———. 1952. Observations on the pilot whale in captivity. J. Mamm., 33:321–334.

Leatherwood, S., R. R. Reeves, W. F. Perrin, and W. E. Evans. 1982. Whales, dolphins, and porpoises of the eastern north Pacific and adjacent Arctic waters. NOAA Tech. Rept. NMFS Circ., 444:123–129.

Mead, J. G., W. A. Walker, and W. J. Houck. 1982. Biological observations on *Mesoplodon carlhubbsi* (Cetacea: Ziphiidae). Smithson. Contrib. Zoology, 344:1–25.

Mercer, M. C. 1975. Modified Leslie-DeLury population models of the long-finned pilot whale (*Globicephala melaena*) and annual production of the short-finned squid (*Illex illecebrosus*) based on their interaction at Newfoundland. J. Fish. Res. Board Canada, 32:1145–1154.

Norman, J. R., and F. C. Fraser. 1937. Giant fishes, whales, and dolphins. C.P. Putnam's Sons, New York, 361 pp.

Norris, K. S., and J. H. Prescott. 1961. Observations on Pacific cetaceans of Californian and Mexican waters. Univ. California Publ. Zool., 63: 291–402.

Perrin, W. F., R. R. Warner, C. H. Fiscus, and D. B. Holts. 1973. Stomach contents of porpoise, *Stenella spp.*, and yellowfin tuna, *Thunnus albacares*, in mixed-species aggregations. Fish. Bull., 71:1077–1092.

Recksiek, C. W., and F. W. Frey. 1978. Biological, oceanographic, and acoustic aspects of the market squid, *Loligo opalescens*, Berry. Calif. Dept. Fish and Game, Fish. Bull., 169:1–185.

Reilly, S. B. 1977. The distribution of pilot whales, *Globicephala macrorhynchus* Gray 1826, in the eastern tropical Pacific. Unpubl. M.S. thesis, California State Polytechnic Univ., San Luis Obispo, 80 pp.

———. 1978. Pilot whale. Pp. 112–119, *in* Marine mammals of eastern North Pacific and Arctic waters (D. Haley, ed.). Pacific Search Press, Seattle, Washington, 256 pp.

Rice, D. W. 1963. Progress report on biological studies of the larger cetacea in the waters off California. Norsk Hvalfangst-Tidende, 52:181–187.

Roper, F. E., and R. E. Young. 1975. Vertical distribution of pelagic cephalopods. Smithson. Contrib. Zoology, 209:1–51.

Sergeant, D. E. 1962. The biology of the pilot or pothead whale *Globicephala melaena* (Traill) in Newfoundland waters. Bull. Fish. Res. Board Canada, 132, 84 pp.

Sergeant, D. E., and H. D. Fisher. 1957. The smaller Cetacea of eastern Canadian waters. J. Fish. Res. Board Canada, 14:83–115.

Tricas, T. C. 1979. Relationship of the blue shark, *Prionace glauca*, and its prey species near Santa Catalina Island, California. Fish. Bull., 77:175–182.

Voss, N. A. 1969. A monograph of the Cephalopoda of the North Atlantic. The family Histioteutidae. Bull. Mar. Science, 19:713–867.

Wolff, G. A. 1982. A beak key for eight eastern tropical Pacific cephalopod species with relationships between their beak dimensions and size. Fish. Bull., 80:357–370.

Young, R. E. 1972. The systematics and aerial distribution of pelagic cephalopods from the seas off southern California. Smithson. Contrib. Zoology, 97:1–159.

Submitted 19 October 1984. Accepted 11 March 1985.

8583

THE USE OF AERIAL PHOTOGRAPHS FOR ESTIMATING SCHOOL SIZES OF CETACEANS

by

Michael D. Scott[1], Wayne L. Perryman[2], and William G. Clark [3]

ABSTRACT

The accuracy and precision of dolphin school size estimates based on aerial photograph counts were examined using data collected on recent aerial and ship surveys. These estimates were found to be accurate during a 1979 research cruise aboard a tuna purse-seiner; dolphin schools were photographed from the ship's helicopter, encircled with the purse-seine, and then counted as the dolphins were released from the net. A comparison of photographic estimates with these counts indicated that the relationship was fairly close and gave no indication of significantly differing from 1:1. During a 1980 aerial study, photographic estimates from different schools, passes, and camera formats were compared and were found to be quite precise, with a standard deviation of approximately 6% of school size.

Photographic estimates were also compared with estimates made by aerial observers. Most observers tended to underestimate school size, particularly for large schools. The variability among observers was high, indicating that observers should be individually calibrated.

INTRODUCTION

School size is an important factor in the estimation of density and abundance of cetaceans. For dolphin species in the eastern tropical Pacific (ETP), aerial surveys have been used to provide data on the densities of schools and on average school sizes. School size data are typically based on counts or estimates by observers aboard the aircraft.

Observer estimates of large aggregations of animals, however, can be greatly in error. Chattin (1952) has described such estimates fairly accurately as "a wild guess plus ten per cent." Lavigne, Øritsland, and Falconer (1977) presented 134 observers with slides of large numbers of dots and aerial slides of pinniped groups hauled out on ice and demonstrated a tendency for these observers to overestimate. Ray and Wartzok (1980) showed similar results for observer estimates of photographs of pinnipeds and cetaceans. Brown (1971), however, showed that observers underestimated large numbers of objects presented on photographs. Heyland (1972) compared aerial observer estimates of geese with aerial photographs taken at the same time, and found that the observers underestimated the number of geese present. Similarly, Sinclair (1973) compared photographic and observer estimates of African buffalo (*Syncerus caffer*) and found that the observer estimates

---

[1] Inter-American Tropical Tuna Commission, c/o Scripps Institution of Oceanography, La Jolla, CA 92037

[2] Southwest Fisheries Center, NOAA, P.O. Box 271, La Jolla, CA 92038

[3] School of Fisheries, University of Washington, Seattle, WA 98195

varied considerably in accuracy, but usually underestimated herd size, particularly for large herds of over 500 animals. Withrow (1982) found similar results for large groups (>200) of hauled-out Stellar sea lions (*Eumetopias jubatus*). Such disparity in results makes it difficult to generalize about observer estimates.

Aerial photography has been increasingly used to collect cetacean group size data (Heyland, 1974; Ray and Wartzok, 1980; R. Wells, unpublished data). Not every school encountered, however, can be successfully photographed. Factors such as sea state, sun glare, water clarity, or behavior of the animals can obscure portions of the school, making the photographs unsuitable for analysis. Thus observer estimates, although often unsatisfactory for large aggregations, must often be relied upon for school size data.

Aerial photographs were taken of dolphin schools during four surveys in the ETP (Table 1). One of these surveys was designed to determine the accuracy of estimates derived from the photographs. The precision of the photographic estimates was determined from the results of another survey in which estimates made from photographs taken by cameras with different formats, on different passes, and by different readers were compared. Data from all four surveys allowed the comparison of both aerial observer and photographic estimates.

This study deals with those questions that can be answered by statistical analysis of the above data, such as:

1) Do estimates derived from photographs accurately depict the true school size?
2) Do photographs taken with the same camera on successive passes over the same school yield statistically indistinguishable estimates of school size?
3) Do the different camera types yield different school size estimates?
4) Are there systematic differences among observers in visual estimates?
5) Can the observer estimates be calibrated by the photographic estimates of those schools for which both kinds of estimates are available?

MATERIALS AND METHODS

Field methods

During 1979, a study was conducted by the Inter-American Tropical Tuna Commission (IATTC) to investigate the accuracy and precision of observer estimates made from the tuna purse seiner, M/V *Gina Anne* (Allen *et al.*, 1980). Observers on board the *Gina Anne* independently estimated the sizes of dolphin schools which were captured by the purse seiner. The captured dolphins were then counted by two to four observers as the dolphins were released over the net during the "backdown" procedure (Figure 1). These observers counted from small boats stationed along the backdown area. An estimate of the total school size was obtained by adding the backdown count, the estimated number of dolphins which escaped capture, and the number of dolphins killed, if any, during the set. The backdown counts were later compared with the shipboard observer estimates.

These dolphin schools were also photographed by National Marine Fisheries Service (NMFS) personnel from the *Gina Anne*'s Bell-47 helicopter with a vertically-mounted KA-51A 127-mm (5-inch) camera and a handheld Hasselblad 500 EL/M 70-mm camera. Whenever possible, the helicopter made multiple photographic passes over the schools at altitudes of 215-335 m and at speeds of 65-70 knots. Estimates of school size based on counts made from the photographs were compared to the estimates based on backdown counts so that the accuracy of the aerial photographic estimates could be assessed. Aerial estimates of school size were also made by one to three observers and these estimates were compared with both the photographic estimates and the backdown counts.

In 1979, aerial photographs were taken as part of a NMFS aerial survey for dolphins in the ETP (Jackson, 1980). A four-engine PBY-5A Catalina airplane was used for this survey; flights were based from airports in Mexico, Costa Rica, El Salvador, Guatemala, Ecuador, and Peru. Photographs were taken with a vertically mounted K–17C 229-mm (9-inch) camera and a handheld Hasselblad 70-mm camera. Several photographic passes were made over schools at altitudes of 240-305 m and at speeds of 90-100 knots. Observers on board recorded notes on school behavior and formations. The schools were later circled so that the observers could estimate school size and identify species.

Estimates were usually based on some type of count. Individual animals could be counted in very small schools, but usually subgroupings which contained approximately equal numbers of animals were counted in larger schools. Thus, the larger the school, the larger the subgroupings had to be. For large schools containing thousands of animals, an observer may have counted in increments of 200 or more. These estimates (by up to six observers per school) were made independently and not discussed until after the field study had been completed. Not all of the schools for which school size estimates were made could be successfully photographed.

An aerial photogrammetric study was also conducted by the IATTC, with personnel and equipment support from the NMFS, in 1980. The study was designed primarily to test the feasibility of measuring dolphin lengths from aerial photographs (Anonymous, 1981). In addition, one to four observers made independent school size estimates which were compared with school size estimates made from the photographs. In this study, a KA-45A 127-mm camera, a KA-62A 127-mm camera, a KC1B 229-mm camera, and four Hasselblad 70-mm cameras were vertically mounted aboard a twin-engine Beechcraft AT-11 airplane. The photographs taken with the KA-45A camera were not used, however, due to a camera malfunction. Photographic passes were made at altitudes of 240–275 m at speeds of 90–100 knots. The schools were circled at an altitude of 150 m to get observer estimates of school size.

Photographs were also taken during a 1981 NMFS aerial survey designed to test the effects of environmental conditions on numbers of schools sighted (Holt, 1983). Photographs were taken of dolphin schools off the coast of Costa Rica with a KA-62A 127-mm camera and four Hasselblad 70-mm cameras vertically-mounted aboard a Beechcraft AT-11 airplane. The methods for obtaining photographs and observer estimates were the same as for the 1980 IATTC study.

Photographic counts

Processed photographs from all surveys were reviewed on a light table to eliminate imagery which was of poor quality or which did not contain all the boundaries of the school. Most of the photographs judged acceptable for analysis were viewed at 6–12x magnification on Variscan Mark II rear-projectors located at the Earth Resources Observation System (EROS) facility in Bay Saint Louis, Mississippi. Images of individual animals were independently marked by two to five readers on acetate mounted on the screen. Slides taken on the 1979 *Gina Anne* study with the Hasselblad camera were viewed with a 70-mm slide projector and marked on a large pad of drawing paper.

The pass was the unit on which the estimate was based, and usually the school was contained on two to three frames from a single pass. The central frame which contained all or most of the school was counted first. Adjoining frames were then overlaid on the plots of the central frame and dolphins not previously counted were added to the plot. The overlap between frames thus allowed questionable images to be re-examined on adjoining frames and allowed counts of animals which may have been too deep to be counted on other frames. Counts of outlying subgroups which appeared in some passes, but not on others, were included in the school size estimates of the passes in which the subgroups were missing.

Two types of data were recorded by the photograph readers. One was the actual number of dolphins counted in each pass (the sum of all dolphins plotted); the other was an estimate based on the actual count, but including an additional percentage, usually small, to incorporate dolphins that were not observed. A number of factors were considered in deriving the added percentage. These included the quality of the photograph, the amount of sun glare or splashes that might obscure dolphins, and the number of dolphins that were diving or swimming well below the surface as observed in the photographs or recorded in the field notes. The counts were therefore usually viewed as underestimates of the school size, particularly as the detectability of the dolphins decreased. Reader variability is present in both the counts and the estimates.

RESULTS

Accuracy of photographic estimates

Five schools which were photographed during the *Gina Anne* experiment were compared with the backdown counts. The photographic estimates and the backdown counts are presented in Table 2. The slope of the regression (constrained to pass through the origin) of photographic estimate on backdown count was 1.06, with 95% confidence interval (0.90, 1.22) and $R^2 = 0.79$. Although only five data points were available, the relationship between the two gave no indication of differing significantly from 1:1.

It should be noted that the backdown counts are not an absolute "ground truth." It was possible that dolphins were under- or over-counted when a large, tight group of animals was backed out through a single "counting sector." The error due to this, however, is likely to be small. Another source of error is that dolphins sometimes evaded capture after the photographs were taken. The number of dolphins in these groups (usually small groups of 10–40 animals) were estimated by the shipboard observers (Table 2).

While the photographic estimates of school sizes sampled during the *Gina Anne* study ranged from 161 to 396, inferential evidence indicates that the photographic estimates may be accurate for larger school sizes as well. During the 1980 IATTC study, two schools were observed merging into a single school. The two schools were each photographed individually prior to their merging, and then photographed again after they had merged. The sum of the average photographic estimates for the smaller, separate schools (573 and 530) was fairly close to the average estimate for the larger school (1265), indicating that the photographic estimates were likely to be consistent among large and small schools.

Analyses of variance of photographic estimates

During the four surveys a total of 151 schools were photographed, of which 71 (47%) were in photographs of good enough quality to be used in the analysis. The average counts and the average best estimates from the photographs are presented in Table 3.

Analyses of variance were conducted to measure the effect of several factors on photographic estimates of school size (Clark, 1984). Since the variance among readings of the same photograph was greater for large schools than small ones, a logarithmic transformation was used to standardize the within-cell variances. Bartlett's test did not show significant heterogeneity of variances in the logarithms of the photographic estimates, so these were used in all the analyses. Roughly speaking, a difference between cells in the logarithms of the estimates can be regarded as a proportional difference.

The sources of variation among the photographic estimates which were examined included:

1) Reading. Different readers usually obtained different estimates from a single pass. These differences among readings of the same photograph measure the minimum uncertainty inherent in the method. For purposes of variance analysis, they provided the within-cell variance with which other effects were compared.

2) Pass. Tests were conducted to determine whether there were significant differences, on average, among estimates based on photographs taken with the same

camera on different passes over the same school.

3) Camera format. Tests were conducted to determine whether there were significant differences, on average, among estimates based on photographs taken by cameras with different "formats" or frame sizes (70 mm, 127 mm, or 229 mm) on the same passes over the same school.

4) School. There were obviously large differences among schools in estimates of school size, and these were quite consistent among passes and formats. While there was no doubt that the effect of school was large and significant, this factor necessarily appeared in all the variance analyses so that it could be estimated and then removed to test those effects in question—pass and camera format.

In terms of the analysis of variance, a mixed model with nesting was used: camera format was treated as a fixed effect to be tested for significance and estimated if found significant, while school and pass were treated as random effects with pass nested within school. Only for schools photographed during the 1980 IATTC study in which multiple passes were made and all three camera formats were used was there an opportunity to treat the effects of school, pass, format, and reading simultaneously.

Effect of pass — In order to use as much data as possible, an analysis of variance was done for each camera format separately (Table 4). Treating the formats separately for this purpose also simplified the model, since only school, pass, and reading remained as sources of variance. The analysis for each camera format used the estimates of all schools with at least two readings from each of at least two passes when the camera in question was operated. The 9-inch camera used in 1979 could not be treated at all because it was not operated successfully on more than one pass over any school.

For each of the three formats, the variance analyses showed that the effect of pass was significant ($P < .005$). The effect of pass, however, is not large (6–8% of school size), and barely exceeds the variation due to reading, which is close to 5% of school size for all three formats. School accounts for about 99% of the total variance in each of the three sets of data.

Since an aircraft making repeated passes over a school affects the behavior of the animals, pass could be treated as a covariate instead as a variance component (Table 5). When it was, the slope was positive and significant within each camera format, which meant there was a significant tendency for photographic estimates to increase from one pass to the next:

	229-mm format	*127-mm format*	*70-mm format*
Estimated slope	.018	.011	.038
95% confidence interval	.004–.032	.003–.020	.012–.064

Once again it should be noticed that while the effect of pass is significant, it is small, amounting to 1–2% of school size per pass.

Since the effect of pass was significant within each format, it could not be eliminated from the model. The way in which it was handled thereafter, however, depended on the nature of the effect. There were two possibilities at the extremes:

1) The effect of pass was consistent among formats. In this case it would not be possible to compare estimates obtained with different formats on different passes, since the effects of pass and format would be confounded.

2) The effect of pass was not consistent among formats. In this case it would be possible to compare estimates obtained with different formats on different passes since, for purposes of testing the effect of format, the effect of pass would simply add to the error variance.

Since pass was significant as a covariate within each format, the first possibility could not be excluded altogether. In order to decompose the effect of pass into a consistent portion and a residual representing interaction, an analysis of variance was done on only the 11 schools that permitted all effects to be estimated simultaneously (Table 6). These schools were photographed in 1980 with both the 229-mm and 127-mm cameras on at least two passes. Both portions were significant, but the consistent effect of pass accounted for three quarters of the variance associated with pass. The effect of pass was therefore found to be largely consistent among formats.

Effect of format — Since the effect of pass was consistent among formats, the only good test of format was restricted to passes on which at least two cameras were operated successfully. This requirement effectively restricted the comparison to the same set of 11 schools referred to above. In the analysis of variance of those estimates (Table 6), format was significant as a fixed effect ($P = .04$), but again the effect was small, .015. This means that on average the estimates made from 229-mm photographs were 1.5% greater than the estimates made from 127-mm photographs.

Precision of average photographic estimates

For a particular school and format, the variance of an average photographic estimate is smaller than the variance of a single photographic estimate. In this situation, let

n_p = the number of passes over the school

n_r = the number of readings per pass

σ_p^2, σ_r^2 = the corresponding variance components of the log estimate y.

It can be shown that:

$$V(\bar{y}) = \frac{\sigma_r^2}{n_r n_p} + \frac{\sigma_p^2}{n_p}$$

With $n_r = n_p = 2$, and with $\sigma_r = .05$ and $\sigma_p = .08$ as above, the standard deviation of the average photographic estimate for a school is $S(\bar{y}) = .06$ or about 6% of school size. Therefore, even if differences due to camera format add 1–2%, the average photographic estimate of school size is still very precise.

In what follows, the average photographic estimate will be treated essentially as a fixed point, regardless of the format or number of passes involved, because the variance of photographic estimates is so small compared with the variance of observer estimates.

Comparison with observer estimates

The important question concerning observer estimates is whether there is a consistent relationship between observer and photographic estimates of a given school. If there is, the relationship can be used to adjust observer estimates of the schools that were not photographed. If there is not, the interpretation of the observer estimates is problematic.

The quantity of interest here is therefore not an observer estimate itself, but the difference between an observer estimate and the average photographic estimate of the same school. For practical purposes this difference can be thought of as the error in the observer estimate, since the average photographic estimate has a variance much smaller than the variance of observer estimates of a given school. Treating the difference as an error assumes that the bias of the average photographic estimate is small or nil.

Like the photographic estimates, the errors of the observer estimates have variances that increase with school size. To standardize the variances, each observer estimate was divided by the average photographic estimate of that school, and this ratio was used in all the analyses. Algebraically, this quantity is:

$$\begin{aligned}\text{Ratio} &= \frac{\text{Observer estimate}}{\text{Average photographic estimate}}\\ &= \frac{\text{Average photographic estimate} + \text{Error of observer estimate}}{\text{Average photographic estimate}}\\ &= 1 + \frac{\text{Error observer estimate}}{\text{Average photographic estimate}}\end{aligned}$$

Working with the ratio is therefore equivalent to working with the *relative* error (which can be either positive or negative) of the visual estimate. The sources of variance in this ratio are:

1) School size. To categorize this effect, schools were divided into five size

groups according to average photographic estimates: 1–99, 100–199, 200–499, 500–999, and ≥1000. These divisions were chosen because they provided a reasonably even distribution of schools among the five categories.

2) Observer. There were 13 observers in these studies, but most were represented by rather few estimates. Only the estimates of three observers (from the 1980 IATTC study) provided adequate coverage of the school size categories and adequate homogeneity of variance to carry out the analysis.

In addition, there may be a significant effect due to individual school, but as this effect was not of interest, it was not estimated (i.e. in the analysis of variance, it was left as part of the error term).

A scatter diagram of all estimates by the 13 observers and corresponding average photographic estimates (Figure 2, Table 7) shows that despite some scatter, the observer estimates as a group are fairly accurate for small schools (up to about 200 animals), but that the majority are low for larger schools. This suggests a curvilinear relationship between observer estimate and school size, and consequently accounts for some of the variance in the ratios of observer estimate to average photographic estimate.

Only three observers had large samples of estimates over a broad range of school sizes. When this three-observer subset was analyzed (Table 8), all factors (observer, school size, and the interaction) were found to be highly significant, with mean ratios of relative error as follows:

School Size	*Observer 1*	*Observer 2*	*Observer 3*
1–99	.96	.85	.70
100-199	.93	.84	.64
200-499	1.00	.66	.71
500-999	.88	.76	.49
1000+	.65	.45	.36

When only the first two school size categories were included in the analysis, school size was not significant, but observer and the interaction were still highly significant. With only the first three school size categories in the analysis, school size was again highly significant.

Unlike pass and format in the case of observer estimates, the significant differences here are not small. Even within school size categories, the differences are not a few percent of school size but a few tens of percent.

DISCUSSION

The results of the *Gina Anne* experiment indicate that estimates based on photographic counts are likely to reflect accurately the actual sizes of cetacean schools. Since only five schools could be compared, more data are needed to confirm these results. In particular, schools in which 100% of the animals are captured are needed to reduce the error associated with observers having to estimate numbers of evading dolphins in addition to counting them during backdown. In this study, however, it was thought that this error was likely to be small because the group sizes of escaping dolphins were usually small and perhaps more likely to be estimated accurately.

The analysis of variance of the photo estimates from the 1980 IATTC study showed that all possible sources of variation were significant—school, format, pass, and the interactions—but that the effect of school dwarfed all the rest of them. This allowed different passes, along with different estimates by the readers, to be considered as replicates. The precision analysis subsequently indicated that the photographic estimates have a standard deviation approximately 6% of school size and thus are quite precise.

The interpretation of the observer estimates, however, is problematic. The general relationship between observer and photographic estimates appears to be curvilinear and suggests that most observers tend to underestimate large schools. Some observers, however, tended to estimate high, and sometimes very high. The results of the analysis of variance of the three-observer subset indicated that this relationship varies among observers, and varies widely. These results may even understate the differences among observers, as the three observers in the subset all happened to estimate low on average. In some school size categories, therefore, it seems likely that the average differences among some observers could amount to much more than the 10–30% of school size indicated by the three-observer subset.

These results and studies by other researchers (Brown, 1971; Heyland, 1972; Sinclair, 1973; Lavigne, Øritsland, and Falconer, 1977; Ray and Wartzok, 1980; Withrow, 1982) indicate that observer estimates can be highly variable. Two methods have been used to calibrate observer estimates, however. Caughley, Sinclair, and Scott-Kemmis (1976) adjusted for bias on an observer-by-observer basis by measuring the performance of each aerial observer in the field where the population size (in this case, a herd of sheep) was known. While their study focused on observer bias at detecting animals, this approach has been applied to group size estimates as well (Withrow, 1982). Large sample sizes over the whole range of school sizes are needed, however, to calibrate the observers. Given the effort needed to calibrate the observers, it is reasonable to assume that a constant cadre of observers would be available for the required surveys.

A second approach is to train observers with slides or photographs of aggregations of known size, allowing the observers to calibrate themselves. Aerial observers have been successfully trained in this manner for surveys of terrestrial animals (Brown, 1971; Sinclair, 1973; Norton-Griffiths, 1978; Dirschl, Norton-Griffiths, and Wetmore. 1981) and hauled-out pinnipeds (Withrow, 1982). The IATTC has also used cine film of known-size dolphin schools taken during the *Gina Anne* cruise to train shipboard observers.

Our data suggest the occurrence of self-training by Observer 1. This observer participated in the 1979 NMFS survey, the *Gina Anne* study (as an aerial observer), and the 1980 IATTC study. In addition, he was a reader of the photographs after each study. For schools of less than 400 animals (the largest group photographed during the *Gina Anne* study and, thus, the subset which could provide a uniform comparison among the three studies), his bias was −16.1% during the 1979 study, +19.9% during the *Gina Anne* study, and −2.0% during the 1980 study. It can be argued that this observer's performance was due to the self-calibration allowed by comparing his previous estimates with the photographic counts.

This points out the likely value of observer experience in accurately estimating school size. Yet the question remains, what constitutes experience in this case? Aerial observers may have spent many hours in the air watching cetacean schools, but may never have had the opportunity to compare their estimates with any form of ground truth, particularly for very large aggregations. Thus, these observers may reliably give the same estimates for schools of the same size, but these estimates may not accurately reflect the true school size. Perhaps our notion of "experience" needs to be re-examined to include calibration of observer estimates against counts from aerial photographs.

ACKNOWLEDGEMENTS

The authors gratefully acknowledge the following individuals who participated in these surveys as pilots, observers, or readers: S. Alexander, E. Barham, W. Brinkerhoff, R. De Rosa, T. Flynn, L. Hansen, R. Holt, T. Jackson, C. Jardin, J. Laake, S. Leatherwood, J. Niehaus, C. Oliver, J. Olson, F. Ralston, J. Rutledge, R. Stives, and W. Walker. We also are grateful to Captain Pete Balestrieri and the crew of the M/V *Gina Anne* whose willing cooperation and assistance made it possible to do the shipboard and helicopter study. We also thank the staff of the EROS facility at Bay St. Louis, Mississippi, for their help and the use of their Variscan projectors. Funding for the study was provided by the IATTC; camera equipment was provided by the NMFS. The analysis by W. Clark was supported in part with funds provided by the U.S. Marine Mammal Commission. The following people reviewed the manuscript and gave much useful advice: W. Bayliff, D. DeMaster, M. Hall, P. Hammond, A. Hohn, R. Holt, J. Laake, C. Peterson, G. Scott, and P. Tomlinson.

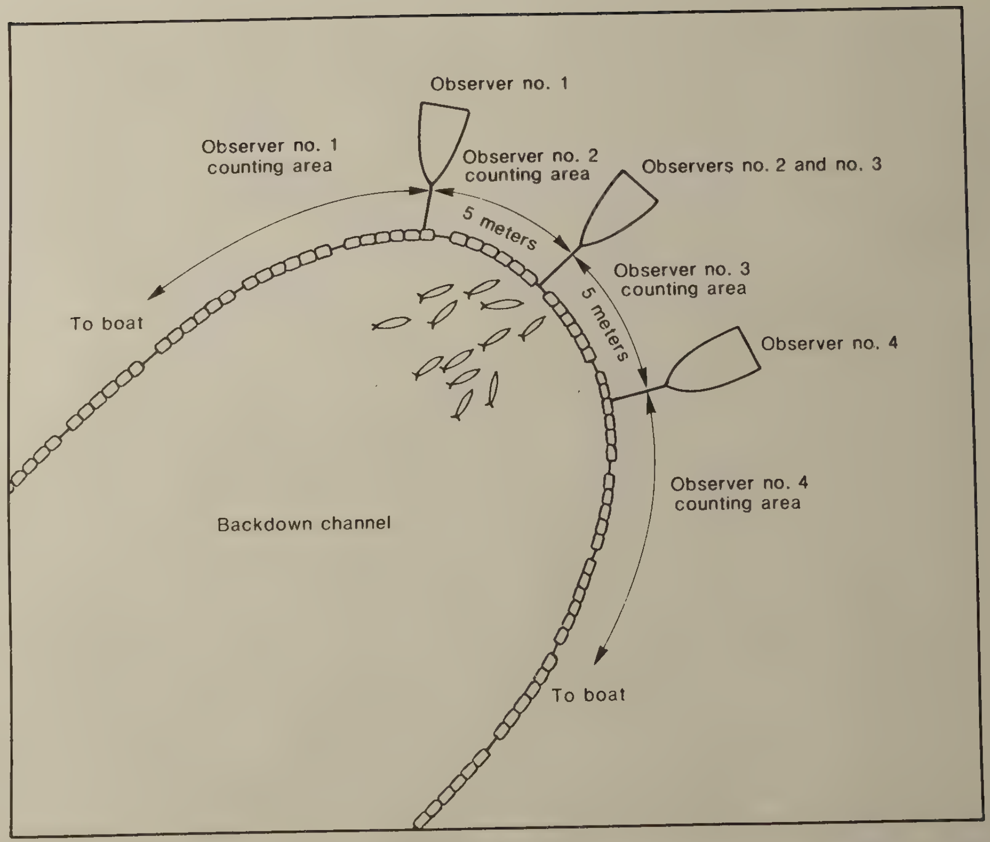
Observer no. 1
Observer no. 1 counting area
Observer no. 2 counting area
Observers no. 2 and no. 3
5 meters
Observer no. 3 counting area
5 meters
Observer no. 4
To boat
Observer no. 4 counting area
Backdown channel
To boat

FIGURE 1. Positions of speedboats and observers during the backdown procedure on the 1979 *Gina Anne* cruise (modified from Allen et al., 1980).

FIGURA 1. Posición de los observadores y de las lanchas durante la maniobra del retroceso en el crucero de 1979 del *Gina Anne* (modificada de Allen et al., 1980).

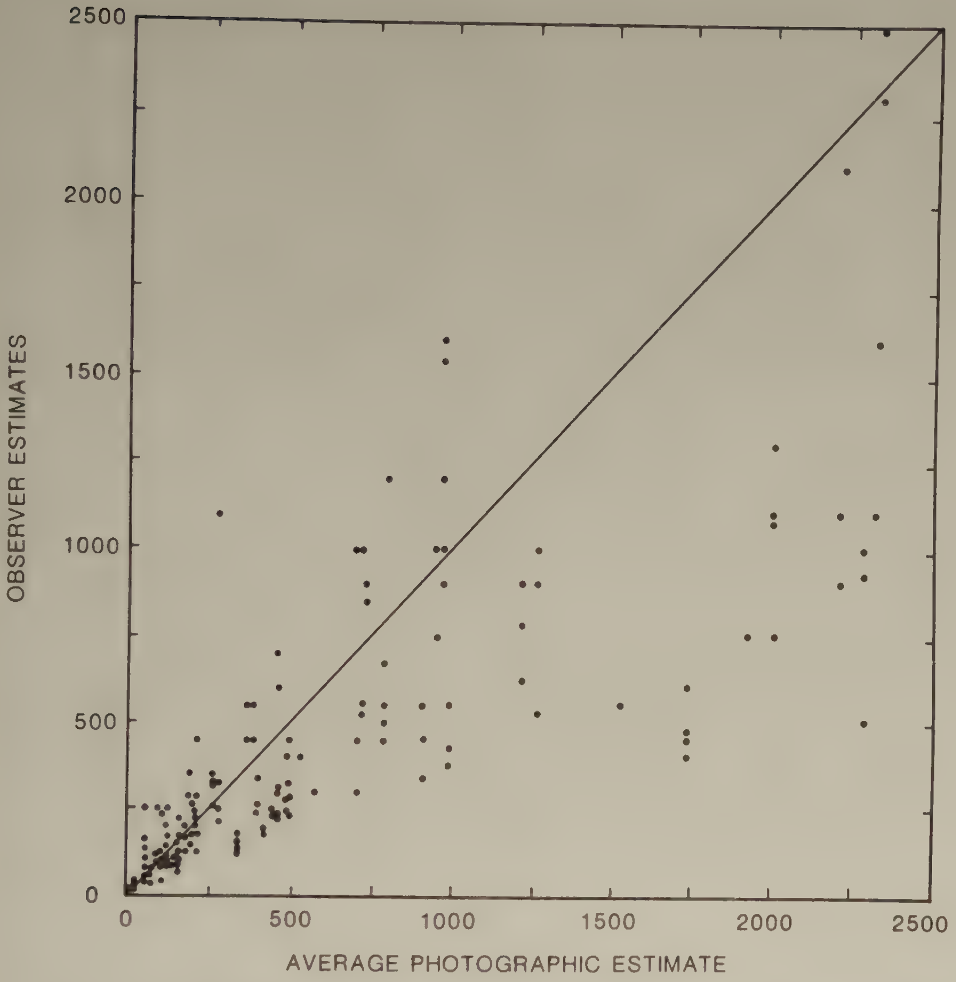

FIGURE 2. Comparison of visual estimates made by aerial observers and the corresponding average photographic estimates of cetacean schools. Not shown are observer estimates of 2500, 4000, 4200, and 4800 for a school with an average photographic estimate of 6028. The diagonal line is the 1:1 bisector.

FIGURA 2. Comparación de las estimaciones visuales hechas por los observadores a bordo de las aeronaves y el promedio correspondiente de las estimaciones fotográficas de los cardúmenes de cetáceos. No se presentan las estimaciones de los observadores de 2500, 4000, 4200 y 4800 de un cardumen con un promedio estimado fotográfico de 6028. La línea bisectriz es de 1:1.

TABLE 1. Studies during which aerial photographs were taken.

Study	Aircraft	Cameras	Total no. of observers	Area covered
1979 aerial survey	PBY-5A Catalina	K-17C 229-mm camera; Hasselblad 70-mm camera	6	Off the coasts of Mexico, Central America, and South America, to 750 nm offshore
1979 *Gina Anne* study	Bell-47 helicopter	KA-51A 127-mm camera; Hasselblad 70-mm camera	3	Off the coast of Mexico, to 800 nm offshore
1980 aerial photogrammetric study	Beechcraft AT-11	KC1B 229-mm camera; KA-62A 127-mm camera; KA-45A 127-mm camera; 4 Hasselblad 70-mm cameras	5	Off the coast of Mexico, to 200 nm offshore
1981 aerial survey	Beechcraft AT-11	KA-62A 127-mm camera; 4 Hasselblad 70-mm cameras	6	Off the coast of Costa Rica, to 56 nm offshore

TABLA 1. Estudios durante los cuales se tomaron fotografías aéreas.

Estudio	Aeronave	Cámara	No. total de observadores	Zona abarcada
Reconocimiento aéreo de 1979	Catalina PBY-5A	cámara K-17C de 229 mm; cámara Hasselblad de 70 mm	6	frente a las costas de México, la América Central y Sudamérica, hasta 750 mn mar afuera
Estudio *Gina Anne* de 1979	Helicóptero Bell-47	cámara KA-51A de 127 mm; cámara Hasselblad de 70mm	3	frente a la costa de México, hasta 800 mn mar afuera
Estudio fotogramétrico aéreo de 1980	Beechcraft AT-11	cámara KC1B de 229 mm; cámara KA-62A de 127 mm; cámara KA-45A de 127 mm; 4 cámaras Hasselblad de 70 mm	5	frente a la costa de México, hasta 200 mn mar afuera
Reconocimiento aéreo de 1981	Beechcraft AT-11	cámara KA-62A de 127 mm; 4 cámaras Hasselblad de 70 mm	6	frente a la costa de Costa Rica, hasta 56 mn mar afuera

TABLE 2. Comparison of school size estimates based on backdown counts and photographs from the 1979 *Gina Anne* cruise.

TABLA 2. Comparación de las estimaciones de la magnitud del cardumen, basadas en los cálculos del retroceso y en las fotografías del crucero *Gina Anne* de 1979.

Species Especie	Backdown count Cálculo del retroceso	Percent of school captured (estimated) % capturado del cardumen (estimado)	Estimated total school size Estimación de la magnitud total del cardumen	Average estimate from photographs Estimación promedio según las fotografías
Stenella longirostris	119	83%	144	201
Mixed *S. longirostris* and *S. attenuata*	239	71%	339	396
Mixed *S. attenuata* and *S. longirostris*	195	80%	243	216
S. attenuata	143	100%	143	161
S. attenuata	90	34%	264	238

TABLE 3. Counts and estimates of dolphin school size from aerial photographs taken during four surveys, 1979-1981.

TABLA 3. Cálculos y estimaciones de la magnitud de los cardúmenes de delfines según fotografías aéreas tomadas durante cuatro reconocimientos, 1979-1981.

School number	Species	Average photographic count	Average photographic estimate
Número del cardumen	Especie	Promedio del cálculo fotográfico	Promedio de la estimación fotográfica
1979 Gina Anne *Study* *Estudio del* Gina Anne *1979*			
6	*Stenella longirostris* and *S. attenuata*	339	362
31	*Steno bredanensis*	52	55
40	*S. attenuata*	73	80
72	*S. longirostris*	182	190
91	*S. longirostris* and *S. attenuata*	55	62
100	*S. longirostris* and *S. attenuata*	147	153
110	*S. attenuata* and *S. longirostris*	380	396
127	*S. longirostris*	124	127
147	*S. longirostris*	186	214
159	*S. attenuata*	141	150
171	*S. attenuata* and *S. longirostris*	194	204
1979 NMFS Aerial Survey *Reconocimiento Aéreo del NMFS 1979*			
4	*S. attenuata*	124	125
31	*Tursiops truncatus*	24	24
33	*T. truncatus*	16	17
34	*S. attentuata*	251	277
47	*S. longirostris*	57	59
78	*S. attenuata*	99	107
81	*S. longirostris*	870	973
82	*S. longirostris*	2212	2332
137	*S. longirostris*	58	60
141	*Delphinus delphis*	89	94
143	*T. truncatus*	71	72
176	*D. delphis*	144	154
198	*S. attenuata*	110	119
383	*D. delphis*	90	100
384	*D. delphis*	98	107
1980 Aerial Photogrammetric Study *Estudio Aéreo Fotogramétrico 1980*			
2	*S. attenuata*	174	181
4	*S. attenuata*	206	213
8	*D. delphis*	446	455
9	*D. delphis*	432	441
14	*S. longirostris*	484	499
17	*Feresa attenuata*	24	24
24	*S. attenuata* and *S. longirostris*	159	165

TABLE 3. (Continued)
TABLA 3. (Continuación)

25	*F. attenuata*	68	68
26	*S. attenuata*	131	141
32	*S. longirostris* and *S. attenuata*	298	307
35	*F. attenuata*	24	26
38	*S. longirostris*	202	210
39	*F. attenuata*	73	74
41	*S. longirostris* and *S. attenuata*	64	68
44	*S. longirostris*	148	156
45	*Peponocephala electra*	704	730
46	*S. longirostris* and *S. attenuata*	364	377
47	*S. longirostris* and *S. attenuata*	250	262
48	*S. attenuata* and *S. longirostris*	704	722
51	*F. attenuata*	14	15
54	*F. attenuata*	56	58
63	*S. longirostris*	2136	2219
67	*S. longirostris*	542	573
68	*S. longirostris*	508	530
67 & 68	*S. longirostris*	1212	1265
70	*S. longirostris*	1466	1525
71	*S. longirostris*	1850	1935
72	*S. attenuata*	324	336
75	*S. longirostris*	916	956
77	*S. longirostris*	152	158
78	*S. longirostris*	50	53
80	*S. attenuata* and *S. longirostris*	667	703
83	*S. longirostris*	756	800
85	*S. longirostris* and *S. attenuata*	472	492
86	*S. longirostris*	472	484
87	*S. longirostris*	5754	6028
88	*S. longirostris*	1175	1215
90	*S. longirostris*	1692	1737
92	*S. longirostris*	967	989
93	*S. longirostris*	888	913
94	*S. longirostris*	1967	2014
95	*S. longirostris*	2240	2294
99	*S. longirostris*	738	786
1981 Aerial Survey *Reconocimiento Aéreo 1981*			
60	*S. attenuata*	171	176
235	*S. longirostris*	444	458

TABLE 4. ANOVA tables for the logarithms of the photographic estimates within camera format; pass treated as a nested factor (from Clark, 1984).

TABLA 4. Tablas del análisis de la varianza (ANOVA) de los logaritmos de las estimaciones fotográficas en el formato de la cámara; las pasadas se consideran como un factor anidado (de Clark, 1984).

Source Fuente	SS SC	df gl	MS CM	F F	P(F) P(F)
229-mm camera (1980) *Cámara de 229 mm (1980)*					
School Cardumen	52.55	12	4.380	263.58	<.005
Pass within school Pasada en el cardumen	.57	35	.016	5.85	<.005
Reading Lectura	.15	52	.003		
127-mm camera *Cámara de 127 mm*					
School Cardumen	316.01	33	9.576	737.17	<.005
Pass within school Pasada en el cardumen	.92	73	.013	6.19	<.005
Reading Lectura	.24	120	.002		
70-mm camera *Cámara de 70 mm*					
School Cardumen	33.13	4	8.283	544.51	<.005
Pass within school Pasada en el cardumen	.11	7	.015	6.90	<.005
Reading Lectura	.08	37	.002		

TABLE 5. ANOVA tables for the logarithms of photographic estimates within camera format; pass treated as a covariate (from Clark, 1984).

TABLA 5. Tablas del análisis de la varianza (ANOVA) de los logaritmos de las estimaciones fotográficas en el formato de la cámara; las pasadas se consideran como una covariante (de Clark, 1984).

Source	**SS**	**df**	**MS**	**F**	**P(F)**
Fuente	**SC**	**gl**	**CM**	**F**	**P(F)**
229-mm camera (1980) *Cámara de 229 mm (1980)*					
School Cardumen	52.52	12	4.377	563.99	<.005
Pass Pasada	.05	1	.051	6.55	.012
Reading Lectura	.67	86			
127-mm camera *Cámara de 127 mm*					
School Cardumen	316.04	33	9.577	1638.86	<.005
Pass Pasada	.04	1	.038	6.46	.012
Reading Lectura	1.12	192	.006		
70-mm camera *Cámara de 70 mm*					
School Cardumen	31.04	4	7.760	2117.06	<.005
Pass Pasada	.03	1	.031	8.57	.005
Reading Lectura	.16	43	.004		

TABLE 6. ANOVA table for the logarithms of photographic estimates of the 11 schools photographed in 1980 with both the 229-mm and 127-mm cameras on at least two passes (from Clark, 1984).

TABLA 6. Tabla del análisis de la varianza (ANOVA) de los logaritmos de las estimaciones fotográficas de los 11 cardúmenes fotografiados en 1980, con ambas cámaras la de 229 mm y 127 mm, por lo menos en dos pases (de Clark, 1984).

Source	**SS**	**df**	**MS**	**F**	**P(F)**
Fuente	**SC**	**gl**	**CM**	**F**	**P(F)**
School Cardumen	90.43	10	9.043	4029.39	<.005
Pass within school Pasada en el cardumen	.59	28	.021	9.39	<.005
Camera format Formato de la cámara	.01	1	.010	4.31	.041
Reading Lectura	.19	84	.002		

TABLE 7. Average photographic estimates and observer estimates of dolphin school sizes.

TABLA 7 Promedio de las estimaciones fotográficas y de las estimaciones de los observadores de la magnitud de los cardúmenes de delfines.

1979 Gina Anne Study
Estudio Gina Anne 1979

School number Número del cardumen	Average photographic estimate Promedio de la estimación fotográfica	Observer estimates Estimaciones de los observadores *Obs. 1*	*Obs. 15*	*Obs. 16*
6	362	450	550	
31	55	58		
40	80	80		
72	190	285	350	144
91	62	75		
100	153	143		
110	396	240	260	339
127	127	185	250	
147	214	275	450	243
159	150	115	175	143
171	204	285	175	264

1979 Aerial Survey
Reconocimiento aéreo 1979

School number Número del cardumen	Average photographic estimate Promedio de la estimación fotográfica	*Obs. 1*	*Obs. 3*	*Obs. 4*	*Obs. 5*	*Obs. 6*	*Obs. 8*	*Obs. 10*
4	125	140		130	170	95	200	
31	24				28	35	40	
33	17				19	18	20	19
34	277	210			1100	325	250	300
47	59			80	165	80	120	
78	107	80		80	235	110	120	100
81	973	900		1600	1540	1200	1000	1200
82	2332	1100		2500	1500	2300	1500	1600
137	60			130		110	250	
141	94					250	80	
143	72			75	102			
176	154	70		100		125	80	130
198	119	100		130	200		140	
383	100	90		115		95		125
384	107	85	45					

1980 Aerial Photogrammetric Study
Estudio Aéreo Fotogramétrico 1980

School number Número del cardumen	Average photographic estimate Promedio de la estimación fotográfica	*Obs. 1*	*Obs. 2*	*Obs. 3*	*Obs. 11*	*Obs. 12*
2	181	165	125	150		
4	213		125	200		
8	455	310	220	300		
9	441		225	250		
14	499		175	190		
17	24	20	28	23	32	

TABLE 7. (Continued)
TABLA 7. (Continuación)

24	165	150	175		125	
25	69	50	50		40	
26	141	135	150	80	130	
32	307	285		175	275	
35	26	30	22		20	
38	210	240	225			
39	74	60	35	40	90	
41	68	95	80		70	
44	156	130	140	130		
45	730	850	900			
46	377	550	450			
47	262	350	260	325	320	
48	722	1060	530	350	560	
51	15	15	14			
54	58	35	45	35		
63	2219	2100	900	1100		
67	573		300			
68	530		400			
67 & 68	1265	900		525		1000
70	1525		550			
71	1935		750			
72	336	175	120	135		150
75	956	750	700			1000
77	158	140	80	85		225
78	53	42	38			45
80	703		450	300		1000
83	800		1200			
85	492	325	240	280		450
86	484	275	230			400
87	6028	4800	4200	2500		4000
88	1215	780	620			900
90	1737	600	475	450		400
92	989	550	425			375
93	913	450	340	450		550
94	2014	1300	1075	750		1100
95	2294	1400	925	500		1000
99	786	675	500	450		550

1981 Aerial Survey
Reconocimiento Aéreo 1981

		Obs. 8	*Obs. 10*	*Obs. 13*
60	176	200	200	
235	458	600	700	600

TABLE 8. ANOVA tables for the ratio of visual estimate to average photographic estimate for schools estimated by Observers 1, 2, and 3 (from Clark, 1984).

TABLA 8. Tablas del análisis de la varianza (ANOVA) que corresponden a la razón entre la estimación visual y el promedio de la estimación fotográfica de los cardúmenes estimados por los observadores 1, 2 y 3 (de Clark, 1984).

Source	**SS**	**df**	**MS**	**F**	**P(F)**
Fuente	**SC**	**gl**	**CM**	**F**	**P(F)**
Case I. All schools included in the analysis *I Caso. Todos los cardúmenes incluídos en el análisis*					
Observer Observador	14.49	2	7.247	101.30	<.005
School size Magnitud del cardumen	3.41	4	.853	11.92	<.005
Interaction Interacción	57.21	9	6.357	88.85	<.005
Residual Residual	7.58	106	.072		
Case II. Only schools <500 animals included in the analysis *II Caso. Solo cardúmenes <500 animales incluídos en el análisis*					
Observer Observador	13.02	2	6.511	82.59	<.005
School size Magnitud del cardumen	1.04	2	.518	6.57	<.005
Interaction Interacción	43.21	5	8.643	109.62	<.005
Residual Residual	5.44	69	.079		
Case III. Only schools <200 animals included in the analysis *III Caso. Solo cardúmenes <200 animales incluídos en el análisis*					
Observer Observador	11.05	2	5.523	95.25	<.005
School size Magnitud del cardumen	.03	1	.027	.47	.496
Interaction Interacción	25.10	3	8.366	144.28	<.005
Residual Residual	2.38	41	.058		

EL EMPLEO DE FOTOGRAFIAS AEREAS PARA ESTIMAR LA MAGNITUD DE LOS CARDUMENES DE LOS CETACEOS

por

Michael D. Scott[1], Wayne L. Perryman[2] y William G. Clark[3]

EXTRACTO

Se examinó la exactitud y la precisión de las estimaciones de la magnitud de los cardúmenes de delfines basadas en el cálculo de las fotografías aéreas, usando los datos obtenidos en los últimos reconocimientos aéreos y de los barcos. En 1979, durante un crucero de investigación en un cerquero atunero, se encontró que estas estimaciones eran acertadas; se fotografiaron los cardúmenes de delfines desde un helicóptero del barco, cercados con la red y luego se contaron a medida que se libraban los delfines de la red. Una comparación de las estimaciones fotográficas con estos cálculos indicó que la relación era bastante aproximada y no hubo indicación que se diferenció significativamente de la razón 1:1. Durante un estudio aéreo en 1980, se compararon las estimaciones fotográficas de diferentes cardúmenes, en los pases y los formatos de las cámaras y se encontró que eran bastante precisos, con una desviación normal de cerca del 6% de la magnitud del cardumen.

Se compararon también las estimaciones fotográficas con las estimaciones realizadas por los observadores aéreos. La mayoría de los observadores tienden a subestimar la magnitud de los cardúmenes, especialmente los cardúmenes grandes. La variabilidad entre los observadores fue elevada, lo que indica que se deben calibrar individualmente los datos de observadores.

INTRODUCCION

La magnitud del cardumen es un factor importante en la estimación de la densidad y la abundancia de los cetáceos. En lo que se refiere a las especies de delfines en el Océano Pacífico oriental (OPO), los reconocimientos aéreos se han empleado para proveer datos sobre la densidad de los cardúmenes y el promedio de la magnitud de los mismos. Los datos de la magnitud de los cardúmenes se basan típicamente en los cálculos o las estimaciones de los observadores a bordo de aeronaves.

Sin embargo, las estimaciones de los observadores de grandes congregaciones de animales, pueden ser muy erradas. Chattin (1952) ha descrito dichas estimaciones muy acertadamente como "una suposición infundada más el diez por ciento". Lavigne, Øritsland y Falconer (1977) presentaron a 134 observadores diapositivas en las que había un gran número de puntos y diapositivas aéreas de grupos de pinnípedos que se encontraban sobre el hielo y demostraron la tendencia que tienen estos observadores de sobreestimación. Ray y Wartzok (1980) indicaron resultados similares en las estimaciones de los observadores en fotografías de pinnípedos y cetáceos. Brown (1971), sin embargo, demostró que los observadores subestiman grandes números de objetos presentados en las fotografías. Heyland (1972) comparó las estimaciones aéreas de gansos de los observadores con fotografías aéreas tomadas al mismo tiempo y encontró que los observadores subestimaron el número actual de los gansos. Similarmente, Sinclair (1973) comparó las estimaciones de los observadores y las fotográficas de los búfalos (*Syncerus caffer*) africanos y encontró que las estimaciones de los observadores variaban considerablemente en precisión y que comúnmente subestimaban la magnitud del rebaño, especialmente en rebaños grandes de más de 500 animales. Withrow (1982) encontró resultados similares en grupos grandes (>200) de leones marinos Stellar (*Eumetopias jubatus*) fuera del agua. Esta disparidad en los resultados hace que sea difícil hablar en general de las estimaciones de los observadores.

---

[1] Comisión Interamericana del Atún Tropical, c/o Scripps Institution of Oceanography, La Jolla, CA 92037

[2] Southwest Fisheries Center, NOAA, P.O. Box 271, La Jolla, CA 92038

[3] School of Fisheries, University of Washington, Seattle, WA 98195

Se han empleado cada vez más las fotografías aéreas para obtener datos de la magnitud de los grupos de cetáceos (Heyland, 1974; Ray y Wartzok, 1980; R. Wells, datos inéditos). Sin embargo, no puede fotografiarse con éxito cada cardumen encontrado. Tales factores como el estado del mar, el resplandor del sol, la claridad del agua o el comportamiento de los animales pueden obscurecer porciones del cardumen, haciendo que las fotografías sean inservibles para el análisis. Por consiguiente, hay que confiar a menudo en las estimaciones de los observadores para obtener los datos de la magnitud del cardumen, aunque estas estimaciones son frecuentemente deficientes en lo que se refiere a congregaciones grandes.

Durante cuatro reconocimientos en el Océano Pacífico oriental se tomaron fotografías aéreas de cardúmenes de delfines (Tabla 1). Se proyectó uno de estos reconocimientos para determinar la precisión de las estimaciones derivadas de las fotografías. La precisión de las estimaciones fotográficas se determinó según los resultados de otro reconocimiento en el que se compararon las estimaciones obtenidas de las fotografías tomadas por cámaras de diferentes formatos, en diferentes pases y por diferentes lectores. Los datos de los cuatro reconocimientos permitieron la comparación de las estimaciones tanto de los observadores aéreos como de las fotografías.

Este estudio trata de aquellas cuestiones que pueden contestarse mediante el análisis estadístico de los datos anteriores, como son:

1) Describen acertadamente la magnitud real del cardumen las estimaciones derivadas de las fotografías?
2) Producen estimaciones estadísticamente indistinguibles de la magnitud del cardumen las fotografías tomadas con la misma cámara en pases sucesivos?
3) Producen diferentes estimaciones de la magnitud de los cardúmenes los diferentes tipos de cámara?

4) Existen diferencias sistemáticas entre los observadores en las estimaciones visuales?
5) Se pueden calibrar las estimaciones de los observadores mediante las estimaciones fotográficas de esos cardúmenes para los que se tienen ambas clases de estimaciones?

MATERIALES Y METODOS

Métodos usados en el campo

En 1979, la Comisión Interamericana del Atún Tropical (CIAT) realizó un estudio para investigar la exactitud y precisión de las estimaciones de los observadores obtenidas desde un cerquero atunero, *Gina Anne* (Allen, *et al.*, 1980). Los observadores a bordo del *Gina Anne* estimaron independientemente la magnitud de los cardúmenes de delfines capturados por el cerquero. Luego los delfines capturados fueron contados por dos, tres o cuatro observadores a medida que se liberaban los delfines sobre la red durante la maniobra del ''retroceso'' (Figura 1). Estos observadores contaban desde pequeños botes estacionados a lo largo del área de retroceso. Se obtuvo una estimación de la magnitud total del cardumen al agregar el cálculo de los observadores que se encontraban en los botes, el número estimado de delfines que no fue capturado y la cantidad de delfines muertos, si es que ocurrió alguna mortalidad durante el lance. Más tarde se compararon los cálculos del retroceso con las estimaciones de los observadores a bordo.

Estos cardúmenes de delfines fueron también fotografiados por el personal del National Marine Fisheries Service (NMFS) en el helicóptero Bell-47 del *Gina Anne* con una cámara KA-51A de 127 mm (5 pulgadas) montada verticalmente y una cámara manual Hasselblad 500 EL/M de 70 mm. Cuantas veces fue posible, el helicóptero realizó varios pases fotográficos sobre los cardúmenes a altitudes de 215–336 m y a velocidades de 65–70 nudos. Con el fin de evaluar la precisión de las estimaciones fotográficas aéreas, se compararon las estimaciones de la magnitud de los cardúmenes basadas en los cálculos hechos según las fotografías con las estimaciones basadas en los cálculos del retroceso. Las estimaciones aéreas de la magnitud de los cardúmenes fueron hechas por uno, dos o tres observadores y estas estimaciones se compararon tanto con las estimaciones fotográficas como con los cálculos del retroceso.

En 1979, se tomaron fotografías aéreas como parte de un reconocimiento aéreo de delfines en el Océano Pacífico oriental del NMFS (Jackson, 1980). Se usó un avión cuadrimotor Catalina PBY-5A en este reconocimiento; los vuelos se iniciaban en aeropuertos de México, Costa Rica, El Salvador, Guatemala, el Ecuador y Perú. Se tomaron fotografías con una cámara K-17C de 229 mm (9 pulgadas) montada verticalmente y una cámara manual Hasselblad de 70 mm. Se hicieron varios pases fotográficos sobre cardúmenes a alturas de 240–305 m y a velocidades de 90–100 nudos. Los observadores a bordo anotaron el comportamiento de los cardúmenes y la formación de los mismos. Luego se voló alrededor de ellos para que los observadores pudieran identificar las especies y estimar la magnitud del cardumen.

Las estimaciones se basaron generalmente en algún tipo de cálculo. Fue posible contar animales individuales en cardúmenes muy pequeños, pero usualmente se contaron subgrupos que incluían aproximadamente cantidades iguales de animales en cardúmenes grandes. Así que cuanto más grande fuera el cardumen tenían que ser más grandes los subgrupos. Puede que un observador haya contado agregaciones de 200 o más animales en cardúmenes grandes con miles de animales. Estas estimaciones (hasta de 6 observadores por cardumen) se hicieron independientemente y no se discutieron hasta que se terminó el estudio preliminar. No se pudieron fotografiar con éxito todos los cardúmenes de los que se hicieron estimaciones de la magnitud.

En 1980, la CIAT realizó también un estudio aéreo fotogamétrico, con personal y equipo del NMFS. Este estudio se designó principalmente para comprobar la posibilidad de medir la longitud de los delfines según las fotografías aéreas (Anónimo, 1981). Además, de uno a cuatro observadores hicieron estimaciones independientes de la magnitud de los cardúmenes las que se compararon con las estimaciones de la magnitud de los cardúmenes hechas según las fotografías. En este estudio, a bordo de un avión bimotor Beechcraft AT-11, se montaron verticalmente una cámara KA-45A de 127 mm, una cámara KA-62A de 127 mm, una cámara KC1B de 229 mm y cuatro cámaras Hasselblad de 70 mm. Sin embargo, las fotografías tomadas con la cámara KA-45A, no se usaron, debido a una avería en la cámara. Los pases fotográficos se hicieron a altitudes de 240–275 m a velocidades de 90–100 nudos. Se voló alrededor de los cardúmenes a una altura de 150 m para obtener las estimaciones de los observadores de la magnitud del cardumen.

En 1981, se tomaron también fotografías durante un reconocimiento aéreo del NMFS, proyectado para comprobar los efectos de las condiciones ambientales sobre la cantidad de cardúmenes vistos (Holt, 1983). Se tomaron fotografías de cardúmenes de delfines frente a la costa de Costa Rica con una cámara KA-62A de 127 mm y cuatro cámaras Hasselblad de 70 mm, montadas verticalmente a bordo de un avión Beechcraft AT-11. Los métodos para obtener las fotografías y las estimaciones de los observadores fueron iguales a los del estudio de la CIAT de 1980.

Cálculos fotográficos

Se examinaron las fotografías procesadas de todos los reconocimientos en una mesa iluminada para eliminar las imágenes de mala calidad o que no contenían todos los límites de los cardúmenes. La mayoría de las fotografías que se juzgaron aceptables para el análisis fueron ampliadas a 6–12x en proyectores de proyección Variscan Mark II, localizados en las oficinas del Earth Resources Observation System (EROS) en Bay Saint Louis, Mississippi. Las imágenes de animales individuales fueron marcadas independientemente hasta por cinco lectores en una película de acetato montada en la pantalla. Las diapositivas tomadas en el estudio de 1979, en el *Gina Anne* con la cámara Hasselblad, se vieron con un proyector de diapositivas de 70 mm y fueron marcadas en un cuaderno grande de papel de dibujo.

El pase fue la unidad en que se basó la estimación y generalmente el cardumen estaba incluído en dos o tres cuadros en un solo pase. Se calculó primero el cuadro central que incluía todo o la mayoría del cardumen. Los cuadros adjuntos se sobrepusieron en los gráficos del cuadro central y los delfines que no se habían contado anteriormente se agregaban al gráfico. La sobreposición entre los cuadros permitía entonces que se volvieran a examinar las imágenes dudosas en los cuadros adyacentes y permitía contar los animales que tal vez estaban a demasiada profundidad para ser contados en los otros cuadros. El cálculo de los subgrupos distantes que aparecieron en algunos pases, pero no en otros, se incluyeron en las estimaciones de la magnitud del cardumen en los pases en que faltaban los subgrupos.

Los lectores de las fotografías registraron dos tipos de datos. Uno fue el número actual de delfines contado en cada pase (la suma de todos los delfines graficados); el otro fue una estimación basada en el cálculo actual, pero incluyendo otro porcentaje, comúnmente pequeño, para incorporar los delfines que no se habían observado. Se consideró un número de factores al calcular el porcentaje agregado. Estos incluían la calidad de la fotografía, la cantidad de resplandor solar o el salpicado que pudiera velar a los delfines y el número de delfines que se estaban zambullendo o nadando muy por debajo de la superficie como se observó en las fotografías o en las anotaciones registradas. Por consiguiente, los cálculos se consideraron usualmente como subestimaciones de la magnitud del cardumen, especialmente a medida que los delfines eran menos visibles. La variabilidad de los lectores se encuentra presente tanto en los cálculos como en las estimaciones.

RESULTADOS

Precisión de las estimaciones fotográficas

Cinco cardúmenes que fueron fotografiados durante el experimento del *Gina Anne* fueron comparados con los cálculos del retroceso. En la Tabla 2 se presentan las estimaciones fotográficas y los cálculos del retroceso. El gradiente de la regresión (forzado a pasar a través del origen) de la estimación fotográfica sobre el cálculo del retroceso fue de 1.06, con un intervalo de confianza del 95% (0.90, 1.22) y $R^2 = 0.79$. Aunque solo se dispuso de cinco puntos de referencia, la relación entre los dos no indicó que se diferenciaron significativamente de la razón 1:1.

Debe observarse que los cálculos del retroceso no son "absolutamente precisos". Existía la posibilidad de que los delfines hubieran sido subcalculados o se hubieran contado en exceso cuando un grupo denso de animales hubiera pasado a través de un solo "sector de cálculo". Sin embargo, el error debido a ésto, parece que sea pequeño. Otra fuente de error es que los delfines algunas veces evaden la captura después de que se han tomado las fotografías. El número de delfines en estos grupos (comúnmente grupos pequeños de 10-40 animales) fue estimado por los observadores a bordo del barco (Tabla 2).

Aunque las estimaciones fotográficas de la magnitud de los cardúmenes muestreados durante el estudio del *Gina Anne* fluctuaron de 161 a 396, la evidencia deducida indica que las estimaciones fotográficas pueden también ser acertadas en cardúmenes más grandes. Durante el estudio de 1980, de la CIAT, se observaron dos cardúmenes que se estaban incorporando en uno solo. Los dos cardúmenes fueron fotografiados cada uno antes de incorporarse y luego se volvieron a fotografiar cuando ya se habían unido. La suma del promedio de las estimaciones fotográficas de los cardúmenes más pequeños separados (573 y 530) fue bastante próxima al promedio de la estimación del cardumen más grande (1265), lo que indica que las estimaciones fotográficas eran probablemente consistentes entre los cardúmenes pequeños y grandes.

Análisis de la varianza de las estimaciones fotográficas

Durante los cuatro reconocimientos se fotografió un total de 151 cardúmenes, de los cuales 71 (47%) se encontraban en fotografías de una calidad lo suficientemente buena para usarlas en el análisis. El promedio de los cálculos y el promedio de las mejores estimaciones de las fotografías se presentan en la Tabla 3.

Se hicieron los análisis de la varianza para calcular el efecto de varios factores en las estimaciones fotográficas de la magnitud del cardumen (Clark, 1984). Como la varianza entre las lecturas de la misma fotografía fue mayor con relación a los grandes cardúmenes que los pequeños, se empleó una transformación logarítmica para normalizar las varianzas entre las casillas. La prueba de Bartlett no indicó una heterogeneidad significante de la varianza en los logaritmos de las estimaciones fotográficas, así que se usaron éstas en todos los análisis. Más o menos hablando, una diferencia entre las casillas en los logaritmos de las estimaciones puede considerarse como una diferencia proporcional.

Las fuentes de variación entre las estimaciones fotográficas que fueron examinadas incluían:

1) La lectura. Los diferentes lectores comúnmente obtuvieron diferentes estimaciones en un solo pase. Estas diferencias entre las lecturas de la misma fotografía evalúan la duda mínima inherente de este método. Para los objetivos del análisis de la varianza, suministraron la varianza entre las casillas, la que se comparó con los otros efectos.

2) El pase. Se realizaron pruebas para determinar si, en promedio, existía una diferencia significativa entre las estimaciones basadas en las fotografías tomadas con la misma cámara en diferentes pases sobre el mismo cardumen.

3) Formato de la cámara. Se hicieron pruebas para determinar si había, en promedio, una diferencia significativa entre las estimaciones basadas en las fotografías tomadas por cámaras con diferentes formatos (70 mm, 127 mm o 229 mm) en los mismos pases sobre el mismo cardumen.

4) Cardumen. Evidentemente hubo grandes diferencias entre los cardúmenes en las estimaciones de la magnitud de éstos y fueron bastante consistentes entre los pases y los formatos. Aunque no existió duda de que el efecto del cardumen fue grande y significante, este factor apareció necesariamente en todos los análisis de la varianza para poderlo estimar y luego se eliminó para probar los efectos de los pases y el formato de las cámaras.

En términos del análisis de la varianza, se empleó un modelo mixto anidado: el formato de la cámara se trató como un efecto fijo que había que examinar para ver si era significante y estimarlo si se encontraba significante, mientras que los cardúmenes y los pases se trataron como efectos aleatorios con pases anidados dentro del cardumen. Solo en los cardúmenes fotografiados durante el estudio de la CIAT de 1980, en el que se hicieron pases múltiples y se emplearon los tres formatos de las cámaras, hubo la oportunidad de tratar simultáneamente los efectos de los cardúmenes, los pases, los formatos y las lecturas.

Los efectos de los pases—Con el fin de usar tantos datos como fuera posible, se hizo un análisis de la varianza separadamente para cada formato (Tabla 4). Al tratar separadamente los formatos con este fin, se simplificó también el modelo, ya que solo el cardumen, el pase y la lectura permanecieron como fuentes de varianza. En el análisis de cada formato de cámara se usaron las estimaciones de todos los cardúmenes que tenían por lo menos dos lecturas de cada pase (siempre que hubiera un mínimo de dos pases) cuando se estaba usando la cámara de que se trataba. No se pudo tratar la cámara de 9-pulgadas empleada en 1979, porque no se usó con éxito en más de un pase sobre cualquier cardumen.

El análisis de la varianza indicó en cada uno de los tres formatos, que el efecto del pase era significativo ($P<.005$). Sin embargo, el efecto del pase no es muy grande (6–8% de la magnitud del cardumen) y apenas excede la variación debida a la lectura, que es cerca del 5% de la magnitud del cardumen en todos los tres formatos. El cardumen es responsable por aproximadamente el 99% de la varianza total en cada una de las tres series de datos.

Como una aeronave que hace pases repetidos sobre un cardumen afecta el comportamiento de los animales, se pueden considerar los pases como una covariante en lugar de un componente de la varianza (Tabla 5). Cuando lo fue, el gradiente fue positivo y significativo en cada formato de cámara, lo que significa que hubo una tendencia significativa en las estimaciones fotográficas de aumentar de un pase al otro:

	Formato de 229 mm	*Formato de 127 mm*	*Formato de 70 mm*
Gradiente estimado	.018	.011	.038
Intervalo de confianza del 95%	.004–.032	.003–.020	.012–.064

De nuevo, debe observarse que aunque el efecto del pase es significativo, es pequeño (1–2% de la magnitud del cardumen por pase).

Como el efecto del pase fue significativo dentro de cada formato, no pudo eliminarse del modelo. Sin embargo, la manera en que fue manejado más tarde dependió de la naturaleza del efecto. Hubo dos posibilidades en los extremos:

1) El efecto de los pases fue consistente entre los formatos: En este caso no sería posible comparar las estimaciones obtenidas con diferentes formatos en diferentes pases, ya que podrían confundirse los efectos del pase y del formato.

2) El efecto de los pases no fue consistente entre los formatos: En este caso, sería posible comparar las estimaciones obtenidas con diferentes formatos en diferentes pases, ya que al examinar el efecto del formato, el efecto del pase aumentaría sencillamente el error de la varianza.

Como el pase fue significativo como un covariante dentro de cada formato, no se pudo excluir totalmente la primera posibilidad. Con el fin de desintegrar el efecto del pase en una porción consistente y en un residuo representante de la interacción, se hizo un análisis de la varianza solo en 11 cardúmenes que permitieron que se estimaran todos los efectos simultáneamente (Tabla 6). Estos cardúmenes fueron fotografiados en 1980, por lo menos en dos pases, tanto con cámaras de 229 mm como de 127 mm. Ambas porciones fueron significantes, pero el efecto consistente del pase es responsable por tres cuartos de la varianza asociada con el pase. Se encontró, por consiguiente, que el efecto del pase era casi uniforme entre los formatos.

Efecto del formato — Como el efecto del pase fue uniforme entre los formatos, la única prueba buena del formato fue limitada a los pases en los que por lo menos dos cámaras habían funcionado con éxito. En efecto, este requisito limitó la comparación en tal forma, que solo se pudo usar la misma serie de 11 cardúmenes nombrada anteriormente. En el análisis de la varianza de esas estimaciones (Tabla 6), el formato fue significante como un efecto fijo ($P = .04$), pero de nuevo el efecto fue pequeño, .015. Esto significa que las estimaciones hechas según las fotografías de 229 mm fueron, en promedio, 1.5% superiores a las estimaciones hechas de fotografías de 127 mm.

Precisión del promedio de las estimaciones fotográficas

En un formato y cardumen particular, la varianza del promedio de una estimación fotográfica es más pequeña que la varianza de una sola estimación fotográfica. En este caso,

n_p = el número de pases sobre el cardumen
n_r = el número de lecturas por pase
σ_p^2, σ_r^2 = los componentes correspondientes de la varianza de la estimación logarítmica de y.

Puede indicarse que:

$$V(\bar{y}) = \frac{\sigma_r^2}{n_r n_p} + \frac{\sigma_p^2}{n_p}$$

Con $n_r = n_p = 2$, y con $\sigma_r = .05$ y $\sigma_p = .08$ como antes, la desviación normal del promedio de la estimación fotográfica de un cardumen es $S(\bar{y}) = .06$ o sea cerca del 6% de la magnitud del cardumen. Por consiguiente, aún si las diferencias debidas al formato de la cámara agregan del 1–2%, el promedio de la estimación fotográfica de la magnitud del cardumen continúa siendo muy preciso.

En lo que sigue, el promedio de la estimación fotográfica se tratará esencialmente como un punto fijo, sin considerar el formato o el número de pases incluídos, debido a que la varianza de las estimaciones fotográficas es tan pequeña comparada con la varianza de las estimaciones de los observadores.

Comparación con las estimaciones de los observadores

Una cuestión importante referente a las estimaciones de los observadores es si existe una relación consistente entre las estimaciones de los observadores y las fotográficas de un cardumen determinado. Si existe, se puede usar la relación para ajustar las estimaciones de los observadores de cardúmenes que no fueron fotografiados. Si no existe, la interpretación de las estimaciones de los observadores es problemática.

El interés aquí no es, por consiguiente, la estimación en sí del observador, pero la diferencia entre una estimación del observador y el promedio de la estimación fotográfica del mismo cardumen. Con fines prácticos esta diferencia puede considerarse como el error en la estimación del observador, ya que el promedio de la estimación fotográfica tiene una varianza mucho más pequeña que la varianza de las estimaciones del observador de un cardumen determinado. Al tratar la diferencia como un error se supone que el sesgo del promedio de la estimación fotográfica es pequeño o no existe.

Igual que las estimaciones fotográficas, los errores de las estimaciones de los observadores tienen varianzas que aumentan con la magnitud del cardumen. Para normalizar las varianzas, cada estimación de los observadores fue dividida por el promedio de la estimación fotográfica de ese cardumen y esta razón se empleó en todos los análisis. Algebraícamente, esta cantidad es:

$$
\begin{aligned}
\text{Razón} &= \frac{\text{Estimación del observador}}{\text{Promedio de la estimación fotográfica}} \\
&= \frac{\text{Promedio estimación fotográfica} + \text{error estimación observador}}{\text{Promedio de la estimación fotográfica}} \\
&= 1 + \frac{\text{Error de la estimación del observador}}{\text{Promedio de la estimación fotográfica}}
\end{aligned}
$$

Trabajar con la razón es, por consiguiente, equivalente a trabajar con el error *relativo* (que puede ser ya sea positivo o negativo) de la estimación visual. Las fuentes de varianza en esta razón son:

1) Magnitud del cardumen. Para categorizar este efecto, se dividieron los cardúmenes en cinco grupos de magnitud de acuerdo al promedio de las estimaciones fotográficas: 1–99, 100–199, 200–499, 500–999 y ≥1000. Se escogieron estas divisiones porque proveen una distribución razonablemente uniforme de los cardúmenes entre las cinco categorías.

2) Observador. En estos estudios hubo 13 observadores, pero la mayoría presentaron más bien pocas estimaciones. Solo las estimaciones de tres observadores (del estudio de 1980, de la CIAT) suministraron un abarcamiento adecuado de las categorías de magnitud de los cardúmenes y una homogeneidad adecuada de la varianza para realizar este análisis.

Además, puede que haya un efecto significante debido a los cardúmenes individuales, pero como este efecto no era de interés, no fue estimado (es decir, en el análisis de la varianza se dejó como parte del término de error).

Un diagrama de dispersión de todas las estimaciones de los 13 observadores y el promedio correspondiente de las estimaciones fotográficas (Figura 2, Tabla 7) indica que a pesar de alguna dispersión, las estimaciones de los observadores como grupo son bastante precisas para los pequeños cardúmenes (hasta de unos 200 animales), pero la mayoría son bajas para los cardúmenes más grandes. Esto indica una relación curvilineal entre la estimación del observador y la magnitud del cardumen y por consiguiente es responsable por parte de la varianza en las proporciones de la estimación del observador con relación al promedio de la estimación fotográfica.

Solo tres observadores tenían grandes muestras de estimaciones sobre una amplia distribución de las magnitudes de los cardúmenes. Cuando se analizó esta subserie de los tres observadores (Tabla 8) se encontró que todos los factores (observador, magnitud del cardumen y la interacción) eran altamente significantes, con proporciones medias del error relativo como sigue:

Magnitud del cardumen	*1 Observador*	*2 Observador*	*3 Observador*
1–99	.96	.85	.70
100-199	.93	.84	.64
200-499	1.00	.66	.71
500-999	.88	.76	.49
1000+	.65	.45	.36

Cuando se incluyeron en el análisis solo las dos primeras categorías de la magnitud de los cardúmenes, ésta no fue significativa, pero el observador y la interacción fueron altamente significativas. Con solo las tres primeras categorías de la magnitud de los cardúmenes en el análisis, la magnitud del cardumen fue de nuevo altamente significativa.

A diferencia de los pases y formatos en el caso de las estimaciones de los observadores, las diferencias significativas aquí no son pequeñas. Aún dentro de las categorías de la magnitud de los cardúmenes, las diferencias no son de unos pocos por ciento de la magnitud del cardumen pero aproximadamente entre el 10 y 30 por ciento.

DISCUSION

Los resultados del experimento del *Gina Anne* indicaron que las estimaciones basadas en los cálculos fotográficos reflejan probablemente con precisión la magnitud actual de los cardúmenes de cetáceos. Como solo pudieron compararse cinco cardúmenes, se necesitan más datos para confirmar estos resultados. Se necesitan especialmente, cardúmenes en los que se capturan 100% de los animales para reducir el error asociado con la estimación de los observadores al contar los animales evasivos además de contarlos durante el retroceso. Sin embargo, en este estudio, se pensó que este error era más bien pequeño debido a que la magnitud de los grupos de los delfines que se escapaban era comúnmente pequeño y tal vez con más probabilidad de ser estimados correctamente.

El análisis de la varianza de las estimaciones de las fotografías del estudio de 1980 de la CIAT indicó que todas las fuentes posibles de variación eran significativas–cardumen, formato, pase y las interacciones–pero que el efecto del cardumen minimizó todo el resto de ellas. Esto permitió considerar diferentes pases, junto con diferentes estimaciones de los lectores como réplicas. El análisis de la precisión indicó posteriormente que las estimaciones fotográficas tienen una desviación normal aproximadamente del 6% de la magnitud del cardumen y por lo tanto son bastante precisas.

Sin embargo, la interpretación de las estimaciones de los observadores es problemática. La relación general entre las estimaciones de los observadores y las fotográficas parece ser curvilineal e indica que la mayoría de los observadores tienden a subestimar los cardúmenes grandes. Sin embargo, algunos observadores, tienden a hacer una estimación elevada, algunas veces demasiado alta. Los resultados de los análisis de la varianza de la subserie de los tres observadores indicaron que esta relación varía entre los observadores, variando ampliamente. Estos resultados pueden aún exponer inadecuadamente las diferencias entre los observadores, ya que los tres observadores en la subserie subestimaron, en promedio, la magnitud de los cardúmenes. Por consiguiente, en algunas categorías de la magnitud de los cardúmenes, parece probable que el promedio de las diferencias entre algunos observadores pueden sumar mucho más que el 10–30% de la magnitud del cardumen indicada en la subserie de los tres observadores.

Estos resultados y estudios por otros investigadores (Brown, 1971; Heyland, 1972; Sinclair, 1973; Lavigne, Øritsland, y Falconer, 1977; Ray y Wartzok, 1980; Withrow, 1982) indican que las estimaciones de los observadores pueden ser muy variables. Sin embargo, se han empleado dos métodos para evaluar las estimaciones de los observadores. Caughley, Sinclair y Scott-Kemmis (1976) ajustaron sus datos de acuerdo al sesgo de cada observador, al calcular el desempeño de cada observador aéreo en el campo en el que se conocía la magnitud de la población (en este caso, un rebaño de ovejas). Aunque su estudio se centralizó en el sesgo de los observadores al descubrir los animales, este método ha sido también aplicado a las estimaciones de la magnitud de los grupos (Withrow, 1982). Sin embargo, se necesitan muestras de gran magnitud sobre toda una escala de la magnitud de los cardúmenes para calibrar los datos de los observadores. Si se tiene en cuenta el trabajo necesario para calibrar las estimacione s de los observadores, es razonable suponer que se podría disponer de un conjunto continuo de observadores para los reconocimientos necesarios.

Otro método es entrenar los observadores con diapositivas o fotografías de agregaciones de magnitud conocida, permitiendo que los observadores hagan sus propias evaluaciones. Se ha tenido éxito en entrenar a los observadores aéreos en esta forma para reconocimientos de animales terrestres (Brown, 1971; Sinclair, 1973; Norton-Griffiths, 1978; Dirschl, Norton-Griffiths y Wetmore, 1981) y de pinnípedos en las playas (Withrow, 1982). La CIAT ha usado también una película de delfines en cardúmenes de magnitud conocida, tomada durante el crucero del *Gina Anne* para entrenar observadores.

En el caso del primer observador nuestros datos indican los efectos de la experiencia anterior en la estimación de la magnitud de los cardúmenes. Este observador participó en el reconocimiento de 1979, del NMFS, en el estudio del *Gina Anne* (como un observador aéreo) y en el estudio de 1980, de la CIAT. Además, fue un lector de las fotografías después de cada estudio. En cardúmenes de menos de 400 animales (el grupo más grande fotografiado durante el estudio del *Gina Anne* y, por lo tanto, la subserie que podía proveer una comparación uniforme entre los tres estudios), su sesgo fue −16.1% durante el estudio de 1979, +19.9% durante el estudio del *Gina Anne* y −2.0% durante el estudio de 1980. Puede argumentarse que el desempeño de este observador se debió a su experiencia previa que le permitió comparar sus estimaciones anteriores con los cálculos fotográficos.

Esto indica el valor probable de la experiencia del observador en estimar correctamente la magnitud del cardumen. Pero queda la cuestión, qué constituye la experiencia en este caso? Puede que los observadores aéreos hayan gastado muchas horas en el aire mirando los cardúmenes de cetáceos, pero puede que nunca hayan tenido la oportunidad de comparar sus estimaciones con ninguna forma de información sólida, especialmente en agregaciones muy grandes. Por consiguiente, estos observadores pueden confiadamente dar las mismas estimaciones para cardúmenes de la misma magnitud, pero estas estimaciones puede que no reflejen precisamente la verdadera magnitud del cardumen. Tal vez sea necesario volver a examinar nuestro concepto de la "experiencia" para incluir la evaluación de las estimaciones de los observadores contra los cálculos de las fotografías aéreas.

RECONOCIMIENTO

Los autores reconocen y agradecen a las siguientes personas que participaron en estos reconocimientos como pilotos, observadores o lectores: S. Alexander, E. Barham, W. Brinkerhoff, R. De Rosa, T. Flynn, L. Hansen, R. Holt, T. Jackson,

C. Jardin, J. Laake, S. Leatherwood, J. Niehaus, C. Oliver, J. Olson, F. Ralston, J. Rutledge, R. Stives y W. Walker. Agradecemos también al Capitán Pete Balestrieri y a la tripulación del *Gina Anne* cuya colaboración y ayuda hicieron posible el estudio a bordo del barco y el helicóptero. Damos también las gracias al personal de las oficinas de EROS en Bay de St. Louis, Mississippi, por su ayuda y el uso de los proyectores Variscan. Los fondos para este estudio fueron provistos por la CIAT; el equipo de las cámaras fue provisto por el NMFS. El análisis de W. Clark fue subvencionado en parte por los fondos provistos por la Comisión de Mamíferos Marinos de los EEUU. Las siguientes personas examinaron el manuscrito y prestaron consejos útiles: W. Bayliff, D. DeMaster, M. Hall, P. Hammond, A. Hohn, R. Holt, J. Laake, C. L. Peterson, G. Scott y P. Tomlinson.

LITERATURE CITED — BIBLIOGRAFIA CITADA

Allen, R.L., D.A. Bratten, J.L. Laake, J.F. Lambert, W.L. Perryman, and M.D. Scott. 1980. Report on estimating the size of dolphin schools, based on data obtained during a charter cruise of the M/V *Gina Anne*, October 11–November 25, 1979. Inter-Amer. Trop. Tuna Comm., Data Rep., 6: 1–28.

Anonymous. 1981. Annual Report of the Inter-American Tropical Tuna Commission 1980 (in English and Spanish). pp. 49–50.

Brown, R.G.B. 1971. Experiments on the counting behaviour of waterfowl observers. Canadian Wildlife Service '71, Dept. of Environ. Ottawa, Canada. p. 20.

Caughley, G., R. Sinclair, and D. Scott-Kemmis. 1976. Experiments in aerial survey. J. Wildl. Mngmt. *40*(2): 290–300.

Chattin J.E. 1952. Appraisal of California waterfowl concentrations by aerial photography. Trans. of the 17th N. Amer. Wildl. Conf. pp. 421–426.

Clark, W.G. 1984. Analysis of variance of photographic and visual estimates of dolphin school size. U.S. Nat. Mar. Fish. Serv. SWFC Admin. Rep. No. LJ-84-11C. 36 pp.

Dirschl, H.J., M. Norton-Griffiths, and S.P. Wetmore. 1981. Training observers for aerial surveys of herbivores. Wildl. Soc. Bull. *9*(2):108–115.

Heyland, J.D. 1972. Vertical aerial photography as an aid in wildlife population studies. Proc. First Canadian. Symp. on Remote Sensing. pp. 121–136.

Heyland, J.D. 1974. Aspects of the biology of beluga (*Delphinapterus leucas* Pallas) interpreted from vertical aerial photographs. Proc. of the Second Canadian Symp. on Remote Sensing. pp. 373–390.

Holt, R.S. 1983. Report of porpoise experiment testing detection of on-track schools (PET DOTS) March 7–April 5, 1981. NMFS Tech. Memo. NOAA-TM-NMFS-SWFC-27. 80 pp.

Jackson, T. 1980. Trip report: Porpoise population aerial survey of the eastern tropical Pacific Ocean, January 22–April 25, 1979. U.S. Nat. Mar. Fish. Serv. SWFC Admin. Rep. No. LJ-80-1. 74 pp.

Lavigne, D.M., N.A. Øritsland, and A. Falconer. 1977. Remote Sensing and Ecosystem Management. Skrifter nr. 166, Norsk Polarinstitutt. 51 pp.

Norton-Griffiths, M. 1978. Counting Animals. African Wildlife Leadership Foundation, Nairobi, Kenya. 139 pp.

Ray, G.C. and D. Wartzok. 1980. Remote sensing of marine mammals of Beringea. Contract Report NAS 2–9300 to the U.S. National Aeronautics and Space Administration. 77 pp.

Sinclair, A.R.E. 1973. Population increases of buffalo and wildebeest in the Serengeti. E. Afr. Wildl. J. 11:93–107.

Withrow, D.E. 1982. Using aerial surveys, ground truth methodology, and haul out behavior to census Stellar sea lions, *Eumatopias jubatus*. M.S. thesis, Univ. of Washington. 105 pp.

8584

Drift Bottle Makes Long Journey

by Richard S. Shomura
Director of the Southwest Fisheries Center's Honolulu Laboratory

■ A drift bottle released from the NOAA ship *TOWNSEND CROMWELL* on February 4, 1973, near Christmas Island was recovered recently. It had drifted more than 4,600 miles to a beach on the northeast coast of Mindanao, a southern island in the Philippines.

Actually, the bottle was found over a year ago on June 15, 1983, by a Philippine resident named Cesar L. Cabrera. Cabrera found the bottle at a spot called White Beach in Cagwait, a town located in Surigao Sur on Mindanao. It is not clear whether Cabrera himself returned the identification card that was inserted in the bottle, since the card was enclosed in an envelope that had the following return address: 4th Mun. Circuit Trial Court of Cagwait-Bayabas, Cagwait, Surigao del Sur. Also, it is not clear why the finder (or sender) waited over a year to mail the card to the Honolulu Laboratory (the envelope was postmarked September 12, 1984).

Information on the general direction of surface currents in the ocean can be surmised from the drift of floating objects such as flotsam, logs and glass balls used as floats in fishing gear. In most instances, however, information on currents obtained from observations on such floating objects is incomplete because the locality and the time the drift started are not known. Also, it is difficult to compute the speed of currents based on these serendipitous observations because the effects of winds on drifting objects are not known. To overcome these uncertainities, oceanographers many years ago introduced drift bottles to study surface currents. These bottles are tightly sealed and weighted with sand so that they will be nearly immersed and not be influenced by winds. The bottles contain cards that are numbered for identification and provide space for the finder to fill in information on date and location of finding.

This particular drift bottle that ended upon the Mindanao Island beach was one of 840 released a few miles north, east and south of Christmas Island on February 4, 1973. The bottles were part of an experiment devised by Richard A. Barkley, an oceanographer who was then on the staff of the Honolulu Laboratory, to study the pattern of surface currents around oceanic islands. Christmas Island was selected for this study because it provided a relatively simple situation: A single small island that had no other intruding islands located "upstream" in the strong regular flow of the westerly North Equatorial Current. One bottle was recovered at sea the next day after it had traveled around the north coast of the island and then west. Twelve bottles were recovered from the windward beach on Christmas Island on February 11 and 12, 1973. Other areas of Christmas Island and other islands in the Line Islands group (Fanning, Washington, and Palmyra) were searched, but no other bottles were found.

In its westward travel in the grasp of the North Equatorial Current the bottle must have passed by numerous islands in the equatorial Pacific Ocean on its way to Mindanao. For about 1,500 miles in the area immediately west of Christmas Island there are relatively few islands. However, further west in the path that the bottle presumably took are the numerous islands of the Gilbert Islands, the Marshalls, Federated States of Micronesia and the Republic of Belau. But somehow the bottle avoided washing ashore on the beaches of all these islands and made its way to the Philippines.

Although the time elapsed between the time of release and recovery is over 10 years, Shomura speculates that the actual journey time may have taken less time than that. The bottle may have been lying undiscovered on the Mindanao beach for a number of years, especially if White Beach is in a remote, relatively uninhabited part of Mindanao. Other drift experiments have shown that bottles released near the equator in the central Pacific Ocean traveled at speeds of more than 36 miles a day, so it is possible that this bottle could have made the journey of over 4,600 miles in about 128 days. It is also possible, of course, that although the bottle was under the primary influence of the North Equatorial Current, it could also have been affected by local currents near islands and thus taken much longer to reach the Philippines. So even though no information was obtainable on the speed of the drift for this bottle, the direction of drift was determined and conforms to what is known of the surface currents in the equatorial Pacific. But perhaps more interesting is what is not known: all the possible meanderings of the bottle during its long journey from Christmas Island to Mindanao.

. . . **Richard**

8585

A Case History of an Anti-El Niño to El Niño Transition on Plankton and Nekton Distribution and Abundances

Paul E. Smith
National Marine Fisheries Service

Introduction

The management of coastal pelagic schooling fishes is complicated by vast changes in recruitment and availability. While an El Niño event can be a tragic economic event in the history of a fishery, it can also be a natural experiment for biological oceanographic monitoring to gather important dynamic information. The motivation and funding to monitor an event like "El Niño" usually arrives after the onset is well in place (McGowan, 1984). To find a time when, by chance, the onset of an El Niño was well monitored, we must return to the 1955-9 event.

While there seems little doubt of the magnitude of the 1983-84 El Niño event, the anchovy population continued to spawn eggs at the same rate in 1983-4 as in 1980-2 (Fiedler, et al., MS) (Table 1). Although the process of spawning is energy intensive (Hunter and Leong, 1981), spawning continued as the apparent production of the anchovy habitat declined (McGowan, 1984; Fiedler, 1984). Local catches were also reduced for the coastal pelagic and continental shelf fishes and increased for tropical and temperate tunas as expected for these oceanic conditions (Table 2). The comparable increase of tropical fish catch in 1957 compared to the average of the previous five years was barracuda 2.4 x, yellowtail 4.6 x, bonito 5.6 x, yellowfin tuna 18.8 x skipjack tuna 82.3 x, and dolphinfish 876.6 x, for only the first nine months of the year. Young sardine were noted in the live anchovy bait catch along the entire coast from San Diego to Monterey Bay for the first time in years. (Anon. 1958).

Reexamination of a Case History

The 1957-9 El Niño was discussed in the "Rancho Santa Fe Symposium". The report of that meeting, and particularly the personal contacts between quantitative and theoretical meteorologists and oceanographers, launched the discipline of "air-sea} interaction (Sette and Isaacs, 1960). A biological study of great magnitude (3,461 plankton observations on 20

Table 1. Northern anchovy (Engraulis mordax) central population reproduction parameters.

PART A Cruise	Spawning area (Sq. mi.)	Spawning biomass '000 t	 g/m^2	Mortality rate z	 %/d
Mar. 1980	19000	870	13	.453	36
Feb. 1981	23000	635	8	.138	13
Apr. 1981	17000	372	6	nil	nil
Feb. 1982	24000	415	5	.158	15
Feb. 1983	28000*	652	7	.184	17
Mar. 1984	18000	309	5	.170	16

PART B Cruise	Female weight g	Specific fecundity m-eggs/d/t	Mean interval days
Mar. 1980	17	30	7
Feb. 1981	13	33	9
Apr. 1981	16	34	8
Feb. 1982	19	33	8
Feb. 1983	11	24	11
Mar. 1984	12	42	6

*About half the area of the state of Washington.

cruises quarterly for five years separated into 18 taxonomic groups) was begun as a result of that climatic change (CalCOFI atlases by Isaacs, Fleminger and Miller, 1969; Isaacs, Fleminger and Miller, 1971; and Fleminger, Isaacs and Wyllie, 1974) and a principle components analysis was reported by Colebrook (19777).

I have divided the fishes of the CalCOFI region into those which occupy an area larger than the CalCOFI survey; those which inhabit the coastal currents of the eastern boundary; and those which are mostly confined to the continental shelf. Most of the fish we have studied are planktivorous so I have included a brief section on plankton. In the "High Seas" category, I have included the tunas, the jack mackerel, the saury, and the mesopelagic fishes. In the fishes of the coastal currents, I have included anchovy, sardine, and Pacific mackerel. The flatfishes and rockfishes are considered under the heading "continental shelf" fishes. Hake are included as continental shelf fishes for the purpose of this paper because that is where most of the feeding takes place (Bailey, et al., 1982). The primary reason for dividing the fishes into these categories is to more precisely interpret the effects of El Niño.

Table 2. Commercial landings from California waters.

Species	1982			1983			Weight ratio
	Rank	Weight	Value	Rank	Weight	Value	
Coastal Pelagics		117.5	18.8		59.1	12.8	0.50
Mackerel	1	54.9	10.1	1	48.8	9.1	0.89
Market squid	4	16.3	3.6	14	1.4	0.6	0.09
Northern anchovy	2	42.1	1.9	10	4.1	0.4	0.10
Pacific bonito	15	2.1	1.0	12	3.2	1.3	1.52
Pacific hake	21	1.0	0.2	17	1.0	0.2	1.00
Thresher shark	20	1.1	2.0	20	0.6	1.2	0.55
Shelf & Slope		76.8	67.1		54.5	43.8	0.71
Chinook salmon	11	3.3	18.8	25	0.4	1.8	0.12
Dover sole	6	10.0	5.1	5	8.4	4.1	0.84
Dungeness crab	12	3.0	7.2	18	0.9	3.1	0.30
English sole	18	1.4	1.0	15	1.2	0.8	0.86
Lingcod	19	1.4	0.7	19	0.8	0.5	0.57
Pacific herring	5	10.3	9.7	6	8.0	12.5	0.78
Petrale sole	22	0.8	1.0	23	0.6	0.8	0.75
Rex sole	25	0.7	0.5	21	0.6	0.5	0.86
Rock crab	unrank	-	-	22	0.6	1.1	+
Rockfish	3	21.8	10.6	4	14.0	8.6	0.64
Rockfish (b-c*)	14	2.3	1.0	11	3.5	1.8	1.52
Rockfish (t*)	16	2.0	1.0	13	1.7	0.8	0.85
Sablefish	7	9.5	5.2	8	6.1	3.2	0.64
Sea urchin	8	8.3	3.1	7	7.2	3.3	0.87
Shrimp (po*)	17	2.0	2.2	24	0.5	0.9	0.25
Temperate Tuna		3.4	4.7		4.5	5.7	1.67
Albacore tuna	13	2.7	3.9	9	4.5	5.7	1.67
Bluefin tuna	24	0.7	0.8	unrank	-	-	-
Tropical tuna		9.7	14.8		37.7	39.9	3.89
Skipjack tuna	10	3.9	3.7	2	18.8	15.3	4.82
Swordfish	23	0.8	5.1	16	1.0	5.7	1.25
Yellowfin tuna	9	5.0	6.0	3	17.9	18.9	3.58

Weight is in thousands of metric tons.
Value is in millions of dollars to the fishermen.
Mackerel is Pacific mackerel and jack mackerel combined.
b-c bocaccio and chilipepper rockfish.
po Pacific Ocean shrimp.
t thornyhead rockfish.

Nekton

High seas

Bluefin tuna. Yamanaka (1984) noted an inverse correlation between the catch rate of young bluefin tuna (_Thunnus thynnus_) off Japan and the United States. In particular there appeared to be a

Table 3. Crude composition of zooplankton in the upper 140 m of the California Current

Functional group	1956		1958		Weight		
	Rank	Weight	Rank	Weight	Ratio	Change	%
Copepoda	2	27.9	1	14.2	0.51	-13.7	12
Chaetognatha	4	6.3	2	4.4	0.70	-1.9	2
Siphonophora	5	6.1	3	3.6	0.59	-2.5	2
Thaliacea	1	91.4	4	3.3	0.04	-88.1	74
Euphausiacea	3	7.1	5	3.2	0.45	-3.9	3
Medusae	6	3.1	6	1.2	0.39	-1.9	2
Decapoda	10	1.2	7	0.6	0.50	-0.6	
Pteropoda	14	0.3	8	0.6	2.00	0.3	
Radiolaria	9	1.4	9	0.4	0.29	-1.0	
Crustacean larvae	12	0.8	10	0.3	0.38	-0.5	
Amphipoda	7	1.8	11	0.2	0.11	-1.6	1
Larvacea	11	0.9	12	0.2	0.22	-0.7	
Ostracoda	13	0.4	13	0.2	0.50	-0.2	
Ctenophora	8	1.5	14	0.2	0.13	-1.3	1
Cladocera	17	0.02	15	0.2	10.00	0.18	
Heteropoda	15	0.1	16	0.1	1.00	=	
Mysidacea	16	0.03	17	0.01	0.33	-0.02	
TOTAL		150.35		32.91	0.22	-117.44	100

Weight is in grams per 1000 cubic meters to 140 meters depth.
Change is the difference in grams between 1956 and 1958.
% is the category change as a percent of sum of categories change.

low rate of return of juveniles to Japan during the El Niño periods. He postulated that during the El Niño more juvenile bluefin migrated to the Pacific coast of America than usual and then those fish migrated to the southern hemisphere off Chile. He also pointed out that the Japanese sardine migrated out to the albacore tuna fishing grounds during the recent El Niño.

Albacore tuna. Like the bluefin tuna, some albacore are trans-Pacific migrants in the temperate zone. The 1957-8 El Niño was associated with inverse trends in the California sport boat and Canadian jigboat catches; between 1955 and 1959 the annual catches of the sport boats was 577, 482, 304, 48, and nil tons, the Canadian jigboats nil, 17, 8, 74, and 212 tons (Laurs 1983). It is now thought that local water clarity may play a large role in determining the feeding migration patterns (Fiedler, Laurs and Montgomery, MS) of albacore and the catch by different method. Changes in prey distribution, vertical and geographic, and local temperature gradients must also have an effect on fishing success on albacore and the distribution of all the oceanic properties is altered by El Niño.

Tropical scombroids. Major predators from the tropics inhabit California Current waters warmer than 20°C. This includes skipjack, bigeye, and yellowfin tunas and the billfish (Katsuwonus pelamis, Thunnus obesus, Thunnus albacares, Makaira indica, and

Xiphias gladius). The northerly extent of these species appears to be limited by surface temperature. Blackburn (1965) found that the existence of a suitable temperature was not always accompanied by the presence of tropical predators. Schaeffer (1960) considered the chief cause of the occurrence of tropical tunas off California to be active migration during warm conditions because the warming at that time was due to heat exchange rather than advection of warm water.

Jack mackerel. The abundance of larvae of jack mackerel declined from an area averaged 2 per square meter in 1950-1957 to fewer than 0.3 per square meter between 1958 and 1960 (MacCall and Stauffer, 19883). The relative recruitment strength of the stock in 1958 was 2 times that in 1959 and 1960. It is obvious that the abundance of larvae of this species is not effective as an index of spawning biomass but is instead responsive to several environmental influences. Since the outer and northern range of spawning is not normally encompassed by the larval surveys, the variation may signal changes in the degree of overlap of the survey area and the spawning area. The change of temperature, alone, is probably incapable of exerting more than a two-fold influence on development rate, thus the 5-7 fold change is probably indicative of a change in fecundity rather than a change in spawning biomass. During the radical change between 1957 and 1958, the primary difference appeared to be the number of samples with large numbers of larvae, suggesting a change in reproductive per capita output (Ahlstrom, 1969). Cursory examination of the larval mortality rate between 3 and 11 mm does not reveal an obvious change between 1957 and 1959 but this constancy could be confounded with an abnormal growth rate.

It is not clear whether jack mackerel changes its distribution in relation to temperature directly to its temperature-related food. The food of another jack mackerel species in a similar current system off the Pacific coast of South America, (Konchina, 1983) consists of primarily Euphausiids (54%), fish (20%), decapods (12%), copepods (7%), and cephalopods (5%). Of the fish 40% were engraulids, 25% were gonostomatids, and 20% were normanichthyids. Almost all oft he euphausiid shrimps were Nyctiphanes simplex. The seasonal maximum of fish in jack mackerel was in August (Southern hemisphere winter) at 35% owing to the addition of Vinciguerria lucetia. He described the feeding interaction between hake and jack mackerel overlapping mainly in the feeding on engraulids and occasionally Vinciguerria lucetia. Thus, to understand the effect of El Niño on jack mackerel one would have to observe changes in euphausiids, and at least 3 groups of fish.

Saury. Saury spawning below 30° north latitude virtually ceased between 1957 and 1960. Either the adult fish were not there or they were unable gain sufficient surplus energy to spawn. This species exhibits a trans-Pacific distribution and is thought to be a zooplankton feeder (Smith and Ahlstrom, 1973). There was also a small decline in the abundance of eggs off southern and central California. This could be explained by more rapid hatching time in the warmer water. Another explanation would be that the zooplankton abundance was lowered which changed the per capita rate of spawning. Also, the northward migration of tropical predatory birds, fish and mammals could be a contributing cause of the decreased abundance of eggs by predation on the spawning adults or consumption of egg masses. Off Japan saury may be replaced by incursions of *Scomber japonicus* (Schaeffer, 1980); although this occurred in 1958 off Japan it was determined whether some oceanic boundary of the saury habitat shifted or the Pacific mackerel population expanded its range into the saury habitat.

Mesopelagic fishes. Even though the main effects of the El Niño may be above the habitat of the adult mesopelagic fishes, the larvae of some mesopelagic fishes inhabit the upper mixed layer. An examination of an atlas of the most common mesopelagic fishes (Ahlstrom, 1972) reveals several different responses to the onset of the 1957-59 El Niño.

Three of the mesopelagic species have epipelagic (100 m or less) larvae. One of the most massive distributional changes occurred with *Vinciguerria lucetia*. Its major concentrations were restricted to south of 30°N in the anti-Niño period 1955-56 and it spread to the oceanic areas off San Francisco to 35 north latitude by 1960. Primarily because of its increased "overlap" with the CalCOFI survey area, the abundance of *V. lucetia* increased an order of magnitude between 1956 and 1959. In a similar but less extensive change of geographic distribution larvae of *Triphoturus mexicanus*, tripled in apparent abundance through a 240 nautical mile northward shift. Larvae of a third species, *Stenobrachius leucopsaurus*, did not appear to respond in any way to either the anti-Niño or Niño; the southern limit of distribution remained off San Diego through the entire period.

Two of the mesopelagic species also have mesopelagic larvae. The number of larval *Leuroglossus stilbius* declined by 6-fold between 1957 and 1958; this appeared to be caused by the decline in spawning in a southern center off Punta Eugenia, Baja California as the northern limits did not appear to shift. *Bathylagus wesethi* larvae doubled in apparent abundance during the niño period, apparently by slight increases in abundance in spawning centers and by drawing closer to the coast. The larvae of *Bathylagus ochotensis*, a subarctic species, decreased slightly during the warming apparently due to a withdrawal from the coast and to the north. The depth distribution of this species is not well known.

Engraulis. The onset of El Niños in 1957-9 (Fig. 1) and 1982-3 (Table 1) had remarkably little effect on the apparent production of eggs and larvae. In fact the "anti-El Niño" with its colder waters and invasion of subarctic fauna appears to have a negative effect on the abundance of these planktivorous fishes. In 1957-9 increase with the onset of El Niño. There were large increases in the abundance of larvae off central California and moderate increases off the southern California coast more than 300 km. In the egg production time series from 1980 to 19884 there continued to be production rates of more than 200 eggs per square meter per day throughout the Los Angeles Bight. In addition, during El Niño in 1983, there were more than 100 eggs produced per square meter per day from 200 km to 250 km offshore. Similar rates were sustained in 1984 out to 200 km. Therefore, the prediction of diminished northern anchovy fecundity caused the apparent low zooplankton volume and chlorophyll (McGowan, 1983; 1984) has not been substantiated. Similarly, in 1957-9, the diminished primary production and zooplankton volume was met with equal or greater spawning of northern anchovy (Smith and Eppley, 1982) in the Los Angeles Bight area.

Sardinops. As with the anchovy, the sardine Sardinops caerulea, appears to be adversely affected by the cold "anti-El Niño" and favored by El Niño (Fig. 2). Murphy (1960) used temperature as a "convenient index" for other oceanic properties in his discussion of the sardine. He stated that "...cooler temperatures along the California Current are associated with accelerated southward transport, and more vigorous upwelling with its attendant offshore movement of water. Plankton densities are increased." He noted that the warm years of the late 30's and early 40's appeared to have been favorable for sardine recruitment and the cooler years 1943-1956 were accompanied by a precipitous and sustained decline in the species. The species reached a spawning biomass of 2 million tons during the El Niño of 1941. However, in the El Niño of 1982-3 off Chile, the large Sardinops population failed to recover its normal fat content in the summer and in the next spawning season the fat content of the population was again reduced by a factor of 2 (Vidal, Chile Pesquero, December 1983 p. 13).

Scomber. A high rate of parent per capita recruitment occurred in the years 1958-60 (Parrish and MacCall, 1978; Schaeffer, 1980). While the catch records of Pacific and jack mackerel are frequently combined for statistical purposes, the species are radically different. The life span of the jack mackerel is several times tnat of the Pacific mackerel and the adult phase of the jack mackerel is found in transitional waters between the Central Water Mass of the North Pacific and the West Wind Drift and California Current. Juvenile jack mackerel school with Pacific mackerel in the coastal currents off California but at the age of 3 or 4 they resume the high seas distribution characteristic of their parents. There they live for about 25 years (MacCall and Stauffer, 1981). Pacific mackerel live in the coastal current region of the subtropical and temperate zone of the Gulf of California, Baja California and southern California. The maximum age of Pacific mackerel is 11 years (Schaeffer, 1980) and they probably remain in the coastal currents region.

Despite the increased recruitment of Pacific mackerel in the 1957-9 Niño the sport catch off California was 1/2 normal in this period. The Mexican catch of Pacific mackerel declined by a factor of 5 in 1957 and declined yet another factor of 5 in 1958. These conflicting facts are probably explained by a more northerly distribution of this species at this time so that they are unavailable to the fishery from the traditional ports.

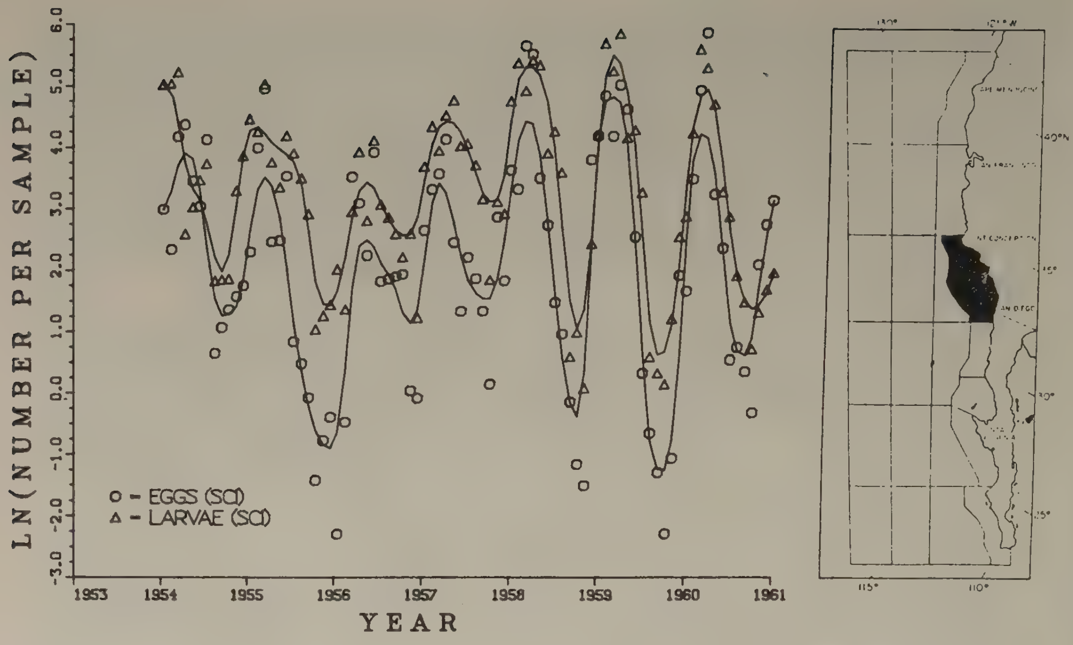

Figure 1. The increase of anchovy spawning between 1954 and 1960 in the southern California inshore region. The circles are at the natural log of the monthly average egg abundance for all stations in the region. The triangles are at the natural log of the monthly average larvae abundance for all stations in the region. The line is a resistant non-parametric smoother for these points (Velleman, 1980).

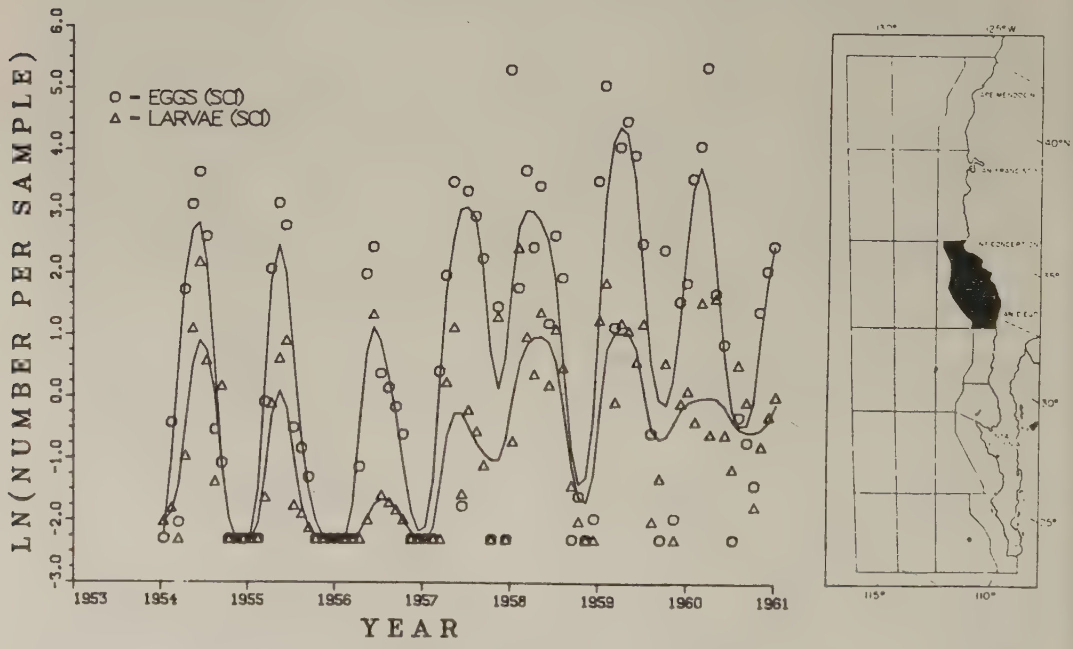

Figure 2. The increase of sardine spawning between 1954 and 1960 in the southern California inshore region. The circles are at the natural log of the monthly average egg abundance for all stations in the region. The triangles are at the natural log of monthly average larvae abundance for all stations in the region. The line is a resistant non-parametric smoother for these points.

Detailed studies of growth have not been conducted on the Pacific mackerel so changes in length at age which are observed for this species (smaller during El Niño) may be due to greater survival of the smaller members of the cohort, or smaller members of the population transported in from the southern, more subtropical sectors of the distribution (Klingbeil, pers. comm.) or larger fish migrating to the north.

Pleuroncodes. The red crab, *Pleuroncodes planipes*, is a benthic animal of the Gulf of California and the south Baja California continental shelf (Longhurst, 1966). During most years the juvenile pelagic phase drifts back and forth in the coastal currents over the adult habitat but important numbers of offspring are entrained in the California Current extension and carried into the tropics. During El Niño, similarly important numbers are carried north as far as southern California in a band 160 km wide and in a narrow coastal strip into waters off central California. New data from trawling for anchovy adults shows a similar northerly transport (Fig. 3) of red crab juveniles offshore. Although sightings of red crab are at the surface, it is not known at what depth the organisms are transported. Since the adults live in depths as great as 300 meters it is conceivable that some transport is in the California Undercurrent. The pelagic phase of red crab is about 2 years in duration but mature individuals have not been collected off Alta California thus the origin of all the young is considered to be at 25°N latitude or 1000 km south of where many young are transported (Boyd, 1967).

Shelf Fauna

The fishes and invertebrates of the continental borderland are likely to exhibit some diversity of response to El Niño. Planktivorous species or older organisms may be in part be isolated from the immediate effects of a brief El Niño. In general hake are mesopelagic spawners which feed on the continental shelf, the rockfish as a group are pelagic over canyons and around islands and the flatfish are demersal over the gentler slopes of the continental margin. The time series of larval catches of these species may permit identification of some changes associated with El Niño.

Merluccius. The Pacific hake does not continuously occupy the zone of coastal currents (Bailey et al., 1982). During the spring and summer, the adult population migrates 1000 km northward to feed on the continental shelf of the north temperate eastern north Pacific. Depending on the age structure and the temperature at depth (Smith, 1975), the hake migrate to various distances to the south in the fall and spawning is conducted in winter. Since the onset of the El Niño was in April 1957, the first year of effect on hake larvae was in 1958. An index of larvae from winter abundance in 1954-1960 was 5, 8, 14, 21, 8, 2, 3. That portion of the larval index in the region seaward of about 300 km for the same years is 2, 4, 11, 15, 3, .1, and .9. The survival of the 1957-9 spawn to fishable age was low relative to 1960 and 1961.

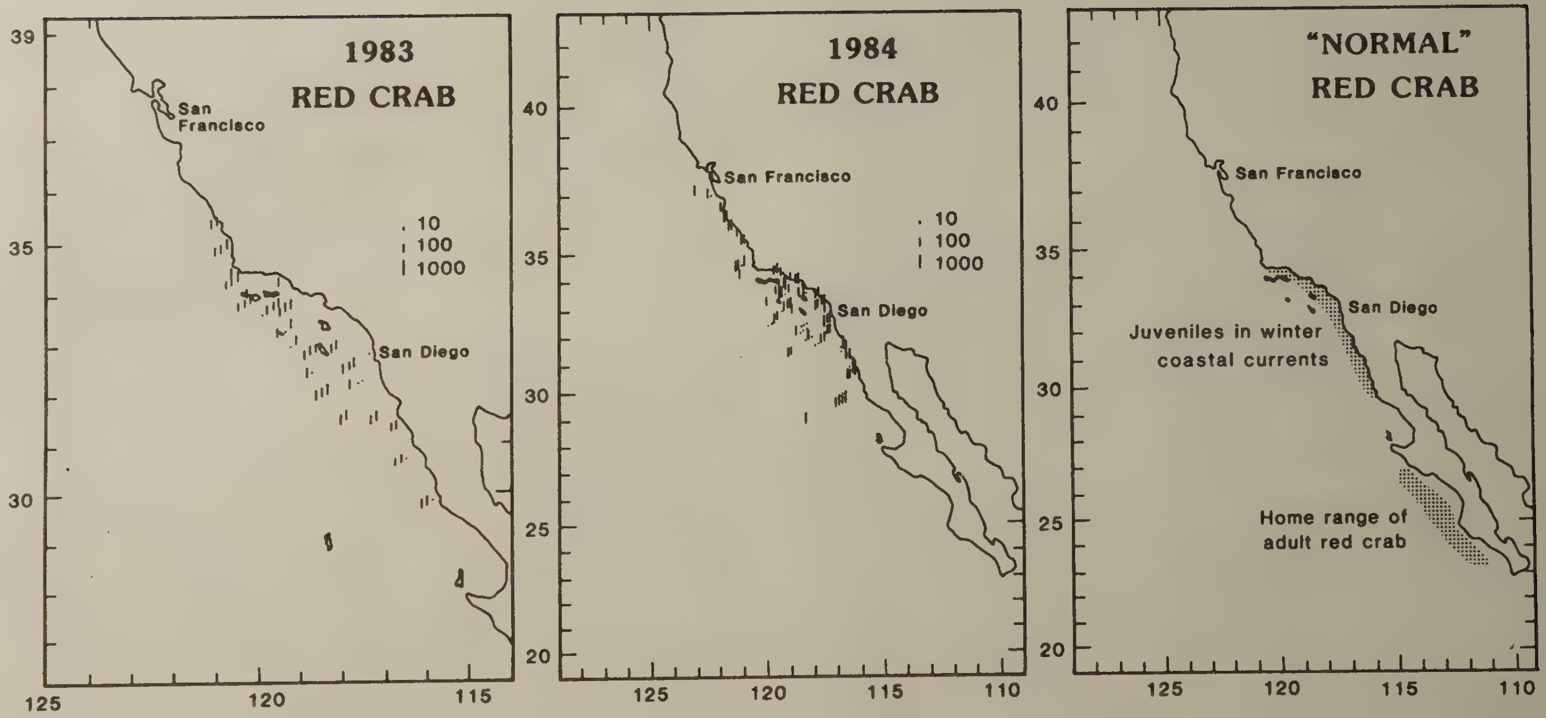
1983
RED CRAB
San Francisco
San Diego
. 10
ı 100
l 1000
39
35
30
125
120
115
1984
RED CRAB
40
25
20
110
"NORMAL"
RED CRAB
Juveniles in winter coastal currents
Home range of adult red crab

Figure 3. Temperate distribution of red crab. a) juveniles caught in near surface trawls in 1983; b) juveniles caught in near surface trawls in 1984; c) normal range and adult habitat. For maps of trawling effort see Picquelle and Hewitt, 1984 and Hewitt, 1984.

Since the larval index was high in 1957, the per capita survival of spawn must have been extremely low for that year.

Rockfish. The first effects of the 1957-9 El Niño on the production of rockfish larvae were noted in 1958. Since the onset of El Niño condition was in April of 1957 after the most rockfish births (rockfish bear live young) had occurred for the year. At 42°N there was an apparent increase in the number of rockfish larvae in 1958. At 37°N there were moderate decreases in 1958 and 1959. At 32°N the number of rockfish larvae per stations decreased by more than half in 1958 and again by a factor of three in 1959. The decline of larvae was similar at 27°N. There were no obvious effects of El Niño on the commercial fishery. The decline in larval abundance may have been caused by the decline of the productivity of the waters adjacent to the continental shelf. The El Niño may have had a profound effect on the reproductive rate of this group of species. A description of these time series is found in Ahlstrom, Moser and Sandknop (1978). This arctic to temperate genus has 69 species in the eastern North Pacific and about 40 species are taken in commercial and sports fisheries in California.

Flatfishes. Of eight kinds of flatfishes that Ahlstrom and Moser (1975) analyzed only four showed major declines in abundance during El Niño of 1957-9. The species which declined less than 2-fold (possible temperature/development rate effect) were the California halibut, Paralichthys californicus, English sole, Parophrys vetulus, Rex sole, Glyptocephalus zachirus, and the Dover sole, Microstomus pacificus. The species which appeared to change more drastically were the speckled sanddab, Citharichthys stigmaeus, other sanddabs, Citharichthys spp., slender sole, Lyopsetta exilis and the turbots, Pleuronichthys spp. It would be interesting to know the feeding habits of these two groups and what mechanism differentiates their response to El Niño.

Plankton

The plankton sampling program of CalCOFI was designed to quantitatively capture the eggs and early larval stages of fishes which occupy the euphotic zone. Thus, observations of organisms which occur in and deeper than the 140-m depth of the CalCOFI oblique tows must be interpreted cautiously. For example, the adults of many euphausiids substantially evaded the bridled ring-net, even at night, and most euphausiids range throughout the upper 600 meters (Brinton and Townsend, 1981). Important amounts of copepod biomass were not retained by the .505 mm mesh apertures of the CalCOFI standard net. Important fractions of the zooplankton are totally destroyed by contact with the filtering surface under tow and others are extruded from the mesh during vigorous washing. Thaliaceans shrink greatly before the displacement volume is taken in many samples the large thaliaceans were discarded before fixation owing to the lack of adequate containers and fixative (Thrailkill, pers. comm.). Planning and sample design, like that conducted for the eggs and larvae of sardine, would be a prerequisite for a quantitative analysis of any of the 500 or so populations now captured in the fish egg and larva surveys. Still the regularity of the sample techniques has permitted advanced analysis and important conclusions about widespread biological oceanographic phenomena and much of the interpretation is based on the strength of the non-seasonal changes during the 1957-9 Niño and the cooler period which preceded it (Bernal, 1981).

As pointed out by Smith (1971) most of the change in zooplankton volume during the El Niño of 1957-59 was caused by a radical diminution in the volume of thaliaceans (salps, pyrosomes and doliolids) and larvaceans. This category comprised 75% of the zooplankton in October of 1956 and by April of 1958 this category was only 7%. The crustaceans had during the same period risen from 17% to 60%. These relative changes in plankton group composition cannot be interpreted in terms of productivity since changes in standing crop merely represent changes in the relative rates of natality, growth and mortality. One would need to know much more about the demographics of the planktonic populations and the vulnerability of the life stages to sampling to make useful inferences about zooplankton production.

Thaliaceans dominated plankton collections in the California Current region in 1956 being more than triple the quantity of copepods and 13 times the volume of euphausiids. The rank order was thaliaceans, copepods, and euphausiids. By 1958 the copepods had decreased to 50%, the euphausiids had decreased to 45%, and the Thaliaceans had decreased to 4% of their volumes. Table 3 lists these functional groups with the other 14 for comparison. Following the climatic shift, copepods became the most abundant group in the biomass and the thaliaceans and euphausiids were nearly equal at fourth and fifth rank abundance. The chaetognaths had risen from fourth to second rank and the siphonophores had risen from fifth to third rank.

Thaliaceans. Thaliaceans were most abundant seaward of 150 km in the main branch of the California Current (Figure 4). The annual average reached a maximum of 200 grams per 1000 m^3 in 1956 and decreased to less than 10 grams per 1000 m^3 by 1958 and in 1959. The annual average temperature shifted from 14 to 16.5° degrees in this outer region over the same period (Fig. 5). Alongshore thaliaceans changed from 140 cc per 1000 m^3 in 1956 to nil in 1958 and remained there in 1959 in the Vizcaino Bay region (Fig. 6). There were parallel temperature rises along the entire coast (Fig. 7).

During the actual onset of El Niño in April of 1957, the thaliacean displacement volume declined 20-fold between April and July. In a similar period in 1956 the thaliaceans increased 5-fold in the southern California section.

Copepods and Euphausiids. Across the coastal currents and main branch of the California Current the annual average abundance of copepods decreased from about 50 and 10 grams per 1000 m^3 in 1955-57 to about 20 and 6 grams per 1000 m^3 in 1958-9 (Fig. 8).

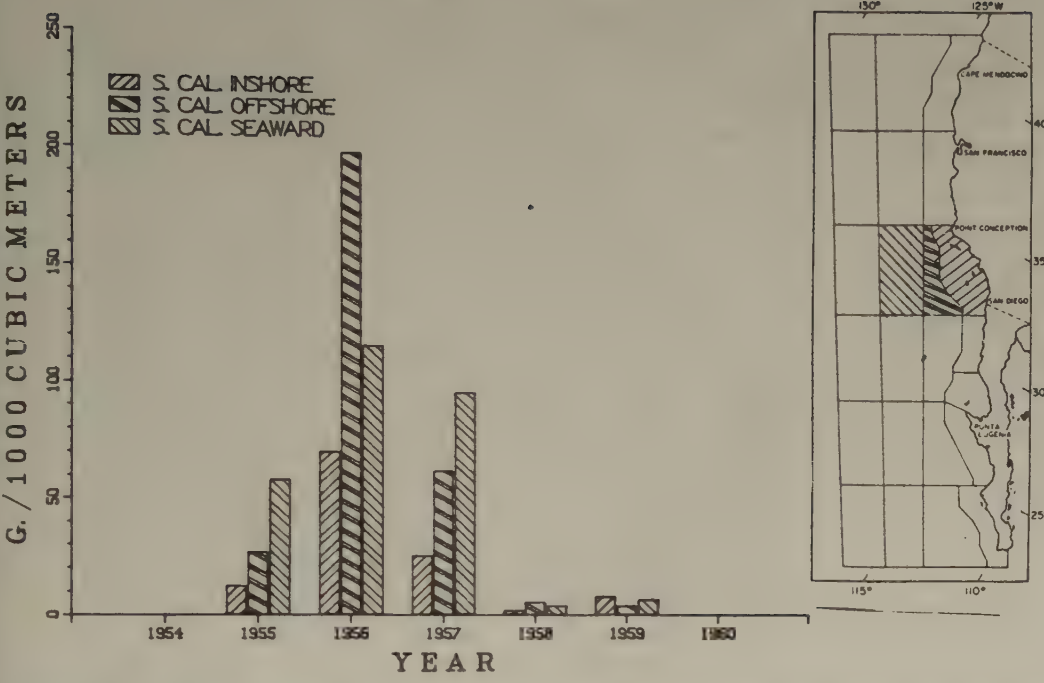

Figure 4. The decrease of thaliacean displacement volume between 1955 and 1959. The first bar is the volume calculated from the average of all stations in the southern California inshore region for the entire year. The second bar is the same value for the southern California offshore region. The third bar is the same value for the southern California seaward region.

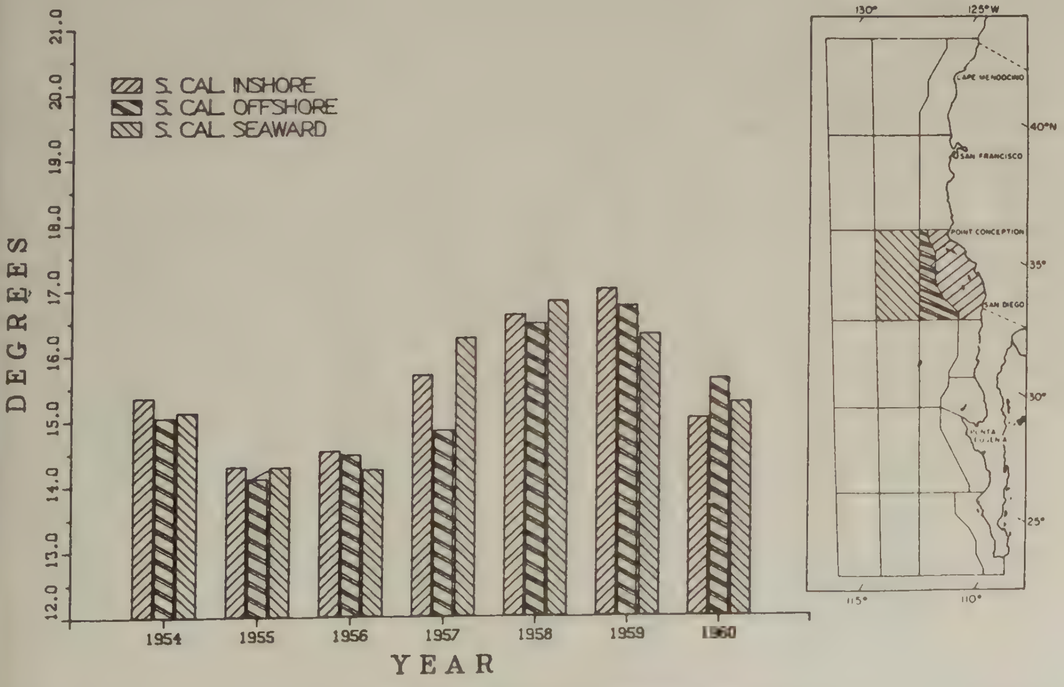

Figure 5. The increase of 10 meter temperatures between 1954 and 1960. The first bar is the 10 m temperature calculated from the average of all stations in the southern California inshore region for the entire year. The second bar is the same value for the southern California offshore region. The third bar is the same value for the southern California seaward region.

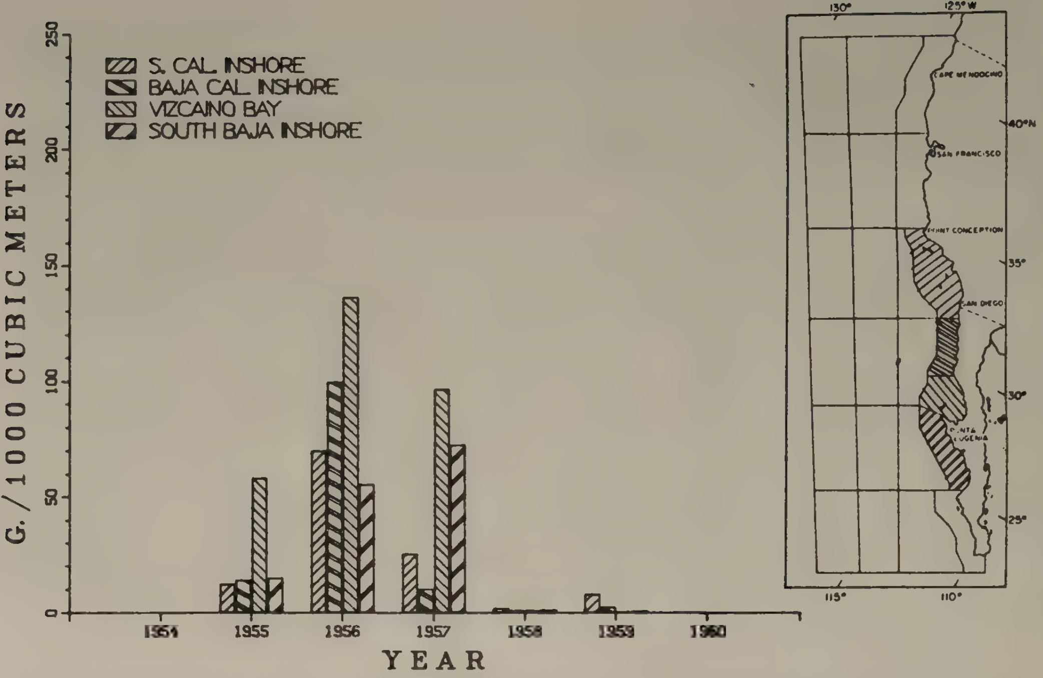

Figure 6. The decrease of thaliacean displacement volume between 1955 and 1959. The first bar is the volume calculated from the average of all stations in the Southern California inshore region for the entire year. The second bar is the same value for the Baja California inshore region. The third bar is the same value for the Sebastian Vizcaino Bay region. The fourth bar is the same value for the south Baja inshore region.

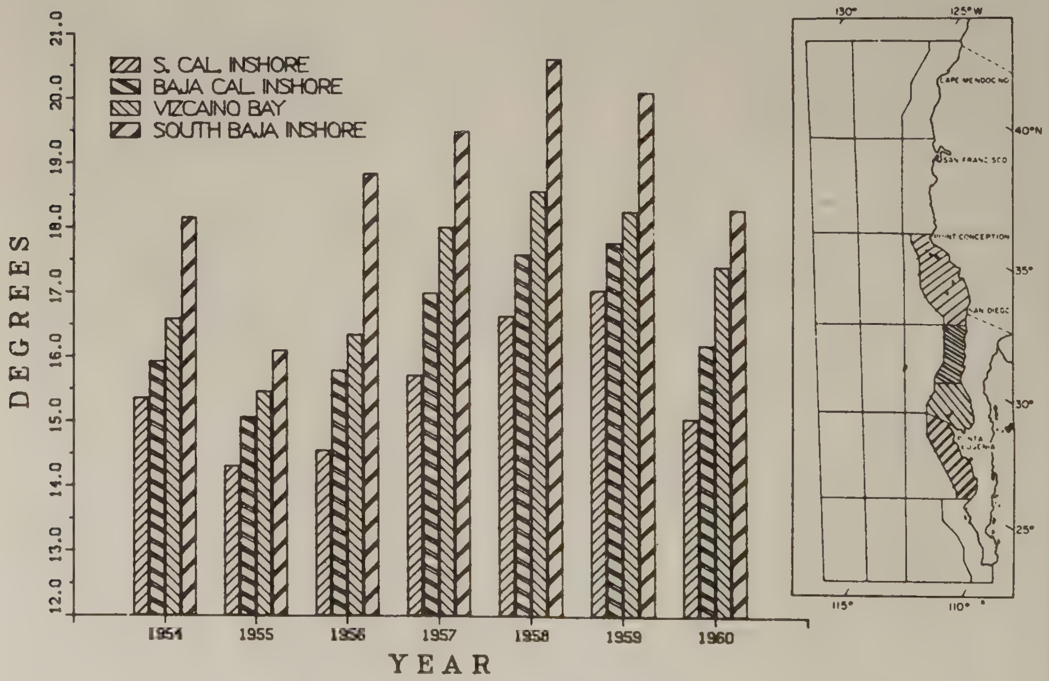

Figure 7. The increase of 10 m temperatures between 1954 and 1960. The first bar is the average 10 m temperature calculated from all stations in the southern California inshore region for the entire year. The second bar is the same value for the Baja California inshore region. The third bar is the same value for the Sebastian Vizcaino Bay region. The fourth bar is the same value for the south Baja inshore region.

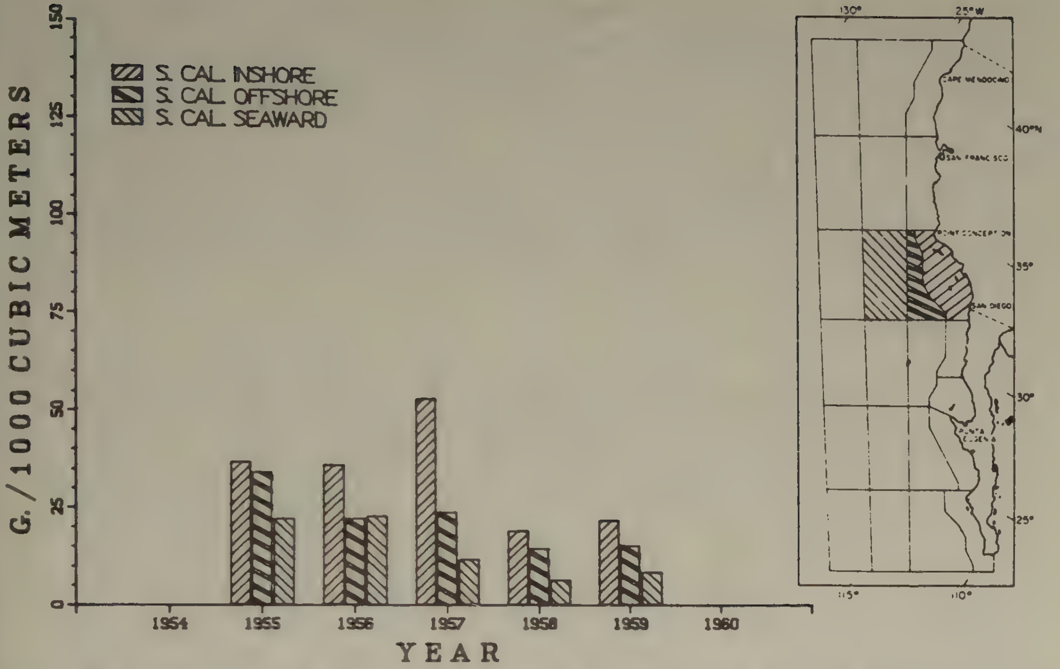

Figure 8. The decrease of copepod displacement volume between 1955 and 1959. The first bar is the volume calculated from the average of all stations in the southern California inshore region for the entire year. The second bar is the same value for the southern California offshore region. The third bar is the same value for the southern California seaward region.

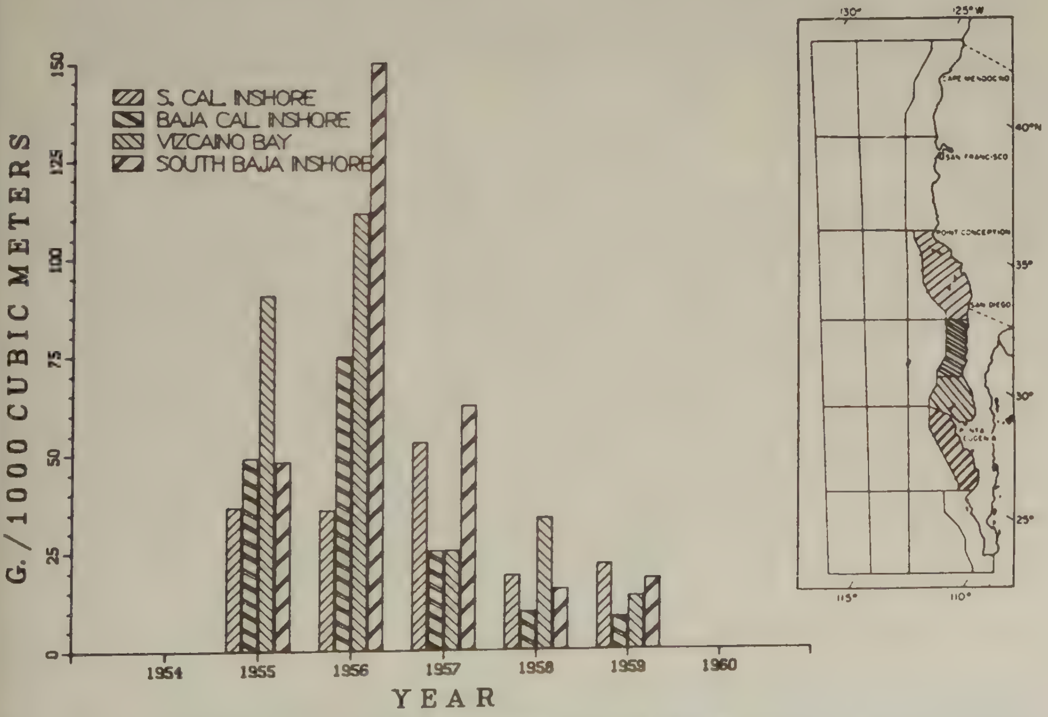

Figure 9. The decrease of copepod displacement volume between 1955 and 1959. The first bar is the volume calculated from the average of all stations in the southern California inshore region for the entire year. The second bar is the same value for the Baja California inshore region. The third bar is the same value for the Sebastian Vizcaino bay region. The fourth bar is the same value for the southa Baja inshore region.

Southward along the coast in the coastal currents zone the decrease in the southerly regions was more dramatic for the copepods, from 140 grams per 1000 m^3 to 20 (Fig. 9). Euphausiids decreased by a factor of three (Fig. 10 and 11).

During the onset of El Niño in April 1957, the inshore copepods decreased by a factor of 4 and the euphausiids decreased by a factor of 3 by July. In the same period in 1956 the volumes were equal over the 3 month span in the southern California inshore area.

Presumed Secondary Production

While secondary production is difficult to infer from zooplankton displacement volume, it may be interesting to note that the slope of the seasonal increase of zooplankton is similar in the southern California inshore area in the years 1955 through 1959 (Fig. 12 and 13). One can infer from this that the reproductive capacity less the predation rate favored increases in zooplankton volume both when the system was dominated by thaliaceans and when dominated by copepods. The second figure is a display of the adjacent month differences displayed as ratios. In this area one can expect sustained increases from 10 to 60% per month in the winter and spring months whether the system is dominated by thaliaceans or copepods and at either the 14° temperature of the 1955-56 period or the 16.5° temperature of the Niño period. Since the currents are sluggish in this area one would expect local growth to dominate over transport as a factor in this rate of increase, transport in the gyre is largely from the south and west with only minor entrainment of the California Current as indicated from the offshore position (270 km at line 90) of salinity less than 33.4% (Bernal, 1981).

Primary Production

Unfortunately, there were no primary production estimates at the time of the 1957-9 El Niño. There are no spatially and temporally coherent time series of an area the size of the California Current region. A coastal time series reported by Smith and Eppley (1982) did capture one extremely high phytoplankton production rate of 1.41 g C per m^2 per day in June of 1975 and a relatively low value of 0.1 g C per m^2 per day in October of 1976 and February 1977. Assuming the Scripps Pier Temperature Anomaly was related to primary production in the same way in the years 1955-59, the annual average production declined from 0.4 to 0.2 g C per m^2 per day and December minima of 0.1 were obtained in 1957 and 1958. There appeared to be moderate agreement in the change in values of zooplankton volume over the same period Table 4.

Summary and Recommendation for Future Study

Re-examination of the more thoroughly sampled transition from anti- to El Niño conditions in 1955-9 suggests answers to the question "Why was the effect on anchovy spawning so moderate in

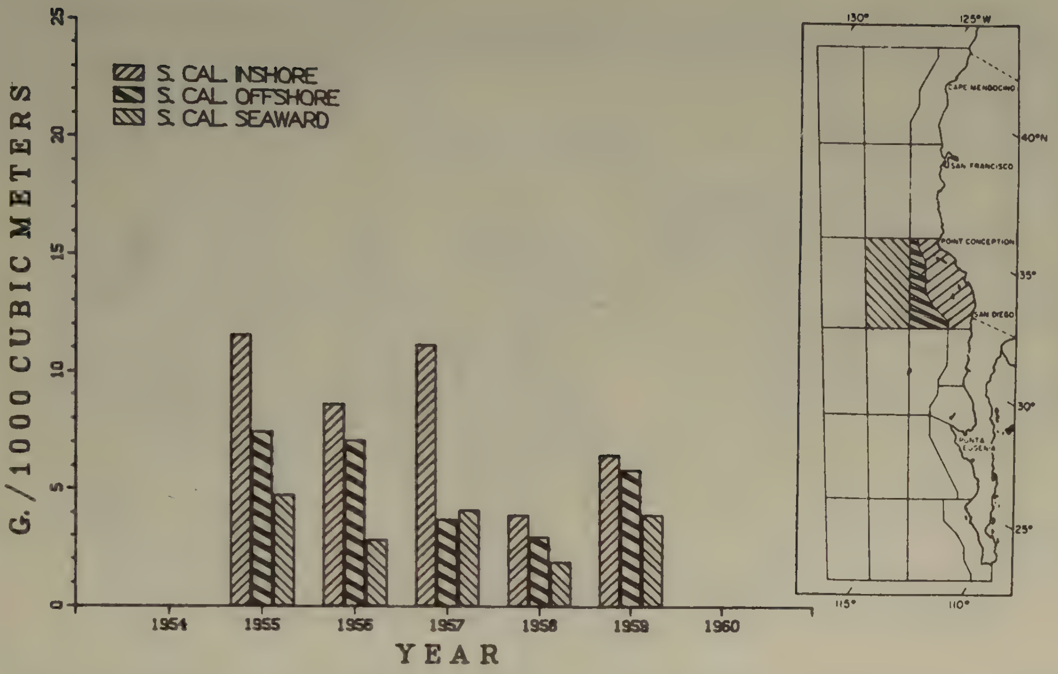

Figure 10. The decrease of euphausiid displacement volume between 1955 and 1959. The first bar is the volume calculated from the average of all stations in the southern California inshore region for the entire year. The second bar is the same value for the southern California offshore region. The third bar is the same value for the southern California seaward region.

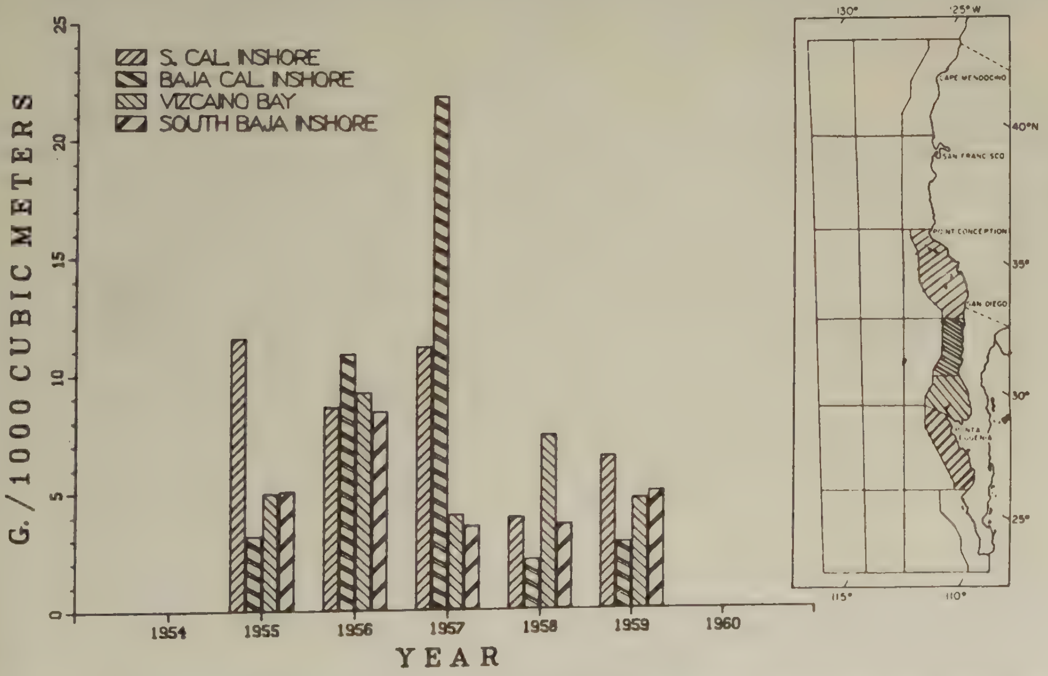

Figure 11. The decrease of euphausiid displacement volume between 1955 and 1959. The first bar is the volume calculated from the average of all stations in the southern California inshore region for the entire year. The second bar is the same value for the Baja California inshore region. The third bar is the same value for the Sebastian Vizcaino Bay region. The fourth bar is the same value for the south Baja inshore region.

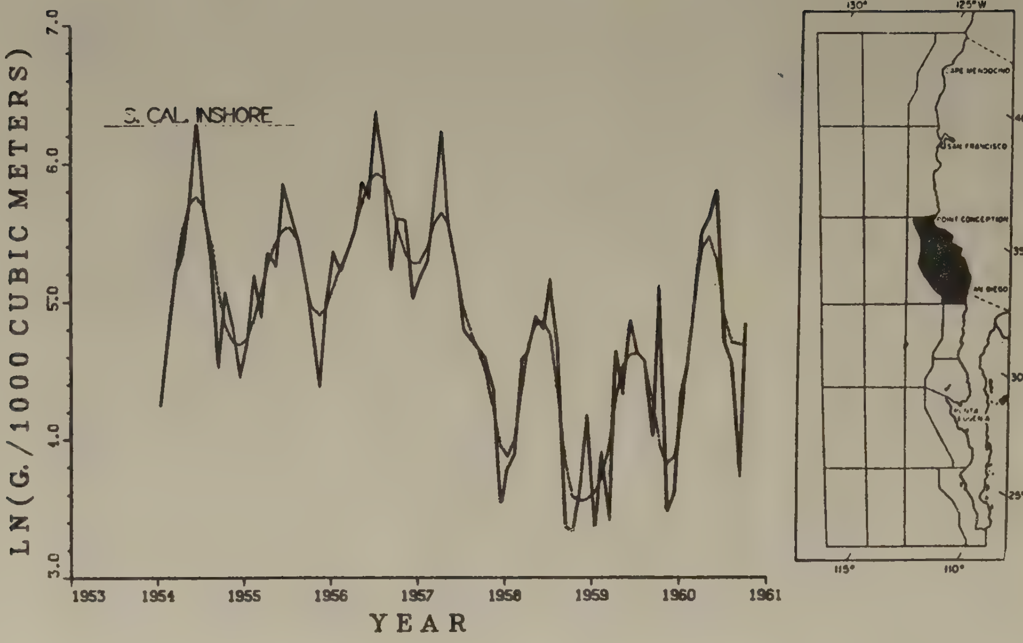

Figure 12. The time series of small zooplankton volume between 1954 and 1960 in the southern California inshore region. The jagged line is the natural log of the average of all stations on a monthly interval with missing values (about 10% mostly August or September) interpolated linearly. The smooth line is a resistant non-parametric smoother for these points. The similarity of seasonal slopes in anti-Niño (1954-60) and Niño (1958-59) years is an indication that the growth rate per unit initial zooplankton volume is similar for both conditions.

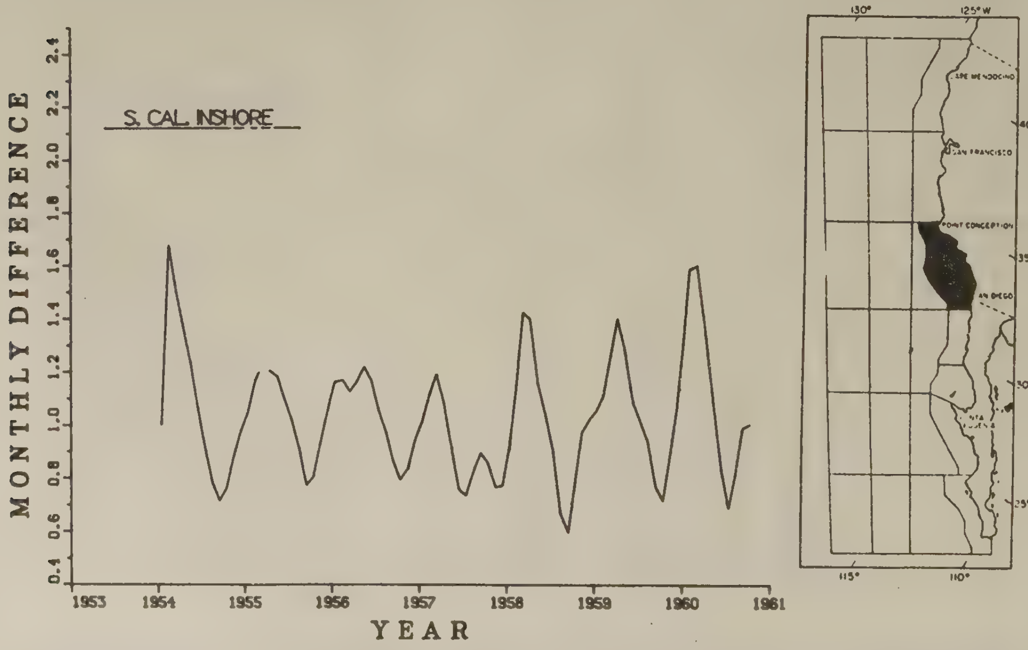

Figure 13. The time series of monthly differences of small zooplankton volume expressed as a ratio between the displacement volume of a given month and that of the previous month in the southern California inshore region from 1954 to 1960. Raw, interpolated and smoothed data in Figure 12.

Table 4. Comparison of estimated primary production and zooplankton standing stock during the 1955-9 transition from anti-Niño tc• Niño.

		Primary production g C/m^2/day	Zooplankton standing stock g/m^2	Change g/m^2/qtr
1955	March	0.5	11	-
	June	0.7	25	14
	September	0.3	13	-12
	December	0.3	13	0
1956	March	0.5	17	4
	June	0.7	42	25
	September	0.4	23	-19
	December	0.2	23	
1957	March	0.3	17	-6
	June	0.5		
	September	0.3	6	-8
	December	0.1	5	-1
1958	March	0.2	7	2
	June	0.6	11	4
	September	0.3	2	-9
	December	0.1	2	0
1959	March	0.2	5	3
	June	0.3	9	4
	September	0.2	7	-2

1983-4?" The energy required for anchovy spawning could have been "gleaned" from local island and coastal enriched areas which would be inadequately represented in wide-scale oceanic surveys. Anchovy, Pacific mackerel, and sardines may draw substantially on stored reserve energy from preceding seasons (Smith and Eppley, 1982) and may delay growth (Table 1b.) Another possibility is that diminished populations of salps, daliaids and pyrosomes (thaliaceans) allowed greater production of other herbivores, like crustaceans which are in the anchovy food chain.

Given these elements of resilience in the anchovy, Pacific mackerel, and sardine populations, one can speculate on why the spawn production of jack mackerel and saury was so low following the 1957 onset of El Niño. The jack mackerel spawning adults occupy the same habitat as the thaliaceans. This area is so broad and homogeneous that the twenty-fold decline in thaliaceans signaled a similar seven-fold decline in larval production by jack mackerel. This could have been mediated by the production of crustacea on which jack mackerel depend in part, or by the withdrawal of key mesopelagic fishes toward the north without equivalent replacement from the south. I would favor the mesopelagic fish explanation because the zooplankton predator, saury, did not change its spawn production rate markedly. Thus the mobility of the jack mackerel was not adequate to compensate for the scale of El Niño event in the main and outer branches of the California Current.

The responses of the hake, rockfish and flatfish to the onset of the El Niño appear similar. The hake feeds along the continental shelf of the British Columbia, Washington, Oregon and northern California coastlines. In the 1955-59 anti-and El Niño transition the main branch of the California Current impinged on these continental borderlands and the rockfish and flatfish are permanent members of that continental border. Thus the similarity of response was probably mediated by the interruption of the usual high rate of primary and secondary productivity usually ascribed to these coastal areas. Since these fishes and the jack mackerel all prey on the sardines and anchovies, one must assume that the predation withdrawn to the north roughly counterbalanced the added predation from the tropical and temperate tunas during the Niño.

References

Ahlstrom, E.H. 1969. Distributional atlas of fish larvae in the California Current Region; jack mackerel, _Trachurus symmetricus_, and Pacific hake, _Merluccius productus_, 1951 through 1966. CalCOFI Atlas No. 11.

Ahlstrom, E.H. 1972. Distributional atlas of fish larvae in the California Current Region, six common mesopelagic fishes - _Vinciguerria lucetia_, _Triphoturus mexicanus_, _Stenobrachius leucopsaurus_, _Leuroglossus stilbius_, _Bathylagus wesethi_, and _Bathylagus ochotensis_, 1955 through 1960. CalCOFI Atlas No. 17.

Ahlstrom, E.H. and H.G. Moser. 1975. Distributional atlas of fish larvae in the California Current region, flatfishes, 1955 through 1960. CalCOFI Atlas No. 23.

Ahlstrom, E.H., H.G. Moser, and E.M. Sandknop. 1978. Distributional atlas of fish larvae in the California Current region, rockfishes, _Sebastes_ spp., 1950 through 1975. CalCOFI Atlas No. 26.

Anon. 1958. Report of activities: California Dept. of Fish and Game. CalCOFI Rept. VI;9-14.

Bailey, K.M., R.C. Francis, and P.R. Stevens. 1982. The life history and fishery of Pacific whiting, _Merluccius productus_. CalCOFI Rep., Vol. 23:81-98.

Bernal, P.A. 1981. A review of the low-frequency response of the pelagic ecosystem in the California Current. CalCOFI Rept. 22:49-62.

Blackburn, M. 1965. Oceanography and the ecology of tunas. Oceanogr. Mar. Biol. Ann. Rev. 3:299-322.

Boyd, C.M. 1967. The benthic and pelagic habitats of the red crab, *Pleuroncodes planipes*. Pacific Science 21:394-403.

Colebrook, J.M. 1977. Annual fluctuations in biomass of taxonomic groups of zooplankton in the California Current, 1955-1959. U.S. Fishery Bull., 75:357-368.

Fiedler, P.C. 1984. Satellite observations of the 1982-83 El Niño along the U.S. Pacific Coast. Science 224:1251-1254.

Fiedler, P.C., R.M. Laurs, and D.R. Montgomery. MS. Albacore catch distribution relative to environmental features observed from satellite.

Fleminger, A., J.D. Isaacs, and J.G. Wyllie. 1974. Zooplankton biomass measurements from CalCOFI Cruises of July 1955 to 1959 and remarks on comparison with results from October, January, and April cruises of 1955 to 1959. CalCOFI Atlas No. 21, 118 p.

Hewitt, R.P. 1984. 1984 Spawning biomass of northern anchovy. SWFC Admin. Rept. LJ-84-18, La Jolla, CA 92038, 26 p.

Hunter, J.R., and R. Leong. 1981. The spawning energetics of female northern anchovy, *Engraulis mordax*. Fish. Bull. U.S., 79:215-230.

Isaacs, J.D., A. Fleminger, and J.K. Miller. 1971. Distributional atlas of zooplankton biomass in the California Current Region, winter 1955-1959. CalCOFI Atlas No. 14, 122 p.

Konchina, Y.V. 1983. The feeding niche of the hake, *Merluccius gayi* (Merlucciidae), and the jack mackerel, *Trachurus symmetricus* (Carangidae), in the trophic system of the Peruvian coastal upwelling. Translation copyright Scripta Publishing Co. 87-98 pp.

Laurs, R.M. 1983. The north Pacific albacore--an important visitor to California Current waters. CalCOFI Rep. XXIV, 99-106 pp.

Loeb, V.J., P.E. Smith, and H.G. Moser. 1983. Recurrent groups of larval fish species in the California Current area. CalCOFI Rep. 24:152-164.

Longhurst, A.R. 1967. The pelagic phase of *Pleuroncodes planipes* Stimpson (Crustacean, Galatheidae) in the California Current. CalCOFI Rep. 11, 142-154.

MacCall, A.D., and G.D. Stauffer. 1983. Biology and fishery potential of jack mackerel (*Trachurus symmetricus*). CalCOFI Rep. Vol. XXIV, 46-56.

McGowan, J.A. 1983. El Niño and biological production in the California Current. Trop. Ocean-Atmos. Newsletter #21 p. 23.

________________. 1984. The California El Niño, 1983. Oceanus 27(2):48-51.

Methot, R.D. Jr., 1981. Spatial covariation of daily growth rates of larval northern anchovy, *Engraulis mordax*, and northern lampfish, *Stenobrachius leucopsarus*. Rapp. P.-v. Reun. Cons. int. Explor. Mer, 178:424-431.

Murphy, G.I. 1960. Oceanography and variations in the Pacific sardine population. CalCOFI Rep. 8:55-64.

Mysak, L.A., W.W. Hsieh, T.R. Parsons. 1982. On the relationship between interannual baroclinic waves and fish populations in the northeast Pacific. Biological Oceanography 2(1):63-103.

Picquelle, S.J. and R.P. Hewitt. 1984. The 1983 spawning biomass of the northern anchovy. CalCOFI Rep. 25:16-27.

Schaeffer, M.B. 1960. Tuna oceanography programs in the tropical central and eastern Pacific. CalCOFI Rep. 8:41-44.

Sette, O.E., and J.D. Isaacs (eds.). 1960. Symposium on the changing Pacific Ocean in 1957-1958. CalCOFI Rep. VII:14-217.

Smith, P.E. 1971. Distributional atlas of zooplankton volume in the California Current region, 1951 through 1966. CalCOFI Atlas No. 13.

Smith, P.E. and E.H. Ahlstrom. 1973. Saury as a latent resource of the California Current., CalCOFI Rep. XIV:88-130.

Smith, P.E. and R.W. Eppley. 1982. Primary production and the anchovy population in the Southern California Bight; comparison of time series. Limnol. Oceanog. 27(1):1-17.

Velleman, P. 1980. Definition and comparison of robust nonlinear data smoothers. J. Am. Stat. Assn. 75:609-615.

8586

ANCHOVY EGG DISPERSAL AND MORTALITY AS INFERRED FROM CLOSE-INTERVAL OBSERVATIONS

PAUL E. SMITH AND ROGER P. HEWITT
National Marine Fisheries Service
Southwest Fisheries Center
P.O. Box 271
La Jolla, California 92038

> *Kiil*. Millions of tons of water come down that river. How do you know the day you made your tests there wasn't something unusual about the water?
>
> *Stockman*. No, I took too many samples.
>
> *Kiil*.How do you know? Why couldn't those little animals have clotted up only in the patch of water you souped out of the river? How do you know the rest of it wasn't pure?
>
> *Stockman*. It's not probable . . . .
>
> *An Enemy of the People*[1]

ABSTRACT

The oceanic boundary currents and continental borderlands that anchovy inhabit comprise diverse spatial and temporal scales of motion. Repetitive sampling at close intervals has been conducted to explore the sources and intensity of variance of observations and maximize the effectiveness of a management-oriented sampling program. The critical scale of repetitive sampling occurs when adjacent observations are so interdependent that they do not improve the precision of the abundance estimates. Sampling studies indicate that the scale of anchovy egg interdependence is on the order of several hundred meters for some days and somewhat less than this in the first few hours after spawning. Spatial correlation appears to diminish rapidly at scales larger than 2,000 m. The minimum distance between stations in the California egg production cruises is 7,500 m; in the Peru egg production survey it was 5,500 m.

In general, large structures in the ocean persist longer than small ones. One simple parameterization of this phenomenon is that a 600-m structure persists for 6 hours in the ocean and that structures of 2,800, 27,000, 147,000 m persist for a day, a week, and a month, respectively. From simple considerations, if the average value of food abundance is too low for larval fish to survive, the useful scale of oceanic feature that contains sufficient food is about 27 km if the food is required for a week, or 147 km if the food is required for a month. The critical scale of these features becomes smaller if production within the structure exceeds consumption and washout. The influence of persistence on survival may diminish as juveniles gain the ability to graze in schools and swim through larger intervening distances between favorable patches. We believe that experimental repetitive sampling supports the general scale for the passive dispersion of eggs: no obvious interrelations between interannual changes in these features and egg and larval survival were noted for the first 20 days of life. The consequences of a laterally incoherent and dissipated habitat may be delayed to the late larval and juvenile stages.

Will we be able to observe the later life stages with the same intensity and accuracy that we have observed the embryonic stages?

RESUMEN

Las corrientes oceánicas de margen y los aledaños continentales que habita la anchoveta sufren movimientos de diferentes escalas temporales y espaciales. Se condujeron muestreos replicados a intervalos reducidos con el fin de explorar las fuentes e intensidad de la varianza de las observaciones y maximizar la eficacia de un programa de muestreo orientado hacia el manejo del recurso. La escala crítica del muestreo repetitivo ocurre cuando las observaciones adyacentes son tan interdependientes que no aumentan la precisión de las estimaciones de abundancia. Muestreos experimentales indican que la escala de interdependencia para los huevos de la anchoveta es del orden de varios centenares de metros durante algunos días, y algo menor en las primeras horas después del desove. La correlación espacial parece disminuir rápidamente a escalas mayores de 2000 m. La distancia mínima entre estaciones en las campañas californianas de producción de huevos es de 7500 m; en los estudios peruanos de producción de huevos era de 5500 m. En general, las estructuras oceánicas mayores son más persistentes que las pequeñas. Una expresión cuantitativa sencilla de este fenómeno consiste en que estructuras de 600 m persisten en el océano durante 6 horas, mientras que aquéllas de 2,800, 27,000 y 147,000 m persisten durante un día, una semana, y un mes, respectivamente. Partiendo de consideraciones simples se deduce que si la abundancia promedio de alimento es demasiado baja para la supervivencia de las larvas

---

[1] Henrik Ibsen. *An Enemy of the People*. An adaptation for the American stage by Arthur Miller. Dramatists Play Service, Inc., New York, 1951.

de peces, la escala útil de la estructura oceánica que contiene alimento suficiente es de, aproximadamente, 27 km, si el alimento es requerido para una semana, o 147 km si lo es para un mes. La escala crítica de estas características disminuye si la producción dentro de la estructura excede al consumo y la exportación. La influencia de esta persistencia en la supervivencia puede disminuir a medida que los juveniles van adquiriendo la capacidad de alimentarse en cardúmenes y de nadar distancias mayores entre lugares favorables. Creemos que el muestreo repetitivo experimental concuerda con la escala general de dispersión pasiva de los huevos: no se observaron interrelaciones obvias entre cambios interanuales en estas características y la supervivencia de huevos y larvas durante los primeros 20 días de vida. Las consecuencias de un hábitat lateralmente incoherente y disipado pueden ser pospuestas hasta los estados larvales avanzados y los juveniles.

¿Podremos observar los estados de desarrollo tardíos con al misma intensidad y precisión con que observamos los estados embrionarios?

INTRODUCTION

Demands on oceanic sampling have rapidly increased from the simple detection and description of resources (Ahlstrom 1968; Hempel 1973; Smith and Richardson 1977) to the testing of hypotheses on the causes of recruitment failure in dynamic coastal areas like the California Current (Lasker 1975; Vlymen 1977; Parrish and MacCall 1978; Lasker and Zweifel 1978; Parrish et al. 1981; Smith 1981; Hewitt 1981; Bakun and Parrish 1982). Smith (1981) described sampling strategies for testing several hypothesized sources of year-class failure; the sources include larval transport, critical period, predation including cannibalism, starvation, unfavorable distribution pattern, and parental deficiencies at the time of spawning. Success in the studies underway have encouraged international organizations (Bakun et al. 1982) to compare dynamic areas like the eastern boundaries of the oceans off South America and Africa with respect to the causes of massive fluctuations in fish reproductive success. These studies require additional work on efficient delineation of distribution and biomass estimation. Because of the nature of the survival mechanisms postulated, directed work on spatial pattern, turbulent diffusion, transport, and survival is also needed.

The spatial pattern of plankton may be considered from the aspects of interpreting existing samples and the strategy of future sampling (Silliman 1946; Sette and Ahlstrom 1948; Taft 1960; Zweifel and Smith 1981). Another aspect of spatial pattern of plankton is the interaction between predator and prey, in particular where food aggregations are necessary for sufficient feeding rates (Lasker 1975; Vlymen 1977; Lasker and Zweifel 1978; Hewitt 1981). Lastly, schooling coastal pelagic fishes proceed through a planktonic phase of weeks to months, and the eventual retention of viable concentrations of juveniles near the coast may be controlled by rates of turbulent diffusion and cross-shelf transport during the spawning season (Smith 1973; Smith and Lasker 1978; Parrish and MacCall 1978; Hewitt 1982; Bakun and Parrish 1982; Smith 1985).

The scale of spatial pattern contains additional information about the recent history and near future of the pelagic aggregation. For example, if individual (0.3 m) spawning pelagic fish like sardines are found in populations (1,000 km), school groups (10 km), schools (100 m), and spawning "cliques" (30 m), one can infer from the rate of dispersal by turbulent diffusion that the major sources of variance in samples are from individuals, cliques, and schools rather than from school groups and populations based on the length-scale assumptions (Smith 1973). Since this pattern of eggs imposed by the spawning and fertilization behavior of the adults persists several days into the larval stage, one may postulate that similar features like diatom patches or grazed gaps in diatom layers would persist equally long in the pelagic environment (Okubo 1971).

It is the purpose of this symposium to explore similarities among the eastern boundary areas of the world oceans, because these contain the potential of tens of millions of tons annual catch of schooling coastal pelagic engraulids, clupeids, scombrids, and carangids. These fisheries are generally not managed and are subject to large natural fluctuations, which seem to be augmented by present fishing practices (Murphy 1977; Smith 1981; Bakun and Parrish 1982; Lasker 1985; Smith 1985). Our objective in this paper is to present a small-scale empirical study of anchovy egg dispersal in a coastal site. The study may then be considered in the context of large-scale environmental features and biological surveys. We believe that existing techniques can be modified to measure offshore drift and dispersal within the coastal habitat and thus describe the habitat of schooling coastal pelagic fish in eastern boundary habitats.

METHODS

The methods used for close-interval sampling of the anchovy population off California are described in detail in Lasker (1984), Smith and Hewitt (1984), Smith, Flerx, and Hewitt (1984) and Moser and Ahlstrom (1984). We will only briefly describe the planning and conduct of the cruise, station activity, the

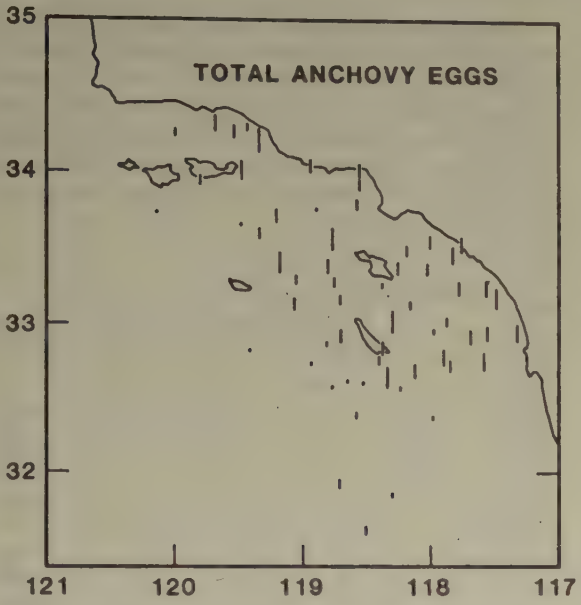

Figure 1. The survey area off southern California. Ordinate values are degrees north latitude, and the abscissa values are degrees west longitude. The lengths of the bars are proportional to the log of the number of anchovy eggs per 0.05 square meters as an average of eight replicates at each station. (See Table 5 for data.)

net, the procedures for sorting, staging and aging the eggs, and the data analysis.

Cruise

The cruise was planned to encompass the spawning habitat of the central population of the northern anchovy (*Engraulis mordax*) with groups of eight samples at stations 20 miles apart in the cross-shelf direction and 40 miles apart parallel to the general run of the coast. Unfortunately, the 25-m motor vessel (*Scorpius*) chartered for this cruise was not competent to occupy the preplanned stations in the weather of January 1979; therefore, stations in the general area of the spawning were occupied at haphazard positions that could be approached from safe harbors among the islands of the Southern California Bight. The stations that had at least one egg in eight tows are plotted in Figure 1 as "sticks" with height proportional to the log of the mean number of total anchovy eggs per observation.

On station we recorded position, cast a 10-m Nansen bottle with reversing thermometer to estimate the temperature, and made eight vertical plankton tows to a wire length of 70 m and back. The positions, date, and time of arrival at the station and the 10-m temperature are listed in Appendix Table 1. To maintain position on the station (relative to the water) as closely as possible, the officers of the vessel were instructed to keep the 45-kg weight on 10-m, 3/16″ cable vertical between casts and tows for the entire duration of the station. The usual interval between vertical tows was 12 minutes, but occasionally repeat tows and delays between tows lengthened that period. The distribution of intervals between adjacent tows is depicted in a histogram in Appendix Table 2; this average interval will be used to interpret all tows.

The Tow

Of the 12 minutes between the initiation of tows, 3-5 minutes were involved with lowering and raising the net, another 5 minutes was required to wash the net and concentrate the sample in the cod end, and 4-5 minutes was needed to preserve the sample in Formalin and label the sample bottle. The winch on the charter vessel was incapable of obtaining the 70-m-per-minute towing rate specified for the project, and rates were commonly in the range of 25 to 40 m per minute.

The plankton net was based on the original design of anchovy egg net (Smith et al. 1968) and modified for vertical towing (Hewitt 1983; Smith et al. 1984). As the original net in the vertical tow series, it differed from the present design by being a single net, with mesh aperture area of 0.333-mm nylon mesh. The mesh-aperture-to-mouth-aperture ratio was 8.7:1, of which 35% was in the terminal conical portion of the net and 65% was in the cylindrical portion to reduce length and facilitate self-cleaning under tow. Nets were washed from the outside by a moderate rate of flow.

Laboratory Work

Anchovy eggs were sorted from samples with a dissecting microscope at a magnification of about 10 × (Kramer et al 1972; Smith and Richardson 1977). The sorted eggs were subsequently staged using criteria of Moser and Ahlstrom (1984). Ages were estimated from the temperature-specific stage development rate (Ahlstrom 1943; Zweifel and Lasker 1976; Lo 1984), the actual time of tow, and the 10-m temperature on the station.

Data Analysis

Descriptive statistics were performed on the UCSD-VAX using Minitab. A correlation matrix on all ages of egg for all 60 tows was performed, yielding 7 correlation coefficients for adjacent columns, 6 for tows 24 minutes apart, 5 for tows 36 minutes apart, etc. Negative binomial parameter estimates were accomplished using the iterative techniques described in Southwood (1978). The BASIC program implemented on the UCSD-VAX to estimate the negative binomial parameters is listed in the Appendix.

TABLE 1
Replicate Observations of Anchovy Eggs
< One Day Old

	Replicate Number								
Row	1	2	3	4	5	6	7	8	Average
1	1	2	4	9	23	3	15	64	15.125
2	0	0	1	0	0	0	1	0	0.250
3	0	0	0	0	0	2	3	17	2.750
4	4	5	0	8	7	8	10	12	6.750
5	0	0	0	0	0	0	0	0	0.000
6	4	2	7	0	0	0	0	0	1.625
7	0	0	0	0	0	0	0	0	0.000
8	1	0	0	0	0	0	0	0	0.125
9	0	0	0	0	0	0	0	0	0.000
10	0	0	0	0	0	0	0	0	0.000
11	1	0	0	0	1	0	1	0	0.375
12	0	0	0	0	1	3	0	5	1.125
13	0	0	0	0	0	0	0	0	0.000
14	0	0	0	0	0	0	0	0	0.000
15	30	39	51	0	0	0	0	0	15.000
16	0	0	0	0	0	0	0	0	0.000
17	0	0	0	0	0	0	0	1	0.125
18	0	0	0	0	0	0	0	0	0.000
19	13	6	20	6	4	6	0	0	6.875
20	0	0	0	0	0	0	0	0	0.000
21	0	0	0	0	0	0	0	0	0.000
22	0	0	0	0	0	0	0	0	0.000

RESULTS

We will consider three aspects of the data. The first will be the data set itself. Secondly, we will describe the data and a possible probability-generating distribution from which it may have been drawn. Thirdly, we will consider one interpretation of the change of the data with time.

The Data Set

The data set consists of four ages of egg, and the distribution of total eggs. The four ages of egg are those eggs less than 8 hours old, 1 day old, 2 days old, and 3 days old. These sets are from the same 8 replicates of 60 observations containing at least one anchovy egg per station.

Eggs produced in the first 8 hours after the onset of spawning are considered separately in the analysis of egg production because incidence and abundance are underestimated. (Smith and Hewitt 1984) In Table 1, it may be seen that of the 60 samples considered, only 22 were in the initial 8-hour period. In no case does a large sample observation continue across the entire set of eight observations on the station. For example, in row 1, replicates 5, 7, and 8 indicate that the ship drifted into a patch, whereas rows 15 and 19 indicate that the ship drifted out of a patch.

The chief difference for one-day-old eggs (Table 2) is that in most observations, the set of replicates is usually taken entirely within or outside of a patch. There are still instances, such as row 49, that indicate drifting out, but most show moderate changes within replicates on station. There are no visible differences in Tables 3 or 4 from Table 2 in terms of continuity of observations on station.

TABLE 2
Replicate Observations of Anchovy Eggs
One Day Old

	Replicate Number								
Row	1	2	3	4	5	6	7	8	Average
1	3	3	3	6	2	2	1	3	2.875
2	2	1	3	4	3	3	0	5	2.625
3	8	5	7	7	6	10	5	13	7.625
4	0	0	0	0	0	0	0	0	0.000
5	0	0	0	0	0	0	0	0	0.000
6	0	1	2	0	4	2	1	2	1.500
7	12	10	10	6	5	3	4	6	7.000
8	5	1	6	6	4	2	10	5	4.875
9	0	0	0	2	0	0	0	1	0.375
10	0	0	0	0	0	0	0	0	0.000
11	9	3	2	2	0	0	3	0	2.375
12	12	23	12	4	7	5	7	5	9.375
13	0	1	0	2	3	3	1	1	1.375
14	0	1	0	0	1	2	0	0	0.500
15	2	5	2	3	0	1	2	0	1.875
16	6	8	3	6	2	6	4	5	5.000
17	3	3	1	2	3	2	0	4	2.250
18	2	0	1	0	1	2	2	2	1.250
19	18	26	21	33	21	32	22	23	24.500
20	0	0	0	0	0	0	0	0	0.000
21	1	3	3	3	2	0	1	0	1.625
22	2	2	9	5	4	4	9	8	5.375
23	0	1	1	1	0	1	3	1	1.000
24	0	0	0	0	0	0	0	0	0.000
25	0	0	0	0	0	0	0	0	0.000
26	0	0	0	0	0	0	0	0	0.000
27	1	0	0	1	0	4	5	1	1.500
28	2	1	0	0	0	0	1	1	0.625
29	4	2	5	0	3	3	0	4	2.625
30	15	5	13	16	10	13	12	6	11.250
31	14	12	11	11	9	7	8	5	9.625
32	0	0	2	1	0	0	0	0	0.375
33	0	0	0	0	0	0	0	0	0.000
34	0	0	0	1	0	0	1	0	0.250
35	2	0	0	1	0	1	0	0	0.500
36	1	2	0	3	0	0	0	0	0.750
37	0	0	0	0	0	0	1	0	0.125
38	17	11	22	26	37	27	20	30	23.750
39	5	8	12	4	6	4	3	3	5.625
40	3	2	3	2	0	3	3	1	2.125
41	0	1	0	2	2	0	0	1	0.750

(continued)

TABLE 2 (continued)

Row	Replicate Number 1	2	3	4	5	6	7	8	Average
42	0	0	0	0	0	0	0	0	0.000
43	0	1	0	0	0	0	0	1	0.250
44	1	4	0	3	5	3	4	3	2.875
45	7	4	4	1	3	2	2	3	3.250
46	0	0	0	0	0	0	0	1	0.125
47	1	1	2	1	1	3	1	5	1.875
48	0	0	0	0	0	0	0	0	0.000
49	3	22	3	0	0	0	0	0	3.500
50	0	0	0	0	0	0	0	0	0.000
51	0	0	1	0	0	0	0	0	0.125
52	0	0	0	0	0	0	0	0	0.000
53	0	0	0	0	0	0	0	0	0.000
54	5	4	3	0	3	2	2	3	2.750
55	0	0	1	0	2	0	0	0	0.375
56	1	2	3	2	4	3	3	4	2.750
57	64	65	64	63	48	82	54	48	61.000
58	1	0	0	2	1	1	5	3	1.625
59	11	20	5	20	20	12	22	18	16.000
60	5	10	8	5	5	7	4	7	6.375

TABLE 3
Replicate Observations of Anchovy Eggs
Two Days Old

Row	Replicate Number 1	2	3	4	5	6	7	8	Average
1	0	1	0	1	0	2	1	1	0.750
2	0	2	0	1	1	1	1	1	0.875
3	0	1	2	0	1	1	0	1	0.750
4	2	0	2	1	1	0	2	1	1.125
5	0	2	1	1	3	0	1	3	1.375
6	3	5	5	6	8	15	14	12	8.500
7	2	2	0	4	2	2	1	0	1.625
8	6	12	11	8	12	9	10	9	9.625
9	0	0	0	0	0	0	0	0	0.000
10	0	0	0	0	0	0	0	0	0.000
11	0	0	0	0	0	1	0	0	0.125
12	0	0	0	0	0	0	0	0	0.000
13	1	1	3	0	0	0	3	2	1.250
14	2	3	5	0	6	7	4	10	4.625
15	1	2	2	0	4	2	1	2	1.750
16	5	2	6	2	2	1	3	2	2.875
17	0	0	0	2	4	4	4	4	2.250
18	1	1	2	0	1	1	1	2	1.125
19	6	14	11	12	12	9	5	9	9.750
20	1	2	2	1	0	3	1	1	1.375
21	7	5	7	2	2	5	1	5	4.250
22	26	32	46	30	17	9	14	13	23.375
23	1	2	2	2	0	0	2	0	1.125
24	0	0	0	0	0	0	0	1	0.125
25	0	0	0	1	0	0	0	0	0.125
26	0	0	0	0	1	0	0	0	0.125
27	1	0	6	4	2	2	10	3	3.500
28	3	2	6	4	1	0	3	6	3.125
29	34	35	40	30	36	39	35	35	35.500
30	7	3	1	2	3	4	1	7	3.500
31	22	10	13	11	15	21	9	12	14.125
32	3	3	2	3	3	3	3	0	2.500
33	0	0	0	0	0	0	0	0	0.000
34	4	1	1	3	1	0	0	0	1.250
35	0	0	0	0	0	0	0	0	0.000
36	0	1	0	0	0	0	0	0	0.125
37	2	0	1	0	0	0	0	0	0.375
38	5	4	3	15	21	15	9	13	10.625
39	0	0	0	0	0	0	0	0	0.000
40	3	3	1	0	2	0	2	3	1.750
41	0	0	0	0	0	0	0	0	0.000
42	1	0	0	0	0	0	0	0	0.125
43	1	1	0	1	0	0	1	2	0.750
44	4	4	9	5	2	8	2	11	5.625
45	0	0	0	0	0	3	2	2	0.875
46	0	0	0	0	0	0	1	1	0.250
47	39	21	39	21	18	48	16	22	28.000
48	0	0	0	0	0	1	0	0	0.125
49	0	2	1	0	2	0	2	0	0.875
50	6	4	4	10	7	4	8	5	6.000
51	2	4	6	4	1	2	4	2	3.125
52	0	0	0	0	0	0	0	0	0.000
53	0	0	0	0	0	0	0	0	0.000
54	27	22	21	0	8	11	4	4	12.125
55	0	0	0	0	0	0	0	0	0.000
56	22	14	6	9	6	4	6	1	8.500
57	96	117	94	89	84	119	111	91	100.125
58	12	3	9	6	3	4	5	9	6.375
59	8	6	2	4	4	2	9	5	5.000
60	1	5	6	4	4	5	12	10	5.875

Table 5 contains the values for all ages of anchovy egg within each station set. At these temperatures, one may expect three ages of egg within close proximity. In this set, only rows 33, 52, and 53 had none of the three ages identified: row 10 had neither one- nor two-day-old eggs, row 35 had neither two- nor three-day-old eggs, and rows 24, 26, 42, and 50 had neither one- nor three-day-old eggs.

In summary, there is coherence among the replicate stations of anchovy eggs older than eight hours. This indicates that the scale of the pattern is large relative to the drift of the research vessel and the layers of water below over periods of one to two hours.

TABLE 4
Replicate Observations of Anchovy Eggs Three Days Old

	Replicate Number								
Row	1	2	3	4	5	6	7	8	Average
1	0	0	0	0	0	0	0	0	0.000
2	0	0	0	0	0	0	0	0	0.000
3	3	4	4	2	1	3	0	2	2.375
4	1	0	4	3	3	1	0	2	1.750
5	3	4	5	4	4	4	1	11	4.500
6	3	0	2	1	2	2	2	2	1.750
7	2	6	9	4	3	3	3	2	4.000
8	1	1	5	2	3	5	5	5	3.375
9	0	0	0	0	0	0	0	0	0.000
10	0	0	0	0	0	0	0	1	0.125
11	5	4	0	3	1	1	4	9	3.375
12	9	11	8	5	8	1	5	5	6.500
13	1	2	2	1	1	3	3	2	1.875
14	2	4	5	3	2	7	2	4	3.625
15	1	0	1	0	0	0	0	1	0.375
16	8	5	3	5	10	6	8	3	6.000
17	9	3	3	0	1	0	1	1	2.250
18	1	0	3	0	1	0	3	0	1.000
19	17	16	15	20	10	10	11	5	13.000
20	4	5	8	4	3	7	5	2	4.750
21	13	7	6	4	9	7	7	3	7.000
22	24	16	16	10	8	9	4	6	11.625
23	1	3	1	2	0	4	1	2	1.750
24	0	0	0	0	0	0	0	0	0.000
25	0	3	0	0	0	0	0	0	0.375
26	0	0	0	0	0	0	0	0	0.000
27	5	0	9	6	6	5	11	10	6.500
28	1	1	0	1	1	0	1	0	0.625
29	21	17	15	23	14	11	14	17	16.500
30	20	6	18	22	9	11	3	9	12.250
31	6	4	5	4	5	2	7	1	4.250
32	1	0	0	1	0	1	1	0	0.500
33	0	0	0	0	0	0	0	0	0.000
34	0	0	1	0	0	1	0	0	0.250
35	0	0	0	0	0	0	0	0	0.000
36	0	0	0	0	0	0	0	0	0.000
37	0	1	1	1	1	0	0	0	0.500
38	3	4	5	4	3	2	4	5	3.750
39	0	0	0	0	0	0	0	0	0.000
40	0	0	0	1	0	0	1	1	0.375
41	0	0	0	0	0	0	0	0	0.000
42	0	0	0	0	0	0	0	0	0.000
43	4	8	4	7	8	5	3	11	6.250
44	2	5	5	2	5	5	6	12	5.250
45	0	1	0	0	1	0	2	2	0.750
46	0	0	0	0	2	1	2	0	0.625
47	25	29	32	43	41	53	52	45	40.000
48	1	2	4	1	0	1	1	0	1.250
49	1	1	0	0	0	0	0	0	0.250
50	0	0	0	0	0	0	0	0	0.000

(continued)

TABLE 4 (continued)

	Replicate Number								
Row	1	2	3	4	5	6	7	8	Average
51	61	69	75	84	76	62	61	68	69.500
52	0	0	0	0	0	0	0	0	0.000
53	0	0	0	0	0	0	0	0	0.000
54	10	10	12	0	5	8	2	5	6.500
55	120	86	119	107	136	114	104	102	111.000
56	0	0	0	0	0	0	0	0	0.000
57	22	26	16	34	16	28	42	26	26.250
58	1	2	2	6	1	5	3	3	2.875
59	3	8	5	2	6	3	3	3	4.125
60	7	12	12	14	9	12	15	17	12.250

TABLE 5
Replicate Observations of Anchovy Eggs All Ages Plus Disintegrated

	Replicate Number								
Row	1	2	3	4	5	6	7	8	Average
1	4	6	7	16	25	7	17	68	18.750
2	2	3	3	5	4	4	1	6	3.500
3	14	11	13	10	8	14	5	16	11.375
4	4	0	8	5	4	1	4	3	3.625
5	3	6	6	6	7	4	2	14	6.000
6	6	6	9	7	14	19	17	16	11.750
7	16	18	19	14	10	10	11	25	15.375
8	17	19	22	24	26	24	35	31	24.750
9	0	0	0	2	0	0	0	1	0.375
10	0	0	0	0	0	1	0	2	0.375
11	15	7	2	5	1	2	7	10	6.125
12	21	34	21	9	16	5	12	10	16.000
13	2	4	7	4	4	11	8	8	6.000
14	4	8	10	3	9	16	6	14	8.750
15	4	7	5	4	4	3	3	3	4.125
16	19	15	12	13	14	13	15	10	13.875
17	19	9	13	7	15	7	5	11	10.750
18	9	9	18	12	8	13	10	7	10.750
19	56	74	63	74	53	64	48	44	59.500
20	6	7	12	6	3	11	7	3	6.875
21	22	15	16	9	13	12	9	8	13.000
22	57	58	76	50	32	27	30	30	45.000
23	2	6	7	5	0	10	7	4	5.125
24	0	0	0	0	0	0	0	1	0.125
25	1	3	0	2	0	0	0	0	0.750
26	0	0	0	0	1	0	0	0	0.125
27	8	14	15	11	9	11	27	14	13.625
28	9	6	6	5	3	0	6	7	5.250
29	59	54	60	54	53	54	50	58	55.250
30	42	15	32	37	22	28	20	22	27.250
31	42	26	29	26	30	33	24	23	29.125
32	4	3	5	6	4	4	4	5	4.375
33	3	0	0	2	1	0	1	0	0.875

(continued)

TABLE 5 (continued)

	Replicate Number								
Row	1	2	3	4	5	6	7	8	Average
34	4	1	2	4	1	1	1	0	1.750
35	2	0	0	1	0	1	0	0	0.500
36	1	3	0	3	1	4	3	2	2.125
37	2	1	2	1	1	0	1	0	1.000
38	56	58	81	48	64	49	34	50	55.000
39	5	8	12	4	6	4	3	3	5.625
40	6	5	4	3	2	3	6	6	4.375
41	0	1	0	2	2	0	0	1	0.750
42	1	0	0	0	0	0	0	0	0.125
43	5	10	4	8	8	5	4	14	7.250
44	7	13	14	10	12	16	12	26	13.750
45	20	11	24	7	8	11	6	7	11.750
46	0	1	2	1	2	3	4	2	1.875
47	66	52	73	65	60	104	72	73	70.625
48	1	2	4	1	0	2	2	0	1.500
49	4	25	4	4	8	4	4	1	6.750
50	6	4	4	10	7	4	8	5	6.000
51	63	73	82	88	77	64	65	70	72.750
52	1	0	0	0	0	0	0	0	0.125
53	0	0	1	0	0	0	0	1	0.250
54	47	39	43	1	18	23	9	13	24.125
55	120	87	122	109	138	116	104	102	112.250
56	23	16	9	11	10	8	10	6	11.625
57	182	208	174	187	148	229	208	165	187.625
58	15	6	11	16	8	10	13	16	11.875
59	29	39	13	27	31	20	37	29	28.125
60	13	27	27	23	19	24	32	34	24.875

Data Summary

Owing to the wide range of numbers of eggs per sample, Tables 6, 7, and 8 are divided into classes whose boundaries encompass factors of four rather than unit frequencies. The general appearance of similarity among the replicate sets above is confirmed in the data summary table and the parameters calculated from them. The primary difference among the distributions of the eight replicates and the distribution of the mean of eight is the lower threshold (0.125 rather than 1 per .05 m^2) for the mean of eight samples on a station. Whereas one would expect the mean of the means to be the same as the mean of the replicates, one would expect the variance of the observations to be eight times the variance of the means of eight; instead, the variance of the means of eight is indistinguishable from the variances of the individual sets for one-, two- and three-day-old eggs.

The estimates of the negative binomial factor *k* are the same from replicate to replicate and between the means of eight and the eight replicates (Tables 6, 7, and 8). Thus the estimation of the negative binomial parameters, mean, and *k* from small sets of observations with high variance is relatively robust when small sample sizes are used. Furthermore, the negative binomial *k* is well estimated from the fraction of zero observations, and even the "moments" estimate (from the mean and variance) is reasonably close to the others and relatively stable under these conditions.

The distribution of the total eggs (Table 9) differs

TABLE 6
Anchovy Egg Sample Frequency Distribution
One-Day-Old Eggs

	Replicate Number								
Eggs/0.05 m2	1	2	3	4	5	6	7	8	Mean
0	26	24	27	25	29	27	27	25	13
0.0625 – 0.25	—	—	—	—	—	—	—	—	3
0.25 – 1	—	—	—	—	—	—	—	—	10
1 – 4	17	19	18	19	15	20	17	17	20
4 – 16	14	12	12	11	12	10	12	14	10
16 – 64	2	4	2	5	4	2	4	4	4
64 – 256	1	1	1	—	—	1	—	—	—
Mean	4.1	4.6	4.1	4.3	3.9	4.3	3.8	3.9	4.1
Variance	83.5	99.0	85.9	97.8	70.7	136.9	69.1	64.2	81.4
Neg. binomial									
k(0)	.321	.274	.277	.260	.283	.269	.327	.285	.312
k(1)	.158	.195	.163	.157	.118	.145	.155	.170	.202
k(2)	.264	.256	.254	.217	.234	.237	.252	.244	.296

k(0) is the parameter of the negative binomial distribution as estimated from the proportion of '0' values.
k(1) is the parameter of the negative binomial distribution as estimated from the sample mean and variance ('moments' estimate).
k(2) is the maximum likelihood estimator (Southwood 1966).

TABLE 7
Anchovy Egg Sample Frequency Distribution
Two-Day-Old Eggs

	Replicate Number								
Eggs/0.05 m2	1	2	3	4	5	6	7	8	Mean
0	24	22	24	27	24	26	20	22	10
0.0625 – 0.25	—	—	—	—	—	—	—	—	7
0.25 – 1	—	—	—	—	—	—	—	—	8
1 – 4	18	21	16	14	19	15	21	18	17
4 – 16	11	12	15	15	12	15	16	17	14
16 – 64	6	4	4	3	4	3	2	2	3
64 – 256	1	1	1	1	1	1	1	1	1
Mean	6.1	5.9	6.3	5.0	5.0	6.1	5.4	5.4	5.7
Variance	213.2	265.7	222.0	163.8	148.8	292.4	225.0	163.8	198.8
Neg. binomial									
k(0)	.299	.347	.295	.268	.329	.262	.417	.363	.318
k(1)	.180	.134	.184	.157	.174	.130	.133	.184	.157
k(2)	.248	.276	.255	.241	.301	.227	.327	.316	.280

k(0) is the parameter of the negative binomial distribution as estimated from the proportion of '0' values.
k(1) is the parameter of the negative binomial distribution as estimated from the sample mean and variance ('moments' estimate).
k(2) is the maximum likelihood estimator (Southwood 1966).

from that of any of the individual nights' spawning. In the individual age groups the frequency of observations decreases from the "0" class to the "64-256" eggs per observation class. In the total eggs observations, the frequency increases from the "0" class to the "4-16" class and then descends. Even when each station has at least one egg in eight samples, the number of observations with "0" eggs in each of the replicates varied from 10% to 18%.

We concluded that nearly uniform results would have been obtained from any set of replicates. Also, the frequency distribution of the total is a composite of the day-class observations and may in fact exhibit a different type of distribution when three days' egg

TABLE 8
Anchovy Egg Sample Frequency Distribution
Three-Day-Old Eggs

	Replicate Number								
Eggs/0.05 m2	1	2	3	4	5	6	7	8	Mean
0	22	25	24	25	24	25	23	24	15
0.0625 – 0.25	—	—	—	—	—	—	—	—	1
0.25 – 1	—	—	—	—	—	—	—	—	10
1 – 4	19	11	10	15	17	14	19	17	13
4 – 16	11	17	20	13	15	17	14	13	16
16 – 64	7	5	4	5	2	3	3	4	3
64 – 256	1	2	2	2	2	1	1	2	2
Mean	7.0	6.4	7.3	7.3	6.9	6.7	6.7	6.8	6.9
Variance	316.8	216.1	334.9	346.0	412.1	316.8	295.8	278.9	302.8
Neg. binomial									
k(0)	.321	.274	.277	.260	.283	.269	.327	.285	.283
k(1)	.158	.195	.163	.157	.118	.145	.155	.170	.157
k(2)	.264	.256	.254	.217	.234	.237	.252	.244	.257

k(0) is the parameter of the negative binomial distribution as estimated from the proportion of '0' values.
k(1) is the parameter of the negative binomial distribution as estimated from the sample mean and variance ('moments' estimate).
k(2) is the maximum likelihood estimator (Southwood 1966).

TABLE 9
Anchovy Egg Sample Frequency Distribution
All Ages Plus Disintegrated

Eggs/0.05 m2	Replicate Number								Mean
	1	2	3	4	5	6	7	8	
0	7	10	11	6	10	11	10	9	—
0.0625 – 0.25	—	—	—	—	—	—	—	—	4
0.25 – 1	—	—	—	—	—	—	—	—	7
1 – 4	12	9	6	12	11	9	9	12	7
4 – 16	21	24	25	27	23	23	25	20	26
16 – 64	17	13	12	10	12	12	12	14	12
64 – 256	3	4	6	5	4	5	4	5	4
Mean	19.1	18.9	20.1	17.8	17.1	18.5	17.1	18.3	18.4
Variance	979.7	1049.8	1049.8	1004.9	852.6	1303.2	1024.0	829.4	961.0

production is present. This may be expected to differ for eggs that hatch in a day or persist for weeks.

Interpretation of Time Series

The correlation between recent observations of newly spawned eggs ends at intervals greater than 24 minutes, whereas one-day-old eggs have a persistent correlation over the entire 84-minute interval between the first and eighth tows (Figure 2). The coherence among tows increases gradually with the age of eggs. Coefficients of correlation over .24, or coefficients of determination over .06 are significant with 60 observations.

The time and space scales of controlled ship's drift in 1-2 hours are small in comparison with the change of distribution of a patch of eggs more than one day old. The scale of deposition of the eggs and their subsequent dispersal for a few hours is of significantly smaller scale. Lastly, since eggs are part of the totally passive plankton, these results suggest that other passive plankton patches, or gaps, would have been equally coherent and slowly changing with time, and that aggregating organisms would have had to expend relatively little energy in maintaining a patch under these conditions.

DISCUSSION

The unusual circumstances of this set of observations have led to a new appreciation for the origin of small-scale distribution of anchovy eggs and the three-day persistence of this distribution. The scale and intensity of this pattern may have important consequences, both for comparative sampling of the habitats of the eastern boundary currents, and for interpreting predation. Because this set of samples was taken for other purposes, we will discuss the relations between these observations and similar observations, the implications of the persistence of pattern, and what sampling design and effort are necessary to advance the pattern studies to an analytical level.

Sampling Consequences

The high variability of plankton samples has been attributed to variations in towing procedure (Windsor and Walford 1936); heterogeneous water masses (Windsor and Clarke 1940; Cassie 1959); and aggregations of organisms (Ricker 1937; Langford 1938; Barnes and Marshall 1951). In particular, sardine eggs, which last in the plankton only a few days, are known to be aggregated at spawning (Silliman 1946; Taft 1960) and diffuse away from school-sized (tens to hundreds of meters diameter) patches, which persist for several days (Smith 1973). Aggregations of organisms and heterogeneous water masses occur at several scales and may persist over various time periods (Haury et al. 1978), and our perception of the pattern is profoundly influenced by frequency and duration of cruises, the spacing between stations, and the width and trajectory of the sampling instruments as well as the length of tow (Weibe 1972).

Number of samples. The required number of observations can be determined for a first approximation from an existing set (Santander et al. 1982) or from a pilot cruise. In general, pattern is small-scale relative to the distribution of the species, so a pilot study of spawning pattern can be conducted in a small area (100 × 100 km). The results of this study indicate that one must be separated from an area by either space (km) or time (days) to gather a valid replicate versus a redundant sample. The same is true of the pilot study conducted on existing sample results.

If a study requires precise data on a single day's spawning, the variance of the total eggs will be an underestimate of the individual day's spawning by the ratio of the persistence of the egg and the sample variance of the total eggs: for an egg that persists 3

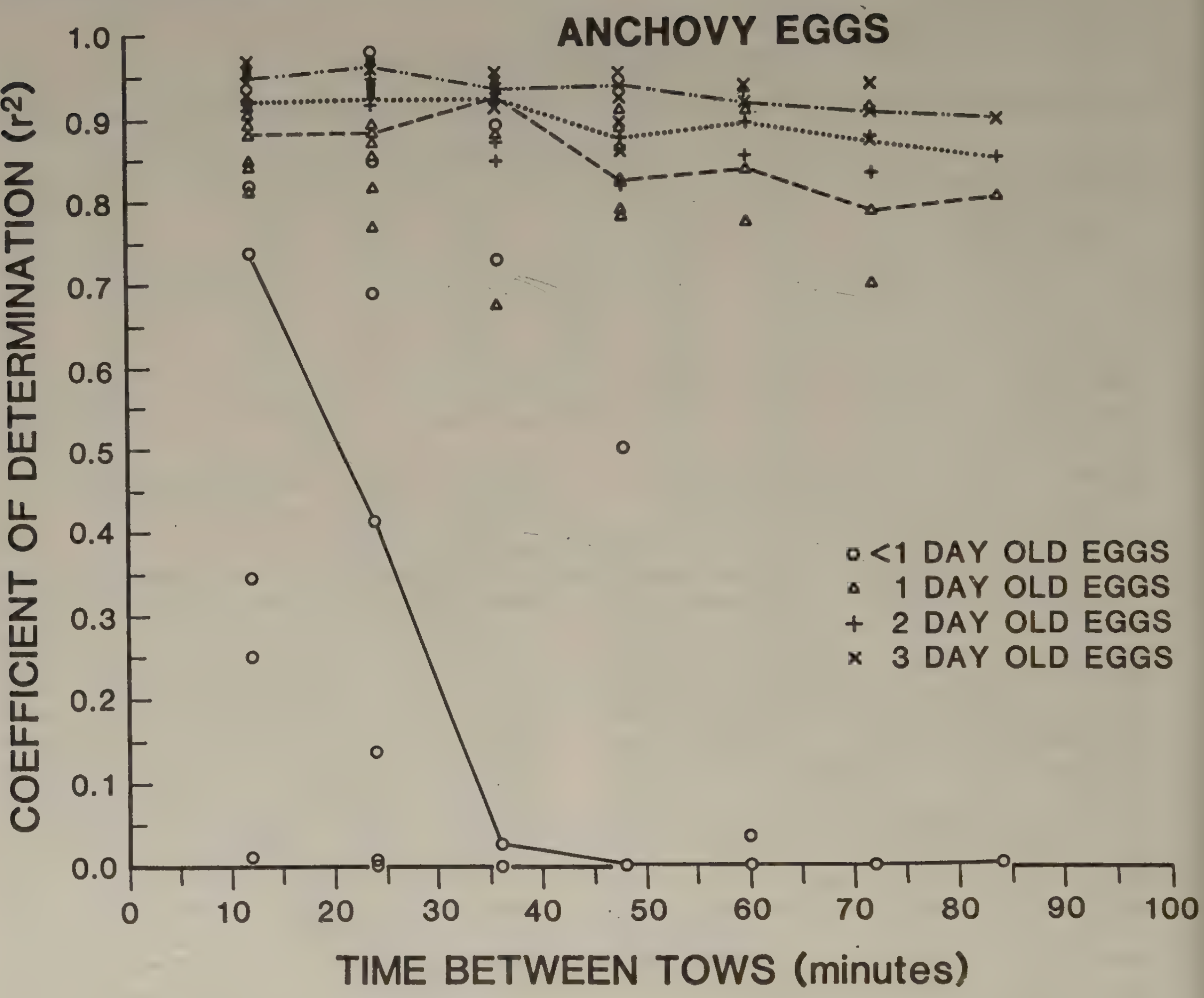

Figure 2. The persistence of correlation between tows as a function of time between tows. Points are from individual values of coefficient of determination for adjacent tows (7 sets), tows separated by 24 minutes (6 sets), tows separated by 36 minutes (5 sets), etc. The lines connect the medians of each interval. (For simplicity, only the nominal interval is graphed: the actual intervals varied from 6 to 36 minutes, with 92% of intervals between 9 and 17 minutes and 51% between 11 and 13 minutes. For complete distribution see Appendix Table 2.)

days, the variance of the total eggs can be multiplied by three to estimate the required number of samples for a given standard error. If the study requires 200 observations to suitably estimate the total number of eggs, it would require 346 samples to estimate the number of eggs spawned in a single day. To describe the onset of spawning between 1800 and 0200 hours with equal precision, it would take a similar number of samples each hour.

Geographic position of samples. Anchovy spawning habitats seem to vary considerably in different eastern boundary currents. The spawning habitat off North America comprises broad regions in relatively permanent gyrals. The spawning habitat off Peru is relatively narrow (Santander et al. 1982; Smith et al. 1983); the spawning habitat off South Africa appears to be a fast-moving coastal jet (Shelton and Hutchings 1982). The current practice is to make 1,000 observations per survey off California (Smith and Hewitt 1984). This may be the minimum required when one considers that the sample must encompass the spawning area, obtain a representative mean, and provide an estimate of egg mortality. Where the spawning habitat is too narrow to provide sufficiently independent adjacent samples, as in Peru, it may be necessary to occupy the habitat more than once. Where the habitat

TABLE 10
Ocean and Atmospheric Predictability Time for Different Scales of Motion

Scale	Predictability time	
	Atmosphere	Ocean
10 m	—	10 min.
100 m	3 min.	1.5 hr
1 km	13 min.	10 hr
10 km	1 hr	3 days
100 km	4 hr	3 weeks
1000 km	1 day	4 months
10000 km	5.5 days	x years

Modified from Platt et al. (1977)

is extremely dynamic, it may be necessary to expand the pattern with time to accommodate the rapidly moving jet and evaluate the survivors.

Consequences for the Study of Pattern

The egg distribution of schooled, coastal, pelagic spawning fish sufficiently resembles coastal plankton blooms like red tide (Kierstad and Slobodkin 1953; Wroblewski 1984) to allow evaluation of the influence of turbulent diffusion and transport at spawning time (Lasker 1975; Bakun and Parrish 1982). The 60 samples reported here (480 observations in samples of 8 per station) are not sufficiently numerous to describe even mortality, so we may expect the number of samples necessary to exceed 200 if interannual variations are relatively large. The assembly of 5 years of egg distribution observations (1,666 positive samples) was adequate to estimate mortality and dispersal (Smith and Hewitt 1984). There was no evidence of offshore transport in the 3-day period for which eggs persist: transport may be inferred from the distribution of older versus younger larvae (Smith 1972 [sardine, Fig. 6; anchovy, Fig. 7]; Hewitt and Methot 1982 [anchovy, Tab. 4, Fig. 15]). Because of this latter phenomenon, higher volumes will have to be filtered over longer distances than used for the vertical tows, to effectively describe transport. Also, the observations must be extended over time to describe transport in the mesoscale.

Predictability in the Eastern Boundary

A new process of modeling, empirical measurements specified by models, and modification of models based on new measurements is beginning (Bakun et al. 1982). For eastern boundary currents the models will have an atmospheric component, an oceanographic component, and a series of biological effects. We must remember that some causative factors in the air and ocean will remain unpredictable over certain space and time scales; thus biological responses will remain unpredictable. The nature of the problem of matching these time and space scales may be seen in Table 10. It seems reasonable to conclude from correlation of replicate samples for eggs less than 8 hours old that the pattern which yielded this result was on the order of hundreds of meters or the space scale of a fish school (perhaps in motion during spawning). Thus there is a new opportunity to design process-oriented cruises with the goal of determining the most important time and space scales of organisms of known age and distributional heterogeneity.

LITERATURE CITED

Ahlstrom, E.H. 1943. Influence of temperature on the rate of development of pilchard eggs in nature. *In* O.E. Sette, (ed.), Studies on the Pacific pilchard or sardine (*Sardinops caerulea*). U.S. Dept. of Interior Spec. Sci. Rep. 15. Reissued 1950.

———. 1968. An evaluation of the fishery resources available to California fishermen. Univ. Wash. Publ. Fish. (New Series) 4:65-80.

Bakun, A., and R.H. Parrish. 1982. Transport, turbulence, and pelagic fish in the California and Peru current systems. CalCOFI Rep. 24:99-112.

Bakun, A., J. Beyer, D. Pauly, J.G. Pope, and G.D. Sharp, 1982. Ocean sciences in relation to living resources. Can. J. Fish. Aquat. Sci. 39:1059-1070.

Barnes, H., and S.M. Marshall. 1951. On the variability of replicate plankton samples and some applications of restricted periods. J. Mar. Biol. Assoc. U.K. 30:233-263.

Cassie, R.M., 1959. Micro-distribution of plankton. N.Z.J. Science 2:398-409.

Haury, L.R., J.A. McGowan, and P.H. Wiebe. 1978. Patterns and processes in the time-space scales of plankton distributions. *In* J.H. Steele (ed.), Spatial pattern in plankton communities. Plenum Publ. Corp. New York, p. 277-327.

Hempel, G. 1973. Fish eggs and larval studies (contribution to a manual). FAO Fish Tech. Paper. 122, 82 p.

Hewitt, R.P. 1981. The value of pattern in the distribution of young fish. Rapp. P.-v. Réun. Cons. Int. Explor. Mer 178:229-236.

———. 1982. Spatial pattern and survival of anchovy larvae: implications of adult reproductive strategy. Ph.D. dissertation, University of California, San Diego, 187 p.

———. 1983. Roll, heave and vertical ichthyoplankton tows. Ocean Science and Engineering 8:41-51.

Hewitt, R.P., and R.D. Methot, Jr. 1982. Distribution and mortality of northern anchovy larvae in 1978 and 1979. CalCOFI Rep., 23:226-245.

Kierstad, H., and L.B. Slobodkin. 1953. The size of water masses containing plankton blooms. J. Mar. Res. 12:141-147.

Kramer, D., M.J. Kalin, E.G. Stevens, J.R. Thraillkill, and J. Zweifel. 1972. Collecting and processing data on fish eggs and larvae in the California Current region. NOAA Tech. Rep. NMFS Circ. 370.

Langford, R.R. 1938. Diurnal and seasonal changes in the distribution of the limnetic crustacea of Lake Nipissing, Ontario. Publ. Ontario Fish. Res. Lab., 56:1-142.

Lasker, R. 1975. Field criteria for survival of anchovy larvae: the relation between inshore chlorophyll maximum layers and successful first feeding. Fish. Bull., U.S. 73:453-462.

———. 1984. An egg production method for anchovy biomass assessment. *In* An egg production method for estimating spawning biomass of pelagic fish: application to the northern anchovy (*Engraulis mordax*). Southwest Fisheries Center Admin. Rep. LJ-84-37.

———. 1985. What limits clupeoid production?. Can. J. Fish. Aquat. Sci. 42 (Suppl. 1):31-38.

Lasker, R., and J.R. Zweifel. 1978. Growth and survival of patches containing different proportions of large and small prey. *In* J.H. Steele (ed.), Spatial pattern in plankton communities. Plenum Publishing Corp., New York, p. 329-354.

Lo, N.C.H. 1984. A model for temperature-dependent northern anchovy egg development and an automated procedure for the assignment of age to staged eggs. *In* R. Lasker (ed.), An egg production method for estimating spawning biomass of pelagic fish: application to the northern anchovy (*Engraulis mordax*) Southwest Fisheries Center Admin. Rep. LJ-84-37.

Moser, H.G., and E.H. Ahlstrom. 1984. Staging anchovy eggs. *In* R. Lasker, (ed.), An egg production method for estimating spawning biomass of pelagic fish: application to the northern anchovy (*Engraulis mordax*) Southwest Fisheries Center Admin. Rep. LJ-84-37.

Murphy, G.I. 1977. Clupeoids. *In* J.A. Gulland (ed.), Fish population dynamics. John Wiley & Sons, New York, p. 283-308.

Okubo, A. 1971. Oceanic diffusion diagrams. Deep-Sea Res. 18:789-802.

Parrish, R.H., and A.D. MacCall. 1978. Climatic variation and exploitation in the Pacific mackerel fishery. Calif. Fish Game Fish Bull. 167:1-110.

Parrish, R.H., C.S. Nelson, and A. Bakun. 1981. Transport mechanisms and reproductive success of fishes in the California Current. Biol. Oceanog. 1(2):175-203.

Platt, T., K.L. Denman, and A.D. Jassby, 1977. Modeling the productivity of phytoplankton. *In* E.D. Goldberg (ed.), The sea: ideas and observations on progress in the study of the seas. Vol. VI. John Wiley & Sons, New York, p. 807-856.

Ricker, W.E. 1937. Statistical treatment of sampling processes useful in enumeration of plankton organisms. Arch. Hydrobiol. 31:68-84.

Santander, H., P. E. Smith, and J. Alheit. 1982. Determinación del esfuerzo de muestreo requierido para el estimado de producción de huevos de anchoveta (*Engraulis ringens*), al frente al Peru. Bol. Inst. Mar. Peru Callao 7(1):1-18.

Sette, O.E., and E.H. Ahlstrom. 1948. Estimations of abundance of the eggs of the Pacific pilchard (*Sardinops caerulea*) off southern California during 1940 and 1941. J. Mar. Res. 7:511-542.

Shelton, P.A., and L. Hutchings. 1982. Transport of anchovy, *Engraulis capensis* Gilchrist, eggs and early larvae by a frontal jet current. J. Cons. Int. Explor. Mer 40:185-198.

Silliman, R.P. 1946. A study of variability in plankton tow-net catches of Pacific pilchard, *Sardinops caerulea*, eggs. J. Mar. Res. 6:74-83.

Smith, P.E. 1972. The increase in spawning biomass of northern anchovy, *Engraulis mordax*. Fish. Bull. U.S. 70:849-874.

———. 1973. The mortality and dispersal of sardine eggs and larvae. Rapp. P.-v. Réun. Cons. Int. Explor. Mer 164:282-292.

———. 1981. Sampling to determine anchovy larval mortality in the sea. *In* R. Lasker (ed.), Marine fish larvae. Univ. Wash. Press, Seattle, p. 12-21.

———. 1985. Year-class strength and survival of O-group clupeoids. Can. J. Fish. Aquat. Sci. 42 (Suppl. 1):69-82.

Smith, P.E., and R.P. Hewitt. 1984. Sea survey design and analysis for an egg production method of anchovy biomass assessment. *In* R. Lasker (ed.), An egg production method for estimating spawning biomass of pelagic fish: application to the northern anchovy (*Engraulis mordax*) Southwest Fisheries Center Admin. Rep. LJ-84-37.

Smith, P.E., and R. Lasker. 1978. Position of larval fish in an ecosystem. Rapp. P.-v. Réun. Cons. Int. Explor. Mer 173:77-84.

Smith, P.E., and S.L. Richardson. 1977. Standard techniques for pelagic fish egg and larva surveys. FAO Fisheries Tech. Pap. 175, 100 p.

Smith, P.E., R.C. Counts, and R.I. Clutter. 1968. Changes in filtering efficiency of plankton nets due to clogging under tow. J. Cons. Perm. Int. Explor. Mer 32:232-248.

Smith, P.E., W.C. Flerx, and R.P. Hewitt. 1984. The CalCOFI vertical egg tow (CalVET) net. *In* R. Lasker (ed), An egg production method for estimating spawning biomass of pelagic fish: application to the northern anchovy (*Engraulis mordax*). Southwest Fisheries Center Admin. Rep. LJ-84-37.

Smith, P.E., H. Santander, and J. Alheit. 1983. Comparison of egg sample probability distributions of the anchovy (*Engraulis ringens*) and sardine (*Sardinops sagax*) off Peru and the anchovy (*Engraulis mordax*) and the sardine (*Sardinops caerulea*) off California. *In* G.D. Sharp and J. Csirke (eds.), Proceedings of the expert consultation to examine changes in abundance and species composition of neritic fish resources. FAO Fish. Rep. 291 Vol 3:1027-1038.

Southwood, T.R.E. 1966. Ecological methods. Methuen, London, 391 p.

———. 1978. Ecological methods. John Wiley & Sons, New York, 524 p.

Taft, B.A. 1960. A statistical study of the estimation of abundance of sardine (*Sardinops caerulea*) eggs, Limnol. Oceanog. 5:254-264.

Vlymen, W.J. 1977. A mathematical model of the relationship between larval anchovy, *Engraulis mordax*, growth, prey microdistribution, and larval behaviour. Environ. Biol. Fishes 2:211-233.

Wiebe, P.H. 1972. A field investigation of the relationship between length of tow, size of net and sampling error. J. Cons. Perm. Int. Explor. Mer 34:268-275.

Winsor, C.P. and G.L. Clarke. 1940. A statistical study of variation in the catch of plankton nets. J. Mar. Res. 3:1-34.

Winsor, C.P. and L.A. Walford. 1936. Sampling variations in the use of plankton nets. J. Cons. Int. Explor. Mer 11:190-204.

Wroblewski, J. 1984. Formulation of growth and mortality of larval northern anchovy in a turbulent feeding environment. Mar. Ecol. Prog. Ser. 20:1-12.

Zweifel, J.R., and R. Lasker. 1976. Prehatch and posthatch growth of fishes—a general model. U.S. Fish. Bull. 74:609-621.

Zweifel, J.R., and P.E. Smith. 1981. Estimates of abundance and mortality of larval anchovy (1951-75): application of a new method. Rapp. P.-v. Réun. Cons. Int. Explor. Mer 178:248-259.

APPENDIX

TABLE 1
Station Data for Replicate Series

CalCOFI line	CalCOFI station	Date	Time	10-meter temperature
90.0	28.0	790122	2043	14.8
82.0	47.0	790127	0810	13.1
83.0	42.0	790127	1254	13.6
83.0	40.6	790127	1832	13.5
87.0	35.0	790128	0645	13.7
89.6	34.6	790128	1419	14.1
93.0	30.0	790129	1855	13.8
93.0	35.0	790129	2313	14.1
93.0	40.0	790130	0337	14.4
93.0	45.0	790130	0757	13.2
89.5	41.0	790131	0959	13.2
88.4	40.6	790131	1413	13.5
89.2	32.9	790201	0813	13.6
90.1	32.0	790201	1150	13.7
90.8	35.1	790201	1549	14.0
91.7	39.8	790201	2057	13.9
90.6	42.8	790202	0127	14.0
88.9	45.3	790202	0632	12.9
87.6	44.7	790202	1031	13.2
86.3	44.8	790202	1905	13.0
86.1	42.6	790203	0010	13.1
84.3	43.4	790203	1108	13.0
83.8	47.2	790203	1444	13.1
83.9	52.3	790203	1839	13.1
89.4	51.2	790204	0947	13.4
91.9	44.2	790204	1855	13.3
92.9	38.1	790204	2346	13.6
91.9	32.8	790205	0423	13.6
92.2	27.7	790205	0817	13.5
93.5	27.4	790205	1142	14.0
93.8	31.8	790206	1945	14.3
91.9	40.6	790207	0728	13.8
90.8	46.5	790207	1222	13.2
90.5	44.2	790207	2127	13.8
92.2	42.9	790208	0845	14.1
93.1	45.2	790208	1717	13.8
91.8	45.8	790208	2104	13.9
92.7	40.9	790209	0126	13.9
94.9	50.2	790209	1802	13.7
96.7	50.2	790209	2213	14.3
96.0	45.9	790210	0319	14.2
94.4	38.6	790210	1106	13.9
93.3	34.7	790210	1526	14.4
92.8	31.6	790210	1859	13.9
91.2	30.2	790211	0040	12.4
91.9	34.3	790211	0540	14.1
91.2	37.8	790211	0939	14.7
89.7	36.5	790211	1400	14.7
88.9	40.7	790211	1739	13.8
88.2	43.9	790212	1519	14.0
87.8	39.1	790212	1907	13.3
86.4	38.5	790212	2300	13.7
85.6	45.8	790213	0749	13.2
82.5	43.3	790214	0640	13.4
83.8	40.6	790214	1050	13.8
85.2	37.2	790214	1452	13.9
86.5	33.9	790214	1920	13.8
89.4	30.6	790215	0320	13.8
90.2	29.3	790215	0655	14.0
91.7	28.0	790215	1050	14.9

TABLE 2
Distribution of Intervals between Tows

Interval between tows (min)	Proportion of observations	
6	.011	*
8	.017	**
10	.089	*******
12	.511	************************************
14	.260	*******************
16	.060	*****
18	.026	**
20	0	
22	.017	**
24	0	
26	.003	*
28	0	
30	0	
32	.003	*
34	0	
36	0	
38	.003	*

TABLE 3
Program to Estimate Parameters of a Negative Binomial Distribution

Original program by Hewitt Tektronix (1977)
Converted by Smith to TRS-80 (1980)
Converted by Smith to VAX (1982)

```
10  rem uses three methods for estimating k of negative binomial”
20  K=0
30  K1=0
40  K2=0
50  PRINT“Enter total number of observations in sample, number of”
60  PRINT“zero observations, mean and standard deviation of all”
70  PRINT“observations.”
80  INPUT N,Z,M,S
85  V=S*S
90  PRINT “trial k = ”;
100 INPUT K
110 X= −LOG(Z/N)/K−LOG(1+M/K)
120 PRINT“residual = ”;X
130 PRINT “press enter for another trial, otherwise any key”
140 INPUT Q$
150 IF Q$=“ ” GO TO 90
160 K1=(M*M)/(V−M)
170 PRINT“Enter the observation frequency table: first value”
180 PRINT“then frequency thus 15,6 - - enter 999,0 when finished”
190 DIM I1(1000),R(1000)
200 I=1
210 PRINT I; “value = ”;
220 INPUT I1(I)
230 IF I1(I)=999 THEN 290
240 PRINT “frequency = ”;
250 INPUT R(I)
260 A=I
270 I=I+1
280 GO TO 210
290 PRINT “trial K = ”;
300 INPUT K2
310 B=1
320 U=0
330 FOR J = 1 TO A
340 Q=0
350 FOR I = B TO A
360 Q=R(I)+Q
370 NEXT I
380 V=Q/(K2+J−1)
390 U = U + V
400 B=B+1
410 NEXT J
420 X=N*LOG(1+M/K2)−U
430 PRINT “residual = ”; X
440 PRINT “want another iteration?”
450 INPUT Q$
460 IF Q$=“ ” GO TO 290
470 PRINT “from the proportion of zeroes ..................................................... ”; K
480 PRINT “by the method of moments .......................................................... ”; K1
490 PRINT “by maximum likelihood ............................................................. ”; K2
500 END
```

8587

Sea Survey Design and Analysis for an Egg Production Method of Anchovy Biomass Assessment

PAUL E. SMITH and ROGER P. HEWITT[1]
Southwest Fisheries Center,
National Marine Fisheries Service, NOAA,
P.O. Box 271,
La Jolla, CA 92038

ABSTRACT

A sea survey of spawning habitat is described for the northern anchovy, *Engraulis mordax*. The central population occurs within a permanent gyral circulation off southern California and in the adjacent nearshore and main branches of the California Current. The geographic scope of spawning is maximal in winter and spring, and its extent appears to be a function of population biomass.

About 8 hours after the onset of spawning it becomes possible to obtain effective samples: adult data can be used for about a day and egg data for a little more than 2 days to estimate vital rates, such as egg production and mortality. The spawning process is so patchy and dynamic that it has not yet been possible to gather useful data on adults or eggs during the spawning interval.

The population egg production rate is determined by a survey using about 1,000 vertical plankton tows of 3.5 m^3 between 70 m depth and the surface. The array of samples is intended to be representative and inclusive of the entire spawning area. Observations of the number of eggs per sample represent a contagious distribution (patchy), and the assumptions necessary for a "normal" or "log-normal" model are not met. The assumption of independence of sample parameters (mean and variance) is not supported with either model. The probability distribution most closely approximated is the "negative binomial." The parameters of that distribution change with the age of the egg.

The Southwest Fisheries Center Egg Production Method was initiated with much historical, geographic, and biological data obtained in the California Cooperative Oceanic Fisheries Investigations (CalCOFI). It should be possible to initiate an egg production method on other species in other regions without this vast time-series of data. Preliminary laboratory work, field surveys, and analyses are described for research at other temperatures and for the diagnosis of egg production for species which spawn at all times of day rather than nocturnally. The geographic limits of spawning should initially be described from oblique plankton tows filtering larger volumes of water (500-1,000 m^3). Also, differences in spawning patch intensity may require observations of more than the 3.5 m^3 which is adequate for the anchovy in this region.

THE SPAWNING PROCESS

Spawning Area

The northern anchovy, *Engraulis mordax*, spawns within the regional eastern boundary current, the California Current system. Figure 1 is a series of overplots of all samples of anchovy eggs collected from 1951 to 1981. These serve to describe the maximum spatial distribution of spawning in each bimonthly period. Spawning occurs primarily nearshore of the main branch (Hickey 1979) of the California Current. The main branch of the California Current is 300 km off Washington and Oregon (lat. 45°N), 430 km off Cape Mendocino (lat. 39°N), 270 km off Point Conception (lat. 34°N), 240 km off northern Baja California (lat. 30°N), and 200 km off Cape San Lazaro (lat. 25°N).

The boundaries of the main branch of the California Current shift in position and are indistinct at every season. The 1950-78 average in a section normal to the coast at lat. 32°N reveals the three branches of the California Current postulated by Hickey (1979) (Lynn et al. 1982). The speeds of the surface currents at the cores of these three zones are given in Table 1. It may be inferred from Figure 1 that the nearshore zone of the California Current system is the most consistent spawning site of the northern anchovy and that virtually no spawning takes place in the outer zone or in the main branch at the season of heaviest southward flow.

Table 1.—Zones of the California Current.

	Outer		Main		Inner	
Month	u[1]	d[2]	u	d	u	d
January	[3]+3.5	600	− 6.9	400	3.5	100
April	−5.2	500	− 6.9	250	−5.2	50
July	−3.5	700	−12.0	250	6.9	100
October	−2.6	700	− 6.1	400	5.2	100

[1] u is the current speed at the core in kilometers/day.

[2] d is the distance of the core from the coast at CalCOFI line 90 (see Lynn et al. 1982) in kilometers

[3] indicates Equatorward flow.

In addition to the large-scale features, there are local environmental events which appear to influence the pelagic spawning population. Temperature (Lasker et al. 1981; Fiedler 1983) and surface chlorophyll concentration estimated from analysis of satellite infrared images (Pelaez and Guan 1982; Fiedler 1983) appear to be important in fine-scale distributions. In the short period in which satellite image analysis has been possible, 0.2 mg/m^3 appears to be a lower limit of chlorophyll in which anchovy spawning takes place (Fiedler 1983). There also appears to be some diminution of incidence of eggs at temperatures below 13.5°C (Fiedler 1983) although temperatures as low as 11°C are not lethal for anchovy eggs. It also appears that a certain amount of stability in terms of mixing (Lasker 1975; Bakun and Parrish 1982; Smith and Lasker 1978) and absence of offshore and southerly transport (Hewitt and Methot 1982; Power 1983) are favorable to the establishment and maintenance of spawning areas.

Population size also appears to control the spawning area (Ahlstrom 1965; MacCall 1983). There is anchovy spawning further offshore and north when the biomass is large, but the spawning area appears to contract toward the Los Angeles Bight when the biomass is smaller. A simple description of this (MacCall 1983) would be that a 100,000-ton spawning biomass would extend off-

---

[1] Present address: Commanding Officer, NOAA Ship *Miller Freeman*, Pacific Marine Center, 1801 Fairview Ave. East, Seattle, WA 98102.

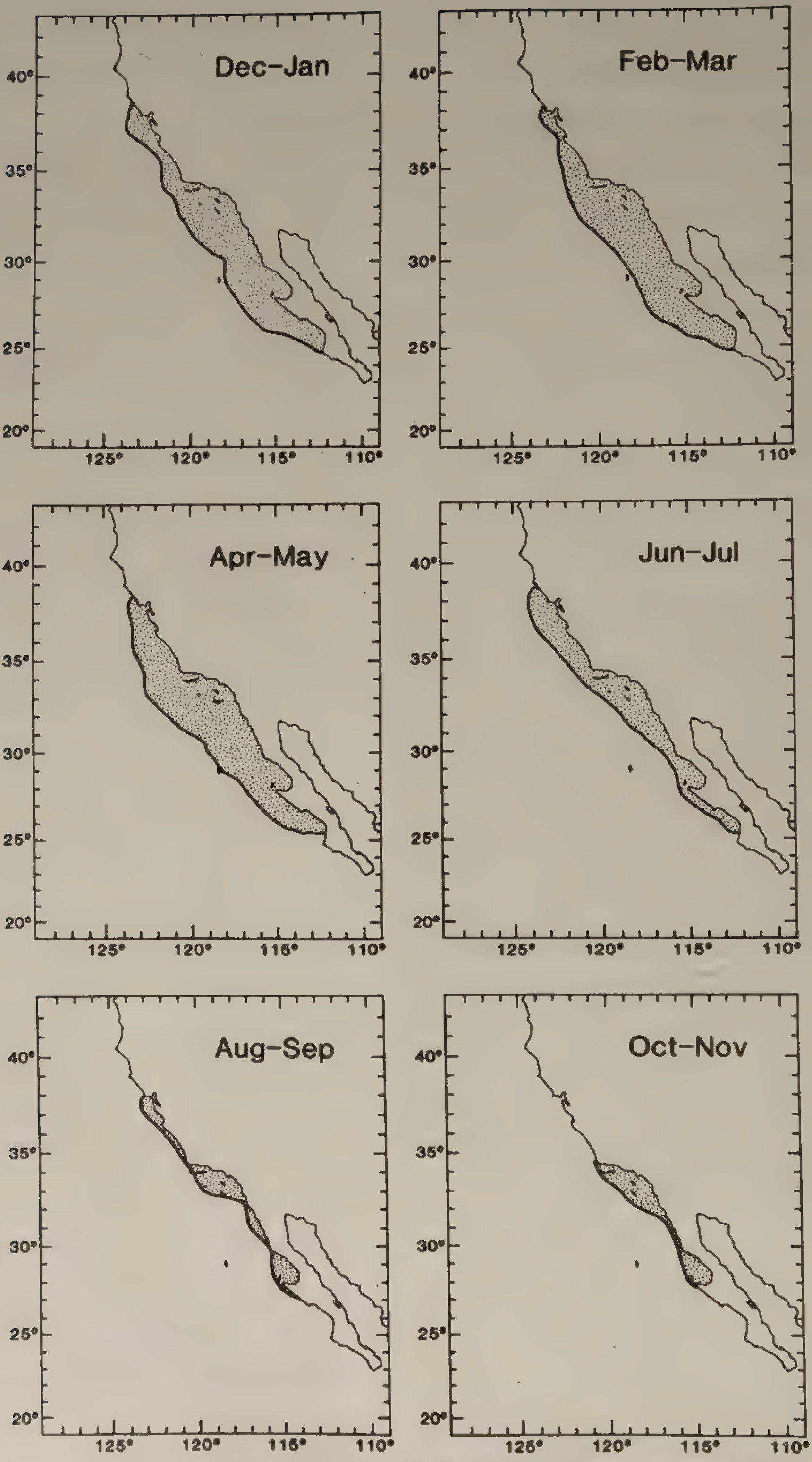
Dec–Jan
Feb–Mar
Apr–May
Jun–Jul
Aug–Sep
Oct–Nov
40°
35°
30°
25°
20°
125°
120°
115°
110°

Figure 1.—Long-term spawning range of the northern anchovy as estimated from approximately 30,000 observations of anchovy eggs taken from a larger area between 1951 and 1983. For maps of all observations between 1951 and 1979 consult CalCOFI Atlases 9 and 28 (Kramer and Ahlstrom 1968; Hewitt 1980).

shore only 260 km, but a 1-million ton spawning biomass would extend offshore 360 km.

Spawning Season

Some anchovy spawning takes place at every time of the year, but winter and spring are times of the most active spawning.

THE SAMPLING PROCESS

Catchability and Vulnerability of Adults

Epipelagic schooling fish are difficult to sample quantitatively. At times the sample trawls have been placed based on sonar mapping the previous day. At other times the samples have been taken where newly spawned eggs were detected by preliminary examination of plankton samples. Uniform samples of all tows conducted for the purpose of estimating egg production represent the 7 to 40-m depth range. The upper limit is set by the minimum depth at which a midwater trawl can be fished.

One aspect of the variation in catchability can be illustrated by examination of the variation in the sex ratio. If one considers the data on 362 observations for which sex ratio was determined between 1977 and 1982, there is an interesting distribution of sex ratios and standard deviations of sex ratio by time of day (Table 2; Hunter and Macewicz 1980). For comparison, the overall mean of sex ratios is 0.497 with a standard deviation of 0.233 and a standard error of the mean ratio of 0.012.

The dispersion of values, about 50% female, is wider than one would expect of a binomial sampling error distribution with 10-30 specimens, thus we believe that the phenomenon reflects actual biological features of the anchovy schooling and behavior pattern. In further support of this idea, the distribution about 50% is skewed to the side of underestimation of females and the bias arises from a peak time 2200-2359 which coincides with the maximum spawning activity as seen from the surveys of stage I and II eggs (see Moser and Ahlstrom 1985). The strength and prevalence of this spawning behavior are demonstrated by the fact that a 5% overall bias in sex ratio may be caused by only 10-15% of females and their attendant males.

We postulate that during the spawning act more males than gravid females are present, and this leads to temporal and spatial heterogeneity; also, the collection of samples with a trawl from a volume which is 15 m thick, 15 m wide, and 2,000 m long has considerable chance of mixing these proportions by transecting spawning and nonspawning clusters. Thus it is that the modal catch category, 43 of 362 samples, is at 50% female. The binomial sampling theorem for fish sample sizes of 10-30 fish would indicate that about 6% of the samples would yield <30% female and also 6% would yield >70% female. The actual observations are given in Table 3.

For the use made of the adult data at present, the sex ratio bias (see Hunter et al. 1985) is not thought to be of any great importance: the ratio of 1-d postovulatory gonads is used for the inverse of the daily spawning fraction, and the sex ratio is determined to be 50% because there is no weight differentiation by sex and the numeric ratio is likely to be 50% as well. In another section (Alheit 1985) we shall see that the Peruvian adult sampling system with purse seiner exhibits no bias, and we assume that the explanation lies with the evasion of the trawl or the depth distribution of the sexes. In general, the commercial fishery exhibits a sex ratio of the order of 60% female, and the sea survey has a ratio of 50% female (Mais 1974).

The inference that changes in catchability and vulnerability of the adults are controlled somewhat by the spawning act is strongly supported by the coincidence of spawning detected in the sea. Statistics are available from 3,936 observations between 1980 and 1983 of which 1,666 had 1 or more anchovy eggs. Prior to the first cellular division (Stage I eggs, see Moser and Ahlstrom 1985) there are small numbers of observations and these reflect the temporal distribution of spawning in much the same way as the adult sex ratio variance (Table 4).

Table 2.—Percent females in trawl catches of northern anchovy at different times of day.

Time of day	No. of samples	% females	SD (%)
1800-1959	77	52.6	18.9
2000-2159	88	47.0	27.9
2200-2359	80	45.3	26.0
0000-0159	64	50.5	22.2
0200-0359	24	50.4	17.7
0400-0559	21	57.1	11.1
0600+	8	65.6	14.7

Table 3.—Actual and expected catches of females of northern anchovy at different times of day during spawning.

Mean time (h)	No. of samples	No. of samples expected at <30% and >70%	No. samples observed <30% female	No. samples observed >70% female
1900	77	5	6	13
2100	88	5	26	19
2300	80	5	22	12
0100	64	4	9	11
0300	24	1	1	3
0500	21	1	0	3
0600+	8	1	0	3

Table 4.—Percent positive egg captures and mean number of northern anchovy per tow by time of day.

Time	Observations	Positive samples	% positive	Mean no.
1800-1959	142	5	3.5	0.120
2000-2159	135	26	19.3	0.919
2200-2359	147	48	32.7	3.265
0000-0159	152	33	21.7	3.303
0200-0359	151	22	14.6	0.464
0400-0559	132	8	6.1	0.462
0600-0759	137	6	4.4	0.153
0800-0959	129	1	0.8	0.008
1000-1159	129	5	3.9	0.039
1200-1359	133	2	1.5	0.023
1400-1559	128	2	1.6	0.016
1600-1759	151	1	0.7	0.007

Sampling Requirements for Egg Survey

The egg survey supplies two values to the spawning biomass estimate: The size of the spawning area and the daily production of eggs per unit area. When establishing standards for the survey of egg production, it is necessary to consider the inclusion of the entire spawning area, the representativeness of the samples within the area, and the sufficiency of the number of observations for the required precision.

There is an obvious bias associated with egg production outside the surveyed area. The product of the survey area and the egg production/unit area is unbiased even if the survey is much larger than the spawning area. That is, as the surveyed area outside the spawning area increases there is a corresponding decrease in the mean number of eggs produced/unit of survey area. However, a secondary objective of the Southwest Fisheries Center Egg Production Method is to determine the error distribution of each estimated parameter. The Central Limit Theorem is not valid in reduction of standard-error-of-the-mean value with increasing number of observations if those values are spatially coherent. If there was a broad contiguous and continuous area of observations with no eggs in the observations, the standard error would be correspondingly biased as an underestimate.

It is not necessary to know the nature of the underlying distribution of observations to use the Central Limit Theorem to estimate the error distribution of the mean. However, it may be useful to consider some probability-generating distributions in order to forecast what an adequate number of observations would be, given the sample variance and the objectives of the survey. As an example of the differences one might encounter, consider: If the eggs were distributed such that the observations produced a "Normal" distribution, then with each sample one would obtain an independent estimate of the population mean and the population variance; if the eggs were distributed such that the observations produced a "Poisson" distribution, then the estimated mean of the population would simultaneously produce an estimate of the variance of the population (equal to the mean); if the eggs were distributed with areas of high density and areas with no eggs at all such that the presence of one egg would predict the presence of other eggs in the sample so that a "Negative Binomial" distribution of observations obtains, one would need many independent observations to obtain a mean number of eggs/unit area with a normal distribution of standard error of the mean. Thus the expense of effort of estimation-per-unit precision is much lower with "Normal" and "Poisson" distributions than it would be with an underlying "Negative Binomial" distribution. To diagnose this, one needs to compare the variance and mean of several estimates. If the variance is independent of the mean, the distribution is "Normal"; if the variance is a power function of the mean, the distribution is probably "Negative Binomial," although there are other possibilities. For a first approximation, the "Negative Binomial" appears to be a useful working model for design of the egg production survey to determine the mean and variance of the egg production parameters.

The establishment of the "Negative Binomial" model of underlying distribution of observations does not support speculation as to the scale or origin of the patchiness, and thus no single set of samples can be used to interpret pattern.

For the purpose of determining sampling requirements for an egg survey, it is necessary only to show that the number of samples is adequate to describe the mean and standard error of the production of eggs per unit area. A second level of analysis and sampling is necessary to jointly describe the scale and intensity of the patchiness and so allow speculation and research as to the processes which underlie the observed pattern. Knowledge of scale of the "patches" and intervening "spaces" and their shapes is necessary for further work.

We discuss the description of pattern below merely to emphasize what we would need to know to interpret processes such as:

1. The interannual variability in patch scale possibly caused by differences in fecundity attributable to such parameters as batch size, interval between spawnings, and age composition of spawners;
2. The geographic variability in the scale and intensity of predation;
3. The interaction of patch scales and numbers of anchovy eggs with patch scales and numbers of their principal predators, including adults within the school, adults and juveniles in other schools of the same species, and other noncannibalistic predators on anchovy eggs;
4. The relevance of interaction between the sampler size and the anchovy egg patch scale in order to transfer these sample designs to other anchovy populations or to other species; and
5. The comparison of vertical samples to older oblique samples, or the effects of taking samples of different size and shape on survey efficiency.

One reason that the standard sampling tactic (the vertical egg tow on a systematic grid) is not fully effective for advanced description of pattern is that observations are taken at one size scale and separated by a fixed distance. If we take the characteristics of the negative binomial—the mean, the coefficient of patchiness, "*k*", and the percent of the area, *P*(0), with no eggs—only the mean is a characteristic of the sampled population; *k* and *P*(0) result from interactions between the scale of the sampler and the scale of the patches of eggs. For example, if the vertical sampler mouth opening were progressively increased from 0.05 m^2 to 10 m^2, we would expect the probability of "zero" observations to decrease. The decrease would depend on what fraction of the interpatch spaces were between 25 cm (the diameter of the smaller sampler) and 357 cm (the diameter of the larger sampler). For *k* the equation for the population is:

$$k_i = \frac{\mu_i^2}{\sigma_i^2 - \mu_i}$$

where k_i is the scale-dependent coefficient of patchiness, μ_i is the population mean of all possible areas for sample size "*i*", and σ_i is the population variance for that set. If the true scale of anchovy egg pattern were approximately the same as the larger sampler, the sample variance would increase under the influence of larger observations and there would be a concomitant diminution of the variance from the effect of the larger sampler lying across more patch boundaries and thus integrating patch and space densities. If the true scale of the anchovy egg patches were smaller than the larger sampler, the variance would decrease because all observations would integrate some space densities. If the true scale of the anchovy egg patches were greatly larger than either sampler, the derived *k*'s would tend to be indistinguishable.

Lastly, if the true scale of the anchovy egg pattern is larger than the spatial interval between stations, the variance will be less because adjacent observations will be more similar than observations chosen at random.

There is evidence that several scales of pattern exist which probably originate from different processes. The smallest scale is imposed by the process of fertilization and is at the scale of a single female or a small group of females. The next scale dimension is imposed by the general schooling habit. The largest scale within the subpopulation is called the "school group" and it may contain several thousand schools of juveniles and adults in varying degrees of spawning condition. For the purposes of this discussion we can label these scales, meters, hundreds of meters, and thousands of meters: the biogeographic boundaries of the entire interbreeding subpopulation (central subpopulation of the northern anchovy) is 400 km cross-shore and 1,000 km along the coast.

The larger scales are of practical concern for the egg production method using the Central Limit Theorem; namely, the effect of multiple observations forming a normal distribution of the standard error of the mean is diminished by coherence among adjacent observations. Preliminary analyses of replicate egg samples (Smith and Hewitt 1985) indicate that cross-shore observation transects with observations separated by only 500-1,000 m would be coherent, while observations in excess of 5,000 m apart are independent of the major persistent source of patchiness at the "school" scale, 100-1,000 m. School groups have not yet been positively identified by the egg production surveys, but they are obvious from aerial and wide-ranging sonar mapping surveys (Fiedler 1978; Smith 1978).

To summarize, sample design decisions for the Southwest Fisheries Center Egg Production Method of biomass assessment have been based on prior knowledge, e.g., 1) the anchovy's spawning season, 2) the spawning area, 3) size of the school groups, and 4) size of the schools.

The volume of one observation is 3.5 m^3 or 1/20 m^2 between 70 m and the surface. The distance between observations is 4 nmi in the cross-shore direction and 10 or 20 nmi in the alongshore plane. For the central subpopulation of the northern anchovy, the recommended sampling area is 200 mi cross-shore and 600 mi alongshore.

Random vs. Centric Systematic Area Sampling

The sample design for the egg production method does not use random sampling: the lines are fixed in cross-shore positions which conform to historical surveys of biological and oceanographic features which can be measured only with straight sections at or near right-angles to the coast. The danger with fixed transects is that characteristics, such as proximity to a canyon or upwelling site, the passage close to an island, or the aversion to stations in shipping lanes, all adversely affect the necessary assumption that all objects to be sampled have had an equal opportunity to appear in a sample. Another problem is the regular spacing of systematic samples: if the alongshore or cross-shore spacing coincides with any periodic element in the distribution of the organisms being sampled, then the possibility exists for bias through oversampling some phases of the spatial periodism. For example, if the number of organisms varied like a sine wave, it is possible that regularly placed samples will hit the peaks or troughs in the distribution, thereby over- or underestimating the population. In a strict sense, statistical limits cannot be established with sets of systematic samples: there is some evidence (Milne 1959) that for periodic differences to be important, they would have to be obvious. Milne (1959) stated "...with proper caution, one will not go very far wrong, if wrong at all, in treating the centric-systematic-area sample as if it were random."

INITIATING AN EGG PRODUCTION PROCEDURE

The Southwest Fisheries Center Egg Production Method was created using new principles of sampling and mortality analysis of anchovy eggs in the sea and residual gonadal tissues indicating recent ovulation. There existed a wealth of data on the geographic distribution of adults (Mais 1974) and the geographic and temporal distribution of anchovy spawn (Kramer and Ahlstrom 1968). It should not be necessary to repeat the CalCOFI effort at each site and for each species to develop egg production procedures for other species in other geographic areas. It is the purpose of this section to describe minimal initial steps for the egg production method.

Initiation of Field Sampling

Observations of larger larvae (5-10 mm) from high-volume oblique tows (ca. 1,000 m^3) would be superior to the CalVET (3.5 m^3) tows for establishing the regional boundaries and season optimum for the egg production method for a given species. For widespread pelagic species exhibiting multiple spawning, interstation distances of 40-120 nmi should suffice (74-222 km) to delimit spatially the spawning area. Monthly, bimonthly, or seasonal surveys should be sufficient.

Laboratory and Field Studies of Spawning Behavior

While it is conceivable that temperature-dependent rates of egg development can be derived from the analysis of field samples and ancillary depth and temperature data, it is recommended that laboratory-controlled temperature experiments be used to establish the temperature-dependent rate model. In particular, the extremes of temperature may be difficult to observe adequately in the field in any given year.

In the field, even when there is no main time of day for spawning, it is possible to determine the number of eggs spawned per day by:

$$N_t = N_0 \int_{-\infty}^{t} \exp[-Z(t-x)] f(x)\, dx$$

where N_t is the number of eggs in a particular stage and later stages at time t; N_0 is the total number entering the series; $\exp[-Z(t-x)]$ is the probability that an egg at time x is still alive at time t; Z is the constant age-specific death rate; and $f(x)$ is the frequency of the stage at time x (Manly 1974). The actual frequency function can be inserted in the equation. For example, a normal distribution of spawning time would yield the equation:

$$N_t = N_0 \exp(-Zt) \int_{-\infty}^{t-\mu/\sigma} (2\pi)^{-1/2} \exp(-1/2x^2)\, dx$$

One must, of course, have more than four samples to solve this equation (Manly 1974).

When regional and seasonal criteria for spawning have been established, there must be an intensive field study to find the sample distribution in time and space which will be sufficiently precise for the purposes of egg production estimate of spawning biomass. The conditions which must be noted from the data set are (after Southwood 1978): 1) Distribution of the time of spawning, 2) variability of survival rates, 3) stage-dependent sampling efficiency, 4) duration of stages, and 5) probability distribution of eggs as a function of time and age.

Working assumptions for the central population of the northern anchovy at lat. 33°N in March are:

1) Spawning occurs between 1800 and 0200, essentially normally distributed with a midpoint of 2200 hours.
2) The survival rate is assumed to be constant between 0200 of the first day after spawning until hatching begins (normally 60 h).
3) All stages are sampled with equal efficiency, but the period when spawning is actually occurring or after hatching begins is excluded from survival stimulation.
4) Duration of egg stages is proportional to a single temperature (usually the surface temperature).
5) The probability distribution of eggs/unit surface area is completely characterized by the two parameters of the negative binomial distribution, the arithmetic mean and the dispersion parameter *k*, a function of the population mean and variance. These parameters are age-specific, the mean decreasing with age and *k* increasing with age.

The last assumption must be considered for the regression method of estimating the precision of the slope and intercept estimates, as there are, as yet, no formal solutions for regression equations under these conditions.

Staging Eggs in Other Species or in Tropical or Arctic Habitats

The anatomical description of the 11 stages of eggs is given for anchovy in Moser and Ahlstrom (1985). Also, an experimental definition of the mid-age of each stage and the conversion of stage, time-of-tow, and temperature information are described by Lo (1985). We here describe some approaches to fishes whose spawning behavior and definition of stages are dissimilar to the anchovy.

The possible number of discrete stages assigned to the continuum of embryonic development is ultimately determined by the presence of recognizable anatomical features. For example, although not used in this work, the 2-cell, 4-cell, and 8-cell stages of the embryonic development could be used to follow population features immediately after fertilization. For convenience the nominal hatching time of 60 h has been divided into 11 stages for a mean duration of about 6 h. If one were dealing with a tropical fish with a hatching time of 20 h, it would seem more reasonable to maintain the number of arbitrarily defined stages at 10 or so, rather than to reduce the number of stages to 3 of about 6-h length. Similarly in the Arctic situation, where hatching may take several weeks, one may need to pool several days' spawning to gain sufficient sample sizes to estimate mortality rate and egg production.

Were the stages equal in duration and spawned at an instant, one would easily see the progression of these stages with time. Since the period of spawning is approximately 1/4 d, and the duration of the stages is from 2 to 9 h, the system used here was originated for the sardine (Ahlstrom 1943) temperature-specific development rate and later applied to the anchovy (see below). Since these are both temperture-zone clupeoid fishes, the rationale for these stages is listed below for the purpose of using this technique for fishes in other latitudes or taxa.

While it has not been possible to obtain exact information on fertilization time or the exact timing of the transitions between stages, it is possible to combine quantitative laboratory and field data to make a best description of the major events in embryogenesis. This description can then be used to design definitive work in the laboratory or field as needed for future studies on these or other fish. We base all of the arbitrary descriptions on a starting time of 1800 (6 p.m.) for onset of spawning, with the midpoint of spawning at 2200 (10 p.m.), and finishing at 0200 (2 a.m.). Bolin (1936) observed that cell cleavage in the anchovy embryo occurred at approximately half-hour intervals, thus we assume that the interval between fertilization and first cleavage is about 0.5 h. Since the duration of the Stage II eggs from first cleavage until the onset of epiboly or cellular overgrowth of the yolk is about 7 h and the number of Stage II eggs collected is about seven times the number of Stage I eggs, we assume that the Stage I egg persists about 1 h or 0.5 h to be fertilized and 0.5 h more until the first cleavage.

Table 5 is from a summary of all field data taken in 1980-83, with 1,666 samples positive for some stage of anchovy egg. For each of the first five stages, the mean number of eggs per 0.05 m^2 is listed for each of 12 2-h periods, and next to each abundance is the cumulative percentage from the onset of the stage to the end of 24 h. For the cumulative percentage of each stage the point at which 5% of the eggs have appeared, 50% and 95% points on the cumulative curve are listed at the bottom of the table. The cumulative effects of temperature have little effect on the early stages. The sets included here are from all temperatures encountered in the surveys, mostly between 13° and 16.5°C in these years with an average temperature of 15.4°C.

In the laboratory experiment, it was not convenient to constrain the gravid anchovies, thus it is not known for certain when the first spawning begins under controlled conditions. Following spawning in the laboratory, the eggs were collected in the outflow in a passive net and were transferred into containers with temperatures controlled at approximately 13.5°, 15.1°, and 16.3°C. This means that the early stages concluded their development at a common temperature of about 15°C and were subsequently placed in controlled temperatures. Thus, for the tables which follow, the temperature is that at which most of Stage III and all of the ensuing stages were passed. The original data were somewhat more finely grouped, but low numbers of specimens in some categories and brevity made some lengthening of observation intervals desirable. To unify these numbers, the raw data were converted to numbers per hundred collected at each time interval, and then the numbers were summed for each stage and the cumulative sum at each reported interval was divided by the total to yield the tabled value of cumulative percent. The 0 in the table means that no specimens of that stage were spotted before that interval; the 1.000 means that no specimens in that stage were found after that interval. All Stage I eggs had developed before the eggs were caught at the outflow and most Stage II and some Stage III eggs were present before the systematic counting and staging began. The experiment was terminated before all larvae had reached the 3.5-mm length.

The actual times of day of the important events were injection of hormones in the afternoon of the preceding day and collection of the eggs in the morning. The first staging ensued at about 1300.

For any small set of anchovy samples, Stage I and Stage XI appear to be too short for any analytical purpose: each appears to be about an hour long. The other stages probably last between 5 and 13 h, and these durations diminish with increasing temperature and development. Thus for other species in lower and higher water temperature, the detection and use of a daily cycle of spawning should include redefined stages which are markedly shorter than one day at the beginning of development. The ensuing stages can be longer as is convenient for data gathering and storage.

Table 5.—Tabulation of field abundance of northern anchovy eggs as a function of time in hours after spawning; 00 refers to the mid-point of spawning.

	Stages									
	I		II		III		IV		V	
Age in hours	eggs/ 0.05m²	cum. %	eggs/ 0.05 m²	cum. %	eggs/ 0.05 m²	cum. %	eggs/ 0.05 m²	cum. %	eggs/ 0.05 m²	cum. %
−04-02	0.120	0.014	0.113	0.002						
−02-00	0.919	0.118	1.511	0.026						
00-02	3.265	0.490	6.252	0.125						
02-04	3.303	0.866	11.612	0.308						
04-06	0.464	0.919	10.298	0.471						
06-08	0.462	0.972	8.932	0.613	0.197	0.004				
08-10	0.153	0.989	11.358	0.792	2.029	0.047				
10-12	0.008	0.990	7.426	0.910	4.767	0.149				
12-14	0.039	0.995	3.969	0.973	5.178	0.259	0.109	0.003		
14-16	0.023	0.997	1.023	0.989	7.474	0.419	0.316	0.013		
16-18	0.016	0.999	0.258	0.993	8.945	0.609	1.109	0.048		
18-20	0.007	1.000	0.450	1.000	8.762	0.796	2.378	0.121		
20-22					2.831	0.856	5.056	0.278	0.873	0.026
22-24					1.926	0.897	5.911	0.462	2.482	0.102
24-26					3.408	0.970	7.388	0.691	2.599	0.108
26-28					1.105	0.994	6.842	0.903	3.421	0.284
28-30					0.298	1.000	1.411	0.947	4.570	0.422
30-32							0.318	0.957	5.576	0.576
32-34							1.241	0.995	5.263	0.751
34-36							0.155	1.000	3.318	0.851
36-38									2.078	0.914
38-40									1.181	0.950
40-42									1.109	0.984
42-44									0.543	1.000
Age at which										
5% appeared	−1.5 h		0.5 h		10 h		18 h		22.5 h	
50% appeared	0.0		6.0		16		24		30	
95% appeared	4.5		13.5		25.5		31		40	

Abnormal Embryos

There appears to be a need for stages which can be recognized even with a distorted specimen. A large fraction of the anchovy eggs are decidedly abnormal and stage classification is quite difficult. We have sought to modify sample washing and fixation to diminish this problem, but the specimens are distorted when fresh and alive (Sandknop and Stevens[2]). Also these abnormal embryos do not seem to be associated with any particular stage or age of egg. Table 9 is a correlation matrix for the disintegrated eggs and the aged ones. The highest correlation is between disintegrated and total eggs, and even this shows no more than 7% of the number of disintegrated eggs can be predicted from the number of eggs in a sample.

Table 6.—Correlation matrix among categories of northern anchovy eggs.

Age of eggs	<8 h	1 d	2 d	3 d	4 d	DIS+[1]
1 d	0.101					
2 d	0.029	0.396				
3 d	−0.022	0.176	0.277			
4 d	−0.024	0.029	0.002	0.325		
DIS+	0.045	0.150	0.143	0.111	0.073	
Total eggs	0.388	0.786	0.737	0.465	0.130	0.258

[1] DIS = disintegrated eggs but with chorion intact.

The time in the field of the proportion of the spawning area covered by spawn (Fig. 2), the mean number of eggs per observation, the standard deviation, the standard error of the mean (Fig. 3), and the dispersion coefficient *k* of the negative binomial (Fig. 4) are consistent with the anchovy laboratory data and that for the Pacific sardine analyzed by Ahlstrom (1943).

SUGGESTIONS FOR FUTURE RESEARCH

Three characteristics of the anchovy make the assignment of ages possible: One is that the anchovy egg is demonstrably spawned during a limited period in each day; another factor is that stages have been assigned so that their duration is about one-third of a day so that ages can be unequivocally assigned if the temperature and time of tow is known; lastly, the total incubation time is about 3 d (see Table 7).

This leads one to the questions: How would one estimate egg production if the eggs were produced at all hours of the day? How would one proceed if the total incubation time were <1 d?—more than 10 d?

Research on these questions could proceed along these lines. For the case of the long incubation period, it is not necessary to follow the course of mortality through the entire incubation period. For example, if the incubation period were 14 d and the ages of eggs could readily be determined for only 3 d, the mortality and production rate from that period would suffice for an estimate of the production of spawn; the ensuing stages of eggs would not even have to be counted or staged.

---

[2] E. M. Sandknop, Biological Technician, and E. L. Stevens, Fishery Biologist, Southwest Fisheries Center, National Marine Fisheries Service, NOAA, P.O. Box 271, La Jolla, CA 92038, pers. commun. Dec. 1981.

The rate of production could probably be estimated without knowing the time-of-day of spawning. For example, in Table 8 estimates of rate of production could be determined solely from empirical abundance information and incubation time. For the purpose of this exercise, I have assumed that the 11 stages are incubated in 66 h, or 6 h/stage. Deviations of abundance from the regression estimate of abundance are of two kinds: Sampling variability and duration differences from the even duration assumption. If sampling variability is ignored, then stage lengths longer or shorter than the average stage duration can be estimated.

ACKNOWLEDGMENTS

We would like to acknowledge the assistance of Carol Kimbrell for organizing and conducting the temperature laboratory experiments, H. Geoffrey Moser and his staff for providing data on staged eggs, Nancy Lo, Susan Picquelle, and Gary Stauffer for determining the age of eggs from field samples, James R. Thrailkill, Rich Charter, and William C. Flerx for planning and conducting the field surveys, designing and constructing the sampling equipment, and Cynthia Meyer and Celeste Santos for entering and checking the egg survey data. We are particularly grateful to Richard Methot who read an early draft of this manuscript.

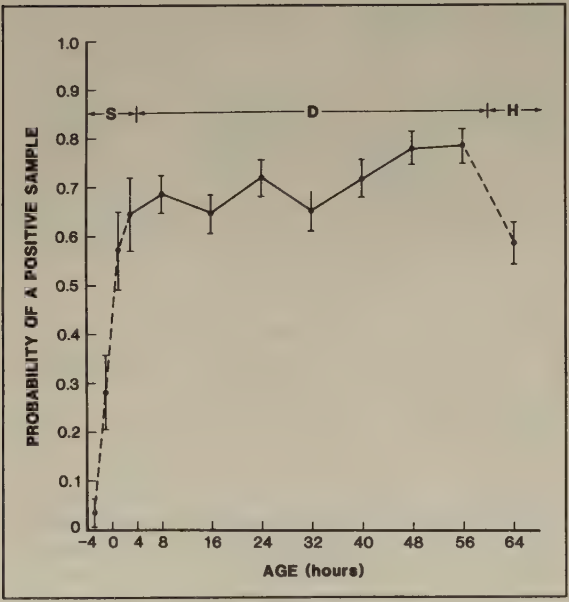

Figure 2.—Time course of proportional occurrence (number of observations with eggs of a given age divided by the number of observations with any age anchovy egg). Dashed lines under "S" indicate observations during the spawning period. The dashed line under "H" represents observations during the hatching period. The process assumed to control the solid line under "D" is dispersal.

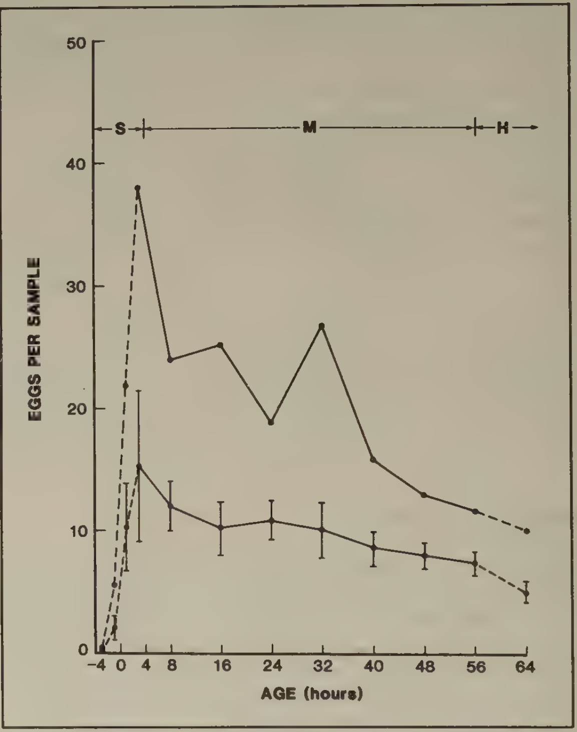

Figure 3.—Time course of the primary statistical parameters, the arithmetic mean (below), the standard deviation of the observations (above), and the standard error of the mean (cross-bars on the arithmetic mean line). Within ages the standard deviation is believed to be a function of the mean, and this function of the mean changes with time owing to dispersal (see Figure 4). Standard error of the mean bars are ±2 (or approximately the 95% limits). For this illustration the number of observations is 1,666 taken between 1980 and 1983 as part of the egg production method estimate of anchovy spawning biomass. The dashed lines under "S" and "H" represent spawning and hatching as in Figure 2. The principal process controlling the slopes of the standard deviation and mean under "M" is mortality. The convergence of the standard deviation and mean lines is caused by dispersal of eggs.

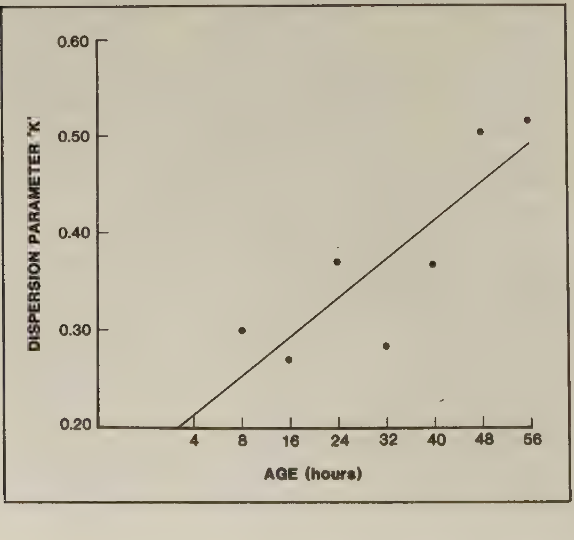

Figure 4.—Negative binomial distribution is represented by two parameters: the arithmetic mean (see Figure 3) and "k", the "dispersion parameter." The points represent maximum-likelihood fits to sample data in seven 8-h intervals which contain samples unbiased by spawning or hatching. The line represents the linear least-squares fit to these points.

Table 7.—Cumulative incidence of laboratory-spawned and reared northern anchovy eggs and larvae.

Age	Stage of development							Larvae	
(h)	IV	V	VI	VII	VIII	IX	X	2.5 mm	3.0 mm
16	0				**at 13.5°C**				
24	0.226	0							
32	0.812	0.204	0						
40	0.995	0.723	0.128	0	0				
48	1.000	0.985	0.759	0.265	0.032	0			
56		1.000	0.992	0.907	0.552	0.032	0	0	
64			1.000	1.000	1.000	0.684	0.174	0.100	0
72						0.947	0.802	0.292	0.004
80						1.000	1.000	0.724	0.014
88								0.880	0.271
96								0.975	0.554
104								1.000	0.763
112									0.843
120									0.888
128									0.977
136									1.000
16	0.028	0			**at 15.1°C**				
24	0.591	0.010	0						
32	0.963	0.505	0.075						
40	1.000	0.965	0.459	0	0				
48		1.000	0.974	0.458	0.016	0			
56			1.000	0.981	0.874	0.273	0	0	
64				1.000	0.976	0.929	0.500	0.145	0
72					1.000	1.000	1.000	0.436	0.078
80								1.000	0.230
88									0.527
96									0.810
104									0.868
112									1.000
16	0.025	0			**at 16.3°C**				
24	0.766	0.069	0						
32	0.944	0.881	0.231	0					
40	1.000	1.000	0.923	0.570	0.037	0			
48			1.000	0.974	0.880	0.210	0	0	
56				1.000	1.000	0.746	0.387	0.250	0.004
64						1.000	1.000	0.625	0.046
72								0.837	0.367
80								1.000	0.685
88									0.930
96									1.000

Table 8.—Empirically derived stage durations of northern anchovy eggs.

Stage	$\bar{X}$	2SE	4X	T	RE	D	CUM	F	L	d
I	0.77	0.28	3.08	3	13.78	1.34	0- 1.34	0.67	—	
II	5.34	0.80	21.36	9	12.85	9.98	1.34-11.32	6.33	6.42	−0.09
III	3.86	0.76	15.44	15	11.98	7.73	11.32-19.05	15.19	13.55	1.64
IV	2.79	0.48	11.16	21	11.17	6.00	19.05-25.05	22.05	21.12	0.93
V	2.75	0.62	11.00	27	10.41	6.34	25.05-31.39	28.22	30.70	−2.48
VI	3.06	0.44	12.24	33	9.71	7.56	31.39-38.95	35.17	39.24	−4.07
VII	2.28	0.36	9.12	39	9.05	6.04	38.95-44.99	41.97	47.13	−5.16
VIII	1.65	0.22	6.60	45	8.44	4.69	44.99-49.68	47.34	52.07	−4.73
IX	2.45	0.14	9.80	51	7.87	7.47	49.68-57.15	53.42	56.28	−2.86
X	1.86	0.10	7.44	57	7.34	5.92	57.15-63.07	60.11	62.63	−2.52
XI	0.44	0.074	1.76	63	6.84	1.54	63.07-64.61	63.84	65.65	−1.81

$\bar{X}$ = mean number of eggs by stage (n = 1,666) per observation
SE = standard error of number of eggs by stage.
4X = daily production by stage if duration is 6 h per stage.
T = midtime of stage if duration is 6 h per stage.
RE = regression estimate of abundance (first approximation).
D = duration of stage in hours if regression error is ignored.
CUM = cumulated age of stages in hours.
F = midtime of each stage estimated from field data.
L = midtime of each stage estimated from lab experiment.
d = difference in hours.

LITERATURE CITED

AHLSTROM, E. H.

1943. Studies on the Pacific pilchard or sardine (*Sardinops caerulea*). 4. Influence of temperature on the rate of development of pilchard eggs in nature. U.S. Fish Wildl. Serv. SSR 23, 26 p.

1965. A review of the effects of the environment on the Pacific sardine. *In* Intl. Comm. Northwest Atlantic Fisheries Spec. Publ. 6, p. 53-74.

ALHEIT, J.

1985. Spawning frequency of Peruvian anchovies taken with a purse seine. *In* R. Lasker (editor), An egg production method for estimating spawning biomass of pelagic fish: Application to the northern anchovy, *Engraulis mordax*, p. 59-61. U.S. Dep. Commer., NOAA Tech. Rep. NMFS 36.

BAKUN, A., and R. H. PARRISH.

1982. Turbulence, transport, and pelagic fish in the California and Peru Current Systems. Calif. Coop. Oceanic Fish. Invest. Rep. 23:99-112.

BOLIN, R. L.

1936. Embryonic and early larval stages of the California anchovy, *Engraulis mordax*, Girard. Calif. Fish Game 22:314-321.

FIEDLER, P. C.

1978. The precision of simulated transect surveys of northern anchovy, *Engraulis mordax*, school groups. Fish. Bull., U.S. 76:679-685.

1983. Satellite remote sensing of the habitat of spawning anchovy in the Southern California Bight. Calif. Coop. Oceanic Fish. Invest. Rep. 24:202-209.

HEWITT, R. P.

1980. Distributional atlas of fish larvae in the California Current region; northern anchovy, *Engraulis mordax* (Girard), 1966 through 1979. CalCOFI Atlas 28, 101 p.

HEWITT, R. P., and R. D. METHOT, JR.

1982. Distribution and mortality of northern anchovy larvae in 1978 and 1979. Calif. Coop. Oceanic Fish. Invest. Rep. 23:226-245.

HICKEY, B. M.

1979. The California Current System - hypotheses and facts. Progress in Oceanography 8(4):191-279.

HUNTER, J. R., and B. J. MACEWICZ.

1980. Sexual maturity, batch fecundity, spawning frequency and temporal pattern of spawning for the northern anchovy *Engraulis mordax* during the 1979 spawning season. Calif. Coop. Oceanic Fish. Invest. Rep. 21:139-149.

HUNTER, J. R., N. C. H. LO, and R. J. H. LEONG.

1985. Batch fecundity in multiple spawning fishes. *In* R. Lasker (editor), An egg production method for estimating spawning biomass of pelagic fish: Application to the northern anchovy, *Engraulis mordax*, p. 67-77. U.S. Dep. Commer., NOAA Tech. Rep. NMFS 36.

KRAMER, D., and E. H. AHLSTROM.

1968. Distributional atlas of fish larvae in the California Current region: northern anchovy, *Engraulis mordax* (Girard). 1951 through 1965. CalCOFI Atlas 9, 269 p.

LASKER, R.

1975. Field criteria for survival of anchovy larvae: the relation between inshore chlorphyll maximum layers and successful first feeding. Fish. Bull., U.S. 73:453-462.

LASKER, R., J. PELAEZ, and R. M. LAURS.

1981. The use of satellite infrared imagery for describing ocean processes in relation to spawning of the northern anchovy (*Engraulis mordax*). Remote Sensing of Environment 11:439-453.

LO, N. C. H.

1985. A model for temperature-dependent northern anchovy egg development and an automated procedure for the assignment of age to staged eggs. *In* R. Lasker (editor), An egg production method for estimating spawning biomass of pelagic fish: Application to the northern anchovy, *Engraulis mordax*, p. 43-50. U.S. Dep. Commer., NOAA Tech. Rep. NMFS 36.

LYNN, R. J., K. A. BLISS, and L. E. EBER.

1982. Vertical and horizontal distributions of seasonal mean temperature, salinity, sigma-t, stability, dynamic height, oxygen and oxygen saturation in the California Current, 1950-1978. CalCOFI Atlas 30, 513 p.

MacCALL, A. D.

1983. Population models of habitat selection, with application to the northern anchovy. Ph.D. Thesis, Univ. Calif. San Diego, 170 p.

MAIS, K. F.

1974. Pelagic fish surveys in the California Current. Calif. Dep. Fish Game, Fish Bull. 162, 72 p.

MANLY, B. F. J.

1974. A note on the Richards, Waloff and Spradbery method for estimating stage specific mortality rates in insect population. Biom. Zeitschr. 17:77-83.

MILNE, A. A.

1959. The centric systematic area-sample treated as a random sample. Biometrics 15(2):270-297.

MOSER, H. G., and E. H. AHLSTROM.

1985. Staging anchovy eggs. *In* R. Lasker (editor), An egg production method for estimating spawning biomass of pelagic fish: Application to the northern anchovy, *Engraulis mordax*, p. 37-41. U.S. Dep. Commer., NOAA Tech. Rep. NMFS 36.

PELAEZ, J., and F. GUAN.

1982. California Current chlorophyll measurements from satellite data. Calif. Coop. Oceanic Fish. Invest. Rep. 23:212-225.

POWER, J.

1983. Larval anchovy (*Engraulis mordax*) drift in the California Current. Results of a simulation model. Natl. Mar. Fish. Serv., NOAA, Southw. Fish. Cent., La Jolla, CA, Admin. Rep. LJ-83-23, 36 p.

SMITH, P. E.

1978. Biological effects of ocean variability: time and space scales of biological response. Rapp. P.-V. Réun. Cons. Int. Explor. Mer 173:117-127.

SMITH, P.E., and R. P HEWITT.

1985. Anchovy egg dispersal and mortality as inferred from close-interval observations. Calif. Coop. Oceanic Fish. Invest. Rep. 26:97-110.

SMITH, P. E., and R. LASKER.

1978. Position of larval fish in an ecosystem. Rapp. P.-V. Réun. Cons. Int. Explor. Mer 173:77-84.

SOUTHWOOD, T. R. E.

1978. Ecological Methods: With particular reference to the study of insect populations. Chapman and Hall, Lond., 524 p.

8588

The CalCOFI Vertical Egg Tow (CalVET) Net

PAUL E. SMITH, WILLIAM FLERX,
and ROGER P. HEWITT[1]
Southwest Fisheries Center,
National Marine Fisheries Service, NOAA,
P.O. Box 271, La Jolla, CA 92038

ABSTRACT

The vertical egg tow (CalVET) net was devised by CalCOFI (California Cooperative Oceanic Fisheries Investigations) to estimate egg production in the central subpopulation of northern anchovy and similar fishes. This paper describes the sampling characteristics of the net and its interaction with physical and distributional features of the anchovy egg. Problems discussed include the horizontal patchiness of the eggs and intensity of their distribution, volume and depth distribution of the water filtered, egg retention, and towing characteristics of the net.

The mouth area of the CalVET net is 0.05 m^2; the tow is vertical to minimize the volume of water filtered per unit depth; the mesh size of 0.150 mm is selected for total retention of the anchovy eggs under all likely conditions. The mesh area of the net is three times the mouth area in the conical portion and five times the mouth area in the cylinder. The conical mesh is the minimum size necessary for highly efficient filtration, while the cylindrical portion reduces the probability of the net clogging during a single tow. A flowmeter detects sequential clogging of the net during a series of tows. The net is lowered and raised rapidly to diminish the effects of ship drift and undersea currents which impose uneven trajectories on the net. The net is probably not capable of sampling active larvae 5 mm or longer, owing to the small mouth size and the disturbance to the net's path from the towing wire.

Design and working drawings of the frame and net are included.

HORIZONTAL PATCHINESS

We assume that eggs are released in the open sea by the gravid females of a northern anchovy school in close proximity to one another where they are fertilized by males. Previous samples of anchovy and sardine eggs indicated that most are found at densities of 1,000 to 5,000 eggs/m^2 when spawned, although only a small proportion of the samples actually contained eggs at these densities (Smith 1973; Smith and Richardson 1977:84). There is also evidence that most eggs are found in the upper 70 m of the water column (Ahlstrom 1959; Pommeranz and Moser 1983).

To shorten the sorting time for samples, we used a small net, 0.05 m^2 in cross section. To reduce the time spent sorting out the anchovy eggs from plankton, we used a vertical tow through the upper 70 m rather than a normal oblique tow, since a vertical tow captures far less extraneous plankton. Sample simulations on existing data for unstaged and staged anchovy eggs indicated that adequate sample precision could be obtained with 500 to 1,000 positive egg samples.

Previous studies by sonar, oblique plankton tow samples, and observations of spawning in the laboratory indicated three contributors to horizontal patchiness of anchovy eggs in the sea: 1) The act of fertilization; 2) the schooling habit; and 3) the propensity of schools to be contagiously distributed. The expected scale of horizontal patchiness from the act of fertilization is of the order of meters to tens of meters. The expected scale of horizontal patchiness from the schooling habit ranges from hundreds to thousands of meters. The expected scale of patchiness from the school group scale is of the order of kilometers to tens of kilometers. A study using eight replicate tows per station identified the school scale as the primary source of variance. Samples replicated at the same station indicated that only during the first half day after spawning was the fertilization swarm a significant source of variance relative to the school-size scale. To achieve statistical independence among adjacent samples, we decided to space the samples at least 3 km apart. The most usual spacing between samples has been 6 km in the offshore-onshore direction and about 16 or 32 km in the alongshore direction.

DEPTH DISTRIBUTION OF WATER FILTERED

The design objective of the CalVET tow was to filter a uniform and measured volume of water for each increment of depth from 70 m to the surface. The chief barriers to this goal are 1) ship drift and undersea currents, 2) clogging of the net, and 3) cyclic vertical motions of the towing wire caused by the heave and roll of the ship (Hewitt 1983).

The primary effect of ship drift and undersea currents is to distort the distribution of water filtered/unit surface area to a given depth. The ideal tow as designated here is to sample about 50 L water/m of depth to a depth of 70 m, or to near-bottom in shallow waters. First of all, ship drift and undersea currents diminish the depth attained with the fixed length of towing wire. For example, if the wire has strayed from the vertical by 30°, 70 m of wire will achieve only 61 m depth. Similarly 5° stray will affect the depth attained by less than 1 m. Secondly, ship drift and undersea currents change the angle of stray with time. For example, the net when vertical will filter 50 L water/m of depth, and at 30° the net will filter 58 L water/m of depth. Our usual experience is that the oversampling occurs in the upper layers relative to the deeper layers. In the recommended sample series all tows are repeated when the angle of stray has exceeded 30°.

---

[1] Present address: Commanding Officer, NOAA Ship *Miller Freeman*, Pacific Marine Center, 1801 Fairview Ave. East, Seattle, WA 98102.

The most important specification in this category is that the net must emerge from the water at right angles to the surface. It is known from horizontal samples at the surface that great concentrations of eggs may exist there, thus to drag the net along the surface toward the ship is to risk vast oversampling of the eggs.

The chief error caused by clogging of the meshes of the net is the relative undersampling of the shallow vs. deep water in an ascending vertical tow. It is conceivable that a net which is filtering 50 L/m of depth might clog in the upper layers and filter 40 or fewer liters per m of depth (Smith et al. 1968). The viscous resistance of the filtering surface requires that about three times as much mesh aperture as mouth aperture is required to filter water efficiently. For this reason the CalVET net is fitted with a truncated conical portion which contains three times as much mesh aperture area as the opening of the net. Since the mesh chosen is about 46% open area, the 0.15 m^2 aperture area of the conical section is achieved with 0.33 m^2 of mesh. In addition, to diminish the danger of the net changing filtration efficiency during the tow due to clogging, the net is fitted with a mesh cylinder with five times the mesh aperture area compared with the mouth opening of the net. This should be ample for a tow this length and with this mesh size (0.333 mm; see below) in coastal waters off California.

Filtering efficiencies of 97% are possible with simple net apertures. Efficiencies of 100% and more are possible with inverted conical net entrances like the original Hensen net. The complicated Hensen technique was not chosen because the filtration efficiency becomes a function of net speed, and the placement of the flowmeter in the flow section to obtain a representative sample of water filtered is poorly understood. Also, reverse cone structures increase the lateral drag of the net and worsen the consequences of ship drift and undersea currents. The design of the CalVET net makes clogging unlikely within a tow; thus the use of a flowmeter is not required to verify the constant filtration of water per unit depth. However, nylon nets are subject to sequential clogging in a series of tows, and flowmeters are recommended to ascertain and correct this problem. Deviations of flowmeter revolutions of 10% or more should be cause for exchange or careful washing of the net. For example, a calibration factor of 0.273 m/revolution of the flowmeter would predict that 256 revolutions be characteristic of a suitable tow from 70 m to the surface. Flow readings of 231 revolutions for the full tow, or 3.3 revolutions/m of wire out in shallow tows, would indicate that a sequence of clogging between tows may have begun.

Another retention problem with vertical net tows relative to horizontal and oblique tows is the direct connection of the net to the ship. The roll and heave of the ship could at times impart velocities to the net less than or in excess of design expectations. Several consequences are possible between motion of the net and the ship's roll and heave. The most serious problem is noted with simultaneous roll and heave downward when the net containing eggs approaches the surface (Hewitt 1983). Should the downward velocity exceed the recovery rate of the net, the net would collapse from below, there would be reverse filtration of water through the mesh apertures, and the eggs would be expelled from the mouth of the net. Probably the next most important danger is that when the net containing eggs approaches the surface, the simultaneous roll and heave upward will add the speed of the ship's motion to the already high speed of the net recovery wire. In this case, the eggs lying on the mesh might be ruptured or extruded through the mesh apertures. Quantitatively less important, perhaps, is the likelihood that a net at depth might be propelled upward fast enough to filter water and turn the flowmeter, thus oversampling the volume at that depth. The flowmeter is normally jammed against the mesh on the downward path. To diminish these effects, the net is lowered at 1-1.2 m/s and recovered at the same speed. In this way we achieve a depth of 70 m in 1 min and recover at the same speed. The net is stopped for 10 s at the bottom. Tows which vary substantially from this regimen should be repeated.

RETENTION OF ANCHOVY EGGS

The main considerations in retention of anchovy eggs by the CalVET net are the relative size of the egg, the mesh aperture, and the filtration velocity. The minimum dimension of the northern anchovy's egg is about 0.65-0.85 mm in February, and 0.55-0.80 mm in August (Smith and Richardson 1977:61). Such an object should be fully retained by mesh sizes <0.4 mm according to the "diagonal rule." The diagonal rule states that the minimum dimension of the object to be sampled should be greater than the diagonal of the mesh aperture. Absolute retention is affected also by the filtration velocity. For example, the CalVET net proceeds through the water at a nominal velocity of 70 m/min. The active filtering surface is about three times the net mouth area, thus the filtration velocity is 1.2 m/s divided by 3, or 0.4 m/s. This is a high filtration velocity relative to the normal oblique tows. Thus the net mesh size for the CalVET was selected to be 0.150 mm. The main reason for the high net velocity is to diminish the time for errors of ship drift and undersea current to accumulate.

DESIGN AND WORKING DRAWINGS OF THE CalVET NET

The CalVET frame and net are much smaller than traditional ichthyoplankton nets: 0.25 m diameter mouth opening (0.05 m^2 mouth area) and the total length of the net is <1.5 m. The net is lowered to a depth of 70 m and retrieved vertically at 70 m/min; strict controls govern the field procedures, and a tow is rejected if the wire strays too far from the vertical or if the retrieval rate is too fast or too slow. The results from field testing the gear in 1979 indicated a very high degree of fidelity among eight replicates at a single station; the test was conducted over 70 stations and within a 200-fold range in egg abundance.

Figures 1-5 describe the bongo-type (PAIROVET) version of the CalVET sampler. The frame was designed to facilitate comparison of nets constructed of various materials and to provide replicate observations when using similar nets; it has become one of the standard samplers used by the Southwest Fisheries Center. The frame is constructed of 6061-T6 aluminum with stainless steel fittings. The nets are nylon mesh attached to the frame with adjustable stainless steel strapping. The cod end is removable and attached to the rest of the net by means of a plastic collar. The net and cod end are sewn inside a "sleeve" constructed of 2-mm mesh vinyl-coated polyester (not shown) to protect them from abrasion.

Nets of several mesh sizes have been used by the Southwest Fisheries Center. All have been constructed using the dimensions shown in the figure; total area of net material is 0.95 m^2. With the exception of the 0.035-mm mesh, all of the net materials have approximately the same porosity, i.e., the portion of the net area which is open. Smith et al. (1968) suggested that adequate filtering efficiency can be maintained in coastal waters if the ratio of aperture area to mouth area is at least 3.4 for a net of the proportions described. Thus, these nets may be expected to perform well with the exception of the very fine (0.035 mm) mesh net which may clog in turbid coastal waters (Table 1).

Table 1.—Ratio of aperture area to mouth area for various net mesh sizes. Nets with mesh <0.333 mm are protected by a 2-mm mesh nylon sheath. See text.

Mesh (mm)	Total area (m^2)	Porosity	Aperture area (m^2)	Aperture area/ mouth area
0.035	0.95	0.16	0.15	3.04
0.075	0.95	0.45	0.43	8.55
0.150	0.95	0.51	0.48	9.69
0.250	0.95	0.49	0.47	9.31
0.333	0.95	0.46	0.44	8.74
0.505	0.95	0.49	0.47	9.37

LITERATURE CITED

ALHSTROM, E. H.
1959. Vertical distribution of pelagic fish eggs and larvae off California and Baja California. Fish. Bull., U.S. 60:106-146.

HEWITT, R.
1983. Roll, heave and vertical ichthyoplankton tows. Ocean Sci. Eng. 8:41-51.

POMMERANZ, T., and H. G. MOSER.
1983. Vertical distribution study. R/V *Ellen B. Scripps*, March 19-April 4, 1980. Technical tow data and environmental observations and preliminary data lists and summaries of vertical distribution of northern anchovy (*Engraulis mordax*) eggs and larvae. Southw. Fish. Cent., Natl. Mar. Fish. Serv., NOAA, P.O. Box 271, La Jolla, CA 92038, Admin. Rep. LJ-83-01, 368 p.

SMITH, P. E.
1973. The mortality and dispersal of sardine eggs and larvae. Rapp. P.-v. Reun. Cons. int. Explor. Mer 164:282-292.

SMITH, P. E., R. C. COUNTS, and R. I. CLUTTER.
1968. Changes in filtering efficiency of plankton nets due to clogging under tow. J. Cons. Perm. Int. Explor. Mer 32:232-248.

SMITH, P. E., and S. L. RICHARDSON.
1977. Standard techniques for pelagic fish egg and larva surveys. FAO Fish. Tech. Pap. 175, 100 p.

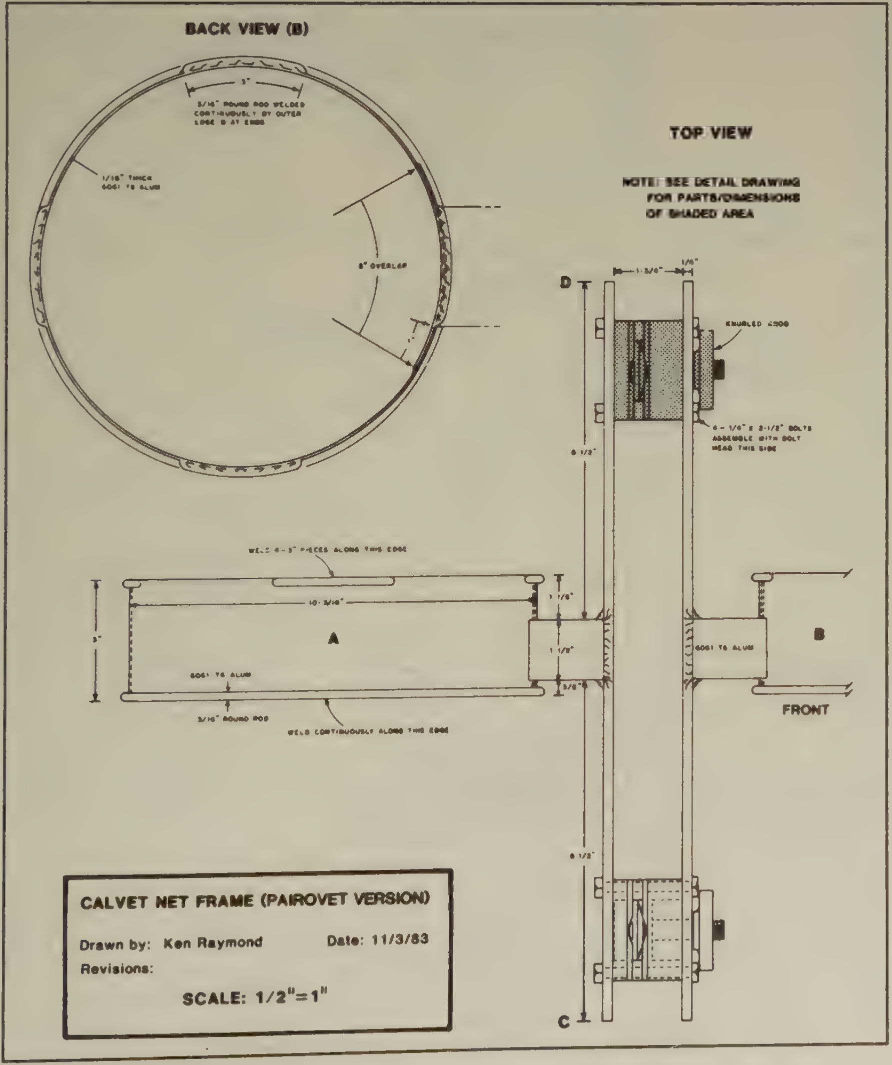
BACK VIEW (B)
3"
3/16" ROUND ROD WELDED CONTINUOUSLY BY OUTER EDGE & AT ENDS
1/16" THICK 6061 T6 ALUM
8" OVERLAP
1"
TOP VIEW
NOTE: SEE DETAIL DRAWING FOR PARTS/DIMENSIONS OF SHADED AREA
D
1-3/4"
1/8"
KNURLED KNOB
4 - 1/4" x 2-1/2" BOLTS ASSEMBLE WITH BOLT HEAD THIS SIDE
8 1/2"
WELD 4 - 3" PIECES ALONG THIS EDGE
10-3/16"
3"
A
6061 T6 ALUM
3/16" ROUND ROD
WELD CONTINUOUSLY ALONG THIS EDGE
1 1/8"
1 1/8"
3/8"
6061 T6 ALUM
B
FRONT
8 1/2"
C
CALVET NET FRAME (PAIROVET VERSION)
Drawn by: Ken Raymond
Date: 11/3/83
Revisions:
SCALE: 1/2"=1"

Figure 1.—Back and top view of PAIROVET version of CalVET net frame.

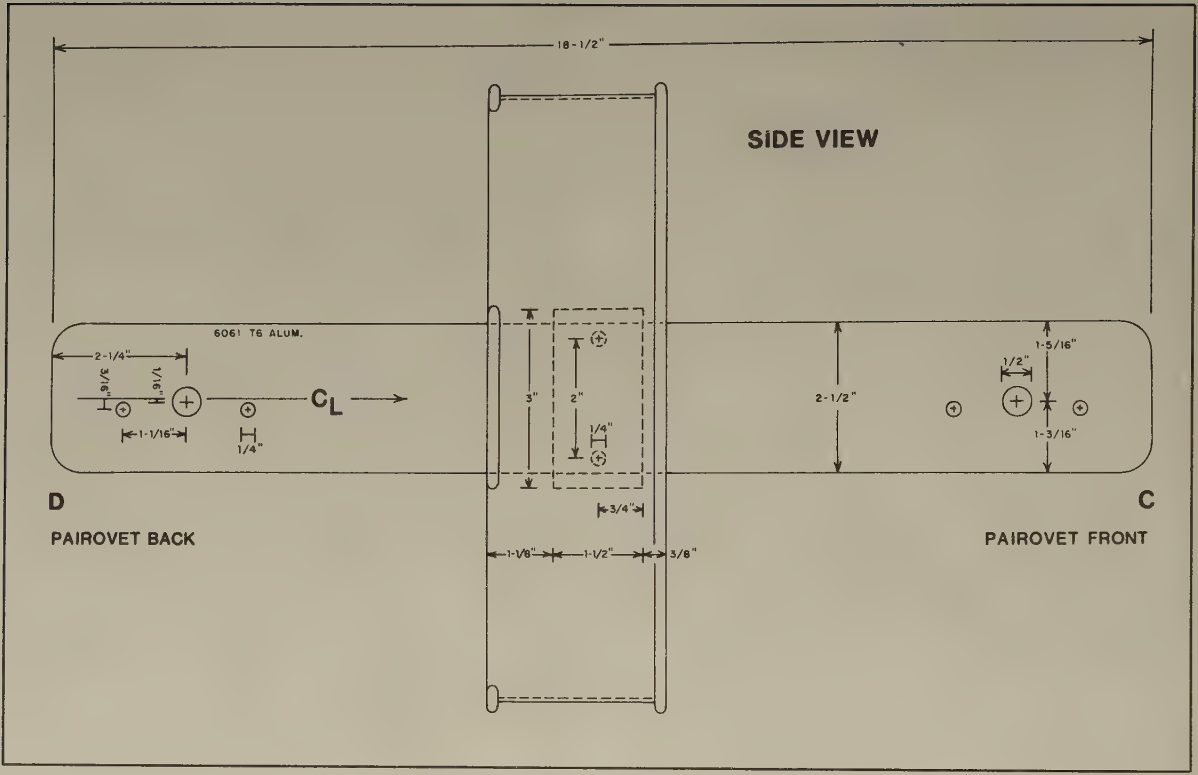
18-1/2"
SIDE VIEW
6061 T6 ALUM.
2-1/4"
3/16"
1/16"
C_L
1-1/16"
1/4"
3"
2"
1/4"
2-1/2"
1-5/16"
1/2"
1-3/16"
D
C
PAIROVET BACK
PAIROVET FRONT
3/4"
1-1/8"
1-1/2"
3/8"

Figure 2.—Side view of PAIROVET net frame.

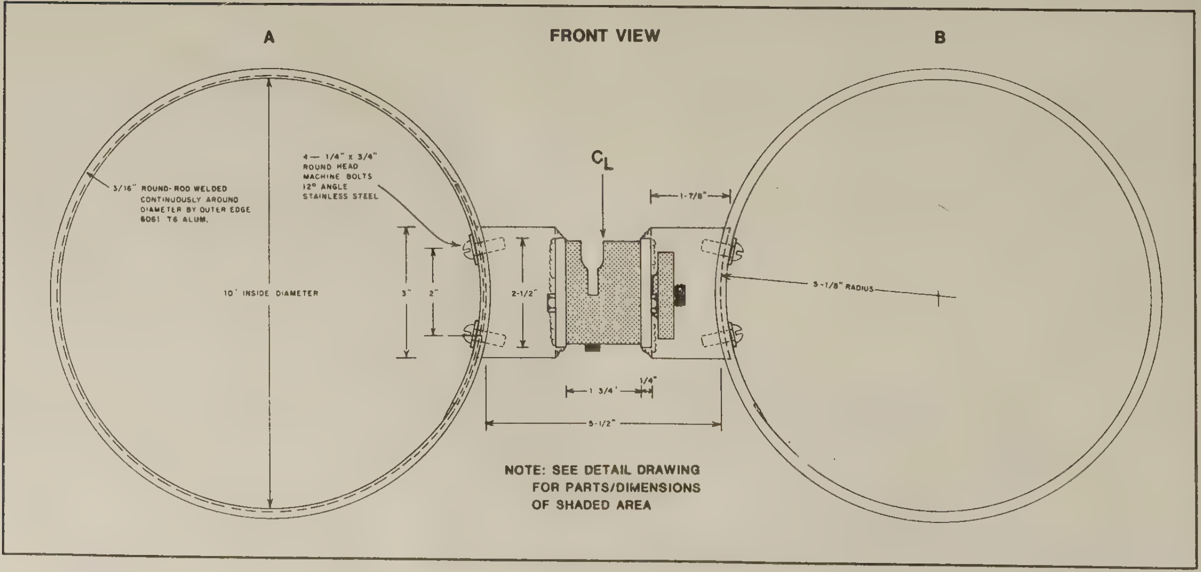
A
FRONT VIEW
B
3/16" ROUND-ROD WELDED CONTINUOUSLY AROUND DIAMETER BY OUTER EDGE 6061 T6 ALUM.
4— 1/4" x 3/4" ROUND HEAD MACHINE BOLTS 12° ANGLE STAINLESS STEEL
C_L
1-7/8"
10" INSIDE DIAMETER
3"
2"
2-1/2"
5-1/8" RADIUS
1 3/4"
1/4"
5-1/2"
NOTE: SEE DETAIL DRAWING FOR PARTS/DIMENSIONS OF SHADED AREA

Figure 3.—Front view of PAIROVET net frame.

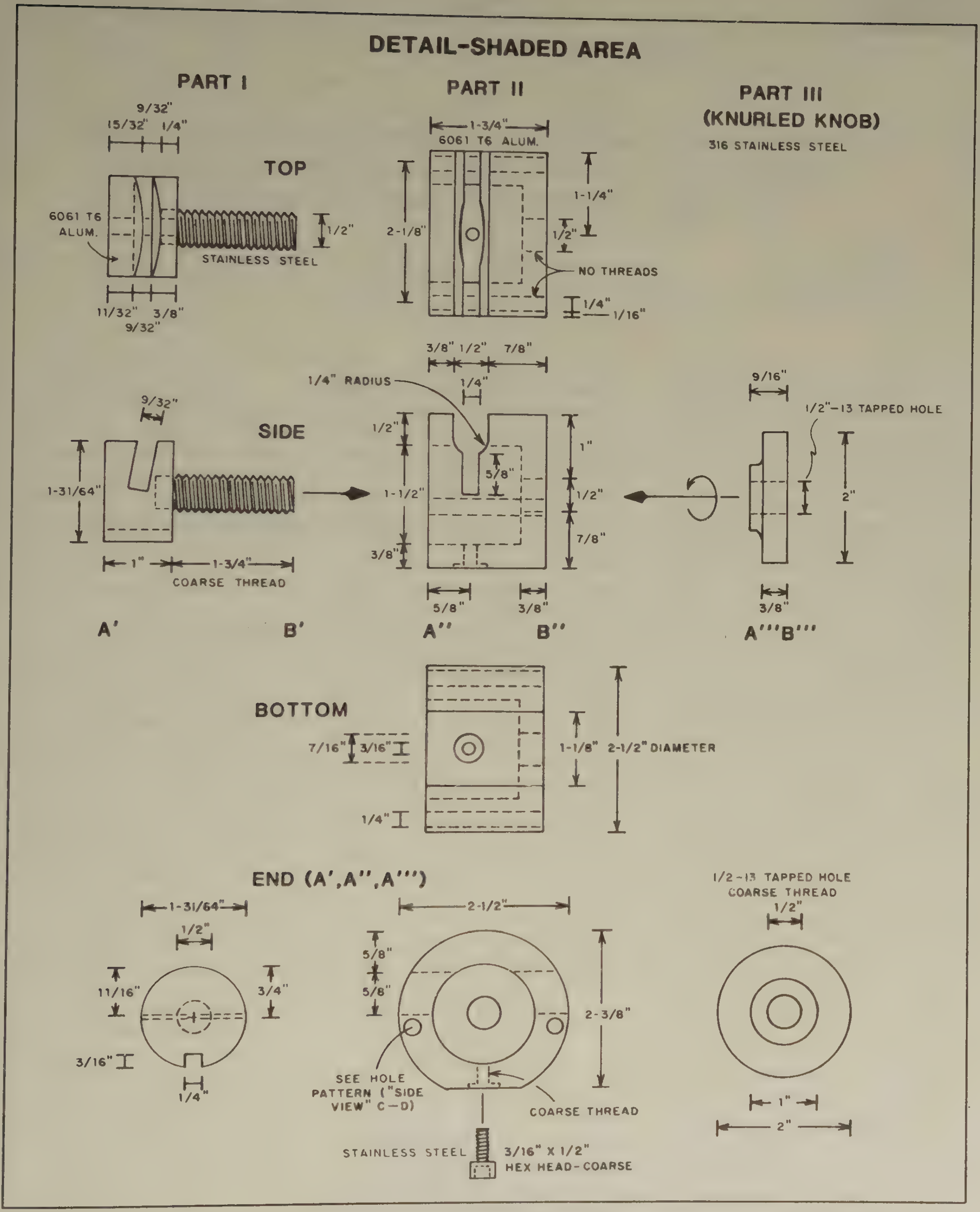
DETAIL-SHADED AREA
PART I
PART II
PART III
(KNURLED KNOB)
316 STAINLESS STEEL
9/32"
15/32"
1/4"
TOP
6061 T6
ALUM.
1/2"
STAINLESS STEEL
11/32"
3/8"
9/32"
1-3/4"
6061 T6 ALUM.
2-1/8"
1-1/4"
1/2"
NO THREADS
1/4"
1/16"
3/8"
1/2"
7/8"
1/4" RADIUS
1/4"
9/32"
SIDE
1/2"
1-31/64"
5/8"
1-1/2"
1"
1/2"
7/8"
3/8"
1"
1-3/4"
COARSE THREAD
5/8"
3/8"
9/16"
1/2"-13 TAPPED HOLE
2"
3/8"
A'
B'
A''
B''
A'''B'''
BOTTOM
7/16"
3/16"
1-1/8"
2-1/2" DIAMETER
1/4"
END (A',A'',A''')
1-31/64"
1/2"
11/16"
3/4"
3/16"
1/4"
2-1/2"
5/8"
5/8"
2-3/8"
SEE HOLE PATTERN ("SIDE VIEW" C—D)
COARSE THREAD
STAINLESS STEEL
3/16" X 1/2"
HEX HEAD-COARSE
1/2-13 TAPPED HOLE
COARSE THREAD
1/2"
1"
2"

Figure 4.—Detailed view of wire attachment for PAIROVET net frame. "Shaded area" refers to Figure 3.

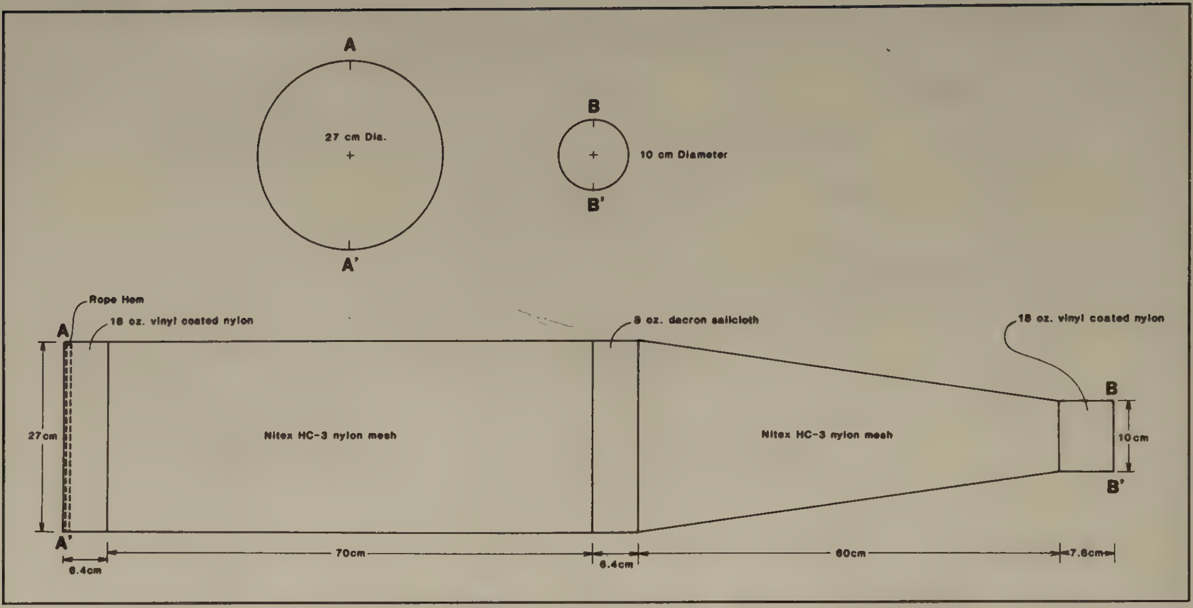
A
27 cm Dia.
A'
B
10 cm Diameter
B'
Rope Hem
18 oz. vinyl coated nylon
A
A'
27cm
Nitex HC-3 nylon mesh
9 oz. dacron sailcloth
Nitex HC-3 nylon mesh
18 oz. vinyl coated nylon
B
B'
10cm
6.4cm
70cm
6.4cm
60cm
7.6cm

Figure 5.—CalVET net dimensions. For nets with mesh sizes <0.333 mm, a protective sheath of 2-mm mesh nylon is used. See Table 1.

8589

Relationship of Sea Surface Temperature Isotherm Patterns off Northwestern Mexico to the Catch of Striped Marlin, *Tetrapturus audax*, off Southern California

JAMES L. SQUIRE, Jr.

Introduction

The relationship of sea surface temperatures to the availability of striped marlin, *Tetrapturus audax*, off southern California has interested both fishery researchers and recreational billfish fishermen. The establishment of a reasonable correspondence would provide an indicator of variations in catch resulting from anomalous environmental conditions.

Uda (1957) outlined the basic biological principles of the association between the environment, as represented by one parameter, sea surface temperature (SST), to the catch of tunas, Scombridae; and billfishes, Istiophoridae. In his paper, he discussed some of the principles of fish distribution for such larger pelagics as tunas and billfishes, including the one which states that "marine organisms are distributed according to the variable environment (hydrobiological) conditions which they require for successful development." This paper describes one such association between the distribution of striped marlin and sea surface temperature.

Many researchers have reviewed the migration of pelagic species off the North American west coast (yellowtail, *Seriola lalandei*; Pacific bonito, *Sarda chiliensis*; Pacific barracuda, *Sphyraena argentea*; white seabass, *Atractoscion nobilis*; and skipjack tuna, *Euthynnus pelamis*) into more northern latitudes during years of anomalous warm sea surface temperatures (Hubbs and Schultz, 1929; Walford, 1931; Radovich, 1961). The number of studies comparing the catches of coastal northeast Pacific pelagic species to SST changes is limited and the more recent ones are by Radovich (1961, 1975) and Squire (1982).

Several studies relate striped marlin catch to SST. Squire (1974) made a comparison of striped marlin catch rates in southern California from 1963 through 1970 for periods with either continuous or discontinuous 68°F (20.0°C) and 70°F (21.1°C) isotherm extensions into the southern California area from the south or southwest. Bimonthly temperature charts produced by the NMFS Southwest Fisheries Center, La Jolla, Calif., were used in the 1963-70 analysis. The current analysis extends the hypothesis which was first described in the 1974 study. In that study, Squire speculated that the continuity of isotherm patterns crossing the Pacific Ocean from the west and recurving northward into southern California waters may have a greater influence on the catch of striped marlin than sea surface temperature observed in fishing areas off southern California.

SST Climatology vs. Striped Marlin Catch

Uda (1957) provided a range of sea surface temperatures for a number of oceanic pelagic species of tunas and billfishes, including those for striped marlin. Optimum SST's for striped marlin, determined from commercial longline catch data, ranged from 18.5°C (64.4°F) to 24°C (75.1°F), with a minimum and maximum range of temperature from 16°C (60.8°F) to 29°C (84.2°F).

Studies of SST associated with catch of striped marlin off southern California (catch temperature) in the early 1970's were made by Squire (1974) and Talbot and Wares (1975). These studies used SST measurements from airborne infrared equipment or nearshore and shipboard measurements, and the striped marlin catch off southern California as recorded by the major billfish clubs. Striped marlin catch data for both studies were obtained from the records of one or more of the following organizations: The Tuna Club, Avalon, Catalina Island, Calif.; Balboa Angling Club, Balboa, Calif.; and The Marlin Club, San Diego, Calif.

Mean catch-temperature for striped marlin landed at San Diego was calculated by Squire (1974) based on temperature data derived from monthly airborne infrared SST surveys of southern California waters in 1963-68 (Squire, 1971) and catch location data for the same period obtained from records of The Marlin Club, San Diego, Calif. Catch-temperature for a sample size of 3,595 fish ranged from 61°F (16.1°C) to 73.0°F (22.8°C) with a mean catch temperature of 67.8°F (19.9°C) and a standard deviation of 0.5°F (0.9°C). This temperature is slightly below the midpoint (69.7°F or 20.8°C) of the optimum temperature range for striped marlin as defined by Uda (1957).

In their study on striped marlin catch-temperature, Talbot and Wares (1975) used SST data recorded at Scripps Pier, located at the Scripps Institution of Oceanography, La Jolla, Calif. They made three statistical tests from the data.

James L. Squire, Jr., is with the Southwest Fisheries Center, National Marine Fisheries Service, NOAA, P.O. Box 271, La Jolla, CA 92038.

Landings of striped marlin during the month of August from 1960 through 1970 at Avalon, Balboa, and San Diego were compared with sea surface temperatures at Scripps Pier. Correlation coefficients (r^2) (Snedecor, 1956) between SST and landings were 0.39 for Avalon, 0.26 for San Diego, and 0.35 for Balboa landings. Only the correlation for Avalon landings was significant (1 percent level).

In the second approach, Talbot and Wares (1975) used mean monthly SST's determined from Scripps Pier data for June through September (1960-70) and landings at Avalon, Balboa, and San Diego. Correlation coefficients were 0.47 for Avalon, 0.39 for Balboa, and 0.50 for San Diego. Correlation with the Avalon data was significant at the 1 percent level, and with San Diego data at the 5 percent level. Balboa catch data were not significantly correlated with Scripps SST data.

In the third test, Talbot and Wares (1975) used SST data developed bimonthly from 1947 through 1966 by the National Marine Fisheries Service, La Jolla, Calif., for three areas of 2° longitude by 2° latitude off southern California. The three areas included the major striped marlin catch areas off southern California. Correlation coefficients between SST and catches for the three areas were 0.42 for Avalon, 0.42 for Balboa, and 0.32 for San Diego. None of the coefficients was significant at the 5 percent level. Based on the available data, Talbot and Wares (1975) found that only 15-25 percent of the variation in striped marlin catch was related to SST changes off southern California. In the discussion, they stated that since a small amount of variation could be attributed to SST changes, other factors were more important than local water temperatures in determining catch of striped marlin in southern California waters.

Important Fishery Characteristics

The southern California sport fishing season for striped marlin extends from late July to early November, the months of latitudinal warming. Normally, no catches are recorded for the period from December through early June. Angler catch rates in this area are 4-5 times lower than those observed about the southern tip of Baja California Sur, Mexico, where striped marlin are caught during all months of the year by both sportfishermen and commercial longliners.

High catch rates for striped marlin have been recorded by Japanese longline operations off the southern portion of the Baja California Sur, Mexico, peninsula during all months of the year. Japanese longline data from commercial and exploratory operations show low hooking rates for striped marlin west and southwest of southern California within the California Current region during all months of the year (Anonymous, 1964-80).

The results of tagging striped marlin in the recreational fishery about the southern tip of Baja California Sur, Mexico, indicate some movement from this area toward the northwest or southern California in early summer. Some of the striped marlin tagged off the east coast of the southern tip of the Baja California peninsula have been recovered off Magdalena Bay, Mexico, northwest of the southern tip of Baja California Sur, and off southern California. The precise migration route of these tagged fish is unknown; however, the relatively short period of time between tagging off Baja California Sur, Mexico, and recovery off Magdalena Bay and southern California indicate movement to the northwest during the late spring and early summer season.

Important Oceanographic Characteristics

The ocean off southern California, sometimes called the Southern California Bight, supports a major sportfishing area for striped marlin. The general boundaries of the Bight extend from Point Conception to near the northwestern border of Baja California, Mexico. The marine environment of the Bight is different from the areas along the west coast immediate to the northwest and the southeast. From studies of current patterns off southern California using drift bottles and cards by Tibby (1939), Schwartzlose (1963), Reid et al. (1958), and Squire (1977), it was determined that in the Bight a counterclockwise current pattern was sometimes evident. The southern California Bight has numerous eddies due to the effects of the chain of offshore islands.

Studies of sea surface temperature using an airborne infrared radiometer off southern California from Point Arguello to Pta. Salsipuedes, Mexico (near lat. 32°N), were conducted from 1963 to 1979 by the NMFS in cooperation with the U.S. Coast Guard (Squire, 1971). These temperature surveys covered the major fishing areas for striped marlin off southern California. During the late summer and early fall months, the period when striped marlin catches are made, temperature survey data indicate the warmest temperature to be in the Gulf of Santa Catalina. Based on catch records from 1960 to 1981, September is the month of greatest striped marlin catch in numbers. Airborne SST survey results showing a typical distribution of SST isotherms off southern California for September 1966 (from an airborne survey on 9-14-66) are shown in Figure 1. The 5-year average temperature isotherms observed in 10′ longitude by 10′ latitude areas for September airborne surveys (1963-67) are shown in Figure 2. Included in Figure 2 is an outline of the major striped marlin fishing areas off southern California.

Sea surface temperatures within the Southern California Bight are usually warmer during the summer, when compared with sea surface temperatures to the area north of Point Conception or south of the area near the U.S.-Mexico border. On many of the airborne infrared monthly charts (Squire, 1971) and the 5-year average chart, colder temperatures have been recorded (Fig. 1 and 2) denoting significant upwelling to the north and south of San Diego.

SST Isotherm Patterns and Their Relation to Catch

Talbot and Wares' (1975) study dealt with the correlation between the catch in the high catch rate areas and the sea surface temperatures at Scripps Pier as an indicator of the trend of temperature in the major fishing areas. Temperatures observed at Scripps Pier, La Jolla, Calif., were in most cases not the same

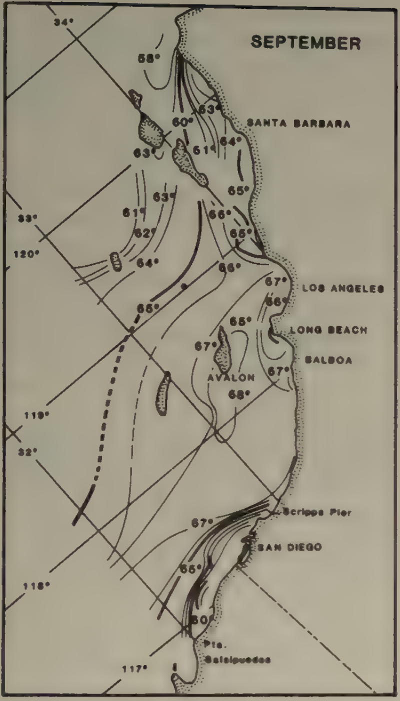
SEPTEMBER
34°
33°
32°
120°
119°
118°
117°
SANTA BARBARA
LOS ANGELES
LONG BEACH
BALBOA
AVALON
Scripps Pier
SAN DIEGO
Pta. Salsipuedes
58°
60°
61°
62°
63°
64°
65°
66°
67°
68°

Figure 1.—Infrared sea surface temperature isotherms off southern California typical of those observed by airborne infrared sea surface surrvey during the late summer. Survey is for 14 September 1966.

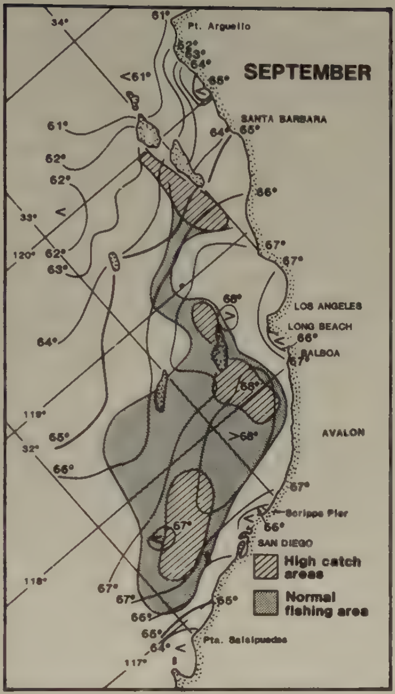
SEPTEMBER
Pt. Arguello
34°
33°
32°
120°
119°
118°
117°
SANTA BARBARA
LOS ANGELES
LONG BEACH
BALBOA
AVALON
Scripps Pier
SAN DIEGO
Pta. Salsipuedes
<61°
61°
62°
63°
64°
65°
66°
67°
68°
>68°
High catch areas
Normal fishing area

Figure 2.—Five-year mean sea temperature distribution (°F) for September airborne surveys conducted 1963-67 with outline of normal and high catch areas for striped marlin.

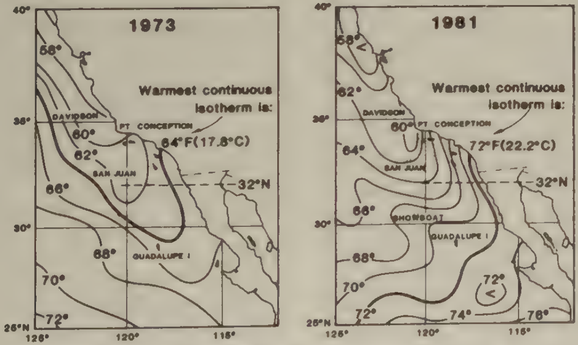
1973
Warmest continuous isotherm is:
64°F(17.8°C)
DAVIDSON
PT CONCEPTION
SAN JUAN
GUADALUPE I
-32°N
58°
60°
62°
66°
68°
70°
72°
40°
35°
30°
25°N
125°
120°
115°
1981
Warmest continuous isotherm is:
72°F(22.2°C)
DAVIDSON
PT CONCEPTION
SAN JUAN
SHOWBOAT
GUADALUPE I
-32°N
58°
62°
60°
64°
66°
68°
70°
72°
74°
76°

Figure 3.—Biweekly sea surface isotherm charts issued by the NMFS Southwest Fisheries Center showing examples of interception of isotherms at lat. 32°N for 16-30 September 1973 and 16-30 September 1981.

as those observed in the major fishing areas for striped marlin as shown in Figure 2. Since comparisons of SST data and catch for the southern California area have provided a rather inconclusive correlation, it was evident that striped marlin catch off southern California should be examined in relation to other environmental features. Thus, I decided to study the relationship between variation in catch and the changes in climatology of the ocean area off northwestern Baja California.

Sea surface temperature isotherm charts in 2°F (1.1°C) increments representing boundaries of areas having a mean temperature range for biweekly periods from July through November 1960-81 were used to determine the climatology of the area. These charts, which were published by the NMFS Southwest Fisheries Center, La Jolla, Calif., were examined to determine the warmest isotherm that extends continuously into southern California waters from the area south and west of a line extending off the coast at lat. 32°N (near Pta. Salsipuedes, Mexico). Examples of the warmest continuous isotherm are found on the charts for 16-30 September during 1973 and 1982 (Figure 3). That period in 1973 (Fig. 3) was characterized by low temperatures during the fishing season. For the same time period in 1981 (Fig. 3), very warm sea surface temperatures were observed. For the 1973 chart (Fig. 3) an example of the warmest continuous isotherm extending into southern California from the south or southwest at lat. 32°N is 64°F (18°C), and for the 1981 chart (Fig. 3), the warmest continuous isotherm observed was 72°F (22.2°C).

Catch data by biweekly periods from June through November 1960-81 were collected from The Marlin Club, San Diego, Calif. A total of 10,807 striped marlin were recorded during the 22-year period. Striped marlin landed during periods when isotherms of 62° - 72°F (16.7° - 22.2°C) were observed to be continuous into southern California at lat. 32°N were recorded. The frequency of striped marlin landings during different isotherm regimes for each 2-week period 16-31 July through 16-31 October 1960-81 is given in Table 1.

A linear regression was fitted in which the predictor variable was isotherm temperature (Table 1, column 1) and the criterion variable was mean number of striped marlin per 2-week period (Table 1, column 4). The results

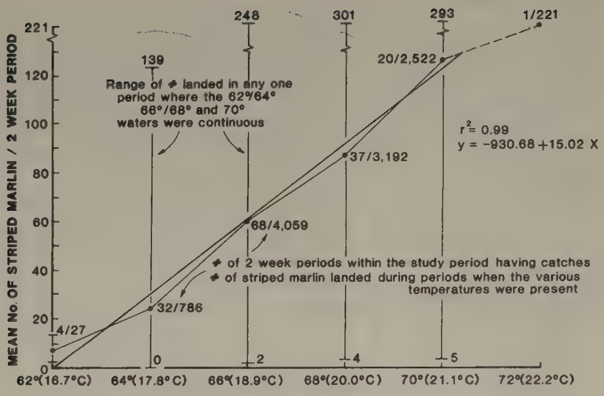

Figure 4.—Average number of striped marlin caught during 2-week periods (16-31 July through 16-31 October) and during periods when isotherms 62° - 70°F (16.7° - 21.2°C) were continuous at lat. 32°N. Data for 72°F (22.2°C) represent only one occurrence (16-30 September 1981) during the 1960-81 period. Range of catch observed within 2-week period for each isotherm is given.

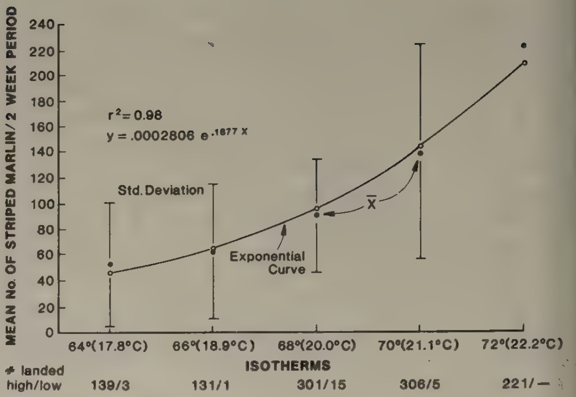

Figure 5.—Average number of striped marlin caught during 2-week periods, (1-15 August through 16-31 September) minimum and maximum number of striped marlin landed during each temperature, calculation of exponential curve and standard deviation of the mean catch observed for each temperature.

Table 1.—Number of striped marlin caught off southern California and number of periods from 16-31 July through 16-31 October when the 62°F-72°F (16.7° - 22.2°C) isotherms were the warmest isotherms continuous into southern California waters from the south, southwest, or west at lat. 32°N, 1960-81.

Isotherm °F(°C)	No. of 2-week periods when isotherms were present	Total no. of striped marlin landed	Mean no. of striped marlin per 2-week period
62°(16.7°)	4	27	6.8
64°(17.8°)	32	786	24.6
66°(18.9°)	68	4,059	59.7
68°(20.0°)	37	3,192	86.3
70°(21.1°)	20	2,522	126.1
72°(22.2°)	1	221	221.0

are presented in Figure 4. The relationship between mean catch data and the occurrence of progressively warmer isotherms is linear ($r^2 = 0.99$). However, the variation in catch (criterion) was substantial during periods when the 62° - 72°F (16.7° - 22.2°C) isotherms were continuous.

Examination of catch and temperature data of some of the larger pelagic fishes (yellowtail and Pacific bonito) off southern California by Squire (1982) indicates that the migration of fish northward from off Mexico during late spring and early summer is more related to increasing sea surface temperatures than is movement south out of southern California during the fall period of decreasing sea surface temperature. Therefore, the relationship between the catch of fish latitudinally or north-south along the coast may be more related to warming during the first part of the fishing season. To examine this possibility for striped marlin, isotherm data were plotted for the biweekly periods 1-15 August through 16-31 September (Figure 5). The curve of catch vs. temperature (Fig. 5) increases at an exponential rate, indicating that for isotherms 64°F (17.8°C) through 72°F (22.2°C) average catches increased from 46 to 208 striped marlin per period, respectively. However, the variation about the isotherm mean temperature (Fig. 5) is considerable. Therefore, results from the use of the isotherm position as a predictor of catch during any 2-week period (1-15 August – 16-31 September) could be highly variable.

Summary and Conclusions

The sport fishery catch of striped marlin off southern California during the period July through October appears to be related to sea surface temperatures observed off the Pacific coast of northwestern Mexico. Isotherms that are continuous into southern California waters from the west or southwest at 68°F (20.0°C) and above tend to be accompanied by an increase in catch; the peak continuous temperature isotherm observed in 1981 (72°F or 22.2°C) was accompanied by an increase in catch. Data also show a high variability in catch relative to any continuous isotherm during the 2-week periods. Therefore, any short-term prediction of catch based on continuous isotherm data may yield highly variable results.

Striped marlin are common to subtropical and tropical waters of lower latitudes than southern California. Sea surface temperatures in these high catch rate areas (commercial and recreational fisheries) are higher than temperatures observed to the south of the Southern California Bight. From available catch and temperature data (1960-81) and observations of the temperature range of striped marlin, it is reasonable to assume that the ocean temperatures, as defined by continuous isotherms extending into southern California from the south or southwest, never attain values that would result in a maximum catch off southern California because catches appear to be increasing at the peak continuous isotherm recorded (72°C or 22.2°C).

Acknowledgments

I wish to extend my appreciation to The Marlin Club, San Diego, Calif., for making the catch data available, and to Norman Bartoo, Steve Reilly, Forrest Miller, David Au, and Earl Weber for manuscript review and suggestions for analysis.

Literature Cited

Anonymous 1964-80. Annual reports of effort and catch statistics by area on Japanese tuna longline fishery. Fish. Res. Dep., Fish. Agency Jpn., var. pagin.

Hubbs, C. L., and L. P. Schultz. 1929. The northward occurrence of southern forms of marine life along the Pacific coast in 1926. Calif. Fish Game, 15(3):234-240.

Radovich, J. 1961. Relationships of some marine organisms of the northeast Pacific to water temperatures, particularly during 1957 through 1959. Calif. Dep. Fish Game, Fish Bull. 112, 62 p.

________. 1975. Water temperature and fish distribution: An epilogue to the warm water years. *In* Symposium on climate change in the northeastern Pacific. Proc. 13th Pac. Sci. Congr. Aug. 18-30, 1975 Univ. B.C., Vancouver, 22 p.

Reid, J. L., Jr., G. I. Roden, and J. G. Wyllie. 1958. Studies of the California Current System. Calif. Coop. Oceanic Fish. Invest. Prog. Rep., 1 July 1956-1 January 1958, p. 27-56.

Schwartzlose, R. A. 1963. Nearshore currents of the western United States and Baja California as measured by drift bottles. Calif. Coop. Oceanic Fish. Invest. Rep. 9:15-22.

Snedecor, G. W. 1956. Statistical methods. The Iowa State Press, Ames, 534 p.

Squire, J. L. 1971. Measurements of sea surface temperature on the eastern Pacific continental shelf using airborne infrared radiometry, August 1963-July 1968. U.S. Coast Guard Oceanogr. Rep. 47 (CG373-47), 229 p.

________. 1974. Catch distribution and related sea surface temperature for striped marlin, *Tetrapturus audax*, caught off San Diego, California. *In* R. S. Shomura and F. Williams (editors), Proc. Int. Billfish Symp., Kailua-Kona, Hawaii, 9-12 August 1972. Part 2. Review and contributed papers, p. 188-193. U.S. Dep. Commer., NOAA Tech. Rep. NMFS SSRF-675.

________. 1977. Surface currents as determined by drift card releases over the continental shelf off central and southern California. U.S. Dep. Commer., Tech. Rep. NMFS SSRF 718, 12 p.

________. 1982. Catch temperature for some important marine species off California. U.S. Dep. Commer., NOAA Tech. Rep. NMFS SSRF 759, 19 p.

Talbot, G. B., and P. G. Wares. 1975. Fishery for billfish off southern California and Mexico, 1903-69. Trans. Am. Fish. Soc. 104(1):1-12.

Tibby, R. B. 1939. Report on returns of drift bottles released off southern California, 1937. Calif. Dep. Fish Game, Fish Bull. 55, 36 p.

Uda, M. 1957. A consideration on the long years trend of fisheries fluctuation in relation to sea conditions. Bull. Jpn. Soc. Sci. Fish. 23(7-8): 368-372.

Walford, L. A. 1931. Northward occurrence of southern fish off San Pedro in 1931. Calif. Fish Game 17(4):402-405.

8590

Procedures for Sorting, Staging, and Ageing Eggs

GARY STAUFFER and SUSAN PICQUELLE[1]
Southwest Fisheries Center,
National Marine Fisheries Service, NOAA,
P.O. Box 271, La Jolla, CA 92038

ABSTRACT

Estimation of the daily production of eggs spawned is based on data for the number of eggs sampled during the plankton survey. This requires that the age of individual eggs be determined. To accomplish this, eggs of the surveyed species must be sorted out of the plankton samples, staged according to their state of embryonic development, and aged. The initial step in processing the plankton samples is removing the fish eggs and larvae and identifying the eggs of the target species. The second step is assigning each egg to a stage of embryonic development and counting the number of eggs of each stage for each plankton sample. Once all the samples have been staged, ages are assigned separately to each sample of the staged eggs based on a stage/temperature/age key, station temperature, and time of station occupancy. This procedure is subject to a number of sources of error that should be kept in mind and evaluated for each application.

INTRODUCTION

The daily production of eggs spawned into the sea is estimated by regressing a mortality model to density data on the number of eggs at age derived from plankton samples. To generate the egg density data, the fish eggs (and larvae) of the target species must be sorted from the plankton samples, staged on the basis of embryonic development, and aged. This process can begin as soon as the plankton samples have been transferred to the laboratory. At the Southwest Fisheries Center (SWFC), this procedure for the eggs and larvae of northern anchovies is carried out by three separate groups.

SORTING

The method of sorting eggs and larvae from the CalVET[2] samples are similar to the procedures outlined by Kramer et al. (1972) and Smith and Richardson (1977). The volume of plankton in CalVET samples was not measured. In this survey, plankton volumes were quite small because of the size of the CalVET net and the short duration of the tow and were not necessary for estimation of spawning biomass.

The plankton samples must be sorted by personnel trained in the identification of fish eggs and larvae particularly of those species from the survey area. Sorters are responsible for cross-checking the inside and outside labels of each sample jar as it is processed. It is critical that sample identification numbers written on all data forms filled out by the sorters match those on the sample jar labels. Sorters are responsible for picking out the eggs and larvae for all species and identifying the target species. At the SWFC, eggs and larvae of the target species are placed in 2-dr vials, filled with diluted Formalin, capped, and labeled with station identification numbers. Additional station data to be recorded on the staged egg data forms are water temperature and time of collection. These data are necessary for ageing the staged eggs at a later date.

Depending on the objectives of a particular survey, other species may also be sorted. Egg counts and possibly larval lengths of the target species are recorded on staged egg data forms. Sorting time per sample depends on the volume and quality of plankton and the quantity of ichthyoplankton in the samples. A sorter at the SWFC can process about eight CalVET samples per day. If processing of the plankton samples is on a strict schedule as it is at the SWFC, then it is advisable to sort first the samples collected at stations with the highest expected density of eggs.

STAGING

The second step in processing eggs of the target species is the assigning of an embryonic developmental stage to each egg. More training, experience, and time are required to accurately stage the embryonic development of fish eggs. The 2-dr vials containing sorted eggs of the target species and the respective staged egg data forms are turned over to a second group responsible for staging eggs at the SWFC.

Working with each sample separately, the technician pipettes or empties the eggs in a vial into a petri dish and sorts the eggs under a binocular dissecting scope into groups for each standardized developmental stage that spans incubation from time of fertilization to hatching, as described in Moser and Ahlstrom (1985). Eggs with disintegrated embryos are often difficult to stage and require special attention (see Moser and Ahlstrom 1985). In some samples, as much as 50% of the eggs could be disintegrated and difficult to stage. The number of eggs in each stage group are counted and recorded on the staged egg data sheet. The number of eggs for which it is impossible to assess the embryonic condition must be recorded also. The sum of the number of eggs staged should equal the earlier sorter's count. If not, then all groups should be recounted and any discrepancies accounted for and noted. When the staging of a sample is completed, all the eggs must be returned to the vial and the sample archived in a storage area.

---

[1] Present addresses: Northwest and Alaska Fisheries Center, National Marine Fisheries Service, NOAA, 7600 Sand Point Way NE, Seattle, WA 98115.

[2] For a description of the CalVET net, see Smith et al. (1985).

AGEING

Once all the station samples have been staged, the completed staged data forms can be turned over to a team which assigns ages to the staged eggs. Although this group of two or three people need not be skilled in identification of eggs and larvae or egg stages, they must understand the daily spawning cycle and the effect of temperature on development rate. It is recommended that each team member age the eggs for all stations independently of the others. This serves as a check of potential ageing errors and biases that could result from subjective decisions on likely ages of eggs for which the day of spawning is not obvious.

Assigning ages to eggs based on the stage of embryonic development is a relatively straightforward procedure if spawning occurs within a brief time interval during the 24-h daily cycle and if the duration of egg stages is less than a day for the range of temperatures observed during the survey. If either one of these conditions is not the case in any particular application, then the procedure described here will have to be modified in order to estimate daily rate of egg production in the sea.

Before the ageing step can begin, the team must specify the hour of peak spawning within the daily cycle to determine time zero for egg development. This can be determined from the time of day that newly fertilized eggs appear in the egg collections and from observations on the spawning behavior or condition of the adults. A stage/temperature/age key as described in Lo (1985, fig. 2) must be available for the target species of the survey. This key represents embryonic growth curves for each developmental stage, relating time to develop with temperature. From these curves, the time or age from fertilization to time of collection can be estimated given the stage of development and station surface temperature, which is assumed to be the temperature at which the egg was incubated. The age of an egg can be calculated by estimating its age in whole days and then adding on the portion of a day that has elapsed between peak spawning hour and the time of day the sample was collected. For northern anchovies off California, the peak spawning hour is set at 2200. Thus eggs need be aged only to the nearest day and then adjusted for the portion of the day between sampling and peak spawning.

The benefit of having all spawning occur in the same short interval each day is that the ages of the eggs within each sample are separated by 24-h increments. Because the duration of any particular stage is much less than 24 h, the distribution of eggs of a single sample over the different developmental stages should form distinct groups or modes with unrepresented stages separating each group. One can then assume that each group is separated by 24 h. This pattern is extremely helpful in assigning whole-day ages to groups of eggs within a sample. However, this pattern becomes blurred for samples taken from colder temperatures where the duration of each stage is longer and the modes or groups of eggs may overlap. This pattern is also less clear for the advanced stages because the ages are assigned with less precision. The longer the incubation time, the more inflated the variance in the age key becomes as the effects of variability in growth rate and environmental factors accrue.

These two problems are partially avoided by truncating the data series and eliminating the eggs older than a specific age. The primary reason for doing this is to avoid the time period when eggs begin to hatch into larvae and are no longer available for sampling. Truncation of egg density data for eggs older than the age at which the onset of hatching is expected for the warmer temperatures encountered on the survey insures that mortality is the only process contributing to the decline in egg abundance. This also eliminates eggs for which the procedure of assigning ages has the greatest uncertainty.

For the northern anchovy surveys conducted by the SWFC, time was saved by taking temperture data at the surface only, at most stations. The recorded temperature data represent the maximum incubation temperatures that eggs would likely encounter in the upper mixed layer, where anchovy eggs are found. In a few cases, eggs could have been assigned to either one of two spawning days based on the age key. In these cases, the older age was assigned based on the assumption that the egg was probably incubated at a temperature colder than the surface waters. However, the majority of eggs closely corresponded to the predicted age suggested by the embryonic growth curves and by the separation of egg-stage modes.

Plankton samples collected during the spawning hours will undersample the new eggs until spawning is completed for the daily spawning period. To avoid underestimating daily egg production from the mortality model, egg densities of the youngest ages exclude samples collected during the spawning period. For northern anchovies this period was between 1800 and 0200. These samples do provide data on eggs older than approximately one-half day (for further discussion see Picquelle and Stauffer 1985).

After assignment of ages by all team members working independently of one another, the staged egg data forms were sorted into convenient time and temperature strata. The team as a group examined the data forms for each stratum for consistency among samples in the assigned age of each stage. At this time, discrepancies between the ages assigned by different team members and among stations with similar conditions were discussed and rectified. This final comparison is very important to minimize any differences among the team, to reduce errors, and to insure that the determinations from the age key are consistent throughout the ageing exercise.

The ageing step can be automated using a computer. Based on the stage/temperature/age key, a reference table can be constructed and included in a computer program. The table should contain the estimated ages of eggs for each of the 11 stages at temperatures ranging from 10° to 22°C, sampled at any time throughout a 24-h period. Ages are assigned to stages according to the reference table.

The advantages of the automated system are twofold. 1) It saves time: the current manual system requires about 1 wk of manpower to age the eggs, enter the data, and build the data files for the estimation of daily egg mortality and egg production; the automated system requires one-half day at most to process the staged eggs and produce a daily egg mortality curve. 2) It standardizes the method: the automated system eliminates the subjectivity of human judgment and variation resulting from operator error, thus the accuracy of the egg production and the egg mortality estimate can be improved (see Lo 1985).

ASSUMPTIONS AND SOURCES OF ERROR

1) Anchovy eggs are easily distinguished because of the oblate spheroid shape. As a result, the sorting procedure for anchovy eggs is quite accurate and relatively efficient. The sorting of spherical eggs of other species may require more skill and resorting to check for accuracy if there is a potential confusion with other species.

2) Often a high fraction of the fish eggs have disrupted or disintegrated embryos. In these cases, the developmental stage must be determined by additional criteria. For the northern anchovy example, it was assumed that this condition occurred during the plankton tow and that eggs in this category had a similar mortality history. The validity of this assumption should be examined in each application of the egg production method.

3) The assumption that 100% of the eggs are retained by the plankton net should be tested. Also, the catching process and fixation may stimulate the eggs to hatch.

4) The mortality model assumes that all egg stages including unfertilized eggs have the same rate of mortality. If unfertilized eggs make up only a small fraction of the total eggs, and if they persist in the water column for <1 d, then it is probably sufficient to assign them as 1-d-old eggs. This ignores the bias in the estimate of daily egg production created by the different mortality rates of unfertilized eggs and the inability to age unfertilized eggs. On the other hand, if unfertilized eggs are not an insignificant fraction of the total, then the egg production mortality model must be modified to account for them.

5) The ageing of staged eggs is facilitated by a short spawning interval within a daily period. Assigning ages to embryonic stages will become less reliable as the spawning interval makes up a greater fraction of the daily period. Stage durations of <12 h at the usual incubation temperature facilitates the assigning of daily ages to staged eggs. If embryonic development is slow, which is often the case at low temperatures, then there is a good possibility that eggs at a single stage could have resulted from more than a single spawning episode. If this occurs, then the arbitrary stages described here must be divided further.

6) The duration of an egg stage is a function of the incubation temperature. The measured temperature at a plankton station may not be the actual temperature at which the collected eggs were incubated within the water column. The temperature measurement must be representative of the temperature at which the majority of the eggs incubate. This requires a study of the vertical distribution of eggs compared with the temperature depth profile.

LITERATURE CITED

KRAMER, D., M. M. KALIN, E. G. STEVENS, J. R. THRAILKILL, and J. R. ZWEIFEL.

1972. Collecting and processing data on fish eggs and larvae in the California Current region. U.S. Dep. Commer., NOAA Tech. Rep. NMFS Circ. 370, 38 p.

LO, N. C. H.

1985. A model for temperature-dependent northern anchovy egg development and an automated procedure for the assignment of age to staged eggs. *In* R. Lasker (editor), An egg production method for estimating spawning biomass of pelagic fish: Application to the northern anchovy, *Engraulis mordax*, p. 43-50. U.S. Dep. Commer., NOAA Tech. Rep. NMFS 36.

MOSER, H. G., and E. H. AHLSTROM.

1985. Staging anchovy eggs. *In* R. Lasker (editor), An egg production method for estimating spawning biomass of pelagic fish: Application to the northern anchovy, *Engraulis mordax*, p. 37-41. U.S. Dep. Commer., NOAA Tech. Rep. NMFS 36.

PICQUELLE, S., and G. STAUFFER.

1985. Parameter estimation for an egg production method of northern anchovy biomass assessment. *In* R. Lasker (editor), An egg production method for estimating spawning biomass of pelagic fish: Application to the northern anchovy, *Engraulis mordax*, p. 7-15. U.S. Dep. Commer., NOAA Tech. Rep. NMFS 36.

SMITH, P. E., and S. L. RICHARDSON.

1977. Standard techniques for pelagic fish egg and larva surveys. FAO Fish. Tech. Pap. 175, 100 p.

SMITH, P. E., W. FLERX, and R. HEWITT.

1985. The CalCOFI vertical egg tow (CalVET) net. *In* R. Lasker (editor), An egg production method for estimating spawning biomass of pelagic fish: Application to the northern anchovy, *Engraulis mordax*, p. 27-32. U.S. Dep. Commer., NOAA Tech. Rep. NMFS 36.

8591

DESCRIPTIONS OF LARVAE OF CALIFORNIA YELLOWTAIL, *SERIOLA LALANDI*, AND THREE OTHER CARANGIDS FROM THE EASTERN TROPICAL PACIFIC: *CHLOROSCOMBRUS ORQUETA*, *CARANX CABALLUS*, AND *CARANX SEXFASCIATUS*

BARBARA Y. SUMIDA, H. GEOFFREY MOSER, AND ELBERT H. AHLSTROM
National Marine Fisheries Service
Southwest Fisheries Center
P.O. Box 271
La Jolla, California 92038

ABSTRACT

Larvae are described for four species of jacks, family Carangidae. Three of these, *Seriola lalandi* (California yellowtail), *Chloroscombrus orqueta*, and *Caranx caballus*, occur in the CalCOFI region. A fourth species, *Caranx sexfasciatus*, occurs from Mazatlan, Mexico, to Panama. Species are distinguished by a combination of morphological, pigmentary, and meristic characters. Larval body morphs range from slender *S. lalandi*, with a relatively elongate gut, to deep-bodied *C. sexfasciatus*, with a triangular gut mass. Pigmentation patterns are characteristic for early stages of each species, but all except *C. orqueta* become heavily pigmented in late stages of development.

RESUMEN

Se describen las larvas de 4 especies de carángidos (Carangidae). Tres de ellas, *Seriola lalandi* (jurel), *Chloroscombrus orqueta*, y *Caranx caballus* se encuentran en la región de la CalCOFI. La cuarta especie, *Caranx sexfasciatus*, se encuentra desde Mazatlán, México, hasta Panamá. Las especies se distinguen por una combinación de rasgos morfológicos, pigmentarios, y merísticos. Los Tipos de larva varían desde delgados, como *S. lalandi*, son vísceras relativamente elongadas, hasta altos, como *C. sexfasciatus*, con una masa visceral triangular. Los patrones de pigmentación son característicos para los estadios tempranos de cada especie, pero todos, excepto *C. orqueta*, se vuelven fuertemente pigmentadas en los estadios de desarrollo tardíos.

INTRODUCTION

Numerous species of carangid fishes occur in the eastern Pacific, but with the exception of jack mackerel (*Trachurus symmetricus*), these species spawn in tropical or subtropical waters. Few species spawn far enough north to occur in the CalCOFI sampling region. One species, the California yellowtail, *Seriola lalandi*, supports an important recreational fishery off southern California and Baja California, and it briefly supported a commercial fishery during the 1950s (MacCall et al. 1976). Larvae of *Seriola* species from other regions of the world have been described (see literature review in Laroche et al. 1984), but larvae of eastern Pacific *Seriola lalandi* have not previously been described[1]. This paper also describes larvae of two other carangids, *Chloroscombrus orqueta* and *Caranx caballus*, occurring in the CalCOFI region, and a third carangid, *Caranx sexfasciatus*, which occurs to the south.

MATERIALS AND METHODS

Larvae used in this work were obtained from various plankton collections made in the eastern tropical Pacific, including those of CalCOFI, EASTROPAC, the Inter-American Tropical Tuna Commission, Bureau of Sport Fisheries and Wildlife, and Scripps Tuna Oceanography cruises. In addition, specimens of *Chloroscombrus orqueta*, dipnetted near San Carlos Bay in the Gulf of California, were provided by Robert Behrstock, formerly of Humboldt State University. Several small larval *Seriola lalandi* reared at the Southwest Fisheries Center's La Jolla laboratory were also examined.

Developmental series were assembled for each species, and morphological and pigmentation changes were described using the methods and terminology of Moser and Ahlstrom (1970) and Ahlstrom et al. (1976). Body lengths given in the text and tables represent notochord length in preflexion- and flexion-stage larvae, and standard length in postflexion larvae and juveniles. Descriptions of fin formation were limited by the condition of the specimens, because many had become decalcified in preservative over prolonged storage. A limited number of specimens were successfully stained, allowing observation of meristic characters and head spination.

[Manuscript received March 8, 1985.]

---

[1] Seven of the illustrations in this paper originally were included in a manuscript by E.H. Ahlstrom and B.Y. Sumida entitled "Early life history studies of eastern Pacific carangids." This manuscript was prepared for a symposium held in Ensenada, Mexico, in February 1975, the proceedings of which were not published. The manuscript is a general summary of some ontogenetic and adult taxonomic characters of nine carangid genera that occur in the eastern Pacific. It is now available as Southwest Fisheries Center Administrative Report LJ-85-02.

TABLE 1
Comparative Morphometry of Five Species of Carangid Larvae

	Snout-anus length / Body length	Head length / Body length	Eye diameter / Head length	Snout length / Head length	Body depth / Body length
Seriola lalandi					
A	*59.6 ±1.34(58-61)	28.2 ±1.30(27-30)	31.0 ±1.87(28-33)	30.2 ±2.28(28-33)	19.4 ±0.55(19-20)
B	61.5 ±0.58(61-62)	31.5 ±1.00(30-32)	30.8 ±1.50(29-32)	30.5 ±1.00(29-31)	23.2 ±2.06(21-26)
C	63.8 ±1.68(62-66)	34.6 ±1.40(32-36)	30.7 ±2.14(28-34)	27.1 ±2.61(24-31)	29.7 ±1.50(27-31)
D	60	31	32	26	29
Trachurus symmetricus	calculated from Ahlstrom & Ball (1954) (Size categories were given equal weighting in calculating means; standard deviation not calculable from data as published.)				
A	56.6 (54-58)	25.2 (17-32)	41.6 (36-51)	No snout lengths measured	21.4 (16-26)
B	59.3 (58-61)	33.2 (30-35)	35.8 (34-37)		26.7 (25-28)
C	58.0 (55-60)	36.2 (35-38)	34.0 (32-37)		27.4 (26-28)
D	54.0	29.5 (28-31)	32.0 (31-33)		24.5 (24-25)
Chloroscombrus orqueta					
A	57.3 ±2.31(56-60)	32.7 ±2.52(30-35)	31.7 ±0.58(31-32)	30.7 ±3.21(27-33)	35.0 ±4.36(30-38)
B	57.2 ±0.96(56-58)	38.0 ±0.82(37-39)	36.0 ±1.82(34-38)	28.0 ±0.82(27-29)	41.5 ±3.00(39-45)
C	50.4 ±3.36(44-55)	34.8 ±2.52(30-38)	36.4 ±2.73(32-40)	25.8 ±2.09(23-28)	43.4 ±1.63(41-46)
D	40.5 ±2.12(39-42)	30.5 ±2.12(29-32)	33.0 ±1.41(32-34)	28.0 ±1.41(27-29)	42.0 ±0.00(42)
Caranx caballus					
A	59.7 ±1.53(58-61)	34.3 ±1.53(33-36)	28.3 ±0.58(28-29)	29.3 ±2.31(28-32)	34.3 ±2.31(33-37)
B	57.0 ±2.00(55-59)	35.0 ±1.73(33-36)	33.0 ±1.73(31-34)	27.0 ±2.00(25-29)	42.0 ±1.73(41-44)
C	55.0 ±1.76(52-58)	35.9 ±1.60(33-38)	34.8 ±2.78(30-40)	25.1 ±3.48(21-32)	43.9 ±1.73(42-46)
D	52	36	35	26	39
Caranx sexfasciatus					
A	54.6 ±1.14(53-56)	32.0 ±3.08(29-37)	31.6 ±2.30(28-34)	29.0 ±2.34(27-33)	35.4 ±4.93(29-42)
B	58.3 ±1.53(57-60)	35.3 ±2.52(33-38)	33.3 ±2.08(31-35)	29.0 ±1.73(27-30)	50.3 ±5.51(45-56)
C	57.1 ±3.81(51-62)	37.6 ±1.84(34-40)	34.8 ±1.69(33-38)	25.5 ±2.88(20-28)	53.2 ±2.20(49-57)
D	48.0 ±2.83(46-50)	32.5 ±2.12(31-34)	33.5 ±2.12(32-35)	25.0 ±1.41(24-26)	43.5 ±3.54(41-46)

*Mean, standard deviation, and range expressed as percentage of body length or head length. A, preflexion; B, flexion; C, postflexion; D, juvenile.

DESCRIPTIONS

Seriola lalandi

Literature. Brownell (1979) illustrated an egg and two reared yolk-sac larvae, which he tentatively identified as *S. lalandi*, from waters off South Africa. The egg measured 1.44 mm in diameter with an oil globule diameter of 0.32 mm.

Distinguishing features. *Seriola lalandi* larvae are slender-bodied and heavily pigmented, lack a supraoccipital crest, and develop the largest number of dorsal fin rays (31-39) among eastern Pacific carangids. The combination of these characters distinguishes *S. lalandi* from all other carangid larvae in the CalCOFI region except for larvae of *Seriola rivoliana*, which co-occur with *S. lalandi* in the southernmost extent of its range, and are presently undescribed.

Morphology and meristics. Early larvae of *S. lalandi* are slender-bodied; body depth at the base of the pectoral fin averages 19% to 23% in preflexion and flexion stages, increasing to about 30% in postflexion and juvenile stages (Table 1). Early stages of *S. lalandi* <10.0 mm are more slender than those of jack mackerel (*Trachurus symmetricus*), in which body depth ranges from 21% to 27% of body length (Table 1, Figure 1).

The gut is comparatively elongate; it increases in length relative to total body length during the larval period, then becomes relatively shorter in juveniles (Tables 1 and 2; Figure 2). The slender gut of early *S. lalandi* differs from the rounded mass found in *Caranx* and *Chloroscombrus*, and from the intermediate robust but somewhat elongate form in *T. symmetricus*. The intestinal coil begins to form at the end of the yolk-sac period at a position about one-fourth of the cleithrum-anus distance. The posterior margin of the

TABLE 2
Measurements (mm) of *Seriola lalandi*

Station	Body length	Snout-anus length	Head length	Eye diameter	Snout length	Body depth at pectoral fin base
6706-S-130.35	4.2 yolk-sac	2.2	0.52	0.26	0.10	0.36
5707-P-107.60	4.4	2.6	1.2	0.38	0.36	0.84
5708-B-113.35	5.2	3.0	1.4	0.46	0.40	1.0
6007-H-133.30	5.9	3.6	1.7	0.47	0.48	1.1
5707-P-107.60	6.1	3.7	1.8	0.56	0.60	1.2
6007-H-133.30	6.4	3.8	1.8	0.56	0.58	1.3
5909-B-133.25	6.6	4.0	2.1	0.64	0.66	1.5
5707-0-110.70	6.9	4.2	2.2	0.64	0.68	1.6
6007-H-133.30	7.2	4.5	2.2	0.70	0.64	1.5
6608-J-123.40	8.6	5.3	2.8	0.90	0.86	2.2
5608-B-130.45	8.9	5.6	3.1	0.92	0.92	2.4
7205-JD-130.80	9.8	6.5	3.5	1.1	0.88	3.0
Baja Calif.	10.9	7.2	3.8	1.3	1.0	3.2
8108-NH-106.7.45	13.7	8.8	4.9	1.6	1.2	4.2
6008-B-137.30	17.9	11.2	6.1	1.8	1.7	5.5
Mazatlan Proj.	20.0	12.9	6.8	1.9	2.1	6.1
Mazatlan Proj.	22.4	14.0	7.2	2.1	1.9	6.5
Cr. 79-DSJ	26.7 juv.	16.0	8.2	2.7	2.2	7.8

Specimens between dashed lines are undergoing notochord flexion.

loop extends posteriad gradually to reach about two-thirds of the cleithrum-anus distance at the beginning of notochord flexion. During this process the gut mass becomes somewhat deeper, tapering posteriad, but retains its elongate shape. By completion of notochord flexion the loop has reached the rectum, about three-fourths of the cleithrum-anus distance, and the entire gut region has become covered by well-developed body-wall musculature.

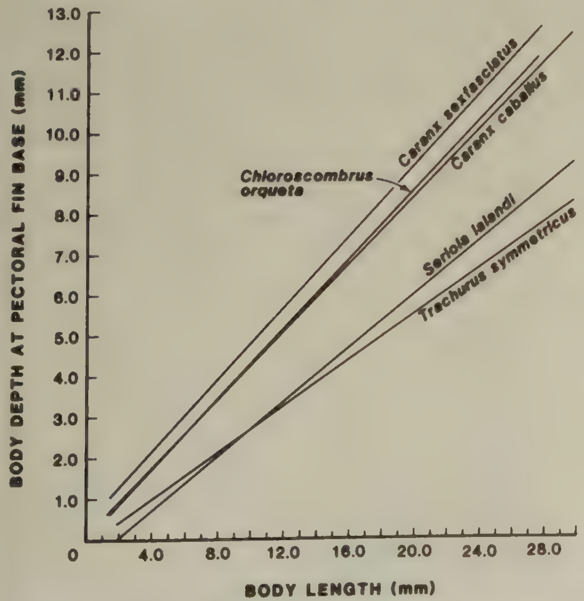

Figure 1. Regression of body depth at pectoral fin base on body length in five species of carangid larvae.

Relative head length increases gradually during larval development ($\bar{x}$ = 28% of body length in preflexion and 35% in postflexion stages) and decreases slightly in early juveniles. Relative eye diameter changes little during development, and relative snout length decreases slightly.

Head spines develop on the following bones: preopercle, frontal, posttemporal, and supracleithrum. Two series of spines develop on the preopercle, one along its posterior margin and one along a ridge just anterior to the margin. The first spine forms at the angle of the posterior margin at about 4.3 mm body length. This becomes the largest preopercular spine, its length reaching 9% of the body length at about 10 mm SL. At about 4.6 mm the first spine in the anterior series forms on the ridge in a position directly anterior to the angle spine of the posterior preopercular series.

Larvae about 5 mm long have developed two additional spines on the posterior margin of the preopercle, one on either side of the angle spine. A second spine forms on the ridge in association with the margin spine below the angle. The spines on either side of the angle spine are about one-half the length of the latter. Also at this stage the frontal bone begins to project above

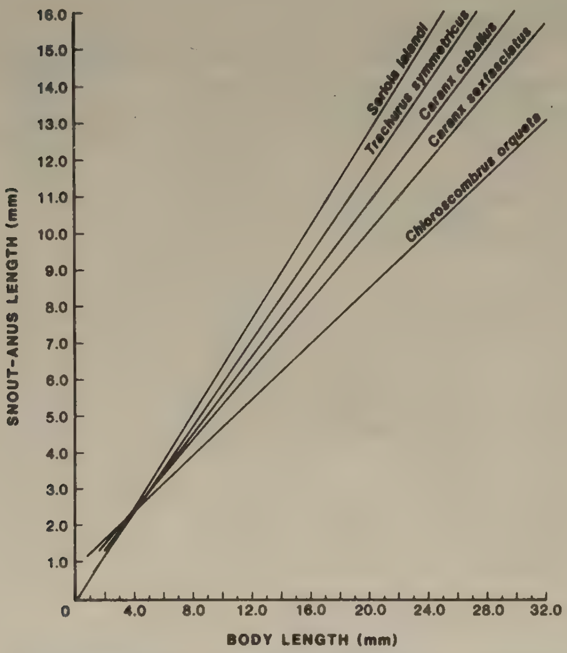

Figure 2. Regression of snout-anus length on body length in five species of carangid larvae.

the eye, forming a supraocular crest, which bears a spine.

Larvae about 6 mm long have added a small spine to each end of the preopercular margin series and begin to develop a single spine on the posttemporal and on the supracleithrum about midway between the posttemporal spine and the pectoral fin base. Also, a prominent longitudinal ridge is present on the pterotic bone.

At the completion of notochord flexion (~8.6 mm), an additional spine is present at each end of the preopercular series, and two more posttemporal spines have developed, one adjacent to the original spine and the other anteroventral to them. At this stage the full head-spine complement is present, and the spines remain prominent until about 13 mm SL, when most of them begin to diminish in size. The two spines on the preopercular ridge are the first to be lost, followed by the outer spines of the preopercular margin series and the supraocular spine. By 26 mm SL only the preopercular spines near the angle are prominent.

Meristic counts of stained specimens are presented in Table 3.

Pigmentation. Seriola lalandi is moderately pigmented in early stages, becoming heavily pigmented during the larval period. Serial melanophores outline the dorsal and ventral body margins of approximately 80% of the length of the body in yolk-sac larvae (Figure 3A-C). These melanophores become expanded and prominent in the preflexion stage (~4.5 mm), extending anteriorly over the snout and posteriorly around the tip of the tail. The melanophores along the tail tip are minute, dispersing outwardly onto the finfold of the developing caudal fin with ensuing growth. Other pigmentation in preflexion larvae includes a lateral midline series on the body and a series on the ventral midline along the isthmus in a continuum with melanophores below the gut (Figure 3D, E). Pigmentation increases rapidly over much of the head and body in early flexion larvae >6.6 mm, and these areas become almost completely covered with melanophores, except for the fin membranes and the posteriormost portion of the body. In larvae ≥7.0 mm, melanophores appear along the edge of the developing dorsal and anal fin pterygiophores. The melanophore pattern undergoes little change in postflexion larvae except for augmented pigmentation on the dorsal, anal, and pelvic fin membranes (Figure 4). By 14.0 mm, melanophores extend over most of the caudal peduncle, which is completely pigmented by 18.0 mm.

The strongly banded pattern exhibited by juveniles apparently forms rapidly, since it is lacking in a 22.4-mm specimen but present in a 24.5-mm specimen (Figure 4C).

Chloroscombrus orqueta

Literature. Larvae of *Chloroscombrus orqueta* have not been described previously.

Distinguishing features. Early *Chloroscombrus orqueta* larvae closely resemble some *Caranx* species in body morph and pigmentation, but have a diagnostic melanophore pattern on the dorsal body margin composed of four melanophores positioned on myomeres 1, 3, 9, and 14. Another feature is a small spine on the pterotic bone in larvae 7.5-11.0 mm. Larvae of *C. orqueta* also develop more dorsal and anal fin rays (25-30 rays for each fin) than any other *Caranx* species in the eastern Pacific.

Morphology and meristics. Chloroscombrus orqueta larvae are deep-bodied, increasing in body depth during all stages of larval development (Table 4; Figure 1). Relative body depth averages 35% in preflexion larvae, and about 42% in later stages (Table 1). Snout-anus distance is about 57% of body length in preflexion and flexion larvae. This is similar to other species described herein; however, in postflexion stages and juveniles the terminal segment of the gut in *C. orqueta* curves more anteriad, resulting in the shortest mean snout-anus length among the species discussed (Table 1; Figure 2). The gut loop is well

TABLE 3
Meristics of Stained *Seriola lalandi*

Station	Body length (mm)	Dorsal fin	Anal fin	Pectoral fin	Caudal fin	Pelvic fin	Branchiostegals
7808-VA-137.35	3.2	—	—	—	—	—	—
5707-B-120.75	3.9	—	—	—	—	—	—
6907-G-117.50	4.1	—	—	—	—	—	—
5609-B-120.45	4.3	—	—	—	—	—	—
5707-0-110.70	4.6	—	—	—	—	—	—
5408-C-130.45	4.9	—	—	—	—	—	4
5807-93.50	5.2	—	—	—	—	—	—
6007-H-133.30	5.6	—	—	—	—	—	4
5707-P-110.55	5.7	—	—	—	0+1+1+0	—	6
5906-0-123.60	6.0	—	—	—	0+1+1+0	—	7
5408-C-117.35	6.3	—	—	—	0+2+2+0	—	7
5707-0-110.70	6.9	10	12	6	0+6+5+0	—	7
6007-H-133.30	7.2	16	7	7	0+6+5+0	—	7
6608-J-123.40	8.6	VII,27	I+I,16	13	1+9+8+1	—	7
7205-J-130.80	9.8	VI,36	II+I,21	14	4+9+8+4	I,4	7
Off Baja Calif.	10.9	VII+I,35	II+I,21	19	5+9+8+5	I,5	7
8108-NH-106.7.45	13.7	VII+I,34	II+I,21	20	9+9+8+9	I,5	7
6008-B-137.30	17.9	VII+I,33	II+I,20	21	12+9+8+12	I,5	7
Mazatlan proj., 6-3-S	20.0	VII+I,36	II+I,22	21	12+9+8+12	I,5	7
RV/DSJ Cr. 79	26.7 juv.	VII+I,31	II+I,21	22	10+9+8+10	I,5	7

Specimens between dashed lines are undergoing notochord flexion.

formed in our smallest larvae (2.7 mm), and the posterior edge of the loop extends to about 60% of the cleithrum-anus distance. During this stage the gut mass lies in a longitudinal plane. By 3 mm, the ascending portion of the loop extends above the gut mass, and the rectal portion descends ventroposteriad at about a 45° angle. The loop portion increases in diameter and in relative mass and occupies most of the perivisceral cavity by about 4.0 mm. At this stage the rectal portion is oriented vertically and curves around the posterior edge of the coil. The gut and the prominent gas bladder above it form a triangular mass with sides of about equal length. The gut mass becomes more rounded with continued development, and by 8.0 mm the body-wall musculature is well developed.

Relative head length increases during preflexion and flexion stages ($\bar{x}$ = 33%-38% of body length), but decreases ($\bar{x}$ = 35%-30%) thereafter. Relative eye diameter increases during larval development and decreases slightly in juveniles. Relative snout length decreases in progressive larval stages but increases slightly in the juvenile stage (Tables 1 and 4).

Head spines develop on the following bones: preopercle, frontal, posttemporal, supracleithrum, and pterotic. Small larvae (2.7 mm) bear a large spine at the angle of the preopercular margin and three smaller spines below the angle. By 3.0 mm, larvae have two more spines above the angle. Larvae >3 mm have a fourth and fifth spine below the angle and a third spine above the angle. By 4 mm, a sixth spine is added below the angle and a fourth above the angle. By 5 mm, larvae have a fifth spine above the angle. Larvae larger than 8.0 mm have 8-10 spines below the angle and 6-7 above the angle. The angle spine reaches a

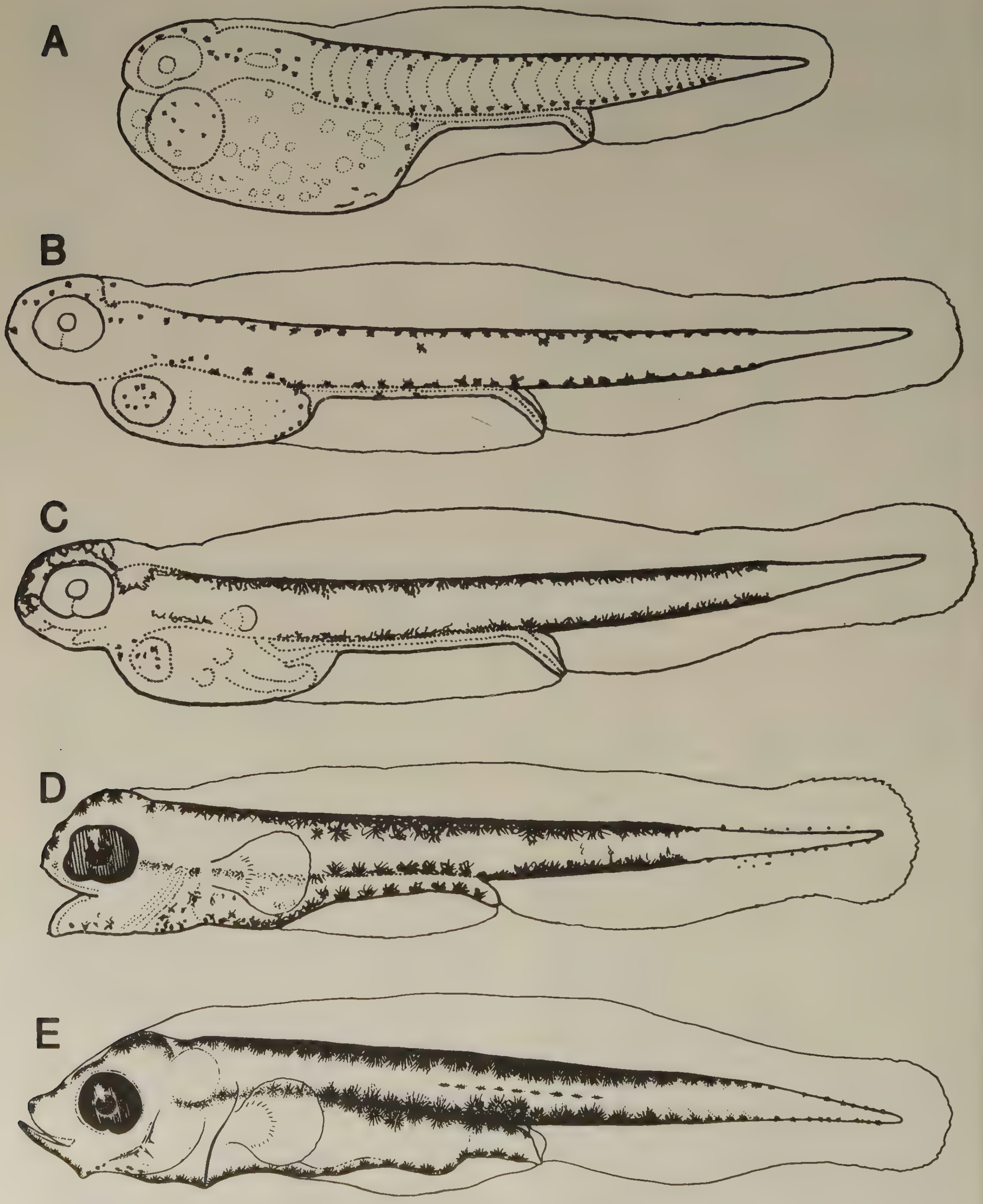

Figure 3. Early larvae of *Seriola lalandi*: *A*, 2.8 mm; *B*, 3.8 mm; *C*, 3.8 mm; *D*, 3.5 mm; *E*, 4.6 mm.

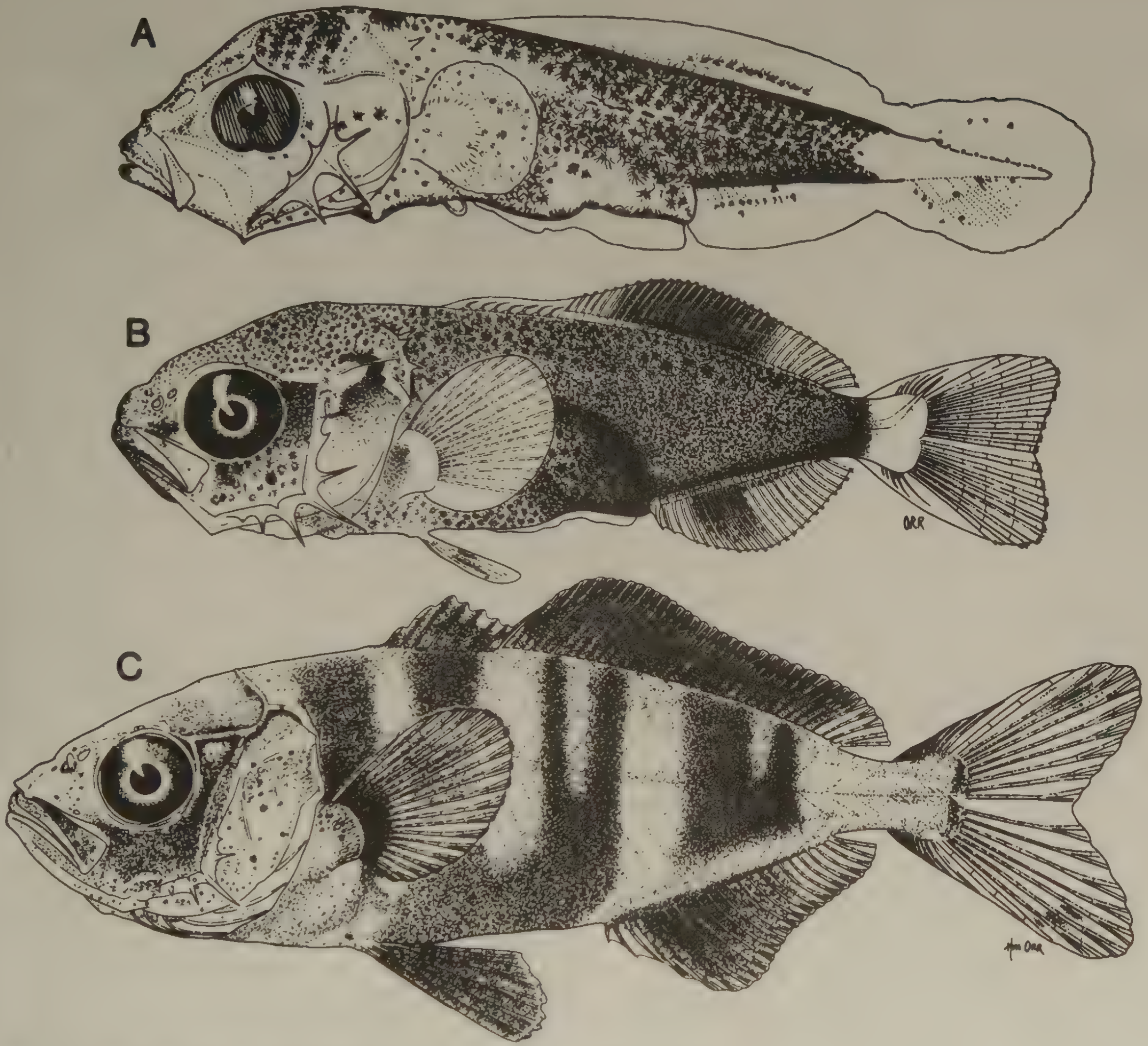

Figure 4. Larvae and early juvenile of *Seriola lalandi*: *A*, 7.0 mm; *B*, 11.7 mm; *C*, 24.5-mm juvenile.

maximum relative length of about 15% of the body length in 3-mm larvae, is reduced to 8%-11% of body length in 4-7-mm larvae, and then decreases abruptly in relative size. The spines above and below the angle spine are about one-half its length, and the others decrease in size gradually toward each end of the series. The uppermost margin spines begin to disappear at about 13 mm; by 16 mm only the spine adjacent to the angle remains in the upper series. Specimens larger than 20 mm retain only the angle spine.

Larvae <3.0 mm have 4 small spines on the lower part of the preopercular ridge. These spines increase in number to a maximum of 9-11 on the lower limb and 3-4 on the upper limb of the ridge in 6-11-mm larvae. Thereafter they decrease in number and are absent by 15 mm.

By about 3.0 mm, larvae have single spines on the posttemporal, supracleithrum, and on the supraocular shelf (frontal bone). Additional posttemporal spines appear by 5 mm, and in larvae >6.6 mm there are 4 spines arranged in an arc on the lower region of the bone. Larvae ≥7.0 mm form additional supracleithral spines, and larvae >8.0 mm have 4 spines arranged in a vertical series on the upper region of the bone. Larvae 8-11 mm in length have a maximum of 9-11

TABLE 4
Measurements (mm) of *Chloroscombrus orqueta*

Station	Body length	Snout-anus length	Head length	Eye diameter	Snout length	Body depth at pectoral fin base
B-5608-137.23	2.7	1.5	0.80	0.26	0.26	0.82
B-5608-137.23	3.0	1.8	0.98	0.30	0.32	1.1
B-5608-137.23	3.4	1.9	1.2	0.38	0.32	1.3
ETP 13.019	3.7	2.1	1.4	0.54	0.38	1.6
ETP 13.019	4.0	2.3	1.5	0.56	0.44	1.8
TO 59-1 #46	4.1	2.4	1.6	0.54	0.44	1.6
TO 59-1 #46	4.6	2.6	1.7	0.60	0.48	1.8
ETP 13.019	5.1	2.7	1.8	0.70	0.48	2.1
ETP 13.019	5.3	2.9	2.0	0.72	0.54	2.2
ETP 13.019	5.9	3.2	2.2	0.76	0.60	2.5
TO 59-1 #46	6.6	3.3	2.3	0.84	0.64	2.8
TO 59-1 #35	7.2	3.6	2.4	0.92	0.60	3.1
TO 59-1 #35	8.0	4.2	2.9	1.0	0.66	3.6
ETP 13.021	8.3	4.3	3.1	1.0	0.72	3.6
ETP 13.019	9.8	5.0	3.5	1.2	1.0	4.2
RAB S-14	11.4	5.5	4.0	1.6	1.0	5.2
ETP 13.019	13.4	6.2	4.0	1.5	1.1	6.0
RAB 71-III (a,b)	15.2	6.7	4.7	1.9	1.1	6.8
Rab S-14	23.5 juv.	9.8	7.5	2.4	2.2	9.8
RAB S-2	29.7 juv.	11.5	8.6	2.9	2.3	12.4

Specimens between dashed lines are undergoing notochord flexion.

spines on the supraocular shelf. Specimens >15 mm lack supraocular spines, and the posttemporal and supracleithral spines become obsolescent at about the same stage.

Small larvae <3.0 mm possess a supraoccipital crest with a scalloped margin. By about 3.0 mm it has developed to its maximum relative size, extends from the midregion of the optic lobes to the second myoseptum, and has formed 10-12 rounded projections. By about 8.0 mm it is much reduced in size and is restricted to the occipital region, and is lost by 13.0 mm.

A small spine-bearing ridge develops on the pterotic bone at about 7.5 mm. A maximum of two spines appear on the ridge. The ridge is absent in specimens larger than 11.0 mm.

Meristic counts of stained material are presented in Table 5.

Pigmentation. Chloroscombrus larvae are lightly pigmented and resemble larvae of some *Caranx* species; however, they may be distinguished by characters discussed below. Pigmentation on preflexion and flexion larvae (~2.6-4.6 mm) is found in the following areas: (1) head—region of the midbrain and jaws; (2) abdomen—over the gas bladder, dorsally over the free portion of the gut terminus, ventrally on the gut wall, and along the margin of the preanal finfold; (3) body—dorsally and ventrally on the body margin, along the lateral midline, internally above the notochord medial to the midline pigment, and a melanophore or two below the developing caudal fin (Figure 5A-C). This is a typical pattern for many early carangid larvae, but a diagnostic melanophore pattern for preflexion and early flexion *C. orqueta* is the dorsal body margin pigment consisting of four melanophores positioned over myomeres 1, 3, 9, and 14 (Figure 5A, B). This character occurs in other *Chloroscombrus* species—*C. cosmopolita* in the eastern Atlantic (Aboussouan 1968) and *C. chrysurus* in the western Atlantic and Gulf of Mexico[2].

Pigmentation gradually increases in postflexion larvae (>5.0 mm), particularly in the head and trunk region (Figures 5D and 6A). Melanophores along the dorsal body margin increase in number to form a continuous dashed line of pigment by 7.2 mm. Myoseptal pigmentation on the ventral surface of the body is first evident at about 5.0 mm (Figure 5D), positioned below the lateral midline streak; internal

---

[2] Laroche, W.A., D. Ruple, and S.L. Richardson. MS. Young carangid fishes from the Gulf of Mexico: a generic diagnosis of larvae, with additional descriptive notes including early development of three species. Gulf Coast Research Lab., Ocean Springs, MS 39564.

TABLE 5
Meristics of Stained *Chloroscombrus orqueta*

Station	Body length (mm)	Dorsal fin	Anal fin	Pectoral fin	Caudal fin	Pelvic fin	Branchiostegals
5608-B-137.23	2.7	—	—	—	—	—	6
Cabo Blanco, Costa Rica 10 miS	2.9	—	—	—	—	—	6
5608-B-137.23	3.0	—	—	—	—	—	7
P-42-130.30	3.2	anlagen	anlagen	—	—	—	7
5608-B-137.23	3.4	anlagen	anlagen	—	0+2+2+0	—	7
P-42-130.30	3.7	anlagen	anlagen	—	0+4+4+0	—	7
ETP 13.019	4.0	VII+I,11	II+I,16	5	0+8+7+0	—	7
ETP 13.019	4.3	VII+I,18	II+I,18	7	0+8+7+0	—	7
ETP 13.019	4.5	VIII+I,22	II+I,23	10	2+9+8+2	—	7
ETP 13.019	5.1	VIII+I,23	II+I,20	12	2+9+8+2	—	7
ETP 13.019	5.6	VIII+I,22	II+I,22	12	2+9+8+2	—	7
TO 59-1 #46	5.9	VIII+I,26	II+I,25	15	3+9+8+3	I,2	7
TO 59-1 #46	6.6	VIII+I,26	II+I,25	14	4+9+8+4	I,2	7
ETP 60.295	7.5	VIII+I,28	II+I,28	20	6+9+8+6	I,3	7
TO 59-1 #35	7.7	VIII+I,26	II+I,25	19	7+9+8+7	I,4	7
TO 59-1 #35	8.0	VIII+I,26	II+I,25	20	6+9+8+6	I,4	7
ETP 13.021	8.3	VIII+I,27	II+I,26	20	8+9+8+8	I,5	7
Cabo Blanco, Costa Rica 10 miS	8.7	VIII+I,27	II+I,28	20	9+9+8+9	I,5	7
RABMEX S-13	9.5	VIII+I,28	II+I,28	21	9+9+8+9	I,5	7
RABMEX 71 III (a,b)	10.2	VIII+I,28	II+I,27	20	9+9+8+9	I,5	7
RABMEX S-14	11.0	VIII+I,27	II+I,26	20	9+9+8+9	I,5	7
RABMEX S-14	12.2	VIII+I,28	II+I,26	21	10+9+8+10	I,5	7
RABMEX S-13	13.2	VIII+I,28	II+I,26	21	9+9+8+9	I,5	7
RABMEX 71 III (a,b)	15.2	VIII+I,28	II+I,29	20	10+9+8+9	I,5	7
RABMEX S-10	15.7	VIII+I,28	II+I,27	21	9+9+8+9	I,5	7
RABMEX S-14	23.5	VIII+I,28	II+I,26	20	9+9+8+9	I,5	7
RABMEX S-2	29.7	VIII+I,28	II+I,28	20	9+9+8+9	I,5	7

Specimens between dashed lines are undergoing notochord flexion.

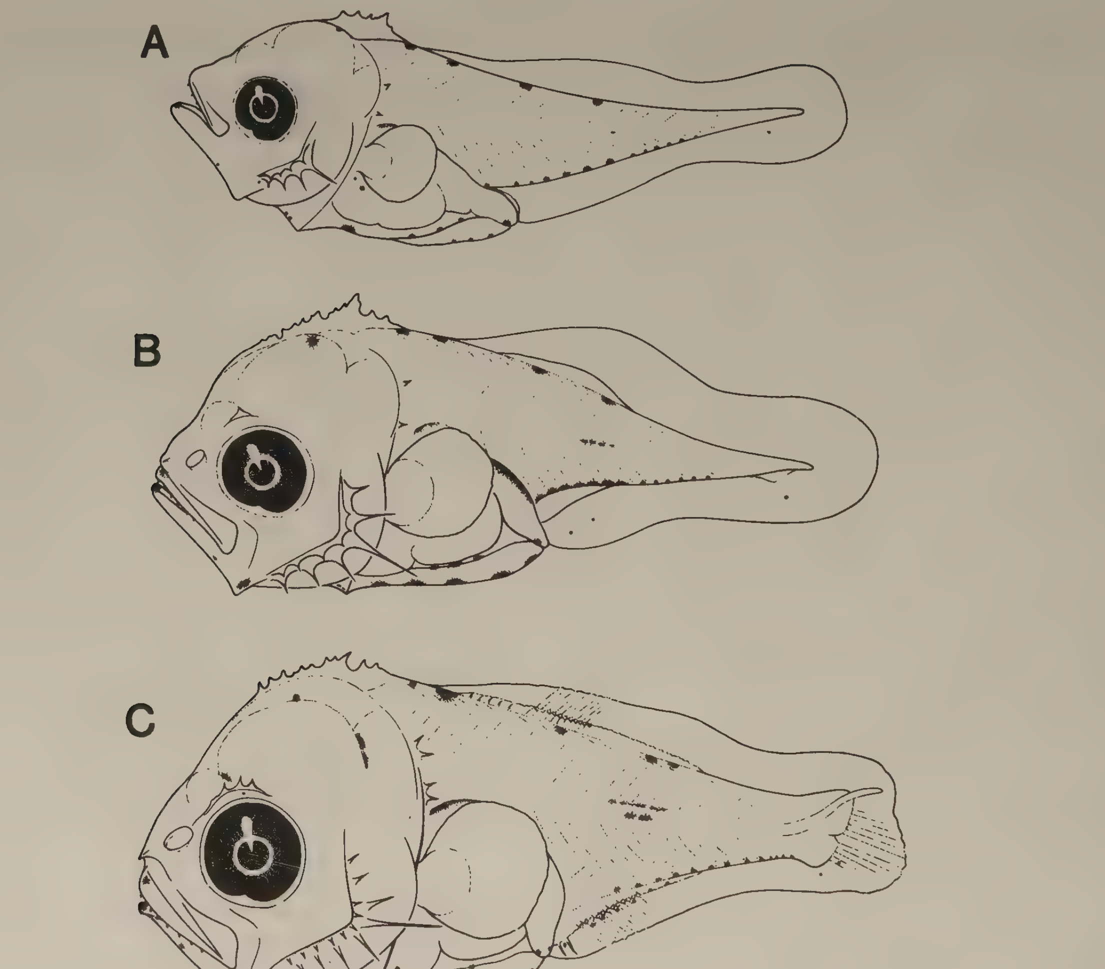

Figure 5. Larvae of *Chloroscombrus orqueta*: *A*, 2.7 mm; *B*, 2.9 mm; *C*, 3.7 mm; *D*, 5.1 mm.

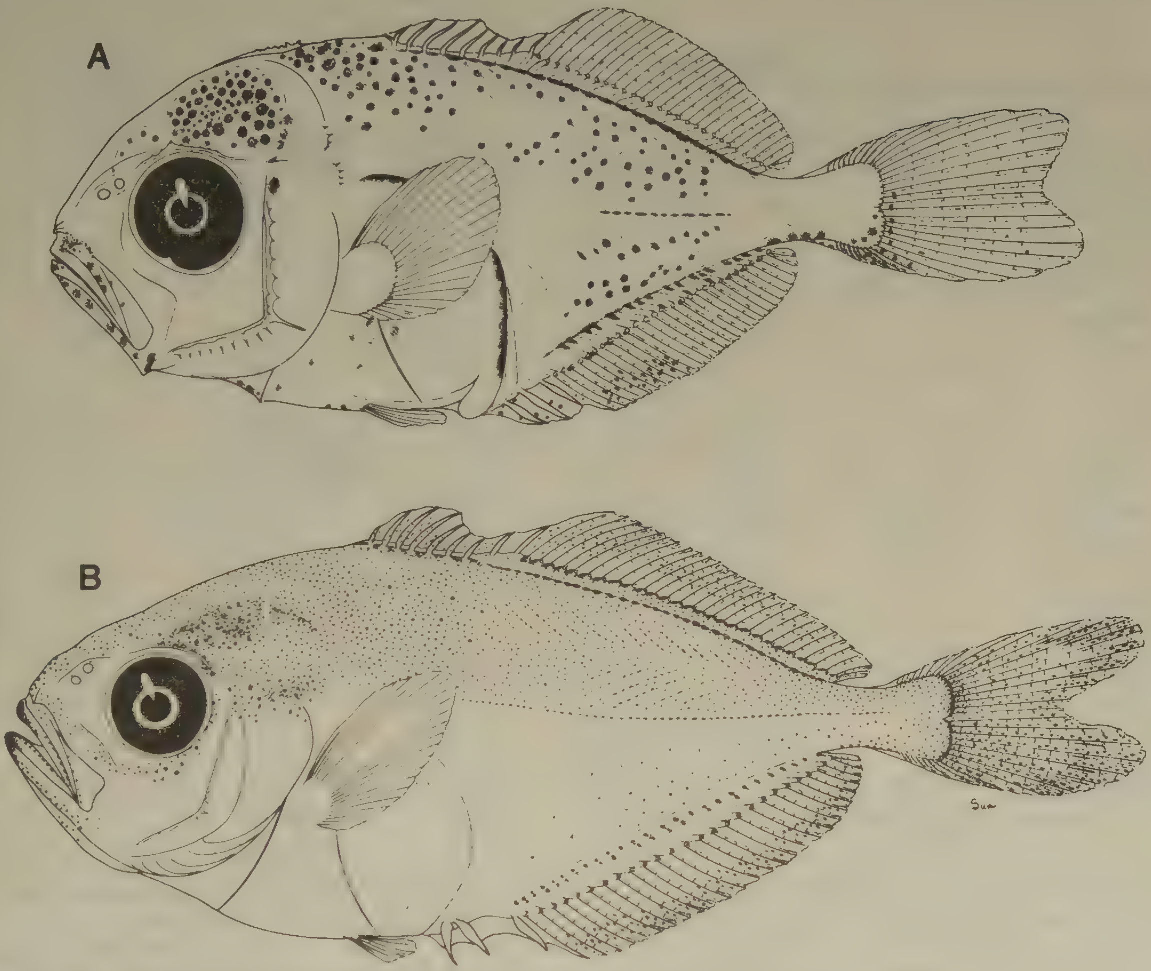

Figure 6. Postflexion larva and early juvenile of *Chloroscombrus orqueta*: *A*, 10.2 mm; *B*, 23.5-mm juvenile.

pigmentation above the spinal column also develops at this time, but is obscured by overlying body musculature. Myoseptal pigmentation on the dorsal surface of the body as well as melanophores in the shoulder region appear later, at about 7.2 mm.

By the early juvenile stage (~23.5 mm; Figure 6B), pigmentation is confined to the dorsolateral half of the head and body region, and remains sparse or lacking on the ventrolateral half. Fin pigmentation initially develops on the anal and caudal fins by about 10.0 mm, and concentrates on the musculature overlying the pterygiophores of the dorsal and anal fins and on the distal margins of the dorsal, anal, and caudal fins in early juvenile stages (Figure 6A, B). The pectoral fins lack pigment throughout the larval and juvenile period.

Caranx caballus

Literature. Larvae of *Caranx caballus* have not been previously described.

Distinguishing features. Caranx caballus larvae are distinguishable by their pigmentation pattern and meristic count of 25 vertebrae. The body morph of early larvae resembles that of *Chloroscombrus orqueta*; however, differences in pigmentation, particularly on the dorsal body margin, differentiate the species. Small *Caranx caballus* (to ~4.0 mm) possess opposing dorsal, lateral, and ventral pigmentation streaks on the body and lack the four characteristic melanophores on the dorsal body margin of early *Chloroscombrus orqueta* larvae.

Morphology and meristics. Relative body proportions of *Caranx caballus* larvae are similar to those of

TABLE 6
Measurements (mm) of *Caranx caballus*

Station	Body length	Snout-anus length	Head length	Eye diameter	Snout length	Body depth at pectoral fin base
ETP 46.135	3.0	1.8	1.0	0.28	0.32	1.0
ETP 46.135	3.6	2.2	1.3	0.36	0.36	1.2
Cabo Blanco, Costa Rica	3.8	2.2	1.3	0.38	0.36	1.4
Cabo Blanco, Costa Rica	3.9	2.3	1.4	0.44	0.38	1.7
" "	4.4	2.5	1.6	0.54	0.40	1.8
TO 59-1 #38 surf.	4.9	2.7	1.6	0.54	0.46	2.0
Cabo Blanco, Costa Rica	5.0	2.7	1.7	0.56	0.46	2.1
" "	5.4	3.0	2.0	0.60	0.64	2.3
Mazatlan 8, Sta. 6	6.3	3.5	2.2	0.76	0.64	2.8
ETP 47.040	7.8	4.4	2.9	1.0	0.68	3.6
67-2, N19	9.3	5.2	3.4	1.2	0.72	4.2
67-2, N19	10.9	6.0	4.2	1.5	1.0	5.0
ETP 47.019	11.7	6.8	4.3	1.4	1.1	5.4
67-2, N19	13.2	7.2	4.8	1.7	1.2	5.7
67-2, N50	16.7	8.9	5.5	2.2	1.2	7.0
67-2, N50	18.4	9.5	6.4	2.4	1.4	7.7
RABMEX S-13	21.7 juv.	11.4	7.7	2.7	2.0	8.5

Specimens between dashed lines are undergoing notochord flexion.

Chloroscombrus orqueta at equivalent stages of development (Tables 1 and 6). Larvae are deep-bodied (Figure 1); relative body depth increases throughout the larval period and decreases slightly in juveniles. Relative snout-anus distance decreases throughout the larval period. Gut development is similar to that described for *C. orqueta*. Relative head length and eye diameter increase during the larval period, while relative snout length decreases.

Spines develop on the preopercle, posttemporal, and supracleithrum. By 3.0 mm, larvae have a large spine at the angle, three below the angle, and one above the angle on the preopercular margin. Larvae 5-6 mm have up to 5 spines below the angle, 7-17-mm larvae have 6-7 spines, and 18-24-mm larvae have 8-9 spines below the angle. The number of spines above the angle increases to about 2 in 4-mm larvae, 4 in 5-8-mm larvae, and 5-6 in larger larvae. The angle spine is relatively largest in 3-mm larvae (10% of body length) and becomes relatively smaller gradually in later larval stages. Larvae ≤3.0 mm develop 3 spines below the angle of the preopercular ridge, and 4-8-mm larvae have 5 spines. Larvae 3-8 mm have only a single spine above the angle. Larvae larger than 8 mm resorb all preopercular ridge spines.

By 3 mm, larvae form a single posttemporal and a supracleithral spine, and develop no additional posttemporal spines; however, by 5.0 mm, a second supracleithral spine appears. Larvae lose both types of spines at about 10 mm.

By 3 mm a supraoccipital crest is present. It extends from the midregion of the optic lobes to the second myoseptum and has wide irregular serrations. After notochord flexion it is restricted to the occipital region and is absent in larvae larger than 8.0 mm. Postflexion larvae develop a supraocular shelf and pterotic ridge, but they do not develop spines.

Table 7 provides meristic counts of stained specimens.

Pigmentation. Pigmentation on *C. caballus* larvae is sparse in early stages, with a generalized pattern of opposing dorsal, lateral, and ventral streaks on the body, and melanophores on the top of the head and over the abdominal region (Figure 7). Preflexion and flexion larvae are characterized by a few melanophores in the ventral region of the gut. These mela-

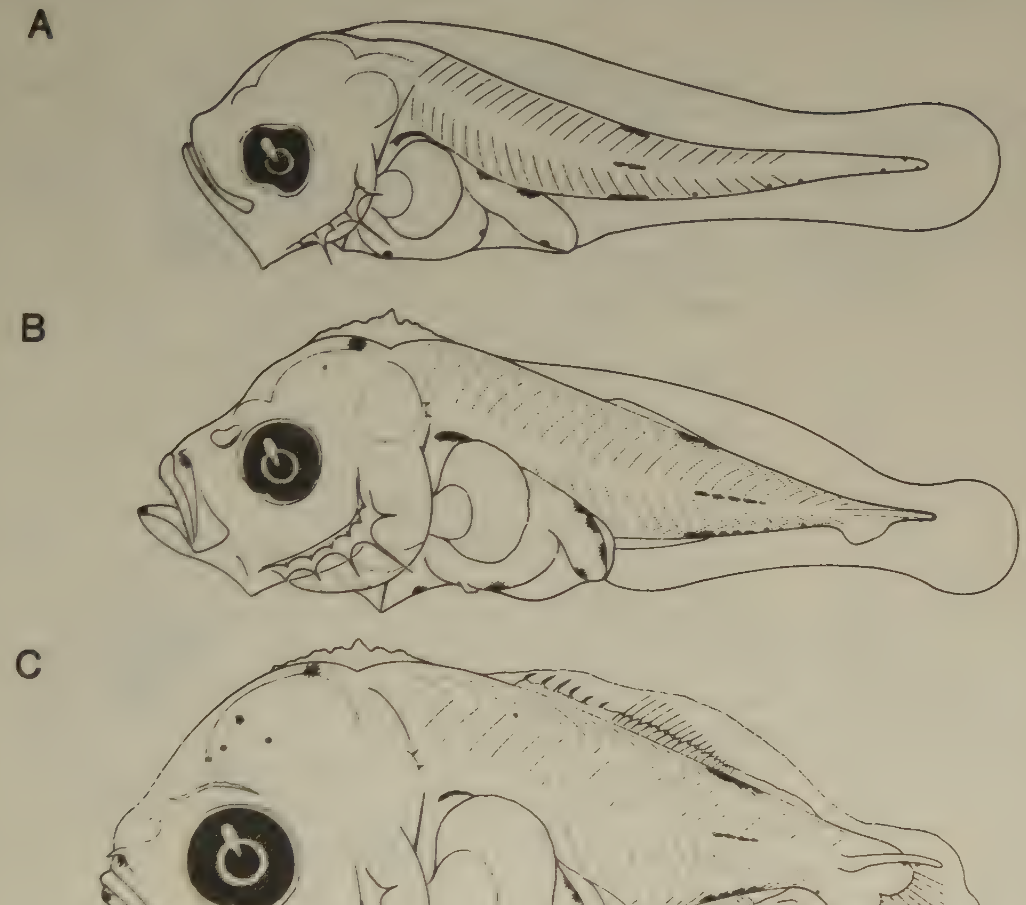

Figure 7. Larvae of *Caranx caballus*: *A*, 2.3 mm; *B*, 3.6 mm; *C*, 3.9 mm; *D*, 4.4 mm.

TABLE 7
Meristics of Stained *Caranx caballus*

Station	Body length (mm)	Dorsal fin	Anal fin	Pectoral fin	Caudal fin	Pelvic fin	Branchiostegals
ETP 46.135	3.0	—	—	—	—	—	5
TO 58-1 #59	4.0	V,13	II+I,10	—	0+4+4+0	—	7
#59	4.2	anlagen	anlagen	—	0+5+5+0	—	7
Cabo Blanco, Costa Rica	4.4	VIII+I,20	II+I,14	9	2+9+8+2	I,2	7
Cabo Blanco, Costa Rica	5.0	VIII+I,21	II+I,19	13	3+9+8+2	I,4	7
67-2 #19	6.2	VIII+I,21	II+I,18	16	4+9+8+5	I,5	7
Cabo Blanco, Costa Rica	6.7	VIII+I,23	II+I,19	17	5+9+8+5	I,5	7
Cabo Blanco, Costa Rica	7.7	VIII+I,22	II+I,20	20	6+9+8+6	I,5	7
67-1, N-22	8.6	VIII+I,22	II+I,19	20	8+9+8+8	I,5	7
67-2, #19	9.3	VIII+I,22	II+I,19	22	9+9+8+9	I,5	7
67-2, #19	10.9	VIII+I,22	II+I,19	22	9+9+8+9	I,5	7
ETP 47.019	11.7	VIII+I,23	II+I,20	22	9+9+8+9	I,5	7
67-1, N-2	13.0	VIII+I,23	II+I,19	22	9+9+8+9	I,5	7
67-2, #27A	13.9	VIII+I,23	II+I,20	22	9+9+8+9	I,5	7
ETP 14.014	16.9	VIII+I,23	II+I,19	22	9+9+8+9	I,5	7
67-2, N-50	18.4	VIII+I,23	II+I,19	22	9+9+8+9	I,5	7
ETP 14.014	23.5 juv.	VIII+I,24	II+I,20	22	9+9+8+9	I,5	7

Specimens between dashed lines are undergoing notochord flexion.

nophores are usually in an anterior, median, and posterior (next to the anus) position along the ventral margin of the gut area, with additional pigmentation along the upper section of the terminal segment of the gut.

During notochord flexion (~3.9-4.9 mm), melanophores become lightly scattered over the head and body (Figures 7C, D and 8A) in contrast to the dense pigmentation that covers all but the posterior sections of the tail in postflexion specimens. Postflexion larvae (6.3-8.5 mm) develop a cluster of pigment around the lateral midline streak (Figure 8B), which is obscured in later stages by heavy pigmentation over the trunk. Beginning at about 13.0 mm, melanophores begin forming in the middle of the caudal peduncle, and subsequently spread to the margins of the peduncle.

Bars of pigmentation are first evident on the body in specimens about 17.0 mm long (Figure 8C), persisting into the juvenile stage. Because of the heavy background pigment over the entire surface of the body, these bars are not as prominent as those in *C. sexfasciatus*.

Fin pigmentation is heavy and conspicuous on the fin membranes of the spinous dorsal, spinous portion of the anal, and the pelvic fins in postflexion larvae from about 10.5 mm through the juvenile stage. Pigment first appears on the anal and pelvic fins by about 5.5 mm and on the spinous dorsal fin by about 6.2 mm.

Caranx sexfasciatus

Literature. Larvae of *Caranx sexfasciatus* have not been previously described.

Distinguishing features. A unique feature of

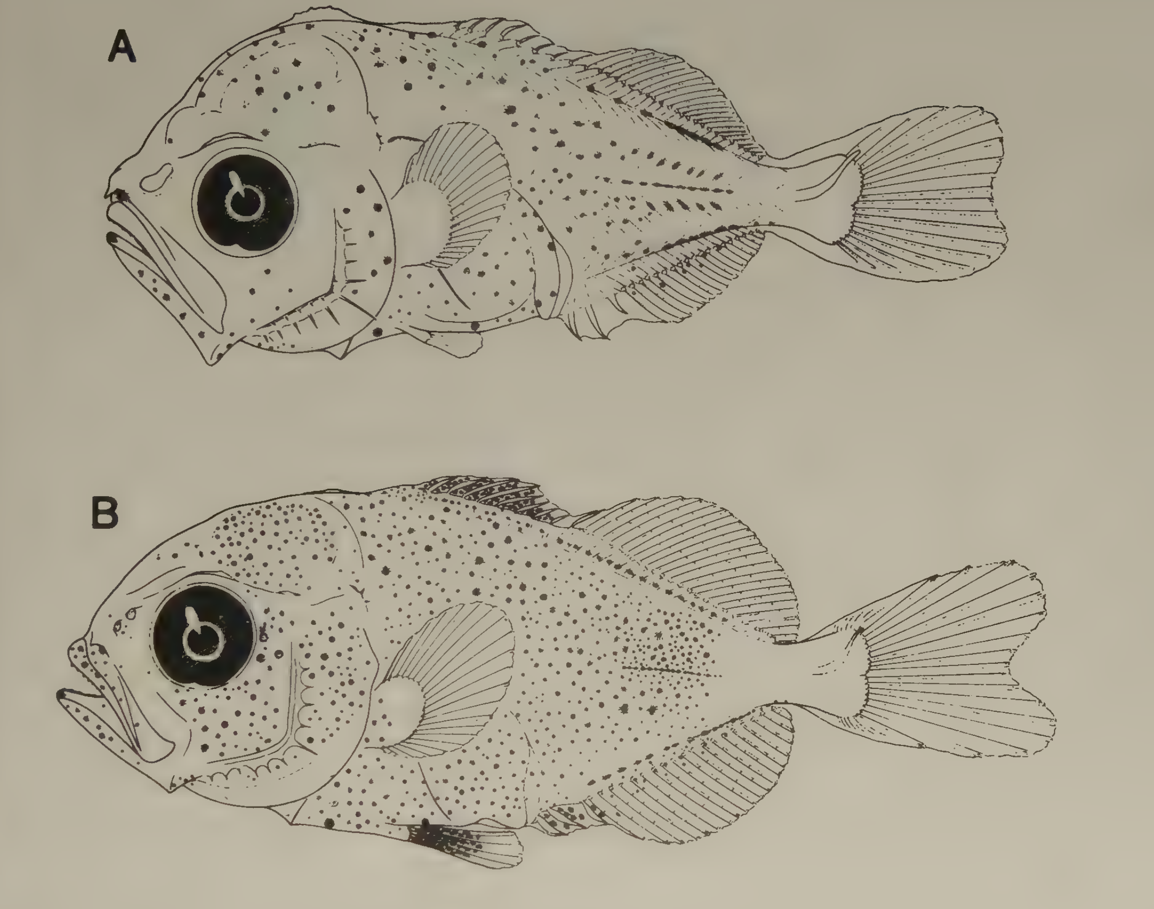

Figure 8. Postflexion larvae of *Caranx caballus*: *A*, 4.9 mm; *B*, 8.4 mm; *C*, 17.0 mm.

TABLE 8
Measurements (mm) of *Caranx sexfasciatus*

Station	Body length	Snout-anus length	Head length	Eye diameter	Snout length	Body depth at pectoral fin base
7205-JD 157G.150	2.6	1.4	0.76	0.24	0.22	0.76
ETP 13.019	3.0	1.6	0.90	0.30	0.24	1.0
7205-157G.150	3.1	1.7	1.0	0.34	0.28	1.1
7205-157G.150	3.4	1.9	1.1	0.34	0.36	1.3
TO 58-1 #69	3.8	2.1	1.4	0.40	0.40	1.6
ETP 13.019	4.0	2.3	1.4	0.44	0.42	2.0
Cabo Blanco, Costa Rica	4.2	2.4	1.4	0.48	0.42	1.9
TO 59-1 #35	4.5	2.7	1.7	0.60	0.46	2.5
TO 58-1 #69	4.6	2.8	1.8	0.60	0.50	2.5
Mazatlan 5-14-0	4.8	2.8	1.7	0.60	0.46	2.5
Cabo Blanco, Costa Rica	5.3	3.3	2.1	0.70	0.50	2.8
ETP 12.033	5.9	3.3	2.0	0.72	0.56	2.9
ETP 46.134	6.6	4.0	2.6	0.88	0.68	3.6
ETP 30.114	7.7	4.2	2.9	1.0	0.80	4.4
7205-G-157G.150	8.5	5.1	3.2	1.2	0.76	4.6
ETP 47.019	9.4	5.1	3.6	1.3	0.80	5.2
ETP 14.232	12.5	6.4	4.6	1.5	0.91	6.6
TO 5801 #141	15.4	8.4	5.8	2.1	1.6	7.8
SIO 64-140	22.8 juv.	11.4	7.7	2.5	2.0	10.5
67-2, N51	30.4 juv.	14.0	9.5	3.3	2.3	12.4

Specimens between dashed lines are undergoing notochord flexion.

Caranx sexfasciatus larvae is a conspicuously pigmented supraoccipital crest. All other described carangid larvae with a supraoccipital crest lack pigment on this structure. Another distinctive character in larvae larger than about 3.4 mm is a preanal finfold that is covered with pigment until resorption of the finfold at about 10.0 mm. Larvae are considerably deep-bodied following notochord flexion, and possess the smallest number of anal fin rays (15-17) among *Caranx* species in the eastern Pacific.

Morphology and meristics. Preflexion larvae of *C. sexfasciatus* are of moderate body depth, but become markedly deep-bodied in later stages (Tables 1 and 8; Figure 1). Body depth averages 35% of body length in preflexion larvae, but increases to over 50% of body length in flexion and postflexion larvae, diminishing to about 44% in early juveniles.

Relative gut length, head length, and eye diameter increase slightly in the larval period, but diminish in juveniles. Relative snout length remains constant at about 29% in preflexion- and flexion-stage larvae, decreasing to about 25% in postflexion larvae and juveniles. Gut development is similar to that described for *C. orqueta*.

As in *C. caballus*, spines develop on the preopercle, posttemporal, and supracleithrum. Small larvae <3 mm have a large spine at the angle of the preopercular margin, 2 below the angle, and 1 above the angle. Postflexion larvae up to about 8.5 mm develop 4 spines below the angle; 9-12-mm larvae have 5 spines; and specimens larger than 13 mm have 6 spines. The number above the angle increases to 3-4 in postflexion larvae up to about 9.0 mm and is reduced to 1 or none in specimens larger than 12 mm. The angle spine is relatively largest in 3-mm larvae (maximum of 15% of body length) and subsequently decreases gradually in relative size. Larvae ≤3 mm develop 4 spines below the angle of the preopercular ridge; by 6.0 mm, 4-5 spines are present. These spines are lost in larvae >6.0 mm. A single spine is present above the angle of the ridge until the completion of notochord flexion (~4.5 mm), after which there is none.

By 4.0 mm, larvae have a single spine on the su-

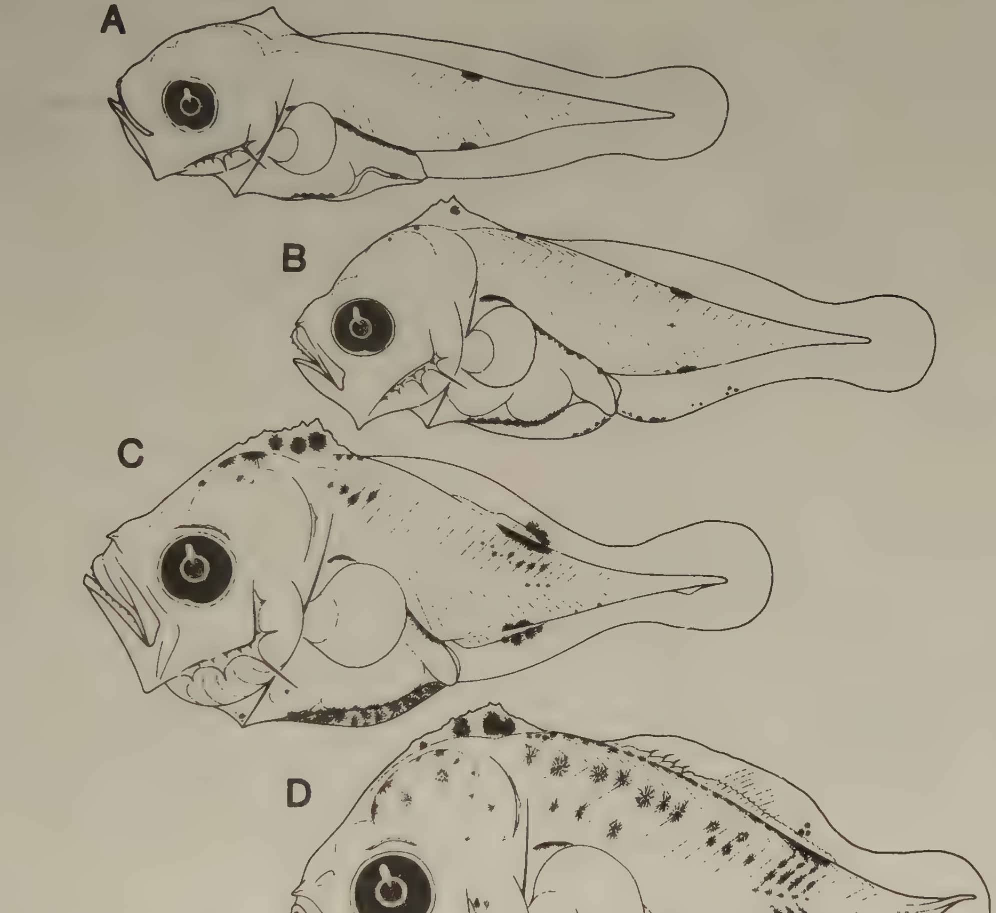

Figure 9. Larvae of *Caranx sexfasciatus*: *A*, 2.6 mm; *B*, 3.0 mm; *C*, 3.4 mm; *D*, 4.0 mm; *E*, 4.2 mm.

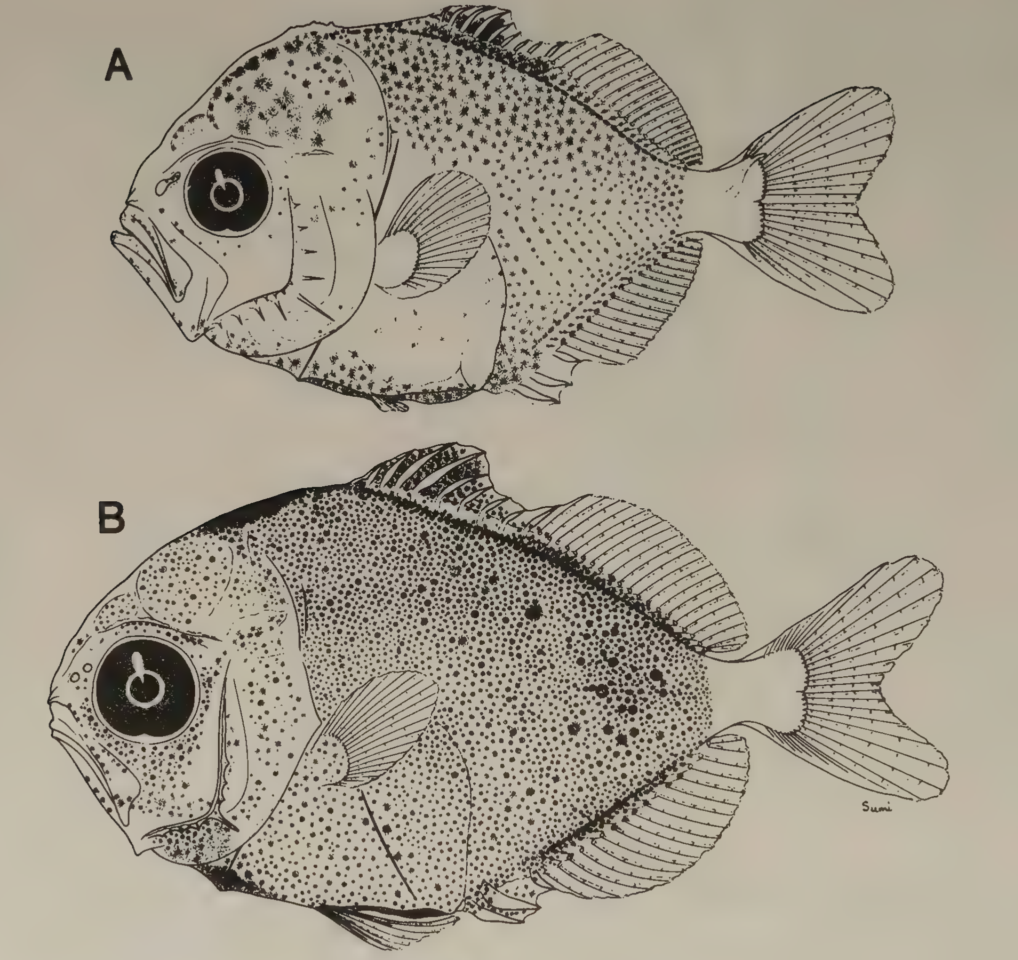

Figure 10. Postflexion larvae of *Caranx sexfasciatus*: *A*, 5.5 mm; *B*, 9.4 mm; *C*, 15.4 mm.

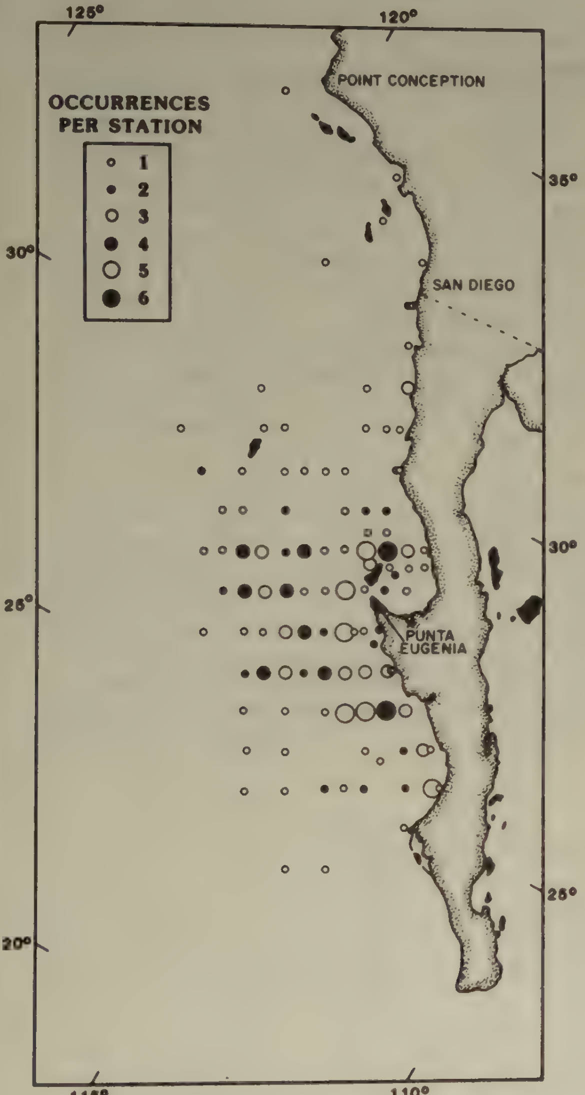

Figure 11. Pooled numbers of occurrences of larvae of *Seriola lalandi* in standard CalCOFI tows taken from 1954 to 1969.

pracleithrum; it remains until about 12.0 mm. At about 4.5 mm, a single posttemporal spine forms directly above the supracleithral spine and is variously present or absent in larvae up to about 8.5 mm, after which it is absent.

Our smallest larvae, <3.0 mm long, have developed a small supraoccipital crest. It enlarges rapidly to its maximum development at about 3.0 mm. It is triangular, with a peak above the occipital region and a convex forward margin, sometimes with minute serrations. It becomes flat and inconspicuous during notochord flexion and is absent in larvae larger than 8.0 mm. An inconspicuous supraocular crest and pterotic ridge develop in postflexion larvae, but these do not develop spines.

Meristic counts of stained specimens are presented in Table 9.

Pigmentation. Caranx sexfasciatus larvae possess striking melanistic pigment on the supraoccipital crest, a character unique among larval carangids that have been described. Our smallest specimens, 2.4-2.6 mm in length, have no pigmentation on the supraoccipital crest, but a single melanophore appears there by 3.0 mm (Figure 9A, B). Melanophores on the crest increase in number and intensity during the larval period until the crest is completely resorbed by 8.0 mm (Figures 9 and 10).

Another distinctive character in larvae larger than about 3.4 mm is a preanal finfold that is completely pigmented until resorption of the finfold at about 10.0 mm. Other pigmentation on early *C. sexfasciatus* consists of a pattern typical for many carangid larvae, with opposing dorsal, lateral, and ventral streaks on the body, as well as pigment on the head and abdominal region. Pigmentation spreads rapidly on the head and body in postflexion larvae (Figures 9E and 10), resulting in a very heavily pigmented body, with the exception of the caudal peduncle. By 15.4 mm, the caudal peduncle is pigmented, and the body exhibits the dark vertical stripes characteristic of the juvenile stage (Figure 10C).

Fin pigmentation remains sparse except for the spinous dorsal fin, which is pigmented early in the larval period, at about 5.5 mm. Pigmentation on this fin persists and intensifies to the late juvenile stage. The anterior portion of the anal fin is also pigmented in the early stages, but the pigment is transitory.

DISTRIBUTION

Seriola lalandi is reported to range from southern Washington to Chile, including the Gulf of California (Miller and Lea 1976); however, the larval distribution is limited to warmer waters. Within all CalCOFI plankton tows taken from 1954-69, *S. lalandi* larvae occurred in 206 samples. The northernmost occurrence was off Point Conception in July 1965; incidence was highest off central Baja California, where larvae were found in a broad band from nearshore to about 200 miles offshore (Figure 11). Incidence of yellowtail larvae was low off southern California (4% of occurrences) compared to Baja California, which had 96% of the occurrences.

Yellowtail larvae were collected from April to October, with 83% of the occurrences in July and

TABLE 9
Meristics of Stained *Caranx sexfasciatus* Larvae

Station	Body length (mm)	Dorsal fin	Anal fin	Pectoral fin	Caudal fin	Pelvic fin	Branchiostegals
7205-157G.150	2.5	—	—	—	—	—	—
7205-157G.150	2.7	—	—	—	—	—	4
7205-157G.150	3.0	—	—	—	—	—	6
75.04 Sta. 8	3.5	—	—	—	—	—	7
TO 59-1 #35	4.7	IX,15	II+I,11	8	1+9+8+1	—	7
Cabo Blanco, Costa Rica	5.3	VIII+I,19	II+I,15	14	4+9+8+4	bud	7
ETP 12.033	5.9	VIII+I,19	II+I,16	15	3+9+8+3	bud	7
75.04 Sta. 2	6.1	VII+I,19	II+I,15	15	5+9+8+5	bud	7
ETP 30.114	7.7	VIII+I,19	II+I,16	18	7+9+8+7	I,3	7
Costa Rica 37-2	9.0	VIII+I,20	II+I,15	20	8+9+8+8	I,5	7
ETP 14.232	12.5	VIII+I,19	II+I,16	21	9+9+8+9	I,5	7
TO 58-1 #69	13.7	VIII+I,20	II+I,17	21	9+9+8+9	I,5	7

Dashed line separates preflexion from postflexion larvae.

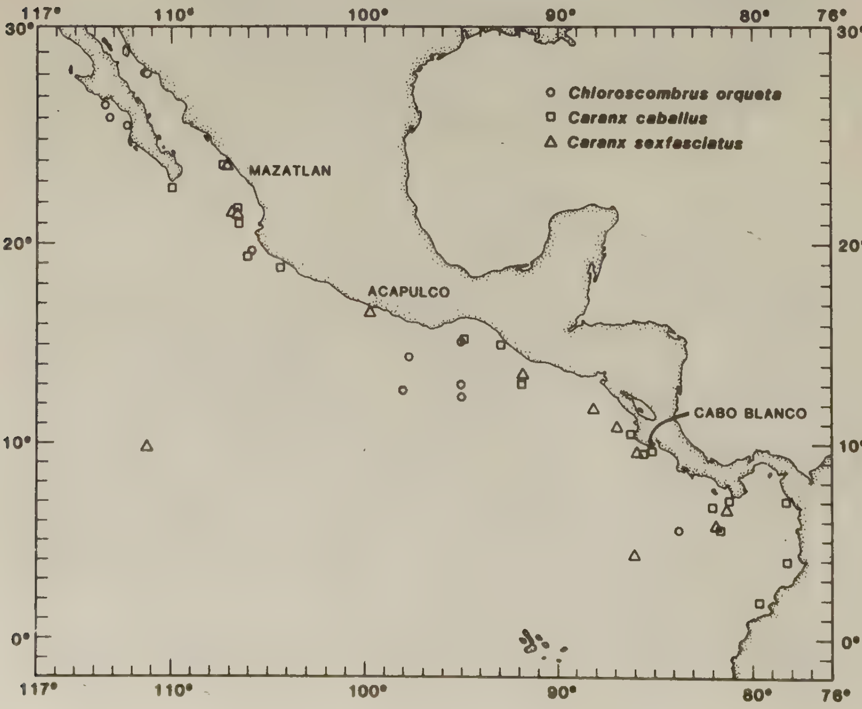
117°
110°
100°
90°
80°
76°
30°
20°
10°
0°
○ Chloroscombrus orqueta
□ Caranx caballus
△ Caranx sexfasciatus
MAZATLAN
ACAPULCO
CABO BLANCO

Figure 12. Occurrences of larvae of *Chloroscombrus orqueta*, *Caranx caballus*, and *Caranx sexfasciatus*. Omitted in this figure are a cluster of *Chloroscombrus orqueta* occurrences near San Carlos Bay, Gulf of California, and clusters of occurrences of the above three species off Cabo Blanco, Costa Rica.

August. This seasonal pattern correlates with the spawning period, reported to be in the spring and summer (Walford 1974). In their observations of maturing ova, Smith and Paul (1960) concluded that spawning generally begins in July and continues until October.

The size-frequency distribution of yellowtail larvae collected in CalCOFI samples in 1954-69 was narrow, with a mean length of 4.1 mm ± 1.16 SD and a range of 2.8-17.9 mm for the 429 larvae measured.

Figure 12 shows localities where larvae of *Chloroscombrus orqueta*, *Caranx caballus*, and *Caranx sexfasciatus* were taken. Of these three species, *Chloroscombrus orqueta* and *Caranx caballus* range as far north as southern California (Hubbs et al. 1979; Miller and Lea 1976), but none of our larvae was taken north of Baja California.

ACKNOWLEDGMENTS

We extend our sincere thanks to Henry Orr and Roy Allen for illustration and drafting assistance, and to George Mattson, who illustrated many of the early *Seriola* larvae. We are indebted to David Ambrose, Elaine Sandknop, and Elizabeth Stevens, who verified identifications of yellowtail larvae; to Rich Charter and Larry Zins, who kindly assisted with the CalCOFI data base; and to the SWFC Technical Support Group for typing the manuscript.

LITERATURE CITED

Aboussouan, A. 1968. Oeufs et larves de teleosteen de l'ouest africain VI. Larves de *Chloroscombrus chrysurus* (Linne) et de *Blepharis crinitus* (Mitchill) (Carangidae). Bull. Inst. Fondam Afr. Noire, Ser. A. 30(3):226-237.

Ahlstrom, E.H., and O.P. Ball. 1954. Description of eggs and larvae of jack mackerel (*Trachurus symmetricus*) and distribution and abundance of larvae in 1950 and 1951. Fish. Bull., U.S. 56(97):209-245.

Ahlstrom, E.H., J.L. Butler, and B.Y. Sumida. 1976. Pelagic stromateoid fishes (Pisces, Perciformes) of the eastern Pacific: kinds, distributions, and early life histories and observations on five of these from the Northwest Atlantic. Bull. Mar. Sci. 26(3):285-402.

Brownell, C.L. 1979. Stages in the early development of 40 marine fish species with pelagic eggs from the Cape of Good Hope. Ichthyol. Bull., J.L.B. Smith Inst. Ichthyol., Rhodes Univ. 40, 84 p.

Hubbs, C.L., W.I. Follett, and L.J. Dempster. 1979. List of the fishes of California. Occ. Pap. Calif. Acad. Sci. 133, 51 p.

Laroche, W.A., W.F. Smith-Vaniz, and S.L. Richardson. 1984. Carangidae: development. *In* H.G. Moser, W.J. Richards, D.M. Cohen, M.P. Fahay, A.W. Kendall, Jr., and S.L. Richardson (eds.), Ontogeny and systematics of fishes. Spec. Publ. No. 1, Amer. Soc. Ichthyol. Herpetol., p. 510-522.

MacCall, A.D., G.D. Stauffer, and J.P. Troadec. 1976. Southern California recreational and commercial marine fisheries. Mar. Fish. Rev. 38(1): 1-32.

Miller, D.J., and R.N. Lea. 1976. Guide to the coastal marine fishes of California. Calif. Dept. Fish Game Fish Bull. 157, 249 p.

Moser, H. G., and E.H. Ahlstrom. 1970. Development of lanternfishes (family Myctophidae) in the California Current. Part I. Species with narrow-eyed larvae. Nat. Hist. Mus. Los Angeles Cty. Sci. Bull. 7, 145 p.

Smith, E.J., Jr., and C.V. Paul. 1960. Maturity and fecundity. *In* J.L. Baxter (ed.), A study of the yellowtail *Seriola dorsalis* (Gill). Calif. Dept. Fish Game Fish Bull. 110:46-52.

Walford, L.A. 1974. Marine game fishes of the Pacific coast from Alaska to the equator. Reprinted for the Smithsonian Institution by T.F.H. Publ. Neptune City, N.J., 205 p.

8592

OBSERVER EFFECT ON INCIDENTAL DOLPHIN MORTALITY IN THE EASTERN TROPICAL PACIFIC TUNA FISHERY

Bruce E. Wahlen[1] and Tim D. Smith[2]

ABSTRACT

Scientific observers placed aboard a sample of purse seine vessels collect data that are used to estimate the total number of dolphins killed incidentally in the eastern tropical Pacific tuna fishery. If the presence of these observers, who are not crew members, affects incidental kill levels, then the kill estimates will be biased. To test for the existence of such an observer effect, we compared dolphin kill data that had been recorded by observers who differed in levels of obtrusiveness according to their purposes for data collection. Some observers were placed on board primarily to collect data for estimating the total number of dolphins killed annually. Other observers collected data both for that purpose and for monitoring compliance with dolphin-release regulations. Our results confirm that the presence of an observer does affect dolphin kill. The primary effect is an increase in the proportion of sets with no dolphins killed, and a decrease in the proportion of sets with one to nine dolphins killed. While the magnitude of the effect of observers cannot be estimated from our data, estimates of total dolphin mortality based on data collected by the scientific observers are biased downward.

Schools of dolphins of several species, primarily *Stenella attenuata* and *S. longirostris*, have been used since the late 1950s by purse seine fishermen in the eastern tropical Pacific Ocean (ETP) to locate and catch yellowfin tuna, *Thunnus albacares*. Perrin (1969) described the process of deploying, or setting, the net around the tuna and dolphins, and then releasing the dolphins while retaining the tuna. Significant numbers of dolphins have been killed incidentally in this fishery by becoming entangled in the purse seines (Smith 1983).

The National Marine Fisheries Service (NMFS) and the Inter-American Tropical Tuna Commission (IATTC) place scientific observers who are not crew members aboard a sample of tuna purse seine vessels to collect data related to dolphin kill. Both the NMFS and IATTC have used the data collected by these scientific observers to estimate the total number of dolphins killed annually by the entire tuna purse seine fleet (Lo et al. 1982; Hammond and Tsai 1983).

Additionally, the NMFS uses these data to monitor dolphin kills relative to annual kill limits established for the U.S. registered fleet (Lo et al. 1982). Periodic estimates of the cumulative numbers of dolphins killed are compared with the annual limit. If the limit is exceeded, U.S. vessels must stop fishing on the affected populations for the remainder of the year.

Data collected by the NMFS observers have also been used to monitor compliance of vessel operators with dolphin-release regulations, including the release of all live dolphins from the net (Federal Register 1977, 1980). Until recently, data collected by an NMFS observer could be used as evidence to prosecute vessel operators for violations of these regulations.

Observer effects have been defined in a general context as measurement procedures which influence and thereby change the behavior of the subject (Johnson and Bolstad 1973, p. 38). Researchers have encountered such effects in a variety of empirical sciences, including psychology (Johnson and Bolstad 1973), social science (Webb et al. 1966, p. 18), and biology (Ricker 1975, p. 87).

We defined an observer effect on the number of dolphins killed as a differential in levels of dolphin kill between trips made with and without a scientific observer. The existence of such a differential would introduce a bias into estimates of the total number of dolphins killed (Smith 1983; Powers[3]). Large numbers of sets involving dolphins (dolphin sets) are made each year (Punsly 1983), so even a moderate observer effect could result in a substan-

---

[1] Southwest Fisheries Center La Jolla Laboratory, National Marine Fisheries Service, NOAA, P.O. Box 271, La Jolla, CA 92038.

[2] Southwest Fisheries Center La Jolla Laboratory, National Marine Fisheries Service, NOAA, P.O. Box 271, La Jolla, CA; present address: Northeast Fisheries Center Woods Laboratory, National Marine Fisheries Service, NOAA, Woods Hole, MA 02543.

[3] Powers, J. E. 1979. A discussion of incidental mortality by unobserved United States purse seiners. Unpubl. manuscr., 7 p. Southwest Fisheries Center La Jolla Laboratory, National Marine Fisheries Service, NOAA, P.O. Box 271, La Jolla, CA 92038.

Manuscript accepted November 1984.
FISHERY BULLETIN: VOL. 83, NO. 4, 1985.

tial bias in the estimates of annual dolphin kill.

Directly testing for the existence of an observer effect on dolphin kills would require comparison of covert observations with observations by NMFS and IATTC observers. Based on the large difference between the kill rate observed covertly by one crew member and the kill rates recorded by NMFS observers during other fishing trips made by the same operator and vessel, Smith (1983) speculated that a large observer effect existed. We investigated the significance of the difference in kill rates reported by Smith (1983) by grouping NMFS-observed trips into sequences of trips with common operator and vessel. A few of these sequences of NMFS-observed trips revealed between-trip kill rate differences as large or larger than in the sequence that included the covert observations.

The existence of an observer effect can be indirectly tested without relying on data from covert observers. Johnson and Bolstad (1973) established the existence of an observer effect by comparing measurements made by observers with various levels of obtrusiveness to the human subjects whose responses were being measured. They concluded that the differences in the responses measured by observers with different levels of obtrusiveness implied that the observer's presence had affected the subjects' behavior. They noted, however, that the magnitude of an observer effect cannot be estimated using this approach.

Following this indirect approach, we tested for the existence of an observer effect on the numbers of dolphins killed by comparing dolphin kill data collected by scientific observers who differed in their purposes of data collection, and hence, in their levels of obtrusiveness.

DATA

The scientific observers were placed aboard a random sample of U.S. registered tuna purse seine vessels (Lo et al. 1982). Assignment of an NMFS or IATTC observer to vessels in the sample was also made randomly, subject to the constraint that any vessel sampled twice within a calendar year would be accompanied by an NMFS observer on at most one trip (Table 1).

Information collected for each NMFS- or IATTC-sampled fishing trip included departure date and data pertaining to each set (such as set type, date, and location), and for dolphin sets, the number of dolphins killed. Data available to the authors from NMFS-sampled trips included all of this information. However, data available from IATTC-sampled trips did not include departure date, and set dates were available only to the quarter of the year.

While the data items collected by both types of scientific observer have been similar over the years, for NMFS observers the purposes of the data collection changed after March 1981. The primary purposes of data collection, as explained to each vessel operator at a placement meeting held prior to departure, were as follows: 1) On NMFS-sampled trips begun from 1978 through March 1981, data were collected for estimating the annual kill of dolphins and for monitoring compliance with dolphin-release regulations; 2) on NMFS-sampled trips begun after March 1981 through the end of 1982, the data were still used for estimating dolphin kills but were no longer used to monitor compliance with dolphin-release regulations[4]; 3) on all IATTC-sampled trips, since the inception of that sampling program in 1979, data were collected for estimating total kill but were never collected for monitoring compliance with dolphin-release regulations.

As described above, the data collected by both NMFS and IATTC observers to estimate total dolphin kill can be used by the NMFS to halt fishing by U.S. vessels on specific dolphin populations for the remainder of the year. The data collected before March 1981 by the NMFS observers for monitoring compliance with dolphin-release regulations, however, can be used by the NMFS as evidence to prosecute operators who failed to comply. Thus, the operators are likely to be more conscious of the presence of an observer who is collecting data both for estimating dolphin kill and for monitoring com-

TABLE 1.—Number of observed fishing trips which made at least one dolphin set from 1978 through 1982, by observer type and year. NMFS totals are subdivided according to departure date of trips (previous year, Jan.-Mar., Apr.-Dec.) and exclude trips in which fishing gear research was conducted.

Observer type	1978	1979	1980	1981	1982
NMFS					
Previous year	5	4	3	3	7
Jan.-Mar.	44	33	15	7	13
Apr.-Dec.	56	32	28	28	18
Total	105	69	46	38	38
IATTC	0	31	57	58	44
Total	105	100	103	96	82

---

[4] The change in data collection purposes of NMFS observers after March 1981 was prompted by a court order forbidding the NMFS from using data collected by observers for monitoring compliance with dolphin-release regulations. No NMFS observers were placed on fishing trips begun from 1983 through part of 1984 because of a subsequent court order forbidding placement of NMFS observers without a search warrant.

pliance with dolphin-release regulations than an observer who is collecting data only for estimating dolphin kill. That this is the case is implied by the constraint in the sampling procedure that any vessel sampled twice within a calendar year may be accompanied by an NMFS observer on at most one trip.

METHODS

We tested for the existence of an observer effect on dolphin kills by comparing the number of killed dolphins recorded by more obtrusive observers with the number recorded by less obtrusive observers. We considered observers who collected data both for estimating dolphin kill and for monitoring compliance with dolphin-release regulations to be more obtrusive to vessel operators than observers who collected data only for estimating dolphin kill. Thus, we compared kills recorded by (1a) NMFS observers before and after March 1981, and (1b) NMFS and IATTC observers before March 1981. As a control, we compared the number of killed dolphins recorded by observers of equal obtrusiveness. That is, we compared kills recorded by (2a) IATTC observers before and after March 1981, and (2b) NMFS and IATTC observers after March 1981.

The frequency distributions of numbers of dolphins killed were extremely skewed, with very long right tails (Fig . 1). Normality assumptions were violated so strongly by these skewed distributions that ANOVA tests for differences in means, particularly one-sided tests, would be difficult to interpret (Glass et al. 1972). Therefore, we tested for differences in the percent of dolphin sets in which no dolphins were killed (zero-kill sets). This percent relates directly to the regulation requiring release of all live dolphins, and is a dominant feature of the dolphin kill distributions.

When comparing frequency distributions, we entertained the null hypothesis of equality of percent zero-kill sets. When comparing observers of different obtrusiveness levels, we tested this hypothesis against a one-sided alternative that distributions from more obtrusive observers had a higher percent

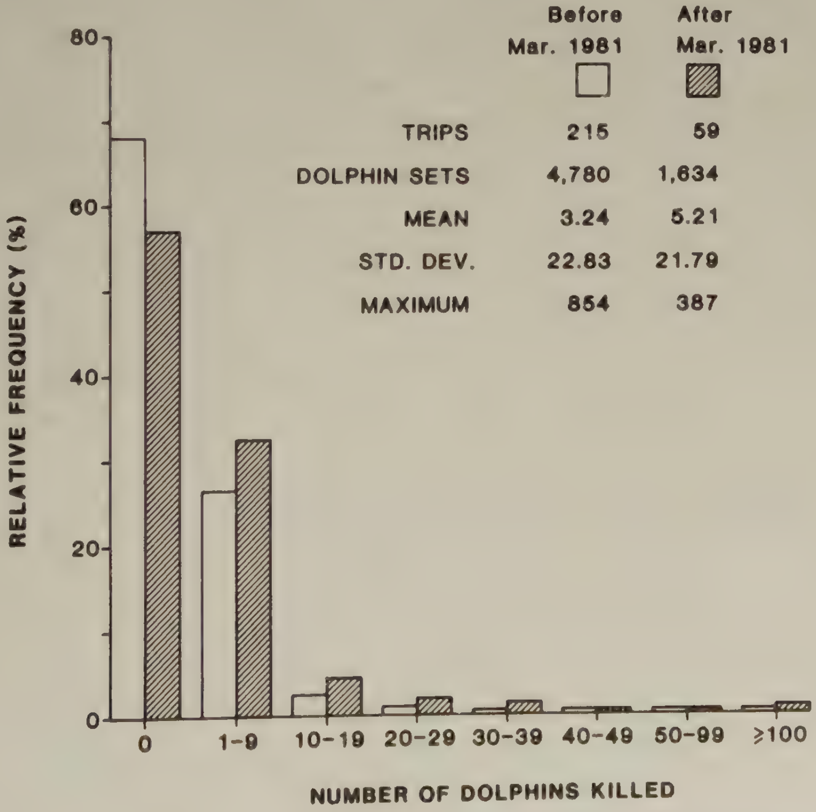

FIGURE 1.—Relative frequency distributions of number of dolphins killed incidentally during sets of NMFS-observed trips, 1978 through 1982, by trip departure date.

of zero-kill sets than distributions from less obtrusive observers. When comparing distributions from observers of equal obtrusiveness, we tested the null hypothesis against the two-sided alternate of inequality (Table 2). Results from all of our tests are reported at the 0.05 significance level.

TABLE 2.—Alternate hypotheses to the null hypothesis of equality of percent zero-kill sets for each of four comparisons, where Before and After refer to before or after March 1981. See text for details.

Comparison	Alternate hypothesis
1a. NMFS before vs NMFS after	Before > After
2a. IATTC before vs IATTC after	Before ≠ After
1b. NMFS before vs IATTC before	NMFS > IATTC
2b. NMFS after vs IATTC after	NMFS ≠ IATTC

For two-sided tests of differences in percents, we used the standard chi-square (χ^2) statistic with one degree of freedom (df). For one-sided tests, we used the square root of the chi-square statistic (Z), which is approximately normal (Snedecor and Cochran 1980, p. 126-127). In some instances, the expected cell frequencies were less than the traditionally accepted minimum of five. However, recent Monte Carlo results (Fienberg 1980, p. 172) suggest that the chi-squared distribution is an adequate approximation at the 0.05 significance level even when minimum expected values are as low as one.

While the sampling of vessels was nearly random, the actual sample obtained may not have been representative of factors affecting dolphin kills. It has been demonstrated that within the ETP, dolphin kills vary among three geographic areas[5] (Fig. 2) and by periods within the year (Lo et al. 1982). We divided the year into two periods: January-March and April-December. This division corresponds to the date of the change in data collection purposes of NMFS observers in 1981, and also tends to equalize sample size since vessels in this fishery are more active in the early part of the year.

We stratified the data by area and period of the year to account for biases due to possible nonrepresentativeness of the sample with respect to these two factors. When data on numbers of dolphins killed were available in all six area-period strata, we made overall two-sided tests for differences in per-

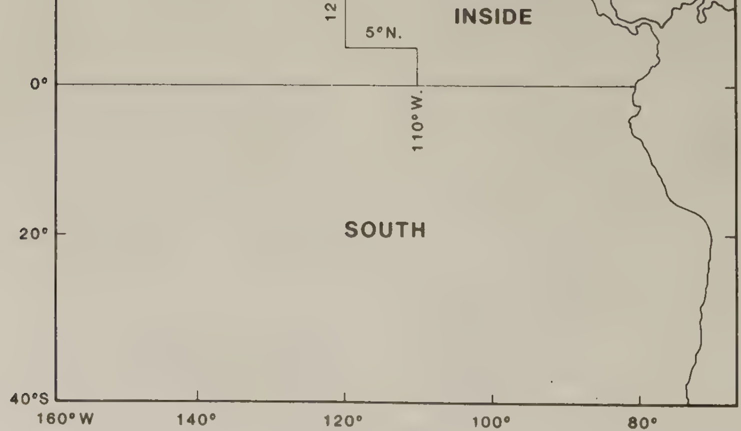

FIGURE 2.—The three areas of the eastern tropical Pacific used to stratify the data, bounded by lat. 40°N., long. 160°W., lat. 40°S., and the western coastline of the North and South American Continents.

---

[5] K.-T. Tsai, Inter-American Tropical Tuna Commission, c/o Scripps Institute of Oceanography, La Jolla, CA 92093, pers. commun. December 1983.

cent zero-kill sets (conditional on period of the year and geographic area) by summing chi-square values and degrees of freedom from each stratum. When observations were not available in one of the strata, or when the alternative was one-sided, an overall test based on the chi-square statistic was not possible. In those cases, results of the tests within each stratum were considered separately.

RESULTS

The first two comparisons of frequency distributions test for differences in the percent of zero-kill sets in data collected by observers on trips begun before compared with trips begun after the change in NMFS observer data collection purposes in March 1981 (Comparisons 1a and 2a, Table 2). The last two comparisons test for differences in the percent of zero-kill sets in data collected by observers on trips begun during the same time period (Comparisons 1b and 2b, Table 2).

Before versus After

The percent of zero-kill sets for NMFS-observed trips was higher before March 1981 than after that date (Fig. 1), and within all area-period strata with complete data, the percent of zero-kill sets was larger before March 1981 (Table 3). The one-sided test of this difference (Comparison 1a, Table 2) was significant within four of the five area-period strata which had complete data, and was very nearly significant within the fifth (Table 3). Thus, the percent of zero-kill sets recorded by NMFS observers was significantly larger before March 1981.

The significant difference in percent of zero-kill sets for NMFS observers before compared with after March 1981 could be due to the change in data collection purposes of NMFS observers which occurred then. Alternatively, the difference could be due to a temporal decline begun before that date.

Allowing for period, the data prior to March 1981 do not show a pronounced trend for any of the three areas (Fig. 3). Although there appears to be a decline in the South for Period 2, this is unreliable as it depends entirely on the 1980 and 1981 data points representing a total of only 17 sets. Similarly, there seems to be a declining trend for the two northern areas. However, for the North Inside area the Period 1 points show no decline, and the possible decline of Period 2 points depends on the 1980 Period 2 point. A 95% confidence interval about this point (observed percent ±2 × standard error), however, is large relative to the difference between it and the Period 2 point of 1979. Further, any such declining trend in Period 2 points for the North Inside area is not reflected in the low 1978 point. A similar argument can be made for North Outside area data to reject the alternative explanation of the difference in percent zero-kill sets before and after March 1981 being the result of a temporal trend begun prior to March 1981.

That the differences in percent of zero-kill sets for NMFS-observed trips was not due to a temporal trend was also tested by comparing the percent of such sets for IATTC-observed trips before and after March 1981. The percent of zero-kill sets for IATTC-observed trips was higher before March 1981, but within the six area-period strata the differences were not consistent (Table 4). The two-sided test (Comparison 2a, Table 2) was significant within only one of the six area-period strata (Period 1, South), and the sample size within that stratum was very small (Table 4). The overall conditional test given area and period was not significant. Thus, IATTC-observed trips with dolphin sets from 1979 through 1982 did

TABLE 3.—Numbers of dolphin sets (*n*) made during NMFS-observed trips, 1978 through 1982. Sets are classified by trip departure date relative to March 1981 (before or after) and to period (1 = Jan.-Mar., 2 = Apr.-Dec.), by area of set (North Inside, North Outside, South), and by numbers of dolphins killed (0, >0). Percents of column totals (%), expected frequencies (*e*), and the statistic *Z* are also tabulated. Values of $Z > 1.64$ are significant, as indicated by an asterisk.

		Period 1						Period 2							
		North Inside		North Outside		South		North Inside		North Outside		South		Total	
Kill		Before	After	Before	After	Before	After	Before	After	Before	After	Before	After	Before	After
0	*n*	1,498	226	0	21	107	0	972	421	591	229	86	33	3,254	930
	%	72.9	62.1	—	52.5	61.1	0.0	69.4	62.7	60.4	55.7	50.6	23.1	68.1	56.9
	e	1,464.7	259.3	0	21	104.0	3.0	941.9	451.1	577.4	242.6	64.6	54.4	—	—
>0	*n*	558	138	0	19	68	5	429	250	387	182	84	110	1,526	704
	%	27.1	37.9	—	47.5	38.9	100.0	30.6	37.3	39.6	44.3	49.4	76.9	31.9	43.1
	e	591.3	104.7	0	19	71.0	2.0	459.1	219.9	400.6	168.4	105.4	88.6	—	—
Total	*n*	2,056	364	0	40	175	5	1,401	671	978	411	170	143	4,780	1,634
	Z	4.18*		—		2.75*		3.01*		1.63		4.99*		—[1]	

[1] Computation of overall test statistic not possible because of one-sided alternative, and because of lack of data in one stratum (Period 1, North Outside).

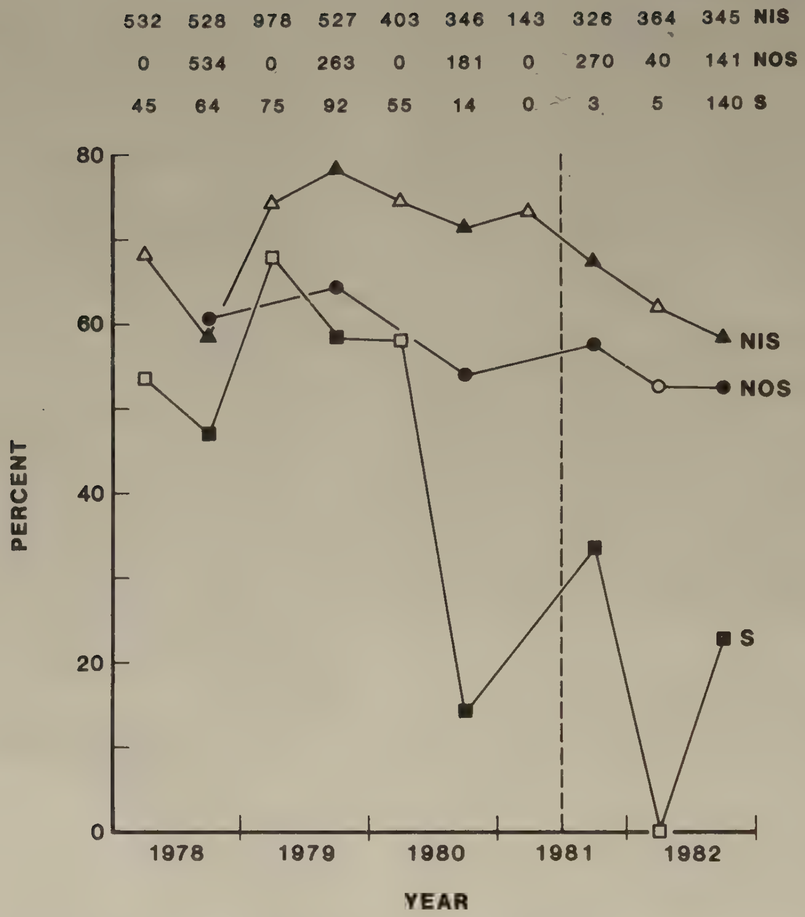

FIGURE 3.—Number of dolphin sets (upper portion) and percent of zero-kill dolphin sets (lower portion) for each of 3 areas (NIS = North Inside, NOS = North Outside, S = South) by period within year (open symbol = Jan.-Mar., closed symbol = Apr.-Dec.). Data are from NMFS-observed trips, 1978 through 1982. Vertical line separates data before and after March 1981.

TABLE 4.—Numbers of dolphin sets (*n*) made from 1979 through 1982, during IATTC-observed trips. Sets are classified by date of set relative to March 1981 (before or after) and to period (1 = Jan.-Mar., 2 = Apr.-Dec), by area of set (North Inside, North Outside, South), and by numbers of dolphins killed (0, >0). Percents of column totals (%), expected frequencies (*e*), and the statistic χ^2 with degrees of freedom (df) are also tabulated. Values of $\chi^2 > 3.84$ (1 df) or 12.59 (6 df) are significant, as indicated by an asterisk.

		Period 1						Period 2							
		North Inside		North Outside		South		North Inside		North Outside		South		Total	
Kill		Before	After	Before	After	Before	After	Before	After	Before	After	Before	After	Before	After
0	*n*	537	188	9	3	13	3	709	721	291	328	5	35	1,564	1,278
	%	67.1	71.2	26.5	14.3	38.2	12.0	70.0	70.1	58.7	55.6	33.3	24.1	65.4	61.6
	e	545.1	179.9	7.4	4.6	9.2	6.8	709.8	720.2	282,7	336.3	3.8	36.2	—	—
>0	*n*	263	76	25	18	21	22	304	307	205	262	10	110	828	795
	%	32.9	28.8	73.5	85.7	61.8	88.0	30.0	29.9	41.3	44.4	66.7	75.9	34.6	38.4
	e	254.9	84.1	26.6	16.4	24.8	18.2	303.2	307.8	213.3	253.7	11.2	108.8	—	—
Total	*n*	800	264	34	21	34	25	1,013	1,028	496	590	15	145	2,392	2,073
	χ^2	1.53		1.13		5.02*		0.01		1.04		0.61		9.34	
	df	1		1		1		1		1		1		6	

not differ significantly in their percent of zero-kill sets before or after March 1981.

Same Time Period

Before March 1981 the percent of zero-kill sets was higher for NMFS-observed trips than for IATTC-observed trips (Fig. 4), and within all area-period strata with complete data, the percent of zero-kill sets was larger for the NMFS observers (Table 5). The one-sided test (Comparison 1b, Table 2) was significant within four of the five area-period strata which had complete data (Table 5). Thus, for trips making dolphin sets from 1979 through March 1981, NMFS observers recorded a significantly higher percent of zero-kill sets than did IATTC observers.

According to our hypothesis, the difference in percent of zero-kill sets between NMFS- and IATTC-observed trips before March 1981 should have disappeared after March 1981 when the purposes for data collection of NMFS observers became nearly the same as for IATTC observers. After March 1981 the percent of zero-kill sets was higher for IATTC-observed trips than for NMFS-observed trips (Fig. 5), but within the six area-period strata the differences were not consistent (Table 6). The two-sided test (Comparison 2b, Table 2) was significant within only one of the six area-period strata (Period 1, North Inside), yet this one chi-square statistic was so large that the overall conditional test for all six strata was also significant (Table 6). It is difficult to interpret the overall result in this situation because of the extraordinary influence of one stratum. However, after March 1981 the percent of zero-kill sets on NMFS-observed trips was clearly not higher than on IATTC-observed trips.

While one would expect the mean number of dolphins killed to decrease when the percent of zero-kill sets increases, this is not necessarily so because of the sensitivity of the mean of a sample to the maximum value in the sample. For instance, in Figure 4 the NMFS maximum is nearly twice that of the IATTC, resulting in a larger NMFS mean despite the higher percent of zero-kill sets in the NMFS sample.

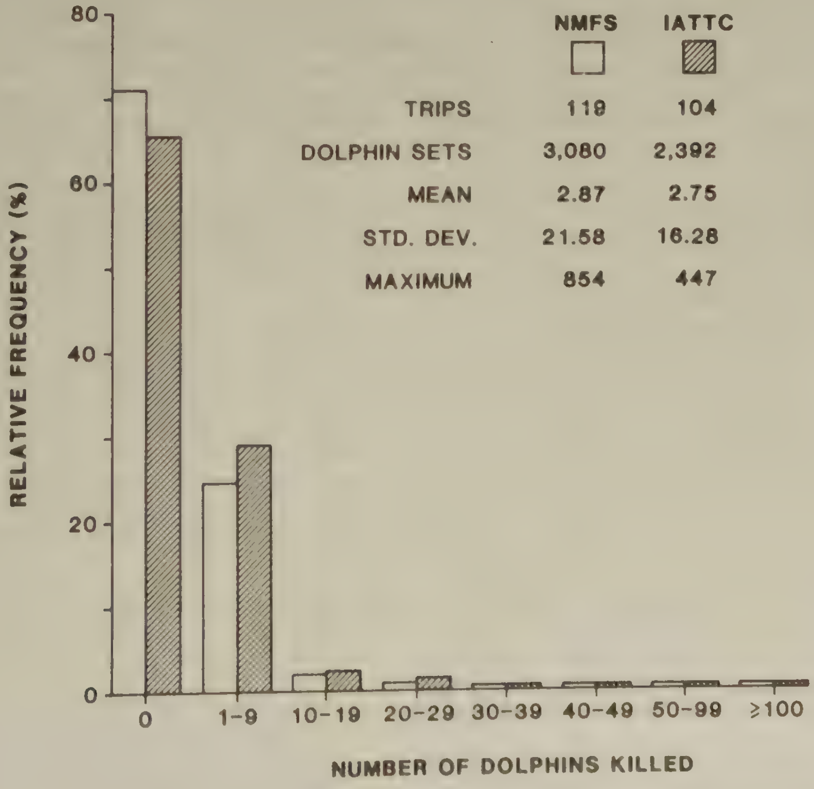

FIGURE 4.—Relative frequency distributions of number of dolphins killed incidentally during sets made from 1979 through March 1981, by observer type.

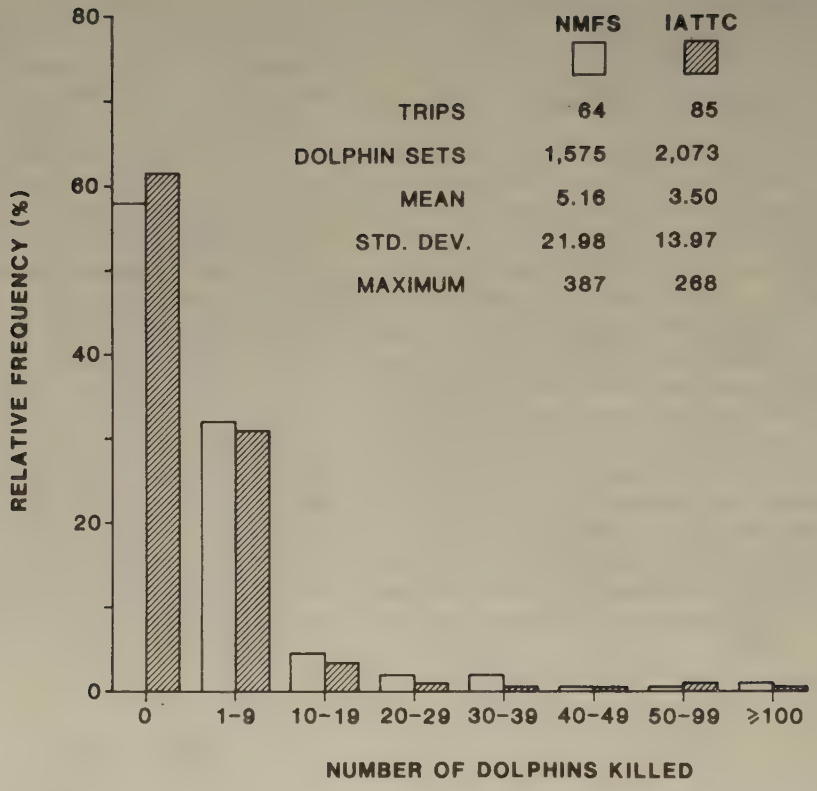

FIGURE 5.—Relative frequency distributions of number of dolphins killed incidentally during sets made after March 1981 through 1982, by observer type.

TABLE 5.—Numbers of dolphin sets (*n*) made from 1979 through March 1981. Sets are classified by observer type (NMFS, IATTC), by area of set (North Inside, North Outside, South), by date of set relative to period (1 = Jan.-Mar., 2 = Apr.-Dec.), and by numbers of dolphins killed (0, >0). Percents of column totals (%), expected frequencies (e), and the statistic *Z* are also tabulated. Values of $Z > 1.64$ are significant, as indicated by an asterisk.

		Period 1						Period 2							
		North Inside		North Outside		South		North Inside		North Outside		South		Total	
Kill		NMFS	IATTC	NMFS	IATTC	NMFS	IATTC	NMFS	IATTC	NMFS	IATTC	NMFS	IATTC	NMFS	IATTC
0	*n*	820	537	0	9	96	13	942	709	267	291	62	5	2,187	1,564
	%	72.7	67.1	—	26.5	53.9	38.2	76.8	70.0	60.1	58.7	59.6	33.3	71.0	65.4
	e	793.9	563.1	0	9	91.5	17.5	904.0	747.0	263.6	294.4	58.6	8.4	—	—
>0	*n*	308	263	0	25	82	21	284	304	177	205	42	10	893	828
	%	27.3	32.9	—	73.5	46.1	61.8	23.2	30.0	39.9	41.3	40.4	66.7	29.0	34.6
	e	334.1	236.9	0	25	86.5	16.5	322.0	266.0	180.4	201.6	45.4	6.6	—	—
Total	*n*	1,128	800	0	34	178	34	1,226	1,013	444	496	104	15	3,080	2,392
	Z	2.64*		—		1.68*		3.66*		0.46		1.92*		—[1]	

[1] Computation of overall test statistic not possible because of one-sided alternative, and because of lack of data in one stratum (Period 1, North Outside).

DISCUSSION AND CONCLUSIONS

We established the existence of an observer effect on the number of dolphins killed incidentally in the ETP yellowfin tuna fishery by following two lines of argument. First, we demonstrated a decrease in the percent of sets with no dolphins killed on NMFS-observed trips after March 1981, when monitoring compliance with dolphin-release regulations was removed as a data collection purpose (Table 3). We further showed that this difference was not due to a temporal trend in fishing conditions by examin-

TABLE 6.—Numbers of dolphin sets (*n*) made from April 1981 through 1982. Sets are classified by observer type (NMFS, IATTC), by area of set (North Inside, North Outside, South), by date of set relative to period (1 = Jan.-Mar., 2 = Apr.-Dec.), and by numbers of dolphins killed (0, >0). Percents of column totals (%), expected frequencies (*e*), and the statistic χ^2 with degrees of freedom (df) are also tabulated. Values of $\chi^2 > 3.84$ (1 df) or 12.59 (6 df) are significant, as indicated by an asterisk.

		Period 1						Period 2							
		North Inside		North Outside		South		North Inside		North Outside		South		Total	
Kill		NMFS	IATTC	NMFS	IATTC	NMFS	IATTC	NMFS	IATTC	NMFS	IATTC	NMFS	IATTC	NMFS	IATTC
0	*n*	193	188	1	3	1	3	455	721	249	328	13	35	912	1,278
	%	55.6	71.2	14.3	14.3	10.0	12.0	66.4	70.1	56.1	55.6	15.9	24.1	57.9	61.6
	e	216.4	164.6	1.0	3.0	1.1	2.9	470.3	705.7	247.8	329.2	17.3	30.7	—	—
>0	*n*	154	76	6	18	9	22	230	307	195	262	69	110	663	795
	%	44.4	28.8	85.7	85.7	90.0	88.0	33.6	29.9	43.9	44.4	84.1	75.9	42.1	38.4
	e	130.6	99.4	6.0	18.0	8.9	22.1	214.7	322.3	196.2	260.8	64.7	114.3	—	—
Total	*n*	347	264	7	21	10	25	685	1,028	444	590	82	145	1,575	2,073
	χ^2	15.53*		0.00		0.03		2.63		0.02		2.16		20.37*	
	df	1		1		1		1		1		1		6	

ing the data by period (Fig. 3) and by demonstrating the lack of a corresponding change in data collected by IATTC observers (Table 4).

Second, we demonstrated that before March 1981 the percent of sets with no dolphins killed was higher for NMFS observers collecting data both for estimating dolphin kill and for monitoring compliance with dolphin-release regulations than for IATTC observers collecting data only for estimating dolphin kill (Table 5). To validate this comparison we also demonstrated that the difference disappeared, or perhaps was reversed, following March 1981 when monitoring compliance with dolphin-release regulations was removed from the NMFS observers' responsibilities (Table 6). Following Johnson and Bolstad (1973), these differences in the data collected by observers differing in their purposes of data collection, and hence in their obtrusiveness, imply the existence of an observer effect.

In making these comparisons, we stratified the data to account for possible differences in fishing conditions in different geographic areas and throughout the year because both area and time of year are important determinants of dolphin mortality. Thus, the differences in the percent of zero-kill sets which we identified cannot be attributed to nonrepresentativeness of the data with respect to area and time of year.

We did not attempt to test for other differences in the frequency distributions of kills, such as changes in the percent of moderate or large kill sets. Sets with large numbers of dolphins killed are rare, and are generally associated with unusual circumstances, such as mechanical failures. The percent of sets with 1-9 dolphins killed appears to vary inversely with the percent of sets with zero dolphins killed (Figs. 1, 4, 5).

Powers et al.[6] showed that the use of some dolphin-release procedures significantly reduces dolphin mortality. Thus, more time and effort expended by the operator on release of dolphins could result in an increase in the frequency of sets with no dolphins killed, and a corresponding decrease in the frequency of sets with 1-9 dolphins killed. A greater tendency for vessel operators to take the additional time in the presence of an observer collecting data for monitoring compliance with dolphin-release regulations could account for the differences we have demonstrated.

The significantly different relative frequency of zero-kill sets recorded by NMFS observers after March 1981 (Table 6) was not expected under our hypothesis. As noted above, this difference was localized to one area-period stratum, and the other five strata were consistent with the null hypothesis of no difference. Either this difference is merely a sampling anomaly, or there are differences between observers in more recent years that we have not taken into account.

Gulland (1983, p. 111) described a method of testing for the existence of a tagging effect that is analogous to our indirect method of testing for an observer effect. He suggested comparing the proportions of tags returned from fish tagged under poor and good conditions. In both Gulland's and our methods, the absolute magnitude of the effects cannot be estimated. For instance, in Gulland's example improvement in the conditions under which tags are applied is unlikely to eliminate entirely the tagging effect. Similarly, the reduction in observer obtrusiveness after March 1981 is unlikely to have eliminated entirely the observer effect because the data collected by scientific observers after 1981 were still used to monitor dolphin kills relative to annual kill limits. Observers collecting data that could not be used for monitoring kill limits would be even less obtrusive than the scientific observers, and covert observers would be, of course, completely unobtrusive.

---

[6] Powers, J. E., N. C. H. Lo, and B. E. Wahlen. 1979. A statistical analysis on effectiveness of porpoise rescue procedures in reducing incidental mortality. Southwest Fish. Cent. La Jolla Lab., Natl. Mar. Fish. Serv., NOAA, Admin. Rep. LJ-79-7, 29 p.

Based on our analysis, we would expect that the frequency of zero-kill sets would be lower on unobserved vessels than on vessels with a scientific observer. This lower frequency of zero-kill sets, coupled with an increased frequency of sets with 1-9 dolphins killed, suggests that the average kill rate on unobserved vessels would be higher. Estimates of total kill, based on the average kill rates from the scientific observers, would therefore be underestimated.

ACKNOWLEDGMENTS

We gratefully acknowledge the assistance of M. M. Croom in providing data and in early discussions of the problem. We also acknowledge the assistance of K. E. Wallace and J. S. Cole in providing data. We are indebted to D. G. Chapman and W. F. Perrin for suggesting analytical methods. We also appreciate the helpful reviews by F. G. Alverson, I. Barrett, P. S. Hammond, R. S. Holt, N. C. H. Lo, N. A. Mendes, J. M. Michalski, G. T. Sakagawa, and K.-T. Tsai, as well as the reveiws by two anonymous individuals.

LITERATURE CITED

FEDERAL REGISTER.
1977. Department of Commerce, NOAA, Taking of marine mammals incidental to commercial fishing operations; final decision and final regulations. Fed. Regist. 42(247):64548-64560.

FEDERAL REGISTER.
1980. Department of Commerce, NOAA, Taking of marine mammals incidental to commercial fishing operations—permits, etc. Fed. Regist. 45(213):72178-72196.

FIENBERG, S. E.
1980. The analysis of cross-classified categorical data. 2d ed. MIT Press, Cambridge, MA, 198 p.

GLASS, G. V., P. D. PECKHAM, AND J. R. SANDERS.
1972. Consequences of failure to meet assumptions underlying the fixed effects analyses of variance and covariance. Rev. Educ. Res. 42(3):237-288.

GULLAND, J. A.
1983. Fish stock assessment: a manual of basic methods. John Wiley and Sons, N.Y., 223 p.

HAMMOND, P. S., AND K.-T. TSAI.
1983. Dolphin mortality incidental to purse-seining for tunas in the eastern Pacific Ocean, 1979-81. Rep. Int. Whaling Comm. 33:589-597.

JOHNSON, S. M., AND O. D. BOLSTAD.
1973. Methodological issues in naturalistic observation: some problems and solutions for field research. *In* L. A. Hamerlynck, L. C. Handy, and E. J. Mash (editors), Behavior change: methodology, concepts, and practice, p. 7-67. Research Press, Champaign, IL.

LO, N. C. H., J. E. POWERS, AND B. E. WAHLEN.
1982. Estimating and monitoring incidental dolphin mortality in the eastern tropical Pacific tuna purse seine fishery. Fish. Bull., U.S. 80:396-401.

PERRIN, W. F.
1969. Using porpoise to catch tuna. World Fishing 18(6): 42-45.

PUNSLY, R. G.
1983. Estimation of the number of purse-seiner sets on tuna associated with dolphins in the eastern Pacific Ocean during 1959-1980. [In Engl. and Span.] Inter-Am. Trop. Tuna Comm. Bull. 18:229-299.

RICKER, W. E.
1975. Computation and interpretation of biological statistics of fish populations. Bull. Fish. Res. Board Can. 191, 382 p.

SMITH, T. D.
1983. Changes in size of three dolphin (*Stenella* spp.) populations in the eastern tropical Pacific. Fish. Bull., U.S. 81:1-13.

SNEDECOR, G. W., AND W. G. COCHRAN.
1980. Statistical methods. 7th ed. Iowa State University Press, Ames, IA, 507 p.

WEBB, E. J., D. T. CAMPBELL, R. D. SCHWARTZ, AND L. SECHREST.
1966. Unobtrusive measures: a survey of non-reactive research in the social sciences. Rand McNally, Chic., 225 p.

8593

Chapter 20

Magnetoreception and Biomineralization of Magnetite

Fish

MICHAEL M. WALKER, JOSEPH L. KIRSCHVINK, and
ANDREW E. DIZON

1. Introduction 417
2. Magnetic Sensitivity in Yellowfin Tuna 419
3. Detection of Magnetic Material in Fish 422
4. Characterization of the Magnetic Material 426
5. Identification and Analysis of the Magnetic Material 429
6. Discussion 431
References 434

1. Introduction

Many species from different taxa respond to one or more features of the geomagnetic field (Keeton, 1971, 1972; Lindauer and Martin, 1972; Wiltschko, 1972; Walcott and Green, 1974; Martin and Lindauer, 1977; Quinn, 1980; Wiltschko *et al.*, 1981). These responses fall into two general categories: responses to magnetic field direction and to magnetic field intensity. Magnetic compass responses include the vanishing bearings of homing pigeons (Walcott and Green, 1974) and directional preferences of migratory species in orientation arena experiments (Wiltschko, 1972; Tesch, 1974; Quinn, 1980). The postulated magnetic intensity, or "map", response (Gould, 1980, 1982; Moore, 1980; Walcott, 1980) refers to the apparent ability of homing pigeons to determine their position to within a kilometer or two using some feature related to geomagnetic field intensity. This response has been inferred from the vanishing bearings and homing speeds of birds released at geomagnetic field anomalies and during magnetic storms (Keeton, 1969, 1971, 1972; Gould, 1980, 1982; Walcott, 1980). Gould (Chapter 12, this volume) provides a full discussion of this research.

Experimental evidence is accumulating that fish also possess a magnetic compass and that they can learn to respond to magnetic fields in conditioning experiments. Quinn

---

MICHAEL M. WALKER • Southwest Fisheries Center Honolulu Laboratory, National Marine Fisheries Service, National Oceanic and Atmospheric Administration, Honolulu, Hawaii 96812, and Department of Zoology, University of Hawaii, Honolulu, Hawaii 96822. JOSEPH L. KIRSCHVINK • Division of Geological and Planetary Sciences, California Institute of Technology, Pasadena, California 91125. ANDREW E. DIZON • Southwest Fisheries Center La Jolla Laboratory, National Marine Fisheries Service, National Oceanic and Atmospheric Administration, La Jolla, California 92038.

(1980), Quinn *et al.* (1981), and Quinn and Brannon (1982) demonstrated unconditioned compass responses in sockeye salmon fry and smolts. Fish held in the center of four-armed wooden tanks (Quinn, 1980; Quinn *et al.*, 1981), or circular arenas with eight escape traps (Quinn and Brannon, 1982) were released and allowed to enter the tank arm or escape trap corresponding to their directional preference. In the absence of visual cues, the fish made their preferences using magnetic field cues. These preferences were appropriate for bringing the fish to their nursery lake or its downstream outlet.

Kalmijn (1978) conditioned a response to magnetic field direction in the ray, *Urolophus halleri*, in which the fish were rewarded for entering an enclosure in the magnetic east and punished for entering an identical enclosure placed in the magnetic west of the experimental tank. When the magnetic field direction in the tank was reversed randomly, the fish selected the enclosure in the magnetic east of the tank with accuracies of up to 90% in training sessions.

There are two central problems in the study of magnetic sensitivity in animals. The first is that many of the behavioral results obtained so far are subject to methodological criticisms, may be unreproducible, and tell little about the functioning of the sense (Emlen, 1975; Able, 1980; Griffin, 1982). The second is that as yet it is unknown how and where the magnetic field is detected (Able, 1980). Thus, it is difficult to design and conduct explicit experiments to obtain the necessary behavioral, anatomical, and neurophysiological proofs of the existence of the sense, and to analyze its capacities.

Conditioning experiments can provide the necessary reproducibility and power for unequivocal demonstration of the existence of a magnetic sense. However, attempts to condition animals to magnetic fields have largely failed (Able, 1980). Where conditioning has been obtained (Reille, 1968; Bookman, 1977; Phillips, 1977; Kalmijn, 1978), either the experiments were unreproducible (Kreithen and Keeton, 1974; Beaugrand, 1976; Griffin, 1982) or subsequent psychophysical analyses of the sense were not carried out (Phillips, 1977; Kalmijn, 1978). These inconsistent results suggest that the experimental designs may have been inappropriate for demonstrating responses to magnetic fields (Ossenkopp and Barbeito, 1978). Thus, it is not yet possible to reject or accept without reservation the hypothesis that animals can detect magnetic fields. Further attempts must be made to obtain robust, reproducible responses to magnetic field stimuli and to identify their sensory bases.

Any hypothesis seeking to explain geomagnetic field sensitivity in animals must provide a mechanism by which the action of the geomagnetic field can bring about orderly displacement of the electrical potential of a receptor cell membrane. That is, the geomagnetic field must act on the magnetoreceptor cell with a neural coupling energy greater than the background thermal energy, kT (Jungerman and Rosenblum, 1980). The mechanism must also explain both the general compass response and the very high sensitivities inferred for detection of changes in magnetic field intensity (Martin and Lindauer, 1977; Gould, 1980, 1982). Finally, the hypothesis should make testable predictions concerning magnetoreceptor operation.

Among the hypotheses for magnetoreception that have been suggested are forms of electrical induction (Kalmijn, 1974; Jungerman and Rosenblum, 1980); optical pumping (Leask, 1977); liquid crystal effects (Russo and Caldwell, 1971); and biological superconductivity (Cope, 1971, 1973). These hypotheses demonstrate stimulus energies sufficient to depolarize the membrane of a receptor cell and make geomagnetic field detection possible. However, few explain both the directional responses to magnetic fields made by animals and the sensitivity to very small variations in magnetic field intensity exhibited by homing pigeons and other birds (Southern, 1978, Gould, 1980, 1982; Walcott, 1980). In addition, there may be a lack of evidence for receptor cells which behave in the required fashion (e.g., Cope, 1973). Finally, magnetoreception is sometimes known to occur under conditions where special requirements of the hypotheses are not met (Quinn *et al.*, 1981).

We do not intend to dismiss this theoretical work prematurely. However, the difficulties with these hypothesized transduction mechanisms summarized above suggest that the older and simpler ferromagnetic transduction hypothesis warrants further examination.

The possibility that the force exerted on magnetic particles could be transduced to the nervous system has been independently suggested by Ising (1945), Lowenstam (1962), and Keeton (1972). Support for the idea came with the discovery of magnetite in magnetotactic bacteria (Frankel *et al.*, 1979; Frankel and Blakemore, 1980), and in bees (Gould *et al.*, 1978), birds (Walcott *et al.*, 1979; Presti and Pettigrew, 1980), and mammals (Zoeger *et al.*, 1981). Theoretical analyses (Yorke, 1979, 1981; Kirschvink and Gould, 1981) show that where the magnetite is present in a suitable form and in sufficient quantities, it could provide the basis for a very sensitive magnetoreceptor system capable of deriving information about direction and intensity of the geomagnetic field. Important predictions of these analyses are (1) that the magnetoreceptors should not be dependent on special conditions other than the presence of a magnetic field to function (Yorke, 1981), (2) that there should be separate compass and intensity receptors (Kirschvink and Walker, this volume), and (3) that compass accuracy and threshold sensitivity to intensity changes should be constrained by the physical properties of the magnetite crystals (Kirschvink and Walker, this volume).

The primary tests of the magnetite-based magnetoreception hypothesis must be behavioral and physiological. However, there are physical tests described in this chapter that bear on the structure and function of a magnetite-based magnetoreceptor. Such tests include magnetometry experiments designed to identify deposits of magnetite within the bodies of different organisms, and to analyze the size, shape, and arrangement of the crystals. Extraction and analysis of diffraction spectra of the magnetic material provide us with a second means of identifying the mineral. Extraction also provides measurements of the size and shape of individual crystals and information about the biomineralization process.

A feature of these studies is the very small amounts of material involved and the ease with which contaminants can affect the results of experiments (Quinn *et al.*, 1981; Jones and MacFadden, 1982; Walker *et al.*, this volume). Thus, it is important in testing for the presence of magnetite in biologic samples to test for the presence of contaminants wherever possible. Methods for doing this in whole tissues include testing for the effect of vigorous washing and ultrasonic cleaning on the magnetic properties of samples used in magnetometry experiments (Jones and MacFadden, 1982) and testing for the magnetic properties of ferromagnetic contaminants (Kirschvink *et al.*, 1985; Walker *et al.*, this volume). Assaying for trace elements associated with geologic and artificial ferromagnetic materials and examining the morphology of isolated crystals provide further means of determining the origin of the crystals.

This paper reports results of our studies of magnetoreception and its possible transduction mechanism in the yellowfin tuna, *Thunnus albacares*, and other pelagic fish. We obtained reproducible responses to earth-strength magnetic fields in the yellowfin tuna using an orthodox discrimination training procedure (Woodard and Bitterman, 1974). Using a variety of magnetometric and mineralogic techniques, we have detected, extracted, and characterized magnetite within the yellowfin tuna and other pelagic fishes. Although these studies are not as complete as we would desire, they do permit us to compare results between species from different orders, providing us with a more general insight into the putative magnetoreceptor system of fish. We then consider the results in relation to magnetoreception and magnetite biomineralization.

2. Magnetic Sensitivity in Yellowfin Tuna

The first hypothesis to test in magnetic field conditioning experiments is that animals can distinguish between different magnetic field stimuli. The procedures chosen should therefore be appropriate to measure simple distinguishability of different magnetic fields. Decisions are required on experimental situation, testing procedure, response measure, response produced, and stimuli to be distinguished. Once it is established that the stimuli are distinguishable, different hypotheses will dictate different choices among these components of learning experiments (Kling, 1971).

Learning is detected as a relatively permanent change in behavior resulting from conditions of practice (Kling, 1971). Thus, in discrimination learning experiments, some measurable bit of behavior is modified by experience gained by the subjects during testing. In unitary, or go-no go, procedures, a single, generalized response is defined and then either positively or negatively reinforced under different stimulus conditions. Discrimination learning is then measured by comparing the readiness with which the response is expressed between the stimulus conditions (Bitterman, 1966). In choice procedures, two discrete responses that cannot be produced together are defined. In one stimulus condition, one of the responses is rewarded and the other punished. In the alternate stimulus condition, the consequences of the two responses are reversed. Discrimination is detected from the choices the animal makes between the alternate responses under the different stimulus conditions (Bitterman, 1966).

The approaches used to study magnetic field conditioning in animals can be summarized as follows. Fields were uniform and movement was restricted, limiting the subject's ability to sample the magnetic field environment (Meyer and Lambe, 1966; Reille, 1968; Kreithen and Keeton, 1974). Magnetic field polarity was the most commonly used discriminative stimulus (Phillips, 1977; Kalmijn, 1978; Griffin, 1982). The subject animal was usually required to make a choice between two alternate responses and, with one exception (Meyer and Lambe, 1966), multiple responding was not required (Bookman, 1977; Kalmijn, 1978; Griffin, 1982).

Magnetic fields are pervasive stimuli that can only be presented singly—first one, then the other—in experimental situations. Choice conditioning experiments using stimuli, such as magnetic fields, that can only be presented singly are among the most difficult discrimination problems that can be presented to experimental animals (Mackintosh, 1974) and will often fail with well-understood, salient stimuli (Bitterman, 1979). In choice procedures, trials most commonly end after the first response by the subject (e.g., Bookman, 1977; Kalmijn, 1978). However, discrimination will be sharpened if subjects are required to produce multiple responses (Bitterman, 1979), as often occurs in unitary procedures. Unitary discriminative training procedures are therefore more appropriate than choice procedures for use with magnetic fields. They should permit the subjects freedom of movement (Kreithen and Keeton, 1974), and sufficient time to sample the magnetic field environment and to produce multiple responses during trials.

For conditioning yellowfin tuna to magnetic fields, we defined a single response, required the fish to produce that response more than once, rewarded that response under one set of magnetic field conditions and not under another, and compared the readiness with which the response was expressed under the two conditions. The fish were required to swim through a 60 × 30-cm pipe frame lowered into their tank for 30-sec trial periods and retracted for intertrial periods. Within the trial periods the fish were able to swim repeatedly through the frame. Thus, the measure of behavior compared between the stimulus conditions was the rate of performance of the conditioned response. The primary advantage of rate as a measure of discrimination is its sensitivity: it can vary widely and rapidly in response to changes in experimental conditions and can accommodate short-term variability in behavior (Kling, 1971).

These experiments were conducted at the Kewalo Research Facility of the Southwest Fisheries Center Honolulu Laboratory, National Marine Fisheries Service. The fish used were captive juvenile yellowfin tuna (40- to 50-cm fork length) tested individually in one of two cylindrical test tanks (6-m diameter, 0.75-m depth). The experimental tanks contained no metal and each had 100 turns of No. 18 AWG magnet wire wrapped around its perimeter. A 1-A direct current passed through these wires added a vertical magnetic field to the background field. This field was nonuniform, adding from 10 μT in the center to 50 μT at the edge of each tank. The pipe frame, the magnetic field, and a semiautomatic feeder mounted at the side of each tank (Jemison *et al.*, 1982) were operated by mechanical and electrical linkages from an experimental control room. The control room was physically isolated from the experimental tank and was darkened during experiments. The fish were observed through small viewing ports, and their responses were recorded manually.

The differences between the two magnetic fields used in the discrimination experiments were as follows. The local Hawaiian field was uniform throughout the tanks. That is, inclination, declination, and total field intensity were the same at any point in the area occupied by the fish. The altered field introduced significant radially-oriented gradients of both intensity and inclination within the tanks. These experiments therefore provided the fish with two very different magnetic fields as discriminative stimuli. The fish could conceivably monitor differences in magnetic field inclination, intensity, or the gradients in these two parameters to make the discrimination.

In discrimination testing, a trial began with simultaneous presentation of the pipe frame and either the reinforced (S^+) or nonreinforced (S^-) stimulus. All responses by the fish within each 30-sec trial period were counted. In S^+ trials the fish was rewarded with a piece of food immediately following the first response after 30 sec. In S^- trials, a 10-sec penalty timer started at the end of the trial period. The timer was reset by each subsequent response by the fish until either the penalty time elapsed or a total of 30 sec of penalty had accumulated. Thus, response to S^- was penalized by extending the trial without any possibility of the fish obtaining food. The fish were given 30-trial training sessions held once daily. In any trial session the S^+ and S^- were presented 15 times, with no more than three S^+ or S^- trials in succession. Testing was balanced by training two fish with the normal Hawaiian field and two with the altered field as S^+.

Discrimination between the two magnetic field conditions became evident after two 30-trial sessions (Fig. 1). During the first day of testing, the response rates to the two stimuli exhibited by the fish fluctuated randomly about each other. By the end of the second day, the fish began to show a higher rate of response to the reinforced than to the nonreinforced stimulus. Some individuals showed higher response rates during nonreinforced trials just before beginning to make the discrimination. However, all individuals showed consistently higher rates of response to S^+ than to S^- on the third and fourth days of training, suggesting that they were correctly anticipating the onset of positive or nonreinforcement.

All the fish completed at least 120 trials over four or more days of testing. An analysis of variance comparing S^+ and S^- response rates over 120 trials divided into blocks of before and after 60 trials (the first two and the third and fourth training sessions) yielded an $F_{1,3}$ stimuli $= 7.61$, $p = 0.07$ and an $F_{1,3}$ stimuli by blocks $= 102.55$, $p = 0.002$. All other comparisons within the analysis did not approach significance. The main effect (stimuli) failed to be statistically significant. This is attributed to the small differences in response rates between S^+ and S^- and to the variability of responding compared with the mean rate of response. Dividing the data into blocks demonstrated that the behavior of the fish on the third and fourth days of testing was different from their behavior over the first 2 days, and that the change in behavior that occurred was dependent on the discriminative stimuli. Thus, the behavior of the fish changed as a result of their learning that production of the response had different outcomes under different magnetic field conditions.

To test whether the fish were responding to possible equipment- or observer-related cues, control trials were conducted with one fish. One of the wires connecting the power supply to the coil around the tank was disconnected and all other procedures followed as before. The response rates during reinforced and nonreinforced trials fluctuated randomly about each other during this period (Fig. 2). When the circuit between the power supply

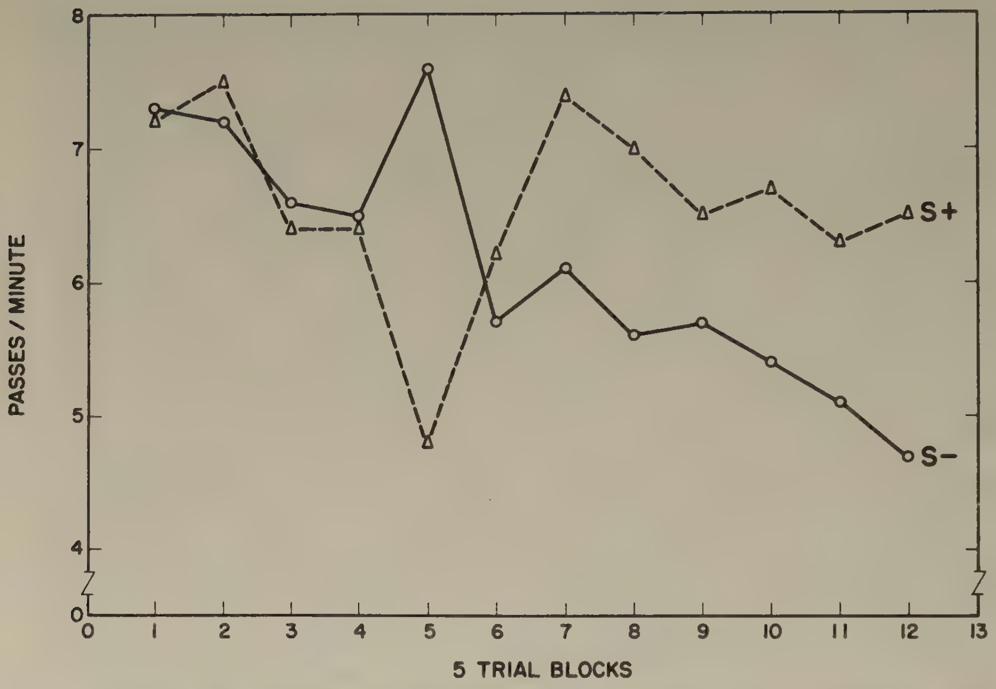

Figure 1. Magnetic field discrimination learning in yellowfin tuna. Each point is the average of five S^+ or S^- trials for the four fish tested. Data from Walker (1984).

and the coil was reestablished, the fish was again able to anticipate positive and nonreinforcement and respond accordingly (Fig. 2). However, the separation between response rates was less than before the control trials were conducted. In subsequent experiments run using double-blind procedures, two fish were easily able to discriminate between the two magnetic fields (Walker, 1984). From these results we conclude that the fish used only the magnetic fields presented to anticipate the onset of positive or nonreinforcement.

3. Detection of Magnetic Material in Fish

As noted above, to act in magnetoreception, the energy of interaction between magnetite particles and the geomagnetic field must bring about the orderly displacement of the potential of a receptor cell membrane. Kirschvink and Walker (this volume) assume that, at the receptor level, energetic considerations are of primary importance and show that single-domain particles are best suited for use in magnetite-based magnetoreception by animals. To transduce the energy of their interaction with the geomagnetic field to the nervous system, the particles must be at least partly free to move. They will then be aligned by an external field and their position or movement will transform magnetic field stimuli to mechanical stimuli (Kirschvink and Walker, this volume).

Freedom of the magnetite crystals in magnetoreceptor organelles to rotate and their small mass mean that, in the absence of an external field, their orientation will be ran-

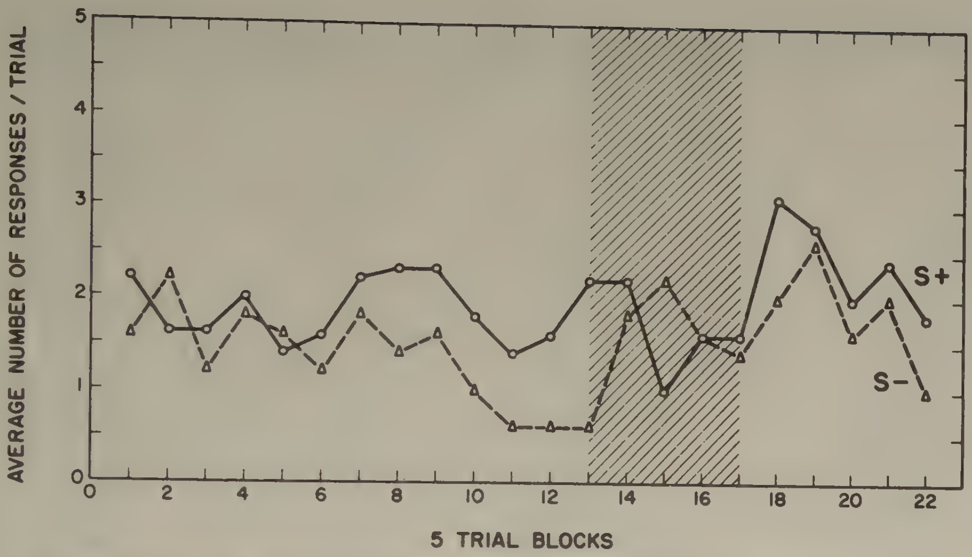

Figure 2. Magnetic field discrimination learning in individual yellowfin tuna. Shaded region in plot indicates control tests. Data from Walker (1984).

domized by thermal agitation. The particle moments will therefore cancel and not be detectable. Consequently, magnetite-based magnetoreceptor organelles will exhibit no natural remanent magnetization (NRM) in the null field environment of a superconducting magnetometer. Freezing biologic samples prevents any magnetic particles present from moving. Their moments can be realigned by momentary exposure to a strong magnetic field (>0.3 T) and will then sum to produce a net moment, the saturation isothermal remanent magnetization (sIRM).

The sIRM has been the basic sample measurement in our biomagnetic studies. Presence of magnetic material in a sample will be demonstrated by a ratio of the signal from the magnetized sample to the background signal in the magnetometer, designated the signal-to-noise (S/N) ratio, greater than unity. A scaling effect on the S/N ratio can result from sample size: Large samples are more likely than small samples to have large S/N ratios. To take account of this effect, we determined relative concentrations of magnetic material, or intensity of magnetization, in different samples by dividing their moments by their mass. In this case a reverse scaling effect could occur. Small samples with moments within or close to the background noise in the magnetometer may appear more intensely magnetized than larger samples with high S/N ratios. Determining whether or not a sample is magnetic using either of these measures alone is arbitrary. Consequently, we chose to recognize as magnetic only samples which gave both high S/N ratios and intensities of magnetization.

To distinguish magnetic material with a possible magnetoreceptive function from other deposits, we sought to identify a tissue having the following characteristics: (1) It should have a high remanent magnetic moment (or high S/N ratio) concentrated in a small volume of sample (indicated by high intensity of magnetization) compared with other tissues from the same fish; (2) the anatomic position of the magnetic tissue must be consistent from fish to fish; and (3) the bulk magnetic properties, including particle coercivity, should be similar in different individuals and in different species of fish.

Our first studies set out to determine whether magnetic material is consistently localized at any point in the body of the yellowfin tuna. Tissue and organ samples, including

Table I. Saturation Moments, Signal-to-Noise Ratios, and Intensities of Magnetization for Tissue and Organ Samples from Different Yellowfin Tuna[a]

Sample	Mean moment (pAm^2) ± S.D. (*N*)	Signal/noise	Intensity (pT) ± S.D. (*N*)
Liver	105.0 ± 134.4 (2)	2.1	1.8
Pyloric cecum	49.6 ± 50.0 (3)	1.0	3.5
Intestine	14.5 ± 20.5 (2)	0.3	4.8
Red muscle	184.0 ± 274.7 (3)	3.7	3.5
White muscle	155.0 ± 211.2 (6)	3.1	5.7 ± 5.3 (3)
Brain	36.4 ± 50.3 (5)	0.7	7.5
Gill	95.0 ± 143.4 (6)	1.9	20.6
Skin	41.7 ± 80.1 (6)	0.8	35.7
Peduncle tendon	120.0 ± 169.7 (2)	2.4	41.4
Frontal bone	202.0 ± 129.0 (6)	4.0	103.6 ± 86.9 (2)
Pectoral fin	325.0 ± 427.0 (2)	6.5	62.5
Posterior brain case	375.0 ± 455.0 (6)	7.5	ND
Dorsal fin	400.0 ± 628.5 (5)	8.0	ND
Cardiac muscle	500.0 ± 707.1 (2)	10.0	4.5
Eye	1242.5 ± 1052.6 (4)	24.9	13.7 ± 14.1 (2)
Dermethmoid bone	1320.6 ± 867.5 (15)	26.4	127.0 ± 86.7 (7)

[a] Variability estimates are standard deviations and numbers in parentheses are the number of samples measured for the saturation moments and intensities of magnetization. Intensity estimates for many samples came from one fish only; "ND" indicates no data. Signal-to-noise ratios were calculated by dividing the mean saturation moment by the maximum background noise (50 pAm^2) in the magnetometer. Samples are grouped into those which were clearly nonmagnetic, those which were magnetic from their signal-to-noise ratio or their intensity of magnetization only, and those which were magnetic from both measures.

bones of the body and skull, skin, sense organs, viscera, and swimming muscles, were dissected from three fish (fork length 40–50 cm) with glass microtome knives and handled with nonmetallic tools in a magnetically shielded, dust-free, clean room. Although subsequent dissections focused on the magnetic tissue, other samples were measured in all fish. Samples were washed in glass-distilled water, frozen in liquid nitrogen, exposed to strong fields from a cobalt–samarium magnet or an air-core impulse solenoid, and tested for IRM in a superconducting magnetometer. Techniques for laboratory preparation and dissection of tissue samples have been described elsewhere (Kirschvink, 1983; Walker et *al.*, this volume).

Six tissue or organ samples showed neither high S/N ratios nor high intensities of magnetization (Table I). Seven other samples had moments less than 10 times the background noise in the magnetometer. However, because of the scaling effect caused by their small mass, these samples showed high intensities of magnetization. Cardiac muscle and eye samples acquired high moments but had relatively low intensities of magnetization. Subdivision and remeasurement showed that the moments acquired by eye samples were not associated with the lens, retina, or optic nerve. Because all these tissue samples were either clearly nonmagnetic, appeared magnetic from one measure only, or were not reproducible in different fish, it seemed unlikely that they would come from a sensory organ; for this reason we focused our work on tissues that acquired large, reproducible moments.

Only the dermethmoid bone gave high values for all measures of magnetization used in all fish examined (Table I). A scatter diagram, plotting intensity of magnetization against S/N ratio for the data presented in Table I, clearly identified the dermethmoid bone as the most magnetic sample measured. Subdivision and remeasurement of the dermethmoids

Table II. Saturation Isothermal Remanent Magnetization in Selected Tissues of Different Fish[a]

Species	Number sampled	Tissue IRM (pAm^2)		
		Dermethmoid	Muscle	Eye
Thunnus albacares	16	260–3000	20–500	100–2600
T. alalunga	2	100–200	30	1700
T. obesus	1	480	400	ND[b]
Sarda orientalis	1	1500	700–1200	5000
Scomber sp.	1	1750	60	90
Makaira nigricans	4	110–170	ND	ND
Oncorhynchus tshawytscha[c]	4	310–360	50–73	100–2300
Engraulis mordax	5	235–2850	40–170	ND

[a] Background signal in magnetometer 10–50 pAm^2.

[b] ND, no data.

[c] Olfactory rosette and brain always nonmagnetic in *O. tshawytscha*; other tissues, especially viscera, variable in all species.

in a number of fish suggested that the magnetic material was contained in tissue in a sinus formed within the bone.

Taken alone, the S/N ratio data could lead to the conclusion that many tissues are magnetic in the yellowfin tuna. However, most samples were only occasionally magnetic and often vigorous washing or ultrasonic cleaning would reduce the IRM acquired by such samples. This suggests the presence of external contaminants in samples where the cleaning procedure reduced the moment and anomalous deposits of magnetic material where it did not.

We then tested for the presence of magnetic material in the bodies of other pelagic fish species. We chose to ignore many of the corresponding tissues that were nonmagnetic in the yellowfin tuna, and concentrated instead on those associated with the head. As in the yellowfin tuna, these experiments did not identify or characterize the magnetic material but they did allow us to (1) identify tissues that were magnetic in all individuals, (2) identify tissues that were probably magnetic due to the presence of contaminants, and (3) identify areas that may have been magnetic due to the presence of anomalous deposits of magnetic material.

Fish from the orders Perciformes (families Scombridae, Istiophoridae, Coryphaenidae), Clupeiformes (family Engraulidae), and Salmoniformes (family Salmonidae), all had magnetic material associated with the dermethmoid bone or the anterior region of the skull (Table II). The sIRM values ranged between 100 and 3000 pAm^2 for dermethmoid bones from nine species of pelagic fish. Most of these sIRM values fell in the range from 100 to 1000 pAm^2, being most consistent among individuals for the blue marlin, *Makaira nigricans*, and chinook salmon, *Oncorhynchus tshawytscha*.

In our survey of different species, we worked mostly with the heads of fish. These heads had often been cut with either a metal saw or a knife, which could easily have contaminated tissues in the region of the cuts (see Bauer *et al.*, this volume). Where we were able to work with whole fish, only tissues in contact with the environment frequently acquired magnetic moments (Table II). For example, the northern anchovy, *Engraulis mordax*, we studied were obtained whole from the Southwest Fisheries Center La Jolla Laboratory, National Marine Fisheries Service. Their gills and guts frequently acquired moments. Vigorous rinsing with distilled water sometimes led to loss of the sIRM acquired by these tissues. Muscle samples, which could not have been exposed to the environment, were not magnetic in any of the anchovies we examined. Magnetic muscle samples in the heads of two chinook salmon could have been contaminated by knife cuts but did not lose their moments after cleaning. The moments acquired by these samples may therefore be due to biochemical deposits of magnetic material, and a number of tests will be necessary to characterize them. Walker *et al.* (this volume) describe these tests and discuss the analysis of a tissue contaminated by saw cuts. Here we focus on tests conducted on the dermethmoid tissue in a number of species.

4. Characterization of the Magnetic Material

Studies of the acquisition and loss of magnetization by samples permitted us to identify tentatively the source of the sIRM in the dermethmoid bone of the yellowfin tuna and to make inferences on the organization of the magnetic crystals. A prediction of the magnetite-based magnetoreception hypothesis is that the particles are free to move and that their orientation will be randomized by thermal agitation at room temperature in a null field environment. If the dermethmoid bone is the site of magnetoreceptor organelles, it should possess no NRM and its acquired moment should be lost if it is allowed to thaw. The frozen dermethmoid bones of seven yellowfin tuna first were tested for NRM. We magnetized these samples, allowed them to warm to room temperature, and measured their moments at 5 min-intervals as they thawed. Four of these samples were then washed, refrozen, and subjected to progressively increasing magnetic fields in an impulse magnetizer (Kirschvink,

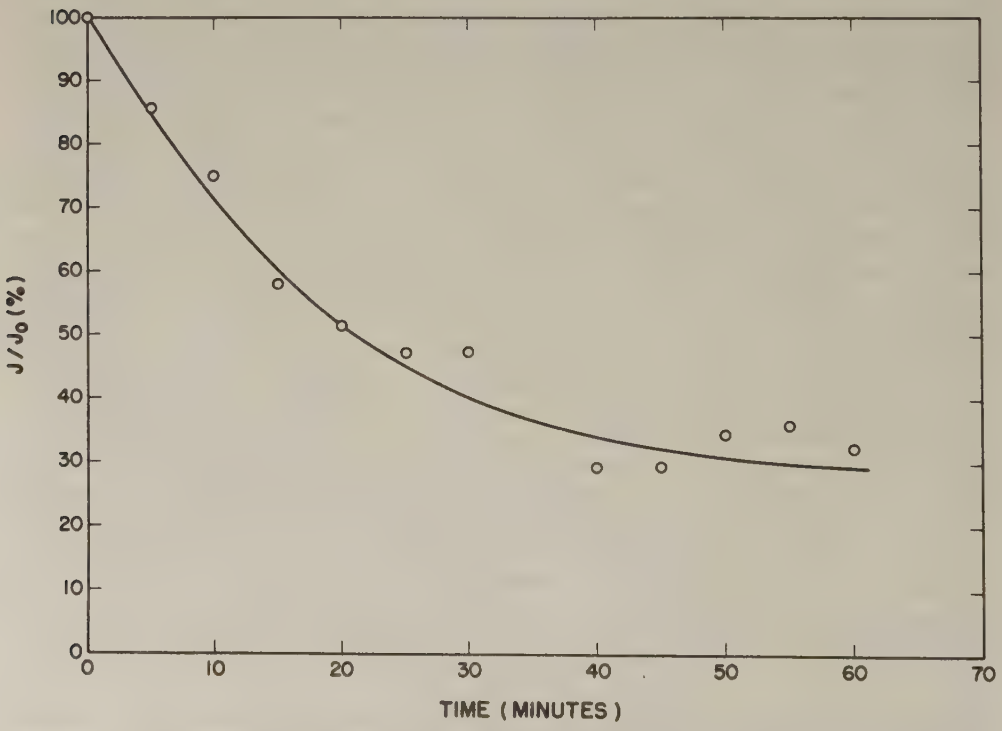

Figure 3. Loss of remanent magnetization with time on warming from liquid nitrogen temperature (77°K) to room temperature (293°K) in the dermethmoid tissues of seven yellowfin tuna. Only two measurements were taken at 35 min.

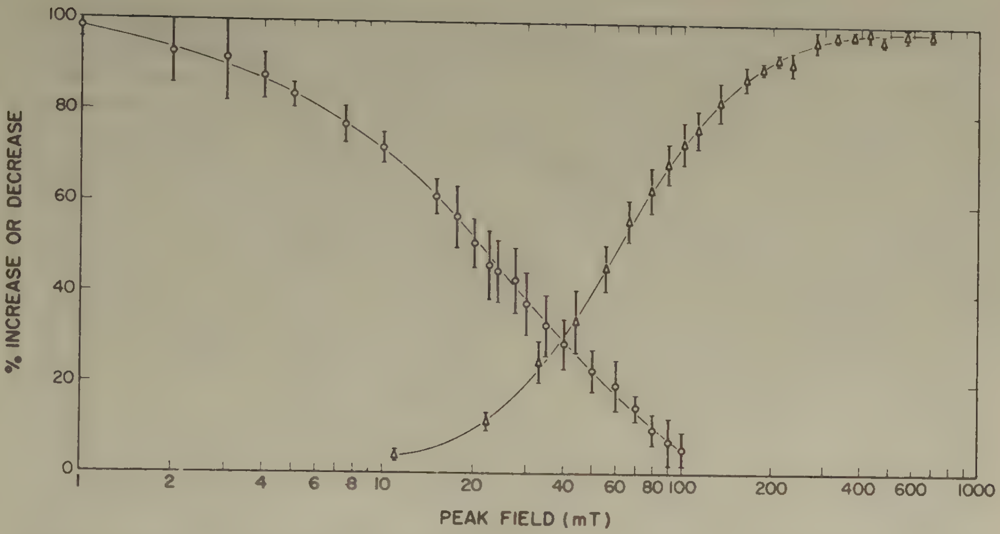

Figure 4. Progressive acquisition and loss of remanent magnetization by the dermethmoid tissues of four yellowfin tuna. Vertical bars indicate standard errors. The ordinate and abscissa of the intersection point are approximately 30% ($R = 0.3$) and 40 mT, respectively (see text). From Walker *et al.* (1984).

1983). This procedure was followed by progressive alternating field (AF) demagnetization of the samples after they were saturated. After each step in these magnetization and demagnetization experiments, we remeasured the moments of the samples.

The frozen dermethmoid bones of the yellowfin tuna showed no NRM (moments 3–30 pA m^2). After saturation, all showed an exponential decay with time in the moments they retained (Fig. 3). This suggests that the orientation of the crystals was randomized by thermal agitation as the tissue thawed. From this observation we conclude that the crystals are at least partly free to rotate.

The dermethmoid tissues of four yellowfin tuna acquired virtually all of their remanence in fields less than 200 mT and lost it again in unblocking fields between 10 and 100 mT (Fig. 4). The relatively narrow range of fields over which the dermethmoid tissues acquired and lost remanent magnetization is consistent with the acquired moments resulting from single-domain crystals of magnetite. However, the estimates of median coercivity of the magnetic particles obtained from the two methods differed significantly. This discrepancy results from interactions between the magnetic particles.

The AF demagnetization curve for a dispersion of noninteracting single-domain crystals should be symmetrical about the 50% level with the IRM acquisition curve. Asymmetry in the two curves implies that the neighboring particles are sufficiently close for their magnetic moments to interact to aid AF demagnetization and inhibit IRM acquisition (Cisowski, 1981). These interaction effects lead to under- and overestimates of the median microscopic coercivities of the crystals, respectively. Cisowski (1981) found that the shift toward higher coercive fields in the IRM curve, and the shift to lower coercive fields in the AF demagnetization curve are almost exactly the same. As a result, the abscissa of the intersection point is independent of the interaction effect and provides an estimate of the remanent coercive field. This has a value of 40 mT for the crystals in the yellowfin tuna dermethmoid tissue. The crystals therefore fit into the single-domain magnetite region with particle lengths of approximately 50 nm and axial ratios of about 0.8 in the Butler–Banerjee diagram (see Fig. 4 in Kirschvink and Walker, this volume). Depending on the size dis-

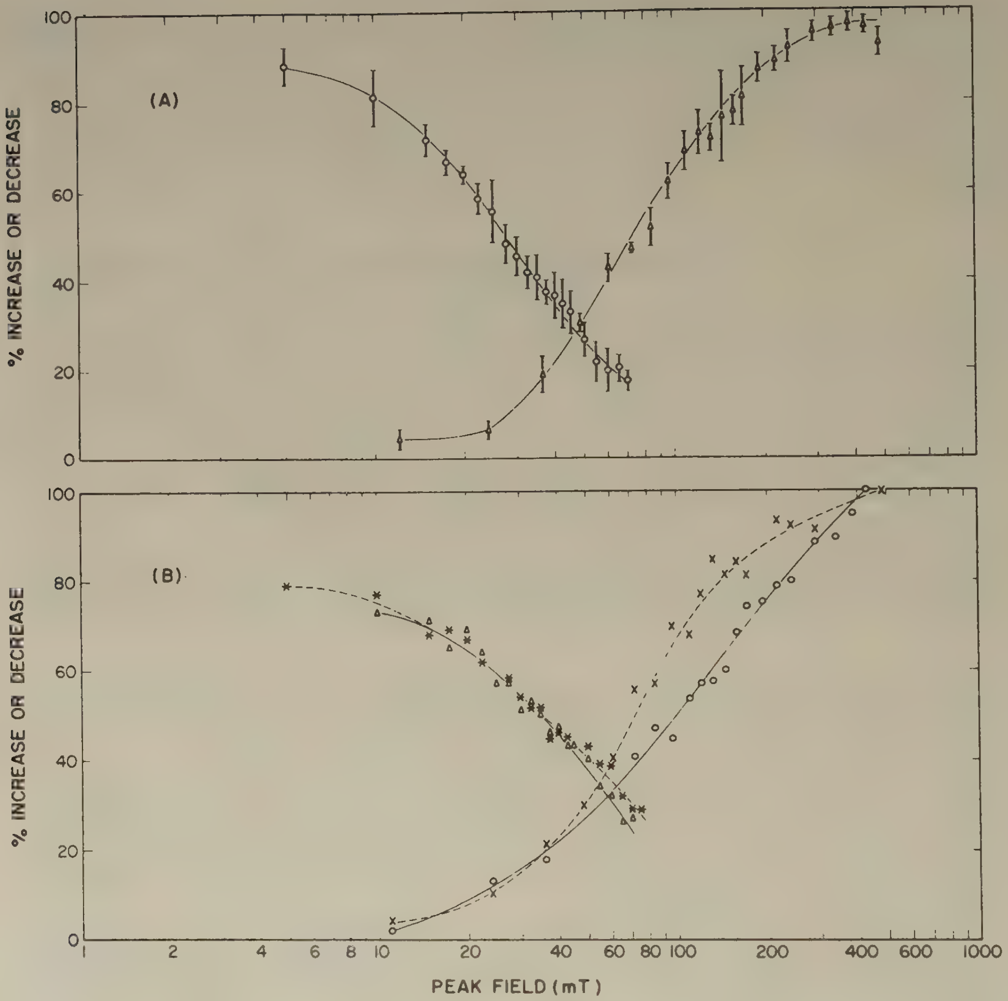

Figure 5. Progressive acquisition and loss of remanent magnetization by the dermethmoid bones of (A) four chinook salmon and (B) one chub mackerel (dashed lines) and one striped bonito (solid lines). Vertical bars in (A) indicate standard errors. R values are 0.32 (chinook salmon), 0.37 (chub mackerel), and 0.32 (striped bonito). Estimates of median coercivities of the magnetic particles taken from the abscissae of the intersection points are 46 mT (chinook salmon), 58 mT (chub mackerel), and 60 mT (striped bonito).

tribution of particles, between 1 million and 100 million crystals would be necessary to produce the sIRMs observed. These numbers are comparable to the estimates of the number of single-domain crystals possessed by honeybees (Gould *et al.*, 1978) and homing pigeons (Walcott *et al.*, 1979).

The intersection of the AF demagnetization and IRM acquisition curves for the tuna dermethmoids is at approximately 30% magnetization [or $R = 0.3$ as discussed by Cisowski (1981)] (Fig. 4). This is well below the value of 0.5 expected for completely noninteracting single-domains. The crystals of magnetite in the dermethmoid tissue of the yellowfin tuna therefore interact significantly and are about as closely associated as the crystals in the semidispersed powder ($R = 0.3$) studied by Cisowski (1981).

Comparative data are available for a number of species. The IRM acquisition and AF demagnetization curves (Fig. 5) for dermethmoid samples from individual chub mackerel, *Scomber japonicus*, and striped bonito, *Sarda orientalis*, and for four chinook salmon are almost identical in form to those obtained for the yellowfin tuna. The AF demagnetization curves for the dermethmoids of two blue marlin were also very similar to the other AF demagnetization curves and gave a median coercivity estimate of 18 mT (Walker, unpublished data). These results give particle length estimates of 50–60 nm and axial ratios of 0.5–0.8 for magnetite particles in all these fish. The consistency of the results in species of very different sizes and from different orders argues against the possibility that their dermethmoids contain contaminants. We have carried out a number of tests which conclusively exclude contaminants as the source of remanence in the dermethmoid tissue of the yellowfin tuna and which further demonstrate the high degree of control exercised over the deposition of the magnetic particles.

The IRM acquisition and AF demagnetization curves for yellowfin tuna, chinook salmon, striped bonito, and chub mackerel are very flat at fields less than 10 mT and also at fields greater than 200 mT. This excludes multidomain magnetites, commonly found in igneous rocks and laboratory dust, as the source of remanence in the dermethmoid tissues. Multidomain magnetites are magnetically soft (Kirschvink, 1983) and acquire or lose magnetization in much lower fields than did the dermethmoid tissues of these pelagic fishes. The flattening of the IRM acquisition curves above 200 mT excludes hematite and many iron alloys, which will continue to acquire remanence in fields above 1 T. Therefore, we can exclude almost all ferromagnetic minerals except maghemite and synthetic magnetite as the source of remanence in the dermethmoid tissues of pelagic fishes. The extraction and analyses of the magnetic particles discussed next enable us to exclude even these possible sources of magnetic remanence.

5. Identification and Analysis of the Magnetic Material

The extraction techniques discussed by Walker *et al.* (this volume) permitted a number of distinctive assays for magnetite in the tuna dermethmoid tissue. Magnetic particles extracted from the tissue were black, both to the naked eye and when viewed under a dissecting microscope. This excluded maghemite as a possible source of the remanence in the dermethmoid tissue and strongly suggested that the only magnetic mineral present was magnetite. In an attempt to determine whether normally nonmagnetic tissues also contained finely dispersed magnetic material, a large sample (about 10 g) of the white muscle of one fish was digested using the same techniques. No magnetic particles were obtained, presumably because any particles present in the swimming muscle must have been present in concentrations too small to be extracted using these techniques.

X-ray diffraction, the technique used to identify the crystals, depends on the interaction between the collimated X-ray beam, the ions in the mineral, and their orientation in the crystal lattice. The beam enters the sample and is scattered at angles characteristic of the position of each ion in the lattice. The scattered beam is detected by X-ray photographic film which, after development, shows a series of concentric arcs. The distance of each arc from the center is thus characteristic of the structure and composition of the sample crystals. From these distances are calculated the distances (known as *d* spacings) between adjacent ions in the unit cell of the lattice.

X-ray diffraction of the magnetic material extracted from the dermethmoid tissue of the yellowfin tuna uniquely identified magnetite as the source of remanence (Fig. 6). The

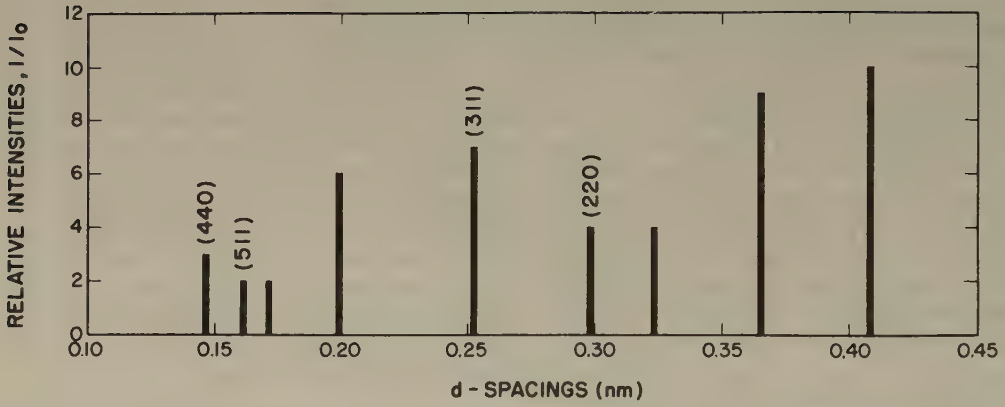

Figure 6. X-ray diffraction data for magnetite extracted from tissue contained within the dermethmoid bone sinus of the yellowfin tuna. Vertical lines indicate relative intensities of lines in the diffraction pattern. Numbers in parentheses indicate lines associated with magnetite and the crystal axis giving rise to each line.

lattice parameter estimated from X-ray diffraction is 0.8358 ± 0.004 nm (reference value 0.8396 nm). The origin of the lines not associated with magnetite in the pattern is unknown, although they do not arise from any known ferromagnetic mineral. Two possible sources of these lines are connective tissue associated with the crystal aggregate and insoluble proteins involved in an organic matrix in which the crystals are deposited (Weiner *et al.*, 1983).

Electron microprobe analysis of aggregated crystals showed that the magnetite from the yellowfin tuna is remarkably pure. The crystals contained no measurable titanium and almost no manganese (Table III), which are common components of geologic magnetites. The crystals also contained no measurable chromium, excluding many possible synthetic ferromagnetic minerals. As in the magnetometry studies, we can thus rule out almost all nonbiologic origins for the magnetite crystals found in the tuna.

We were able to use transmission electron microscope (TEM) studies to measure the size and shape of the isolated magnetite particles. These crystals averaged 45 nm in length, 38 nm in diameter, and had a subcubic form (Fig. 7). The crystals are thus single-domains and conform to the size and axial ratio ranges predicted from their coercivities (see above).

Table III. Electron Microprobe Analyses of Magnetite Particles isolated from Yellowfin Tuna

Oxide	Magnetite standard (NMNH 11487)	Weight (%) of sample
FeO	90.9	86.3 + 7.7
TiO_2	0.2	0.0 ± 0.0
Cr_2O_3	<0.25	0.0 ± 0.0
MnO	<0.0	0.2 ± 0.1
CaO	—	0.2 ± 0.0
Total	91.4	86.7

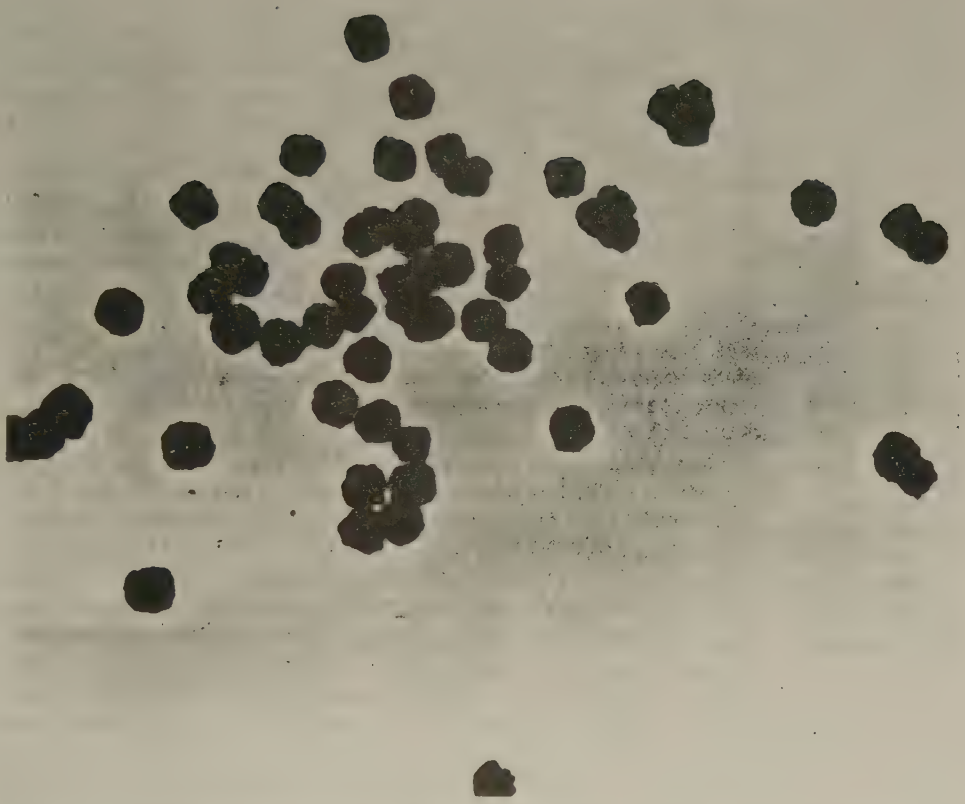

Figure 7. Free magnetite grains extracted from the dermethmoid tissue of the yellowfin tuna. Transmission electron micrograph courtesy of R. S.-B. Chang. From Walker *et al.* (1984).

Their morphology differs from the octahedral crystal form found in all nonbiogenic magnetites. On the basis of this crystal form, we conclude that these crystals could not have come from nonbiologic sources, but must have a biogenic origin. This is consistent with the results obtained from the different approaches used in this study. The evidence from a variety of methods for biogenic origin of the crystals gives us greater confidence when discussing our results and their implications for magnetoreception and magnetite biomineralization in fish.

6. Discussion

There is a growing body of evidence that fish respond to magnetic fields. Elasmobranch (Kalmijn, 1978) and teleost (this study) fish have been conditioned to respond to magnetic field stimuli while salmoniform (Quinn, 1980; Quinn *et al.*, 1981; Quinn and Brannon, 1982) and anguilliform (Tesch, 1974) fish have shown unconditioned directional responses to magnetic fields. Directional responses imply that fish possess a magnetic compass. The conditioning experiment reported here (Figs. 1 and 2) provided changes in magnetic field intensity, intensity gradients, and inclination to fish being conditioned to discriminate between magnetic fields. Thus, it is possible that the fish responded to intensity or intensity gradients in these experiments. There is an important need for further conditioning experiments to test the responses of fish to these components of the geomagnetic field and to test the predictions of the ferromagnetic magnetoreception hypothesis (Kirschvink and Walker, this volume).

It has not yet been established that fish use the geomagnetic field for direction finding or navigation in the ocean. Quinn (1982) presents arguments that migrating Pacific salmon must be able to navigate to achieve the distances traveled in the time taken to return from the open ocean to the North American coast. Quinn goes on to suggest that these fish may use a compass and a magnetic map based on a bicoordinate grid of magnetic field inclination and declination for navigation.

There is some field evidence that fish are able to determine their position and swimming direction, although the sensory bases for these abilities are unknown. Short-term tracking experiments show that a number of different pelagic fishes, including swordfish, *Xiphias gladius* (Carey and Robison, 1981), and Atlantic salmon, *Salmo salar* (Smith *et al.*, 1981), maintain relatively constant compass courses for substantial periods (up to several days in the swordfish tracked by Carey and Robison). In addition, skipjack tuna (Yuen, 1970) and swordfish (Carey and Robison, 1981) make diurnal return movements to discrete areas (shallow banks) without retracing their outward path. The sensory mechanism or mechanisms responsible for guiding these movements are as yet unknown. However, the ability of fish to detect magnetic fields suggests that the possibility that they use the geomagnetic field to guide their movements is worth serious experimental investigation.

The lack of feasible transduction mechanisms to explain magnetoreception has hindered the testing of hypotheses concerning magnetic sensitivity in animals. One mechanism for transduction of magnetic field information to the nervous system has been suggested for the elasmobranchs by Kalmijn (1974, 1978). On the basis of his theoretical analysis, Kalmijn (1974) predicted that the elasmobranchs should be able to detect magnetic fields using their ampullae of Lorenzini. This prediction appeared to be borne out by his later successful conditioning of rays to respond to magnetic fields (Kalmijn, 1978). However, the critical behavioral experiment to determine whether or not electrical field information is necessary for magnetoreception in the elasmobranchs has yet to be carried out.

Discovery of single-domain magnetite in a variety of metazoan groups provides the basis for a general magnetoreception mechanism suitable for use in both aquatic and terrestrial environments. In the vertebrates, single-domain magnetite has been found in the anterior dura mater membrane or in association with the ethmoid areas of the skull (Baker, Chapter 26; this volume; Bauer *et al.*, this volume; Mather, this volume; Perry *et al.*, this volume). We have found single-domain magnetite with virtually identical magnetic properties in the dermethmoid tissue of representatives of different orders of teleost fish. Our studies of the magnetite crystals in the yellowfin tuna showed that the crystals average 45 nm in length by 38 nm in diameter (Fig. 7) and are arranged in interacting arrays that appear at least partly free to rotate. These results enable us to refine our predictions concerning magnetoreceptor organization and sensitivity in fish.

The magnetic properties of the magnetite crystals will determine and constrain the operation of magnetite-based magnetoreceptor organelles (Kirschvink and Walker, this volume). From the dimensions of the crystals extracted from the yellowfin tuna, we can calculate that 8.5×10^7 particles are necessary to produce the mean remanence observed in the dermethmoid tissue. The energy of interaction of the individual crystals with the geomagnetic field will be about 0.1 kT (see Fig. 4 in Kirschvink and Walker, this volume). To achieve coupling energies with the geomagnetic field large enough for detection by the nervous system, the crystals must therefore be organized into interacting arrays. Depending on the numbers of crystals in the arrays, the maximum theoretical sensitivity of a magnetite-based magnetoreception system in fish can easily be estimated (Yorke, 1981). The apparent freedom of the crystal arrays to rotate suggests that a mechanoreceptor monitoring position or movement of the arrays is a suitable means to link the magnetite crystals to the nervous system.

The appeal of the ferromagnetic magnetoreception hypothesis is that it can theoretically account for the responses to magnetic fields exhibited in such diverse groups as the bacteria (Frankel and Blakemore, 1980), algae (Lins de Barros *et al.*, 1981; Lins de Barros and Esquivel, this volume), bees (Lindauer and Martin, 1972), fish (Quinn, 1980), and birds (Keeton, 1969). In the unicellular organisms and honeybees, the hypothesis has been tested experimentally (Kalmijn, 1981; Kirschvink, 1981; Frankel *et al.*, this volume). For fish, some indirect evidence for the hypothesis is also available. Quinn *et al.* (1981) state that the magnetoreceptor of the sockeye salmon must be able to function in the dark, in salt and fresh water, in the absence of water flow, and be evolutionarily adaptable to magnetic field reversals. Although not a test of the hypothesis, these behaviorally determined constraints argue against the optical pumping and electrical induction hypotheses for magnetoreception (Leask, 1977; Kalmijn, 1978) and are all compatible with possession by the salmon of a ferromagnetic magnetoreceptor (Kirschvink *et al.*, 1985).

The case for magnetite-based magnetoreception in metazoans will not be proven until linkage of the crystals to functioning sensory nerves transmitting magnetic field information to the central nervous system has been demonstrated. However, the discovery of biogenic magnetite, suitable for use in magnetoreception in different vertebrate and invertebrate organisms, cracks the conceptual nut concerning a general magnetic sensory mechanism and provides a good working hypothesis for the testing of many ideas about magnetoreception. Substantial support for the hypothesis will come from experiments that test for ferromagnetic effects on behavioral responses to magnetic fields. Kirschvink and Walker (this volume) suggest experiments to estimate the magnetic moments of magnetite-based magnetoreceptors and to test the theoretical constraints on ferromagnetic compass and intensity receptors.

The variety of techniques used in these studies provided us with a number of internal checks on our work. Through magnetometry studies we were able not only to identify those areas of the bodies of fish that were magnetic, but also to show that the sIRM acquired by the dermethmoid tissue was due to single-domain particles and not to magnetically very soft or very hard contaminants. The microprobe analyses showed that the crystals from the yellowfin tuna contained almost none of the impurities characteristic of geologic magnetites. Finally, the unique nonoctahedral morphology of the crystals compared with the octahedral crystal form of all other magnetites demonstrates the biogenic origin of the crystals seen in TEM (Fig. 7; Lowenstam and Kirschvink, this volume).

Our studies on the magnetite crystals extracted from yellowfin tuna bear on the process of magnetite biomineralization. The diffraction spectra show that the crystals are very pure, implying that they are formed under close chemical control. The crystals are also very uniform in size and shape. These properties are characteristic of biominerals formed under matrix-mediated control (Lowenstam, 1981; Lowenstam and Kirschvink, this volume).

The only well-studied examples of magnetite biomineralization are in the chitons and bacteria. These organisms appear to lay down a template of organic matrix and biochemically precipitate magnetite within it under enzymatic control (Kirschvink and Lowenstam, 1979; Balkwill *et al.*, 1980; Nesson and Lowenstam, this volume). Matrix-mediated biomineralization may be the mechanism for magnetite precipitation in fish as it could provide the means for control of the size, shape, and composition necessary for use of the crystals in magnetoreception. Locations of the crystals and their site of deposition in intact tissues could provide us with valuable understanding of both their biomineralization and their role in magnetoreception.

Biomineralization processes have a long evolutionary history. The widespread use of very similar matrix-mediated biomineralization processes in metazoans for skeleton building from the late Precambrian period (Weiner *et al.*, 1983) suggests a common origin for matrix-mediated biomineralization dating to the early Precambrian (Lowenstam and Weiner, 1983). Magnetite, presumably formed by matrix-mediated biomineralization, has now been identified in many phylogenetically distant metazoan groups. From arguments similar to those advanced by Lowenstam and Weiner (1983), two interpretations of the appearance of magnetite in these groups can now be offered. Biogenic magnetite in the metazoans arose from a long history in the Precambrian which predates the differentiation of the metazoan phyla, or it arose from multiple, independent origins in the late Precambrian, after the divergence of the metazoan phyla. Resolution of the problem of the origin of biogenic magnetite in the metazoans may depend on identification of biogenic magnetites of clear metazoan origin from before the late Precambrian.

Lowenstam and Weiner (1983) suggest that the ability to produce magnetite evolved in the early Precambrian as a means of iron storage in the reducing environment of that time. In bacteria possessing magnetite crystals, the ability to perform directed swimming responses may have provided selective advantages for magnetotaxis, even before the advent of an oxygen-rich environment. In the metazoans, it seems necessary to postulate selection operating on an association between magnetite crystals and sensory nerves as the origin of magnetoreception. This assumes that magnetite played some other, prior role in the body of the organism. Other studies have reported the presence of magnetite or magnetic material which does not have an apparent magnetoreceptive function (e.g., Presti and Pettigrew, 1980) and which may be lost in anemic individuals (Baker *et al.*, 1983). Study of these deposits and the sites and conditions under which they form may elucidate the early functions of magnetite in the metazoans.

ACKNOWLEDGMENTS. Heinz A. Lowenstam and Anjanette Perry provided helpful discussions during the course of this research. We are greatly indebted to Charles E. Helsley, Barbara H. Keating, Li Chung Ming, and Michael O. Garcia of the Hawaii Institute of Geophysics, University of Hawaii, for the use of paleomagnetic laboratory facilities and assistance with X-ray diffraction and electron microprobe analyses. Shih-Bin Robin Chang and Karla A. Peterson carried out the transmission electron microscope study and assisted in magnetometry experiments at the California Institute of Technology. Research funds and facilities were most generously provided by the Southwest Fisheries Center Honolulu Laboratory, National Marine Fisheries Service. This research was supported in part by a graduate study award from the East–West Center, Honolulu, and a grant from Sigma Xi to M.M.W. This is Contribution No. 3938 from the Division of Geological and Planetary Sciences, California Institute of Technology.

References

Able, K. P., 1980, Mechanisms of orientation, navigation, and homing, in: *Animal Migration, Orientation, and Navigation* (S. A. Gauthreaux, Jr., ed.), Academic Press, New York, p. 283–373.

Baker, R. R., Mather, J. G., and Kennaugh, J. H., 1983, Magnetic bones in human sinuses, *Nature* **301**:78–80.

Balkwill, D. L., Maratea, D., and Blakemore, R. P., 1980, Ultrastructure of a magnetotactic spirillum, *J. Bacteriol.* **141**:1399–1408.

Beaugrand, J. P., 1976, An attempt to confirm magnetic sensitivity in the pigeon, *Columba livia*, *J. Comp. Physiol. A* **110**:343–355.

Bitterman, M. E., 1966, Animal learning, in: *Experimental Methods and Instrumentation in Psychology* (J. B. Sidowski, ed.), McGraw–Hill, New York, pp. 451–484.

Bitterman, M. E., 1979, Discrimination, in: *Animal Learning: Survey and Analysis* (M. E. Bitterman, V. M. LoLordo, J. B. Overmier, and M. F. Rashotte, eds.), Plenum Press, New York, pp. 413–443.

Bookman, M. A., 1977, Sensitivity of the homing pigeon to an earth-strength magnetic field, *Nature* **267**:340–342.

Carey, F. G., and Robison, B. H., 1981, Daily patterns in the activities of swordfish, *Xiphias gladius*, observed by acoustic telemetry, *U. S. Fish Bull.* **79**:277–292.

Cisowski, S., 1981, Interacting vs. non-interacting single-domain behavior in natural and synthetic samples, *Phys. Earth Planet. Inter.* **26**:56–62.

Cope, F. W., 1971, Evidence from activation energies for superconductive tunneling in biological systems at physiological temperatures, *Physiol. Chem. Phys.* **3**:403–410.

Cope, F. W., 1973, Biological sensitivity to weak magnetic fields due to biological superconductive Josephson junctions?, *Physiol. Chem. Phys.* **5**:173–176.

Emlen, S. T., 1975, Migration: Orientation and navigation, in: *Avian Biology*, Volume V (D. S. Farner, J. R. King, and K. C. Parkes, eds.), Academic Press, New York, pp. 129–219.

Frankel, R. B., and Blakemore, R. P., 1980, Navigational compass in magnetic bacteria, *J. Magn. Magn. Mater.* **15–18**:1561–1564.

Frankel, R. B., Blakemore, R. P., and Wolfe, R. S., 1979, Magnetite in freshwater magnetotactic bacteria, *Science* **203**:1355–1356.

Gould, J. L., 1980, The case for magnetic sensitivity in birds and bees (such as it is), *Am. Sci.* **68**:256–267.

Gould, J. L., 1982, The map sense of pigeons, *Nature* **296**:205–211.

Gould, J. L., Kirschvink, J. L., and Deffeyes, K. S., 1978, Bees have magnetic remanence, *Science* **201**:1026–1028.

Griffin, D. R., 1982, Ecology of migration: Is magnetic orientation a reality?, *Q. Rev. Biol.* **57**(3):293–295.

Ising, G., 1945, Die physikalische Moglichkeit eines tierischen Orientierungssinnes auf Basis der Erdrotation, *Ark. Mat. Astron. Fys.* **32A**(18):1–23.

Jemison, H. A., III, Dizon, A. E., and Walker, M. M., 1982, An automatic feeder for liquids and wet or dry solids, *Behav. Res. Methods Instrum.* **24**(1):54–55.

Jones, D. S., and MacFadden, B. J., 1982, Induced magnetization in the monarch butterfly, *Danaus plexippus* (Insecta, Lepidoptera), *J. Exp. Biol.* **96**:1–9.

Jungerman, R. L., and Rosenblum, B., 1980, Magnetic induction for the sensing of magnetic fields by animals—An analysis, *J. Theor. Biol.* **87**:25–32.

Kalmijn, A. J., 1974, The detection of electric fields from inanimate and animate sources other than electric organs, in: *Handbook of Sensory Physiology*, Volume III/3 (A. Fessard, ed.), Springer-Verlag, Berlin, pp. 147–200.

Kalmijn, A. J., 1978, Experimental evidence of geomagnetic orientation in elasmobranch fishes, in: *Animal Migration, Navigation, and Homing*, (K. Schmidt-Koenig and W. T. Keeton, eds.), Springer-Verlag, Berlin, pp. 347–353.

Kalmijn, A. J., 1981, Biophysics of geomagnetic field detection, *IEEE Trans. Magn.* **Mag-17**:113–1124.

Keeton, W. T., 1969, Orientation by pigeons: Is the sun necessary?, *Science* **165**:922–928.

Keeton, W. T., 1971, Magnets interfere with pigeon homing, *Proc. Natl. Acad. Sci. USA*, **68**:102–106.

Keeton, W. T., 1972, Effects of magnets on pigeon homing, in: *Animal Orientation and Navigation* (S. R. Galler, K. Schmidt-Koenig, G. J. Jacobs, and R. E. Belleville, eds.), NASA SP-262, U.S. Government Printing Office, Washington, D.C., pp. 579–594.

Kirschvink, J. L., 1981, The horizontal magnetic dance of the honeybee is compatible with a single-domain ferromagnetic magnetoreceptor, *BioSystems* **14**:193–203.

Kirschvink, J. L., 1983, Biogenic ferrimagnetism: A new biomagnetism, in: *Biomagnetism: An Interdisciplinary Approach* (S. Williamson, ed.), Plenum Press, New York, pp. 501–532.

Kirschvink, J. L., and Gould, J. L., 1981, Biogenic magnetite as a basis for magnetic field detection in animals, *Biosystems* **13**:181–201.

Kirschvink, J. L., and Lowenstam, H. A., 1979, Mineralization and magnetization of chiton teeth: Paleomagnetic, sedimentologic, and biologic implications of organic magnetite, *Earth Planet. Sci. Lett.* **44**:193–204.

Kirschvink, J. L., Walker, M. M., Chang, S.-B. R., Dizon, A. E., and Peterson, K. A., 1985, Chains of single-domain magnetite particles in chinook salmon, *Oncorhynchus tshawytscha*, *J. Comp. Physiol. A.*, in press.

Kling, J. W., 1971, Learning: Introductory survey, in: *Woodworth & Schlosberg's Experimental Psychology* (J. W. Kling and L. A. Riggs, eds.), Holt, Rinehart & Winston, New York, pp. 551–613.

Kreithen, M. L., and Keeton, W. T., 1974, Attempts to condition homing pigeons to magnetic stimuli, *J. Comp. Physiol. A* **91**:355–362.

Leask, M. J. M., 1977, A physicochemical mechanism for magnetic field detection by migratory birds and homing pigeons, *Nature* **267**:144–145.

Lindauer, M., and Martin, H., 1972, Magnetic effect on dancing bees, in: *Animal Orientation and Navigation* (S. R. Galler, K. Schmidt-Koenig, G. J. Jacobs, and R. E. Belleville, eds.), NASA SP-262, U.S. Government Printing Office, Washington, D. C., pp. 559–567.

Lins de Barros, H. G. P., Esquivel, D. M. S., Danon, J., and Oliveira, L. P. H., 1981, Magnetotactic algae, *Acad. Bras. Cienc. Notas Fis.* CBPF-NF-048/81.

Lowenstam, H. A., 1962, Magnetite in denticle capping in recent chitons (Polyplacophora), *Geol. Soc. Am. Bull.* **73**:435–438.

Lowenstam, H. A., 1981, Minerals formed by organisms, *Science*, **211**:1126–1131.

Lowenstam, H. A., and Weiner, S., 1983, Mineralization by organisms and the evolution of biomineralization, in: *Biomineralization and Biological Metal Accumulation* (P. Westbroek and E. W. de Jong, eds.), Reidel, Dordrecht, pp. 191–203.

Mackintosh, N. J., 1974, *The Psychology of Animal Learning*, Academic Press, New York.

Martin, M., and Lindauer, M., 1977, The effect of the earth's magnetic field on gravity orientation in the honey bee (*Apis mellifica*), *J. Comp. Physiol. A* **122**:145–187.

Meyer, M. E., and Lambe, D. R., 1966, Sensitivity of the pigeon to changes in the magnetic field, *Psychon. Sci.* **5**(9):349–350.

Moore, B. R., 1980, Is the homing pigeon's map geomagnetic?, *Nature* **285**:69–70.

Ossenkopp, K.-P., and Barbeito, R., 1978, Bird orientation and the geomagnetic field: A review, *Neurosci. Biobehav. Rev.* **2**:255–270.

Phillips, J. B., 1977, Use of the earth's magnetic field by orienting cave salamanders (*Eurycea lucifuga*), *J. Comp. Physiol. A* **121**:273–288.

Presti, D., and Pettigrew, J. D., 1980, Ferromagnetic coupling to muscle receptors as a basis for geomagnetic field sensitivity in animals, *Nature* **285**:99–101.

Quinn, T. P., 1980, Evidence for celestial and magnetic compass orientation in lake migrating sockeye salmon fry, *J. Comp. Physiol. A* **137**:243–248.

Quinn, T. P., 1982, A model for salmon navigation on the high seas, in: *Proceedings of the Salmon and Trout Migratory Behavior Symposium*, (E. L. Brannon and E. O. Salo, eds.), pp. 229–237.

Quinn, T. P., and Brannon, E. L., 1982, The use of celestial and magnetic cues by orienting sockeye salmon smolts, *J. Comp. Physiol. A* **147**:547–552.

Quinn, T. P., Merrill, R. T., and Brannon, E. L., 1981, Magnetic field detection in sockeye salmon, *J. Exp. Zool.* **217**:137–142.

Reille, A., 1968, Essai de mise en évidence d'une sensibilité du pigeon au champ magnétique à l'aide d'un conditionnement nociceptif, *J. Physiol. (Paris)* **60**:85–92.

Russo, F., and Caldwell, W. E., 1971, Biomagnetic phenomena: Some implications for the behavioral and neurophysiological sciences, *Genet. Psychol. Monogr.* **84**:177–243.

Smith, G. W., Hawkins, A. D., Urquhart, G. G., and Shearer, W. M., 1981, Orientation and energetic efficiency in the offshore movements of returning Atlantic salmon, *Salmo salar* L., *Scott. Fish. Res.* Rep. 21, ISSN 0308 8022.

Southern, W. E., 1978, Orientation of ring-billed gull chicks: A reevaluation, in: *Animal Migration, Navigation, and Homing*, (K. Schmidt-Koenig and W. T. Keeton, eds.), Springer-Verlag, Berlin, pp. 311–317.

Tesch, F.-W., 1974, Influence of geomagnetism and salinity on the directional choice of eels, *Helgol. Wiss. Meeresunters.* **26**:382–395.

Walcott, C., 1980, Magnetic orientation in homing pigeons, *IEEE Trans. Magn.* **Mag-16**:1008–1013.

Walcott, C., and Green, R. P., 1974, Orientation of homing pigeons altered by a change in the direction of an applied magnetic field, *Science* **184**:180–182.

Walcott, C., Gould, J. L., and Kirschvink, J. L., 1979, Pigeons have magnets, *Science* **205**:1027–1029.

Walker, M. M., 1984, Learned magnetic field discrimination in yellowfin tuna, *Thunnus albacares*, *J. Comp. Physiol. A.* **155**:673–679.

Walker, M. M., Kirschvink, J. L., Chang, S.-B. R., and Dizon, A. E., 1984, A candidate magnetic sense organ in the yellowfin tuna, *Thunnus albacares*, *Science* **224**:751–753.

Weiner, S., Traub, W., and Lowenstam, H. A., 1983, Organic matrix in calcified exoskeletons, in: *Biomineralization and Biological Metal Accumulation* (P. Westbroek and E. W. de Jong, eds.), Reidel, Dordrecht.

Wiltschko, R., Nohr, D., and Wiltschko, W., 1981, Pigeons with a deficient sun compass use the magnetic compass, Science **214**:343–345.

Wiltschko, W., 1972, The influence of magnetic total intensity and inclination on directions preferred by migrating European robins (*Erithacus rubecula*), in: *Animal Orientation and Navigation* (S. R. Galler, K., Schmidt-Koenig, G. J. Jacobs, and R. E. Belleville, eds.), NASA SP-262, U. S. Government Printing Office, Washington, D.C., pp. 569–577.

Woodward, W. T., and Bitterman, M. E., 1974, A discrete-trials/fixed-interval method of discrimination training, *Behav. Res. Methods Instrum.* **6**:389–392.

Yorke, E. D., 1979, A possible magnetic transducer in birds, *J. Theor. Biol.* **77**:101–105.

Yorke, E. D., 1981, Sensitivity of pigeons to small magnetic field variations, *J. Theor. Biol.* **89**:533–537.

Yuen, H. S. H., 1970, Behavior of skipjack tuna, *Katsuwonus pelamis*, as determined by tracking with ultrasonic devices, *J. Fish. Res. Board Can.* **27**:2071–2079.

Zoeger, J., Dunn, J. R., and Fuller, M., 1981, Magnetic material in the head of the common Pacific dolphin, *Science* **213**:892–894.

8594

Chapter 5

Detection, Extraction, and Characterization of Biogenic Magnetite

MICHAEL M. WALKER, JOSEPH L. KIRSCHVINK,
ANJANETTE PERRY, and ANDREW E. DIZON

1. Introduction 155
2. Magnetometry Studies 156
3. Extraction and Characterization of Biogenic Magnetite 160
4. Discussion 163
5. Summary 164
References 165

1. Introduction

Several difficulties arise when attempts are made to characterize the deposits of magnetite found in metazoans. We are usually forced to deal with very small amounts of material, dispersed in tissues, using indirect methods that are subject to contamination. Magnetite crystals in the abdomens of bees (Gould *et al.*, 1978), and in the heads of pigeons (Walcott *et al.*, 1979), and other vertebrates (Bauer *et al.*, this volume; Perry *et al.*, this volume; Walker *et al.*, this volume) are submicroscopic (<100 nm), occupy a combined volume of 10^{-10} to 10^{-8} cm^3, and have a mass of 1–100 ng. In organisms of up to 100 kg or more, detecting such quantities of magnetite from its magnetic properties depends on the crystals being highly concentrated in small, recognizable structures, and not uniformly dispersed throughout all the tissues. Extraction and recovery of the crystals likewise depend on their being sufficiently concentrated to be magnetically detectable.

The failure to recognize contaminants and the influence they can have on results of biomagnetic studies has greatly hindered our progress in understanding the origin and functions of biogenic magnetite. Magnetite is a common industrial pollutant and can often find its way onto the external body surface or into the gut of higher animals (Kirschvink, 1983). A typical 100-nm crystal of the type found in bees and pigeons (Gould *et al.*, 1978; Walcott *et al.*, 1979) has a moment of about 0.5 fAm^2 whereas a 10-μm dust-sized particle

---

MICHAEL M. WALKER and ANDREW E. DIZON • Southwest Fisheries Center La Jolla Laboratory, National Marine Fisheries Service, National Oceanic and Atmospheric Administration, La Jolla, California 92038. JOSEPH L. KIRSCHVINK • Division of Geological and Planetary Sciences, California Institute of Technology, Pasadena, California 91125. ANJANETTE PERRY • Department of Oceanography, University of Hawaii, Honolulu, Hawaii 96822.

may have moments of up to 500 pAm^2. The moment of the multidomain particle is well within the 1–10 pAm^2 sensitivity limits of the superconducting magnetometers currently in use whereas the moments of 10^3 to 10^4 of the single-domain particles must be aligned to be detectable. Other ferro- or ferrimagnetic contaminants are frequently present within the laboratory environment, particularly in paleomagnetic laboratories where rock samples tend to leave a fine dust that is often rich in magnetic contaminants. The ease with which contaminants can enter at all stages of biomagnetic studies dictates that we not only adopt procedures to minimize the risk of contamination but that we specifically distinguish between contaminants and true biochemical precipitates. It is therefore necessary to identify those properties that are likely to be unique to biogenic magnetite.

Interest in biogenic magnetite has focused on its potential use in the transduction of the geomagnetic field to the nervous system. Kirschvink and Walker (this volume) argue that the physical properties of the crystals are of primary importance and that single-domain crystals are the most likely form of magnetite for use in magnetoreception. This constraint should result in a restricted size-frequency distribution of the magnetite particles. Magnetite particles suitable for magnetoreception should therefore have coercivities greater than that of multidomain magnetite (<20 mT; Zoeger *et al.*, 1981) and less than the theoretical maximum for single-domain magnetite (300 mT; McElhinny, 1973). Superparamagnetic particles of biogenic magnetite (Gould *et al.*, 1978) are difficult to detect without special facilities. Thus, in searching for magnetite suitable for use in magnetoreception, we are primarily attempting to distinguish between single-domain and multidomain particles.

There is as yet no evidence that magnetite in the gut or the environment can naturally enter the bloodstream and be transported to the places it is detected. Any such particles used for magnetoreception are most likely produced within the organisms themselves, presumably by enzyme catalysis. The specificity of enzyme pathways would be expected to result in biogenic magnetite containing few of the impurities associated with geologic magnetite or metals used to harden iron alloys (Lowenstam and Weiner, 1983). Magnetite particles suitable for magnetoreception can therefore be reasonably expected to possess physical and chemical properties distinguishing them from geologic and synthetic magnetites.

Magnetite or magnetic material without apparent magnetoreceptive function has been detected in a variety of tissues in different species (Lowenstam, 1962; Presti and Pettigrew, 1980; Kirschvink, 1981; Kirschvink *et al.*, 1982). Except in the chitons, where magnetite is used to harden radular teeth (Lowenstam, 1962), the function of these deposits is unknown. Hypotheses are that the deposits store excess iron or that they may have a pathologic origin (Lowenstam and Weiner, 1983). It is therefore more difficult to predict characteristics that will distinguish them from other magnetites. However, it is important that attention be given to these deposits because they may predate the use of magnetite for magnetoreception (Kirschvink and Gould, 1981; Walker *et al.*, this volume).

This chapter reviews the techniques which are in common use for detecting and characterizing biogenic magnetite. Procedures for avoidance of contamination and examples of specific tests for contaminants that are easy to conduct are included. Finally, we attempt to identify further techniques that may prove useful in detecting, extracting, and analyzing biogenic magnetite.

2. Magnetometry Studies

As noted above and by other authors in this volume, accidental contamination of samples is a major problem in the search for biogenic magnetite. When working in paleomagnetic laboratories, we have sought to minimize the risks of contamination by thoroughly scrubbing and lining the walls, roof, and floor with thin polyethylene sheets. The recent development of a clean laboratory specifically designed for biomagnetic studies eliminates many of the contamination problems previously experienced (Kirschvink, 1983). We still find, however, that contamination can enter in lint on the clothing or in the hair of people using the laboratory. In the future, we hope to eliminate even this source of contamination by wearing lint-free garments and by using a deionized water shower.

Nonmagnetic tools are a must in carrying out dissections in preparation for measurements in the magnetometer. Typical metal dissection tools such as bone saws, scalpels, and forceps can leave trails of highly magnetic particles behind them. Even tools made from nonferrous metals such as aluminum or copper often contain small ferromagnetic inclusions sufficient to prevent their use in dissections. Magnetic particles left in tissues by these tools can easily be detected but can only be recognized from extensive tests of their magnetic properties (see below).

Wood, plastic, and glass seem to be the materials most suitable for tools used in dissections. We found glass microtome knives convenient for dissection and easily obtained from electron microscopy laboratories. Disposable wood chopsticks are ideal for handling tissue samples of the sizes measured in the magnetometer. Although they will acquire magnetic moments, frequent washing and replacement of the chopsticks minimizes the risk that they will pick up and transfer contaminants to samples. Frequent washing in glass-distilled water and extended ultrasonic cleaning in either glass-distilled water or 6 N HCl of nondisposable equipment that comes in contact with the samples also serve to minimize contamination.

The risk of contamination is further reduced if dissections are made from whole carcasses rather than sections that have been reduced in size using metal saws or knives (Walker *et al.*, this volume). Saws appear to inject magnetic particles well into tissues. These particles may be dispersed further during dissection and their presence and contribution to tissue moments cannot be determined other than by extensive tests. We have also found from our work with fish that juvenile or subadult animals with incompletely ossified bones are easier to dissect than adults. In large, thick-boned species such as the blue marlin, *Makaira nigricans*, the easiest way to gain access to structures within the skull was to score along bone sutures with a glass knife and break the bones apart. In turtles and cetaceans, a rubber mallet or wooden-jawed vice was necessary to crack the skull bones to provide access to the dura mater membrane (Bauer *et al.*, this volume; Perry *et al.*, this volume). Such techniques, while effective, make accurate localization and identification of magnetite-containing structures difficult.

After tissue samples have been dissected and washed in glass-distilled water, several of their magnetic properties are of interest. These include the natural remanent magnetization (NRM), saturation isothermal remanent magnetization (sIRM), and rate at which magnetization is acquired or lost in progressively increased aligning or randomizing fields. Before a tissue sample can be measured, it must be frozen so that any small magnetic particles present will be immobilized. Otherwise, in the null field environment of the magnetometer, the orientation of any magnetic particles suspended in a viscous medium will be randomized by Brownian motion and any moments due to alignment of the particles will be lost.

Simply freezing a sample is sufficient only for measuring its NRM. Determination of other magnetic properties requires that the sample be magnetized prior to measurement. When inducing the sIRM in a sample, it is desirable to expose it to a strong uniform field in excess of 300 mT. In our early work we attempted to do this using a cobalt–samarium magnet. Unfortunately, it is difficult to obtain homogeneous magnetization of large samples using this method because of the rapid decay of field strength with distance from the magnet. Inhomogeneous magnetization can lead to underestimates of the amount of magnetic material present, making it possible to miss potentially important magnetic structures. An air core solenoid delivering homogeneous fields of up to several Tesla has proven very reliable in uniformly magnetizing samples for measurement in the magnetometer. This solenoid also makes possible the progressive magnetization of samples in coercivity studies (Kirschvink, 1983).

Great care is necessary in the choice of sample holders for magnetometry experiments. The mylar, glass, or polyethylene plastic tubes commonly used by paleomagnetists are adequate for use with biomagnetic samples, although they will acquire spurious moments and contribute to background noise in the magnetometer. They will also acquire magnetic moments if exposed to strong magnetic fields, so that samples must be magnetized separately from these holders and then loaded for measurement. Consequently, it is difficult to maintain the same orientation of the sample to components of the process (solenoids and magnetometer detection coils) in repeated measurements.

We have found two simple methods of attaching samples to a holder that maintain constant orientation of the sample relative to the axes of the solenoids and magnetometer pickup coils. A magnetized, frozen sample can be attached to the moistened end of a white cotton thread and lowered vertically into the magnetometer. If thoroughly cleaned, the thread does not show any NRM and can be used for repeated measurements such as alternating field (AF) demagnetization. However, the "clean" threads may sometimes gain moments if exposed to strong fields. Another method of loading the samples for rapid IRM acquisition studies was therefore required. We found that a more effective sample holder was a hook made of quartz glass fiber. The hook was inserted into the unfrozen tissue and left within it throughout all the measurements. With this apparatus and the air core impulse or AF solenoid mounted in line on the magnetometer, we were able to automate our experiments and minimize time spent handling samples during repeated measurements. Control experiments conducted with the quartz fiber hook attached to an ice cube showed that the fiber possessed no natural moment and did not acquire a moment even in high inducing fields. However, such fibers have the disadvantage that they are fragile and break easily.

There are several paleomagnetic techniques that can be adapted for identifying and characterizing the properties of biogenic magnetite. The most important of these is to determine the coercivity spectrum of the particles present in a tissue sample. The coercive field of a magnetite particle is the minimum intensity of an external field required to flip the moment of the particle from one of its stable orientations in the long axis of the particle to the other. The range of applied fields over which a sample acquires or loses magnetization is dependent on the coercivities of the magnetic particles present in the sample. Thus, the coercivity spectrum can eliminate a variety of minerals like hematite and goethite as possible sources of remanence, and can give information concerning the size and shape of any magnetite fraction present.

Two methods are available for determining the coercivity spectrum of particles present in a sample: progressive IRM acquisition and AF demagnetization. An external field, B, will shift the moments of magnetite particles with coercive fields less than $B \cos \theta$, where θ is the angle between the particle and field vector directions. In IRM acquisition experiments, the moments of particles in a sample are aligned by progressively increased fields. In AF demagnetization experiments, the orientation of aligned moments of particles with coercivities less than the peak applied field is randomized by sinusoidally oscillating fields which slowly decrease in magnitude. Although the use of the cotton thread or quartz fiber techniques described above makes these iterative measurements relatively easy, they make it impossible to correct for the effect of the angle between the direction of the crystal axes and the applied fields and cause slight overestimation of the coercivities of the particles. However, for distinguishing single-domain magnetite from multidomain particles, and also from high-coercivity minerals such as hematite, this error can be ignored. Thus, acquisition

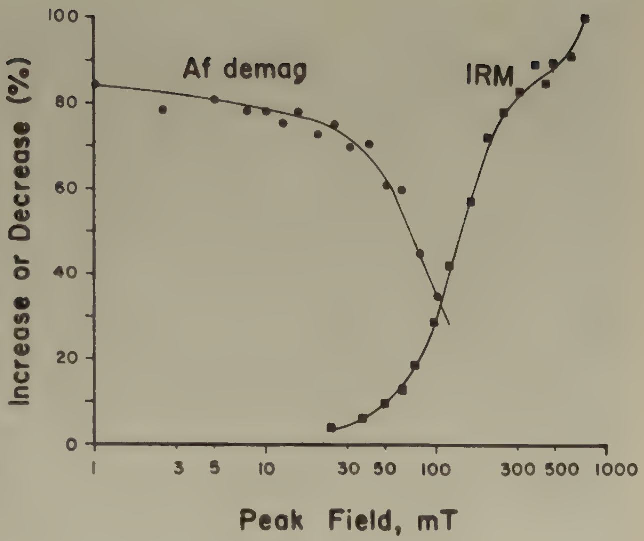

Figure 1. Comparison of IRM acquisition and AF demagnetization experiments on an ethmoid region sample from a human. 100% represents saturation magnetization and 0% represents the natural remanent magnetization of the sample. Sample supplied by R. R. Baker (Department of Zoology, University of Manchester).

of IRM in fields less than 20 mT or greater than 300 mT will indicate the presence of magnetic contaminants in samples.

Plotting the results of IRM acquisition and AF demagnetization experiments together can reveal much about the nature of the magnetic particles. For single-domain particles of the type predicted for use in magnetoreception, magnetization will be acquired or lost over a relatively small range of fields. Where all the particles are of single-domain size and uniformly dispersed throughout a sample, the two curves should be mirror images of each other over the same ranges of intensity of the applied fields. Where the crystals are sufficiently close to interact with each other, IRM acquisition is inhibited and AF demagnetization is aided (Cisowski, 1981). Thus asymmetry of the curves about the 50% magnetization point indicates the degree of interaction of the particles.

An example is given in Fig. 1 of the use of IRM acquisition to detect high-coercivity contaminants in a sample of bones and tissue from the ethmoid region of a human head. When we first tested this sample, we believed it had been dissected using nonmagnetic instruments. However, the sample turned out to be far more magnetic than any other biological sample we have examined (moments $>10^4$ pA m^2). The IRM acquisition curve was incompatible with the presence of magnetite alone, as the sample did not become saturated by 300 mT but continued to acquire magnetization up to fields of 800 mT. The AF demagnetization curve also showed the extraordinary stability of the magnetic material present in the sample. The tissue retained the majority of its magnetization up to fields of 100 mT, the upper limit of our demagnetization unit. From these data we could only conclude that there must have been high-coercivity contaminants in the tissue. On checking, R. R. Baker (Department of Zoology, University of Manchester, personal communication, 1982) discovered that an assistant had inadvertently trimmed the sample with a band saw. It would thus be impossible to conclude that biogenic magnetic particles contained within the sample had been detected and identified as magnetite suitable for use in magnetoreception.

Where suitable facilities are available, several other techniques have proven or should prove useful in identifying and characterizing magnetite present in biologic samples. The identity of the mineral can be determined from its Curie temperature, a procedure used to identify magnetite in pigeons and honeybees (Gould *et al.*, 1978; Walcott *et al.*, 1979).

The loss of IRM on warming through the isotropic point of magnetite has been used to identify multidomain magnetite in the Pacific dolphin (Zoeger *et al.*, 1981). As it distinguishes single-domain from multidomain material, this test is potentially very useful in demonstrating the presence of contaminants in biologic samples. Finally, the presence of superparamagnetic crystals can be demonstrated by continuously monitoring the remanent moment of a sample versus temperature as it warms from liquid nitrogen temperature (77°K) to room temperature (293–298°K). Freezing the samples to liquid nitrogen temperature shifts the boundary between single-domain and superparamagnetic behavior toward smaller particle sizes. Thus, as the crystals warm through their single-domain/superparamagnetic transition, they will lose their stable remanence. A drop in total moment will accompany this transition and the temperature at which it occurs will indicate the approximate sizes of the crystals. This experiment demonstrated the presence of over 10^8 such particles with sizes of 30–35 nm in the honeybee (Kirschvink and Gould, 1981) as well as in one species of chiton (Kirschvink and Lowenstam, 1979).

3. Extraction and Characterization of Biogenic Magnetite

Much can be learned about the nature and organization of the magnetic material discovered in biologic samples using its bulk magnetic properties as discussed above. However, it is eventually necessary to extract the material from the sample and apply a range of techniques to its identification and characterization. Areas of highest magnetite concentration must be accurately identified if sufficient quantities of material are to be obtained for analysis. In the fish this was done by magnetometric studies that exhaustively sampled the tissues of one species, the yellowfin tuna, *Thunnus albacares*, until tissues containing high magnetic remanence could be reliably located (Walker and Dizon, 1981; Walker *et al.*, this volume). We were able to identify one specific and relatively small structure, the dermethmoid bone, that was always magnetic in the tuna and in all the fish species subsequently examined. Our experiments showed that the magnetite was concentrated in tissue contained within a sinus formed within the dermethmoid bone.

In other vertebrates, magnetite appeared to be concentrated in the dura mater (Bauer *et al.*, this volume; Perry *et al.*, this volume) or in a region of the skull similar to the fish (Mather and Baker, 1981; Baker *et al.*, 1983; Baker, Chapter 26, this volume; Mather, this volume). In the turtles and cetaceans, subdivision of the dura revealed localization of magnetic material within its anterior portions. Concentration on these regions made for efficient extraction of magnetite in the green turtle, *Chelonia mydas* (Perry *et al.*, this volume).

For invertebrates the situation is less clear. Deposits of magnetite or magnetic material have been located from magnetometry and coercivity studies in the abdomen of the honeybee (Gould *et al.*, 1978) and in the head-thorax of the monarch butterfly (Jones and MacFadden, 1982). There appears to be no reason why magnetite should not be detected in the bodies of other invertebrate groups. If easily accessible magnetite-containing structures can be identified, the generally smaller size of invertebrates compared to vertebrates could make them more suitable for magnetite extraction studies.

Once the magnetic structures have been identified, it is a simple matter to dissect and combine a number of them for magnetite extraction. In this way we were able to treat the dermethmoid tissues of up to five yellowfin tuna at once. The tissues were ground with a little distilled water in a glass tissue grinder or in a test tube using a nonmagnetic pestle. In the tuna this released fat and oil droplets into suspension. These were removed by adding anhydrous ether to the suspension and shaking vigorously. After the aqueous and ether phases separated, the ether was decanted and replaced. This procedure was repeated until the aqueous phase became clear.

After ether extraction, the suspension was centrifuged, the aqueous supernatant removed, and 5% Millipore* filtered hypochlorite solution (commercial bleach) added. The mixture was centrifuged and the hypochlorite replaced periodically either until the tissue disappeared completely or until no further digestion occurred. When digestion was complete, the suspension was centrifuged and the supernatant replaced with distilled water. This washing procedure was repeated at least five times. In the tuna a white residue associated with the magnetic material remained after tissue digestion. Treatment with buffered EDTA (pH 7.1) carried out in similar fashion to the hypochlorite digestion freed the crystals from the residue. They could then be separated magnetically from the residue under a dissecting microscope.

To remove the magnetic particles for analysis, we held them in suspension using a cobalt–samarium magnet held to the side of the test tube, and then pipetted them onto a slide coated with xylene-based cement. The water in which the crystals were pipetted onto the slide was allowed to evaporate and a second layer of cement covering the first applied. The crystals were thus sealed in a cement sandwich which could be cut out, removed from the slide, and placed in the beam of a mini-Debye Scherrer X-ray camera. For electron microprobe analysis we pipetted the crystals onto clean microscope slides, allowed them to dry completely, and transferred them to slides coated with epoxy resin. It was then a simple matter to cure the resin, polish the crystals, and coat them with carbon for electron microprobe analyses. Similarly, aggregates can be pipetted onto plugs and prepared for examination in the scanning electron microscope (SEM) (see Perry *et al.*, this volume).

We exposed the crystals to Mo K_α X-irradiation (48–72 hr) in the mini-Debye Scherrer camera. Development of the film and measurement of the band patterns was then routine (see Perry *et al.*, this volume; Walker *et al.*, this volume). The procedure for electron microprobe analyses was more complex. These analyses determine the elemental composition of minerals and permit tests of the purity and origin of the magnetite crystals. A survey using EDAX probe was an appropriate beginning point as it indicated all the elements present and their relative proportions in any sample (see Perry *et al.*, this volume). Key elements were then selected for quantitative analyses. In the tuna and turtle, we analyzed for oxides of iron against a magnetite standard and for oxides of rare earth metals such as titanium and manganese, which are commonly found as impurities in geologic magnetite (Perry *et al.*, this volume; Walker *et al.*, this volume). We also chose to analyze for calcium in an attempt to determine how closely the residue remaining after hypochlorite digestion was associated with particle aggregates in the tuna.

Our analyses of the magnetite from the green turtle and the tuna showed that there were very few oxides other than oxides of iron in the material. Although the standard (NMNH 11487) used in the quantitative analyses was an unusually pure geologic magnetite (M. O. Garcia, Hawaii Institute of Geophysics, University of Hawaii, personal communication), it still contained measurable oxides of the rare earth metals titanium and chromium, whereas the biologic magnetites did not (see Perry *et al.*, this volume; Walker *et al.*, this volume). These data, taken with the absence of nickel from the turtle samples (Perry *et al.*, this volume) and very small amounts of manganese in magnetite from both the tuna and the turtles, strongly suggested to us that the magnetite was neither synthetic nor geologic in origin.

The very small amounts of material obtained by digestion made it impossible to use the approach developed by Towe (this volume) for preparing the crystals for transmission electron microscopy (TEM). Chang (Division of Geology and Planetary Science, California Institute of Technology, personal communication) developed a method for obtaining dis-

---

* Reference to trade names does not imply endorsement by the National Marine Fisheries Service, NOAA.

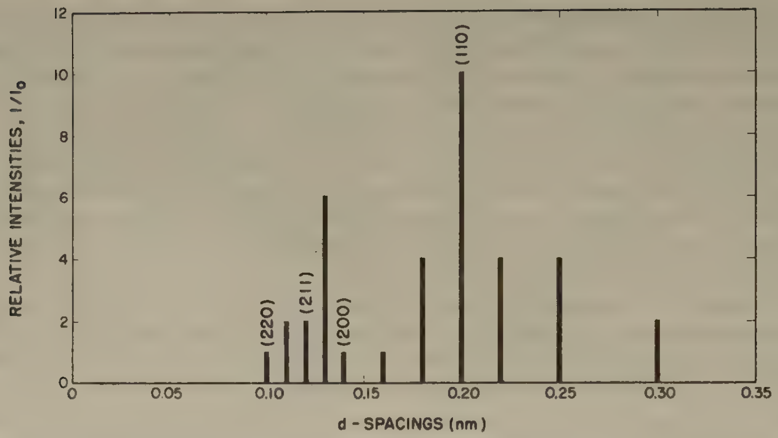

Figure 2. X-ray diffraction data for magnetic particles extracted from mouse tumors supplied by F. L. Tabrah and S. Batkin (John A. Burns School of Medicine, University of Hawaii). Vertical lines indicate relative intensities of the lines in the diffraction pattern. Numbers in parentheses indicate lines associated with metallic iron and the crystal plane giving rise to each line. Lines at *d* spacings of 0.30 and 0.25 nm could come from either magnetite or maghemite. The sources of the remaining lines in the pattern are unknown.

persed crystals that compensated for this limitation. The aggregated crystals were pipetted onto carbon-coated copper mesh grids and dispersed in an alternating magnetic field (100 mT). The grids were then air-dried and prepared for examination in TEM (see Walker *et al.*, this volume).

Extraction of the magnetic material immediately produced a substantial amount of information that assisted in its identification. For example, the color of the particles extracted from the tuna and the turtle was sufficient to exclude maghemite. Maghemite has magnetic properties similar to magnetite and therefore cannot be excluded as a source of magnetic remanence by coercivity studies. However, tests were still necessary to identify the crystals uniquely, demonstrate their biologic origin, and to exclude the possibility that contaminants may have entered during dissection or extraction. For example, the particles extracted from the yellowfin tuna and green turtle were uniquely identified as magnetite by X-ray diffraction (Perry *et al.*, this volume; Walker *et al.*, this volume). In contrast, X-ray diffraction of magnetic material extracted from tumors that had been shown to contain probable single-domain magnetite crystals revealed native iron, and a mineral that could have been magnetite or maghemite (Fig. 2). On the basis of color, maghemite could be excluded. However, the iron was presumably a contaminant arising from an as yet unrecognized source.

Diffraction patterns are not conclusive proof of the origin of magnetite particles extracted from tissues, and care is necessary in their interpretation. Pure, fine-grained magnetite powders such as those predicted for use in magnetoreception will ideally yield sharp, unambiguous diffraction patterns. Streaking of the spots or lines in X-ray and electron diffraction patterns could arise from more than one source. Towe and Moench (1981) suggest that vacancy defects in the crystal structure could have caused streaking of an electron diffraction pattern taken from single-domain magnetite crystals purified from magnetotactic bacteria. However, multidomain particles could also give streaked diffraction patterns. Therefore, procedures that combine identification of the particles with determination of their domain state are necessary. Electron diffraction and measurement of the size and shape of isolated crystals can be conducted on the same samples mounted on copper mesh grids. Thus, although electron diffraction is a more cumbersome technique than X-ray diffraction, it does provide a conclusive test of the origin of the particles when carried out in conjunction with determination of their size and morphology (Towe, this volume; Walker *et al.*, this volume).

4. Discussion

The magnetometric methods developed so far permit detection and characterization of the bulk properties of concentrations of magnetite in organisms. It is also now possible to conduct analyses of polycrystalline aggregates and isolated crystals of magnetite extracted from magnetic tissues. An important conclusion arising from these studies is that although it is relatively easy to detect the presence of magnetic material in organisms, it is far more difficult to determine its origin and what, if anything, it does. We have attempted to define a theoretical basis for determining what the form of biogenic magnetite used in magnetoreception should be, and the experimental evidence to date has been consistent with the theory. This permitted refinement of the hypothesis on the organization of magnetite-based magnetoreceptor organelles (Kirschvink and Gould, 1981; Kirschvink *et al.*, in press; Kirschvink and Walker, this volume; Walker *et al.*, this volume), providing opportunities for further tests of the ferromagnetic magnetoreception hypothesis.

An important result of this work is the demonstration of the need to test for contaminants at all stages of the research, and to check for consistency of results obtained from different techniques. The differences between the bulk magnetic properties of the dura mater of the Pacific dolphin (Zoeger *et al.*, 1981), the sample shown in Fig. 1, and the ethmoid tissues of pelagic fish (Walker *et al.*, this volume) illustrate quite clearly the effects contaminants can have on magnetometry results. The mouse tumors from which we extracted magnetic particles had previously been shown to be magnetic and probably to contain single-domain magnetite (Kirschvink *et al.*, 1982). X-ray diffraction of the magnetic particles extracted from one of the tumor strains demonstrated the presence of native iron, with the possible presence of magnetite. The presence of iron conflicts with the magnetometry data and suggests that contaminants may have entered during the extraction. Thus, magnetic material detected in tissues and obtained by extractions should be shown to be biogenic by independent means wherever possible.

The property of biogenic magnetite crystals that truly sets them apart from their synthetic and geologic counterparts is their nonoctahedral crystal morphology in TEM (Towe and Moench, 1981; Matsuda *et al.*, 1983; Walker *et al.*, this volume), a property not essential to the magnetite-based magnetoreception hypothesis. This observation suggests that the distinctive properties of biogenic magnetite arise from the biomineralization process. In line with this, it seems reasonable that the chemical composition of biogenic magnetite would be different from geologic magnetite. A potentially much more important characteristic is the ratio of the oxygen isotopes present in biologic compared with nonbiologic magnetite (Lowenstam and Kirschvink, this volume). At present, technology and availability of material limit the utility of oxygen isotopes for the recognition of biogenic magnetites. Currently available mass spectrometers require a minimum of about 20 μg of sample, which is the equivalent of quantitative extraction of the magnetite from the dermethmoid tissue of at least 100 yellowfin tuna. The potential for entry of contaminants in such a large-scale extraction is enormous. An ion microprobe may require less sample than a mass spectrometer and we are investigating the adaptation of this apparatus for analysis of biogenic magnetites.

Thus, a substantial case can be made for our ability to determine what is and is not biogenic magnetite suitable for use in magnetoreception. This does not imply that the case for magnetite-based magnetoreception is proven. However, the approach that has helped in recognition of magnetite suitable for magnetoreception may prove useful in predicting the important properties of other deposits of magnetite found in metazoans. Characterization of these deposits is important because they may predate the use of magnetite in magnetoreception (Kirschvink and Gould, 1981; Walker *et al.*, this volume), and because it is necessary to be able to distinguish the two from each other and from contaminants.

Simple hypotheses for the origin of biogenic magnetite are that it constitutes some form of iron storage or is deposited pathologically (Lowenstam and Weiner, 1983; Walker *et al.*, this volume). In support of these hypotheses is the observation that anomalous deposits of magnetic material are found more frequently in larger and older organisms (J. G. Mather, Department of Zoology, University of Manchester, personal communication, 1981; Perry, unpublished data; Walker, unpublished data). Crystal size and form may be less important in these cases than in magnetite used in magnetoreception. Presumably, enzyme catalysis will be necessary to precipitate the mineral, so the deposits are still likely to be chemically distinctive. Study of the biomineralization of other storage or pathologically formed minerals may be instructive in helping predict the likely properties of biogenic magnetite not used in magnetoreception. This may also assist in predicting where such deposits are likely to form and in their subsequent detection.

By carrying out studies with magnetite specifically in mind, we risk failing to recognize other interesting biologically formed magnetic minerals. In recent years the number of known biogenic minerals has increased substantially (Lowenstam, 1981; Lowenstam and Kirschvink, this volume). In carrying out biomagnetic studies, we should therefore be prepared to adopt appropriate approaches for correct identification and characterization of other magnetic minerals. The basic magnetometric techniques suitable for detecting these minerals are already well established through paleomagnetic studies. Buffered enzyme extractions aimed at digesting specific components of magnetic tissues may be a suitable approach for extracting magnetic minerals unaltered. The specific methods for detecting, extracting, and characterizing biogenic magnetite have undergone considerable development in the last year or two. We expect this development to accelerate as interest in biomineralization grows and hope that this chapter serves as a stimulus to development of new, more efficient approaches.

5. Summary

Magnetite detected in cells or tissues is part of a recently described class of biologically formed minerals and provides a possible physical basis for magnetoreception in living organisms. Detection of magnetic material alone adds little to understanding of either the biomineralization process or the possible use of the material in magnetoreception. Further progress requires development of procedures that will distinguish between magnetic contaminants and biologic precipitates in tissue. Hypotheses concerning the nature and role of the magnetic material can then be tested.

This chapter considers the special case of magnetite that is likely to be used in magnetoreception and attempts to define properties that will distinguish it from geologic and synthetic magnetites. Methods developed to detect and characterize the magnetic properties of such material and to distinguish it from contaminants are then described. A similar approach is used to develop techniques for extraction, identification, and characterization of the properties of individual crystals and crystal aggregates. Examples of tests that have identified magnetic material other than magnetite that could be used in magnetoreception are given for magnetometry, extraction, and histologic studies.

The studies demonstrate that the biomineralization process is responsible for producing the key distinguishing features of biologically formed magnetite. Although invasive

and noninvasive techniques can distinguish between biologic and nonbiologic magnetite, use of both approaches at once can provide considerably more information on the nature of the magnetic material as well as checks on results obtained by either set of techniques. Extension of the approaches developed in this chapter to other magnetic minerals with other possible roles in the physiology of the living organism could be equally fruitful.

Acknowledgments. We are greatly indebted to Charles E. Helsley, Barbara H. Keating, and Li Chung Ming, Hawaii Institute of Geophysics, University of Hawaii, for the use of paleomagnetic laboratory facilities and assistance with X-ray diffraction analyses. Karla A. Peterson assisted in magnetometry experiments at the California Institute of Technology. Research funds and facilities were most generously provided by the Southwest Fisheries Center Honolulu Laboratory, National Marine Fisheries Service, NOAA. This research was supported in part by a graduate study award from the East–West Center, Honolulu, and a grant from Sigma Xi to M.M.W. This is Contribution No. 3939 from the Division of Geological and Planetary Sciences, California Institute of Technology.

References

Baker, R. R., Mather, J. G., and Kennaugh, J. H., 1983, Magnetic bones in human sinuses, *Nature* **301**:78–80.

Cisowski, S., 1981, Interacting vs. non-interacting single-domain behavior in natural and synthetic samples, *Phys. Earth Planet. Inter.* **26**:56–62.

Gould, J. L., Kirschvink, J. L., and Deffeyes, K. S,. 1978, Bees have magnetic remanence, *Science*, **201**:1026–1028.

Jones, D. S., and MacFadden, B. J., 1982, Induced magnetization in the monarch butterfly, *Danaus plexippus* (Insecta, Lepidoptera), *J. Exp. Biol.* **96**:1–9.

Kirschvink, J. L., 1981, Ferromagnetic crystals (magnetite?) in human tissue, *J. Exp. Biol.* **92**:333–335.

Kirschvink, J. L., 1983, Biogenic ferrimagnetism: A new biomagnetism, in: *Biomagnetism: An Interdisciplinary Approach* (S. J. Williamson, G.-L. Romani, L. Kaufman, and I. Modena, eds.), Plenum Press, New York, pp. 501–532.

Kirschvink, J., and Gould, J. L., 1981, Biogenic magnetite as a basis for magnetic field detection in animals, *BioSystems* **13**:181–201.

Kirschvink, J. L., and Lowenstam, H., A., 1979, Mineralization and magnetization of chiton teeth: Paleomagnetic, sedimentologic, and biologic implications of organic magnetite, *Earth Planet. Sci. Lett.* **44**:193–204.

Kirschvink, J. L., Tabrah, F. L., and Batkin, S., 1982, Ferromagnetism in two mouse tumours, *J. Exp. Biol.* **101**:321–326.

Kirschvink, J. L., Walker, M. M., Chang, S.-B. R., Dizon, A. E., and Peterson, K. A., Chains of single-domain magnetite particles in chinook salmon, *Oncorhynchus tshawytscha*, *J. Comp. Physiol.*, in press.

Kuterbach, D. A., Walcott, B., Reeder, R. J., and Frankel, R. B., 1982, Iron-containing cells in the honey bee (*Apis mellifera*), *Science* **218**:695–697.

Lowenstam, H. A., 1962, Magnetite in denticle capping in recent chitons (Polyplacophora), *Geol. Soc. Am. Bull.* **73**:435–438.

Lowenstam, H. A., 1981, Minerals formed by organisms, *Science* **211**:1126–1131.

Lowenstam, H. A., and Weiner, S., 1983, Mineralization by organisms and the evolution of biomineralization, in: *Biomineralization and Biological Metal Accumulation* (P. Westbroek and E. W. de Jong, eds.), Reidel, Dordrecht, pp. 191–203.

McElhinny, M. W., 1973, *Paleomagnetism and Plate Tectonics*, Cambridge University Press, London.

Mather, J. G., and Baker, R. R., 1981, Magnetic sense of direction in woodmice for route-based navigation, *Nature* **291**:152–155.

Matsuda, T., Endo, J., Osakabe, N., Tonomura, A., and Arii, T., 1983, Morphology and structure of biogenic magnetite particles, *Nature* **302**:411–412.

Presti, D., and Pettigrew, J. D., 1980, Ferromagnetic coupling to muscle receptors as a basis for geomagnetic field sensitivity in animals, *Nature* **285**:99–101.

Towe, K. M., and Moench, T. T., 1981, Electron-optical characterization of bacterial magnetite, *Earth Planet. Sci Lett.* **52**:213–220.

Walcott, C., Gould, J. L., and Kirschvink, J. L., 1979, Pigeons have magnets, *Science* **205**:1027–1029.

Walker, M. M., and Dizon, A. E., 1981, Identification of magnetite in tuna, *Eos* **62**:850.

Zoeger, J. Dunn, J. R., and Fuller, M., 1981, Magnetic material in the head of the common Pacific dolphin, *Science* **213**:892–894.

8595

The Thermal Ecology of Basking Green Turtles *(Chelonia mydas)*

Grant Recipient: G. Causey Whittow, Pacific Biomedical Research Center, Kewalo Marine Laboratory, Honolulu, Hawaii.[1]

Grant 1765: For a study of the thermal ecology of Hawaiian green turtles.

Although terrestrial basking is common among freshwater aquatic turtles (Boyer, 1965; Moll and Legler, 1971; Terpin et al., 1979), the only sea turtle that basks in the sun, on land, is the green turtle *(Chelonia mydas)*. Furthermore, only certain populations of green turtles have been reported to bask (Balazs, 1979). Among these, the Hawaiian population may be the most important in terms of numbers of turtles and the consistency of their basking behavior. Little is known about the biology of basking sea turtles. Balazs and Ross (1974) reported that six-month-old turtles kept in a tank at the Hawaii Institute of Marine Biology basked when given the opportunity, although animals of this age do not bask under natural conditions. In a later report, Balazs (1977) described the nocturnal basking behavior of green turtles at Necker Island in the northwestern Hawaiian Islands. Balazs (1979) reported that, at French Frigate Shoals, also in the northwestern Hawaiian Islands, the incidence of diurnal basking was highest during the breeding season of the turtles, when, presumably, the number of turtles present at French Frigate Shoals was highest. The purpose of the present investigation was to study the thermal aspects of basking in Hawaiian green turtles in the hope of discovering why the turtles bask.

METHODS

The site of the study was French Frigate Shoals, in the northwestern Hawaiian Islands. French Frigate Shoals is an atoll consisting of a crescent-shaped reef and approximately 12 small sand islands (Figure 1). Of these islands, Trig and Whale-Skate are favored for basking while East Island, which is the main site for nesting, is used particularly during the egg-laying season. Most observations in the present investigation were made on Trig Island. Captive green turtles were studied at the Kewalo Marine Laboratory (University of Hawaii), the Hawaii Institute of Marine Biology (University of Hawaii), and Sea Life Park, an oceanarium on Oahu, Hawaii. On both Trig and Whale-Skate Islands, the procedure was to observe a single turtle and to keep a complete dossier of its movements, behavior, orientation with respect to that of the sun and wind, and its respiratory pattern, from the time of its emergence to the time of either its return to the ocean or when the observer left the island. Records were also kept of the temperature of a 15.2-cm black globe, the temperature of the sand surface, and the magnetic compass bearing of the sun and wind. Great care was taken to ensure that the turtle was not aware of the observer. This was usually achieved by lying prone behind vegetation. If the observer was seen by the turtle it appeared to remain alert, with its eyes open; but the profile of an observer standing close to a turtle would invariably provoke it to return to the sea.

---

[1] Co-investigator for this project was George H. Balazs, Hawaii Institute of Marine Biology, University of Hawaii, Honolulu, Hawaii.

The black globe (Casella & Co., London), painted with Nextel Black Velvet coating (Minnesota Mining Co.), was suspended 10 cm above the surface of the sand to approximate the midpoint of the turtle. The ratio-

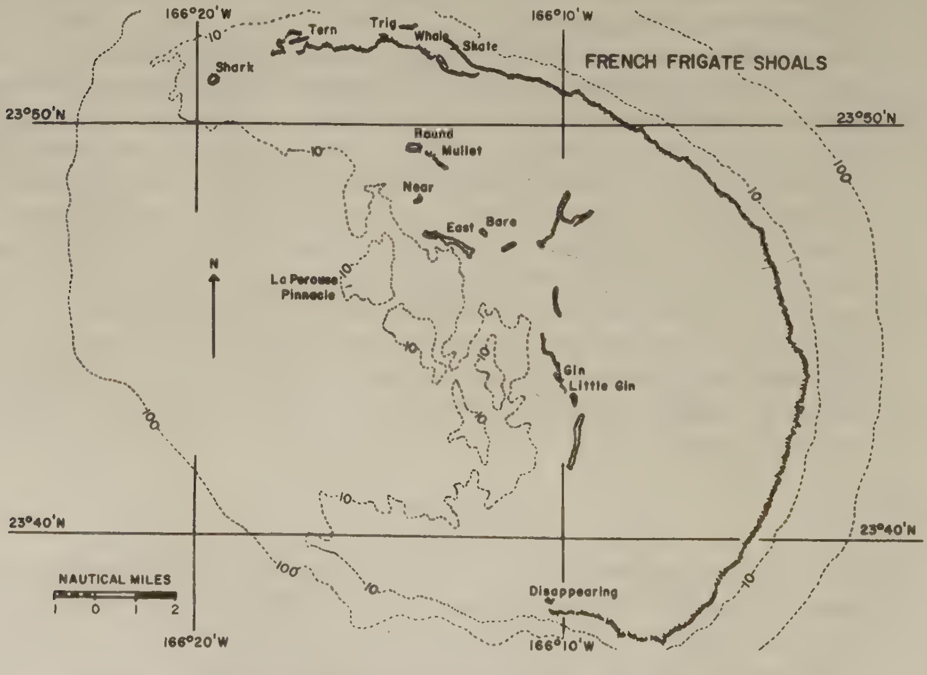
166°20'W
10
Tern
Trig
Whale
Skate
166°10'W
FRENCH FRIGATE SHOALS
Shark
23°50'N
23°50'N
Round
Mullet
10
Near
East
Bare
10
N
La Perouse Pinnacle
10
Gin
Little Gin
100
100
23°40'N
23°40'N
NAUTICAL MILES
1 0 1 2
166°20'W
100
10
Disappearing
166°10'W
10

FIGURE 1. French Frigate Shoals showing Trig and Whale-Skate Islands.

nale for its use in field studies on the thermal ecology of basking turtles is similar to that for its use in field studies of basking seals (Whittow, 1978).

Sand surface temperatures, were measured with mercury thermometers; surface temperatures of carapace and plastron, with a Barnes Portable Infrared Thermometer (Model PRT-10-L), as described previously (Whittow, 1978).

The interval between breaths was measured with a stopwatch, using binoculars; most basking turtles raise their heads at each breath, which facilitates counting the number of breaths.

The orientation of the turtle was recorded with the aid of a sighting pocket compass. A compass was also used to measure the bearing of the sun and the direction of the wind, as described previously (Whittow, 1978).

RESULTS

Thermal Profile of the Basking Beach. On Trig Island, and also on Whale-Skate, the turtles prefer the side of the island facing the outer reef, and it is rare to see a basking turtle on the opposite side of the island. The basking beach also happened to be the beach facing the prevailing northeast trade winds. In Figure 2 the sand and black-globe temperatures are shown for both the basking beach and the beach not favored for basking. The data for the two sides of the island were obtained on the same day, so that they are directly comparable. It may be seen from Figure 2 that there was a striking difference between the thermal conditions on the basking beach and the opposite side of the island. This was true for both islands. Sand temperatures were lower, and black globe temperatures strikingly lower, on the beach favored by the turtles for basking. The basking beach faced the wind but, for the great part of the time, faced away from the sun—factors that probably contributed in large part to the cooler conditions on the basking beach. The slopes of the beaches, which may have a bearing on the amount of solar radiation incident on the turtles, were slightly different: 7° for the basking beach on both Trig and Whale-Skate, as opposed to 11.5° (Whale-Skate) and 9.3° (Trig) for the beaches where basking was rare.

Basking Behavior. The turtles began to come ashore to bask at midmorning and continued to do so during the afternoon. The duration of basking varied considerably. Some evidence was obtained that the duration of basking was greater, the lower the mean black-globe temperature while the turtle was basking (Figure 3). While the turtles were ashore they were extremely inactive. The only discernible movements were raising of the head each time that the turtle breathed, and sand flipping.

Breathing Pattern. The characteristic pattern of breathing in the basking turtles consisted of single respirations alternating with long periods of apnea (breath-holding). The mean duration of the breath-hold in the turtles at French Frigate Shoals was 219.2 sec, as shown below, but the range of values was considerable (50 to 635 sec). There did not appear

	French Frigate Shoals	Kewalo Marine Laboratory	Sea Life Park
Mean (sec)	219.2	227.8	217.4
Standard deviation	123.1	130.1	106.4
No. of observations	138	13	14

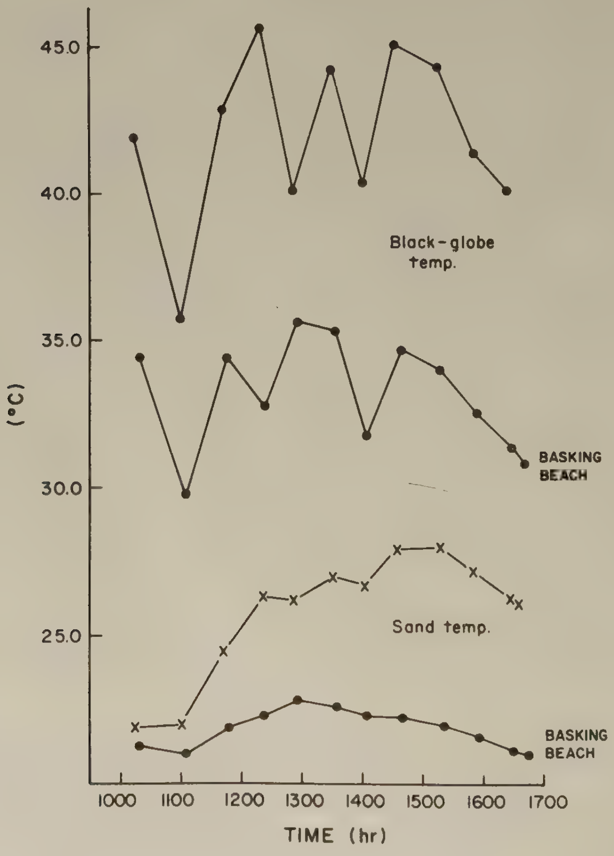

Figure 2. Sand and black-globe temperatures on the basking beach at Trig, and also on the beach not favored by basking turtles.

to be any trend in the respiratory pattern related to duration of basking. The breath-hold times recorded for captive animals at the Kewalo Marine Laboratory and Sea Life Park were within the range of those at French Frigate Shoals. So also were the times of voluntary submergence of the captive turtles in water, measured on seven occasions. On an eighth occasion, however, a captive turtle remained under water for 1032 sec. Most turtles raised their heads during a respiration, and many of them moved the head to one side. The turtles seemed more alert when taking a breath, and any small movements made by the turtles were executed immediately following a breath.

Sand Flipping. Many turtles flipped sand onto their carapaces with

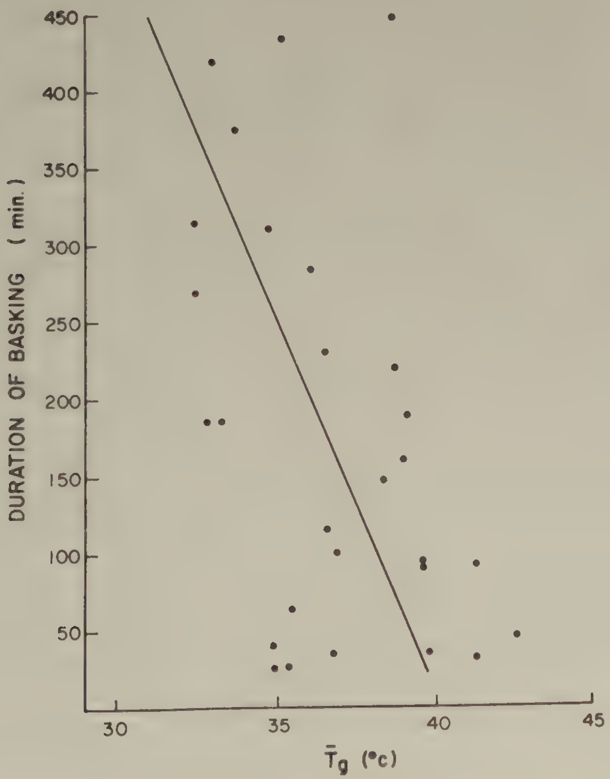

FIGURE 3. Relationship between the duration of basking and the mean black-globe temperature ($\bar{T}g$) during the basking period. Each point represents a separate turtle. The line is the fitted regression line ($y = 975{\cdot}96 - 21{\cdot}67\,x$).

their front flippers during basking. Because of the smooth surface and rounded contours of the carapace, little sand usually remained on the carapace, but it tended to accumulate on the edges. Continued vigorous sand flipping could cover as much as one third of the carapace with sand. Sand flipping did not occur until the carapace was dry, and it occurred more frequently on very hot days. On relatively cool, cloudy days, sand flipping was not seen. Simultaneous measurements of the temperature of the sand-covered carapace and of the uncovered carapace revealed that the latter could be 10°C warmer than the sand on the carapace. A variation of sand-flipping behavior was seen in the captive turtle at the Kewalo Marine Laboratory. This turtle was provided with a wooden basking ramp and it very often basked parallel to and close to the edge of the water in its tank. In this position, it was able to flip water over its carapace with one of its flippers.

Orientation. No evidence was obtained that the turtles changed their orientation with respect to either the sun or wind. The turtles very often remained in the same position for long periods of time; this was usually the position that they had adopted on first emerging from the ocean.

Carapace Temperature. The carapace temperatures of basking turtles at French Frigate Shoals, and of captive turtles, are given below:

	N	$\bar{x}$	S.D.	RANGE
French Frigate Shoals	38	34.5	4.0	25.0-42.3
Kewalo Marine Laboratory, Honolulu	16	37.3	2.4	32.0-40.0
Sea Life Park, Oahu	20	37.8	2.3	35.0-42.8

The measurements were obtained under widely varying conditions but they were all made when the carapace was dry and exposed to direct solar radiation. The mean carapace temperature was slightly higher in the captive turtles, possibly reflecting the hotter conditions prevailing in their more southerly situation. In many ways, the ranges of values shown above are more instructive than the means of the values. The lowest temperature (25°C) was obtained in the late afternoon when conditions on the beach were relatively cool. The highest temperatures (40.0 to 42.8°C) suggest that the turtles may be absorbing a significant amount of solar radiation.

Rectal Temperature. The number of measurements of rectal temperature was limited by the consideration that, unlike other observations and measurements in this study, it involved interference with the animal. Results on 17 animals were:

N	x̄	S.D.	Range
17	28.7	1.4	26.9-31.3

As in the case of the carapace temperature measurements, the values were obtained under a variety of conditions and the mean value is probably less informative than the highest reading (31.3°C). This value was 5°C higher than the ocean temperature. Higher rectal temperatures might have been recorded if more measurements had been made. Assuming that the mean body temperature of the turtle was 31.3°C, that the specific heat of the tissues was 0.83, and that the turtle's body temperature was close to that of the ocean when it emerged to bask, it was calculated that the turtle had stored 465 kcal of heat during basking. This calculation was based on an estimated body weight of 112 kg, derived from measurements of the turtle's linear dimensions. The estimated weight of the turtle was also used to obtain a value for the resting metabolic rate of the turtle (Prange, 1976). It transpired from these calculations that the quantity of heat stored by the turtle was more than 12 times the hourly metabolic rate of a turtle of these dimensions.

Shade, Cloud, Rain. There is no shade on the beaches at French Frigate Shoals, and turtles clearly do not leave the ocean in order to seek shade. At Sea Life Park, part of the basking area was shaded by a tree, and it is interesting that on one particularly hot, still day, two turtles were observed to bask in the shade.

Turtles were never observed to bask when it was raining. In fact, on Trig Island two basking turtles were observed to return to the ocean during a brief, heavy rain. Captive turtles did not bask during prolonged heavy rain, either. In both captive turtles and the turtles at French Frigate Shoals, the incidence of basking was high on the first sunny day following stormy, rainy weather. Turtles that had emerged from the ocean to bask during sunny weather remained ashore with the advent of cloudy conditions. On occasion, turtles—both captive animals and those at French Frigate Shoals—were seen to bask in cloudy weather.

CONCLUSIONS

The observations made in this study suggest that basking green turtles may absorb a significant amount of solar radiation. However, the effect of any absorbed heat is lessened by the selection of a relatively cool beach and by the complete inactivity of the turtles, apart from thermoregulatory behavior. These factors may enable the turtles to stay on the beach for a longer period of time than they would ordinarily. Freshwater aquatic turtles are believed to derive a number of benefits from basking, including synthesis of vitamin D, destruction of algae, and improvement of digestion (Boyer, 1965; Moll and Legler, 1971; Gatten, 1974). To these might be added, for Hawaiian green turtles, evasion of predatory tiger sharks. The basking behavior of Hawaiian green turtles may in fact be made possible by the prevalence of the northeast trade winds and the highly reflective, cool, white sand of the northwestern Hawaiian Islands. A similar conclusion was made with regard to the thermoregulatory behavior of the Hawaiian monk seal, which shares the basking beaches with the turtles (Whittow, 1978).

REFERENCES

Balazs, G. H.

1977. Ecological aspects of green turtles at Necker Island. 27 pp. University of Hawaii, Hawaii Institute of Marine Biology.

1979. Synopsis of biological data on the green turtle in the Hawaiian Islands. National Marine Fisheries Service Report.

Balazs, G. H., and Ross, E.

1974. Observations on the basking habit in the captive juvenile Pacific green turtle. Copeia, no. 2, pp. 542-544.

Boyer, D. R.

1965. Ecology of the basking habit in turtles. Ecology, vol. 46, pp. 99-118.

Gatten, R. E.

1974. Effect of nutritional status on the preferred body temperature of the turtles *Pseudomys scripta* and *Terrapene ornata*. Copeia, no. 4, pp. 912-917.

Moll, E. O., and Legler, J. M.

1971. The life history of a Neotropical slider turtle *Pseudomys scripta* (Schoepff), in Panama. Bull. Los Angeles County Museum Natural History, no. 11, pp. 72-79.

Prange, H. D.

1976. Energetics of swimming of a sea turtle. Journ. Exp. Biol., vol. 64, pp. 1-12.

Terpin, K. M.; Spotila, J. R.; and Foley, R. E.

1979. Thermoregulatory adaptations and heat energy budget analyses of the American alligator, *Alligator mississippiensis*. Physiol. Zool., vol. 52, pp. 296-312.

Whittow, G. C.

1978. Thermoregulatory behavior of the Hawaiian monk seal *(Monachus schauinslandi)*. Pacific Sci., vol. 32, pp. 47-60.

G. Causey Whittow
George H. Balazs

8596

SKELETOCHRONOLOGICAL AGE ESTIMATES FOR HAWAIIAN GREEN TURTLES

Age estimates of Hawaiian *Chelonia mydas* indicate that turtles resident to different foraging pastures may reach adult size at significantly different ages (Balazs 1980). These age estimates were derived entirely from growth rates of wild animals recaptured one or more times. An independent method of age estimation seemed desirable to test the estimates derived from growth data. The tentative success of the skeletochronological technique (Zug et al. 1983, in press) offered such an opportunity.

Humeri were available from 10 Hawaiian *Chelonia* that died from various causes over the past 9 years, and a single green turtle from Canton Island (lat. 2°50'S, long. 171°43'W) in the Phoenix Group. More humeri are currently being obtained for additional analysis. The bones were prepared and examined as outlined in Zug et al. (1983). The skeletochronological age estimates were made without knowledge of age or specific provenance of the specimens.

Of the 11 specimens, minimum age could be estimated for 9 (Table 1). The bone sections from the remaining two were homogenous in appearance and had no evidence of periosteal laminae (cyclic marks of skeletal growth, MSG's). We can offer no satisfactory explanation for the absence of MSG's, but their absence is observed in other reptiles (*Caretta*, *Iguana*) (Zug, unpubl. obs.). The number of MSG's visible in bone sections of the other Chelonia ranges from 1 to 16 (median 3; mean 4.6).

Age estimates from sections with few MSG's would seem less reliable than estimates from sections with numerous MSG's. In general, the extreme — low and high — estimates are associated with few MSG's per section. The linear regression for the entire Hawaiian sample is $Y = 52.03 + 0.329X$ ($r = 0.66$) and for this sample without the centenarian $Y = 40.69 + 0.746X$ ($r = 0.92$), where Y is carapace length in centimeters and X is age in years. Thus, only the

135-yr estimate deviates strongly from the other estimates.

Table 1. Body dimensions and age estimates of Chelonia mydas. Abbreviations: CL, carapace length, straight line; HL, maximum length of humerus; M & F, male and female; Sk and K, age estimates from skeletochronology and known age, respectively.

			Age Estimate		
CL	HL	Sex	Sk	K	Provenance
			Oahu Island		
33.6	6.3	?	?	2	Lanikai
45.1	8.7	?	(4)		Reef Runway
54.0	11.4	?	18		Bellows
74.8	15.6	M	(135)		Barbers Point
88.8	19.4	F	43		Kaneohe Bay
92.7*	19.3	M	81		Bellows
93.0	19.2	F	(66)		Waikiki
			Hawaii Island		
39.4	8.0	?	(17)		Kau District
52.4	11.1	?	13		Kau District
			Northwestern Hawaiian Islands		
41.0	7.6	?	?		French Frigate Shoals
			Phoenix Group		
90.0	20.2	F	15		Canton Island

*The only over-the-curve carapace length measurement.
() Age estimated from one or two MSG's

Although these age estimates are most tentative, they suggest several general observations. Mark and recapture growth data indicate that the Kau turtles grow considerably faster than the Oahu turtles (Balazs 1982); the skeletochronological estimates suggest slow growth and late maturity for turtles at both locations. If sexual maturity occurs at carapace length greater than 81 cm, Hawaiian turtles may require 40-50 yr to reach that size. The Canton Island turtle derives from considerably warmer waters and its estimated age indicates much faster growth and earlier maturity.

Balazs, G. H. 1980. Synopsis of biological data on the green turtle in the Hawaiian Islands. US Dep. Commer., NOAA Tech. Memo. NMFS, NOAA-TM-NMFS-SWFC-7, 141p.

Balazs, G. H. 1982. Growth rates of immature green turtles in the Hawaiian Archipelago. pp. 117-126 In K. A. Bjorndal (ed.) Biology and Conservation of Sea Turtles, Smithsonian Institution Press, Washington, DC.

Zug, G. R., A. Wynn and C. Ruckdeschel. 1983. Age estimates of Cumberland Island loggerhead sea turtles. MTN 25:9-11.

Zug, G. R., A. Wynn and C. Ruckdeschel. In press. Age determination of loggerhead sea turtles, Caretta caretta, by incremental growth marks in the skeleton. Smithsonian Contrib. Zool.

GEORGE R. ZUG, Department of Vertebrate Zoology, National Museum of Natural History, Smithsonian Institution, Washington, DC 20560 USA

GEORGE H. BALAZS, Southwest Fisheries Center Honolulu Laboratory, National Marine Fisheries Service, NOAA, PO Box 3830, Honolulu, HI 96812 USA.

GPO 684-443/18018